FY13 ANNUAL PROGRESS REPORT

Los Alamos NATIONAL LABORATORY EST. 1943

Laboratory Directed Research and Development

Los Alamos National Laboratory

This page intentionally left blank.

About the Cover

ChemCam is the Chemistry and Camera instrument, one of 11 science instruments onboard the NASA Mars Science Laboratory rover, Curiosity. As the name implies, ChemCam is actually two different instruments combined as one: a Laser-Induced Breakdown Spectrometer (LIBS) and a Remote Micro Imager (RMI). The purpose of the LIBS instrument is to provide elemental compositions of rock and soil, while the RMI will give ChemCam scientists high-resolution images of the sampling areas of the rocks and soil that LIBS targets.

The LIBS technology was developed at Los Alamos National Laboratory with early support from the LDRD program. The research focused on LIBS technique for detection work in hazardous environments. A 2010 LDRD project explored direct application of LIBS on the ChemCam instrument, including LIBS detection limitations in Mars and Venus environments. Today LDRD is exploring the applications of this technology for finding and analyzing nuclear materials.

Los Alamos
NATIONAL LABORATORY
EST.1943

Disclaimer

Issued March 2014

Structure of this Report

In accordance with U.S. Department of Energy Order (DOE) 413.2B, the Laboratory Directed Research and Development (LDRD) annual report for fiscal year 2013 (FY13) provides summaries of each LDRD-funded project for the fiscal year, as well as full final reports on completed projects. The report is organized as follows:

Overview: An introduction to the LDRD Program at Los Alamos National Laboratory (LANL), the program's structure and strategic value, the LDRD portfolio management process, and highlights of outstanding accomplishments by LDRD researchers.

Project Summaries: The project summaries are organized first by science and technology categories: Physics, Chemistry and Material Sciences, Environmental and Biological Sciences, Information Science and Technology, and Technology. Within each category, summaries are organized by LDRD component in the following order: Directed Research (DR, Exploratory Research (ER), Early Career Research (ECR), and Postdoctoral Research and Development (PRD). Full final reports are included at the end of each section.

Projects are listed in numerical order according to their project identification number, which consists of three parts. The first is the fiscal year in which the project began; the second is a unique numerical identifier; and the third identifies the project component.

Acknowledgements

Technical Review
William Priedhorsky
Jeanne Robinson
Lennett Rendon

Publication Editor and Designer
Andrea Maestas

Team Contributors
Stephen Schultz
Lisa Lujan
Susan Whittington
Debbie Martinez
Peter Haase

Table of Contents

Environmental and Biological Sciences

Information Science and Technology

Physics

Technology

Laboratory Directed Research & Development: Making every mission possible

by William Priedhorsky, Los Alamos LDRD Program Manager

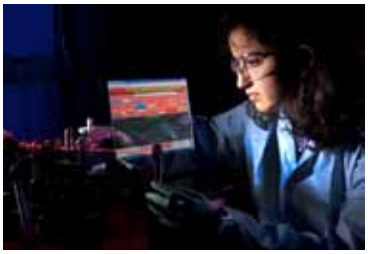

R&D is one of the best investments a country can make. In his 2013 remarks to the National Academy of Sciences, President Obama said, "With the pace of technological innovation today, we can't afford to stand still for a year or two years or three years. We've got to seize every opportunity we have to stay ahead. And we can't let other countries win the race for ideas and technology of the future." The national laboratories have been entrusted with the role of serving as incubators for innovation — places where novel solutions to resolve future national security challenges are cultivated, directed, and sustained. The Laboratory Directed Research and Development program at Los Alamos National Laboratory has a fundamental role in maintaining intellectual vitality and innovation in our enduring capabilities. It is also critical in anticipating and addressing technical challenges that would otherwise compromise the Laboratory's ability to execute its missions to

- ensure the safety and reliability of U.S. nuclear deterrent,
- reduce the threat of weapons of mass destruction, proliferation, and terrorism, and
- solve national problems in defense, energy, environment, and infrastructure.

These missions demand that we *anticipate, innovate, and deliver* to solve the unsolved and know the unknown. We seek innovation that can drive breakthroughs in mission performance, whether that mission demands prediction of weapons aging, the remediation of legacy contamination, or the mitigation of transnational terrorism.

At Los Alamos, LDRD is an open market for ideas, inspired by mission. We succeed because of the diversity of our investments, which mix applied and fundamental research. Although no single project can guarantee results, the aggregate results of LDRD investment drive the Laboratory forward. The LDRD program is extremely important in the recruitment and retention of technical staff, as well as for our postdoc pipeline and collaborations with academia. Many of the innovations and technological advances that put Los Alamos on the map are built upon the quality and success of the LDRD program.

Our missions require breadth and depth in science and technology. Their complexity demands a span of excellence that crosses nearly every discipline in science. For example, the core nuclear weapons program demands prediction and control of materials in extreme conditions, computing at the petascale and soon the exascale, the understanding of turbulent fluid flow, miniaturized smart sensors, and advances in nuclear and high-energy density physics.

By investing in LDRD, Los Alamos builds its vision: to be the National Security Science Laboratory of choice, ready to take on whatever complex issue the nation asks of us.

Laboratory Directed Research and Development is the most prestigious source of research and development funding at the Los Alamos National Laboratory. It follows a strategic guidance derived from the missions of the U.S. Department of Energy, the National Nuclear Security Administration, and the Laboratory. To execute that strategy, the Los Alamos LDRD program creates a free market for ideas that draws upon the bottom-up creativity of the Laboratory's best and brightest researchers. The combination of strategic guidance and free-market competition provides a continual stream of capabilities that position the Laboratory to accomplish its missions.

The LDRD program provides the Laboratory Director with the opportunity to strategically invest in forward-thinking, potentially high-payoff research that strengthens the Laboratory's capabilities for national problems. Funded in FY13 with approximately 6.9% of the Laboratory's overall budget, the LDRD program makes it possible for researchers to pursue cutting-edge research and development. This in turn enables the Laboratory to anticipate, innovate, and deliver world-class science, technology, and engineering.

Program Structure

The Los Alamos LDRD program is organized into four program components with distinct institutional objectives: Directed Research (DR), flagship investments in mission solutions; Exploratory Research (ER), smaller projects that invest in people and skills that underpin key Laboratory capabilities; Early Career Research (ECR), supporting the development of early-career researchers; and Postdoctoral Research and Development (PRD), recruiting bright, qualified, early-career scientists and engineers. In FY13, the LDRD program funded 300 projects with total costs of $145.7 million. These projects were selected through a rigorous and highly competitive peer-review process and are reviewed formally and informally throughout the fiscal year.

Directed Research

The DR component makes long-range investments in multidisciplinary scientific projects in key competency or technology-development areas vital to LDRD's long-term ability to execute Laboratory missions. In FY13, LDRD funded 54 DR projects, which represents approximately 56% of the program's research funds. Directed Research projects are typically funded up to a maximum of $1.8M per year for three years.

The DR component is guided by the LDRD Strategic Investment Plan, which is in turn guided by eight Grand Challenges that define the advances in science and technology that are needed to address Los Alamos missions. In FY13, the LDRD Program Office engaged thought leaders across the Laboratory to restructure the DR component for the upcoming fiscal year. The new scheme consists of five Focus Areas that map directly to the Los Alamos science pillars, plus two additional multi-competencies not captured by the pillars. The new structure applies to the FY14 LDRD program plan.

Exploratory Research

The ER component is focused on developing and maintaining technical staff competencies in key strategic disciplines that form the foundation of the Laboratory's readiness for future national missions. Largely focused on a single discipline, ER projects explore highly innovative ideas that underpin Laboratory programs. In FY13, LDRD funded 135 ER projects, which represents approximately 34% of the program's research funds. Exploratory Research projects are typically funded up to a maximum of $390K per year for three years.

Unlike DR proposals, division endorsements are not required for ER proposals; instead, this component of the LDRD program is operated as an open and competitive path for every staff member to pursue funding for his/her great idea. The ER component is a critical channel for purely bottom-up creativity at the Laboratory. Nonetheless, it is strongly driven by mission needs via the definition of the 12 ER research categories, and the assignment of investment between them.

Early Career Research

The ECR component of the LDRD program is designed to strengthen the Laboratory's scientific workforce by providing support to exceptional staff members during their crucial early career years. The intent is to aid in the sometimes challenging transition from postdoc to full-time staff member, and to stimulate research in disciplines supported by the LDRD program. In FY13, the LDRD program funded 28 ECR projects, which represents approximately 3% of the programs research funds. Early Career Research projects are funded up to $225K per year for two years, and only up to 60% of their overall funding can be from the LDRD program.

Postdoc Research and Development

The PRD component ensures the vitality of the Laboratory by recruiting outstanding researchers. Through this investment, the LDRD program funds postdoctoral fellows to work under the mentorship of PIs on high-quality projects. The primary criterion for selection of LDRD-supported postdocs is the raw scientific and technical talent of the candidate, with the exact specialty of the candidate a

Directed Research Grand Challenges	Mission Impact
Beyond the Standard Model	Sensitive instrumentation and tools to manipulate massive data volumes, in support of national security missions
Materials: Discovery Science to Strategic Applications	Energy sources, efficiency and storage; sensing for threat reduction; materials underpinnings of stockpile security
Complex Biological Systems	Energy, national security, health and the environment
Information Science and Technology	Overarching capability supporting all Laboratory missions
Earth and Energy Systems	Energy and climate security
Nuclear Performance	Stockpile safety, surety and reliability
Sensing and Measurement Science for Global Security	Nuclear weapons of mass destruction, space situational awareness, global environmental treaty monitoring, and emerging threats
Engineered Systems	Systems-level solutions for all missions

Exploratory Research Technical Categories	Laboratory Capability
Biological, Biochemical, and Cognitive Sciences	Biosciences
Chemistry and Chemical Sciences	Chemistry
Computational and Numerical Methods	Information and knowledge sciences, computer and computational sciences
Computer Science, Mathematics, and Data Science	High-performance computing, data analysis, and data-driven science
Defects and Interfaces in Materials	Theoretical, computation and modeling, and experimental methods to understand defects and interfaces in materials
Earth and Environmental Sciences and Space Physics	Earth and space sciences
Engineering Applications	Weapons science and engineering, advanced manufacturing, sensors, and remote sensing
Emergent Phenomena in Materials Functionality	Theory, computation and modelling, and experimental methods to understand behavior of materials
High-energy Density, Plasma, and Fluid Physics	High-energy density plasmas and fluids and beams
Measurement Science, Instrumentation, and Diagnostics	Measurement methods that enable new scientific discovery
Nuclear and Particle Physics, Astrophysics, and Cosmology	Nuclear physics, astrophysics, and cosmology
Quantum and Optical Science	Fundamental interactions and excitations in atomic, optical, and molecular systems

secondary factor. In FY13, LDRD funded 82 PRD projects, which represents 6% of the program's research funds. These postdocs are supported full-time for two years.

In addition to approximately 47 Director's Postdocs, the LDRD program supported 17 distinguished postdoctoral fellows at a higher salary and for a three-year term. Distinguished postdoctoral fellow candidates typically show evidence of solving a major problem or providing a new approach or insight to a major problem and show evidence of having a major impact in their research field. To recognize their role as future science and technology leaders, these appointments are named after some of the greatest leaders of the Laboratory's past.

More postdocs are hired through DR and ER projects than directly through PRD appointments. Counting both avenues, the LDRD program supported 61% of the 596 postdocs at the Laboratory in FY13.

Postdoctoral Research and Development Projects

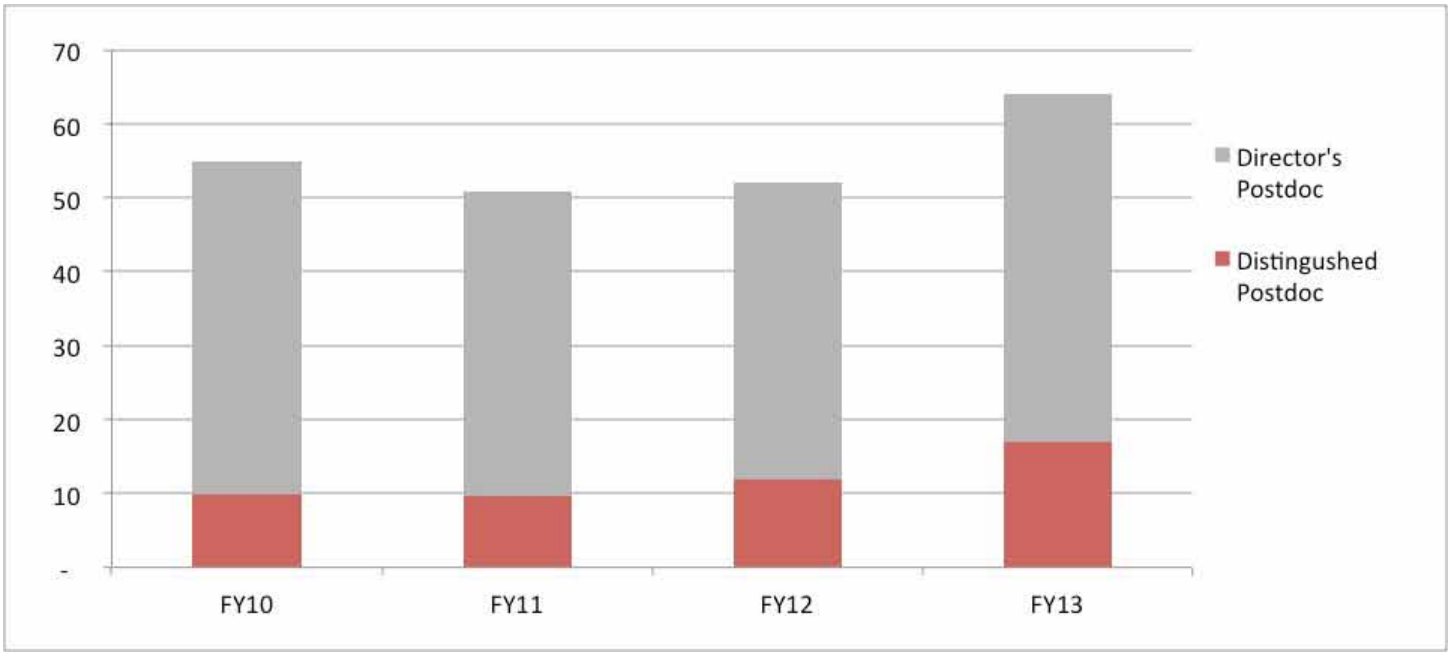

An intense burst of laser energy slams into an extremely thin foil target to produce neutrons at Los Alamos National Laboratory's TRIDENT laser facility during a recent experiment, which proved that laser-driven neutrons can be used to detect and interdict smuggled nuclear materials.

First nuclear material detection by short-pulse-laser-driven neutron source

Los Alamos researchers successfully demonstrated for the first time that laser-generated neutrons can be enlisted as a useful tool for national security.

The international research team used the short-pulse laser at Los Alamos' TRIDENT facility to generate a neutron beam with novel characteristics that interrogated a closed container to confirm the presence and quantity of nuclear material inside. The successful experiment paves the way for creation of a table-top-sized or truck-mounted neutron generator that could be installed at strategic locations worldwide to thwart smugglers trafficking in nuclear materials.

See this scientific achievement in motion on the Laboratory's You Tube page.

Program Reserve

Most LDRD investments are selected in a rigorous, multi-step peer-review process during the nine months preceding the new fiscal year. However, in a fast-changing world, there are needs that cannot wait until the next cycle of competition. The LDRD Program Office holds a reserve each year for these needs. This reserve is small on a program basis, but allows the opportunity to make modest investments that address new opportunities. In FY13, the reserve budget was approximately $3.2M.

Reserve decisions are guided by strategic priorities articulated by Division Leaders, Associate Directors, and more senior management. They are also informed by the just-concluded competitive cycle, in which selection panels sometimes identify ideas that are exciting but just not mature enough for a full-scale investment. Reserve is held foremost to exploit opportunity, rather than fix problems, and the expectation is that reserve projects will be the first step in a chain that leads to bigger things.

Reserve Project Delivers Results

Numerous space probes have taken advantage of radioisotope thermoelectric generators (RTGs) powered by plutonium. However, the end of the Cold War brought about a shortage of plutonium. In collaboration with NASA Glenn Research Center and National Security Technologies, a team of LDRD researchers developed an alternative type of nuclear reactor, one that uses plentiful uranium as its fuel source. Known as KiloPower, the reactor has six major components: a reactor core, core reflector, a rod to start the reactor, heat pipes to move energy, radiation shielding and Stirling engines to provide power. Measuring just 1 ft, the fast reactor uses neutrons with a high-energy range, in excess of 0.2 meV, to produce fission and employs heat pipes to remove heat from the core. The heat pipes transfer the heat to a Stirling-engine power-conversion system. The Stirling engine then produces 500 to 1,500 W of electricity over 15 to 30 years.

With KiloPower, it is possible for NASA and other governmental and industrial organizations to continue developing probes and spacecraft for deep-space exploration.

Researchers test novel power system for space travel

A team of Los Alamos researchers developed a small-space reactor known as KiloPower that can provide long-term power—approximately 15 to 30 years—to a deep-space probe or satellite. To produce electricity, KiloPower uses a nuclear fission system as a heat source that transfers heat via a heat pipe to a small Stirling-engine-based power convertor to produce electricity.

KiloPower uses plentiful uranium instead of scarce plutonium; generates 500 to 1,500 watts of electricity; and minimizes hazards and guarantees performance as a result of its safe and simple design. With KiloPower, it is possible for NASA and other government and industrial organizations to continue developing probes and spacecraft for the exploration of deep space. Other applications include providing power on the surfaces of planets, mobile power for forward-operating bases (of interest to the Department of Defense), and power in remote locations of interest to intelligence agencies.

Los Alamos research on the project was funded by the LDRD program. NASA Glenn and NSTec also used internal support to fund their contributions to the experiment.

“Perhaps one of the more important aspects of this experiment is that it was taken from concept to completion in 6 months for less than a million dollars,” said Los Alamos engineer David Dixon. “We wanted to show that with a tightly-knit and focused team, it is possible to successfully perform practical reactor testing.”

See this scientific achievement in motion on the Laboratory’s You Tube page.

Project Budgets

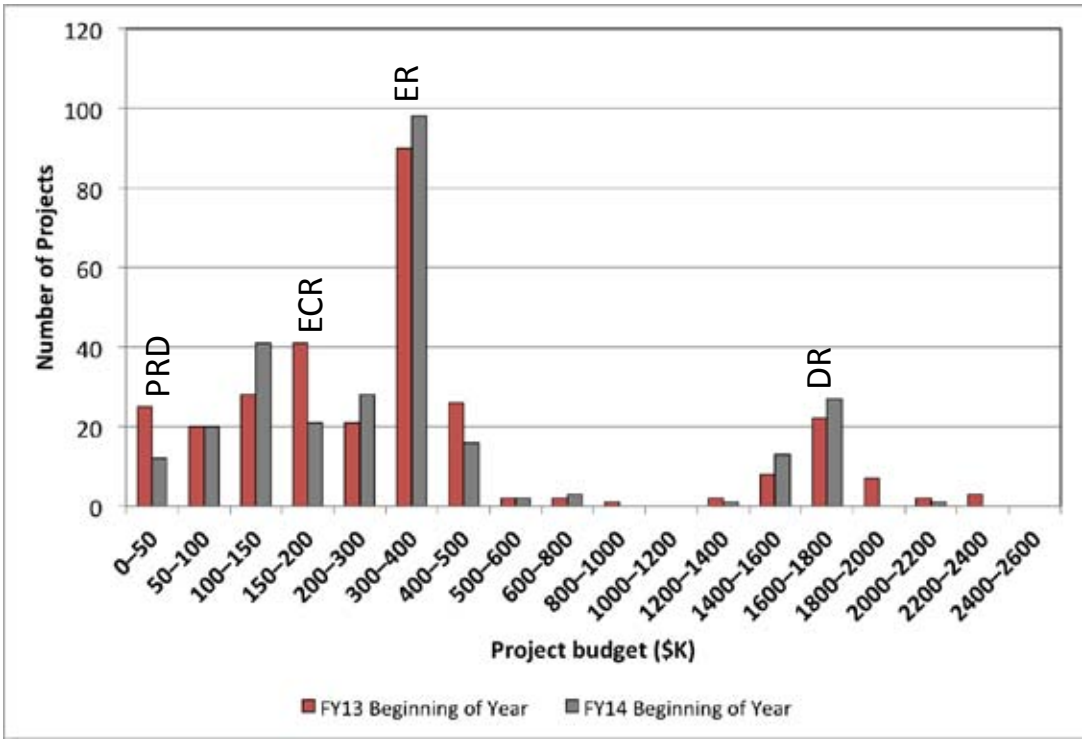

Senior management reviews project sizes annually with a goal of keeping projects as small as possible, while still accomplishing our strategic objectives. Typical project sizes for each LDRD component are identified above.

Protecting ports, borders, and critical infrastructure

The Multi-Mode Passive Detection System (MMPDS) combines technology invented by scientists at Los Alamos with private sector investment and expertise from Decision Sciences, to deliver totally safe, effective and reliable automated scanning to speedily detect both shielded and unshielded nuclear and radiological threats. Additional modality enables explosive and contraband detection. Harnessing the natural occurrence of muons in the atmosphere, MMPDS tracks muons through even heavily shielded materials and computes a 3-D image of what is being scanned. In combination with a gamma radiation detector, MMPDS can scan a typical 40-foot shipping container in 45 seconds, on average, providing accurate and safe scanning while facilitating the flow of commerce. The MMPDS technology produces no ionizing radiation, meaning it is completely safe for people, animals, plants and food. MMPDS modular construction enables the system to be scaled up or down to scan any type of vehicle, rail cars and cargo containers.

A key driver behind the success of MMPDS is a technology called muon tomography. Muons are naturally occurring cosmic ray-induced particles that continuously rain down from the Earth's upper atmosphere, harmlessly penetrating everything they touch. MMPDS tracks these muons, detecting and recording their deflection signatures with advanced proprietary software and algorithms as they pass through an object within the MMPDS. LDRD investment in muon tomography dates back to 2001.

The Laboratory granted Decision Sciences Corporation exclusive commercial license for muon tomography, and the technology won a 2013 R&D 100 Award. Watch a *Nova* segment about MMPDS on the Decision Sciences website.

The Los Alamos LDRD portfolio reflects diversity at all levels, from innovative projects that span the DOE missions, to a diverse pool of researchers that range from early career to senior scientist.

LDRD Researchers Across Divisions and Directorates

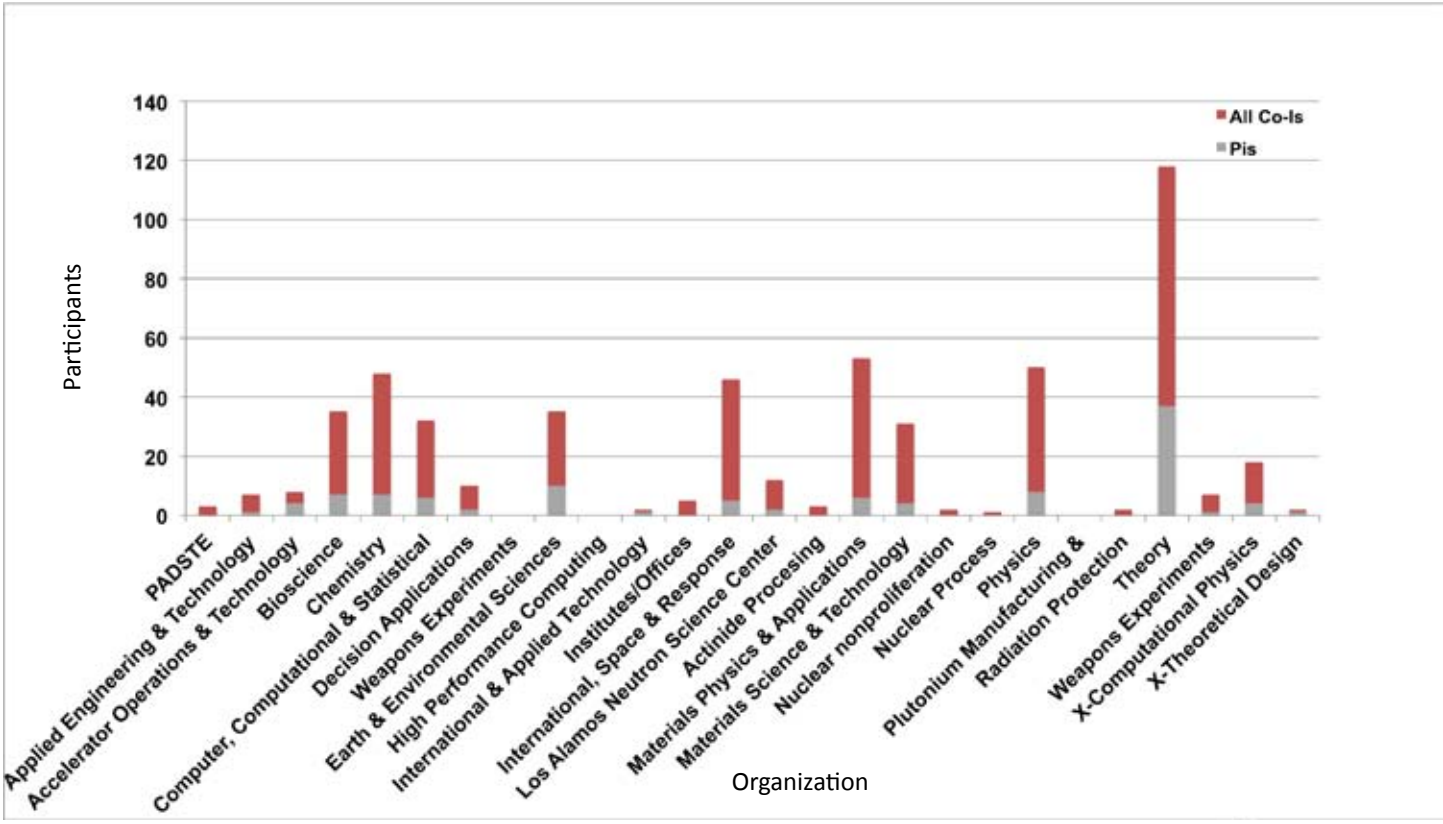

LDRD Supports Researchers at All Career Stages

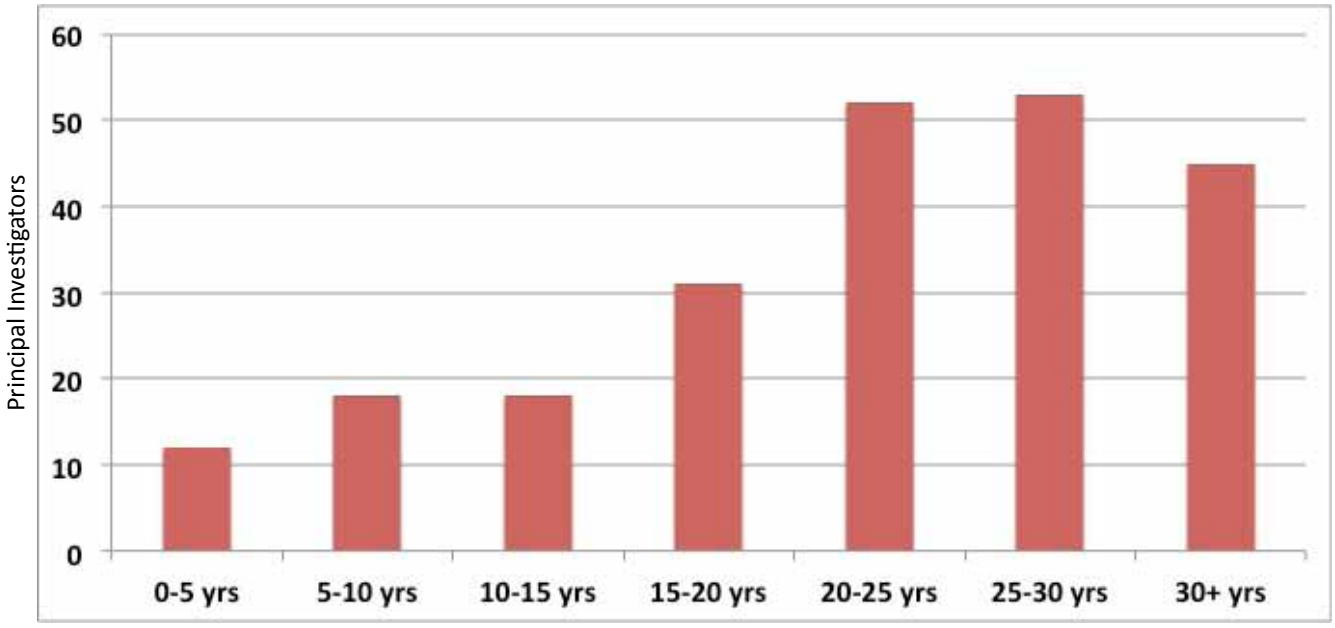

Project Selection

The LDRD program is the vehicle by which the Laboratory harvests the ideas of some of our best and brightest scientists and engineers to execute DOE/NNSA missions. This bottom-up approach is balanced by a program management strategy in which Senior Laboratory leadership sets science and technology priorities, then opens an LDRD competition for ideas across the breadth of the Laboratory. Panels formed from the Laboratory's intellectual leaders rigorously review proposals. Conflict of interest is carefully regulated, and evaluation criteria include innovation and creativity, potential scientific impact, viability of the research approach, qualifications of the team and leadership, and potential impact on Laboratory missions. The selection processes are modeled on best practices established by the National Science Foundation (NSF) and National Institutes of Health (NIH).

To guarantee fairness and transparency, and to ensure that the strongest proposals are funded, the selection panels include managers and technical staff drawn from the full range of technical divisions. Serving on an LDRD selection panel is often a starting point on the path to leadership roles in the scientific community. Past LDRD panelists have gone on to be Laboratory Fellows, division leaders, program directors, association Fellows, and chief scientists, while others have become leaders in academia.

Independent project appraisals

In FY13, the LDRD Program Office conducted an appraisal of every ongoing project it intended to fund in the next fiscal year. The primary objective is to assess progress and provide peer input to help PIs maintain the highest quality of work. The appraisals also help the LDRD Program Office monitor and manage the program portfolio. In addition to formal project appraisals, which are conducted annually, the LDRD Program Director and Deputy Program Director meet informally with PIs in their labs at least once a year to discuss their projects. The purpose of these one-on-one meetings is to give PIs individualized assistance and to determine what the LDRD Program Office can do to positively impact the success of the project. Every DR project has also been assigned a Program Development Mentor to assist the transition of LDRD successes to mission. Any weaknesses are actively addressed, and the project leader is asked to respond to the report with a revised project plan.

Continuing DR projects are appraised every year of the life of the project, with at least one of the reviews including external reviewers. The internal-external review is open to all Laboratory staff and leaders. Four project appraisers – two internal and two external – are nominated by the PI and approved by the LDRD Program Director. When possible, the appraisal is held as part of a broader workshop hosted by the Laboratory.

Written appraisals, held in the LDRD archives, address: (1) Brief summary of accomplishments; (2) Assessment of quality of science and technology, relevance to Laboratory and national missions, progress toward goals and milestones, project leadership, and the degree to which the project may establish or sustain a position of scientific leadership for the Laboratory; and (3) Recommendations by the committee for changes in the scope or approach of the project. The criteria for the most important point – number (2) above – are derived from criteria developed by the National Academy of Science to assess all federally sponsored research.

Continuing ER and ECR projects are appraised in their first and second years. The LDRD Deputy Program Director collaborates with the technical divisions to conduct project appraisals. Like DRs, the projects are appraised according to the Federal criteria of quality, performance, leadership, and relevance.

LDRD service provides benefit to all

The mission of the Laboratory is to solve the nation's most difficult national security problems. By their nature, these problems lack a well-defined path to solution. In fact, the path is often completely unknown. It is rare that such creative work is done alone; the ideas and results from many colleagues are needed, often drawn out in conferences, hallway conversations, journals, and seminars. LDRD is an internal arena in which Laboratory staff serve as peer reviewers and play a key role of interaction in the scientific process. Proposal selection panelists are chosen for their subject-matter expertise, and the discussions in which they engage are not only critical to the LDRD process, but they also provide an opportunity for panelists to educate themselves on the latest results and practices, and expose themselves to opportunities for collaboration. As noted in an evaluation of peer review conducted by the UK House of Commons, "Peer review is regarded as an integral part of a researcher's professional activity; it helps them become part of the research community."

DR Project Appraisal Highlights

Plutonium-242: A National Resource for the Fundamental Understanding of *5f* Electrons (20120024DR)

"The project team has established new experimental and theoretical capabilities to study plutonium materials that are clearly aligned with the missions of the Laboratory and key parts of the Plutonium Science and Research Strategy Implementation Plan. This project contributes important work to maintaining Los Alamos as the NNSA Plutonium Center of Excellence."

Dynamic Earthquake Triggering, Granular Physics and Earthquake Forecasting (20120007DR)

"The project is well conceived in that it consists of laboratory, simulation, and observational efforts that are lead by experts and employ students and early career scientists. Further, the team of scientists from diverse backgrounds and numerous, including international, institutions have done an admirable job coordinating efforts. For example, modeling efforts are focused on understanding experimental results through accurate reproduction of the experimental setup at other institutions. Scientists often want to solve the most interesting problem to them, personally, and it is the exception rather than the norm when this level of cooperation is found. "

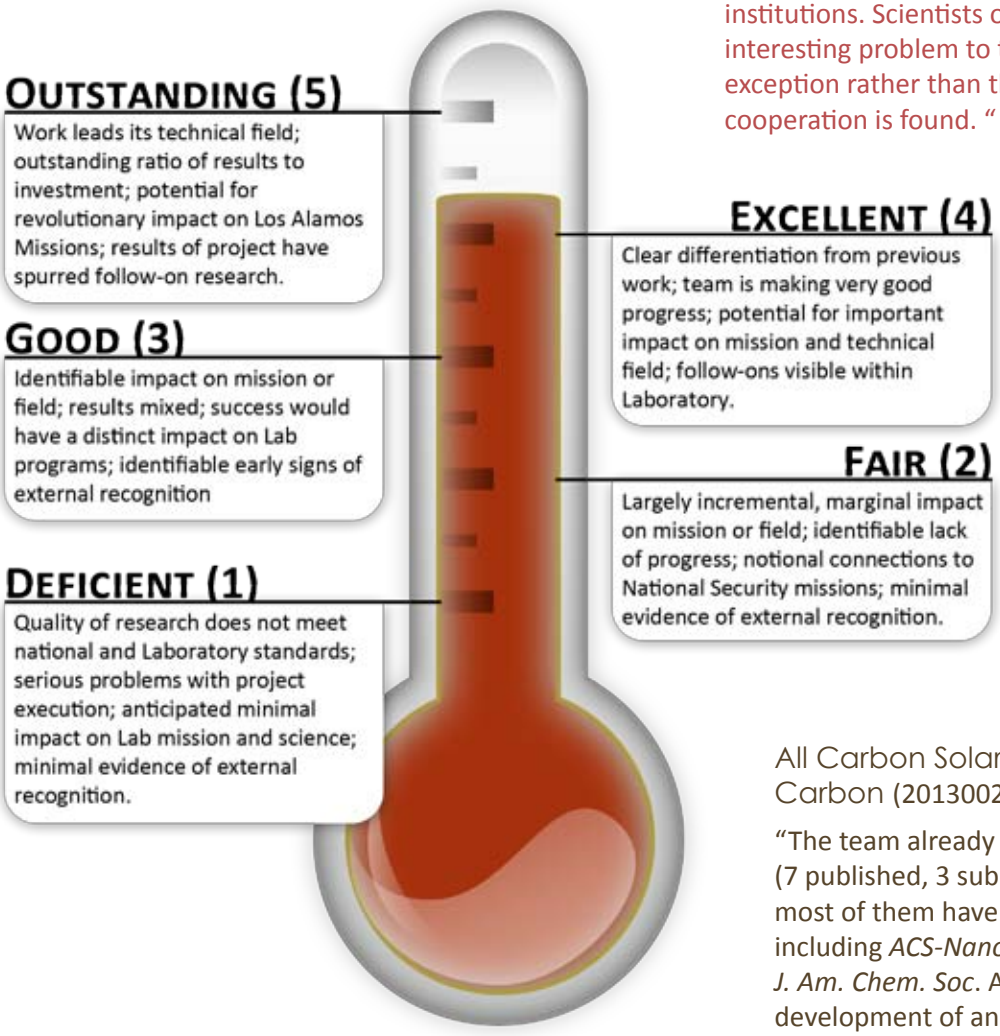

Analysis of FY13 DR project appraisals showed an average score of 4.3, which is between excellent and outstanding. This average reflects 21 appraisals.

All Carbon Solar Cells: Fighting Carbon with Carbon (20130026DR)

"The team already has 17 publications to their credit (7 published, 3 submitted and 7 in preparation) and most of them have appeared in journals of high impact, including *ACS-Nano, NanoLett, Phys. Rev. Lett.*, and *J. Am. Chem. Soc*. An essential breakthrough was the development of an aqueous two phase (ATP) method for isolating single chirality nanotubes."

Genetically Encoded Materials: Libraries of Stimuli-Responsive Polymers (20120029DR)

"The results of this project have the potential to have a significant impact within the technical field. In particular, the development of combinatorial methods producing libraries of mono-disperse polymers of known structure is unprecedented, and could be a transformational technology in combinatorial synthesis. The results...also have potential to impact a broad range of other technological areas including electronics and sensors. Internally, the significance of the results from this project have been recognized by the LANL Technology Transfer Department as they have fast tracked this work for patent protection."

Mission Relevance

Mission relevance is one of the most important criteria in the evaluation of a potential LDRD project; it is carefully considered in project selection, and it is tracked annually through the data sheet process. Many of the technologies that put Los Alamos on the map have deep roots in LDRD and are valuable to DOE/NNSA mission areas of nuclear security, energy security, environmental remediation, and scientific discovery and innovation. LDRD work also benefits the national security missions of the Department of Homeland Security, the Department of Defense, and Other Federal Agencies. As a result, the scientific advances and technology innovations from LDRD provide multiple benefits to all Los Alamos stakeholders, consistent with Congressional intent and the Laboratory's scientific strategy.

FY13 LDRD Investment in DOE Missions ($M)

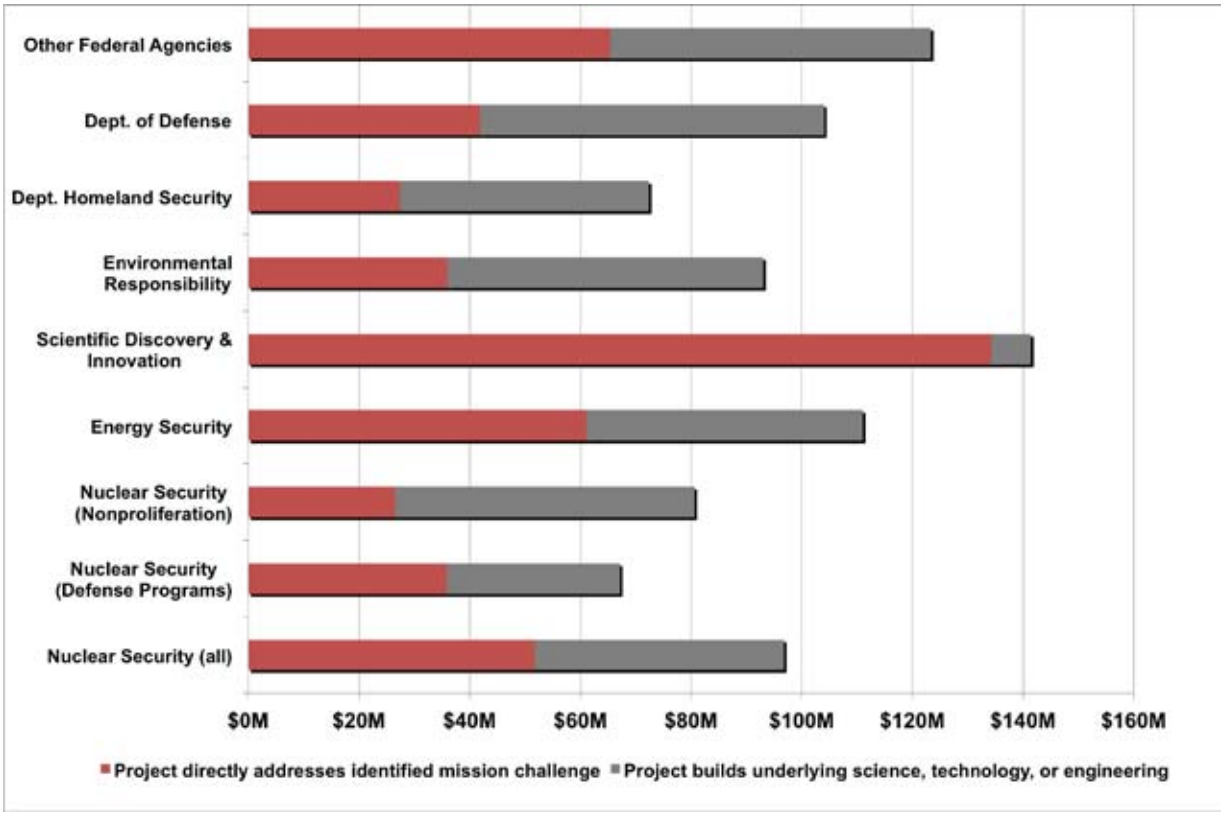

The chart above shows the mission relevance of the$145.7M FY13 LDRD portfolio. The dollar amounts total more than 100 percent of the total FY13 budget because many LDRD projects impact and have relevance to more than one mission area.

The Los Alamos LDRD program plan includes a list of every project to be funded in the upcoming fiscal year and indicates which mission areas the project will impact.

The NASA Mars Science Laboratory rover Curiosity launched November 25, 2011, and landed on Mars in Gale Crater on August 5, 2012. Since its landing, Curiosity has been assessing whether the Martian environment ever was, or is, capable of supporting microbial life. Like its predecessors, the Curiosity rover will rely on proven technology, as well as new, innovative technologies to carry out its mission. Curiosity represents the next big step in the exploration of Mars because it will:

- demonstrate the ability to land a very large, heavy rover to the surface of Mars (which could be used for a future Mars Sample Return mission that would collect rocks and soils and send them back to Earth for laboratory analysis)
- demonstrate the ability to land more precisely in a 20-kilometer (12.4-mile) landing circle and
- demonstrate long-range mobility on the surface of the red planet (5-20 kilometers or about 3 to 12 miles) for the collection of more diverse samples and studies.

Technology development makes missions possible. Each Mars mission is part of a continuing chain of innovation. Each relies on past missions for proven technologies and contributes its own innovations to future missions. This chain allows NASA to push the boundaries of what is currently possible, while still relying on proven technologies.

ChemCam

ChemCam is the Chemistry and Camera instrument, one of 11 science instruments onboard Curiosity. As the name implies, ChemCam is actually two different instruments combined as one: a Laser-Induced Breakdown Spectrometer (LIBS) and a Remote Micro Imager (RMI). The purpose of the LIBS instrument is to provide elemental compositions of rock and soil, while the RMI will give ChemCam scientists high-resolution images of the sampling areas of the rocks and soil that LIBS targets.

Simply stated, ChemCam will tell us what the rocks are made of in the Curiosity rover's landing region. The primary objectives of ChemCam are to rapidly analyze rocks and soil to determine their compositions and to identify samples that would be of greatest interest to scientists for analysis by other instruments onboard Curiosity.

Determining the composition of rocks on the Martian surface is usually a laborious, time-consuming task, even for advanced spacecraft such as the Mars Exploration Rovers Spirit and Opportunity. Most rocks on the surface of Mars are covered with a layer of dust. Many rocks are also covered with a layer of material that has been altered by wind and possibly water. To determine the true composition of a rock, spacecraft must first clear away the dust and the altered layer of rock. This involves the spacecraft rolling up to the rock and using a tool to clear away the unwanted layers. Dust can be easily removed but altered layers of rock usually need to be removed by grinding away the material. Another obstacle is the rock grinder. They wear down. In fact the rock grinders on the previous MER rovers wore down long ago. When conducting a Mars mission, this seemingly menial task may require at least one day's worth of operations, a long time by mission standards. ChemCam, with its unique laser system, will be able to perform the same task in a fraction of the time and without having to be in contact with the rock.

LDRD Investment Made ChemCam Possible

The LIBS technology was developed at Los Alamos National Laboratory with early support from the LDRD program. The research focused on LIBS technique for detection work in hazardous environments. A 2010 LDRD project explored direct application of LIBS on the ChemCam instrument, including LIBS detection limitations in Mars and Venus environments. Today LDRD is exploring the applications of this technology for finding and analyzing nuclear materials. The multi-mission nature of this LDRD work is representative of the large majority of the LDRD portfolio, which boasts numerous projects with results that impact several mission areas.

Mission Impact

LDRD delivers capabilities and explores solutions for all Los Alamos missions: Nuclear Security, Global Security, Energy Security, and Scientific Discovery. In some cases these lead to clearly identified follow-on projects. In part, this can be attributed to the program development mentors who help transition these projects from LDRD to external funding.

Putting a quantitative metric on mission impact is difficult. The obvious metric (follow-on funding) omits other benefits like new ideas and approaches that feed into ongoing work. Counting dollars is also imperfect because, although LDRD is part of what enables new mission solutions, the Laboratory brings other assets to bear, including facilities, ideas, and personnel from a range of programs. Nonetheless, admittedly rough numbers show that projects active in FY13 played an important part on the path to $53M of externally funded R&D. This number will grow with time as follow-on funding is often acquired after projects end.

The path from LDRD to mission is clearly demonstrated by follow-on projects from sponsors that range, inside DOE, from the nuclear weapons program to nonproliferation programs, applied energy programs, and the Office of Science, and more broadly, across a range of sponsors that include DoD (DARPA, ONR, and DTRA), DHS and DNDO, NIH and CDC, classified agencies, and a suite of industrial partners. The capabilities sustained by these external sponsors feed back once again to enable the Laboratory's execution of NNSA missions.

Here we highlight two successful projects that acquired external funding in FY13:

TerraMajic

Vision is one of the most challenging and intriguing problems in artificial intelligence and computer science. Advances in the field have hinged on three fundamental challenges: (1) how to create mathematical models of natural video sequences that can generate and interpret the visual scene; (2) how to learn image feature representations in such models across many spatial and temporal scales and for many object categories; and, (3) how to exploit the sheer size and richness of large-scale video datasets now becoming available. These three problems not only need to be solved together but are now within reach as a result of new theoretical, experimental and computational advances. Los Alamos researchers developed novel video analysis models and algorithms that are expected to approach human analyst performance and will surpass human speed.

An LDRD research project titled *Hierarchical Sparse Models for Robust Analysis of Video Data* brings together world-class researchers in statistical modeling, computer vision, and high performance computing. Their Video Analysis Search Technology (VAST) is being developed for integration into an intelligence system for the DoD and other communities.

Early LDRD investment in VAST exercised and strengthened Laboratory capabilities in image analysis, biosecurity, and data analysis and pattern recognition, and serves critical Federal and industry sponsors.

Uniquely combining Magnetic Resonance Imaging (MRI) and X-ray technology, LDRD scientists unlocked new threat technology that could make airport travel faster and safer. This advanced technology, called MagRay, builds on previous Lab technology, captures measurements of MRI, which is better suited for screening liquids than traditional baggage scanners, alongside x-ray density, and a new parameter—proton content—that is not available in either x-ray or MRI alone.

Traditional baggage scanners, which use x-rays, have limited sensitivity for liquid discrimination, whereas MagRay quickly and accurately distinguishes between liquids that visually appear identical. For example, what appears to be a bottle of white wine could potentially be nitromethane, a clear liquid that can be used to make an explosive. The operator interface is straightforward: A red light signals a hazardous liquid; a green light signals a benign liquid. The technology could eliminate the need for the 3.4-oz container limitation (the 3-1-1 rule) for travelers.

Early LDRD investment in the MRI technology used in MagRay supported the Laboratory's global security mission and Science of Signatures pillar. The Department of Homeland Security is supporting the development of MagRay for use in airports across the nation.

Awards and Recognitions

The LDRD program supports some of the Laboratory's most accomplished researchers, as well as many of its most promising young scientists and engineers. In the past year, LDRD researchers received many awards and recognitions, including R&D 100 Awards; fellowships from professional associations; poster, publication, and research awards; and many more. Here we highlight only a few.

Zelenay receives Research Award from the Electrochemical Society

The Energy Technology Division of The Electrochemical Society presented the Research Award to Piotr Zelenay. The award recognizes his "outstanding and original contributions to the science and technology of energy-related research areas that include scientific and technological aspects of fossil fuels and alternative energy sources, energy management and environmental consequences of energy utilization."

Currently PI on an LDRD DR project, Zelenay's research focuses on polymer electrolyte fuel cells (PEFCs), including the direct-methanol fuel cell (DMFC), precious-metal/non-precious metal electrocatalysis, membrane and membrane-electrode assembly development, and performance optimization of fuel cell materials and components. He is the recipient of a 2003 Laboratory Distinguished Performance Award and a 10-time recipient of the Laboratory's Patent & Licensing Award. He garnered a 2010 DOE Hydrogen Program R&D Award in recognition of outstanding contributions to fuel cell technologies, and 2001 DOE "Energy 100" and "Energy @23" awards for fuel cells for transportation. He has authored more than 100 scientific papers, holds six patents, and serves on the editorial board of the Springer journal Electrocatalysis.

Jaqueline Kiplinger selected as Subdivision Chair in the American Chemical Society

Jaqueline L. Kiplinger was selected to serve as the chair-elect for the Organometallic Subdivision of the American Chemical Society (ACS) Division of Inorganic Chemistry. She will act as a liaison between the Division and the organometallic community, proposing symposia for future ACS meetings and communicating opportunities for Division support for organometallic conferences. The Division of Inorganic Chemistry represents a diverse body of scientists – organometallic, bioinorganic, solid-state, materials, nanoscience and coordination chemists – devoted to understanding and promoting the richness of the chemistry of the elements.

Currently an LDRD PI, Kiplinger is internationally recognized as a scientific leader in actinide and lanthanide chemistry. She is a Fellow of the American Association for the Advancement of Science and the Royal Society of Chemistry, and she has received two R&D 100 Awards, a Los Alamos Fellows Prize for Research, and a Los Alamos Distinguished Mentor Award. She has served on the Editorial Board for the American Chemical Society journal Organometallics and as an Alternate Councilor for the ACS Division of Inorganic Chemistry. Kiplinger has published nearly 80 journal articles and has received more than 2100 citations.

José Olivares elected to Board of Directors of the Algae Biomass Organization

The Algae Biomass Organization (ABO) chose José Olivares to serve on its Board of Directors. The ABO is a non-profit organization whose mission is to promote the development of viable commercial markets for renewable and sustainable commodities derived from algae. ABO's board guides the organization to educate the general public, policy makers, and industry about the benefits of algae to address energy security, food production and stainability, and to advocate for policies that can accelerate the development of commercial markets for products made from algae.

Olivares' research focus has been primarily in instrumentation for mass spectrometry and biological and chemical sensor development for national security and health related applications. He is the Division Leader for the Bioscience Division and serves on the DR Strategy Team. He is the Executive Director of the National Alliance for Advanced Biofuels and Bioproducts, a consortium of 40 institutions funded by the DOE - Energy Efficiency and Renewable Energy Office of Biomass Programs. Olivares is an adjunct member of The Danforth Plant Science Center, a non-profit institution dedicated to plant research for food and energy, and co-Editor-in-Chief of the scientific journal Algal Research.

Performance Metrics

The LDRD program is a key resource for addressing the long-term science and technology goals of the Laboratory, as well as for enhancing the scientific capabilities of Laboratory staff. Through careful investment of LDRD funds, the Laboratory builds its reputation, recruits and retains excellent scientists and engineers, and prepares to meet evolving national needs. The impacts of the LDRD program are particularly evident in the number of publications and citations resulting from LDRD-funded research, the number of postdoctoral candidates supported by the program, and the number of awards LDRD researchers received.

Publications

The numerous publications made possible with LDRD funding help the Laboratory maintain a strong presence and scientific reputation in the broader scientific community. In FY13, LDRD researchers generated 534 peer-reviewed publications, accounting for 24% of the Laboratory's total. The quality of these publications is evidenced by the number of times they were cited. LDRD publications published in FY13 were cited 481 times, accounting for 38% of the Laboratory's citations, as well as one of the Laboratory's top 10 cited publications. With increased efforts to collect post-project performance metrics, LDRD publication and citation counts increase year-to-year. Recent analysis of citations since the inception of the LDRD program reveals 13 of the top 50 high cited publications are linked to LDRD.

Peer-Reviewed Publications				
	FY10	**FY11**	**FY12**	**FY13**
LANL Pubs	1741	2079	2119	2263
LDRD Supported	408	452	458	534
% due to LDRD	23%	22%	22%	24%

Citations				
	FY10	**FY11**	**FY12**	**FY13**
LANL Citations	14416	6899	3373	1278
LDRD Supported	3944	1866	1096	481
% due to LDRD	27%	27%	32%	38%
Top 10 Most Highly Cited Publications				
LDRD Supported	4	4	1	2

Patents and Disclosures

Another indication of the cutting-edge nature of the research funded by LDRD is the contribution the program makes to the intellectual property of the Laboratory. In FY13, LDRD-supported research resulted in 32 patents, 42% of the Laboratory's total, and 30 disclosures, 27% of the Laboratory's total.

Patents Granted				
	FY10	**FY11**	**FY12**	**FY13**
LANL Patents	61	59	72	77
LDRD Supported	15	15	11	32
% due to LDRD	24%	25%	15%	42%

Disclosures				
	FY10	**FY11**	**FY12**	**FY13**
LANL Disclosures	116	129	103	110
LDRD Supported	16	28	34	30
% due to LDRD	21%	22%	33%	27%

Postdoctoral Support

LDRD remains an important vehicle for recruiting the brightest researchers to the Laboratory, where they become innovators and scientific leaders. In FY13, LDRD supported 367 postdocs, accounting for 61% of the Laboratory's total.

Postdoc Support				
	FY10	**FY11**	**FY12**	**FY13**
LANL Postdocs	547	580	581	596
LDRD Supported	325	330	349	367
% due to LDRD	59%	57%	60%	61%

Postdoc Conversions				
	FY10	**FY11**	**FY12**	**FY13**
LANL Conversions	53	44	41	57
LDRD Supported	33	17	21	34
% due to LDRD	62%	39%	51%	59%

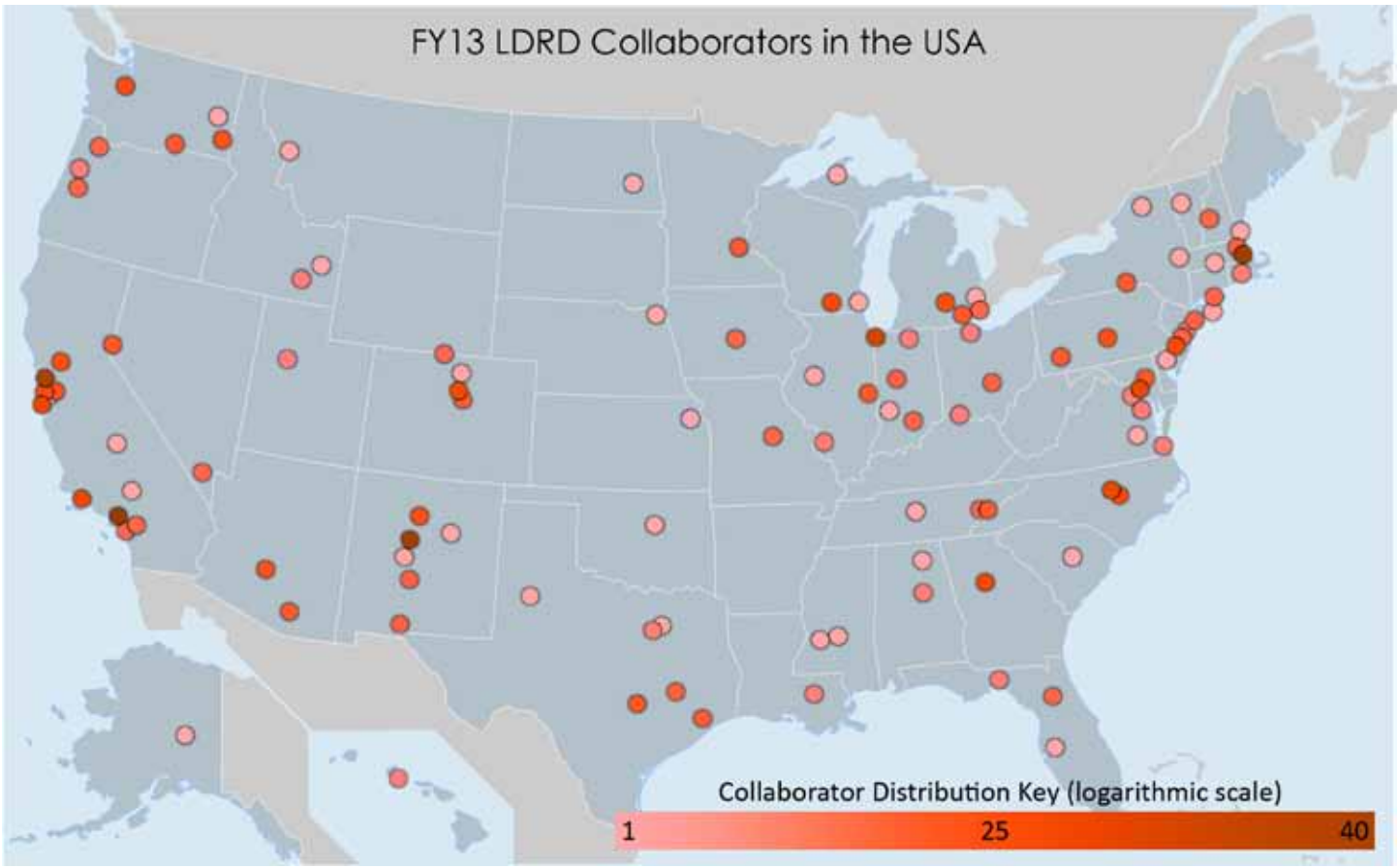

External collaborations are often critical to a successful LDRD project. Formal collaborations between LDRD and researchers at other national laboratories, academia, and industry enable access to world-leading facilities and knowledge. Such collaborations enable LDRD researchers to be active and prominent members of the broad scientific community. There were more than 1,000 external collaborators associated with FY13 LDRD projects, many of which involved no exchange of funds.

Bette Korber developed a component of a new vaccine against HIV that is now being tested in monkeys.

New global HIV vaccine design shows promise in pre-clinical trials

The considerable diversity of HIV worldwide represents a critical challenge for designing an effective HIV vaccine. Now, it appears that a vaccine bioinformatically optimized for immunologic coverage of global HIV diversity, called a mosaic vaccine and designed by Los Alamos researcher Bette Korber and her team may confer protection from infection.

These vaccines are specifically designed to present the most common forms of parts of the virus that can be recognized by the immune system. This new insight regarding a mosaic vaccine's ability to protect from infection is the result of work by a scientific team led by Beth Israel Deaconess Medical Center (BIDMC), including Los Alamos LDRD researchers. The study, which was conducted in monkeys, was published in the journal *Cell*.

"These data suggest a path forward for the development of a global HIV vaccine and give us hope that such a vaccine might indeed be possible," says lead author Dan H. Barouch, MD, PhD, the director of the Center for Virology and Vaccine Research at BIDMC and professor of medicine at Harvard Medical School. "We are planning to advance this HIV vaccine candidate into clinical trials next year," he adds.

Chemistry and Material Sciences

Energy Storage

Fernando H. Garzon
20120003DR

Introduction

The storage of energy from intermittent renewable energy sources to supply the irreducible base needed by electrical utilities is a critical limitation to widespread of renewable energy. Ammonia has been proposed by many as a carbon-free energy carrier and storage medium (NH_3 holds 14 MJ/liter, 10-100 times more than the best battery). However, current methods of ammonia production have high capital costs, low to moderate efficiency, and are not scalable to utility levels. Our main goals are to: 1) Improve our theoretical understanding of nitrogen reduction on surfaces, multi-electron transfer to adsorbed molecules, and proton transport in anhydrous electrolytes. 2) Develop, characterize and optimize new materials for electrolytes and electrocatalysts for ammonia electrosynthesis. 3) Demonstrate improved efficiency of scalable ammonia electrosynthesis concepts.

Benefit to National Security Missions

Los Alamos National Laboratory has a stated mission in the area of Energy Security. This project directly supports the Laboratory's grand challenges in Energy and Earth Systems and Materials, coupling to the themes of energy storage, interfaces, emergent properties, and nanotechnology. Success will lead us to the design principles for materials to be used in the next generation of electrochemical energy storage systems with substantially improved efficiency. The work is expected to lead to follow-on proposals in BES in the areas of new materials, interfaces, emergent properties, energy conversion, and energy storage. In the applied area, such as ARPA-E, DOE-EERE, and DOE-OE, this work will position LANL to lead or be a strong team member with ANL for the development of improved transportation, local, and distributed-grid-level electrical storage systems. The low cost synthesis of ammonia from renewable energy is also of importance to the USDA.

Progress

A number of major accomplishments were achieved in FY2013. The high pressure experimental research capability of the Laboratory was enhanced by the completion of a high pressure reaction chemistry facility. The facility, located in MPA- Division, includes a custom designed high pressure systems (200 atm) to perform gas adsorption, infrared spectroscopy of surfaces and high pressure electrochemical experimentation. The laboratory now can safely perform ammonia synthesis, characterize ammonia adsorption in nonaqueous electrolytes, determine the reaction species and intermediates on electrochemical catalyst surfaces and measure fundamental thermodynamic properties of ionic liquid electrolyte ammonia mixtures. The team also developed a high temperature electrochemical experimental capability for characterization of solid proton conductor based electrochemical reactors and an RF magnetron in situ thin film sputter deposition capability suitable for the creation of nanoscale catalytic electrode materials relevant to the needs of the project.

Important milestones were achieved with the newly developed experimental capabilities. The deposition systems yielded high surface area molybdenum nitride thin films on a variety of substrates. The crystal structure morphology and surface chemistry of these nanoscale electrode materials were characterized by electron microscopy, X-ray diffraction, X-ray photoemission spectroscopy and gas adsorption measurements. New indium tin pyrophosphate and strontium cerate proton conducting membranes were synthesized and characterized. The proton conduction mechanism of tin pyrophosphate is currently under debate within the scientific community. Experiments and theoretical modeling conducted by LANL determined that the protons moved by a grain boundary transport mechanism and yielded several pre-

sentations and publications. A large number of indium tin pyrophosphate materials with varying metal to phosphate ratios were synthesized using solution precipitation methods developed and patented by LANL. The crystal structures, surface areas and ionic conductivities as a function of temperature, and gas composition were determined by electrochemical transport measurements. Our data clearly showed that no structural changes in the crystalline phase were occurring as the sample composition was varied from stoichiometric to excess phosphate compositions. However the presence of a phosphate-rich grain boundary phase was detected and the measured proton conductivity was a strong function of the grain boundary phase.

The strontium cerate proton conducting materials with electro-catalytic electrodes were incorporated into small scale electrochemical reactors for measurements of ammonia electrochemical synthesis from nitrogen and hydrogen feedstock materials. The reactors successfully electrosynthesized ammonia. Protonic ionic liquids were prepared and purified for low temperature liquid electrolyte cells. Ionic conductivity of the protic ionic liquids was characterized using AC impedance spectroscopy and the thermal stability was determined.

Neutron vibrational spectroscopy is a powerful tool for investigating the surface reactions occurring on the ammonia synthesis catalysts. The technique requires relatively large homogenous samples, thus we developed nanosynthesis methods to yield large quantities of well-characterized molybdenum nitride catalysts for our upcoming LANSCE run cycle. The nanosynthesis and characterization was presented and published in FY13.

Future Work

In the following fiscal year we will continue our electrocatalyst materials development and electrode optimization for ammonia synthesis. We will test our high surface area thin film molybdenum nitride thin films deposited on conductive support materials in electrochemical cells containing ionic liquid electrolytes and on solid oxide proton conductors. Continued electrolyte studies will include ionic transport measurements on protic ionic liquids particularly ammonia -ionic liquid interaction studies at high pressures in our new test facility. We will measure the solubility of ammonia in protic ionic liquids, and characterize how the the binary mixture properties change with composition. Solid state electrochemical cells will be fabricated using thin ceramic and polymer reinforced solid electrolyte membranes. Liquid cells will be fabricated for pressurized studies of the nitrogen reduction electrochemistry of nitrogen. Cyclic voltammetry and AC impedance spectroscopy will characterize ionic transport in these systems. The ammonia synthesis conversion rate will be evaluated by DC polarization measurements and optimized by alterations of the electrochemical cell design.

As the Los Alamos Neutron Scattering Facility is now operational this year, supporting studies will include structural neutron diffraction studies of the molybdenum nitride electrode materials and solid electrolytes. Neutron vibration spectroscopy will characterize the proton dynamics is the pyrophosphate material. IR spectroscopy and NMR spectroscopy of the ionic liquid -ammonia systems will provide molecular information about the interactions of ammonia with the protonic ionic liquids.

Theoretical studies will include Density Functional Theory based calculations of the nitrogen reduction reaction on metal nitride surfaces and studies to elucidate the ionic transport mechanisms in both solid and liquid electrolyte systems. Pathways for homogenous nitrogen catalysis on metal centered organic catalysts will evaluated using molecular dynamics.

Conclusion

This project will investigate the conversion of electrical energy into liquid fuel, greatly increasing our ability to store GWhs of energy onsite. The project will increase our fundamental understanding of nitrogen reduction chemistry, decrease the cost of plant fertilizer from renewable resources, and enable the more efficient utilization of intermittent renewable energy sources. The project will expand our theoretical knowledge of a meaningful electrosynthetic process, charge transfer theory, and emergent ion transport properties at nanoscale interfaces.

Publications

Kreller, C. R., M. S. Wilson, R. Mukundan, E. L. Brosha, and F. H. Garzon. Stability and Conductivity of In3+-Doped SnP2O7 with Varying Phosphorous to Metal Ratios. 2013. ECS ELECTROCHEMISTRY LETTERS. 2 (9): F61.

Kreller, C. R., M. S. Wilson, and F. H. Garzon. Enhancing the Protonic Conductivity of Tin Pyrophosphates by Increasing Phosphate Content . 2013. Electrochemical Society Transactions. 57 (11): 1009.

Kreller, C. R., R. Mukundan, and F. H. Garzon. Electrosynthesis of Ammonia using Solid-State Proton Conductors. To appear in 224 Meeting of the Electrochemical Society. (San Francisco, 27 Oct.-4 Nov.).

Ogumi, Z., H. Matsuoka, F. Garzon, H. Kim, L. J. Wan, K. Tamao, and M. Nakamura. Electrochemistry 80th Anniversary Special Issue. 2013. ELECTROCHEMISTRY. 81 (3): 140.

Sansinena, J. M., J. Chilstunoff, N. C. Tomson, J. M. Boncella, and F. H. Garzon. Ionic Liquids for Ammonia Electrosynthesis and Energy Storage . Presented at 224th Meeting of the Electrochemical Society. (San Francisco, 27 Oct- 4 Nov. 2013).

Organic Electronic Materials: Designing and Creating Functional Interfaces

Sergei Tretiak
20120019DR

Introduction

The description of disordered organic materials and the interfaces between these materials presents an exciting challenge that requires the establishment of new approaches lying between those of condensed matter (which typically relies on crystal periodicity) and molecular chemistry (which typically relies on small system size). We have developed new theoretical tools and mastered sophisticated experimental techniques, which together will enable a quantitative jump in our understanding of physical and dynamical processes in disordered organic electronic materials. By manipulating both the nanostructure of the molecular building blocks and the structure of the interfaces between them through synthetic and fabrication processes, we aim to engineer materials and fabricate devices with emergent properties and unprecedented efficiencies. The proposed interdisciplinary research harnesses the group's unique depth of expertise in theory (spanning all length scales from molecular electronic structure simulations to mesoscale device modeling), time- and spatially resolved spectroscopic and transport measurements, organic synthesis, device fabrication and characterization.

Benefit to National Security Missions

The project objectives will be achieved through integration of LANL strengths in theory, spectroscopy, chemistry, high-performance computing, and materials science on multiple length-/time-scales, thereby realizing the vision of "co-design" and directly aligning with the MaRIE goal to "couple theory, experiment, and simulation tools." The outcome will favorably position the Lab for future investments in the strategic field of Organic Functional Materials, with application to a range of sensing missions including, potentially, nuclear nonproliferation. We primarily address the Materials: Discovery Science to Strategic Applications challenge by (i) a thorough understanding of dynamical processes at interfaces, (ii) their application to control of the material functionality and (iii) by discovering emergent phenomena in complex systems. The project also strongly supports the Energy and Earth Systems challenges by providing design strategies for molecular materials suitable for clean energy production.

Progress

During the second year of the project our effort focused on several research directions, including synthesis, device fabrication and characterization, and theoretical modeling. Our synthetic efforts result in synthesized and characterized series of thiophene oligomer derivatives: terthiophene, quatertiophene and pentathiophene derivatives with thiolated and syloxinated end group. The latter allow for covalent bonding to the Au/Ag and glass substrate surfaces, respectively. In particular, Scanning Tunneling Microscope (STM) characterization of self-assembled monolayer (SAM) thin films on single crystalline gold surfaces, reveal a surprising fact that only specific oligomers from the family are able to organize into ordered monolayers, as opposite to the globular structures. These properties make clear differences on the device performance (as described below) due to changing the underlying interface structure.

Ongoing quantum-chemical simulations are able to rationalize the observed phenomena. Our device fabrication and spectroscopic efforts focused on four fundamental processes that determine the performance of typical organic photovoltaic devices. Typically exciton dissociation rate is faster than it needs to be by several orders of magnitude, and charge transfer state recombination is also too fast. We inserted a LiF insulating layer between the donor and acceptor layer in a prototypical system (tetracene(Tc)/fullerene bi-layer) and find that there is an optimum thickness of the insulator layer for improving device performance. We applied ultrafast pump-probe spectroscopy to follow the dynamics of singlet and triplet excitons induced by ultrashort laser pulse

absorption in thin Tc/fullerene films. These studies reveal a complex dynamics of multiple excited states and present a first spectroscopic evidence of timescales and pathways related to the exciplex formation in this system. We further study donor/acceptor bi-layers (such as the MTDATA/Bphen and P3HT/C60) by photoconductivity and PL/TRPL experiments (Thrust 2).

These experiments are performed on films and prototype devices to understand the effect of electric field on energetic and dynamic of charge-separated (exciplex) states. Our studies reveal a clear presence of luminescent interfacial exciplex state. Spectroscopic studies in the presence of magnetic field brought unique information on emission dependence on the applied magnetic field evidencing impact of hyperfine interactions in the dynamics of spin states. Concurrent electronic structure studies interpret the underlying phenomena in terms of 'hot' and 'cold' exciplex states.

We further study the effects of inserting an insulating layer at the interface of the P3HT/C60 pair. By incorporating a thin insulating LiF layer we are able to decrease the exciplex recombination rate and to decrease the exciplex binding energy that results in a dramatic increase in photocurrent by two orders of magnitude. Insertion of well-ordered monolayers of thiophene oligomers (see above), increase photocurrent even further. This already suggests new synthetic strategies targeting optimization of energy conversion efficiency and minimizing losses in organic semiconductor devices. Our theoretical modeling span multiple time and length timescales.

Using our LANL-developed Non-Adiabatic Excited State Dynamics (NA-ESMD) code we investigate energy transfer processes in several polymeric systems and discover multiple channels in energy transport, which emphasizes complexity of this process going beyond simple Foerser-like phenomenological approaches. We are finalizing development of a computational platform to simulate the electronic (e.g., photoexcitation) and vibrational dynamics of large organic molecules within a complex environment.

This Quantum Mechanics/Classical Mechanics (QM/MM) computational framework combines available codes for classical molecular dynamics of large organic systems with accurate simulations of excited state dynamics using the NA-ESMD code. One the larger scale, our developed multiscale macroscopic charge transport models 'bridging the gap' between local properties of the polaron and exciton (nanoscale) and mesoscopic charge mobilities and exciton (micron-scale) are currently being extended to disordered inhomogeneous systems.

Finally, to evaluate the influence of interfaces on the device performance, we have applied a physics-based one-dimensional model to assess the effect of incorporating a thin tunnel barrier between the electron and hole transport layers of organic photovoltaic devices. The results evidence that by optimally choosing the insulating layer thickness, the organic solar cell power efficiency can be significantly improved. The results of our first and second year work have been summarized in 25 articles published/submitted to the international journals. Several student and postdoc hires were also made.

Future Work

In the third year of the project we will continue joint experimental/theoretical studies of well-ordered materials to evaluate the impact of aggregation on the electronic properties (Thrust 1). In particular, we will construct a self-assembled monolayer of thiophene oligomers at air-water interface and on various substrates and conduct various optical and structural characterizations of self-assemblies. By incorporation synthesized self-assemblies into device architectures as built in interfaces, we will further study impacts of these interfaces on the device performances and will obtain valuable insights, establishes correlation between interfacial structure and charge transfer dynamics.

Spectroscopic measurement (e.g., photoluminescence (PL) and time-resolved PL (TRPL) study) will provide understanding of the effect of electric field on charge separation and recombination processes. Our supplemental theoretical modeling using the LANL-developed NA-ESMD code and multiscale transport models will provide details of structure/property relationships and will help understanding of underlying electronic dynamics.

We will further study donor/acceptor bi-layers (such as the MTDATA/Bphen) by photoconductivity and PL/TRPL experiments (Thrust 2). These experiments will be performed not only on films but also on prototype devices to understand the effect of electric field on energetic and dynamic of charge-separated (exciplex) states.

We will also attempt to tune the lifetimes of exciplexes by incorporating a tunnel barriers in the interface. The concurrent theoretical modeling will use the organic interface device model developed in FY12 to interpret current-voltage and capacitance-voltage measurements on bilayer organic devices. Finally, we will finalize development of theoretical tools (Quantum Mechanics/Molecular Mechanics (computational platform for modeling excited state dynamics beyond the Born-Oppenheimer approximation and extend organic interface device model to describe

bulk heterojunction organic solar cells) and experimental capabilities (a time-resolved Optical Parametric Oscillator system at NHMFL).

Conclusion

Our effort will focus on the fundamental and applied science of organic π-conjugated materials including films and blends of conducting polymers, small molecules, fullerenes, and graphene, all of technological importance, present-day or anticipated. If successful, this will significantly advance the knowledge and development of multifunctional organic π-conjugated materials towards their use in a variety of additional applications. Moreover, the theoretical tools/experimental techniques that we develop and experience we gain will be readily applicable to a multitude of soft materials in the future focus of LANL mission impact.

Publications

Alberti, S. F., V. D. Kleiman, T. Nelson, A. E. Roitberg, and S. Tretiak. Shishiodoshi unidirectional energy transfer mechanism in phenylene ethynylene dendrimers. 2012. Journal of Chemical Physics. 137: 22A526.

Campbell, I. H., and B. K. Crone. Improving an organic photodiode by incorporating a tunnel barrier between the donor and acceptor layers. 2012. APPLIED PHYSICS LETTERS. 101 (2): 023301.

Clark, J., T. Nelson, S. Tretiak, G. Cirmi, and G. Lanzani. Femtosecond torsional relaxation. 2012. Nature Physics. 8 (3): 225.

Fernandez-Alberti, S., A. Roitberg, T. Nelson, and S. Tretiak. Identification of unavoided crossings in nonadiabatic photoexcited dynamics involving multiple electronic states in polyatomic conjugated molecules. 2012. Journal of Chemical Physics. 137 (1): 014512 (10 pp.).

Furmanchuk, A., J. Leszczynski, S. Tretiak, and S. Kilina. Morphology and optical response of carbon nanotubes functionalized by conjugated polymers. 2012. Journal of Physical Chemistry C. 116 (12): 6831.

Gorshkov, V. N., S. Tretiak, and D. Mozyrsky. Semiclassical Monte-Carlo approach for modelling non-adiabatic dynamics in extended molecules. 2013. NATURE COMMUNICATIONS. 4: -.

Kilina, S., E. Batista, A. Saxena, D. L. Smith, R. L. Martin, and S. Tretiak. Effect of Packing on Formation of Deep Carrier Traps in Amorphous Conjugated Polymers. 2013. Journal of Physical Chemistry Letters. 4: 1453.

Kilina, S., J. Ramirez, and S. Tretiak. Brightening of the lowest exciton in carbon nanotubes via chemical functionalization. 2012. Nano Letters. 12 (5): 2306.

Liu, F. L., B. K. Crone, P. P. Ruden, and D. L. Smith. Control of interface microscopic processes in organic bilayer structures and their effect on device performance. 2013. Journal of Applied Physics. 113: 044516.

Liu, F., P. Paul. Ruden, I. H. Campbell, and D. Smith. Electrostatic capacitance in single and double layer organic diodes. 2012. APPLIED PHYSICS LETTERS. 101 (2): 023501.

Liu, F., P. Paul. Ruden, I. H. Campbell, and D. Smith. Device model for electronic processes at organic/organic interfaces. 2012. JOURNAL OF APPLIED PHYSICS. 111 (9): 094507.

Nayyar, I. H., E. R. Batista, S. Tretiak, A. Saxena, D. L. Smith, and R. L. Martin. Effect of trans- and cis-isomeric defects on the localization of the charged excitations in -conjugated organic polymers. 2013. JOURNAL OF POLYMER SCIENCE PART B-POLYMER PHYSICS. 51 (12): 935.

Nayyar, I., E. Batista, S. Tretiak, A. Saxena, D. L. Smith, and R. L. Martin. Role of Geometric Distortion and Polarization in Localizing Electronic Excitations in Conjugated Polymers. 2013. Journal of Chemical Theory and Computations. 9: 1144.

Nelson, T., S. Fernandez-Alberti, A. E. Roitberg, and S. Tretiak. Nonadiabatic excited-state molecular dynamics: Treatment of electronic decoherence. 2013. JOURNAL OF CHEMICAL PHYSICS. 138 (22): -.

Nelson, T., S. Fernandez-Alberti, A. E. Roitberg, and S. Tretiak. Conformational disorder in energy transfer: beyond Forster theory. 2013. PHYSICAL CHEMISTRY CHEMICAL PHYSICS. 15 (23): 9245.

Nelson, T., S. Fernandez-Alberti, V. Chernyak, A. Roitberg, and S. Tretiak. Nonadiabatic excited-state molecular dynamics: Numerical tests of convergence and parameters. 2012. Journal of Chemical Physics. 136 (5): 054108.

Park, Y. I., C. Y. Kuo, J. S. Martinez, Y. S. Park, O. Postupna, A. Zhugayevych, S. Kim, J. Park, S. Tretiak, and H. L. Wang. Tailored Electronic Structure and Optical Properties of Conjugated Systems through Aggregates and Dipole-Dipole Interactions. 2013. ACS APPLIED MATERIALS & INTERFACES. 5 (11): 4685.

Sheng, C. X., S. Singh, A. Gambetta, T. Drori, M. Tong, S. Tretiak, and Z. V. Vardeny. Ultrafast intersystem-crossing in platinum containing pi-conjugated polymers with tunable spin-orbit coupling. 2013. SCIENTIFIC REPORTS. 3: -.

Soler, M. A., A. E. Roitberg, T. Nelson, S. Tretiak, and S. F. Alberti. Analysis of state-specific vibrations coupled

to the unidirectional energy transfer in conjugated dendrimers. 2012. Journal of Physical Chemistry A. 116: 9802.

Zhugayevych, A., O. Postupna, R. Bakus , G. Welch, G. Bazan, and S. Tretiak. Ab-initio study of a molecular crystal for photovoltaics: light absorption, exciton and charge carrier transport. 4920. Journal of Physical Chemistry C. 117: 2013.

Plutonium-242: A National Resource for the Fundamental Understanding of 5*f* Electrons

Eric D. Bauer
20120024DR

Introduction

Plutonium is arguably the most complex element in the periodic table. Plutonium's complex electronic structure is due to its position in the actinide series where 5f electrons move from being tied to the atoms (localization) to freely moving around the metal (itineracy). Understanding the behavior of the 5f electrons at this crossover poses a significant challenge to the condensed matter community. As a major step to address the challenge of understanding the 5f electrons of Pu, we will synthesize high-purity single crystals of delta-242Pu and 242Pu-based compounds to, for the first time: 1) use advanced photon spectroscopies to determine the valence of Pu's 5f electrons, which will significantly constrain current theories of Pu electronic states; 2) apply novel photon spectroscopy and neutron scattering techniques to determine the magnetic configuration of delta-Pu's 5f electrons and their charge/spin fluctuations, resolving a decades-long debate; and 3) perform seminal measurements of the electronic band structure of delta-Pu using our unique angle-resolved photoemission capability to significantly constrain equation of state models. The fundamental and comprehensive understanding of the 5f electrons of Pu obtained through this integrated effort in experiment and theory will provide the scientific basis for Pu's equation of state, phase stability, and phase transformation kinetics under extreme conditions.This national program will stretch the Lab's expertise in characterizing and modeling complex materials, as well as revitalize plutonium science in this country and make it an attractive field of study for the next generation of LANL scientists; it is a crucial step towards fulfilling LANL's role as the Plutonium Center of Excellence and the Plutonium Science Strategy.

Benefit to National Security Missions

The fundamental understanding of plutonium obtained from this project will provide the scientific underpinning for the Lab's core missions of stockpile sustainability and materials science, directly addresses the Materials Grand Challenge with an emphasis on the emergent phenomena arising from Pu's 5f electrons. A Plutonium Science Strategy has recently been developed as part of the Plutonium Center of Excellence. The cutting edge research contained within this project for a fundamental understanding of the 5f electrons of plutonium specifically address many aspects of the Plutonium Science Strategy. Our program will assert LANL leadership in Pu science and stretch the Lab's capability base in new directions through the development of a robust, long-term delta-Pu single crystal grain growth capability and determination of Pu's electronic structure using the most sophisticated experimental and theoretical techniques available. Plutonium science also supports nuclear nonproliferation, nuclear energy, and environmental remediation.

Progress

This year, we have performed seminal measurements of the magnetic fluctuation spectrum in large polycrystalline samples of delta-242^Pu (22 g) and 242^PuCoGa$_5$ (15 g) at the Spallation Neutron Source at Oak Ridge National Laboratory. In particular, we found evidence for magnetic scattering centered at 90 meV and derived a magnetic form factor—for the first time ever. This result implies that the Kondo effect (i.e., a fluctuating magnetic moment) is the origin of the missing magnetism in delta-Pu, resolving a debate that has persisted for more than 20 years. Experiments on 242^PuCoGa$_5$ were successful and preliminary analysis of the data suggests additional scattering at very low energy (1 meV) deep in the superconducting state. Further analysis is ongoing.

We were successful in our attempts to grow large single grains of delta-Pu up to 1.3 mm in diameter. Starting with fine-grained Ga-stabilized delta-Pu, we strained the material between 2-4%, then annealed for 100 hours at about 400 C. This produced a number of large single grains, a couple of which are large enough to

carry out band structure measurements of delta-Pu via angle-resolved photoemission (ARPES) for the first time. We have begun to harvest two of the large grains and will collect our initial ARPES before the end of the fiscal year. In parallel, we performed two de Haas van Alphen (dHvA) measurements to probe the Fermi surface on very small delta-Pu grains (100 microns) at the National High Magnetic Field Laboratory using a novel technique involving a micro-silicon cantilever. While these first two attempts were not successful, we plan to measure the Fermi surface with this technique in the new modulation coils, which improves the sensitivity of the technique by more than an order of magnitude.

We carried out a number of measurements on the $PuMIn_5$ and $PuMGa_5$ (M=Co, Rh) superconductors to investigate the effects of the 30% volume collapse from PuRhIn5 to $PuCoGa_5$, which is similar to the volume difference between alpha-Pu and delta-Pu. By performing resonant ultrasound measurements on a single crystal of $PuCoGa_5$, which is most similar to delta-Pu, we extracted all six elastic constants of this tetragonal system. Analysis of the superconducting and normal states reveal that only the compressional modes show an anomaly below Tc and further indicate an unusual softening of the lattice below 50 K. These results suggest that valence fluctuations may mediate the superconductivity in $PuCoGa_5$. Extensive measurements on the PuRh(In1-xCdx)5 single crystals reveal that long-range antiferromagnetic (AFM) order is found for x>0.07 Cd with a narrow region of coexistent superconductivity and AFM order. This is the first example of such interplay between superconductivity and magnetism in a plutonium compound. To further explore the nature of the 5f electrons of plutonium in these materials, we performed angle-resolved photoemission (ARPES) and x-ray photoemission spectroscopy (XPS) measurements on single crystals of $PuCoIn_5$, $PuPt_2In_7$, and $PuCoGa_5$. These experiments reveal the degree of localization of the Pu 5f electrons. The ARPES measurements also reveal the electronic band structure, which when compared to dynamical mean field theory, delineate the degree of hybridization of the 5f and conduction electron states that characterize the strong electronic correlations in these materials.

We continue to search for the direct Pu-239 nuclear magnetic resonance (NMR) signal in a number of Pu intermetallic compounds. Preliminary results for observing the Pu-239 signal in the superconductor $PuCoGa_5$ look promising for observing this fingerprint of plutonium's nucleus will allow us to study its 5f electrons, which play a decisive role in controlling the degree of localization/itineracy of its 5f electrons.

In a three-pronged effort, the theoretical work for the project spans the range from providing exact solutions in the extreme itinerant limit (local density approximation), to the localized limit (hybrid functionals), and in between these limits where the Coulomb repulsion and kinetic energies of the 5f electrons are comparable dynamical mean field theory (DMFT). In a tour de force effort, we recently completed calculations on alpha-Pu, for the first time, within the framework of density functional theory (DFT) and the generalized gradient approximation (GGA) together with dynamical mean-field theory (DMFT). In short, alpha Pu appears to have the capacity to simultaneously have multiple degrees of electron localization/delocalization of Pu 5f electrons within this elemental phase of Pu.

Future Work

For the next fiscal year, we will focus on the following goals:

1. Harvest large single grains of delta-Pu prepared by the strain-anneal technique for first-ever measurement of delta-Pu band structure via angle resolved photoemission experiments.
2. Perform measurements of the angular momentum components of of delta-Pu at the Advanced Photon Source to determine magnetic configuration its the 5f electrons.
3. Perform de Haas van Alphen measurements on small, readily available single grains of delta-Pu using a new modulation coil for improved sensitivity at the National High Magnetic Field Laboratory.
4. Carry out measurements of the phonon dispersions on single grains of delta-Pu at the Advanced Photon Source to determine the softening of the specific phonon mode related to the delta-alpha phase transitions.
5. Investigate origin of multiconfigurational ground state recently observed by our team in alpha-Pu and delta-Pu through combination of dynamical mean field theory and detailed x-ray absorption spectroscopy measurements.
6. Perform inelastic neutron scattering measurements on delta-242^Pu and 242^PuCoGa5 and various neutron facilities (Spallation Neutron Source, Neutron Center for Research, and again at LANL).
7. Search for the Pu-239 direct NMR signal in various Pu-based superconductors and magnets to reveal the nature of the 5f electrons in these materials.

Conclusion

The complex behavior of Pu arising from its unique position in the periodic table remains an enigma to this day and poses one of the most significant challenges to DOE's national security missions. Sustaining the aging nuclear stockpile at significantly reduced levels demands a fundamental understanding of Pu's 5f electrons beyond what is currently known. Our approach consists of performing experiments on single crystals of delta-Pu and Pu compounds containing the isotope Pu-242. Our work will provide a fundamental and comprehensive understanding of plutonium necessary for the continued success of DOE's stockpile sustainability and other national security missions.

Publications

Bauer, E. D., P. H. Tobash, J. N. Mitchell, and J. L. Sarrao. Single crystal growth of plutonium compounds from molten metal fluxes. 2012. Philosophical MagazinePhilosophical Magazine. 92 (19-21): 2466.

Bauer, E. D., P. H. Tobash, J. N. Mitchell, and J. L. Sarrao. Single crystal growth of plutonium compounds from molten metal fluxes. 2012. Philosophical MagazinePhilosophical Magazine. 92 (19-21): 2466.

Booth, C. H., Y. Jiang, D. L. Wang, J. N. Mitchell, P. H. Tobash, E. D. Bauer, M. A. Wall, P. G. Allen, D. Sokaras, D. Nordlund, T. C. Weng, M. A. Torrez, and J. L. Sarrao. Multiconfigurational nature of 5f orbitals in uranium and plutonium intermetallics. 2012. Proceedings of the National Academy of Sciences of the United States of AmericaProceedings of the National Academy of Sciences of the United States of America. 109 (26): 10205.

Haga, Y., E. D. Bauer, P. H. Tobash, J. N. Mitchell, O. Ayala-Valenzuela, R. D. McDonald, C. H. Mielke, and Z. Fisk. Shubnikov-de Haas oscillation in PuIn3. 2013. Journal of the Korean Physical SocietyJournal of the Korean Physical Society. 63 (3): 380.

II, M. F. Beaux, J. J. Joyce, T. Durakiewicz, K. S. Graham, E. D. Bauer, P. H. Tobash, and S. Richmond. Electronic Structure, Localization and 5f Occupancy in Pu Materials. Mate.

Jian-Xin, Z., P. H. Tobash, E. D. Bauer, F. Ronning, B. L. Scott, K. Haule, G. Kotliar, R. C. Albers, and J. M. Wills. Electronic structure and correlation effects in PuColn 5 as compared to PuCoGa 5. 2012. Europhysics LettersEurophysics Letters. 97 (5): 57001 (5 pp.).

Mitchell, T. E., J. P. Hirth, D. S. Schwartz, and J. N. Mitchell. The beta-to-alpha phase transformation in plutonium. 2013. Acta MaterialiaActa Materialia. 61: 2895.

Rudin, S. P.. Density Functional Theory Calculation Study of the Entangled Crystal, Magnetic, and Electronic Structures of PuGa3 . 2013. arXiv:1307.0762arXiv:1307.0762 .

Wang, C. C., M. D. Jones, and J. Zhu. Fermi surface topology and de Haas–van Alphen orbits in PuIn_{3} and PuSn_{3} compounds. 2013. Physical Review BPhysical Review B. 88 (12): 125106.

Yasuoka, H., G. Koutroulakis, H. Chudo, S. Richmond, D. K. Veirs, A. I. Smith, E. D. Bauer, J. D. Thompson, G. D. Jarvinen, and D. L. Clark. Observation of Pu-239 Nuclear Magnetic Resonance. 2012. ScienceScience. 336 (6083): 901.

Yasuoka, H., G. Koutroulakis, H. Chudo, S. Richmond, D. K. Veirs, A. I. Smith, E. D. Bauer, J. D. Thompson, G. D. Jarvinen, and D. L. Clark. Observation of Pu-239 Nuclear Magnetic Resonance. 2012. ScienceScience. 336 (6083): 901.

Zhu, J., R. C. Albers, K. Haule, G. Kotliar, and J. M. Wills. Site-selective electronic correlation in α-plutonium metal. 2013. Nat CommunNat Commun. (in press).

Modern Challenges in Actinide Science

Albert Migliori
20120167DR

Introduction

The purpose of Modern Challenges in Actinide Science is to support cutting-edge research for targeted tasks at the forefront of actinide science today that directly support LANL missions.

Broadly defined, this project supports experimental and theoretical research that underlies LANL missions in fundamental actinide science (all aspects), nuclear weapons, nuclear energy and energy security, nuclear safeguards and detection of actinide materials, nuclear nonproliferation and forensics, fate and transport of actinides in the environment, interactions of actinides with biological systems, and nuclear waste management--all deemed strategic for the Laboratory. Some of these will be in areas that will enhance the "plutonium center of excellence" designation for Los Alamos. Other areas will support MaRIE and the "LANL-LLNL Plutonium Science and Research Strategy." Noting that "actinides" are more than just plutonium, and that the "other" actinides are exceptionally important for forensics, environmental-related missions, biological and waste management issues and more, a balance will be maintained among the many actinide research areas chosen for this project.

For definiteness, the project will support research in sub-tasks as described above, identified and worked on by LANL postdoctoral fellows. Each sub-task, and the postdoctoral fellow proposing it, will be evaluated by a selection team that will judge the proposed work for scientific merit, relevance to LANL mission, and quality of the applicant, with precedence among equal-quality proposals given to areas important to LANL missions identified above that are underrepresented.

Benefit to National Security Missions

"Modern Challenges in Actinide Science" will support scientific discovery and innovation, environmental remediation, nuclear waste management, nuclear energy, nuclear forensics, nuclear weapons, nonproliferation, and the associated agencies by studying the important modern experimental, engineering, technical, and theoretical questions that govern the properties of actinides. Because each of the mission-relevant areas has as an irreducible central component of the actinide elements, research on modern scientific challenges in actinides is a required component of each of the relevant areas. It is expected that the selected sub-tasks will each lead to knowledge and capabilities that will attract internal and external funding where new science merits it and where that science is instrumental in resolving technical and engineering issues.

Progress

- The projects led by postdoctoral fellows in the last year have resulted in 28 publications.
- Resonant Ultrasound Studies of plutonium elastic moduli versus temperature and time required advances in the analysis of huge amounts of data. These advances enabled studies of the temperature dependence of the elastic moduli of superconductors with unprecedented precision. The result is the discovery of a new thermodynamic phase in high temperature superconductors, "Bounding the pseudogap with a line of phase transitions in YBa2Cu3O6+δ," Nature 498, 75-77 (2013).
- Work to date has indicated that installation of a third U=E multiple bond may lead to highly reactive species, necessitating more research into the groups of atoms used to occupy the remainder of the metal's coordination sphere.
- A comprehensive study of the materials PuCoIn5 and PuIn3 has been completed and the relevant manuscripts will be submitted to Journal of Physics: Condensed Matter within a couple of months.
- Discovery of the direct plutonium-239 Nuclear Magnetic Resonance (NMR) signal, published in

the jounal Science: First observation of 239Pu NMR in any material, reported by Yasuoka et al., Science, 2012, 336 (6083): 901-904. The use of NMR to direct observe plutonium-239 in the solid state and perhaps solution opens up a powerful new window to observe the chemical and electronic behavior of plutonium for many applications.

- Our photoluminescent measurements on Cs2NpO-2Cl4 doped into a Cs2UO2Cl4 matrix (referred to as Cs2U(Np)O2Cl4) revealed energy transfer between the Cs2UO2Cl4 host matrix and the Cs2NpO2Cl4 analyte. The energy transfer results in a large increase in the near-IR luminance intensity from Cs2NpO2Cl4. To study this effect in a quantitative way we produced a series of Cs2U(Np)O2Cl4 crystals containing varying amounts of Cs2NpO2Cl4. This allowed us to gain an understanding of the mechanisms which are involved in the transfer of energy between actinide-containing molecules and to develop a model for the energy transfer in this system. We have recently produced the analogous plutonium-containing Cs2U(Pu)O2Cl4 system and are preparing to studying energy transfer in this system as well.
- Synthesized a new type of carboxyl-functionalized pyrazolium ionic liquid that may have useful properties for dissolving and separating actinide metal ions and characterized the new ionic liquid with spectroscopic methods. Studied the uranyl(VI) coordination chemistry with a carboxyl-functionalized phosphonium ionic liquid using various spectroscopic methods. Three papers were published on this work.
- We have observed the first ever signal from ultracold neutron-generated fission in actinides.
- Published a paper describing the electronic structure of several novel uranium compounds in the Journal of the American Chemical Society.
- Developed capabilities to collect solution-phase sulfur K-edge X-ray absorption spectroscopic measurements. All measurements to date have been with solid materials.
- Synthesized and analyzed a series of transition metal dithiophosphinate complexes using X-ray absorption spectroscopy to lay the foundation for analyzing f-element dithiophosphinate complexes.
- Synthesized a novel dithiophosphinate extractant that we anticipate will provide better separation factors for separation trivalent actinides from lanthanides. This could be useful for the recycle of actinides in an advanced nuclear energy system.
- We have investigated multiple routes to generating U(VI) tris(imido) complexes (imido = [R-N=]2–; R = alkyl, aryl), for the purpose of discovering a general route into these species. Protonolysis reactions of the U(VI) bis(imido) carbene species U(NAr)2(dppmS2)(t-Bu2bpy) (Ar = aryl groups; dppmS2 = 1,1-bis(thiodiphenylphosphino)methane dianion; t-Bu2bpy = 4,4'-di-tert-butyl-2,2'-bipyridyl) with acidic amines liberates free H2dppmS2, but we have been unable to positively identify the uranium-containing product from this reaction. Attempts at hydrogen-atom abstraction reactions from low-valent uranium amides have resulted in either electron transfer from a U(III) pentakis-arylamide or unidentified products in the cases of U(IV) imido amides. Further work will continue in this area to generate suitable starting materials for investigating hydrogen-atom abstraction chemistry. We have also investigated the formation of bis(imido)-oxo or dioxo-imido U(VI) complexes using nitrite salts as O1– sources, but the only products isolated from these reactions are uranyl (UO22+) derivatives, suggesting that undesired chemistry is occurring with the imido group.
- Development and programming of analytical methods needed to conduct project-related measurements
- Preliminary actinide measurements involving selected test materials. To date, such measurements have consistently shown the proposed sources to be superior to traditional approaches, with as much as a 2400% enhancement in sample utilization being recorded at trace loading levels (e.g. picograms).

Future Work

- Study the complexation of actinides in new ionic liquids with X-ray diffraction analysis and spectroscopic methods such as Raman, FT-IR, UV-vis-NIR and NMR.
- Continue focus on developing synthetic methods for generating small molecule analogs to UO3. Expand to the study of imido complexes of uranium that could serve as synthetic precursors for molecular UO3 analogs.
- Submit manuscripts relevant to the study of unconventional superconductivity and exotic magnetism in a series of Pu-based heavy-fermion superconductors. Complete the study of at least four compounds, specifically PuCl6, PuCoGa5, PuSb2, and δ-Pu.
- Develop procedure for manufacture of thin foils of Pu-239 and other actinides, commission a detection system for materials sputtered from the actinide foils, & perform first characterizations using the ultracold

neutron source.

- Perform a series of measurements in which the slow dynamics of defects in Pu metal is studied via evolution of elastic moduli of a crystal.

- Continue photoluminescent measurements on Cs2NpO2Cl4 doped into a Cs2UO2Cl4 matrix. Synthesize crystals of Cs2PuO2Cl4 doped into a Cs2UO2Cl4 matrix. Perform theoretical calculations on Cs2PuO2Cl4.

- Evaluate impact of the spectroscopic overlap of strontium Kα line on plutonium quantification. Investigate potential approaches to compensate for the strontium interference. Conduct laboratory validation, including assessment of precision, accuracy, & limit of detection for use of monochromatic wavelength dispersive XRF (MWDXRF) & micro XRF (MXRF).

- Expand efforts to enhance the detection of plutonium & americium in thermal ionization mass spectrometry measurements, focusing on construction & testing of 2nd generation sources to characterize increased sample detection abilities/needs for various materials. Exploit improved sample utilization to address current challenges in plutonium chronometry.

- Synthesize f-element complexes with dithiophosphinate ligands. Analyze samples from f-metal-ion reactions with dithiophosphinates by EXAFS. Complete the synthesis of a new family of extractants that we anticipate will provide better actinide separation factors.

Conclusion

It is expected that between 12 and 16 individual research tasks will be active on average during the period of the project. Each is expected to produce peer-reviewed publications and an internal LANL seminar each year for which the sub-task is active. It is intended that these sub-tasks cover all areas of actinide science that are relevant to LANL missions. It is important to note that not all areas will be covered at any one time, and that precedence for underrepresented areas will be given.

Publications

Ashley, K. R., S. M. Bowen, J. W. Oldham, Jr., A. C. Olson, S. A. Kozimor, and A. R. Schake. Quantifying abundances of long-lived 155Eu and 151Sm fission products using gamma- and liquid scintillation counting spectroscopies. Analytical Chemistry.

Beaux, M. F., J. J. Joyce, T. Durakiewicz, K. S. Graham, E. D. Bauer, J. N. Mitchell, P. H. Tobash, and S. Richmond. Electronic structure, localization, and 5f occupany in Pu materials. 2012. MRS Proceedings. 1444 (2012): 123.

Beaux, M. F., T. Durakiewicz, L. Moreschini, M. Grioni, F. Offi, G. Monaco, G. Panaccione, J. J. Joyce, E. D. Bauer, J. L. Sarrao, M. T. Butterfield, and E. Guziewicz. Electronic structure of single crystal UPd3, UGe2, and USb2 from hard X-ray and angle-resolved photoelectron spectroscopy. 2011. Journal of Electron Spectroscopy and Related Phenomena. 184 (8-10): 517.

Bejger, C., Y. H. Tian, B. J. Barker, K. S. Boland, B. L. Scott, E. R. Batista, S. A. Kozimor, and J. L. Sessler. Synthesis and characterization of a tetrathiafulvalene-salphen actinide complex. 2013. Dalton Transactions. 42: 6716.

Boland, K., S. Conradson, A. Costello, A. Gaunt, S. Kozimor, I. May, S. Reilly, and D. Schnaars. Stabilising pentavalent actinides-visible-near infrared and X-ray absorption spectroscopic studies of the utility of the [(Np3W4O15)(H2O)(3)(MW9O33)(3)](18-)(M = Sb, Bi) structural type. 2012. DALTON TRANSACTIONS. 41 (7): 2003.

Chen, X. Y., G. S. Goff, B. L. Scott, and W. Runde. Comparison of structural Variations of Ln(III) compounds with (pyrazol-1-yl)acetic acid. To appear in Polyhedron.

Chen, X., G. S. Goff, M. Quiroz-Guzman, D. P. Fagnant, Jr., J. F. Brennecke, B. L. Scott, and W. Runde. Directed nucleation of monomeric and dimeric uranium(VI) complexes with a room termperature carboxyl-functionaled phosphonium ionic liquid. 2012. Chemical Communications. 49 (19): 1903.

Chen, X., G. S. Goff, W. C. Ewing, B. L. Scott, and W. Runde. Solid-state and solution-state coordination chemistry of Lanthanide(III) complexes with alpha-hydroxyisobutyric acid. 2013. Inorganic Chemistry. 52 (6): 3217.

Chen, X., G. S. Goff, W. C. Ewing, B. L. Scott, and W. Runde. Solid-state and solution-state coordination chemistry of Lanthanide(III) complexes with alpha-hydroxyisobutyric acid. 2012. Inorganic Chemistry. 51: 13254.

Coleman, M. E., E. M. Bond, W. A. Moody, and L. Tandon. The analysis of uranium-232: comparison of radiochemical techniques and an improved method by alpha spectrometry. 2013. JOURNAL OF RADIOANALYTICAL AND NUCLEAR CHEMISTRY. 296 (1): 483.

Dakovski, G., Y. Li, S. Gilbertson, G. Rodriguez, A. Balatsky, J. Zhu, K. Gofryk, E. Bauer, P. Tobash, A. Taylor, J. Sarrao, P. Oppeneer, P. Riseborough, J. Mydosh, and T. Durakiewicz. Anomalous femtosecond quasiparticle

dynamics of hidden order state in URu2Si2. 2011. PHYSICAL REVIEW B. 84 (16): 161103.

Daly, S., J. Keith, E. Batista, K. Boland, D. Clark, S. Kozimor, and R. Martin. Sulfur K-edge X-ray absorption spectroscopy and time-dependent density functional theory of dithiophosphinate extractants: Minor actinide selectivity and electronic structure correlations. 2012. Journal of the American Chemical Society. 134 (35): 14408.

Daly, S., J. Keith, E. Batista, K. Boland, S. Kozimor, R. Martin, and B. Scott. Probing Ni[S2PR2](2) Electronic Structure to Generate Insight Relevant to Minor Actinide Extraction Chemistry. 2012. INORGANIC CHEMISTRY. 51 (14): 7551.

Daly, S., J. Klaehn, K. Boland, S. Kozimor, M. MacInnes, D. Peterman, and B. Scott. NMR spectroscopy and structural characterization of dithiophosphinate ligands relevant to minor actinide extraction processes. 2012. Dalton Transactions. 41 (7): 2163.

Gianetti, T. L., G. Nocton, S. G. Minasian, N. C. Tomson, A. L. D. Kilcoyne, S. A. Kozimor, D. K. Shuh, T. Tyliszczak, R. G. Bergman, and J. Arnold. Diniobium inverted sandwich complexes with μ-η6:η6-arene ligands: synthesis, kinetics of formation, and electronic structure. 2012. Journal of the American Chemical Society. 135 (8): 3224.

He, H. M., D. A. Andersson, D. D. Allred, and K. D. Rector. Determination of the Insulation Gap of Uranium Oxides by Spectroscopic Ellipsometry and Density Functional Theory. 2013. JOURNAL OF PHYSICAL CHEMISTRY C. 117 (32): 16540.

He, H., P. Wang, D. D. Allred, M. P. Wilkerson, J. Majewski, and K. D. Rector. Characterization of chemical speciation in ultra thin uranium oxide films. 2012. Analytical Chemistry. 84 (23): 10380.

Jiang, Yu, C. H. Booth, P. H. Tobash, K. Gofryk, M. A. Torrez, F. Ronning, E. D. Bauer, and J. D. Thompson. Magnetic Frustration Effects in Uranium Intermetallics. 2011. In International Conference on Strongly Correlated Electron Systems (SCES 2010) ; 27 June-2 July 2010 ; Santa Fe, NM, USA. Vol. 273, p. 012036 (4 pp.).

Jilek, R., L. Spencer, R. Lewis, B. Scott, T. Hayton, and J. Boncella. A Direct Route to Bis(imido)uranium(V) Halides via Metathesis of Uranium Tetrachloride. 2012. Journal of the American Chemical Society. 134 (24): 9876.

Knezevic, M., I. J. Beyerlein, D. W. Brown, T. A. Sisneros, and C. N. Tome. A polycrystal plasticity model for predicting mechanical response and texture evolution during strain-path changes: Application to beryllium. 2013. INTERNATIONAL JOURNAL OF PLASTICITY. 49: 185.

Knezevic, M., I. J. Beyerlein, T. Nizolek, N. A. Mara, and T. M. Pollock. Anomalous basal slip activity in zirconium under high-strain deformation. 2013. Materials Research Letters. 1 (3): 133.

Knezevic, M., J. S. Carpenter, and R. J. McCabe. Deformation behavior of the cobalt-based superalloy Haynes 25: Experimental characterization and crystal plasticity modeling. To appear in Acta Materialia.

Knezevic, M., R. A. Lebensohn, O. Cazacu, B. Revil-Baudard, G. Proust, S. Vogel, and M. E. Nixon. Modeling bending of α-titanium with embedded crystal plasticity and analytical yield surface formulations in implicit finite elements. 2013. Materials Science and Engineering A. 564 (1 March): 116.

Knezevic, M., R. J. McCabe, C. N. Tome, R. A. Lebensohn, S. R. Chen, C. M. Cady, G. T. Gray, and B. Mihaila. Modeling mechanical response and texture evolution of alpha-uranium as a function of strain rate and temperature using polycrystal plasticity. 2013. INTERNATIONAL JOURNAL OF PLASTICITY. 43: 70.

Knezevic, M., R. J. McCabe, R. A. Lebensohn, C. N. Tome, C. Liu, M. L. Lovato, and B. Mihaila. Integration of self-consistent polycrystal plasticity with dislocation density based hardening laws within an implicit finite element framework: Application to low-symmetry metals. 2013. JOURNAL OF THE MECHANICS AND PHYSICS OF SOLIDS. 61 (10): 2034.

Knezevic, M., R. J. McCabe, R. A. Lebensohn, C. N. Tome, and B. Mihailia. Modeling mechanical response and texture evolution of α-uranium as a function of strain rate and temperature using polycrystal plasticity. 2013. International Journal of Plasticity. 43 (April): 70.

Koutroulakis, G., H. Chudo, H. Yasuoka, P. H. Tobash, H. N. Mitchell, E. D. Bauer, and J. D. Thompson. Microscopy properties of the heavy-fermion superconductor PuCoIn5: An NQR study. New Journal of Physics.

Koutroulakis, G., H. Chudo, H. Yasuoka, P. H. Tobash, J. N. Mitchell, E. D. Bauer, and J. D. Thompson. Itinerant weak antiferromagnetism in PuIn3 explored by 115In NQR. Journal of Physics - Condensed Matter.

McCleskey, T. M., E. Bauer, Q. X. Jia, A. K. Burrell, B. L. Scott, S. D. Conradson, A. Mueller, L. Roy, X. D. Wen, G. E. Scuseria, and R. L. Martin. Optical band gap of NpO2 and PuO2 from optical absorbance of epitaxial films. 2013. JOURNAL OF APPLIED PHYSICS. 113 (1): -.

Minasian, S. G., J. M. Keith, E. R. Batista, D. L. Clark, S. A. Kozimor, R. L. Martin, and D. K. Shuh. The importance

of φ-orbital mixing in thorocene and uranocene determined from carbon K-edge X-Ray absorption spectroscopy and time-dependent density functional theory. Agnewandte Chemie.

Minasian, S. G., J. M. Keith, E. R. Batista, K. S. Boland, J. A. Bradley, S. R. Daly, W. W. Lukens, J. Nordlund, G. T. Seidler, D. Sokaras, G. L. Wagner, T. C. Weng, P. Yang, S. A. Kozimor, R. L. Martin, D. K. Shuh, and T. Tyliszczak. Orbital mixing in metal-oxygen multiple bonds evaluatied using oxygen K-edge spectroscopy and DFT. Nature Chemistry.

Minasian, S., J. Keith, E. Batista, K. Boland, D. Clark, S. Conradson, S. Kozimor, R. Martin, D. Schwarz, D. Shuh, G. Wagner, M. Wilkerson, L. Wolfsberg, and P. Yang. Determining relative f and d orbital contributions to M-Cl covalency in MCl₆²⁻ (M = Ti, Zr, Hf, U) and UOCl₅ ⁻ using Cl K-edge X-ray absorption spectroscopy and time-dependent density functional theory. 2012. Journal of the American Chemical Society. 134 (12): 5586.

Minasian, S., K. Boland, R. Feller, A. Gaunt, S. Kozimor, I. May, S. Reilly, B. Scott, and D. Shuh. Synthesis and Structure of (Ph4P)(2)MCl6 (M = Ti, Zr, Hf, Th, U, Np, Pu). 2012. INORGANIC CHEMISTRY. 51 (10): 5728.

Monreal, M. J., R. K. Thomson, T. Cantat, N. E. Travia, B. L. Scott, and J. L. Kiplinger. UI4(1,4-dioxane)(2), [UCl4(1,4-dioxane)](2), and UI3(1,4-dioxane)(1.5): stable and versatile starting materials for low- and high-valent uranium chemistry . 2012. Organometallics. 30 (7): 2031.

Monreal, M. J., R. K. Thomson, T. Cantat, N. E. Travia, B. L. Scott, and J. L. Kiplinger. UI4(1,4-dioxane)(2), [UCl4(1,4-dioxane)](2), and UI3(1,4-dioxane)(1.5): Stable and Versatile Starting Materials for Low- and High-Valent Uranium Chemistry. 2011. ORGANOMETALLICS. 30 (7): 2031.

Nerikar, P. V., L. A. Casillas Trujillo, D. A. Andersson, C. Unal, B. P. Uberuaga, C. R. Stanek, D. C. Parfitt, R. W. Grimes, and S. B. Sinnott. Segregation of xenon to dislocations and grain boundaries in uranium dioxide. 2011. Journal Name: Physical Review. B, Condensed Matter and Materials Physics. 84 (17): Medium: X; Size: page(s) 17410.

Olson, A. C., J. M. Keith, E. M. Batista, K. S. Boland, S. R. Daly, S. A. Kozimor, M. M. MacInnes, R. L. Martin, and B. L. Scott. Using solution- and solid-state S K-edge X-ray absorption spectroscopy with Density Functional Theory to evaluate M-S bonding for MS42. (M = Cr, Mo, W) dianions. Inorganic Chemistry.

Park, W. K., P. H. Tobash, F. Ronning, E. D. Bauer, J. L. Sarrao, J. D. Thompson, and L. H. Greene. Observation of the Hybridization Gap and Fano Resonance in the Kondo Lattice URu₂Si₂. 2012. Physical Review Letters. 108 (24): 246403 (5 pp.).

Rim, K. R., D. Eom, S. W. Chan, M. Flytzani-Stephanopoulow, G. W. Flynn, and E. R. Batista. Scanning tunneling microscopy and theoretical study of water adsorption on Fe3O4: Implications for catalysis. 2012. Journal of the American Chemical Society. 134 (46): 18979.

Romanchuk, A. Y., S. N. Kalmykov, A. V. Egorov, Y. V. Zubavichus, A. A. Shiryaev, O. N. Batuk, S. D. Conradson, D. A. Pankratov, and I. A. Presnyakov. Formation of crystalline PuO2+xnH2O nanoparticles upon sorption of Pu(V,VI) onto hematite. 2013. Geochimica et Cosmochimica Acta. 121: 29.

Shekhter, A., B. J. Ramshaw, R. Liang, W. N. Hardy, D. A. Bonn, F. F. Balakirev, R. D. McDonald, J. B. Betts, S. C. RIggs, and A. Migliori. Bounding the pseudogap with a line of phase transitions in YBa2Cu3O6+δ . 2013. Nature. 498: 75.

Spencer, L. P., S. G. Minasian, R. E. Jilek, E. R. Batista, K. S. Boland, J. M. Boncella, S. D. Conradson, D. L. Clark, R. L. Gdula, T. W. Hayton, S. A. Kozimor, R. L. Martin, M. A. McInnes, A. C. Olson, B. L. Scott, D. K. Shuh, and P. Yang. Tetrahalide complexes of the [U(NR)2]2+ ion: synthesis, theory, and Cl K-edge X-ray absorption spectroscopy. 2013. Journal of the American Chemical Society. 135 (6): 2279.

Stanley, F. E., K. J. Spencer, D. S. Schwartz, M. G. Watrous, and J. E. Delmore. Investigating enhanced thorium ionization in TIMS using Re/Pt porous ion emitters. Journal of Radioanalytical and Nuclear Chemstry.

Teng, B. T., F. M. Wu, W. X. Huang, X. D. Wen, L. H. Zhao, and J. F. Luo. A DFT study of the structures of aux clusters on a CeO2(III) surface. 2012. A European Journal of Chemical Physics and Physical Chemistry. 13 (5): 1261.

Thomson, R., C. Graves, B. Scott, and J. Kiplinger. Straightforward and efficient oxidation of tris(aryloxide) and tris(amide) uranium(III) complexes using copper(I) halide reagents. 2011. INORGANIC CHEMISTRY COMMUNICATIONS. 14 (11): 1742.

Thomson, R., M. Monreal, J. Masuda, B. Scott, and J. Kiplinger. Lutetium gets a crown: Synthesis, structure and reaction chemistry of the separated ion pair complex, [Li(12-crown-4)₂][(C₅Me ₅)₂LuMe₂]. 2011. Journal of Organometallic Chemistry. 696 (25): 3966.

Tobash, P., F. Ronning, J. D. Thompson, B. L. Scott, P. J. Moll, B. Batlogg, and E. D. Bauer. Single crystal study of the heavy-fermion antiferromagnet CePt ₂In₇. 2012. Journal of Physics Condensed Matter. 24 (1): 015601.

Travia, N. E., M. J. Monreal, B. L. Scott, and J. L. Kiplinger. Thorium-mediated ring-opening of tetrahydrofuran and the development of a new starting material for thorium chemistry: preparation, crystal structure, and chemistry of ThI4(DME)4. 2012. Dalton Transactions. 2012 (41): 14514.

Ueland, B. G., C. F. Miclea, Y. Kato, O. Ayala-Valenzuela, R. D. McDonald, R. Okazaki, P. H. Tobash, M. A. Torrez, F. Ronning, R. Movshovich, Z. Fisk, E. D. Bauer, I. Martin, and J. D. Thompson. Controllable chirality-induced geometrical Hall effect in a frustrated highly-correlated metal. 2012. Nature Communications. 3: 1067.

Vasudevan, K. V., B. L. Scott, R. Marti-Arbona, and J. C. Gordon. Decamethylsamarocene-mediated reductive coupling of the (1R,2R)-N,N'-Bis(2- pyridylmethylene) cyclohexane-1,2-diamine ligand . European Journal of Inorganic Chemistry.

Vasudevan, K. V., N. C. Smythe, B. L. Scott, and J. C. Gordon. Metallopolymer formation using the (1R,2R)-N,N'-bis(2-pyridylmethylene)- cyclohexane-1,2-diamine (BPID) ligand class. 2012. Dalton Transactions. 42 (14): 4768.

Vasudevan, K., B. Scott, and J. Gordon. Main-group element compounds derived from the (1R,2R)-N,N ,Äô-bis(2-pyridylmethylene)cyclohexane-1,2-diamine (BPID) ligand. 2012. MAIN GROUP CHEMISTRY. 11 (1, SI): 45.

Vasudevan, K., N. Smith, B. Scott, B. Bennett, R. Muenchausen, and J. Gordon. Ionic liquid mediated routes to polydentate oxygen-donor adducts of cerium(iii) bromide. 2012. Dalton Transactions. 41 (7): 1924.

Wang, S. W., M. Tang, L. L. Zhang, G. L. Xiao, K. S. Brinkman, and F. L. Chen. Irradiation effect on the structure change for Sr2Fe1.5Mo0.5O6-delta perovskite ceramic. 2013. JOURNAL OF ALLOYS AND COMPOUNDS. 578: 170.

Wen, X. D., R. Hoffmann, and N. W. Ashcroft. Two-dimensional CdSe nanosheets and their interaction with stabilizing ligands. 2012. Advanced Materials. 25 (2): 261.

Wen, X. D., R. L. Martin, G. E. Scuseria, S. P. Rudin, E. R. Batista, and A. K. Burrell. Screened hybrid and DFT plus U studies of the structural, electronic, and optical properties of U3O8. 2013. JOURNAL OF PHYSICS-CONDENSED MATTER. 25 (2): 025501.

Wen, X. D., R. L. Martin, L. E. Roy, G. E. Scuseria, S. P. Rudin, E. R. Batista, T. M. McCleskey, B. L. Scott, E. Bauer, J. J. Joyce, and T. Durakiewicz. Effect of spin-orbit coupling on actinide dioxides, AnO2 (An=Th, Pa, U, Np, Pu and Am): A screened hybrid density functional study. 2012. Journal of Chemical Physics. 137 (15): 154707.

Wen, X. D., R. L. Martin, T. M. Henderson, and G. E. Scuseria. Density functional theory studies of the electronic structure of solid state actinide oxides. 2013. Chemical Review. 113 (2): 1063.

Wen, X. D., S. P. Rudin, E. R. Batista, D. L. Clark, G. E. Scuseria, and R. L. Martin. Rotational rehybridization and the high temperature phase of UC2. 2012. Inorganic Chemistry. 51 (23): 12650.

Wen, X., T. Yang, R. Hoffmann, N. W. Ashcroft, R. Martin, S. Rudin, and J. Zhu. Graphane nanotubes. 2012. ACS Nano. 6 (8): 7142.

Yang, Y., J. Saiers, N. Xu, S. Minasian, T. Tyliszczak, S. Kozimor, D. Shuh, and M. Barnett. Impact of natural organic matter on uranium transport through saturated geologic materials: From molecular to column scale. 2012. Environmental Science and Technology. 46 (11): 5931.

Yasuoka, H., G. Koutroulakis, H. Chudo, S. Richmond, D. K. Veirs, A. I. Smith, E. D. Bauer, E. D. Thompson, G. D. Jarvinen, and D. L. Clarks. Observation of ²³⁹Pu Nuclear Magnetic Resonance. 2012. Science. 336 (6083): 901.

Zhao, Y., B. T. Teng, X. D. Wen, L. H. Zhao, and M. F. Luo. A theoretical evaluation and comparison of MxCe1−xO2−δ(M = Au, Pd, Pt, and Rh) catalysts. 2012. Catalysis Communications. 27: 63.

Zhao, Y., B. T. Teng, X. D. Wen, L. H. Zhao, and M. F. Luo. Superoxide and peroxide species on CeO2(111), and their oxidation roles. 2012. Journal of Physical Chemistry. 116: 15986.

Accelerating Materials Certification Through Co-design

Jack S. Shlachter
20120707DR

Introduction

The goal of this project is to make progress towards the grand challenge goal of predictive process-aware materials performance through a focus on "co-design." Co-design traditionally refers to the simultaneous optimization of hardware and software in computer science; here, we broaden the definition of co-design to include the integrated coupling of multi-scale theory, computation/information science & technology techniques (including data visualization), and experiment. We propose a series of four coupled thrusts to achieve our goal. We will i) build on past successes to pursue the co-design of micro-mechanical models to improve predictive capability in regimes of high-pressures and strain rates with a focus on Zr and Ti, ii) develop, in parallel with thrust i, a co-design framework for multi-scale models focused on radiation damage evolution, in particular creep-related phenomena, iii) utilize ion beam irradiation as a means of accelerating materials damage, including providing key data for thrust ii, and iv) explore the foundations of coherent x-ray diffractive imaging in order to translate physical observables into model inputs in support of thrusts i and ii. In this thrust structure, the project leadership's principal responsibility is fostering integration and collaboration among these thrusts. This management plan will yield synergies not possible through a series of discrete projects.

Benefit to National Security Missions

The need to predict and control materials in extremes spans the full range of DOE missions from weapons performance to energy security. Further, successful nuclear weapons program approaches to certification of materials performance (and the associated quantification of performance margins and uncertainty) have not e.g., been translated to nuclear energy materials certification challenges. In this project, we will address specific process-aware materials performance challenges in our enduring nuclear weapons stockpile and work to develop a paradigm for accelerated materials certification for fusion energy.

Progress

On the major experimental/modeling effort under this project, the Dynamic Materials Performance effort, we have significant findings from polycrystal experiments and single crystal simulations on how phase transformation is preceded by deformation modes and the dependence on shock direction. Through this work we have identified a need for single crystal experiment measurements. For the balance of this year, we will focus on single crystal measurements + estimation of barrier energies + preliminary results from our microstructural model.

Our Linac Coherent Light Source (LCLS) jumpstart activities, crucial to demonstrating use of an x-ray free electron laser (XFEL), the experiment has been completed, and the data analysis will be continued until it is ready for publication. In late breaking news – the proposal to use the LCLS for Run 8 was ranked in the top group and is expected to receive beamtime.

Measurement of temperature in extreme environments is a major R&D activity for developing advanced certification of materials. In the first of our three thermometry activities, the spontaneous Raman approach, we are currently performing continuous wave measurements to 900 K accompanied by writing automated data acquisition and analysis software. Pulsed measurements on statically heated samples will be performed over the next few months. We have constructed a cell capable of testing static samples from liquid nitrogen to >900 K. We have assembled a Stokes/anti-Stokes Raman Detection system, written LabView acquisition software, and tested several algorithms for fluorescent background subtraction and real time (few Hz) conversion to temperature. This is being tested with CW lasers currently, but is

mobile for transition to the microsecond and nanosecond laser laboratories. We have measured Raman spectra/temperatures of quartz to 900 K. We have performed maintenance to restore operation to the microsecond laser, which is now performing normally.

Calculations relating experimental observations to theoretical predictions of parametric effects have begun. The static temperature test cell, spectrometers, detectors, and lasers were all assembled from available equipment for cost savings.

A second approach to measuring temperatures involves analyzing subtleties in the diffraction signals. This work is titled Separation of Deformation, Particle Shape and Temperature Factors from Nuclear Motion Data. Initial analysis on Cu and Ta samples has shifted to Zr simulations in the Dynamic Materials Performance effort though the phase transformation is complicating our analysis (a very large number of defects structures are generated that excessively blur the peaks). The transfer of initial amounts of this data has recently occurred and we have begun our SOMERIF structural analysis on this. One staff member had previously written a more sophisticated diffraction calculation program that integrates over many time steps and can include particle shape factors and realistic detector scenarios. This is very well suited for our application. The initial temperature analysis will likely revert back to Cu samples for the proof of principle. We are now agreed on a path forward and will be ramping up the efforts.

On the radiation front, our LANL/TAMU collaboration continues its activities in the Ion Beam Materials Laboratory (IBML). The corrosion chamber design and off-site test is being done at the TAMU in collaboration with INL and LANL. The chamber will be installed in the IBML in July/August and the irradiation experiment is scheduled in the Aug./Sept. time frame. Finally, our UCSD collaboration is developing. We estimate that it will take some time to design, install, and conduct first wall materials research on this unique and novel capability.

Future Work

Work in FY14 will build on and extend scope initiated in FY12 and continued in FY13. In particular, we will i) pursue the co-design of micro-mechanical models to improve predictive capability in regimes of high-pressures and strain rates with a focus on Zr and Ti, ii) develop a co-design framework for multi-scale models focused on radiation damage evolution, in particular creep-related phenomena, iii) utilize ion beam irradiation as a means of accelerating materials damage, including providing key data for thrust ii, and iv) explore the foundations of coherent x-ray diffractive imaging in order to translate physical observables into model inputs in support of thrusts i and ii.

Conclusion

The need to predict and control materials in extremes spans the full range of DOE missions from weapons performance to energy security. Further, successful nuclear weapons program approaches to certification of materials performance (and the associated quantification of performance margins and uncertainty) have not e.g., been translated to nuclear energy materials certification challenges. Through this project, we will develop theoretical models and identify physical observables that can be measured by experiment to test these models that when taken together will accelerate the rate at which we can design and discover new materials to meet these certification challenges.

Fighting Carbon with Carbon: All-Carbon Nanomaterial Photovoltaics

Stephen K. Doorn
20130026DR

Introduction

Our pioneering development of graphene oxide and compositionally-defined bundles of carbon nanotubes as new optical materials has revealed new photophysical behaviors that indicate these carbon nanomaterials possess many properties of ideal light harvesters for thin-film photovoltaic applications. These benefits include more efficient light absorption than molecular chromophores, tunability of optical and electrochemical properties to match the solar emission spectrum and allow optimization of interfacial charge flow between other device materials, and extremely efficient photogeneration of long-lived free charges available for collection as electrical power. Our findings create a compelling opportunity to create new photovoltaic device types. These will be designed to specifically exploit the potential our newly-introduced materials hold for overcoming current bottlenecks in solar-energy harvesting performance imposed by the limitations of currently used light-harvesting chromophores. By project end we will harness these properties within functioning phtovoltaic device prototypes based on two complementary platforms suitable for follow-on development. In establishing these prototype platforms, our primary goals will be to:

1. Demonstrate for the first time the benefits of carbon nanomaterials (CNM) as active light harvesting components.
2. Demonstrate that CNM can be used to overcome key performance limitations of solar cells.
3. Demonstrate the potential of integrated CNM-based photovoltaic devices.

To meet these goals we will: i) Establish the fundamental photophysical and electrochemical behaviors of CNM chromophores and the means to control and tune the associated energy and charge flows. ii) Establish the principles for CNM materials integration into functioning photovoltaic devices. iii) Pursue these objectives within the context of the interfacial interactions dictated by two primary device architectures we view as the most promising for realizing all-CNM photovoltaics. These include a layered thin-film platform and a dye-sensitized solar cell configuration, where our CNM become the active dye.

Benefit to National Security Missions

Our effort introduces a promising new approach that will enhance LANL's portfolio in renewable energy research, which must continue to grow and strengthen to meet the critical energy challenges facing the nation. Success will contribute to reducing climate disruption threats while ensuring our nation's future energy security and thus national security. Our approach does not rely on rare, isolated, or politically inaccessible resources. We thus will be pioneering new earth-abundant materials to solve energy problems, while developing/controlling new multifunctional semiconductor and photonics materials. Beyond energy-harvesting applications, advances from our effort will also impact threat reduction needs through detector and sensors development and photonics applications, all of which rely on similar photophysical processes as will be studied here.

Our discovery position in the emerging areas of graphene oxide and defined-composition nanotube bundles as optical nanomaterials also places us at the forefront of such areas as probing their photophysical properties, understanding and controlling energy and charge flow in these systems, and determining how these dynamical processes are defined by the interfacial interactions of multiple materials. With relevant behaviors and interactions arising and playing out across nm to um length scales and dynamical processes occurring from fs to ms timescales, these questions go to the heart of understanding functional behaviors that are defined at the mesoscale. Thus, our studies also address DOE Office of Science needs for improved basic understanding of

materials and fundamental chemistry for materials control.

Progress

Carbon Nanotube (CNT) PV Architecture

Several devices have been prepared from CNT enriched in (6,5) structures generated via density gradient purification. While the sample is nearly pure (6,5), sufficient metal contamination in the material has been found to effectively short-out our PV devices through production of metallic networked percolation pathways. The devices, however, have proved valuable in indicating film thickness requirements and demonstrating the need for enhanced purification. New separations approaches have been hit hard and include gel chromatography, which shows good metals removal, but yields short tubes. Polymer-based separations also show good metal removal and selectivity, but give low yields and tricky processing. One highlight is the polymer MehPPV, which shows interesting potential for light collection sensitization at wavelengths not absorbed by our CNTs. Our newest approach is based on two-phase extraction and is already giving pure (6,5) and significant metal reduction in one separation step (manuscript in preparation). Samples of enriched material from each approach are now being incorporated into second generation devices.

Fundamental Exciton Behavior

Understanding transport of optical excitations and free charges is essential for optimizing PV devices. We have revealed for the first time via our ability to directly image exciton diffusion that CNT exciton transport proceeds via an incoherent hopping mechanism (published in Nano Letters). We have also revealed the detailed nature of environmental dipole interactions that lead to exciton dissociation (published in J. Am. Chem. Soc.). Related theory is showing an enhanced free carrier generation in the presence of low-level dopants (published in J. Phys. Chem. Lett.) and points towards an approach to enhance free-carrier generation from photo-excitations. Direct imaging techniques are also revealing novel biexciton behaviors. We are also probing optical states in single chirality bundles. New Raman results show evidence for long-lived excited states oriented perpendicular to typical CNT excitations that can enhance charge transport to collection interfaces. LANL-unique nonadiabatic excited state dynamics modeling is revealing unique localization of optical excitations in CNT analogues.

Graphene Oxide (GO)

We are probing the nature of GO optical states and how they respond to changes in their chemical environment using photoluminescence (PL) imaging of single flakes. Follow-on studies are targeting site-selective spectroscopy to correlate PL spectra directly to chemical species. An especially exciting result is finding GO photoconductivity (PC) in devices: a prerequisite to PV function. Correlated spatial mapping of photoconductivity surprisingly reveals response is located away from collection electrodes, showing an internal potential is developed. Paired with electrostatic force microscopy (EFM) measurements, we correlate PC response with topological features and see that topological defects create built-in potentials that drive photogenerated charge carriers to collection electrodes (manuscript in preparation). The results provide a strategy for device architectures based on interleaved GO and reduced-GO regions we can generate via laser heating-based lithographic patterning. GO thermodynamics relevant to activity of functional groups and potential O-migration are being explored theoretically. The results also tie to oxygen doping of CNTs as model systems for charge trapping in devices.

Dye Sensitized Solar Cell (DSSC) Architectures

A primary challenge in CNM-based DSSC devices arises from the optimized TiO2 films having pore sizes of ~20 nm, constraining how we integrate CNMs for optimizing interactions for charge transfer reactions. We focus on three routes. Co-sintering of long CNTs is being enabled by optimizing CNT surface chemistry. Acid-based cutting is being used to reduce CNT lengths to the same scale as the TiO2 pores and is looking to be a very promising approach. Cutting introduces carboxylate groups, ideal for binding to TiO2. Furthermore, low-level surface passification is found to turn on CNT PL, demonstrating their optical properties are retained. We also are pursuing nanoscale graphene flakes as light-harvesting chromophores. Their synthesis is a complex multi-step process. We have just finished synthesis of all precursors. Finally, we are pursuing a chemical vapor deposition route for synthesis as well.

New Capability Development

All optical components are assembled for our super-resolution photocurrent imaging apparatus, which can now be used for standard correlated photocurrent imaging. Testing of the anti-phase beam shaping to give 50 nm resolution is proceeding. Our transient absorbance system is now assembled. We have installed a new state-of-the-art Raman triple monochromator to further explore CNT bundle interactions.

Future Work

Our continuing goals are organized by three interconnected areas: Materials Development and Characterization, Development of Fabrication/Integration Procedures, and Studies of Exciton and Charge Transfer/Transport.
In the area of Materials Development and Characteriza-

tion, we will target generation of nanotube and graphene oxide materials and films with specific characteristics. For graphene oxide the effort will include development of methods for isolation of flakes with defined dimensions using density gradient approaches and defining film morphologies from such isolated materials. In parallel, theoretical and experimental efforts will be aimed at understanding and tuning graphene oxide optical and electrochemical behavior. For nanotubes, effort will be directed at improved separations for limiting metallic content in semiconducting films, and defining morphology and makeup of nanotube-based films. In support of development of dye sensitized cell architectures, we will continue development of solid state electrolytes, mapping of relevant nanotube band structures and probing charge transfer reactions at TiO2 interfaces.

For Development of Fabrication/Integration Procedures our separations methods will provide metal-free nanotube material for devices. For our film-based devices, we will then focus on defining film morphologies, optimizing initial band offsets, controlling materials content, and devising bulk heterojunction geometries for optimized materials interactions. For dye sensitized cells, we will be optimizing strategies for chemical coupling of nanotubes, graphene oxide, and nanographene flakes to nanostructured TiO2. For Exciton/Charge Transfer and Transport Studies, while test devices are progressing, we will in parallel focus on putting in place the proposed capabilities for capacitive photo-current imaging spectroscopies paired with super-resolution techniques. Once in place we will then proceed with characterization of charge transport behavior in the first-generation test devices. Paired with theory, we will use the results to help define directions for optimization towards second-generation devices.

Conclusion

By project's end we expect to i) establish the fundamental photophysical behaviors of our new optical nanomaterials for use as active light-harvesting materials and how to tune these behaviors, ii) establish the principles for carbon nanomaterials integration into functioning photovoltaic devices, and iii) establish the most promising device architectures for follow-on development. The result will be a promising new approach to photovoltaic energy harvesting that overcomes many current limitations. The effort will also create new understanding of the optical behaviors of our new class of materials to advance other applications while also developing powerful new techniques for nanomaterials characterization.

Publications

Arnold, M. S., J. L. Blackburn, J. J. Crochet, S. K. Doorn, J. G. Duque, A. Mohite, and H. Telg. Recent developments in the photophysics of single-walled carbon nanotubes for their use as active and passive material elements in thin film photovoltaics. 2013. Physical Chemistry Chemical Physics. 15: 14896.

Crochet, J. J., J. G. Duque, J. H. Werner, B. Lounis, L. Cognet, and S. K. Doorn. Disorder limited exciton transport in colloidal single-wall carbon nanotubes. 2012. Nano Letters. 12: 5091.

Duque, J. G., L. Oudjedi, J. J. Crochet, S. Tretiak, B. Lounis, S. K. Doorn, and L. Cognet. Mechanism of electrolyte-induced brightening in single-wall carbon nanotubes. 2013. Journal of the American Chemical Society. 135: 3379.

Sau, J. D., J. J. Crochet, S. K. Doorn, and M. L. Cohen. Multiparticle exciton ionization in shallow doped carbon nanotubes. 2013. Physical Chemistry Letters. 4: 982.

Solenov, D., C. Junkermeier, R. L. Reinecke, and K. A. Velizhanin. Tunable adsorbate-adsorbate interactions on graphene. 2013. Physical Review Letters. 111: 115502.

Design Principles for Materials with Magnetic Functionality

Joe D. Thompson
20130052DR

Introduction

Advanced materials have been and will continue to be essential for the country to remain globally competitive and to ensure our energy and defense security. Magnetism underpins many energy-efficient technologies, notably wind turbines and 'green' automobiles, but magnetism is an intrinsically complex and delicate collective-electron function that is reflected in the multiple electronic properties of materials that must be satisfied simultaneously to produce useful function. Magnets presently used in these technologies rely on nationally critical rare and expensive elements, and despite decades of making-and-measuring to find new magnetic materials that are free of those critical elements, this approach has not been successful. Progress requires a strategy based on scientific principles that ultimately will allow the design of suitable replacement magnetic materials. With remarkable recent advances in quantum chemistry and in modeling the consequences of complex electronic properties as well as our ability to test predictions with new experimental techniques, the discovery, understanding and application of principles for control of strong magnetic properties in metals rich in earth-abundant elements is within grasp. In a closed loop of state-of-the-art computation, theoretical modeling, materials synthesis, and in-depth measurements, we will determine and test scientific principles that will allow the designed control of magnetic properties in advanced materials suitable for application in energy-efficient technologies.

Benefit to National Security Missions

The computationally motivated, experimentally validated design of new materials with specified functionality has emerged as a major scientific challenge for materials physics and chemistry, a challenge that must be met to satisfy ever increasing demands for advanced materials that underpin the Nation's energy security and competitiveness. Strongly magnetic materials are key to numerous energy-efficient technologies, but their useful function presently relies on rare and expensive elements. We will discover scientific principles that will allow designed control of materials that are strongly magnetic and free of critical rare elements. The same techniques for rational materials design may eventually benefit the weapons program.

Progress

In a closed loop of computation, theoretical modeling, materials synthesis, and experimental validation, we have studied in detail a family of rare-earth-free materials with compositions T23-xT'xZ6, where T is a 3d-element (Cr, Mn, Fe, Co and Ni), T' is a heavier 4d- or 5d-element and Z=B, C, or Al. Density functional electronic structure and ordered magnetic moment have been calculated for 35 new variants of this family, and based on these calculations, the most promising materials have been made and their magnetic properties have been measured. Trends in magnetic properties predicted from the calculations are supported qualitatively, and often quantitatively, by experiments. Though many of these materials have large saturated magnetic moments and high ferromagnetic ordering temperatures, which are desirable characteristics, none of these materials has a large coercive field. As we have shown from theoretical modeling, the relatively strong hybridization between T and T' electrons and the absence of strong crystalline electric fields in the cubic structure of these materials cause the spin-orbit coupling, and hence coercive magnetic field, to be small, which renders the magnetic figure of merit of this family of materials to be insufficient for technological applications. This family will not be pursued further, but other materials hold more promise as we have found from the over 100 density functional calculations on approximately 50 different materials. Motivated by these calculations, we have synthesized 65 samples and measured the magnetic properties of the 34 most promising materials. This study is on-going.

In a parallel effort, we have focused on understanding the origin of a modestly large coercive magnetic field in YCo5, which has been known for many years; however, the mechanism responsible for its coercive field is not known. From theoretical modeling and density functional calculations on YCo5, we have three important predictions: (1) hexagonal or tetragonal crystal symmetry favors a large orbital magnetic moment and hence coercive field; (2) the electronic configuration of Co also lends itself to a substantial orbital moment; and, (3) a Coulomb interaction of 2eV or greater is important for inducing a large orbital moment on the Co electrons. Preliminary photoemission experiments support the third prediction and planned x-ray circular dicroism experiments will test the second one. On the basis of these guiding principles, we have begun a study of two new families of materials that form in the Mo5SiB2 and Ti3Co5B2 structure types as well as used total energy and magnetic anisotropy energy calculations to predict that a new material ScCo5 might be very promising. Experiments are underway to test this prediction. In addition, an entirely new approach has begun that uses the local density approximation plus dynamical mean field theory (LDA+DMFT) to calculate realistic Coulomb, crystal-field, and spin-orbit interactions on multiple d-electron orbitals. Such a calculation on multiple orbitals has never been attempted but will be a powerful predictive tool of magnetic functionality.

Besides scientific progress, this project also has pursued programmatic funding opportunities. In response to the DOE call for a Critical Materials Hub proposal, we participated actively in the Laboratory's response to that call. Though the proposal was among the few finalists, it was not selected for funding. In coordination with Laboratory ARPA-E program managers, the concept of this project was discussed with two APRA-E program offices, the Rare-Earth Alternatives in Critical Technologies and the Vehicle Technology office. Both considered our concept attractive, but both also judged that it was premature to invest in it at this time. Finally, one team member has been requested to serve as a guest editor of the special issue of the Journal of Physics: Condensed Matter that will be devoted to rare-earth replacement magnets. Another team member will contribute an invited review to this special issue that summarizes our scientific approach to developing design principles for the predictive control of magnetic functionality and the success that this approach has realized.

Future Work

We will apply our state-of-the-art capabilities of electronic structure calculations, many-electron modeling, materials synthesis and detailed experimental measurements to develop a predictive understanding of crystal-chemical conditions that favor strong ferromagnetic properties in new and known rare-earth-free materials that are identified through calculations and simulations. Specifically, we will explore theoretically and experimentally families of materials that form in hexagonal or tetragonal crystal structures and that are rich in magnetic Co and Fe. We will predict their magnetic properties and validate those predictions by combinations of magnetization, magnetic force microscopy, magnetic circular dicrosim and photoemission experiments. In parallel, we will develop new computational algorithms that more accurately predict the intrinsic spin-orbit coupling, and hence magnetic anisotropy energy, that must be optimized in materials to have a sufficiently large magnetic figure of merit to be technologically useful. Results of these calculations will be tested experimentally. By iteratively closing compute, make, model and measure loops, we expect to refine the initial set of design principles developed in the first year of this project for predicting strongly ferromagnetic properties of material devoid of rare-earth elements.

Conclusion

State-of-the-art calculations of electronic structure and magnetic anisotropy, coupled with the solution of theoretical models of complex electronic interactions, will be tested experimentally to establish scientific principles that allow the designed control of the crystal structure and chemical make-up of new materials with magnetic properties favorable for strong magnetism in metallic compounds that do not contain nationally critical elements.

Publications

Ronning, F., and J. L. Sarrao. Material's prediction scores a hit. Physics Viewpoint.

Non-Precious Metal Electrocatalysts for Clean Energy

Piotr Zelenay
20130065DR

Introduction

In order to fully realize the clean energy conversion and storage technologies (fuel cells, metal-air batteries, water electrolyzers for hydrogen generation), highly active, durable, and inexpensive non-precious metal electrocatalysts are needed for oxygen reduction reaction (ORR) and oxygen evolution reaction (OER). In this project, we respond to that grand challenge in electrocatalysis by combining experimental and multi-scale modeling approaches for the purpose of (1) elucidating the nature of the ORR and OER active catalytic sites on the surface of non-precious metal catalysts, (2) probing the interplay between meso- and nanoscale controls on electrocatalyst performance, and (3) designing and synthesizing catalysts with the structure optimized for maximum oxygen reduction/evolution activity and required performance stability.

Active site characterization from density functional theory and model system experiments will provide insights into ORR & OER reaction mechanisms and the molecular nature of the active site. Mesoscale/multiphysics studies using lattice Boltzmann method (LBM) will guide the synthesis towards materials with appropriate physicochemical properties. Ultimately, information generated from the theory and characterization of model systems will be used to tune precursors for the design and synthesis of ultra-high performance catalysts. Advanced characterization using nitric oxide (NO) probes, iron-specific nuclear resonance vibrational spectroscopy (NRVS), and other methods will be combined with theory to further tune catalyst performance. Stabilization and promotion of optimal active sites will be investigated by the employment of carbon and non-carbon (i.e. oxide) template structures.

Research in this project will advance the fundamentals of oxygen electrocatalysis and develop novel materials and concepts for energy applications. The proposed effort directly tackles two top research priorities in the LDRD Energy & Earth Systems Challenge, including the need to utilize earth-abundant elements in place of precious metals. Ultimately, this proposed work will also position LANL to target major new initiatives in clean-energy catalysis in the future.

Benefit to National Security Missions

This research directly supports the Los Alamos LDRD Energy & Earth Systems Grand Challenge "concepts and materials for clean energy". In particular, it tackles the top research priorities of "new materials, for energy applications, containing earth-abundant elements that mimic properties of rare and expensive materials" and "energy generation and efficiency". This research will enable sustainable and low-cost energy devices with enhanced energy efficiency/capacities, which will position LANL to target new initiatives in meso-scale catalysis, scheduled to be announced by DOE-BES in the near future.

In particular, this research is A-relevant to the DOE-EERE mission of developing alternative energy sources, especially for transportation and stationary applications (fuel cells, hydrogen generation). By being directly relevant to renewable energy this research earns the highest mark in the energy security category. Finally, this effort focuses on the fundamental understanding of materials for two possibly most challenging reactions in electrochemistry, oxygen reduction and evolution, using a combination of modeling, experimentation with model systems, and catalyst development. This makes this project very highly relevant to both basic understanding of materials and fundamental chemistry.

Progress

Model Systems

To achieve the goal of rational synthesis of non-precious metal catalyst (NPMC) systems for oxygen reduction reaction (ORR), we have focused our efforts on the synthe-

sis of model systems based on graphene (G) and graphene oxide (GO). We know that N-doped GO shows higher ORR activity compared to pure GO. Therefore, we have developed processes to make nitrogen-doped graphene oxide (nGO), characterized by a variety of techniques including XPS, thermo gravimetric analysis, electron microscopy and electrochemical techniques. The data obtained has been used to guide subsequent syntheses of the next-generation nGOs. Our results indicate that the total amount of nitrogen, typically 5-12 at%, has minimal effect on ORR activity. However, the location of the nitrogen in the graphene lattice seems to have more influence on catalytic activity, which is consistent with the theory. We also know that reduction of nGO starts above 200°C, but higher synthesis temperatures (850°C) are required to improve its catalytic properties towards ORR. Electron microscopy collected shows that as the samples are heated the graphene sheets become more isolated, i.e. exfoliated, indicating that surface area increases with temperature, which could explain some the catalytic activity improvements.

Theory

Static and dynamic density functional theory calculations have been used to investigate the properties of the active site(s) in model systems. ORR pathways have been determined for a series of transition metals and transition metal clusters incorporated into the carbon-nitrogen framework. From this analysis we have been developing generalized scaling laws so that a descriptor-based framework can be rapidly used to optimize catalyst active site design. Ab initio molecular dynamics simulations have been performed to investigate the role of solvent in modifying the reaction pathway and/or the identity of the active site, in particular probing the stability of these sites in aqueous media. Kinetic models based on the detailed molecular-level reaction pathways are being developed to support the lattice-Boltzman mesoscale model (LBM).

We have developed a new lattice Boltzmann framework for pore-scale investigation of multicomponent multiphase reactive transport that can handle large density ratios between liquid and gas phases. It can predict vapor to liquid condensation, as well as oxygen and water vapor transfer and heterogeneous surface chemical reactions. The activation energy obtained from the DFT simulations will be used to calculate the reaction rate constant that will in turn be used in the LBM simulation, leading to a true multiscale model.

Catalyst Synthesis

We pursue three approaches to the development of ORR catalysts with enhanced performance. The first two approaches are based on high-temperature routes, involving (i) graphene and (ii) carbon meso- and nanotubes. We have established the synthesis-structure-activity correlations by varying the synthesis conditions: support, nitrogen precursor, heating temperature, and transition metal and its content. We have experimentally verified that by controlling the level and type of nitrogen functionalities we can substantially improve the ORR activity and durability of nGO-rich structures. This generates much needed input for the model system design and modeling efforts (above) in terms of the impact doped nitrogen functionalities have on the catalyst ORR activity. We have also studied electrode structures of the graphene and tube-based catalysts to understand the relationship between the 3D mesoscale catalyst structure, mass-transport effects, and active-site kinetics. This data is used as an input for theoretical effort based on DFT calculations and LBM.

The high-temperature route provides relatively little control over the exact structure and population of the ORR active sites. Therefore, in our third approach, we have focused on designing molecules as active-site mimics, characterizing these sites spectroscopically and ultimately gaining more control over the active site preparation. We have been building molecular mimics of the active sites by coordinating extended aromatic ligands with N-donor atoms to Fe. Initially, we attempted to use relatively simple ligands, such as phenanthroline, with weak-field co-ligands incorporated to encourage the complex to be high-spin and to confer square-planar geometry. This has been extended further to slightly larger ligands which similar properties, such as isoeilatin and dibenzoeilatin. While it is clear that these ligands complex Fe, full characterization has been hampered by low solubility and mixed stoichiometry of the reaction products. We are currently trying to incorporate additional functional groups to increase the solubility and thereby improve the characterization.

Future Work

Research in this project will be performed in three main tasks, with the following goals in the first year:

Molecular Level Insights into the Nature of Non-Precious Metal Active ORR and OER Sites

We will establish a capability in the synthesis of model electrocatalyst systems based on nitrogen-doped graphene and graphene oxide (GO) functionalized with non-precious metals and synthesize first samples of both types. Those samples will be characterized using spectroscopic and imaging tools to identify the most active reaction sites.
In the part of effort devoted to the modeling of graphene systems we will start using density functional theory (DFT) calculations to assign experimental spectra and interrogate active-site geometry and electronic structure. Based

on the understanding obtained from DFT, modifications will be made to the graphene/GO systems to test particular aspects of the theory. Together, this will provide a preliminary scientific model critical for optimization of non-precious metal ORR, OER, and bifunctional ORR/OER electrocatalysts.

Theory and Optimization of the Mesoscale Catalyst Structure

In this task, fundamental kinetic quantities for active sites, based on DFT, will be reconciled with mass-transport phenomena via the mesoscale lattice Boltzmann method (LBM). The initial model will be developed and validated using experimental techniques developed at LANL. One class of measurements will provide model inputs, and includes porosimetry (hydrophobic/hydrophilic pores), TEM (particle size distribution), X-ray tomography (gas diffusion layer mesostructure). Another class will be used to validate outputs, including electrochemical impedance spectroscopy, helium/oxygen diffusivity, and neutron radiography.

Rational Design and Synthesis of Next-Generation NPMCs

Based on work derived from the initial studies of the model graphene electrocatalysts, as well as past results, the design, synthesis and optimization of new non-precious metal electrocatalysts will begin. Carbon and non-carbon templates (i.e. oxides) will be investigated for the stabilization and promotion of active sites.

Conclusion

The primary outcome of this project will be a fundamental understanding of non-precious metal ORR and OER catalysis in electrochemical energy systems. It will include reaction mechanisms, active-site structures, and synthesis-structure-reactivity correlations. In particular, integration of modeling of the active site with mesoscale theory will allow coupling of intrinsic site reactivity with mesostructure-sensitive kinetics, providing “real-world” activity directly comparable to the experimental measurements. First-principles calculations will assist in interpreting spectroscopic and electrochemical signatures emerging from characterization studies. The fundamental understanding of electrocatalysis will be used to design, synthesize, and demonstrate next-generation Non Precious Metal Catalysts with high performance and durability.

Publications

Chen, L., Q. Kang, Y. L. He, W. Tao, and P. Zelenay. Pore-scale simulation of sater vapor generation, condensation, and transport in the cathode of a proton exchange membrane fuel cell. To appear in ECS Transactions.

Chen, L., Q. Kang, Y. L. He, and W. Tao. A critical review of the pseudopotential multiphase lattice Boltzmann model: methods and applications. International Journal of Heat and Mass Transfer.

Chen, L., Y. L. He, Q. Kang, and W. Tao. Coupled numerical approach combining finite volume and lattice Boltzmann methods for multi-scale multi-physicochemical processes. 2013. Journal of Computational Physics. 255: 83.

Chung, H. T., J. H. Won, and P. Zelenay. Active and stable carbon nanotube/nanoparticle composite electrocatalyst for oxygen reduction. 2013. NATURE COMMUNICATIONS. 4: -.

Elbaz, L., G. Wu, and P. Zelenay. Heat-treated non-precious-metal-based catalysts for oxygen reduction. 2013. In Electrocatalysis in fuel cells: A non- and low-platinum approach. Edited by Shao, M.. , p. 231. London: Springer-Verlag.

Holby, E. F., G. Wu, P. Zelenay, and C. D. Taylor. Modeling non-precious metal matalyst mtructures and mheir relationship to ORR activity. To appear in ECS Transactions.

Hussey, D. S., D. L. Jacobson, D. Liu, B. Khaykovich, M. V. Gubarev, D. Spernjak, G. Wu, J. Fairweather, R. Mukundan, R. Lujan, P. Zelenay, and R. L. Borup. Neutron imaging of water transport in polymer-electrolyte membranes and membrane-electrode assemblies. To appear in ECS Transactions.

Wu, G., and P. Zelenay. Nanostructured Nonprecious Metal Catalysts for Oxygen Reduction Reaction. 2013. ACCOUNTS OF CHEMICAL RESEARCH. 46 (8): 1878.

Yamaguchi, H., J. Granstrom, W. Nie, H. Sojoudi, T. Fujita, D. Voiry, M. Chen, G. Gupta, A. D. Mohite, S. Graham, and M. Chhowalla. Reduced graphene oxide thin films as ultrabarriers for organic electronics. 2013. Advanced Energy Materials. : DOI: 10.1002/aenm.201300986.

Phase Stability of Multi-Component Nanocomposites under Irradiation

Blas P. Uberuaga
20130118DR

Introduction

We propose to design multi-component nano-composite materials that resist radiation-induced solute redistribution (RISR) and thus maintain stable nano-phases at extremes of high dose irradiation at elevated temperatures. The next generation of nuclear energy systems will not be possible without the development of such new materials. Further, the accident at the nuclear plant at Fukushima demonstrates the need for advanced clad materials that not only can sustain high burn-up but are also resistant to other phenomena such as corrosion.

The design of materials that are essentially "immune to radiation", as called for by DOE, is one of the grand challenges in the materials science discipline. This is because energetic radiation damages a material by a variety of very different mechanisms, such as void swelling, embrittlement, irradiation creep, and phase instabilities from radiation induced solute redistribution (RISR). Typically, the solution for one problem either has no effect on or exacerbates the other damage mechanisms. For example, using interfaces as sinks for vacancies and interstitials can reduce void swelling but the same interfaces that mitigate void swelling can increase RISR.

RISR causes phase instabilities that lead to catastrophic failure through embrittlement, fracture and corrosion. We propose an innovative solution to the chronic problem of radiation-induced phase instability: nanocomposite materials design via interfaces that minimize defect fluxes, which is the origin of RISR. We hypothesize several factors we can use to control defect fluxes and suppress RISR. We propose a materials co-design R&D approach where experiments and multi-scale modeling are closely integrated to test our hypotheses, develop a fundamental understanding of RISR to interfaces, and advance design principles for next-generation materials for nuclear energy applications that maintain chemical composition profiles that are critical for many materials properties in extreme environments.

Benefit to National Security Missions

Our aim is to develop a basic understanding of a primary damage failure mode in materials under irradiation: radiation-induced solute redistribution. This leads to phase separation, dissolution of important secondary phases, and changes in chemical composition that accelerate materials failure in nuclear energy systems. By developing a basic understanding of these materials, we will formulate design principles that will allow us to propose future nuclear energy materials that resist such damage and failure.

That this is a fundamental materials approach, this is clearly relevant to the DOE Office of Science, particularly Basic Energy Sciences (BES). If successful, the types of materials we would propose would also be of interest to Fusion Energy Sciences (FES) with in the Office of Science, as well as the Office of Nuclear Energy, which is more focused on fission energy systems.

This work would enhance energy security by enabling future generation nuclear energy systems that are more robust and thus more politically and socially acceptable as replacements for fossil energy sources. Further, by developing more radiation tolerant claddings, nuclear fuel could be burned to greater amounts, reducing the quantity of spent fuel in storage and the consequent load on any future nuclear waste repository.
Fuel cycle research of this sort builds capability for nuclear nonproliferation in general.

Progress

We have begun work on two main efforts.
The first involves model systems of Ni-Al alloys, to mimic Inconel materials. This involves two primary tasks. The first is atomistic scale modeling, which consists of accelerated molecular dynamics (AMD) simulations of diffusion in disordered alloys, atomistic simulations of Al segregation to Ni grain boundaries, an assessment

of potentials for the Ni-Al phase diagram, and atomistic modeling of the role of alloying elements on the stability of Ni3Al precipitates within Ni. This is complemented by experimental studies which involve the growth, characterization, and implantation studies of Ni/Ni3Al multilayers. The experimental effort just began as the experimental postdoc has just joined LANL. In the AMD simulations, we find that defects interact only weakly with Al atoms, and that diffusion must occur via random encounters rather than the formation of defect complexes. The atomistic simulations of segregation show that Al only weakly segregates to model boundaries, but once it does, begins repelling other Al, forming somewhat complex ordered structures at the boundary that can be validated with transmission electron microscopy (TEM).

The second effort involves model metal/oxide systems to mimic nanostructured ferritic alloys (NFAs). Again, there are two primary tasks. The first involves multiscale modeling, using density functional theory (DFT) to examine the structure and chemistry of the interface between Fe and TiO2 and Fe and Y2O3, the two model systems we have focused on initially. The output from these calculations will be used to parameterize a phase field model of alloy redistribution under irradiation. In conjunction, we are performing experimental studies on multilayer materials such as Fe/Y2O3/Fe/TiO2/Fe/MgO, in which the Fe layers are doped with Cr, to understand how Cr segregates to these interfaces. We will soon irradiated these materials in the Ion Beam Materials Laboratory (IBML) at LANL and characterize how the Cr redistributes under irradiation. In conjunction with these efforts, we have performed neutron reflectometry of Fe/TiO2 and Fe/Y2O3 interfaces and will be analyzing that data this summer. Regarding the multilayer materials, we have characterized the atomic structure of the Fe(Cr)/MgO, Fe(Cr)/Y2O3, and Fe(Cr)/TiO2 interfaces. We are currently determining the local oxygen content at those interfaces using analytical microscopy techniques. The DFT calculations have pointed to several high-level governing rules that determine the propensity of alloying element segregation to metal/oxide interfaces, based on Hume-Rothery Rules and Ellingham Diagrams. This provides a quick predictive estimate of which elements will segregate to a given interface.

In parallel, we are characterizing real engineering materials, particularly 14YWT, to compare with the results on our model materials described above.

There are three side projects related to these main tasks. First, we are developed spatially parallel accelerated molecular dynamics methods to extend the system size that these methods can be applied to, which should prove useful for studying complex alloys under irradiation. We are also in the initial stages of planning atom probe tomography experiments, with the University of Michigan, to complement our TEM characterization efforts at LANL. Emmanuelle Marquis (UMich) will visit in July to coordinate these activities. Finally, we are also exploring the use of mechanical alloying coupled with levitation melting to synthesize three-dimensional nanocomposites of the same composition as our multilayer morphologies.

In addition, to perform some of the irradiations, we had to complete modifications of the Tandem accelerator in the IBML in order to perform higher energy implantations/irradiations at higher temperatures that are more relevant for nuclear energy applications. We also installed a pyrometer to measure the temperature of the sample during the implantations/irradiations.

We have put in place two subcontracts (MIT and UMich) and hired multiple new postdocs to perform the work on this project. We are also organizing a course on the use of Idaho National Laboratory's MARMOT phase field simulation code which will provide the necessary framework to perform the phase field simulations.

Future Work

During the next fiscal year, we will focus on two primary tasks.

The first is developing a multiscale model that incorporates atomistic information into a mesoscale description of the material to understand how solute redistribution changes as a function of microstructure during irradiation. This will be done for two metallic model systems, Fe and Ni alloys, which have real engineering counterparts in nuclear energy systems. A critical component of this modeling effort will be to determine to what extent a simplified description of the chemical interactions within the alloy system can be used to develop an accurate kinetic model of the solutes within the defect fields produced during irradiation, as this will be key for the next step: the development of such a model for metal/oxide composites. The modeling development will be focused on four areas: 1) defect thermodynamics in and around boundaries in the different model materials, 2) the coupling of solutes with those defects, 3) the redistribution of solutes near a given grain boundary, and 4) incorporation the atomistic information into a mesoscale model that determines how the solutes redistribute in a complex microstructure.

The second task will be to perform experiments on the exact same model systems as are being examined theoretically. We will synthesize polycrystalline materials, both

Fe and Ni, with various amounts of solute elements. We will characterize the materials pre and post irradiation to understand how the elements have redistributed. This will include SIMS, XRD, and TEM, the later particularly focused on determining how the segregation depends on boundary type. These results will then be compared to the modeling to determine to what extent the modeling has captured the important phenomena and develop design principles on what features of the microstructure, as detailed by the hypotheses in our proposal, control radiation-induced solute redistribution.

Conclusion

The goal of this project is to understand and control the atomic scale processes that lead to redistribution of elements in complex alloys during irradiation. The key results of this project will be (i) development of a multi-length and multi-time scale model to predict solute/elemental redistribution in a given alloy as a function of interface properties and spacing, (ii) tests of the hypotheses correlating the interface properties to RISR in nanocomposites, and (iii) development of figures-of-merit from the integrated results of all the hypotheses.

Radioparagenesis: Robust Nuclear Waste Form Design and Novel Materials Discovery

Christopher R. Stanek
20110009DR

Abstract

Of the outstanding issues currently preventing expansion of nuclear energy, nuclear waste disposal possesses the highest potential to benefit from technological advances. By verifying the concept of radioparagenesis, we will introduce a new way of thinking about nuclear waste disposal. Specifically, not only can robust waste forms be designed to withstand radiation damage and chemical evolution, but also computational tools predicting the performance of waste in a repository setting can be made significantly more reliable. The goal of this project is to validate and verify the new concept of "radioparagenesis." Radioparagenesis was recently discovered by our team, and is the formation of unconventional crystal structures (e.g. rocksalt BaCl) for compounds formed during the chemical transmutation that occurs during radioactive decay. The technical approach of this project consists of experimental and theoretical components. The experimental component relies on the Isotope Production Facility (IPF) at LANL to synthesize accelerated fission product analogues that decay quickly enough (as opposed to actual fission products of interest to the nuclear energy community, whose decay dictates hundred year experiments) for observation. We employ complementary first principles calculations to predict the result of the accelerated experiment. Verification of this phenomenon will allow us to drastically improve the predictability of nuclear waste form performance as well as the backward design robust waste forms. In addition to providing a potential innovative solution to the nuclear waste problem, radioparagenetic phases may also exhibit interesting materials properties for non-nuclear applications.

Background and Research Objectives

In order to develop a predictive capability to design radiation tolerant and chemically robust nuclear waste forms (and in the process, remove a significant obstacle limiting the expansion of nuclear energy), we must first solve a fundament materials science question: What is the impact of daughter product formation on the stability of solids comprised of radioactive isotopes? In order to answer this question, we require a multidisciplinary approach integrating first principles modeling with the synthesis and characterization of small and highly radioactive samples. Once we understand the effects of radioparagenesis we can use the insight to evaluate and design waste forms. We have pursued three tasks that correspond to each of the following goals: (1) develop a new branch of physics and chemistry associated with our recent discovery of radioparagenesis, (2) utilize the insights gained to design robust nuclear waste forms, and (3) discover and characterize heretofore unobserved materials with potentially interesting properties. We have designed these goals to guide and focus the exploration that occurs after a significant discovery – in this case the discovery of radioparagenesis, which we define as: the formation of compounds, often unconventional (e.g. BaCl in the rocksalt structure), due to the chemical transmutation that occurs during radioactive decay.

For over thirty years, crystalline ceramic nuclear waste forms have been proposed for the encapsulation of specific fission products. Faced with the necessity to predict the long-term behavior of these waste forms, researchers have focused on candidate compositions that exhibit: (1) geological analogues, thus suggesting long-term stability, e.g. Synroc, (2) resistance to radiation damage (either using accelerated isotopes or by ion irradiation) and (3) leaching resistance. However, these studies have not yet adequately accounted for the chemical and physical changes that will occur in the waste form during fission product transmutation, i.e. the conversion of one element or isotope into another, in this case during radioactive decay. Indeed, for many fission products, waste form performance may be dominated by transmutation effects. The selection criteria for a candidate waste form discussed above may address the performance of the waste form very early in its life, but lack the predictive power required to evaluate the performance of the

waste form far in to the future.

For as long as ceramic waste forms have been considered, researchers have recognized what Vance, nearly 30 years ago, called the "transmutation problem," i.e. the deleterious effects on waste form performance due to the formation of chemically disparate daughter products. In the same year as the Vance work, which outlined potential deleterious effects due to transmutation (for example due to the different valence and ionic radius of parent and daughter isotopes), Gray published in Nature the results of an experimental attempt to determine the role of daughter product formation on candidate waste form stability. Since consideration of actual fission products would require experiments lasting one hundred years or more, Gray identified two approaches to accelerate the phenomenon using either (1) separation of short-lived isotopes, or (2) neutron irradiation of non-radioactive material to activate short-lived isotopes. Gray pursued the second option - claiming that the first was "prohibitively expensive" - and found no significant change in waste form properties. However, only a small fraction of transmutation (~10% of that expected in actual waste) had occurred and, the experiment did not reproduce typical waste form conditions (e.g. neutron damage was annealed). Since the work of Vance and Gray, the transmutation problem has remained essentially dormant, not because the problem has been solved, but rather, because there has been no clear path forward for further investigation. In fact, an important point about these previous studies is that although the investigators were certainly aware of the transmutation issue, they were only able to ask rhetorical questions. With new experimental (e.g. Isotope Production Facility (IPF)) and theoretical tools (e.g. density functional theory (DFT)) that exist today, we have an important opportunity to not only ask these questions, but also provide answers via methods that were recently thought to be impossible (e.g. we have started Gray's "prohibitively expensive" experiment in an LDRD feasibility study). Furthermore, IPF experiments are "cleaner" in that the samples are isotopically purer, free from neutron radiation induced damage (not present in actual waste) and more representative of the separations and nuclear waste form processes.

To maximize the potential for success of this LDRD DR project, we originally organized it to consist of three integrated components, relying upon unique LANL strengths in radiochemistry and characterization of radioactive material; earth and energy systems; and computational materials science, respectively. These tasks are: (1) Experimental Verification of Radioparagenesis, (2) Robust Waste Form Design and Evaluation, and (3) Exploration of Novel Materials and Their Properties. During the course of the project, we made several slight course corrections. For example, Task 3 was refocused to more generally study the implications of radioparagenesis to include novel materials and new directions subtasks. Furthermore, our original emphasis on X-ray diffraction in Task 2 was augmented to include electron microscopy in order to take advantage of reduced sample volume (in order to minimize radioactivity).

Scientific Approach and Accomplishments

The major accomplishment of this project has been the establishment of a new capability to study accelerated chemical aging samples. This has required the integration of radiochemistry (for sample synthesis) and materials science (for sample characterization). The ability to synthesize very small samples for characterization via e.g. electron microscopy in relatively open areas (such as the Materials Science Laboratory) has allowed for unique studies to be performed. For example, we have very recently studied isotopically pure Lu-177 samples, the details of which are below.

Lu-177 decays primarily through 0.497 MeV beta radiation, and has a half-life of 6.65 days, and is currently used in nuclear medicine f. It decays to Hf-177, which is stable. From a coordination chemistry perspective, Lu-177 meets the requirements we have defined for accelerated aging studies, namely: (1) half-life must be conducive to experimental investigation, (2) the daughter product must be chemically distinct, (3) the radioactivity must be sufficiently low such that it can be handled, and (4) the isotope must be available. In this case, Lu is a rigidly 3+ cation while Hf is rigidly 4+, thus satisfying criterion 2. The beta radiation associated with Lu-177 is relatively low, and can be shielded especially for small transmission electron microscopy samples, which satisfies criterion #3. Importantly, we negotiated with colleagues at the Missouri University Research Reactor (MURR) for us to receive Lu-177 for only the shipping cost, which very elegantly satisfies requirement #4. The very short half-life of Lu-177 however requires extreme choreography of experimental activities. As an example, for the first experiment we performed on Lu-177, the sample arrived via FedEx from MURR on 6/18/13. The sample was purified in the TA-48 hot cells before dawn on 6/19/13 (to remove daughter product grown in during shipping). The sample was oxidized (to Lu2O3) and the TEM sample produced in the evening of 6/19/13 (Figure 1). The sample was shipped from TA-48 to the Materials Science Laboratory in TA-3 early on 6/20/13, at which time we began to accumulate TEM date. This experiment has required significant RCT and line management support.

Figure 1. Laura Wolfsberg (C-IIAC) and Jeff Aguiar (MST-8), rehearsing the loading procedure of the Lu-177 TEM sample in to a retractable holder through a shielded plexiglass box. Note the camera providing real time imagery of the sample in the laptop screen.

We are still in the process of analyzing the Lu-177 data, and have performed a second experiment in order to confirm initial results. However, the preliminary results are very exciting. We have obtained diffraction patterns, chemistry and even atomic resolution images (Figure 2) for the sample over the course of 6 half lives. From the diffraction data, it seems as though the phases present do not correspond exactly to equilibrium phase diagrams, see Figure 3. In fact, there is a particular phase that we believe we have observed that has not been observed in nature – although further analysis (including comparison to DFT calculations) is required to confirm.

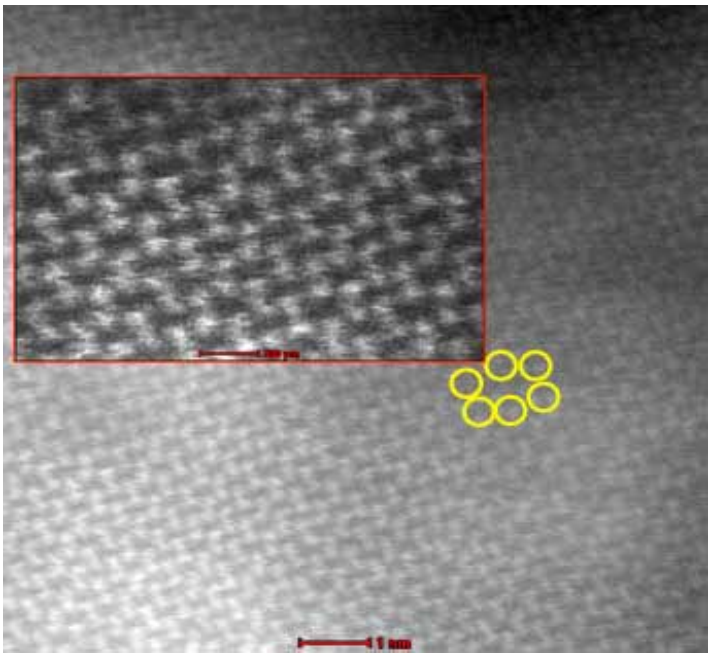

Figure 2. STEM image of 177Lu2-xHfxO3 sample.

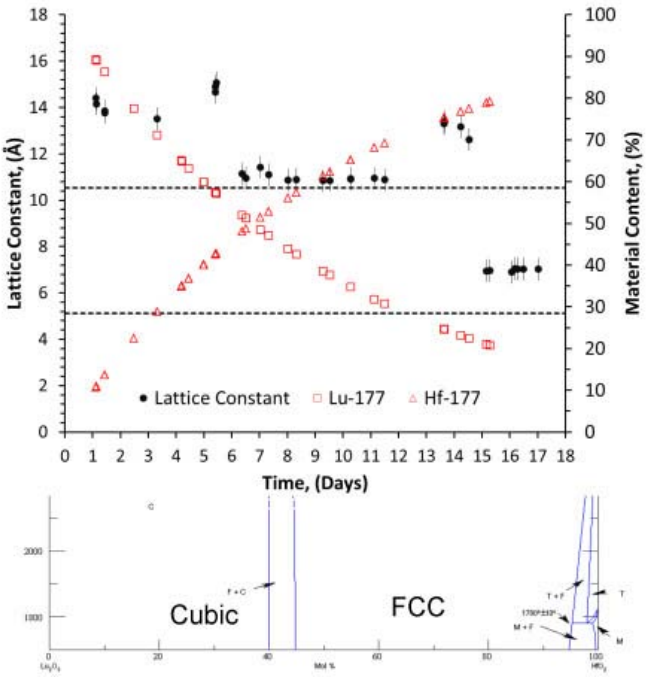

Figure 3. The black circles in the top image correspond to lattice constant of 177Lu2-xHfxO3 sample, plotted as a function of time (Lu-177 half-life = 6.65 days). The concentration of Lu and Hf are shown as open red squares and triangles respectively. It is clear from this figure that there are at least 4 separate phases that occur. These phases are compared to the equilibrium phase diagram represented in the lower image. It is also clear that there is not agreement between the measured data and the equilibrium phase diagram, suggesting the transmutation is resulting in non-equilibrium behavior.

In addition to accelerated chemical aging, we have also studied the impact of daughter product formation on the stability of waste forms in a repository setting. This has been done by linking DFT results of surface energetics and reactivity, with Lattice-Boltzmann pore scale models. For example, we have calculated the segregation of Ba to CsCl surfaces (Ba is the daughter product of Cs-137, an important short-lived fission product) see Figure 4, the influence of Ba on the formation of surface defects, and the interaction of water on both clean CsCl and Ba-doped surfaces. Importantly, we have found that the incorporation of Ba in the subsurface dramatically reduces the energy to form surface defects or, alternatively, to rip them off the surface. This effect results in enhanced leaching when the daughter is present. This effect has been demonstrated using Lattice-Boltzmann approaches, see Figure 5. This result demonstrates the dramatic effect that daughter products can have on waste form performance, even when not resulting in a phase change.

Several other related studies have been conducted related to the chemical effects associated with transmutation or daughter product formation. For example, we have syn-

thesized Fe-55 rich samples for experimental characterization. In addition to studying the effects of the formation of Mn (daughter product), we have also loaded these samples in to a range of diamond anvil cells to study the combined effect of chemical strain due to daughter product and applied pressure. We have also use density functional theory to examine the effect of C-14 transmutation on DNA stability. The human body contains 20 ng of radioactive 14C, generating 4000 decays per second of which 20–30 occur in nuclear DNA. We have found differences in behavior between DNA and RNA that might suggest justification for genetic code evolution. Finally, we are working with colleagues at Idaho National Laboratory to examine a ~50 year old sample 137CsCl in order to compare our accelerated chemical aging results to actual fission product waste forms of a certain age. This study will continue in FY14 via INL LDRD support.

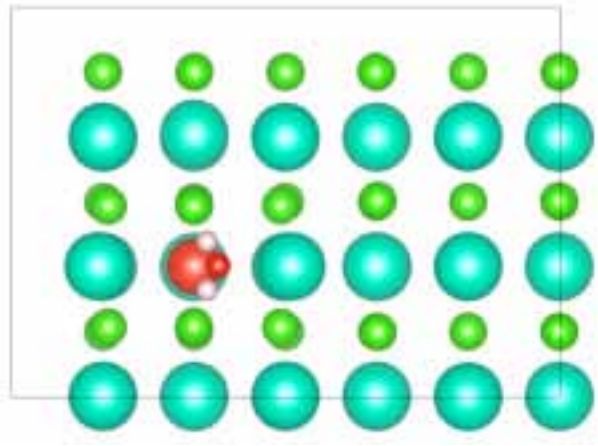

Figure 4. Schematic of atomistic simulations performed on the effect of Ba (daughter product) on CsCl surface stability in the presence of water.

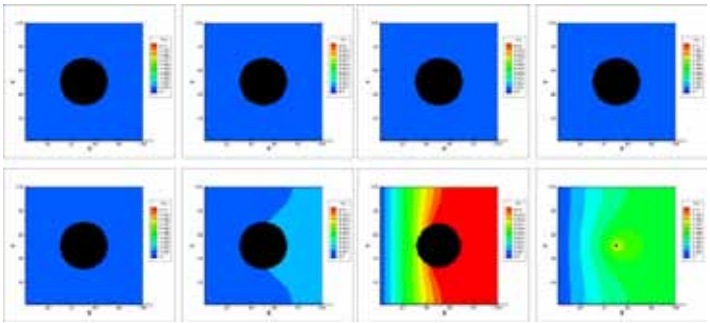

Figure 5. Dissolution of CsCl into water at 20oC. Reaction rate constant is calculated without considering Ba effect (E=1.4eV, top); and is calculated considering Ba effect (bottom). From left to right: time=0, 10, 20, and 30 years. The frequency factor (A) in the Arrhenius equation is 1.e11; initial domain is 10cmX10cm, and initial diameter of the CsCl particle is 4 cm. Initial concentration of CsCl is 0.1mol/L; concentration at the left boundary is set at 0.1 mol/L; the right boundary is the exit; and top and bottom boundaries are nonreactive walls.

Impact on National Missions

A critical problem for DOE-NE is providing a solution for nuclear waste disposal. This is evidenced by the recent Blue Ribbon Commission report on nuclear waste disposal as well as guidance from DOE to focus on " long-term, science-based R&D of technologies with the potential to produce beneficial changes to the manner in which the nuclear fuel cycle and nuclear waste is managed." This project directly fits this description. This project also addresses issues of fundamental materials science, using computer simulation to design materials with engineered functionality.

In addition to civilian nuclear waste, In the 1970s and 1980s large quantities of 137Cs (t 1/2 = 30 yr) and 90Sr (t1/2 = 29 yr) were extracted from spent nuclear fuel at Hanford in Washington State, and synthesized into capsules of CsCl and SrF2. Even though many of the capsules have aged for more than one half-life, they still account for around one-third of the radioactivity at the Hanford site and are the most significant source of radiation in the United States outside of a reactor. Stored underwater due to the radiation field, monitoring primarily consists of engineering-type "clunk-tests" which assess swelling associated with radiation damage, gas evolution, and/or phase decomposition. Aside from health-and-safety considerations, the Hanford capsules are scientifically interesting from a solid-state chemistry viewpoint, since the stable daughter isotopes differ markedly in oxidation state and size to the parent. These large changes in local chemistry have the potential to compromise a nuclear waste form over time by inducing large volume changes and disrupting the crystalline lattice. Again, studies performed in this project directly address the transmutation issue present in this defense waste.

Publications

Costa, G. C. C., H. W. Xu, and A. Navrotsky. Thermochemistry of Barium Hollandites. 2013. JOURNAL OF THE AMERICAN CERAMIC SOCIETY. 96 (5): 1554.

Jiang, C., B. P. Uberuaga, K. E. Sickafus, F. M. Nortier, J. J. Kitten, N. A. Marks, and C. R. Stanek. Using "radioparagenesis'' to design robust nuclear waste forms. 2010. ENERGY & ENVIRONMENTAL SCIENCE. 3 (1): 130.

Jiang, C., C. R. Stanek, N. A. Marks, K. E. Sickafus, and B. P. Uberuaga. Radioparagenesis: The formation of novel compounds and crystalline structures via radioactive decay. 2010. PHILOSOPHICAL MAGAZINE LETTERS. 90 (6): 435.

Jiang, C., C. R. Stanek, N. A. Marks, K. E. Sickafus, and B. P. Uberuaga. Predicting from first principles the chemical evolution of crystalline compounds due to radioactive

decay: The case of the transformation of CsCl to BaCl. 2009. PHYSICAL REVIEW B. 79 (13): -.

Marks, N. A., D. J. Carter, M. Sassi, A. L. Rohl, K. E. Sickafus, B. P. Uberuaga, and C. R. Stanek. Chemical evolution via beta decay: a case study in strontium-90. 2013. JOURNAL OF PHYSICS-CONDENSED MATTER. 25 (6): -.

Sassi, M., B. P. Uberuaga, C. R. Stanek, and N. A. Marks. Transmutation in (SrF2)-Sr-90: A density functional theory study of phase stability in ZrF2. 2012. PHYSICAL REVIEW B. 85 (9): 094104.

Stanek, C. R., B. P. Uberuaga, B. L. Scott, R. K. Feller, and N. A. Marks. Accelerated chemical aging of crystalline nuclear waste forms. 2012. CURRENT OPINION IN SOLID STATE & MATERIALS SCIENCE. 16 (3, SI): 126.

Uberuaga, B. P., C. Jiang, C. R. Stanek, K. E. Sickafus, N. A. Marks, D. J. Carter, and A. L. Rohl. Implications of transmutation on the defect chemistry in crystalline waste forms. 2010. NUCLEAR INSTRUMENTS & METHODS IN PHYSICS RESEARCH SECTION B-BEAM INTERACTIONS WITH MATERIALS AND ATOMS. 268 (19): 3261.

Winkler, B., C. R. Stanek, W. A. Taylor, L. Wolfsberg, B. L. Scott, R. M. Dickerson, W. Morgenroth, and L. Bayarjargal. Synthesis and characterization of (Fe2O3)-Fe-55 for the investigation of radioparagenesis. 2013. SOLID STATE SCIENCES. 18: 58.

Zhang, F., J. D. Gale, B. P. Uberuaga, C. R. Stanek, and N. A. Marks. Importance of dispersion in density functional calculations of cesium chloride and its related halides. 2013. PHYSICAL REVIEW B. 88 (5): -.

Hydrogen Effects in Delta-Stabilized Pu Alloys: Fundamental Thermodynamics and Interactions at Reduced Dimensionality

Daniel S. Schwartz
20110011DR

Abstract

Hydrogen is known to strongly interact with plutonium and its alloys. Our data from a variety of diffraction techniques coupled with immersion density measurements shows that hydrogen induces a high vacancy concentration, 10-3- 10-4, in Pu-2 atomic % Ga alloys. We feel that the high vacancy concentration is an incipient form of the Superabundant Vacancy phenomenon. Modeling of hydrogen-vacancy structures using density functional techniques suggest that the complex formed by introducing multiple hydrogen atoms into a Pu vacancy is a stable, low-energy structure. Increasing the Ga concentration to 7 atomic % effectively shuts down the vacancy-stabilizing ability of hydrogen.

Background and Research Objectives

Plutonium-based alloys exhibit complex behaviors that have puzzled materials scientists since they were first produced in the 1940's. LANL Pu scientists are tasked with cutting through this complexity and developing an understanding of Pu alloys that will allow effective management of the Nation's aging nuclear stockpile. This project focused specifically on expanding our understanding of the influence of dissolved hydrogen on the structure and behavior of Pu alloys. The urgency for the project is the fact that much of the Pu in the stockpile contains significant amounts of hydrogen, with 0.5 – 1.0 atomic % being typical. Despite the high amounts of hydrogen in our Pu alloy stream, our understanding of the effects of hydrogen dissolved in the Pu alloys lattice is rudimentary.

Hydrogen is known to have a profound effect on defect properties in many metal systems, where it both creates and stabilizes vacancy structures at high concentrations [1]. Vacancies, i.e. sites in the crystal lattice where atoms are missing, can be a trap for hydrogen in the lattice, where the hydrogen atoms and the vacancy defect mutually stabilize each other. In some metals, this effect can be extreme and is called the Superabundant Vacancy (SAV) phenomenon. Our goal in this project was to investigate the effects of hydrogen in Pu-Ga alloys, as a function of both hydrogen and Ga content. We were particularly interested to search for SAV behavior in these alloys.

Scientific Approach and Accomplishments

With the cooperation of the plutonium manufacturing team in the plutonium facility at LANL, we prepared three different alloys for this project in kilogram quantities. The alloys included pure Pu, which was electro-refined twice to maximize purity, a Pu-2 atomic % Ga (Pu-2Ga) alloy, and a Pu-7 atomic % Ga (Pu-7Ga) alloy. Ga is commonly added to Pu alloys to stabilize the face centered cubic δ-Pu phase, which is a much more ductile, machinable, and generally easier to handle form of Pu. At room temperature, pure Pu has the monoclinic crystal structure (the α-Pu phase) which is quite brittle. The Pu-7Ga alloy (Figure 1) is approximately at the Ga concentration where δ-Pu is most stable at room temperature [2]. The ability to make significant quantities of Pu alloys is a unique LANL capability, and we consider the preparation of our project alloys a great success.

The alloys were exposed to hydrogen (or deuterium) using a Sieverts' apparatus, which is a furnace capable of heating samples while they are exposed to precisely measured quantities of gas. The temperature and pressure are accurately measured, yielding the pressure-temperature diagram for the specimen, from which it can be determined exactly how much hydrogen was absorbed by the specimen. As the hydrogen pressure is increased over a Pu specimen, three stages are typically observed: 1) hydrogen being absorbed in the Pu lattice, 2) the nucleation and growth of PuH2 in the Pu specimen, and 3) the completion of the hydriding process, where the entire specimen is PuH2. In this program, we exclusively focused on the first region, where hydrogen is in solution in the Pu lattice, but no hydride has formed.

Figure 1. A portion of the Pu-7 atomic % Ga casting produced for this project.

Our first goal was to quantify the concentration of vacancies in our alloys, as function of Ga and H content. We used a method first developed to quantify the vacancy concentration in metals as they approach their melting point [3]. This technique involves comparing the bulk density of a specimen to its density determined by X-ray Diffraction (XRD). The comparison is sensitive to vacancies because the atomic lattice in a metal contracts in the presence of vacancies, i.e. there is an apparent increase in density, while the bulk density actually decreases because many lattice sites are vacant (Figure 2). Our bulk density measurements are made using the Archimedes immersion method, which is highly accurate for specimens in the 1 - 10 gram weight range. XRD measurements yield a very accurate value for the lattice parameter, i.e. the atomic spacing in the sample's lattice, typically on the order of 200 ppm error. We first held several Pu-2Ga specimens at 450°C in vacuum for several days to uniformly distribute the Ga throughout the specimens. After slow cooling, we measured the density and XRD lattice parameter of the specimens. Then we used the Sieverts' apparatus to charge the specimens with 1 atomic % hydrogen, and remeasured the density and XRD lattice parameter. A clear decrease in bulk density was measured (~0.45% decrease), while the density based on XRD measurements increased (~0.4%). For further confirmation, we performed similar lattice parameter measurements on H-charged and pure Pu-2Ga using both neutron diffraction at LANL's neutron accelerator and synchrotron diffraction at the Stanford Synchrotron Radiation Lightsource. In both cases, 1 atomic % hydrogen in Pu-2Ga resulted in a ~0.4% density increase, based on the measured lattice parameters. This is a classic indication that the lattice contains a significant quantity of vacancies. We estimate from these numbers that the vacancy concentration is in the 10-3 to 10-4 range. This is a strikingly high vacancy concentration. For comparison, well-annealed gold at room temperature will have a vacancy concentration on the order of 10-17!

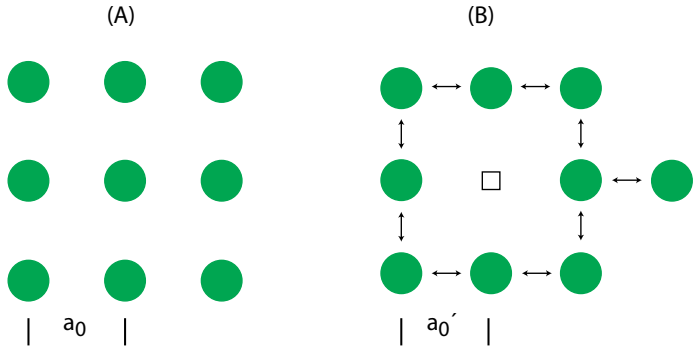

Figure 2. (A) Schematic of a perfect Pu lattice. The lattice parameter, a0, can be measured by XRD. (B) When a vacancy forms (marked by □) a Pu atom moves from its site to a different location in the Pu lattice, leaving a vacant lattice site. The vacancy causes the lattice to collapse slightly, so XRD measures a smaller lattice spacing (a0´ < a0). However, the overall volume of the ensemble of atoms becomes larger, because the atom formerly at the vacancy finds a new site to occupy. Therefore, the XRD measurements show a densification of the lattice, while bulk density measurements show a decrease in density. This differential indicates the presence of vacancies.

As a further check, we took the hydrogen-charged specimen back into the Sieverts' apparatus and removed the hydrogen by vacuum annealing at 450°C. We subsequently remeasured the XRD lattice parameter for the dehydrogenated specimen, and it had returned to a value close to its initial, hydrogen-free value. The results indicate that the vacancy concentration had returned to its normal level after hydrogen removal. This series of measurements is the first distinct evidence for hydrogen-induced vacancies in Pu alloys.

In parallel with our experimental efforts, we performed a variety of calculations to examine the energetics and atomic structure of hydrogen-vacancy complexes in the Pu system. Density functional theory (DFT) was used to calculate the energy of different plausible hydrogen-vacancy

structures. DFT calculations are based on fundamental quantum mechanics and yield electronic configurations and energies. The calculations are complex for atoms with large numbers of electrons like Pu, where f-orbitals must be included in the process, and the computation cells are limited to ~30 atoms. The effect of introducing hydrogen atoms into a vacancy in Pu was systematically examined by putting from 1 to 8 hydrogen atoms into a cell of Pu atoms with a vacancy site at its center (Figure 3). The energies of the resulting hydrogen-vacancy complexes were calculated, and the atoms were allowed to move to minimize the cell energy and reveal where the hydrogen atoms preferentially bind to the Pu vacancy. The hydrogen atoms were found to avoid the center and bind to the edges of the vacant site. Several hydrogen atoms may coexist in the vacant site with only weak hydrogen-hydrogen atom interactions. It was not until 4 hydrogen atoms were introduced into the vacancy that significant crowding (i.e. strong electronic interaction) of the hydrogen atoms took place (Figure 3e). Hydrogen atoms were observed to monotonically reduce the energy of formation for vacancy-hydrogen complexes. The calculations thus support the idea that hydrogen stabilizes vacancies in Pu through the formation of a low-energy hydrogen-vacancy complex, most likely with multiple hydrogen atoms associated with each complex.

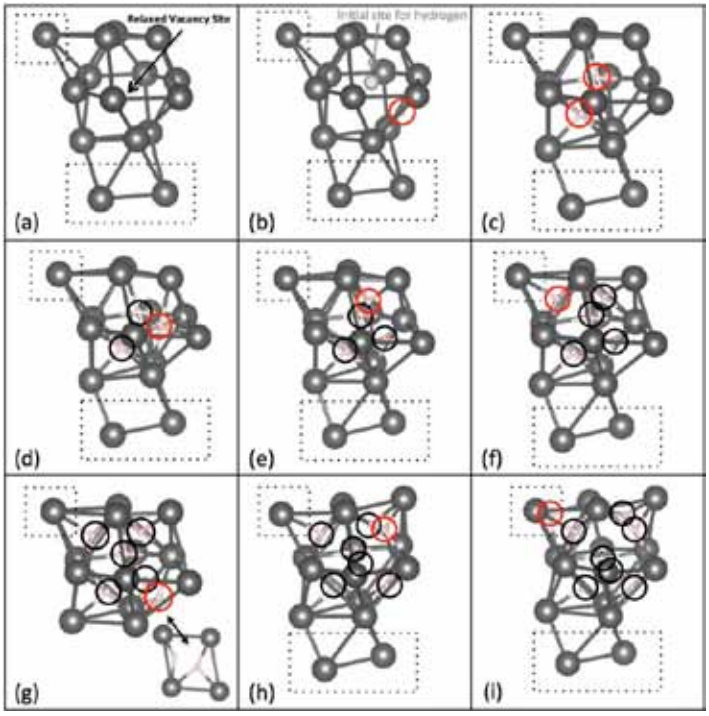

Figure 3. Calculational cells for increasing numbers of hydrogen atoms (0 to 8 H atoms) in a Pu vacancy used for density functional calculations. The Pu atoms are gray, and the hydrogen atoms are circled.

The concentration of hydrogen-stabilized vacancies that we measure in our Pu alloys is much lower than that in the SAV systems described by Fukai [1], which can approach 30 at. %. We are operating at far lower hydrogen pressures, but the basic processes responsible for the SAV phenomenon are active, i.e. hydrogen-vacancy complexes having lower energy than isolated vacancies and interstitial hydrogen. We consider the hydrogen-vacancy structures in our Pu alloys an incipient form of the SAV phenomenon.

We revived the Positron Annihilation Lifetime Spectroscopy (PALS) instrument at LANL for this project. PALS is one of the few analytical techniques capable of giving direct information about atomic level defects with volumes of ~1 nm3 and is therefore ideal for probing our hydrogen-vacancy complexes. Positrons directed into a material will penetrate hundreds of micrometers into the bulk and annihilate preferentially at regions of excess volume in the crystal lattice (e.g. vacancies). The lifetime of the positron can be measured accurately, and is directly related to the volume of the annihilating defect. Lifetime measurements are coupled with DFT calculations of the electron and positron density for expected defects, such as single vacancies and hydrogen-vacancy complexes. Accurate calculations of the positron lifetime can be made from the charge density values, and a good match of measured lifetime to a calculated value is convincing evidence that the defects are the calculated type. We successfully developed the ability to perform such calculations at LANL, and calculated very accurate lifetimes for aluminum as a test.

While we had good success resuscitating the PALS system and performing the necessary calculations, our results on Pu specimens were not satisfactory. We performed PALS on Pu-2Ga and Pu-7Ga alloys, both hydrogen-free and with 1 atomic % hydrogen. Our results were not consistent with calculated lifetimes, which were significantly lower than the measured values. In addition, we did not see a meaningful effect on lifetime due to the addition of hydrogen. We believe that a mixture of instrument errors and the electronic complexity of Pu are confusing our results. Nevertheless, we support the future use of PALS to probe hydrogen-vacancy complexes in Pu, as it should be able to give us information about the volume of the complexes which is otherwise unattainable.

Hydrogen that is dissolved in Pu alloys must first pass through the sample surface. Therefore, a key part of understanding hydrogen in Pu alloys is understanding how hydrogen interacts with the Pu surface. X-ray Photoemission Spectroscopy (XPS) is a powerful tool for examining atomic species and charge states in the top few nm of the specimen surface. XPS was used to study the surface of hydrogen-free Pu-7Ga. This alloy was chosen because we believed its well-known oxidation resistance and phase stability would make it a simple starting point, from which we

could better understand the behavior of the more complex hydrogen-charged materials. However, the surface of Pu-7Ga was not simple. As received, the surface was a complex mixture of PuO2 and Ga oxide, along with fluorine, carbon, and other elements picked up from the glovebox environment where the Pu-7Ga specimens are prepared. Surfaces are prepared for XPS analysis by sputter cleaning with argon ions, which removes incidental contaminants, and sputtering was successful in removing fluorine, carbon, and copper from the surface. However, even extended sputtering did not remove the oxide layer. We conclude that much of the surface oxide comes from oxygen in the Pu bulk moving to the surface, even at room temperature.

We used a related technique, Photoemission Spectroscopy (PES) to get information about the electronic structure of δ-phase Pu, and δ-Pu in the presence of hydrogen. A key finding was that δ-Pu has a multivalent electron structure, i.e. the f-orbital contains a mixture of 5f 5 and 5f 6 electronic states. With this more detailed understanding of pure δ-Pu electronic structure, we addressed the question of how hydrogen interacts with Pu to modify the electronic structure. PES spectra were taken from δ-Pu in the presence of hydrogen gas at a range of temperatures from 20K to 300K. At the lowest temperatures, H and Pu weakly interact indicative of simple physiosorption of hydrogen on the Pu surface. At 300K, there are clear signs of chemical bonding between H and Pu, specifically in the disruption of the 5f 5 component of the multivalent f-orbital. The chemical bonding of H and Pu at 300K was detectable at very low concentrations of hydrogen, so it is clear that the ingress of hydrogen into the Pu lattice is easy and involves an electronic interaction between the two species.

The system we are studying is a ternary with three components: Pu, Ga, and H. We found that the effects of hydrogen in Pu cannot be separated from Ga. Increasing Ga in the system to 7 atomic % effectively switched off the vacancy-stabilizing ability of hydrogen. We measured no increase in vacancy concentration when Pu-7Ga was charged with hydrogen. In general, Pu with high amounts of Ga behaves in a more normal way. We determined that many of the well-known [4] anomalous thermodynamic properties of Pu-2Ga disappear at high Ga concentrations. We developed computational frameworks in this project with promise to help understand the anomalous effects of Ga, which will continue to influence the field well beyond the term and scope of this project.

Impact on National Missions

The findings of this project have important ramifications for the understanding of how plutonium in the Nation's nuclear weapons stockpile is aging. LANL and LLNL plutonium scientists have been tasked with assessing the state of the Pu stockpile as it ages. While these efforts have been quite rigorous over the past decades, they have not dealt with or recognized the prevalence of hydrogen in the Pu metal. Relatively straightforward and conservative calculations suggest that the damage field produced by alpha-decay in 239Pu will interact with ~2% of the hydrogen-vacancy defects per year in a specimen with the typical concentration of 10-3 that we measured. Even without any understanding of what results from this interaction, it seems clear that the intrinsic defect structure of the stockpile Pu needs to be considered to understand Pu aging at the fundamental level.

Our project also had an impact on the development and maintenance of Pu facilities at LANL. The positron annihilation system in particular was resurrected and used for Pu measurements for the first time at LANL. Additionally, this project involved three early career scientists, supporting the goal of maintaining a stream of plutonium scientists for the future.

References

1. Fukai, Y.. Formation of superabundant vacancies in M-H alloys and some of its consequences: a review. 2003. JOURNAL OF ALLOYS AND COMPOUNDS. 356: 263.
2. Timofeeva, L. F.. Phase transformations in Pu-Ga and Pu-Al alloys Effects of pressure and temperature on kinetics of delta-phase decomposition. 2007. JOURNAL OF ALLOYS AND COMPOUNDS. 444: 124.
3. SIEGEL, R. W.. VACANCY CONCENTRATIONS IN METALS. 1978. JOURNAL OF NUCLEAR MATERIALS. 69-7 (1-2): 117.
4. Hecker, S. S., D. R. Harbur, and T. G. Zocco. Phase stability and phase transformations in Pu-Ga alloys. 2004. PROGRESS IN MATERIALS SCIENCE. 49 (3-4): 429.

Publications

Beaux, M. F., J. J. Joyce, T. Durakiewicz, K. S. Graham, E. D. Bauer, J. N. Mitchell, P. H. Tobash, and S. Richmond. Electronic Structure, Localization and 5f Occupancy in Pu Materials. 2012. ACTINIDES AND NUCLEAR ENERGY MATERIALS. 1444: 123.

Joyce, J. J., T. Durakiewicz, K. S. Graham, E. D. Bauer, D. P. Moore, J. N. Mitchell, J. A. Kennison, R. L. Martin, L. E. Roy, and G. E. Scuseria. Pu Electronic Structure and Photoelectron Spectroscopy. 2011. In International Conference on Strongly Correlated Electron Systems (SCES 2010) ; 27 June-2 July 2010 ; Santa Fe, NM, USA. Vol. 273, p. 012023 (5 pp.).

Joyce, J. J., T. Durakiewicz, K. S. Graham, M. F. Beaux II, E.

D. Bauer, D. P. Moore, J. N. Mitchell, P. H. Tobash, and S. Richmond. Delta-Pu electronic structure and valence. Phys. Rev. Lett..

Lee, T., M. I. Baskes, A. C. Lawson, S. D. Conradson, S. P. Chen, A. Caro, S. M. Valone, and C. D. Taylor. Atomistic modeling of thermodynamic properties of Pu-Ga alloys based on Invar mechanism. Phys. Rev. B.

Mitchell, J. N., F. J. Freibert, D. S. Schwartz, and T. E. Mitchell. Diverse phase transformation behavior in pure plutonium. Presented at Plutonium Futures - The Science 2012. (Cambridge UK, 15-20 July).

Mitchell, J. N., F. J. Freibert, and D. S. Schwartz. Phase Transitions in Pure Plutonium. 2012. ACTINIDES AND NUCLEAR ENERGY MATERIALS. 1444: 159.

Richmond, S., D. S. Schwartz, A. I. Smith, and A. L. Costello. New observations supporting the existence of the superabundant vacancy phenomenon in delta-Pu metal. Presented at Plutonium Futures - The Science 2012. (Cambridge UK, 15-20 July 2012).

Schwartz, D. S., S. Richmond, A. I. Smith, A. Costello, and C. D. Taylor. Hydrogen-Vacancy Effects in Pu-2 at. % Ga Alloys. 2012. ACTINIDES AND NUCLEAR ENERGY MATERIALS. 1444: 183.

Schwartz, D. S., S. Richmond, A. I. Smith, and W. D. Peach. Hydrogen effects in Pu-Ga Alloys: preliminary thermodynamic and microstructural analysis of Pu-7 at. % Ga. Presented at Plutonium Futures 2012. (Cambridge, UK, 15-20 July).

Smith, A. I., S. Richmond, K. L. Page, J. Siewenie, and T. Saleh. First look at local structural evolution of hydrogen loaded delta 239Pu-2at.%-Ga alloys. Presented at Plutonium Futures - The Science 2012. (Cambridge UK, 15-20 July).

Taylor, C.. Surface segregation and adsorption effects of iron-technetium alloys from first-principles. 2011. Journal of Nuclear Materials. 408 (2): 183.

Taylor, C. D., S. C. Hernandez, M. F. Francis, D. S. Schwartz, and A. K. Ray. Hydrogen trapping in delta-Pu: insights from electronic structure calculations. 2013. JOURNAL OF PHYSICS-CONDENSED MATTER. 25 (26): -.

Valone, S.. Quantum Mechanical Origins of the Iczkowski-Margrave Model of Chemical Potential. 2011. JOURNAL OF CHEMICAL THEORY AND COMPUTATION. 7 (7): 2253.

Valone, S. M., S. R. Atlas, and M. I. Baskes. Fragment Hamiltonian model potential for nickel: metallic character and defects in crystalline lattices. Modeling and Simulation in Materials Science and Engineering.

Venhaus, T.. X-ray photoelectron spectroscopy of 7-at.% gallium δ-stabilized plutonium. Presented at Actinides 2013, Karlsruhe, Germany. (Karlsruhe, 21-26 July, 2013).

First Reactions: Simple Molecule Chemistry Behind the Shock Front

Dana M. Dattelbaum
20110012DR

Abstract

Understanding the behaviors of materials in extreme environments is foundational for predicting the response of weapons materials, creating environmentally tolerant properties, and potentially exploiting extreme conditions to tailor materials functionality. Furthermore, the increasing diversity in long-term NNSA mission drivers, and needs for increasing fidelity of weapons physics models, will continue to drive research into dynamic materials performance under the extreme conditions encountered under shock loading. Significant gaps in our knowledge remain regarding the general principles of shock-induced chemical reactions, and the specifics of bond-changing steps under these conditions. Through in situ measurements of shock wave structures and spectroscopic signatures, this synergistic LDRD project has shed light on the details of chemical reactions behind the shock front in simple chemical structures. These include reaction thresholds/rates and their state sensitivities, as well as electronic changes leading to and associated with chemical bond changes, and predicted reaction mechanisms. The outcome of this work is a better understanding of how chemical reactions proceed under shock compression.

Background and Research Objectives

Molecular bonding is defined by strong intramolecular covalent bonds, and weaker intermolecular forces (hydrogen bonding, van der Waals, dipole-dipole). Application of pressure results in dramatic volume reductions, overcoming repulsive intermolecular interactions, and potentially new chemical reaction pathways and products[1-4]. Today, the interrogation of new chemical structures at static high pressures is commonplace[1, 3-4]. Shock compression creates extreme compression conditions on a rapid (ps) timescale, invoking additional effects on local chemical structures, including unique steric and electronic structures, shock heating, and transient non-equilibrium partitioning of kinetic energy behind the front[1,2,5,8]. If the first chemical reactions were better understood, our predictive capabilities for the dynamic response of materials would be dramatically improved, and further, shock-driven reactivity could be designed into new molecules for use under these conditions. However, there remain significant challenges to understanding and predicting chemical reactivity under these conditions; most notably the harsh in situ conditions, short temporal existence of reactants and intermediates, and single-event nature of shock compression experimentation.

Foundational work[10-21] established that many organic materials react readily under shock compression, even those that do not readily react under thermal or catalytic conditions such as styrene, tetrahydrofuran, benzene, and tetrachloroethylene. The goals of this project are to predict, measure and quantify the details associated with the first reactions behind a shock front for a selection of relevant functional groups (such as O-O, O-H, C=C, C≡C, C≡N, and ring structures). Theory and experiment are matched in length and time scales, with different shock compression platforms (gas gun-driven plate impact, and direct laser shock drive) providing sustained shocks on duration from 100s ps to microseconds in time. The objectives of the project are to quantify the time scales of processes behind the shock front leading to and associated with chemical bond breaking, predict and measure electronic states, volume changes and temperatures for direct comparison to experiment, and to understand reaction activation barriers and mechanisms under shock compression.

Scientific Approach and Accomplishments

A synergistic theoretical-experimental effort focusing on shock-driven reactivity of simple chemical structures has been established to quantify the mechanisms, length- and timescales of the processes associated with chemical reactions behind a shock front. This approach combines new computational methods in many-atom reactive molecular dynamics, with application of pico-

second-to-microsecond time-resolved experimental diagnostics during shock compression. In this project, we have focused on predicting and interrogating shock-induced chemical reactions in three classes of molecular compounds: oxygen-rich molecules (H2O2, HCOOH), unsaturated structures (e.g. C=C, C≡C, C≡N), and ring (saturated and unsaturated) structures. We have chosen simple chemical structures because they are computationally tractable, and in many cases, their thermodynamic properties and static high-pressure responses are reasonably well-characterized, offering benchmarks for the dynamic experiments. They represent functional groups present in most molecular solids, and offer an opportunity to establish a foundational knowledge of comparative group reactivity.

Shock-compression experiments were performed using both gas gun-driven and laser-driven shock compression platforms, launching shock waves into the materials with sustained durations ranging from ~350 picoseconds to several microseconds. Experiments and theory were matched in length and time scale to the processes occurring following shock compression. At the earliest time/length scales, laser-driven shock compression with ultrafast (ps) probes of electronic and bonding changes[7, 28-30] were matched to quantum molecular dynamics (LATTE) simulations[8, 22-23] at the same conditions. From nanoseconds-to-microseconds behind the front, measurement of in situ wave dynamics, and global reaction rates were interpreted with calculated temperatures from inert and product equations of state.[5,6,25,27] The dynamic experiments were benchmarked to static high pressure-temperature experiments of pressure- and temperature-driven chemical reactions using in situ synchrotron-based diagnostics of structure and bonding (x-ray diffraction, infrared spectroscopy).[24, 26] As a result of this focused LDRD effort, the major accomplishments toward understanding shock-driven reactivity are:

1. We have quantified many of the details of shock-driven reactions for a number of simple molecular structures. These include defining the timescales of induction times, electronic structure, and bonding changes behind the front. We have also defined the reaction thresholds on the principal shock adiabat (Hugoniot) for a large variety of chemical functional groups, volume changes leading to and associated with chemical reactions, and global reaction rates as a function of shock input condition;

2. We have developed and applied in situ spectroscopic diagnostics to measure electronic and structural changes in shocked organic liquids from ps-to-microsecond timescales behind the shock front.;

3. We have developed a novel quantum reactive molecular dynamics approach (LATTE) with significant improvements in energy conservation and scaling, parameterized the potentials for C, H, N, and O, and simulated shock-driven chemistry in simple molecules, validated against and guiding experiments on the same timescale;

4. We have demonstrated a bridging of the temporal and spatial scales of chemical reactions behind the shock front through shock temperature-sensitive global reaction rates.

Reaction thresholds and dynamics via wave evolution
The mechanical variables (Us, up, P, V) associated with shock-induced chemical reactions, and their kinetic evolution have been quantified under sustained shock conditions using LANL large bore single- and two-stage light gas guns. Reaction threshold conditions on the principal Hugoniot have been quantified by in situ measurements of the reactive flow, including the first wave state on the unreacted Hugoniot.[5, 25, 26] In doing so, we have established an order of reactivity for a variety of chemical functional groups and simple molecules as a function of shock pressure on the principal Hugoniot, including –C=C-, -C≡C-, -C-H, -C=O, and O-O motifs.[5, 6, 7] For example, unsaturated structures (such as C=C and C≡C) were found to react at modest shock input conditions (4-7 GPa). Aromatic structures were more stable, reacting at > 10 GPa, and saturated molecules appear to be the most stable (including C-C, C-H, O-O). Multiple wave structures resulting from volume changes associated with shock-driven chemical reactions, provide information about reaction thresholds, densities of intermediate and product states, and global reaction rates. Figure 1a shows example shock wave profiles (in particle velocity vs. time) of one of the molecules studied, acrylonitrile (CH3C≡N) shocked to 7.6 GPa. As seen in the Figure 1a, over measurable time and distance, the input shock wave evolves into a 3-wave structure, indicating at least 2 higher density products are formed behind the shock front with volume reductions of 5 and 6% for the first and second reaction step, respectively. [5] The threshold or “cusp” condition for acrylonitrile was found to be at ~ 5.6 GPa and 850 K.

From the evolution of shock wave profiles as a function of varying shock input strength, reaction induction times and global reaction rates for transformation of initial molecules to states of higher density were quantified. Figure 1(b) shows example wave profiles from 5 different shock experiments on acrylonitrile above 6 GPa; shock stress is given (in GPa) next to each profile. It is observed that the wave dynamics, and thus the reaction rates, vary substantially over a small range of shock input conditions; e.g. from 6

to 8.9 GPa. The risetimes of the reactive waves, Figure 1b, are related to the global reaction rates of the reactions. For acrylonitrile, the global reaction rates are ~1.0-1.7 × 107 s-1 near the reaction threshold, with reactions occurring over 10s of nanoseconds at 6-8 GPa.[5] However, the reactions are readily accelerated by shock input condition, reaching 109 s-1 by 18 GPa[5, 7]. This is due to the state sensitivities of the reactions to shock pressure, and more importantly, shock temperature. Figure 2 shows the measured and calculated reaction rates for the two reactions in acrylonitrile as a function of calculated shock temperature, illustrating the shock state (P,T) sensitivities of the reaction rates[5].

Probes of chemistry in the first ½ nanosecond

Ultrafast spectroscopic probes coupled to laser-driven shock compression allows for evolution in electronic and bonding structures behind the shock front at early times. Shocked states were diagnosed using ultrafast dynamic ellipsometry, and evidence of "cusps" or non-linearities in the shock adiabat due to chemical reaction were observed at higher input conditions than in the gas gun-driven experiments, due to the shorter timescales sampled by the laser shock experiments[7, 28-30]. Ultrafast transient absorption measurements were performed for the same series of simple molecular structures as described above[7]. The transient absorption spectra reveal new insights into electronic structure changes following shock compression. For example, a continuous red shift of the absorption band, consistent with shock-induced band gap closure, was not observed for any compound studied [7]. Rather, transient absorption features in the range 400-800 nm were observed for molecules undergoing chemical reaction, such as acrylonitrile shocked above 12 GPa, Figure 3, and phenylacetylene shocked above 10 GPa. Coincident with the growth of the visible absorption feature in phenylacetylene, the transmitted shock wave measurements exhibited a volume collapse that occurred exclusively in the high stress region of the shock. This is consistent with a densification reaction observed in gas gun embedded gauge measurements of shocked phenylacetylene, but the stress state was much higher and the reaction time much faster in the laser shock experiments.[7] In addition to direct observation of electronic absorption changes associated with compression and chemical reaction to form products, the transient absorption experiments indicate that at modest pressures, induction times of 50-100 picoseconds are observed behind the shock front. An ultrafast CARS (Coherent Anti-Stokes Raman Spectroscopy) diagnostic was also coupled to the laser-driven shock platform for probing bonding changes behind the front. The CARS diagnostic was demonstrated with single shot sensitivity on micron-thick shocked samples.

Reactive molecular dynamics simulations: LATTE

A new reactive molecular dynamics capability based on semi-empirical methods (self-consistent field-tight binding level) has been developed to allow for long-duration (ns) molecular dynamics simulations of molecular chemistry under simulated shock conditions.[8, 22, 23] Optimal scaling of computation cost with system size was achieved through sparse matrix algebra methods,[8] and by porting the computationally-expensive algorithms to high performance, many-core graphics cards. These novel approaches allow for realization of simulations with the thousands of atoms that are required for explicit resolution of a shock front, and the transient non-equilibrium phenomena it invokes.[8] Shock simulations were performed on the same molecular compounds as focused on by the experimental effort, with specific focus on acrylonitrile, phenylacetylene, formic acid, and benzene. Figure 4 shows the results from LATTE simulations on acrylonitrile. The simulations in Figure 4a show the computational cell before, and at simulated shock compression at >10 GPa. Shock compression at this P,T condition results in bond cleavage and polymerization of acrylonitrile to form polyacrylonitrile. The simulations results, Figure 4b and 4c, show HOMO-LUMO gap reduction following shock compression, and the number of atoms incorporated into the growing polyacrylonitrile product. Following shock compression, an induction time is observed, and reduction of the HOMO-LUMO gap (by over an eV) associated with closure of the chemical potential, and reaction to form the product(s). The simulations are directly consistent with the observed densification reactions observed in the gas gun and laser experiments, and visible-centered absorption feature that appears as reaction proceeds.

LATTE was further extended to extract Raman spectra "on-the-fly" from simulations for the first time in order to track reaction pathways and their kinetics via coupled theory and experiment. Spectra were computed by the extension of the tight-binding formalism to incorporate into the Hamiltonian a dependence on an external electric field. The polarizability tensor was computed at intervals as the gradient of the total energy with respect to the applied field and Raman intensities by the Fourier transform of its time correlation function. This new capability is of tremendous significance to objectives in understanding chemistry in dynamic extreme conditions, because for the first time theory and experiment will coincide in terms of temporal (ps to ns) and spatial (multi-nm) scales as well as in the diagnostic information that can be extracted.

High pressure synthesis and "dynamic" diamond anvil cell experiments

Definition of the static P/T phase diagrams, and high pres-

sure reactivity of a large number of simple organic molecules was performed using x-ray microdiffraction techniques at the HP-CAT beamline at the Advanced Photon Source, and the U2A beamline at the National Synchrotron Light Source to aid in interpretation of the dynamic experiments. The materials studied to date include: t-butyl acetylene, ethynyl trimethylsilylacetylene, hydrazine, acrylonitrile, benzonitrile, formic acid, nitrobenzene, and aniline.[24, 26, 31] Overall, reaction thresholds of pressure-driven chemistry were found to be greater than under shock conditions by at least 4 GPa, due to the temperature and strain rate differences. Raising the temperatures at high pressures was found to decrease the reaction thresholds in pressure to be close to shock conditions. New polymer materials were also synthesized by high pressure and/or high P/T conditions in diamond anvil cells, and recovered to ambient conditions. Examples include the glassy poly(t-butyl acetylene), and opaque poly(ethynyl trimethylsilane) polymers.[26] Furthermore, using the new 3.5 generation synchrotron PETRA-III (Hamburg, Germany), organic materials were rapidly ramp-compressed through the liquid-solid transition and reaction (polymerization) thresholds while simultaneously measuring time-resolved full angle-dispersive x-ray diffraction patterns at strain rates up to 10-2 s-1.

Impact on National Missions

Predicting the evolution of chemical reactions in extreme environments underpins our ability to perform weapons assessments through predicting how materials behave under dynamic compression, and the development of realistic EOS and reactive burn models that capture shock-driven chemistry. An improved fundamental knowledge is also the only means of enabling the design of new materials. As such, the themes of this LDRD project are directly aligned with Stockpile Stewardship and related National Security missions. Nationally, this work can also be tied to Office of Science priority research directions in thermo-mechanical extremes, as outlined by the recent Materials under Extreme Environments report,[1] and National user facilities such as the Linear Coherent Light Source (LCLS), HP-CAT and DCS beamlines[2,3] at the Advanced Photon Source, and National Synchrotron Light Source. New diagnostics of matter in extreme conditions, including ultrafast transient absorption and coherent anti-Stokes Raman spectroscopy, and transient Raman spectroscopies coupled to single- and two-stage light gas guns at Los Alamos, have been developed, as well as new triggering methods for timing high latency diagnostics (flash lamp-pumped lasers, accelerator-generated x-rays and protons) to shock conditions.[9] Time-resolved (few-100s ms) x-ray diffraction at strain rates up to 102 s-1 within high pressure diamond anvil cells was also demonstrated.

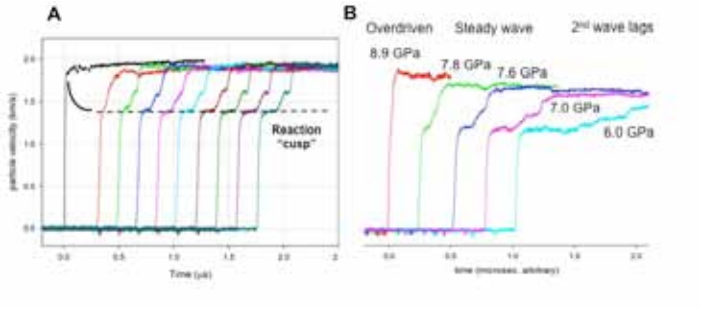

Figure 1. (A) Particle velocity wave profiles measured in acrylonitrile shocked to 7.6 GPa. A three-wave structure indicative of the formation of two higher density products is observed. (B) Particle velocity wave profiles from five shock compression experiments on acrylonitrile at varying shock input strengths (listed next to the profile in GPa). The shock-driven reactions are quite sensitive to the shock input condition and span a range of wave dynamics from 6.0- 8.9 GPa.

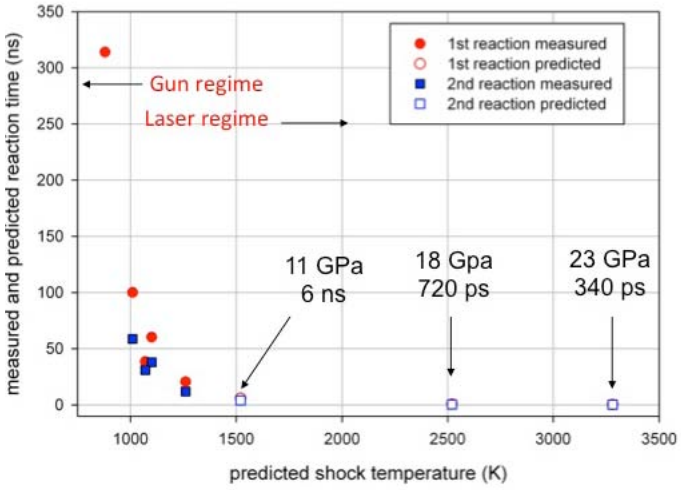

Figure 2. Measured and predicted reaction time (in nanoseconds) for acrylonitrile as a function of predicted initial shock temperature. The reactions are found to be highly state sensitive.

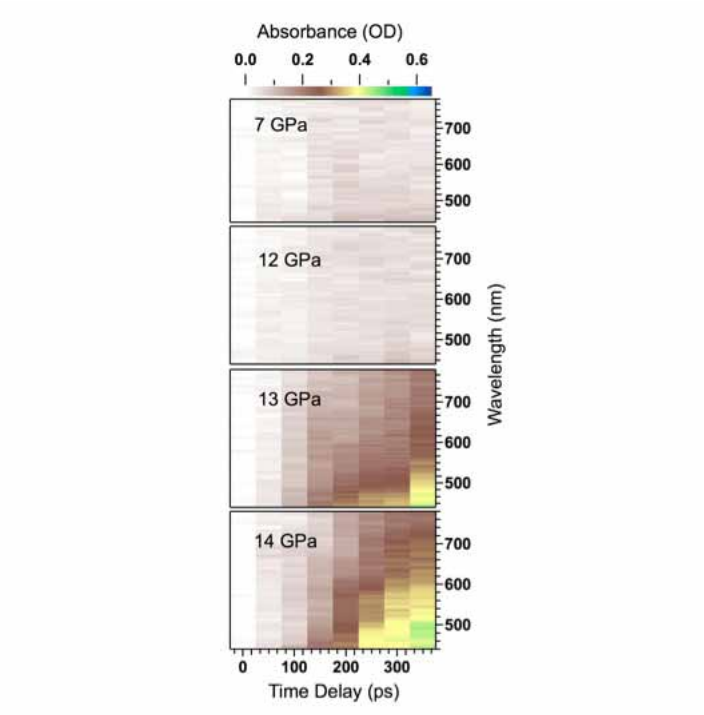

Figure 3. Time-resolved transient absorption spectra (in wavelength) as a function of time following shock compression of acrylonitrile. A visible absorption is observed at shock input conditions above 13 GPa associated with shock-driven reactions.

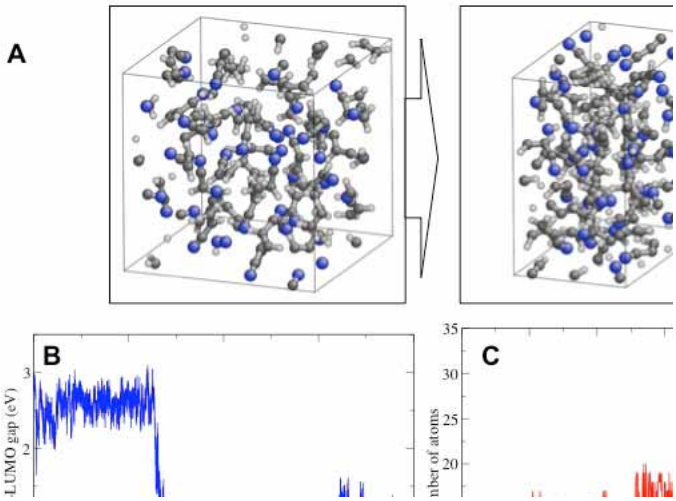

Figure 4. (A) LATTE simulation of acrylonitrile before (left) and after (right) simulated shock compression. The shock compression event results in a decrease in the HOMO-LUMO gap (B) with time, and polymerization of acrylonitrile with time (C). (C) indicates the number of atoms in the polymer chain as a function to time to > 50 picoseconds.

References

1. Wadsworth, J., G. Crabtree, and R. J. Hemley. Materials under Extreme Environments. 2007. Department of Energy Office of Science, Basic Energy Sciences report.
2. New Research Opportunities in Dynamic Compression Science. 2012. Dynamic Compression Sector at the Advanced Photon Source, Washington State University and DOE/NNSA.
3. Advances in Matter under Extreme Conditions - HPCAT Workshop Report. 2013. High Pressure Collaborative Access Team, Advanced Photon Source, Argonne National Laboratory.
4. Hemley, R. J.. Effects of high pressure on molecules. 2000. Annual Reviews of Physical Chemistry. 51: 763.
5. Dattelbaum, D. M., and S. A. Sheffield. Shock-induced chemical reactions in simple organic molecules. 2012. (Chicago, IL, 26 June - 01 July 2011). Vol. 1426p. 627. Chicago, IL: American Institute of Physics.
6. Manner, V. W., S. A. Sheffield, D. M. Dattelbaum, and D. B. Stahl. Shock compression of formic acid. 2012. (Chicago, IL, 26 June - 01 July, 2011). Vol. 1426p. 201. Chicago, IL: American Institute of Physics.
7. Dang, N. C., C. A. Bolme, D. S. Moore, and S. D. McGrane. Shock Induced Chemistry In Liquids Studied With Ultrafast Dynamic Ellipsometry And Visible Transient Absorption Spectroscopy. 2012. Journal of Physical Chemistry A. 116 (42): 10301.
8. Cawkwell, M. J., and A. M. N. Niklasson. Energy Conserving, Linear Scaling Born-Oppenheimer Molecular Dynamics. 2012. Journal of Chemical Physics. 137: 134105.
9. Goodwin, P. M., B. Marshall, G. D. Stevens, and D. M. Dattelbaum. A Non-Invasive Method for Tracking the Position and Velocity of Gas Gun-Launched Projectiles Using External-Surface Transient Strain Measurements with Optical Fiber-Bragg Gratings. 2013. Review of Scientific Instruments. 84 (3): 035002.
10. Dremin, A. N., and L. V. Babare. The shock wave chemistry of organic substances. 1982. AIP Conference Proceedings. 78: 27.
11. Dremin, A. N., and L. V. Babare. On the shock polymerization process. 1984. Le Journal de Physique Colloques. 45: C8.
12. Vakushev, V. V., S. S. Nabatov, and O. B. Yakusheva. Physical properties and conversion of acrylonitrile at high dynamic pressures. 1974. Fizika Goreniya i Vzryva. 10: 583.
13. Sheffield, S. A., and G. E. Duvall. Response of liquid carbon disulfide to shock compression: equation of state

at normal and high densities. 1983. Journal of Chemical Physics. 79: 1981.

14. Sheffield, S. A.. Response of liquid carbon disulfide to shock compression. II. Experimental design and measured Hugoniot information. 1984. Journal of Chemical Physics. 81: 3048.

15. Dick, R. D.. Shock wave compression of benzene, carbon bisulfide, carbon tetrachloride, and liquid nitrogen. 1970. Journal of Chemical Physics. 52: 6021.

16. Dick, R. D.. Shock compression data for liquids. I. Six hydrocarbon compounds. 1979. Journal of Chemical Physics. 71: 3203.

17. Graham, R. A., and B. W. Dodson. Shock-induced organic chemistry. 1981. APS conference on shock waves in condensed matter. : 0.

18. Graham, R. A., and B. W. Dodson. Bibliography on shock-induced chemistry. 1980. Sandia National Laboratory Report SAND-80-1642.

19. Nellis, W. J., F. H. Ree, R. J. Trainor, A. C. Mitchell, and M. B. Boslough. Equation of state and optical luminosity of benzene, polybutene, and polyethylene shocked to 210 GPa (2.1 Mbar). 1984. Journal of Chemical Physics. 80: 2789.

20. Sheffield, S. A., D. M. Dattelbaum, R. R. Alcon, D. L. Robbins, D. B. Stahl, and R. L. Gustavsen. Shock-induced chemical reaction in organic and silicon-based liquids. 2006. AIP Conference Proceedings. : 921.

21. Sheffield, S. A., and R. R. Alcon. Shock-induced reaction in several liquids. 1989. American Physical Society topical conference on shock compression of condensed matter. : 683.

22. Niklasson, A. M. N.. Extended Born-Oppenheimer molecular dynamics. 2008. Physical Review Letters. 100: 123004.

23. Odell, A., A. Delin, B. Johansson, M. J. Cawkwell, and A. M. N. Niklasson. Geometric integration in Born-Oppenheimer Molecular Dynamics. 2011. Journal of Chemical Physics. 135: 224105.

24. Chellappa, R., and D. M. Dattelbaum. Hydrogen bonding in hydrazine to 20 GPa. Journal of Physical Chemistry.

25. Dattelbaum, D. M., S. A. Sheffield, J. D. Coe, and M. A. Margevicius. Shock-induced chemistry of phenylacetylene. J. Phys.: Conf. Series.

26. Chellappa, R. S., D. M. Dattelbaum, S. A. Sheffield, and D. L. Robbins. Pressure-induced polymerization in substituted acetylenes. 2012. (Chicago, IL, 26 June-01 July, 2011). Vol. 1426p. 1421. Chicago, IL: American Institute of Physics.

27. Dattelbaum, D. M., S. A. Sheffield, J. D. Coe, M. A. Margevicious, and M. J. Cawkwell. Shock-driven chemistry in phenylacetylene. to be submitted to Journal of Physical Chemistry.

28. Schulze, P. A., N. C. Dang, C. A. Bolme, K. E. Brown, and S. D. McGrane. Shock hugoniot equations of state for binary ideal (toluene/fluorobenzene) and non-ideal (ethanol/water) liquid mixtures. 2013. Journal of Physical Chemistry A. 117 (29): 6158.

29. McGrane, S. D., D. S. Moore, D. J. Funk, and R. L. Rabie. Spectrally modified chirped pulse generation of sustained shock waves. 2002. Applied Physics Letters. : 3919.

30. McGrane, S. D., D. S. Moore, and D. J. Funk. Sub-picosecond shock interferometry of transparent thin films. 2003. Journal of Applied Physics. : 5063.

31. Manner, V. W., R. S. Chellappa, S. A. Sheffield, Z. Liu, and D. M. Dattelbaum. High pressure far-infrared spectroscopic studies of hydrogen bonding in formic acid. 2013. Applied Spectroscopy. 67 (9): 1080.

Publications

Bishop, M. M., R. S. Chellappa, M. Pravica, J. D. Coe, Z. Liu, D. M. Dattelbaum, and Y. Vohra. 1,1-diamino-2,2-dinitroethylene under high pressure-temperature. 2012. Journal of Chemical Physics. 137 (17): 174304.

Cawkwell, M. J., E. J. Sanville, S. M. Mniszewski, and A. M. N. Niklasson. Self-Consistent Tight-binding Molecular Dynamics Simulations of Shock-Induced Reactions in Hydrocarbons. 2012. In American Physical Society Shock Compression of Condensed Matter Topical Group Meeting. (Chicago, IL, 26 June-01 July 2011). Vol. 1426, p. 1295. Chicago, IL: American Institute of Physics.

Cawkwell, M. J., E. J. Sanville, S. M. Mniszewski, and A. M. N. Niklasson. Computing the density matrix in electronic structure theory on graphics processing units. 2012. Journal of Chemical Theory and Computation. 2012 (8): 4094.

Cawkwell, M. J., and A. M. N. Niklasson. Energy Conserving, Linear Scaling Born-Oppenheimer Molecular Dynamics. 2012. Journal of Chemical Physics. 137: 134105.

Chellappa, R. S., D. M. Dattelbaum, N. Velisavljevic, and S. A. Sheffield. The phase diagram of ammonium nitrate. 2012. Journal of Chemical Physics. 137: 064504.

Chellappa, R. S., D. M. Dattelbaum, S. A. Sheffield, and D. L. Robbins. Pressure-induced polymerization in substituted acetylenes. 2012. In American Physical Society Shock Compression of Condensed Matter Topical Group meeting. (Chicago, IL, 26 June-01 July, 2011). Vol. 1426, p. 1421. Chicago, IL: American Institute of Physics.

Chellappa, R., and D. M. Dattelbaum. Hydrogen bonding in hydrazine to 20 GPa. Journal of Physical Chemistry.

Dang, N. C., C. A. Bolme, D. S. Moore, and S. D. McGrane. Shock Induced Chemistry In Liquids Studied With Ultrafast Dynamic Ellipsometry And Visible Transient Absorption Spectroscopy. 2012. Journal of Physical Chemistry A. 116 (42): 10301.

Dang, N. C., C. A. Bolme, D. S. Moore, and S. D. McGrane. Temperature measurements in condensed phases using non-resonant femtosecond stimulated Raman scattering. 2013. Journal of Raman Spectroscopy. 44 (3): 433.

Dattelbaum, D. M., R. S. Chellappa, P. R. Bowden, J. D. Coe, and M. A. Margevicious. Chemical stability of molten 2,4,6-trinitrotoluene at high pressure. Applied Physics Letters.

Dattelbaum, D. M., S. A. Sheffield, J. D. Coe, M. A. Margevicious, and M. J. Cawkwell. Shock-driven chemistry in phenylacetylene. to be submitted to Journal of Physical Chemistry.

Dattelbaum, D. M., S. A. Sheffield, J. D. Coe, and M. A. Margevicius. Shock-induced chemistry of phenylacetylene. J. Phys.: Conf. Series.

Dattelbaum, D. M., and S. A. Sheffield. Shock-induced chemical reactions in simple organic molecules. 2012. In American Physical Society Shock Compression of Condensed Matter Topical Group meeting. (Chicago, IL, 26 June - 01 July 2011). Vol. 1426, p. 627. Chicago, IL: American Institute of Physics.

Davidson, A., R. Chellappa, D. M. Dattelbaum, and C. S. Yoo. Pressure-induced isostructural metastable phase transition of ammonium nitrate. 2011. Journal of Physical Chemistry. 115: 11889.

Davidson, A., R. Dias, C. S. Yoo, and D. M. Dattelbaum. “Stubborn” Triaminotrinitrobenzene (TATB): Unusually High Chemical Stability of a Molecular Solid to 150 GPa . 2011. J. Chem. Phys.. 135: 174507.

Goodwin, P. M., B. Marshall, G. D. Stevens, and D. M. Dattelbaum. A Non-Invasive Method for Tracking the Position and Velocity of Gas Gun-Launched Projectiles Using External-Surface Transient Strain Measurements with Optical Fiber-Bragg Gratings. 2013. Review of Scientific Instruments. 84 (3): 035002.

Manner, V. W., R. S. Chellappa, S. A. Sheffield, Z. Liu, and D. M. Dattelbaum. High pressure far-infrared spectroscopic studies of hydrogen bonding in formic acid. 2013. Applied Spectroscopy. 67 (9): 1080.

Manner, V. W., S. A. Sheffield, D. M. Dattelbaum, and D. B. Stahl. Shock compression of formic acid. 2012. In American Physical Society Shock Compression of Condensed Matter Topical Group meeting. (Chicago, IL, 26 June - 01 July, 2011). Vol. 1426, p. 201. Chicago, IL: American Institute of Physics.

Niklasson, A. M. N., and M. J. Cawkwell. Fast Quantum Molecular Dynamics. 2012. Physics Review B. 86 (17): 174308.

Odell, A., A. Delin, B. Johansson, M. J. Cawkwell, and A. M. N. Niklasson. Geometric integration in Born-Oppenheimer Molecular Dynamics. 2011. Journal of Chemical Physics. 135: 224105.

Schulze, P. A., N. C. Dang, C. A. Bolme, K. E. Brown, and S. D. McGrane. Shock hugoniot equations of state for binary ideal (toluene/fluorobenzene) and non-ideal (ethanol/water) liquid mixtures. 2013. Journal of Physical Chemistry A. 117 (29): 6158.

Innovative and Validated Sub-micron to Meso-scale Modeling of the Evolution of Interface Structure and Properties under Extreme Strains

Irene J. Beyerlein
20110029DR

Abstract

Nanocomposite materials are an exciting class of materials that have proven to be ten times stronger, more corrosion and radiation resistant than traditional metals [1,2]. These are bulk-sized composites comprised internally of nano-sized metallic crystals and a high density of bi-metal interfaces. As materials for next generation applications are expected to push the envelope and exhibit predictable lifetime performance in extreme environments for longer service-lives than are attainable with today's materials, nanostructured composite metals have become an attractive candidate.

Designing nanostructural materials for operation in extreme environments for future energy and defense applications requires the development of a predictive capability for both material synthesis and mechanical performance. In this program, we developed innovative synthesis and multi-scale modeling techniques for two-phase metal composites. Both techniques will for the first time permit development of scientifically guided synthesis routes needed for a targeted set of desired interfacial properties.

Background and Research Objectives

Metals need to be far stronger and more thermally stable than those in use today in order to have a profound impact on energy efficiency in future automotive, aircraft, power generation, and nuclear and non-nuclear military and defense applications. A promising way forward has been to shrink the grain size of metals down to nanoscale dimensions.

Nanostructuring via severe plastic deformation (SPD) has become a popular way of fabricating nanomaterials in structural size scales [3,4]. This grain refining technique is a top-down process that can transform a traditional coarse-grained metal to a nanocrystalline metal without changing the original dimensions of the sample [3]. Experiments have shown that the resulting increases in the fraction of grain boundaries can lead to several-fold increases in strength [2,3]. Impressive though this result may be, the grain boundaries created by mechanical processing are disordered (high energy, tangled networks of defects) [3] and unstable in high temperatures. Consequently, they do not retain their superior strength in high temperature.

Our objective in this project was to develop a multi-scale model for processing of two-phase composites. The model aimed to predict the processing route that provides for the 'right' interfaces—those that are stable in strain and at high temperature. Unlike prior work using SPD on one metal, we applied a SPD process to a composite consisting of two dissimilar metals. The idea is that compared to grain boundaries, the bimetal interfaces would be much more stable under elevated temperatures and when spaced several nanometers apart, would be effective barriers to dislocation motion. Ultimately, the model designs the interfaces needed for creating a strong and thermally stable nanostructured metal.

Scientific Approach and Accomplishments

Our scientific approach consisted of developing a novel processing technique for making bulk nanomaterials and a multi-scale processing model for designing the routes taken by this technique.

Regarding this first, we fabricated Cu-Nb nanocomposite materials in bulk form (>cm3) with a processing technique called accumulative roll bonding (ARB) [2,4]. To prevent the introduction of oxides to the interfaces, a specially designed ARB process was used [2]. Our ARB process delivers two-phased (Cu-Nb) samples with controllable layer thicknesses from submicron to the nanoscale (down to 10 nm) [5,6]. Figure 1 shows many typical nanolayered microstructures manufactured by this technique. The samples shown differ in the spacing between the Cu-Nb interfaces [5-7]. The size of the samples from which these micrographs were taken was

several orders of magnitude larger (cm3). Therefore, the ARB process combines an unprecedented level of control of nm-scale structure with the ability to fabricate large volumes of material.

For the second technique, we developed the first two-phase composite crystal plasticity finite element model [8,9]. Displacement and traction continuity are enforced at the interface throughout deformation. In this way, the interface provides a 'kinematic constraint' on the deformation of the two adjoining crystals, just as in the experiment. While the total deformation state is two-dimensional (i.e., plane strain condition of the ARB process), the deformation of the crystals is fully three-dimensional (out-of-plane plastic deformation is allowed). The constitutive laws used for both Cu and Nb follow an anisotropic elastic and rate-dependent crystal plasticity formulation, which is given in [9]. Plastic deformation is accommodated by dislocation glide and normal slip is assumed, wherein slip system activation is correlated with the resolved shear stress. Our model employs slip system flow kinetics based on the notion of thermally activated dislocation glide. In this classical scenario, dislocations glide from one pinning point to another and use a combination of thermal activation and mechanical stress to overcome each pinning site. In the Cu-Nb bicrystal simulations that follow, we make available the 12 {111}<110> slip systems in Cu and the 12 {110}<111> slip systems and 12 {112}<111> slip systems in Nb [28]. The thermal activation slip rate model introduces material parameters for each allowable slip family in Cu and in Nb. The calibrated material parameters are given in [9] and were determined by fitting to a large suite of tests with widely varying temperature and strain rate.

Together with these two techniques we made the following three accomplishments:

Accomplishment #1: We discovered that nanocomposites with stable interfaces can evolve from extreme mechanical deformation. The textures of these nanocomposites were measured by neutron diffraction at LANL's LANSCE facility [4]. The remarkable findings were that the textures were unusually sharp and significantly different from the theoretical rolling textures expected of Cu or Nb alone. We further analyzed via TEM the nanocomposite interfaces at different stages in the SPD process [10]. Remarkably, in spite of exposure to extreme straining, the same interface prevailed over the entire sample and exhibited a regular structure at the atomic level (Figure 2). We also proved that the interfaces were stable up to 600 C, which is half the melting temperature of Cu [10]. Our demonstration that nanocomposites with stable interfaces can evolve from extreme mechanical deformation promotes development of innovative manufacturing methods for novel metals in sizes suitable for car bodies and aircraft and structures in nuclear reactors.

Accomplishment #2: The evolution to a predominant interface seen above is not anticipated. It is not expected that an SPD process can actually lead to ordered interfaces. We hypothesized that the interface characters that are mechanically stable (that is preferred in SPD) are associated with plastically stable orientations on both sides of the interface and low formation energy interfaces. These two things need to be satisfied concurrently, plastic stability in both orientations and creation of low energy interfaces, which imposes a severe constraint on which interfaces will be stable.

To study the plastic stability of interfaces during rolling of Cu-Nb, our multi-scale model was employed to model texture evolution during rolling [9]. An elastically anisotropic and rate-dependent plasticity law was employed for both Cu and Nb [9]. Cu was assumed to deform on the {111}<110> slip systems and Nb on both the {110}<111> and {112}<111> slip systems.

For validation, we first tested the model on traditional composites, containing relatively thick micron scale Cu and Nb layers, where several grains span an individual layer, measured textures corresponded to the theoretical textures of rolling Cu or Nb alone [4]. The CPFE model [9] in Figure 3 was able to effectively predict this texture development in both the Cu and Nb phases within a two-phase Cu-Nb multilayer, containing only a few grains through-thickness. More details on the model development and experiments used for input and validation can be found in [9].

Once validated, we applied the model to the nanolayered Cu-Nb composite comprised of alternating single crystalline layers [8]. Consistent with experiment, the interfaces were enforced to maintain compatibility at all times during deformation. Using this model geometry, the rolling stability of many interface characters was tested [8] and of these a handful were found to be mechanically stable and maintain their character to within 10 degrees. Specifically, for the {112}fcc||{112}bcc KS interface the Cu crystal tilted ~6º and the Nb ~3º about the TD. As confirmation, deviations of up to 10º from {112}Cu||{112} Nb KS interfaces have been reported in the actual samples [11,12]. The most stable interface tested was the {110}<001>Cu||{112}<110>Nb interface, which begins to emerge at the finest scales, 10 nm [10] (Figure 4). For these same interfaces, we calculated the corresponding formation energy using molecular dynamics. In plotting on a map the formation energy and plasticity stability for all interfaces, see Figure 5, we found that the most stable

interfaces seen experimentally lay in a 'regime' of stability with low formation energy and high plastic stability. This newly discovered "regime of mechanical interface stability" can be explored to design synthesis techniques for nanocomposites

Accomplishment #3: Based on the two foregoing accomplishments, we were able to further demonstrate that it is possible to achieve atomic-level tuning of material interfaces via macro-level control of the manufacturing process. Combining our new modeling tools and synthesis techniques, we predicted that either atomically faceted or atomically flat interfaces can be successfully created in bulk nano-laminar Cu-Nb composites via severe plastic deformation (SPD). As mentioned earlier, this would not have been thought possible before since usually SPD techniques leave internal interfaces thermally unstable and structurally disordered. We confirmed our hypothesis by demonstrating in the laboratory that interfaces can be tailored to be atomically regular in structure. We then carried out mechanical and thermal stability tests to prove that the nanostructured materials we designed possessed a combination of superior strength and thermal stability. This third accomplishment implies that improvement in thermal stability of the material can be achieved by optimizing the manufacturing processes. The ability to alter the manufacturing route to create two significantly different interfaces that produce outstanding performance is unprecedented.

Impact on National Missions

The results of our project will have the following impacts on national missions.

First, our demonstration that interfaces can be tuned via extreme mechanical deformation promotes development of innovative manufacturing methods for novel metals eventually in sizes suitable for car bodies and aircraft.

Second, the knowledge and modeling capability provided by this program will enable design and synthesis of a new class of advanced materials by methods that are no longer prohibitively expensive or incapable of producing sufficient material quantities.

Third, the predictive tools developed will accelerate the development of interface-dominant materials by reducing the number of experimental iterations and laboratory tests required to bring them into practice, impacting a wide range of industries: automotive, aircraft and power generation turbines, and both nuclear and non-nuclear military and defense applications.

Fourth, the President's Council of Advisors for Science and Technology very recently issued the "Report to the President on Capturing Domestic Competitive Advantage in Advanced Manufacturing". Our research is aligned with their recommendation to increase R&D funding in "Advanced Materials Design, Synthesis and Processing" and "Nanomanufacturing" for ultra-strong, lightweight materials that could have future implications for private business and address manufacturing challenges in the private sector. Additionally, this research more than ever answers the recent 2012 DOE-BES report entitled "From Quanta to the Continuum: Opportunities for the Mesoscale" and their priority research directions is "Mastering Defect Mesostructure and its Evolution" with science that controls meso-scale behavior by understanding defect structures and their underlying mechanisms.

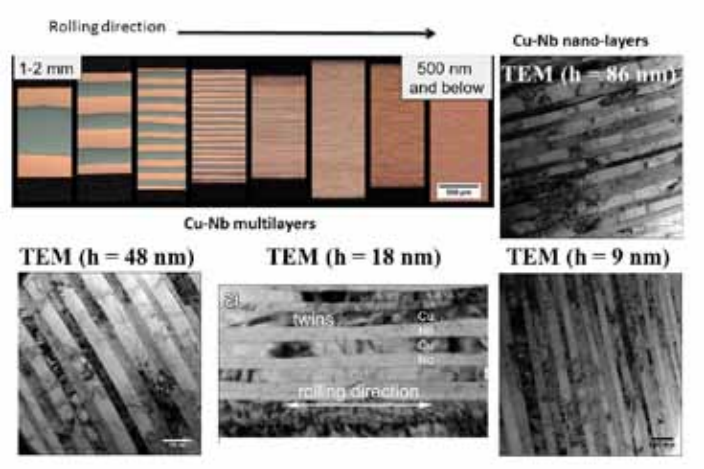

Figure 1. Multilayered Cu-Nb composite fabricated by our specially designed accumulative roll bonding technique.

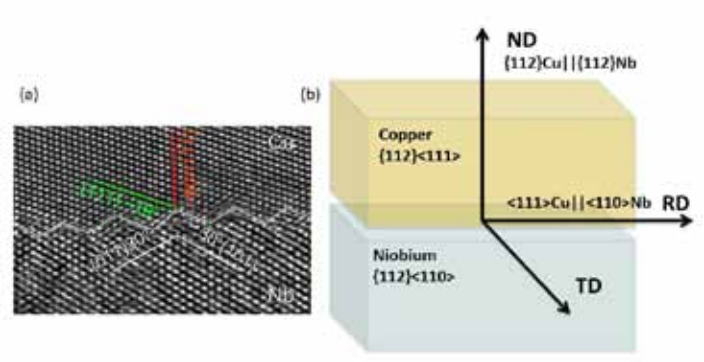

Figure 2. (a) high resolution transmission electron micrograph of the {112}fcc||{112}bcc <110>fcc||<111>bcc interface prevailing in the ARB Cu-Nb nanolayered composites and a (b) schematic of this interface.

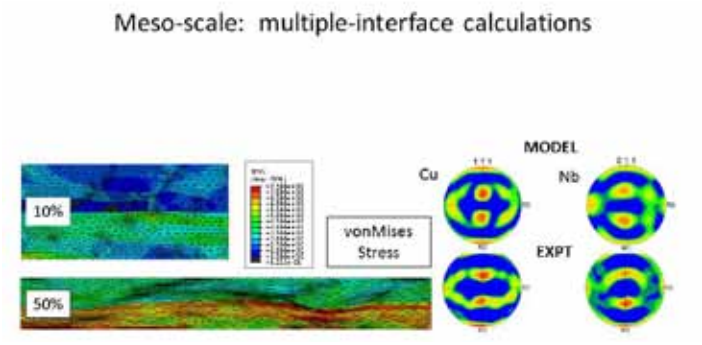

Figure 3. Crystal plasticity finite element calculation of Cu-Nb multilayer composite in rolling (a) Inhomogeneous deformation fields during deformation. Calculation shown assumes that the Cu-Nb interfaces are kinematically constrained to remain bonded during deformation and (b) agreement with measurements of texture development.

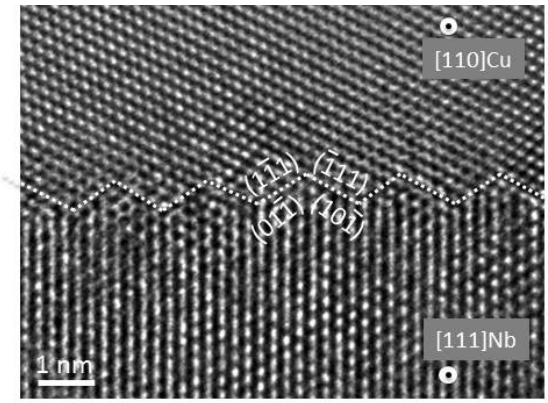

Figure 4. Most stable interface predicted and made by our program

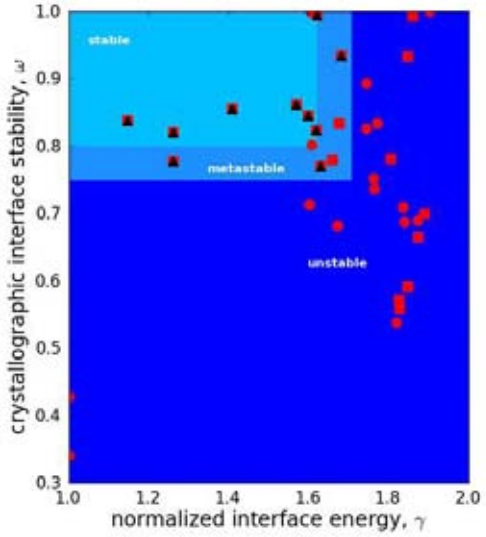

Figure 5. Map plotting a measure of plastic stability against interface formation energy. The most stable interfaces are found in the top left hand corner of the map. In agreement, interfaces produced by our synthesis technqiue fall in this regime of the map.

References

1. Misra, A., and R. G. Hoagland. Effects of elevated temperature annealing on the structure and hardness of copper/niobium nanolayered films. 2005. Journal of Materials Research. 20: 2046.

2. Hansen, B. L., J. S. Carpenter, S. D. Sintay, C. A. Bronkhorst, R. J. McCabe, J. R. Mayeur, H. M. Mourad, I. J. Beyerlein, N. A. Mara, S. R. Chen, and G. T. Gray. Modeling the texture evolution of Cu/Nb layered composites during rolling. 2013. INTERNATIONAL JOURNAL OF PLASTICITY. 49: 71.

3. Valiev, R. Z., and T. G. Langdon. Principles of equal-channel angular pressing as a processing tool for grain refinement. 2006. PROGRESS IN MATERIALS SCIENCE. 51 (7): 881.

4. Carpenter, J. S., S. C. Vogel, J. E. LeDonne, D. L. Hammon, I. J. Beyerlein, and N. A. Mara. Bulk texture evolution of Cu-Nb nanolamellar composites during accumulative roll bonding. 2012. ACTA MATERIALIA. 60 (4): 1576.

5. Zheng, S. J., I. J. Beyerlein, J. Wang, J. S. Carpenter, W. Z. Han, and N. A. Mara. Deformation twinning mechanisms from bimetal interfaces as revealed by in situ straining in the TEM. 2012. ACTA MATERIALIA. 60 (16): 5858.

6. Carpenter, J. S., R. J. McCabe, I. J. Beyerlein, T. A. Wynn, and N. A. Mara. A wedge-mounting technique for nanoscale electron backscatter diffraction. 2013. JOURNAL OF APPLIED PHYSICS. 113 (9): -.

7. Beyerlein, I. J., N. A. Mara, J. S. Carpenter, T. Nizolek, W. M. Mook, T. A. Wynn, R. J. McCabe, J. R. Mayeur, K. Kang, S. J. Zheng, J. Wang, and T. M. Pollock. Interface-driven microstructure development and ultra high strength of bulk nanostructured Cu-Nb multilayers fabricated by severe plastic deformation. 2013. JOURNAL OF MATERIALS RESEARCH. 28 (13): 1799.

8. Mayeur, J. R., I. J. Beyerlein, C. A. Bronkhorst, H. M. Mourad, and B. L. Hansen. A crystal plasticity study of heterophase interface character stability of Cu/Nb bicrystals. 2013. INTERNATIONAL JOURNAL OF PLASTICITY. 48: 72.

9. Hansen, B. L., J. S. Carpenter, S. D. Sintay, C. A. Bronkhorst, R. J. McCabe, J. R. Mayeur, H. M. Mourad, I. J. Beyerlein, N. A. Mara, S. R. Chen, and G. T. Gray. Modeling the texture evolution of Cu/Nb layered composites during rolling. 2013. INTERNATIONAL JOURNAL OF PLASTICITY. 49: 71.

10. Zheng, S. J., I. J. Beyerlein, J. S. Carpenter, K. W. Kang, J. Wang, W. Z. Han, and N. A. Mara. High-strength and thermally stable bulk nanolayered composites due to twin-induced interfaces. 2013. NATURE COMMUNICATIONS. 4: -.

11. Kang, K., J. Wang, and I. J. Beyerlein. Atomic structure variations of mechanically stable fcc-bcc interfaces. 2012. JOURNAL OF APPLIED PHYSICS. 111 (5): -.

12. Carpenter, J. S., X. Liu, A. Darbal, N. T. Nuhfer, R. J. McCabe, S. C. Vogel, J. E. LeDonne, A. D. Rollett, K. Barmak, I. J. Beyerlein, and N. A. Mara. A comparison of texture results obtained using precession electron diffraction and neutron diffraction methods at diminishing length scales in ordered bimetallic nanolamellar composites. 2012. SCRIPTA MATERIALIA. 67 (4): 336.

Publications

Al-Maharbi, M., I. Karaman, I. J. Beyerlein, D. Foley, K. T. Hartwig, L. J. Kecskes, and S. N. Mathaudhu. Microstructure, crystallographic texture, and plastic anisotropy evolution in an Mg alloy during equal channel angular extrusion processing. 2011. Materials Science and Engineering A. 528 (25-26): 7616.

Beyerlein, I. J., N. A. Mara, J. Wang, J. S. Carpenter, S. J. Zheng, W. Z. Han, R. F. Zhang, K. Kang, T. Nizolek, and T. M. Pollock. Structure-Property-Functionality of Bimetal Interfaces. 2012. Journal of Materials. 64: 1192.

Carpenter, J. S., S. C. Vogel, J. LeDonne, D. L. Hammon, I. J. Beyerlein, and N. A. Mara. Bulk texture evolution of Cu-Nb nanolamellar composites during accumulative roll bonding. 2012. Acta Materialia. 60: 1576.

Carpenter, J. S., X. Liu, A. Darbal, N. T. Nuhfer, R. J. McCabe, S. C. Vogel, J. E. LeDonne, A. D. Rollett, K. Barmak, I. J. Beyerlein, and N. A. Mara. A comparison of texture results obtained using precession electron diffraction and neutron diffraction methods at diminishing length scales in ordered bimetallic nanolamellar composites. 2012. Scripta Materialia. 67: 336.

Chen, X., I. J. Beyerlein, and L. C. Brinson. Bridged crack models for the toughness of composites reinforced with curved nanotubes. 2011. Journal of the Mechanics and Physics of Solids. 59 (9): 1938.

Chu, H. J., C. Zhou, J. Wang, and I. J. Beyerlein. An analytical model for the critical shell thickness in core/shell nanowires based on crystallographic slip. 2012. Journal of the Mechanics and Physics of Solids. 60: 418–431.

Chu, H. J., E. Pan, J. Wang, and I. J. Beyerlein. Three-dimensional elastic fields due to a dislocation loop in an anisotropic bi-material . 2012. Journal of Applied Mechanics. 79: 021011.

Chu, H. J., E. Pan, J. Wang, and I. J. Beyerlein. Three-dimensional elastic displacements induced by a dislocation of polygonal shape in anisotropic elastic crystals . 2011. International Journal of Soilds and Structures. 48: 1164.

Chu, H. J., E. Pan, X. Han, J. Wang, and I. J. Beyerlein. Elastic fields of dislocation loops in three-dimensional anisotropic bi-materials. 2012. Journal of the Mechanics and Physics of Solids. 60: 418.

Chu, H. J., J. Wang, C. Z. Zhou, and I. J. Beyerlein. Misfit Strain Relaxation Mechanisms in Core/Shell Nanowires. 2013. Journal of Materials. 64: 1227.

Chu, H. J., J. Wang, C. Zhou, and I. J. Beyerlein. Self-energy of elliptical dislocation loops in anisotropic crystals and its application for defect-free core/shell nanowires. 2011. Acta Materialia. 59: 7114.

Chu, H. J., J. Wang, I. J. Beyerlein, and E. Pan. Anisotropic Bimaterial Models Incorporating Atomistic-scale Physics for the Interfaces-Dislocation Interactions using Green's Function Method. 2013. International Journal of Plasticity. 41: 1.

Chu, H. J., J. Wang, and I. J. Beyerlein. Anomalous reactions of a supersonic coplanar dislocation dipole: bypass or twinning?. 2012. Scripta Materialia. 67: 69.

Hansen, B. L., J. S. Carpenter, S. D. Sintay, C. A. Bronkhorst, R. J. McCabe, J. R. Mayeur, H. M. Mourad, I. J. Beyerlein, N. A. Mara, S. R. Chen, and G. T. Gray III. Modeling the Texture Evolution of Cu/Nb Layered Composites during Rolling . 2013. International Journal of Plasticity. 49: 71.

Hunter, A., I. J. Beyerlein, T. C. Germann, and M. Koslowski. Influence of the stacking fault energy surface on extended partials with a 3D phase field dislocations model. 2011. Physical Review B. 84 (14): 144108.

Kang, K., J. Wang, S. J. Zheng, and I. J. Beyerlein. Minimum energy structures of faceted, incoherent interfaces. 2012. Journal of Applied Physics. 112: 073501.

Kang, K., J. Wang, and I. J. Beyerlein. Atomic structure variations of mechanically stable interfaces. 2012. Journal of Applied Physics. 111: 053531.

Lee, S. B., J. E. LeDonne, S. C. V. Lim, I. J. Beyerlein, and A. D. Rollett. The five-parameter Heterophase Interface Character Distribution (HICD) of physical vapor-deposited and accumulative roll-bonded Cu-Nb multilayer composites. 2012. Acta Materialia. 60: 1747.

Mara, N. A., I. J. Beyerlein, J. S. Carpenter, and J. Wang. Interfacially driven deformation twinning in bulk Cu-Ag composites. . 2012. Journal of Materials. 64: 1218.

Mayeur, J. R., I. J. Beyerlein, C. A. Bronkhorst, H. M. Mourad, and B. L. Hansen. A crystal plasticity study of interfacial stability of CuNb bicrystals. 2013. International Journal of Plasticity. 48: 72.

Wang, J., I. J. Beyerlein, N. A. Mara, and D. Bhattacharyya. Interface-facilitated deformation twinning in copper within submicron Ag-Cu multilayered composites. 2011. Scripta Materialia. 64: 1083.

Wang, J., K. Kang, R. F. Zhang, S. J. Zheng, I. J. Beyerlein, and N. A. Mara. Structure and property of interfaces in ARB Cu/Nb laminated composites. 2012. Journal of Materials. 64: 1208.

Xu, X. F., K. Hu, I. J. Beyerlein, and G. Deodatis. Statistical strength of hierarchical carbon nanotube composites. 2011. International Journal for Uncertainty Quantification. 1 (4): 279.

Zhou, C., I. J. Beyerlein, and R. LeSar. Plastic deformation mechanisms of FCC single crystals at small scales. 2011. Acta Materialia. 59 (20): 7673.

Next Generation Ionic Liquids for Plutonium Science, Separation, and Production

George S. Goff
20110083DR

Abstract

Most experts agree that nuclear energy will continue to play a significant role throughout the 20th century and beyond, yet the key to sustainable nuclear power lies in the proper management of nuclear waste. Whether looking at the direct disposal of used nuclear fuel (UNF) or reprocessing and recycling of U (and/or Pu and the minor actinides), disposition and stability of Pu waste forms, formation of advanced reactor fuels, or the purification of Pu for weapons applications, understanding the underlying chemistry of Pu is vital for an accurate evaluation of nuclear fuel cycle options and responsible stewardship of our existing stockpile of nuclear weapons.

Ionic liquids (ILs) are low-melting salts, often containing an asymmetrical organic cation and an organic or inorganic anion. There is an emerging interest in ILs for potential applications in the separation of actinides from UNF, electrochemical separation of actinide ions, and solid-state coordination studies of the actinides. Due to the wide range of tunable physical properties, ILs have the potential to stabilize unusual oxidation states and unique structural motifs not readily accessible in conventional aqueous media. The chemistry of Pu in ionic liquids remains a highly undeveloped field, with the potential to discover revolutionary separation schemes to displace currently used separation technologies. Our research program combined experimental measurements and theoretical modeling to develop the requisite structural, thermodynamic, and kinetic parameters needed to evaluate the feasibility of using ionic liquids for separating plutonium from a variety of matrices.

Background and Research Objectives

Conventional processing of used nuclear fuel is based on the 60-year-old, aqueous/organic PUREX process to partition the actinides and fission products. This process is highly complex, has a large facility footprint, and employs organic diluents and extractants which are susceptible to radiation damage. Pyrochemical processing was developed during the 1940-50s to produce Pu metal for weapons applications. Later, this technology was investigated for use in partitioning the actinides from metal reactor fuels, and is one of the three production-scale techniques currently used at the Plutonium Facility at TA-55 for the production of plutonium metal [1]. Pyroprocessing of nuclear materials generally involves dissolution into molten salts (generally a mixture of alkali or alkaline earth chlorides or fluorides) at temperatures above 500°C, followed by selective recovery of actinides by electroreduction at the cathode [2]. Several disadvantages have prevented pyroprocessing from replacing PUREX including high temperature operations, batch operation, highly corrosive solvents, and lower decontamination factors [2]. More recently, ILs have been proposed as alternative solvents for liquid-liquid extractions [3-6] and as electrolyte solutions for the electrodeposition of transition metals and actinides including reprocessing of used nuclear fuel [5, 7, 8]. Identifying ILs with sufficient radiation stability, solubility, and electrochemical windows for performing U and Pu electroplating would revolutionize conventional pyroprocessing technologies.

Nearly all early studies of actinides in ILs used the first generation haloaluminate ILs [5, 9, 10]. These ILs generally have a low solubility for U, and electrochemical windows that are insufficient to electroplate either U or Np metals, and thus are not suitable for process applications.[5] Since the discovery of water-stable second generation ILs in the mid 1990s, ILs have been studied to be used as solvents for separations, catalysis, and in electrolytic processes, due to their negligible vapor pressure, non-flammability, low corrosivity, and wide range of thermal stability and electrochemical windows (up to 6 V compared to 2-3 V for water) [11].

In contrast to aqueous and conventional organic solutions, solvation of metal cations is a critical process in ILs that determines the effective charge and thermodynam-

ic properties of the cationic metal complex. Model predictions indicate solvation of the metal cations occurs via the formation of subsequent alternating shells of IL-anions and cations, but there is currently no experimental validation of these results. Solvation mechanisms have been studied by ab initio molecular dynamics simulations for U and Eu, but no studies have been performed for the transuranium elements.

Studies on the radiation stability of ILs remain rare and radiolysis products for most ILs are not well known. An early study with 1,3-alkylmethylimidazolium chloride (C2, C4, and C6mmim) and nitrate showed a 15 times higher stability than tributyl phosphate/kerosene solvents (used in PUREX) when subjected to alpha and gamma radiation [12]. More recently, imidazolium, pyridininium, and quaternary ammonium ILs showed less than 1% decomposition when exposed to gamma-radiation dose equivalent to 1 year of processing used nuclear fuel [13]. While the bulk IL showed strong radiation stability, all ILs investigated showed an increase in the UV-vis absorption spectra and a narrowing of the electrochemical window. Data in the literature are insufficient to understand radiolysis mechanisms or predict stability for a given structure.

Scientific Approach and Accomplishments

This LDRD project focused on understanding the fundamental chemical and physical phenomena such as solvation, solubility, electronic structure of f-element complexes, and electrochemical reduction and plating processes. Specifically, this project focused on identifying ionic liquids suitable for electrochemically separating Pu from the other light actinides (Th, U, Np, Am, Cm) as well as the light actinides from the lanthanides. We employed a multifaceted approach to study the structural, thermodynamic, and kinetic behavior of Pu in ILs in order to demonstrate the feasibility of using ILs for advanced Pu separations. Our approach combined single-crystal X-ray diffraction studies with a variety of spectroscopic tools (UV-vis-NIR, FT-IR, Raman, NMR) to probe the behavior of actinides in ILs. Our efforts utilized both conventional ILs as well as functionalized ILs that incorporated metal centers into the structure of the IL to improve solubility and tune the electrochemical window for separations. Molecular modeling was integrated with experiments by using measured results to validate calculations, and calculations were used to identify appropriate IL candidates for experimental studies. Quantum mechanical calculations enabled us to understand the stability, solvation, redox behavior, spectroscopic signatures, and electronic structures of actinide complexes. The following sections briefly describe some of the scientific highlights of our work.

Synthesis and Characterization of Novel ILs and Actinide Compounds: This project has synthesized and characterized a number of novel ILs containing functional groups to complex actinides. One approach was to incorporate into the structure of the ionic liquids ligands that have traditionally been used as actinide or lanthanide separating agents. Oxalate has long been used as a precipitating agent for Pu, and a number of ILs containing the oxalate anion were synthesized (manuscript in preparation). These ILs had very high viscosities, making them impractical for most applications, which was largely overcome by decreasing the size of the cation or protonating the oxalate anion to the monovalent bioxalate anion. Alpha-hydroxyisobutyric acid (HIBA) is a characteristic human metabolite which has long been used to separate individual actinides and lanthanides from complex mixtures. Despite being used in lanthanide separations for over 55 years, prior to our work there was only one reported crystal structure for lanthanide-HIBA complex. We were able to isolate lanthanide-HIBA complexes across the lanthanide series which were characterized by both single crystal and powder X-ray diffraction studies [14]. ILs were synthesized using HIBA as the anion, and also tethered to a quaternary amine in the cation. Preliminary results indicate coordination of the actinides to the HIBA group, which would allow us to tune whether the metal center is incorporated into the cation or the anion of the IL.

A number of other novel ILs were synthesized which contain a carboxyl group in the cation. Most previous work was focused on ammonium-based cations, which gave fairly narrow electrochemical windows and possess melting points above room temperature. We improved upon these ILs by changing the nitrogen center in the cation to a phosphorous center [15]. The carboxyl-functionalized phosphonium ionic liquid (IL), [HCTMP][Tf2N], enabled the directed nucleation of either monomeric or dimeric uranyl(VI) compounds, shown in Figure 1. This new IL is the first carboxyl-functionalized IL which is liquid at room temperature and exhibits a wider electrochemical window and lower melting point than its ammonium analogue. Melting points for the monomeric and dimeric uranium compounds were both below 100°C, making these the first confirmed uranium-based ILs reported in the literature.

Molecular Dynamics of Actinides in ILs: Molecular dynamics (MD) simulations of actinide-containing materials can provide valuable information about the interactions between actinides and ionic liquids which can be difficult to obtain experimentally. MD simulations can directly compute properties such as viscosities and electrical conductivities, phase equilibria (liquid-liquid or solid-liquid), and the partitioning of ions between different phases. The accuracy

of these simulations depends solely on the ability of the force field (model interaction potential) to mimic the true interaction potential of the system. The number of force fields available to model molecular interactions in common actinide systems is minuscule to non–existent and most were developed and optimized to study solid uranium oxides. In collaboration with the University of Notre Dame, a set of classical potentials was developed to model interactions with water with uranium, neptunium, plutonium, and americium in the +V and +VI oxidation states [16]. These are the first reported potentials for Np, Pu, and Am. These potentials were utilized in MD simulations to predict the interactions of uranyl(V/VI) and plutonyl(V/VI) with water in ionic liquids,[17] and the results were validated by spectroscopic measurements. Figure 2 shows the competition between water and the anion of the IL to complex the actinide over a range of water concentrations. This project established the ability to perform MD simulations on actinides in ILs, as well as to successfully predict the speciation of an actinide in a complex multi-component environment for the first time.

Prediction of Electrochemical Windows of ILs: At the beginning of this project, computational methods existed to predict certain physical properties of ILs, but there were no methods to predict the electrochemical stability. The electrochemical window corresponds to the range of voltages that can be applied to an IL before it irreversibly decomposes (e.g. the cation will reduce and the anion will oxidize). Having a predictive capability to accurately describe the redox behavior of an IL is key to being able to identify and screen and develop novel ILs with an electrochemical window wide enough to allow the electroplating of Pu. Modeling IL systems is more challenging than standard polarizable solvents (such as water), which can be adequately described with a polarizable continuum model. Due to the low dielectric constants and the ionized nature of ILs, the response due to a change in oxidation state is the rearrangement of the solvent environment rather than a change in polarization. Our methodology for predicting the electrochemical window uses a combination of quantum-mechanics and molecular mechanics (QM/MM) approaches in order to be able to explicitly simulate a large region of the solvent. A single anion-cation pair is simulated using QM and the surrounding environment is modeled with MM, for which force-fields have been developed previously by other authors. With this approach we have successfully calculated electrochemical windows in good agreement with experimental data for a range of conventional ILs [18], and a manuscript is in preparation expanding this methodology to ILs containing functional groups such as carboxylate. This work successfully established the methodology to predict electrochemical windows for ILs for a wide range of applications beyond Pu separations, including other areas of interest such as lithium batteries and fuel cells.

Electrochemistry of Actinides and Lanthanides in ILs: Electrochemical studies performed under this LDRD project had several specific goals including identifying ILs with sufficient electrochemical windows to allow for deposition of actinides, understanding how to manipulate ILs to extend the ECWs to enable electroplating, and identifying minimum potentials and temperatures for An plating from these ILs. We have identified a number of ILs with sufficiently broad electrochemical windows to enable electrorecovery of actinides. Most studies were performed using the bistriflimide anion, which has exceptional (electro) chemical stability and only weakly coordinates the actinide centers. Cyclic voltammetry studies for U and Pu in piperidinium- and imidazolium-based ILs reveal a series of ill-defined reduction peaks and quasi-reversible stripping peaks. Bulk deposition experiments indicate that both U and Pu can be recovered from ILs. Under most conditions the bulk deposits, such as those shown in Figure 3, are amorphous. Annealing the samples improves the crystallinity, and X-ray diffraction and SEM/EDX characterization reveal this deposit to be UO2. Studies with lanthanides, which are important fission products in used nuclear fuel, show that the lanthanides are significantly more difficult to electroplate, and studies with mixed samples of U and lanthanides indicate the feasibility of selectively recovering the U while the lanthanides remain in solution. This provides the scientific basis for a possible IL-based electrorecovery process for processing UNF.

Radiation Stability of ILs: While a significant amount of work has been reported on the stability of ILs subjected to gamma-radiation, only one previous report examined the effect of alpha-radiolysis on the stability of ILs, which is the primary decay mode for many actinides [12]. Radiolysis of organic materials is known to produce hydrogen gas, which can present significant safety hazards in industrial applications. Very few studies have quantified H2 production, and those only focused on gamma-radiation. Experiments performed under this LDRD with collaborators at the University of Notre Dame Radiation Laboratory measured the yield of H2 production using 5 MeV He ions (for alpha-radiation) and a Shepherd Co-60 gamma source for a range of IL and IL related compounds [19]. The results indicated that the ILs behaved like conventional organic materials, with H2 yield decreasing for aromatic compounds. While the H2 production was higher for alpha radiation, the rates were relatively independent for aliphatic amines. In fact quaternary ammonium ILs showed significantly lower H2 production than their analogous aliphatic hydrocarbon

compounds, indicating that this family of ILs could posses superior radiation stability.

Impact on National Missions

This project addresses LANL's weapons and energy security missions. Understanding actinide behavior in non-conventional solvents can lead to revolutionary nuclear material processing technologies that can reduce costs, proliferation risks, and environmental impacts, and eventually contribute to a sustainable nuclear energy portfolio. Expanding the scientific understanding of Pu and actinide chemistry is central to LANL's leadership in Pu science and its function as the NNSA Plutonium Center of Excellence. Developing advanced separation technologies for used fuel, other nuclear materials, or high value isotopes such as Pu-242 supports LANL's Plutonium Science and Research Strategy, and is of interest to NNSA and several DOE Offices. The scientific challenge of understanding the radiation-induced degradation of ionic liquids in extreme radiation environments as found in used nuclear fuel reprocessing is of great important to the MaRIE mission. Training a new generation of actinide chemists as postdocs is a critical aspect identified across the DOE complex. This project provided partial or full funding for 9 postdocs, and six students.

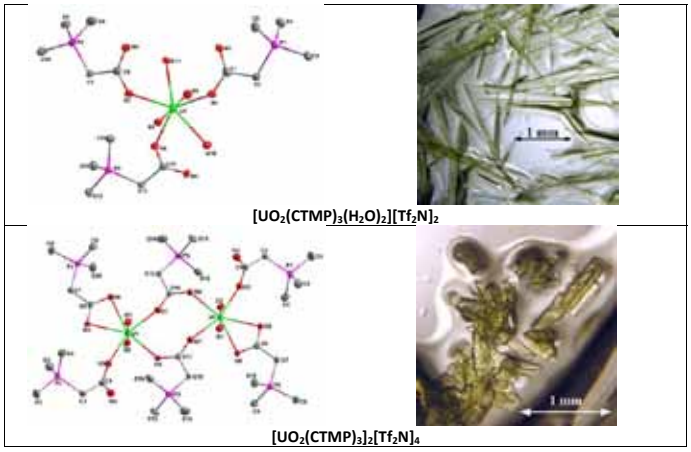

Figure 1. Photographs and thermal ellipsoids showing the structure of the cationic units in the monomeric compound [UO2(CTMP)3(H2O)2]2+ (upper) and the dimeric compound [UO2(CTMP)3]24+ (lower). The hydrogen atoms have been removed for clarity.

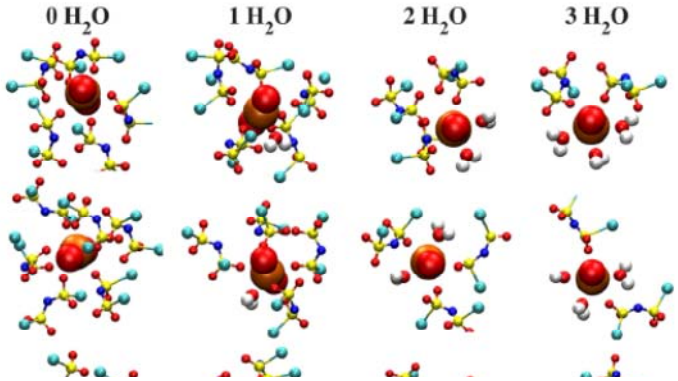

Figure 2. Simulation snapshots showing coordination of water and bistriflimide to plutonium(VI) in the first solvation shell. Plutonium (orange), oxygen (red), hydrogen (white), nitrogen (blue), sulfur (yellow), and CF3 (cyan).

Figure 3. Electrodeposited U from the IL [PMP][Tf2N] (left) and [EMIM][Tf2N] (right) and Pu from the IL [EMIM][Tf2N] (right).

References

1. Clark, D., G. Jarvinen, C. Kowalczyk, J. Rubin, and M. Stroud. Plutonium Processing at Los Alamos. 2008. Actinide Research Quarterly. 3: 1.

2. Nuclear Technology Review 2008. 2008.

3. Huddleston, J. G., and R. D. Rogers. Room temperature ionic liquids as novel media for 'clean' liquid-liquid extraction. 1998. Chemical Communications. (16): 1765.

4. Visser, A. E., R. P. Swatloski, S. T. Griffin, D. H. Hartman, and R. D. Rogers. Liquid/liquid extraction of metal ions in room temperature ionic liquids. 2001. Separation Science and Technology. 36 (5 & 6): 785.

5. Cocalia, V. A., K. E. Gutowski, and R. D. Rogers. The coordination chemistry of actinides in ionic liquids: A review of experiment and simulation. 2006. Coordination Chemistry Reviews. 250 (7-8): 755.

6. Dietz, M. L., and J. A. Dzielawa. Ion-exchange as a mode of cation transfer into room-temperature ionic liquids containing crown ethers: implications for the 'greenness' of ionic liquids as diluents in liquid-liquid extraction. 2001. Chemical Communications. (20): 2124.

7. Schubert, T., S. Z. El Abedin, A. P. Abbott, K. J. McKenzie, K. S. Ryder, and F. Endres. Electrodeposition of metals. 2008.

8. Venkatesan, K. A., T. G. Srinivasan, and P. R. Rao. A review on the electrochemical applications of room

temperature ionic liquids in nuclear fuel cycle. 2009. J. Nucl. Radiochem. Sci.. 10 (1): R1.

9. Trulove, P. C., and R. A. Mantz. Electrochemical properties of ionic liquids. 2008.

10. Binnemans, K.. Lanthanides and Actinides in Ionic Liquids. 2007. Chemical Reviews. 107 (6): 2592.

11. Forsyth, S. A., J. M. Pringle, and D. R. MacFarlane. Ionic Liquids-An Overview. 2004. Aust. J. Chem.. 57 (2): 113.

12. Allen, D., G. Baston, A. E. Bradley, T. Gorman, A. Haile, I. Hamblett, J. E. Hatter, M. J. Healey, B. Hodgson, R. Lewin, K. V. Lovell, B. Newton, W. R. Pitner, D. W. Rooney, D. Sanders, K. R. Seddon, H. E. Sims, and R. C. Thied. An investigation of the radiochemical stability of ionic liquids. 2002. Green Chem.. 4 (2): 152.

13. Bridges, N., A. Visser, M. Williamson, J. Mickalonis, and T. Adams. Effects of gamma radiation on electrochemical properties of ionic liquids. 2010. Radiochimica Acta. 98: 243.

14. Chen, X., G. S. Goff, W. C. Ewing, B. L. Scott, and W. Runde. Solid-State and Solution-State Coordination Chemistry of Lanthanide(III) Complexes with α-Hydroxyisobutyric Acid. 2012. Inorg. Chem.. 51 (24): 13254.

15. Chen, X., G. S. Goff, M. Quiroz-Guzman, D. P. Fagnant, J. F. Brennecke, B. L. Scott, and W. Runde. Directed nucleation of monomeric and dimeric uranium(VI) complexes with a room temperature carboxyl-functionalized phosphonium ionic liquid. 2013. Chemical Communications. 49 (19): 1903.

16. Maerzke, K. A., G. S. Goff, W. H. Runde, W. F. Schneider, and E. J. Maginn. Structure and Dynamics of Uranyl(VI) and Plutonyl(VI) Cations in Ionic Liquid/Water Mixtures via Molecular Dynamics Simulations. 2013. J. Phys. Chem. B. 117 (37): 10852.

17. Pomogaev, V., S. P. Tiwari, N. Rai, G. S. Goff, W. Runde, W. F. Schneider, and E. J. Maginn. Development and application of effective pairwise potentials for UO2n+, NpO2n+, PuO2n+, and AmO2n+ (n = 1, 2) ions with water. 2013. Phys. Chem. Chem. Phys.. 15 (38): 15954.

18. Tian, Y., G. S. Goff, W. H. Runde, and E. R. Batista. Exploring Electrochemical Windows of Room-Temperature Ionic Liquids: A Computational Study. 2012. J. Phys. Chem. B. 116 (39): 11943.

19. Dhiman, S. B., G. S. Goff, W. Runde, and J. A. LaVerne. Hydrogen Production in Aromatic and Aliphatic Ionic Liquids. 2013. J. Phys. Chem. B. 117 (22): 6782.

Publications

Carney, B. D., X. Chen, G. S. Goff, H. He, W. Runde, B. L. Scott, and L. A. Seaman. Ionic Liquids for Actinide Processing. Invited presentation at 2013 Chemistry Capability Review. (Los Alamos, NM, 9-12 June 2013).

Chen, X., G. S. Goff, B. L. Scott, M. T. Janicke, and W. Runde. Solid-state and solution-state coordination chemistry of lanthanide(III) complexes with (pyrazol-1-yl)acetic acid. 2013. Inorganic Chemistry. 52: 3217.

Chen, X., G. S. Goff, B. L. Scott, and W. Runde. Comparison of structural variations of Lanthanide(III) compounds with (pyrazol-1-yl)acetic acid. Polyhedron.

Chen, X., G. S. Goff, B. L. Scott, and W. Runde. Comparison of structural variations of Ln(III) compounds with (pyrazol-1-yl)acetic acid. To appear in Polyhedron.

Chen, X., G. S. Goff, M. Quiroz-Guzman, D. P. Fagnant, Jr, B. L. Scott, and W. Runde. Directed nucleation of monomeric and dimeric uranium(VI) complexes with a room temperature carboxyl-functionalized phosphonium ionic liquid. 2013. Chemical Communications. 49 (19): 1873.

Chen, X., G. S. Goff, W. C. Ewing, B. L. Scott, and W. Runde. Solid-state and solution-state coordination chemistry of lanthanide(III) complexes with alpha-hydroxyisobutyric acid. 2012. Inorganic Chemistry. 51 (24): 13254.

Dhiman, S. B., G. S. Goff, W. Runde, and J. A. LaVerne. Hydrogen Production in Aromatic and Aliphatic Ionic Liquids. 2013. Journal of Physical Chemistry B. 117: 6782.

Dhiman, S., and J. A. LaVerne. Hydrogen production in the gamma-ray and helium-ion radiolysis of ionic liquids . Presented at Radiation Chemistry Gordon Research Conference. (Andover, NH, July 29 - August 3, 2012).

Fagnant, D. P., G. S. Goff, B. L. Scott, W. Runde, and J. F. Brennecke. Switchable phase behavior of [HBet][Tf2N]-H2O upon neodymium loading: implications for lanthanide separations. 2013. Inorganic Chemistry. 52 (2): 549.

Goff, G. S., X. Chen, K. M. Long, B. L. Scott, G. D. Jarvinen, W. Runde, D. F. Fagnant, Jr., and J. F. Brennecke. Ionic Liquids for Advanced Nuclear Fuel Cycles. Invited presentation at 2012 LDRD Day. (Pojoaque, NM, 23 Oct. 2012).

Goff, G. S., X. Chen, K. M. Long, W. C. Ewing, G. D. Jarvinen, and W. Runde. Development of ionic liquids for the electrochemical separations of actinides. Presented at 36th Actinide Separations Conference. (Chattanooga, TN, 22-24 May, 2012).

Jarvinen, G. D., and D. L. Clark. Fundamental Studies of Metal Complexation and Higher-Order Structures in Separation Systems. Invited presentation at 37th Actinide Separations Conference. (Spokane, WA, 25-27 June 2013).

Joyce, E. L., and L. D. Schulte. Plutonium reprocessing requirements and considerations for ionic liquid development . 2011. Los Alamos National Laboratory Report, LA-CP 11-01479.

Long, K. M., G. S. Goff, and W. H. Runde. Exploring the chemistry of transuranic elements in ionic liquids. Presented at 242nd ACS National Meeting & Exposition. (Denver, CO, United States, August 28-September 1, 2).

Maerzke, K. A., G. S. Goff, W. Runde, W. F. Schneider, and E. J. Maginn. Structure and Dynamics of Uranyl and Plutonyl in Ionic Liquid/Water Mixtures via Molecular Dynamics Simulations. 2013. Journal of Physical Chemistry B. 117 (37): 10852–10868.

Maerzke, K. A., W. F. Schneider, and E. J. Maginn. Molecular dynamics simulations of uranyl and plutonyl coordination in water/ionic liquid mixtures. Presented at American Chemical Society Annual Meeting. (New Orleans, LA, April 2013).

Pomogaev, V., N. Rai, S. P. Tiwari, W. Schneider, and E. Maginn. Formation energies and PES of uranyl and plutonyl hydrated complexes to develop effective potentials for condensed phase simulations. Presented at 14th International Congress of Quantum Chemistry. (Boulder, CO, 25-30 June, 2012).

Pomogaev, V., S. P. Tiwari, N. Rai, G. S. Goff, W. Runde, W. F. Schneider, and E. J. Maginn. Development and Application of Effective Potentials for UO2n+, NpO2n+, PuO2n+, and AmO2n+ (n = 1,2) Ions with Water. 2013. Physical Chemistry Chemical Physics. 15 (38): 15954.

Tian, Y., G. S. Goff, W. Runde, and E. R. Batista. Exploring electrochemical windows of room-temperature ionic liquids: a computational study. 2012. Journal of Physical Chemistry B. 116 (39): 11943.

Tian, Y., and E. R. Batista. Exploring electrochemical windows of room-temperature ionic liquids by hybrid QM-MM method and thermodynamics calculations. Presented at 243rd ACS National Meeting & Exposition. (San Diego, CA, March 25-29, 2012).

Functional Materials by Design: Explosives with Tailored Optical Response Properties

Robert J. Scharff
20130006DR

Abstract

We offer an innovative approach to establish design principles and a scientific methodology for generating photoactive energetic materials with controllable optical functionality. The project aims to increase the controllability of chemical dynamics in novel photoactive materials through a concerted experimental and theoretical effort that characterizes the dynamics of energy localization, chemical bond activation, and chemical reactions. This approach will provide critical insight on how to manipulate electronic structure through synthesis in order to generate the desired material response to overcome mechanisms that limit controllability. We have proposed a three-part solution for the design of photoactive energetic materials for quantum optical initiation. The first part involves the development of new explosives derivatized with an optical chromophore. The optimization of optical response properties of the photon-absorbing chromophore enables efficient coupling of the laser field to the explosive and facilitates control of excited state dynamics. The second part addresses the need for the elucidation of electron-vibrational dynamics following photoexcitation. Our feasibility studies support our main idea that exothermic chemical reactions could be achieved photochemically. The third part of the project uses femtosecond laser pulse-shaping quantum control to optimize photodissociation quantum yields and photoinitiation of exothermic explosive chemistry.

Background and Research Objectives

Laser ignition of explosives materials is of considerable interest for both commercial and defense purposes [1-3]. Current efforts to initiate explosives with lasers are driven by the increase in electrical safety requirements of weapons. Ideally, an insensitive (e.g., to spark, friction, fire, lightning flash) explosive could only be initiated with a laser. While it is possible to initiate explosives with a laser, the process is indirect and requires high laser energies [3-10]. There are also applications that use very sensitive explosives that can be initiated with only a flash of light [11, 12]. For laser initiation of pentaerythritol tetranitrate (PETN) [3-10], several established routes to couple a laser field to the explosive are utilized [13]: (i) the beam directly impinges on an explosive target resulting in a thermal response [9,10]. (ii) The beam directly impinges on an explosive target that contains absorbing particles used to create local “hot spot” regions where chemical reactions develop [4-6]. (iii) The beam is fiber-optically coupled to the explosive through a metal layer sputter coated to the end of the fiber [3, 7, 8]. The laser pulse vaporizes the metal layer to create a plasma that inputs a quasi isentropic compression wave into the explosive. In the all instances, the mechanism of initiation is not a direct photochemical process, but rather an indirect, shock-less deflagration (burning)-to-detonation transition (DDT). The problems with current optical initiation schemes are: (i) high energies are required, (ii) initiation is “indirect”, and (iii) initiation of the chemical reaction is not “controllable”.

While a programmatic need exists for the development of optical isolation techniques to enhance the safety of the enduring U.S. nuclear stockpile, even greater programmatic needs exist for quantum controlled explosive initiation (QCI) in future surety applications and other technologies. In order to achieve QCI, we have proposed a key innovation: engineer new explosive materials specifically optimized for quantum control of photochemical decomposition. Optical control can only be effective in newly designed materials that are synthesized to take advantage of such control. To date, our efforts have focused on making new explosive materials with energetic optical chromophores, calculating the non-linear optical response properties, and validating those calculations with ultrafast optical techniques. These results have established the platform from which we can now envision creating new explosives with controllable optical functionality for next generation explosive applications.

Photochemistry is the key to control. The term photo-

chemistry applies to chemical reactions that are induced by light-matter interactions. Upon absorption of light, the ground state population in a molecular system can transfer to an electronically excited state where a subsequent chemical reaction ensues. Classic examples of 1-photon induced photochemistry are the Norrish reactions with ketones and aldehydes [14, 15]; 3D microfabrication with nonlinear photoinitiator polymers is an example of 2-photon induced photochemistry [16-23]. Broadly defined, the term "nonlinear" includes simultaneous multi-photon absorption, cascaded 1-photon absorptions, and "pump-dump" processes; all of which are physical mechanisms that can be optimized to control chemical dynamics.

Our project develops an alternate initiation scheme that uses ultrashort (<100 fs) optical pulses to trigger and control a net exothermic photochemical-to-DDT reaction. Our scheme provides a significant improvement to current laser ignition schemes because of the direct absorption of the laser field by the explosive and increased optical sensitivity that allows the energy of the excitation source to be reduced. Furthermore, the wide spectral bandwidth of ultrashort optical pulses makes it possible to control chemical reactions [24-26] responsible for explosive decomposition.

Scientific Approach and Accomplishments

Understanding and controlling excited state dynamics (spatial energy transfer, excitation localization/delocalization, and/or charge separation) lies at the heart of all our efforts to design photoactive materials with desired functionality. While this design approach has become the standard for many technological applications (e.g., solar energy harvesting), a similar approach will be required to achieve quantum control of photoactive energetic materials. Through FY13, we have amassed theoretical and experimental results that demonstrate key elements of our hypothesis, mitigate the level of risk, and provide feasibility for our research plan. We have utilized LDRD FY13 Reserve to (i) synthesize new explosive materials with energetic optical chromophores, (ii) validate their optical response properties through experiment and simulation, and (iii) develop critical experimental capabilities to measure time dependent photoexcited molecular dynamics. Synthesis: We have expanded our chemical basis set for added flexibility in the preparation of photoactive energetics for quantum control. Preliminary results on chromophore-derivatized explosive prototypes indicate favorable trends in the computed and measured two photon absorption spectra, and current excited state molecular dynamics calculations demonstrate the plausibility of our hypothesized mechanism for photoinitiation [27]. Theory: Our theoretical modeling suggests that materials possessing large linear or nonlinear optical susceptibilities are ideal for photoactive energetic materials due to their potential for rapid energy redistribution during relaxation from excited states above S1. Also, we have formulated a novel theoretical algorithm that describes coherent photoexcited state dynamics, a critical innovation necessary to model quantum control experiments [28]. Characterization and control: In FY13, we have developed an excited state femtosecond stimulated Raman spectroscopy diagnostic (ES-FSRS) [29] that we have coupled to our existing UV/near-IR shaped pulse quantum control experiment. This represents a unique, advanced spectroscopic capability for characterization and control of excited state molecular dynamics. Preliminary results on nitromethane demonstrate our new capability to measure real-time molecular changes due to excited state photochemistry, and also illustrate how "off the shelf" explosives lack large optical cross-sections that lead to decomposition (Figure 1).

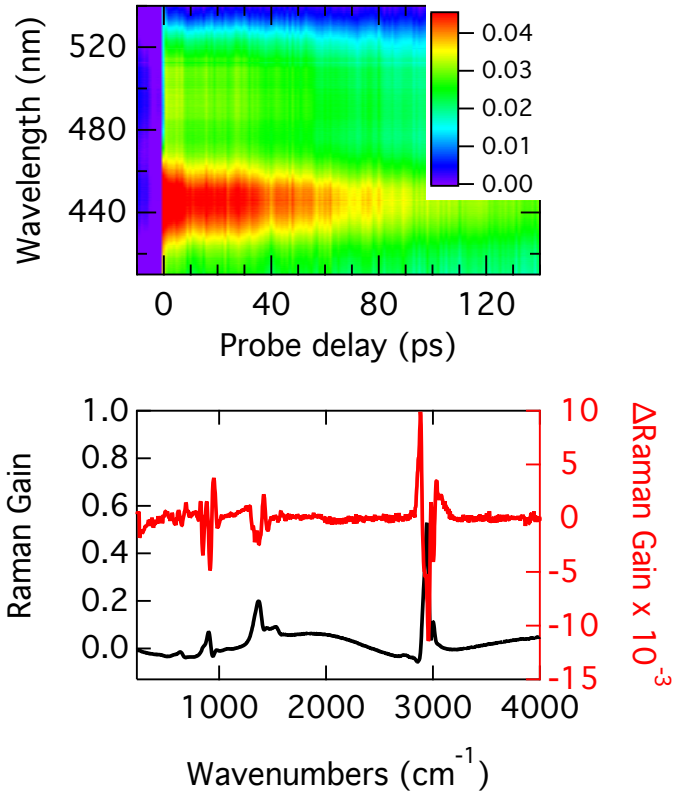

Figure 1. Nitromethane photochemistry. Time resolved transient absorption (top) quantifies excited state dynamics, but the broad features generally do not definitively identify molecular species. The FSRS spectrum (bottom, black) and the ES-FSRS spectrum (red curve is FSRS of products – reactants) have sharp peaks corresponding to specific bonds, and small changes in bonding are observed.

Impact on National Missions

Nuclear stockpile aging and enhanced surety are two of the primary concerns for the Weapons Program. The development of photoactive energetic materials that initiate through the quantum control of photochemistry addresses future surety themes outlined in the FY12 SSMP and provides an enabling technology for future Directed Stockpile Work [30, 31]. The theory-guided synthesis of energetic materials tailored for optical response would be unprecedented and unique to LANL, paving the way for the future creation of novel optical explosives that perform like RDX (1,3,5-trinitro-1,3,5-triazacyclohexane) yet are insensitive to mechanical and thermal stimuli. Since there are no insensitive photoactive explosives currently, producing new insensitive photoactive explosives will generate licensable technology opportunities for direct optical initiation detonators, quantum control detonators, and conventional light sensitive explosive applications. The design of photoactive materials for quantum controlled initiation offers modern technology that will address future requirements [30] for "direct optical initiation or other advanced initiation approaches" above and beyond those of current optical isolation techniques [1, 3, 7]. More safe and secure control of explosives also has Department of Defense applications.

References

1. Clarke, S. A., C. D. Landon, M. J. Murphy, M. E. Martinez, T. A. Mason, and K. A. Thomas. Detonator Performance Characterization Using Multi-frame Laser Schlieren Imaging. 2009. APS Topical Conference on Shock Compression of Condensed Matter. 1195: 663.

2. Akinci, A. A., S. A. Clarke, K. A. Thomas, and A. C. Munger. Optical initiation spot size effects in low-density PETN. 2006. SPIE Optical Technologires for Arming, Safing, Fuzing, and Firing II. 6287: 628709.

3. Akinci, A., K. Thomas, A. Munger, L. Nunn, S. Clarke, M. Johnson, J. Kennedy, and D. Montoya. On the development of a laser detonator. 2005. SPIE Optical Technologies for Arming, Safing, Fuzing, and Firing. 5871: 1.

4. Aluker, E. D., A. G. Krechetov, A. Y. Mitrofanov, and D. R. Nurmukhametov. Photochemical and Photothermal Dissociation of PETN during Laser Initiation. 2011. Russian Journal of Physical Chemistry B. 5 (4): 658.

5. Aluker, E. D., G. M. Belokurov, A. G. Krechetov, A. Y. Mitrofanov, and D. R. Nurmukhametov. Laser initiation of PETN containing light-scattering additives. 2010. Technical Physics Letters. 36 (3): 285.

6. Aduev, B. P., D. R. Nurmukhametov, and A. V. Puzynin. Laser initiation of a mixture of PETN with NiC nanoparticles at elevated temperatures. 2010. Russian Journal of Physical Chemistry B. 4 (3): 452.

7. Stewart, D. S., K. A. Thomas, S. Clarke, H. Mallett, E. Martin, M. Martinez, A. Munger, and J. Saenz. On the initiation mechanism in exploding bridgewire and laser detonators. 2006. AIP Conference Proceedings. 845 (1): 471.

8. Nagayama, K., K. Inou, and M. Nakahara. Initiation of PETN high explosive by pulse laser-induced high-temperature plasma. 2001. In Impact Engineering and Application, Vols I and II. Edited by Chiba, A., S. Tanimura, and K. Hokamoto. , p. 515. Oxford: Elsevier.

9. Tarzhanov, V. I., A. D. Zinchenko, V. I. Sdobnov, B. B. Tokarev, A. I. Pogrebov, and A. A. Volkova. Laser initiation of PETN. 1996. Combustion Explosion and Shock Waves. 32 (4): 454.

10. Bykhalo, A. I., E. V. Zhuzhukalo, N. G. Kovalskii, A. N. Kolomiiskii, V. V. Korobov, A. D. Rozhkov, and A. I. Yudin. INITIATION OF PETN BY HIGH-POWER LASER-RADIATION. 1985. Combustion Explosion and Shock Waves. 21 (4): 481.

11. Benham, R.. Preliminary experiments using light-initiated high explosive for driving thin flyer plates. 1980.

12. Benham, R.. A new LIHE (Light Initiated High Explosive) test capability for spherical targets. 1987.

13. Bourne, N. K.. On the laser ignition and initiation of explosives. 2001. Proceedings of the Royal Society A - Mathematical, Physical, and Engineering Sciences. 457 (2010): 1401.

14. Norrish, R. G., and C. H. Bamford. Photodecomposition of aldehydes and ketones. 1936. Nature. 138: 1016.

15. Norrish, R. G., and C. H. Bamford. Photo-decomposition of aldehydes and ketones. 1937. Nature. 140: 195.

16. Baldacchini, T., H. Chen, R. A. Farrer, M. J. Previte, J. Moser, M. J. Naughton, and J. T. Fourkas. Multiphoton photopolymerization with a Ti : sapphire oscillator. 2002. Edited by G. S. Edwards, J. Neev, A. Ostendorf, and J. C. Sutherland. Vol. 4633, p. 136.

17. Baldacchini, T., R. A. Farrer, J. Moser, J. T. Fourkas, and M. J. Naughton. Efficient multiphoton polymerization for the fabrication of 3-dimensional microstructures. 2003. Synthetic Metals. 135 (1-3): 11.

18. Belfield, K. D., and K. J. Schafer. Two-photon photoinitiated polymerization. 2003. Edited by K. D. Belfield, and

J. V. Crivello. Vol. 847, p. 464.

19. Engelhardt, S., Y. Hu, N. Seiler, D. Riester, W. Meyer, H. Krueger, M. Wehner, E. Bremus-Koebberling, and A. Gillner. 3D-Microfabrication of Polymer-Protein Hybrid Structures with a Q-Switched Microlaser. 2011. Journal of Laser Micro Nanoengineering. 6 (1): 54.

20. Gu, J., W. Yulan, W. Chen, X. Dong, X. Duan, and S. Kawata. Carbazole-based 1D and 2D hemicyanines: synthesis, two-photon absorption properties and application for two-photon photopolymerization 3D lithography. 2007. New Journal of Chemistry. 31 (1): 63.

21. Ovsianikov, A., A. Deiwick, S. Van Vlierberghe, P. Dubruel, L. Moeller, G. Draeger, and B. Chichkov. Laser Fabrication of Three-Dimensional CAD Scaffolds from Photosensitive Gelatin for Applications in Tissue Engineering. 2011. Biomacromolecules. 12 (4): 851.

22. Ovsianikov, A., M. Malinauskas, S. Schlie, B. Chichkov, S. Gittard, R. Narayan, M. Loebler, K. Sternberg, K. P. Schmitz, and A. Haverich. Three-dimensional laser micro- and nano-structuring of acrylated poly(ethylene glycol) materials and evaluation of their cytoxicity for tissue engineering applications. 2011. Acta Biomaterialia. 7 (3): 967.

23. Steenhusen, S., T. Stichel, R. Houbertz, and G. Sextl. Multi-photon polymerization of inorganic-organic hybrid polymers using visible or IR ultra-fast laser pulses for optical or (opto-)electronic devices. 2010. Edited by W. V. Schoenfeld, J. J. Wang, M. Loncar, and T. J. Suleski. Vol. 7591.

24. Brumer, P., and M. Shapiro. Control of unimolecular reactions using coherent light. 1986. Chemical Physics Letters. 126 (6): 541.

25. Tannor, D. J., R. Kosloff, and S. A. Rice. Coherent pulse sequence induced control of selectivity of reactions: Exact quantum mechanical calculations. 1986. The Journal of Chemical Physics. 85 (10): 5805.

26. Tannor, D. J., and S. A. Rice. Control of selectivity of chemical reaction via control of wave packet evolution. 1985. Journal of Chemical Physics. 83 (10): 5013.

27. Nelson, T., and S. Tretiak. NA-ESMD calculation of explosive prototype. 2012. Theoretical Division, LANL, unpublished work. : 1.

28. Mozyrsky, D., V. Gorshkov, and S. Tretiak. manuscript under review. Nature Physics.

29. Kukura, P., D. W. McCamant, and R. A. Mathies. Femtosecond stimulated Raman spectroscopy. 2013. Annual Review of Physical Chemistry.

30. FY12 Stockpile Stewardship and Management Plan, U. S. Department of Energy. 2011.

31. Guidice, S. J.. Weapons Engineering Capability Review. 2012.

Alternative Explosives Signatures for Detection

David S. Moore
20130086DR

Abstract

The events at the Boston Marathon finish line this past April graphically illustrate the difficulties we face as a nation to find and neutralize explosive devices before they are used. Our toolset is massive and diverse, from intelligence, counter-intelligence, and persistent surveillance to regulation of explosives and precursors, X-ray imaging, and metal detection, yet it fails in many situations, including venues without controlled access like the streets of any city. Our adversaries are agile and adapt by countering every new technology that achieves some level of success (metal detectors, RF jammers, hand swipes/ IMS technology, X-ray imaging). Our project aims to fill a major gap in our arsenal, by detecting the bulk explosive itself. This proposed capability is potentially disruptive to current evasion-of- detection tactics, because it exploits the nonlinear coupling of penetrating GHz-to-THz electromagnetic radiation to explosives and detection of the alternative signatures that are generated.

We performed proof-of-principle studies that show a connection between local chemical energy release and local nonlinearities that can be exploited to differentiate inerts from explosive materials. The experiments and theory were designed to correlate the changes in effective permittivity caused by the presence or absence of a local source term with activation energy at hot spots. The ultimate goal is to develop fundamental principles that define the processes and signatures, which will guide the design of a prototype detection system with area-scanning capability from safe standoff distances.

Background and Research Objectives

The detection of explosives is a pressing current problem, both at home and abroad. The Washington Post series “Left of Boom” succinctly outlines the latest evolution of the use of IEDs (improvised explosive devices) especially in Iraq and Afghanistan, and the progress of counter-IED technologies [1]. Each new technology has been countered by our adversaries with great agility, so that a suite of technologies must be deployed in order to cover the multitude of possible threat scenarios. A serious gap is evident in this suite of technologies – that of detecting the bulk explosive using non-ionizing radiation – the gap that the work described in this proposal is intended to fill. The characteristic of explosives that we exploit is the intrinsic property that defines an explosive – its metastable chemical energy that can be quickly released on command (shock, friction, spark). The work addressed the high-risk aspect of this novel explosive detection in the GHz to THz electromagnetic (EM) frequency range by performing proof-of-principle studies. First, we measured reflected power from pressed powder samples of HMX and sugar (each with as close to the same particle size distribution as feasible, which was measured using micro-computed X-ray tomography) as a function incident EM amplitude. Second, the reflected power data were related to theoretical results. These utilized macroscopic models for the EM response of crystalline materials using effective medium theory, with the difference between inerts and explosives being an activation energy barrier that can be overcome in small local regions by sufficiently strong excitation, thereby releasing energy and locally increasing the temperature. This response in turn modifies the effective electric permittivity and thereby the reflected power, providing the connection to the experiment.

Scientific Approach and Accomplishments

We performed experiments and developed theory intended to show a connection between local chemical energy release and local nonlinearities that can be exploited to differentiate inerts from explosive materials using GHz frequency stimulation. Experimentally, we measured the reflected power from pressed powder samples of inert and explosive materials prepared with the same particle size distribution. We observed distinctly different time dependent GHz reflectivity from pressed HMX and pressed sugar – chemically similar except one is an explosive and the other an inert (Figure 1). Note the very

similar behavior of four different samples of HMX and the very similar behavior of the three different samples of sugar, along side the significantly different behavior of HMX compared to sugar. Pre- and post-mortem micro-CT images of the two materials show voids in the HMX sample caused by local reactivity due to the locally high temperatures under GHz irradiation. Note that the GHz source was only on for a short time, so that even though the peak power was high, the duty cycle and therefore also the deposited average power was low. A simple theory was developed based on macroscopic Maxwell equations and effective medium theory for anisotropic materials, resulting in effective permittivity tensors that reveal the frequency and temperature dependent response of the materials to external EM waves (dotted lines in Figure 1).

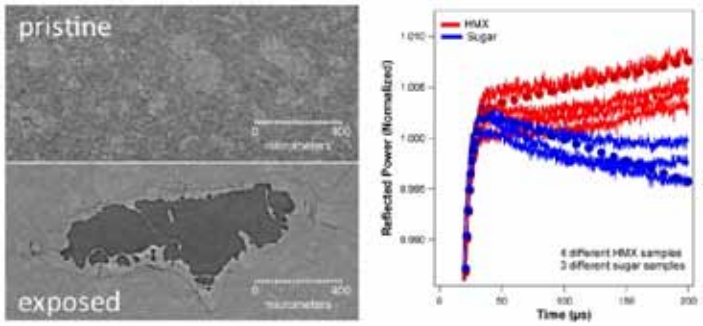

Figure 1. Micro-CT image of a pristine (left top) and an exposed (left bottom) HMX sample showing void growth; Reflected power versus time for 11 GHz irradiation at 500 W (simple theory = dots) showing distinctly different behavior of HMX and sugar.

We also obtained reflected power data on these same samples as a function of excitation power, showing different behavior for the explosive compared to the inert (Figure 2).

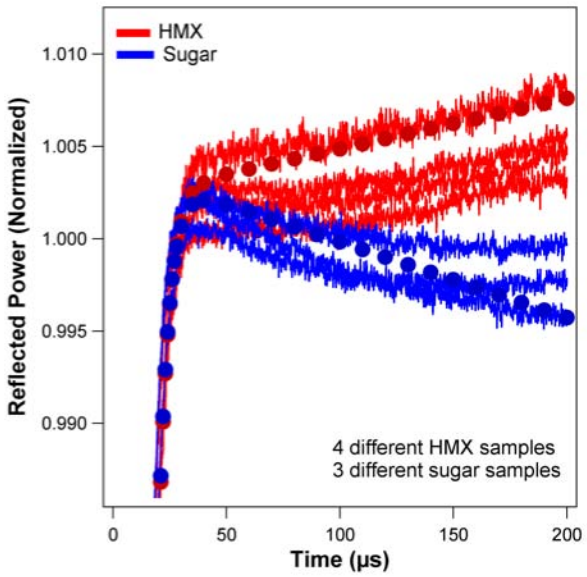

Figure 2. Reflected power versus time for 11 GHz irradiation at three different incident powers. The HMX shows a nonlinear increase in reflected power with increasing incident power, while the sugar does not.

The power levels involved are less than or similar to everyday EM exposures. For a detection system with output power of 10 kW, pulse duration of 1 μs and a spot size on target of 50 cm diameter, the peak intensity is greater than 2 W/cm2. However, thousands of these 1 μs pulses a minute at this intensity do not exceed the FCC average irradiance allowance of 5 mW/cm2. In addition, a typical cell phone emits about 20 mW/cm2 at a distance of 2.2 cm from the antenna, larger than the irradiance from these stimulation sources. Finally, finite element modeling of these experiments shows only small temperature increases (even a much longer and stronger 100 ms pulse at 43 W/cm2 increases an HMX sample temperature by less than 2 ˚C), so the probability of accidentally setting off the explosive during detection is very low.

Impact on National Missions

The results described above are the first step towards explosive detection in frequency regimes capable of penetrating non-metallic packaging, clothing, or camouflage to interrogate bulk explosives, filling a capability gap in the current suite of counter-IED technologies, which includes X-ray imaging, metal detection, trace analysis, intelligence, and persistent surveillance. These GHz range EM frequencies have not been investigated for standoff detection until recently. The ultimate aim of the work is to obtain the characteristics and parameters needed for forward deployment of an actual detector system. Subsequent LDRD work (new start FY2014) will jump-start new modeling capabilities at LANL that will enable predictive theory of elasto-electric coupling with chemical energy release at hot spots in explosives. We at LANL are breaking ground for the detection of alternate signatures using GHz-to-THz frequencies integrated with modeling of elasto-electric coupling including chemical energy release at hot spots and thermal diffusion.

This project represents a transformational approach to uncovering the direct explosive signal type applicable to the Discover Signatures and Revolutionize Measurement components of the Science of Signatures pillar. The overarching goal of the project directly supports LANL's long-term objective of discovery of the next generation of materials signatures of explosives within its global security mission. The deep fundamental understanding of energy absorption and subsequent responses are applicable to MaRIE's "Decadal Challenges for Predicting and Controlling Materials Performance in Extremes" for the design and control of

energy release in explosives. This work along with that to be performed in the FY2014 new start Directed Research project will develop a new framework for a unified description of explosives' hot spots coupled to the local mechanical, thermal and electromagnetic signatures. Understanding and controlling the material functionality of defects and crystalline interfaces is important for hot spots and their signatures and underpins the Materials for the Future pillar with the focus area Defects and Interfaces, as well as the priority area 2 for advanced (THz) spectroscopies. There are a number of agencies interested in the results of this research, including the Office of Naval Research (ONR – Code 30), Department of Homeland Security (DHS – S&T Explosives), and Joint IED Defeat Organization (JIEDDO). Jon Schoonover, a LANL Global Security program manager, is mentoring the project and helping with transition. The results and data obtained in FY2013 resulted in a full LDRD FY2014 new start DR project, whose results will eventually enable transition to a product for controlled access portals or vehicle mounted systems including stimulation source(s), antenna arrays and thermal detectors, or as an add-on to ground penetrating radar systems.

References

1. Atkinson, R.. About Left of Boom: The Fight Against Roadside Bombs. 2007. The Washington Post.

Room Temperature Oxidation and Corrosion of Plutonium

Alison L. Pugmire
20130738ECR

Introduction

Currently, a systematic investigation of plutonium corrosion under room temperature, pressure and humidity has yet to be performed. This work proposes to use a carefully controlled environment to form the oxide layer on well-characterized Pu metal samples. At various times during the corrosion process, a combination of spectroscopic tools will probe both the surface layer (spectroscopic ellipsometry, SE; Auger electron spectroscopy, AES; x-ray photoelectron spectroscopy, XPS) and the bulk material (x-ray diffraction, XRD; x-ray absorption fine structure, XAFS). This work will also aim to address a long-standing issue with plutonium metal experiments: variability in the sample preparation and resultant reproducibility. These issues will be addressed by utilizing a consistent and controlled preparation method and conducting the experiments on multiple samples to ensure repeatable and, more importantly, reliable results.
Many questions remain regarding the room temperature/pressure mechanism of plutonium corrosion. What is the chemical composition of the corrosion products (PuO2, Pu2O3, etc.)? Is the surface layer oxide crystalline PuO2 or an amorphous oxide mixture as recent investigations indicate? Is Pu2O3 present at the PuO2-metal interface? Why are seemingly different results obtained for ultra-high vacuum conditions versus "real world", ambient conditions? The proposed work aims to answer these fundamental questions with a comprehensive surface and bulk layer study at conditions most relevant to the storage and use of plutonium: near room temperature and pressure.

Benefit to National Security Missions

Los Alamos National Laboratory (LANL) is the premier institution for plutonium science, with a rich history of excellence in actinide research and development, pit manufacturing, and surveillance. The laboratory's mission is to "ensure the safety, security, and effectiveness of the U.S. nuclear deterrent." The core of this mission is to ensure the reliability and performance of the nation's weapons systems currently in the stockpile. Interest in the health of the nuclear stockpile has been heightened in recent months due to the Department of Energy (DOE) and LANL's recent commitment to pit reuse. As stated by LANL Director Charlie McMillan in a June 27, 2012 All-Hands Meeting, "Pit reuse is now a certification 'grand challenge, one of the most complicated we have ever faced." Plutonium corrosion has been identified as a key issue in pit aging and reuse, and the current state of corrosion knowledge has been recognized as limited at best. Thus, this research directly addresses the laboratory's mission to en-sure the effectiveness of the stockpile and the challenges facing certification of pits for reuse.

Progress

Year 1 focused on developing a sample preparation method, utilizing in-house techniques to structurally and chemically characterize the samples, and submit proposals for off-site XAFS experiments for Year 2.

Accomplishments from the first half of Year 1 (FY2013 2nd, 3rd quarters) are listed and organized in accordance with the Year 1 objectives.

Task 1: Determine the optimal samples and sample preparation method

- The first set of stock material (Sample Set 1) was identified and collected
- A preparation method was chosen and tested on Sample Set 1 (mechanical polishing followed by electropolishing)
- A duplicate sample of one exposure condition was also selected to test reproducibility
- Based on the results of Tasks 2-4, the second set of stock materials (Sample Set 2) was identified to be tested in the latter part of Year 1/Year 2

Task 2: Determine the optimal exposure conditions

- Three optimal sample exposure conditions were chosen (wet air, dry air, wet argon environment)
- An optimal sample exposure time was selected (~30 days) based on the samples ident-fied in Task 1 and literature review
- Set up of exposure containers was completed and tested (Task 3)

Task 3: Exposure Experiments

- The first set of exposure experiments were completed (30 day cycle)
- Samples were characterized using various x-ray spectroscopies (x-ray photoelectron, XPS, and x-ray absorption, XAFS, in collaboration with the project's collaborator)
- Surface quality of Sample Set 1 was determined using XPS and XAFS
- Technique limitations (probe depth, etc) were identified and will guide and aid in the co-ordination of multiple techniques in end of Year 1/Year 2 experiments
- XPS and XAFS data analysis from these experiments is on-going, but initial results are guiding the preparation/setup/exposure of the second set of experiments with the second set of stock material (Sample Set 2)

Task 4: Submit Beam Time Proposals

- An off-site XAFS beam time proposal was prepared and submitted at the first available deadline (June 1, 2013)

Future Work

Year 2 will continue the structural and chemical characterization of the corrosion process using in-house capabilities and off-site synchrotron experiments. The tasks and goals to be accomplished in the next fiscal year (FY14 1st, 2nd, 3rd, and 4th quarters) are listed.

Task 1: Determine additional samples and other potential sample preparation methods

- Identify and collect additional stock materials (Sample Set 2 (see progress section), Sample Set 3, etc.)
- If relevant or needed, test other preparation methods (e.g. mechanical polishing with no electropolishing)
- Identify the advantages/disadvantages of preparation methods based on "real world" surface relevance, reproducibility, and experimental results
- Determine 1) surface quality 2) sample pedigree of different stock materials and sample preparation

Task 2: Exposure Experiments

- Expose additional stock materials to same exposure time initially tested (~30 days)
- Based on initial experiments, determine additional relevant exposure times
- Characterize samples using in-house techniques
- Incorporate more characterization techniques not employed in first set of exposures (XRD, Auger)

Task 3: Analyze Spectroscopic Data and Interpret results

- Analyze data collected throughout FY13 and FY14 (XRD, XAFS, XPS, Auger)

Task 4: Determine Future Work and Develop a Proposed Corrosion Mechanism

- Based on the results from Tasks 2 and 3, determine optimal structural and characteriza-tion techniques most appropriate and most useful for potential future work
- Based on the results from Tasks 2 and 3, propose a room temperature corrosion mechanism

Conclusion

The goals of this research are to study the ambient oxidation/corrosion mechanism of plutonium using a systematic approach to prepare the specimens; develop the oxide layer as a function of humidity, oxygen content, and exposure; and study the oxide layer using multiple techniques. Expected results include determination of the chemical (e.g. PuO2, Pu2O3, and/or PuOxCy) and structural composition (e.g. crystalline or amorphous) of the surface and bulk oxide layer. These results will help develop a comprehensive picture of the corrosion mechanism, impacting our understanding of Pu aging in the stockpile.

Publications

Booth, C. H., Y. Jiang, S. A. Medling, D. L. Wang, A. L. Costello, D. S. Schwartz, J. N. Mitchell, P. H. Tobash, E. D. Bauer, S. K. McCall, M. A. Wall, and P. G. Allen. Self-irradiation damage to the local structure of plutonium and plutonium intermetallics. 2013. JOURNAL OF APPLIED PHYSICS. 113 (9): -.

Pugmire, A. L.. Spectroscopic Analysis of Actinyl Systems. To appear in Actinide Research Quarterly.

Pugmire, D. L., H. G. Garcia Flores, and A. L. Costello. The room temperature oxidation/corrosion of delta plutonium. Presented at XIII International Workshop: Fundamental Properties of Plutonium. (Sarov, Russia, 8-13 Sept. 2013).

Novel Mesoscale Modeling Approach for Investigating Energetically Driven Nanoscale Defect/Interface Interactions

Abigail Hunter
20130745ECR

Introduction

In nanomaterials (grain sizes less than 100nm), experimental studies and atomistic simulations show that when the characteristic length scale (ex: layer thickness, grain size) decreases many deformation mechanisms arise that are not active in bulk and coarse-grained material counterparts, such as dislocation emission and absorption at grain boundaries and interfaces, dislocation pile-ups, confined layer slip, and deformation twinning. These alternative deformation mechanisms, along with grain boundaries and bimetallic interfaces, can result in unique material behavior including high strength and improved ductility. As applications for nano-devices increases, there is not only a growing need to ensure reliability, but also the opportunity to engineer materials for specific applications, however a predictive model to address these issues still does not exist.

This project is focused on investigating nanoscale defect/interface interactions, such as nucleation and growth of deformation twins, and dislocation dynamics as controlled by interfaces through development of an innovative three-dimensional (3D) phase field dislocation dynamics (PFDD) mesoscale model that links atomic-scale and nanoscale physics. This model is unique at Los Alamos National Laboratory (LANL), and has great potential to answer many questions about the effects of deformation twinning, and the impact of grain boundaries and heterophase interfaces on dislocation and material strength behavior. The goals of this project include innovative extensions of the 3D PFDD model that will not only be new in the scientific community, but will also answer many questions about dislocation behavior on the nanoscale, particularly at interfaces. Model advancements as part of this project include: incorporation of temperature dependence, implementation of a complex description of nanolayer interfaces, and reformulation to account for body-centered cubic (bcc) crystal structures. Development of this computational tool will enable the study of deformation mechanisms at interfaces not possible with current mesoscale methods.

Benefit to National Security Missions

Understanding the effects of defects and interfaces on material behavior as materials age becomes increasingly important for determining the performance, reliability, and safety of weapon systems. Los Alamos National Laboratory (LANL) has advanced atomistic and continuum simulation tools, however, it is not clear how to connect information on these two very different length scales. Hence, there remains a computational gap at the mesoscale that translates into a gap in our understanding of material deformation. The phase field dislocation dynamics (PFDD) model aims to fill this gap, and produce predictive multiscale simulations crucial for stockpile stewardship.

The goals of this proposal include innovative extensions of the PFDD model that will not only be new in the scientific community, but will also answer many questions about dislocation behavior on the nanoscale, particularly at interfaces. The proposed model advancements will be extensions that have not yet been achieved by current phase field dislocation models. These advancements will enable the PFDD model to investigate many defect/interface deformation mechanisms not possible with current mesoscale methods.

Progress

The primary goal of this project is to investigate nanoscale defect/interface interactions, such as nucleation and growth of deformation twins, and dislocation dynamics as controlled by interfaces through development of an innovative three-dimensional (3D) phase field dislocation dynamics (PFDD) mesoscale model that links atomic-scale and nanoscale physics. This model is unique to Los Alamos National Laboratory (LANL) and the novel extensions of the PFDD model achieved as part of this project will be both new to the scientific

community and answer many questions about dislocation behavior on the nanoscale, particularly at interfaces. Three specific goals are highlighted in this project: (1) investigate the effects of grain size variation and temperature dependence on deformation twinning in face-centered cubic (fcc) materials, such as copper, nickel, gold, and silver, (2) study dislocation behaviors in fcc/fcc multilayers, and (3) account for dislocation behavior in base-centered cubic (bcc) materials, such as tantalum, steel, chromium, and niobium.

Over the past year, much progress has been made toward achieving these three goals. While work in all three areas has begun, focus of the project in the first year has been surrounding fcc/fcc interfaces, which is the primary goal of the project (collaborator: Irene Beyerlein- T-3). This topic initiated a collaboration with Dr. Marisol Koslowski at Purdue University. A two-layer PFDD model has been developed that accounts for differences in material properties between two metallic layers. Currently, this new algorithm is being extended to a parallel PFDD code and numerical considerations are being addressed. In parallel with modification to the PFDD code itself, MD simulations of copper/nickel interfaces have been completed (collaborator: Ruifeng Zhang – Iowa State). This also included development of a cross-potential for nickel (collaborator: Xiang-Yang (Ben) Liu-MST-8). These simulations provide key information for the development of a complex description of the interface region between two nanolayers. Furthermore, information from these simulations will be directly incorporated into the PFDD model in order to accurately describe dislocation behavior across the interface. This summer (July 2013) a Purdue student, Yifei Zeng, will come to LANL and focus on the implementation of a complex energy landscape into the PFDD model in order to investigate defect behavior in this region.

Studying deformation twinning is another key goal of this project (collaborator: Irene Beyerlein- T-3). Current efforts include simulations studying the formation of deformation twins in copper, nickel, and silver. More specifically, we are investigating the emergence of twins from grain boundaries in several different initial defect configurations proposed in literature. This work also investigates the effects of grain size variation, and material variation on the emergence of deformation twins in fcc metals.

The final goal of this project requires reformulation of the PFDD model to account for a different material crystal class, bcc. Initial reformulation of the model has begun, in particular, modification of crystallographic considerations such as number of slip planes and general geometry. Next steps include simulations of perfect dislocations in bcc metals, followed by development and implementation of a complex description for extended dislocation cores.
This project has resulted in several collaborations including those spanning divisions/groups within LANL, and external academic relationships. Several publications are currently underway, in addition to those already published or submitted:

Three other papers are currently being written that address two-layer twin formation, an analytical model that describes dislocation formation from grain boundaries, and combined DFT-PFDD simulations that investigate partial dislocation dependence on material variations.

Future Work

The goals of this projectl include innovative extensions of the three-dimensional (3D) phase field dislocation dynamics (PFDD) model that will not only be new in the scientific community, but will also answer many questions about dislocation behavior on the nanoscale, particularly at interfaces. Three specific goals are highlighted in this project:

1. Investigate the effects of grain size variation and temperature dependence on deformation twinning in face-centered cubic (fcc) materials, such as copper, nickel, gold, and silver. This goal requires that temperature dependence be included in the current PFDD model framework through the material parameters and energy functional. With this model advancement, it will be possible to study the transition between slip and deformation twinning deformation mechanisms.
2. Study dislocation behaviors in face-centered cubic (fcc)/fcc multilayers. Modeling dislocation behavior across nanolayer interfaces has never been attempted with a phase field model. A complex description of a bi-material interface must be implemented into the current PFDD framework in order to study defect/interface interactions. This model advancement will present opportunities to study other interfaces in fcc materials such as grain boundaries.
3. Account for dislocation behavior in base-centered cubic (bcc) materials, such as tantalum, steel, chromium, and niobium. This final goal requires a complete reformulation of the current 3D PFDD model, making it the first model of its kind applied to bcc materials. Describing the dislocation core in bcc materials will be both the most difficult challenge to overcome in achieving this goal, and the most important component for accurately modeling dislocation behavior in bcc materials. The PFDD model has a direct connection with atomistic simulation tools, which is particularly advantageous in addressing this problem.

Conclusion

The primary goal of this proposal is to investigate nanoscale defect/interface interactions, such as nucleation and growth of deformation twins, and dislocation dynamics as controlled by interfaces through development of an innovative three-dimensional (3D) phase field dislocation dynamics (PFDD) mesoscale model that links atomic-scale and nanoscale physics. Model advancements as part of this project include: incorporation of temperature dependence, implementation of a complex description of nanolayer interfaces, and reformulation to account for body-centered cubic (bcc) crystal structures. Development of this computational tool will enable the study of deformation mechanisms at interfaces not possible with current mesoscale methods.

Publications

Hunter, A., R. F. Zhang, I. J. Beyerlein, T. C. Germann, and M. Koslowski. Dependence of equilibrium stacking fault width in fcc metals on the gamma-surface. 2013. MODELLING AND SIMULATION IN MATERIALS SCIENCE AND ENGINEERING. 21 (2): -.

Hunter, A., R. F. Zhang, and I. J. Beyerlein. Universal scaling law for the dislocation core size in fcc metals. Physical Review Letters.

Hunter, A., and I. J. Beyerlein. Unprecedented grain size effect on stacking fault width. 2013. Applied Physics Letters Materials. 1: 032109.

Magnetic Field Effects on Convection-Modified Solid-Liquid Interfaces

Amy J. Clarke
20130755ECR

Introduction

In-situ characterization techniques are now affording direct interrogation of opaque materials during synthesis and processing, in part because of pioneering first experiments performed by this team to monitor metallic alloy melting and solidification using x-rays and protons. Feedback from in-situ characterization will enable in-process adjustments to control solidification and microstructure evolution and permit the advancement of solidification theory and the development of predictive solidification and microstructure evolution models. This project extends our methodology to explore the influence of magnetic field on the solid-liquid interface of metallic alloys during solidification, demonstrating a new approach to further control microstructure evolution during processing. In the proposed project, we wish to directly observe the impact of controlled alloy melt fluid flow on the solid-liquid interface during solidification. Melt flows interact with solid interfaces at a variety of length scales, from the macro-scale down to the micro-scale dendritic tips to influence solute segregation and microstructure evolution. The dynamic equilibrium present at the solid-liquid interface is critical to morphology selection, and we intend to probe the selection criteria for important types of flow geometries. Specific flows in metallic systems will be achieved by controlling geometry, heat flux, and the application of magnetic field. The solid-liquid interface shape, local composition, and the influence of magnetic field on the microstructure evolution during processing will be determined from in-situ imaging using synchrotron x-ray radiography at Argonne National Laboratory's Advanced Photon Source.

Benefit to National Security Missions

Convection of an alloy melt during casting mold filling plays a critical role in the solute segregation that develops at the macro-scale, whereas localized convection cells that develop during solidification drastically influence micro-scale solute segregation and morphological and microstructure evolution. Application of a magnetic field during solidification provides an opportunity to control alloy melt fluid flow characteristics and the interface shape and dynamic equilibrium at that interface. Materials for the future, including the creation of materials with application-tailored properties to achieve controlled functionality by directed synthesis and processing, is one of three science pillars at Los Alamos National Laboratory. Controlling materials synthesis and processing and the design of materials functionality through the exploitation of defects and interfaces, understanding the dynamic evolution of materials, defect structures, and interfaces, and the use of novel characterization techniques, especially at extremes, are priorities listed in Los Alamos National Laboratory's Directed Research and Development Defects and Interfaces in Materials (DIM) Exploratory Research Category. These priorities are also reflected in the laboratory's Matter-Radiation Interactions in Extremes (MaRIE) Signature Facility vision, and are deeply rooted in nationally recognized needs identified by the U.S. DOE Basic Energy Sciences, The National Academies, and the White House Office of Science and Technology Policy's Materials Genome Initiative (MGI).

Progress

The broad goal of this program is to better understand the impact of fluid flow on solid-liquid interfaces during solidification and melting by using magnetic field as a way to change the flow characteristics. To satisfy these goals, furnaces and crucibles must be built; upon initiation of this program in January of 2013, design of these parts began. We first re-examined the flow conditions from the dynamic imaging data which prompted the idea for the proposed work and reviewed relevant information available in the literature. Three types of flow conditions have been selected for further study. Two involve the development of natural convection patterns in the melt, and a third flow condition will be based upon forced fluid flow, which will have direct relevance to ap-

plications ranging from casting to microfluidics. The first iteration of one of our experimental designs will promote 2D convection cells and is currently being constructed. Potential designs for a forced-flow crucible are currently being modeled to determine desired heat flow conditions. A portable 0.3T permanent magnet has been acquired and will be used for the planned experiments. An adjustable-power electromagnet is currently being installed for access to high fields up to 1.5T. Considering the progress in the design of crucible geometries and the acquisition of sufficient magnetic field capabilities, we are currently on pace with our original schedule.

Future Work

The application of magnetic field has significant potential to influence alloy melt fluid flow, heat transfer, and the shape of the solid-liquid interface to affect morphological (and microstructure) evolution during solidification. The role of liquid motion on solid-liquid interface characteristics will be examined and real-time x-ray imaging at a national user facility will capture the effects. Fiscal Year 2013 will be dedicated to developing the experimental capabilities needed for these experiments. Furnace and casting geometry design will commence immediately. Geometry and heat flow conditions will be designed at Los Alamos National Laboratory utilizing multiple characterization methods, including experimental validation, imaging, and finite element simulation. The goal for the Fiscal Year 2013 design phase and experimentation is to develop a response surface of characteristics, such as liquid velocities, as a function of our control parameters, so that a high degree of reproducibility is achieved. Ex-situ microstructural analysis will provide the preliminary validation. Along with experimental platform design, candidate materials will also be selected based upon the experimental results. In this way, the sampling ranges may be optimized to fully explore the theoretical response space. We anticipate identification of at least two alloy or composite systems to use as the primary focus of experimentation during the second year of this project. The specific Fiscal Year 2013 tasks include: the design and fabrication of furnace geometries; validation of designs and measurement of achievable flow velocity ranges; and the selection of candidate alloys. The real-time imaging experiments will be performed in Fiscal Year 2014; analysis of the image sequences and data visualization will start in the same year.

Conclusion

In this project, we will explore the role of magnetic field on solid-liquid interfaces during solidification. The influence of different fluid flow regimes on solid-liquid interface shape, solute segregation, and morphology evolution will be studied. We will use synchrotron x-ray imaging to create movies of the solid-liquid interface during solidification, and will demonstrate the potential of magnetic field to modify the interface characteristics. The use of magnetic field during solidification will provide a set of broadly applicable microstructure and property control schemes for the creation of structural alloys.

Understanding The Catalytic Conversion of Oligosaccharides to Fuels and Chemical Feedstocks

Andrew Sutton
20130757ECR

Introduction

A procedure to produce branched alkanes containing ten and eleven carbon atoms from starch in two steps using mild acidic conditions with lanthanide and palladium catalysts is known. The reaction proceeds well at 200 oC under moderate pressure of H2 (200 psi); however, the mechanism and the identity of any reaction intermediates are unknown. If the steps involved in this general reaction can be better understood, routes that obviate the need for expensive catalysts as well as the use of ambient reaction conditions might be achievable.

Benefit to National Security Missions

The work to be carried out develops the understanding of fundamental chemical reactions (i.e. Fundamental Chemistry Mission) with direct relevance to biomass derived substrates to produce fuels and chemical feedstocks. Development of competitive alternative energy sources and feedstocks directly impact our national security mission.

Progress

We have made progress identifying a selection of intermediates in the HDO reaction of the triketone. We have used labeled products to follow the reaction pathway and we now have a clearer understanding of the initial deoxygenation steps. This has been applied to the Garcia-Gonzales reaction and we have further modified the HDO of that reaction to progress in a step-wise reaction exhibiting much more control. We have investigated a range of different reaction conditions and have screened different Bronsted acids to perform the transformations. We have also moved to industrially relevant solvents which have further improved the process.

Future Work

Due to the two year time frame for the project, all components will be performed in tandem. These tasks are:

1. Identification and isolation of possible intermediates
2. Use of isotopically enriched substrates for mechanistic investigation
3. Theoretical calculations of likely reaction pathways with input from experimental work, and validation of these pathways through Tasks 1 and 2
4. Use of knowledge obtained from Tasks 1, 2 and 3 to start developing NPMCs for the hydrogenation and HDO reaction chemistries, designed to achieve transformations to the intermediates identified in Tasks 1 and 2
5. Task 4 will also address the isolation of intermediates with applicability to feedstocks

Conclusion

We expect to gain a more detailed understanding of hydrodeoxygenation reaction mechanisms involved in alkane production from biomass and to develop an insight into potential new catalysts for performing these transformations.

Publications

King, A. E., A. D. Sutton, and E. Batista. Mechanistic Insights into the Palladium-Catalyzed Reduction of Pentanone to Pentane: Insights into a Biomass-to-Fuel Conversion Process. TBD.

Effects of Joining Processes on Bimetal Interface Content and Radiation Damage Resistance

John S. Carpenter
20130764ECR

Introduction

A fundamental study of the effect of pre-existing interfacial structure on the joinability and resulting material properties of bulk nanostructured metals (BNM) is proposed. BNMs, due to the nanometer length scale, have material properties and behaviors that arise as a result of two factors: 1) interfacial type and 2) interfacial density. Success has been achieved in fabricating strong and lightweight BNMs with industrial methods that exhibit properties that far exceed those of bulk metals through purposeful manipulation of both interfacial density and interface type. In order for BNMs to be used in engineering applications, however, the reaction of the interfacial density and interface type to industrial joining processes must be evaluated.

The Cu-Nb bimetallic multilayer nanocomposite system has been selected as the model system for the proposed work. Controlled interfacial structures and controlled nanoscale interfacial densities in a bulk sheet form appropriate for joining studies have been demonstrated at LANL. Understanding the physics that govern the dynamic and thermal stability of interfaces in Cu-Nb nanolamellar material will be valuable for the joining of any material, BNM or otherwise, where interfaces comprise the primary control on material behavior and properties.

Cu-Nb multilayers also exhibit outstanding material behavior such as high strength, thermal stability, and ultrahigh resistance to both shock and radiation damage. Given the properties exhibited by Cu-Nb composites, a range of potential applications exist such as nuclear fuel cladding, armor for defense applications, and as a strong, lightweight structural material in transportation. A secondary goal of this proposal, therefore, is to explore methods for joining Cu-Nb nanolamellar material in order to unlock its potential as a lightweight manufacturable nanolayered composite.

Benefit to National Security Missions

Fossil Energy, DOD, Commerce and Transportation
If joining of bulk nanostructured metals (BNMs) is successful, this class of materials could reduce vehicle weight significantly without compromising and, perhaps, enhancing safety. These materials are lightweight, strong, and resistant to shock damage making BNMs useful in reducing weight of both civilian passenger cars and military vehicles. This reduction in weight would reduce the amount of fossil fuels needed providing more fossil energy security.

Nuclear Energy

Materials in nuclear fuel reactors experience extreme radiation and temperatures over their lifetimes. BNMs have exhibited 'self-healing' interfaces that both remove radiation damage and provide thermal stability. These interfaces would enable significantly improved safety, performance, and lifetime length for future advanced reactor and fuel cycle design.

Basic Understanding of Materials

Although it is clear that interfacial type and density control properties in BNMs, the stability of these interfaces under joining conditions has not been well-studied. Only recently has a BNM with tailored interfacial types and densities been fabricated. With this material in hand, concentrated studies on the relative stability and dynamics of various interfacial structures can commence.

Matter-Radiation Interactions in Extremes (MaRIE) Signature Facility

This study will investigate the stability of a well-controlled and well-characterized microstructure under the extreme conditions of radiation and joining. The current study will make use of ex situ characterization techniques that provide static properties. These results could form a seed study for future work at the MaRIE

facility where in situ techniques could be used to manufacture specific microstructures under dynamic control.

Progress

The overall goal of the project is to study the effect of pre-existing interfacial structure on the joinability and resulting material properties of bulk nanostructured metals (BNM). Success has been achieved in fabricating strong and lightweight BNMs with industrial methods that exhibit properties that far exceed those of bulk metals through purposeful manipulation of both interfacial density and interface type. In order for BNMs to be used in engineering applications, however, the reaction of the interfacial density and interface type to industrial joining processes must be evaluated.

In order to study this, two welding techniques – fusion welding and friction stir welding (FSW) - were used on Cu-Nb bimetallic multilayer composites with varying nominal layer thicknesses. Cu and Nb are immiscible and the controlled geometry of the composites provides an embedded measurement tool allowing microstructural changes due to welding to be evaluated. Over the course of the first five months of funding, work has commenced towards achieving the four goals seen in the technical description. Progress to this point will be described in the context of these four goals. In addition, three Cu-Nb multilayer materials have been investigated to this point – material A) multilayer with nominal layer thicknesses (h) of 20 um, material B) multilayer with h = 300 nm, and material C) multilayer with h = 30 nm.

Identify differences in welding parameters that can be associated with interfacial type and density

Eight different sets of weld parameters were utilized during fusion welding in order to investigate how material A reacted to standard welding techniques. Delamination between layers as well as substantial porosity was noted for all sets of weld parameters. In addition, complete melting of the Cu phase occurred leading to a loss of layered geometry in the weld and heat affected zone. These results showed that standard welding techniques do not present a usable technique for joining nanostructured metals while maintaining the integrity of the overall material and the unique properties that stem from the nanostructured grains.

FSW was performed on the same material utilized in the fusion welding studies. Successful welding was achieved with results indicating that Cu did not melt in order to accomplish joining. Instead, the layered structure was refined and mixed in the welded area from layers on the order of 20 um thick to layers ~200 nm thick. Welding of Cu-Nb material with similar interfacial structure, but a higher density (material B) was then attempted. The tooling needed to be redesigned and significant changes in weld parameters were also required to successfully weld this material. Refinement was again noted in the weld nugget but the length scale of the refined microstructure was now less than 80 nm. When similar weld parameters were used on material C, successful welding was not achieved as the material tore, instead. Further work is needed in tool redesign and weld parameter selection that will allow joining of the 30 nm material.

Investigate stability of interfacial types and densities under the effects of joining

Due to the length scale involved, the interfacial types and densities in the welded zone are currently being studied using a combination of electron microscopy based techniques. This work is ongoing and will form the bulk of the work over the final part of the first year.

Investigate stability of mechanical properties after joining

Mechanical properties were tested in the parent material, in the weld affected zone, and in the welded zone, or nugget, with nanoindentation. Measured hardnesses within the weld nugget for the material B were 200% greater than the parent material and 20% greater than the strongest Cu-Nb multilayer composite fabricated thus far (a Cu-Nb multilayer with nominal layer thicknesses of 7 nm). This increase in strength is consistent with a grain size < 5nm in the welded zone and might indicate that performing FSW on a whole sheet of Cu-Nb multilayer nanocomposite could lead to improved mechanical properties.

Publicize results

Two talks (one invited) will be given at two materials science conferences over the next six months. A peer-reviewed journal publication detailing the results obtained to this point is in preparation.

Future Work

The goals of this project will be accomplished through completing the following tasks:

- Utilize two joining techniques, friction stir welding and fusion welding, to fabricate three joined sheets of Cu-Nb multilayer nanocomposite with each sheet exhibiting differences in interfacial type or density prior to welding.
- Characterize interfacial type and density after joining through the use of diffraction, electron microscopy and optical microscopy techniques.
- Utilize nanoindentation in order to characterize the relative hardness between joined and unjoined regions.

- Submit results to a peer-reviewed journal.
- Present results in a conference talk.

Conclusion

The technical goal is to join two sheets of Cu-Nb bimetallic multilayer nanocomposites such that properties like strength, radiation damage resistance, and thermal stability are maintained or enhanced. Joining will be attempted on Cu-Nb materials that exhibit three different interfacial types and two different interfacial densities. Through this study the relative effect of interfacial type and density on joinability can be studied as well as the stability of various interfaces under extreme strain. In addition, if joining is successful while maintaining the material properties, the last hurdle inhibiting bulk metallic nanocomposites from use as structural materials will have been overcome.

Probing Interface Reactions of Calcite Nanocrystals at Elevated Temperatures and Pressures

Katharine L. Page
20130772ECR

Introduction

Calcite (the most stable form of calcium carbonate, CaCO3) is an important mineral phase in both environmental systems and energy applications. Calcium carbonate is considered the long-term sink for atmospheric carbon dioxide (CO2), and thus the process by which CO2 is trapped and transformed to stable carbonate minerals is of great fundamental and practical interest. The main goal of this project will be to isolate and characterize the atomic interface structures that facilitate precipitation and dissolution of carbonate species under conditions found in underground reservoirs for CO2 sequestration.

There are many challenges to probing the relevant interface reactions experimentally: in bulk carbonate systems, the solid/fluid interface represents a very small proportion of the total system, resulting in low signal strength for many experimental measurements. Additionally, standard diffraction (the usual means of determining atomic structure) is intrinsically insufficient due to the amorphous nature of the fluid phase and the non-periodic/highly disordered interface with the solid phase. As a further complication, the sequestering of CO2 in underground reservoirs occurs under hot, pressurized conditions. Appropriate sample environments further reduce signal from the interface. All these factors have hindered progress in experimentally probing the atomic interface structures controlling precipitation and dissolution of carbonates at crustal conditions. We will use advanced scattering techniques based on neutron total scattering measurements to target the atomic structure at the interface between the mineral calcite (and other carbonate species) and water/carbon dioxide fluids at elevated temperatures and pressures. The approach will involve a size dependent (and therefore surface area dependent) set of carefully characterized nanocrystalline samples, high pressure and temperature sample environment development for local structure measurements, and differential neutron total scattering measurements with fluid-solid mixtures. Along the way we will advance techniques based on neutron diffraction for characterizing the atomic structure at the interfaces of fluids and nanomaterials.

Benefit to National Security Missions

Understanding the behavior of mineral interfaces in geothermal fluids is important for expanding many of the earth's energy options, including geothermal production, hydrocarbon extraction, and geologic carbon sequestration. Successful study of the interface reactions in the CaCO3/D2O/CO2 system directly supports the missions of reducing climate and energy impacts, and enabling environmental remediation and restoration.

Sample environment capabilities and modeling methodology developed with this work will also provide new or improved research tools for probing complex materials, relevant to the MARIE and NNSA missions of LANL and the DOE Office of Science, as well as DOE Fossil Energy, and Nuclear Energy Programs. For instance, the temperature and pressure regimes and length scales of interest in this study are directly applicable to optimizing hydrocarbon extraction from oil and gas reservoirs and understanding corrosion and scaling in nuclear reactors.

Progress

The project scope has four tasks associated with it: (1) careful synthesis and characterization of size dependent nanocrystalline carbonate materials; (2) development of high pressure and temperature cells compatible with local structure measurements; (3) neutron total scattering measurements of calcite-fluid solutions at elevated pressure and temperature; and (4) a data simulation and data modeling effort to interpret experimental results.

Task 1: In the last several months we have identified that very small and monodisperse calcite nanocrystal samples are quite difficult to synthesize. Nonetheless, a large (100 gram) calcite nanoparticulate sample with an average particle diameter of 40 nm has been prepared at the Lujan Center by a senior adviser for this project, Dr. Luke Daemon. This sample has been characterized by laboratory x-ray diffraction, thermogravimetric analysis, transmission electron microscopy (for morphology), and surface area measurements. Plans for both mechanical milling and digestive ripening of this sample have been made in hopes to produce smaller and larger average particle size samples, respectively. In addition, an external collaboration has been formed with Dr. Andrew Villegas-Jimenez at the Carnegie Institute of Washington to leverage his recent successes in producing high purity calcium carbonate samples of homogenous nanometer size without using chemical additives.

Task 2: The PI, in consultation with the Lujan Center's sample environment, high pressure, and mechanical design teams, has completed the engineering design of a series of high pressure and temperature cells compatible with neutron total scattering measurements (which require a very low and stable background scattering signal). The suite of gas pressure cells includes both mechanically weaker but proven vanadium material designs and mechanically stronger but unproven titanium-zirconium marerial designs, as well as several different cell thicknesses. Finite element analysis was applied to the final designs to validate safety factors for experimental measurements. Specifically, we have designed a 200 bar pressure cell for operation at room temperature and below, a 400 bar pressure cell for operation up to 500 K, and an 800 bar pressure cell for operation up to 750 K. The three generations of designs will be assembled and tested in July. Successful prototypes will be tested in situ on the NPDF beamline in August and September of this year, in hopes to identify the best compromise of high temperature/pressure conditions and low and stable background scattering.

Task 3: Four days of neutron scattering beamtime have been awarded through the Lujan Center's competitive proposal review process to investigate the first series of nanoparticulate calcite samples with the commissioned high temperature and high pressure cells on the NPDF instrument. Measurements will be scheduled for September and October of this year. Complementary X-ray total scattering experiments have also been scheduled at beamline 11-ID-B at the Advanced Photon Source, Argonne National Laboratory for the middle of August. The X-ray measurements will only be completed at ambient conditions.

Task 4: Neutron and X-ray data simulation at ambient conditions (to establish and benchmark signal sensitivity for CaCO3-D2O/CO2 fluid/solid interfaces) is in early stages. Two data modeling approaches and software suites are currently being compared and evaluated for their utility. Additional Accomplishments: In a recent unrelated visit to Oak Ridge National Laboratory (ORNL), the PI became aware of relevant research led by Dr. David Wesolowski, Dr. Andrew Stack, and Dr. Gernot Rother in the Geochemistry and Interfacial Science Group within the Chemical Science Division. The idea of following calcite and carbonate mineral growth within controlled pore glass (CPG) substrates with capabilities developed in this project was nucleated. The lack of experimental data for tracking the role of water on the structural stability and transformation of the metastable hydrous amorphous calcium carbonate (ACC) to calcite was also discussed as an area the present capabilities could address. Plans for collaborative and follow-on research are being discussed.

Finally, a postdoctoral associate offer has been accepted by Dr. Hsiu-Wen Wang, a skilled mineralogist, geochemist, and neutron scatterer, to join the PI in completing this project. She will begin work at LANL in August 2013, pending completion of all LANL hiring protocols.

Future Work

Tasks and goals for the next fiscal year include:

Task 1: completion of the synthesis and characterization of size dependent nanocrystalline calcite materials. We will complete preparation of a size-dependent series of five or more homogenous and narrow size-distribution carbonate nanocrystal powders. The size series will provide an increasing availability of surface area for liquid-surface interaction per sample. The materials will be characterized by laboratory x-ray diffraction, thermogravimetric analysis, transmission electron microscopy (for morphology), and surface area measurements.

Task 2: We will continue development of high pressure and temperature cells compatible with local structure measurements. Specifically, in the comping year three design prototypes will be commissioned and evaluated for compatibility with the project goals. Any needed modifications will be addressed in the upcoming 2013 run cycle of the Lujan Neutron Scattering Center.

Task 3: Neutron total scattering measurements will be completed for the initial series of calcite nanocrystal samples, and for calcite-fluid solutions at elevated pressure and temperature by differential scattering techniques (by subtracting the signals separately collected for the solid

particles and D2O/CO2 fluid from the scattering signal of each solution). Complementary x-ray total scattering measurements will also be completed for the series of nanocrystal samples at ambient conditions.

Task 4: A data simulation and data modeling effort will be initiated to interpret the experimental results. Interpretation of the results will involve both data simulation at ambient conditions (to establish and benchmark signal sensitivity for CaCO3-D2O/CO2 fluid/solid interfaces) and data modeling at all experimental conditions accessed. Two data modeling approaches and software suites will be evaluated for their utility.

The feasibility of studying carbonate-mineral growth within controlled pore glass (CPG) substrates with developed capabilities will also be investigated. If feasible, the transformation of the metastable amorphous calcium carbonate (ACC) species to stable calcite species may be tracked.

Conclusion

We will isolate and characterize the atomic interface structures that determine precipitation and dissolution of carbonate species under conditions found in underground reservoirs. Conversion of CO2 into solid carbonate phases will provide the largest storage capacity within porous sandstone saline aquifers, and prevent leakage through cracks and fissures in shale and salt capping layers. Understanding the species (composition and structure), conditions (temperature and pressure), and processes involved in the formation of stable carbonate minerals will aid modelers in building more realistic simulations, help to predict the success of geologic repositories, and assist in identifying candidate sites for sequestration.

Exploiting Non-Innocent Ligands in Catalysis: New Base Metal Catalysts for the Reduction of Carbon Dioxide

Susan K. Hanson
20110537ECR

Abstract

Transition metal catalysts could have a transformative impact on renewable energy technologies, but the majority of effective catalysts are based on scarce and expensive precious metals. The replacement of precious metal catalysts with earth-abundant metals is thus a key goal of sustainable and green chemistry, and was a primary focus of this project. This project evaluated the hypothesis that by designing catalysts that incorporated "non-innocent" ligands (ligands which could participate in the reaction as proton donors or acceptors via metal-ligand cooperativity), it would be possible to enhance the reactivity of earth-abundant metals.

Several different iron, nickel, and cobalt complexes were synthesized and the reactivity of these complexes was evaluated. The most promising results were obtained with nickel and cobalt complexes of a PNP pincer ligand. Two different nickel hydride complexes were prepared and shown to catalyze the hydrogenation of olefins under mild conditions. Both cationic and neutral cobalt(II) alkyl complexes of the cooperative pincer ligand PNHPCy (PNHPCy = bis(dicyclo-hexyl¬ethyl)amine) were synthesized. The cationic cobalt(II) alkyl compound was shown to be a catalyst for the hydrogenation of both olefins and substrates with polar multiple bonds (ketones, aldehydes, and imines). In addition, the cobalt catalyst showed a surprising and remarkable tolerance for different functional groups and water, suggesting its promise for energy related transformations. This discovery of a versatile, earth abundant metal cobalt hydrogenation catalyst was an important breakthrough. Subsequent work demonstrated that the cobalt complex could also catalyze the acceptorless dehydrogenation of alcohols, a reaction that has applications in hydrogen storage and generation. Detailed studies of the reactivity of the cobalt catalyst provided important insights into the reaction mechanism.

Overall, the results of these studies confirm that it may be possible to enhance the reactivity of earth-abundant metals by using "non-innocent" ligands capable of metal-ligand cooperativity. In addition, the results underscore the potential of cobalt complexes to replace precious metals as catalysts for energy-related transformations. By enabling more effective and sustainable renewable energy technologies, earth abundant metal catalysts could have an important impact on domestic energy security.

Background and Research Objectives

Amidst concerns over increasing carbon dioxide emissions, worldwide energy consumption is projected to nearly double over the next 30 years. To meet growing worldwide demands for energy without further increasing atmospheric carbon dioxide levels, it will be necessary to more effectively utilize non-petroleum based feedstocks. However, the conversions of renewable feedstocks to fuels, including the reduction of carbon dioxide, are challenging reactions, requiring a catalyst to perform a complex series of chemical steps. New and more effective catalysts could improve our ability to harness renewable resources.

Transition metal catalysts promise to enable key transformations in renewable energy technologies, such as biofuel production, carbon dioxide reduction, and hydrogen storage and generation. However, current catalytic technologies are based on rare and expensive precious metals (Pt, Pd, Ir, Rh, and Ru). For widespread applications in energy technologies, there may not be enough of these precious metals available in the world to meet the anticipated demand. Consequently, a major goal of sustainable chemistry is to develop alternatives to precious metal catalysts based on inexpensive, readily available, and earth-abundant metals such as iron, cobalt, or nickel.

The goal of this proposal was to synthesize a new family of earth-abundant metal complexes of Ni, Co, and Fe,

and develop these complexes as catalysts for hydrogenation reactions and the reduction of carbon dioxide. The initial hypothesis was that incorporating a tethered base (proton acceptor) in the metal coordination sphere would increase catalytic activity or enable new reaction modes. The objective of this work was to prepare complexes of such "non-innocent" ligands and investigate if altering the ligand framework around a non-precious metal center could result in better catalysts.

Scientific Approach and Accomplishments

In initial work, a number of different ligand candidates were evaluated in reactions with iron, cobalt, and nickel metals. The most promising approach involved the synthesis of nickel and cobalt complexes of the ligand PNHPCy (PNHPCy = bis(dicyclohexylethyl)amine). Use of the PNHPCy ligand posed several advantages; including a meridonal tridentate coordination mode and large steric bulk, both of which could help stabilize highly reactive species or intermediates. The PNHPCy ligand also had the potential to participate in the reaction in a "non-innocent" fashion via the basic central nitrogen of the pincer ligand (Figure 1).

Using the ligand PNHPCy, two new nickel hydride complexes were synthesized (complexes 1 and 2, Figure 2). These complexes were tested as catalysts for the hydrogenation of substrates with C=C and C=O bonds. The cationic nickel(II) hydride complex was an active catalyst for the hydrogenation of olefins, although only limited reactivity was observed with substrates with C=O bonds. Mechanistic experiments indicated that the increased reactivity of the nickel complex with olefins may be due to an increased propensity of olefins to undergo insertion into the Ni-H bond (C=O insertion into the nickel-hydride bond was not observed). A full paper describing this work was published in the European Journal of Inorganic Chemistry.

Neutral and cationic cobalt(II) alkyl complexes 3 and 4 of the ligand PNHPCy were synthesized and evaluated as hydrogenation catalysts (Figure 2). The cationic cobalt(II) alkyl complex 4 was a highly active catalyst for the hydrogenation of olefins. Carbon-heteroatom (C=O, C=N) bonds were also reduced under mild conditions using 4 as a catalyst. Additional experiments probed the functional group tolerance of the cobalt catalyst. Surprisingly, catalyst 4 was not completely deactivated by water or oxygen functional groups. These results suggest the promise of 4 as an earth-abundant metal catalyst, since the ability to tolerate oxygenated substrates will be critical for application in energy-related technologies. Details of this work were published and featured on the cover of the journal Angewantde Chemie International Edition (Figure 3). A patent application was filed describing the nickel and cobalt complexes and their catalytic activity.

Mechanistic experiments were performed to gain insight into the cobalt-catalyzed reactions. The role of metal-ligand cooperativity in the reactions was assessed by comparing the reactivity of cobalt catalyst 4 with the analogue 5, where the central nitrogen of the ligand is substituted with a methyl group (Figure 4). If the N-H group on the ligand plays an important role in the catalytic cycle, a suppression in catalytic activity would be expected using 5. In fact, catalyst 5 showed diminished reactivity relative to 4 in the low temperature hydrogenation of ketones, suggesting an important role for metal-ligand cooperativity and the "non-innocence" of the ligand. The full set of experiments and mechanistic insights gained from this work are described in a full paper published in the Journal of the American Chemical Society.

Additional work explored the potential of cobalt complexes to catalyze the acceptorless dehydrogenation of alcohols, and the transfer hydrogenation of C=O and C=N bonds. These reactions have application in energy related technologies, including hydrogen storage and generation and as a selective and low-temperature route to generate hydrogen from biomass-derived alcohols and carbohydrates. The full results were published in the journals Organic Letters and Chemical Communications.

In conclusion, using a "non-innocent" ligand was evaluated as a strategy for enhancing the reactivity of earth-abundant metals. Using such ligands, new and active examples of nickel and cobalt hydrogenation catalysts were developed. The development of the cobalt catalyst was particularly significant, given its high activity under mild conditions and robust functional group tolerance. These features of the cobalt catalyst suggest that it could have important applications in energy-related technologies. Overall, the design of effective earth-abundant metal catalysts for the hydrogenation of C=C and C=O bonds is a key step forward in our ability to more efficiently and cost-effectively utilize renewable resources like carbon dioxide.

Impact on National Missions

In a recent 2013 address to the nation, President Obama stated that "the only way for America's energy supply to be truly secure is by permanently reducing our dependence on oil…We have to discover and produce cleaner, renewable sources of energy with less of the carbon pollution that threatens our climate. And we have to do it quickly." In order to effectively use renewable sources of carbon (non-food biomass or carbon dioxide) as fuels, new catalytic technologies are needed. In demonstrating that it is possible to use inexpensive, earth-abundant metals like nickel and cobalt as catalysts for these applications, this

work has provided an important conceptual and technological advance. The work is relevant to Office of Basic Energy Sciences mission priorities.

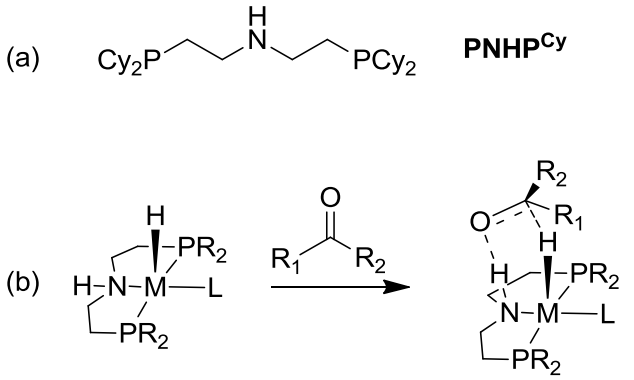

Figure 1. (a) The "non-innocent" PNP pincer ligand and (b) its proposed ability to participate in a reaction by metal-ligand cooperativity.

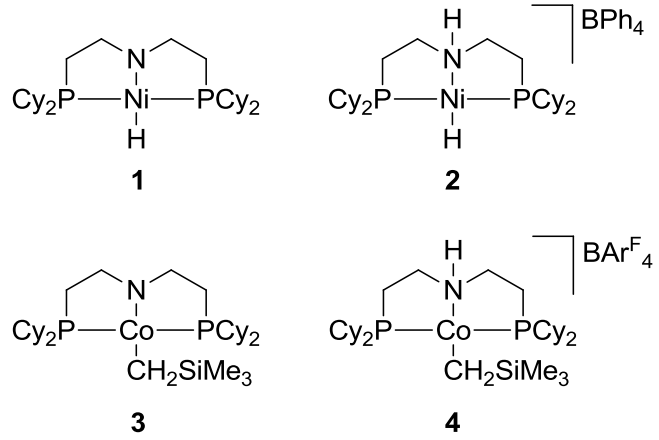

Figure 2. New nickel(II) hydride and cobalt(II) alkyl complexes synthesized and found to be active catalysts for hydrogenation reactions.

Figure 3. Cobalt-catalyzed hydrogenation reactions featured on the cover of Angewandte Chemie International Edition.

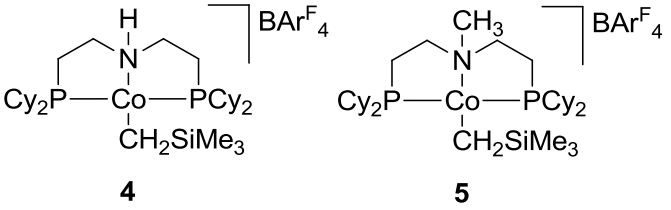

Figure 4. Comparison of the reactivity of cobalt complexes 4 and 5 provided insights into the role of metal-ligand cooperativity and the "non-innocent" ligand in the catalytic reactions. The two complexes differ in the substitution at the central nitrogen of the pincer ligand (N-H vs. N-methyl).

Publications

Lucas, M., S. Hanson, G. Wagner, D. Kimball, and K. Rector. Evidence for room temperature delignification of wood using hydrogen peroxide and manganese acetate as a catalyst. 2012. Bioresource Technology. 119: 174.

Vasudevan, K. V., B. L. Scott, and S. K. Hanson. Alkene Hydrogenation Catalyzed by Nickel Hydride Complexes of an Aliphatic PNP Pincer Ligand. 2012. European Journal of Inorganic Chemistry. : 4898.

Zhang, G., B. L. Scott, and S. K. Hanson. Mild and homogeneous cobalt-catalyzed hydrogenation of C=C, C=O, and C=N bonds. 2013. Angewandte Chemie International Edition. 51: 12102.

Zhang, G., K. V. Vasudevan, B. L. Scott, and S. K. Hanson. Understanding the mechanisms of cobalt-catalyzed hydrogenation and dehydrogenation reactions. 2013. Journal of the American Chemical Society. 135: 8668.

Zhang, G., and S. K. Hanson. Cobalt-catalyzed acceptorless alcohol dehydrogenation: synthesis of imines from alcohols and amines . 2013. Organic Letters. 15: 650.

Zhang, G., and S. K. Hanson. Cobalt-catalyzed transfer hydrogenation of C=O and C=N bonds. Chemical Communications.

Advanced Materials for Exploring New Electronic and Optical Behaviors in Single-walled Carbon Nanotube Systems

Juan Duque
20120502ECR

Abstract

A general challenge in generating functional materials from nanoscale components is integrating them into useful composites that retain or enhance the properties of interest. Because the unique electronic and optical properties of single-walled carbon nanotubes (SWCNT) are highly sensitive to environmental effects, incorporating SWCNTs into useful composites which retain and/or enhance the photophysical properties for optoelectronics and sensing applications is still a major challenge.

Background and Research Objectives

The photophysical properties of SWNTs are highly stable and excitonic in nature, with discrete levels below the single-particle excitation spectra. While long radiative lifetimes (~ns) suggest higher photoluminescence (PL) quantum yields (QY), only modest QY ~7-20% have been reported, as consequence of the lack of homogeneity in the optical properties at the ensemble level and the strong environmental sensitivity. Emerging data indicates high mobility of the exciton in 1-D along the SWNT surface efficiently quenches PL by rapidly carrying excitons to defect sites where they dissociate into free charge carriers. Moreover, environmental perturbations can also couple emissive states (dark) with optically allowed states (bright) affecting exciton behavior. Although these photo-generated carriers are of interest for energy harvesting, PL QY is compromised since exciton binding and exciton diffusion behaviors are directly affected. A key capability in meeting these challenges is the ability to tune interfacial behaviors and obtain photoluminescent solution- and surfactant-free systems with minimal and/or controllable perturbations from the local environment; the presence of aqueous media and suspending agents such as surfactants and polymers masks the intrinsic photophysical behavior of the tubes.

The ability to tune interfacial behaviors presents a rich opportunity for engineering and optimizing SWNT optical response since surfactant structure, access to the tube surface, and reactivity with other organic molecules can be controlled. Recent reports have shown that multi-functional materials may be obtained by tailoring interactions between tubes and other species. Of particular interest is to study the charge transfer (CT) and energy transfer (ET) behavior in these multi-component materials. When studying ET behaviors, important material functionality can be extracted including interstitial spacing, inter-particle coupling, and percolation. For instance, Förster resonant ET (FRET) in bundles of different bandgap semiconducting tubes has resulted in diameter dependent exciton ET. Similar FRET observations have been reported with quantum dots, polymers, and metal porphyrins. However, a major drawback is the lack of control of the bundle size, tube type, and interactions. Thus, the general challenge of generating functional materials from nanoscale components and integrating them into useful composites that retain or enhance the properties of interest still remains. Nevertheless, ET is the basis for understanding how to build up more complex interactions within systems.

If properly prepared, aerogels can offer the alternative of having a solution- and surfactant-free environment where the inter-particle interactions may be controlled. Aerogel preparation methods can be modified to optimize interstitial distances and optical density, as well as tune the pore size distribution, thus allowing significant degrees of freedom for engineering of the desired properties. Although SWNT-aerogel composites have been investigated for their mechanical and electronic properties, no reports to date have demonstrated SWNT-aerogels with an observable emission signal. Recently, here at LANL, we developed SWNT-aerogel nanocomposites with tunable local environmental interactions. These nanocomposites exhibit a behavior characteristic of non-interacting samples in the absence of solution and surfactants. These silica matrices are of particular importance because they provide the first bulk-phase platform to develop a fundamental understanding of the

link between SWNT interfacial chemistry and underlying photophysical behaviors, while also providing a suitable matrix for development of relevant applications. This work pioneers the currently unexplored area of SWNTs in solution- and surfactant-free systems for basic research as well as for energy and optoelectronics applications.

Engineering material functionality through interfacial interactions is a major component in developing the next generation of composites for energy harvesting, sensing, and photonic applications. A general challenge in generating functional materials from nanoscale components is integrating them into useful composites that retain or enhance the properties of interest. Here, we aim to design and engineer the functionality of nano-structured materials, specifically SWNT nanocomposites, by tuning interfacial behaviors and interactions (such as surfactant structure, dopants, and matrix composition), thus controlling intertube and matrix interactions.

Scientific Approach and Accomplishments

We used an innovative method developed here at LANL by our team to obtain highly fluorescent and low density SWCNT-aerogel mesocomposites. The approach provides a rationale for tailoring SWCNT photophysical response via interfacial chemistry.

Using this mesomaterials we monitored the interaction of molecules inside and outside carbon nanotubes and the effect of confinement. Moreover, we examined the changes in dielectric environment due to local environment (Figure 1).

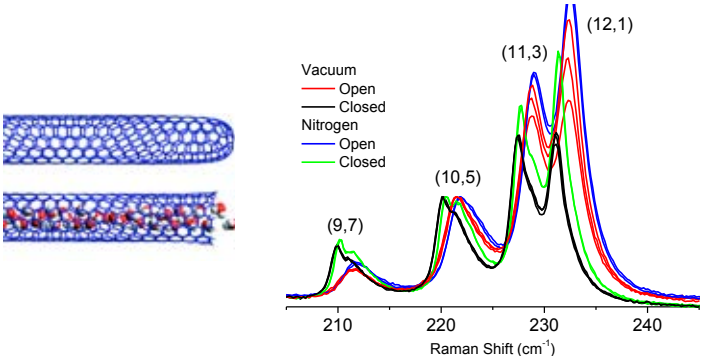

Figure 1. Raman spectra of carbon nanotubes empty and filled with water.

We also studied the energy transfer of nanotubes and rare-earth ions. Formation and evolution of highly photoluminescent complexes of rare-earth ions (REI) and bile salt molecules is observed in a crowded environment of silica hydrogels. By comparing the behavior of REI complexes in bulk solution and small compartments inside the hydrogel, the nature of the 5x-longer lifetime of REIs was understood. The effect is due to binding of REI to surfactant molecules followed by formation of a closed shell micelle, completely screening REIs from the water molecules. The process is shown to be slowed down in the crowded environment of a hydrogel.

We studied behavior of Tb ions in different environments. We found that Tb ions quickly form long-lived PL complexes in solution containing surfactant (DOC) molecules. This process is faster than the diffusion through the DOC/SWNT silica hydrogel. The PL lifetime in these complexes increases to 2.3 ms for DOC/SWNT hydrogel with time. Similar changes of the shape of Tb lines of steady-state PL spectra in DOC bulk solution and DOC/SWNT silica gel, compared to TbCl3 water solution, suggest the formation of DOC micelles in both cases (Figure 2).

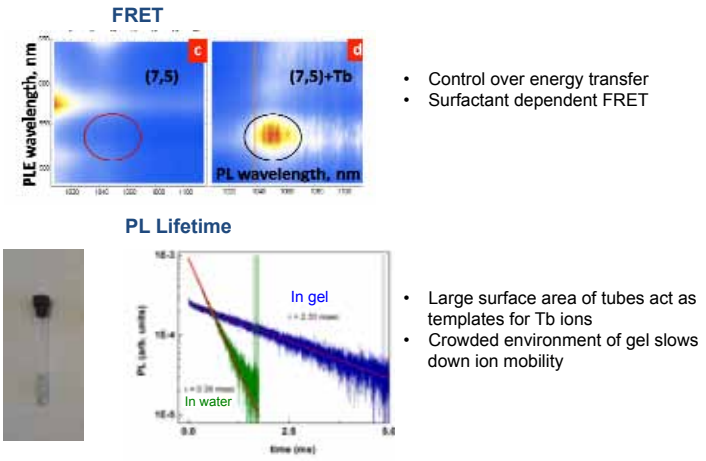

Figure 2. Lifetime of rare-earth ions inside hydrogels.

As result of this work we have establish several collaborations inside LANL but also with universities, which have resulted in data for upcoming publications.

Impact on National Missions

This work focused on the development of new mesocomposites with tunable and desire properties for sensing and photonics applications. Through my early career project I was able to establish and maintain two capabilities very important to the mission of the laboratory:

The unique and extensive resonant Raman excitation capability (with wavelengths extending from 350 to 1000 nm) at LANL's Integrated Spectroscopy Laboratory (residing in Chemistry Division) is recognized worldwide. This capability has fostered both internal and external (national and international) collaborations, which have resulted in significant discoveries appearing in well-over 100 peer-reviewed publications in high-profile journals including Nature journals, Phys. Rev. Lett., J. Am. Chem. Soc., etc. The impacted subject areas have spanned many disciplines and include

nanoscience (carbon nanotubes, graphene, quantum-dots, nanowires), thin film development, actinide chemistry, plasmonic materials, biophysics, and inorganic photo- and coordination chemistry among others, putting the laboratory at the vanguard in nanophotonics, optoelectronics, materials, chemistry, and biosciences research.

Nevertheless, a major drawback with the system was the lack of a microscope that couples all of the excitation wavelengths, namely a continuous excitation, high-resolution Resonance Raman microscope. The ability to spatially resolve Raman features with multiple excitation wavelengths in one experiment will allow correlation of a wide range of optical features with morphological differences in materials. This is vital to understanding the optical, electronic, and catalytic properties, among others, of materials, particles, and molecules. The addition of a confocal microscope in conjunction with this project is at the forefront of Raman research, opening the door to new groundbreaking studies, and makes the new spatially correlated Raman, Fluorescence and Absorption Microscope a vital tool to materials researchers in support of our national security mission.

Publications

Arnold, M. S., J. L. Blackburn, J. J. Crochet, S. K. Doorn, J. G. Duque, A. Mohite, and H. Telg. Recent developments in the photophysics of single-walled carbon nanotubes for their use as active and passive material elements in thin film photovoltaics. 2013. Physical Chemistry Chemical PhysicsPhysical Chemistry Chemical Physics. 15 (36): 14896.

Crochet, J. J., J. G. Duque, J. H. Werner, B. Lounis, L. Cognet, and S. K. Doorn. Disorder Limited Exciton Transport in Colloidal Single-Wall Carbon Nanotubes. 2012. Nano LettersNano Letters. 12 (10): 5091.

Crochet, J. J., J. G. Duque, J. H. Werner, and S. K. Doorn. Photoluminescence imaging of electronic-impurity-induced exciton quenching in single-walled carbon nanotubes. 2012. Nature NanotechnologyNature Nanotechnology. 7 (2): 126.

Crochet, J., J. Duque, J. Werner, and S. Doorn. Photoluminescence imaging of electronic-impurity-induced exciton quenching in single-walled carbon nanotubes. 2012. NATURE NANOTECHNOLOGY. 7 (7): 126.

Duque, J. G., G. Gupta, L. Cognet, B. Lounis, S. K. Doorn, and A. M. Dattelbaum. New Route to Fluorescent Single-Walled Carbon Nanotube/Silica Nanocomposites: Balancing Fluorescence Intensity and Environmental Sensitivity. 2011. Journal of Physical Chemistry CJournal of Physical Chemistry C. 115 (31): 15147.

Duque, J. G., H. Telg, H. Chen, A. K. Swan, A. P. Shreve, X. M. Tu, M. Zheng, and S. K. Doorn. Quantum Interference between the Third and Fourth Exciton States in Semiconducting Carbon Nanotubes Using Resonance Raman Spectroscopy. 2012. Physical Review Letters-Physical Review Letters. 108 (11).

Duque, J. G., L. Oudjedi, J. J. Crochet, S. Tretiak, B. Lounis, S. K. Doorn, and L. Cognet. Mechanism of Electrolyte-Induced Brightening in Single-Wall Carbon Nanotubes. 2013. Journal of the American Chemical SocietyJournal of the American Chemical Society. 135 (9): 3379.

Duque, J., and e. et al. Fluorescent Single-Walled Carbon Nanotube Aerogels in Surfactant-free Environments. 2011. ACS Nano. 5 (8): 6686.

Haroz, E. H., J. G. Duque, B. Y. Lu, P. Nikolaev, S. Arepalli, R. H. Hauge, S. K. Doorn, and J. Kono. Unique Origin of Colors of Armchair Carbon Nanotubes. 2012. Journal of the American Chemical SocietyJournal of the American Chemical Society. 134 (10): 4461.

Haroz, E. H., J. G. Duque, W. D. Rice, C. G. Densmore, J. Kono, and S. K. Doorn. Resonant Raman spectroscopy of armchair carbon nanotubes: Absence of broad G(-) feature. 2011. Physical Review BPhysical Review B. 84 (12).

Haroz, E. H., J. G. Duque, X. M. Tu, M. Zheng, A. R. Walker, R. H. Hauge, S. K. Doorn, and J. Kono. Fundamental optical processes in armchair carbon nanotubes. 2013. NanoscaleNanoscale. 5 (4): 1411.

Telg, H., J. G. Duque, M. Staiger, X. M. Tu, F. Hennrich, M. M. Kappes, M. Zheng, J. Maultzsch, C. Thomsen, and S. K. Doorn. Chiral Index Dependence of the G(+) and G(-) Raman Modes in Semiconducting Carbon Nanotubes. 2012. Acs NanoAcs Nano. 6 (1): 904.

Valence, Coordination and Reactivity at Interfaces

Christopher D. Taylor
20120510ECR

Abstract

Metal/oxide interfaces are critical to technological applications in heterophase junctions, metal/support interactions in catalysis, stability of electrocatalysts, the corrosion of materials, and thin-film technologies. The physics controlling such interfaces is opaque: band-bending and interface dipoles, redox chemistry, interdiffusion, and interfacial energy considerations obfuscate the construction of clear predictive models. Furthermore, the complexity of the interface structure and redox chemistry places it at the very limits of what we can tackle using first-principles, electronic-structure based models. Accordingly, we propose that theory should begin by simulating known configurations of the metal/oxide interface, obtained from well-defined, in situ, high-resolution surface science measurements. Several such case studies have appeared in the recent literature, for the cases of oxide films grown on Mg, Ni, and Pu metal. Consequently, we have constructed first-principles models for these experimentally determined interfacial structures and quantify the interfaces in terms of valence (charge states at the interface), coordination (structure and local bonding at the interface) and reactivity (interfacial energies). In doing so, we provide fundamental information concerning the charge states of ions that exist at this interface (somewhere between a metallic and an ionic state), demonstrate new capabilities for understanding interfacial (two-dimensional) systems, and open up new materials design concepts for exercising control over interfaces in metal/oxide and metal/ceramic systems. This first-principles data is foundational for developing new capabilities in the molecular dynamics simulation of charge-transfer systems relevant to electrocatalysis, metal/ceramic interfaces, and energy generation.

Background and Research Objectives

Surface states and interfaces critically define materials behavior and response. Electrocatalysis by nanoparticles, for example, can be limited by oxidation states that emerge under electrochemical conditions unique to the particles' size.[1] Redox reactions and interdiffusion at heterophase junctions can change the nature of charge transport, modify surface dipoles and create new compounds at the interphase.[2] Furthermore, it has been known for some time that metal stability is conferred by formation of passive oxide films.[3]

High-Resolution Characterization: In situ electrochemical scanning tunneling microscopy (EC-STM) and X-ray asdorption spectroscopy (XAS) provide information about the structure and composition of materials/environment interfaces. EC-STM has been applied to characterize monolayer growth, epitaxial relations and electrochemical potentials associated with passivation.[4, 5] The atomic resolution provides insights into preferred coordination at these interfaces, but does not answer questions regarding valence or transport. Pugmire and co-workers demonstrated with XAS that the Pu metal/oxide interface consists of a sub-stoichiometric Pu2O3-y phase that lies somewhere between metallic Pu and the sesquioxide Pu2O3.[6] Valence and coordination information of thin oxide layers have been gleaned for platinum metal nanoparticles in fuel cells via X-ray probe techniques.[7] Experimental characterization provides a starting point for theory to probe the nature of intermediate states and the kinetics of transformations.

Modeling Oxide Growth: The process of oxidation has been described by several models, the most definitive of which is the point defect model (PDM) of Macdonald et al.[8, 9] Fundamental is the rate-dependence of oxide film growth via transport of vacancies across the film, from the metal to the environment. Although PDM is "deterministic",[10] there is, at present, no easy way to determine the rates of many of these processes from first-principles, other than by electronic structure computations.

Such computations applied to metal/oxide interfaces are ambitious as system representations must be large

enough to take into account relative orientations of the two interfaces and the presence of defects. Coarse-grained approaches, such as combining interatomic potentials for metals with Coulomb potentials,[11] can provide some means for simulating defect transport,[12] but the physics that defines the intermediate states – lying somewhere in between that of a metal and an ion – lies beyond the scope of these methods. While innovative frameworks for capturing these "superposition" (ionic+metallic) states are being developed by Valone in MST-8/LANL[13] the implementation of such models requires verifiable electronic structure data to construct the model Hamiltonian. By studying selected systems for which high-resolution measurements of the interface are available, we have created a first-principles framework.

Scientific Approach and Accomplishments

First-principles studies of electrochemical interfaces: Our research team had begun systematic development of first-principles approaches for modeling the materials/environment interface.[14-18] Using first-principles calculation, atomistic simulation, MD and constrained optimization we investigated factors controlling metal dissolution.[19, 20] The strength of metal-metal interactions was related to local coordination and alloy composition. In this work, we generalized this approach to look not only at dissolution of metals (Fe alloys) but also the formation of oxides on metals (Mg, Ni, Pu).

Incipient Magnesium Oxidation

Oxide initiation on metal surfaces has been characterized in four-steps[21-33]. O2 dissociates over a metal surface to form chemisorbed oxygen[34-36]. These oxygen atoms sit over high-coordination hollow sites on the atomistically corrugated surface planes[21]. Repulsive interactions between surface O atoms results in a 2-dimensional phase[25-29]. Further oxygen exposure enhances oxygen coverage, leading to new 2-dimensional phases that accommodate pair-wise interactions. Once a critical surface coverage occurs, oxygen atoms ingress[33] sub-surface[30, 31]. In the third step subsurface oxygen atoms experience mutual attraction and combine to form oxide nuclei[30-32]. Further uptake of oxygen at the surface leads to bulk oxide formation[21]. This process is self-limiting, with a critical concentration required before the system can pass to the next stage of oxide formation.

While magnesium may be considered one of the simplest metals (i.e. 2s2 electron configuration) its oxide formation is not consistent with this scheme [25, 37-40]. In the first stages O2 dissociates to form chemisorbed oxygen, O*. Rather than adsorbing on the surface, the oxygen atoms appear to immediately chemisorb subsurface [17, 18]. These oxygen atoms attract and form hexagonal clusters that co-exist with clean magnesium surface[25]. This behavior is distinct from the general outline above, suggesting an alternative model for oxidation.[37, 38]. Therefore, Mg oxidation was considered an attractive model system to begin application of our method.

When comparing our findings to the four step process described above distinctives for Mg emerge immediately: The subsurface tetrahedral (tet-1) is, in fact, most stable: adsorption at the surface sites (atop, bridge, and hcp) is unstable. In addition to this distinctive, O*-O* interactions are unique in that they are attractive, not repulsive. In the progression from single, to three- and seven-atom clusters, there is an accumulative effect of progressively stronger binding, i.e. a thermodynamic driving force accelerates MgO cluster nucleation. When the work function of these structures was calculated, the tetrahedral-1 clusters uniquely demonstrate a reduced work function. This explains the previous determination of a diminished work function upon initial surface oxidation obtained using both photoelectric and Kelvin probe techniques[37, 38, 41].

The differential binding provides further insight into the mechanisms of oxide nucleation (Figure 1). The differential binding energies indicate that the smallest clusters grow laterally, and the 7-atom clusters grow subsurface. The 10-atom nucleus grows in a non-trivial pattern, intercalating further oxygen atoms within the Mg plane. The multilayer oxide has been previously studied using experiment and theory[42, 43]. Schröder et al. used x-ray photoelectron diffraction, single scattering cluster[44], and DFT to study oxide structure on Mg(0001).[39, 40] They found that the multilayered oxide was a mixed 2 and 3 ML structure on top of an almost undistorted Mg(0001) surface. The Mg-O layers were reconstructed into a "graphite-like" structure. Our work shows that this structure emerges from oxidation of the O10 nuclei.

Applying first principles thermodynamics[45-47] we find that attractive Mg-O interactions result in phase separation. This prediction is supported by experiment - transmission electron microscope images of O2/Mg(0001) show formation of MgO platelets separated by regions of free metal[48, 49]. Phase separation results in a renewal of reactive metal surface and persistence of oxidation until the surface is completely populated with oxide nuclei: there is no immediate monolayer or sub-monolayer pre-passivation, hence the strong reactivity of Mg to oxidation.

Extensions beyond LDRD include study of Mg-alloy systems, critical to development of lightweight alloys for biomedical, transportation and aerospace. Opportunities are being pursued with NIH and Boeing.

Multi-layer Oxides on Nickel

Generally corrosion-resistant, nickel alloys are susceptible to localized corrosion. Proper elucidation of the problem requires detailed understanding of the passive film, which can be begun by establishing a first-principles program to simulate oxide/metal interfaces on nickel alloys. Oxide formation on nickel surfaces was studied using first principles electronic structure calculations. As for Mg, our desire was to understand the transition from nickel to nickel oxide, and quantify oxide formation in terms of valence, coordination and reactivity.

In the case of nickel, DFT methods need to be well-tested to ensure electronic structure is determined correctly. For instance, it is known that band gaps for nickel oxide are incorrectly determined from conventional DFT, but self-energy corrections remedy this problem.[50] Conversely, metallic phases of nickel are well-described by conventional DFT, but self-energy corrections introduce significant errors.

We first studied single oxygen atom adsorption on a (2x2) unit cell of Ni(111). Single oxygen adsorption at an fcc site on the Ni(111) was the most stable when performing both PBE (conventional DFT) and PBE+U (DFT with self-energy corrections). Higher charge transfer from nickel to oxygen was observed in all PBE+U calculations. Three oxygen atoms were placed along the (111) plane on the Ni(111) surface. There was no reorganization in the PBE calculated geometry, maintaining (111) site coordination, akin to experimental geometries with hydrated surfaces. The PBE+U calculations led to a reconstruction of the Ni(111) surface. A nickel atom terminated octopolar reconstruction was observed, similar to the p(2 x 2) reconstruction predicted by Wolf and has subsequently been observed experimentally. [51-55] This suggests that the nickel atoms at the surface do adopt more of a nickel-oxide like structure, since PBE+U leads to a structure that resembles experiment.

We considered a Ni(111) surface covered by an entire monolayer of NiO. We observed a reconstruction of the surface using PBE that resulted in an oxygen terminated octopolar structure. Two of the three PBE+U variations resulted in oxygen terminated octopolar-like structures, but with nickel clusters visible. Calculations with all interface Ni atoms treated with the self-energy correction resulted in the preservation of the (111) plane ordering with higher binding energy and charge transfer to the oxygen atoms. The preference for no reconstruction tracks more with the OH termination of nickel oxidation seen in ex-situ environments as being stable and more favorable than oxygen terminated surfaces.[4, 5] The agreement between these latter calculations and the STM results[4, 5] implies that all interface atoms undergo a transition in electronic structure to become oxide-like.

From the energetic analysis, nickel oxidation adopts the conventional scheme described above. Oxidation initiates at three-fold hollow sites, higher exposure leads to step-site migration and geometries that maximize oxygen-oxygen distances and/or provide metallic screening. As bilayers form, the system adopts a non-oxygen terminated surface that prevents reaction with the oxide layer and further surface oxidation.

Initial Oxidation of Plutonium

Passivation of plutonium is relevant to laboratory missions. The sequence of chemisorption steps leading up to monolayer oxide formation on δ-Pu(111) was simulated via DFT. As in nickel, chemisorption begins by occupation of oxygen at a three fold hollow site, a configuration maintained up to 0.75 ML. At 1.0 ML, significant reconstruction takes place, pushing Pu into an α-like configuration. The oxygen-plutonium binding relationships move towards a preference for four-fold coordination (Figure 2).

The sequential chemisorption steps are exothermic in nature, suggestive of the high reactivity towards oxygen and the difficulty encountered in surface science studies when deoxygenated surfaces are desired.[56, 57] Thermodynamic analysis implies a preference for uniform oxidation as opposed to islanding, consistent with the experimental finding that there is a continuum in oxide stoichiometries across the metal/oxide interface.[58]

Differences in local coordination and structure are correlated with charge transfer. The Pu-O interaction involves charge transfer, mostly from s and d states of Pu to oxygen, but also involving back-bonding from oxygen back to the Pu p and f states. Classical electrostatic models overestimate the extent to which oxygen polarizes the surface. The quantum mechanical (Bader [59-61]) analysis provides a consistent charge state for oxygen throughout all the interactions – from low to high coverage – and charge transfer is principally confined to the top monolayer of Pu atoms and the chemisorbed O. The maximum charge state induced on Pu for the reconstructed 1.0 ML system is +1.8 electrons, suggestive of an emerging Pu_2O_3 phase. Experiment suggests that there exist a range of oxidation states in the passive oxide film: PuO (an oxidation state of (II), Pu_2O_3 (an oxidation state of (III)) and, finally, PuO_2.[57, 58, 62]

The variety of charge states emerging from this quantum mechanically based study, and the flexibility to reconstruction provide some insight as to how the diversity in stoichiometries comes about and provides the foundation for further studies of metal/multilayer systems.[63, 64]

Coordination, Valence and Reactivity on Iron
The process of dissolution entails a change in the charge state of the atom at the interface between a material and its environment. The dissolution process on iron-based alloys was simulated by vertically displacing a surface adatom above the lowest energy Fe(110) surface.

The energy curve that controls the reactivity of metal atoms during dissolution can be divided into three distinct regions or stages.(Figure 3a) In the early stage of displacement (stage I – elevation of adatoms is less than 1.0 Å), the energy is controlled by strong metal surface bonding and the work is paid to the potential energy required for stretching the interatomic bonds. If the height is not constrained, there is a tendency for adatoms to be drawn back to the surface, therefore the bond stretching in this stage could be regarded as elastic, i.e. reversible. If the adatom is constrained it tends to draw surface atoms towards itself. The middle part of the energy curve (stage II – adatom's elevation between 1.0 and 2.5 Å) corresponds to the region of bond breaking. During this stage, a certain amount of energy is increasingly required for breaking the bonds and separating the adatom from the surface. In the last part of the curve (stage III - elevation is greater than 2.5 Å), the energy curve is stable, indicating a "free zone" in which the adspecies energy is determined by the formation of bonds with surrounding solvents (if any). The work of separation increases in the order of Cr < Fe < Mo adatom. In other words, the dissolution of adsorbed Mo is relatively more difficult than that of Fe and Cr in the same circumstance.

With no solvents, the native adsorbed atom (Fe in this study) is neutrally charged (Figure 3c). When the material is an alloy, electronegativity differences result in charge transfer. Cr and Mo, respectively, have positive and negative charges in adsorbed states on the Fe surface. The valence orbitals of Mo are more fully occupied by electrons than those of Cr are. As a result, Mo adsorption is more stable.

We simulated the role of water as a source of OH ions. Chemically, one would expect this to lower the energy penalty as some of the Fe atom's dangling bonds will be saturated through bonding to OH. Fe is considered to bind to two hydroxyl ions and the simulation procedure conducted as above. In this case, the shortest Fe-Fe bond of the adatom is 2.40 Å, which is longer than that of the stand-alone adatom but a little shorter than that of bulk atoms. When the elevation is less than 1.0 Å, the energy changes of Fe and Fe(OH)2 are almost identical (Figure 3a). If the altitude of Fe(OH)2 is raised further, the formation of bonds with hydroxide groups alleviates the bond-breaking process and results in a noticeable reduction of dissolution energy. This observation is consistent with the "make-before-break" mechanism observed for copper dissolution [65].

Impact on National Missions

The interplay of valence, coordination and reactivity that corresponds to the transformation of metals into oxides or dissolved ions touches aspects of LANL Mission and Capabilities ranging from aging of actinide materials, through to thin film fabrication, catalysis, energy generation, and nuclear fuel materials. The techniques and theory that we have demonstrated and advanced in this work are anticipated to open up new directions to explore the role of processing techniques such as alloying, grain-boundary engineering, surface texturing and thin-film fabrication to create materials with "smart interfaces." Already, there have been impacts from this work in the study of oxide-strengthened metal alloys, corrosion simulations developed in partnership with US industries, and in a recently awarded LDRD-DR effort aimed at exploring surface chemistry mechanisms on plutonium surfaces.

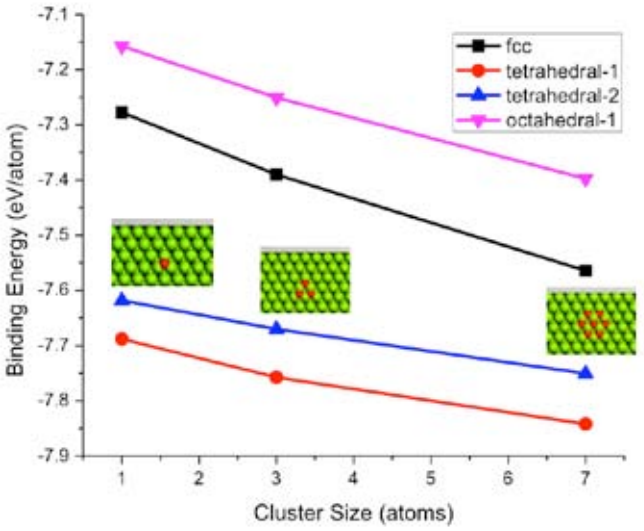

Figure 1. Differential binding energy of oxygen clusters on Mg(0001) shows the tendency for oxygen to cluster, forming areas on the surface that are oxygen rich (passivated) and oxygen deficient (reactive).

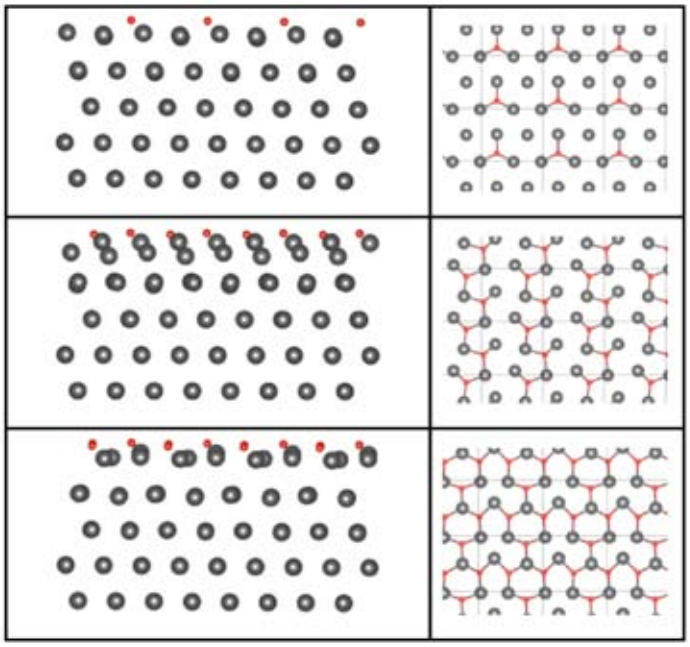

Figure 2. Chemisorption of oxygen on delta-Pu(111) at 0.25 (top), 0.50 (middle) and 0.75 (bottom) monolayers, shown in side (left) and top (right) views.

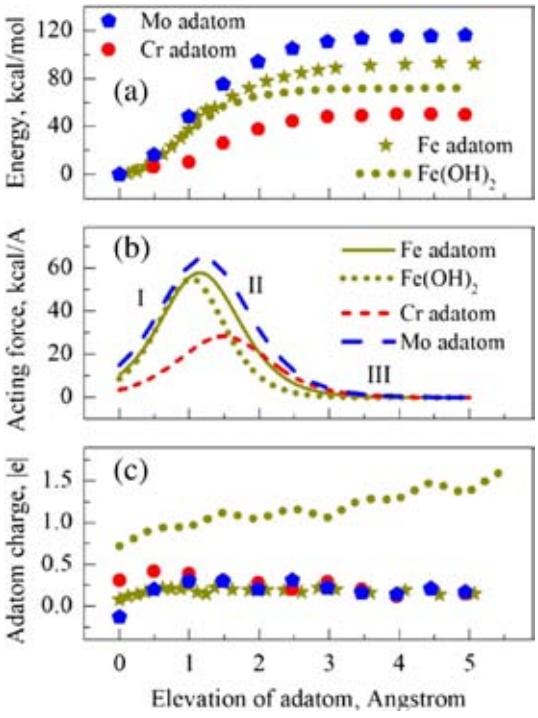

Figure 3. (a) Energies of dissolution (bond-breaking) of iron, chromium and molybdenum adatoms in proximity to a (1 1 0) iron surface, (b) Force acting on the adatoms calculated from desorption energy, (c) charges determined by Bader method for iron, chromium and molybdenum adatoms while being 'dragged' away from the (1 1 0) iron surface. Fig. (c) has the same legend as in (a).

References

1. 1, J. K. A.U. Goonewardene. An STM study of the oxidation of Mg(0001). 2002. Surface ScienceSurface Science. 501: 9.

2. Barbier, A., C. Mocuta, H. Kuhlenbeck, K. F. Peters, B. Richter, and G. Renaud. Atomic structure of the polar NiO(111)-p(2 x 2) surface. 2000. Physical Review LettersPhysical Review Letters. 84 (13): 2897.

3. Barbier, A., G. Renaud, C. Mocuta, and A. Stierle. Structural investigation of the dynamics of the NiO(111) surface by GIXS. 1999. Surface ScienceSurface Science. 433: 761.

4. Behler, J., B. Delley, S. Lorenz, K. Reuter, and M. Scheffler. Dissociation of O_{2} at Al(111): The Role of Spin Selection Rules. 2005. Physical Review LettersPhysical Review Letters. 94 (3): 036104.

5. Bungaro, C., . , P. Ballone, and W. Kress. Early Oxidation Stages of Mg(0001): A Density Functional Study. 1997. Physical Review LettersPhysical review letters. 79 (22): 4.

6. Campbell, T. J., G. Aral, S. Ogata, R. K. Kalia, A. Nakano, and P. Vashishta. Oxidation of aluminum nanoclusters. 2005. Phys. Rev. BPhys. Rev. B. 71 (205413-2).

7. Carley, A. F., P. R. Davies, K. R. Harikumar, R. V. Jones, and M. W. Roberts. Oxygen States at Magnesium and Copper Surfaces Revealed by Scanning Tunneling Microscopy and Surface Reactivity. 2003. Topics in CatalysisTopics in Catalysis. 24 (1): 51.

8. Carley, A. F., P. R. Davies, R. V. Jones, K. R. Harikumar, and M. W. Roberts. Atom resolved evidence for a defective chemisorbed oxygen state at a Mg(0001) surface. 2002. Chemical CommunicationsChemical Communications. (18): 2020.

9. Chao, C. Y., L. F. Lin, and D. D. Macdonald. A point defect model for anodic passive films: I. Film growth kinetics. 1981. J. Electrochem. Soc.J. Electrochem. Soc.. 128: 1187.

10. Cox, L.. X-ray photoemission study of δ-Pu stabilized by 1 wt.% Ga: Electronic structure and sputter-induced surface phase transformation. 1988. Physical Review BPhysical Review B. 37 (14): 8480.

11. Dinh, L. N., J. M. Haschke, C. K. Saw, P. G. Allen, and W. McLean II. Pu. 2011. J. Nuc. Mater.J. Nuc. Mater.. 408: 171.

12. Dudarev, S. L., G. A. Botton, S. Y. Savrasov, C. J. Humphreys, and A. P. Sutton. Electron-energy-loss spectra and the structural stability of nickel oxide: An LSDA+U study. 1998. Physical Review BPhysical Review B. 57 (3): 1505.

13. Ebensperger, C., and B. Meyer. First-principles study of the reconstruction and hydroxylation of the polar NiO(111) surface. 2011. Physica Status Solidi B-Basic Solid State PhysicsPhysica Status Solidi B-Basic Solid State Physics. 248 (10): 2229.

14. Fadley, C.S.. 1990.

15. Fehlner, F. P., and M. J. Graham. Thin oxide formation on metals. 2002.

16. Flores, H. G., and D. L. Pugmire. The growth and evolution of thin oxide films on δ-plutonium surfaces. 2010. IOP Conference Series: Materials Science and EngineeringIOP Conference Series: Materials Science and Engineering. 9: 012038.

17. Flores, H. G., P. Roussel, D. P. Moore, and D. L. Pugmire. Characterization and stability of thin oxide films on plutonium surfaces. 2011. Surface ScienceSurface Science. 605 (3-4): 314.

18. Friebel, D., D. J. Miller, C. P. O'Grady, T. Anniyev, J. Bargar, U. Bergmann, H. Ogasawara, K. T. Wikfeldt, L. G. Pettersson, and A. Nilsson. In situ X-ray probing reveals fingerprints of surface platinum oxide. 2011. Phys. Chem. Chem. Phys.Phys. Chem. Chem. Phys.. 13: 262.

19. Fu, Q., and T. Wagner. Interaction of nanostructured metal overlayers with oxide surfaces. 2007. Surf. Sci. Rep.Surf. Sci. Rep.. 62: 431.

20. Ganduglia-Pirovano, M. V., K. Reuter, and M. Scheffler. Stability of subsurface oxygen at Rh(111). 2002. Physical Review BPhysical Review B. 65 (24): 245426.

21. Flores, H. G. Garcia, P. Roussel, D. P. Moore, and D. L. Pugmire. Characterization and stability of thin oxide films on plutonium surfaces. 2011. Surf. Sci.Surf. Sci.. 605: 314.

22. Gesell, T. F., and E. T. Arakawa. Work function changes during oxygen chemisorption on fresh magnesium surfaces. 1972. Surface ScienceSurface Science. 33 (2): 419.

23. Getman, Rachel B., . , and William F. Schneider. Thermodynamics of Environment-Dependent Oxygen Chemisorption on Pt(111). 2008. Journal of Physical Chemistry CJournal of Physical Chemistry C. 112: 14.

24. ., , . , and . . Abstractive dissociation of oxygen over Al(111): A nonadiabatic quantum model. 2012. Journal of Chemical PhysicsJournal of Chemical Physics. 120 (8): 19.

25. Gileadi, E.. Can an electrode reaction occur without electron transfer across the metal/solution interface?. 2004. Chemical Physics LettersChemical Physics Letters. 393 (4-6): 421.

26. Haschke, J. M., and T. H. Allen. Plutonium hydride, sesquioxide and monoxide monohydride: pyrophoricity and catalysis of plutonium corrosion. 2001. J. Alloys. Comp.J. Alloys. Comp.. 320: 58.

27. Hawkins, J. M., J. F. Weaver, and A. Asthagiri. Density functional theory study of the initial oxidation of the Pt(111) surface. 2009. Physical Review BPhysical Review B. 79 (12): 125434.

28. Hayden, B. E., E. Schweizer, R. Kötz, and A. M. Bradshaw. The early stages of oxidation of magnesium single crystal surfaces. 1981. Surface ScienceSurface Science. 111 (1): 26.

29. Henkelman, G., A. Arnaldsson, and H. Jonsson. A fast and robust algorithm for Bader decomposition of charge density. 2006. Computational Materials ScienceComputational Materials Science. 36 (3): 354.

30. Holby, Edward F., . , and . . Thermodynamics and Hysteresis of Oxide Formation and Removal on Platinum (111) Surfaces. 2012. The Journal of Physical Chemistry CThe Journal of Physical Chemistry C.

31. Lee, D.D., J.H. Choy, and J.K. Lee. Computer generation of binary and ternary phase diagrams via a convex hull method . 1992. Journal of Phase EquilibriaJournal of Phase Equilibria. 13 (4): 7.

32. Lin, L. F., C. Y. Chao, and D. D. Macdonald. A point defect model for anodic passive films: II. Chemical breakdown and pit initiation. 1981. J. Electrochem. Soc.J. Electrochem. Soc.. 128: 1194.

33. Lindroos, M., H. Pfnur, G. Held, and D. Menzel. Adsorbate induced reconstruciton by stron chemisorption - Ru(001) p(2x2)-O. 1989. Surface ScienceSurface Science. 222 (2-3): 451.

34. Macdonald, D. D.. The history of the point defect model for the passive state: a brief review of film growth aspects. 2011. Electrochim. ActaElectrochim. Acta. 56: 1761.

35. Namba, H., J. Darville, and J. M. Gilles. A model for the

oxidation of Mg(0001) based upon LEED, AES, ELS and work function measurements. 1981. Surface Science-Surface Science. 108 (3): 446.

36. Pfnur, H., G. Held, M. Lindroos, and D. Menzel. Oxygen induced reconstruction of close-packed surface - a LEED0IV study on Ru(001)-p(2x1)O. 1989. Surface ScienceSurface Science. 220 (1): 43.

37. Reuter, K.. Nanometer and sub-nanometer thin oxide films at surfaces of late transition metals. 2004. Los Alamos National Laboratory, Preprint Archive, Condensed MatterLos Alamos National Laboratory, Preprint Archive, Condensed Matter. : 1.

38. Reuter, K., M. V. Ganduglia-Pirovano, C. Stampfl, and M. Scheffler. Metastable precursors during the oxidation of the Ru(0001) surface. 2002. Physical Review B (Condensed Matter and Materials Physics)Physical Review B (Condensed Matter and Materials Physics). 65 (16): 165403/1.

39. Reuter, K., and M. Scheffler. First-Principles Atomistic Thermodynamics for Oxidation Catalysis: Surface Phase Diagrams and Catalytically Interesting Regions. 2003. Physical Review LettersPhysical Review Letters. 90 (4): 046103/1.

40. Reuter, K., and M. Scheffler. Oxide formation at the surface of late 4d transition metals: insights from first-principles atomistic thermodynamics. 2004. Applied Physics A: Materials Science & ProcessingApplied Physics A: Materials Science & Processing. 78 (6): 793.

41. Richmond, S., J. S. Bridgewater, J. W. Ward, and T. H. Allen. The solubility of hydrogen and deuterium in alloyed, unalloyed and impure plutonium metal. 2010. IOP Conference Series: Materials Science and EngineeringIOP Conference Series: Materials Science and Engineering. 9: 012036.

42. Sanville, E., S. D. Kenny, R. Smith, and G. Henkelman. Improved grid-based algorithm for Bader charge allocation. 2007. Journal of Computational ChemistryJournal of Computational Chemistry. 28 (5): 899.

43. ., , . , and . . O adsorption and incipient oxidation of the Mg(0001) surface. 2004. Physical Review B (Condensed Matter and Materials Physics)Physical Review B (Condensed Matter and Materials Physics). 69: 8.

44. ., , . , and . . Mg(0001) surface oxidation: a two-dimensional oxide phase. 2004. Physical Review B (Condensed Matter and Materials Physics)Physical Review B (Condensed Matter and Materials Physics). 69: 4.

45. Schwoebel, R. L.. Oxide Formation on Magnesium Single Crystals. I. Kinetics of Growth. 1963. Journal of Applied PhysicsJournal of Applied Physics. 34 (9): 2776.

46. Schwoebel, R. L.. Oxide Formation on Magnesium Single Crystals. II. Structure and Orientation. 1963. Journal of Applied PhysicsJournal of Applied Physics. 34 (9): 2784.

47. Seyeux, A., V. Maurice, L. H. Klein, and P. Marcus. In situ scanning tunneling microscopy study of the initial stages of growth and of the structure of the passive film on Ni(111) in 1 mM NaOH(aq). 2005. J. Solid State Electrochem.J. Solid State Electrochem.. 9: 337.

48. Streitz, F. H., and J. W. Mintmire. Electrostatic potential for metal-oxide surfaces and interfaces. 1994. Phys. Rev. BPhys. Rev. B. 50: 11996.

49. Surnev, L., G. Rangelov, and G. Bliznakov. Interaction of oxygen with a Ru(OO1) surface. 1985. Surface Science-Surface Science. 159 (2–3): 299.

50. Tang, L., B. Han, K. Persson, C. Friesen, T. He, K. Sieradzki, and G. Ceder. Electrochemical stability of nanometer-scale Pt particles in acidic environments. 2010. J. Am. Chem. Soc.J. Am. Chem. Soc.. 132: 596.

51. Tang, W., E. Sanville, and G. Henkelman. A grid-based Bader analysis algorithm without lattice bias. 2009. Journal of Physics-Condensed MatterJournal of Physics-Condensed Matter. 21 (8).

52. Taylor, C. D.. The transition from metal-metal bonding to metal-solvent interactions during a dissolution event as assessed from electronic structure. 2009. Chem. Phys. Lett.Chem. Phys. Lett.. 469: 99.

53. Taylor, C. D.. Cohesive Relations for Surface Atoms in the Iron-Technetium Binary System. J. Alloys Comp.J. Alloys Comp.. Submitted.

54. Taylor, C. D., M. Janik, M. Neurock, and R. G. Kelly. Ab Initio Simulations of the Electrochemical Activation of Water . 2006. Mol. Sim.Mol. Sim.. 33: 429.

55. Taylor, C. D., R. G. Kelly, and M. Neurock. First-Principles Calculations of the Electrochemical Reactions of Water at an Immersed Ni(111)/H2O Interface. 2006. J. Electrochem. Soc.J. Electrochem. Soc.. 153: E207.

56. Taylor, C. D., R. G. Kelly, and M. Neurock. First-principles prediction of equilibrium potentials for water activation by a series of metals. 2007. J. Electrochem. Soc.J. Electrochem. Soc.. 154 (12): F217.

57. Taylor, C. D., M. Neurock, and J. R. Scully. First-principles investigation of the fundamental corrosion properties of a model Cu38 nanoparticle and the (111), (113) surfaces. 2008. J. Electrochem. Soc.J. Electrochem. Soc.. 155: C407.

58. Taylor, C. D., S. Wasileski, J. W. Fanjoy, J. Filhol, and M. Neurock. First principles reaction modeling of the electrochemical interface: Consideration and calculation of a tunable surface potential from atomic and electronic structure. 2006. Phys. Rev. B.Phys. Rev. B.. 73: 165402.

59. Todorova, M., W. X. Li, M. V. Ganduglia-Pirovano, C. Stampfl, K. Reuter, and M. Scheffler. Role of subsurface oxygen in oxide formation at transition metal surfaces. 2002. Physical Review LettersPhysical Review Letters. 89 (9): 961031.

60. Todorova, M., K. Reuter, and M. Scheffler. Density-functional theory study of the initial oxygen incorporation in Pd(111). 2005. Physical Review B: Condensed Matter and Materials PhysicsPhysical Review B: Condensed Matter and Materials Physics. 71 (19): 195403/1.

61. Valone, S. M., and S. R. Atlas. Energy dependence on fractional charge for strongly interacting subsystems. 2006. Phys. Rev. Lett.Phys. Rev. Lett.. 97: 256402.

62. Wei-Xue, L., C. Stampfl, and M. Scheffler. Subsurface oxygen and surface oxide formation at Ag(111): a density-functional theory investigation. 2003. Physical Review B (Condensed Matter and Materials Physics) Physical Review B (Condensed Matter and Materials Physics). 67 (4): 45408.

63. Wiame, F., V. Maurice, and P. Marcus. Initial stages of oxidation of Cu(111). 2007. Surf. Sci.Surf. Sci.. 601: 1193.

64. Wolf, D.. Reconstruction of NaCl surfaces from a dipolar solution to the Madelung problem. 1992. Physical Review LettersPhysical Review Letters. 68 (22): 3315.

65. Zhang, W. B., and B. Y. Tang. Stability of the polar NiO(111) surface. 2008. Journal of Chemical Physics-Journal of Chemical Physics. 128 (12).

Publications

Francis, M. F., and C. D. Taylor. Materials Science and Engineering, Los Alamos National Labs, Los Alamos, New Mexico, USA. 2013. First-principles insights into the structure of the incipient magnesium oxide and its instability to decomposition: Oxgen chemisorption to Mg (0001) and thermodynamic stability. Physical Review B . 87 (87): 13.

Rossi, M., and C. Taylor. Atomistic modeling of ISCC in fuel-pellet interactions. 2011. In 242nd National Meeting of the American-Chemical-Society (ACS) ; 20110828 - 20110901 ; Denver, CO. Vol. 242.

Taylor, C.. Connections between the energy functional and interaction potentials for materials simulations. 2011. ABSTRACTS OF PAPERS OF THE AMERICAN CHEMICAL SOCIETY. 242.

Plasmas of Magnetic Monopoles in Artificial Spin Ice: Designing Frustration, Engineering Magnetricity

Cristiano Nisoli
20120516ECR

Abstract

At the end of this project we have realized our goal: proving that artificial spin ice contains bona fide monopoles in artificial spin ice, emerging as relevant degrees of freedom of its low-energy dynamics, endowed of magnetic charge, and interact through Coulomb force. We have shown formation of crystallites of magnetic charges in kagome spin ice much similar to an ionic crystal. Moving beyond our initial aim, we have also proposed new topologies meant to predict and control monopole dynamics via the concept of "emergent" frustration. We have designed these new geometries, studied them theoretically, analytically and numerically, and realized them experimentally. The experiments completely validated out predictions: this lead to the proof of emergent frustration, of screening of monopoles by embedded magnetic charges and of formation of magnetic polarons. We have published our theoretical and experimental results on Nature, Phys. Rev. Lett., New Journal of Physics (Invited). Further work is under submission to Nature Physics. The PI has also cemented his leadership in this field, which he cofounded, by authoring a Review of Modern Physics. This LDRD grant funded an undergraduate student from UNV Reno, Muir Morrison, who has worked with the PI for a full year and was later admitted in prestigious graduate programs, including Cornell, Caltech, Berkley (he is at Caltech as of July 2013). The PI has also collaborated with a graduate student (Tammie Nelson, T-1, now Director's Fellow) and with Gia-Wei Chern (T-4, Oppenheimer Fellow). Some of the results of this work have been reported in a LANL press release.

Background and Research Objectives

In 2006, a joint theoretical and experimental collaboration between the PI and P. Schiffer's group (now at UI Urbana) at Penn State University, presented a new class of frustrated magnetic artificial materials, called "Artificial Spin Ice" [1-17] (Figure 1). Artificial spin ice is a two-dimensional array of elongated single-domain permalloy nano-islands whose shape anisotropy defines Ising-like spins arranged along the sides of a regular lattice. Unlike naturally occurring magnetically frustrated materials such as the spin ice pyrochlores, ASI remarkably allows imaging of its microstate, therefore providing a direct experimental benchmark to theoretical tre¬atments, and can be engineered into different geometries, to explore new phenomena and effects. Since its introduction, ASI has been used successfully to study frustration [1-10], and extension of thermodynamics to granular systems governed by non-trivial interactions [2, 5, 8] topological defects [13, 17], information encoding [6], and anomalous topological hall effect connected to emerging chirality [18]. It also became preferred ground for direct imaging of a new striking fractionalization phenomenon: "magnetic monopoles" [18-26]. This novel excitation, endowed with a quantized magnetic charge, introduced by C. Castelnovo and collaborators [19] in 2007, and then detected in rare heart pyrochlores [20] (including currents of magnetic monopoles [19-25]) was soon after directly visualized in ASI [13-15].

In this project we had posed the following series of scientific questions:

Are observed ASI monopoles "real" magnetic monopoles? While there is little doubt that magnetic monopoles of spin ice rightfully deserve their name [13-20], the situation for ASI is entirely different. ASI observed topological excitations do correspond structurally to the magnetic monopoles of spin ice (Figure 3), insofar as one can attribute somehow formally a "net magnetic charge" to the excited vertices. Yet questions remains: do they interact as coulomb charges? Are there signatures of this interaction in the experimental data? (..) are ASI magnetic monopoles "physical"?

Of course monopoles as elementary particles have never been found in Nature, despite a long search since Dirac's early predictions. We asked here whether one could prove the existence of magnetic monopoles, as el-

ementary excitations and low-energy degrees of freedom, emerging in artificial spin ice arrays as a particular case of fractionalization, or deconfinement of quasi-particles that together are seen as comprising the fundamental unit of the system, in this case the north and south poles of a nanomagnet.

We therefore proposed:

Our primary goal is to show theoretically and experimentally that ASI monopoles do indeed interact as coulomb charges and respond to external magnetic fields just as electrical charges respond to electrical fields (…). We will prove the existence of magnetic monopoles in Artificial Spin Ice (ASI).

Scientific Approach and Accomplishments

Our main goal was to prove the bona-fide (see above) nature of ASI monopoles. We believed small signatures of monopoles were buried into old data and we proposed to refine our out of equilibrium theory [2, 5, 8] to reveal those signals. While we pursued this route, new developments in the field suggested to us a better way to achieve our results in a more solid way. Since the beginning (2006) artificial spin ice was disordered through a protocol of AC demagnetization, which we had developed especially to lower the interisland magnetic interaction [5]. The PI had previously demonstrated [3, 6] that this method produces a well-defined statistical ensemble, which can be predicted in terms of an effective thermodynamics [2, 8]. Meanwhile researchers at Leeds attempted true thermalization during growth [14]. The PI explained those results (New Journal of Physics, dedicated issue, 2012, invited). An idea emerged: reaching true thermalization by heating the material in the narrow temperature window (about 10 Celsius) below the Curie temperature of the nanoisland, but above their blocking temperature. By engineering the material such that the blocking temperature would sit low enough in the phase diagram of artificial spin ice, it was possible to create a thermal spin ensemble able to access low entropy regions. For the kagome geometry, the odd coordination of the lattice means that each vertex in the ice phase supports a magnetic charge, either positive or negative. One thus expects (and can prove) that such charges would rearrange in a sort of ionic crystal as the entropy is lowered. We were able to witness such charge crystallization (Figure 2), which provided a much clearer proof of the existence and interaction of these emergent magnetic charges than the route we initially detailed in the proposal. This result was published in Nature on August 2013 and featured in a LANL press release.

Confident that we would reach our initial goal (which reviewers had considered perhaps too ambitious) we worked in parallel to exploit this new technique. We concentrated on a material-by-design approach that would allow us to control the properties of these magnetic charges. All the studies of artificial spin ice so far had used simple geometries (square, hexagonal, ladder). These were not chosen for their austere beauty, but because of limits in nanofabrication. As limits were progressively lifted, the PI saw that the time was ripe to introduce novel topologies. These take advantage of emergent rather than direct frustration.

Frustration in artificial spin ice comes from the impossibility of minimizing all the interactions between nearest neighboring nanoislands. However because of the anisotropy of the magnetic interaction, the degeneracy of this frustration is lifted in most geometric arrangement. Degeneracy of the manifold is essential for magnetic charges: one can prove that, in a non-degenerate phase, magnetic monopoles are energetically confined by their Dirac strings.

The PI devised a new way to achieve degeneracy, through an emergent frustration. There each vertex of the lattice has a defined minimal energy, however it is impossible to allocate all vertices in their ground state: excitations are topologically protected (Figure 3). Without indulging too much on the details, one can show that this different, emergent frustration leads to a different behavior of monopole excitations. They can effectively be screened by an embedded magnetic charge and the monopole dressed by the charge forms a bound magnetic polaron.

We offered general mathematical criteria to assess emergent vertex-frustration, and we studied in depth (analytically and numerically) some of the lattices. For one of our design we assisted experimentalists in fabrication and analysis. The “Shakti” lattice was then realized experimentally (to be submitted to Nature Physics) , thermally annealed with our new technique, and all of our predictions (submitted to Phys. Rev. Lett.) were validated. The emergent frustration revealed the predicted manifold, and monopoles indeed formed magnetic polarons (Figures 4, 5).

In conclusion

- We developed a new experimental design that directly revealed monopoles! (New Journal of Physics 2012)
- We actually SAW monopoles interacting and reorganizing (Nature, 2013)
- As a consequence, we realized the need of “Monopole-Oriented Geometries” (New Journal of Physics 2013, Phys. Rev. Lett, submitted)
- One of these geometries have been realized and

showed monopole screening (to be submitted to Nature Physics)

Impact on National Missions

Magnetic technology generally concerns itself with manipulation of localized dipolar degrees of freedom. The ability to build materials containing delocalized monopolar charges is very exciting with possible technological implications in data storage and computation, and can lead to materials with needed and emergent functionality including unprecedented sensitivity for sensing and control in national security missions. This work demonstrates a direction in condensed matter physics that is quite opposite to what has been done in the last six decades or so. Instead of imagining an emergent theoretical description to model the behavior of a naturegiven material and validating it indirectly, we engineer materials of desired emergent properties that can be visualized directly. DOE and LDRD alike have largely invoked this material-by-design approach that replaces serendipity with design, assisted by a mesoscopic analysis.

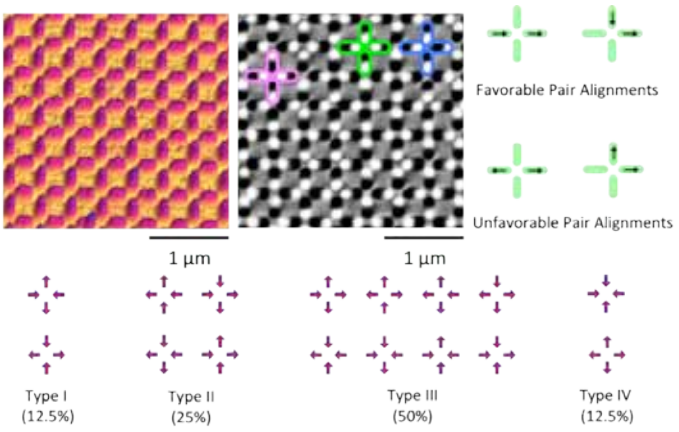

Figure 1. Artificial Spin Ice (shown on top left as an AFM image) allows for direct visualization of its magnetic degrees of freedom through MFM (top center) and other techniques (see below in the text). Energetically favorable and unfavorable dipole interactions are described in the top right. Bottom: four legged vertices have 2^4=16 possible moment configurations, which separate into four symmetry-distinct types, shown here with the relative frequency, which corresponds to random assignation of the moments. Note that even in the low energy configurations, some interactions are frustrated, but the lack of degeneracy beside spin inversion in Type I vertices provides an ordered antiferromagnetic ground state [1].

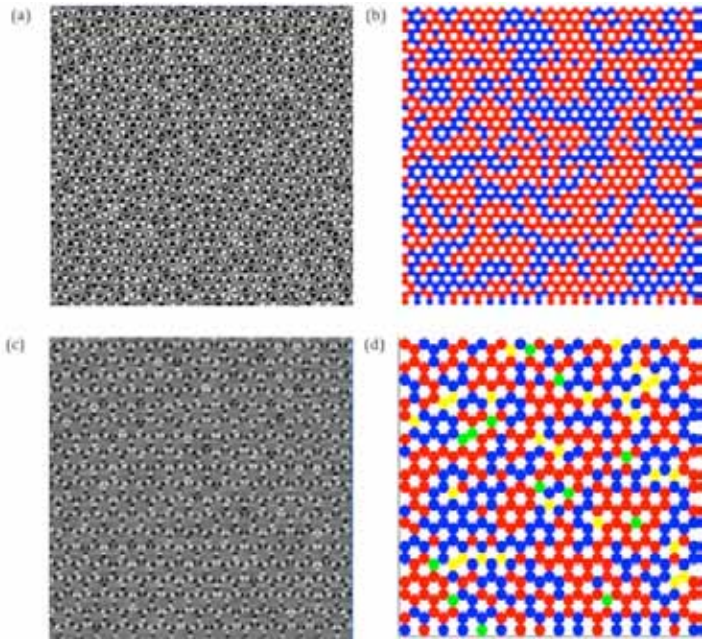

Figure 2. Emergent domains of ordered magnetic charges in artificial kagome spin ice. (a, c) MFM images of thermally annealed artificial kagome spin ice with lattice parameter of 260 nm and 490 nm. (b, d) Maps of the distribution of magnetic charge in (a, c). Red and blue dots correspond to vertices belonging to each of the two degenerate magnetic charge-ordered states described in the text. Green and yellow dots represent the +3 and -3 excitations. Figure S11 in Supplementary Information reproduces these maps but also includes vectors representing the magnetic moments of the islands comprising the lattices (Nature 2013).

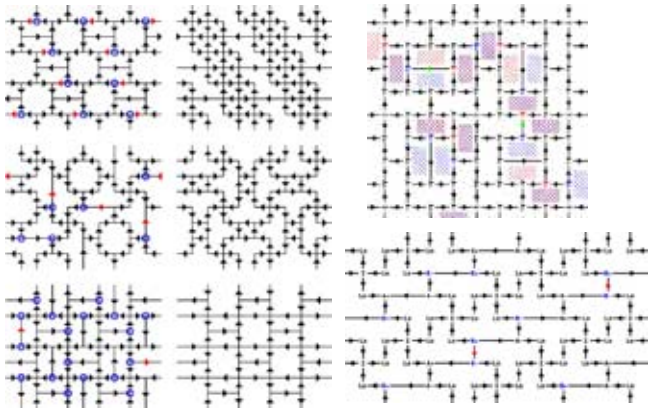

Figure 3. Vertex-frustrated and non-frustrated lattices based on perpendicular vertices. Lattices on the left are frustrated while those at the centeer, despite the apparent similarity of the lattices, are not. The unhappy vertices are circled (blue), while red spins may be chosen in either direction without changing the energy of the configuration: that is not the only source of degeneracy, as other allocations of the unhappy vertices are degenerate. The 'staggered brickwork' lattice (top left) has a 'trivial' degeneracy, which can be mapped into a system of independent spins. In contrast, the 'pinwheel' (middle left) and 'shakti' lattices (lower left) possess more complex degeneracy. The ice manifold of the shakti lattice can be mapped into an emergent six vertex

model. On the top right the Santa Fe lattice can be mapped into an eight vertex model. Both show monopole crystallization. On the bottom right, the Tetris lattice show a sliding phase in its ice manifold (New Journal of Physics 2013).

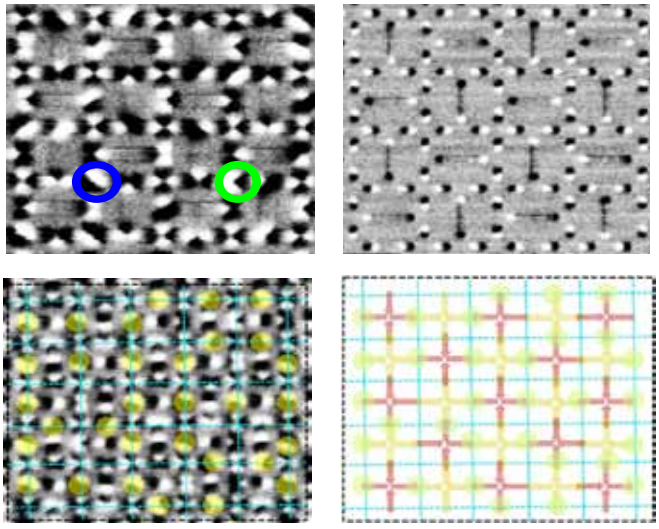

Figure 4. Top: MFM images of thermally annealed shakti 2 lattices with lattice constant a = 360 nm (left) and 800 nm (right). Most of the four-island vertices in the 360 nm lattice are in the Type I configuration; there are a few higher-energy Type II (blue circle) and Type III (green circle) vertices. Note how the (light contrast) Type III vertex circled in green is surrounded by four three-island vertices with dark contrast. This is an example of the monopole screening described in the text. Bottom: a portion of completely annealed Shakti 1 (right) employed to reveal emergent frustration in the ice manifold; the reticulate of turquois lines define the plaquettes, each supporting two and only two unhappy vertices, Type II'; the assignation of topologically protected defect on each plaquette corresponds to an emergent six-vertex, ice-rule model (right) in which red arrows point toward a defect, whereas yellow arrows point away from it (unpublished).

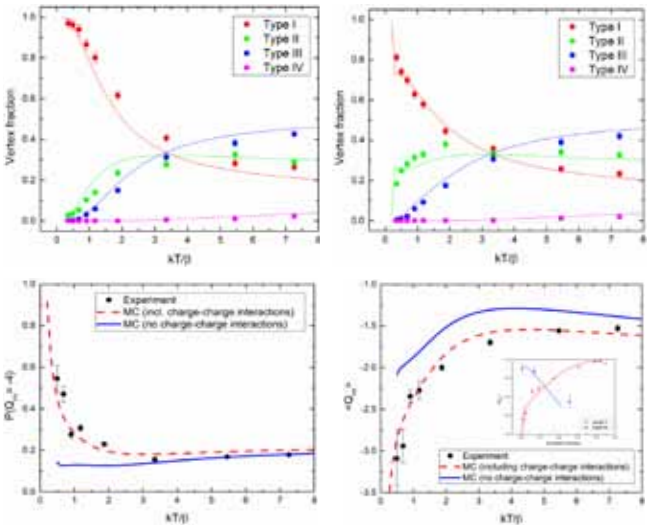

Figure 5. Top: Our theoretical predictions and experimental data on the vertex population of the Shakti lattice. Bottom: Charge screening of magnetic monopoles: theory vs. experiment.

References

1. Wang, R. F., C. Nisoli, R. S. Freitas, J. Li, W. McConville, B. J. Cooley, M. S. Lund, N. Samarth, C. Leighton, V. H. Crespi, and P. Schiffer. Artificial 'spin ice' in a geometrically frustrated lattice of nanoscale ferromagnetic islands. 2006. NATURE. 439 (7074): 303.

2. Nisoli, C., R. F. Wang, J. Li, W. F. McConville, P. E. Lammert, P. Schiffer, and V. H. Crespi. Ground state lost but degeneracy found: The effective thermodynamics of artificial spin ice. 2007. PHYSICAL REVIEW LETTERS. 98 (21): -.

3. Wang, R. F., J. Li, W. McConville, C. Nisoli, X. Ke, J. W. Freeland, V. Rose, M. Grimsditch, P. Lammert, V. H. Crespi, and P. Schiffer. Demagnetization protocols for frustrated interacting nanomagnet arrays. 2007. JOURNAL OF APPLIED PHYSICS. 101 (9): -.

4. Wang, R. F., C. Nisoli, R. S. Freitas, J. Li, W. McConville, B. J. Cooley, M. S. Lund, N. Samarth, C. Leighton, V. H. Crespi, and P. Schiffer. Artificial 'spin ice' in a geometrically frustrated lattice of nanoscale ferromagnetic islands (vol 439, pg 303, 2006). 2007. NATURE. 446 (7131): 102.

5. Ke, X., J. Li, C. Nisoli, P. E. Lammert, W. McConville, R. F. Wang, V. H. Crespi, and P. Schiffer. Energy minimization and ac demagnetization in a nanomagnet array. 2008. PHYSICAL REVIEW LETTERS. 101 (3): -.

6. Lammert, P. E., X. L. Ke, J. Li, C. Nisoli, D. M. Garand, V. H. Crespi, and P. Schiffer. Direct entropy determination and application to artificial spin ice. 2010. NATURE PHYSICS. 6 (10): 786.

7. Li, J., S. Zhang, J. Bartell, C. Nisoli, X. Ke, P. E. Lammert, V. H. Crespi, and P. Schiffer. Comparing frustrated and unfrustrated clusters of single-domain ferromagnetic islands. 2010. PHYSICAL REVIEW B. 82 (13): -.

8. Nisoli, C., J. Li, X. L. Ke, D. Garand, P. Schiffer, and V. H. Crespi. Effective Temperature in an Interacting Vertex System: Theory and Experiment on Artificial Spin Ice. 2010. PHYSICAL REVIEW LETTERS. 105 (4): -.

9. Li, J., X. Ke, S. Zhang, D. Garand, C. Nisoli, P. Lammert, V. H. Crespi, and P. Schiffer. Comparing artificial frustrated magnets by tuning the symmetry of nanoscale permalloy arrays. 2010. PHYSICAL REVIEW B. 81 (9): -.

10. Ke, X. L., J. Li, S. Zhang, C. Nisoli, V. H. Crespi, and P. Schiffer. Tuning magnetic frustration of nanomagnets in triangular-lattice geometry. 2008. APPLIED PHYSICS LETTERS. 93 (25): -.

11. Ke, X., J. Li, C. Nisoli, P. E. Lammert, W. McConville, R. F. Wang, V. H. Crespi, and P. Schiffer. Energy minimization and ac demagnetization in a nanomagnet array. 2008. PHYSICAL REVIEW LETTERS. 101 (3): -.

12. Wang, R. F., J. Li, W. McConville, C. Nisoli, X. Ke, J. W. Freeland, V. Rose, M. Grimsditch, P. Lammert, V. H. Crespi, and P. Schiffer. Demagnetization protocols for frustrated interacting nanomagnet arrays. 2007. JOURNAL OF APPLIED PHYSICS. 101 (9): -.

13. Mengotti, E., L. J. Heyderman, A. F. Rodriguez, F. Nolting, R. V. Hugli, and H. B. Braun. Real-space observation of emergent magnetic monopoles and associated Dirac strings in artificial kagome spin ice. 2011. NATURE PHYSICS. 7 (1): 68.

14. Morgan, J. P., A. Stein, S. Langridge, and C. H. Marrows. Thermal ground-state ordering and elementary excitations in artificial magnetic square ice. 2011. NATURE PHYSICS. 7 (1): 75.

15. Ladak, S., D. E. Read, G. K. Perkins, L. F. Cohen, and W. R. Branford. Direct observation of magnetic monopole defects in an artificial spin-ice system. 2010. NATURE PHYSICS. 6 (5): 359.

16. Farhan, A., P. M. Derlet, A. Kleibert, A. Balan, R. V. Chopdekar, M. Wyss, L. Anghinolfi, F. Nolting, and L. J. Heyderman. Exploring hyper-cubic energy landscapes in thermally active finite artificial spin-ice systems. 2013. NATURE PHYSICS. 9 (6): 375.

17. Mengotti, E., L. J. Heyderman, A. F. Rodriguez, F. Nolting, R. V. Hugli, and H. B. Braun. Real-space observation of emergent magnetic monopoles and associated Dirac strings in artificial kagome spin ice. 2011. NATURE PHYSICS. 7 (1): 68.

18. Branford, W. R., S. Ladak, D. E. Read, K. Zeissler, and L. F. Cohen. Emerging Chirality in Artificial Spin Ice. 2012. SCIENCE. 335 (6076): 1597.

19. Castelnovo, C., R. Moessner, and S. L. Sondhi. Magnetic monopoles in spin ice. 2008. NATURE. 451 (7174): 42.

20. Morris, D. J. P., D. A. Tennant, S. A. Grigera, B. Klemke, C. Castelnovo, R. Moessner, C. Czternasty, M. Meissner, K. C. Rule, J. U. Hoffmann, K. Kiefer, S. Gerischer, D. Slobinsky, and R. S. Perry. Dirac Strings and Magnetic Monopoles in the Spin Ice Dy2Ti2O7. 2009. SCIENCE. 326 (5951): 411.

21. Bramwell, S. T.. MAGNETIC MONOPOLES Magnetricity near the speed of light. 2012. NATURE PHYSICS. 8 (10): 703.

22. Giblin, S. R., S. T. Bramwell, P. C. W. Holdsworth, D. Prabhakaran, and I. Terry. Creation and measurement of long-lived magnetic monopole currents in spin ice. 2011. NATURE PHYSICS. 7 (3): 252.

23. Fennell, T., S. T. Bramwell, D. F. McMorrow, P. Manuel, and A. R. Wildes. Pinch points and Kasteleyn transitions in kagome ice. 2007. NATURE PHYSICS. 3 (8): 566.

24. Bramwell, S. T.. A spin on cool complexity. 2006. NATURE PHYSICS. 2 (4): 219.

25. Bramwell, S. T., S. R. Giblin, S. Calder, R. Aldus, D. Prabhakaran, and T. Fennell. Measurement of the charge and current of magnetic monopoles in spin ice. 2009. NATURE. 461 (7266): 956.

26. Fennell, T., P. P. Deen, A. R. Wildes, K. Schmalzl, D. Prabhakaran, A. T. Boothroyd, R. J. Aldus, D. F. McMorrow, and S. T. Bramwell. Magnetic Coulomb Phase in the Spin Ice Ho2Ti2O7. 2009. SCIENCE. 326 (5951): 415.

Publications

Chern, G. W., M. Morrison, and C. Nisoli. Engineering Degeneracy: a Critical Ground State for Artificial Spin I. Physical Review Letters.

Gilbert, I., G. W. Chern, C. Nisoli, and P. Schiffer. Emergent Frustration in Artificial Spin Ice: Magnetic Polarons and Charge Ordering. . 2013. To be submitted to Nature Physics.

Lammert, P., V. Crespi, and C. Nisoli. Gibbsianizing nonequilibrium dynamics of artificial spin ice and other spin systems. 2012. New Journal of Physics. 14 (4): 045009 (19 pp.).

Morrison, M., T. R. Nelson, and C. Nisoli. Unhappy vertices in artificial spin ice: new degeneracies from vertex-frustration. (Invited). 2013. New Journal of Physics. 15 (4): 045009 .

Nisoli, C.. On thermalization of magnetic nano-arrays at fabrication. 2012. New Journal of Physics. 14: 35017.

Nisoli, C., R. Moessner, and P. Schiffer. Artificial spin ice: Designing and imaging magnetic frustration . To appear in Review of Modern Physics.

Zhang, S., I. Gilbert, C. Nisoli, G. W. Chern, M. J. Erickson, L. O'Brien, C. Leighton, P. E. Lammert, V. H. Crespi, and P. Schiffer. Crystallites of magnetic charges in artificial spin ice. 2013. NATURE. 500 (7464): 553.

Zhang, S., J. Li, I. Gilbert, J. Bartell, M. Erickson, Y. Pan, P.

Lammert, C. Nisoli, K. K. Kohli, R. Misra, V. Crespi, N. Samarth, C. Leighton, and P. Schiffer. Perpendicular magnetization and generic realization of the ising model in artificial spin ice. 2012. Physical Review Letters. 109 (8): 087201.

Zhang, S., J. Li, J. Bartell, X. Ke, C. Nisoli, P. Lammert, V. Crespi, and P. Schiffer. Ignoring your neighbors: Moment correlations dominated by indirect or distant interactions in an ordered nanomagnet array. 2011. Physical Review Letters. 107 (11): 117204.

Valence-Fluctuation-Mediated Superconductivity in Heavy-Fermion Materials

Marc Janoschek
20120525ECR

Abstract

The belief that room temperature superconductivity – the holy grail of condensed matter physics – is within reach, originated in the surprising discovery of unconventional superconductivity in the high-Tc cuprate materials at temperatures up to 160 K, and has been recently refuel by the high-Tc ¬iron-pnictides. Here our current understanding of superconductivity is based on a theory by Bardeen, Cooper and Schrieffer (BCS) who were able to show that superconductivity develops in materials that exhibit an arbitrarily weak attractive force between electrons (that usually strongly repel each other), that consequently leads to the formation of electron pairs, the so-called Cooper pairs. These pairs can travel through a solid without resistance due to the remarkable properties of quantum physics. While we understand that in conventional superconductors collective atomic vibrations (phonons) provide the required pairing interaction, this also implies that their superconducting transitions temperatures are very low. The high superconducting transition temperatures frequently found in unconventional superconductors showed that a new "super-glue" must mediate unconventional superconductivity. Because unconventional superconductivity is usually found in vicinity of magnetism, the major contender for the new pairing glue are magnetic fluctuations (magnetic analog of phonons). However, a "smoking gun"-experiment for that scenario is still missing, and notably, the abundance of emergent electronic phenomena that is generally found in conjunction with unconventional superconductivity suggests that other pairing glues should exist. In this early-career project we have investigated the recently proposed alternative mechanism of valence-fluctuation-driven superconductivity. We have used a new neutron scattering technique called Larmor diffraction to shed some light on this issue. Our results show that Larmor diffraction is a useful technique to study the physics of strongly correlated electron compounds more broadly, and more specifically add to the evidence that valence fluctuations may indeed play role in mediating unconventional superconductivity.

Background and Research Objectives

A common theme found in many materials exhibiting unconventional superconductivity is the existence of a zero-temperature magnetic instability. At the instability, a nonmagnetic state can be smoothly transformed into a magnetically ordered state as function of a non-thermal control parameter such as chemical substitution, or pressure. On the nonmagnetic side of the instability, the magnetic moments are randomly oriented and there is no correlation between neighboring moments. When the magnetic state is approached, magnetic fluctuations arise that correlate moments over increasing length scales. The fluctuations are strongest right at the magnetic instability and the associated correlation length becomes infinite resulting in the onset of magnetic order (Figure 1). It is precisely these fluctuations that are thought to mediate the unconventional superconductivity. In this picture, a symmetric dome of superconductivity emerges around the instability. The highest transition temperature is expected at the instability, where the fluctuations become strongest (Figure 1(a)) [1-4].

While it is clear that proximity to a magnetic instability and the associated magnetic fluctuations play an important role in mediating unconventional superconductivity, there are also growing experimental and theoretical indications that magnetic fluctuations by themselves may not be a sufficient condition for unconventional superconductivity: (i) In many cases, the highest superconducting transition temperature (TS) occurs far away from where the magnetic fluctuations are the strongest. (ii) Only for few materials such as CeCu2Si2 [5] and YBa2Cu3O6.6 [6], it has been reported that magnetic fluctuations are strong enough to mediate unconventional superconductivity. On the other hand there are many calculations that demonstrate that magnetic fluctuations alone may be too weak [7, 8]. (iii) Various ordered states and exotic behavior emerge in the vicinity of supercon-

ductivity that has been proposed to drive unconventional superconductivity. Examples for other superconducting glues include: charge loop-and stripe order [9,10], electronic nematic ordering [11,12], and valence fluctuations [13,14]. The main obstacle in identifying such alternative pairing mechanisms is that it is generally not possible to measure the associated fluctuations that are thought to mediate the SC. However, the proposal of valence fluctuation mediated superconductivity may represent a tangible way to overcome this issue.

Valence fluctuations occur frequently in materials that contain actinide or rare earth ions, where the valence (basically the net charge of the ions) of the electron shells may change continuously or discontinuously as a function of temperature, external pressure or chemical composition [15]. In these materials, the valence electrons do not participate in the bonding of different ions and stay localized. In contrast, the bonding is assumed by electrons in lower electron shells that form a conduction band. The change of the valence of the actinide/rare earth ions is then promoted by the so-called Kondo effect that leads to a partial delocalization of the valence electrons into the conduction band [16]. If the strength of the Kondo effect is increased by application of temperature, external pressure, or chemical composition, this may lead to a macroscopic phase transition, where all actinide/rare earth sites collectively change their valence. If the change of valence at the transition occurs smoothly, it is expected that strong valence fluctuations emerge, similar to the magnetic fluctuations near to a magnetic phase transition. As illustrated in Figure 2 this may lead to a weak attractive interaction between two conduction electrons, and in turn to unconventional superconductivity [13,17].

Here the outstanding scientific problem lies in the identification of such a valence transition in the presence of unconventional superconductivity. While a recently developed theoretical frame work showed that valence fluctuations should be strong enough to mediate unconventional superconductivity, so far only indirect proof has been demonstrated as we will summarize in the following. The archetypal compound that has been investigated in this context is CeCu2Si2. CeCu2Si2 exhibits below a superconducting transition temperature Tc = 0.7 K [18] that shows a distinct pressure dependence: Tc remains constant up to pressures of roughly 2 GPa, where it increases abruptly to 2.25 K followed by a slow decrease towards zero [19,20]. By substituting Ge on the Si site the superconducting phase disintegrates into two distinct domes as shown in Figure 3a [14]. This has led to the view that the SC at ambient pressures is due to magnetic fluctuations, whereas the dome at high pressures is due to valence fluctuations as corroborated by various transport and thermal measurements that agree with the theory of valence fluctuations [13,17].

A similar case is the material CeRhIn5 that shows magnetic order below a temperature TN = 3.8 K [21]. As illustrated in Figure 3b the magnetism is abruptly suppressed for pressures larger than P1 = 1.77 GPa, while superconductivity appears in a broad dome that roughly extends between 1.5 and 4.5 GPa and reaches the maximal superconducting transition temperature Tc = 2.3 K at P2 = 2.3 GPa [22]. The difference between P1 and P2 is peculiar; if the superconductivity were mediated solely by magnetic fluctuations, one would naively expect both to be identical. Interestingly, the magnetic order reappears between P1 and P2, coexisting with superconductivity, when a magnetic field is applied [23], suggesting that superconductivity inhibits the magnetism at zero magnetic field instead of relying on it. Substitution of Co in CeRh1−xCoxIn5 suppresses the magnetic order at $x \approx 0.8$ and superconductivity appears for $0.4 \leq x \leq 1$. Tc remains at 1.5 K for $0.4 \leq x \leq 0.75$ and increases to 2.2 K for $x > 0.75$ [24], similar to pressure for CeCu2Si2. The application of pressure eliminates the magnetic phase for increasing x while enlarging the superconducting dome, indicating that superconductivity in CeRh1−xCoxIn5 exist without being in the vicinity magnetic fluctuations [25]. Identical to CeCu2Si2, the transport measurements agree with the theory for valence-fluctuation-mediated superconductivity. However, the most promising evidence for valence fluctuations driving the superconductivity in CeRhIn5 is a change in the electronic structure at P2 [26] in accord with theory [27]. Finally, a last contender for valence-mediated superconductivity is the material PuCoGa5 that is isostructural to CeRhIn5. However, the presence of plutonium in this compounds makes more detailed investigations complicated, and not much data is currently available [28].

While investigations on these materials certainly suggest valence fluctuation are viable as a candidate for a superconducting glue, microscopic evidence remains absent, and it is easy to identify why. As discussed above a valence transition corresponds to partial release of a valence electron on a rare earth or actinide ion into the valence band. The loss of a valence electron reduces the size of the ion, and consequently a subtle reduction of the size of the material will occur at the valence transition. This reduction in size can be easily and precisely measured at ambient pressure. However, conventional types of measurement, such as capacitive dilatometry, cannot be used at high pressures, where the valence transitions are expected to occur in the materials discussed above [29]. The goal of this early-career research project was therefore to demonstrate a new way to of measuring small changes in the

lattice parameters that can be employed at high pressure while working on the outstanding scientific problem of valence-fluctuation mediated superconductivity.

Scientific Approach and Accomplishments

We have used a novel neutron scattering method called Larmor diffraction that may be used in combination with high pressure cells at low temperature. Conventional neutron diffraction methods don't reach the resolution of other methods such as dilatometry for measurements of the lattice parameter of a material that are required for detecting a subtle valence transition. On the other hand neutron diffraction is highly suitable for high pressure work because neutrons penetrate deeply into materials because they are neutral (i.e. they are not decelerated by the charges of the ions and electrons present in any material), and thus pressure cells are transparent to them. Larmor diffraction combines both worlds by using the small magnetic moment that is carried by a neutron and precess a magnetic field. As we show in Figure 4a and b, changes of a lattice parameter d can be encoded in this precession, and enhance the resolution in measuring changes of the lattice parameter Δd/d to 10-5 which approaches conventional methods such as dilatometry [29].

For the scope of this project the material CeRhIn5 represented the ideal candidate to look for valence-mediated superconductivity. Single crystals of very high quality can be easily synthesized, which preclude problems from disorder. In contrast, CeCu2Si2 silicon has to be substituted with germanium to tune the material to the putative valence transition. Further, in CeCu2Si2 the putative valence transition occurs at very high pressures that are currently not accessible with neutron scattering. In Figure 4c we show Larmor diffraction measurements carried out at ambient pressure and compare them to data obtained be means of conventional dilatomtry. This result demonstrates that Larmor diffraction is in excellent agreement with conventional methods.

Our Larmor diffraction measurements carried out at temperatures below 30 K and for various pressures are shown in Figure 5. Before we discuss the data, we want to point out that the measurement of one complete data set at a single pressure takes between 7-10 days. The only neutron instrument world-wide that is setup to perform Larmor diffraction measurements on a routine basis is situated at FRM II research reactor in Munich, Germany, and neutron beam time for the measurements carried out during this early-career project had to be obtained through the proposal system at Munich, which is open to the international neutron user community. We obtained a total of 46 days of beam time within less than two years, which is a considerable achievement by itself. We note that a day of neutron beam time costs about $10k, and consequently the PI has obtained in the order of $400k additional funding to carry out this project.

As explained and illustrated in Figure 5 we are able to pick up the major features of the phase diagram of CeRhIn5 such as the antiferromagnetic and superconducting transition temperatures. More interestingly, the Larmor diffraction measurements show oscillations below a temperature Tx ≈ 10 K and in vicinity of the pressure P2 at which the putative valence transition has been postulated. In this pressure and temperature regime corresponds to the temperature where transport measurements detect increased scattering in the electron system, which has been speculated to emerge because of charge/valence fluctuations (cf. Figure 5a) [30]. Finally, at a pressure of 1.9 GPa, which is the highest pressure at which we were able to perform measurements so far, we see a distinct change in the low temperature behavior of the lattice parameters as explained in detail in Figure 5b. This change is in agreement with the expectations for a valence transition, but ultimately more measurements at higher pressures will need to be carried out to confirm this behavior.

Impact on National Missions

Pressure is an important and well-defined tuning parameter for the study of strongly correlated electron systems and is the 'cleanest' way to tune between different quantum ground states. Neutron scattering on the other hand is an excellent microscopic probe that is able to extract information on multiple relevant energy scales from the bulk of the sample, such as spin fluctuations, crystal field excitations and lattice degrees of freedom. A key element of this proposal is to answer an outstanding scientific problem while advancing neutron scattering experiments to higher pressures. This line of inquiry will be of great importance for future research on novel electronic materials broadly, and specifically for the neutron scattering efforts funded by the Department of Energy's Office of Basic Energy Science (OBES). As highlighted in last year's report of OBES "neutron scattering is among the most powerful tools for characterizing matter to understand and develop new materials and chemistries," and has "applications in geology, biology, and physics" [31]. To provide US scientists with access to this powerful probe DOE alone operates three large neutron user facilities at the Los Alamos and Oak Ridge National Laboratories, with an annual budget of ~250M$ (~30% of budget for all OBES user facilities) where scientific users can carry out their research using neutrons. During the last decade OBES also invested well over ~$1B in the construction of the newest of these three national user facilities, namely the Spallation Neutron Source at

Oak Ridge. We note, that advanced neutron scattering techniques such as Larmor diffraction are currently not available at any of the U.S.'s neutron sources, and building expertise in such techniques through projects such as this one will be critical to our ability to maintain the science and technology leadership of the U.S. Finally, we point out that discussion with program managers about follow on funding for the program of inquiry initiated in this LDRD project has already begun.

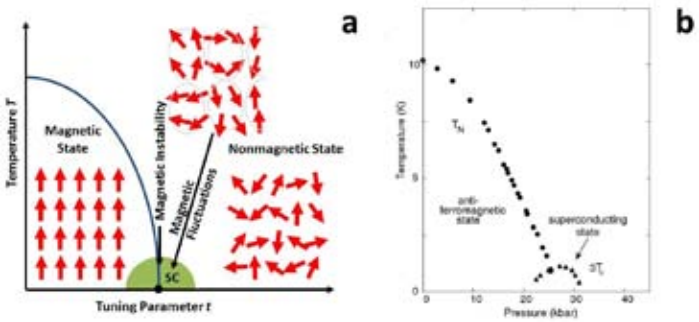

Figure 1. The concept of unconventional superconductivity mediated by magnetic fluctuations is illustrated. a A schematic phase diagram demonstrating magnetic-fluctuation-mediated superconductivity as function of temperature T and control parameter t. t can be pressure P, or chemical substitution x. Manipulating t, the material can be smoothly tuned from a nonmagnetic into a magnetic state separated by a zero-temperature magnetic instability. In the nonmagnetic phase the magnetic moments are randomly oriented and not correlated to their neighbors (right inset), whereas in the magnetic phase they are macroscopically ordered (here ferromagnetically, left inset). Approaching the instability from the nonmagnetic side, magnetic fluctuations arise that correlate fluctuating moments over increasing length scales (here denoted by the grey circles in the top inset). Right at the instability the fluctuations are strongest, and the correlation length becomes macroscopic, triggering the onset of magnetic order. The fluctuations are also believed to serve as the glue for the Cooper pairs, resulting in a symmetric dome of superconductivity (SC) around the instability (green shade).7-10 b Experimentally determined phase diagram for the compound CePd2Si2 showing that this kind of picture has indeed been found for several compounds.

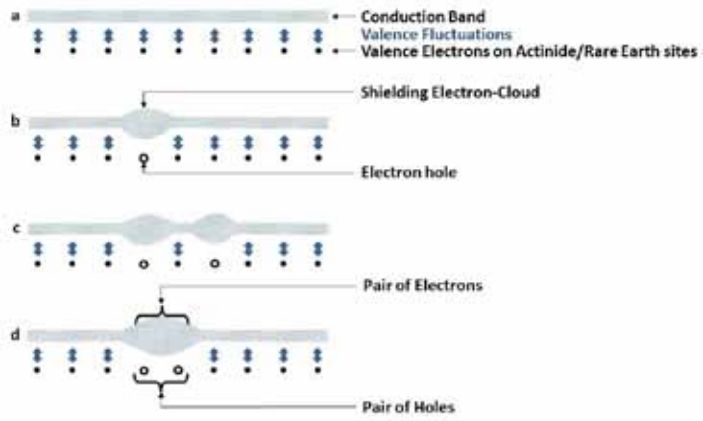

Figure 2. We illustrate the concept of valence-fluctuation-mediated unconventional superconductivity in a metallic sample containing actinide or rare earth ions. a In the conduction band electrons can move freely therefore allowing to conduct electricity. In contrast, the valence electrons on the actinide/rare earth sites are localized (black dotes) and do not move throughout the material. b As indicated by the blue arrows the valence electrons may hop into and out of the conduction due to valence fluctuations. As indicated by the empty circle, if the valence electron hops into the conduction band, an electron hole carrying a positive charge is generated at the actinide/rare earth ion site. The movable conduction electrons are attracted by this positive charge leading to cloud of conduction electrons shielding the hole. c In case more than one hole exist, the two holes (or shielding electron clouds) repel each other. d Energetically it is more favorable to move the two holes in a neighboring configuration, in which the holes can be screened more efficiently. This effectively leads to an attractive interaction between to electrons, and would therefore lead to Cooper pairs and superconductivity.

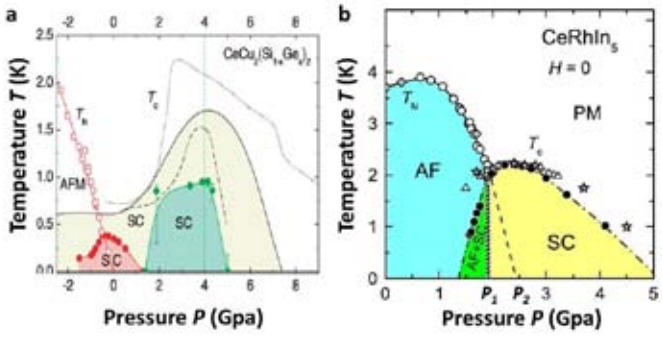

Figure 3. The pressure P vs temperature T phase diagrams of the putative valence-fluctuation-mediated superconductors a CeCu2(Si1-xGex)2 and b CeRhIn5 are shown (see text for details).

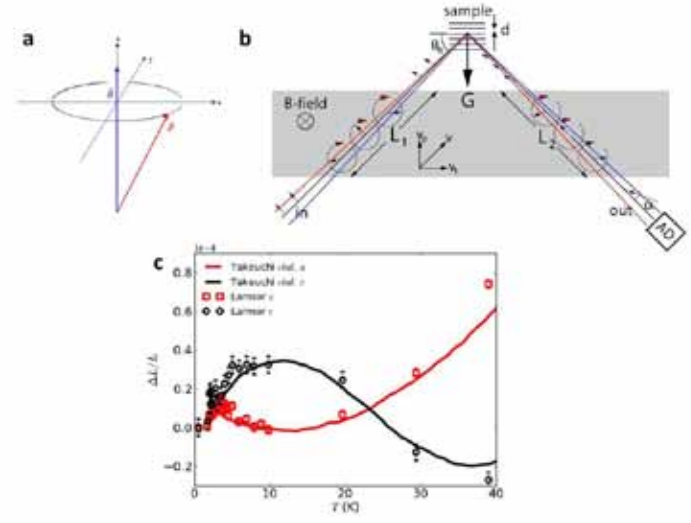

Figure 4. The principle behind the Larmor diffraction method is illustrated. a Neutrons exhibit a small magnetic moment (red arrow) that precesses in the presence of a magnetic field (blue arrow) similarly to a gyroscope performing precessions in the gravitational field of earth. b This effect can be used to measure

changes in the lattice parameter d of a material precisely. Hereby the neutrons are scattered of the lattice planes of the material of interest. However, the neutrons incident on the sample (marked with "in"), and the neutrons scattered off the sample (marked with "out") move through a magnetic field (grey area) in which the magnetic moments of the neutrons preccess. It turns out that the total number of precessions the neutrons carry out while moving through this setup is directly proportional to the lattice parameter d of the sample. The number of precession is dependent on d because the path length through the magnetic field changes as function of d. This setup can measure changes of a lattice parameter with a precision of 10-5 or better and can be used in combination with pressure cells, because pressure cells are transparent for neutrons. C We show the results of our Larmor diffraction measurements on the material CeRhIn5 at ambient pressure (empty symbols) in comparison with the results by Takeuchi et al. obtained by conventional dilatometry (solid lines).

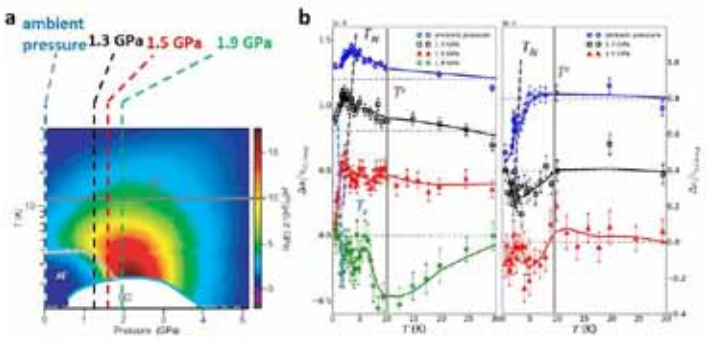

Figure 5. The results of this project are illustrated. a A modified pressure P vs temperature T phase diagram is show. "AF" and "SC" denote the antiferromagnetic and superconducting phases. The colored dash lines represent the pressures at which we have carried out the Larmor diffraction measurements (shown in b). The color scale in the background shows the electrical resistivity normalized to the electrical resistivity at 5.2 GPa [30], and represents the amount of electron scattering observed in the sample as function of pressure. Blue represents lowest scattering and red the highest. The electron scattering is maximal below a temperature Tx ≈ 10 K and around P2 = 2.3 GPa. b The change of the tetragonal lattice parameters a and c of CeRhIn5 is shown for various pressures and below T = 30 K. As indicated by the purple and light blue dash lines the transition temperatures to the antiferromagnetic and superconductings state can be seen in our data. Further below Tx,, where electrical resistivity shows additional scattering, we see oscillations in Delta a/a and Delta c/c that become stronger when approaching P2. Further, at the pressure P = 1.9 GPa (the highest pressure for which we recorded data) the behavior for the c lattice parameter changes significantly: instead of a slow increase below ≈ 25 K a large decrease below ≈ 30 K. We note that from the data shown other contribution such as lattice vibrations were subtracted.

References

1. Mathur, N. D., F. M. Grosche, S. R. Julian, I. R. Walker, D. M. Freye, R. K. W. Haselwimmer, and G. G. Lonzarich. Magnetically mediated superconductivity in heavy fermion compounds. 1998. NATURE. 394 (6688): 39.

2. Paglione, J., and R. L. Greene. High-Temperature Superconductivity in Iron-Based Materials. 2010. Nature Physics. 6: 645.

3. MONTHOUX, P., A. V. BALATSKY, and D. PINES. TOWARD A THEORY OF HIGH-TEMPERATURE SUPERCONDUCTIVITY IN THE ANTIFERROMAGNETICALLY CORRELATED CUPRATE OXIDES. 1991. PHYSICAL REVIEW LETTERS. 67 (24): 3448.

4. Zaanen, J.. A modern, but way too short history of the theory of superconductivity at a high temperature. 2011. In 100 years of superconductivity. Edited by Rochella, H., and P. H. Kes. , p. 10. Boca Raton: Taylor & Francis.

5. Stockert, O., J. Arndt, E. Faulhaber, C. Geibel, H. S. Jeevan, S. Kirchner, M. Loewenhaupt, K. Schmalzl, W. Schmidt, Q. Si, and F. Steglich. Magnetically driven superconductivity in CeCu2Si2. 02. Nature Physics. 7 (2): 119.

6. Dahm, T., V. Hinkov, S. V. Borisenko, A. A. Kordyuk, V. B. Zabolotnyy, J. Fink, B. Buchner, D. J. Scalapino, W. Hanke, and B. Keimer. Strength of the spin-fluctuation-mediated pairing interaction in a high-temperature superconductor. 2009. NATURE PHYSICS. 5 (3): 217.

7. Kee, H. Y., S. A. Kivelson, and G. Aeppli. Spin-1 neutron resonance peak cannot account for electronic anomalies in the cuprate superconductors. 2002. PHYSICAL REVIEW LETTERS. 88 (25): -.

8. Eschrig, M.. The effect of collective spin-1 excitations on electronic spectra in high-T-c superconductors. 2006. ADVANCES IN PHYSICS. 55 (1-2): 47.

9. Varma, C. M.. Non-Fermi-liquid states and pairing instability of a general model of copper oxide metals. 1997. PHYSICAL REVIEW B. 55 (21): 14554.

10. Li, Y., V. Baledent, G. Yu, N. Barisic, K. Hradil, R. A. Mole, Y. Sidis, P. Steffens, X. Zhao, P. Bourges, and M. Greven. Hidden magnetic excitation in the pseudogap phase of a high-T-c superconductor. 2010. NATURE. 468 (7321): 283.

11. Chuang, T. M., M. P. Allan, J. Lee, Y. Xie, N. Ni, S. L. Bud'ko, G. S. Boebinger, P. C. Canfield, and J. C. Davis. Nematic Electronic Structure in the "Parent" State of the Iron-Based Superconductor Ca(Fe1-xCox)(2)As-2. 2010. SCIENCE. 327 (5962): 181.

12. Kasahara, S., H. J. Shi, K. Hashimoto, S. Tonegawa, Y.

Mizukami, T. Shibauchi, K. Sugimoto, T. Fukuda, T. Terashima, A. H. Nevidomskyy, and Y. Matsuda. Electronic nematicity above the structural and superconducting transition in BaFe2(As1-xPx)(2). 2012. NATURE. 486 (7403): 382.

13. Onishi, Y., and K. Miyake. Enhanced valence fluctuations caused by f-c Coulomb interaction in Ce-based heavy electrons: Possible origin of pressure-induced enhancement of superconducting transition temperature in CeCu2Ge2 and related compounds. 2000. JOURNAL OF THE PHYSICAL SOCIETY OF JAPAN. 69 (12): 3955.

14. Yuan, H. Q., F. M. Grosche, M. Deppe, C. Geibel, G. Sparn, and F. Steglich. Observation of two distinct superconducting phases in CeCu2Si2. 2003. SCIENCE. 302 (5653): 2104.

15. ROBINSON, J. M.. VALENCE TRANSITIONS AND INTERMEDIATE VALENCE STATES IN RARE-EARTH AND ACTINIDE MATERIALS. 1979. PHYSICS REPORTS-REVIEW SECTION OF PHYSICS LETTERS. 51 (1): 1.

16. Coleman, P.. Heavy Fermions: electrons at the edge of magnetism. 2007. In Handbook of magnetism and advanced magnetic materials. Edited by Kronmüller, H., and S. Parkin. Vol. I, p. 95. published online: John Wiley & Son, Ltd.

17. Holmes, A. T., D. Jaccard, and K. Miyake. Signatures of valence fluctuations in CeCu2Si2 under high pressure. 2004. PHYSICAL REVIEW B. 69 (2): -.

18. STEGLICH, F., J. AARTS, C. D. BREDL, W. LIEKE, D. MESCHEDE, W. FRANZ, and H. SCHAFER. SUPERCONDUCTIVITY IN THE PRESENCE OF STRONG PAULI PARAMAGNETISM - CECU2SI2. 1979. PHYSICAL REVIEW LETTERS. 43 (25): 1892.

19. BELLARBI, B., A. BENOIT, D. JACCARD, J. M. MIGNOT, and H. F. BRAUN. HIGH-PRESSURE VALENCE INSTABILITY AND TC MAXIMUM IN SUPERCONDUCTING CECU2SI2. 1984. PHYSICAL REVIEW B. 30 (3): 1182.

20. THOMAS, F., J. THOMASSON, C. AYACHE, C. GEIBEL, and F. STEGLICH. PRECISE DETERMINATION OF THE PRESSURE-DEPENDENCE OF T(C) IN THE HEAVY-FERMION SUPERCONDUCTOR CECU2SI2. 1993. PHYSICA B-CONDENSED MATTER. 186-88: 303.

21. Bao, W., P. G. Pagliuso, J. L. Sarrao, J. D. Thompson, Z. Fisk, J. W. Lynn, and R. W. Erwin. Incommensurate magnetic structure of CeRhIn5. 2000. PHYSICAL REVIEW B. 62 (22): 14621.

22. Knebel, G., D. Aoki, J. P. Brison, and J. Flouquet. The Quantum Critical Point in CeRhIn5: A Resistivity Study. 2008. JOURNAL OF THE PHYSICAL SOCIETY OF JAPAN. 77 (11): -.

23. Park, T., F. Ronning, H. Q. Yuan, M. B. Salamon, R. Movshovich, J. L. Sarrao, and J. D. Thompson. Hidden magnetism and quantum criticality in the heavy fermion superconductor CeRhIn5. 2006. NATURE. 440 (7080): 65.

24. Zapf, V. S., E. J. Freeman, E. D. Bauer, J. Petricka, C. Sirvent, N. A. Frederick, R. P. Dickey, and M. B. Maple. Coexistence of superconductivity and antiferromagnetism in CeRh1-xCoxIn5. 2002. PHYSICAL REVIEW B. 65 (1): -.

25. Jeffries, J. R., N. A. Frederick, E. D. Bauer, H. Kimura, V. S. Zapf, K. D. Hof, T. A. Sayles, and M. B. Maple. Superconductivity and non-Fermi liquid behavior near antiferromagnetic quantum critical points in CeRh1-xCoxIn5. 2005. PHYSICAL REVIEW B. 72 (2): -.

26. Shishido, H., R. Settai, S. Hashimoto, T. Kubo, H. Harima, and Y. Onukia. de Haas-van Alphen effect in CeRhIn5 under pressure. 2005. PHYSICA B-CONDENSED MATTER. 359: 184.

27. Watanabe, S., and K. Miyake. Quantum Valence Criticality as an Origin of Unconventional Critical Phenomena. 2010. PHYSICAL REVIEW LETTERS. 105 (18): -.

28. Bauer, E. D., M. M. Altarawneh, P. H. Tobash, K. Gofryk, O. E. Ayala-Valenzuela, J. N. Mitchell, R. D. McDonald, C. H. Mielke, F. Ronning, J. C. Griveau, E. Colineau, R. Eloirdi, R. Caciuffo, B. L. Scott, O. Janka, S. M. Kauzlarich, and J. D. Thompson. Localized 5f electrons in superconducting PuCoIn5: consequences for superconductivity in PuCoGa5. 2012. JOURNAL OF PHYSICS-CONDENSED MATTER. 24 (5): -.

29. Pfleiderer, C., P. Boni, T. Keller, U. K. Rossler, and A. Rosch. Non-Fermi liquid metal without quantum criticality. 2007. SCIENCE. 316 (5833): 1871.

30. Park, T., V. A. Sidorov, F. Ronning, J. X. Zhu, Y. Tokiwa, H. Lee, E. D. Bauer, R. Movshovich, J. L. Sarrao, and J. D. Thompson. Isotropic quantum scattering and unconventional superconductivity. 2008. NATURE. 456 (7220): 366.

31. Basic Energy Sciences 2011 summary report. 2011. U.S. DOE 2011. Basic Energy Sciences 2011 Summary Report.

Understanding Earth's Deep Water Cycle: Neutron Diffraction and Calorimetric Studies of Hydrous Minerals

Hongwu Xu
20110190ER

Introduction

As part of the global hydrologic cycle, the Earth's deep water cycle plays a significant role in many geological processes, including arc volcanism, deep focus seismicity, and, in a larger context, the evolution of our planet. To understand Earth's deep water cycle, it is essential to determine the stability and fate of hydrous minerals, which occur in hydrated oceanic crust, when the crust is subducted into the mantle via the mechanism of plate tectonics. The aim of this research is to characterize the crystal structures, mechanical properties, thermodynamic stability and phase equilibria of a number of important hydrous minerals using neutron and synchrotron x-ray diffraction at simultaneous high-pressure (P) and high-temperature (T) conditions (high P-T neutron diffraction is a unique capability at LANL), together with high-T solution calorimetry. Specifically, we will examine three groups of minerals: 1) simple hydroxides; 2) oceanic crust minerals; and 3) potential hydrous mantle minerals. In particular, since these minerals contain large amounts of light elements, particularly hydrogen, neutron diffraction is an ideal tool for such studies. Systematic measurements of these minerals using neutron diffraction coupled with our cutting-edge high P-T technique at LANSCE will yield valuable information such as hydrogen positions and displacement parameters that cannot be obtained with other methods. The obtained results will provide important parameters for models of Earth's deep water cycle and thus will shed light on mechanisms underlying the storage, fate and dynamics of water in the Earth's interior.

Benefit to National Security Missions

Successful execution of this project will contribute greatly to the fundamental understanding of Earth's deep cycling of water, CO2 and other volatiles and its related geological activities including volcanism and seismicity. This work is also an essential part of studies of the global water cycle which integrates physical, chemical, and biological processes that sustain ecosystems and influence climate, hazardous events, and related global change. The unique neutron and calorimetric capabilities developed/optimized in this research will have a wide range of applications in materials science, physics, chemistry, Earth and environmental sciences, and thus will strengthen key capabilities required for future Laboratory mission areas in plutonium science, energy security and environmental remediation. Potential future sponsors for water/volatile cycle research include NASA, DOE's Office of Science, and NSF. We will closely engage appropriate program managers in the Lab and the DOE complex throughout the project.

Progress

First, we conducted high-pressure synchrotron infrared (IR) spectroscopic experiments of brucite (Mg(OD)2) and hydrous phase A (Mg7Si2O8(OD)6) using diamond-anvil cell (DAC) techniques. Second, we carried out synchrotron X-ray diffraction (XRD) measurements of Ni(OD)2 and Ni(OH)2 at high pressure (P) and temperature (T) using multi-anvil techniques. Third, we performed analyses of high P-T synchrotron XRD and neutron diffraction (collected previously) data of jarosite (KFe3(SO4)2(OD)6). The goals were to study the structures and stability of these phases at high-P high-T conditions. Hydrous phase A is a potential host for water in the Earth's mantle, and simple hydroxides (brucite and nickel hydroxide) are present as component units in the structures of complex hydrous minerals. Jarosite occurs on Mars, which is considered as a strong evidence for the existence of water (and life) in ancient Mars. Hence, studying the structures and stability of these minerals at relevant P-T conditions will provide important insights into the mechanisms of water storage in the deep Earth and Mars (if the same plate tectonic mechanism is operating).

High-P synchrotron IR spectroscopy of brucite and phase A: IR spectra of Mg(OD)2 and Mg7Si2O8(OD)6 were col-

lected from 600 to 8000 cm-1 in frequency at pressures up to 31 GPa. Although both samples are nominally deuterated phases, their IR spectra indicate that they contain small amounts of OH, presumably due to the exchange of D by H from moisture during sample synthesis/handling. Because IR spectroscopy is more sensitive to OH than OD, the presence of small amounts of OH results in significant IR signals arising from OH. Thus the samples can be used for studying both OD and OH vibrational properties. No phase transition was obvious in brucite on compression; however, starting from 2.2 GPa, a new IR band (2687 cm–1) associated with OD appeared and its intensity increased with pressure. For Phase A. a phase transition was observed at 12 GPa, as evidenced by the slope changes in variations of OH/OD band frequencies with pressure.

High P-T synchrotron XRD of Ni(OD)2 and Ni(OH)2: The reported bulk moduli for nickel hydroxide exhibit a wide range, from about 52 to 88 GPa. One possible reason is the use of Ni(OD)2 versus Ni(OH)2. To determine the possible H/D isotope effect, we carried out synchrotron XRD on Ni(OD)2 and Ni(OH)2 at identical P-T conditions. At a given condition, unit-cell parameters a and c of Ni(OH)2 are larger than those of Ni(OD)2. The resulted smaller unit-cell volumes for Ni(OD)2 imply that the structure may preferentially incorporates D over H at high pressure. Furthermore, Ni(OD)2 is only slightly more compressible than Ni(OH)2 (primarily along the c-axis). Thus the discrepancies in reported bulk moduli are not due to H/D isotope effect. In fact, for the same Ni(OD)2 sample, we obtained a bulk modulus of 148.4 GPa using DAC synchrotron XRD and a value of 57.3 GPa with toroidal-anvil-cell neutron diffraction. This is likely due to differences in stress state and diffraction geometry between the two techniques.

High P-T synchrotron X-ray/neutron diffraction of jarosite: Several sets of measurements were performed to 9 GPa and 1273 K to map out jarosite P-T stability regions. For example, at 9.1 GPa, jarosite was stable up to 824 K, but then decomposed partially into yavapaiite, hematite and water at 839 K. This dehydroxylation temperature is much higher than that at ambient pressure (between 550 and 575 K), suggesting a positive P-T slope for the dehydroxylation reaction. At a given pressure, the c dimension of jarosite expands at a rate more rapidly than that for a. Similar to the behavior at room pressure, this anisotropy is largely due to the ease of tilting the Fe(O,OD)6 octahedra about the a-axes, which results in rapid increase in the (001) layer thickness with temperature. However, the magnitudes of the thermal expansion are smaller than those at ambient pressure, apparently due to the confining effect.

Other activities: 1) High-T synchrotron XRD was conducted to 1066 K on polyhalite (K2MgCa2(SO4)4·2H2O), an important mineral coexisting with salt crystals in salt repositories. 2) Two clathrate hydrates containing CO gas molecules were synthesized and characterized at high-P low-T conditions; 3) A piston-cylinder apparatus that can reach 4 GPa and 2373 K (a new materials synthesis capability at LANL) was installed.

Future Work

During the extension period (FY14) of this project, we will focus our efforts on neutron diffraction studies of hydrous phase A, an important host phase for water in the Earth's mantle. A deuterated sample, Mg7Si2O8(OD)6, has been synthesized specifically for neutron measurements, to avoid large incoherent scattering of H, which would cause high backgrounds of neutron diffraction patterns. We intend to determine the crystal structure, thermo-mechanical properties and thermodynamic stability of this phase at high pressure (P) and/or high temperature (T). Neutron diffraction, which detects the nucleus rather than electron cloud and can sense light elements, represents a powerful tool for locating hydrogen/deuterium positions in hydrous minerals. With our unique high P-T neutron capability (up to 10 GPa and 1800 K) at LANSCE, we have successfully conducted experiments on various materials/minerals aimed at refining their atomic positions and thermal parameters at high P-T conditions. In addition, we plan to perform high P-T synchrotron X-ray diffraction experiments on this phase using multi-anvil and diamond-anvil cell techniques, which are complementary to neutron methods and allow measurements at higher pressures. Lastly, we will complete analyses of the obtained synchrotron infrared spectroscopy data of phase A (as well as brucite), summarize the results, and prepare manuscripts for publication (including those on synchrotron X-ray and neutron diffraction results of brucite, nickel hydroxide and jarosite). The overall goal is, via integrated, multi-technical approaches, to determine the effects of water on phase relations and stability, physical properties and melting temperatures of related minerals – a critical issue for understanding Earth's deep volatile cycle. For follow-up projects, we will continue to explore the application of high P-T diffraction and spectroscopy methods to studies of minerals (e.g., clay and clathrate hydrate) important to Earth, environmental and energy systems, such as enhanced geothermal systems and salt repositories (such as WIPP).

Conclusion

Using neutron/synchrotron x-ray diffraction and solution calorimetry, we will determine crystal structures, elastic properties, thermodynamic stability and phase equilibria of a number of oceanic crust and mantle hydrous minerals

at high P-T conditions. In particular, we will characterize hydrogen bonding in these minerals, which plays a key role in their thermodynamic stability, dehydration processes and phase relations. These results will help construct phase diagrams of hydrous peridotite in MgO-SiO2-H2O and related systems at mantle conditions and will thus shed lights on the mechanisms of volatile circulation through the mantle and the origins of the arc volcanoes and deep focus earthquakes.

Publications

Xu, H. W., Y. S. Zhao, J. Z. Zhang, Y. J. Wang, D. D. Hickmott, L. L. Daemen, M. A. Hartl, and L. P. Wang. Anisotropic elasticity of jarosite: A high-P synchrotron XRD study. 2010. AMERICAN MINERALOGIST. 95 (1): 19.

Xu, H. W., Y. S. Zhao, S. C. Vogel, D. D. Hickmott, L. L. Daemen, and M. A. Hartl. Thermal expansion and decomposition of jarosite: a high-temperature neutron diffraction study. 2010. PHYSICS AND CHEMISTRY OF MINERALS. 37 (2): 73.

Xu, H., D. D. Hickmott, Y. Zhao, J. Zhang, Q. Wei, S. C. Vogel, and L. Wang. High-P/T synchrotron X-ray and neutron diffraction study of carbonate minerals. 2010. GEOCHIMICA ET COSMOCHIMICA ACTA. 74 (12): A1159.

Xu, H., D. Hickmott, J. Zhang, Y. Zhao, S. Vogel, and L. Daemen. Structure and stability of nickel hydroxide at high T-P conditions. Presented at Goldschmidt 2011. (Prague, Czech Republic, 14-19 Aug. 2011).

Xu, H., Y. Zhao, D. D. Hickmott, N. J. Lane, S. C. Vogel, J. Zhang, and L. L. Daemen. High-temperature neutron diffraction study of deuterated brucite. 2013. Physics and Chemistry of Minerals. : 10.1007/s00269.

Zhu, J. L., H. W. Xu, J. Z. Zhang, C. Q. Jin, L. P. Wang, and Y. S. Zhao. Thermal equations of state and phase relation of PbTiO3: A high P-T synchrotron x-ray diffraction study. 2011. JOURNAL OF APPLIED PHYSICS. 110 (8): -.

Zhu, J. L., S. M. Feng, Q. Q. Liu, J. Z. Zhang, H. W. Xu, Y. C. Li, X. D. Li, J. Liu, Q. Z. Huang, Y. S. Zhao, and C. Q. Jin. Temperature and pressure effects of multiferroic Bi2NiTiO6 compound. 2013. JOURNAL OF APPLIED PHYSICS. 113 (14): -.

Zhu, J. L., Z. J. Lin, J. Z. Zhang, H. W. Xu, S. C. Vogel, C. Q. Jin, and Y. S. Zhao. High pressure neutron and synchrotron X-ray diffraction studies of tetragonal LaFeAsO0.9F0.1. 2012. HIGH PRESSURE RESEARCH. 32 (3): 405.

Developing Potentials for Atomistic Modeling of Defect Phenomena at Metal-Ceramic Interfaces

Steven M. Valone
20120053ER

Introduction

The goal of this project is to understand defect interactions with metal-ceramic interfaces at an atomistic level by means of a new, unified model for both metals and ceramics. Defects e.g., point defects or line defects (dislocations), interacting with complex interfaces, influence many interfacial properties and the resulting material performance. The response of metal-ceramic interfaces to defects, whether generated from fabrication, cascade damage from irradiation, or materials deformation processes, are complicated by the disparity in the materials in intimate contact. However many defects, their movements, and mutual interactions can not be observed directly via experiments due to the short-time scales involved. It is then desirable to understand the physical processes and dynamics at the atomistic level via simulations such as molecular dynamics (MD) and conventional or off-lattice-kinetic Monte-Carlo. All atomistic simulations require interatomic potentials to describe the interactions among atoms, or the bonding. Attaining this goal requires the development of a unified atomistic model for both metals and ceramics as a central objective. For mixed bonds environment such as the metal/ceramic interfaces, it is well known that there are charge transfer issues that have puzzled the atomistic modeling community for many years. How to tackle the issue with physical principles, and its potential impact on understanding mixed-material interfaces, prompts the writing of this ER project. A spin-off of broad importance to materials modeling will be high fidelity interatomic potentials that describe the metallic, ionic, and covalent bonds in one, unified model. The model is to reduce to, or otherwise approximate, established models for these individual classes of materials.

Benefit to National Security Missions

Atomistic modeling capability is hugely important to predictive science capabilities in general. Nearly every multi-scale modeling proposal around the world for the last 5 years assumes the availability of atomistic models for complex materials that in fact are not in evidence. Campaigns 1 and 2, BES, Waste Storage programs (Veirs), and other LDRD projects have interests in the success of this project. If this project is successful, the new modeling tool will open new vistas for coupling mechanical and electronic structure responses of nanoscale materials that we cannot attempt now because the atomistic models do not have the right physics and the electronic structure methods cannot accommodate the time and length scales of interfacial interactions and heterogeneity.

Progress

The second stage of the Fragment Hamiltonian (FH) model of Ni metal was revised from the model produced in the first year of the project (2012) because we learned new properties of the model. That is we came to understand that the main components of the FH model pertained to charge-transfer hopping, rather than intra-band hopping in the sense of tight-binding theory. The "intra-band hopping" energies appear in a different part of the model than what we had first thought. The Ni paper had to be revised and is now ready for submission. The results of the model show that several 3d phases Ni can be modeled well with the FH model, as can most other 3d structures, such as monovacancies and faulted fcc lattices (ie half-way between fcc and hcp). Lower dimensional structures (1d and 2d lattices, surfaces, grain boundaries) are not as well represented with this first version of the FH model. Postdoc Ghanshyam Pilania was hired in March 2013 from Ramprasad's group at UConn. Our first pass at expanding the FH model to a metal/metal-oxide system, namely Be/BeO, was undertaken. Pilania developed the essential database of information for the Be/BeO composite system from electronic structure calculations. Baskes and Liu developed and applied the methodology to use the electronic structure data to produce an FH model of the mixed system. This work is on-going.

In addition, Pilania was able to identify the lattice parameters at which a metal-insulator transition occurred in lattices of 1, 2 and 3 dimensions. As expected, this pattern, based on spatial dimensions, is observed in both Be lattices and BeO lattices and is expected in essentially all crystalline materials. These dimensional dependencies are important to capture in the model, both for reasons of fidelity and for validation with electronic properties. Our first effort to capture the opening and closing of an energy gap in the FH model was restricted to a 1d chain model. Two cases were considered. The first case corresponds to a large lattice spacing and atomic-like energy levels. In this case, the hopping energies are close to zero (atoms are stuck in a neutral state). There are energy gaps between clusters of energy levels analogous to "HOMO-LUMO" gaps. The second case corresponds to a compressed lattice and bands of energy levels. In this second case, the same hopping energies were allowed to increase to values comparable to the gaps in the first case. The gaps closed in a way that is reminiscent to the way a multi-band tight binding model behaves.

Because we were able to capture some form of energy-gap closure in the FH model, Baskes proceeded to develop a model of the basic energy scales in the model so as to possess both neighbor-coordination and dimensionality dependencies. For this reason, we are able to represent structures of all three dimensionalities in Be. The Ni model still needs to be revised. Pilania was able to devise a method analyze the results of electronic structure calculations that directly measures covalency as an output. He did so by deconstructing the electron density output from an electronic structure calculation according the ansatz of the FH model. The analysis works well for any one material like Be or BeO. However, we are still experiencing some inconsistency when we compare estimates of covalency for Be and for Be in BeO. As we have refined the details of the FH model, Ben Liu has been developing the LAMMPS computer code (from SNL) that is serving as the repository for the FH model. The code is being and has been used to estimate defect energies for more complex structures (relaxed surfaces, grain boundaries, vacancies) than what can be estimated analytically. Valone presented invited talks at the Institute for Pure and Applied Mathematics at UCLA and at U of Az.

Future Work

The first stage of the Fragment Hamiltonian (FH) model of Ni metal was revised from the model produced in the first year of the project (2012) because we learned new properties of the model. A paper is being prepared at the same time and is to be submitted in the next month (July 2013). General characteristics of the model will be expanded to a metal/metal-oxide systems, namely Be/BeO and Ni/NiO. The second stage of the model for Ni/NiO is being conducted with the idea of using fits to spectroscopic measures, such as XPS, PES, and EELS, in order to devise a model of the composite system. Our ability to use such data comes from the "tight-binding-like" interpretation of the FH model. Postdoc Ghanshyam Pilania will developing information for both composite systems, and learning to analyze the results of electronic structure calculations to directly measure covalency as an output. The model derived in this way are to be tested with a 1d chain model. As we refine the details of the FH model, Ben Liu will continue to develop the LAMMPS computer code. The code will be used to estimate defect energies for more complex structures (relaxed surfaces, grain boundaries, vacancies) than what can be estimated analytically. Force fields will be added to the code in the coming FY. Invited talks have been accepted at the ACerS and TMS next Winter by both Valone and Pilania. Also Valone was invited to contribute to a book chapter on potential energy surfaces and atomistic methods, being edited by colleagues at the University of Az. The FH model will be featured. That task is to be completed during the end of the first quarter of FY2014.

Conclusion

Understanding metal-ceramic interfaces and defect interactions are of great importance to applications of interest: radiation damage resistance, mechanical behavior, and novel electronic materials. Understanding the mechanistics of why some materials can withstand high-level irradiation damage is of great interest for designing better materials. Metal-ceramic interfaces are of high interest for their extraordinary mechanical behavior. Finally, metal-ceramic layered materials can often have surprising electronic properties, as for example, the giant room-temperature magneto-resistance in single-crystal Fe/MgO/Fe magnetic tunnel junctions. The outcome of the project will be a new model that describes the atomistic level for both of these disparate materials.

Publications

Kolluri, K., M. J. Demkowicz, R. G. Hoagland, and X. Y. Liu. Behavior of vacancies and interstitials at semicoherent interfaces. 2013. Journal of Metals. 65 (3): 374.

Liu, X. Y.. Interphase Defects, Structures, and Phase Stability. 2013. Journal of Metals. 65 (3): 358.

Valone, S. M., K. Muralidharan, and K. Runge. Interatomic Potentials Including Chemistry. To appear in Multiscale Paradigms in Integrated Computational Materials Science and Engineering. Edited by Deymier, P. A..

Valone, S. M., S. R. Atlas, and M. I. Baskes. Embedded atom

method potentials from the fragment hamiltonian model: Crystalline phases and surfaces of nickel. 2012. LA-UR 2012-01180.

Valone, S. M., and S. R. Atlas. Density and spectral-density matrices in atomistic-scale models. 2012. LA-UR-2012-22846.

Yadav, S. K., R. Ramprasad, A. Misra, and X. Y. Liu. Core structure and Peierls stress of edge and screw dislocations in TiN: A density functional theory study. (submitted to Acta Mater.) LA-UR-13-25179.

Yadav, S. K., R. Ramprasad, J. Wang, A. Misra, and X. Y. Liu. First-principles study of Cu/TiN and Al/TiN interfaces: weak vs strong interfaces. LA-UR-13-27331 (submitted to Modelling and Simulation in Materials Science and Engineering).

Yadav, S. K., X. Y. Liu, J. Wang, R. Ramprasad, A. Misra, and R. G. Hoagland. First-principles density functional theory study of generalized stacking faults in TiN and MgO. submitted to Philosophical Magazine (LA-UR-13-22557).

From Waste to Fuels and Feedstocks: Reduction of CO_2 Using Main-Group Catalysts

Andrew Sutton
20120197ER

Introduction

Carbon dioxide (CO2) is the greenhouse gas of greatest concern in climate change, but it could also be the most abundant C1 building block on the planet if its capture and conversion to a useful feedstock under mild conditions can be realized. In this proposal, we outline the pathway by which we believe this conversion can be accomplished catalytically. By eschewing the use of expensive and rare precious metals and using main-group (p-block) compounds instead, the process that we are proposing will be amenable to future implementation on a global scale. We aim to accomplish this conversion using main-group compounds in the form of frustrated Lewis pairs (FLPs, i.e. a Lewis acid/base pair that cannot form self-adducts) to support the hydrogenation of CO2 to yield methanol (MeOH). We will use our experience with the H2 fuel carrier ammonia borane (AB) to design a regenerable system. Ultimately, we envision a double FLP reaction pathway that is capable of the single-stage conversion of a H2/CO2 input stream into MeOH and H2O via simultaneous H2 cleavage and CO2 activation. Throughout this project, we will be advancing scientific knowledge on the mechanism of interaction and reaction in these systems.

Benefit to National Security Missions

Due to concern over CO2 as a greenhouse gas, the DOE has taken steps to develop the conversion of CO2 to value-added products such as fuels and feedstocks. In order to do this effectively on a large scale, cost and material availability must be considered. Moving away from precious metals to main-group elements as catalysts would enable us to develop a catalytic system for CO2 reduction which would not only be relatively cost-efficient, but also support the DOE & LANL Grand Challenges. Finally, better understanding of these reaction mechanisms may enhance our ability to mitigate other waste streams.

Progress

A technician has been employed part time and extensive screening of Lewis Acids and Lewis Bases has been carried out and this large range has been exposed to CO2 for binding property analysis. The best system is still the one discovered with aluminum and phosphines from our initial studies and efforts to impart water and air stability have been progressing well.

New ligands have been designed and synthesized and computational analysis has given us confidence these will be robust and catalytically active species.
We have also started utilizing bidentate Lewis Bases in water and air stable systems and hope these will also show excellent CO2 binding affinities.

Future Work

We have developed several new frustrated Lewis pairs (FLPs) that we have shown via 13C NMR and IR to bind CO2. These systems need to be further developed to reduce CO2 to methanol using H2, ammonia borane or other good reducing agent to enable the full sequestration and reduction of CO2 to be performed. We also need to impart increased aqueous and acid tolerance to our FLP systems.

Conclusion

The scale of CO2 production creates significant problems in capture and sequestration as there is little short-term economic incentive to do so and the quantities involved are large. The work we propose will address this issue by developing chemistry to convert CO2 into a value-added molecule, MeOH, which is a C1 feedstock. In the course of this work, we expect to advance our understanding of multi-electron reduction chemistry using abundant main group materials. From this knowledge base, we will be able to expand our investigations into

other chemistries such as the activation of small molecules and C-C bond forming reactions.

Publications

Smythe, N. C., A. D. Sutton, D. A. Dixon, and B. Zelenay. Aluminum Oxide Frustrated Lewis Pairs for CO2 Conversion to Methanol. To appear in TBD.

First Principles Many-body Approaches to Strongly Correlated Actinide Metals

Jianxin Zhu
20120232ER

Introduction

Since the early days of the Manhattan Project, it has long been a cherished goal, often thought impossible, to have an accurate first-principles, parameter-free, capability to calculate and predict, anywhere in the phase diagram, the materials properties of plutonium (Pu), which has an extremely anomalous metallurgy. The complexity of Pu metals is closely related to the unique position of Pu in the last row of periodic table, where the 5f electrons of Pu are borderline between being either itinerant or localized. This implies the presence of strong electronic correlation in these materials.

Recent development of the combination of the local density approximation (LDA) and dynamical mean field theory (DMFT), so called the LDA+DMFT method, has advanced our understanding of emergent phenomena like metal-Mott-insulator transitions with structure information in strongly correlated materials. However, the LDA+DMFT suffers from the weaknesses with the uncertainty of screened local Coulomb interactions and the issue introduced by a double-counting correction. In this project we will develop a first-principles version of DMFT, which will be combined with the quasiparticle GW theory. GW refers to the theory that predicts electronic energy for ground and excited states of materials. In the latter framework, the screened local Coulomb interactions are calculated on the fly with no adjustable parameters. The development of this theory will thus form a fundamental basis for new advances in our understanding of the superconductivity, magnetic and heavy fermion behaviors, and many other anomalous properties of strongly correlated d- and f-electron materials. It will replace the “empirical” nature of current predictions with a new theory that has controllable approximations, and as such can be systematically improved. We focus on the application to actinide materials. This new theoretical technique will position LANL to be a leader in actinides theory in specific, and materials theory and simulations in general.

Benefit to National Security Missions

The development of a new first-principles electronic-structure method for strongly correlated actinide materials that can accurately calculate effects of electronic correlations on physical properties at any given temperature and pressure will have immediate application in a variety of NW, energy, high-performance (exascale) computing, and IS&T missions at the Laboratory. In the energy arena, for example, this will enable accurate materials predictions for actinide oxide fuels. Once the basic method is established and validated, future program development will be needed to generalize it in order to calculate various specific materials properties of interest. For example, a phonon module should be developed so that effects of thermal vibrations on the free energy at finite temperatures can be calculated.The code should also be generalized and exploited as an accurate method to calculate phase diagrams of relevant materials. Elastic constants and mechanical properties could also be calculated.

Progress

We have calculated the LDA and relativistic quasi-particle self-energy (GW) renormalized band structure of U, Np, Pu, and extended Pu systems. With increasing lattice constants and partially filled f-orbitals, these systems allow us to understand the correlation physics from itinerant to localization limit. With 5f electrons, the spin-orbit coupling is non-negligible in these systems and the Fermi energy is very close to the spin-orbit split. For quasi-particle correction, we have therefore employed a scalar relativistic extension of single shot GW approximation. We have also estimated average screened Coulomb interaction U in the static limit for all systems. In the weakly interacting localized electronic systems, GW self-energy is well known to incorporate the dynamic correlation in both long- and short-range limit. With increasing U, such dynamical quasi-particle correction becomes over-burdened in the short range limit and thus calls for

proper atomic treatment, which is widely addressed by various versions of dynamical mean field theory (DMFT). Our first-principles GW calculations thus benchmark correlation strength in the light actinides from itinerant-to-localized systems including the spin-orbit coupling effects. We have also developed an intermediate Coulomb-U coupling model for intermetallic actinides to capture their electronic structure properties affected by electron correlations. This model is based on material-specific ab-initio band structure from which correlation effects are computed via self-consistent GW-based self-energy corrections arising from spin fluctuations.

We applied this approach to four isostructural intermetallic actinides PuCoIn5, PuCoGa5, PuRhGa5 belonging to the Pu-115 family, and UCoGa5, a member of the U-115 family. The 115 families share the property of spin-orbit split density of states enabling substantial spin fluctuations around 0.5 eV, whose feedback effect on the electronic structure creates mass renormalization and electronic 'hot spots', i.e., regions of large spectral weight in momentum-energy space.

A detailed comparison was provided for the angle-resolved and angle-integrated photoemission spectra and de Haas-van Alphen experimental data as available. The results suggested that this class of actinides is adequately described by the intermediate Coulomb interaction regime, where both itinerant and incoherent features coexist in the electronic structure.

Future Work

In the next fiscal year, we will continue applying the GW+SO method to investigate the electronic structures of many heavy fermion systems including some new actinide-based topological insulators, e.g., PuSb. We are particularly interested in looking into the bulk energy gap in these systems. We will start exploring the possibility of calculating the total energy within the GW Green's function formalism, which is important to the study of equilibrium volume of actinides. Therefore, our short term priority is to develop this methodology which can be built upon the existing scalar relativistic GW code.

We plan to integrate our SO+GW method in a self-consistent GW+DMFT(CTQMC) formalism which will not only allow us to study the strongly correlated systems or metal-to-insulator(MIT) transitions from first-principles, but also enable us to understand electronic structure associated more complicated Kondo like physics in actinide systems. In parallel, we plan to extend the GW-based self-energy method based on spin fluctuations necessary for identifying the electronic hot spots at the Fermi surface that lead to a superconducting instability. We anticipate predicting the symmetry of the dominant pairing channel(s) and classifying the most important Fermi surface sheets for nesting.

Conclusion

This project will integrate GW methods with DMFT techniques to generate a first-principles, parameter free method that can accurately calculate electronic correlation effects for any material at any temperature and atomic volume. This code will enable us to confidently predict trends in correlation effects systematically for different crystalline phases of elemental actinides as well as for classes of different actinide compounds.

It will provide us with a tool to confidently understand many anomalous properties in actinide metals. It will provide a general-purpose electronic structure method that can also be applied to related correlated transition metal and rare-earth compounds.

Publications

Ahmed, T., R. C. Albers, A. V. Balatsky, C. Friedrich, and J. Zhu. GW quasiparticle calculations with spin-orbit coupling for the light actinides. 2013. arXiv.org.

Das, T.. Interaction induced staggered spin-orbit order in two-dimensional electron gas. 2012. Physical Review Letters. 109: 246406.

Das, T.. Staggered spin-orbit order: A new paradigm of broken symmetry phase of matter. 2013. Journal of Superconductivity and Novel Magnetism. 26: 1673.

Das, T., J. Zhu, T. Durakiewicz, J. J. Joyce, and M. J. Graf. Materials specific electronic correlation effects and spectral weight `hot spots' in inter metallic actinides. 2012. In 2012 MRS Spring Meeting. (San Francisco, 9-13 April, 2012). Vol. 1444, p. 169. Cambridge: Cambridge University Press.

Das, T., J. Zhu, and M. J. Graf. Spin fluctuations and the peak-dip-hump feature in the photoemission spectrum of actinides. 2012. Physical Review Letters. 108: 017001.

Das, T., J. Zhu, and M. J. Graf. The electronic structure and self-consistent spin-fluctuation corrections of inter metallic actinides. 2013. Journal of Materials Research. 28: 659.

Das, T., T. Durakiewicz, J. Zhu, J. J. Joyce, J. L. Sarrao, and M. J. Graf. Imaging the formation of high-energy dispersion anomaly in the actinide UCoGa5. 2013. Physical Review X. 2: 041012.

Nica, E. M., K. Ingersent, J. Zhu, and Q. Si. Quantum critical Kondo destruction in the Bose-Fermi Kondo model with a local transverse field. 2013. Physical Review B. 88: 014414.

Ronning, F., J. Zhu, M. J. Graf, R. C. Albers, H. Rhee, and W. E. Pickett. Superconducting gap structure of the 115's revisited. 2012. Journal of Physics: Condensed Matter. 24: 294206.

Svane, A., R. C. Albers, N. E. Christensen, M. van Schilfgaarde, A. N. Chantis, and J. Zhu. The electronic correlation strength of Pu. 2013. Physical Review B. 87: 045109.

Zhu, L., and J. Zhu. Singularity in self-energy and composite fermion excitations of interacting electrons. 2013. Physical Review B. 87: 085120.

Lanthanum Bromide Glass Ceramics for Gamma-Ray Spectroscopy

Markus P. Hehlen
20120246ER

Introduction

Our goal is to demonstrate a novel rugged lanthanum bromide glass-ceramic scintillator for gamma-ray spectroscopy. This is important because the best and most desired gamma-ray scintillator available today– cerium-doped lanthanum bromide (LaBr3:Ce3+) – is an extremely hygroscopic crystal that is difficult to grow and a challenge to handle. The resulting high cost, small size, and few suppliers limit its use to a small number of specialized detectors. What is urgently needed is a gamma-ray scintillator with LaBr3:Ce3+ performance that is chemically inert, mechanically rugged, and that can be manufactured economically in large size. If successful, we will be the first to demonstrate such a material. This would be a breakthrough in scintillator research and a game-changer for a broad range of customers who rely on gamma-ray spectroscopy in a wide range of homeland security, non-proliferation, and intelligence applications.Our primary research objective is to fabricate a chemically inert and mechanically rugged oxide glass matrix in which we grow in situ a high density of LaBr3:Ce3+ nano-crystals. The resulting scintillating glass ceramic will be optically transparent and encapsulate the hygroscopic LaBr3:Ce3+.Such a material is novel and does not currently exist. Its fabrication requires special synthesis methods because bromides react readily with water and oxides in undesired ways. We will use non-hydrolytic sol-gel (NHSG) processing as an anhydrous, low-temperature, and scalable synthesis route to this new class of nano-composite materials.

Benefit to National Security Missions

Scintillators are currently used in numerous types of radiation detection systems for basic science, medical imaging, non-destructive evaluation, and radiation detection. This projects seeks to enable a breakthrough in scintillators that would directly benefit all of these areas. Our prime goal is to break the price-performance correlation in radiation detection materials by breaking the single crystal-performance correlation.The use of scalable synthesis techniques that do not require long time periods and expensive equipment suggests that these glass ceramic scintillators can be produced at costs at least 20× lower than respective crystals. At the same time, the high-Z and high light output of these materials will preserve good performance. This is of interest to our homeland security, nuclear nonproliferation, and space systems customers.

Progress

The main goal of the project is to create for the first time a material that contains nano-particles of a high-performance halide scintillator (such as LaBr3:Ce) dispersed in a chemically inert silica matrix. Our baseline approach was to utilize a non-hydrolytic sol-gel (NHSG) synthesis to form the silica matrix in the presence of dissolved LaBr3:Ce, followed by heat treatment to induce the precipitation of LaBr3:Ce nano-crystals. NHSG synthesis is attractive because it allows for the solution-based formation of a silica-based glass at room temperature under the exclusion of water, which would readily react in undesired ways with LaBr3:Ce. The focus in the first half of FY13 was on completing the development of the NHSG process. We successfully fabricated transparent silica-gels with this method. A setback was encountered when we observed that the solubility for LaBr3:Ce in the starting solutions was insufficient. This initiated an extensive experimental campaign that exhaustively tested various starting reactants, the process temperature, and several additional solvents for their ability to dissolve LaBr3:Ce. We concluded that the LaBr3:Ce solubility was too low in any of the NHSG chemistry to obtain the required large mass fraction of LaBr3:Ce needed in the solution for the final application.

This extensive sol-gel synthesis effort led us to discover an alternative sol-gel approach to a nano-structured scintillator. LSO:Ce is a bright gamma-ray scintillator with

an energy resolution comparable to NaI:Tl but 6 times shorter decay time. Being able to produce it via a low-cost sol-gel process would be very attractive for a number of applications. We found that an LSO:Ce based nano-structured glass ceramic can be fabricated with a sol-gel process that uses regular siloxane chemistry. Our first experiments yielded relatively transparent gels with the required high concentration of the lutetium precursor. This process is currently being systematically optimized with the goal of scaling it up to larger sample sizes (several cubic centimeters) in FY14 for subsequent measurement of scintillation photon yield and energy resolution.

We have also initiated scintillator syntheses using mesoporous silica. These materials are silica-glass monoliths that contain a network of open pores with pore sizes of <10 nm and are therefore optically transparent. They lend themselves to infusion of the pores with scintillator materials to form a highly loaded nano-structured scintillator. This approach has not been reported before. We have successfully filled a large fraction of the available pore volume (28 vol% for Vycor) with LaBr3:Ce and SrI2:Eu (two highly efficient scintillators) using immersion of the mesoporous silica in the respective halide melt. The resulting composites exhibit bright photo- and radioluminescence, which are pre-requisites for efficient gamma-ray scintillation. This development currently focuses on developing the process parameters to obtain composites with high optical transparency.

Our work in FY13 has also resulted in two accepted publications in the Journal of Luminescence, an accepted publication in Optical Materials, and an invited presentation at the Phosphor Global Summit.

Future Work

The following goals and associated tasks are scheduled for next fiscal year.

Sol-gel process development

The sol-gel process development for LSO scintillator will be completed. The goal is to produce a nano-structured scintillator sample of sufficient size to measure a gamma-ray spectrum and determine the energy resolution of this composite material. This involves optimization of the sol-gel chemistry as well as the parameters for the heat treatment of the gel. This effort is guided by a diverse set of optical and structural characterization methods.

Infused meso-porous silica

Encouraged by our first results in FY13, we will pursue this alternate method of fabricating a nano-structured scintillator. We will tune the process to maximize transmission and measure a gamma-ray spectrum determine the energy resolution of this composite material. This effort is guided by a diverse set of optical and structural characterization methods.

Both these development efforts will allow us to obtain the first nano-structured glass ceramic samples that may offer a lower cost way to high resolution scintillators compared to bulk crystals. We will publish this work in peer-reviewed papers and, if possible, present at an international conference (ICL'2014).

Conclusion

We expect to fabricate a transparent silica glass ceramic containing a 50-60% volume fraction of <10 nm diameter LaBr3:Ce3+ nano-crystals. This nano-composite material will have scintillation performance that rivals that of LaBr3:Ce3+ single-crystal. Success will be achieved when we have demonstrated (1) an energy resolution of <3.5% at 662 keV, (2) a scattering length of ≥10 cm at the 380 nm scintillation wavelength, and (3) stability against hydrolysis in ambient air over a period of 1 month. Achieving this would constitute a breakthrough in scintillator research and would result in publications/presentations, patents, follow-on funding, and interest by commercial companies.

Publications

Blair, M. W., M. Fasoli, S. C. Tornga, A. Vedda, N. A. Smith, B. L. Bennett, M. P. Hehlen, and R. E. Muenchausen. Nanophosphor GdOBr:Ce via combustion synthesis: luminescence results. 2013. PHYSICA STATUS SOLIDI C: CURRENT TOPICS IN SOLID STATE PHYSICS, VOL 10, NO 2. 10 (2): 227.

Hehlen, M. P.. Short Course: Fundamentals of rare-earth spectroscopy. 2013. In Phosphor Global Summit 2013. (New Orleans, 18-20 March 2013). , p. 1. Falmouth, ME: Smithers.

Hehlen, M. P., M. G. Brik, and K. W. Kramer. 50th anniversary of the Judd-Ofelt theory: An experimentalist's view of the formalism and its application. 2013. JOURNAL OF LUMINESCENCE. 136: 221.

Hehlen, M. P., N. A. Smith, M. W. Blair, A. Li, S. Stange, R. D. Gilbertson, E. A. McKigney, and R. E. Muenchausen. Nanocomposite scintillators. Nanocomposite, ceramic and thin-film scintillators. Edited by Nikl, M..

Lakshminarayana, G., E. M. Weis, A. C. Lira, U. Caldino, D. J. Williams, and M. P. Hehlen. Cross Relaxation in rare-earth-doped oxyfluoride glasses. 2013. JOURNAL OF LUMINESCENCE. 139: 132.

Lakshminarayana, G., E. M. Weis, B. L. Bennett, A. Labouriau, D. J. Williams, J. G. Duque, M. Sheik-Bahae, and M.

P. Hehlen. Structural, thermal, and luminescence properties of cerium-fluoride-rich oxyfluoride glasses. 2012. OPTICAL MATERIALS. 35 (2): 117.

Li, A., N. Smith, M. P. Hehlen, E. A. McKigney, and R. Gardner. Light yield measurement method for milled nanosize inorganic crystals. 2012. Applied Radiation and Isotopes. 70: 1219.

Vasudevan, K. V., W. L. Boncher, N. A. Smith, M. W. Blair, B. L. Scott, B. L. Bennett, M. P. Hehlen, R. E. Muenchausen, and J. C. Gordon. Nitrile-supported coordination polymers of Cerium (III) Bromide. To appear in Inorganic Chemistry.

Are Nanoscale Foams Radiations Resistant?

Jose A. Caro
20120250ER

Introduction

The search in recent years of materials with improved radiations response has been based on engineering nanoscale features that act as efficient sinks for irradiation created defects, such as the Nanostructured Ferritic Alloys (NFA), or Oxide Dispersion Strengthened (ODS) steels. Similarly, the search of materials with improved mechanical properties (mainly strength) has been based on engineering nanoscale features that inhibit dislocation motion over long distances, typically by decreasing grain size to the nm range. These strategies have given impressive results by increasing radiation tolerance and hardness compared to coarse grain counterparts.

By shifting from internal interfaces in bulk materials to surface derived phenomena in nanoporous materials, a field that has not been explored so far, a new understanding of radiation tolerance and strengthening will be obtained. Foams with filament and porous sizes in the range of nanometers are ideal systems to study these effects and could provide insight on designing the ultimate material regarding perfect sink strength offered by the surface of the pores, and ultimate strength offered by dislocation free ligaments.

The goal of this project is to investigate the role of surface-to-volume ratio on the irradiation and mechanical properties of nanoscale foams. We will prove that high surface density nano-foams can be tailored to become simultaneously radiation tolerant and ultra-strong.

Benefit to National Security Missions

This work will lead to improved understanding and control of defects and interfaces, which is a critical capability for the Laboratory's mission in energy security, specifically in the area of where defects and interfaces control phenomena such as radiation hardness of materials in nuclear reactors. It will also provide insight into how interfaces and defects play an important role in the functionality of nano-structured materials. There is also a close connection to MaRIE, which has a focus on materials in extreme irradiation environments; LANL will benefit from supporting research that explores the fundamental science of radiation tolerance in materials. Developing a basic understanding in the area of this project will place us in a strategic position to seek future funding from the DOE Office of Nuclear Energy and Office of Basic Energy Science.

Progress

In previous work, we studied the response of nanoporous gold (np-Au) foams under irradiation at room temperature and different dose-rates [E. Fu, et al. APL 101 (2012) 191607]. Our experimental findings show that 400 keV Ne++ ion irradiation for a total dose of 1 dpa leads to the formation of Stacking Fault Tetrahedra (SFTs) at high and intermediate dose-rate, while no SFTs are formed at low dose-rate. An atomic-view of the process based on Molecular Dynamics simulations (MD) shows that vacancy migration distance and nanofoams ligament size play a key role in explaining the dose-rate dependent defect accumulation.

In the past months, we continued this study by investigating the mechanical response of nanofoams under irradiation. These investigations have two parts: 1) computer simulations studies in which we observe that nanofoams soften under irradiation and 2) experimental indentation studies which are in good agreement with this prediction.

A paper was published on the deformation mechanism of the ligaments that forms the nanofoam [L. Zepeda-Ruiz, et al., APL (2013) in press]. MD simulations of Au nanopillars under compression in the unirradiated (defect-free) and irradiated condition (with a SFT at the center of the nanopillar) show that SFTs play an important role in the deformation. Upon applied stress,

plastic deformation originates at the SFT, which becomes an almost inexhaustible source of dislocations. These results indicate that the presence of SFTs in Au ligaments after irradiation will induce a decrease of yield stress under compression, reducing its yield strength.

np-Au deformation behavior under compression was studied before and after ion irradiation at room temperature. Nanoporous gold specimens were prepared by chemically dealloying in nitric acid ~ 100 micron thick Au30/Ag70 thin films deposited on a multilayered substrate. Preliminary characterization and nanoindentation test results obtained as a function of etching time and irradiation conditions confirm that: 1) np-Au hardness decreases as ligament size increases (Hall Petch effect) and 2) np-Au hardness decreases under irradiation indicating that metallic foams soften under irradiation in very good agreement with previous computational simulations.

We presented our work in two conferences (MRS 2012, and TMS 2013) and have three papers in preparation.

Future Work

On the experimental side we will irradiate foam samples with different projectiles to explore the dependence of damage on the recoil spectrum. This variable is the last we proposed to explore. On the irradiated samples we will perform high resolution microscopy to determine the damage and nano indentation to determine the hardening. On the computational side, we will perform large scale simulations of damage on foams containing stacking fault tetrahedra to confirm the experimental findings and provide a quantitative explanation.

We will write and publish the work already done on mechanical properties of irradiated foams, and on the recoil spectrum dependence of damage.

Conclusion

This work will break new ground in understanding the basic physics of material response under radiation conditions where the architectural dimensions of the material are smaller than the typical size of the collision event that characterize the radiation damage. It will lead to improved understanding and control of defects and interfaces, specifically in the area of where defects and interfaces control phenomena such as radiation hardness of materials in nuclear reactors. It will also provide insight into how interfaces and defects play an important role in the functionality of nano-structured materials.

Publications

Caro, M., E. G. Fu, L. Zepeda-Ruiz, W. Mook, Y. Q. Wang, J. K. Baldwin, C. Sheehan, E. Bringa, M. Nastasi, and A. Caro. Radiation response of nano-scale gold foams. Invited presentation at 8th Pacific Rim International Congress for Advanced Materials and Processing (PRICM-8). (Waikoloa, HI, 4-9 Aug., 2013).

Caro, M., E. G. Fu, L. Zepeda-Ruiz, Y. Q. Wang, J. K. Baldwin, C. Sheehan, E. Bringa, M. Nastasi, and A. Caro. Radiation effects in nanoporous gold. Presented at TMS Annual Meeting Symp. on Functional Nanomaterials. (San Antonio, TX, 3-7 Mar., 2013).

Caro, M., E. G. Fu, L. Zepeda-Ruiz, Y. Q. Wang, K. Baldwin, E. Bringa, M. Nastasi, and A. Caro. Characterization of a window of radiation resistance in nanoporous gold. Presented at 2012 MRS Fall Meeting Symp. MM, Materials under Extreme Environments. (Boston, MA, 25 Nov. - 30 Dec., 2012).

Caro, M., W. M. Mook, E. G. Fu, Y. Q. Wang, J. K. Baldwin, C. Sheehan, L. Zepeda-Ruiz, E. Bringa, and M. Nastasi. Radiation effects on mechanical properties of nanoscale gold foams. Presented at CINT Workshop . (Santa Fe, NM, 24-26 Sep., 2013).

Farkas, D., A. Caro, E. Bringa, and D. Crowson. Mechanical response of nanoporous gold. 2013. Acta Materialia. 61: 3249.

Fu, E. G., L. Zepeda-Ruiz, M. Caro, Y. Q. Wang, E. Bringa, J. Baldwin, M. Nastasi, and A. Caro. Temperature dependent radiation response of nanoporous (np) Au foams. Presented at Computer Simulation of Radiation Effects in Solids COSIRES 2012. (Santa Fe, NM, 24-29 June, 2012).

Fu, E., M. Caro, L. A. Zepeda-Ruiz, Y. Q. Wang, K. Baldwin, E. Bringa, M. Nastasi, and A. Caro. Surface effects on the radiation response of nanoporous Au foams. 2012. Applied Physics Letters. 101: 191607.

Fu, E., M. Caro, Y. Q. Wang, M. Nastasi, L. Zepeda-Ruiz, E. Bringa, K. Baldwin, and A. Caro. Nanofoams Response to Radiation Damage. Invited presentation at CAARI 2012, 22nd Int. Conf. on the Application of Accelerators in Research and Industry. (Fort Worth, TX, USA, 5-10 August 2012).

Fu, E., M. Caro, Y. Q. Wang, M. Nastasi, and A. Caro. Irradiation Response and Stability of Nanoporous Materials. Presented at 18th International Conference on Ion Beam Modification of Materials (IBMM 2012). (Qingdao, China, September 2-7 2012).

Zepeda-Ruiz, L., E. Martinez, M. Caro, E. G. Fu, and A. Caro. Deformation mechanisms of irradiated metallic nanofoams. 2013. Applied Physics Letters. 103: 31909.

A Novel Mo-99 Separation Process Designed for Next Generation Medical Isotope Production

Iain May
20120255ER

Introduction

Mo-99 is a radioactive isotope that decays to Tc-99m, the most important radioisotope in nuclear medicine. Two front runner technologies for the domestic production of Mo-99 are based on the fission of U-235 in mildly acidic low enriched uranium (LEU) solutions, in either nitrate or sulfate media. Both require the extraction of trace amounts of Mo-99 (low mass of material but high specific radioactivity) from a vast excess of uranium. The current most technically advanced chemical process for this separation involves two inorganic columns designed to recover a crude Mo-99 product and a combined precipitation and solvent extraction process to purify the LEU fuel for recycle.

We proposed to develop a novel separation process that will allow efficient Mo-99 recovery after production, recycle of LEU fuel and the generation of a waste stream that can readily be converted to low level waste (LLW). The flowsheet we envision comprises steps that are known individually but have not previously been integrated into an overall process. We will evaluate specialized apparatus for several of these individual operations, including utilizing automation where possible. Our objective will be to prove that this "inventive application" of apparatus and individual chemical separations into an integrated process flow can successfully separate Mo-99, at the bench top scale, from LEU solutions irradiated at LANSCE (Los Alamos Neutron Science Center). Irradiated solution tests will be used to evaluate the best chemical processing conditions for efficient Mo-99 recovery and LEU fuel recycle.

Benefit to National Security Missions

The US requires the domestic production of Mo-99 from Low Enriched Uranium (LEU), both to ensure continuous supply of this important medical isotope and to eliminate dependence on the international use of High Enriched Uranium (HEU) for Mo-99 production. Developing a US Mo-99 domestic supply thus addresses two national security needs, secure medical isotope production and lowered proliferation concerns through elimination of HEU use. By providing a separation science solution to Mo-99 recovery from two of the front runner technologies for US based Mo-99 production LANL will be positioned to support the supply of Mo-99 in this country for decades to come, of direct interest to the NA21 Global Threat Reduction Initiative.

Progress

In our original proposal the end of FY 2013 milestone was to 'prove efficient separation of Mo-99 from uranium in nitrate and/or sulfate media.' This milestone has been met, we have performed the experiments that indicate that medical isotope Mo-99 can be successfully recovered from a vast excess of irradiated Low Enriched Uranium (LEU) using our novel flow sheet. This technology can potentially be applied to the separation of Mo-99 generated as a fission product from LEU solution fuels. Using Mo-99 milked from a Tc-99m generator we proved 'proof of concept' that our novel separation technology could be applied to the separation of Mo-99 from a mildly acidic uranium nitrate solution. The next step was to prove that this separation could still be achieved in the presence of the full suite of fission products generated during irradiation of a Low Enriched Uranium (LEU) solution. This required the development of a new sample irradiation capability at Target 4 LANSCE, developed in part for this project. Target 4 represents a new sample irradiation capability at LANSCE, the contribution made through this proposal towards this capability development directly supported the collection of technical data for this project - no augmentation.

The Mo-99 generated in the irradiated uranium nitrate solution was successfully separated from the vast excess of low enriched uranium. While the % recovery of Mo-99 was not as high as we were aiming (> 85 %), further pro-

cess optimization allowed us to get very close to achieving our target through a subsequent Mo-99/depleted uranium trial.

While the major technical development FY13 was the Target 4 sample irradiation capability, significant advances in analytical chemistry procedures were also made in support of the separation chemistry. This included developing a spectroscopic uranium analysis capability that allowed for quick, and accurate, analysis of uranium concentration. Also, a literature analytical procedure for acidity analysis was refined and adapted for our specific application.
We had previously submitted an Idea to LANL Tech Transfer based on our novel separation process and, based on FY13 results we have initiated the process for submission of patent protection. Once our intellectual property has been protected we will seek to publish our work in high impact chemical science/technology peer reviewed journals.
During FY13 we took the decision to focus solely on recovery of Mo-99 from irradiated LEU nitrate solution fuels, and we did not continue pursuing research into LEU sulfate solutions. In the summer of FY12 initial testing with our newly installed semi-automated separation equipment revealed complexities in the uranium sulfate chemistry that were not present with the uranium nitrate chemistry. When writing the original proposal we acknowledged that the sulfate chemistry could be challenging, but in FY14 we plan to return to uranium sulfate fuel to evaluate the feasibility of applying our separation technology for this fuel.

Future Work

Patent Protection
We plan to submit a patent, protecting the intellectual property associated with our novel technology for medical isotope Mo-99 recovery from irradiated Low Enriched Uranium (LEU).

Advances in Flow Sheet Separation Chemistry
We want to confirm that we can recover >85 % Mo-99 from an irradiated LEU solution in dilute nitric acid, while obtaining near quantitative recovery of the uranium for recycle. This will involve additional flowsheet chemistry refinements. Secondly, we wish to turn our attention to more careful control of other fission product contaminants of the Mo-99 product. Of most relevance is I-131, an isotope that partitions between numerous product and waste streams in Mo-99 recovery processes from enriched uranium targets. We have ideas for chemical control that could be very efficient, when coupled with our novel separation technology. Finally, we will evaluate additional purification steps for the LEU product post-recovery of Mo-99. Our FY13 results indicate that it should be possible to obtain a higher purity LEU product, enhancing the attractiveness of fuel recycle.

Evaluate Mo-99 Recovery from LEU Sulfate Fuel
We plan experiments to evaluate the possibility of our novel flow sheet being adapted to the successful recovery of Mo-99 from an irradiated LEU solution in dilute sulfate media.

Communication of Results
We have communicated results obtained in this project to the NA-21 Global Threat Reduction Initiative, who could provide follow up funding to apply our research to commercial Mo-99 production programs. Research performed in this project could also find application in Spent Nuclear Fuel Reprocessing, and the automated chemical processing applied here could be applicable to many chemistry projects. Therefore, once patent protection is in place we will seek to present our results to a wider audience through conference presentations and peer reviewed publications.

Conclusion

Mo-99 decays to Tc-99m, the most commonly utilized radioisotope in nuclear medicine. 50,000 procedures are performed every day here in the US with Mo-99, but the short radioactive half life of this isotope leads to rapid shortages when there are interruptions to production. Currently the US is entirely dependent on increasingly unreliable foreign suppliers and there is an urgent need to develop domestic production and purification processes. Our goal will be to develop a separation process for Mo-99 that will complement Mo-99 production technologies based on U-235 fission that are being developed here in the US with low enriched uranium.

Ultrafast Spectro-microscopy for Nanoscale Magnetic Domain Imaging

Richard L. Sandberg
20120278ER

Introduction

Our goal is to develop an ultrafast soft X-ray coherent diffractive imaging (CDI) microscope for magnetic materials. Our novel design will use high harmonic generation (HHG) as a tabletop coherent soft X-ray (SXR) source. Complete characterization of the magnetic inhomogeneity and its non-equilibrium dynamics holds the key to understanding of the exotic properties of complex magnetic and other nanostructured materials. Tools that image element-specific magnetization dynamics at the spatial and temporal scales of electron-spin-lattice interactions (fs-to-ps) are therefore essential for further progress in complex material science.

While time-resolved X-ray magnetic linear and circular dichroism microscopies(tr-XMLD/tr-XMCD) have proven to be powerful techniques to unveil magnetic properties of a broad class of materials, they have relied on larger synchrotron X-ray sources and had a limited temporal resolution (>ps), far from the fundamental timescales of the underpinning physical processes.

Despite recent progress in the development of femtosecond X-ray imaging techniques, ultrafast time-resolved imaging of magnetic material structure has never been demonstrated to our knowledge. The magnetic x-ray CDI (mCXDI) microscope proposed here will be capable of resolving ultrafast processes such as charge relaxation and spin ordering at the nanometer (sub-50 nm) spatial and femtosecond (<30 fs) time scales. This technique will fill the gap between electron, scanning probe, and optical photon imaging technologies and will provide an unprecedented combination of elemental specificity, sensitivity to ferromagnetic and anti-ferromagnetic spin ordering, and the ability to probe material dynamics at the fundamental space and timescales.

The development of time-resolved X-ray dynamic imaging is still at the early demonstration phase and significant impact for ongoing and future LANL programs in nanoscale imaging of heterogeneous complex materials at LANL and worldwide is envisioned with this microscope.

Benefit to National Security Missions

The proposed integration of “table-top” ultrafast magneto-optical X-ray spectroscopy and coherent X-ray imaging will provide LANL with a novel capability to investigate the dynamics of the magnetic ordering in a broad class of materials at the fundamental time and spatial scales and place LANL at the forefront of this field. This project will also enable an important characterization capability for MaRIE, LANL’s future signature facility, since the ability to unravel functionality in novel materials with coherent X-rays is an important competence underpinning MaRIE’s M4 facility. This work will directly address the LDRD Grand Challenge in Materials. In the long term, our work will be directly applicable to exploration of spin ordering in actinide and other mission-relevant materials, which aid in determine material functionality. Furthermore, development of ultrafast magnetic CXDI will introduce a unique capability to the LANL-based CMIME-EFRC and CINT and will attract more users to this facility.

Progress

The goals of the first year and a half of this project focused on building the table-top magnetic coherent X-ray diffractive imaging (mCXDI) system, optimizing the X-ray magnetic linear dichroism (XMLD) signal spectroscopically, and completing the first static imaging studies of non-magnetic (initially) and then magnetic samples. At the time of writing this report in June – about one and a half years through this project – we are slightly behind in achieving all of these goals due to several challenges we have had. However, we have made good progress recently and believe we can still achieve all of the goals of the project in the next year and one half.

Last year we highlighted the successful design and

integration of the mCXDI chamber into the existing time-resolved, spectroscopic high harmonic generation (HHG) system. We also mentioned initial studies that were performed on an antiferromagnetic strontium-doped manganite film (SrMnO3). Those studies lead us to an upgrade in the laser system that has greatly increased its flux and usefulness. Furthermore, we developed a robust broadband phase retrieval algorithm for inverting the collected diffraction patterns into high resolution images. We have begun efforts to use this algorithm on actual soft x-ray (SXR) diffraction patterns.

With the fully operational mCXDI chamber, we have conducted many studies on test patterns to optimize the coherence and flux. We are proud to report that the soft x-ray flux available from the upgraded laser setup appears to have approximately an order of magnitude higher flux at the magnetically important iron M-edge (55 eV) than previous sources used for such efforts.

During this last year we have also designed and purchased multilayer soft x-ray mirrors that have made our chamber more versatile. However, the coherence of the source has been limited due to challenges in alignment and vibration in the HHG source that we did not discover and correct until recently. These vibrations had prevented reconstruction of high quality, high resolution (sub-100 nm) SXR images of the test samples. Beside test objects, a gold-chromium test sample was designed and lithographically patterned that will allow us to demonstrate absorption contrast dichroism imaging. This type of imaging will allow elemental specific imaging of nanometer scale samples – a potential first for a tabletop source. We are currently finishing the collection of this data and expect to have two papers submitted by the end of this FY. Furthermore, these initial studies were highlighted in an invited talk at a Special Symposium on coherent diffractive imaging at the TMS 2013 Conference.

Additionally, this year we have identified and designed a transmissive magnetic sample geometry under a CINT User Proposal with Quanxi Jia. These samples are currently being manufactured and include a thin layer of multiferroic and antiferromagnetic (AFM) bismuth ferrite (BiFeO3 or BFO). In the coming weeks, we expect to begin studies on these samples in order to determine their optimal contrast and magnetic domain structure. These samples will also be an excellent candidate for time-resolved imaging in FY14. Additionally, in collaboration with Steve Conradson (MST-8), we have begun x-ray absorption fine structure (XAFS) studies at the SLAC SSRL synchrotron on BFO samples doped with strain inducing SmO3 nanopillars. These studies will aid our efforts at imaging AFM domains in at least two ways: 1st, these XAFS studies will tell us about the effect of strain-inducing elements on the local atomic structure of the materials, a critical direction for the future of multiferroic materials like BFO, and 2nd, these initial studies open the door to pursuing coherent diffractive imaging at the SSRL. To this effect, a user proposal has been submitted to the SSRL for coherent scattering and imaging studies of BFO and other multiferroic materials in collaboration with Alex Reid of SLAC.

Future Work

Our goals for the next FY will be to conclude and publish static imaging demonstrations, conduct time resolved studies of magnetic materials, and conduct complementary static studies of antiferromagnetic (AFM) materials at synchrotrons. First, throughout the rest of this FY and in the beginning of FY14, we plan on finishing the static imaging experiments already begun on three samples: static test patterns, absorption contrast gold/chromium patterns, and thin film bismuth ferrite, BiFeO3 (BFO). Imaging the antiferromagnetic domain structure of a material like BFO will be a first on either a tabletop or synchrotron x-ray source. These results will be finished and written up in the next few months. Additional imaging of static AFM materials such as SrMnO3 (SMO) or other xMnO3 materials will also be pursued.

The bulk of the efforts during the last FY of this project will be dedicated to time-resolved imaging of novel magnetic materials. We will begin with laser driven demagnetization studies of BFO or SMO. We stress that such studies have not been demonstrated in a time resolved fashion on any existing X-ray source. As a complementary effort to the tabletop source, we have also submitted a user proposal for beamtime at the SLAC SSRL synchrotron. During FY14, we have planned a series of coherent scattering and imaging experiments on AFM materials that will avail of the higher flux and contrast at the L-edges (~700 eV) not currently accessible on our tabletop source. These first experiments, combined with tabletop results, will be combined into a user proposal for time resolved studies at the LCLS X-ray Free Electron Laser (XFEL) at SLAC.

Conclusion

Our proposed tabletop magnetic coherent x-ray diffractive imaging (mCXDI) microscope will fill the urgent need of ultrafast and nanoscale probes to address several materials challenges, especially novel magnetic materials that will have a large impact on wide ranging technology from information storage to energy applications. Therefore, we expect this work to have significant impact in both materials science and ultrafast nano-probe development both

for the LANL and worldwide community. Additionally, this work will aid in providing a stepping stone capability towards understanding materials under extremes – a category which has critical and cross cutting applications to our energy security.

Publications

Barber, J. L., R. L. Sandberg, C. W. Barnes, and R. L. Sheffield. Diffractive Imaging at Large Fresnel number: The Challenge of Dynamic Mesoscale Imaging with Hard X rays. Phys. Rev. B.

Sandberg, R. L., Z. F. Huang, R. Xu, J. A. Rodriguez, and J. W. Miao. Studies of Materials at the Nanometer Scale Using Coherent X-Ray Diffraction Imaging. 2013. JOM. 65 (9): 1208.

Unlocking Plasmons in Graphene

Kirill A. Velizhanin
20120300ER

Introduction

A plasmon is the collective movement of electrons in a conducting material, i.e., a metal. Controlling the movement of plasmons can have many potential applications in fields such as telecomunications, sensing and renewable energy. Graphene, which is a newly isolated form of carbon that is only a one atom thick sheet, holds promise to become a useful material for such plasmonic applications due to its high electrical conductivity and its unique electronic and mechanical properties. However, systematic studies of the plasmons in graphene have not been performed to date. Thus, the goal of our project is to provide a fundamental understanding of the plasmon's in graphene using a combined theoretical and experimental approach to "unlock" its potential for future applications. We will experimentally measure several critical parameters (e.g., plasmon dispersion relation and lifetime) under a variety of conditions. These parameters will be used to theoretically predict the behavior of plasmons in graphene.

With this knowledge, we will then attempt to control the plasmons in graphene through the addition of semiconductor or metal nanoparticles onto the graphene surface, as well as by patterning or functionalizing the substrate supporting the graphene film. These features will provide a rudimentary means for spatial confinement and directing of plasmons in graphene. Direct visualization of graphene plasmons will be performed with advanced optical characterization tools. The detailed understanding of plasmons in graphene gained from this work is expected to allow us to predict how to optimize graphene-based devices for a variety of applications.

Benefit to National Security Missions

The work will directly support a LANL Materials Grand Challenge directed at "Control of electronic or photonic functionality…". Further, this work supports ongoing efforts in T-Division and the Center for Integrated Nanotechnologies focused on understanding/manipulating optical plasmons for new applications. In particular, this work will bring new capabilities to CINT that may be made available to new users, which directly supports our DOE-BES mission. Ultimately, the work proposed here could lead to breakthrough capabilities for optical switching, signal processing and active metamaterial applications that would be of interest to a variety of sponsors including BES, as well as lead to new intellectual property.

Progress

Surface plasmons on a single-layer graphene reside in the infrared range of the spectrum, depending on the exact amount of doping. The success of the experimental component of this ER project relies heavily on the availability of high-quality graphene samples with the ability to control the amount of doping. An experimental postdoc, Akhilesh Singh, has been hired (started March 2013) to accomplish the graphene synthesis, fabrication of graphene-based devices and their optical characterization. To date, Dr. Singh has been able to accomplish the chemical vapor deposition (CVD) synthesis of good quality graphene samples with a few 100 µm continuous single layer flakes. This has been confirmed with optical microscope and Raman measurements. This contributes to the Lab (and CINT) capabilities in synthesis of novel materials with unique properties.

Defects/functionalization have to be introduced to graphene in order to couple the external optical long-wavelength excitation to short-wavelength graphene plasmons. We have continued the studies of the interactions between graphene surface and adsorbate/ligand molecules. In particular, D. Yarotski has applied scanning tunneling microscopy to determine the quality of the CVD-grown graphene samples. The images reveal atomically flat graphene surface that exhibits periodic Moiré patterns. These patterns confirm the presence of single

layer graphene and are induced by the lattice constant mismatch between graphene and a substrate. We are currently working on mapping the spatial distribution of fluorine molecules bonded to graphene as a function of doping flux and exposure time. These results will be used to optimize graphene functionalization approaches and create covalently bonded fluorine 'mediators' between graphene and other nano-to-microscale adsorbants relevant to its electro-optical applications.

The optical characterization of graphene samples and the interferometric time-resolved measurements of plasmons propagation in graphene require new experimental tools in LANL and CINT labs. A high-end infrared optical microscope and spectrometer were set up in the ultrafast optical spectroscopy lab at CINT by A. Efimov. The spectrometer features step-scan capability so the system will be used in the interferometric experiments on plasmon propagation. Preliminary experiments indicate superior signal-to-noise and drift resistance as compared to the previous systems used.

Electrical gate-dependent measurements on the gated graphene samples were performed using a microscope probe station from Agilent. It was found that presently all the samples tested posses a substantial level of p-doping potentially indicating large levels of defects and adsorbates. Vacuum measurements are ongoing.

On the theory side, we have continued investigating the properties of plasmons in graphene and their dependence on such graphene parameters as doping level and concentration of defects. Specifically, K. Velizhanin has published a paper on the interaction of charge carrier with defects/adsorbates on graphene. An interaction of graphene plasmons with semiconductor quantum dots have been studied by us recently.

In particular, we have demonstrated the strong enhancement of resonance energy transfer between quantum dots in the presence of graphene as compared to the standard Forster resonance energy transfer. This finding might become of use in applications of hybrid graphene-based materials in photovoltaics. The theory paper on strong interaction of excitons in semiconductor nanostructures (e.g., quantum wells) and plasmons in graphene is currently in preparation.

Overall we feel that the progress within experimental and theoretical components of the project is very good. The recent additions of such capabilities to the project as successful CVD graphene growth, optical microscope/spectrometer and scanning tunneling microscope studies, as well as thorough theoretical analysis of efficiency of plasmon excitation and propagation in graphene put us well on our way to study, analyze and model plasmonic response of graphene-based devices.

Future Work

Both theoretical and experimental efforts during the next fiscal year will be focused on increasing the efficiency of plasmon propagation and plasmon excitation in graphene. The former task will incorporate the fabrication high-mobility graphene samples (using both chemical vapour deposition and exfoliation techniques). On the theory side, various mechanism of plasmon energy losses will by studied (e.g., defect scattering, phonons), so that the sample fabriction can be guided.

The latter task, i.e., efficient plasmon excitation in graphene, will involve theoretical (and, subsequently, experimental) design of defects in graphene in order to achieve the efficient coupling between laser beam and plasmons. Semiconductor quantum dots are easy to use in a laboratory, but they do not provide very efficient photon-plasmon coupling.

Our preliminary theoretical analysis shows that in-graphene voids (holes, tranches) can drastically increase the efficiency of this coupling. During the next year, theory will focus on accurate quantitative studies and optimization of plasmon excitation by in-graphene voids. Fabrication of graphene samples with incorporated voids (made by means of lithography or focused ion beam etching), optical characterization of such samples and observation of plasmon propagation in such structures will constitute the experimental efforts.

Conclusion

We expect to directly measure, for the first time, the critical parameters needed to describe the collective movement of electrons, i.e., plasmons, in graphene. We will also study the behavior of plasmons in graphene in the presence of controlled defects, such as nanoparticles, as well as under applied external electrical fields. We will use this knowledge to optimize predictive tools needed to theoretically describe plasmons in graphene. We expect that this predictive capability will allow us to design new graphene-based devices for practical applications that may lead to new break throughs in fields such as telecommuication, photovoltaics and sensing.

Publications

Solenov, D., and K. Velizhanin. Adsorbate Transport on Graphene by Electromigration. 2012. Phys. Rev. Lett.. 109

(9): 095504.

Velizhanin, K. A., and T. V. Shahbazyan. Long-range plasmon-assisted energy transfer over doped graphene. 2012. Phys. Rev. B. 86: 245432.

Velizhanin, K., and A. Efimov. Probing plasmons in graphene by resonance energy transfer. 2011. Phys. Rev. B. 84 (8): 085401.

Plasmon-exciton Interactions in Single-wall Carbon Nanotube – Metal Nanostructure Complexes

Han Htoon
20120330ER

Introduction

Single-wall carbon nanotubes (SWNTs), a graphene sheet rolled up to form a tube of ~1 nm in diameter and tens of microns in length, represent a nanoscale laboratory for exploring emerging quantum phenomena in an ideal one dimensional (1D) system. Intense research efforts focused on the optical properties of SWNTs in the past decade have revealed novel phenomena such as the Aharanov-Bohm effect, violation of the Condon approximation, and coherent exciton energy transfer. Here, aiming toward establishing a new branch in this very active research field, we propose to investigate the interaction of two different fundamental optical excitations, namely, 1D excitons of SWNTs (electron-hole pairs) and plasmons (collective excitations of charge density waves supported by metallic nanostructures). Although plasmon-exciton interactions has been investigated intensely in nanocrystals, quantum dots, molecules and quantum wells, so far very few studies have been conducted on SWNTs. This study possesses tremendous potential for revealing never before seen phenomena that lie at the interface of classical electrodynamics and quantum mechanics. The non-linear Fano effect (constructive and destructive interference of a narrow discrete resonance with a broad spectral line) and exciton induced transparency (an analog of electromagnetically induced transparency) represent two examples of the theoretically predicted phenomena we expect to encounter in this study. In addition, as this investigation is reaching into unexplored areas, we also expect the emergence of completely unpredicted phenomena.

Benefit to National Security Missions

The novel physical phenomena we aim to explore in this project will pave the way to tailor not only the spontaneous optical excitation and emission processes but also the coherent dynamical behaviors of SWNT-metal nanostructure complexes for applications ranging from bio/chemo sensing to quantum information processing. This project, therefore, directly addresses a LANL 2011 Material Grand Challenge, “Understanding and Control of Emergent Functionality Using Extrinsic Techniques.” Furthermore the SWNT-metal nanostructure complexes could also have potential to bring transformational breakthrough in light emitting as well as light harvesting applications. This project therefore addresses “Energy and Earth System” grand challenge, “Concepts and Materials for Clean Energy.

Progress

Fabrication of SWNT-metal nanostructure complexes

The team designed several metal-dielectric- metal (MDM) plasmonic cavity arrays with resonances aligned to the emission of SWNTs, and developed an e-beam lithography process for fabrication of these structures on transparent quartz substrates. We also successfully incorporated nanocrystal quantum dots into MDM cavities. Collaborations are ongoing with C-PCS to adapt this scheme for incorporation of polymer wrapped SWNT into MDM cavities. We expect to achieve SWNT-MDM coupled structures in a few months.

Acquisition of superconducting nanowire single photon detection system (SNSPD)

With the financial support of CINT, we are acquiring the SNSPD system capable of performing time tagged time correlated photon counting experiments on large diameter SWNT emitting at wavelengths beyond 1 μm (cost: ~180K). This instrument will allow us to investigate plasmon exciton interactions at 1.3 and 1.5 micron telecommunication wavelength regimes.

Studies of plasmon induced localization

A publication is underway to report on the observation of plasmon induced location of excitons in SWNTs coupled to the atomically smooth gold pyramids that is reported in the last year progress reports.

The team is also finishing up the preparation of two theoretical papers explaining this plasmon induced exciton localization effect.

Investigation of Plasmonic effects on exciton diffusion, recombination dynamics and photon emission statistics
The team is conducted PL imaging, time resolved PL and photon-correlation spectroscopy studies on individual stand-alone SWNT as well as SWNT-metal nanostructures complexes to understand the competing role of exciton diffusion and Auger Recombination in defining photon emission statistics of SWNTs. These studies revealed that (1) the efficiency of Auger recombination decreases with the increase of exciton diffusion length, (2) a strong photon anti-bunching can only be achieved in short SWNTs in which the exciton diffusion is limited by the non-radiative recombination at the end of the SWNTs and (3) coupling to a metallic nanostructure can lead to increase of multi-exciton emission. A model was successfully developed to describe the interplay of exciton-exciton Auger annihilation and one dimensional exciton diffusion to explain the first two findings. These results were presented at the APS March meeting in 2013 and WONTON.

A new single nanotube imaging microscope was assembled in the last year. The capability of the microscope was expanded to do simultaneous "two-color" imaging on InGaAs (For NIR emission) and EM-CCD (for visible emission) cameras with wide area or confocal excitation of nanotubes and to obtain single-tube and even single-site spectra along the length of an individual SWNT. Significant progresses were also made towards characterizing the emission characteristics of oxygen doped SWNTs. These will serve as a baseline for probing interaction of dopant optical behaviors with plasmonic structures. In particular, it will be interesting to compare spectral response of exciton localized at dopant sites with respect to that of exciton localized at plasmonic hotspots.

Future Work

Interactions of two different fundamental optical excitations often lead to the emergence of new phenomena that cannot be observed in neither of the original excitations. The interaction between the optical excitation of a quantum emitter (exciton) and a propagating excitation of charge density waves on the surface of a conductor (plasmon), represents one such instance. Phenomena that lie at the interface of classical electrodynamics and quantum mechanics such as enhancement of emission rates and exciton Rabi splitting have emerged in the study of this interaction in variety of nanostructures. In addition to being important for fundamental reason, these phenomena exhibit tremendous potential for technological applications ranging from solid state lighting to quantum communication as they provide handles to manipulate not only spontaneous emission rates but also quantum coherent dynamics and photon emission statistics.

So far very few studies on plasmon-exciton interaction have been conducted on single walled carbon nanotubes (SWNTs). Because of the SWNT's unique one dimensional electronic structure, the manifestation of this interaction is bound to be different at the fundamental level and therefore holds great potential for the emergence of unexpected phenomena. To this end here we propose to investigate plasmon-exciton interactions in high quality, well-defined SWNTs. In this study, we will first develop two novel approaches- plasmon induced trapping and chemical assembly- to controllably couple SWNTs to variety of metallic nanostructures. We will then apply a suite of advance single nanostructure optical spectroscopy approaches to explore the effect of plasmon on diffusion localization and recombination dynamic of 1D excitons. In addition we will also exploit the strong transition dipole moments of SWNT's 1D exciton to explore phenomena of strong interaction regimes such as nonlinear Fano effect and exciton induced transparency. We will also apply hybrid quantum-mechanical-semiclassical approaches to model the exciton-plasmon dynamic in 1 D systems.

Conclusion

Through this project, we expect to attain the capability to manipulate various aspects of light-SWNT interactions that hold the key to the realization of a variety of technological applications. Specifically we expect to attain the capability to tailor both spontaneous optical excitation and emission processes. This capability will bring transformational breakthroughs in the utilization of SWNTs in photonic, chemo/bio sensing and light-harvesting applications. Furthermore, this study is also expected to shed new light on the manipulation of coherent dynamics and photon emission statistics of SWNTs and lay the foundation for their applications in quantum information processing and communication applications.

Publications

Cherqui, C.. Plasmon assisted polaron effects in carbon nanotubes. Student Award Presentation . Invited presentation at TSRC Workshop on Nanomaterials: Theory and Computation. (Telluride, July 16-20, 2012).

Cherqui, C., D. H. Dunlap, and A. Piryatinski. Diffusion of Plasmon-Exciton Polaron. Presented at APS March Meeting. (Boston, Feg 27- March 2, 2012).

Crochet, J. J.. Exciton transport and manipulation in colloidal semiconducting carbon nanotubes. Invited pre-

sentation at 5th Workshop on Nanotube Optics and Nanospectroscopy. (Santa Fe, 16-20 June, 2013).

Doorn, S. K.. Surface Chemistry of Carbon Nanotubes: Photoluminescence Probes at the Ensemble, Single-Tube, and Single-Site Levels. Invited presentation at Telluride Science Research Center Workshop on The Chemistry and Physics of Defects in Carbon Nanotubes. (Telluride, CO, 8-12 July, 2013).

Doorn, S. K.. Exciton transport and manipulation in colloidal semiconducting carbon nanotubes. Invited presentation at 223rd Electrochemical Society Meeting. (Toronto, Canada, 12-16 May, 2013).

Doorn, S. K.. Surface chemistry of carbon nanotubes: Enabling novel composite materials and studies of dopant chemistry at the 1-D interface. Invited presentation at Lehigh University, Physics Colloquium. (Lehigh University, 3 Oct, 2013).

Ma, X., J. G. Duque, J. J. Crochet, S. K. Doorn, and H. Htoon. Photon Statistics of Single Carbon Nanotubes at Room Temperature. 2013. In American Physical Society, March Meeting, . (Blatimore, MD, 18-22 March, 2013). Vol. 58, p. 1. Baltimore, MD: American Physical Society.

Ma, X., J. G. Duque, J. J. Crochet, S. K. Doorn, and H. Htoon. Influences of exciton diffusion and exciton-exciton annihilation on photon emission statistics of carbon nanotubes. Presented at 5th Workshop on Nanotube Optics and Nanospectroscopy. (Santa Fe, June 16-20).

Piryantinski, A.. Localized Surface-Plasmon Effect on Exciton Transport and Radiative Properties in 1D Nanostructures. Invited presentation at TSRC Workshop on Nonequilibrium Phenomena, Nonadiabatic Dynamics and Spectroscopy. (Telluride, CO, 21-25 July, 2013).

Piryantinski, A.. Surface-Plasmon Assisted Charge Carrier and Exciton Transport in 1D Nanostructures. Invited presentation at Seminar, Department of Physics, University of Wyoming. (Laramine, 26 April, 2013).

Piryantinski, A., C. Chirque, and D. Dunlap. Surface-Plasmon Assisted Charge Carrier and Exciton Transport in 1D Nanostructures. Presented at 5th Workshop on Nanotube Optics and Nanospectroscopy. (Santa Fe, 16-20 June, 2013).

Piryatinsko, A.. Surface-Plasmon Assisted Charge Carrier and Exciton Transport in 1D Nanostructures. Invited presentation at TSRC Workshop on Nanomaterials: Theory and Computation . (Telluride, 16-20 July, 2012).

Novel Inverted Nanoshells for Multimodal Diagnostic Imaging and Cancer Therapy

Jennifer A. Hollingsworth
20120365ER

Introduction

The overarching goal is to design and implement a new nanoparticle-based platform for combined multimodal imaging and cancer therapy. The approach is to encapsulate within a metal shell a semiconductor and/or lanthanide (Ln)-comprising core that affords both fluorescence and magnetic resonance (MR) contrast capabilities. The metal shell also serves dual duty, simultaneously enhancing fluorescence originating in the core and generating heat upon optical activation for photothermal cancer therapy. In contrast with other nanoparticle-based approaches that aim to couple diagnostics with therapy, this approach affords greater simplicity, smaller/tunable particle sizes, enhanced optical performance, and biocompatibility. Our design strategy is guided by modeling studies, which revealed the transformative potential of "inverted" nanoshell (INS) structures for enhancing a fluorophore's emission. The inverted geometry places the emitter at the center of a metal shell, where the optical intensity enhancement is strong and uniform. In contrast, the field enhancement outside a metal shell structure, though very large at the surface of the metal, drops off quickly and non-uniformly with distance from the metal. Here, we take advantage of the internal field enhancements by placing our fluorophores on the inside of a metal nanoshell, advancing the state-of-the-art in fluorophore probe design, while at the same time combining this concept with an additional imaging functionality (MR) and a therapy functionality (photothermal). We will demonstrate proof-of-concept deep-tissue imaging and selective hyperthermal cancer-cell ablation using peptide-INS conjugates.

Benefit to National Security Missions

In addressing our overarching goal to develop and test novel inverted nanoshell nanoparticles for coupled multimodal imaging and photothermal cancer therapy, we will concurrently build new capabilities in optical nanomaterials and advanced imaging in complex media (ensemble to single-particle, static to real-time), significantly improve our understanding of interactions at the nano-bio interface, and provide proof-of-concept for a new approach to realizing simultaneous imaging/therapy.

Combined, this agenda advances basic understanding of materials and basic health research at a nationally competitive level. It capitalizes on, advances, and unifies three LANL technologies: patented giant quantum dots, patented 3D particle tracking, and human tissue models. The work will be of strong interest to DOE Office of Science with respect to new optical materials design/development, with applications beyond biosciences to efficient lighting, light-based communications technologies, low-threshold lasing, single-photon sources for quantum cryptography, etc., as they incorporate additional functionality, while solving the remaining outstanding flaws of more conventional emitters. It will also be directly relevant to the needs of DHHS agencies, even beyond the direct goal of advancing nanoparticles for combined imaging/therapy, where predicting and controlling nanoparticle mediated activity at the molecular, cellular and tissue levels has implications for a range of future applications from nano-enabled bio/chem-sensors to non-invasive drug delivery and "battle suit medicine." Also along these lines, the new dual-purpose nanomaterials developed here can find implementation beyond cancer, e.g., in the targeted treatment of non-cancerous diseased tissue.

Progress

INS synthesis

While silica (SiO_2) shell growth onto giant quantum dot (gQD) emitters has proven successful for a range of SiO_2 thicknesses (10 nm initially and more recently 13, 15, and 20 nm), successful addition of the targeted gold (Au) shell has been more elusive. We define success as the ability to apply a uniform/thin Au shell to all

nanoparticles without emitter quenching. We continue to work out the required chemistry for controlled Au shell growth onto these relatively large gQD/SiO2 nanocrystals, but of primary concern is the tendency of the Au reduction step to afford nearly complete suppression of emission even without complete Au shell coverage on the nanocrystals. Extensive characterization by transmission electron microscopy (TEM) at different stages of Au reduction and growth has allowed us to confirm that the source of gQD quenching is attachment of Au ions at the gQD surface and nucleation of Au nanoparticles directly onto the gQD. The ability of the Au ions to penetrate the SiO2 shell likely results from the porosity of this amorphous layer, as indicated by recent literature suggesting that the SiO2 is porous to ions/small molecules. We have attempted several approaches to limit/prevent the transport of Au ions to the gQD surface: (1) "seal" the SiO2 against ion penetration by (a) addition/optimization of multiple layers of polyelectrolyte – recent improvements affording highly charged/stable layers (zeta potential ~±40) or (b) growth of a crystalline oxide (ZnGa2O4) onto the gQD surface (completed–awaiting characterization) or onto the SiO2 surface, and (2) increase the SiO2 thickness (>10 nm). The latter approach combined with highly ionic polyelectrolyte coverage has recently afforded Au-coated gQDs that retain much of their emission despite exhibiting almost exclusively Au-absorption features. We are awaiting TEM analysis to confirm the structure affording this very promising result.

Spectroscopic evaluations

We have quantified brightness per particle (BPP) using fluorescence correlation spectroscopy (FCS) and developed BPP curves as a function of laser power for four different laser sources. The lasers thus far investigated include 405 and 470 nm pulsed, and 488 and 532 nm continuous wave (CW). The tracking studies discussed below were primarily obtained using a 470 nm pulsed laser, with laser power optimized to achieve maximum BPP. It was subsequently determined that by using a CW source we could avoid QD saturation, allowing continuously increasing QD BPPs with increasing laser power, even for the 532 nm CW source despite the minimal gQD absorption cross-section at this wavelength. Using CW sources, we expect to further improve the already dramatically increased tracking times (below), and, significantly, use of "redder" 532-nm source will reduce background emission/unintended cell damage.

Cell targeting/tissue mimics

Focusing on peptide-conjugation chemistry, the gQDs were functionalized with bis(DHLA)-PEG-COOH ligands (provided by NRL colleagues). Carboxyl termination was used to facilitate 1-Ethyl-3-(3-dimethylaminopropyl)carbodiimide (EDC)-mediated coupling (semi-stable amine-reactive N-hydroxysuccinimide ester intermediate) to Neutravidin. Gels confirmed gQD-Neutravidin coupling (1% agarose gel, 120 V, 60 min). Following conjugation to the cell-targeting agent, cell-binding specificity was determined – targeted-to-untargeted ratio of 4-to-1. With this level of specificity, we were able to conduct extensive 3D particle-tracking/cell-association experiments, obtaining many 10's of successful tracks affording an average tracking duration 20-fold higher than commercial QDs, dramatically improving our chances for successfully observing QD (or INS)-cell interactions. To further improve cell targeting, we are improving our conjugation chemistry for enhanced cell specificity (to equal commercial QDs' ~10-to-1), replacing Neutravidin with Streptavidin (promising: significantly improved gel-filtration chromatograms).

We have also made progress in developing suitable cell-matrix composites that afford sufficiently low viscosity to observe QD mobility combined with retention of good cell growth. Specifically, we have evaluated the penetration efficiency of our gQDs (INS surrogates) through decreasing concentrations of matrigel: 9.5 - 3 ng/mL, finding lower concentrations (3 – 5 ng/mL) to be more favorable for gQD penetration. 3T3 cells were grown in the optimal matrigel suspension, and gQDs evaluated for penetration-efficiency and non-specific binding/phagocytosis by cells. We are currently assessing non-specific gQD-cell binding in this environment and will proceed with specific-binding experiments. gQDs were evaluated for cytotoxicity and found to be non-cytotoxic in the relevant concentration range – important for distinguishing future "intentional" cell toxicity.

Future Work

Guided by theory/optical-spectroscopy characterizations, we will synthesize and study enhancement and/or damping effects as a function of core size, spacer-layer thickness, and metal-shell thickness toward optimized structures. As the emitting "core" material, we will utilize two types of nanocrystals: our unique "giant" (g-QDs) (focus to date) and either lanthanide or manganese-doped QDs. We now have two g-QDs to explore: CdSe/CdS g-QDs that can be tuned to emit in the far-red and InP/CdS g-QDs that emit in the near-infrared. Both are appropriate wavelengths for deep-tissue imaging. Time permitting, we will incorporate a paramagnetic material to add MR-imaging functionality.

To assess the significance of any ensemble-level absorption/emission enhancements observed in Task 1 for deep-tissue fluorescence imaging, we aim to obtain 1 and 2-photon action cross sections for individual particles using fluorescence correlation spectroscopy (FCS) and time-correlated single-photon counting (TCSPC) measurements, where "action" cross sections effectively include

both quantum yield and absorption characteristics of the material, which are both critical for effective detection through distance (i.e., a biological tissue). In all cases, we will compare the action-cross-sections for both the emitting core and the INS form. The most promising candidates will be incorporated into "tissue mimics" to investigate imaging in a more realistic environment (tissue complexity will be tuned) and as a function of depth/imaging mode (1- or 2-photon).

Toward our goal to establish proof-of-concept cancer-cell targeting/photothermal therapy, we have worked out the required peptide conjugation chemistry that will enable the INS to selectively target and eliminate cancer cells in a matrix of normal cells. We now aim to establish this capability for mixtures of cancerous and normal cells embedded in a collagen-matrix (co-culture tissue-like matrix), then transitioning to re-constructed cancerous tissue.

Conclusion

We anticipate three advances impacting both basic and applied biosciences. First, we will establish materials-design principles for advanced multimodal-imaging/therapy nanoparticles. The approach is flexible and can be applied to different imaging agents, e.g., as new, "greener" NQDs are developed, these can be incorporated into the design motif, or different MR contrast agents could be use. We will establish a dual-imaging capability for deep-tissue studies, including a novel capability for real-time tracking of nanoparticle-based cell targeting. Lastly, we will establish the materials and photoactivation requirements for selective cancer cell hyperthermal ablation that is applicable to multiple cancer types and other diseases.

Publications

Hollingsworth, J. A.. Heterostructured Quantum Dots: From Molecular Probes Toward Cancer Therapy. Invited presentation at Nanoparticle Synthesis and Applications Cancer Imaging and Treatment Symposium . (University of New Mexico, Albuquerque, 16 Aug. 2013).

Hollingsworth, J. A., J. H. Werner, H. Htoon, A. Piryatinski, R. Schaller, Y. Ghosh, A. M. Dennis, A. M. Keller, B. Mangum, and D. C. Hannah. Non-blinking "giant" quantum dots: Ideal probes for real-time three-dimensional tracking. 2013. In CLEO:2013. (San Jose, CA, 9-14 June 2013). Vol. CLEO:QELS Fundamental Sci, p. Biophotonics (QTu1P). OSA Optics InfoBase: The Optical Society.

Hollingsworth, J. A., J. Werner, R. Iyer, N. Karan, A. Keller, A. Nagy, Y. Ghosh, and J. L. Casson. Novel inverted nanoshells for multimodal diagnostic imaging and cancer therapy. Invited presentation at Los Alamos National Laboratory Laboratory Directed Research and Development Day. (Santa Fe, October 23, 2012).

Keller, A. M., Y. Ghosh, M. E. Phipps, D. S. Lidke, B. S. Wilson, J. A. Hollingsworth, and J. H. Werner. 3-dimensional tracking of blinking-suppressed quantum dots in live cells. 2013. In Biophysical Society 57th Annual Meeting. (Philadelphia , February 2-6, 2013). , p. 1. Conference Abstracts: Biophysical Society.

Keller, A. M., Y. Ghosh, M. S. DeVore, M. E. Phipps, M. H. Stewart, D. S. Lidke, B. S. Wilson, J. A. Hollingsworth, and J. H. Werner. 3-Dimensional Tracking of Non-blinking 'Giant' Quantum Dots in Live Cells. Nature Nanotechnology.

Park, Y. S., Y. Ghosh, P. Xu, N. H. Mack, H. L. Wang, J. A. Hollingsworth, and H. Htoon. Single-nanocrystal photoluminescence spectroscopy studies of plasmon-multiexciton interactions at low temperature. 2013. The Journal of Physical Chemistry Letters. 4: 1465.

Forensic Archaeology of a Manhattan Project Era Nuclear Site

Warren J. Oldham
20120459ER

Introduction

The goal of this research is to develop accurate and precise methods for characterizing nuclear sites, including those that have undergone demolition and decontamination efforts intended to mask nuclear proliferation activity. This will be achieved by reconstructing the weapons production activities that occurred during the historic Manhattan Project at the plutonium processing facility previously located near Ashley Pond in downtown Los Alamos. This represents a significant experimental challenge since environmental samples collected near this location inevitably contain mixtures of plutonium that originate from a variety sources and were deposited at various times between 1944 and 2011. We propose here to make use of this unique site to develop a systematic approach for reconstructing nuclear process activities, even when complicated isotopic compositions exist. Specific scientific goals include: Developing methods for identifying trace levels of radionuclides that are associated single source terms in areas where large regional contributions of actinides and fission products are present. Demonstrating for the first time that relationships exist between actinides and stable isotopes that contain unique insight associated with process history and intent of the nuclear material. Conducting carefully designed experiments that advance current methods for age dating and accounting for global fallout contributions to radioanalytical measurements.

Benefit to National Security Missions

Analytical methods that enhance the detection and isotopic characterization of trace-level plutonium in the environment support LANL's core mission in nuclear nonproliferation and treaty verification. In the future the laboratory may be tasked with monitoring compliance with additional international agreements including the Fissile Materials Cut-off Treaty and the Comprehensive Test Ban Treaty. The analytical and evaluation techniques pioneered in this research will provide a technical foundation to position the laboratory as a credible national resource to support these expanded program requirements.

Progress

The ubiquitous and persistent background resulting from fallout during the era of atmospheric nuclear testing complicates analytical detection of low-level emissions resulting from modern nuclear activities. This project aims to develop a novel sampling and analysis strategy to distinguish local signatures from global fallout based on improved understanding of actinide geochemistry and environmental behavior. Our work has shown that rusty metal adsorbs trace actinides in the environment through natural weathering processes to facilitate ultra-low plutonium detection using a simple and robust analytical method. We hypothesized that if industrial effluents are more easily mobilized than global fallout, then analysis of the surface oxide coating of discarded metal objects could reveal a local source-term of interest.

During FY13 this idea was directly tested using a "case study" approach focused on the former site of original Manhattan Project Era laboratories near Ashley Pond. This site included the world's first plutonium processing and fabrication facility that operated in support of the war effort from 1943 to 1945. Although this area was ultimately remediated for unrestricted public access, we suspected that the ultra-sensitive nature of the iron-oxide adsorption process might be used to detect faint plutonium signatures from the Manhattan Project. We've now shown that rusty bottle caps (contemporary origin) collected within the boundaries of the former TA-1 site, reveal ultra-low $^{240}Pu/^{239}Pu$ atom ratios representing Pu from the earliest years of the U.S. nuclear weapons program. Although local sample concentrations were not appreciably elevated compared to regional background examples, isotopic measurements ($^{240}Pu/^{239}Pu$) for TA-1

samples varied from 0.0036 to 0.050 compared to 0.168 ± 0.012 for regional collections. The results of this study suggest that the novel surface oxide sampling strategy can be used to selectively identify local nuclear signatures even when only trace-level contamination is present. The work was presented at the most recent LDRD Day at Buffalo Thunder Casino and formed the basis of a PADSTE Science Highlight (2-20-2013). The work was also a featured highlight on the LDRD Homepage.

The results of the "rusty bottle cap" study have changed our thinking about what is central to faint signature detection. We believe that relative mobility is the key concept for environmental monitoring efforts. Our work suggests that the chemical form of industrial contaminants compared to nuclear fallout will ultimately control relative environmental mobility. To rigorously test this idea, we aim to conduct careful laboratory based experiments comparing aqueous mobility of plutonium contained within these two distinct sample types. While well-characterized standard reference materials containing industrial contamination are available from NIST (e.g. SRM 4353 Rocky Flats Soil), analogous nuclear fallout standards are not readily available. To solve this problem, we have identified SRM 1648a (Urban Particulate) as a new, previously unrecognized source of atmospheric fallout from nuclear weapons testing. The material was originally collected by NIST using an industrial scale baghouse during 1976 and 1977 in St. Louis, MO and inadvertently contains significant concentration of nuclear fallout from Chinese and French nuclear tests. Plutonium and americium concentrations as well as isotopic compositions were determined during FY13. These measurements will form the basis for comparisons with natural matrix standards containing plutonium contamination derived from industrial releases. The analytical study of SRM 1648a was presented at the American Chemical Society meeting in New Orleans, LA within a dedicated session on Nuclear Forensics.

Developing methods for quantitatively evaluating long-lived lanthanide fission products, i.e. ^{151}Sm and ^{155}Eu, from environmental samples offers opportunity to advance theories regarding the fate-and-transport of electropositive and radioactive metals in environmental systems. While this method can be applied in analysis of nuclear waste and assessment of environmental contamination sites, its application toward nuclear forensics is of particular importance given that ^{151}Sm and ^{155}Eu ($t_{½}$ = 90 and 4.75 y, respectively) can be used to assess fission events that happened long ago. Over the last two years we have developed a chemical purification process that provided highly pure lanthanide concentrates from which individual fractions of ^{151}Sm and ^{155}Eu were isolated in high yield and excellent purity using high performance liquid chromatography. The ^{151}Sm and ^{155}Eu analytes were quantified using liquid scintillation counting and γ-spectroscopy, respectfully. Overall, the procedure represents a robust and accurate method for evaluating abundances of ^{151}Sm and ^{155}Eu in environmental samples.

Future Work

This project aims to develop novel analytical methods to improve detection and interpretation of signatures associated with nuclear activities. The effort is proceeding along three main thrust areas: (1) Trace-level measurements of actinides in the environment associated with discarded rusty iron relics (e.g. nails, bottle caps, etc.). During FY14 measurements of Am-241 and Np-237 compared to Pu-239 and Pu-240 in collections of this type will be completed to determine relative environmental mobility of the different actinide elements. The presence of these anthropogenic radionuclides within the surface oxide coating of rusty artifacts implies aqueous transport from the local environment. The relative concentrations and isotopics measured for rusty metal samples will be compared with adjacent soils to characterize relative mobility, (2) Radioanalytical measurement of Sm-151, combined with Pu isotopics, is being developed to correct for global fallout in mixed samples that also contain a local signature of interest. During FY14, we will validate the radioanalytical methods developed in FY12/13 to measure Sm-151. A significant challenge will be measurement of trace Sm-151 derived from nuclear fallout contained within SRM 1648A. (3) A new capability to simultaneously measure Np-237 and Pu is being developed. During FY14 we will measure the relative ratio of Np-237 and Pu-239 contained in samples collected from TA-18, which formerly contained various critical assemblies used in weapons development work. During the time that these machines were operated, U-238 underwent neutron capture reactions to simultaneously form U-237 and U-239. Today these short-lived isotopes will be detectable as Np-237 and Pu-239, respectively. The relative ratio of these analytes could provide forensic information on the nature of the original activities that were conducted at TA-18.

Conclusion

The research will (1) develop methods for distinguishing trace levels of radionuclides that are associated with nuclear operations from regional and global backgrounds, (2) identify signatures and observables between radionuclide and stable element emissions, and (3) validate methods for identifying proliferation activity in the face of active deception.

Publications

Oldham, W. J., B. S. Matteson, J. L. Miller, C. T. Lake, and M. Attrep. Rusty nails adsorb trace plutonium from the environment. 2013. JOURNAL OF RADIOANALYTICAL AND NUCLEAR CHEMISTRY. 296 (2): 889.

Exploiting Metal/Organic Interfaces as Potential Bulk Heterojuntions: Unlocking the Efficiency of Organic Photovoltaics

Hsing-Lin Wang
20120464ER

Introduction

In this project, we adopt an unorthodox approach to develop organic photovoltaic devices with improved efficiency and reproducibility. We will focus our efforts on the following:

- Developing a unique donor-acceptor interface, bulk heterojunction (BHJ), using nanoporous metals to improve charge separation and collection efficiency. We will synthesized nanoporous metal with control pore size ranges from 10-50 nm, matching the exciton diffusion length in the polymer systems, ~ 5-15 nm, thus ensuring minimal exciton diffusion losses.
- Surface functionalization of nanoporous metals by covalently attaching electron acceptors onto the metal surface, allowing instaneous electron transfer and collection on the metal electrode. This novel approach to the best of our knowledge has never attempted by any other research group.
- Enhancing light absorption by increasing light trapping within the active polymer, as well as synthesizing novel low-band gap polymers with absorption that covers the solar emission from UV to near IR. We plan to develop synthesis of conjugated polymers with low band gap molecules in the backbone structures, and pentathiophene as side chains. Our design entails extension of polymer absorption to encompass the spectra of UV, visible, and near infrared lights, allowing overlaps portions of the solar emission that were previously inaccessible.
- Enhancing hole-transport by design synthesis of conjugated polymer thin films with improved crystallinity. We will extend our synthesis to a variety of semi-rigid side chain structures that are likely to couple with each other and form highly ordered crystalline thin films. Higher crystallinity leads to higher carrier mobility, minimize the possibility of exciton recombination.

Combining the above approach allows solving critical issues that hampering efficiencies of organic photovoltaic devices.

Benefit to National Security Missions

This research allows better understanding of fundamental mechanisms for self-assembly and a viable approach to fabricating nano-assemblies with complex structures and functionality. The proposed study addresses fundamental challenges at the interface between chemistry, materials, and nanotechnology. Success will have widespread impact on the fabrication of photovoltaic devices. The proposed work will strengthen our capability in addressing laboratory missions, particularly in the areas of materials development and energy security. Understanding the underpinning mechanism that dominate charge separation and charge collection efficiencies will form the foundation for developing next generation solar cells with unprecedented high efficiency and support new program development in Office of Science and DARPA.

Progress

Our goals in this project are (a) enhance light absorption due to increased light scattering pathways from the porous metal into the active later and by synthesizing novel low-band gap polymers (b) enhancing light absorption by synthesizing novel low-band gap polymers and by increasing the thickness of organic film and (c) enhancing hole-transport characteristics by synthesizing crystalline polymers. We have made significant progress in all fronts of the project.

Polymer synthesis

For the past three 12 months, we have demonstrated synthesis and characterization of a series of two dimensional polythiophene-based conjugated polymers; alternative copolymers consist of benzo[1,2-b:3,4-b] bithiophene-bithiophene (donor-donor) and benzo[1,2-b:3,4-b]bithiophene-benzothiadiazle (donor-acceptor) as

building blocks for the conjugated polymer main chain. We observe a 0.4 eV difference for the band gap and LUMO level between the donor-acceptor and donor-donor type polymers; however, the HOMO level for the two polymers remained unchanged (~ -5.4 eV), suggesting that the HOMO level was essentially dominated by the benzo[1,2-b:3,4-b]dithiophene (BDT) moieties and the LUMO level and band gap are determined by the nature of the co-monomer. Overall, these 2-D conjugated polymers integrating low band gap molecules in the backbone structures, and oligothiophene as side chains. Such design entails extension of polymer absorption to encompass the spectra of UV, visible, and near infrared lights, allowing overlaps portions of the solar emission that were previously inaccessible.

Fabrication of porous electrodes

We have focused our effort to synthesize nanoporous metal based photovoltaics.

We have synthesized various nanoporous metals including Au, Ag, Ni, and Ti. Nanoporous gold have high work function of 5 eV and small pore size (5-20 nm), therefore resulting in low efficiency. We have recently synthesized nanoporous Titanium by dealloying a Ti/Al alloy. Nanoporous Ti have bigger pore size (60-100 nm) and a low work function of 4.1 eV. Organic polymers easily infiltrate into the pores and the nanoporous Ti acts as a superior electron acceptor. Initial photovoltaics were prepared using a standard donor/acceptor pair e.g. P3HT and PCBM. Initial results reveal that Nanoporous Ti based solar cells have better performance than planar Ti. However these cells exhibit low shunt resistance, which leads to shorting of devices. Nanoporous Titanium (have been reported for first time) will have numerous other applications including Dye sensitized solar cells. We are currently focusing our efforts on optimization of nanoporous based photovoltaics by (a) depositing an oxide layer to prevent shorting (b) lowering the work function of materials.

OPV devices

We then use these polymers to fabricate organic photovoltaic (OPV) devices. The device structure comprise of multilayered ITO as transparent electrode, MoO3 is the hole transporting layer, polythiophene derivative and C60 mixture as electron donor and acceptor, and Ca/Al as another electrode. Polymer solar cells are fabricated using alternating copolymers blended with Phenyl-C71-butyric acid methyl ester (PC71BM) to form donor (D) /acceptor (A) bulk-heterojunction. Our polymers with low band gap and high degree of crystallinity are used for initial optimization. We spun cast polymer/PC71BM blend solution in high boiling point 1,2-dichlorobenzene (oDCB) to achieve an optimized film morphology. The D/A weight ratio was tuned from 1:0.5 up to 1:3.0 to find the optimized composition for efficient charge separation and transportation. As a result, the best performing device (D:A=1:1.5) showed an average power conversion efficiency (PCE) around 3.30% and peak PCE~3.68% with open circuit voltage (Voc)~0.804V short circuit current density (Jsc)~7.24 mA/cm2, fill factor~62.0%. Another polymer system processed under the same condition reveals a superior PCE~4.25%, which is due to the high degree of crystallization as manifested by the UV-Vis absorption spectrum of polymer solutions. Of particular importance is the enhanced absorbance peak at ~600 nm which implies the increase in chain packing and crystallinity. The temperature-dependent photoluminescence spectra show a gradual decrease of the emission peak at 620nm, further validate the crystalline nature of the polymer.

Future Work

- We will perform synthesis and characterization of polythiophene derivatives with optimum absorption that covers wavelength from 300-800 nm.
- Preparation of different Nanoporous Metals including Titanium, Aluminum and Silver that have lower work function with appropriate pore size.
- Infiltrate them with functionalized C-60 using vapor deposition and solution-based techniques.
- Demonstrate a functional OPV

Conclusion

We expect to demonstrate fabrication of bulk heterojunctions (BHJs) with extremely high surface area, controlled pore size and morphology to maximize charge separation and collection efficiencies. Success of this work will allow development of next generation OPV devices with high efficiencies that rival the mono- and polycrystalline Si panels with efficiency ranges from 12-18%. Significantly lower the price for manufacturing and installation, meanwhile reduce the unit price of solar power. This will significantly shorten the time frame originally set by the DOE SunShot Initiative to achieve cost competitive solar energy by 2020.

Publications

Kang, L. L., P. Xu, B. Zhang, H. H. Tsai, X. J. Han, and H. L. Wang. Laser wavelength- and power-dependent plasmon-driven chemical reactions monitored using single particle surface enhanced Raman spectroscopy. 2013. CHEMICAL COMMUNICATIONS. 49 (33): 3389.

Kuo, C. Y., Y. C. Huang, C. Y. Hsiow, Y. W. Yang, C. I. Huang, S. P. Rwei, H. L. Wang, and L. Wang. Effect Side-Chain Architecture on the Optical and Crystalline Properties of

Two-Dimensional Polythiophenes. 2013. MACROMOLECULES. 46 (15): 5985.

Li, Q., P. Xu, B. Zhang, G. Wu, H. T. Zhao, E. G. Fu, and H. L. Wang. Self-supported Pt nanoclusters via galvanic replacement from Cu2O nanocubes as efficient electrocatalysts. 2013. NANOSCALE. 5 (16): 7397.

Park, Y. I., B. Q. Zhang, C. Y. Kuo, J. S. Martinez, J. Park, S. Mallapragada, and H. L. Wang. Stimuli-Responsive Poly-N-isopropylacrylarnide: Phenylene Vinylene Oligomer Conjugate. 2013. JOURNAL OF PHYSICAL CHEMISTRY C. 117 (15): 7757.

Park, Y. S., Y. F. Chen, Y. Ghosh, A. Pirytinski, P. Xu, N. H. Mack, H. L. Wang, V. I. Klimov, J. A. Hollingsworth, and H. Htoon. Strong Photon Bunching in Individual Nanocrystal Quantum Dots Coupled to Rough Silver Film. 2012. In 2012 CONFERENCE ON LASERS AND ELECTRO-OPTICS (CLEO). , p. -.

Park, Y. S., Y. Ghosh, Y. Chen, A. Piryatinski, P. Xu, N. H. Mack, H. L. Wang, V. I. Klimov, J. A. Hollingsworth, and H. Htoon. Super-Poissonian Statistics of Photon Emission from Single CdSe-CdS Core-Shell Nanocrystals Coupled to Metal Nanostructures. 2013. PHYSICAL REVIEW LETTERS. 110 (11): -.

Sasaki, D. Y., N. Zawada, S. F. Gilmore, P. Narasimmaraj, M. A. A. Sanchez, J. C. Stachowiak, C. C. Hayden, H. L. Wang, A. N. Parikh, and A. P. Shreve. Lipid Membrane Domains for the Selective Adsorption and Surface Patterning of Conjugated Polyelectrolytes. 2013. LANGMUIR. 29 (17): 5214.

3-Dimensional Characterization of Nuclear Fuels: Microstructural Evolution under Representative Temperature and Thermal Gradients

Donald W. Brown
20130232ER

Introduction

Recently, interest in nuclear energy in the Unites States has surged with increased efforts to extend the lifetime of the current fleet of reactors and to develop advanced reactors which operate at higher temperatures and use fuel to higher burn-up. Safety margins and predictions of the engineering performance of nuclear reactor fuel rely on modeling codes used to predict dimensional change, stress state and fission gas release as a function of burn-up and temperature history. Thermal conductivity is the single most important material parameter in these codes and is heavily dependent on microstructure e.g. grain morphology, porosity, etc. To date, empirical and phenomenological descriptions of the evolution of the microstructure of fuel materials are used to calculate the thermal conductivity, but this leaves huge uncertainties and necessarily results in large safety margins and inherently inefficient use of resources as well as increased production of waste.

The goal of the proposed research is to advance the understanding of the microstructural evolution of nuclear fuel materials under conditions simulating those perceived during manufacture and in-pile. Specifically, we will monitor grain morphology, pore migration, chemical segregation, and fission gas transport in nuclear fuels under processing temperatures (~1650ºC) and under service conditions (themal gradient of 1000ºC/5mm). Toward this end, we will develop high energy synchrotron x-ray techniques for characterization of fuel under representative temperature conditions. These techniques provide a non-destructive means to monitor the evolution of fuel microstructure under representative conditions. The results will be used by researchers across the nation working on multi-length scale modeling of ceramic nuclear fuels.

Benefit to National Security Missions

The work is directly relevant to DOE NE (nuclear energy) in that it provides data that will be used to validate computational models which are currently being developed as part of DOE NE. It will advance the field of ceramic nuclear fuels specifically, and ceramics in general. The development of the technique is directly relevant to the Materials and Radiation Interaction in Extremes (MaRIE) project in that one would imagine every sample run in the multi-probe diagnostic hall (MPDF) first being characterized with the high energy diffraction microscopy (HEDM) developed herein. This technique development is particularly relevant to the nuclear stockpile mission in that it will focus on specific advances necessary to study high-Z number materials with x-ray diffraction and tomography.

Progress

In FY13 we wrote proposals for and were awarded two rounds of beamtime on beamline 1-ID at the Advanced Photon Source (APS) to complete High energy diffraction microscopy on ceramic uranium dioxide (UO2) and metallic uranium (U) samples. The experiments were run in October of 13 and April of 14. Another proposal will be submitted to the APS for the July 8th deadline. Also, we wrote a proposal and received beamtime for tomographic studies of sintered UO2 samples on beamline 10BM at the APS. Finally, we have prepared and submitted a proposal for Small Angle Neutron Scattering beamtime. (HEDM) experiments on 1ID on UO2+x pellets with varying O content and, in a burgeoning collaboration with Idaho National Lab, metallic U foils were examined. Near field measurements, which map grains by orientation were completed on three samples with different O content (2 off stoiciometric) and 2 metallic uranium foil samples. Simultaneously, we completed tomography on the same samples. Finally, looking forward to in-situ measurements, far field measurements, which can determine orientation and strain in grains, were also completed.

Analysis of the HEDM data has lagged because we have struggled to hire the postdoc/student for this work and to get a contract in place with Livermore, who has the analysis capability in house. The data has been examined to the point that we are sure the analysis can be completed. A new postdoc has accepted the position and will start July 15th. The contract with Livermore is now in place. This will allow analysis of the HEDM data to commence.

Preliminary analysis of the tomography data has been completed and is very promising. By including LANL in-house expertise (James Hunter) and aggressively pursuing real time data analysis, we were able to improve upon the optimization of the instrument setup. It appears we have achieved sub-micron resolution on both UO2 and metallic U samples.

The tomographic experiments on sintered and quenched UO2 cylinders have been completed and analysis is advanced. We are currently preparing a manuscript including this data and previous tomographic measurements supported by earlier LDRD projects. The title will be approximately: "The Use of High Energy Xray Tomography to Characterize Porosity in Ceramic Uranium Dioxide Nuclear Fuel."

Don Brown (PI) has been invited to give a presentation at the Mechanical Evaluation of Stress Using Neutron and Synchrotron Techniques (MECA SENS), in Australia in September, in which this work will be highlighted.

Future Work

- Prepare samples in ex-situ thermal gradient
- Complete Small Angle Neutron Scattering (SANS) measurements during sintering of UO2 samples.
- March 14, Prepare ion bombardment assisted deposition (IBAD) samples with Krypton or Xenon bubbles.
- Complete High Energy Diffraction Microscopy (HEDM) experiments on heat treated samples.
- Complete Small Angle Xray Scattering (SAXS) experiments on IBAD samples.
- Present HEDM results at topical conference and/or publish results in peer reviewed journal.
- Present/publish SANS and SAXS data.

Conclusion

This experimental work will provided the nuclear fuel theoretical community with unprecedented information concerning the microstructural evolution of fuels during usage. We will not only recognize that the grain structure of a ceramic fuel evolves during use, but will also determine kinetics and mechanisms for said motion of the grain. We will understand preferential segregation of fission products to specific grain boundary types. This data will be used by the fuel modeling community represented, for instance by the CASL (Consortium for Advanced Simulation of Light Water Reactors) at LANL, to both drive model development and validate existing models.

Publications

Brown, D. W., L. Balogh, D. Byler, C. M. Hefferan, J. F. Hunter, P. Henesei, S. F. Li, J. Lind, S. R. Niezgoda, and R. M. Suter. Demonstration of near field high energy x-ray diffraction microscopy on high-Z ceramic nuclear fuel material. . To appear in MECA SENS (Approximately Mechanical Evaluation of Stress With Neutron and X-ray Scattering Techniques). (Sydney, Australia, 10-12 Sept 213).

Very Low Temperature Scanning Point Contact Spectroscopy Investigation of Inhomogeneous States on the Nano-scale

Roman Movshovich
20130285ER

Introduction

We will combine our expertise in several Scanning Probe Microscopy (SPM) and Spectroscopy (SPS) techniques and a dilution refrigerator instrumented with a 14 Tesla magnet to develop a novel Low Temperature Scanning Point Contact Spectroscopy (LTSPCS) apparatus. Point Contact Spectroscopy (PCS) has been used extensively for investigating homogeneous superconducting (SC) states in zero magnetic field. Our LTSPCS apparatus will go well beyond this: a sub-nm resolution of the PCS combined with the scanning capability and in-situ control of the force between the PCS tip and the sample, combined with high magnetic field, and very low temperatures environment, will allow us to explore the spatially inhomogeneous states in an unprecedented phase space. Within this proposal we will address some of the hottest topics in correlated electron physics, among them (1) spatial variation of the energy gap in the postulated Fulde-Ferrell-Larkin-Ovchinnikov superconducting state in CeCoIn5, and (2) direct visualization of the high field vortex structures, up till now studied only by Small Angle Neutron Scattering (SANS) techniques, in e.g. CeCoIn5 and UPt3. Our LTSPCS apparatus will be developed on the basis of the combination of techniques and components adapted from a number of different scanning probes, such as a unique all metal tip cantilever (based on cantilevers used for Scanning Tunneling Microscopy (STM)), and fiberoptic interferrometery employed in conventional Magnetic Force Microscopy (MFM) and Atomic Force Microscopy (AFM). The experimental part of this project will be complimented by advances in the theoretical understanding of the details of the FFLO state (especially at the surface), and a substantial increase in our capabilities to model point contact spectroscopy of heavy-fermion superconductors. The unique combination of achieved capabilities will open a new era of correlated electron research at very low temperatures and high fields, and help assure the preeminent position of LANL in this field.

Benefit to National Security Missions

This project addresses the Grand Challenge: “Materials: Discovery Science to Strategic Applications”. It creates new measurement and modeling capabilities in materials science for superconductivity and f-electron physics. The VLTSPCS will ensure LANL’s position of leadership in the area of correlated electron research. It will be directly applicable to investigations of heavy fermion physics, an area of traditionalyl strong interest at LANL due to its focus on f-electron elements, especially the actinide series. Overall, this project supports both themes of Emergent Phenomena and Defects and Interfaces, two of the three areas of the Materials Strategy at LANL. The VLTSPCS will open up avenues for new program development based on the multi-component suite of the Scanned Probes. John Sarrao, former Office of Science Programs Director and MaRIE Capture Manager, is cognizant of the proposed research.

The experimental part of this project cannot be successful without advances in the theoretical understanding of the details of the FFLO state (especially at the surface), and a substantial increase in our capabilities to model point contact spectroscopy of heavy-fermion superconductors. The developed modeling capabilities will allow the interpretation of measurements within this project, and apply to other correlated electron systems as well.

Progress

We have designed the stage for the dilution refrigerator. The stage drawings have been submitted to the shop. We have placed an order for the digital controller that will be used in the SPCS apparatus. We have initiated a leak check, thermometry calibration, and cool-down procedures for operational test of the dilution refrigerator with a new 14 Tesla magnet. The 1K pot fill line of the dilution refrigerator is being rebuilt.
We derived an analytic formulation of the tunneling conductance in the normal state based on our multi-channel

point-contact tunneling model for heavy-fermion materials. This new formulation provides a great simplification over previous formulations and allows us to better understand qualitatively the normal state properties of electrons tunneling from a metallic tip into a heavy-fermion metal beyond numerical results. In addition, we have begun with the construction of a tunneling Hamiltonian that incorporates the magnetic field and other ordered states, such as a spin-density wave. The effects of both magnetic field and spin-density wave in the superconducting phase need to be accounted for when analyzing SPCS measurements in the suspected FFLO phase of CeCoIn5 at low temperatures and high magnetic fields, because of the NMR observation of antiferromagnetic order in the same part of the phase diagram.

Jeehoon Kim will be leaving the lab by August 1. We have initiated a search for his replacement. Neliza Leon-Brito from the Alex DeLosanne's group at the UT Austin has arrived to LANL for training and experimental collaboration with Jeehoon while he is still here.

Future Work

Within the experimental part of our project, we will build the Very Low Temperature Scanning Point Spectroscopy (VLTSPCS) stage and combine it with a dilution refrigerator and 14T magnet. We will demonstrate the scanning capability of our device on NbSe2; image the superconducting vortex (spatial variation of the energy gap) and vortex lattice with the SPCS apparatus.

Within the theoretical part of our project, we will develop the model for the FFLO state in the presence of localized states at the surface and calculate the conductance in the vortex state for fields at arbitrary angle relative to the surface.

Conclusion

We will develop new experimental capability of Very Low Temperature Scanning Point Spectroscopy, together with theoretical modeling support, to image the superconducting energy gap on the sub-nm scale, at temperatures down to few tens of mK, and fields up to 14 T. Visualization of the spatial variation of the superconducting energy gap in CeCoIn5 will settle the controversy of whether the High Field Superconducting (HFSC) phase is a realization of the FFLO state, predicted theoretically in 1960's, or an exotic field-induced magnetic state. We will directly image the vortex lattice of CeCoIn5 and explore its rich and exotic phase diagram.

Publications

Chen, H., Y. Y. Tai, C. S. Ting, M. J. Graf, J. Dai, and J. X. Zhu. Disorder effects in multiorbital s±-wave superconductors: Implication for Zn-doped BaFe2As2 compounds. Phys. Rev. X.

Excited State Quantum Interactions in Carbon Nanotubes

Stephen K. Doorn
20130309ER

Introduction

Our recent first-time demonstration of quantum interference and violation of the Condon approximation in carbon nanotubes (CNTs) overturns long-held assumptions regarding their optical response and opens the way for new quantum physics to be explored in these systems. While these fundamental behaviors are fascinating by themselves, they have the potential to alter relaxation pathways and dynamics underlying anticipated applications in photonics, optoelectronics and energy harvesting. It is therefore important to understand both the origins and consequences of these phenomena in CNTs. Our goal is to understand how the interplay of electronic and vibrational structure in CNTs gives rise to non-Condon and interference behaviors and determine what consequences they hold for observed photophysical responses. We focus on three objectives:

1. Non-Condon Behaviors will be probed for multiple nanotube structures, vibrational modes, and excited states using Raman and modeled with quantum chemical theory to gain an understanding of their origins. Dynamic perturbation of CNT structure will further inform on their origins and reveal routes to control the effect.

2. Dynamic Control of Quantum Interference by strain tuning of the electronic energy spacings that determine interference will allow us to sample all possible interference behaviors while using interference response to probe consequences for underlying photophysical behaviors.

3. Relaxation Pathways and Dynamics will be probed using time-resolved spectroscopies to learn the fate of optical excitations as determined by phonon-mediated electronic state interactions.

Each of these focal areas represents pioneering studies that will open significant new areas of CNT physics for further investigation. No other molecular or condensed-matter system offers the ability to study non-Condon and interference behaviors in such a controlled and systematic way and the information gained here will impact understanding of photophysical behaviors of broad classes of optical materials and serve as a bridge between molecular and condensed matter systems.

Benefit to National Security Missions

Results of this project will have a direct bearing on developing optical and electronic properties of carbon nanotubes for photonic and energy harvesting applications and may also contribute to sensing and spectral tagging applications. As a result this work will have direct relevance to the mission of the DOE-BES funded Center for Integrated Nanotechnologies and the potential applications will be of interest to agencies including NIH, DOE, DHS, and DOD with potential impact on threat reduction and renewable energy missions. Our effort will also drive development and understanding of fundamental surface chemistry of low-dimensional materials. Additionally, the quantum behaviors we will study are found in broad classes of materials, but only carbon nanotubes allow the detailed study that will be pursued in this effort. As a result, the nanotubes serve as ideal model systems for obtaining a basic understanding of several novel quantum behaviors. As such, their study supports DOE goals for expanding fundamental understanding of functional nanomaterials.

Progress

We report progress in 6 separate areas related to the goals of the project

Non-Condon Behavior in Armchair Carbon Nanotubes: We have successfully obtained Raman excitation profiles (REPs) for the (5,5), (6,6), and (7,7) chiralities (so-called armchair metallic structures) of nanotube. Material

enriched in these structures was obtained via two separate enrichment methods and from two separate nanotube source materials. The strong asymmetry in the REPs that was previously observed in semiconducting tubes was found to continue for these metallic structures. The results suggest a continuation of the trend that asymmetry increases with tube diameter and towards large chiral angles and further indicates the behavior is intrinsic and general for all tube types. The results have been submitted to Phys. Rev. B and the manuscript is under revision after a first round of reviews.

Frequency Behavior of the TO Phonon in Armchair Nanotubes

Our work on enriched samples of single armchair structures has allowed us to obtain the first ever detailed frequency values for the TO phonon mode over 6 different structures. Frequencies show a sharp decrease to smaller diameter tubes, but can be modeled by a strongly upshifted response similar to the TO mode of semiconducting tubes. By also probing the response of the frequencies to electrochemical doping we are able to understand the TO behavior as arising from the effects of rehybridization induced by strong tube curvature. Upshifted frequencies result from an anomalie in the phonon dispersion. Our results resolve a controversy in the theoretical community over how to describe electonr-phonon coupling in metallic nanotubes.

Transition and Phonon Mode Dependence of Non-Condon Effects

We have now obtained REPs for the E11 thru E44 (first through fourth exciton transitions) of a wide range of semiconducting tube structures. Additionally, we have this data for the LO, TO, and radial breathing mode (RBM) phonon modes. In all cases except for one, non-Condon-induced asymmetry is observed. For the RBM, surprisingly, we observe no asymmetry. For the LO and TO, we find that as one goes from E11 to E22 excitation the asymmetry increases significantly, but shows no particular trend on going to higher-energy excitations. The results show that we do need to consider how extrinsic effects may impact the non-Condon behavior. Additionally, we have begun quantum chemical modeling to evaluate where differences in non-Condon response for the different phonon modes originates. The experimental part has been written up for publication, which will wait on the theory results.

Probing Double Resonance Raman Response

We have completed theoretical modeling of the double resonance (2D) Raman response for several nanotube chiralities and have performed a detailed comparison to experimental results on the (9,1) structure. The comparison shows the 2D behavior arises from an LO phonon and allows us to confirm our understanding of phonon dispersion in nanotubes. Our next step is to apply similar comparisons for all the tubesfor which we have overlapping theory and experimental data.

Sample Development for Strain-Based Measurements

We require increased amounts of enriched material for our strain-based measurements and are applying a new two-phase extraction method for separations that depends on tuning relative degrees of hydrophobicity/-philicity between different structures. We are already showing good results for isolation of (6,5) tubes and are progressing to isolation of other structures. The strain measurements also require a composite matrix that will transfer applied strain to the constituent nanotubes. We have evaluated PDMS (a silane polymer), which may be suitable but requires tricky processing conditions. We are currently looking into triblock copolymers as an alternative.

Pump-Probe Capability for Evaluating Dynamics Response to Quantum Interference

We are nearing completion of building femtosecond pump-probe capability to evaluate excited state dynamics in single-chirality samples. In particular we are interested in measuring those in the (10,5) tube, which is anticipated to reveal new quantum interference behaviors. This structure requires a pump pulse capable of being tuned to 375 nm. We are currently waiting on a chirped mirror set used to shorten pulses to an anticipated 5 femtoseconds. Once incorporated in the instrument, we will have tunable 5 fs pulses available from 335-430 nm and from 550 to 900 nm.

Future Work

Critical to understanding the origins of the non-Condon effects is determining their dependence on nanotube structure. We expect the effect is related to the curvature of the related band structure, which is a strong function of excitation energy. To confirm this expectation, our investigations will probe the behavior for the first four bright exciton states, using the nanotube G-band vibration as a probe. We will also evaluate the behavior for metallic structures, in order to both extend the generality of the behavior beyond semiconducting structures and to evaluate how the effect may be linked to exciton formation or to non-adiabatic behaviors inherent to other electron-phonon coupling phenomena in metallic structures.

Equally important is determining how vibrational mode and different coupling mechanisms impact the non-Condon response by evaluating the effect over additional modes (not just G-band). Analysis of excitation behavior of the nanotube radial breathing mode (RBM), 2D, and

M modes will be our targets. The resonance behaviors for these vary from direct exciton resonances to double resonance processes that link the nanotube electronic and phonon densities of states. Experimental data will be analyzed and modeled within a 3D evaluation of these state behaviors. The result should help address current controversy about so-called internal and external resonance processes in these materials and will provide further insite into how non-Condon effects arise.

In anticipation of an emphasis on dynamic tuning of interference and non-Condon behaviors for follow-on years, we will also focus effort on development of appropriate sample matrices to enable our envisioned strain-tuning measurements.

Finally, on the theory side of our effort, we will extend our existing modeling of non-Condon effects on the G-plus mode to also include modeling of expected behavior for G-minus and RBM vibrations and establish a foundation for also modeling strain effects.

Conclusion

Our effort will lead to an understanding of how interactions between electronic and vibrational structure in carbon nanotubes (CNTs) leads to quantum interference behaviors and gives rise to breakdown in fundamental descriptions of quantum interactions. These will be pioneering studies in an emerging area of CNT photophysics. The result will allow us to determine what consequences these behaviors have for nanotube optical responses that underlie photonics, optoelectronics, and energy harvesting applications. Ultimately, by revealing the origins and consequences of these new CNT quantum phenomena we will also generate the principles for how we may control them for enabling applications.

Publications

Berciaud, S., X. Li, H. Htoon, L. E. Brus, S. K. Doorn, and T. F. Heinz. Intrinsic line shape of the Raman 2D mode in freestanding graphene monolayers. 2013. Nano Letters. 13: 3517.

Duque, J. G., E. H. Haroz, H. Telg, J. J. Crochet, J. Simpson, A. R. Hight Walker, X. Tu, M. Zheng, J. Kono, and S. K. Doorn. Asymmetric excitation profiles and non-Condon effects in the resonance Raman respons of armchair carbon nanotubes. To appear in Physical Review B.

Haroz, E. H., J. G. Duque, X. Tu, M. Zheng, A. R. Hight Walker, R. H. Hauge, S. K. Doorn, and J. Kono. Fundamental optical processes in armchair carbon nanotubes. 2013. Nanoscale. 5: 1411.

"Upscaling" Nanoscale Thermoelectrics: The Meso-macroscale Design Challenge for Real-World Energy Needs

Jennifer A. Hollingsworth
20130350ER

Introduction

The overarching goal is to address the challenge of scale that is uniquely relevant to nano-enabled thermoelectrics (TEs). Nanoscale phenomena can dramatically alter and improve the fundamental properties of semiconductor materials for applications in TEs, such as the electronic density-of-states (DOS) and charge carrier or phonon mobilities and interactions. However, in contrast with other potential nano-based technologies (lighting, sensing, energy harvesting/storage), TEs requires bulk-scale assemblies to achieve high efficiencies at the device level (cm rather than nm-µm scale). This requirement remains a key challenge to translating properties efficiencies at the nanoscale to practical efficiencies in applications. We aim to bridge this literal, physical gap in nanomaterials integration by developing new synthetic methodologies for interconnecting nanomaterial building blocks into functional networks and composite structures. We will also address an underpinning "knowledge gap" in terms of understanding how the key transport properties—electrical and thermal—change across the extremity of length scales from nano/meso- to macroscale. Though the problem of scale is distinctly paramount for TEs, the synthetic strategies and new principles of multi-scale transport will be applicable to a wide range of nano-enabled technologies. To these ends, we will pursue the following three objectives:

- Assessing and optimizing nanoscale TE functionality by way of baseline studies in single-NW systems of controlled size and surface roughness.
- Understanding and controlling meso-macroscale TE properties of novel branched/networked NW constructs.
- Assessing the viability of aerogels as a NW TEs matrix.

Benefit to National Security Missions

Successful completion of the proposed objectives will provide advances in synthesis, characterization and theory that will lay the foundation for successful, functional translation of nanoscale phenomena to the macroscale, as well as understanding how properties scale with changes in length scale and complexity. More specifically, we will also develop novel functional composites comprising NW networks in aerogels for applications in thermoelectrics. Further, we will establish new non-contact characterization and modeling tools for addressing transport processes from simple to branched NWs and their composites. This aspect of the work contributes directly to DOE Basic Science initiatives and is relevant to the Scientific Discovery and Innovation Mission in the Basic Understanding of Materials.

The work also fundamentally addresses challenges faced by the implementation of nano-enabled thermoelectrics in real-world device architectures, where success would have a clear impact on Mission Relevance in Energy Security (Renewable Energy) and the Environment (Climate and Energy Impact and even "waste" management), as theremoelectrics tackles both waste heat utilization and heat management issues.

Lastly, the new composite materials will be tested and operated at temperature extremes (cold and hot) and entail conversion of energy types (e.g., heat to electricity) and energy translation across interfaces, with direct relevance to complex materials design and characterization for MaRIE. In addition, the technology developed will support longer term development of small-size, rapid-response temperature probes for extreme environments, e.g., explosives.

Progress

Significant progress in both theory and experiment are described below for each objective.

Despite a late start by the primary synthetic chemist on the effort (Dr. Mishra: mid-April arrival), we have already synthesized several of the test materials for project Objective 1 – ultra-narrow and thicker (~40 nm) diameter PbS and PbSe nanowires and surface-roughened nanowires. We have added to our "test systems" with the inclusion of PbSe/PbS tetrapods, which afford in a single nano-construct multiple branch points and, thereby, an additional option for testing our hypotheses pertaining to branching-effects on thermoelectric properties, especially electrical/thermal transport. The tetrapods also inherently contain an internal interface that may further serve to modify carrier/thermal transport as a function of its crystalline quality (expected to be quasi-epitaxial) and the size of the tetrapod arm-lengths/diameters. The tetrapod syntheses entail first synthesizing CdSe/CdS tetrapods then chemically converting these by cation exchange reactions into the desired PbSe/PbS structures. We have to date prepared 6 nm-diameter/35 nm-arm length and 12 nm-diameter/30 nm-arm length CdSe/CdS tetrapods, which have been converted to their PbSe/PbS counterparts.

We have also begun efforts to synthesize Bi2Te3 nanowires. Our goal is to synthesize controlled-diameter nanowires (~5 and ~40 nm) by solution-liquid-solid (SLS) growth, as this method affords facile control over nanowire diameter by simple manipulation of the size of the metal nanoparticles used to "catalyze" nanowire nucleation/layer-by-layer growth/elongation. This approach for Bi2Te3 is not yet known in the literature. To this end, we are attempting to modify or develop new synthetic procedures for "Bi2Te3 quantum dots" for adaptation to SLS growth. Specifically, SLS requires that Bi2Te3 is formed by direct reaction of Bi and Te molecular precursors, rather than reaction through a Bi (or Te) crystalline intermediate (literature approaches). We have to-date performed numerous reactions between different Bi/Te molecular precursors in a range of solvents, mediated by various surfactants over several temperatures. These have been characterized by powder x-ray diffraction (XRD) and transmission electron microscopy (TEM). While XRD shows we are creating crystalline Bi2Te3, morphology remains non-optimal and/or the nanoparticles are aggregated. With a satisfactory approach in hand, we will attempt SLS Bi2Te3-nanowire growth.

We have identified a "test-bed" device-design to use for comparative studies of the different thermoelectric nanomaterials: reported in Wang et al. Nano Lett. 8, 2008, 2283. We will fabricate/test similar devices in CINT using our nanowire/tetrapod series.

Theoretical efforts have begun in earnest to address the key question of how branch points affect carrier/phonon transport. Significantly, members of this ER team have already demonstrated theoretically a key premise of our proposed work. They have developed a model that maps a nanowire network on a two-port network used in the theory of electrical circuits to describe charge-carrier/heat transport in interconnected systems. This model has been implemented into an efficient computational code and allows us to perform simulations at the device-modeling level. The simulations have been performed for Bi2Te3 nanowire-networks and have demonstrated that a network structure enhances thermoelectric figure-of-merit, ZT. Additionally, they have developed a number of numerical microscopic techniques for modeling thermoelectric properties of individual nanowires and the effect of junctions for branched nanowires. These techniques have been applied to Bi2Te3 materials and successfully benchmarked against published data. They have obtained data that has been used as input parameters to the network-simulation code. A manuscript is in preparation (O. Roslyak, A. Piryatinski "Enhanced thermoelectric properties of semiconductor nanowire networks" Nano Letters (in prep), and two oral presentations have been given (O. Roslyak, A. Piryatinski; "Thermoelectric effects in disordered branched nanowires", APS Annual Meeting, 2013; O. Roslyak "Enhanced thermoelectric effect of branched nano-wire trees." Invited lecture, Fordham University).

We have successfully incorporated semiconductor nanowires into an aerogel matrix. Here, we employed "model" nanowires comprising CdSe, as this material was immediately available. We successively increased the concentration of nanowires embedded within the porous aerogel matrix. We have yet to hit a synthetic limit in this process, but are challenged by solvent compatibility issues (differences in preferred solvent for the nanowires compared to the aerogel formation chemistry). Nevertheless, composites-to-date are dark in color (nanowires) but remain uniform in appearance, translucent and structurally sound. We will now extend to thermoelectric-relevant nanowires using modified nano-surface chemistry for enhanced chemical-compatibility.

Future Work

Nanoscale test systems

Using solution-phase methods (low-cost and scalable), we will continue to synthesize NWs that allow us to test nanoscale effects on key TE parameters: the electronic DOS – i.e., ultranarrow sub-10 nm NW diameter versus tens of nms, and carrier/phonon transport – i.e., smooth versus nanoroughened wire surfaces. Additional NW structural/compositional characteristics can be modified to achieve more complete optimization of TE properties, but our aim

here is instead to investigate the translation of nanoscale effects across vast length scales. For this reason, we focus our studies on NW size (quantum confinement) and surface properties.

Meso-macroscale integration/exploration
We will develop new synthetic methods for interconnecting NWs into branched/hyperbranched structures as designed model systems for understanding scaling effects on TE properties. By linking NWs together into progressively more complex assemblies, we will address how branch points affect carrier/phonon transport and whether these processes can be controlled by tuning the NW-NW connection (size, composition or crystal-structure mismatch) and concentration of branch sites. Experimental and theoretical characterizations on individual or small collections of NW branch points will encompass mesoscale processes. Going beyond this, we will further increase NW network complexity (via extreme hyperbranching or gelation condensation chemistry) to access transport processes in complex interconnected NW networks and to investigate non-equilibrium phonon dynamics that may result from bulk disorder & fractional dimensionality.

Aerogel utility
Aerogels are characterized by extremely low thermal conductivity and continuous porosity. They can be molded into pellets and machined. We will optimize NW-aerogel composite chemistry. We aim to assess the utility of aerogels as scalable matrices for bulk-scale NW TEs by establishing basic transport properties of NWs-in-aerogels from single/branched aerogel-embedded NWs to NW networks in an aerogel framework.

Conclusion
The technical goals that will be pursued are:

- Using solution-phase methods, we will synthesize NWs that allow us to test nanoscale effects on key TE parameters: the electronic DOS – i.e., ultranarrow sub-10 nm NW diameters, and carrier/phonon transport – i.e., smooth versus nanoroughened wire surfaces.
- We will develop new synthetic methods for interconnecting NWs (from Obj 1.) into branched and hyperbranched structures as designed model systems for understanding/controlling scaling effects on TE properties.
- We will develop methods for embedding NWs into aerogels and assess the utility of aerogels as scalable matrices to realize bulk-scale NW TEs.

Publications
Roslyak, O.. Enhanced thermoelectric effect of branched nano-wire trees. Invited presentation at Fordham University Seminar. (New York, 12 May 2013).

Roslyak, O., and A. Piryatinski. Thermoelectric effects in disordered branched nano-wires. 2013. In American Physical Society Annual Meeting 2013. (Baltimore, MD, 18-22 March 2013). , p. BAPS.2013.MAR.W12.14. College Park, MD: Bulletin of the American Physical Society.

Roslyak, O., and A. Piryatinski. Enhanced thermoelectric properties of semiconductor nanowire networks. Nano Letters.

Threat Reduction via Nanomaterials: Engineering a Novel SERS Plat-form for Chemical Detection

Nathan H. Mack
20130416ER

Introduction

Surface enhanced Raman spectroscopy (SERS) is an established technique for boosting the intrinsic Raman signal from a molecular compound by binding it to an appropriately designed metal surface. It has the capability for not only ultra-sensitive detection levels, but also provides a molecular fingerprint spectrum that can be used for compound identification. For nearly a decade now, this technique has been studied as a potential break through approach to sensing threat agents (e.g. explosives, chemical weapons, and toxic chemicals). Unfortunately, the processes required to make an effective SERS metal substrate required expensive lithography techniques and were often irreproducible, thereby limiting it's use to carefully controlled laboratory experiments.

Recent developments at LANL have produced a polymer-based metal-nanocomposite that can act as a highly enhancing SERS substrate. We have found it to be sensitive to a variety of organic compounds down to 10^-12 molar concentrations. Additionally, it can be produced at a fraction of the cost and has superior physical and mechanical properties as compared to traditional SERS substrates. This initial work hints that these materials may be ideally suited as a SERS based detection platform as the material can be produced in flexible thin film formats that opens up a wide array of potential detection approaches. In this work, we will exploit these enhanced properties to develop a field-able sensing platform for threat agent detection. We will determine the limits of detection for a variety of explosive residue and chemical agent simulants, develop new process techniques to enable high throughput substrate production, and design a proof of concept sampling system that will be suitable for portable detection applications.

Successful completion of this work will bring SERS to the forefront of detection technologies and have wide applications among DOD, DHS, and other agencies with interest in the detection of chemical species.

Benefit to National Security Missions

This work will have two primary areas of mission relevance which can be extended to any agency interested in the ultra-sensitive detection and identification of chemical species. First, we hope to gain a better understanding of how these novel materials interact with various threat agents (and their simulants). This will include how these chemical species bind to metal surfaces, what their relative affinities are for these surfaces, how these affinities can be enhanced, and what optical signatures can be exploited for chemical identification. All of this falls under the fundamental basic understanding of materials.

Second, this work will have national security and threat reduction mission relevance in that we hope to demonstrate real world detection and identification of various chemical threat agents. This could be applied to portal monitors, airport screening, first responder devices, and be applied to war-fighter support. Additionally, chemical detection and identification will have intelligence and reconnaissance applications.

Progress

One of the greatest challenges to realizing SERS based sensing is the reproducible production of highly enhancing structured metal surfaces at a realistic cost. In order to move our technology beyond TRL1 as well as move towards a more portable form factor (i.e. a test stick or cartridge based substrate), we set out to develop a set of polymer process rules that define how to produce reliable SERS substrates. Initial batches of polymer films were producing SERS sensing substrates that perform, however, they exhibit incomplete coverage of the polymer surface with structured metal, leading to inhomogeneous SERS signals. We altered the process conditions to include both solvent removal, acid doping, and me-

chanical pressing steps, as well as empirically adjusted relative concentrations of the Ag metal precursors to result in a process that yields films with >80% metal coverage. This coverage is high enough such that any voids in the metal film are smaller than the spotsize of our Raman laser, and thus insignificantly affect the resulting SERS signal.

With these films in hand, we are now starting to screen for potential threat agents of interest, starting with simple organophosphate solutions. Initially, these solutions are relatively high in concentration (millimolar); ultimate limits of detection will be resolved once we have a more complete sensing matrix indicating what agents yield the greatest SERS signal. We expect to have this matrix completed for CW simulants by the end of the FY, with similar matrices for home made explosives and energetic materials early in the next FY. We have contacted WX personnel to assist in providing energetic materials for testing.

In parallel, we have been working with ISR-5 to explore new SERS sensing form factors that take advantage of that groups automated production facilities. This approach would automate the polymer processing steps in order to 1) improve batch reproducibility and reliability and 2) enable precise spatial control over polymer deposition by extruding the polyaniline (PANI) from a fine needle prior to solvent removal. This will result in patterned and layered PANI structures that can then be subsequently metalized. Our hope is that we can use these 3d hierarchical structures to further enhanced analyte capture (and retention). Key metrics in this process are the polymer gelation time, as all patterning must be performed prior to the polymer setting as a gel, which could affect subsequent metallization processes.

Finally, we have been investigating the purchase of a portable raman spectrometer to be used for demonstration of real world SERS analyte detection. Typical SERS work in the literature is performed on a highly tuned spectrometer that requires large lasers, microscopes, optics, etc. However, translating results on an expensive research grade spectrometer over to a realistically portable spectrometer often results in failure. We had one vendor visit our labs to demonstrate their portable spectrometer that can be battery powered, and is approximately the size of a carry on luggage bag. This spectrometer performed well as compared to data taken on an identical sample using our research grade Raman system. This spectrometer also has dual wavelength capabilities, which will enable a wider range of analyte detection through the elimination of fluorescence in troublesome samples. This spectrometer is our top choice, but we have sent several samples for demonstration at several vendors' labs and are awaiting their representative spectra. We hope to submit our purchase request within the month and have all acquisitions completed by the end of this FY.

Future Work

In the first year of this project we will have run our nano-composite through a variety of sensitivity tests to determine the lower limits of detection to several threat agents. In the next FY, this work will be extended to include explosives residues and explosive precursors to test for potential applications in detection of energetic materials. Additionally, we will explore surface modification of the sensor surface to affect enhancements in sensitivity. We intend to explore self assembled monolayers to vary the sensor's hydrophobicity and surface charge, as well as ligand based molecules to serve as capture moieties for binding analytes of interest.

On the engineering side of this project, we have developed a reproducible method for batch production of our sensor materials. In the next FY, we will work to develop a new polymer processing approach (based on our batch synthesis approach) that will enable continuous fabrication of ribbons of the nano-composite. These ribbon materials will be verified for sensing capabilities and be used as one component in our proposed sampling scheme. We will study the mechanical properties of laminating this material to a flexible permeable membrane, which will serve to protect the sensing surface and act as a sample compartment for analytes of interest.

Our new portable spectrometer will come online at the beginning of the next FY. Work in this area will focus on fabricating any necessary components to allow us to rapidly analyze test samples for demonstration purposes. Lower limits of detection will be determined using both model analytes as well as analytes from our previously determined detection matrix.

Success in these three areas will enable use to gain valuable information on analyte sensor affinities and spectral responses as well as perform real world demonstrations of threat agent detection to sponsors for follow-on funding in out years.

Conclusion

In this work, we seek to develop our novel nano-composite into a field-able sensing platform for threat agent detection. We will determine this material's limits of detection for a variety of explosive and chemical agent simulants and then use this data to guide the development of a proof of concept sampling system that will be suitable for portable

detection applications. The engineering component of this work will involve developing new process techniques to enable continuous production of the polymer-based material to allow for high throughput substrate production at previously unrealized low costs.

Publications

Kang, L. L., P. Xu, B. Zhang, H. H. Tsai, X. J. Han, and H. L. Wang. Laser wavelength- and power-dependent plasmon-driven chemical reactions monitored using single particle surface enhanced Raman spectroscopy. 2013. CHEMICAL COMMUNICATIONS. 49 (33): 3389.

Kang, L. L., P. Xu, D. T. Chen, B. Zhang, Y. C. Du, X. J. Han, Q. Li, and H. L. Wang. Amino Acid-Assisted Synthesis of Hierarchical Silver Microspheres for Single Particle Surface-Enhanced Raman Spectroscopy. 2013. JOURNAL OF PHYSICAL CHEMISTRY C. 117 (19): 10007.

Li, S. W., P. Xu, Z. Q. Ren, B. Zhang, Y. C. Du, X. J. Han, N. H. Mack, and H. L. Wang. Fabrication of Thorny Au Nanostructures on Polyaniline Surfaces for Sensitive Surface-Enhanced Raman Spectroscopy. 2013. ACS APPLIED MATERIALS & INTERFACES. 5 (1): 49.

Park, Y. S., Y. Ghosh, P. Xu, N. H. Mack, H. L. Wang, J. A. Hollingsworth, and H. Htoon. Single-Nanocrystal Photoluminescence Spectroscopy Studies of Plasmon-Multiexciton Interactions at Low Temperature. 2013. JOURNAL OF PHYSICAL CHEMISTRY LETTERS. 4 (9): 1465.

Park, Y. S., Y. Ghosh, Y. Chen, A. Piryatinski, P. Xu, N. H. Mack, H. L. Wang, V. I. Klimov, J. A. Hollingsworth, and H. Htoon. Super-Poissonian Statistics of Photon Emission from Single CdSe-CdS Core-Shell Nanocrystals Coupled to Metal Nanostructures. 2013. PHYSICAL REVIEW LETTERS. 110 (11): -.

Accurate Interfacial Structures for Atomistic Simulations: Minimizing the Grand-canonical Free Energy

Danny Perez
20130517ER

Introduction

To carry out effective simulations at the atomic scale, it is crucial to know the details of the atomistic structures of materials. Often, obtaining that information experimentally is impractical so simple rules of thumb or geometric constructions are used to fill in the missing details. Sometimes, limited searches are used to explore the neighborhood of these guesses to assess their thermodynamic stability, which is often a good metric of their practical relevance. However, due to the large size of the accessible configuration space, unconstrained searches are scarcely attempted. This problem is even more severe when the number of atoms in the structures of interest is unknown. This is a common case when defects are involved. This inability to thoroughly search the space of possible configurations severely limits the accuracy of atomistic simulations. In this project, we propose to develop efficient sampling algorithms that would allow to systematically and autonomously search for the most relevant structures. Our work will be based on a grand-canonical approach where the number of atoms in the simulation cell is not fixed, but can freely evolve according to its own dynamics, i.e., atoms will be able to dynamically come in and out of the simulation as time passes.

This framework will be coupled to state-of-the-art sampling algorithms that will allow an efficient search of this huge grand-canonical (where the number of atoms is also free to vary) space. Our method will first be demonstrated on problems related to grain boundary and interfaces in materials, a very important class of two- dimensional defects that often significantly affect mechanical properties. Our approach could have a profound impact in the field by leveraging modern simulation techniques to turn the “art” of predicting the atomic structure of materials into a systematic search process. This could dramatically improve the accuracy and predictive power of atomistic simulations.

Benefit to National Security Missions

Atomistic computer simulations play an increasingly important role in the prediction of properties of materials, or in the interpretation of experimental results. However, to be effective, these simulations need adequate starting points that properly represent the most probable atomic-scale structure of the material. This is crucial for a number of the lab’s missions, specially those dealing with materials in extreme conditions. For example, we recently found that adding a small proportion of interstitials to a grain boundary in tungsten (a leading candidate for the first wall of fusion reactors) can dramatically lower the stress at which the boundaries slide, which could lead to creep, but also enhance the ability of the materials to heal radiation-induced defects. To quantify these effects, it is paramount to first identify the structures that are thermodynamically relevant (i.e., who are the most stable). These same challenges exist everywhere atomistic simulations of materials are used. Our proposed methodology will assist in the sampling of the possible structures and greatly help in the identification of the relevant ones. This has the potentials to significantly increase the power of atomistic simulations across a very wide range of problems of direct relevance to the lab’s missions, for example to investigate the properties of cladding materials in nuclear reactors, or to be able to predict the response of polycrystalline materials to shock, to name only a few examples. This capability directly supports mission needs for DOE Office of Science, Nuclear Energy, and MaRIE while enhancing our basic understanding of materials mission.

Progress

The last year was dedicated to assessing the performance of our initial simulation code and to the analysis of the most promising sampling algorithms that could be leveraged to ensure a thorough exploration of the possible atomistic configurations of our system. We have tested approaches based on meta-dynamics, a well-

known sampling algorithm that learns about the features of the system as the simulation proceeds in order to design a bias function that would make sampling more efficient by promoting the exploration of unlikely regions in the space of configurations that can act as pathways to other isolated regions. We have shown that this approach performs well for grain boundaries, and we observe that we are able to add and remove whole layers of the boundary freely, which indicates very good sampling efficiency. Our results demonstrate that for certain boundaries, local reorganizations can lead to relatively small changes in formation energy as more atoms are added or removed from the boundary.

We have also investigated and adopted a novel sampling algorithm, so-called statistical temperature sampling. This algorithm allows us to go beyond the initial expectations of the proposal in that it enables correct finite-temperature sampling, in contrast to zero-temperature sampling as we initially expected (i.e., we can now identify structures that are the most stable at finite temperature, and not only at the absolute zero). This will allow us to investigate thermodynamic effects, such as interface phase transitions, while greatly enhancing the sampling efficiency compared to direct simulation techniques. This method will also allow us to obtain results for a wide range of temperatures from a single simulation. We have implemented the method in our simulation code and demonstrated that it is able to quickly recover the crystalline minimum energy state, even when starting from a completely disordered configuration. This is highly suggestive that a similar performance will be achieved in the case of interfaces. We have begun deriving the grand-canonical variant of this method that will allow for correct sampling in the grand canonical ensemble, i.e., where the number of atoms can freely change during the course of the simulation. This combined approach will lead to very efficient sampling of different configurations with varying numbers of atoms and energies, which will maximize our chances of identifying the most relevant ones for matching experimental conditions. Further, as part of our work, we have discovered links between the meta-dynamics and statistical temperature approaches that went unnoticed up to now. We are now developing a unified picture of these different methods, which will be very important to the field in terms of assessing, comparing, and improving methods. A manuscript detailing our findings is now in preparation.

Finally, we have applied our technique to the investigation of the configuration of point defect clusters in Zirconium, which are of relevance to understanding radiation-induced creep (the slow plastic deformation of materials when exposed to radiation) in the cladding of nuclear fuel. Through a comparison with extensive accelerated molecular dynamics simulations, we have showed that our method can quickly and reliably identify highly non-trivial low-energy configurations, such as a new type of interstitial clusters that consist of delocalized defects in nanoscale triangles located in the basal planes of Zirconium. Interestingly, this defect, which was previously largely overlooked, appears to be very stable, and could therefore be very relevant in applications. We have also demonstrated that different interatomic potentials give drastically different predictions of the clustering of small vacancy clusters. This information will be leveraged by creep modeling activities carried out in T and MST divisions, as part of the CASL Nuclear Energy Hub.

Future Work

During the second FY, we will pursue the derivation and implementation of our statistical temperature sampling scheme that will increase the efficiency of the simulation by promoting the exploration of different configurations, with varying numbers of atoms and energies. We expect that this approach will lead to very efficient sampling, while allowing for a rescaling of the simulation results that will allow us to make predictions over a range of chemical potentials and temperatures from a single simulation. This will go beyond what we expected to be able to achieve during the course of this project, as it will open the door to the study of finite temperature effects, such as phase transitions, on boundaries. This will be a unique method that will greatly expand our current capabilities. Note that the same algorithm can be run both into exploration and accurate sampling mode, which allows for exploration of the possible configurations at a modest cost, and for accurate thermodynamics with a larger investment in computer time.

We will validate and thoroughly test the algorithm. Our main model system at this stage will be a family of grain boundaries in copper. We will also quantify the landscape of defective boundaries and qualitatively assess their thermodynamic relevance in different conditions. This will inform us on the behavior of boundary upon injection of defects, a topic of great relevance to understand radiation damage, for example.

Conclusion

We will develop sampling algorithms based on an innovative grand-canonical approach. These methods will be used to explore the landscape of possible atomic-scale structures of materials. These techniques will allow researchers to systematically, simply, and efficiently search for the most relevant structures, instead on relying to informed

guesses or searches in narrow parameter spaces. These can then be used as the starting points of very high quality atomistic simulations that aim at predicting the behavior of materials. This new capability will first be applied to the exploration of the structure of boundaries and interfaces in materials.

Figure 1. Illustration of a grand-canonical simulation of an interface. Green atoms are fixed and impose a certain kind of boundary. Red atoms are “real”, or “normal”, atoms, while blue atoms are “virtual”, i.e., they are only partially present in the simulation. Whether a certain atom is real or virtual evolves naturally during the simulation.

Understanding and Controlling Magneto-electric Coupling in Multiferroic Materials

Dmitry A. Yarotski
20130525ER

Introduction

The last few decades have seen the discovery of novel classes of correlated electron materials with exotic properties that few would have imagined. Multiferroic materials stand out among them, due to the ability to change their magnetization and/or polarization state with either electric or magnetic fields. This has the potential to revolutionize future energy, sensing and information technologies, as multiferroic circuits will combine the low power consumption and speed of field-effect devices with the permanence of magnetic elements. The remarkable properties of multiferroics emerge from strong coupling between coexisting electric and magnetic orders. Despite recent progress in the synthesis and characterization of single-phase and heterostructured multiferroic materials, the existing understanding of magnetoelectric (ME) coupling mechanisms is still controversial, and the dynamical properties of multiferroics remain practically unexplored. In particular, the role of low-energy excitations (phonons, magnons, etc.) in the emergence of multiferroic functionality has not been clarified.

Our ultimate goal is to leverage the unmatched LANL integration of material synthesis, advanced ultrafast optical techniques and forefront solid-state theory to test the dynamic limits of ME phenomena and reveal the mechanisms governing ME coupling in representative multiferroic materials. In pursuit of this goal, we will use intense THz pulses to directly excite low-energy modes and investigate their effect on magnetic and electric orders in each material.

A unique set of time-resolved optical and soft X-Ray probes will allow unambiguous separation of spin, charge and lattice dynamics, and in conjunction with theoretical modeling will unveil the microscopic origin of ME coupling in multiferroics. This integration of “passive” and “active” broadband ultrafast optical methods with forefront modeling expertise is a unique capability at LANL. The application of this capability to study multiferroic materials is poised to make a broad impact on condensed matter physics and will open new directions in complex materials research.

Benefit to National Security Missions

Our work directly addresses the Grand Scientific Challenges identified in the Basic Energy Sciences Advisory Committee (BESAC) report, which are central to DOE’s missions in energy, science, and security in general, and to the LANL Materials Grand Challenge in particular. The proposed integration of material synthesis, ultrafast optical techniques and forefront condensed matter theory represents the LANL Materials Strategy and should provide LANL, as well as CINT, with the capability to investigate emergent properties of complex materials through observation of the dynamical behavior of relevant order parameters and through selective excitation of the low-energy modes responsible for material functionality. Our thrust to interface materials science with ultrafast THz, optical and X-Ray coherent photon probes represents an essential element in the MaRIE strategy that connects the M4 facility to the Multi-Probe Diagnostic Hall. Proposed experiments will provide critical understanding of the mechanisms of magnetoelectric coupling and thus enable the design and synthesis of new multiferroic materials with controlled functionalities. Materials with tunable and novel functionality are an enabling component in the development of next-generation devices for sensing, information storage, and spintronics applications. We believe that our integrated capabilities in complex material design, synthesis and characterization will be of great interest to multiple sponsors, including DOE-BES, DOD, IC, and industry.

Progress

Using our existing theoretical and experimental expertise in the physics of complex materials, we have made substantial progress in the first year of this project. In particular, our experimental efforts have focused on

elucidating the dynamic coupling between magnetic and electric orders in a number of multiferroic materials by means of broadband ultrafast spectroscopy. We have used optical pump – Terahertz (THz) probe experiments to investigate the dependence of magneto-electric response of Eu0.75Y0.25MnO3 multiferroic compound on temperature. These studies revealed drastic changes in the relaxation dynamics of photo-induced charge carriers when material passes through antiferromagnetic phase transition near Neel temperature of 45K. Onset of magnetic order enhances the energy dissipation from hot carrier to other degrees of freedom as indicated by reduction in relaxation timescales from more than 1 nanosecond at room temperature to ~500 ps below Neel temperature. This behavior clearly reveals strong interaction between the electronic and spin excitations, and should provide more quantitative information about the underpinning mechanisms when ongoing theoretical simulations are completed.

One of the goals of our project is to reveal the role of the low energy excitations in an emergence of magneto-electric coupling. To address this goal, we have established collaboration with Richard Averitt from Boston University. We have used intense THz source available in his laboratory to selectively excite phonon/electromagnon modes in Eu0.75Y0.25MnO3 and TbMn2O5 multiferroic crystals, and to probe the ensuing time-averaged effects on magnetic/electric orders and coupling between them. However, no discernible nonlinear responses were observed in the THz electric fields up to 200 kV/cm. This result does not imply the weakness of nonlinear effects in THz range but is simply the consequence of the limitations of an experimental apparatus where the changes in the short THz pulse are averaged over long periods of time. Dr. Averitt is currently working on introducing high temporal resolution in the system, and we are already scheduled to conduct time-resolved experiments that will allow direct observation of the phonon/electromagnom dynamics. Simultaneously, an experience gained during this work allowed us to accelerate the construction of intense THz source at LANL which will be completed by the end of this year. This new capability will provide access to sub-picosecond THz pulses spanning 0.5-5 THz with electric fields up to 1 MV/cm. Moreover, this system will be coupled with second harmonic/Kerr rotation probes that will enable independent monitoring of the ultrafast dynamics of electric and magnetic orders.

We have also been successful in synthesizing vertically aligned nanocomposite multiferroic films with nanomaze structure. Our results suggest that nanomaze architecture consist of epitaxial phases and presents a novel platform for creating tunable multiferroic functionalities. In addition, novel composite materials were fabricated where components are interfaced in three dimensions, unlike currently used one-dimensional layered structures. Such 3D composite films are expected to improve magneto-electric coupling due to better control of strain fields and proximity effects. We will systematically study the effects of structure and composition on the performance of these materials using conventional techniques and newly developed THz capability.

Experimental advances were matched by theory development aimed at explaining the data and directing the experiment to discovering the mechanisms underpinning multiferroic response. Specifically, we have carried out first-principles calculations of electronic/magnetic structure and optical properties of bulk materials mentioned above as well as new Bi2FeMnO6 crystals. The reveled magnetic structure and its implications on ferroelectric/lattice order helped to identify the signatures of multiple-order interactions that should be observable with ultrafast THz, optical and X-Ray probes. Moreover, we have shown that thinner films have larger magnetic moment than thicker ones thus indicating an importance of the strain effects. These results will provide a solid foundation for modeling more complex heterostructured materials where the interfaces are used to control strain state and order coupling. In addition, the theory will focus more on modeling spin response in X-Ray region to substantiate novel ultrafast coherent X-Ray probes of time-resolved magnetic phenomena in multiferroic materials.

Future Work

In the next year, we will base on our initial success and continue the synergistic theory-synthesis-characterization effort aimed at elucidating the physics of multiferroic materials. We will complete the construction of intense THz source which will provide sub-picosecond THz pulses spanning 0.5-5 THz with electric fields up to 1 MV/cm. This system will be coupled with THz/second harmonic/Kerr rotation probes for the ultrafast dynamics of electric and magnetic orders. We have already demonstrated strong interaction between the electronic and spin excitations in representative Eu0.75Y0.25MnO3 compound using optical pump-THz probe technique. Next, we will apply the new THz capability to this and TbMn2O5 materials to directly excite electromagnon modes and reveal the mechanisms underpinning spin-polarization coupling. Simultaneously, we plan to use ultrashort optical pulses to excite the electronic subsystem in Eu0.75Y0.25MnO3, and TbMn2O5, and probe the timescales of spin order switching with time-resolved x-ray magnetic linear spectroscopy at Mn3+ edge. Similarly, we will investigate magnetic and electric order dynamics in BFO/LCMO bilayer films, which have shown

a promise for building 'artificial' multiferroics. Moreover, recent studies have clearly shown that improved multiferroic functionalities can be achieved by creating 3D composite films. We will systematically synthesize a variety of different vertically aligned nanocomposite films with different chemical compositions, and apply our unique suite of ultrafast techniques guided by theoretical modeling to establish the process-structure-functionality relationship in the 3D composite BFO/LCMO thin films. Further theory development will aim at modeling the influence of strain on the magnetism in these compounds in a hope to uncover the mechanism for the enhancement of the magnetic moment in the thinner films accompanied by the calculations of electronic, magnetic, and optical properties.

Conclusion

We expect to provide a better understanding of the dynamics and origins of magnetoelectric (ME) coupling in multiferroic materials. We will answer three longstanding questions in the basic and applied science of ME systems: 1) How fast can the magnetization/polarization be switched, and how can this be improved? 2) What low-energy excitations are responsible for the strong interactions between electric and magnetic orders? 3) How can we manipulate these excitations to enhance the ME coupling and design better multiferroics? This will enable development of the basic principles of ME material design, with a significant impact on energy and information technologies.

Publications

Aguilar, R. Valdes, Y. M. Sheu, A. J. Taylor, R. P. Prasankumar, and D. A . Yarotski. Time resolved terahertz and second harmonic investigations in multiferroic RMnO3 and RMn2O5. Presented at 2013 March Meeting of The American Physical Society. (Baltimore, MD, 18-22 March, 2013).

Chen, A. P., H. H. Zhou, Z. X. Bi, Y. Y. Zhu, Z. P. Luo, A. Bayraktaroglu, J. Phillips, E. M. Choi, J. L. MacManus-Driscoll, S. J. Pennycook, J. Narayan, Q. X. Jia, X. H. Zhang, and H. Y. Wang. A New Class of Room-Temperature Multiferroic Thin Films with Bismuth-Based Supercell Structure. 2013. ADVANCED MATERIALS. 25 (7): 1028.

Chen, A. P., W. R. Zhang, F. Khatkatay, Q. Su, C. F. Tsai, L. Chen, Q. X. Jia, J. L. MacManus-Driscoll, and H. Wang. Magnetotransport properties of quasi-one-dimensionally channeled vertically aligned heteroepitaxial nanomazes. 2013. APPLIED PHYSICS LETTERS. 102 (9): -.

Chen, A. P., Z. X. Bi, Q. X. Jia, and H. Y. Wang. Microstructure, vertical strain control and tunable functionalities in self-assembled, vertically aligned nanocomposite thin films. 2013. ACTA MATERIALIA. 61 (8): 2783.

Phase Transitions at Extremes: Emergence of Topological Defects

Vivien Zapf
20130601ER

Introduction

Ever since an early metal worker plunged hot iron into water and discovered quench-induced hardening, the importance of speed in phase transitions was clear. A phase transitions is e.g. the process of transforming from solid to liquid or from a non-magnetic to a magnetic state. Phase transitions traversed at extreme speeds are central to many LANL missions. First order transitions (which are abrupt and have latent heat,) are well understood and phenomena such as nucleation and annealing are the basis of vast industries. Second order phase transitions at extreme speeds (which are continuous and have no latent heat) can also produce profound effects on materials. However, our understanding of second order transitions is incomplete. The Kibble-Zurek Mechanism (KZM) was developed starting in 1985, largely at LANL, and describes how rapid quenching can "freeze in" fluctuations in second order phase transitions, creating defects such as domain walls, vortices, etc. These defects are long-lived fossils of transition dynamics, revealing nature of the fluctuations and the symmetry breaking process. KZM applies to second order phase transitions of interest to LANL and DOE from cosmology to magnets to superconductors.

Recent breakthroughs allow us to test KZM in materials with practical importance. We will study KZM in magnets for the first time in theory and experiment. We innovate by using magnetic fields to induce phase transitions with up to eleven orders of magnitude of quench rate. Thus, for the first time, we can test key quantitative prediction of KZM: the dependence of defect density on quench rate. We build on our expertise in a new class of magnets that have the right symmetry to allow spin vortices and other topological defects, testing KZM in both thermal and quantum phase transitions.

Benefit to National Security Missions

This project seeks to understand the formation of vortices and other defects in phase transitions out of equilibrium. This is known as the Kibble Zurek mechanism. We will focus specifically on magnetism, thus enhancing fundamental understanding of materials. These topics fall directly within the purview of the DOE Office of Science. However this theory applies to all phase transitions that are traversed rapidly and out of equlibrium. We will be testing the central quantitative prediction of the Kibble Zurek mechanism, and thus we will be making contributions to other fields in which out-of-equilbrium phase transitions are studied including ferroelectrics, charge-density waves, superconductors, cold atoms, and even cosmology. The Kibble Zurek Mechanism was first proposed in cosmology to explailn the formation of the early universe.

It applies to information science and technolgy because topological defects are a new frontier for quantum computing, and even in a classical context can be used to store and manipulate date. Understanding how to create and manipulate vortices, both wanted and unwanted vortices, is thus important for fields directly impacting information technology including spintronics, quantum computing, and computer memories.

Progress

Success in exploring the Kibble-Zurek mechanism (KZM) as outlined in our proposal requires four ingredients: appropriate compounds, variable-pulse speed magnetic fields, the ability to measure the resultant topological defects, and detailed modeling of the compounds. We describe outline the progress in these four areas below.

Appropriate compounds

We previously suggested NiCl2-4SC(NH2)2 as an excellent candidate compound, and we are conducting experiments now. However, we are also exploring the physical properties of several new magnetic compounds that are candidates for observing the Kibble-Zurek mechanism.

These include CoCl2-4SC(NH2)2, Ca3CoMnO6, REInO3 (RE = rare earth), Ho2CuTiO6 and Er2CuTiO6, and Ni3TeO6. Three papers are in progress on this preliminary characterization and Zapf and Jaime are finalizing a Rev. Mod. Phys. on quantum magnets exhibiting Bose-Einstein Condensation, which are the prime candidates for KZM.

Variable pulse speeds
We have developed new pulse algorithms for our unique 60 T shaped-pulse magnet to achieve the widest possible range of pulse speeds, and tested these on Ca3CoMnO6. This magnet will be the main magnet in which the final tests of the Kibble-Zurek mechanism will be conducted.

Measurements of the KZM effect
Our direct measurements of the KZM effect are stalled for the moment because our optical fiber grating magnetostriction method is not effective at measuring the magnetostriction in the samples most relevant to this ER due to mismatched thermal expansion. We are also learning that magnetostriction measurements transverse to the applied magnetic field are optimal for testing KZM and the optical fiber system does not have the ability to measure transverse magnetostriction in many of our magnets. Therefore we are taking a different tack and developing a method of measuring magnetostriction that uses a piezo-electric cantilever to track the length changes of the sample. This method will be more robust for a wide range of samples, and can be oriented in any direction relative to the applied magnetic field. Initial results strongly suggest that it is at least as sensitive as the optical fiber system, and the first measurements on our candidate systems are commencing this summer and fall.

Theoretical Modeling
We have investigated formation of topological defects following a phase transition in several models relevant to the ongoing experiments. These include formation of topological defects in a quench from a Mott insulator to superfluid, which is most relevant to NiCl2-4SC(NH2)2. Two papers on this subject have been published. We have also developed a simple model that accounts for the winding number in two-dimensional systems through the correlations between pairs of topological topological defects. This has led to re-interpretations of the data of the experiments on tunnel Josephson junctions (and brought them into agreement with the Kibble-Zurek mechanism). Furthermore, Zurek and del Campo are involved in a paper that tests KZM in ion traps, where chains of ions ("Coulomb crystals") can buckle (creating a "zigzag") as a result of a change of the external potential. Topological defects (places where a "zig" is followed by another "zig" rather than a "zag") form in a phase transition that is in the same universality class as Ising model in one dimension. Zurek has also co-authored a review paper with del Campo and Kibble on the interplay between inhomogeneity of the system and KZM.

Future Work
In Fiscal year 2014 we will complete our detailed theory of how the Kibble Zurek Mechanism applies to XY antiferromagnetism for quantum phase transitions in two and three dimensions, and the physical properties being studied experimentally in this ER (see below). Particular attention will be paid to the quantum aspects of the dynamics of phase transitions.

On the experimental side we will complete the development of a magnetostriction measurement method that is compatible with our samples (an unexpected addition to our work). Then we will measure the magnetostriction, the dielectric constant and the ac susceptibility measurements in at variable pulsed speeds for the compound NiCl2-4SC(NH2)2, and then for analog compounds that order magnetically even in zero field, allowing us to pulse the magnetic field first and then measure afterwards in zero field. We will continue exploring new antiferromagnets that are candidates for our KZM investigations due to their XY antiferromagnetism and magneto-electric coupling.

Conclusion
We expect to test the central prediction of the Kibble Zurek Mechanism that topological defects, like vortices, can be induced by rapidly quenching through 2nd order phase transitions. We will study magnetism and perform the first detailed quantitative test of the power-law scaling of vortex density with quench speed. We will develop the theory for magnets and quantum magnets, and perform experiments in the unpredented range of magnetic field quench speeds at the National High Magnetic Field Laboratory.

Publications
Campo, A. Del, and W. Zurek. Universality of phase transition dynamics: topological defects from symmetry breaking. To appear in 80th Birthday Symposium for Tom Kibble.

Campo, A. del, T. Kibble, and W. Zurek. Causality and non-equilibrium second-order phase transitions in inhomogeneous systems. 2013. J. Phys. Condensed Matter. 25: 404210 .

Matlashov, A. N., L. J. Schultz, M. A. Espy, R. H. Kraus, I. M. Savukov, P. L. Volegov, and C. J. Wurden. SQUIDs vs. Induction Coils for Ultra-Low Field Nuclear Magnetic Resonance: Experimental and Simulation Comparison. 2011. IEEE TRANSACTIONS ON APPLIED SUPERCONDUCTIVITY. 21 (3): 465.

Mun, E. D., M. Frontzek, A. Podlesnyak, G. Ehlers, S. Barilo, S. V. Shiryaev, and V. S. Zapf. High magnetic field evolution of ferroelectricity in CuCrO2. Physical Review B.

Oh, Y. S., S. Artyukhin, J. J. Yang, V. S. Zapf, J. W. Kim, D. Vanderbilt, and S. W. Cheong. Colossal magnetoelectricity in a collinear antiferromagnet. Nature Communications.

Pyka, K., J. Keller, H. L. Partner, R. Nigmatullin, T. Burgermeister, D. M. Meier, K. Kuhlmann, A. Retzker, M. B. Plenio, W. H. Zurek, A. del Campo, and T. E. Mehlstaubler. Topological defect formation and spontaneous symmetry breaking in ion Coulomb crystals. 2013. NATURE COMMUNICATIONS. 4: -.

Torrontegui, E., S. Ibanez, S. Martinez-Garaot, M. Modugno, A. del Campo, D. Guery-Odelin, A. Ruschhaupt, X. Chen, and J. G. Muga. Shortcuts to Adiabaticity. 2013. ADVANCES IN ATOMIC, MOLECULAR, AND OPTICAL PHYSICS, VOL 62. 62: 117.

Tsyrulin, N., C. D. Batista, V. S. Zapf, M. Jaime, B. R. Hansen, C. Niedermayer, K. C. Rule, K. Habicht, K. Prokes, K. Kiefer, E. Ressouche, A. Paduan, and M. Kenzelmann. Neutron study of the magnetism in NiCl2 center dot 4SC(NH2)(2). 2013. JOURNAL OF PHYSICS-CONDENSED MATTER. 25 (21): -.

Wulf, E., D. Huvonen, J. W. Kim, A. Paduan-Filho, E. Ressouche, S. Gvasaliya, V. S. Zapf, and A. Zheludev. Criticality in a disordered quantum antiferromagnet by neutron diffraction. Physical Review B.

Zapf, V. S., M. Jaime, and C. D. Batista. Bose-Einstein Condensation in Quantum Magnets. Reviews of Modern Physics.

Zurek, W. H.. Topological relics of symmetry breaking: winding numbers and scaling tilts from random vortex–antivortex pairs. 2013. J. Phys.: Condens. Matter. 25: 404209.

Redox active Catalysts for C-C Coupling Reactions Relevant to Renewable Energy

John C. Gordon
20130672ER

Introduction

An effort to upgrade derivatives of glycerol (essentially a waste molecule produced on a huge scale as a result of biodiesel production) for the synthesis of fuels precursors and higher value chemicals, and to do it using well-defined, inexpensive catalysts based on earth abundant metals is a desirable goal. The research outlined herein targets the development of inexpensive catalysts, comprised of earth abundant metals, which are capable of such biomass derived molecule upgrading.

Precious metals are commonly used in catalysis due to their ability to promote two-electron processes, such as oxidative addition reactions. In contrast however, 1st-row metals tend to undergo one-electron redox changes or promote radical reactions, which has limited their more general use in catalytic chemistries. The proposed work will attempt to use redox active ligands capable of conferring multi-electron redox behavior on cheap and abundant metals, thus potentially applicable to upgrading glycerol based derivatives.

Benefit to National Security Missions

The proposed work will advance our understanding of the chemistry and chemical methods that directly bear upon energy security. Success in this area would seed the development of future approaches to more efficient chemistries, potentially providing a bridge from basic science to global scale energy solutions.

The LDRD funds requested for this project will provide an opportunity for our team to collect results in this high profile area of renewable energy. Results from this exploratory work should prove invaluable in obtaining potential future funding from organizations such as DOE Office of Basic Energy Sciences (Catalysis Science) and DOE Office of Energy Efficiency and Renewnable Energy.

Progress

The concomitant rise in global energy demands and growing concerns over climate change have spurred interest in the development of alternative energy sources as well as less expensive synthetic methods for high-value chemical feedstocks. The development of novel methods for biomass derived molecule conversion is a burgeoning area. We are specifically interested in approaches for the reductive coupling of three-carbon containing ketonic molecules derived from glycerol into six (or higher)-carbon containing molecules as this represents a potential route for both fuel and fine-chemical synthesis from readily-available and inexpensive precursors.

Our approach to the homocoupling of glycerol derivatives involves the use of earth-abundant, first-row transition metals (e.g. iron) supported by redox active ligands. While first-row transition metals typically undergo one-electron redox changes, the coordination of redox active ligands to metals such as iron, facilitates the multi-electron redox changes that are required to promote the desired coupling reactions. It is envisioned that the storage of extra reducing equivalents will more easily permit the reductive coupling of ketonic substrates.

To this end, we have already synthesized a series of both previously published as well as new iron complexes containing redox-active ligands and have begun preliminary reactivity studies designed to establish the ability of reduced iron complexes to affect the coupling of ketones. The most promising complex thus far is a new [FeII(BIAN)Cl2] complex. [FeII(BIAN)Cl2] contains an iron center supported by a bis(aryl)acenapthenequinonediimine (BIAN) ligand. X-ray crystallographic characterization of this molecule reveals a tetrahedral geometry around the iron center, and magnometry and Mössbauer data confirm the divalent oxidation state of iron within this molecule. Cyclic voltammetry reveals two successive one-electron reductive processes; comparison with

the cyclic voltammetry data of the BIAN ligand suggests that the first reduction occurs on the iron center while the second reduction is largely ligand-based.

Exposure of [FeII(BIAN)Cl2] to chemical reductants in the presence of either cyclooctene (cod) or toluene results in the the formation of [Fe(BIAN)(cod)] and [Fe(BIAN)(toluene)] species, respectively. Both species have been characterized via NMR spectroscopy, and the structure of the [Fe(BIAN)(toluene)] species has been confirmed via X-ray crystallography. Examination of both reduced iron species via spectroscopic and magnetic techniques is planned for the future. Computational studies aimed at elucidating their electronic structures are also underway. Finally, exposure of the [Fe(BIAN)(cod)] complex to a slight excess of ketones including benzophenone and acetophenone results in rapid formation of the anticipated coupled products as confirmed by 13C-NMR spectroscopy. Further efforts will attempt to extend this reactivity to both aldehydes and biomass-derived substrates.

Future Work

We will computationally screen existing ligands suitable for desired redox chemistries and attempt to make iron complexes supported by these. We will also design, prepare and synthesize other promising new ligand candidates. If successful in new ligand synthesis, we will also proceed to synthesize and characterize new iron complexes, and begin to test their redox chemistries with standard organic substrates that will serve as models for the biomass derived molecules.

Conclusion

Developing earth abundant metal-catalyzed processes to affect the low cost conversion of biomass derived feedstocks remains a major challenge in the field of energy related chemistry. In part this is due to the inability of first row transition metals to participate in multi-electron redox processes. Success in this project would not only lead to a more fundamental mechanistic understanding of C-C coupling reactions with traditional organic substrates using these classes of metals, but also has the potential, if successful, to convert species derived from a large scale waste by-product of biodiesel (glycerol) into potentially useful fuel precursors and other chemicals.

Novel Chemical Architectures for Supercapacitor Electrolytes: Comparing In Situ Scattering Measurements to Theory and Simulation

Cynthia F. Welch
20130681ER

Introduction
We aim to increase the energy storage density in supercapacitors, a family of devices well suited to the intermittent power generation associated with many renewable sources. We propose that tailoring the size and shape of the electrolyte in supercapacitors to match the electrode surface geometry will lead to enhanced energy densities, forming our central hypothesis. This hypothesis leads us to consider several nano-structured organic electrolytes (NOEs) as candidates for use in supercapacitors, as well as to study their behavior near and in the electrode pores. The novelty of our project lies in optimizing the electrolyte rather than the electrode. Many key questions about the behavior of the electrolytes in the harsh environments near electrodes must be answered for progress to be made. Our access to unique electrochemical sample cells that allow us to probe the in situ behavior of the electrolyte near electrode surfaces and our recent theoretical advances for the proposed electrolyte class provide the key enabling developments.

Thus, we have four major goals:

1. Produce multi-scale descriptions of the NOE materials in device settings
2. Discover the physical principles directing their spatial distribution in heterogeneous media
3. Explore their non-equilibrium route to this distribution upon charging/discharging the device
4. Encapsulate in quantitative expressions the physics dictating their performance

Benefit to National Security Missions

Many processes involved in manufacturing and transporting goods suffer from inefficiencies due to wasted energy. Similarly, many renewable energy sources (such as wind and solar) yield only intermittent electricity generation. We therefore require advanced devices that quickly capture and release stored energy. If their energy densities can be improved, given that supercapacitors may deliver an order of magnitude more power than chemical batteries, they may dramatically improve the performance of dynamic energy capture and reuse systems. Our project aims to improve the energy densities of supercapacitors by tailoring the size and shape of the electrolyte to match the electrode surface geometry. Specifically, we will explore certain dendritic chemistries, which possess all of the key properties needed in a good electrolyte. In addition, several aspects of their physical chemistry recommend them for application in supercapacitors. These characteristics include precisely controlled size and shape, broad range of available sizes, high charge densities, low viscosities at relevant concentrations, and the ability to capture impurities.

Progress

Our goals for Year 1 of the project are as follows:

- Build molecular dynamics (MD) models of charged dendrimers in a salt-water solution. Study both single molecule and blend behaviors at various relative concentrations and generations of growth. Carry out the quantum chemical stability study to introduce relevant fragmentation species into the MD simulations.
- Experimentally validate both the MD and the chemical stability results via chromatography (gel permeation), spectroscopy (NMR, mass spec) and scattering (light, small-angle neutron).
- Use our new theory to extract an effective step length. This information will be used (in Year 2) to construct a field theoretical model to predict the localization of the individual dendrimers onto various pore surface geometries.
- Take the intra-molecular dimensions from the MD results to construct a coarse grained model.

Over the past nine months, we have made significant progress on each of these goals as well as on one of the goals for Year 2. Here are more details regarding our progress toward each of these goals:

We have constructed MD models of poly(propylene imine) (PPI) dendrimers and carried out some single molecule studies. We have also begun the quantum chemical stability studies. MD models of poly(amido amine) (PAMAM) dendrimers will be constructed and studied over the next 3 months. These MD studies are computationally very expensive; therefore, we applied for LANL Institutional Computing time and have now been granted time on several Institutional Computing platforms over the next 2 years. Part of our allocation will be utilized to complete these atomistic MD studies, which will likely continue into Year 2 of the project.

We have purchased several generations of poly(amido amine) (PAMAM) dendrimers and begun the chemical stability studies. Characterization by gel permeation chromatography and NMR spectroscopy will be completed by the end of Year 1. Light scattering studies have been attempted but were unsuccessful due to the small size of the dendrimers, which is at the lower limit of detection for the instrument used. An alternate light scattering instrument has been identified, and we will use this instrument over the next 3 months to make another attempt at characterization by light scattering. A beam time proposal for small-angle neutron scattering studies was submitted and, if granted, will be executed at the end of Year 1 or beginning of Year 2, depending on neutron beam availability and scheduling constraints.

One of us (P. Welch) has written a paper that details the process of extracting an effective step length for dendrimers. This parameter will be used in Year 2 to construct a field theoretical model to predict electrolyte / electrode interactions. The paper has recently received an LA-UR number and will be submitted within the next few weeks to a peer-reviewed journal.

Coarse-grained models of PAMAM and PPI have been constructed. In addition, Brownian dynamic (BD) simulations of these coarse-grained model dendrimers between two flat, oppositely charged electrodes have begun, which was a goal originally slated for Year 2. These simulations have the benefit of being less computationally expensive than the MD studies of (1) above. Therefore, we have been able to explore a large parameter space in the first nine months of the project. Specifically, we have examined the effects of dendrimer concentration, dendrimer generation of growth (or size), electrode surface charge density, and solvent dielectric constant. Each of these parameters has spanned values most relevant to our target application, supercapacitor devices. We are in the process of writing a paper that details the results of these studies, which suggest some interesting phenomena that may be unique to electrolytes with dendritic architectures. We will also build on the results of these studies with additional BD simulations in Year 2, focusing on different pore geometries. Our Institutional Computing allocation has been, and will continue to be, used for these studies.

Future Work

- Carry out Brownian dynamics (BD) simulations on the coarse grained models within the Debye-Hückel and implicit solvent approximations. Examine the behavior of single and multiple molecules in the neighborhood of surfaces with different pore geometries. The surfaces will be modeled as static particles arranged in the desired topologies. Examine the behavior of blends of nano-structured organic electrolytes (NOEs) in the presence of electric fields and model (flat) electrode surfaces. Apply an external electric field and track the phase separation of the two species.
- Using the information on the effective step length obtained in Year 1, construct a field theoretical model using the Edwards path integral formulation to predict the localization of the individual dendrimers onto various pore surface geometries. Extend this approach to multiple molecules, solving for concentration within the pore. Compare the results with the CGM modeling (1 above).
- Devise an extension of the Ginzburg-Landau theory for polymer blends to account for blends of the NOEs in solution and in the presence of an electric field.
- Experimentally challenge the simulations with X-ray and neutron reflectivity experiments of dendrimers at flat electrode surfaces.

Conclusion

This project will produce: 1) A new set of theories for predicting when specific NOEs will partition within pores of various geometries; 2) A new theory for predicting how the environmental parameters dictate the structure of the multilayer arrangement of the NOEs near the electrode; 3) A new theory detailing the dependence of capacitance on the relationship between pore geometry and electrolyte shape; 4) A multi-scale simulation model of a class of supercapacitor devices that may be used as the foundation for a future program at LANL; 5) New insight into the behavior of NOEs in complex environments.

Publications

Welch, P. M.. The escape of a charged dendrimer from an oppositely charged planar surface. To appear in Journal of Chemical Physics.

Welch, P. M., C. F. Welch, and N. J. Henson. The flattening of dendrimers from solutions onto charged surfaces. ACS Macro Letters.

Superconducting Vortices in Magnetic Media

Boris A. Maiorov
20110138ER

Abstract

As electricity demand continues to rise, and environmental constraints become more relevant, it is imperative to enhance the performance of superconductors for applications oriented to energy efficiency and storage. Superconductors have great potential in transmission cables, high field magnets as well as in magnetic storage systems. For that they must be able to carry large electrical currents without dissipation. The maximum dissipationless current, called critical current density Jc, is set by the pining force exerted by different types of defects on vortices, flux-lines that appear in type-II superconductors. Magnetic defects can lead to the so-called magnetic pinning. During this project we studied the effect of a magnetic medium on the pinning and dynamics of the vortex state.

We developed new experimental and theoretical tools that allowed us to understand the interplay between superconducting vortices and magnetic media. To unequivocally study the effect of the magnetic medium we studied system where the magnetic ordering transition takes place inside the superconducting phase, namely ErNi2B2C and ThNi2B2C with Tc~11K and TN=6 and 2K respectively with Tc and TN being the superconducting and Néel transition temperature respectively.

We calculated and measure the magnetic influence of different magnetic phases on Jc. Among relevant results, we found a Jc increase associated with TN in ErNi2B2C. We analyzed the nature of the pinning enhancement as well as its origin in magnetic domains. Theoretically, a new model used to explain the already found increase in Jc at a ferrimagnetic low-temperature phase in ErNi2B2C was developed.

The technical and theoretical advances made in this project are available to other areas of condensed matter physics in the Laboratory. The capabilities developed are being used to explore other superconducting and magnetic systems in complex experimental conditions such as pulsed magnetic fields.

Background and Research Objectives

As electricity demand continues to rise, and environmental constraints become more relevant, it is imperative to enhance the performance of superconductors for applications oriented towards energy efficiency and storage. In most applications, the superconductors are exposed to relatively high magnetic fields (H) that penetrate the material by creating superconducting vortices. Any electric current that flows through the superconductor exerts a Lorentz force (FL) on the vortex that is proportional to the magnitude of the current. When the current density, J, reaches a critical value, Jc, FL becomes strong enough to overcome the pinning force that anchors vortices. Vortex motion leads to energy dissipation, i.e., the material acquires a finite resistivity for J>Jc. The work in this project was aimed to find ways to reduce dissipation using magnetic pinning related routes.

Standard vortex core pinning comes from material defects that create an attractive vortex potential. In particular, magnetic defects can lead to so-called magnetic pinning. In principle, magnetic pinning can significantly increase the value of Jc (in particular at high temperatures) as it can result in pinning energies larger than those achieved by non-magnetic defects (core pinning). However, the interplay between vortices and magnetic media cannot be properly exploited without a comprehensive study that includes both static and dynamical properties of the entire system. Thus, we centered our studies on the effect of a magnetic medium on the dynamics and pinning of the vortex state.

A common problem in previous studies of magnetic pinning is the inability of separating the core (local suppression of the superconducting order parameter) and magnetic contributions. To unequivocally study the effect of the magnetic medium, it is necessary to be able

to induce substantial changes in the magnetic properties. For this purpose, we studied different systems where the magnetic ordering transition takes place inside the superconducting phase. These studies have never been done before.

Scientific Approach and Accomplishments

The idea is to explore the interaction between superconducting vortices and magnetism. This project had two components, a theoretical and experimental. Due to the extremely challenging objectives of passing high amounts of currents to observe the fast vortex movement, extremely clean single crystals were needed and sample fabrication down to microns sized (without contamination or crystalline degradation) was needed. ErB2Ni2C, TmB2Ni2C and LuB2Ni2C single crystals were obtained from Ames Lab, (Dr. Sergey Bud'ko, budko@ameslab.gov). ErNiBC has several magnetic phases that coexist with superconductivity and LuB2Ni2C is non magnetic. We will compare and contrast the results obtained in these single crystals. For achieving the required current densities we were able to fabricate micro bridges to inject high current densities in these very clean crystals. This was done using Focused Ion Beam (FIB) at CINT facilities in Sandia (Figure 1). A separate proposal was submitted to CINT for user facility access. This proposal was approved and renewed. We also developed photolithography masks that allow for short connecting wires (these are made of Pt deposited in-situ by FIB-ID) in order to reduce contact heating. The resulting microbridges show extremely sharp Tc (narrower than that of bulk single crystals) as well as neither reduction of Tc nor increase of resistivity. This achievement solves tremendous efforts to reduce the cross section of single crystals that we made during this project.

We performed measurement of linear and non-linear electrical transport. In the superconducting phase the electric field (E=V/d V=voltage and d=distance) that indicates vortex movement, as a function of current density amplitude (J), which measures the force that acts on the vortices.

We were able to find by performing transport and magnetization measurements of the critical current density Jc in ErNi2B2C single crystals that show strongly enhanced vortex pinning at the Néel temperature TN and low applied fields. The height of the observed Jc peak decreases with increasing magnetic field in clear contrast with that of the peak effect found at the upper critical field. We also performed angular transport measurements of Jc on this compound. They reveal the correlated nature of this pinning enhancement, which we attribute to the formation of antiphase boundaries at TN. [1]. (Figure 2)

This also lead to explore the lower temperature magnetic phase and TmNi2B2C that also has an Antiferromagnetic transition but at lower temperature and with a different crystallographic orientation. A manuscript is in preparation.

In parallel studies of the dynamic of vortices in parallel potential has allowed us to find a universal description including copper- and iron-based superconductors. Besides de minimum in the N values where E=C JN previously found we found a new regime that can be associated to the lock-in angle, this regime is characterized as maximum in N. Field dependence can be fitted reasonable well with models too. Interestingly the same qualitative behavior is found in iron based superconductors, measured in collaboration with IFW (Dresden). A manuscript is in preparation.

Lastly, our measurements in micro-bridges in clean samples have allow us to tailor superficial pinning by cutting some samples at arbitrary angles we were able to 'generate' new maxima in Jc.

We have studied the vortex dynamics in ferromagnetic superconductors and shown that vortices attract each other at large distances due to polarization of the magnetic moments. [2] Vortex clusters are then stabilized in the ground state for a low vortex density. The motion of vortex clusters driven by the Lorentz force excites magnons. These magnon excitations become unstable at a threshold velocity above which domain walls are generated for a slow relaxation of the magnetic moments. The domain walls modulate the vortex configuration. This underlying dynamics of vortices and magnetic moments can be probed by transport measurements. We also discuss a novel way to measure the spectrum of magnetic excitation in magnetic materials using motion of vortex lattice based on the present study [3].

We also found a new type of vortex pinning by enhancing the viscosity of vortex in magnetic superconductors with long relaxation time of magnetization and large magnetic susceptibility. [4] In the absence of current, vortices are dressed by nonuniform magnetic polarization and form vortex-polarons. Under a small current and consequently low Lorentz force, the magnetic polarization follows the vortex motion.(Figure 3) However, at long magnetic relaxation time of magnetization, there is additional dragging force by the magnetization besides the Bardeen-Stephen one, thus the effective viscosity of vortex is significantly enhanced resulting in suppression of dissipation. For a large current, the magnetic polarization cannot follow the vortex motion and the vortex-polaron dissociates, i.e. the magnetization and vortex become decoupled. In the IV characteristic, the decoupling transition shows as a voltage jump and can be identified as a depinning transition.

The polaronic pinning mechanism successfully explains the observed enhancement of critical current in the ErNiBC superconductor at low temperatures. The polaronic pinning can be optimized in magnetic-superconducting multilayers. [5] We show also that vortex-polaron creep is suppressed at low temperatures. [6,7]

Impact on National Missions

The work achieved in this project is related to the Laboratory's Energy Security mission and Materials for the Future science pillar. The knowledge and technical advances produced during this three-year project will aid the LANL materials community in devising ways to harness the functionality provided by a superconducting state in order to address applied energy problems.

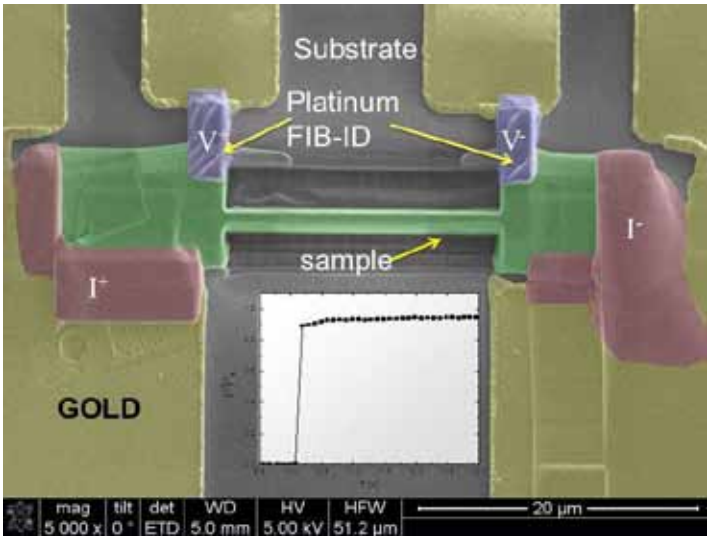

Figure 1. Scanning Electron Microscope image of a micro-bridge of ErBNiC fabricate using Focused Ion Beam. The inset shows the superconducting transition that is extremely sharp and has not suffered any degradation during the fabrication process. (the colors were added for visualization purpose).

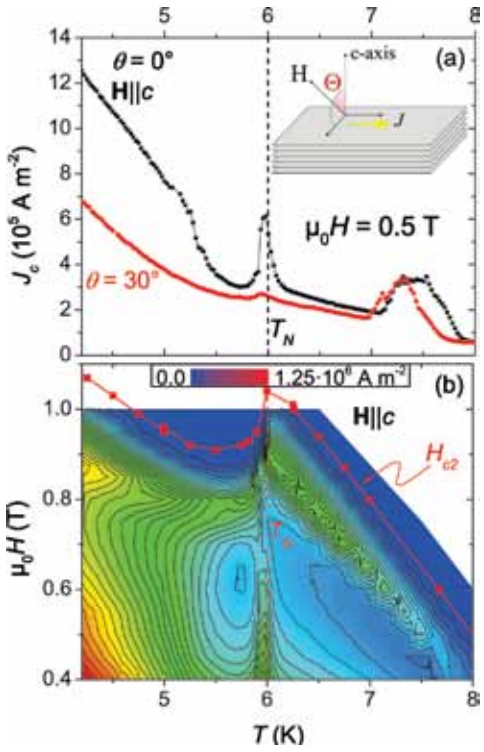

Figure 2. (a) Transport measurements of Jc for H || c and ϑ = 30◦ . A new peak in Jc is observed at T = TN for H || c. The sketch gives the measurement geometry. (b) Contour plot of Jc as a function of temperature and magnetic field H || c showing the field range where the peak at T = T_N is present.

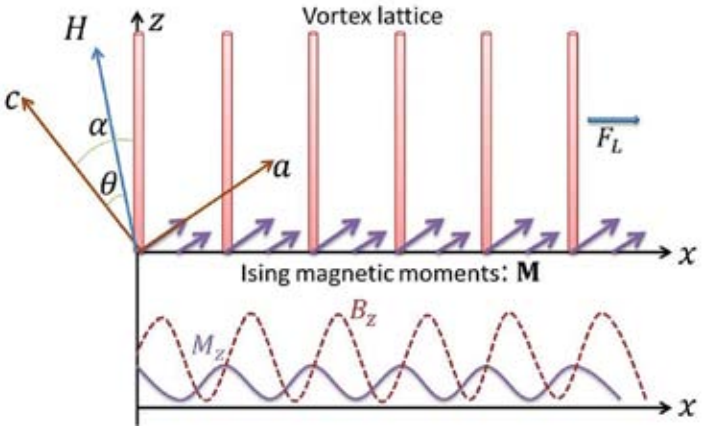

Figure 3. Schematic view of the vortex lattice in the presence of free Ising magnetic moments along the a axis. The vortex lattice is tilted from the applied magnetic fields in the ac plane due to the polarization of the magnetic moments. The vertical columns show the vortex cores. The polarized magnetic moments are nonuniform in space due to the spatial modulation of the vortex lattice magnetic field. Due to the Lorentz force vortices move along the x axis. In moving lattice, there is a phase shift between the magnetic induction (dashed line) associated with the vortex lattice and the magnetization (solid line) caused by the retardation in the response of magnetic moments to the vortex magnetic field.

References

1. Weigand, M., L. Civale, F. J. Baca, Jeehoon Kim, S. L. Bud'ko, P. C. Canfield, and B. Maiorov. Strong enhancement of the critical current at the antiferromagnetic transition in ErNi2B2C single crystals. 2013. Phys. Rev. B. 87: 140506(R).

2. Lin, S. –Z., L. N. Bulaevskii, and C. D. Batista. Vortex dynamics in ferromagnetic superconductors: Vortex clusters, domain walls, and enhanced viscosity. 2012. Phys. Rev. B. 86: 180506.

3. Lin, S. –Z., and L. N. Bulaevskii. Measuring spectrum of spin wave using vortex dynamics. 2012. Phys. Rev. B. 85: 134508.

4. Bulaevskii, L. N., and S. –Z. Lin. Prediction of Polaron-like Vortices and a Dissociation Depinning Transition in Magnetic Superconductors: The Example of ErNi2B2C. 2012. Phys. Rev. Lett.. 109: 027001.

5. Lin, S. –Z., and L. N. Bulaevskii. Enhancement of critical current density in superconducting/magnetic multilayers with slow magnetic relaxation dynamics and large magnetic susceptibility. 2012. Phys. Rev. B. 86: 064523.

6. N.Bulaevskii, L., and S. –Z. Lin. Self-induced pinning of vortices in the presence of ac driving force in magnetic superconductors. 2012. Phys. Rev. B. 86: 224513.

7. Bulaevskii, L. N., and S. -Z. Lin. Polaron-like vortices, dissociation transition and self induced pinning in magnetic superconductors. 2013. JETP. 144: 475.

8. Lin, S. –Z., C. Reichhardt, and A. Saxena. Manipulation of skyrmions in nanodisks with a current pulse and skyrmion rectifier. 2013. Applied Physics Letters. 102: 222405.

9. Lin, S. –Z., and L. N. Bulaevskii. Quantum motion and level quantization of a skyrmion in a pinning potential in chiral magnets. 2013. Applied Physics Letters. 88: 060404.

10. Solovyov, V. F., Q. Li, W. Si, B. Maiorov, T. J. Haugan, J. L. MacManus-Driscoll, H. Yao, Q. X. Jia, and E. D. Specht. Influence of defect-induced biaxial strain on flux pinning in thick YBa${}_{2}$Cu${}_{3}$O${}_{7}$ layers. 2012. Phys. Rev. B. 86: 094511.

Publications

Bulaevskii, L. N., and S. -Z. Lin. Polaron-like vortices, dissociation transition and self induced pinning in magnetic superconductors. 2013. JETP. 144: 475.

Bulaevskii, L. N., and S. Z. Lin. Prediction of Polaronlike Vortices and a Dissociation Depinning Transition in Magnetic Superconductors: The Example of ErNi2B2C. 2012. Physical Review Letters. 102 (2): 027001.

Bulaevskii, L. N., and S. –Z. Lin. Prediction of Polaronlike Vortices and a Dissociation Depinning Transition in Magnetic Superconductors: The Example of ErNi2B2C. 2012. Phys. Rev. Lett.. 109: 027001.

Lin, S. Z., and L. N. Bulaesvskii. Enhancement of critical current density in superconducting-magnetic multi-layers with slow magnetic relaxation dynamics and large magnetic susceptibility. 2012. Physical Review B. 86 (6): 064523.

Lin, S. Z., and L. N. Bulaevskii. Measuring spectrum of spin wave using vortex dynamics. 2012. Physical Review B. 85 (13): 134508 .

Lin, S. –Z., C. Reichhardt, and A. Saxena. Manipulation of skyrmions in nanodisks with a current pulse and skyrmion rectifier. 2013. Applied Physics Letters. 102: 222405.

Lin, S. –Z., L. N. Bulaevskii, and C. D. Batista. Vortex dynamics in ferromagnetic superconductors: Vortex clusters, domain walls, and enhanced viscosity. 2012. Phys. Rev. B. 86: 180506.

Lin, S. –Z., and L. N. Bulaevskii. Quantum motion and level quantization of a skyrmion in a pinning potential in chiral magnets. 2013. Applied Physics Letters. 88: 060404.

N.Bulaevskii, L., and S. –Z. Lin. Self-induced pinning of vortices in the presence of ac driving force in magnetic superconductors. 2012. Phys. Rev. B. 86: 224513.

Solovyov, V. F., Q. Li, W. Si, B. Maiorov, T. J. Haugan, J. L. MacManus-Driscoll, H. Yao, Q. X. Jia, and E. D. Specht. Influence of defect-induced biaxial strain on flux pinning in thick YBa2Cu3O7 layers. 2012. Physical Review B. 86 (09): 094511.

Weigand, M., L. Civale, F. J. Baca, Jeehoon Kim, S. L. Bud'ko, P. C. Canfield, and B. Maiorov. Strong enhancement of the critical current at the antiferromagnetic transition in ErNi2B2C single crystals. 2013. Phys. Rev. B. 87: 140506(R).

Novel Anti-Perovskite Electrolytes for Superionic Lithium Transport

Luc L. Daemen
20110139ER

Abstract

We proposed a novel class of superionic solid electrolyte made of lithium rich anti-perovskites (LiRAP) to work with metallic Li-anode and readily rechargeable cathodes. LiRAP solid electrolytes conduct Li+ ions well at high voltage and high current, providing much enhanced energy density and power capacity for the solid-state battery. The new materials can form rather adaptable solid solutions with immense Li+ vacancies and lattice imperfections in the crystal lattice for fast ionic transporting with low energy barriers. The Li+ mobility of the LIRAP increases to advanced superionic conduction as soft-phonon driven structural phase transitions occur at high temperatures. It overcomes current fluid electrolyte shortcomings of toxic leakage and short circuit burning and offers a much improved electrochemistry safety solution.

Background and Research Objectives

Developing clean and renewable energy is one of the most pressing tasks of humanity. Viability of sustainable energy depends on the effectiveness of electric energy storage (EES), manifested by the slow pace with which the petroleum fuel is replaced with electricity in today's vehicle transportation. High-performance batteries are hence essential for a clean-energy economy. However, the research and development of Li-based battery/capacitor materials for EES applications has progressed only incrementally for the last decade. Current technology of lithium ion battery (LIB) may meet some requirements for the emerging plug-in hybrid electric vehicle market, but provides unsatisfactory performance in terms of vehicle driving range and acceleration. The limitations are largely due to shortcomings of LIB's fluid electrolytes, especially their inability of pairing with a metallic lithium anode – an energy density booster with which a solid electrolyte could team up. Materials that possess superionic lithium conductivity and can serve as solid electrolytes hence have been long sought after. Such materials will have transformational and disruptive effect on the transportation battery market.

The project sought support to further develop our newly invented class of solid Li+ electrolytes for high performance batteries. Lithium-rich Li3OCl, Li3O(Cl,Br) and related anti-perovskites Li3-x-Mx/2O(A1-zA'z)1 (where A and A' are halogens at the dodecahedral site and M is a divalent metal doped at the octahedral vertex) are novel compounds that have been invented recently by the PIs (US & International patent pending; Zhao et al.) and have demonstrated 3D superionic conductivity, a broad working window, economic viability, and environmental friendliness in preliminary studies. These new materials can form rather adaptable solid solutions with immense Li+ vacancies and lattice imperfections for fast ionic transport. The novel anti-perovskites can accommodate a large number of mobile Li+ ions in the crystal lattice with a low energy barrier for ionic hopping. The ionic mobility increases to advanced superionic conduction as phonon-softening structural phase transition occurs at high temperature.

Scientific Approach and Accomplishments

Summary of third-year and project accomplishments:

Synthesis of a solid, Li-rich electrolyte with the anti-perovskite structure for battery and other electrochemical devices such as supercapacitors. Several synthetic routes were developed: solid state reaction, high-pressure, "wet" synthesis in ionic liquids.

Clarification of the synthetic mechanism and identification of defect phases forming during the synthesis. Post-processing to eliminate non-perovskite phases.

Replacement of oxygen by sulfur to obtain novel Li3SX anti-perovskites (X=halogen) similar to the superionic conductor Ag3SX. Aliovalent doping of the sulfur phases. The new class of sulfur-based materials is of importance to sulfur-based baterries (anodes and cathodes). Chemical synthesis, thermal analysis, crystallography, and

electrochemical properties of these new compounds. Most notably, Li3SF was synthesized when attempts at making Li3OF failed. Fluorine is less volatile than Cl or Br in these compounds. The new fluorine-based material will be much more stable for battery applications.

Development and characterization of layered antiperovskites, Li7O2X3 (X=halogen) with higher Li ionic conductivity.

Synthesis of the first set of hybrid, organic-inorganic antiperovskites: Li5O(TP)X where TP = terephthalate anion and X = halogen. These materials, inspired from the parent compounds, are much less moisture-sensitive than the inorganic anti-perovskites. We are partnering with MPA-11 to examine their use in Li air batteries.

Deposition of the first multilayer structures by pulsed laser deposition from a Li3OCl target and characterization of these structures. Important step toward device fabrication.

Electrochemical study of the electrolyte/lithium metal interface to assess the chemical compatibility of lithium anodes (high-energy and high-power density) with the new anti-perovskite electrolytes.

Durability studies on the long term effects of current flow in the antiperovskite electrolytes.

Several difficulties arose, particularly the appearance of non-perovskite phases during the synthesis. These phases blocked Li transport and decreased ionic conductivity. Two post-processing methods were developed to overcome this difficulty. This resulted in a gain of an order of magnitude in Li conductivity.

Highlight: Durability studies (3rd year)

The effects of long term ionic current flow on Li3OCl durability were studied in an electrochemical cell comprising of a pressed pellet of the material between two flat electrodes made of solid lithium. The current was generated by applying triangular wave voltage with an amplitude of ±5 V and 100 mV s 1 sweep rate (cyclic voltammetry) or a constant voltage of up to ±4 V (chronoamperometry) between the electrodes. Full electrochemical characteristic of the cell was measured at specific time intervals using electrochemical impedance spectroscopy.

Cyclic voltammetry was performed at several temperatures ranging from 70 °C to 160 °C. Irrespective of temperature, the measured current initially increased, reaching its maximum value after 20 to 40 cycles (1 - 2 hrs) and then decreased following an approximate logarithmic relationship versus time. The initial current increase most likely originated from establishing a uniform contact between the pellet and the electrodes. We found that the electrical charge passed rather than time elapsed was responsible for the observed current decrease, since the current after a several hour break was typically returning to its value measured before the break. In some cases, even a partial current recovery was observed.

The impedance spectroscopy experiments performed at various temperatures and bias voltages revealed that the Li|Li3OCl|Li cell is best represented by an equivalent circuit comprising of two independent circuits in series corresponding to the electrolyte and its interface(s) with lithium electrode(s) (Figure 1). The circuit representing the electrolyte was further divided into two sub circuits corresponding to the bulk material (resistance R2 and capacitance C1) and its grain boundaries. The latter are best described as a resistor (R4) in parallel with either constant phase element (CPE1) or a pure capacitor. On the other hand, the Li|Li3OCl interface is best represented by a capacitor describing the respective electrical double layer (C3) in parallel with a resistor (R3) characterizing the charge transfer reaction. The transport phenomena associated with the charge transfer, typically described as a Warburg element (Wo), were found negligible under all conditions studied.

While the gradual current decrease following the initial period seemed concordant with the visible formation of a grayish deposit on the surfaces of lithium electrodes facing the solid electrolyte and possible electrode passivation, no proof for such a hypothesis was obtained from electrochemical impedance spectroscopy. We found that the main source of the gradual increase in the overall cell impedance during cyclic voltammetry was not the deposit formed on the electrode surfaces but an increase in the material grain boundary resistance. For instance, in a ~100 hour long experiment at 120 °C with a 1.70 mm x 1 cm (thickness x diameter) Li3OCl pellet the following time independent parameters were obtained: (3.8 ± 0.9) x 105 Ohm for the bulk material resistance, (7.8 ± 2.8) x 10 10 for the grain boundary constant phase element and 0.74 ± 0.04 for its exponential, (4.8 ± 0.1) x 10 11 F for the cell electrical capacity, and (2.4 ± 0.2) x 10 10 F for the Li|Li3OCl double layer capacity. During that time, the grain boundary resistance increased more than two times from (7.3 ± 2.2) x 105 Ohm to (1.8 ± 0.3) x 106 Ohm (Figure 2).

Local “melting” leading to a smaller contribution of the grain boundaries in the measured cell impedance or restructuring of the grain boundaries can be postulated at temperatures ≥ 140 °C. The effect is manifested by a decrease in the measured capacitance of grain boundaries with temperature and by a significant decrease in the grain boundary resistance. The phenomenon has a stronger ef-

fect on the cell impedance than the decrease of the bulk material resistance. For instance, after ~36 hours of cyclic voltammetry at 140 °C and 160 °C, the grain boundary resistance for a 3.56 mm x 1 cm (thickness x diameter) pellet was found to be approximately 10 times lower at 160 °C than at 120 °C, whereas the respective ratio of the bulk material resistance was only ~3.2 (Figure3).

Impact on National Missions

Impact on energy security, industrial partnership with national laboratories, basic research in functional materials and across length scales.

Research on anti-perovskites is now being actively pursued at the University of Texas, Austin in the laboratory of John Goodenough (the inventor of the lithium battery), at the University of Nevada - Las Vegas, and by a private company, Pathion, Inc. based in the Bay Area. A UNLV student is currently pursuing his PhD research on anti-perovskite electrolytes at LANSCE.

Early in 2012, an ARPA-E proposal to develop devices based on the materials developed in the LDRD-ER project was submitted to DOE with a view to short-term commercialization of the electrolyte materials developed at LANL. The proposal was approved by DOE-ARPA-E and research and development under this proposal started a few months ago. The industrial partners are K2Energy and Pathion.

The LDRD-ER project played its intended role perfectly in providing seed funding to develop a novel product. The work done under LDRD-ER funding allowed very clearly for the continuation, extension, and growth of this project with other universities and industrial partners.

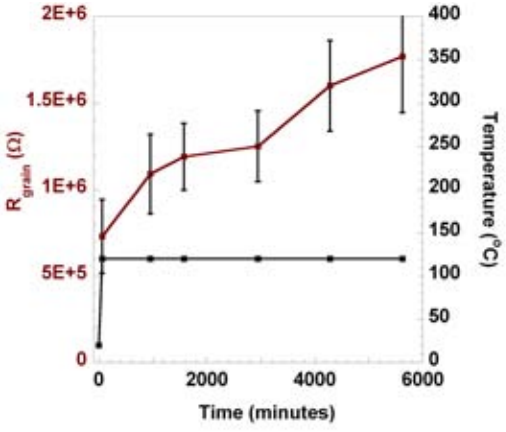

Figure 1. Equivalent circuit of a Li|Li3OCl|Li cell

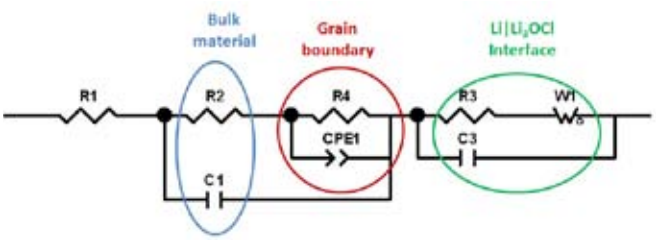

Figure 2. Li3OCl grain boundary resistance as a function of time of voltage cycling between +5 V and 5 V at 120 °C

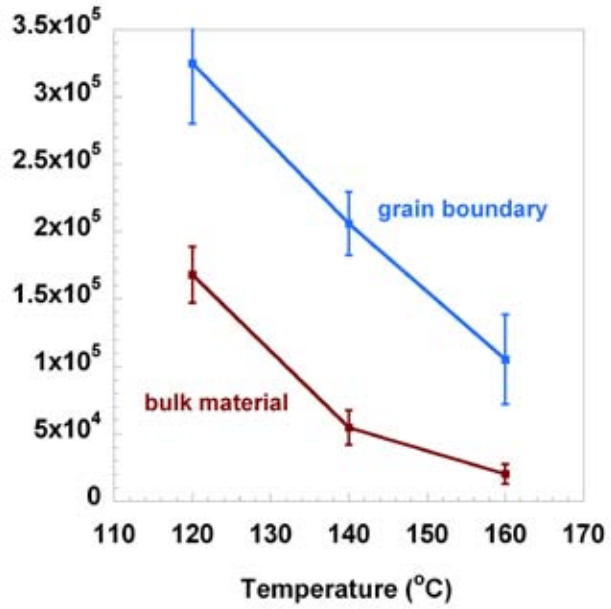

Figure 3. Grain boundary and bulk material resistance of Li3OCl versus temperature for a sample that underwent ~36 hours of voltage cycling between +5 V and 5 V in a Li|Li3OCl|Li cell at 140 °C and 160 °C.

Publications

Xia, C., L. Li, Y. Tian, Q. H. Liu, Y. C. Zhao, L. J. Jia, and Y. D. Li. A high performance composite ionic conducting electrolyte for intermediate temperature fuel cell and evidence for ternary ionic conduction. 2009. JOURNAL OF POWER SOURCES. 188 (1): 156.

Zhao, Y. S., and L. L. Daemen. Superionic Conductivity in Lithium-Rich Anti-Perovskites. 2012. JOURNAL OF THE AMERICAN CHEMICAL SOCIETY. 134 (36): 15042.

Quasiparticle Scattering for Multiscale Modeling of Electronic Materials

Sergei Tretiak
20110212ER

Abstract

This research program promises to develop new theoretical methodologies allowing the quantum chemical techniques that have proven themselves in providing accurate and adequate results in intermediate size molecules to be extended to the world of macromolecules and superstructures. Consequently, the range of treatable molecular systems are to be extended from ~1,000 atoms to at least 10,000-100,000 atoms sized nanostructures, without any substantial information loss or accuracy compromise. The theoretical modeling efficiently uses previously LANL-developed quantum chemical tools, which outperform similar techniques world-wide (Tretiak and Piryatinski). Close synergistic interactions with experiment at LANL and word-wide allow disseminating theoretical findings.

Background and Research Objectives

A quantitative understanding of matter at the nanoscale is a grand-challenge for theory. Over the years, electronic structure calculations, such as density functional theory (DFT), transformed theoretical chemistry, surface science and materials physics and have created a new ability to describe the electronic structure and interatomic forces in molecules with hundreds of atoms. Still, these calculations require atomistic information (electrons and orbitals). Consequently, numerical cost is high, effectively limiting the range of treatable systems by ~1000 atoms. On the other hand, design of functional nanostructures such as photovoltaic unit or nanoscale electronic chip, requires quantum-mechanical modeling of extended systems with millions atoms in size. This challenge calls for development of multiscale approaches. Notably, any reduction of computational complexity is highly non-trivial, since we need to take an advantage of complex quantum-mechanical phenomena, such as delocalized wavefunctions, quantum confinement, and coherences, to achieve new functionalities. In this project we will develop theoretical framework based on the quasiparticle scattering concept, which would allow multiscale modeling of electronic properties on nanomaterials with limited numerical effort. Our theory bridges traditional molecular description (spatially confined wavefunctions, orbitals) with solid-state physics picture (periodic delocalized wavefunctions, quasiparticles) and directly addresses nanostructures spanning intermediate sizes. Scattering calculations include two steps: i) conventional quantum-chemical calculations and/or analysis of experimental data of simple molecular fragments (building blocks ~10-100 atoms in size) to retrieve the quasiparticle properties; and ii) applying scattering theory to large nanostructures to obtain electronic properties of interest. The resulting numerical effort scales cubically with the number of molecular building blocks (not electrons!) in the superstructure.

Scientific Approach and Accomplishments

In the course of this project we have formulated the theoretical foundation of the Exciton Scattering (ES) methodology as illustrated in Figure 1, and have applied this approach to many important electronic materials. First of all, we have applied the ES approach to understand excited-state structure of donor and acceptor substituted conjugated oligomers [1]. Intuitive relationships between the substituent's electron withdrawing or donating ability and the ES parameters have been established. A good agreement of the absorption spectra between the ES approach and the reference quantum-chemical computations demonstrates that the ES approach is qualified for such conjugated push-pull systems [1]. Secondly, we have extended the ES method to include symmetric triple and quadruple joints that connect linear segments on the basis of the phenylacetylene backbone [2]. The obtained scattering matrices that characterize these vertices are used in application of our approach to several test structures, where we find excellent agreement with the transition energies computed by the reference quantum chemistry. We introduce topological charges, associated with the scattering matrices, which help to formulate useful relations between the

number of excitations in the exciton band and the number of repeat units [2,3]. The obtained features of the scattering phases are analyzed in terms of the observed excited state electronic structure [2]. To treat more complicated molecular systems using sophisticated ab initio approaches we have introduce a Natural Atomic Orbital representation to be used with the ES theory, which has broadly expanded applications of our multiscale techniques to a variety of new materials [4].

We further formulated a universal multiscale scattering approach. The scattering equations have been re-formulated in terms of an effective tight-binding model, which is a Hamiltonian describing the parent scattering problem [5]. We further built into this Hamiltonian coupling to phonons and defects (following many previous solid state studies). Electron-vibrational couplings have been extracted from the conventional quantum chemical calculations as we routinely did previously for many molecular systems such as polymers and carbon nanotubes. Such reduced description (an effective lattice model), can be numerically solved, while it retains the accuracy sufficient to describe electronic properties of the material in question. The lattice model has been successfully tested on several molecular systems containing disorder/defect effects and exciton-phonon interactions [6]. The outline of developed methodology as well as our numerous applications to organic electronic materials has been summarized in a large review article to appear in the Accounts of Chemical Research journal [7].

Our scattering model is not limited to organic molecules since it provides a universal description of electronic processes in many nanoscale materials. We have implemented our interband exciton scattering model into a numerical code to simulate the processes of carrier multiplication (CM) (also referred in the literature as the multi-exciton generation) in narrow gap, PbSe and PbS, nanocrystal quantum dots. Using this approach we have performed a systematic study of the CM pathways (as illustrated in Figure 2a,b) in these materials [8,9]. Two fundamentally different processes of multiple-exciton photogeneration (Figure 2a) and subsequent phonon assisted cooling (Figure 2b) are investigated and their contributions to the CM quantum efficiency are determined. The analysis shows that the exciton scattering induced impact ionization dynamics is the main mechanism responsible for the CM during both the photogeneration and the population relaxation events. The results provide insight into experimental data reported in the literature. Another fundamental question that has been addressed in our study is the spectroscopic signatures of the interband exciton scattering and the Coulomb correlations that lead to this process. We have used our exciton scattering theory to calculate the nonlinear coherent response to a sequence of three ultrafast optical pulses and specifically focused on the so-called double-quantum coherence technique, which is proved to be sensitive to the carriers correlations [10]. Finally, we have investigated the exciton collective behavior in ensemble of semiconductor quantum dots interacting through delocalized plasmon mode (Figure 2c). In this situation exciton collective behavior can lead to the formation of spontaneous coherence and under certain conditions the superradiant states as shown in Figure 2d [11].

Impact on National Missions

First and foremost our project upon completion will provide novel computational capabilities critical for understanding light-induced dynamics in many technologically relevant nanostructures. Consequently, we envision extremely broad applications of developed tools, relevant to the current and future LANL/DOE missions. Our project primarily addresses Energy and Earth Systems LANL Grand challenge by providing computational means for molecular materials suitable for clean energy (solar energy capture and energy storage). Secondly, it strongly relates to Materials: Discovery Science to Strategic Applications challenge by discovering emergent phenomena in complex systems. Consequently, proposed activities have potential for extending our program through LANL, and will place us in the excellent position to respond to incoming National Initiatives in energy and materials, particularly BES calls.

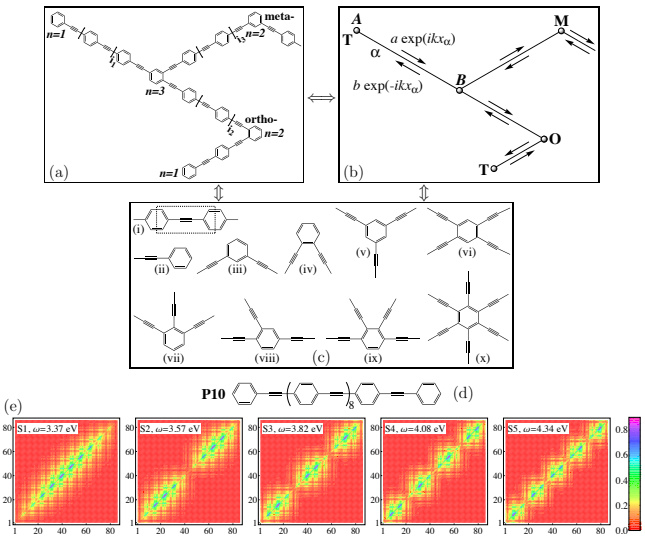

Figure 1. Illustration of the Exciton Scattering (ES) approach. (a) structure of a conjugated molecule; (b) exciton scattering picture on the quasi-1D graph of the molecule; (c) building blocks of phenylacetylene (PA) molecules; (d) linear PA molecule consists of 10 repeat units; (e) exciton-scattering patterns given by the contour plots of transition density matrices from ground state to excited state in the molecule shown in (d).

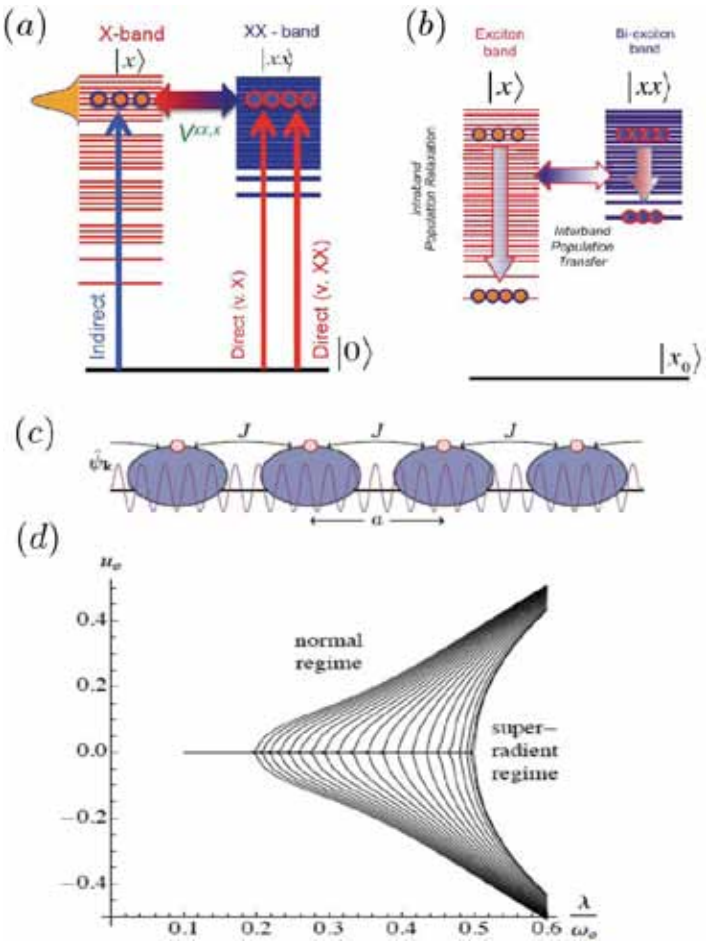

Figure 2. Investigated pathways of the exciton scattering leading to the carrier multiplication processes in semiconductor quantum dots. (a) Indirect and direct photogeneration processes. (b) Population relaxation and Interband population transfer. (c) Semiconductor quantum dots (red) topping metal ellipsoids (blue) whose collective surface-plasmon modes lead to the interaction between the excitons in the quantum dot. (c) Phase diagram showing formation of the exciton superradiant states.

References

1. Li, H., C. Wu, S. Malinin, S. Tretiak, and V. Chernyak. Excited States of Donor and Acceptor Substituted Conjugated Oligomers: a Perspective from the Exciton Scattering Approach. 2010. Journal of Physical Chemistry Letters. 1: 3396 .

2. Li, H., C. Wu, S. Malinin, S. Tretiak, and V. Chernyak. Exciton Scattering on Branching Centers in Conjugated Molecules. 2011. Journal of Physical Chemistry B. 115: 5465 .

3. Catanzaro, M., T. Shi, S. Tretiak, and V. Chernyak. Topological properties of scattering matrices on graphs: counting the number of standing waves in quasi-one-dimensional systems. Physical Review Letters.

4. Li, H., V. Chernyak, and S. Tretiak. Natural Atomic Orbital Representation for Optical Spectra Calculations in the Exciton Scattering Approach. 2012. Journal of Physical Chemistry Letters. 137: 9245 .

5. Li, H., C. Wu, S. V. Malinin, S. Tretiak, and V. Chernyak. Effective tight-binding models for excitons in branched conjugated molecules. 2013. Journal of Chemical Physics. 139: 064109.

6. Li, H., M. Catanzaro, S. Tretiak, and V. Chernyak. Analytical properties of exciton scattering in conjugated molecules and chemistry of substituents. Journal of Physical Chemistry Letters.

7. Li, H., C. Wu, S. V. Malinin, S. Tretiak, and V. Chernyak. Exciton scattering approach for optical spectra calculations in branched conjugated macromolecules. To appear in Accounts on Chemical Research.

8. Velizhanin, K. A., and A. Piryatinski . Numerical Study of Carrier Multiplication Pathways in Nanocrystalline and Bulk Forms of PbSe. 2011. Physical Review Letters. 106: 207401.

9. Velizhanin, K. A., and A. Piryatinski . Probing Interband Coulomb Interactions in Semiconductor Nanostructures with 2D Double-Quantum Coherence Spectroscopy . 2011. Journal of Physical Chemistry B. 115: 5372.

10. Velizhanin, K. A., and A. Piryatinski. Numerical analysis of carrier multiplication mechanisms in nanocrystalline and bulk forms of PbSe and PbS. 2012. Physical Review B. 86: 165319.

11. Bittner, E. R., A. Piryatinski, and D. Dunlap. Thermodynamics of exciton collective behavior. Nano Letters.

Publications

Bittner, E. R., A. Piryatinski, and D. Dunlap. Thermodynamics of exciton collective behavior. Nano Letters.

Catanzaro, M., T. Shi, S. Tretiak, and V. Chernyak. Topological properties of scattering matrices on graphs: counting the number of standing waves in quasi-one-dimensional systems. Physical Review Letters.

Li, H., C. Wu, S. Malinin, S. Tretiak, and V. Chernyak. Excited States of Donor and Acceptor Substituted Conjugated Oligomers: a Perspective from the Exciton Scattering Approach. 2010. Journal of Physical Chemistry Letters. 1: 3396 .

Li, H., C. Wu, S. Malinin, S. Tretiak, and V. Chernyak. Exciton Scattering on Branching Centers in Conjugated Molecules. 2011. Journal of Physical Chemistry B. 115: 5465 .

Li, H., C. Wu, S. V. Malinin, S. Tretiak, and V. Chernyak. Effective tight-binding models for excitons in branched conjugated molecules. 2013. Journal of Chemical Physics. 139: 064109.

Li, H., C. Wu, S. V. Malinin, S. Tretiak, and V. Chernyak. Exciton scattering approach for optical spectra calculations in branched conjugated macromolecules. To appear in Accounts on Chemical Research.

Li, H., M. Catanzaro, S. Tretiak, and V. Chernyak. Analytical properties of exciton scattering in conjugated molecules and chemistry of substituents. Journal of Physical Chemistry Letters.

Li, H., V. Chernyak, and S. Tretiak. Natural Atomic Orbital Representation for Optical Spectra Calculations in the Exciton Scattering Approach. 2012. Journal of Physical Chemistry Letters. 137: 9245 .

Velizhanin, K. A., and A. Piryatinski. Numerical analysis of carrier multiplication mechanisms in nanocrystalline and bulk forms of PbSe and PbS. 2012. Physical Review B. 86: 165319.

Velizhanin, K. A., and A. Piryatinski . Numerical Study of Carrier Multiplication Pathways in Nanocrystalline and Bulk Forms of PbSe. 2011. Physical Review Letters. 106: 207401.

Velizhanin, K. A., and A. Piryatinski . Probing Interband Coulomb Interactions in Semiconductor Nanostructures with 2D Double-Quantum Coherence Spectroscopy . 2011. Journal of Physical Chemistry B. 115: 5372.

Solving the Active Site Conundrum in Oxygen Reduction Catalysis

Piotr Zelenay
20110236ER

Abstract

Given the extremely volatile and generally very high price of Pt and other noble metals over recent years, the development of non-precious metal fuel cell electrocatalysts that meet the Department of Energy targets of high volumetric activity (330 A/cm3) and long-term stability (5,000 hours with cycling) would significantly accelerate energy independence and environmentally benign energy technologies. While non-precious metal catalysts for oxygen reduction reaction (ORR) have been studied for decades, with only incremental improvements made in the total activity, the active catalytic site in such materials remains unknown. LANL-sponsored research, involving pyrolyzed graphitic-metal-nitrogen species, has produced catalysts with the highest activity/durability/selectivity ever reported in non-precious metal electrocatalysis. A focused theoretical and experimental effort has been applied to develop science-based structure-activity relations for these poorly understood and difficult-to-characterize systems. Atomistic modeling was employed in synergy with complementary experimental characterization techniques (electrochemistry, electron paramagnetic resonance, nuclear resonance vibrational spectroscopy and Mößbauer) to elucidate the nature of the active site of non-precious ORR catalysts including structure-property relations, and to employ LANL expertise in synthesis and characterization to develop a non-precious metal catalyst that possesses optimized ORR activity.

Background and Research Objectives

The cost of a Pt cathode oxygen reduction reaction (ORR) catalyst represents the greatest challenge for large-scale introduction of polymer electrolyte fuel cells (PEFCs) for automotive transportation. Except for precious-metal "thrifting" (already close to its limit), replacement of Pt with non-precious metal ORR catalysts is the sole viable solution. Significant progress has been achieved within the past decade with heat-treated N-Metal-C catalysts but closing the gap between non-precious metal and Pt-based ORR catalysts is unlikely to happen without "molecular-level" insight into the structure of the active site(s) and knowledge-based design of future catalysts.

These catalytic systems, derived from polyaniline (PANI) salts of Fe and/or Co, and high surface-area carbon in a high temperature process at ca. 900°C have been shown to possess the field-leading ORR activity (Figure 1). However, for non-precious catalysts to become practical, the activity needs to be improved by approximately 0.1 V, to the level exhibited by Pt-based oxygen-reduction catalysts (blue plot in Figure 1). In order to proceed at a rate faster than traditional Edisonian methods, this will require learning what the active site in these materials is such that design principles can be devised to optimize active site exposure and concentration. Since characterization of the species involved in non-precious metal catalysis is challenging, by virtue of the extreme conditions involved during synthesis, we applied molecular modeling techniques in concert with experimental characterization.

Experimentally, our objective in this project was to transform bulk characterization techniques, e.g., EPR, NRVS, and Mößbauer, into surface-specific tools by using gas surface probes (NO, alkyl peroxides). Molecular modeling provides a powerful complement to these experiments.

Scientific Approach and Accomplishments

Our focus in this work was to determine features of the ORR active site in the non-precious metal catalysts to use as a basis for future rational design of new active site centers that lead to minimal H2O2 production while facilitating high activities and reduction potentials for the four-electron path. Our research approach was to use stochastic search techniques to provide a "short-list" of hypothetical active sites via molecular modeling, and then to calculate, using quantum mechanics, their

associated spectroscopic signatures and theoretical oxidation/reduction reaction activity. This latter activity was calculated from the energy barriers connecting the necessary intermediate states along the reaction path from O2 through to H2O and H2O2. The spectroscopic signatures and active-site configurations were then compared with those obtained using the NRVS (nuclear resonance vibrational spectroscopy) technique, EPR (electron paramagnetic resonance) and Mößbauer spectroscopy.

Next, we present the synthesis of the electrocatalysts and the results of the experimental characterization work. Then we describe the modeling efforts and summarize the findings.

Synthesis of Optimized Electrocatalysts

Commercial carbon blacks were used as supporting materials in polyaniline (PANI-Fe) and cyanamide (CM-Fe) catalysts synthesis. In a typical approach [1-6], carbon supports were treated in hydrochloric acid for 24 hours, to remove metal impurities, and oxidized in 70% nitric acid at 80°C for 8 h for oxygen functionalization. 57FeCl3 and 57Fe(CH3COO)2 were used as iron precursors in PANI-Fe and CM-Fe catalyst synthesis, respectively.

Addition of Chemical Probe Species (NO)

As-prepared Fe catalysts were electrochemically reduced in an O2-free wet box, as shown in Figure 2, to reduce Fe(III) to Fe(II), facilitating binding of NO onto Fe(II) sites. 0.5 M H2SO4 and DI-water were used to purify the NO before it entered the glove bag for NO treatment. Teflon-sealed vials containing solid-state Fe samples were put into a N2-purged polyethylene foil glove-bag and NO flow was connected into the vials by using needles. As the NO adsorption onto Fe sites is rapid, the duration of NO treatment was around 2 min. Then the NO-treated Fe catalysts samples were stored in a liquid N2-filled container and shipped to the Advanced Photon Source (APS) at Argonne National Laboratory and the University of Rochester for NRVS and Mößbauer spectroscopy, respectively.

Electron Paramagnetic Resonance (EPR) and Diffuse Reflectance Infrared Fourier Transform Spectroscopy (DRIFTS)

Six samples of oxidized, reduced and NO-exposed PANI-Fe and CM-Fe catalysts were measured by electron paramagnetic resonance (EPR) spectroscopy showing a signal at g of ca. 4.3 from Fe3+ in a distorted octahedral symmetry [7]. The EPR measurements did not show clear evidence of NO adsorption. One difficulty was the presence of significant bulk Fe that resulted in low sensitivity, obscuring detection of surface Fe. Six new catalysts samples with a smaller concentration of Fe were measured. As seen previously, all samples showed a signal at g = 4.3, as before. The position does not shift significantly for the different samples, indicating there is no significant change in the local environment. Subtracting the spectra of the NO-adsorbed sample from the spectra of the reduced sample yields a weak signal with a hyperfine pattern that could be representative of Fe-NO. However the signal is not clearly distinguishable from background and so not definitive evidence of Fe-NO interaction (Figure 3a).

Diffuse reflectance infrared Fourier transform spectroscopy (DRIFTS) results show changes in the carbon matrix as evidenced by the C≡C peak, and the FTIR results display changes in OH concentration, presumably related to changes in surface chemistry (Figure 3b). There are no absorbance bands evident around 600 cm-1 as expected for Fe-NO, based upon NRVS (below).

The Raman results are typical of graphite samples [8] but do not directly inform about Fe-NO interactions. (Figure 3c,d) The data have been normalized to the G-peak at 1600 cm-1, and this highlights the increase of the D-peak in the reduced and NO absorbed samples. The intensity increase of the D-peak is typical of increasing disorder in the carbon matrix [9]. These studies highlight the challenge in interrogating these non-precious metal catalysts using standard spectroscopy.

Mößbauer Spectroscopy

The 80K 57Fe Mößbauer spectrum of as-prepared CM-Fe-C is shown in Figure 3e-A. Three sextet species are present in as-prepared CM-Fe-C representing ca. 40% of all the iron present with the major sextet species consistent with the formation of bulk iron nitride, FexN. A singlet iron species is also present, previously assigned in PANI-Fe-C to superparamagnetic iron. The remaining iron species (ca. 54%) are well fit by a sum of three doublet iron species consistent with the formation of mono- and/or dimeric iron. Such species are predicted by molecular modeling as strong candidates for the active site. The overall Mösßbauer spectrum, as well as the individual sextet and doublet species present in CM-Fe-C are distinct from those previously identified in PANI-Fe-C, indicating the effect of changing the nitrogen precursor molecule.

Electrochemical reduction of as-prepared CM-Fe-C has a dramatic effect on iron speciation as shown by the changes in the spectrum (Figure 3e-B). Detailed analysis of individual contributions to the Mößbauer spectrum indicated the presence of the same three sextet species and the same singlet species upon reduction. A significant change in the doublet iron species was observed. The change required four doublet species in order to obtain a reasonable fit. Changes in the iron speciation upon reduction occur only within the mono- and dimeric iron doublet species. The

presence of a large isomer shift in the doublet due to the high velocity shoulder on the sextet feature at ca. 3 mm/s is consistent with a high-spin iron(II) species. Upon reduction, the amount of sextet (ca. 54%) and singlet (ca. 9%) iron increased while the amount of doublet iron (ca. 37%) decreased.

Treatment of electrochemically reduced CM-Fe-C with NO was performed in order to evaluate the presence of surface or near-surface, gas-accessible iron species. The Mößbauer spectrum of NO treated CM-Fe-C (Figure 3e-C) exhibits changes in the doublet Mößbauer intensity relative to reduced catalysts, consistent with the perturbation of iron species due to NO treatment. No changes are observed in the sextet or singlet species. NO treatment leads to a change in the doublet iron speciation consistent with the presence of gas accessible reduced iron species. As NO is an analog for O2 for iron ligation, such gas-accessible iron sites should also be capable of binding O2 during ORR.

Nuclear Resonance Vibrational Spectroscopy (NRVS)
The 57Fe samples prepared from optimized PANI-Fe and CM-Fe fuel cell catalysts were analyzed at APS for NRVS activity. This technique provides the unique ability to probe vibrational spectra based upon the environment of specific isotopes, in this case 57Fe, and thus avoids the challenges of optical spectroscopy. The use of NO provides a way to distinguish bulk from surface. Two sets of NRVS spectra were obtained according to two allocations of the competitive beam-time: June 2011 and April 2013 (Figure 4). In both cases there was observed a change in iron speciation upon reduction, whereas NO adsorption resulted in weak changes. It was suggested that NO photolysis may be the cause of the weak signal, as multiple scans lead to a reduced difference spectrum. Strategies to overcome these challenges have been proposed, but beam-time did not permit further measurements. In the first analysis (June 2011), a difference spectrum led to a significant peak around 600 cm-1, which was identified using density functional theory (below). However, in the repeat experiment in April 2013, this spectral feature was not observed, possibly due to NO photolysis.

Modeling and Simulation
Previous experimental results implied that a positive correlation between carbon graphitization, i.e. the C-sp2/sp3 ratio, and activity of synthesized NPMC [10]. Hence, the model system adopted was a graphene "flake" (Figure 5a). This system consisted of 96 C-atoms (before vacancies) and contained zig-zag and armchair H-coordinated edges, allowing the simulation of bulk and edge effects. Based on typical values for N and M concentrations used in NPMC synthesis [3] we inserted 8 N and 2 M atoms into the model system. Calculations were performed using semi-empirical PM6 calculations [11] as implemented in Gaussian '09 [12]. PM6 allowed very rapid energy calculation. A handful of systems were tested using density functional theory [13-17] to help benchmark the accuracy of the relative energies emerging from the PM6 calculation. The Metropolis Monte Carlo algorithm [18] was implemented to screen the results. The flake was kept overall neutral in charge and the spin-state was set to a singlet state and random substitutions of C for vacancies, N or Fe atoms were made. The energies of these random systems were evaluated using PM6. According to Metropolis Monte Carlo, a random perturbation (i.e. atom substitution or swap) from the currently selected structure was accepted if the following criterion was met: $-\Delta E/kT > \ln \mu$ where μ is a random number between 0 and 1. This method, combined with the generation of random initial structures studied in parallel, provided a robust method for exploring active-site configurational space.

One prediction of the semi-empirical potential model was the restructuring of C to form cyclopentane and larger C rings at C vacancy sites (see Figure 5b). These structures are known to be the stable vacancy structures in 2-D C systems [18-20], thus validating our computational method. Examination of the local atomic arrangements about the M (Fe) atoms in the model system shows that Fe clustering at 2nd nearest neighbor sites is thermodynamically preferred (Figure 5c,d). In this cluster, a local N atom (or, in other cases, a C atom) was perturbed from its intermediate lattice site, becoming a bridge atom linking two Fe atoms. N bridged Fe clusters were more stable than C bridged Fe clusters. The consideration of N- or C-bridged binuclear site as the NPMC active site was unexpected and contributes significantly to the literature on this topic, as most hypothesized active sites are based on the "heme" Fe-N4 center. The site we have elucidated has several catalytic advantages: if breaking of the O-O bond is to occur (dissociative ORR pathway) then having two sites in close proximity that can coordinate the O-O bond from each side is advantageous. Furthermore, these sites will be templated by the graphitic network itself. Another motif based on our search is the clustering of vacancies, N atoms, and the bridged two-Fe structures and the apparent preference of these clusters to be positioned close to the flake edge. For this reason, we suggest that active sites will be much more prevalent and accessible at edge-sites of the graphitized carbon matrix.

The motifs, identified and described, above have served as starting points for more accurate, but computationally intensive, DFT studies and further optimization. The stability of vacancies, N-coordinated vacancies, and Fe binding on these defects was studied on 1-D graphene nanorib-

bons as a function of distance from the nanoribbon edge [21]. It was found that N coordination stabilizes the local Fe defect and that such defect complexes were most stable near the edge. These findings are important for catalysis in two respects: (1) N is important in that it stabilizes the Fe defect leading to higher concentrations of these assumed active sites and (2) these sites are most abundant near the ribbon edge where they are most accessible, leading to less transport limited active sites. In addition, by moving a pair of N-coordinated Fe edge defects closer together, it was determined that Fe does prefer to cluster. Using a consistent thermodynamic model, we compared relative stability of nitrogen-coordinated transition-metal atom defects at graphene edges. We have found that the most stable structure is dependent on the nitrogen and transition-metal chemical potential and so, precursors and processing conditions are likely to change the structures that are formed. This theoretical model establishes a direct link between synthesis conditions (N-rich versus Fe-rich) and the molecular products obtained.

By performing a phonon analysis, we determined the vibrational modes of active site candidate structures with NO ligands and discovered that the Fe-NO bond stretch is dependent upon the local nitrogen coordination of the transition metal. The calculated frequencies for the FeN3 active sites agreed well with the experimentally determined Fe-NO bond stretch frequency (using Nuclear Resonance Vibrational Spectroscopy, NRVS, in the June 2011 experiment) while the frequency of FeN4 sites did not.

Impact on National Missions

The development of alternative energy systems is an important component of the current Laboratory mission, as outlined in the LANL Grand Challenge in Energy and Earth Systems. In particular the Grand Challenge calls for "advances in prediction and controlling atom motion and electron distribution", as well as "fundamental advances in […] devices for harvesting, storing and converting energy." Furthermore, the connection between materials structure and ultimate activities relates to the Grand Challenge in Materials to exercise "intentional control of functionality through discovery and application of fundamental materials properties […] from the molecular level." In the current work, we have significantly advanced the molecular level understanding of the operation of these non-precious metal fuel cell catalysts, highlighting a path forward for science-based optimization of the materials and synthesis procedures. Furthermore, we have, for the first-time, provided an atomistic-level view of the structure of these active sites in these highly-efficient catalyst materials that provides the opportunity to apply the same level of rigor that has been applied to the theoretical analysis of the oxygen reduction reaction on precious metal catalysts in the past. These results have been used to initiate an LDRD-DR effort (FY13) to use graphene model systems to advance catalytic activities through rational design.

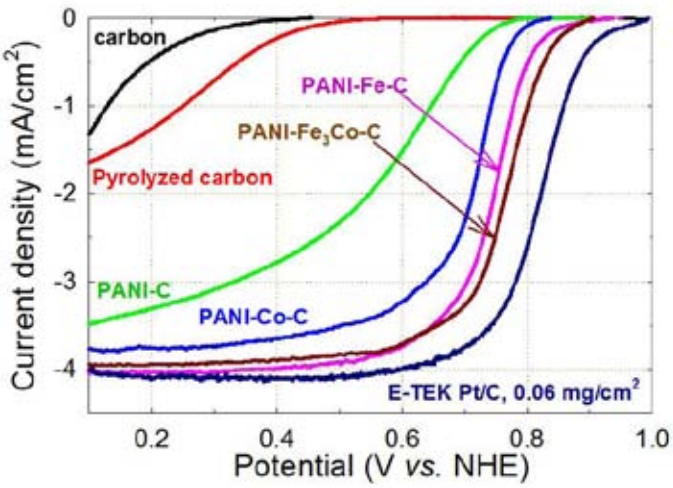

Figure 1. Metal- and nitrogen-modified catalysts have performance characteristics approaching Pt-based systems (rotating-disk electrode data at 25°C).

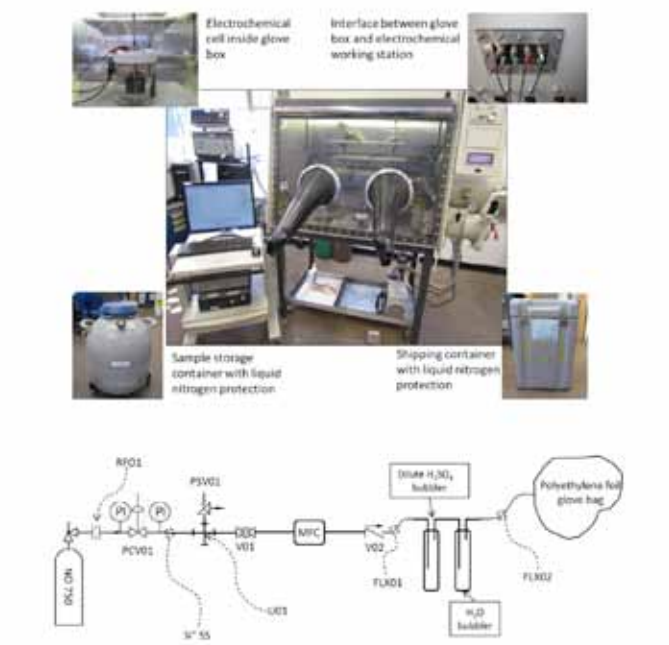

Figure 2. A newly developed experimental setup for an electrochemical reduction treatment of Fe catalysts in an oxygen-free wet box (top) and schematic diagram of a schematic diagram of the homemade experimental setup for the NO treatment of Fe catalysts (bottom).

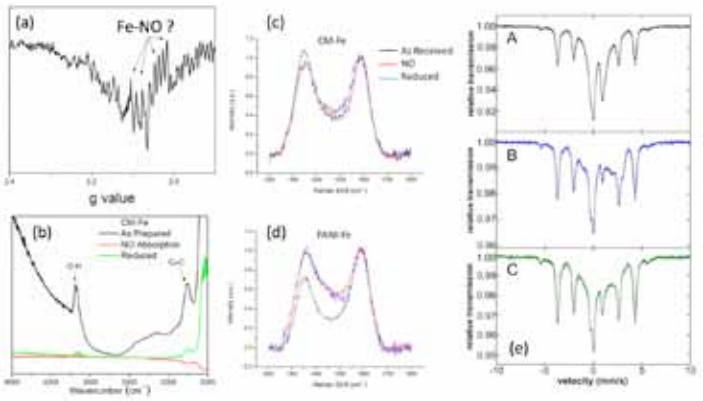

Figure 3. (a) The results of subtracting the spectra of the NO adsorbed on PANI-Fe from the spectra of reduced PANI-Fe. The hyperfine pattern is consistent with a Fe-NO species but the signal is barely distinguishable from the baseline. (b) DRIFTS spectra of CM-Fe showing changes in the C≡C and O-H absorbance values. The vibrations are typical of the catalyst and surface chemistry, respectively. (c,d). Raman spectra of catalyst samples normalized to the G-peak at 1600 cm-1. Data attest to an increase in the D-peak relative to the G-peak indicating and increase in disorder in the carbon matrix. (e). 80 K 57Fe Mößbauer spectra (dots) and best fit (black line) for (A) as-prepared CM-Fe-C, (B) reduced CM-Fe-C, and (C) reduced CM-Fe-C treated with NO.

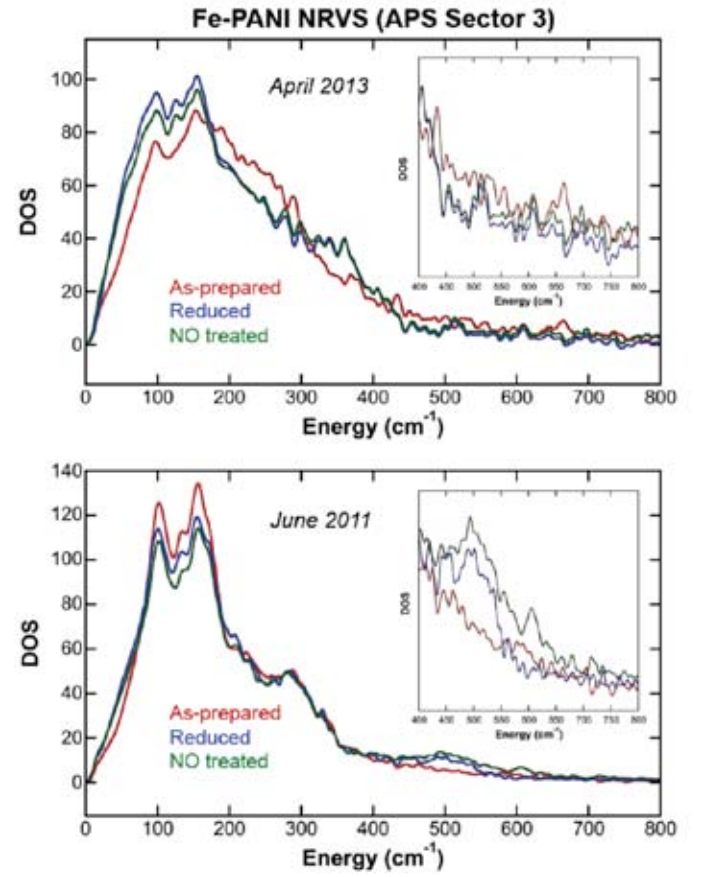

Figure 4. NRVS spectra obtained with two different samples of 57Fe non-precious metal catalysts exposed to NO.

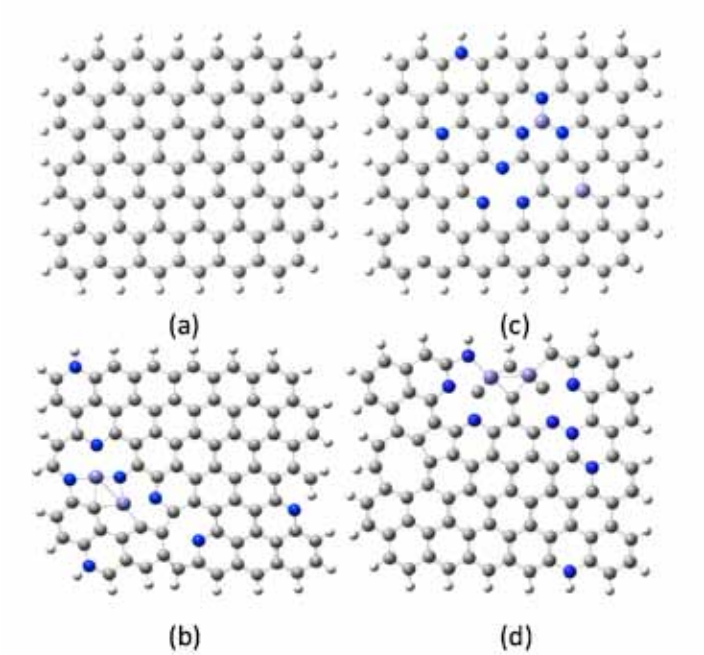

Figure 5. (a) Example of a perfect graphene flake with zig-zag (top and bottom) and armchair (left and right) edges. (b) Example of potential random initial flake structures with 2 vacancies, 8 N, and 2 Fe. Larger spheres represent Fe, blue spheres represent N, and white spheres represent H, C is in gray. (c,d) Two examples of highly stable structures found using the stochastic search algorithm displaying 2nd NN Fe/N/vacancy clusters near the flake edge.

References

1. Metropolis, N., A. W. Rosenbluth, M. N. Rosenbluth, and A. H. Teller. Equations of State Calculations by Fast Computing Machines. 1953. Journal of Chemical Physics. 21: 1087.

2. Kresse, G., and J. Hafner. Ab inito molecular dynamics for liquid metals. 1993. Physical Review BPhysical Review B. 47.

3. Kresse, G., and J. Hafner. Ab initio molecular-dynamics simulation of the liquid-metal,Äìamorphous-semiconductor transition in germanium. 1994. Physical Review BPhysical Review B. 49 (20): 14251.

4. Rao, A. Srinivasa, R. Ramakrishna Reddy, T. V. Ramakrishna Rao, and J. Lakshmana Rao. Electron paramagnetic resonance and optical absorption spectra of Fe3+ ions in alkali cadmium borosulphate glasses. 1995. Solid State Communications. 96 (9): 701.

5. Kresse, G., and . . Efficient iterative schemes for ab initio total-energy calculations using a plane-wave basis set. 1996. Physical Review BPhysical Review B. 54.

6. Perdew, J. P., K. Burke, and M. Ernzerhof. Generalized

gradient approximation made simple. 1996. Physical Review LettersPhysical Review Letters. 77.

7. Perdew, J. P., K. Burke, and M. Ernzerhof. Erratum: Generalized gradient approximation made simple. 1997. Physical Review LettersPhysical Review Letters. 78.

8. El-Barbary, A. A., R. H. Telling, C. P. Ewels, M. I. Heggie, and P. R. Briddon. Structure and energetics of the vacancy in graphite. 2003. Physical Review BPhysical Review B. 68 (14): 144107.

9. Sammalkorpi, M., A. Krasheninnikov, A. Kuronen, K. Nordlund, and K. Kaski. Mechanical properties of carbon nanotubes with vacancies and related defects. 2004. Physical Review BPhysical Review B. 70 (24): 245416.

10. Ferrari, A. C., J. C. Meyer, V. Scardaci, C. Casiraghi, M. Lazzeri, F. Mauri, S. Piscanec, D. Jiang, K. S. Novoselov, S. Roth, and A. K. Geim. Raman Spectrum of Graphene and Graphene Layers. 2006. Physical Review Letters-Physical Review Letters. 97 (18): 187401.

11. Ferrari, A. C.. Raman spectroscopy of graphene and graphite: Disorder, electron–phonon coupling, doping and nonadiabatic effects. 2007. Solid State Communications. 143 (1–2): 47.

12. Stewart, J. P.. Optimization of parameters for semiempirical methods V: Modification of NDDO approximations and application to 70 elements. 2007. Journal of Molecular Modeling. 13 (12): 1173.

13. Chung, H. T., C. M. Johnston, F. H. Garzon, and P. Zelenay. A Non-Precious Electrocatalyst for Oxygen Reduction Based on Simple Heat-Treated Precursors. 2008. ECS TransactionsECS Transactions. 16 (2): 385.

14. Wu, G., Z. Chen, K. Artyushkova, F. H. Garzon, and P. Zelenay. Polyaniline-derived Non-Precious Catalyst for the Polymer Electrolyte Fuel Cell Cathode. 2008. ECS TransactionsECS Transactions. 16 (2): 159.

15. Frisch, M. J., H. Schlegel, G. Scuseria, M. Robb, J. Cheeseman, G. Scalmani, V. Barone, B. Mennucci, G. Petersson, and H. Nakatsuji. Gaussian-09, Revision A. 01. Gaussian. 2009. Inc, Wallingford.

16. Chung, H. T., C. M. Johnston, K. Artyushkova, M. Ferrandon, D. J. Myers, and P. Zelenay. Cyanamide-derived non-precious metal catalyst for oxygen reduction. 2010. Electrochemistry CommunicationsElectrochemistry Communications. 12 (12): 1792.

17. Wu, G., M. A. Nelson, N. H. Mack, S. Ma, P. Sekhar, F. H. Garzon, and P. Zelenay. Titanium dioxide-supported non-precious metal oxygen reduction electrocatalyst. 2010. Chemical CommunicationsChemical Communications. 46 (40): 7489.

18. Jaouen, F., E. Proietti, M. Lefevre, R. Chenitz, J. Dodelet, G. Wu, H. T. Chung, C. M. Johnston, and P. Zelenay. Recent advances in non-precious metal catalysis for oxygen-reduction reaction in polymer electrolyte fuel cells. 2011. Energy & Environmental Science. 4 (1): 114.

19. Wu, G., H. T. Chung, M. Nelson, K. Artyushkova, K. L. More, C. M. Johnston, and P. Zelenay. Graphene-Enriched Co9S8-N-C Non-Precious Metal Catalyst for Oxygen Reduction in Alkaline Media. 2011. ECS TransactionsECS Transactions. 41 (1): 1709.

20. Wu, G., C. M. Johnston, N. H. Mack, K. Artyushkova, M. Ferrandon, M. Nelson, J. S. Lezama-Pacheco, S. D. Conradson, K. L. More, D. J. Myers, and P. Zelenay. Synthesis-structure-performance correlation for polyaniline-Me-C non-precious metal cathode catalysts for oxygen reduction in fuel cells. 2011. Journal of Materials Chemistry. 21 (30): 11392.

21. Holby, E. F., and C. D. Taylor. Control of graphene nanoribbon vacancies by Fe and N dopants: Implications for catalysis. 2012. Applied Physics Letters. 101 (6): 064102.

Publications

Choi, J. H., C. M. Johnston, D. Cao, and P. Zelenay. Se-modified Ru nanoparticles as ORR catalysts. Part 2: evaluation for use as DMFC cathodes. 2011. J. Electroanal. Chem. 662: 267–273 .

Chung, H. T., G. Wu , and P. Zelenay. Nanostructure vs. Reactivity of Non-Precious Metal Oxygen Reduction Catalysts. To appear in Hydrogen and Fuel Cells Zing Conference 2013. (Napa, California, July 12-15, 2013).

Chung, H. T., J. H. Won, and P. Zelenay. Active and Stable Carbon Nanotube/Nanoparticle Composite Electrocatalyst for Oxygen Reduction. 2013. Nat. Commun. 4: 1922.

Chung, H. T., and P. Zelenay. Nitrogen-doped carbon tubes for polymer electrolyte fuel cells and other electrochemical applications (invited lecture). Invited presentation at 13th International Symposium on Polymer Electrolytes (ISPE-13). (Selfoss, Iceland, 26-31 August, 2012).

Elbaz, L., G. Wu, and P. Zelenay. Heat-treated non-precious-metal-based catalysts for oxygen reduction. 2013. In Electrocatalysis in fuel cells: A non- and low-platinum

approach (Springer-Verlag London Limited). Edited by Shao, M.. , p. 213. London: Springer.

Ferrandon, M., A. J. Kropf, D. J. Myers, K. Artyushkova, U. Kramm, P. Bogdanoff, G. Wu, C. M. Johnston, and P. Zelenay. Multi-Technique Characterization of a Polyaniline-Iron-Carbon Oxygen Reduction Catalyst. 2012. J. Phys. Chem. C. : 16001.

Ferrandon, M., X. Wang, A. J. Kropf, D. J. Myers, G. Wu, C. M. Johnston, and P. Zelenay. Stability of Iron Species in Heat -Treated Polyaniline-Iron-Carbon Polymer Electrolyte Fuel Cell Cathode Catalysts. To appear in Electrochim. Acta. : doi:10.1016/j.electacta.

Holby, E. F., C. D. Taylor, G. Wu, and P. Zelenay. Active site modeling: Non-precious metal based catalysts for ORR. Presented at 222nd Meeting of the Electrochemical Society. (Honolulu, Hawaii, 7-12 October, 2012).

Holby, E. F., C. D. Taylor, G. Wu, and P. Zelenay. Modeling Carbon Based Non-Precious Metal Catalyst Active Site Structures for the Oxygen Reduction Reaction in PEFC Cathodes. To appear in 245th National Meeting of the American Chemical Society. (New Orleans, April 9, 2013).

Holby, E. F., G. Wu, P. Zelenay, and C. D. Taylor. Modeling of non-precious metal catalyst active sites (invited lecture). Invited presentation at Los Alamos National Laboratory Materials Theory Seminar. (Los Alamos, New Mexico, 25 July, 2012).

Holby, E. F., G. Wu, P. Zelenay, and C. D. Taylor. Modeling of non-precious metal catalyst active sites (invited lecture). Invited presentation at University of New Mexico Energy Technology Seminar. (Albuquerque, New Mexico, 10 September, 2012).

Holby, E. F., G. Wu, P. Zelenay, and C. D. Taylor. Metropolis Monte Carlo search for non-precious metal catalyst active sites candidates. 2013. ECS Transactions. 50 (2): 1839.

Holby, E. F., J. L. Kneebone, S. L. Daifuku, G. Wu, H. T. Chung, M. L. Neidig, P. Zelenay, and C. D. Taylor. Structure of Fe-Nx-C defects in Non-Precious Oxygen Reduction Reaction Catalysts Elucidated via First-Principles Modeling and Mössbauer Spectroscopy. Nature Materials.

Holby, E. F., and C. D. Taylor. Control of graphene nanoribbon vacancies by Fe and N dopants: Implications for catalysis. 2012. Applied Physics Letters. 101: 06412.

Holby, E., G. Wu, P. Zelenay, and C. Taylor . Modeling Non-Precious Metal Catalyst Structures and Their Relationship to ORR Activity. To appear in 224th Meeting of the Electrochemical Society. (San Francisco, 27 October 2013).

Johnston, C. M., D. Cao, J. H. Choi, P. Babu, F. Garzon, and P. Zelenay. Se-modified Ru nanoparticles as ORR catalysts. Part 1: synthesis and analysis by RRDE and in PEFCs. 2011. J. Electroanal. Chem. 662: 257–266 .

Shi, Z., H. Liu, K. Lee, E. Dy, J. Chlistunoff, M. Blair, P. Zelenay, J. Zhang, and Z. S. Liu. A Theoretical Study of Possible Active Site Structures in Cobalt-Polypyrrole Catalysts for Oxygen Reduction Reaction. 2011. J. Phys. Chem. C. 115: 16672.

Wu, G., C. M. Johnston, N. H. Mack, K. Artyushkova, M. Nelson, M. Ferrandon, J. S. Lezama-Pacheco, S. D. Conradson, K. L. More, D. J. Myers, and P. Zelenay. Synthesis-structure-performance correlation for polyaniline-Me-C non-precious metal cathode catalysts for oxygen reduction in fuel cells. 2011. J. Mater. Chem.. 21: 11392.

Wu, G., K. L. More, C. M. Johnston, and P. Zelenay. High-Performance Electrocatalysts for Oxygen Reduction Derived from Polyaniline, Iron, and Cobalt. 2011. Science. 332: 443.

Wu, G., K. L. More, P. Xu, H. L. Wang, M. Ferrandon, A. J. Kropf, D. J. Myers, S. Ma, C. M. Johnston, and P. Zelenay. Carbon-nanotube-supported graphene-rich non-precious metal oxygen reduction catalyst with enhanced performance durability. 2013. Chem. Commun.. 49 (32): 3291.

Wu, G., M. Nelson, H. Chung, and P. Zelenay. Co9S8-N-C Non-Precious Metal Catalyst for Oxygen Reduction in Alkaline Media. To appear in 220th Meeting of the Electrochemical Society. (Boston, October 9-14, 2011).

Wu, G., and P. Zelenay. Nanostructured Nitrogen-Carbon-Transition-Metal Catalysts for Oxygen Reduction Reaction. 2013. Acc. Chem. Res. 46 (8): 1878–1889.

Zelenay, P.. Non-precious metal catalysts for oxygen reduction (invited lecture). Invited presentation at Tongji University, State Research Center for Fuel Cell Vehicle and Powertrain System Engineering Technologies. (Shanghai, China, 6 September, 2011).

Zelenay, P.. Non-precious Metal catalysts for oxygen reduction (invited lecture). Invited presentation at Nanjing University, Department of Materials Science. (Nanjing, China, 8 September, 2011).

Zelenay, P.. Non-precious metal catalysts for oxygen reduction (invited lecture). Invited presentation at Dalian Institute of Chemical Physics, Chinese Academy of Science. (Dalian, China, 15 September, 2011).

Zelenay, P.. Non-PGM electrocatalysis of oxygen reduction (invited lecture). Invited presentation at Tsinghua Uni-

versity, Institute of Nuclear and New Energy Technology. (Beijing, China, 19 September, 2011).

Zelenay, P.. Non-precious metal catalysts for oxygen reduction in fuel cells: In pursuit of platinum (invited lecture). Invited presentation at Peking University, College of Engineering. (Beijing, China, 20 September, 2011).

Zelenay, P.. Non-precious metal oxygen reduction catalysts for fuel cells (invited lecture). Invited presentation at University of Rochester, Department of Chemical Engineering. (Rochester, NY, 26 October, 2011).

Zelenay, P.. Precious metal-free oxygen reduction catalysts for polymer electrolyte fuel cells (invited lecture). Invited presentation at University of California, UCSB Chemical Engineering Seminar Series. (Santa Barbara, CA, 3 November, 2011).

Zelenay, P.. State of the art in non-precious metal catalysts for fuel cells (invited lecture). Invited presentation at 221st Meeting of the Electrochemical Society. (Seattle, Washington, 6-10 May, 2012).

Zelenay, P.. Oxygen reduction on non-precious metal catalysts: How close are we to a viable system? (invited lecture). Invited presentation at Gordon Research Conference on Fuel Cells. (Smithfield, Rhode Island, 5-10 August, 2012).

Zelenay, P.. High-Performance Electrocatalysts for Oxygen Reduction Derived from Polyaniline, Iron, and Cobalt. To appear in American Physical Society March Meeting in 2013. (Baltimore, Maryland, March 18-22, 2013).

Zelenay, P.. Non-Precious Metal Oxygen Reduction Catalysts: Are We Closing on the Performance Gap to Platinum?. To appear in Hydrogen + Fuel Cells 2011. (Vancouver, Canada, May 15-18, 2011).

Zelenay, P., G. Wu, H. T. Chung, M. Blair, E. F. Holby, C. D. Taylor, and M. L. Neidig. Insight into the possible nature of the active catalytic site in non-precious metal fuel cell ORR catalysis. Presented at 222nd Meeting of the Electrochemical Society. (Honolulu, Hawaii, 7-12 October, 2012).

Zelenay, P., G. Wu, H. T. Chung, M. W. Blair, E. F. Holby, C. D. Taylor, and M. L. Neidig. Oxygen reduction on non-precious metal fuel cell catalysts (invited keynote lecture). Invited presentation at 63rd Annual Meeting of the International Society of Electrochemistry. (Prague, Czech Republic, 19-24 August, 2012).

Zelenay, P., G. Wu, H. T. Chung, and C. M. Johnston . Electrocatalysis of oxygen reduction on non-precious metal fuel cell catalysts (invited keynote lecture). Invited presentation at Electrocatalysis: Present and Future (ELCAT Meeting). (Alicante, Spain, 14-17 November, 2011).

Zelenay, P., G. Wu, Q. Li, and H. T. Chung . The Effect of Carbon Derived from Different Nitrogen Precursors on Oxygen Reduction Activity of Non-Precious Metal ORR Catalysts. To appear in First International Conference on Electrochemical Materials and Technologies for Clean Sustainable Energy. (Guangzhou, China, July 5-9, 2013).

Zelenay, P., H. T. Chung, Q. Li, G. M. Purdy, and G. Wu . Advantages and Limitations of Non-Precious Metal ORR Catalysts in Various Environments. To appear in 64th Annual Meeting of the International Society of Electrochemistry. (Santiago de Querétaro, 8-13 September, 2013).

Zelenay, P., H. T. Chung, Q. Li, and G. Wu. Oxygen reduction at non-precious metal electrocatalysts: Beyond the standard PEFC cathode (invited lecture). Invited presentation at 3rd CARISMA International Conference on Medium and High Temperature Proton Exchange Membrane Fuel Cells. (Copenhagen, Denmark, 3-5 September, 2012).

Innovative Process for Making Ultra-thin Dielectrics

Quinn R. Marksteiner
20110246ER

Abstract
This project set out to fabricate nonlinear dielectrics that exhibited a high degree of nonlinearity (dielectric constant vs. electric field) and low dielectric loss. In addition, we attempted to fabricate these nonlinear materials into very thin slabs (~100 um), which could be used in very high frequency applications such as nonlinear transmission lines. We developed the capability to diagnose and fabricate high quality, low loss nonlinear materials using Barium Strontium Titanate.

Background and Research Objectives
BSTO is a ferroelectric material that has a variety of interesting electromagnetic properties [1]. When the material is below the Curie temperature, it is in the ferroelectric state. In this state the material is very lossy (a large fraction of electromagnetic energy is converted to heat when it interacts with the material), and the material exhibits hysteresis. Above the Curie temperature, the material enters the paraelectric state. In this state, hysteresis disappears and the material becomes less and less lossy as the temperature increases above the Curie point. In this paraelectric state, the material is useful for a wide variety of electromagnetic devices, because if its high dielectric constant, high nonlinearity, and relatively low loss at high frequency. Figure 1 shows our measurement of dielectric constant and loss vs. temperature, and Figure 2 shows our measurement of nonlinearity.

In particular, this project was focused on developing a technique for fabricating high quality ceramic blocks of Barium Strontium Titanate (BSTO) that could be used in a Nonlinear Transmission Line (NLTL). A nonlinear transmission line is a periodic array of nonlinear materials that can convert a capacitive discharge into a narrowband, high frequency radiation [2]. The frequency and performance of a NLTL can be improved if the capacitance in a individual block of BSTO can be brought down. Because of this, a key goal of this project was fabricating very thin slabs of BSTO that still were highly nonlinear and low loss.

Scientific Approach and Accomplishments
The first step to developing high quality materials was to develop useful diagnostics. At the beginning of the project, we were already able to measure the low frequency (< 10 MHz) dielectric constant and loss of the material as a function of temperature. In the first half of the project, we developed a resonant cavity method to measure the high frequency (300 MHz – 2.5 GHz) dielectric constant and loss as a function of temperature [3]. We also developed a test stand to measure the nonlinear dependence of dielectric constant as a function of temperature and electric field strength.

These diagnostics were then used to scan a set of parameters related to the chemical mixture and the fabrication process of the materials. After a large amount of data-taking, it was found that the most important factor that determined the quality of BSTO was the chemical purity of the starting materials [3]. The combination of diagnostic development and optimization of LANL led to LANL having the capability to fabricate large quantities of high quality BSTO.

After developing the capability to diagnose and fabricate high quality bulk ceramics, we begin to work on the fabrication of thin laminates of materials, which could be used to increase the frequency output of a NLTL. The fabrication of thin materials proved to be more difficult than we had anticipated. The supporting material (MgO) tends to have a slightly different coefficient of thermal expansion, which leads to small cracks forming in the BSTO during the baking process. Because BSTO has a very high dielectric constant, even a microscopic crack can significantly degrade the performance of the material.

Although we did not succeed in fabricating thin laminates of BSTO, we did succeed in fabricating laminates

and multilayer laminates of thick materials. These multilayer laminates can be directly metalized, which greatly simplifies the process of constructing a device which consists of a large number of electrically connected slabs of BSTO. Figure 3 shows a picture of one of these laminates.

We have also expanded our capability to diagnose materials, by developing a resonant cavity that can measure the high frequency properties of materials under a DC bias. This work was completed in the last few days of the project, and will be published.

Impact on National Missions

The capabilities developed in this project can support many national missions, particularly with regards to the development of NLTL technology for civilian and military applications. The output of an NLTL is very high power [2], and has the potential to be used as a nonlethal electromagnetic weapon.

BSTO is a material that has a wide variety of applications, many of which are of interest to the lab and the nation. For example, BSTO have been used in dielectric wakefield accelerators, which could lead to significant cost saving for future accelerators such as the MaRIE XFEL.

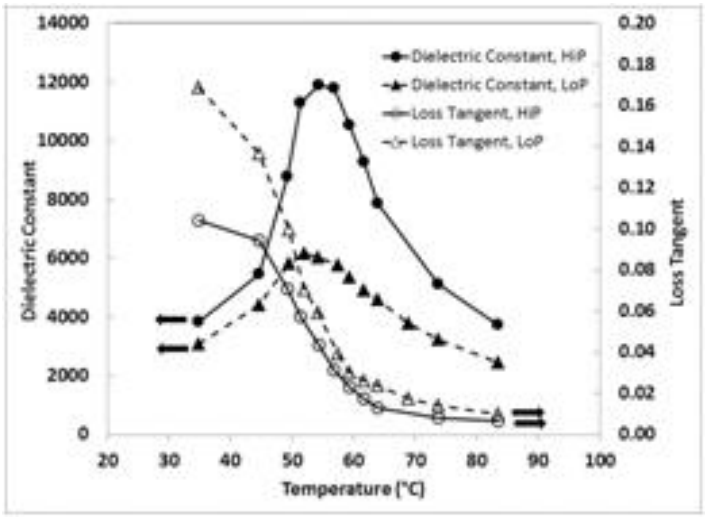

Figure 1. Measurement of dielectric constant and loss vs. temperature.

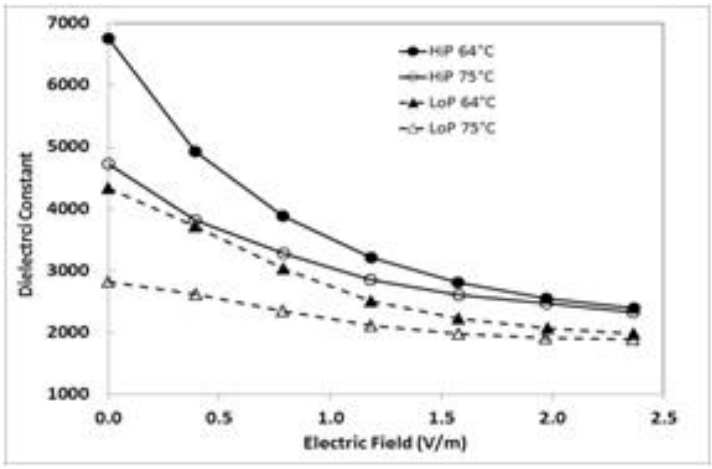

Figure 2. Measurement of dielectric constant vs. bias

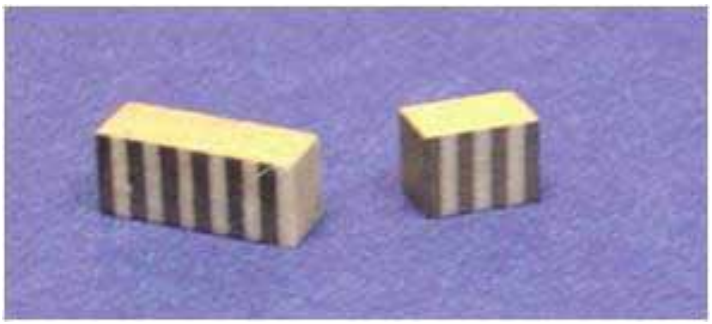

Figure 3. Picture of multilayer laminate.

References

1. Tagantsev, A. K., V. O. Sherman, K. F. Astafiev, J. Venkatesh, and N. Setter. Ferroelectric materials for microwave tunable applications (vol 11, pg 5, 2003). 2005. JOURNAL OF ELECTROCERAMICS. 14 (3): 199.

2. IKEZI, H., S. S. WOJTOWICZ, R. E. WALTZ, J. S. DEGRASSIE, and D. R. BAKER. HIGH-POWER SOLITON GENERATION AT MICROWAVE-FREQUENCIES. 1988. JOURNAL OF APPLIED PHYSICS. 64 (6): 3277.

3. Chen, C. F., Q. R. Marksteiner, G. King, T. A. Wynn, M. B. Treiman, D. A. Dalmas, A. Llobet, W. B. Haynes, D. R. Guidry, and P. A. Papin. Slip casting of sol-gel-synthesized barium strontium zirconium titanate ceramics. 2013. JOURNAL OF MATERIALS SCIENCE. 48 (17): 5788.

4. Publications

5. Chen, C. F., Q. R. Marksteiner, G. King, T. A. Wynn, M. B. Treiman, D. A. Dalmas, A. Llobet, W. B. Haynes, D. R. Guidry, and P. A. Papin. Slip casting of sol-gel-synthesized barium strontium zirconium titanate ceramics. 2013. JOURNAL OF MATERIALS SCIENCE. 48 (17): 5788.

Embedding Plasmonic Nanostructures at Semiconductor Interfaces for Enhancing Photovoltaic Efficiency

Todd L. Williamson
20110290ER

Abstract

The remarkable optical properties and tunability over visible wavelengths of plasmonic nanostructures make them attractive candidates for enhancing the performance of photovoltaic (PV) devices. Measureable improvements in performance and efficiency of inorganic semiconductor-based PV devices have been observed by placing plasmonic nanostructures on either their front or back surface. Ideally, plasmonic nanostructures should be embedded into the active p-n junction in PV devices to achieve new, higher levels of efficiency. The goal of this project was to investigate new mechanisms for enhancing PV efficiency by embedding plasmonic nanoparticles at the p-n junction in InGaN-based semiconductor PV devices whose tunable bandgaps cover nearly the entire solar spectrum making them ideal materials for high efficiency hybrid PVs. Our overall target was to create the first PV devices with plasmonic NPs buried at active semiconductor p-n junction interfaces with tailored properties for higher conversion efficiencies. These PV devices take advantage of near field interactions to manipulate their local electronic fields resulting in enhanced performance. The fundamental advances in materials science and photophysics made through this work will drive the development of novel PV device architectures that far out perform current implementations.

Background and Research Objectives

The emerging field of plasmonics has been facilitated by dramatic advances in control over the design and implementation of nanostructured materials. One distinctive aspect of these advanced materials is their exceptional optical properties relative to bulk and/or molecular counterparts. More specifically, metal nanoparticles are increasingly being utilized for diverse applications that range from biological sensing to implementations of sub-wavelength optical lenses that circumvent the traditional diffraction limit. The key to these materials success has been the efficient control and excitation of plasmonic modes at the particle's surface, which is synthetically defined by their shape, size, and composition. Using these properties, nanostructured metal particles will permit the development of next generation materials that may be employed in numerous sophisticated technologies. Conventional optoelectronic devices, such as photovoltaics (PV) are based on successful charge separation at p-n semiconductor interfaces. Recent approaches to improving efficiencies involve multi layer stacks, use of new and exotic materials, and careful selection of materials with appropriate bandgap energies. However, there are currently no meaningful approaches that address routes for enhancement at the p-n interface. In this work, we have sought to merge conventional optoelectronic semiconductor device geometries with advanced nanostructured metal particle synthetic techniques to produce novel optoelectronic materials that exhibit superior performance characteristics. The primary limiting factor of these nanostructure architectures has been the successful fusion of high-quality, low temperature thin film growth techniques with chemically synthesized, uniform, optically active nanomaterials. This work involved a combination of fabrication and synthetic capabilities available at LANL to produce novel hybrid plasmonic-photovoltaic architectures. This unique approach of embedding plasmonic nanotructures at an active p-n semiconductor interface enables direct manipulation of plasmon-exciton couplings that we desired to utilize for enhanced device performance. Figure 1 shows a schematic of a concept device from this work.

Scientific Approach and Accomplishments

The fabrication of buried plasmonic NPs at semiconductor interfaces involves the combination of vacuum-based thin film growth and solution-based chemical synthesis. Leveraging these two techniques, we have attempted to build novel device architectures for exploiting enhanced photon-plasmon-exciton couplings using four research thrusts:

Nanoparticle synthesis: The targeted plasmonically active PV devices inherently involve a wide variety of NP architectures available through several synthetic approaches. The most rudimentary particle designs involve colloidal Au and Ag that are prepared using standard wet chemical synthetic techniques allowing plasmon excitation across much of the visible spectral region (400nn to 600nm). Increasing the particle complexity using nanoshell particles allows access to a wider range of plasmon energies. Control of overall particle size and dispersion are important for ensuring that well defined plasmon resonances are available at the semiconductor interfaces to observe their interaction with the local electronic band structure.

Semiconductor Film Deposition: The targeted semiconductor system for this work is the InxGa1-xN ternary alloy system. This important semiconductor system has a tunable direct bandgap ranging from 0.7 eV (1800 nm) to 3.4 eV (365 nm), a range that encompasses nearly the entire solar spectrum. In order to take full advantage of plasmon-semiconductor interactions, the resonance frequency and the semiconductor bandgap need to be carefully chosen and optimized to yield the maximum enhancement. InGaN is the only known direct bandgap semiconductor alloy system that has the bandgap tunability over this critical energy range that favorably overlaps with readily achievable plasmon resonance energies. Our film deposition approach utilizes energetic neutral atom beam lithography & epitaxy. ENABLE is a MBE-type film growth technique wherein energetic nitrogen atoms are used to initiate the chemistry required for growth of epitaxial nitride films. Of importance is the ENABLE system's capability of growing semiconductor films at low temperature, critical for successfully incorporating active plasmonic NPs at the semiconductor p-n interfaces. Typical substrate temperatures during growth are ~500 - 600°C, well below the melting temperature of the NPs, but high enough to desorb any insulating ligands from the colloidal synthesis. ENABLE is used for growing both the initial InGaN film (p- or n-type) and the capping film (opposite doping) on top of the plasmonic structures. Plasmonic structures will be deposited in between growth steps.

Nanoparticle Deposition: Some of the plasmonic sensitizers are prepared via solution phase colloidal synthesis, and require efficient means of transfer onto the semiconductor surface using different deposition approaches depending on the particle type and the surface's properties. After evaluating a number of methods, we determined that placing a solution containing the particles on the desired InGaN wafer and then dragging a slide across the surface led to the best distribution and uniformity of coated NPs. In addition to deposition of colloidal NPs, we have also investigated using e-beam lithography to directly pattern structures onto the surface. This process is slower than the colloidal approach, but offered the flexibility of a wider array of geometries and a cleaner process to improve electrical metrics.

Buried Interface characterization: The general approach we have followed to form buried nanostructured PV interfaces relies heavily on a thorough understanding of the photophysics associated with both plasmons and semiconductor excitons. To this end, thorough charac-terization of all thin film growth stages (and their functionalization with plasmonic NPs) is vital for comprehending how the NPs maintain their properties during semiconductor deposition and on the quality of the overgrown semiconductor films. Initially, plasmonic nanostructures on the semiconductor layers were extensively characterized SEM prior to overgrowth of the capping semiconductor layer to determine their surface coverage. Enhanced PV performance should require minimal particle coverage (e.g. on the order of a few percent of a ML) this minimizes lattice defects in overgrown semiconductor layers. XRD was used to examine film crystallinity. Following structural characterization, the devices' electrical properties both with and without illumination were studied.

Accomplishments: This project has had a number of notable accomplishments:

Growth and n and p type doping of InGaN over a wide range of compositions relevant to the goals of this project. See Figures 2 & 3 for electrical data of relevant films.

Growth and evaluation of control junctions (i.e. without NPs) of InGaN

Deposition of uniform colloidal NPs on the surface of InGaN

Deposition of e-beam lithography patterned plasmonic structures on InGaN

Overgrowth of InGaN on top of previously grown InGaN that has been patterned with NPs. The overgrown films did not show any structural degradation by XRD

Impact on National Missions

This work will directly impact LANL's emerging core missions in energy and materials science. The fundamental understandings into plasmon-exciton interactions and their direct manipulation are of broad interest to both the nanomaterials and optoelectronics communities. Applying principles from these the emerging fields of plasmonics and photovoltaics based on InGaN alloys, this work can have direct implications on the next generation of PV tech-

nologies that are of significant interest to energy independence, national security, and environmental missions that are ongoing at LANL and the DOE complex. Direct impact in LANL threat reduction and energy security missions via applications in sensing and improvements in semiconductor-based energy harvesting materials is also possible. This project positions LANL for numerous external follow-on funding calls from various agencies.

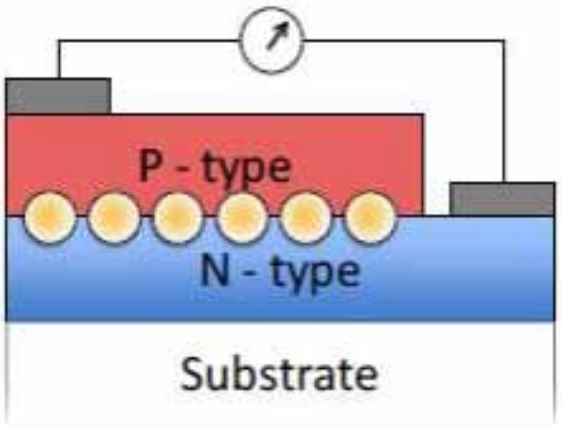

Figure 1. Schematic diagram of a proposed hybrid plasmon-photovoltaic device.

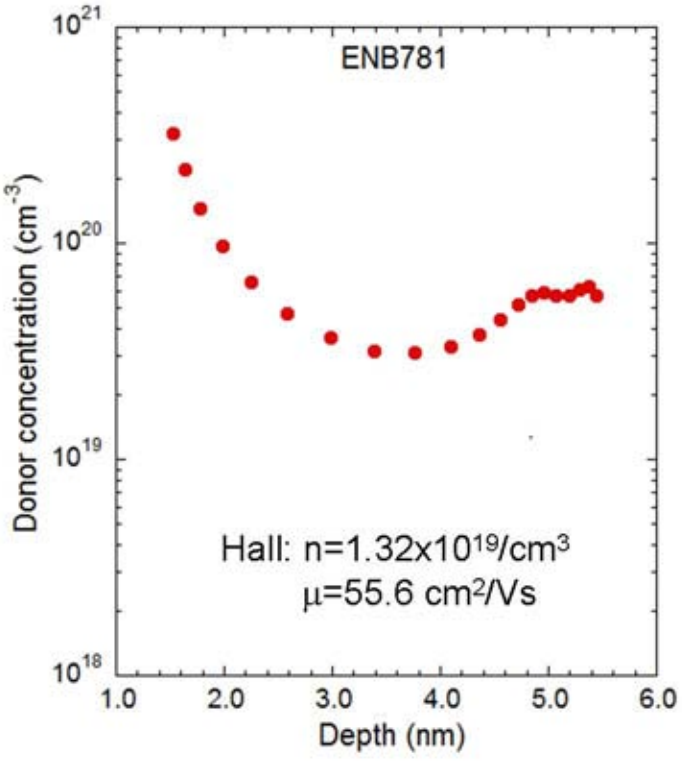

Figure 2. Electrical data from n-type InGaN with ~25% In content and a electronic bandgap of ~2.2 eV.

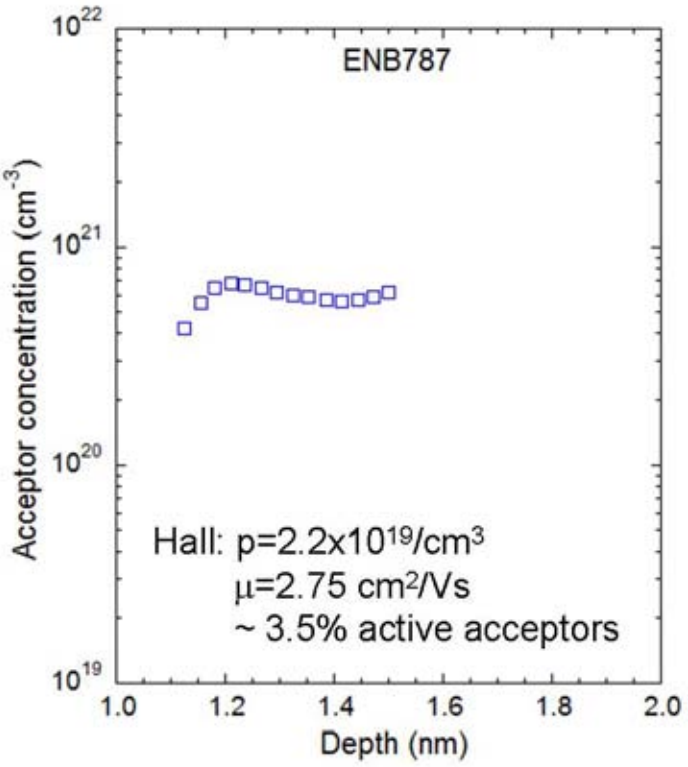

Figure 3. Electrical data from p-type InGaN with ~25% In content and a electronic bandgap of ~2.2 eV.

Publications

Hoffbauer, M. A., T. L. Williamson, J. J. Williams, J. L. Fordham, K. M. Yu, W. Walukiewicz, and L. A. Reichertz. In-rich InGaN thin films: Progress on growth, compositional uniformity, and doping for device applications. 2013. JOURNAL OF VACUUM SCIENCE & TECHNOLOGY B. 31 (3): -.

Williams, J. J., T. L. Williamson, M. A. Hoffbauer, A. M. Fischer, S. M. Goodnick, N. N. Faleev, K. Ghosh, and C. B. Honsberg. Inducing a junction in n-type InxGa(1-x)N. 2013. JOURNAL OF VACUUM SCIENCE & TECHNOLOGY B. 31 (3): -.

Williams, J. J., T. L. Williamson, M. A. Hoffbauer, Y. Wei, N. N. Faleev, and C. Honsberg. Growth of high crystal quality InN by ENABLE-MBE. Physica Status Solidi C.

Williamson, T. L., A. L. Salazar, J. J. Williams, and M. A. Hoffbauer. Improvements in the compositional uniformity of In-rich InxGa1-xN films grown at low temperatures by ENABLE. 2011. PHYSICA STATUS SOLIDI C: CURRENT TOPICS IN SOLID STATE PHYSICS, VOL 8, NO 7-8. 8 (7-8): -.

Williamson, T. L., J. J. Williams, J. C. D. Hubbard, and M. A. Hoffbauer. High In content InxGa1-xN grown by energetic neutral atom beam lithography and epitaxy under slightly N-rich conditions. 2011. JOURNAL OF VACUUM SCIENCE & TECHNOLOGY B. 29 (3): -.

Bio-analogue Catalysts: Evolved Aptazymes for the Hydrolysis of Organophosphorous Compounds

Robert F. Williams
20110338ER

Abstract

Aptamers are nucleic acid binding species capable of recognizing a wide range of target molecules and biological structures with varying conformational flexibilities. Isolated from high diversity combinatorial libraries of synthetic nucleic acids by a rapid iterative selection process, aptamers have been selected for effective binding recognition as well as for a designed catalytic function (enzyme mimic or aptazymes). This catalytic function is universal for multiple classes of phosphorus bonds found in chemical warfare nerve agents (CWAs). Our first selection protocols sought to find aptamers to hydrolyze a P-O bond as an initial target. Additional aptamer libraries were constructed to target other phosphorus bonds such as P-S and P-N bonds and optimum aptazymes were selected for these specific bond types with varying degrees of success. Initially, our three aptazyme classes were designed individually to function on P-O, P-S, and P-N bonds; however, isolated aptazymes were only successful for P-O and moderately successful for P-S bond types. These three bond types represent all known classes of G and V organophosphorus CWAs (e.g. sarin (GB) and VX) as well as the majority of pesticides in commercial use. We believe future inclusion of non-natural nucleosides in the aptamer sequence will allow for enhanced hydrolysis of P-S bond types as well as hydrolysis of the P-N bond type. Our selected apatazymes for P-O bonds are efficient catalysts that hydrolyze a compound with that bond type to eliminate the compound's toxic effects. While initial aptazymes have been shown to effectively catalyze the hydrolysis of organophosphorus compounds with P-O bond types, additional development of aptazymes for P-S and P-N bond types is needed to enhance and increase their binding, catalytic activity, and overall stability.

Background and Research Objectives

Aptamers are nucleic acid (DNA; deoxyribonucleic acid or RNA; ribonucleic acid) binding species capable of recognizing a wide range of target molecules and biological structures. Isolated from high diversity combinatorial libraries of synthetic nucleic acids by a rapid iterative selection process, aptamers can be selected and obtained for effective binding recognition as well as for a designed catalytic function (aptazyme). Systematic evolution of ligands by exponential enrichment (SELEX) is an in vitro selection technique that utilizes combinatorial chemistry to produce nucleic acid ligands with high binding affinity and specificity toward a desired target. The attraction of nucleic acid-based combinatorial chemistry lies in its potential for amplification and directed evolution. Mimicking the process of natural selection in the laboratory setting, repeated cycles of selection for specific high-affinity binding with increasing stringency, followed by polymerase chain reaction (PCR) amplification can lead to the isolation of oligomers 'evolved' to bind tightly and selectively to a target of choice. These selected aptamers have demonstrated a remarkable affinity for their targets, with dissociation constants typically in the micromolar to sub-nanomolar range. For all of their diversity, however, the ability of nucleic acids to perform biological functions such as binding and catalysis is limited when compared to the rich chemical functionality of proteins. To enhance aptamer capabilities, synthetic chemistries for modifying nucleotides have been developed to increase the potential of aptamers for binding, catalysis, and stability.

While this project was designed to develop novel catalysts as enzyme mimics, these catalysts are not designed to hydrolyze the phosphorous-fluorine bond of organophosphorous (OP) compounds (e.g. nerve agents) as has been traditionally done for destruction or decontamination of such OPs. Rather, these enzyme mimics, called aptazymes, were designed to target other specific phosphorous bonds that are ubiquitous in OP compounds such as P-O, P-S, and P-N bonds. Breaking or hydrolyzing these bonds, instead of the reactive P-F bond, produces a highly unstable intermediate that rapidly and spontaneously decomposes to an inert, non-toxic product. This

approach allows a universal capture and breakage of bonds to phosphorous found in all chemical weapon agents (CWAs) as well as all related OP toxic industrial chemicals and materials (TICs/TIMs) such as pesticides. Development of a robust toolbox, which specifically targets bonds for catalytic breakage, has important ramifications for the chemical and pharmaceutical industries, for therapeutic applications, and for our fundamental understanding of biological catalysis.

Construction of DNA aptazymes was predicated, partially, on the recognition of the robust role these molecules have played in the origins of enzymatic function in the evolution of life and their specific abilities to make and break phosphate bonds. With the high structural and functional diversity space available, we proposed that unique aptazymes would identify, recognize, and hydrolyze specifically targeted side chains of OP compounds. Consequently, this project has produced rationally designed, highly effective biological catalysts that mimic naturally occurring enzymes; yet, are more easily manufactured, effectively employed in the field for remediation, can be developed for biomimetic sensor applications, and may be useful in prophylactic roles for both the environment and personnel. Additionally, their continued study will allow development of more complex enzyme mimics by providing a more fundamental understanding of molecular recognition and the role of conformational flexibility in enzyme catalysis.

Also, this project has addressed a critical LANL mission by developing a new technical means to reduce the global threat of existing and emerging CWAs and thwart terrorist attacks that might employ them by providing a new tool to remediate an exposure event.

Scientific Approach and Accomplishments

Our goals for this project were the following:

To construct, using a combinatorial approach, highly efficient and selective bio-analogue catalysts comprised of DNA oligomers (aptamers) that will break a phosphorous (P-O, P-S, or P-N) type bond. These designed enzyme mimics or aptazymes will exhibit molecular recognition and have the ability to degrade, specifically and catalytically, OP compounds with the above types of bonds.

To optimize the catalytic turnovers of these aptazymes by elucidating and understanding the conformational constraints that controls the observed catalysis.

In order to accomplish these goals we attempted to synthesize two general types of analogs that mimic either the transition state (TS) or the ground state (GS) structure of a P-X bond targeted for breakage and use them to challenge our aptazyme libraries. Figure 1 shows the structures of a substituted cyclic phosphoroamidate (TS model) or a phosphate diester (GS model) used for this approach. After coupling to an immobilized support, using standard coupling chemistries, a nucleic acid combinatorial library containing 50-mers or higher, as required, was developed and exposed to the immobilized analogs under controlled conditions of pH, temperature, and ionic strength. A typical uncatalyzed hydrolysis half-life at pH 7 ranges from 10-30 hours for the most reactive class of compounds, depending upon the phosphorous ligands allowing sufficient time to select for binding and enhanced hydrolytic activity. Removal of unbound nucleic acid species, release of bound aptamers, amplification of selected aptamers, and re-exposure to bound targets was sequentially repeated with increasing stringency to produce aptamer structures with optimal binding and, ultimately, hydrolytic rate. Kinetic competition between the selected aptamers and BChE was used to evaluate aptamer efficacy. The sequence of the selected aptamers allows us to synthesize optimal aptazymes, de novo, with high fidelity and low cost.

As shown pictorially in Figure 2, the synthesized combinatorial library, with a diversity of approximately 1015, was bound to a streptavidin gel through a biotin moiety and remained immobilized on the gel unless the desired bond of the phosphonate, phosphate, or transition state analog target molecule was hydrolyzed (Figure 3). The initial library was constructed by template-directed extension of 5'-biotin-d(GGAAAAA)r(linker-target-linker) d-(GGAAGAGATGGCGAC)-3' on 5'-GTGCCAAGCTTAC-CG-N50-100-GTCGCCATCTCTTCC-3' (where N = G, A, T, or C). Extension products were purified by non-denaturing polyacrylamide gel electrophoresis (PAGE). Optimization of the library and increased catalytic efficacy utilized concentration modifications, deletions, and/or changes in ionic strength. Ineffective catalysis obtained in the initial N50 libraries; consequently, the random oligonucleotide region was increased from N50 to N100. Additionally, modifications to extend the linker portion on the aptamer side of the linker-target-linker region were done until binding/hydrolysis was observed. Both linkers were comprised of ~2 kDa polyethene glycol (PEG) units with a short oligonucleotide sequences on either the 3' side for Linker 1 or 5' side for Linker 2. Additionally, Linker 2 terminated on the 5' side with a biotin moiety for attachment to a streptavidin solid support for immobilization. The 5' side of Linker 1 and the 3' side of Linker 2 were functionalized to allow easy covalent incorporation of the target molecules shown in Figure 3. The ligation reaction to couple the target with the linkers utilized the high yielding and extremely efficient Cu(I)-catalyzed Huisgen [2+3] dipolar cycloaddition reaction between an organic azide and a functionalized

acetylene to form a 1,2,3-triazole (Click Chemistry) under mild physiologic conditions. Typically, the azide functionality was attached to PEG Linker 1 (PEG-N3) and the acetylene moiety was incorporated into the ligand side chain attached to the phosphorous coupled to Linker 1 (Figure 3). PEG Linker 2 was prepared with a terminal acetylene moiety (PEG-C≡CH) and attached to a ligand side chain that contains an N3 (Figure 3). Although this procedure can result in dimers, performing the initial coupling reaction, regardless of choice, with a large excess of linker generally prevented this from occuring.

Only when the correct hydrolysis event occurs can the 3' end of the molecule be uncoupled from the biotin; thus allowing removal of the hydrolyzed 3' molecule from the gel. It was ultimately found that using a column of pre-attached libraries resulted in poor recognition although hydrolysis was observed. This was due to our inability to control the spacing of each library unit resulting in cross-reaction by adjacent library units on the column. The solution to this problem was to use a dilute solution of the libraries and then separate all the non-hydrolyzed library units by chromatography on a streptavidin column (vide infra). After elution of the 3'-molecule-linker-target moiety, these oligonucleotide sequences, which showed hydrolytic activity, were amplified by standard PCR, purified, and again subjected to primer template-directed extension to allow for a subsequent round of selection. As more rounds of selection were undertaken, more stringent criteria, such as variations in concentration, metal ion co-factor, salt, temperature, and exposure time, were evoked to enhance the desired catalytic activity and specificity. To guarantee that the aptamer distinguishes between a target and a known closely related molecule (protein, peptide) we employed alternate rounds of positive selection taking only those molecules that bind with negative selection for the related, but undesired molecular targets (taking only those molecules that do not bind).

The first key accomplishment of this project was the design and implementation of a synthetic route to a phosphonate compound that is coupled to a polyethylene glycol linker that ends in a biotin moiety. This was required in order to select a specific phosphorous-ligand (oxygen, sulfur, or nitrogen) bond that will be selectively hydrolyzed by the DNA aptamers. The initial target molecule was a phosphonate that contains the P-O-Linker2-B bond linkage in the ground state. The oxygen is connected to both the phosphorous and the polyethylene glycol linker that ends in the biotin moiety (Linker2-B). Aptamers that successfully hydrolyzed the target P-O bond were recovered for subsequent amplification. On the other side of the phosphorus containing molecule, the DNA aptamer library was attached to the phosphorous through another polyethylene glycol linker (PG-Linker1) through an alkyl bond to the phosphorous (PG-Linker1-C-P). The PG-Linker1-P bond is not hydrolyzable. The second key accomplishment was the synthesis of the complete phosphonate containing polyethylene linkers on both sides of the molecule. One terminated with biotin and the other terminated in an azide functional group (N3-PG-Linker1-C-P-O-Linker2-B. When the complete complex construct was attached to the DNA aptamer library using copper mediated click chemistry, a ground state transition model for hydrolysis was produced (DNA-Library-CCN-PG-Linker1-C-P-O-Linker2-B). A third key accomplishment was design and synthesis of the DNA aptamer library terminating in an alkyne moiety for the click coupling to the azide terminated moiety containing the phosphorus described above. Additionally, the primer molecules for PCR amplification of the selected DNA aptamers were also designed; however, additional design work on these primers to further optimize the amplification of aptamers that show hydrolytic activity is needed. The fourth key accomplishment was a redesign of the selection strategy to take advantage of temperature as a selection stringency parameter and to eliminate the cross-linking interactions caused by high density placement of the complete complex construct (DNA-Library-CCN-PG-Linker1-C-P-O-Linker2-B) on a streptavidin-linked solid support. As mentioned above, if the complex constructs are too close together they can interact with an adjacent DNA aptamer to hydrolyze its neighbor phosphonate rather that the phosphonate to which it is actually attached. This produces aptamers that are not truly competent with correct conformations to the pool of successful aptamers. However, dilute solutions of the DNA aptamer library complexes, first heated to ~85 deg C to denature the aptamers followed by metal addition and cooling to allow the DNA aptamers to refold prior to any reaction, was a successful strategy. Our fifth key accomplishment was the selection and isolation of four competent aptamers that hydrolyzed the P-O bond of the ground state model. These aptazymes, characterized by sequencing and NMR, showed rates of hydrolysis that were approximately 104 to 105 higher than the base hydrolysis rate of diisopropylfluorophosphate in a standard pH7 buffer. One additional aptamer that showed a 102 rate enhancement for methamidophos (P-S bond) was also isolated.

Review board recommendations at the end of the second year suggested our focus in the third year be redirected from our original design protocol to take advantage of adding functionalized dUTP's in the DNA cocktail to produce aptazymes with enhanced binding and catalysis resulting from the enhanced functionalities on the nucleic acids (e.g more protein like). Selection against a transition state analogue was also suggested to be a more important

goal since we had already demonstrated hydrolysis with a ground state model. Unfortunately, problems with personnel turnover and delays in the synthesis of the transition state model compounds did not allow us to complete an optimized selection before the project ended. Nevertheless, hydrolysis was demonstrated but at rates lower than observed with the aptazymes generated with the ground state model. While additional work in this area is warranted to further enhance the catalytic efficacy of these aptazymes and to test them against a wider variety of OP compounds, our results are extremely promising.

Impact on National Missions

The development of technologies that allow for the rapid and specific identification/elimination of chemical threat agents in the environment and mitigation of adverse effects on exposed individuals are essential for threat reduction and mitigation. A primary mission goal of the Laboratory is to develop the technical means to reduce the global threat of existing and emerging chemical and biological weapons of mass destruction and to thwart terrorist attacks that might employ them by providing the necessary science and technology. Consequently, development of effective countermeasures to organophosphorus CWAs, TICs, TIMs, and related compounds are critical to LANL's nonproliferation activities and mission to prevent or reduce the capability for rogue nations or terrorists to do our nation harm. Our systematic experimental approach has provided new tools for the discovery of enzyme-like function, a core objective for our understanding Complex Systems of biological function.

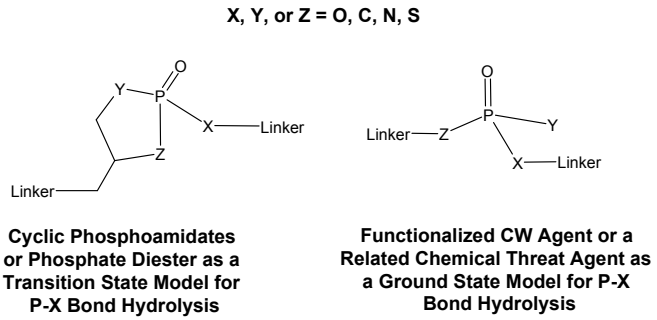

Figure 1. Representations of a Transition State Model and a Ground State Model for DNA Aptamer Selection where the P-X Bond is the Target Bond to Cleave.

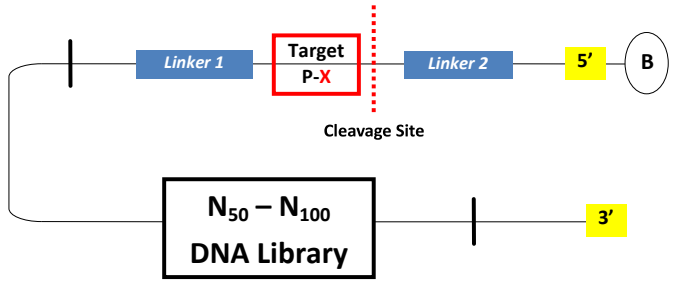

Figure 2. Scheme Describing the Design of the Combinatorial Library of DNA that will Hydrolyze the Target P-X Bond. The 5' End is Connected to a Biotin (B) to Bind to Streptavidin and Linker 1 and 2 are Described in Figure 3. The 50 to 100 Random Sequence Deoxyribonucleic Acid Library.

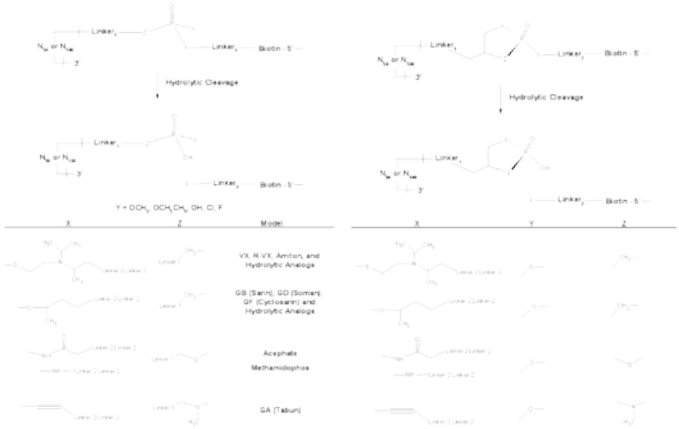

Figure 3. Design of Linker1-Target-Linker2 Used in Selection Scheme for the Ground State Model (Right) and the Transition State Model (Left).

Developing a Mild Catalytic Route for the Reduction of N_2 to NH_3

John C. Gordon
20110358ER

Abstract

The research in this project concerns the development of catalysts capable of supporting the conversion of di-nitrogen (N2) into ammonia under mild conditions using the earth-abundant metal iron (Fe). Largely due to the demands of food production, industrial generation of ammonia (NH3) consumes more than 1 % of the world's energy output as a result of the energetically in-tense conditions employed. Enzymatic ammonia production occurs under ambient temperature and pressure, and translation of this efficiency to a synthetic system would significantly decrease energy production demands. We aim to pursue this goal through a heretofore unexplored reaction manifold designed to maximize nitrogen activation and minimize the number of intermediates necessary for ammonia production. The interdependent use of experiment and theoretical calculations will be used to realize secondary objectives of advancing scientific understanding of dinitrogen functionalization in addition to probing the boundaries thereof, understanding the effect of varied electronic structure on nitrogen reactivity, and exploring new Fe coordination chemistry.

Background and Research Objectives

The research outlined in this project seeks to lower the energetic and economic footprints of NH3 production via the development of base metal catalysts that are capable of converting N2 into NH3 under mild conditions. We are approaching this goal by incorporating lessons learned from previous studies on the bonding and reactivity of N2 and using them to design catalysts that maximize N2 activation and minimize the number of potential intermediates involved in catalytic turnover in order to confer robustness to the catalytic cycle.

In pursuit of this objective, we also aim to advance the current understanding of how electronic configuration and ligand steric bulk affect the ability of iron (Fe) to reductively cleave N2, functionalize the resulting nitride, and release NH3. These catalyst design characteristics can then be optimized to improve catalyst efficiency and efficacy through a feedback loop of experimental and theoretical investigations.

Scientific Approach and Accomplishments

Towards our aims above, we have been using calculations to guide both our design strategies and synthetic efforts related to target catalytic species. We have been able to isolate a very interesting (and rare) example of a di-iron complex containing a bridging N2 ligand, in which the bound N2 fragment appears to be highly activated (based on metric data from the X-ray structure of this molecule, as well as from Raman spectroscopy). Recent calculations are pointing towards the significant reduction of the bond order within the bound N2 fragment, thus consistent with our original hypothesis that a zerovalent di-iron complex should significantly weaken the N2 ligand and promote its susceptibility towards further functionalization. We have also learned more about electron density within this molecule and how this might impact the activation of the N2 moiety and its propensity to undergo reactivity to form NH3 or other reduced nitrogen products.

In parallel with computational work, we have been investigating the chemistry of the Fe2N2 fragment with reagents that should be capable of cleaving the bound N2 ligand, thus forming another of the intermediates necessary to complete our targeted catalytic cycle (a trivalent iron nitride fragment).

We have also invoked the use of Mossbauer spectroscopy as a probe of electronic structure within these iron complexes, as this is a tool that will help rationalizeboth the reactivity of these molecules as well as their electronic structure and bonding properties pointed towards by calculation.

As a result of our work, we are beginning to gain a more detailed picture of the electronic structure of such

classes of metal-bound N2 molecules. In particular we are gaining more insight into which oxidation states and spin states of iron are required for N2 activation, and what kinds of ligands are need to support such molecules.

Impact on National Missions

Developing a process to affect the low cost reduction of N2 to NH3 under mild conditions remains a major challenge in the field of modern chemistry. Although the fundamental chemistries of this transformation have been demonstrated, an economically viable catalyst system that also exhibits reasonable turnover numbers has thus far been elusive. Research in this area of catalysis for energy will both advance our fundamental knowledge about the stepwise reduction of N2 at a cheap and abundant transition metal center and potentially lay the groundwork for a less energy intensive NH3 production scheme than the current Haber-Bosch process. This work directly supports our mission in energy security.

Publications

Mukhopadhyay, T. K., R. K. Feller, F. N. Rein, N. J. Henson, N. C. Smythe, R. J. Trovitch, and J. C. Gordon. Investigation of Formally Zerovalent Triphos Iron Complexes. 2012. ChemCommun (Chemical Communications). 48: 8670.

Determination of Fluid Properties at Carbonate Interfaces - An Integrated Experimental and Theoretical Approach

Donald D. Hickmott
20110363ER

Abstract

Phenomena at the interface between carbonate minerals and CH4-CO2-H2O-rich fluids at elevated pressure (up to 200 MPa) and temperature (up to 400o C) control a number of energy-relevant processes, particularly extraction of hydrocarbons from unconventional oil and gas reservoirs and sequestration of CO2 in deep geologic formations. We developed and tested a novel high pressure-temperature experimental cell for neutron reflectometry of fluid-solid interfaces to 200 MPa and 200o C. The cell has wide application in Earth and energy science and in corrosion studies. Neutron and x-ray studies of calcite thin films in contact with calcite-saturated fluids have revealed positive density anomalies at ambient pressure and temperature consistent with hydrophilic (highly wetting) interactions. Synchrotron x-ray studies also reveal structural rearrangement of the films due to contact with fluids; both amorphization and crystallographic re-orientation are observed. Theoretical calculations using molecular dynamics and kinetic Monte Carlo methods simulate the density anomalies and show that the diffusion of CaCO3 monomers on calcite surfaces with increasing temperature (300-800o K) at elevated pressure is complex. Such diffusion shows a reversal in rate at 600o K related to minimization of the desorption free energy between 600-700o K. Simulations also suggest that two dimensional surface clusters below a critical size of a few nanometers preferentially exist as disaggregated calcite chains; this has ramifications for surface growth and dissolution mechanisms of calcite.

Background and Research Objectives

Understanding and controlling interface processes for carbonate minerals is crucial for a range of energy and environmental applications. Carbonate minerals interact with mixed-volatile H2O-CO2-CH4-rich fluids at elevated pressures (P) and temperatures (T) during extraction of hydrocarbons from carbonate reservoirs, during production of geothermal energy, at some subsurface nuclear waste sites, and during sequestration of CO2 into deep geologic reservoirs. Surprisingly, the fundamental physics of mixed-volatile fluid interactions with carbonate and other minerals at the Ps and Ts of energy extraction remain poorly understood; this is largely due to the extreme difficulties of both doing experiments and developing accurate theoretical methods at such conditions. Thus, the overarching objective of this research is to use integrated experimental and theoretical methods to better understand high P-T carbonate/fluid interface properties, particularly density and related transport properties, as a function of P-T. Density is a particularly important property to understand because it can be related to wettability, which controls fluid flow in Earth's crust. Understanding fluid/mineral interfaces at a fundamental level opens up the possibility of manipulating surface structures and free energies and thereby controlling reaction driving forces and kinetics during fluid-rock interactions. Surface diffusion is crucial in high-surface materials such as shales, due to the potential control on fluid flow (CO2 infiltration or hydrocarbon extraction) by dynamic diffusive processes.

Scientific Approach and Accomplishments

We pursued a combined experimental and theoretical approach to address this key problem. On the experimental side we developed novel high P-T capabilities for neutron investigations of interfaces and began to apply these to calcite (CaCO3) thin films, whereas on the theoretical side we used state-of-the-art molecular dynamics methods to model fluid and interface processes and dynamic transport phenomena at calcite/water interfaces at high P-T.

We developed a novel elevated P-T cell for neutron reflectometry (Figure 1) [1]. Neutron reflectometry is a sensitive method for studying processes at interfaces with angstrom-scale resolution, but has never been applied at the elevated Ts and Ps of hydrocarbon extraction or carbon sequestration. The new cell is constructed of aluminum and can support both aqueous and mixed-

volatile fluids; measurements can be made in-situ while conditions are changing, allowing the study of dynamic processes. The Q range of the cell is 0.31 angstrom-1. Studies of corrosion of an aluminum film demonstrate the ability to probe surface degradation mechanisms and interface reactions at elevated P-T conditions. This cell is capable of studying density profiles near interfaces at Ts up to 200o C and Ps up to 200 MPa; this P-T range represents conditions in the Earth at depths up to ~ 6.5 kilometers under a range of geothermal gradients. The cell represents a new capability for the Los Alamos Neutron Scattering Center (LANSCE) and for the nation; it should be applicable to a range of Earth science problems and to problems in materials science such as high P-T corrosion, catalysis, and materials synthesis.

We applied neutron reflectometry to calcite thin films (Figure 2). A scattered-length-density contrast-matched deuterated water/hydrogenous water mixture was used to highlight density contrasts within a few angstroms of the calcite surface. Initial data shows that the near-surface region in the fluid has elevated density (at room P-T) compared to bulk fluid, suggesting hydrophilic interactions and rapid interface transport at these conditions. The thin films were produced using an atomic-layer chemical vapor deposition (ALCVD) method [2]. We characterized these thin films with a range of analytical techniques, including scanning electron microscopy, surface profilometry, and synchrotron-based surface x-ray scattering methods at the Advanced Photon Source (APS)(Figure 3). The APS results showed: 1) that the calcite thin films were polycrystalline and that their crystallographic orientation was dependent of the conditions during ALCVD; and 2) that the calcite thin films re-oriented during water exposure. Films deposited at 250o C on an alumina buffer layer amorphized in contact with calcite-saturated fluids whereas those deposited directly on single-crystal quartz crystallographically reoriented [3]. Films deposited at higher temperatures are more strongly subject to fluid-induced amorphization. These results suggest careful diagnostics prior to or during high P-T neutron reflectometry are vital. Future elevated P-T neutron reflectometry studies of these calcite films are planned.

The use of inelastic neutron (INS) scattering to probe the disposition of methane on calcite surfaces was explored. INS provided insights into the vibrational spectra of methane monolayers on calcite compared to bulk methane. Such observations may be useful in optimizing methane extraction from carbonate-rich unconventional gas reservoirs.

Molecular dynamics (MD) and kinetic Monte Carlo simulation methods were used to model the calcite (1014) / water interface over a range of Ts (300-800o K) at elevated P (~ 100 MPa) [4]. Water density profiles perpendicular to the calcite surface were determined and showed an elevated density region. The density curve was more affected by T than P with sharp density peaks associated with surface structured water (< 6 angstroms) at lower Ts (< 400o K), suggesting less water ordering at higher Ts. These calculations are consistent with the neutron reflectometry results. At ~ 100 MPa water density decreases monotonically from 1.03 to 0.48 g/cm3 from 300o to 800o K and this change in density affects the solvation of calcite molecules in solution. Calculations of free energy barriers for an extra CaCO3 molecule to desorb from the calcite surface over a range of Ts (300-800o K at ~ 100 MPa) shows that the ratio of the desorption barrier to the thermal energy initially decreases with T and reaches a minimum at 600o K. Above that T the trend reverses due to the relatively faster increase in the barrier which is a result of poor water solvation. This unusual phenomenon also affects the dynamical behavior of the extra CaCO3 molecule at the interface. We calculated the residence times in different surface states (i.e. surface and bulk) to study the diffusion of the CaCO3 monomer at the interface. From the distribution of duration times and the corresponding diffusion coefficients in different states, we generated a family of dynamic trajectories and computed the effective diffusivity as a function of T. The effective diffusivity increases with T to 600o K then begins to decrease (Figure 4) , indicating that the adsorbed species diffuses relatively less through the bulk liquid than on the interface. The calculations also suggest surprising T-dependent crystallographic orientation dependence of diffusion rate on the (1014) surface. The extent of the bulk-mediated diffusion strongly depends on the ambient condition for the calcite/water system.

It has been recently shown that amorphous CaCO3 plays a critical role in the formation of other polymorphs of CaCO3 [5][6]. In order to identify the equilibrium configuration of aqueous calcite (1014) interfaces at different P-T, we applied the parallel tempering method. In parallel tempering, multiple MD trajectories evolve at different Ts. Periodically, any two trajectories can swap configurations using a Metropolis-like Monte Carlo algorithm. Since high-T trajectories explore larger regions of phase space, exchanging configurations can significantly improve sampling at low Ts. As an added bonus, one can show that all the trajectories correctly sample their respective canonical ensemble. We used parallel tempering as implemented in the LAMMPS package to simulate aqueous calcite (1014) interfaces. Various surface coverages (100, 70 and 50%) were studied. We used a chain of 64 Ts ranging from 300o to 1000o K. The results show that incomplete layers are unstable. Instead, the calcite surface tends to form disag-

gregated calcite chains as shown in Figure 5 (a) [top and side views of the original surface are shown in Figure 5 (b) and (d) respectively.] For the same coverage (70%), this result was confirmed by instead starting the simulation from an energetically stable structure [c.f. Figure 5 (c)]. These results have interesting ramifications. They suggest a transition in the morphology of surface clusters can be expected as a function of their size: small clusters would be found in a disaggregated state, but they would eventually adopt a conventional layer structure with increasing size. This could have interesting consequences for calcite growth and dissolution, as the unraveling of such disaggregated calcite structures at steps or kink sites could affect the surface morphology and the growth mode. For geological systems, this surface destabilization process could be common, especially when the P-T vary dramatically. Also, sudden changes in super-saturation could result in rapid precipitation, where clusters (instead of monomers) would deposit on the surface. This suggests that a complex dynamical process, where the interplay between cluster formation and precipitation and crystallization from an amorphous state, would determine the final morphology. This phenomenon is not only fundamental from the geological point of view, but it could also play a crucial role in the mineralization processes that take place in living organisms. While surprising, these observations are consistent with literature results. It has been shown that small CaCO3 particles (<3.8nm in diameter) are amorphous, but that larger ones are crystalline [5]. In our simulation, the cell size is about 2 nm, which is consistent with the amorphous (disaggregated calcite) structure of the surface.

Impact on National Missions

Carbonates, particularly calcite, are extremely important in a range of energy and environmental applications. Interactions of hydrocarbon, carbonic, and aqueous fluids with calcite is a key process during extraction, particularly unconventional extraction, of oil and gas from carbonate reservoirs and in CO2 sequestration. The new capabilities (high P-T cell and theoretical advances) and understanding of interface behavior for carbonates derived from the combination of experiment and theory in this project will allow more rigorous models of chemical interactions during CO2 sequestration and natural gas extraction. Such models may enable optimization of these processes, benefiting the energy security of the nation

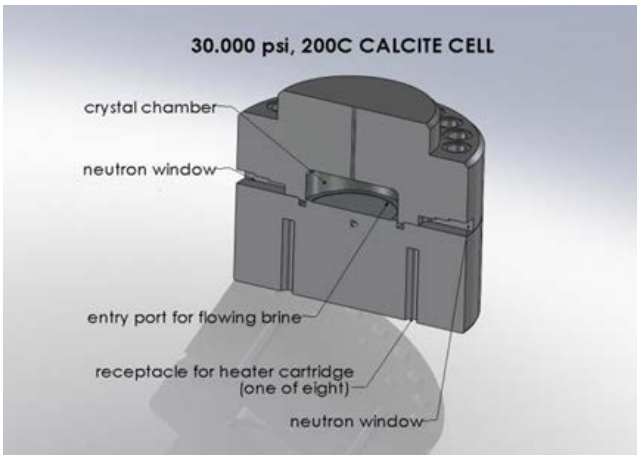

Figure 1. Cross section of aluminum high pressure-temperature cell for neutron reflectometry.

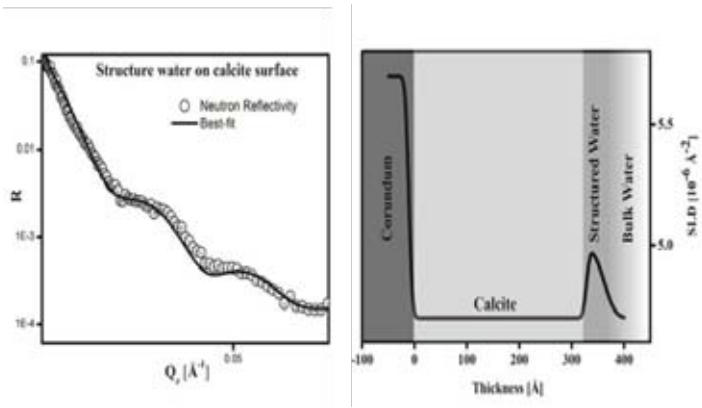

Figure 2. (left) The reflectivity curve for scattered-length-density (SLD) matched water in contact with calcite thin film deposited on Al2O3 substrate. Heavy line represents best-fit calculated SLD profile. (right) Real-space best fit profile.

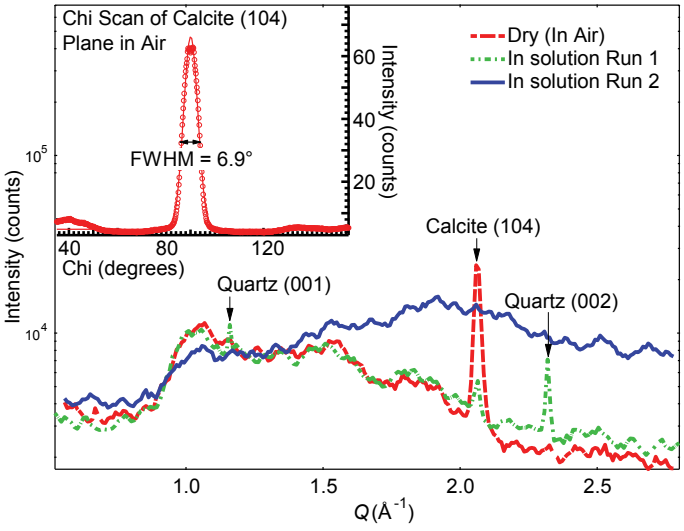

Figure 3. SG-XRD pattern of 250 C atomic layer chemical vapor deposition thin calcite film on an Al2O3 buffer layer on single crystal quartz in air (dry) and in solution (Runs 1 and 2). A chi scan of the calcite (104) plane showing a FWHM of 6.9 is in the upper left corner.

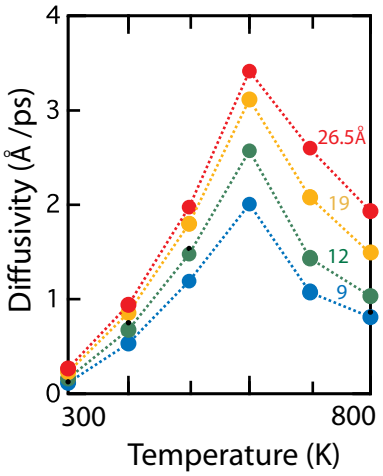

Figure 4. Calculated calcite/fluid interface diffusivities at a range of temperatures for varying water thicknesses.

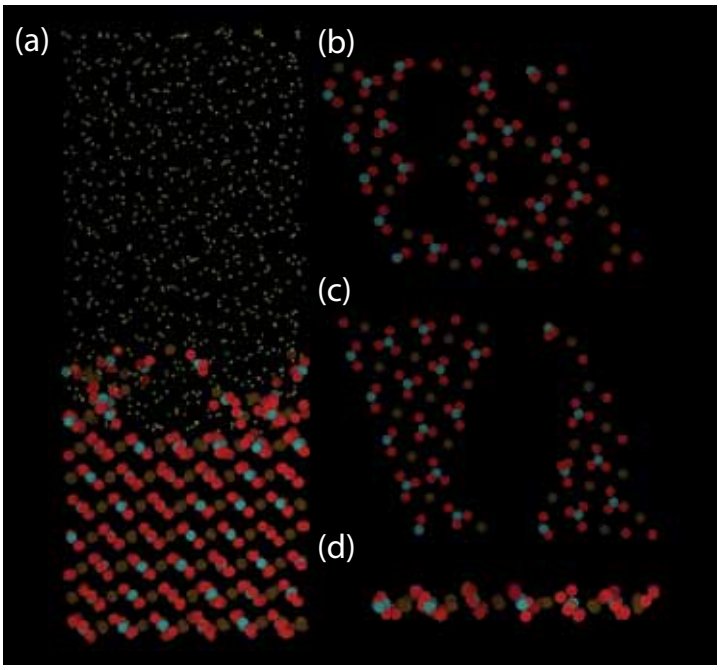

Figure 5. Parallel tempering simulation of a hydrated calcite interface: a) Equilibrium structure of surface with 70% coverage; b), c), d) structures used to initialize the simulation. Brown spheres: Ca; red spheres: O; blue spheres: C; Yellow dots: water molecules.

References

1. Wang, P., A. H. Lerner, M. Taylor, J. K. Baldwin, R. Grubbs, J. Majweski, and D. D. Hickmott. High pressure and high temperature neutron reflectometry cell for solid-fluid interface studies. 2012. European Physical Journal - Plus. 127 (7): 12076.

2. Nilsen, O., H. Fjellvag, and A. Kjekshus. Growth of calcium carbonate by the atomic layer chemical vapour deposition technique. 2004. Thin Solid Films. 450 (2): 240.

3. Wang, P., M. R. Hudak, A. Lerner, R. K. Grubbs, S. Wang, Z. Zhang, E. Karapetrova, D. D. Hickmott, and J. Majewski. X-ray scattering of calcite thin films deposited by atomic layer deposition: studies in air and in calcite saturated water solution. Thin Solid Films.

4. Lu, C. Y., D. Perez, D. D. Hickmott, and A. F. Voter. Insights into microscopic diffusion processes at a solid/fluid interface under supercritical conditions: a study of the aqueous calcite ($10^{-}14$) surface. 2012. Journal of Physical Chemistry C. 116: 25934.

5. Raiteri, P., and J. D. Gale. Water is the key to nonclassical nucleation of amorphous calcium carbonate. 2010. Journal of the American Chemical Society. 132 (49): 17623.

6. Demichelis, R., P. Raiteri, J. D. Gale, D. Quigley, and D. Gebauer. Stable prenucleation mineral clusters are liquid-like ionic polymers. 2011. Nature Communications. 2 (590): 1.

Publications

Hickmott, D. D., A. Lerner, P. Wang, J. Majewski, and M. Taylor. Neutron reflectometry at elevated pressures and temperatures - novel P-T cell and preliminary experiments. Presented at American Geophysical Union Annual Meeting. (San Francisco, 4-9 Dec. 2011).

Lu, C. Y., D. Perez, D. D. Hickmott, and A. F. Voter. Insights into microscopic diffusion processes at a solid/fluid interface under supercritical conditions: a study of the aqueous calcite ($10^{-}14$) surface. 2012. Journal of Physical Chemistry C. 116: 25934.

Lu, C. Y., D. Perez, D. D. Hickmott, and A. F. Voter. Insights into microscopic diffusion processes at a solid/fluid interface under supercritical conditions: a study of the aqueous calcite (1014) surface. Presented at American Chemical Society. (New Orleans, 7-11 April 2013).

Wang, P., A. H. Lerner, M. Taylor, J. K. Baldwin, R. K. Grubbs, J. Majewski, and D. D. Hickmott. High-pressure and high-temperature neutron reflectometry cell for solid-fluid interface studies. 2012. European Physical Journal Plus. 127 (7): 76.

Wang, P., J. Majewski, A. Lerner, M. Taylor, and D. Hickmott. High Pressure and High Temperature Neutron Reflectometry Cell for Solid-fluid Interface Studies . 2012. In American Conference on Neutron Scattering. (Washington, D.C., 24-28 June 2012). , p. 5. Warrendale, PA: Materials Research Society.

Wang, P., M. R. Hudak, A. Lerner, R. K. Grubbs, S. Wang, Z. Zhang, E. Karapetrova, D. D. Hickmott, and J. Majewski. X-ray scattering of calcite thin films deposited by

atomic layer deposition: studies in air and in calcite saturated water solution. Thin Solid Films.

Photo-triggerable Immolative Polymers: A New Modality for Radiation Dosimetry

Robert D. Gilbertson
20110421ER

Abstract

We have been developing a chemical method for radiation detection. Our approach involves the use of a chemical reaction that is initiated by the absorption of ionizing radiation. The material utilizes nanoparticle scintillators to absorb the incident radiation. Upon absorption, a radical chain process is initiated by the excited nanoparticles that results in the cleavage of a chemical bond releasing a small molecule that can be detected in various ways. In this fashion, we have demonstrated the generation of carboxylic acids or amines from ester or carbamate precursors, by exposing these constructs to gamma or X-ray sources.

This class of polymers is non-fluorescent, and can be readily depolymerized by endgroup cleavage. Once the polymer unzips, the aniline monomers that are generated are highly fluorescent. Thus, this reaction sequence can be used as "turn on" radiation sensor. By using neutron-absorbing materials as the radiation antennae, this method should be tunable to neutron detection as well.

Background and Research Objectives

The long-term goal of this project is to develop a new radiation dosimetry method with a high sensitivity for gamma and neutron radiation. Specifically, the target applications of this methodology are personal dosimetry and long dwell time measurements. The work takes advantage of a recently developed class of functional polymers that have been called "self-immolative" polymers. The defining feature of self-immolative polymers is that the polymer backbone, and in some cases the polymer side chains, can be completely depolymerized in a controlled manner when subjected to a single triggering event such that a large number of copies of a single "reporter" molecule are released after a triggering event.

We have developed a chemical system based on these self-immolative polymers that responds to ionizing radiation through the fragmentation of a chemical bond, generating products that can be readily detected, as an odor or as a highly fluorescent product. By relying on a chemical reaction rather than on the emission of light (scintillation) or generation of an electrical signal (semiconductor detector), this method does not require the use of materials that are optically transparent or electrically conductive. The initial work has focused on understanding the fragmentation chemistry well enough to enable the design of self-immolative polymers whose depolymerization reactions can be initiated by ionizing radiation induced bond fragmentation. By choosing a polymer that is non-fluorescent when polymerized but is composed of highly fluorescent monomers, depolymerization of this material will result in the turn on of the fluorescence of the monomers that are generated when the polymer is exposed to ionizing radiation. The intensity of the fluorescence should be proportional to the quantity of radiation absorbed by the material (Figure 1).

Scientific Approach and Accomplishments

The initial phases of the project have involved a large synthetic effort for the preparation of model compounds, immolative polymers, and scintillating nanoparticles. We first prepared a monomeric model compound in order to test the proof of concept of the project. That is, could we initiate cleavage of a polymer system (a monomer in the model case) using the response of scintillating nanoparticles to gamma-ray irradiation. To this end a monomeric immolative model compound with a picolinium trigger was synthesized. In addition to the model compound we also prepared lanthanum fluoride scintillating nanopaticles with a cerium dopant. In the proof of concept experiment a solution of the model compound and scintillating nanoparticles was exposed to gamma-ray irradiation for 30 minutes resulting in 7% fragmentation as measured by integration of proton NMR signals. An additional proof of concept experiment was carried out using a monomeric model compound with a masked fluorescent reporter. When this

compound was exposed to gamma-ray irradiation in the presence of scintillating nanoparticles, 18% fragmentation was observed by NMR and a fluorescent compound was produced (Figure 2).

While this experiment demonstrated the proof of concept of our proposal we observed fragmentation levels much higher than expected based on the radiation flux and assuming 100% efficiency in our triggering system. This led us to investigate the triggering and degradation mechanism more closely. Upon further investigation we made several more interesting observations: 1) the reaction occurred non-scintillating lanthanide nanoparticles were used. 2) Citrate radical species are observed by EPR upon irradiation of the nanoparticles with an X-ray source. 3) The cleavage reaction continues after the sample is removed from the gamma-ray source (and kept in the dark. 4) The reaction is very sensitive to the nature of the stabilizing ligand on the nanoparticle: citrate works best, diethylene glycol shows very small (~1%) of cleavage, unstabilized particles give no observable cleavage. Taken together all of these observations led us to believe that a free radical chain reaction mechanism was responsible for triggering the polymer degradation.

With the results of successful proof of concept experiments in hand we began the synthesis of gamma-ray triggered immolative polymers which should show signal amplification proportional to their molecular weight when cleavage of the trigger is initiated. Polymers up to thirty repeat units in length were produced using slight modifications of the literature procedures (Figure 3). When a solution of this polymer was subjected to gamma-ray irradiation in the presence of scintillating nanoparticles no fragmentation was observed in the NMR spectra. We surmised that impurities present in the polymer solution (due to the difficulties of polymer purification) led to inhibition of the cleavage and/or polymer fragmentation reactions.

In order to determine the root cause of the lack of fragmentation and have better analytical accuracy in doing so, a plan was devised to synthesize a model polymer of 2 repeat units. To date, this model polymer has been synthesized, however it has not yet been exposed to gamma-ray irradiation. We anticipate that this experiment will be carried out and that the results will available in short order.

Our overarching research goal was to develop a radiation dosimetry method based on self-immolative polymers that has a high sensitivity (low minimum detectable dose) for X-ray and gamma radiation, long-term stability, and a simple readout method. We have demonstrated the prop of concept of this idea by the gamma-ray induced cleavage of a picolinium ester (Figure 2). Within this framework, we have shown that a radical chain mechanism is likely occurring in triggering process (radiation→light→photo trigger). We have shown that small molecule cleavage of picolinium esters and carbamates is viable with the systems of nanoparticle, electron shuttle and ascorbic acid developed in this work. We have determined that the dose rates needed for observable chemical reaction are much lower than in other materials that detect radiation via chemical bond cleavage. From this work it is further apparent that further development of the polymer chemistry will be necessary to observe immolative effects in a dosimetry device. Studies on oligomers will be the first step to understanding how this system can be used to induce depolymerization. It is apparent that quantification of the extent of bond fragmentation will be related to the total dose the material receives, a fundamental requirement of dosimetry.

We have demonstrated the proof of concept of the fundamental premise of this proposal and the concept offers the potential for many different applications. We have begun to extend this research to other types of radiation. The use of neutron activated triggers (10B and 7Li) is being pursued to develop new materials for neutron detection. We anticipate our results will lead to new funding opportunities and we will continue to strive to understand the energy transfer efficiency of the triggering process (radiation→light→photo trigger), the triggering mechanisms and how they can be tailored to multiple stimuli, the depolymerization process including ambient environment effects and time constraints, and the optimal readout process.

Impact on National Missions

This work directly supports existing laboratory programs in the development of new radiation detector materials, as well as providing foundation resources for the development of new radiation detector systems. Based on the results of this effort and the potential for signal amplification we have submitted several additional research proposals outside the laboratory to NSF, NA-22, NA-42, and GS sponsors including proposals using immolative polymers for latent fingerprint visualization, explosives detection, and as an aid to enhance photo-dynamic therapy in cancer treatment. We anticipate that positive results from this ER work will enhance our efforts to further develop this work and obtain support from additional funding sources outside the laboratory. These proposals have not been funded as yet. However, recent experience has demonstrated that these sponsors as well as DHS and DTRA are interested in supporting new concepts at relatively high funding levels, but that initial results, such as those obtained through LDRD projects, are crucial in demonstrating the wisdom of a particular approach. Under this strategy, a single

LDRD-ER might spawn two or three new external projects, depending on what additional development is required for individual applications. We are optimistic that we can develop new funding in the future using the results from this LDRD-ER project to generate research proposals for the aforementioned sponsors as well as in the GS arena.

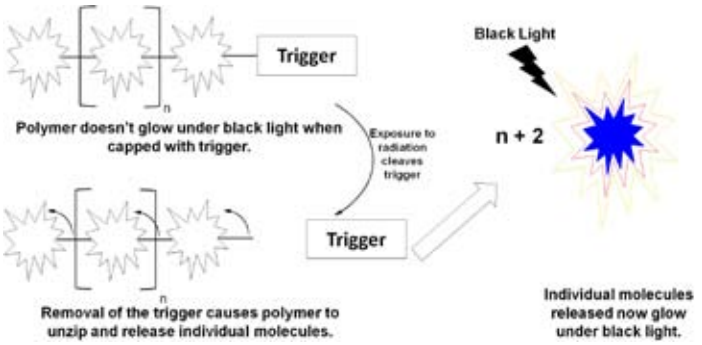

Figure 1. Schematic of a radiation triggered self-immolative polymer degradation.

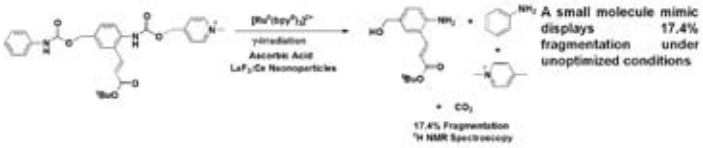

Figure 2. Gamma-ray induced cleavage of a model compound.

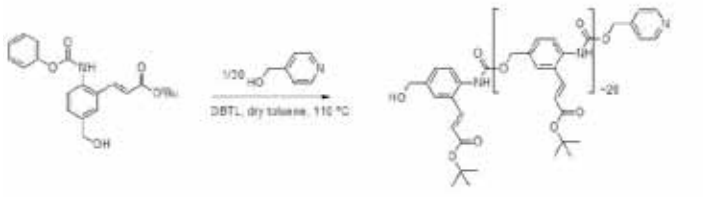

Figure 3. NMR spectra are consistent with a 20 repeat unit polymer.

Publications

Boncella, J. M., L. P. Spencer, and J. B. Edson. Photorelease of primary aliphatic and aromatic amines by visible-light-induced electron transfer. 2011. Organic Letters. 13 (23): 6156.

Cape, J. L., J. B. Edson, L. P. Spencer, M. S. DeClue, H. J. Ziock, S. Maurer, S. Rasmussen, P. A. Monnard, and J. M. Boncella. Phototriggered DNA Phosphoramidate Ligation in a Tandem 5 '-Amine Deprotection/3 '-Imidazole Activated Phosphate Coupling Reaction. 2012. BIOCONJUGATE CHEMISTRY. 23 (10): 2014.

Edson, J. B., D. S. Kuiper, R. D. Gilbertson, and J. M. Boncella. Low level gamma-ray radiation detection: carboxylic acid release from picolinium esters. . Angewandte Chemie International Edition..

Stable Uranium Benzyne Complex

Jaqueline L. Kiplinger
20130793ER

Abstract

The primary focus of this project was to isolate and structurally characterize a stable uranium benzyne complex in both solution and the solid-state. The solid-state structure would provide an important benchmark for future theoretical studies on the bonding and electronic structure in this compound. The electronic structure of a compound, or "what the electrons are doing", governs all its nonnuclear properties, including the chemistry it displays with other substrates. Exploring the chemistry of uranium compounds provides an improved understanding of chemical reactivity, covalency, and the relative roles of 5f- and 6d-orbitals in chemical bonding for the actinides. This project supports LANL's core capability in actinide science, the Lab's Plutonium Strategy, and LANL's Energy Security and Global Security mission areas.

Background and Research Objectives

Benzyne (C6H4) is a reactive species, which features rich and diverse chemistry with numerous organic compounds. Unfortunately, these reactions tend to be difficult to control. However, metals are able to stabilize highly reactive organic fragments and also to activate stable molecules toward selective attack. Although several benzyne complexes of transition metals have been reported [1], few are known for the f-element metals.

Early work by Marks' group at Northwestern showed that the uranium diphenyl complex, (C5Me5)2U(C6H5)2, (1) eliminated benzene at room temperature to generate the benzyne intermediate (C5Me5)2U(benzyne) (2) (Figure 1) [2]. The benzyne complex was very reactive and could not be isolated. However, its existence was determined by the chemistry it performed. Once generated, the benzyne complex reacted with diphenylacetylene to afford the uranindene complex (3). Similar chemistry was reported for the thorium diphenyl complex, (C5Me5)2Th(C6H5)2, but the chemistry required temperatures above 100 °C.

Besides this initial report, the chemistry of uranium benzyne compounds was largely unexplored until recently when Evans and co-workers reported a similar insertion reaction to yield the metallocycle complex 4 by reacting (C5Me5)2U(C6H5)2 (1) with iPrN=C=NPri [3]. During the course of this work, Hayton and co-workers reported a structurally characterized uranium complex containing tethered benzyne ligands but did not explore its reactivity [4].

As shown in Figure 1, we recently discovered that pyridine undergoes C-H activation with the uranium diphenyl complex (1) to give the novel uranium phenyl η2-pyridyl complex, (C5Me5)2U(C6H5)[η2-(N,C)-NC5H4] (5). The dialkyl complexes (C5Me5)2U(CH3)2 and (C5Me5)2U(CH2C6H5)2 also react with pyridine to give the structurally related uranium methyl and benzyl η2-pyridyl complexes, (C5Me5)2U(CH3)[η2-(N,C)-NC5H4] and (C5Me5)2U(CH2C6H5)[η2-(N,C)-NC5H4], respectively. By extension, we initially thought this chemistry was taking place with the diphenyl complex (1). However, it was possible that this chemistry could also be taking place with the uranium benzyne intermediate (2) as illustrated in Figure 1. In support of this proposal, we discovered something completely unexpected when the uranium diphenyl complex (1) was reacted with furan. Instead of reacting by the anticipated C-H cleavage pathway, we obtained an unusual 1H NMR spectrum and a preliminary (highly disordered) X-ray structure that is consistent with the furan-stabilized uranium complex 6 as illustrated in Figure 1. Our preliminary data suggests that we have serendipitously synthesized the first example of a stable uranium benzyne complex.

Since our structural data were not concrete, we performed a reaction with our proposed furan-stabilized uranium benzyne complex (C5Me5)2U(C6H4)(C4H4O) (6). It is known that the "reactive" uranium benzyne complex 2 reacts with diphenyl acetylene at room temperature to give the complex 3 as illustrated in Figure

1 [2]. When complex 6 is reacted with diphenylacetylene at 60-75 °C, complex 3 is produced. This is compelling evidence that we have essentially placed a uranium benzyne complex "in a bottle." This is very exciting as this observation suggests that our benzyne complex is rather stable compared to complex 2. This enhanced stability will provide us with an unparalleled opportunity to probe the chemistry and ultimately understand the electronic structure and bonding of the actinide benzyne functionality.

Scientific Approach and Accomplishments

Initially, we prepared the uranium diphenyl complex, (C5Me5)2U(C6H5)2, (1) using Marks' published procedure which involves the reaction of 3 equivalents of phenyl lithium, Li(C6H5) with (C5Me5)2UCl2 in diethyl ether at -78 °C (Figure 2). However, the synthesis was not reproducible and generated a mixture of the desired complex 1 and a lithium "ate" complex, (1·LiCl(Et2O)x) as shown in Figure 2. This hindered our progress and prevented us from reproducibly accessing the target uranium benzyne complex (C5Me5)2U(C6H4)(C4H4O) (6). To address this problem, we turned to the diphenyl magnesium reagent, Ph2Mg(1,4-dioxane) and reaction of this compound with (C5Me5)2UCl2 afforded pure (C5Me5)2U(C6H5)2, (1). This result represents a new route to (C5Me5)2U(C6H5)2, (1) and is a significant improvement over Marks's original 1981 procedure. From this new synthesis we were able to obtain the first crystal structure of (C5Me5)2U(C6H5)2, (1) (Figure 2).

We anticipated that the uranium benzyne complex would chemically behave differently than transition metal benzyne complexes. The closest analogues are the early transition metal benzyne complexes, which have demonstrated chemical behavior consistent with an ortho-metallated phenyl complex description [1]. Using this bonding description, the benzyne ligand in complex 6 is dianionic. Chemistry is the best way to understand the electronic nature of the benzyne functional group and we planned to survey the chemistry of complex 6 using the reactions outlined in Figure 3.

Unfortunately, despite numerous efforts, to date we have not been able to obtain a crystal structure of the furan-stabilized uranium benzyne complex (C5Me5)2U(C6H4)(C4H4O) (6). This is still a work in progress. The reactions we intended to perform were designed to examine the ability of complex 6 to undergo insertion reactions with a variety of unsaturated substrates to form metallacycles. For example, 6 will likely insert benzonitrile to give the ketimide metallacycle complex 7. Multiple insertions could also take place with complex 6. An ideal substrate to examine this would be carbon dioxide as it is small. Carbonylation of 6 should initially form the dihapto-acyl insertion complex 8. Actinide acyl complexes have been reported and resemble "anchored" Fisher carbene complexes in spectroscopic and chemical properties. However, complex 8 is interesting as it features a second reactive site. Migratory insertion of a second equivalent of CO should give the novel bis-acyl complex 9. It will be interesting to examine the benzyne complex's stability toward oxidation chemistry. By increasing the oxidation state of the uranium metal, the electronic structure, and therefore the chemistry, of the benzyne functional group is expected to change. Our LANL team showed that reaction of uranium(IV) complexes with copper salts is a mild way to synthesize the corresponding uranium(V) systems. Accordingly, reaction of 6 with CuI should give the uranium(V) benzyne iodide complex (10). Similarly, pyridine N-oxide has been shown to promote two electron oxidation of uranium with concomitant oxygen-atom transfer. Thus, reaction of 6 with pyridine N-oxide could yield the uranium(VI) benzyne oxo complex 11. However, an alternative pathway involving C-H activation of the pyridine N-oxide may yield the unusual metallacycle 12. If this latter pathway occurs, then other oxidants such as silver nitrate or nitrous oxide will be employed to yield complex 11. It would also be interesting in future studies to perform simple substitution of the furan donor ligand in complex 6 as a means to tune the reaction chemistry displayed by the benzyne fragment.

Impact on National Missions

Exploring the chemistry of uranium improves our understanding of the electronic structure of the light actinides. Uranium is a member of the actinide series, which marks the emergence of 5f electrons in the valence shell. The roles of these 5f electrons in the various pure phases, alloys, compounds, and molecules can vary from being delocalized (bonding) to being localized (nonbonding). The electronic structure of a material, or "what the electrons are doing", governs all its nonnuclear properties. It dictates the arrangement of the atoms in a molecule and is responsible for its response to light, the magnetic properties, and the bonds formed with other materials. This project supports LANL's Energy Security and Global Security mission areas as well as the Lab's Plutonium Strategy.

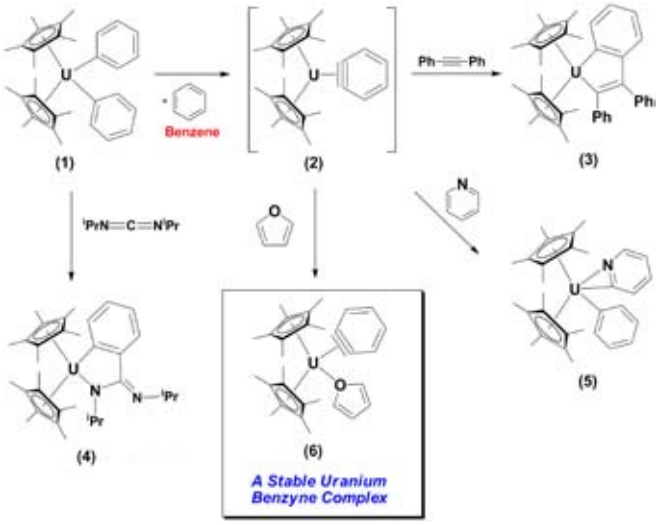

Figure 1. Synthetic procedures for the generation and chemistry of a reactive uranium benzyne complex and the synthesis of a stable uranium benzyne complex.

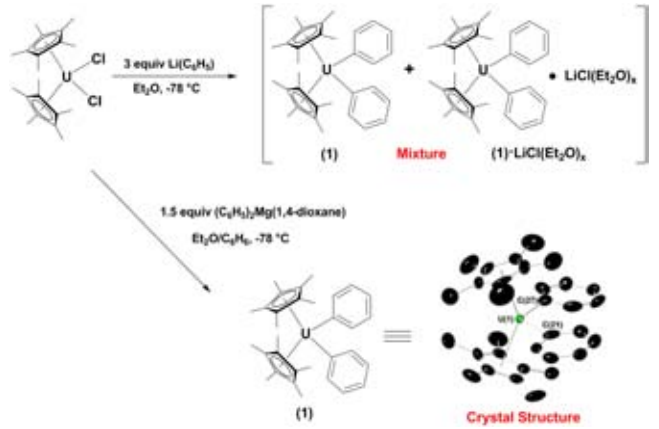

Figure 2. Improved synthetic procedure for the preparation of pure uranium diphenyl complex, (C5Me5)2U(C6H5)2, (1). Also shown is the molecular structure of complex 1.

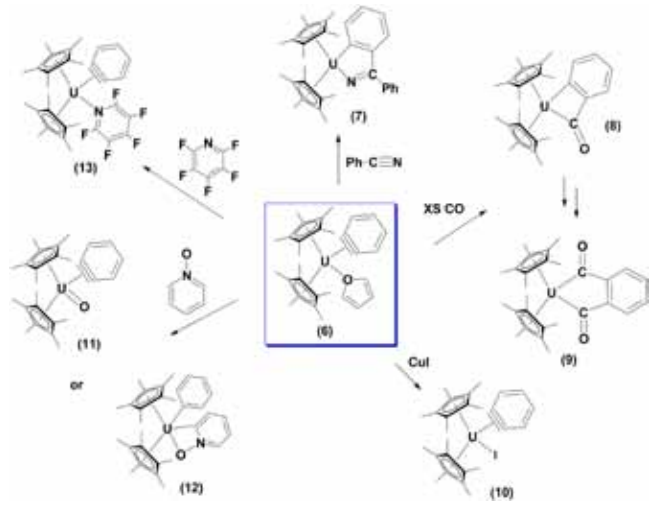

Figure 3. Proposed Synthetic outline to probe the chemistry of a stable uranium benzyne complex.

References

1. Buchwald, S. L., and R. B. Nielsen. Group 4 metal complexes of benzynes, cycloalkynes, acyclic alkynes, and alkenes. 1988. Chemical Reviews. 88: 1047.

2. Fagan, P. J., J. M. Manriquez, E. A. Maatta, A. M. Seyam, and T. J. Marks. Synthesis and properties of bi s(pentamethylcyclopentadienyl) actinide hydrocarbyls and hydrides. A new class of highly reactive f-element organometallic compounds. 1981. Journal of the American Chemical Society. 103: 6650.

3. Evans, W. J., J. R. Walensky, and J. W. Ziller. Insertion of carbodiimides and organic azides into actinide-carbon bonds. 2009. Organometallics . 28: 3350.

4. Seaman, L. A., E. A. Pedrick, T. Tsuchiya, G. Wu, E. Jakubikova, and T. W. Hayton. Comparison of the reactivity of 2-Li-C6H4CH2NMe2 with MCl4 (M=Th, U): Isolation of a thorium aryl complex or a uranium benzyne complex. 2013. Angewandte Chemie, International Edition. 52: 10589.

Characterization of Products from Hydrolysis of UF6

Marianne P. Wilkerson
20130803ER

Abstract

The goal of this project is to develop a fundamental understanding of signatures from products of uranium hexafluoride (UF6) hydrolysis reactions. Uranium hexafluoride is a ubiquitous material in the nuclear enterprise. Due to its volatility, it is essential for isotope separation, and as such, is often a 'fingerprint' for breakout from reactor- or fuel-grade to weapons-grade uranium. A number of studies in the open literature reveal complex chemical reactivity between UF6 and water vapor, and suggest that relative humidity and temperature play a role in the chemical and physical composition of the hydrolysis products and the evolution of these products over time. Additional work suggests that the deposited products may exhibit morphology dependent upon initial UF6 concentration and chemically interact with deposition surfaces. Our limited understanding of the complexity of these systems, however, precludes our ability to develop viable and quantitative signatures from these products. Characterization of these materials produced under a variety of parameters, including relative humidity, temperature, concentration of UF6, and composition of surface depository, will lead to more effective analyses of detectable signatures from UF6 hydrolysis.

Background and Research Objectives

Many technical references report that UF6 reacts with water as follows:

$$UF_6 + 2H_2O \rightarrow UO_2F_2 + 4HF$$

Additional work reveals that the reactivity of UF6 with water is complex, forming a variety of uncharacterized reaction intermediates and products, and is likely dependent upon environmental and release conditions.1,2 However, these studies do not address the chemical compositions of these materials, information that is important for detection of released UF6.

Paffett, Wagner and Wilkerson initiated studies to probe the chemical behavior of these systems under the LDRD-DR, Molecular Forensic Science of Nuclear Materials. A reaction chamber was developed in which to conduct UF6 hydrolysis (Figure 1). This reaction chamber provides the ability to introduce a stream of UF6 into a humidified space or conversely to allow humidity to be added to a chamber filled with UF6. The initial studies revealed that the morphology and chemical speciation of deposited materials are dependent upon atmospheric conditions of temperature and humidity. Images reveal significantly different morphologies between products deposited on carbon tape versus aluminum (Figure 2). Furthermore, these materials readily changed morphologically within days of release, as illustrated in Figure 3.

Careful study of the chemical and morphologic characteristics of hydrolyzed UF6 will enable more effective means of developing tools to detect and quantify release of UF6. Specifically, the studies proposed here will achieve this fundamental understanding through the following:

Generation of hydrolysis products through reactivity controlled as a function of:

- UF6 concentration
- Water vapor pressure
- Temperature
- Rate of water vapor and/or UF6 release
- Reactivity of hydrolysis products with surface depository

Chemical changes in hydrolysis products as a function of

- Temperature
- Relative humidity
- Time

A series of hydrolysis products will be prepared and analyzed through morphologic imaging via Scanning Electron Microscopy, and characterization of chemical speciation through X-ray diffraction analysis and infrared absorption spectroscopy.

Scientific Approach and Accomplishments

The technical approach includes the following:

- Hydrolysis of UF6 on the bench scale as a function of temperature, relative humidity, and composition of surface depository
- Store products under controlled temperature and relative humidity as a function of time
- Image morphology of material for characterization of size and surface homogeneity
- Characterize chemical speciation through infrared absorption and X-ray spectroscopies

Bench scale hydrolysis of UF6 will provide a means for safely conducting these reactions safely and in a controlled environment, permitting the ability to conduct a large number of experiments using varied reaction conditions that one might expect in different natural environments. Vessels developed under a separate WFO project will enable the ability to control exposure of the samples to time, temperature and relative humidity. Measurements of morphology will reveal particle size and homogeneity of the initial and aged hydrolysis products. Chemical speciation (powder X-ray diffraction analysis for phase type and long range order; diffuse reflectance for vibrational signatures; synchrotron-based studies for characterization of amorphous components of the material) will yield complete characterization. Each of these factors will enable more effective detection capabilities for identifying UF6 hydrolysis products and understanding the temporal behavior of these materials.

Through the initial portion of this project, an extensive literature search of publications relevant to hydrolysis of UF6 was conducted. An outline for a publication for peer review was prepared. In addition, these results were shared with potential sponsors of this work. (Please contact M. Wilkerson for additional information.)

The feasibility of characterizing chemical speciation from these particulates was tested. Through initial study under the LDRD-DR Molecular Forensic Science of Nuclear Materials, an experiment was conducted at Beam Line 2-3 at the Stanford Synchrotron Radiation Lightsource to measure X-ray Absorption Spectra from aged material deposited onto aluminum, shown previously in Figure 3. Initial data suggested the formation of different oxidation states of uranium following one week of aging, such that U(IV) was produced under conditions of low temperature (20°F), while U(VI) was the predominant product following aged under conditions of high temperature (90°F). Under this LDRD-Reserve, powder X-ray diffraction measurements were then conducted, and analysis reveals the presence of both UO2F2·xH2O and UOF4 (Figure 4). The stronger intensity of lines from UOF4 is of notable interest.

The majority of the experimental work was not completed due to the September 2013 timeline of a separately funded project utilizing the capability developed for this project (vide supra). Therefore, a portion of the funds (2/3) were returned to the LDRD Program Office, and it is proposed that the experimental portion of this work will be completed in FY2014.

Impact on National Missions

The impact of this project is the ability to correlate environmental conditions (temperature, relative humidity) and depository surface composition with UF6 hydrolysis products. As stated by Andy Erickson (PADGS), "the continued pursuit of Weapons of Mass Destruction (WMD) by numerous proliferant nations is not showing any signs of slowing down. As such, the need to accurately determine whether a nation is pursuing WMD or simply a nuclear fuel cycle is important, as is the ability to locate previously unknown/undeclared uranium facilities... By providing funding for the proposed work, it demonstrates the laboratory's investment in an area of key interest to sponsors, a welcome occurrence in the current funding environment. In addition to answering key scientific questions, the work is timely, as significant government effort is ongoing to develop new signatures for monitoring countries of concern."

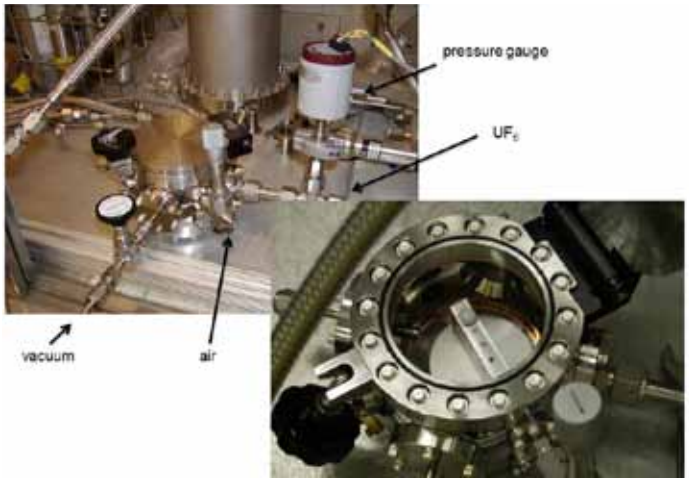

Figure 1. An experimental chamber was designed for laboratory scale experiments to hydrolyze UF6 under controlled temperature and relative humidity.

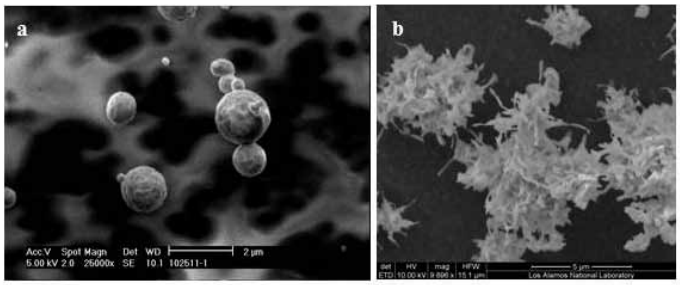

Figure 2. Material released from hydrolyzed UF6 (1 g UF6, 19% relative humidity, room temperature) was directly deposited onto carbon tape (a) and onto aluminum (b).

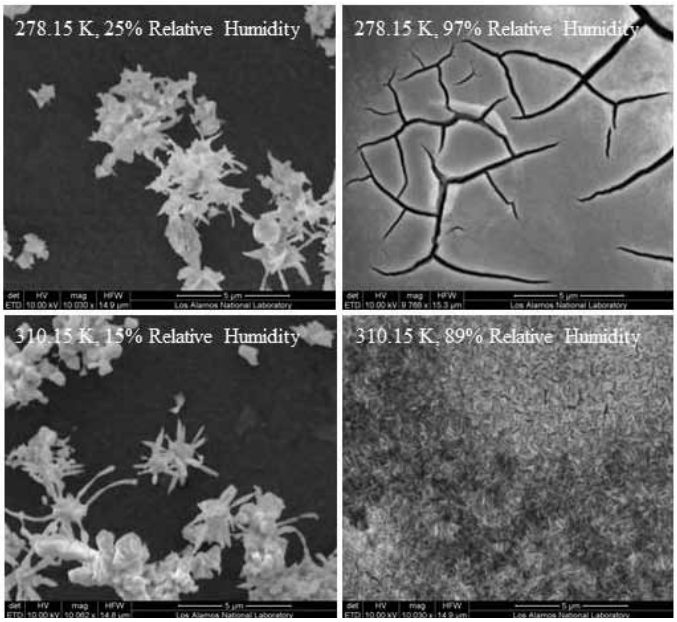

Figure 3. Morphologic images were collected from material released from hydrolyzed UF6 (1 g UF6, 19% relative humidity, room temperature) and then aged at the indicated temperatures and relative humidities after one week.

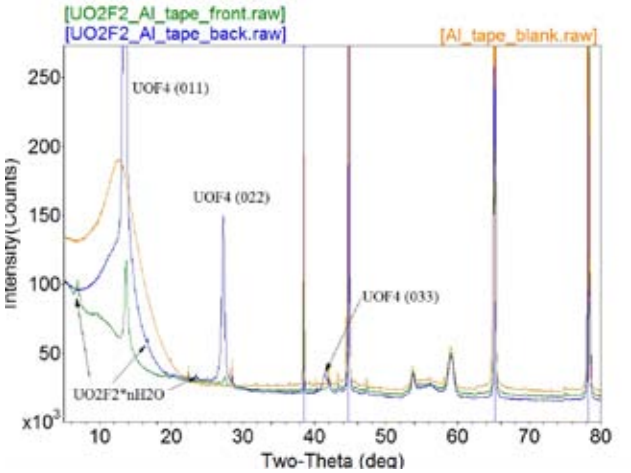

Figure 4. Powder X-ray diffraction analyses of hydrolyzed UF6 deposited onto aluminum reveals the presence of UOF4 and UO2F2-xH2O.

References

1. Bostick, W. D., and W. H. McCulla. Sampling, characterization, and remote sensing of aerosols formed in the atmospheric hydrolysis of uranium hexafluoride. 1985. Journal of Environmental Science and Health. A20 (3): 369.

2. Kips, R.. Development of uranium reference particles for nuclear safeguards and nonproliferation control. 2007.

Publications

Wilkerson, M., M. T. Paffett, and G. L. Wagner. Characterization of Products from Hydrolysis of UF6. To appear in Manuscript in preparation.

Re-invigorating LANL Quantum Computing Research

Antoinette J. Taylor
20130809ER

Abstract

Quantum computing holds great promise of exceptional speed up of computations for applications ranging from national security to pharmaceutical design. Because the basic building block of a Quantum Computer (QC), the qubit, has not been established, there are still many physics experiments to be done to improve on the existing qubits, as well as models and simulations needed to understand the many complex real-world issues surrounding development of a QC. In this project, we propose to reinvigorate QC research at LANL, exploiting its world-class capabilities condensed matter physics (theory and experiment), photonics and QC theory, to enable program development opportunities in this arena. Our proposed research includes proof-of-principal experimental research on spins in quantum dots, topological quantum computing (QC), photonics, and superconducting qubits, as well as fundamental QC theoretical studies. The proposed research builds upon areas where LANL has existing world-class capabilities that will materially advance QC research. We have assembled an exceptional team to execute the proposed research. The proposed work will allow us to re-invigorate our activities in QC and seek external funding that is available in the near term (FY14) and not later, hence the urgency of FY13 LDRD funding.

Background and Research Objectives

Quantum computing holds great promise of exceptional speed up of computations for applications ranging from national security to pharmaceutical design. The field became critical for national security in 1993 when Peter Shor developed an algorithm that provided exponential speed up for factoring large numbers, an algorithm with direct applicability to cryptography. From the mid-1990s to the mid-2000s Los Alamos was arguably the strongest single institution for quantum computing (QC) research. Since that time the Lab has lost some key personnel, but a strong core of experimentalists, theorists, and modelers remains and can be tapped to advance the field. Because the basic building block of a QC, the qubit, has not been established, there are still many physics experiments to be done to improve on the existing qubits, as well as models and simulations needed to understand the many complex real-world issues surrounding development of a QC.

In this project we will pursue proof-of-principal experimental research on topological QC and superconducting qubits, as well as fundamental QC theoretical studies. We believe we have assembled an exceptional team to execute the proposed research. The proposed research builds upon areas where LANL has existing world class capabilities and will materially advance QC research since LANL retains a strong QC theory team, and many materials capabilities not available elsewhere. The proposed work will allow us to re-invigorate our activities in QC.

Scientific Approach and Accomplishments

Fabrication of basic constituents of superconducting qubits and study of their physical properties: The basic component of a QC is a qubit. All types of superconducting (SC) qubits rely in two phenomena, flux quantization and coherent tunneling across Josephson junctions (JJ). Leonardo Civale, Boris Maiorov and Quanxi Jia worked together to perform magnetization and transport studies to explore flux quantization in SC circuits and the properties of Josephson junctions.

The basic idea behind the first experimental study was to use our Magnetic Properties Measurement System (MPMS) SQUID magnetometer to measure the magnetic flux Φ produced by the persistent supercurrents circulating in SC rings as a function of the magnetic field H. The values of Φ are quantized in units of the flux quantum Φ0=2.07x10-7 Gcm2, and the response is periodic in H with periodicity ΔH=Φ0/A, where A is the ring area. The MPMS is not sensitive enough to detect the signal of a single ring, thus we proposed to pattern arrays of 104 to

106 identical rings. The first goal was to implement upgrades in the MPMS to (1) reduce the noise level, and (2) increase the field resolution. L.C. visited Quantum Design, the manufacturer of our SQUID magnetometer to discuss these plans. Regarding the noise, they explained that the main source is the current circulating through the heater of the sample temperature control, and showed us how to reduce it by modifying some software parameters. We tested this method and we have been able to reduce the noise in standard measurements from the typical ~ 2 x 10-7 emu to ~ 5 x 10-8 emu. It is possible to increase the sensitivity by one more order of magnitude by maintaining the sample in a fixed position (rather than scanning it through the detection coils) and processing the raw SQUID signal. We learned to do this without the need to incorporate additional electronics, and we are currently testing the method. Regarding the field resolution, they suggested a simple modification to the magnet circuit (change of the control resistors) that will allow us to increase the field resolution from the standard 0.15 Oe to around 0.01 Oe. We will implement this hardware change in the near future. In parallel, we have discussed the details of the fabrication of the arrays of rings with the colleagues at CINT (SNL) that will pattern them by photolithography. We purchased the Nb ingot needed and are presently designing the masks.

In the second study we fabricated and studied individual high Tc superconductive JJs of different characteristics. Until now, studies of JJs for QC have been almost exclusively focused on low Tc superconductors. The key idea is to take advantage of the fact that high-temperature superconductor (HTS) films develop a natural JJ when deposited on bi-crystal substrates, eliminating the need for multi-step JJ fabrication processes. Although bi-crystal JJs can only be used to build some types of qubits (e.g. phase and charge), the work conducted under this project allows us to establish the basic fabrication needs and setup the measurements capabilities. We have already deposited YBa2Cu3O7 (YBCO) films on two SrTiO3 (100) bi-crystal substrates by Pulsed Laser Deposition. We have chosen bi-crystals with angles of 30°, typically used for YBCO SQUIDs, and 36.8°, which will produce JJs with different parameters (lower coupling, and consequently smaller critical currents). We are currently in the process of patterning the bridges needed for the nonlinear electrical transport studies (I-V characteristics as a function of H and T) on these samples.

Topological quantum computation: The recent discovery of a new class of materials known as topological insulators provides renewed enthusiasm for the prospect of topologically protected qubits for quantum computation. The source of this excitement lies in the potential realization of Majorana fermions, which should exist in properly engineered structures utilizing topological insulators. A material that is a topological insulator (TI) possesses an insulating ground state that is topologically distinct from the vacuum; this necessarily ensures a metallic state at the surface. Unfortunately, all known TI materials possess impurities in the bulk which destroy the topological protection of the surface state. Our route to circumventing this problem is to investigate systems that are topological insulators due to strong correlations, rather than conventional band insulators. Strong correlations can result in much larger insulating gaps in the bulk that would add protection to a metallic surface state, as well as provide a simple mechanism for generating magnetism and/or superconductivity. Our experimental efforts led by Filip Ronning examined whether specific Samarium (Sm) based compounds may act as good host states for Majorana Fermions. Majorana Fermions should have topologically protected non-abelian statistics that some day may be used for quantum computation. We performed three complimentary studies.

First we measured specific heat of 6 powdered SmB6 samples with varying particle size from 40 um to a 1 mm3 single crystal. This compound was selected because it is a well known example of a “Kondo insulator”, a narrow gap material with an energy-gap brought about due to many-body correlations stemming from rare-earth magnetism interacting with charge carriers. The varying surface to volume ratio for different samples should enable us to determine whether a predicted surface state exists. Instead, we observed a decrease in the heat capacity at the lowest temperatures in the more finely powdered samples with higher surface area. This effect is likely due to a thermal decoupling of the sample at the lowest temperatures. Future measurements on LaB6 would help confirm this interpretation.

Second, we used a single crystal piece of SmB6 and at the CINT core in Sandia deposited a 80 nm thick film of Al on its surface. Subsequently, a 100nm wide trench in the Al was cut using a FIB, thereby creating a Josephson junction device. If a topologically protected surface state exists in SmB6, then this Josephson junction should possess Majorana fermions hence modifying its current-phase relation. Our transport measurements on this preliminary sample showed only a very weak superconducting signature (1% of the transport). I-V measurements revealed unstable resistance values. The origin of this behavior is likely in part due to the surface roughness observed in our SEM measurements of order 1 um. Future studies will require enhanced fabrication efforts to reduce sample roughness.

Lastly, with Cristian Batista we calculated the electronic band structure for SmS. This material, like SmB6, is a correlated semi-conductor with an incomplete gap at low tem-

peratures, which may be due to a topologically protected surface state. By inspection the electronic band structure has a band inversion that is a minimal requirement for possessing a topologically protected surface state. Using this band structure as input Cristian Batista is creating a tight binding Hamiltonian and calculating the topologically invariant quantities to determine if indeed a protected surface state must exist in this material.

Fast quantum computation and simulation methods: While quantum computers can efficiently simulate Schrödinger's evolution equation, efficient quantum methods to simulate simple classical processes, such as those determined by partial differential equations, are unknown. Examples are the simulation of the Master or heat equations. The first goal of this project's computational component was to design quantum-computation inspired methods for the efficient simulation of such equations. Our approach is to construct quantum Hamiltonians whose ground states encode the solution to the corresponding time-dependent equation. We also sought efficient quantum methods to prepare the ground states. One such approach is by means of adiabatic quantum computation, in which the ground state is prepared by slow changes in the Hamiltonian interactions.

Together with Director's funded postdoc, Jie Ren (T-4), and a visiting summer student, Fuxiang Li, (from Texas A&M University) Nikolai Sinitsyn performed calculations for the effect that they call the Braid Phase Transition. The latter is a topological phase transition, induced by the measurement apparatus. They discovered that this effect occurs when coupling to the apparatus becomes relatively strong, i.e. this transition indicates the appearance of quantum Zeno effect. This effect sheds new light on the physics of the measurement process by proving that quantum measurement can be considered as a topological critical phenomenon. The results are currently being written as a manuscript. Importantly, it should be possible to observe this unusual phase transition at LANL using the recently developed capability in the spin noise spectroscopy.

Cold atoms provide promising candidates for the quantum simulation of complex many-body Hamiltonians. Two challenges in this scheme are cooling to extremely low temperatures, and overcoming the effects of noise and fluctuations. Postdoc Armin Rahmanisisan's research in quantum simulations has focused on these challenges. He has proposed a scheme based on the optimal control of unitary evolution, which may help extend the limits of atomic cooling beyond the current state of the art. Additionally, He has been investigating the heating effect due to the inherently noisy fluctuations of quantum Hamiltonians and their effects on measurable observables. It is known that quantum (unitary) circuits can be related to condensed matter problems via mappings to "Feynman" Hamiltonians. That is, the ground state of Feynman Hamiltonians have large amplitude with the state output by a quantum circuit. Rolando Somma's efforts in support of this project focused on generalizing this mapping to non-unitary circuits. This opens the door to using exact methods, devised for computing ground state properties, for the simulation of non-unitary circuits.

Diego Dalvit has worked in collaboration with Adolfo del Campo (T-4 JRO Fellow) on issues associated with finding shortcuts to adiabaticity. They also examined ideas to apply similar techniques to problems where the target state is not the ground state with a given excited state. He has also used some of the resources to invite Dr. Federico Spedalieri from the Information Sciences Institute (USC School of Engineering), who is the lead person running the supercomputing D-Wave machine at USC. Dr. Spedalieri visited LANL during September 10-13, and presented a quantum lunch on September 12.

Impact on National Missions

Quantum computing holds great promise of exceptional speed up of computations for applications ranging from national security to pharmaceutical design. The field became critical for national security in 1993 when Peter Shor developed an algorithm that provided exponential speed up for factoring large numbers, an algorithm with direct applicability to cryptography. The proposed work will invigorate quantum computer science and technology at Los Alamos National Laboratory, enabling researchers at the Laboratory advance forefront technology in this arena. The proposed work is tightly tied to the Laboratory's national security and global security missions.

Attosecond Probing of Dynamical States in Solids - Graphene

George Rodriguez
20100633PRD4

Abstract

By combining the time resolved angle resolved photoemission spectroscopy setup (trARPES) [1] at LANL with ultrashort laser pulse generated attosecond pulse trains, the physics of electron dynamics and transport in graphene was studied in the time domain. Graphene was chosen due to the technological interest in its potential applications and unique electronic properties [2-4]. A question of central importance in graphene is how the carriers behave after optical excitation. The trARPES setup gives the ability to answer this through a measurement of the energy and momentum resolved dynamics of the unique linear band structure in graphene, although in a transient way. By promoting carriers above the ground state of the system through optical photoexcitation followed by extreme ultraviolet (XUV) photoemission of the now excited state in a pump-probe configuration, the time evolution of the carrier dynamics could be directly recorded. Additionally, since the pulses in the probe pulse train were cutting-edge sub-femtosecond (fs) pulses, the time domain response was measured with very high temporal resolution – approaching state-of-the-art technology.

Background and Research Objectives

The technique of trARPES has already demonstrated its utility in measuring complex correlated electron materials [5]. The electronic structure of materials is measured as the time evolution of both occupied and unoccupied states within the complex band structure. Luckily, graphene has a relatively simple structure in the vicinity of the Fermi edge with a linearly dispersive set of bands forming the so-called “Dirac point” [6]. While this band structure makes theoretical calculations easier, the continuous nature of the band structure opens the door for many electron-electron and electron-phonon interactions. Scattering of these “quasiparticles” results in a very fast excited state lifetime in comparison to other materials with large bandgaps [7]. Accurately measuring the time domain lifetimes of quasiparticles formed from optical excitation in materials has proven difficult due to the extremely short timescales involved. The powerful technique of trARPES represents the first such experiments on this unique material and has placed LANL in a leading position in this rapidly emerging field.

Combining trAPRES with attosecond pulse trains allows the opportunity to measure the electron transport in graphene with resolution limited only by the number of pulses in the attosecond pulse train. ARPES measures the simultaneous emitted angle and energy of electrons from a sample. Static ARPES measurements have already measured the band structure within the linear regime of graphene [8, 9]. In our experiments, an attosecond pulse train comprised of XUV photons was created through the high harmonic generation process. To the attosecond train, an infrared (IR) pulse was added as a pump for the graphene samples. Figure 1(a) shows a model of the band structure behavior in graphene following optical excitation. At t=0 when the pump and probe beams are overlapped, the optical pulse creates a band of promoted electrons above the Dirac point and a corresponding band of holes below. After a fast thermalization process, the electrons and holes redistribute themselves covering a wider energy range than the original band of promoted carriers. Most of this redistribution has already been theoretically explained [10-12]. As the delay between the pump and probe is increased, snapshots of the population decaying back to the ground state via electron-electron and electron-phonon interactions are made. A direct measurement of the dynamics involved in this process was the goal of this work. While there has been some theoretical work discussing the redistribution of carriers in graphene samples [10, 12], an accurate experimental result was realized for the first time by this work. The technique of trARPES with attosecond pulse trains has greatly increased our understanding of the dynamical processes in both graphene and other similar Dirac materials.

Scientific Approach and Accomplishments

In this work we studied the strongly correlated electron system in graphene on the fastest timescale currently possible, namely an attosecond pulse train. Such short pulses allowed us to accurately measure the relevant quasiparticle dynamics and transient spectral functions in both the energy and time domains simultaneously. Due to the low photoelectron count rates available we chose to look at the graphene samples in an angle integrated mode although the possibility for angle resolved experiments also exists. We looked at two important questions in the studies of graphene (described below), both of which are of significant scientific interest.

1.) Tracing ultrafast separation and coalescence of carriers in graphene with time-resolved photoemission: In graphene, an important question is how the photoexcited carriers behave on ultrashort timescales. Although more recent time-resolved studies have provided a wealth of information [13-15], fundamental questions concerning the quantum descriptions of the transient electron-hole plasma remain. More precisely, two alternative views of the dynamical relaxation are possible. For the first possibility, a very rapid thermalization amongst both the electrons and holes leaves the system at an elevated temperature, the resultant transient state being well-described by a Fermi distribution with unaltered chemical potential, μ, but at raised temperature, T. We will refer to this system as the T* model. A second possibility is that the nonequilibrium carriers form transient populations mimicked by two separate Fermi distributions with distinctly different chemical potentials and temperatures. We will call this system the μ* model. On one hand, the μ* description of the photoexcited electrons and holes allows for phenomena such as terahertz lasing or using graphene in tunable lasers [2, 16]. On the other hand, the observation of phenomena such as ultrafast photoluminescence and studies of carrier multiplication in graphene [15,16] imply fundamentally different quantum descriptions of the photo excited electron hole plasma, more in line with the T* model.

In the experiments, an attosecond pulse train of XUV photons with energy ~30 eV was used. The photons were then incident on a graphene sample grown via the chemical vapor deposition method with very few defects [17, 18]. Since the photon energy was well above the work function of the material, a spectrum of the emitted photoelectrons could be measured by observing the electron's resultant kinetic energy. This spectrum was a reconstruction of the band structure of the graphene and since our method for time-resolved photoemission is a true single photon process, an accurate reconstruction of the electrons and holes could be measured directly. Figure 1(b) shows a plot of the static photoemission spectra for graphene mounted on a substrate. Silicon dioxide was chosen as the substrate to minimize modifications to the electronic structure through substrate interactions [19, 20]. By using a pump pulse with photon energy below the work function of the material (1.55 eV) to first excite the sample, the time-evolution of the carrier and hole dynamics could be measured by simply varying the delay between the 1.55 eV pump pulse and the XUV probe pulse. The inset in Figure 1(b) shows the signal within the linear portion of graphene's band structure.

By measuring the population of emitted photoelectrons in the vicinity of the Dirac point, a map of the material's time-dependent electron transport was produced as seen in Figure 2(a). By extracting the data for graphene from Figure 2(a), we could assign a time varying temperature and chemical potential to the material. The results of this are shown in Figure 2(b). For early times, an ultrafast and large temperature change was measured due to thermal effects of the laser pulse on the graphene sample. This temperature then decayed slowly over a picosecond timescale due to a bottleneck effect of relaxing electrons. More interestingly, the chemical potential exhibited a non-zero behavior at early times followed by decay to zero. This represents a separated carrier distribution more indicative of the μ* model. At later times, the distributions coalesce into a single distribution centered at zero more closely matching the T* model. This demonstrates that both models occur in the samples but are strongly dependent on the timescales involved. The μ* model is more prevalent in ultrafast systems and at early times while the T* model is obvious in relatively slower experiments. Since the trARPES technique allows a direct sampling of the time evolution of the carrier distributions, only this technique combined with an attosecond pulse train was capable of measuring these results. Additional details of these experiments can be seen in References [21, 22].

2.) Direct measurement of quasiparticle lifetimes in graphene in the vicinity of the Dirac point: In a similar experiment to the previous one, graphene samples were again excited with optical photons and probed with ultrashort attosecond pulse trains. In this experiment however, the quasiparticle lifetimes were measured and compared with theory. With this method, we observed a very obvious excitation energy dependence on the relaxation time of graphene. At high energies above the Dirac point, the lifetimes were found to decay much faster than those close to the Dirac point as seen in Figure 3. This was attributed to the reduced phase space volume available for electron-phonon interactions close to the Dirac point in graphene's unique zero-gap band structure [6, 7]. This phenomenon

was further studied by directly measuring the relaxation times of carriers and holes generated in an energy range of +/- 1 eV around the Dirac point. We limited our photon energy to this range since the energy band structure is linear and we can eliminate intraband scattering processes. Our experimental results showed that after excitation, the carriers and holes redistribute themselves on a few fs timescale through various methods [10, 11]. After thermalization, the excited carriers cascade back to the ground state with those closest to the Dirac point relaxing last.

Our experimental results were also compared to a full tight-binding model to give further insight. The model includes many-body interactions which represent the coupling of electronic states to the lattice [23, 24]. These results along with the most recent experimental measurements can be seen in Figure 3 and in References [25, 26]. The resultant theoretical approach gave qualitatively identical results to the experiments. Additional measurements that include the angular dependence of the photoelectrons may yield more insight on which portions of the band structure are responsible for the quasiparticle dynamics while even shorter pulse durations can probe the initial thermalization processes after optical excitation.

Impact on National Missions

The research in this project was aimed at fundamental understanding of electronic structure and behavior of the complex correlated electronic material of graphene and with attosecond prulse trains setting the ultimate temporal resolution. It supported fundamental experiments as a foundation for future energy technologies by improving our understanding of new material properties. Hence, this project embraced the Laboratory's Materials Strategy, as well as the LDRD Grand Challenge in Materials. Broadening our knowledge about electrical transport and the physics of low dimensional electron systems is relevant to the DOE energy security mission, and ultimately National Security, by providing the scientific base for next generation energy efficient technologies. The scientific capabilities demonstrated in this project enhanced the Laboratory's portfolio in these studies for DOE Basic Energy Sciences program in Material Sciences and Engineering.

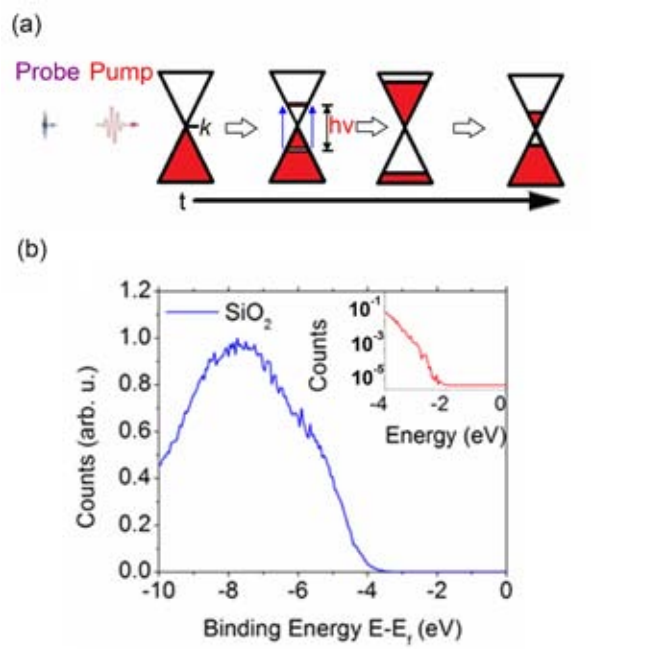

Figure 1. (a) A model of the carrier distributions in the linear region of graphene. The red color represents filled states and the white represents empty states. (b) A plot of the static photoemission signal from the graphene sample mounted on a silicon dioxide substrate. The inset shows the signal on a log plot in the vicinity of the linear portion of the band structure.

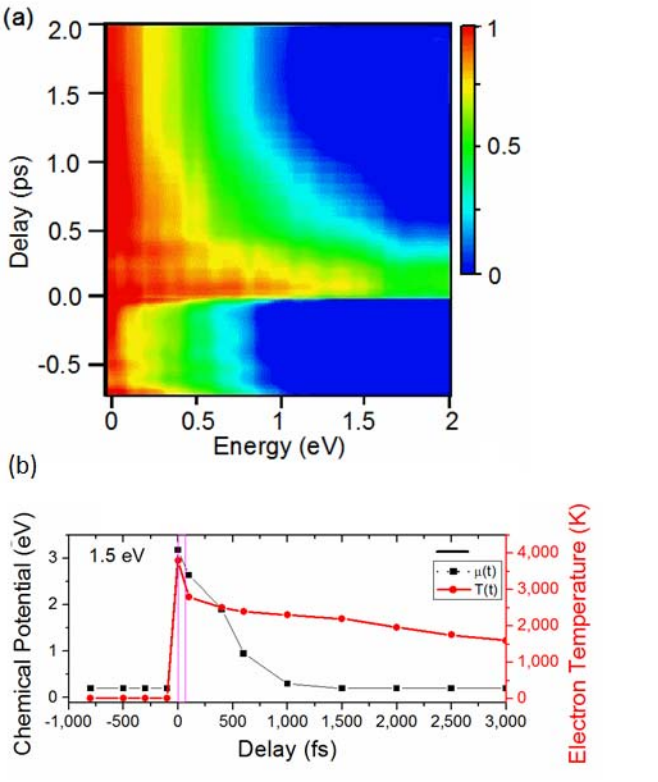

Figure 2. (a) The photoemission signal above the Dirac point in graphene as a function of delay. (b) A plot of the time varying chemical potential (black squares) and temperature (red squares) as extracted from the data in (a).

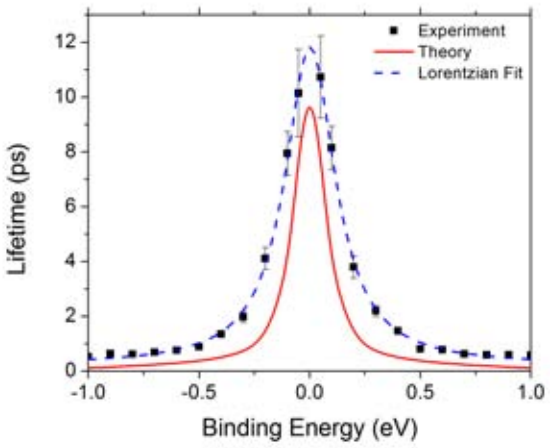

Figure 3. The measured quasiparticle lifetime is shown as the black squares. The blue dashed line represents a Lorentzian fit to the experimental data. The solid red line is the comparison with the theoretical model.

References

1. Dakovski, G. L., Y. Li, T. Durakiewicz, and G. Rodriguez. Tunable ultrafast extreme ultraviolet source for time- and angle-resolved photoemission spectroscopy. 2010. Review of Scientific Instruments. 81 (7): 073108.

2. Sun, Z., D. Popa, T. Hasan, F. Torrisi, F. Wang, E. J. R. Kelleher, J. Travers, V. Nicolosi, and A. C. Ferrari. A stable, wideband tunable, near transform-limited, graphene-mode-locked, ultrafast laser. 2010. Nano Research. 3: 653.

3. Gusynin, V. P., and S. G. Sharapov. Unconventional integer quantum Hall effect in graphene. 2005. PHYSICAL REVIEW LETTERS. 95 (14): 146801.

4. Zhang, Y., Y. Tan, H. Stormer, and P. Kim. Experimental observation of the quantum Hall effect and Berry's phase in graphene. 2005. Nature. 438 (7065): 201.

5. Rohwer, T., S. Hellmann, M. Wiesenmayer, C. Sohrt, A. Stange, B. Slomski, A. Carr, Y. Liu, L. M. Avila, Kalla&uml, S. Mathias, L. Kipp, K. Rossnagel, and M. Bauer. Collapse of long-range charge order tracked by time-resolved photoemission at high momenta. 2011. Nature. 471 (7339): 490.

6. Park, C. H., F. Giustino, C. Spataru, M. Cohen, and S. G. Loiue. Angle-resolved photoemission spectra of graphene from first principles. 2009. Nano Letters. 9: 4243.

7. Bostwick, A., T. Ohta, T. Seyller, K. Horn, and E. Rotenberg. Quasiparticle dynamics in graphene. 2007. NATURE PHYSICS. 3 (1): 36.

8. Zhou, S. Y., G. -H. Gweon, A. V. Fedorov, P. N. First, W. A. De Heer, D. -H. Lee, F. Guinea, A. H. Neto, and A. Lanzara. Substrate-induced bandgap opening in epitaxial graphene. 2007. NATURE MATERIALS. 6 (11): 916.

9. Ohta, T., A. Bostwick, T. Seyller, K. Horn, and E. Rotenberg. Controlling the electronic structure of bilayer graphene. 2006. SCIENCE. 313 (5789): 951.

10. Rana, F.. Electron-hole generation and recombination rates for Coulomb scattering in graphene. 2007. PHYSICAL REVIEW B. 76 (15): 155431.

11. Winzer, T., and E. Malic. Microscopic study of the efficiency of Coulomb and phonon induced relaxation channels in graphene. 2011. Phys. Status Solidi B. 248: 2615.

12. Kim, R., V. Perebeinos, and P. Avouris. Relaxation of optically excited carriers in graphene. 2011. PHYSICAL REVIEW B. 84 (7): 075449.

13. Sun, D., Z. Wu, C. Divin, X. Li, C. Berger, W. de Heer, P. First, and T. Norris. Ultrafast Relaxation of Excited Dirac Fermions in Epitaxial Graphene Using Optical Differential Transmission Spectroscopy. 2008. PHYSICAL REVIEW LETTERS. 101 (15): 157402.

14. Breusing, M., S. Kuehn, T. Winzer, E. Malic, F. Milde, N. Severin, J. P. Rabe, C. Ropers, A. Knorr, and T. Elsaesser. Ultrafast nonequilibrium carrier dynamics in a single graphene layer. 2011. PHYSICAL REVIEW B. 83 (15): 153410.

15. Lui, C. H., K. F. Mak, J. Shan, and T. Heinz. Ultrafast Photoluminescence from Graphene. 2010. PHYSICAL REVIEW LETTERS. 105 (12): 127404.

16. Ryzhii, V., M. Ryzhii, A. Satou, T. Otsuji, A. A. Dubinov, and V. Ya. Aleshkin. Feasibility of terahertz lasing in optically pumped epitaxial multiple graphene layer structures. 2009. JOURNAL OF APPLIED PHYSICS. 106 (8): 084507.

17. Dorn, M., P. Lange, A. Chekushin, N. Severin, and J. P. Rabe. High contrast optical detection of single graphenes on optically transparent substrates. 2010. JOURNAL OF APPLIED PHYSICS. 108 (10): 106101.

18. Ferrari, A. C., J. C. Meyer, V. Scardaci, C. Casiraghi, M. Lazzeri, F. Mauri, S. Piscanec, D. Jiang, K. S. Novoselov, S. Roth, and A. K. Geim. Raman spectrum of graphene and graphene layers. 2006. PHYSICAL REVIEW LETTERS. 97 (18): 187401.

19. Knox, K., S. Wang, A. Morgante, D. Cvetko, A. Locatelli,

T. O. Mentes, M. A. Nino, P. Kim, and R. M. Osgood. Spectromicroscopy of single and multilayer graphene supported by a weakly interacting substrate. 2008. PHYSICAL REVIEW B. 78 (20): 201408.

20. Wang, Y. Y., Z. H. Ni, T. Yu, Z. X. Shen, H. M. Wang, Y. H. Wu, W. Chen, and null. Wee. Raman studies of monolayer graphene: The substrate effect. 2008. JOURNAL OF PHYSICAL CHEMISTRY C. 112 (29): 10637.

21. Gilbertson, S., G. Dakovski, T. Durakiewicz, J. Zhu, K. Dani, A. Mohite, A. Dattelbaum, and G. Rodriguez. Tracing ultrafast separation and coalescence of carrier distributions in graphene with time-resolved photoemission. 2012. Journal of Physical Chemistry Letters. 3 (1): 64.

22. Gilbertson, S., G. Dakovski, J. X. Zhu, K. Dani, A. Dattelbaum, and G. Rodriguez. Separation and recombination of carrier distributions in graphene. Presented at Annual Meeting of the Conference on Lasers and Electro-Optics (CLEO) 2012. (San Jose, CA, 6-11 May 2012).

23. Neto, A. H. Castro, F. Guinea, N. M. Peres, K. S. Novoselov, and A. K. Geim. The electronic properties of graphene. 2009. REVIEWS OF MODERN PHYSICS. 81 (1): 109.

24. Piscanec, S., M. Lazzeri, F. Mauri, A. C. Ferrari, and J. Robertson. Kohn anomalies and electron-phonon interactions in graphite. 2004. PHYSICAL REVIEW LETTERS. 93 (18): 185503.

25. Gilbertson, S., T. Durakiewicz, J. Zhu, A. Mohite, A. Dattelbaum, and G. Rodriguez. Direct measurement of quasiparticle lifetimes in graphene using time-resolved photoemission. 2012. JOURNAL OF VACUUM SCIENCE & TECHNOLOGY B. 30 (3): 03D116.

26. Gilbertson, S., G. Dakovski, T. Durakiewicz, J. X. Zhu, K. Dani, A. Mohite, A. Dattelbaum, and G. Rodriguez. Time resolved carrier distributions in graphene. Presented at American Physical Society March Meeting 2012. (Boston, MA, 27 Feb. - 2 Mar. 2012).

Publications

Gilbertson, S.. Attosecond observation and control of autoionization in helium. Invited presentation at International Symposium on (e,2e), Double Photoionization and Related Topics & 16th International Symposium on Polarization and Correlation in Electronic and Atomic Collisions. (Dublin, Ireland, 4-6 Aug. 2011).

Gilbertson, S., G. Dakovski, J. X. Zhu, K. Dani, A. Dattelbaum, and G. Rodriguez. Separation and recombination of carrier distributions in graphene. Presented at Annual Meeting of the Conference on Lasers and Electro-Optics (CLEO) 2012. (San Jose, CA, 6-11 May 2012).

Gilbertson, S., G. Dakovski, T. Durakiewicz, J. X. Zhu, A. D. Mohite, A. Dattelbaum, and G. Rodriguez. Time resolved carrier distributions in graphene. Presented at American Physical Society March Meeting 2012. (Boston, MA, 27 Feb. - 2 Mar. 2012).

Gilbertson, S., G. Dakovski, T. Durakiewicz, J. Zhu, K. Dani, A. Mohite, A. Dattelbaum, and G. Rodriguez. Tracing ultrafast separation and coalescence of carrier distributions in graphene with time-resolved photoemission. 2012. Journal of Physical Chemistry Letters. 3 (1): 64.

Gilbertson, S., T. Durakiewicz, J. Zhu, A. Mohite, A. Dattelbaum, and G. Rodriguez. Direct measurement of quasiparticle lifetimes in graphene using time-resolved photoemission. 2012. JOURNAL OF VACUUM SCIENCE & TECHNOLOGY B. 30 (3): 03D116.

Mechanistic Investigation of C-C Bond Forming Reactions for the Production of Long Chain Hydrocarbons

Enrique R. Batista
20110542PRD1

Abstract

Due to instabilities in the global supply of crude oil, the development of bio-fuels is a top priority. A critical step toward realization of high energy density bio-fuels is the development of organic fuels that consist of a narrow distribution of longer hydrocarbon chains, which have higher energy density than current bio-fuels like ethanol. The key challenge in the synthesis of long hydrocarbon chains is the formation of new carbon-carbon bonds. One fundamental organic transformation ubiquitous in modern organic chemistry, the aldol condensation, is a carbon-carbon bond-forming reaction involving ketones and aldehydes (species with a C-O double bond, or carbonyl group). Our experimental collaborators have enjoyed some success with a new type of catalyst that can affect this reaction. A mechanistic understanding can lead to new options for improvement and optimization. We will use computational tools to analyze the atomistic aspects of the reaction mechanism and use this understanding to test new possibilities that will then be visited by the experimentalists for testing in the laboratory.

Background and Research Objectives

In an effort to upgrade bio-renewables to high-energy-density fuels and chemical feedstocks we are developing a strategy to convert readily available cellulose-derived polyols (such as hydroxymethyl furfural HMF) to high-density C8-C15 hydrocarbons. This first involves chain lengthening through C-C bond-forming aldol condensations followed by systematic defunctionalization involving such challenges as catalytic ring-opening of furans, removal of oxygen atoms through dehydration and reduction and removal of the resulting unsaturation through hydrogenation. The project consists in a tightly coupled effort with experimental groups, that are synthesizing catalyst molecules, and our computational work aimed at understanding the underlying mechanisms of catalysis. Our effort will inform experimental groups and help them better tailor their efforts.

Scientific Approach and Accomplishments

Detailed mechanistic results derived from theory focusing on the C-C bond-forming step in this process were produced for the piperidine catalyzed aldol condensation between HMF and acetone. The catalytic aldol condensation process was determined to proceed through a six-step mechanism involving a two-step substrate activation, a C-C bond forming step, a two-step release of products/catalyst regeneration followed by an additional dehydration of the products. In order to arrive at this conclusion we had to analyze all possible reactions involving the catalyst and the two substrates as well as the involvement of the solvent molecules during each step of the reaction. This last consideration is usually treated in a very approximated fashion or ignored all together. We found that many of the steps along the reaction pathway require proton transfers, which are catalyzed by clusters of water molecules requiring inclusion of explicit solvent. In addition, this mechanism proceeds through a very reactive zwitterionic intermediate previously believed to react with itself. Our more accurate approach utilizing explicit solvent molecules was used to clarify this confusion in the literature about intermediate steps of this nature in similar reactions. Consideration of those confused intermediate structures would make one believe that a key step in the catalytic process is not possible.

This work has been further expanded to examine the C-C bond-forming step in a related aldol condensation process utilizing bio-derived ethyl levulinate in place of acetone. This procedure also requires an acetic acid co-catalyst and is performed in the absence of water. While the general mechanism has not changed these new reaction conditions present several new problems: 1) Unlike acetone, ethyl levulinate has multiple active cites requiring understanding of the observed regioselectivity; 2) While the general mechanism is believed to be the same, water, which was found to be critical in the previous studies, is no longer present; 3) The role

of the co-catalyst is unknown. Through an examination of the possible reaction pathways we have determined that while reaction at multiple sites in ethyl levulinate leads to thermodynamically stable products, the observed product is the result of substantially lower kinetic barrier. The other two issues were found to solve each other as the acetic acid was found to act as a proton transfer catalyst in the place of water.

Finally, we have moved into studies of O-O bond activation mediated by transition metal complexes. These systems are also of interest in energy fuel cells. A fuel cell recovers stored energy in the form of hydrogen via a four-proton, four-electron reduction of oxygen at the cathode. In an effort to understand this mechanistically complex chemistry, much work has been performed over the last quarter century to develop molecular analogues for the study of oxygen reduction. In biology, oxidase enzymes such as cytochrome c oxidase perform this same chemistry using oxygen as the terminal oxidant. By employing oxygen in this same way, a rich array of aerobic oxidation chemistry has been developed employing palladium catalysts. In all of these chemistries, understanding the precise nature of the reaction of O2 with the given metal complex is crucial to further understanding and advancing these systems.

The initial work has been presented at the Gordon Conference on reaction mechanisms, and at the American Chemical Society National meeting in Denver, CO. A joint experimental/theory paper has been accepted in the peer-reviewed journal Current Organic Chemistry with an exhaustive description of the whole catalytic process. In addition a new joint experimental/theory manuscript is in preparation detailing the mechanistic differences involved with substrate modification, changes in solvent and the addition of co-catalysts. The oxygen activation work was published in two papers in the journal Inorganic Chemistry.

Impact on National Missions

This project includes organic aldol catalysis for carbon-carbon chain extension. Optimization of this process will result in significant impact to the fuels and specialty chemical sectors. Because the approach to producing liquid fuels is based on bio-mass, this project contributed to the carbon-neutral fuel cycle impacting environment and climate missions. The development of efficient catalytic mechanisms for production of biofuels has also been identified as a research need by the Office of Science BES report on “Clean and Efficient Combustion of 21st Century Transportation Fuels”. Having established credibility in the areas of biomass conversion is important for EERE and BES missions in the development of new cycles for biofuels.

References

1. Keith, J. M., J. K. Kim, L. Alexander, R. Wu, R. L. Martin, E. R. Batista, R. Michalczyk, B. Scott, S. K. Hanson, A. D. Sutton, J. C. Gordon, and L. A. P. silks. Solvent-free Organocatalysis Applicable to the Carbon Chain Extension of Carbohydrate Derivatives: Application to the Production of Transportation Fuels. J. of Organic Chemistry.

2. Keith, J. M.. Insertion of Molecular Oxygen into Rh-H: Sterically Induced Mechanistic Crossover Between Radical-Chain and Hydrogen-Atom-Abstraction Pathways. Angew. Chem. Int. Ed..

3. Keith, J. M., T. S. Teets, and D. G. Nocera. O2 Insertion into Group 9 Metal-Hydride Bonds: Evidence for Oxygen Activation through the Hydrogen-Atom-Abstraction Mechanism. 2012. Inorg. Chem.. 51 (17): 9499.

Publications

Daly, S., J. Keith, E. Batista, K. Boland, S. Kozimor, R. Martin, and B. Scott. Probing Ni[S2PR2](2) electronic structure to generate insight relevant to minor actinide extraction chemistry. 2012. Inorganic Chemistry. 51 (14): 7551.

Keith, J. M.. Insertion of Molecular Oxygen into Rh-H: Sterically Induced Mechanistic Crossover Between Radical-Chain and Hydrogen-Atom-Abstraction Pathways. . Angew. Chem. Int. Ed..

Keith, J. M., J. K. Kim, L. Alexander, R. Wu, R. L. Martin, E. R. Batista, R. Michalczyk, B. Scott, S. K. Hanson, A. D. Sutton, J. C. Gordon, and L. A. P. Silks. Solvent-free Organocatalysis Applicable to the Carbon Chain Extension of Carbohydrate Derivatives: Application to the Production of Transportation Fuels. J. of Organic Chemistry.

Keith, J. M., J. K. Kim, L. Alexander, R. Wu, R. L. Martin, E. R. Batista, R. Michalzyk, B. L. Scott, S. K. Hanson, A. D. Sutton, L. A. P. Silks, and J. C. Gordon. Aqueous organocatalysis applicable to the carbon chain extension of carbohydrate derivatives: Application to the production of transportation fuels. To appear in Current Organic Chemistry.

Keith, J. M., T. S. Teets, and D. G. Nocera. O2 Insertion into Group 9 Metal-Hydride Bonds: Evidence for Oxygen Activation through the Hydrogen-Atom-Abstraction Mechanism. 2012. Inorg. Chem.. 51 (17): 9499.

Keith, J., E. Batista, R. Martin, R. Wu, L. Pete. Silks, and J. Gordon. Catalyzed conversion of non-food biomass to fuels: Probing the mechanism of the initial C-C bond forming step. 2011. In 242nd National Meeting of the American-Chemical-Society (ACS) ; 20110828 -

20110901 ; Denver, CO. (Denver, CO, Aug. 28 - Sep. 1st, 2011). Vol. 242, p. 1. Denver, CO: ACS.

Keith, J., and E. Batista. Theoretical Examination of the Thermodynamic Factors in the Selective Extraction of Am3+ from Eu3+ by Dithiophosphinic Acids. 2012. Inorganic Chemistry. 51 (1): 13.

Exploiting the Fermi Surface to Understand Quantum Criticality in Complex Electronic Materials

Eric D. Bauer
20110549PRD1

Abstract

Standard models for simple metals and insulators often fail for strongly interacting electronic systems in which correlations between d- or f-electrons and conduction electrons promote new and unexpected states of matter. An increasingly common example of emergent phenomena in these complex electronic materials (e.g., heavy fermions and high-Tc cuprates) is found when a magnetic phase transition is tuned to absolute zero temperature by an external parameter, such as doping, pressure, or magnetic field. At the resulting quantum critical point, new and distinct states are found. In particular, jiggling of spins of the f-electrons ("spin fluctuations") that are abundant and violent at the quantum critical point lead to unusual behavior that do not follow the expectations for a simple metal. This type of behavior has continued to defy a complete description after nearly 20 years and poses one of the most significant challenges to the condensed matter community. A crucial yet unresolved issue of quantum criticality is what happens to the Fermi surface (the surface of constant energy that dictates the motion of the valence electrons) at the quantum critical point. In general, the Fermi surface is expected to be small in the magnetic state, where the f-electrons are located close to the atomic core (localized) and evolves into a large Fermi surface when the f-electrons on the other side of the quantum critical point. The two leading models of quantum criticality have distinct predictions for this small-to-large Fermi surface crossover—either it is continuous or occurs abruptly. Director's Funded postdoctoral Fellow Ryan Baumbach will synthesize and characterize f-electron compounds that exhibit quantum critical behavior to quantitatively determine the evolution of the Fermi surface volume. This research will lay the scientific foundation for understanding quantum criticality.

Background and Research Objectives

In f-electron materials, novel states of matter emerge from the nearly degenerate kinetic and potential energy of the f-electrons. The two extreme limits of f-electron behavior, i.e., magnetic order or itinerant paramangetism, due to competition between Coulomb repulsion (potential energy) and orbital overlap with neighboring ligands (kinetic energy), respectively, are well-understood phenomena with in standard models for metals. An increasingly common example of emergent phenomena in these complex electronic materials (e.g., heavy fermions and high-Tc cuprates) is found when a magnetic phase transition is tuned to absolute zero temperature by an external parameter, such as doping, pressure, or magnetic field. At the resulting quantum critical point, new and distinct states are found, which cannot be understood by knowing the properties of the two parent magnetic or nonmagnetic states. This type of behavior has continued to defy a complete description after nearly 20 years and poses one of the most significant challenges to the condensed matter community. While many theories have been proposed, these models do not describe all the properties of even a single quantum critical material. A solution to this quantum criticality conundrum will come from carefully designed experiments that distinguish between existing theories and guide in the development of new ones. A crucial yet unresolved issue of quantum criticality is what happens to the Fermi surface (the surface of constant energy that dictates the motion of the valence electrons) at the quantum critical point. The synthesis and characterization of ultra-high purity f-electron compounds that exhibit quantum critical behavior, mainly involving Ce, and U, provides the means to quantitatively determine the evolution of the Fermi surface volume through direct measurements including de Haas van Alphen and Hall effect. This research will lay the scientific foundation for understanding quantum criticality and will play a central role in understanding and exploiting functional complex electronic materials of the 21st century.

Scientific Approach and Accomplishments

Director's Funded Ryan Baumbach's research for this project is focused around two main goals: 1) to search for promising quantum critical f-electron materials and to characterize their properties and 2) explore the Fermi surface of these materials near the quantum critical point. Below is a summary of his accomplishments towards these goals.

Search for New Quantum Critical Systems

Baumbach discovered a new class of materials with the chemical formula LnT2M2X (Ln = La-Nd, T = Ru, Os; M = Al, Ga; X = B, C). These compounds crystallize in a filled variant of the CeMg2Si2–type structure and are closely related to the ubiquitous ThCr2Si2-type structure, which is associated with a large number of systems that exhibit non-Fermi-liquid behavior and quantum criticality. As such, the LnT2M2X materials provide an exciting new avenue for the study of correlated electron physics. Attention has been focused on the CeT2M2X materials, as these are the most likely to exhibit quantum critical behavior. Three compounds: CeRu2Al2B, CeRu2Ga2B, and CeRu2Ga2C have been synthesized. Contrary to what is often observed for Ce-based compounds, these three compounds show pronounced local magnetic moment behavior, resulting in ferromagnetic ordering of the Ce-ions at strikingly high temperatures: i.e., Curie temperatures Tc = 12.8 K, 16.1 K, and 16.7 K for CeRu2Al2B, CeRu2Ga2B, and CeRu2Ga2C, respectively. In addition, CeRu2Al2B undergoes antiferromagnetic ordering at a Neel temperature TN = 14.1 K. The application of a magnetic field H to CeRu2Al2B results in a rich phase diagram that includes three magnetically ordered phases: (1) antiferromagnetic, (2) canted antiferromagnetic, and (3) ferromagnetic, indicating that there are several finely tuned exchange interactions [1-2].

The unit cell volumes for these three compounds decrease in the order CeRu2Al2B, CeRu2Ga2B, CeRu2Ga2C, commensurate with the increase in Tc. This trend suggests that the Ce 4f electrons in these materials localized and magnetic, supporting the point of view that in order to access the quantum critical point, it is necessary to further reduce the unit cell volume. To this end, the temperature (T)–pressure (P) phase diagrams were studied up to pressures of 25 kbar. The evolution of properties with chemical and applied pressure suggests that CeRu2Al2B is furthest from the possible quantum phase transition and CeRu2Ga2C is the nearest to one [3].

To further characterize the microscopic properties of this new class of materials, nuclear magnetic resonance (NMR) studies were performed on the tetragonal Ce-based ferromagnet CeRu2Ga2B. The Knight shifts show an Ising-type anisotropy along the c axis, similar to results from the static susceptibility. The anisotropy of the spin-lattice relaxation rates indicates that the anisotropy of spin fluctuations are also Ising-like along the c-axis. The absolute values and temperature dependence of spin-lattice relaxation rate suggest a well-localized 4f picture for this system: The local moments of Ce ions fluctuate as a result of ferromagnetic intersite coupling above the ferromagnetic transition and individually fluctuate due to intrasite coupling well above Tc [4]. These measurements provide important clues for the microscopic origin of the magnetism in CeRu2Ga2B and point to future directions to tune this new class of magnets to a quantum critical point.

Explore the Fermi surface of these materials near the quantum critical point

In solids containing elements with f-orbitals, the interaction between f-electron spins and those of itinerant electrons leads to the development of low-energy excitations with a heavy effective mass. These excitations are fundamental to the appearance of unconventional superconductivity and non-Fermi liquid behavior observed in actinide- and lanthanide-based compounds. In particular, massive mobile electrons are expected to emerge from complex interactions in a periodic array of f-electron atoms, the Kondo lattice, only at low temperatures— which has never observed directly before. Scanning tunneling microscopy has been used to detect the emergence of heavy excitations with lowering of temperature in a prototypical family of CeMIn5 (M=Co, Rh) heavy fermion compounds, which provides first direct visualization of heavy fermion band structure and developing ground state (Figure 1). Furthermore, these measurements reveal signature of quantum criticality, opening up an entirely new window for understanding this decades-old conundrum found in many classes of energy-saving materials [5].

Baumbach's efforts produced ultra-high purity samples of the Ce2T3X5 (T = transition metal and X = Si, Ge) family of correlated electron compounds, which includes the pressure-induced superconductor Ce2Ni3Ge5. Of these materials, the antiferromagnets Ce2Rh3Ge5 and Ce2Pt3Si5 are particularly interesting (Neel temperature TN = 5.5 K and 6.3 K, respectively). Recent studies at the National High Magnetic Field Laboratory in Los Alamos show that in addition to having similar ordering temperatures and associated magnetic 4f-electron entropy their antiferromagnetic states are suppressed to zero temperature at similar magnetic fields (critical fields Hc = 23 T and 36 T, respectively as shown in Figure 2), suggesting comparable magnetic energy scales in these compounds. In contrast, while the pressure needed to access a quantum critical point (QCP) in Ce2Rh3Ge5 is extremely low (Pc = 5 kbar), the Néel temperature for Ce2Pt3Si5 is insensitive to pressures up to 15

kbar. These results imply that although these compounds are markedly similar, the mechanism that drives the QCP in Ce2Rh3Ge5 is not present in Ce2Pt3Si5. In order address this difference, it is essential to investigate their behavior in the vicinity of their field and pressure driven quantum phase transitions. Preliminary measurements to quantify the shape of the Fermi surface for H > Hc for both of these compounds, have been carried out at low temperatures and high magnetic fields for both of these compounds, as illustrated in (Figure 3). Future measurements at lower temperatures will be performed in April, 2013 to observe the Fermi surface change across the quantum critical point in these Ce2M3X5 materials.

Impact on National Missions

The study of quantum criticality is one of the true frontiers in modern science. Understanding the essential interaction among strongly correlated electron materials is a necessary step for the Laboratory and for DOE to fulfill its missions in energy security. This research will provide the scientific foundation for understanding and exploiting functional complex electronic materials of the 21st century.

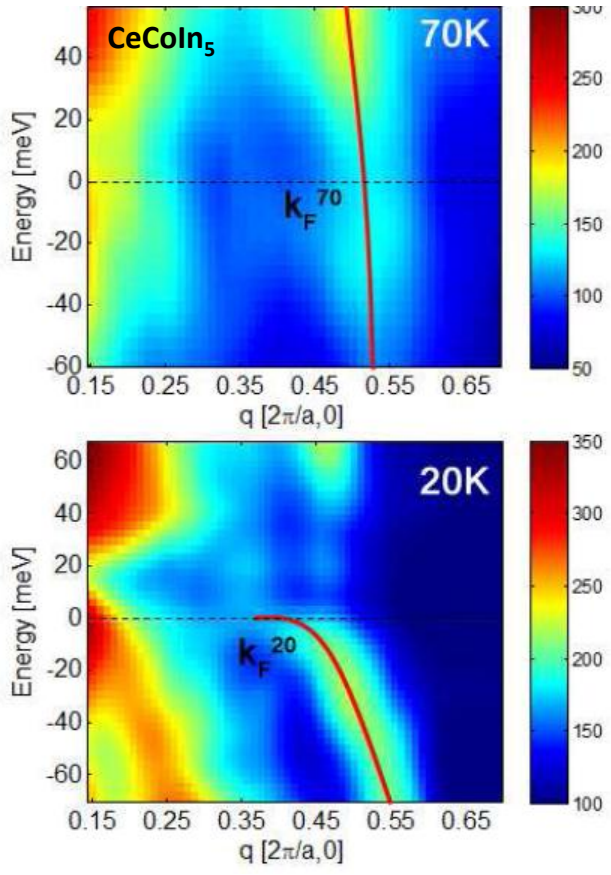

Figure 1. Transition from a small to large Fermi surface in CeCoIn5 determined via scanning tunneling spectroscopy showing the development of the heavy fermion state with decreasing temperature.

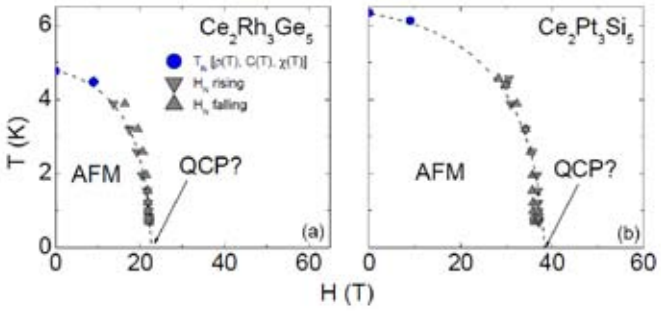

Figure 2. Temperature – magnetic field (T-H) phase diagrams for Ce2Rh3Ge5 and Ce2Pt3Si5. For H < 9 T, data were gathered using electrical resistivity, specific heat, and magnetic susceptibility techniques in DC magnetic fields. Data points at higher magnetic fields were collected in pulsed magnetic fields up to 60 T.

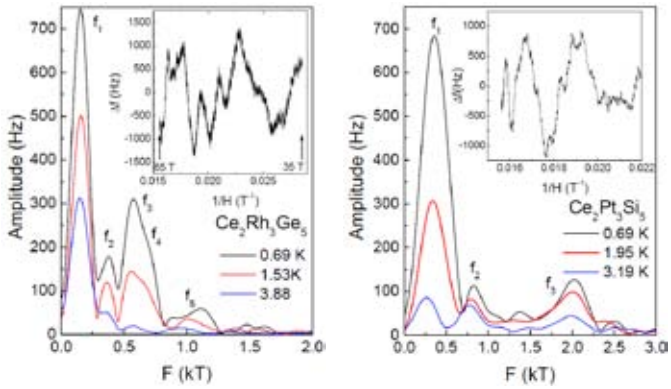

Figure 3. Main panels: Fourier transform of the oscillations in Ce2Rh3Ge5 (left panel) and Ce2Pt3Si5 (right panel) for H > Hc revealing different frequencies corresponding to various Fermi surface sections at several representative temperatures. Insets: Raw tunnel diode oscillator data at 0.69 K (after polynomial background subtraction) showing quantum oscillations.

References

1. Baumbach, R. E., T. Shang, M. Torrez, F. Ronning, J. D. Thompson, and E. D. Bauer. Local moment ferromagnetism in CeRu2Ga2B. 2012. Journal of Physics-Condensed MatterJournal of Physics-Condensed Matter. 24 (18).

2. Baumbach, R. E., H. Chudo, H. Yasuoka, F. Ronning, E. D. Bauer, and J. D. Thompson. CeRu2Al2B: A local- moment 4 f magnet with a complex T-H phase diagram. 2012. Physical Review BPhysical Review B. 85 (9).

3. Baumbach, R. E., X. Lu, F. Ronning, J. D. Thompson, and E. D. Bauer. Pressure tuned ferromagnetism in CeRu2M2X (M = Al, Ga; X = B, C). 2012. Journal of Physics-Condensed MatterJournal of Physics-Condensed Matter. 24 (32).

4. Sakai, H., Y. Tokunaga, S. Kambe, R. E. Baumbach, F.

Ronning, E. D. Bauer, and J. D. Thompson. NMR study for 4f-localized ferromagnet CeRu2Ga2B. 2012. Physical Review BPhysical Review B. 86 (9).

5. Aynajian, P., E. H. da Silva Neto, A. Gyenis, R. E. Baumbach, J. D. Thompson, Z. Fisk, E. D. Bauer, and A. Yazdani. Visualizing heavy fermions emerging in a quantum critical Kondo lattice. 2012. NatureNature. 486 (7402): 201..

Publications

Aynajian, P., E. H. da Silva Neto, A. Gyenis, R. E. Baumbach, J. D. Thompson, Z. Fisk, E. D. Bauer, and A. Yazdani. Visualizing heavy fermions emerging in a quantum critical Kondo lattice. 2012. NatureNature. 486 (7402): 201.

Baumbach, R. E., H. Chudo, H. Yasuoka, F. Ronning, E. D. Bauer, and J. D. Thompson. CeRu2Al2B: A local- moment 4 f magnet with a complex T-H phase diagram. 2012. Physical Review BPhysical Review B. 85 (9).

Baumbach, R. E., T. Shang, M. Torrez, F. Ronning, J. D. Thompson, and E. D. Bauer. Local moment ferromagnetism in CeRu2Ga2B. 2012. Journal of Physics-Condensed MatterJournal of Physics-Condensed Matter. 24 (18).

Baumbach, R. E., X. Lu, F. Ronning, J. D. Thompson, and E. D. Bauer. Pressure tuned ferromagnetism in CeRu2M2X (M = Al, Ga; X = B, C). 2012. Journal of Physics-Condensed MatterJournal of Physics-Condensed Matter. 24 (32).

Sakai, H., Y. Tokunaga, S. Kambe, R. E. Baumbach, F. Ronning, E. D. Bauer, and J. D. Thompson. NMR study for 4f-localized ferromagnet CeRu2Ga2B. 2012. Physical Review BPhysical Review B. 86 (9).

Non-aqueous Organic Materials for Bio-defense

James M. Boncella
20110580PRD2

Abstract

Room-temperature ionic liquids (RTILs) are uniquely composed of cation-anion pairs that form non-volatile, low-density, thermally stable liquids at room temperature, and can be rationally designed such that they interact with biomolecules in highly advantageous ways. We have investigated and reduced to practice the use of RTILs to stabilize, solubilize, and eliminate polymorphs of small molecule drugs, penetrate skin for transdermal drug delivery, eliminate biofilms of pathogenic bacterial, which are antibiotic-resistant due to their nearly impenetrable extracellular matrix, and stabilize carbonic anhydrase, an enzyme useful in some alternative energy strategies, These results are relevant to the LANL mission because we have shown defeat of antibiotic-resistant biofilms, and eight-fold increased thermal stability of drugs to temperature extremes and sunlight exposure. The work has received a follow-on grant to address defense-related needs for skin-based delivery of pharmaceutical agents. Three patent applications and four peer-reviewed publications have also arisen from this work.

Background and Research Objectives

Room-temperature ionic liquids (RTILs), are uniquely composed of cation-anion pairs that form non-volatile, low-density, thermally stable liquids at room temperature, and interact with biomolecules in highly advantageous ways. For example, RTILs, which are neither hydrophobic nor hydrophilic in the traditional definition, can stabilize proteins, solubilize substrates, and improve enzyme or biocatalyst selectivity and activity. These non-aqueous fluid materials can be used to address many areas related to the LANL mission by rational design for application in biological processes. RTILs are unique materials as they are primarily organic in nature, enabling rapid modification to address specific applications. This ability to tune the properties of RTILs renders them extremely powerful new materials and allows investigation into the basic science that drives their functionality as chemical and biological tools. Hydrophobic, protic, and aprotic ionic liquids have been designed, synthesized, and tuned depending upon requirements of the biological system, and applied to diverse problems related to antibiotic-resistant pathogens, biodefense, and bioenergy.

We have developed a new general strategy for producing ionic liquid formulations of cationic pharmaceutical agents that is more robust than the current state of the art and features a simplified synthetic method. Many drugs form crystalline polymorphs that differ in solubility in the acidic stomach environment. Some drugs are poorly absorbed due to low solubility of the crystalline form. Increased bioavailability through drug formulation with ionic liquids would mean smaller effective dosages and would eliminate batch variations due to polymorphism. In addition to circumventing crystal polymorphism issues, ionic liquid formulations of medicines are also useful because they can be designed to stabilize drugs to high temperature or UV irradiation, and improve or control solubility and bioavailability of the drug. We have produced thermally stabilized forms of small molecule drugs as well as trans-dermally bioavailable forms of pharmaceuticals that must otherwise be administrated i.v. in a hospital setting (Figure 1). Materials synthesized have been evaluated on stability vs. time and pH, purity, melting/glass transitions, water-octanol partitioning, and cost effectiveness.

Ionic liquids are not currently used for transdermal applications because they have not been sufficiently studied for drug delivery and cytotoxicity. Our basic research gave rise to a funded project to address these bottlenecks. The funded project is advancing the design of preliminary topical formulations that were developed based on FDA-approved and GRAS (generally recognized as safe ingredients). The properties of these formulations are being optimized and the investigation is leading to a better understanding of the science and design criteria of

controlling transdermal efficacy and improving toxicity to biofilms. This research has also given rise to investigations of the efficacy of ionic liquids in treating infections due to pathogenic biofilms.

Scientific Approach and Accomplishments

The scientific approach has involved the synthesis of over 100 ionic liquids and deep eutectic solvents. We began by using existing principles to design materials with desirable room temperature properties such as a low melting temperature, low viscosity, high or low conductivity, high or low water solubility, low toxicity, or high lipophilicity. We transitioned to relying on our own observations about structure-activity relationships, outlined below, for designing new materials.

The accomplishments of this project have included four peer-reviewed papers. At least two manuscripts destined for peer-review are in preparation, which will bring the total publication number to six. Three patent applications have been filed for materials developed during this project. Specifically, one important accomplishment involved the identification of a novel, unpublished, and eminently patentable synthetic strategy for reliably synthesizing ionic liquids from pharmaceutical salts. Our strategy, one that was previously not identified by the ionic liquid and pharmaceutical formulation research communities, predictably produces ionic liquids from small molecule drugs. Our own initial experiments with the state-of-the-art synthesis of pharmaceutical ionic liquids revealed issues not readily revealed by published literature. The standard syntheses involved metathesis reactions or activation of components by ion exchange columns. The metathesis reactions inevitably produced side products, such as NaCl, which were difficult to remove from the final ionic liquid. The use of ion exchange columns also sometimes introduced impurities, either through material leaching from the columns themselves or because the organic molecules degraded in the presence of the strongly acidic or basic ion exchange resins. The formation of ionic liquids containing active pharmaceutical agents using our newly introduced method has been successful for every pharmaceutical agent that we have tried, as long as the melting point of the standard pharmaceutical salt is less than 300°C. Our strategy for new formulations is defined by four features: 1) inorganic-organic anion-cation pairs instead of organic-organic pairs, 2) IL formation involving chlorometallate speciation in Lewis acids, rather than proton transfer reactions, 3) GRAS-based reagents to speed regulatory approval, and 4) use as starting materials of virtually any active pharmaceutical agent with melting point <300°C. The synthetic method has produced 30 new pharmaceutically relevant ionic liquids, including an agent with potent anti-biofilm activity, starting from four different metallochlorides ($ZnCl_2$, $FeCl_3$, $CoCl_2$, and $SnCl_4$). The use of Lewis-acidic ionic liquids succeeds without production of side products or impurities because the chloride of the pharmaceutical agent combines with $ZnCl_2$ to produce zinc chloride anions and oligomers (Figure 2) that contribute to the disorder and reduced melting temperatures of the system. We also realize benefits of eliminating the use of ion exchange columns due to the extra time it takes to pass reagents through the column, the loss of a certain percentage of reagent to the stickiness of the column and the cost of the column resin.

Completed analyses on these materials (Figure 3), including glass transition temperatures, decomposition temperatures, and viscosity for some ionic liquids synthesized as described, include thermal gravimetric analysis for determination of thermal stability, differential scanning calorimetry for identification of glass transitions and melting temperatures, Raman spectroscopy for detection of zinc chloride speciation, infrared spectroscopy for observation of cation-anion interaction in solution, water-octanol partition coefficients for determination of lipophilicity, mass spectrometry for evaluation of purity and speciation, viscosity measurements, cyclic voltammetry, and determination of electrical conductivity. These results have been published in peer-reviewed journals.

The strategy has produced an agent with an 8-fold increase in shelf life at room temperature and a 10-fold increase in shelf life at 40°C (Figure 4), which also has increased water solubility as compared with the commercially available, crystalline HCl salt. With another agent, we can reduce the number of cells in biofilms derived from clinically isolated, pathogenic P. aeruginosa by three orders of magnitude.

Other accomplishments of this project have included the identification of ionic liquids that allow the activity of the enzyme carbonic anhydrase. This enzyme is of interest for CO_2 conversion and in biofuels applications. Ionic liquids must have low viscosity to allow diffusion into and out of the enzyme active site and may not denature or inhibit the enzyme. Scientific design criteria that were developed to promote carbonic anhydrase activity in ionic liquids included prioritization of ionic liquids with no “active” protons and ionic liquids containing imidazolium derivatives as the cationic component. Moreover, materials with bistrifluoromethylsulfonimide were ultimately eliminated from consideration. Imidazolium derivatives promote the activity of carbonic anhydrase, as has been shown by x-ray crystallography, and bistrifluoromethylsulfonimide is a suspected inhibitor of the enzyme. Preliminary, unpublished results suggest that four ionic liquids with potential for use in a carbonic anhydrase system are 1-hexyl-1-methylimidazolium chloride, ethylammonium nitrate, propylammonium

nitrate, and 1,3-dimethylimidazolium dimethylphosphate.

Another accomplishment of the project is the development of ionic liquid and deep eutectic solvent materials for promoting transdermal delivery of small molecule drugs. We are the first to examine the interaction between neat ionic liquids and mammalian skin. Work is ongoing, but preliminary investigations have revealed two excellent delivery agents, both of which include a terpenoid anion. Tetradecyltrihexylphosphonium cations and choline cations have both been employed in this work to design and produce ionic liquids and deep eutectic solvents with low viscosity, high lipophilicity, low conductivity, low toxicity to human primary lung cells, and high ionic strength.

Another accomplishment of this project is the development of ionic liquid and deep eutectic solvent materials for elimination of clinically derived, pathogenic biofilms of Pseudomonas aeruginosa. We are the first to investigate the toxicity of neat ionic liquids in pathogenic biofilms. The use of neat ionic liquids instead of solvated ionic liquids greatly improves dissolution of the biofilm. A neat ionic liquid contains only cations and anions and has strong hydrogen bond-disrupting capabilities, in contrast with a solvated ionic liquid, which is essentially a highly concentrated aqueous solution and has reduced potential to break down the biofilm extracellular matrix.

Three collaborations have been initiated due to this project. A partnership with biofilm experts at Northern Arizona University (Prof. Andrew Koppisch) has allowed investigation of the antimicrobial effects of our ionic liquids in clinically isolated, biofilm-forming pathogenic bacteria. An effort involving students from Dixie State College of Utah (Prof. Rico Del Sesto) will allow investigation into the prevention of biofilm growth on ionic liquid coated catheters, army uniforms, metal surfaces, and fiberglass plates. Finally, a team effort with transdermal drug delivery experts at the University of California-Santa Barbara (Prof. Samir Mitragotri) is beginning to identify mechanisms for ionic liquid penetration of skin. For the collaboration with UCSB, we have won a two-year grant from this year's highly competitive UC Lab Fee program, a result of the rapid progress of this project to garner further interest in more applied aspects of these materials.

Impact on National Missions

Drugs formulated as ionic liquids will be more stable at extremes of temperature and under exposure to sunlight and should therefore prove more useful for use by the warfighter. Other applications of this work will include addressing defense-related needs for rapid and facile skin-based or oral delivery of antimicrobial, anti-tubercular, and other pharmaceutical agents, as well as addressing national security concerns related to administration of prophylactic agents in the case of a CBRNE attack on the general population.

The creation of new materials from active pharmaceutical compounds is a new area of study with relevance to military and government applications. We have developed these new, biologically-active materials within the two-year project, building a capability that is relevant to several missions. The work has developed our ability to understand and design these new agent tool kits, and has addressed areas where significant intellectual property has been generated.

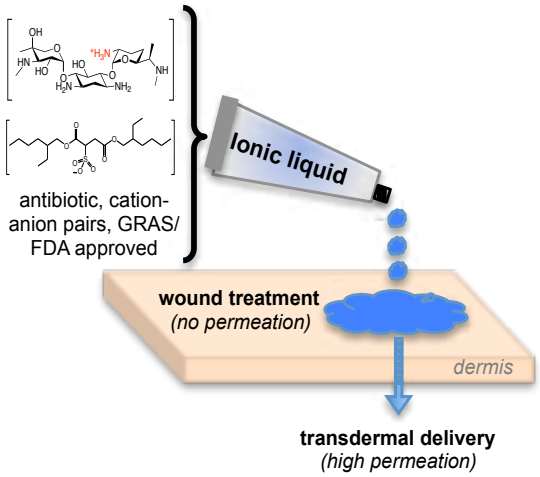

Figure 1. Transdermal drug delivery by IL.

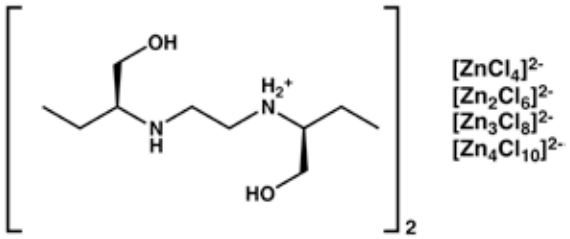

Figure 2. Ethambutol, a pharmaceutical used in the treatment of tuberculosis, is shown along with the zinc chloride species identified by Raman spectroscopy that contribute to the fluidity of the ionic liquid formulation.

ILs formed with two equiv. $ZnCl_2$	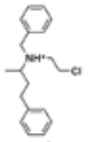 *phenoxybenzamine*	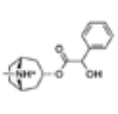 *homatropine*	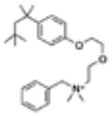 *benzethonium*	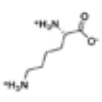 *lysine*	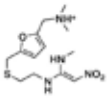 *ranitidine*	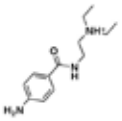 *procainamide*	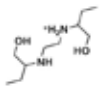 *ethambutol*	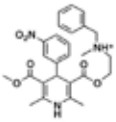 *nicardipine*	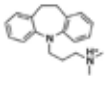 *imipramine*
T_g of IL	30.31°C	62.18°C	8.58°C	-22.57°C	-21.89°C	-16.99°C	13.74°C	39.2°C	24.6°C
T_g of Cl^- salt	122°C	205°C	146°C	263°C	124°C	156°C	183°C	156.7°C	161.6°C
ΔT_g	- 92°C	- 143°C	- 137°C	- 286°C	- 146°C	- 173°C	- 169°C	-117.8°C	-137.0°C
T_{dec} onset, IL	259.0°C	274.5°C	291.8°C	332.8°C	230.9°C	291.0°C	216.5°C	302.2°C	267.2°C
T_{dec} onset, Cl^- salt	213.9°C	266.7°C	181.5°C	267.3°C	216.8°C	279.7°C	250.1°C	226.7°C	245.8°C
ΔT_{dec} onset	+ 45.1°C	+ 7.8°C	+ 110.3°C	+ 55.5°C	+ 14.1°C	+ 11.3°C	- 33.6°C	+75.5°C	+ 21.4°C
IL mass loss, 50-120°C	0.84%	0.32%	0.17%	2.4%	2.4%	0.69%	1.8%	0.01%	1.7%
IL Viscosity, 90°C	ND	ND	8700 cP	24240 cP (at 145°C)	ND	ND	17350 cP	ND	ND
Use of drug	complex regional pain	cocaine analog	anti-pathogen	amino acid	acid reflux	irregular heartbeat	tuberculosis	vascular disorders	potential anti-ebola therapeutic

Figure 3. Summary of properties, including glass transition temperatures, decomposition temperatures, and viscosity for a selection of ionic liquids produced during this project.

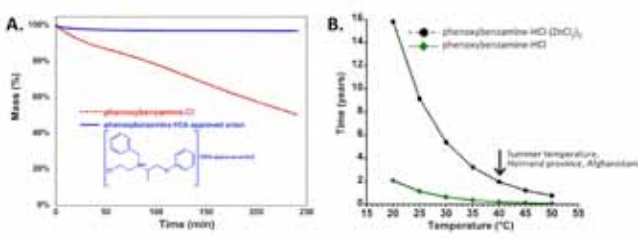

Figure 4. Demonstration of increased thermal stability of amorphous chlorometallate formulations of pharmaceuticals. (A) Thermal stability as measured by mass loss (loss of HCl) over 4 h at 120°C. The solid blue line represents the amorphous formulation and the dotted red line represents the unstabilized small molecule drug. (B) Demonstration of a predicted 8-fold increase in shelf life due to formulation of standard chloride salt pharmaceuticals as metal chloride ionic liquids. These ionic liquid species form due to metal chloride speciation of ZnCl₂ and other pharmaceutically safe salts.

Publications

Lovejoy, K. S., A. J. Lou, L. E. Davis, T. C. Sanchez, S. Iyer, C. A. Corley, J. S. Wilkes, R. K. Feller, D. T. Fox, A. T. Koppisch, and R. E. Del Sesto. Single-Pot Extraction-Analysis of Dyed Wool Fibers with Ionic Liquids. 2012. ANALYTICAL CHEMISTRY. 84 (21): 9169.

Lovejoy, K. S., C. A. Corley, E. K. Cope, M. C. Valentine, J. G. Leid, G. M. Purdy, J. S. Wilkes, A. T. Koppisch, and R. E. Del Sesto. Utilization of Metal Halide Species Ambiguity to Develop Amorphous, Stabilized Pharmaceutical Agents As Ionic Liquids. 2012. CRYSTAL GROWTH & DESIGN. 12 (11): 5357.

Lovejoy, K. S., G. M. Purdy, S. Iyer, T. C. Sanchez, A. Robertson, A. T. Koppisch, and R. E. Del Sesto. Tetraalkylphosphonium-Based Ionic Liquids for a Single-Step Dye Extraction/MALDI MS Analysis Platform. 2011. ANALYTICAL CHEMISTRY. 83 (8): 2921.

Lovejoy, K. S., L. E. Davis, L. M. McClellan, A. M. Lillo, J. D. Welsh, E. N. Schmidt, C. K. Sanders, A. J. Lou, D. T. Fox, A. T. Koppisch, and R. E. Del Sesto. Evaluation of ionic liquids on phototrophic microbes and their use in biofuel extraction and isolation. 2013. JOURNAL OF APPLIED PHYCOLOGY. 25 (4): 973.

Metal Catalysts for Oxidation of Lignocellulose and Reduction of Carbon Dioxide

Susan K. Hanson
20110581PRD2

Abstract

With demand increasing for fossil fuels and concern growing over carbon dioxide emissions, the development of alternative energy sources is a national security priority. Lignocellulose or carbon dioxide might function as a source of renewable feedstocks for a range of commodities; however, technical challenges remain in the catalytic conversion of lignocellulose or carbon dioxide for use in biofuel and chemical applications. This project has focused on replacing traditional catalysts based on precious metals with alternative catalysts based on inexpensive, earth-abundant metals. Vanadium-catalyzed aerobic oxidation has been demonstrated as an approach to break down lignin model compounds, suggesting the potential of vanadium catalysts for converting lignin into more valuable chemicals. A new class of cobalt catalysts has been developed for hydrogenation and dehydrogenation reactions. The cobalt catalysts were shown to reduce several different functional groups, including C=C, C=O, and C=N bonds, under mild conditions, providing an inexpensive alternative to the precious metal catalysts typically used for these reactions. The development of inexpensive, earth-abundant catalysts for both of these processes is an important technical advance in our ability to more efficiently use renewable resources.

Background and Research Objectives

From 2007 to 2035, global energy consumption is projected to increase by 49%. Demand for fossil fuels, fuel costs, carbon dioxide emissions, and concerns over global warming are on the rise. The development of alternative energy sources is thus becoming an increasingly urgent priority for national security. Non-food derived biomass (lignocellulose) and carbon dioxide are the only renewable carbon feedstocks that could be used to replace petroleum as a source of carbon-based fuels and chemicals. However, converting either lignocellulose or carbon dioxide to useful chemicals and fuels is a major challenge. A catalyst (a chemical which enables the desired reaction) is required to produce fuels or other industrial chemicals from lignocellulose or carbon dioxide, but the current catalytic technologies are lacking. More effective and selective catalysts are needed to fully utilize these renewable feedstocks. This project investigated the synthesis of new catalysts for the conversion of lignocellulose and carbon dioxide to useful chemicals and fuels.

Disassembly of lignin

Non food-derived biomass (lignocellulose) is attracting attention as a potential renewable feedstock for production of chemicals and fuels. Efficient transformation of lignocellulose into more valuable products remains a major challenge, particularly due to the difficulties associated with breakdown of lignin. Although some promising selective conversions of cellulose to useful materials have recently been reported, less progress has been made with lignin, which is typically incinerated in the paper and forest industry. New methods to depolymerize lignin would represent a major breakthrough towards the production of bio-derived chemicals and fuels.

The strategy explored in this project was to use an earth-abundant transition metal (vanadium) catalyst to break apart lignin. This approach could lead to selective methods to transform lignin into more useful chemicals and fuels. We selected vanadium for investigation because in oxidation reactions, vanadium complexes are known to break carbon-carbon and carbon-hydrogen bonds.

New vanadium(V) catalysts were synthesized, characterized, and evaluated for the oxidation of lignin model compounds. Specifically, vanadium(V) complexes of the tridentate bis(phenolate)pyridine ligand H2BPP (H2BPP = 2,6-(HOC6H2-2,4-tBu2)2NC5H3) and the bis(phenolate) amine ligand H2BPA (H2BPA = N,N-bis(2-hydroxy-4,5-dimethyl¬benzyl)¬propyl-amine) were prepared (Figure 1). Complexes (BPP)VV(O)(OiPr) and (BPA)VV(O)(OiPr) were evaluated as catalysts for the aerobic oxidation of 4-me-

thoxybenzyl alcohol and arylglycerol β–aryl ether lignin model compounds. The catalytic activities and selectivities of the bis(phenolate) complexes were compared to other related catalysts. Decomposition of the vanadium catalyst resulting from oxidation of the bis(phenol)amine ligand was observed during the attempted aerobic oxidation of lignin model compounds. However, the vanadium complex with the bis(phenolate)pyridine ligand did catalyze the aerobic oxidation of lignin model compounds. Overall, in considering a complete catalytic cycle, the evidence suggests that while the more electron rich bis(phenolate) ligand set may accelerate the reaction of vanadium(IV) with air, the opposite trend is expected for the alcohol oxidation step, which would be promoted by more electron deficient ligands. Designing more active vanadium catalysts for aerobic oxidation reactions will require balancing the electronic requirements of both steps. A paper describing these findings has been published. Another goal of the project was to develop a water-soluble vanadium complex and test its ability to catalyze aerobic oxidation in aqueous solution. Several different approaches were attempted in order to prepare a water-soluble vanadium analogue, and one such catalyst bearing 8-hydroxyquinoline-5-sulfonate ligands was prepared. This complex was tested for the oxidation of lignin model compounds, and a number of other substrates. Our results indicate that certain benzylic alcohols can be oxidized by air in water, using the vanadium catalyst. Overall, these results are a promising indication that it may be possible to develop an environmentally friendly method to break down lignin, using water as a solvent, air as the oxidant, and a vanadium catalyst.

Developing hydrogenation catalysts based on earth-abundant metals

Non-food biomass and carbon dioxide are potential renewable feedstocks, but both contain more oxygen-based functional groups than traditional petroleum-derived feedstocks. To use biomass or carbon dioxide as precursors for chemicals or fuels, removal of the oxygen functionality is needed. Although considerable progress has been made in the catalytic reduction of carbon dioxide and biomass feedstocks, many of the best current processes employ precious metal hydrogenation catalysts (e.g. platinum, ruthenium, rhodium, or iridium). Replacing these precious metal catalysts with earth abundant metals (cobalt or iron) would be a key breakthrough in terms of developing more cost-effective and sustainable processes.

This project focused on the design of earth-abundant metal catalysts for hydrogenation based on iron and cobalt. Prior to this work, few examples of homogeneous Fe, Ni, or Co hydrogenation catalysts were known, and these lacked the high activity, broad substrate scope, and functional group tolerance of more commonly used precious metal catalysts. In this project, iron and cobalt complexes were investigated as catalysts for the hydrogenation of organic substrates. Specifically, a cobalt-based catalytic system for the hydrogenation of alkenes, aldehydes, ketones, and imines was developed (Figure 2). The cobalt system is remarkably active, operating under mild conditions (room temperature or 60 oC). The cobalt catalyst is effective for a wide range of substrates and tolerates alcohol, amine, and carboxylic acid functionalities and water. Mechanistic experiments indicated that the active catalyst is a cobalt(II) hydride complex. These findings have major ramifications for future catalyst development, suggesting the potential of cobalt(II) hydride complexes, which have been largely neglected, to serve as highly active catalysts. A paper describing these findings was featured on the cover of the chemistry journal Angewandte Chemie International Edition (Figure 3).

The new cobalt complexes were also evaluated as catalysts for alcohol dehydrogenation. Alcohol dehydrogenation has applications in energy technologies, like hydrogen storage and production, as a selective and low-temperature route to generate hydrogen from biomass-derived alcohols and carbohydrates. However, previous examples of homogeneous catalysts capable of the acceptorless dehydrogenation of alcohols have been limited exclusively to precious metals (Ru, Rh, Ir, Os). In this project, the first example of a non-precious metal (cobalt) catalyst for the acceptorless dehydrogenation of alcohols was developed. The cobalt catalyst displays comparable activity to previously reported ruthenium catalysts, is active for a wide range of aliphatic and aromatic alcohols, and generates the carbonyl products in high yields, affording hydrogen as the only reaction by-product. Deuterium labeling studies were used to confirm that the alcohol dehydrogenation proceeds through a cobalt-hydride intermediate.

The new cobalt catalysts for hydrogenation and dehydrogenation were an important step forward in the development of cost-effective, viable routes to use alternative carbon sources like biomass or carbon dioxide. However, the mechanisms of these reactions were not known, and it was clear that a better fundamental understanding of the elementary steps involved would be instrumental for rational catalyst design and optimization. Additional experimental studies were carried out that explored the mechanisms of the cobalt-catalyzed hydrogenation and dehydrogenation reactions. Investigations into the role of metal-ligand cooperativity in the reactions, as well as the identification of potential catalytic intermediates and resting states (including an unusual stable cobalt(III) aryl hydride product of C-H bond activation) provided new insights into the catalytic

cycles. Notably, our studies suggested that the hydrogenation of alkenes and the dehydrogenation of alcohols proceeded by different mechanisms, and that both catalytic cycles based on cobalt(II) and cobalt(I)/(III) oxidation states are viable. This part of work has been published as a full article in the Journal of American Chemical Society. Overall, the design of effective earth-abundant metal catalysts for the hydrogenation of C=C and C=O bonds is a key step forward in our ability to more efficiently and cost-effectively utilize renewable resources like lignocellulose or carbon dioxide.

Impact on National Missions

In a recent 2013 address to the nation, President Obama stated that "the only way for America's energy supply to be truly secure is by permanently reducing our dependence on oil…We have to discover and produce cleaner, renewable sources of energy with less of the carbon pollution that threatens our climate. And we have to do it quickly." In order to effectively use renewable sources of carbon (non-food biomass or carbon dioxide) as fuels, new catalytic technologies are needed. In demonstrating that it is possible to use inexpensive, earth-abundant metals like vanadium and cobalt as catalysts for these applications, this work has provided an important conceptual and technological advance. The work is relevant to Office of Basic Energy Sciences mission priorities. DoD relevance is driven by the fact the DoD is aggressively seeking new energy sources for its deployed operations.

(a) (b)

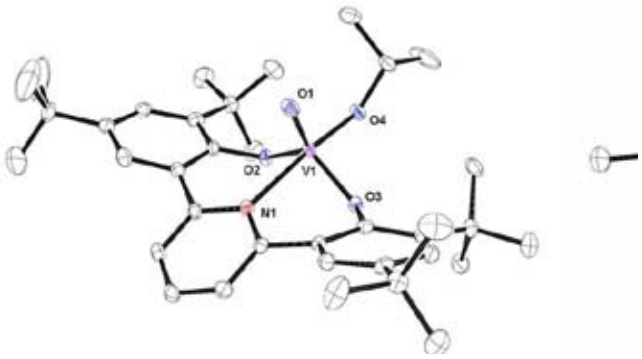

Figure 1. Structures of bis(phenolate)pyridine vanadium complex (a, left) and bis(phenolate)amine vanadium complex (b, right).

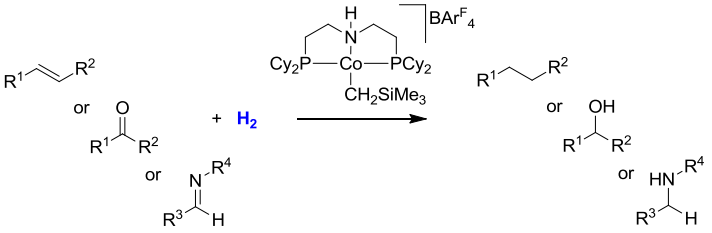

Figure 2. Cobalt catalyst developed for the hydrogenation of C=C, C=O, and C=N bonds.

Figure 3. Cobalt catalysis featured on the cover of Angew. Chem. Int. Ed.

Publications

Zhang, G., B. L. Scott, R. Wu, L. A. Silks, and S. K. Hanson. Aerobic oxidation reactions catalyzed by vanadium complexes of bis(phenolate) ligands. 2012. Inorganic Chemistry. 51 (13): 7354.

Zhang, G., B. L. Scott, and S. K. Hanson. Mild and homogeneous cobalt-catalyzed hydrogenation of C=C, C=O, and C=N bonds. 2012. Angewandte Chemie International Edition. 51: 12102.

Zhang, G., K. V. Vasudevan, B. L. Scott, and S. K. Hanson.

Understanding the mechanisms of cobalt-catalyzed hydrogenation and dehydrogenation reactions. 2013. Journal of the American Chemical Society. 135: 8668.

Zhang, G., and S. K. Hanson. Cobalt-catalyzed acceptorless alcohol dehydrogenation: synthesis of imines from alcohols and amines. 2013. Organic Letters. 15: 650.

Controlled Synthesis and SERS Responses of Metal Nanostructures with Complex Morphologies

Hsing-Lin Wang
20110759PRD4

Abstract

In this project, we aimed at synthesis of metal nanoparticles (1D) and hybrid nanocomposites (2D) with strong plasmonic properties through an extremely facile synthetic platform that is cost effective and time efficient. This synthetic platform allowed us to fabricate metal nanoparticles with a wide range of sizes, structures, and morphologies. These metal nanoparticles have novel optical, sensing, and catalytic properties, resulting from the complex particle morphology, which led to surface, enhanced Raman scattering. Results obtained from this study allowed us to establish correlations between the metal structures and the optical/catalytic properties. The surface enhanced Raman scattering (SERS) technique utilizes surface plasmons generated by the greatly enhanced electromagnetic field at the rough metal surfaces. SERS spectroscopy has been recognized as a powerful tool for chemical analysis and sensing applications due to its high sensitivity and resolution. [1, 2] The development of the SERS technique has enabled a series of applications that was previously not accessible. Another objective of this project was to develop highly efficient SERS substrates based on conducting polymer mediated electrodeless deposition of metal nanoparticles [3] (Figure 1). These substrates were extremely sensitive and showed promise toward detection of several chemicals related to food safety and explosive detection. Moreover, the confinement of SERS on a single metal particle has shown promise in better understanding the catalytic reactivity and demonstrated their use as a heterogeneous catalyst. We also show examples of plasmon assisted catalytic reaction on our SERS substrate toward better understanding the reaction mechanisms induced by laser excitation.

Background and Research Objectives

Surface–enhanced Raman scattering (SERS) utilizes the greatly enhanced electromagnetic fields generated by the excitation of surface plasmons at metal surfaces to enhance the Raman signal of absorbed molecules. This technique has been widely explored as a powerful spectroscopic probe that can provide non–destructive and ultra–sensitive detection of chemical and biological molecules up to single molecule levels. Most recent activities have focused on the SERS properties of metal nanoparticle dimers since the space between the dimers can provide large electromagnetic field enhancements. However, the focus of nanoscience and nanotechnology has gradually shifted from the synthesis of individual components to their assembly into larger systems with well–defined structures. Assemblies of nanoscale building blocks with complex structures usually presents collective optical, electronic, catalytic, and magnetic properties that are distinctly different from the corresponding individual nanoparticles. Self–assemblies of metal nanoparticles based on rational control of non-covalent interactions provide powerful tools for the design of hierarchical structures at length scales from nano– to micrometer size. Therefore, the large–scale controllable synthesis of metal structures with specific morphologies is expected to lead to a greater understanding/validation of underpinning SERS mechanisms involved in complex assemblies with enhanced optical and electronic properties.

The goal of this project was to demonstrate controlled synthesis of self-assembled metal structures with specific complex morphologies through a facile and novel technique trough which metal nanoparticles with a wide range of structures, sizes, and morphologies can be synthesized. We proposed to study the SERS response of these metal nanoparticles for sensitive detection of chemical and biological analytes. We aimed to understand the underpinning mechanism of how metal nanoparticles self-assemble into larger, complex systems with well–defined structures (Figure 2). We synthesized these metal structures using reducing and directing agents without polymer surfactant or capping agents. Structure–property relationships and tunable

photonic responses resulting from the directed assembly of nanoparticles were interpreted.

Another important goal of this project was to demonstrate catalytic properties of these SERS substrates for various chemical reactions. Using surface plasmon to assist chemical reactions has tremendous implications for energy applications. SERS particles irradiated under laser light result in the formation of "hot electrons" which can then reduce the absorbates immobilized on the metal particle surface. We used p-nitrothiophenyl (p-NTP) as model molecules to show dimerization of p-NTP to form azobenzene molecules on SERS substrate. We have shown for the first time, the detailed reaction mechanisms of this dimerization reaction, revealing the catalytic nature of our SERS substrates, which can be applied to reactions with significant energy implications.

Scientific Approach and Accomplishments

Synthesis and characterization

These as–synthesized metal structures have been analyzed with electron microscopy, transmission electron microscopy, and X–ray diffraction. Mapping and imaging using SERS spectra of chemical and biological molecules on the metal structures have been measured with a Raman microscope apparatus. In order to conduct a systematic study of how small molecules impact the self–assembly of metal nanoparticles into larger systems, small inorganic and organic acids, amino acids, and inorganic salts have been employed in the synthesis of the metal structures to develop control over the size and morphology of the metal particles. SERS comparisons, polarization–dependent SERS responses and plasmonic properties of the metal structures with different morphologies were also performed.

Chemical sensing

Through the use of a wide range of metal nanoparticles we synthesized, we have shown applications of these nanoparticles as well as nanocomposites toward detection of chemicals. A clear example is the detection of melamine down to 2 ppm sensitivity (Figure 3). As of today, our SERS substrate is the only substrate capable of detecting melamine with sensitivity reaching 2 ppm. Such results have potentially huge impacts on food safety as our technology represents a new technique of inspecting toxins in dairy products and the method is fast and cheap. This work was published as a featured front cover article in the Journal of Materials Chemistry.[4]

Catalytic applications

We have demonstrated catalytic reactions driven by a single particle on which the kinetics and products can be monitored by SERS spectra. The conversion of p-nitrothiophenyl (p-NTP) into dimerized azobenzene (DMAB) and the wavelength-dependent kinetics has been demonstrated by using three laser excitation wavelengths. The reactivity under 633 nm proceeded much slower than that under 532 nm or 514.5 nm excitation. Further decrease of the laser energy turned off the reaction completely. Our results revealed consistency with previous observation as we use a relatively low power (0.05 mW) of 633 nm excitation laser, conversion of p-NTP to DMAB proceeded extremely slow as compared to that using the high laser power (0.2 mW).

The SEM micrograph of a single micron sized particles comprised of numerous nanosheets and the SERS spectra of p-NTP as a function of time are shown in Figure 4. The surface Plasmon intensity decrease of the ν(NO2) band at 1335 cm-1, and increase of the ν(N=N) bands at 1380 and 1440 cm-1 can be distinguished over a time scale of several hours. The diminished NO2 peak and concomitant increase of the N=N band absorption provided unequivocal evidence of the chemical reaction catalyzed by surface plasmons. The control experiment carried out under the same conditions without the usage of metal particles showed no formation of N=N band frequency. Such drastic change in the reaction clearly associates the reaction itself with the surface plasmon as a catalytic substrate. The modification of the plasmonic properties of the metal particles through variation of the particle morphology was expected to have a huge impact on their catalytic properties. This work has been published in Chemical Communications as featured front cover article.[5]

Impact on National Missions

Our project aimed at developing a facile and novel small molecule–directed synthesis of metal nanoparticles and their self-assemblies with well–defined structures. These studies could open up a new avenue for fabricating complex assembled architectures with emergent properties that were previously inaccessible. The spontaneous organization of nanoparticles into larger systems is of scientific importance as understanding the assembly process on the nanometer scale is of great interest for bottom–up fabrication of functional devices. The advantages of fabricating self–assembled metal complex structures is clear: (1) Superior SERS responses and morphological control over conventional approach via manipulating the organization of small nanoparticles. The emergent, superior optical and catalytic properties can lead to significant reduction of energy use for chemical reactions. Moreover, the catalytic properties also show promise in biofuel and biomass production with much lower cost and faster reaction time. (2) A greater understanding of the self–assembly mechanism that will allow optimization of the SERS response with sensitivities that rival fluorescence at the single molecule

detection level, which will be tremendously important for detection of explosive and toxins and will therefore contribute significantly to the area of threat reduction.

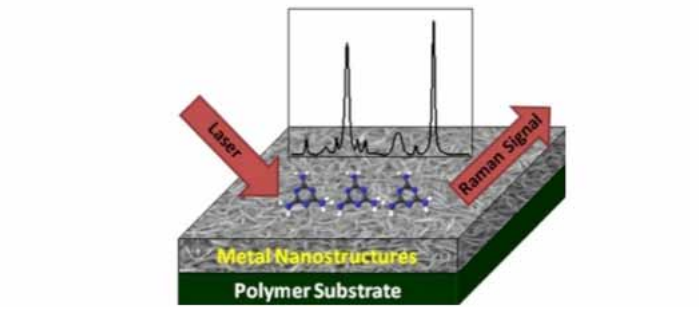

Figure 1. Schematic representation of a SERS substrate comprised of numerous nanosheet assembly on top of a conducting polymer layer.

Figure 2. Schematic illustration of the synthesis of metal particles with well–defined morphologies aided by reducing and directing agents. Variations of the molar ratio between reducing and directing agents, and the timing of adding directing agent to the solution can result in metal particles with four distinct morphologies.

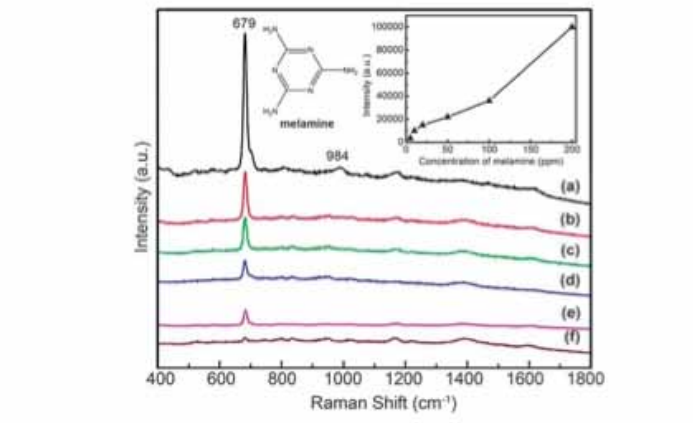

Figure 3. SERS spectra of melamine in different concentrations taken on core–shell Ag wire structures: (a) 200 ppm, (b) 100 ppm, (c) 50 ppm, (d) 20 ppm, (e) 10 ppm, and (f) 5 ppm. Measurements were conducted with a 10 s exposure and 1 mW laser power. Inset shows the relationship between Raman intensity of the 679 cm-1 band and concentration of melamine solution.

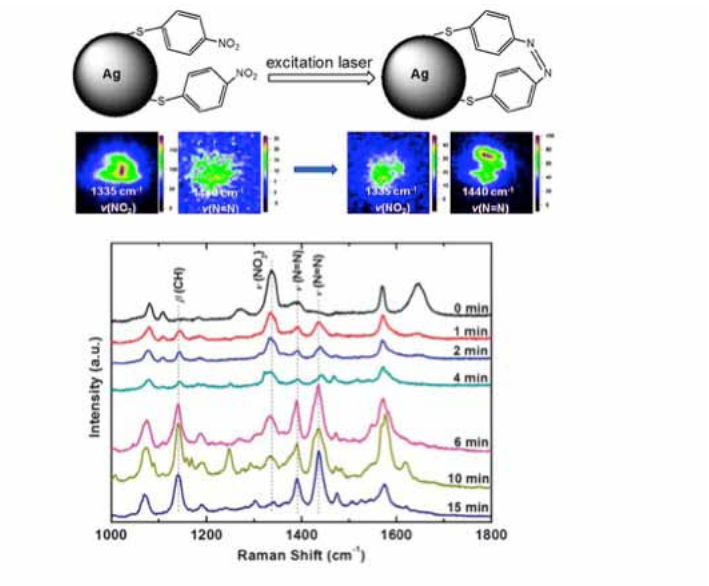

Figure 4. (top) Laser induced dimerization reaction, converting p-nitrothiophenyl (p-NTP) into dimerized azobenzene (DMAB), and (bottom) Time-dependent SERS spectra of p-nitrothiophenol (pNTP) under continuous exposure to the 633 nm laser. The spectra were collected for a single Ag particle, with an integration time of 2 s, and a laser power of 2 mW.

References

1. Lantman, E. M. van Schrojenstein, T. Deckert-Gaudig, A. J. G. Mank, V. Deckert, and B. M. Weckhuysen. Catalytic processes monitored at the nanoscale with tip-enhanced Raman spectroscopy. 2012. NATURE NANOTECHNOLOGY. 7 (9): 583.

2. Casadio, F., M. Leona, J. R. Lombardi, and R. Van Duyne. Identification of Organic Colorants in Fibers, Paints, and Glazes by Surface Enhanced Raman Spectroscopy. 2010. ACCOUNTS OF CHEMICAL RESEARCH. 43 (6): 782.

3. Wang, H. L., W. G. Li, Q. X. Jia, and E. Akhadov. Tailoring conducting polymer chemistry for the chemical deposition of metal particles and clusters. 2007. CHEMISTRY OF MATERIALS. 19 (3): 520.

4. Zhang, B., P. Xu, X. M. Xie, H. Wei, Z. P. Li, N. H. Mack, X. J. Han, H. X. Xu, and H. L. Wang. Acid-directed synthesis of SERS-active hierarchical assemblies of silver nanostructures. 2011. JOURNAL OF MATERIALS CHEMISTRY. 21 (8): 2495.

5. Kang, L. L., P. Xu, B. Zhang, H. H. Tsai, X. J. Han, and H. L. Wang. Laser wavelength- and power-dependent plasmon-driven chemical reactions monitored using single particle surface enhanced Raman spectroscopy. 2013. CHEMICAL COMMUNICATIONS. 49 (33): 3389

Publications

He, J. J., X. J. Han, J. Yan, L. L. Kang, B. Zhang, Y. C. Du, C. K. Dong, H. L. Wang, and P. Xu. Fast fabrication of homogeneous silver nanostructures on hydrazine treated polyaniline films for SERS applications (vol 14, pg 4952, 2012). 2012. CRYSTENGCOMM. 14 (24): 8737.

He, J. J., X. J. Han, J. Yan, L. L. Kang, B. Zhang, Y. C. Du, C. K. Dong, H. L. Wang, and P. Xu. Fast fabrication of homogeneous silver nanostructures on hydrazine treated polyaniline films for SERS applications. 2012. CRYSTENGCOMM. 14 (15): 4952.

He, J., X. Han, J. Yan, L. Kang, B. Zhang, Y. Du, C. Dong, H. Wang, and P. Xu. Fast fabrication of homogeneous silver nanostructures on hydrazine treated polyaniline films for SERS applications. 2012. CRYSTENGCOMM-CRYSTENGCOMM. 14 (15): 4952.

Huang, Y. F., H. S. Shih, C. W. Lin, P. Xu, D. J. Williams, K. J. Ramos, D. E. Hooks, and H. L. Wang. Morphology Control of Cu Crystals on Modified Conjugated Polymer Surfaces. 2012. CRYSTAL GROWTH & DESIGN. 12 (4): 1778.

Huang, Y. F., Y. I. Park, C. Kuo, P. Xu, D. J. Williams, J. Wang, C. W. Lin, and H. L. Wang. Low-Temperature Synthesis of Au/Polyaniline Nanocomposites: Toward Controlled Size, Morphology, and Size Dispersity. 2012. JOURNAL OF PHYSICAL CHEMISTRY C. 116 (20): 11272.

Huang, Y., H. Shih, C. Lin, P. Xu, D. J. Williams, K. J. Ramos, D. E. Hooks, and H. Wang. Morphology Control of Cu Crystals on Modified Conjugated Polymer Surfaces. 2012. CRYSTAL GROWTH & DESIGNCRYSTAL GROWTH & DESIGN. 12 (4): 1778.

Huang, Y., Y. I. Park, C. Kuo, P. Xu, D. J. Williams, J. Wang, C. Lin, and H. Wang. Low-Temperature Synthesis of Au/Polyaniline Nanocomposites: Toward Controlled Size, Morphology, and Size Dispersity. 2012. JOURNAL OF PHYSICAL CHEMISTRY CJOURNAL OF PHYSICAL CHEMISTRY C. 116 (20): 11272.

Jeon, S. H., P. Xu, B. Zhang, N. H. Mack, H. Tsai, L. Y. Chiang, and H. L. Wang. Polymer-assisted preparation of metal nanoparticles with controlled size and morphology. 2011. JOURNAL OF MATERIALS CHEMISTRY. 21 (8): 2550.

Kang, L. L., P. Xu, B. Zhang, H. H. Tsai, X. J. Han, and H. L. Wang. Laser wavelength- and power-dependent plasmon-driven chemical reactions monitored using single particle surface enhanced Raman spectroscopy. 2013. CHEMICAL COMMUNICATIONS. 49 (33): 3389.

Kang, L. L., P. Xu, D. T. Chen, B. Zhang, Y. C. Du, X. J. Han, Q. Li, and H. L. Wang. Amino Acid-Assisted Synthesis of Hierarchical Silver Microspheres for Single Particle Surface-Enhanced Raman Spectroscopy. 2013. JOURNAL OF PHYSICAL CHEMISTRY C. 117 (19): 10007.

Li, Q., P. Xu, B. Zhang, G. Wu, H. T. Zhao, E. G. Fu, and H. L. Wang. Self-supported Pt nanoclusters via galvanic replacement from Cu2O nanocubes as efficient electrocatalysts. 2013. NANOSCALE. 5 (16): 7397.

Li, Q., P. Xu, B. Zhang, H. Tsai, S. J. Zheng, G. Wu, and H. L. Wang. Structure-Dependent Electrocatalytic Properties of Cu2O Nanocrystals for Oxygen Reduction Reaction. 2013. JOURNAL OF PHYSICAL CHEMISTRY C. 117 (27): 13872.

Li, S. W., P. Xu, Z. Q. Ren, B. Zhang, Y. C. Du, X. J. Han, N. H. Mack, and H. L. Wang. Fabrication of Thorny Au Nanostructures on Polyaniline Surfaces for Sensitive Surface-Enhanced Raman Spectroscopy. 2013. ACS APPLIED MATERIALS & INTERFACES. 5 (1): 49.

Mack, N. H., J. A. Bailey, S. K. Doorn, C. A. Chen, H. M. Gau, P. Xu, D. J. Williams, E. A. Akhadov, and H. L. Wang. Mechanistic Study of Silver Nanoparticle Formation on Conducting Polymer Surfaces. 2011. LANGMUIR. 27 (8): 4979.

Park, Y. S., Y. F. Chen, Y. Ghosh, A. Pirytinski, P. Xu, N. H. Mack, H. L. Wang, V. I. Klimov, J. A. Hollingsworth, and H. Htoon. Strong Photon Bunching in Individual Nanocrystal Quantum Dots Coupled to Rough Silver Film. 2012. In 2012 CONFERENCE ON LASERS AND ELECTRO-OPTICS (CLEO). , p. -.

Park, Y. S., Y. Ghosh, P. Xu, N. H. Mack, H. L. Wang, J. A. Hollingsworth, and H. Htoon. Single-Nanocrystal Photoluminescence Spectroscopy Studies of Plasmon-Multiexciton Interactions at Low Temperature. 2013. JOURNAL OF PHYSICAL CHEMISTRY LETTERS. 4 (9): 1465.

Park, Y. S., Y. Ghosh, Y. Chen, A. Piryatinski, P. Xu, N. H. Mack, H. L. Wang, V. I. Klimov, J. A. Hollingsworth, and H. Htoon. Super-Poissonian Statistics of Photon Emission from Single CdSe-CdS Core-Shell Nanocrystals Coupled to Metal Nanostructures. 2013. PHYSICAL REVIEW LETTERS. 110 (11): -.

Wu, G., K. L. More, P. Xu, H. L. Wang, M. Ferrandon, A. J. Kropf, D. J. Myers, S. G. Ma, C. M. Johnston, and P. Zelenay. A carbon-nanotube-supported graphene-rich non-precious metal oxygen reduction catalyst with enhanced performance durability. 2013. CHEMICAL COMMUNICATIONS. 49 (32): 3291.

Xu, P., E. Akhadov, L. Wang, and H. Wang. Sequential chemical deposition of metal alloy jellyfish using polyaniline: redox chemistry at the metal-polymer interface. 2011. CHEMICAL COMMUNICATIONSCHEMICAL COMMUNICATIONS. 47 (38): 10764.

Xu, P., E. Akhadov, L. Y. Wang, and H. L. Wang. Sequential chemical deposition of metal alloy jellyfish using polyaniline: redox chemistry at the metal-polymer interface. 2011. CHEMICAL COMMUNICATIONS. 47 (38): 10764.

Xu, P., K. Chang, Y. I. Park, B. Zhang, L. L. Kang, Y. C. Du, R. S. Iyer, and H. L. Wang. Conjugated polymer mediated synthesis of nanoparticle clusters and core/shell nanoparticles. 2013. POLYMER. 54 (2): 485.

Yan, J., X. Han, J. He, L. Kang, B. Zhang, Y. Du, H. Zhao, C. Dong, H. Wang, and P. Xu. Highly sensitive surface-enhanced Raman spectroscopy (SERS) platforms based on silver nanostructures fabricated on polyaniline membrane surfaces. 2012. ACS Applied Materials and InterfacesACS Applied Materials and Interfaces. 4 (5): 2752.

Yan, J., X. Han, J. He, L. Kang, B. Zhang, Y. Du, H. Zhao, C. Dong, H. Wang, and P. Xu. Highly Sensitive Surface-Enhanced Raman Spectroscopy (SERS) Platforms Based on Silver Nanostructures Fabricated on Polyaniline Membrane Surfaces. 2012. ACS APPLIED MATERIALS & INTERFACESACS APPLIED MATERIALS & INTERFACES. 4 (5): 2752.

Yan, J., X. J. Han, J. J. He, L. L. Kang, B. Zhang, Y. C. Du, H. T. Zhao, C. K. Dong, H. L. Wang, and P. Xu. Highly Sensitive Surface-Enhanced Raman Spectroscopy (SERS) Platforms Based on Silver Nanostructures Fabricated on Polyaniline Membrane Surfaces. 2012. ACS APPLIED MATERIALS & INTERFACES. 4 (5): 2752.

Zhang, B., B. T. Zhao, S. H. Huang, R. Y. Zhang, P. Xu, and H. L. Wang. One-pot interfacial synthesis of Au nanoparticles and Au-polyaniline nanocomposites for catalytic applications (vol 14, pg 1542, 2012). 2012. CRYSTENGCOMM. 14 (24): 8735.

Zhang, B., B. T. Zhao, S. H. Huang, R. Y. Zhang, P. Xu, and H. L. Wang. One-pot interfacial synthesis of Au nanoparticles and Au-polyaniline nanocomposites for catalytic applications. 2012. CRYSTENGCOMM. 14 (5): 1542.

Zhang, B., B. Zhao, S. Huang, R. Zhang, P. Xu, and H. Wang. One-pot interfacial synthesis of Au nanoparticles and Au-polyaniline nanocomposites for catalytic applications. 2012. CRYSTENGCOMMCRYSTENGCOMM. 14 (5): 1542.

Zhang, B., P. Xu, X. M. Xie, H. Wei, Z. P. Li, N. H. Mack, X. J. Han, H. X. Xu, and H. L. Wang. Acid-directed synthesis of SERS-active hierarchical assemblies of silver nanostructures. 2011. JOURNAL OF MATERIALS CHEMISTRY. 21 (8): 2495.

Developing a Materials Strategy for d-electron Heavy Fermion Systems

Filip Ronning
20120749PRD2

Abstract

The physics of strongly correlated d-electron systems is generally believed to be fundamentally the same as their f-electron counterparts with simply larger energy scales due to the more extended d-orbital wave functions and thus larger hybridization. Indeed, for either a single d or f element localized in a metallic host the Kondo effect (the screening of magnetic moments by conduction electrons) will occur. When a lattice of f-elements are embedded in a local host, the Kondo effect occurs in a collective fashion giving rise to electronic excitations that have masses up to 1,000 times that of a free electron. However, while a lattice of f-electrons embedded in a metallic host gives rise to “heavy” electrons, analogous behavior has not been realized in d-electron intermetallics although very strong Coulomb interactions due to proximity to insulating states leads to similar phenomena in transition metal (3d-electron) oxides. By doping iron and cobalt into a non-magnetic host material (SrNi2As2) we demonstrated the single ion Kondo effect, a necessary precondition for heavy fermion behavior. Furthermore, by examining the Fe rich analog in the 10-3-8 compound we found unconventional superconductivity. This work sheds new light on the formation of strong electronic correlations and the emergent phenomena that result from it.

Background and Research Objectives

We are internationally recognized for developing an understanding of the emergent phenomena such as superconductivity that occurs in strongly correlated (f-) electron systems. We are now in a position to move beyond observation to control of these properties. In order to demonstrate control we must be able to recreate the chemical conditions for d-electron systems to mimic the behavior of f-electron systems. This was the challenge and goal of this project. We aimed to find new forms of matter (including superconductivity) in d-electron based systems, and to gain a better understanding of how the Kondo effect works in a lattice.

Scientific Approach and Accomplishments

Ni Ni discovered a new family of superconductors based on Fe (the so-called 10-3-8 family). She grew single crystals, which allowed for an accurate determination of the temperature-composition phase diagram [2,3]. In addition, nuclear magnetic resonance measurements were performed, which demonstrated the presence of magnetism in these materials – a likely ingredient for the mechanism of superconductivity [1]. In addition, Ni Ni doped iron and cobalt into non-magnetic analogs of another member of the Fe-based superconductors with the chemical formula SrNi2As2. Transport and thermodynamic measurements revealed a Kondo effect occurring with iron doping, as was our goal, but not with cobalt. This suggests an additional connection between the Fe-based superconductors, and the f-electron based heavy electron superconductors, which had not been previously considered, and was one of our objectives. Finally, Ni Ni reinvestigated the uranium based heavy electron superconductor U2PtC2. We found evidence for a nearby magnetic state when the system is alloyed with rhodium. This may play an important role for elucidating the superconducting mechanism in this material.

Impact on National Missions

One of the three pillars of the LANL materials strategy is focused on developing the understanding required to achieve controlled functionality of strongly correlated systems that will produce emergent phenomena. We achieved partial understanding by recreating the chemical conditions to create heavy electron physics (well known in f-electron materials) in d-electron materials. This work has potential benefit to nuclear deterrence, global threat reduction, and most immediately, energy security through the potential development of rare earth replacement magnets and novel superconducting materials.

References

1. Zhou, T., G. Koutroulakis, J. Lodico, N. Ni, J. D. Thompson, R. J. Cava, and S. E. Brown. Antiferromagnetic order in Ca10(Pt3As8)(Fe2As2)5 observed by 75As NMR. 2013. Journal of Physics: Condesned Matter. 25: 122201.

2. Ni, N., W. E. Straszheim, D. J. Williams, M. A. Tanatar, R. Prozorov, E. D. Bauer, F. Ronning, J. D. Thompson, and R. J. Cava. Temperature-concentration phase diagram of (Ca1-xLax)10(Pt3As8)(Fe2As2)5 superconductors. 2013. Physical Review B. 87: 060507.

3. Gao, P., L. Sun, N. Ni, J. Guo, Q. Wu, C. Zhang, D. Gu, K. Yang, S. Jiang, R. J. Cava, and Z. Zhao. Scaling of pressure-induced and doping-induced superconductivity in the Ca10(PtnAs8)(Fe2As2)5 arsenides. Nature Communications.

Publications

Gao, P., L. Sun, N. Ni, J. Guo, Q. Wu, C. Zhang, D. Gu, K. Yang, S. Jiang, R. J. Cava, and Z. Zhao. Scaling of pressure-induced and doping-induced superconductivity in the Ca10(PtnAs8)(Fe2As2)5 arsenides. Nature Communications.

Ni, N., W. E. Straszheim, D. J. Williams, M. A. Tanatar, R. Prozorov, E. D. Bauer, F. Ronning, J. D. Thompson, and R. J. Cava. Temperature-concentration phase diagram of (Ca1-xLax)10(Pt3As8)(Fe2As2)5 superconductors. 2013. Physical Review B. 87: 060507.

Zhou, T., G. Koutroulakis, J. Lodico, N. Ni, J. D. Thompson, R. J. Cava, and S. E. Brown. Antiferromagnetic order in Ca10(Pt3As8)(Fe2As2)5 observed by 75As NMR. 2013. Journal of Physics: Condensed Matter. 25: 122201.

Multiferroic Magnetoelectric Hybrid Inorganic-Organic Frameworks

Michael R. Fitzsimmons
20110716PRD2

Introduction

Metal-organic-frameworks are crystalline compounds consisting of metal atoms or clusters coordinated to organic ligands with extended structure in at least one direction. A unique potential of metal-organic-frameworks is to exhibit combinations of properties that might not be possible in purely inorganic and organic systems. This potential is realized by tailoring the polymeric ligand structures comprising the framework and the metal ion captured inside the framework that will allow us to circumnavigate the mutually exclusive problem of achieving ferromagnetism and ferroelectricity in a single inorganic compound.

We will study structurally disordered metal-organic-frameworks which upon application of an external stimulus, i.e. temperature or pressure, result in a polar-ordered structure and ferroelectric behavior. Magnetic transition metals will be used to achieve simultaneous ferromagnetic ordering. Many known examples will also be studied and optimized. For example, we will study potential multiferroic behavior in [Co2(C3H3N2)4]n (zni phase). We will investigate how the lattice distortions, dopant metals, magnetic and electric field, and local bonding environments affect multiferroic behavior and coupling between two ferroic orders in pressure induced amorphous and crystalline phases of this material. Further, chiral ligands will be used to create novel polar materials.

The proposed work will rely heavily on our expertise in metal-organic-framework synthesis, x-ray based characterization techniques, and electric and magnetic transport measurements, and will make extensive use of neutron scattering. Our work will yield compounds, multiferroics, exhibiting a strong magnetoelectric effect by tailoring the metal-organic-framework structures. Devices using multiferroic behavior will be faster, smaller and more sensitive to their environment than present technology. New applications include: secure communication achieved by changing frequencies used to broadcast information in real-time, and the detection of steel moving under the ocean's surface.

Benefit to National Security Missions

Our work will yield compounds called multiferroics exhibiting a strong magnetoelectric effect by tailoring the metal-organic-framework structures. In a field dominated by materials that contain the toxic element lead, metal-organic-frameworks will open new opportunities for the production of lead-free (i.e., green) multiferroic compounds customized for specific technological applications, including but not limited to data storage, photo-voltaic, sensors, and transducers. Devices using multiferroic behavior will be faster, smaller and more sensitive to their environment than present technology. New applications include: secure communication achieved by changing frequencies used to broadcast information in real-time, and the detection of steel moving under the ocean's surface.

In addition, Prashant's work in material science will enhance the reputation of the Lujan Center in the area of the application of neutron scattering techniques in research programs. The Lujan Center is funded as a national user facility for neutron scattering.

Progress

The key accomplishment of this project during the last 12 months would be the realization of giant coupling between magnetism and electric polarization, a much sought after property necessary to satisfy ever growing need for better data storage media and other functional properties otherwise not possible, in metal-organic-frameworks (MOFs) or hybrid inorganic-organic materials.

MOFs are crystalline materials consisting of metal atoms or clusters coordinated to organic ligands with extended

structure in at least one direction. A unique potential of MOFs is to exhibit combinations of properties that might not be possible in purely inorganic and organic systems. This potential is realized by tailoring the polymeric ligand structures comprising the framework and the metal ion captured inside the framework that allows us to circumnavigate the mutually exclusive problem of achieving ferromagnetism and ferroelectricity in a single inorganic compound. We accomplished this in (CH3)2CH2Mn(HCOO)3 a manganese formate framework in which Mn atoms are bridged together by the most basic carboxylate ligand formic acid. This framework contains disordered organic cations in the pores. It is the ordering of these cations that leads to net electric polarization in this material below 180K. Due to the paramagnetic nature of the materials, the magnitude of electric polarization can be enhanced by an applied magnetic field. This is an important breakthrough given that ferroelectricity and ferromagnetism are usually two mutually exclusive properties in a single phase material.

In addition to the scientists at the magnet lab (TA-35), we have also worked with theoretical division. Together we are developing novel MOF materials which would display a strong magnetoelectric coupling via new mechanisms (PRL 108, 097202, 2012). This work is currently in progress where we are applying bottom-up assembly for the realization of the structure required as described in the paper.

Future Work

For the next year, we will continue developing materials with magnetoelectric coupling at close to room temperature. Part of this effort will be to understand the origin of this coupling in mixed valence iron metal organic framework (MOF) that according to our preliminary results is magnetoelectric. Furthermore, there are no well-established methods to quantify this coupling between magnetism and electric polarization, primarily due to the lack of materials with this extraordinary behavior. As part of this project, as we develop new materials with this effect, we hope to quantify this effect and establish benchmarks similar to the existing ones in the field of ferroelectrics (e.g. electric polarization values of potassium dihydrogen phosphate and urea). We will also attempt to make thin films of MOFs, which is an architecture required before these materials could be used for data storage or sensor applications. We will use polarized neutron reflectometry to characterize magnetism of the thin films.

Prashant will also work with Michael Fitzsimmons on polarized neutron reflectometry (PNR). This will be a new technique for Prashant, hence a growth opportunity, which he will apply to his future research as an academic to understand the spin states in technologically relevant hybrid multiferroic materials.

In addition, work will also be carried out at the National High Magnetic Field Lab. Materials studied with PNR will be studied with high magnetic field at the pulse field facility. We will do pulse-field measurements of electric polarization to quantify the coupling between electric polarization and magnetism.

Conclusion

Our work will yield compounds, multiferroics, exhibiting a strong magnetoelectric effect by tailoring the metal-organic-framework structures. In a field dominated by materials that contain the toxic element lead, metal-organic-frameworks will open new opportunities for the production of lead-free (i.e., green) multiferroic compounds customized for specific technological applications, including but not limited to data storage, photo-voltaic, sensors, and transducers. Devices using multiferroic behavior will be faster, smaller and more sensitive to their environment than present technology. New applications include: secure communication achieved by changing frequencies used to broadcast information in real-time, and the detection of steel moving under the ocean's surface.

Publications

Li, W., Z. Zhang, E. Bithell, A. Batsanov, P. Barton, P. Saines, P. Jain, C. Howard, M. Carpenter, and A. Cheetham. Ferroelasticity in a metal-organic framework perovskite; towards a new class of multiferroics. 2013. Acta Materialia. 61: 4928.

Stroppa, A., P. Barone, P. Jain, J. M. Perez-Mato, and S. Picozzi. Hybrid Improper Ferroelectricity in a Multiferroic and Magnetoelectric Metal-Organic Framework. 2013. Advanced Materials. 25: 2284.

Tan, J., P. Jain, and A. Cheetham. Influence of ligand field stabilization energy on the elastic properties of multiferroic MOFs with the perovskite architecture. 2012. Dalton Transactions. 41: 3949.

Thomson, R. I., P. Jain, A. K. Cheetham, and M. A. Carpenter. Elastic relaxation behavior, magnetoelastic coupling, and order-disorder processes in multiferroic metal-organic frameworks. 2012. Physical Review B. 86.

Wang, Z., P. Jain, K. Choi, J. van Tol, A. Cheetham, H. Kroto, H. Koo, H. Zhou, J. Hwang, E. S. Choi, M. Whangbo, and N. Dalal. Dimethylammonium copper formate (CH3)(2)NH2 Cu(HCOO)(3): A metal-organic framework with quasi-one-dimensional antiferromagnetism and magnetostriction. 2013. Physical Review B. 87.

Catalysts Containing Earth Abundant Metals for Energy Applications

John C. Gordon
20110752PRD3

Introduction

Catalytic transformations impact an enormous range of DOE mission areas, for example in the conversion of crude petroleum and biomass into clean burning fuels and materials. Electrocatalysts control the conversion of fuels into energy in fuel cells and batteries and play important roles in the photocatalytic conversion of energy into chemicals and materials. Catalysts are crucial to creating new, energy-efficient routes for the production of basic chemical feedstocks and value-added chemicals. Environmental applications of catalysis science include minimizing unwanted products and transforming toxic chemicals into benign ones, such as the transformation of chlorofluorocarbons into environmentally acceptable refrigerants.

It is well known that Nature utilizes iron-based catalysts contained within the active sites of enzymes to allow a wide array of difficult catalytic bond transformations to occur. Unfortunately our mechanistic understanding of these processes is generally poor. Therefore, expanding our knowledge of rudimentary synthetic and mechanistic molecular iron chemistry is therefore a worthy goal towards the design and scale-up of efficient catalysts capable of promoting energy related processes important to humanity. Thus focus of this particular research will be on the chemistry and development of cheap and earth abundant metal (e.g. iron , cobalt, nickel) catalysts pertinent to a variety of reactions with implications in global scale energy storage and production on the terawatt scale.

Benefit to National Security Missions

These findings will inform the future design of new catalysts relevant to energy, such as in the conversion of methane to methanol and other global-scale reactions with direct energy applications, improvements to which will ultimately benefit society. This is directly aligned with DOE and LANL missions in National and Energy security. In particular, agencies such as OBES (ctalysis program) and EERE (BETO) will likely be interested in such technological approaches.

Progress

In the past year, the project “Catalysts Containing Earth Abundant Metals for Energy Applications” has been advanced from an initial, exploratory concept to the point where we have now developed new, functional cobalt catalytic systems. In the process, several ligand systems were synthesized and examined for complex formation. 6,6’’-Di(Mes)-2,2’:6’,2’’-terpyridine (Mes = 2,4,6-trimethylphenyl) was prepared and the iron(II) and iron(0) derivatives obtained, however the low yield and high expense of the ligand precursor 6,6’’-dibromo-2,2’:6’,2’’-terpyridine forced us to abandon this approach. The proligand 2,6-bis(Mes)-pyridine was synthesized but failed to ligate with Co, Fe or Mn. Attempts were made to prepare 1,10-bis(Mes)-phenanthroline but these failed. The 1,4-diimine family of ligands RN=C(R’)-C(R’)=NR were prepared for R = Mes, Dipp (2,6-di-iso-propylphenyl), Ad (1-adamantyl); R’ = Me, H. Subsequently the new transition metal species M(RN=C(R’)-C(R’)=NR)Cl2 and M(RN=C(R’)-C(R’)=NR)2 (M = Co, R’ = H , R = Ad, Dipp; M = Mn, R’=H, R = Dipp) were prepared and fully characterized. Structural studies using X-ray diffraction methods revealed divalent metal centers and anionic ligand non-innocence in the case of the reduced bis(ligand) complexes. The reactivity of these compounds is under investigation. The new species Fe(AdN=C(H)-C(H)=NAd)Cl2 was also prepared, and was used as a platform to investigate the feasibility of the synthesis of a multiply-bound terminal imido species. Unfortunately, sustained efforts towards this goal did not produce the desired compound, although the new species Fe(AdN=C(H)-C(H)=NAd)(N(SiMe3)2)Cl was obtained during this process and fully characterized.

A new bulky ligand, Mes2NH, has been synthesized

by Buchwald coupling; however, no tractable transition metal derivatives have been currently identified from synthetic efforts. Reaction of the bulky amide LiN(SiMe3)Ad with FeCl2 yielded an unusual tetrameric species {Fe(NSiMe3Ad)}4(O).

The pyridine-diamide ligand [2,6-(DippN(H)CH2)2NC5H3] was prepared and attempts were made to synthesize new Fe and Co catalysts based on this system. Unfortunately, ligation with Fe results in multiple C-C and C-N bond cleavage, yielding an unusual dimeric species in which one arm of the pincer ligand has been broken and two ligands have been fused together via a cis carbon-carbon double bond. At this point the mechanism for the formation of this species is unclear. However this result effectively terminates investigations into this species as a potential catalyst.

Similar work with Co has yielded crystals suitable for X-ray diffraction studies; we are currently waiting for repairs on this instrument in order to carry out structural studies. Given the failure rate of several of these routes to potential new catalysts, attention shifted to synthesizing novel variants on a functioning Co system that had been recently discovered in our group by Drs Susan Hanson and Guoqi Zhang. The new variation on the "PNP" donor ligand involved a tolyl rather than ethylene linker in the backbone, which was expected to decrease the flexibility of the ligand skeleton and change the basicity of the central amine donor. The new complex Co[PNP]CH2SiMe3 was obtained and characterized, and showed a longer Co-N bond, and a lesser degree of sp2-hybdrization at the amide nitrogen, compared with the ethylene linked analogue. These structural and electronic variations led to varied reactivity, and whilst addition of H(OEt2)2BArF to the ethylene linked complexes leads to a protonated amine center in the form {Co[PN(H)P]CH2SiMe3}BArF with the aryl linked ligand, Co[PNP]BArF was observed to form instead. Co[PNP]BArF has been shown to be an effective catalyst for hydrogenation and isomerization of olefins; hydrosilation reactivity is currently under investigation. The analogous iron derivatives, Fe[PNP]CH2SiMe3 and Fe[PNP]Cl have been prepared and characterized, however have not been shown to be active as hydrogenation catalysts. Modification of these catalysts is underway.

In conclusion, a variety of ligands, both known and hitherto unknown, have been prepared and examined for their ability to support molecular catalysts based on first row transition metals. Although many of these systems failed to prove stable, we have discovered that the PNP pincer system supports a diverse range of catalytic systems. Future work will focus on exploring these systems.

Future Work

It is anticipated that by judicious choice of of molecular targets, we will be able to prepare and characterize molecular compounds that exhibit new earth abundant metal (e.g. Fe, Co) based reactivity, including inert bond-activation reactions (e.g. C-H, Si-H, N-N, and H-H bond cleavage) and other novel small molecule transformations pertinent to energy related processes.
We will continue our work into next FY on the design, synthesis and characterization of catalyst targets. The most promising candidates will be screened for reactivity towards small molecule synthons, such as N2, CO, CO2, etc. These findings will inform the future design of new catalysts relevant to energy processes, such as in the conversion of methane to methanol, the conversion of nitrogen into ammonia, and other global-scale chemical processes.

Conclusion

It is anticipated that by judicious choice of of molecular targets, we will be able to prepare and characterize molecular compounds that exhibit new iron-based reactivity, including inert bond-activation reactions (e.g. C-H, Si-H, N-N, and H-H bond cleavage) and other novel small molecule transformations pertinent to energy related processes. These findings will inform the future design of new catalysts relevant to energy, such as in the conversion of methane to methanol, the conversion of nitrogen into ammonia, and other global-scale chemical processes, improvements to which will ultimately benefit society.

Direct Tracking of Charge Carriers in Heterostructured Nanowires

Rohit P. Prasankumar
20110753PRD4

Introduction

Silicon nanowires (SiNWs) have attracted much attention because of their great potential for nanophotonic and nanoelectronic applications. These quasi-one-dimensional (1D) nanosystems have unique properties that depend on their size, shape, and alignment. While time-integrated and time-resolved photoluminescence (PL) experiments have given some insight into the influence of these parameters on NW properties, these measurements have not had sufficient time resolution to resolve several important carrier relaxation processes in these systems, including electron-phonon coupling and inter/intravalley scattering. Therefore, there remains a lack of basic understanding of how light interacts with individual NWs on an ultrashort time scale, which is critical to fully realize their promise for various applications.

To date, inhomogeneities in NW ensembles have made it difficult to unambiguously extract their underlying physics. In this project, by isolating individual nanowires, we avoid complications resulting from the broad size and alignment distribution in nanowire ensembles, allowing us to use ultrafast optical microscopy to directly examine carrier dynamics and carrier velocities in individual NWs with high temporal and spatial resolution in a non-contact manner. Moreover, we can use a hybrid NW-nanoantenna structure in a terahertz (THz)-pump, optical-probe experiment to generate THz field strengths on the order of tens to hundreds of kV/cm at the antenna focus. This will enable us to directly photoexcite transient electron dynamics, allowing us to monitor the resulting carrier populations with ultrafast time resolution and observe novel phenomena such as the dynamic Franz-Keldysh effect.

Our ultrafast optical and THz experiments should thus open pathways to directly study carrier dynamics and charge transport in quasi-1D nanosystems. This research has potential application to NW-based devices, optoelectronics, and sensitive photodetection on both the nanoscale and ultrashort time scales, which will contribute to institutional efforts in nanoscience at LANL.

Benefit to National Security Missions

This research will develop the new capability of ultrafast optical microscopy, which is a general technique that can be applied nearly any biological, chemical, or physical system. The generality of this technique therefore makes it quite interesting to several programs within the DOE Office of Science, and could also appeal to other programs within DOE, DOD, NIH, and NIST. In addition, the understanding of carrier transport across interfaces in nanowires gained here will have a significant impact on solar cell and solid-state lighting applications, as well as the use of these nanowires as high speed nanoscale transistors. Finally, the goals of this project align well with the “Basic Understanding of Materials” mission, and to a lesser extent, the “Renewable Energy” mission at LANL.

Progress

In the past year, we developed a two-dimensional (2D) smart pixel detector to create an ultrafast optical wide field microscope (UOWFM), capable of rapidly acquiring wide field microscopic images with high temporal- and spatial-resolution. As compared to most optical microscopy measurements, which are nearly always performed in a time-integrated mode, our ultrashort pulsed laser-based technique provides femtosecond temporal resolution over a broad energy range. This is realized by combining wide field optical microscopy and ultrafast optical spectroscopy.

As a first step, we acquired time-resolved images of a gold-patterned amorphous silicon film and a single silicon nanowire (NW) to demonstrate the validity of this novel concept. Two different femtosecond laser systems were used to study these different samples, demonstrating the versatility of our approach. In both cases, we

used a unique 2D smart pixel detector array (provided by Heliotis AG) with a 50X (0.50 NA) objective and a zoom lens with variable magnification to image these materials. This 2D array detector performs with sensitivity comparable or better to that of a conventional single pixel detector in these experiments, which allows our UOWFM system to behave like a 'lock-in' camera; essentially, this technique allows one to "look" through an optical microscope with extremely high time resolution. The time-resolved optical images of a single Si NW acquired using UOWFM thus provided valuable insight into carrier dynamics with sub-micron optical resolution, while time-resolved images of a patterned Si film demonstrated our ability to capture information over a large area within a short acquisition time. Importantly, our nanowire imaging results show that our technique works for very small targets with sub-micron spatial resolution, which should be very helpful for nanomaterials research, particularly given the rapid image acquisition time.

Overall, ultrafast optical wide field microscopy combines the non-contact nature and spatial resolution of conventional optical microscopy with the temporal resolution of ultrafast spectroscopy to rapidly and sensitively acquire spatially and temporally resolved images of nearly any sample. Furthermore, ultrafast optical wide field microscopy can, in principle, be used to acquire time-varying images of almost any material that can be imaged with a conventional optical microscope, and can thus be expected to have many future applications in a variety of physical, chemical, and biological systems. Our future work will thus include further optimizing the 2D array detector for this unique application and applying this technique to track space and time varying processes in a variety of systems. This will contribute to LANL's leadership in nanoscience and nanotechnology while supporting the collaboration between LANL and Sandia National Laboratories (through the Center for Integrated Nanotechnologies). Finally, this forefront science and capability development will attract high quality students, postdocs and collaborators to LANL.

In parallel, we built a time-domain terahertz (THz)-probe spectroscopy system, based on an amplified 1 kHz laser, and designed a special hybrid plasmonic NW-nanoantenna device structure that will enable us to study the response of individual semiconductor NWs after both optical and THz photoexcitation. This THz nonlinear spectroscopy capability can be applied to a wide range of problems in photonics and electronics, advancing both fundamental science while potentially impacting engineering applications.

Future Work

Building on our previous work, we expect to investigate ultrafast carrier dynamics in various single nanowire samples, such as semiconductor NW heterostructures, NWs integrated with plasmonic structures, and NWs integrated with other materials, such as graphene. We will do this by extending our system to incorporate a microstructured fiber to generate a white light continuum, which will allow us to tune the probe wavelength throughout the visible and near-infrared relative to a given material's band gap. This will also allow us to directly measure carrier diffusion velocities and coefficients in a wide range of samples, focusing on nanowire-based structures but also extending our capabilities to other materials, such as complex oxide heterostructures and metamaterials. This aspect of our research thus has potential applications in NW-based devices, optoelectronics, and sensitive photodetection by combining measurements at both micrometer distance and femtosecond time scales to reveal the intrinsic properties of these quasi-one-dimensional nanosystems.

In parallel, we will use our newly built THz system to explore the possibility of directly pumping semiconductor NWs with ultrashort, intense THz pulses. We will facilitate this by incorporating a single NW into a hybrid NW-nanoantenna structure, which will enhance the THz field strength enough to produce a measurable signal level (this would normally be difficult since the NW volume is extremely small compared to the THz wavelength). By performing THz-pump, optical-probe experiments on the hybrid NW-nanoantenna structure, we can selectively excite and track electron dynamics with THz peak field strengths on the order of tens of kV/cm and monitor the resulting evolution of the electron population with ultrafast time resolution. This will be a significant advance over typical optical-pump/optical-probe experiments, which investigate both hole and electron dynamics created simultaneously using band-to-band photoexcitation, and may allow us to observe unique phenomena such as the dynamic Franz-Keldysh effect.

Conclusion

Silicon nanowires (SiNWs) have attracted much attention because of their great potential for nanophotonic and nanoelectronic applications. However, to fully realize this promise, an understanding of non-equilibrium carrier dynamics in these quasi-one-dimensional systems, especially on an ultrashort time scale, is critical. Here, we will use ultrafast optical and terahertz (THz) spectroscopy to explore carrier dynamics in individual semiconductor NWs.

This will provide deep insight into the intrinsic properties of semiconductor NWs, enabling their optimization for a variety of applications.

Publications

Prasankumar, R. P.. Tracking charge carriers through space and time in single semiconductor nanowires. Invited presentation at CINT User Workshop. (Albuquerque, 19-20 September 2012).

Prasankumar, R. P.. Tracking charge carriers through space and time in single semiconductor nanowires. Invited presentation at SSL EFRC coffee hour. (Albuquerque, 14 June 2012).

Seo, M. A., J. Yoo, D. E. Perea, S. A. Dayeh, S. T. Picraux, A. J. Taylor, and R. P. Prasankumar. Tracking ultrafast carrier dynamics in single semiconductor nanowire heterostructures. 2013. In 18th International Conference on Ultrafast Phenomena. (Lausanne, Switzerland, 8-13 July 2012). , p. 4030. London: Oxford University Press.

Seo, M. A., J. Yoo, S. A. Dayeh, S. T. Picraux, A. J. Taylor, and R. P. Prasankumar. Mapping carrier diffusion in single silicon core-shell nanowires with ultrafast optical microscopy. 2012. Nano Letters. 12: 6334.

Seo, M. A., J. Yoo, S. A. Dayeh, S. T. Picraux, A. J. Taylor, and R. P. Prasankumar. Tracking charge carriers through space and time in single semiconductor nanowires. Presented at Conference on Lasers and Electro-Optics. (San Jose, CA, 6-11 May, 2012).

Seo, M. A., J. Yoo, S. A. Dayeh, S. T. Picraux, A. J. Taylor, and R. P. Prasankumar. Mapping carrier diffusion in single silicon core-shell nanowires with ultrafast optical microscopy. 2013. In 7th International Conference on Materials for Advanced Technologies. (Singapore, 30th June-5th July, 2013). Vol. 8, p. 128. Singapore: World Scientific.

Seo, M. A., S. A. Dayeh, P. C. Upadhya, J. A. Martinez, B. S. Swartzentruber, S. T. Picraux, A. J. Taylor, and R. P. Prasankumar. Understanding ultrafast carrier dynamics in single quasi-one-dimensional Si nanowires. 2012. APPLIED PHYSICS LETTERS. 100 (7): 071104.

Seo, M. A., S. A. Dayeh, P. C. Upadhya, S. T. Picraux, J. Martinez, B. S. Swartzentruber, A. J. Taylor, R. P. Prasankumar, and IEEE. Polarization anisotropy of transient carrier dynamics in single Si nanowires. 2011. In Conference on Lasers and Electro-Optics (CLEO) ; 20110501 - 20110506 ; Baltimore, MD.

Seo, M. A., S. Boubanga-Tombet, J. Yoo, Z. Ku, A. V. Gin, S. T. Picraux, S. R. J. Brueck, A. J. Taylor, and R. P. Prasankumar. Ultrafast optical wide field microscopy. 2013. Optics Express. 21: 8763.

Fabrication of an All-carbon Solar Cell

Andrew M. Dattelbaum
20120732PRD1

Introduction

Unlike other nanomaterials that degrade in air and loss their functionality, graphene oxide is stable in air. Thus, graphene oxide is a unique nanoscale material that may be functionalized at the atomic level to control the properties of bulk films prepared from the nanoscale building blocks. We will demonstrate that chemical modification of graphene oxide can be used to control the resulting properties of bulk films prepared from the functionalized material. Such functionalization can be used to make graphene oxide that is optimal for new photovoltaic materials, supercapacitors or fuel cell membranes.

Benefit to National Security Missions

This work supports the energy security mission of Los Alamos National Laboratory. Specifically, we will synthesize new carbon nanomaterials that may be useful for a variety of applied energy applications in fuel cells, organic photovoltaic architectures, and supercapacitors. If successful, the work may be useful to a variety of sponsors in the DOD or Intelligence Community. The work also supports the mission of the Center for Integrated Nanotechnologies, which is a DOE Basic Energy Sciences funded user facility located in part at Los Alamos. The Center's goal is to promote nanoscience accessibility across the country by providing access to the expertise and equipment at the facility. This work will eventually lay the foundation for new capabilities that will be available to future users keeping us at the cutting edge of nanoscience work.

Progress

Graphene oxide (GO) ozonation for polymer electrolyte membrane application in Fuel cells

In collaboration with the fuel cell group in MPA-11, we investigated the ozonation process of graphene oxide. We studied the structure of ozonated graphene oxide using a variety of techniques including solid state nuclear magnetic resonance, and it ability to conduct protons in a hydrogen fuel cell. We observed an enhancement in the ability of graphene oxide after the ozonation process was completed. A manuscript based on this result was written and is submitted.

Use of graphene oxide as a nanoscale supercapacitor

We developed a technique that uses a laser to pattern films of graphene oxide to make them act as supercapacitors. The technique uses a mask to simplify the fabrication process, as well as facilitate assembly of the supercapacitor devices, which is the biggest challenge in micro-scale-device fabrication. Devices with three different sizes were fabricated (0.25 mm2, 2.5 mm2, and 25 mm2). An unusual dependence of the capacitance as the area changed was observed (exponential instead of linear, as we initially expected, i.e. the capacitance was better than we thought it would be). We are currently trying to understand this behavior through a series of systematic studies.

Crosslinking of graphene oxide

We are chemically crosslinking graphene oxide sheets to make the bulk films prepared from GO more stable in fuel cell and supercapacitor devices. We are trying to crosslink GO with various chemistries that involve polymers like poly(ethylene) imine and poly(ethylene) glycol. If successful, we will have a much stronger GO-based film that can sustain extreme conditions such as mechanical stretching and water/organic solvent flooding.

Future Work

- Set up a synthesis program at LANL to prepare reduced graphene oxide that can be incorporated into a solar cell device.
- Optimize the overall cell performance by chemical doping or functionalization of the graphene oxide to tailor the interface for controlled characterization of the charge transfer mechanisms in the solar cell.

- Prepare functionalized graphene oxide thin films and work with colleagues in MPA-11 who will determine if they are viable materials for fuel cells.
- Synthesize graphene oxide films and pattern them to test their use as supercapacitors.

Conclusion

If successful, this work would establish a new class of organic photovoltaic devices based on all-carbon nanomaterials. Due to the ability to make large quantities of graphene oxide and its doping flexibility, devices made from this material may lead to more stable and efficient solar cells, supercapacitors or membranes for fuel cells than what is achievable from currently available technology.

Chemically Modifying the Uranyl Ion

Jaqueline L. Kiplinger
20120750PRD2

Introduction

The uranyl ion, [UO2]2+, is the most ubiquitous form of uranium. The metal-oxygen bonds in this linear molecule are incredibly strong, making uranyl complexes very stable. Because uranyl complexes are so stable, they are resistant to modifications–modifications that could lead to easier separations, or improved nuclear fuel reprocessing, for example. In this context, chemically modifying a uranyl complex by connecting a carbon ligand to it is a very challenging but important goal. A molecular uranyl complex containing a metal-carbon bond, also called an organometallic uranyl complex, would be of interest because solid-state uranium carbide materials can be used in the new generation of safer nuclear reactors. We propose to prepare stable organometallic uranyl complexes using a straightforward method. These well-defined molecular compounds will be valuable because they enable a range of experimental and theoretical studies that are not available using solid-state materials.

Benefit to National Security Missions

The goals of this project are (1) to synthesize and characterize a rare uranyl fluoride complex and (2) to use this uranyl fluoride complex to synthesize a uranyl complex containing a uranium–carbon bond. Within the field of actinide chemistry, this work will have a considerable impact, not only because examples of these complexes are so uncommon, but also because the methods we propose will be adaptable for widespread use by the chemistry community, beyond uranyl complexes and across the actinides. More broadly, this chemical achievement will be a major step forward in understanding how to chemically modify the uranyl ion, and the proposed work could lead to essential improvements in processing and separation. Finally, this effort will generate a handful of well-defined complexes of uranyl difluoride. UF6 reacts with water to form uranyl fluoride, which is a hallmark for the presence of UF6 activities. Characterizing and studying the chemistry of these uranyl fluoride compounds could find relevance in the nonproliferation community.

Progress

We attempted to prepare stable uranyl complexes of the type, [L]UO2Cl (where L = bulky ligand). Unfortunately, the ligand we chose ended up reacting with the normally inert UO2 fragment. We will be looking at bulky ligands to try and circumvent this new reaction pathway.
We prepared stable thorium complexes of the type [L]2ThCl2 (where L = bulky ligand) and uranium complexes of the type [L]2UCl2 (where L = bulky ligand). We discovered new synthetic methods for the high-yielding preparation of thorium metallocene dichloride complexes. We started to examine the reaction chemistry of both systems and developed routes to the first thorium azide complexes.

We successfully applied our new method for preparing actinide fluoride bonds by reacting the [L]2UCl2 and [L]2ThCl2 complexes with trimethyltin fluoride (Me3Sn-F). This chemistry yielded the corresponding fluoride complexes [L]2UF2 and [L]2ThF2.

Finally, we discovered a route to the first terminal uranium(III) fluoride complexes. These compounds are remarkable stable, which is in contrast to previous predictions. We began exploring the chemistry of these molecules.

All complexes will be fully characterized using miscellaneous spectroscopic techniques and X-ray diffraction.

Future Work

We will continue to explore avenues to prepare stable uranyl complexes of the type, [L]UO2Cl (where L = bulky ligand). We will be looking at other bulky ligands to try and stabilize a monomeric uranyl fluoride complex.
We will continue to explore the chemistry of the

[L]2ThF2 and [L]2UF2 (where L = bulky ligand) complexes. We will finish and publish a manuscript on the new synthetic method for the high-yielding preparation of thorium metallocene dichloride complexes.

We will finish and publish a manuscript on the synthesis of the first thorium azide complexes.

We will continue to explore the generality of the our new method for preparing actinide fluoride bonds by reacting uranium chloride, bromide and iodide complexes with complexes with trimethyltin fluoride (Me3Sn-F). After this scope is accomplished we will file a patent application. Finally, we will continue to explore the chemistry and properties the first terminal uranium(III) fluoride complexes, which we recently prepared.

Conclusion

The main project goals are (1) to synthesize and characterize a rare uranyl fluoride complex and (2) to use this uranyl fluoride complex to synthesize a uranyl complex containing a uranium–carbon bond. Within the field of actinide chemistry, this work will have a considerable impact, not only because examples of these complexes are so uncommon, but also because the methods we propose will be adaptable for widespread use by the chemistry community, beyond uranyl complexes and across the actinides.

Publications

Monreal, M. J., R. J. Wright, J. T. Golden, D. E. Morris, B. L. Scott, P. P. Power, and J. L. Kiplinger . Thorium(IV) and uranium(IV) halide complexes supported by bulky β-diketiminato ligands. 2013. Organometallics (Invited Article – Special Issue: Recent Advances in Organo-f-Element Chemistry). 32: 1423.

Travia, N. E., M. J. Monreal, B. L. Scott , and J. L. Kiplinger. Thorium-mediated ring-opening of tetrahydrofuran and the development of a new thorium starting material: Preparation and chemistry of ThI4(DME)2. 2012. Dalton Transactions. 41: 14441.

Travia, N. E., M. J. Monreal, B. L. Scott, D. E. Morris , and J. L. Kiplinger. Developing the next generation thorium iodide starting materials. Invited presentation at 243rd American Chemical Society National Meeting. (San Diego, California, 25-29 March 2012).

Travia, N. E., M. J. Monreal, B. L. Scott, and J. L. Kiplinger. A new starting material for thorium chemistry: ThI4(DME)2. Presented at Gordon Research Conference on Inorganic Chemistry. (University of New England, Biddeford, Maine, 17-22 June 2012).

Designing and Probing Novel Materials by Pressure Tuning of Nanocrystals

Hongwu Xu
20120753PRD2

Introduction

Nanocrystals, which are sized between 1 and 100 nm and are structurally defect-free, possess unique properties compared to their bulk counterparts. Pressure tuning of nanocrystals is a novel approach to design, develop and probe new nanostructured materials. At high hydrostatic pressure and/or deviatoric stress, nanocrystals may not only undergo structural transformations to other phases but also coalesce into one-, two- and three-dimensional superlattices and mesostructures, potentially leading to new physical properties.

Using lead chalcogenide (e.g., PbSe) as a model system, this project focuses on investigations of pressure-induced behavior of nanocrystals mainly using small-angle and wide-angle synchrotron X-ray scattering (SAXS and WAXS) coupled with diamond-anvil cell (DAC) techniques. Major tasks include: 1) synthesize series of lead chalcogenide nanocrystals of various particle sizes, morphology and capping ligands using wet-chemical and other methods; 2) characterize the obtained nanoparticle samples using powder X-ray diffraction, scanning and transmission electron microscopy and other methods; and 3) employ several high-pressure techniques including SAXS, WAXS, Raman, absorption and emission spectroscopies to determine pressure-tuned structural stability, phase transformations, mechanical and optical properties of random “amorphous” and assembled ordering nanocrystals. In particular, the combined in-situ high-pressure SAXS and WAXS techniques will allow examination of structural variations in both nanocrystals (atomic structures, WAXS) and their assembled architectures (mesoscale superlattices, SAXS).

The results will shed light on structural mechanisms underlying the formation of novel high-pressure nanophases and their assembled superlattices. This research is expected to open up a new direction in high-pressure nanomaterials science by exploring new phenomena and tuning mechanisms for a wide spectrum of nanoparticles and their building blocks, with great potential for technological applications.

Benefit to National Security Missions

This project represents a research topic with great scientific value and tremendous potential for technological applications. Through the state-of-the-art in-situ high-pressure small- and wide-angle synchrotron X-ray scattering measurements of series of lead chalcogenide nanocrystals, this work will shed important lights on structural mechanisms underlying the formation of novel chalcogenide nanocrystals and their assembled superlattices at high hydrostatic pressure and/or deviatoric stress. More broadly, the results will have applications/implications for controlled nanoparticle synthesis and for design and fabrication of novel structured nanomaterials with potential, enhanced or newly emerging properties. The use of pressure will enable systematic manipulation of the nanophases and their assembled architectures (e.g., interparticle spacing), thereby enabling tuning of their properties for specific applications.

This research is expected to open up a new direction in high-pressure nanomaterials science by exploring new phenomena and tuning mechanisms for a wide spectrum of nanoparticles and their building blocks. Examples of potential applications include catalysts, solar cells, optoelectronic and thermoelectric devices. Using pressure as a tool/variable, this research seeks fundamental understanding of the structures and properties of novel nanomaterials, and is tied to missions in DOE office of Science and NSF, and to all the three themes of LANL’s Materials Grand Challenge (defects and interfaces, extreme environments, and emergent phenomena), as well as MaRIE.

Progress

During the past year, we have made tremendous progress in this project. Specifically, we investigated the roles

of organic capping ligands in controlling the formation of colloidal lead selenide (PbSe) nanoparticle assemblies (or supercrystals), determined the temperature effects, and examined size-dependent phase transition behavior at high pressure.

Roles of capping ligands

Although the presence of organic ligands outside inorganic, colloidal nanoparticles is essential to nanoparticles formation, their roles in controlling self-assembly of the nanoparticles are not well understood. In this work, we specifically designed our experiments to examine how capping ligands affect the symmetry/structure of assembled superlattice. We used monodisperse PbSe nanoparticles with sizes of 9.7 nm, 9.4 nm, 7.3 nm, 5.3 nm and 3.8 nm, which are coated with the same organic ligand - oleic acid. Small-angle X-ray scattering (SAXS) measurements show that these nanoparticles self-assembled into supercrystals via evaporation-induced processes. We observed different packing behaviors for PbSe nanoparticles with different sizes: The smaller nanoparticles (3.8 and 5.3 nm), which have higher ratios of ligand/particle (and are thus softer) tend to form the body-centered-cubic (bcc) superstructures, whereas the larger nanoparticles (7.3, 9.4 and 9.7 nm) with lower ligand/particle ratios adopt the face-centered-cubic (fcc) superstructures. Entropic considerations suggest that these nanoparticles would form the closest packed fcc structure. The formation of the bcc supercrystals from smaller nanoparticles (3.8 and 5.3 nm) was unexpected, indicating the important role that organic ligands may play in the self-assembly process. In addition, the fact that the nanoparticles can orient to produce single supercrystals during the aging period confirms the importance of ligand-ligand interactions in directing the assembly process.

Temperature effects

We further exploited the roles of capping ligands on the assembled superlattices by varying temperature. A series of SAXS measurements were conducted on PbSe supercrystal samples (3.8 and 5.3 nm) after they had been heated at increased temperatures from 25 to 150 °C. The results show that the supercrystal phases underwent a gradual transition from the bcc to fcc structure, implying that the bcc superstructure was metastable and was stabilized due to kinetic reasons. Moreover, as it was unlikely that the PbSe core particles would undergo much change at these relatively low temperatures, the bcc-to-fcc transition may solely arise from structural changes in ligands as well as their interactions between nanoparticles.

Pressure effects

We conducted high-pressure wide-angle X-ray scattering (WAXS) experiments of PbSe nanoparticles using diamond-anvil techniques. The purpose was to study the effects of nanoparticle size on the cubic-to-orthorhombic phase transition at high pressures. With decreasing the particle size from 9.7 nm to 5.3 nm, the phase transition pressure increases from 7 GPa to 11 GPa, which is referred to as the Hall-Petch effect. However, as the particle size is further decreased to 3.8 nm, instead of the conventional cubic-to-orthorhombic transition, the rock-salt PbSe structure became amorphous at about 13 GPa. This behavior is similar to that of PbTe nanoparticles, reported by us recently: Z. Quan, Z. Luo, Y. Wang, H. Xu, C. Wang, Z. Wang, and J. Fang (2013), Pressure-induced switching between amorphization and crystallization in PbTe nanoparticles. Nano Letters (revised).

Future Work

During FY14, we will perform the following tasks:

1. Conduct additional in-situ high-pressure small-angle and wide-angle X-ray scattering experiments of PbSe nanoparticles using diamond anvil cell (DAC) techniques at CHESS, Cornell University. The combined small- and wide-angle synchrotron measurements will allow examination of structural variations, phase transformations and mechanical properties (compressibility or expandability) of both PbSe nanocrystals (atomic-level) and their assembled architectures (meso-scale) as a function of pressure, pressure medium, and nanoparticle size. One goal is to determine the fundamental mechanisms underlying the formation of high-pressure nanocrystal phases and the coalesced mesostructures or superlattices. Another goal is to use pressure as a synthetic tool to obtain novel nanoparticle assembly morphologies such as nanowires, nanosheets, and nanoporous framework structures.
2. Extend our studies of single-component nanoparticle self-assemblies to binary-component systems. Potential systems include lead chalcogenide and metal or magnetic nanoparticles, in which novel couplings/interactions are expected to occur and, as a result, new physical phenomena may emerge. Various factors controlling the co-assembly behavior, including assembly method, ratio of different components, type of metal/magnetic nanoparticles, and external forces (especially pressure), will be investigated. The relations of superlattices to the resulted physical properties will also be explored.
3. Further analyze the SXAS/WAXS data of PbSe nanoparticles collected in FY13, conduct additional experiments (such as electron microscopy) if needed, summarize the results and write papers for publication.

Conclusion

Through the state-of-the-art in-situ small- and wide-angle synchrotron X-ray scattering measurements of series of lead chalcogenide nanocrystals, this research will provide important insights into rational design of related structured nanomaterials with enhanced or newly emerging properties. Specific results include: 1) development of novel routes/procedures for controlled synthesis of lead chalcogenide nanocrystals; 2) characterization of their compositions, sizes, shapes and surface structures; and 3) determination of the formation mechanisms and governing factors responsible for structural stability of high-pressure nanophases and their assembled architectures.

Publications

Quan, Z. W., Z. P. Luo, Y. X. Wang, H. W. Xu, C. Y. Wang, Z. W. Wang, and J. Y. Fang. Pressure-Induced Switching between Amorphization and Crystallization in PbTe Nanoparticles. 2013. NANO LETTERS. 13 (8): 3729.

Functional Soft Materials by Assembling Metallo-biopolymers

Reginaldo C. Rocha
20120765PRD3

Introduction

The extensive use of polygalacturonic acids and alginates in textiles, food, and biomedical industries is based on the high electrostatic charges of the polysaccharide structures and their ability to form multilayer gel-like structures in the presence of metal cations. Evidently, ideal information-rich materials should be able to translate positional and orientational orders beyond the single-molecule level to the next hierarchical level. This project introduces a designed motif of higher-level biopolymer structures where helical polypeptide chains strongly associate by specific sequestration and binding of metal ions. Not only will metal centers bring their rich optical, electronic, and redox capabilities to such biopolymers but also they can play the role of dynamic cross-linkers by assembling multiple polymer strands together. Similarly, secondary structures can be conceived of in the context of the so-called "egg-box model" by replacing intra-stand hydrogen bonds with site-specific placement of metal-based cross-linkers.

Metal-ligand interactions can capture all the salient features of protein-protein interactions (specificity, directionality, symmetry, and reversibility) on a much smaller surface than needed by non-covalent interactions. The reversibility of metal-ligand coordination also allows for the self-correction necessary to produce assemblies with long-range order. Importantly, chemical control and tunability are inherent in this approach, as metal-directed self-assembly is dependent on external stimuli and can be dictated by the choice of metal ions and binding motif. The potentiality of resulting novel materials is determined by the tunability of specific functionalities and responsiveness, as well as the dynamic nature of the supramolecular metallo-biopolymers.

Benefit to National Security Missions

This research supports our National Laboratory missions by providing advancements toward the development and fundamental understanding of novel materials for energy and environment sciences and technologies.

With the development of biopolymer-based functional (nano)materials and their target applications in the areas of renewable energy, biosensing, regenerative medicine, optical and electronic devices, and self-healing systems, this research is highly relevant to the DOE (SC/BES), DOD (DARPA), and DHHS (NIH), in addition to possible deployment and utility to NASA and Intelligence missions. DHS and DTRA also have a vital interest in biodegradable polymers and wound-healing biocompatible materials, which represent an underlying theme in this work. Therefore, through the creation of capabilities and involvement in this new field, our project will lead to funding opportunities from several government agencies. This research also ties directly into the following LANL's LDRD Grand Challenges: "Materials: Discovery Science to Strategic Applications," "Complex Biological Systems," and "Energy & Earth Systems," in addition to its alignment with our DOE's Center for Integrated Nanotechnologies (CINT) missions in nanoscience and nanotechnology.

Progress

A central goal of our proposed work was to construct a library of metal-biopolymer complexes by combining the rich information content of biopolymers with the tunable redox, magnetic, and optical properties of metal-ligand units. Through this approach, we have designed related classes of constructs in which metals can be integrated into biopolymer structures in three different ways: by tethering to the polymer backbone as a preformed complex (class I), by coordination with a preconjugated ligand in a "plug and play" fashion (class II), or by direct coordination of metal ions with polypeptide residues (class III). We have investigated these possibilities by synthesis and characterization of representative members for each of these classes, as summarized

below in our progress to date.

For classes I and II, we have implemented different bioconjugation methods to take advantage of our new ligand units functionalized with -NH2/-COOH groups complementary to the side-chain functionalities of biopolymers that are suitable for carbodiimide coupling chemistry. In class I, we have used alterations in substituent groups on transition metal-terpyridine complexes to modulate their strong metal-to-ligand charge-transfer (MLCT) absorptions across the visible spectral region and associated redox potentials.

We have also developed a suite of transition-metal complexes in which one fixed bidentate ligand having conjugation sites is partnered with other ligands that are varied to achieve improved photophysical and redox properties; these properties can also be tuned by medium conditions, such as pH or solvent. Incorporation of redox and optical features from metal-ligand moieties into the integrated assemblies was clearly shown by electrochemical and photophysical studies.

The most striking results were 1) a large perturbation of the metal-based oxidation potential by hundreds of mV upon bioconjugation, and 2) a three-fold increase in intensity for the MLCT-based photoluminescence upon coacervation of the polypeptides above their transition temperature. Based on systematic structure-property studies, we have surmised that coacervation induces structural restrictions with increased rigidity imposed on the metal-ligand moiety. Combined with the insulation by the surrounding polymer, such structural factors lead to the unique optical and electronic effects observed.

In class II, we have adopted the “plug and play” approach where the side-chain length of the functional groups of a terpyridyl unit has been varied systematically to procure a spectrum of reactive ligands with variable exposure. This functionalized side chain was shown to readily bind to a series of lanthanide ions, resulting in highly photoluminescent metallo-biopolymers both in liquid solutions and in thin films.

The emission spectra of these integrated assemblies cover the entire visible range, raising exciting possibilities for applications into light-emitting materials with individual selection of specific light hues or combined into the generation of white light. In both classes I and II, the successful conjugation of metal-ligand components with polypeptides as well as the introduction of redox/optical properties into specific polymer sites has been evidenced by several techniques such as nuclear resonance spectroscopy, gel electrophoresis, and time-dependent monitoring of the bioconjugation reactions using mass spectrometries (both electrospray ionization and matrix-assisted laser desorption/ionization). To follow on such promising results, we are set out to evaluate these assemblies as to stimuli-responsive characteristics as a function of their emergent redox and optical properties.

In class III, an exciting accomplishment was the development of a method for constructing hybrid organic-inorganic nanocomposites from metal ions such as copper(II)/silver(I) and natively unstructured polypeptides. Characterization by scanning electron microscopy (SEM) clearly shows that some of the tested metal ions induce the formation of well-defined nanostructures (e.g. “nanoflowers”) in phosphate buffer. Our initial studies seem to indicate that the complexes formed between polymers and metal ions become nucleation sites for primary crystals. This interaction then leads to the growth of micrometer-sized flower particles featuring the nano-sized petal shapes. Energy-dispersive X-ray spectroscopy (EDX) confirmed that Cu(II) is the main constituent of the structure, and X-ray photoelectron spectroscopy (XPS) showed that the oxidation state of copper (+2) does not change upon composite formation. Wide-angle X-ray diffraction (XRD) has also been used and revealed that the crystal pattern is similar to Cu3(PO4)2 generated from the mixture of CuSO4 in phosphate buffer. This is an important finding because metal-biopolymer composites encompass materials where blending is a technological approach to generating a complete landscape of biomaterials with specific sets of properties.

Future Work

In this first year of the project, libraries of metal-ligand complexes were created and used as electronically and optically active components into the construction of metallo-biopolymers that were categorized in three classes. By making these novel materials available and structurally characterized, we can next focus on exploring the functionalities emerging from the synergy between such metal sites (transition metals and lanthanides) and biopolymers. Parallel to the detailed understanding to be gained from structure-property relationships, the design and assembly of new derivatives optimized for stimuli-responsive functions will be possible through systematic photophysical, electrochemical, and microscopic studies as a function of key factors such as chemical nature of metal ions, ligand environments, and composition of polypeptides. In addition to our ongoing experimental characterizations, computational modeling will be initiated to support the elucidation of emergent properties arising from the interplay between inorganic moieties and polypeptide structures in the integrated metallo-biopolymer assemblies (as described in the Progress section).

Conclusion

In our metal-directed self-assembly approach, higher-order topologies will be created from association of tailored polypeptide modules. These topologies will arise from incorporation of metal-ligand sites into such modules and dependence of target metallo-biopolymer ensembles on the chemical nature of metal ions as well as ligands and coordination environments. We also aim at developing a detailed understanding of key factors determining function of resulting biomaterials via systematic studies of structure-property relationships. In addition to high-impact fundamental contributions to new areas in soft nanomaterials, outcomes of this project are expected to have great potential for applications in optoelectronics, sensing, and self-healing (bio)materials.

Publications

Balog, E. R., K. Ghosh, Y. Park, H. Wang, R. C. Rocha, and J. S. Martinez. Elastin-like Polymers for Stimuli-Responsive Opto-Electronic Materials. Presented at Materials Research Society (MRS) Spring Meeting. (San Francisco, CA, April 1-5, 2013).

Ghosh, K., E. R. Balog, J. S. Martinez, and R. C. Rocha. Coacervation-Induced Photoluminescence Enhancement in Bio-Polymer Assembies of Elastin-like Polypeptides with Photoactive Metal Complexes. Chem. Comm..

Ghosh, K., E. R. Balog, J. S. Martinez, and R. C. Rocha. Optical and Redox Properties of Novel Conjugates from Elastin-Like Polypeptides and Photoactive Transition-Metal Complexes. Presented at Materials Research Society (MRS) Spring Meeting. (San Francisco, CA, April 1-5, 2013).

Ghosh, K., E. R. Balog, J. S. Martinez, and R. C. Rocha. Metal-Biopolymer Assemblies and Composites From Elastin-like Polypeptides. Presented at Gordon Research Conferences - Polymers Conference. (South Hadley, MA, June 9-14, 2013).

Ghosh, K., E. R. Balog, P. Sista, J. S. Martinez, and R. C. Rocha. Flower-Shaped Nanopatterns from Metal-Biopolymer Assemblies. Biomater. Sci..

Ghosh, K., P. Sista, and R. C. Rocha. Metallo-Biopolymers: Bioconjugation Strategies and Applications. Polym. Chem..

Sista, P., K. Ghosh, J. S. Martinez, and R. C. Rocha. Polythiophenes in Biological Applications. To appear in J. Nanosci. Nanotech..

nTuned Optical Properties of Low-dimensional Carbon Nanomaterials for Energy Harvesting

Stephen K. Doorn
20120766PRD3

Introduction

Low-dimensional carbon nanomaterials such as graphene and carbon nanotubes (CNTs) offer intriguing optical properties which can potentially be incorporated into energy harvesting applications. However, their implementation requires in-depth understandings of the materials optical properties such as fundamental nature of the optically excited states and their relaxation dynamics. Furthermore, tuning of these states by chemical doping will provide flexibility to device design. The primary aim of this research is to evaluate the potential of oxygen doping of these materials for charge/energy transfer processes at the core of photovoltaic needs by first understanding the nature of their optical states, and to demonstrate their ideal chemical structures for photovoltaics. We aim to answer the question: "Can effective functionalization strategies lead to unique optical properties of graphene oxide and CNTs for energy harvesting applications?"

With similar origins for optical properties based in oxygen doping, optical properties of graphene oxide (GO) and oxygen doped nanotubes may display parallel behaviors that lead to better understanding of optical response in both. For GO we will focus on chemically exfoliated flakes as material. Steady-state and time-resolved optical studies will be performed on this material. Our focus will be on defining how chemical modification alters optical response. For oxygen-doped carbon nanotubes, we will also apply steady state and time-resolved spectroscopies. Direct imaging and spectroscopy at the single nanotube and even dopant-site level will also be pursued. Of special interest will be determining the surface mobility of oxygen dopants, how these states interact withe the mobile excitons, and what are their surface dynamics.

Benefit to National Security Missions

Fine tuning of graphene/CNTs with well designed chemical functionalization would open up a pathway for incorporation of these materials into large area, inexpensive, flexible energy harvesting electronics. Understanding their optically excited states and relaxation dynamics will clarify the competition between charge and energy transfer and recombination in these materials, which is crucial in determining their potential for photovoltaics. The results will provide insight for design of novel energy harvesting devices utilizing the unique optical properties of low-dimensional carbon nanomaterials, and makes an important contribution to LANL's mission on sustainable energy. The goals of the project also directly address development of new routes to controlling materials functionality. The same characteristics and underlying behaviors that we will study as related to photovoltaic applications also form the basis for applications of these materials in sensing, imaging, optoelectronics, and photonics. These then also support LANL national security missions and are relevant to programs related to DOE, DOD, DHS, and NIH.

Progress

Our two research thrusts of i) graphene and ii) CNTs (carbon nanotubes) were conducted in parallel to facilitate the understanding of the underlying origin of the oxygen doping induced optical states in low-dimensional carbon nanomaterials. Details of progress made for each thrust are as follows:

Graphene

We fabricated graphene oxide (GO) single nanosheet optoelectronic devices as platforms for understanding the core photophysics of the low-dimensional carbon nanomaterials during energy harvesting device operations. State-of-the-art electron-beam lithography and thin film metal deposition capabilities at the Center for Integrated Nanotechnologies (CINT) were used for the fabrication. Single nanomaterial device fabrication requires time and effort compared to the assembled

film counterpart; however, the obtained information is free from averaging effects, which is essential for the fundamental study of the device. Device characterization using Scanning Photocurrent Microscopy (SPCM) provided photocurrent distribution of the material with high spatial resolution. The SPCM characterization was then correlated with complementary optical properties such as photoluminescence (PL) and Raman spectral mapping measured at the same positions. The results showed clear correlations which gives us insight as to how to design efficient graphene-, and possibly CNT-based photovoltaics. Specifically, regions of strong photocurrent intensity matched well with areas producing high PL, indicating that the origin of photocurrent is most likely the oxygen functional groups of GO. (It is known that oxidized regions of GO have strong PL.) Consistency between low PL intensity region with high Raman intensity region also confirms that high PL intensity region has higher density of oxygen. Further investigations on the origin of high photocurrent in GO will be performed using well-controlled device geometries which contains n- and p-doped regions.

Carbon Nanotubes (CNTs)

We have obtained unique optical properties of CNTs via controlled oxygen doping. By using ozonated water as an oxygenating agent, new optical states with a clear red shift of photoluminescence (PL) were observed for CNT suspensions compared to undoped samples. The shift was observed for both mixed chirality and chirality separated (6,5) CNTs. The type of surfactant used to wrap and disperse CNTs in aqueous suspension was crucial in enabling the doping chemistry to proceed. It is speculated that surfactant dependent morphology of the wrapped CNT surface, determined by the affinity of surfactants to CNTs, plays an important role in achieving the appropriate density of oxygen doping. Investigations on the nature of the shifted optical state are underway by performing temperature dependent PL of chirality enriched (6,5) CNT suspensions, as well as using single molecule spectroscopy to probe the single optical site induced by the oxygen doping. Our temperature dependent measurements are indicating the dopant sites act as trap sites for excitons, with a trapping energy of about 250 meV. Single-tube and single-site imaging and spectroscopy studies are laying the groundwork for further probing the trapping nature of these dopants and how it may lead to novel PL saturation behavior. Magneto-PL and electroluminescence (EL) on oxygen doped CNTs are also planned to gain insight into the nature of the sites and their role in improving CNT optical properties for energy harvesting applications.

Future Work

Development and optical studies of Graphene Oxide (GO)

We will establish approaches to variable functionalization chemistry of GO, with the goal of tunable control over its optical properties. Additional control will be pursued by defining size and shape distributions using density gradient centrifugation approaches. Optical spectra and relaxation behaviors for different functionalization will be established. Development of simple thin film devices will also be established as a platform for probing phto-induced charge generation. Capacitive photocurrent spectroscopy will be used for determining the nature and evolution of photogenerated charges.

Development and optical studies of oxygen-doped carbon nanotubes

The ability to create oxygen doped carbon nanotubes will be established. Incorporation into new gel matrices for enabling certain types of optical measurements will also be pursued. Of particular interest will be probing of exciton optical properties within these doped materials. Studies will include time-resolved, imaging, and temperature dependent measurements at both the ensemble and single-tube levels. Initial focus will be on establishing migration behaviors of dopant-induced states and how these interact with optically generated excitons. Ultimately, incorporation into electro-optic devices will also be pursued.

Conclusion

Fine tuning of graphene/CNTs with well designed chemical functionalization would open up a pathway for incorporation of these materials into large area, inexpensive, flexible energy harvesting electronics.Understanding their optically excited states and relaxation dynamics will clarify the competition between charge and energy transfer and recombination in these materials, which is crucial in determining their potential for photovoltaics. The results will provide insight for design of novel energy harvesting devices utilizing the unique optical properties of low-dimensional carbon nanomaterials, and makes an important contribution to LANL's mission on sustainable energy as well as to the world's energy needs.

Enhanced Structural Robustness in Metal/Nonmetal Nanocomposites using Bio-inspired Structure Design

Amit Misra
20120769PRD3

Introduction

Nanocomposites of a metal (copper) and a non-metal (carbon or carbide or nitride) will be synthesized using physical vapor deposition following bio-inspired design of sandwich structures. The crystallinity and morphology of the non-metallic phase and the relative thicknesses of the two phases will be varied. The strength and crack growth resistance will be measured using a variety of nanomechanical testing such as hardness, stiffness, compression and notched bend tests. Scanning and transmission electron microscopy will be used to characterize the structure and morphology of the constituent phases and the interaction of defects such as dislocations and cracks with the metal / non-metal interfaces.

The scientific impact of this research will be that, for the first time, metal-carbon composites possessing a combination of high strength, high resilience and high fracture toughness will be developed. While the current state-of-the-art relies on the "small is stronger" paradigm to increase the hardness of soft metals via refinement of grain size, this will push the frontiers in designing materials with unprecedented levels of strength and fracture toughness.

Benefit to National Security Missions

The proposed work is directly aligned with the grand challenges and scientific issues outlined in the BESAC report of DOE, Office of Science titled "Directing matter and energy: five grand challenges for science and the imagination" and the Basic Research Needs (BRN) workshop series, specifically: Advanced Nuclear Energy Systems (ANES); and Materials Under Extreme Environment (MUEE). Some specific scientific questions from these reports that are pertinent to this LDRD project are: How do we make hard matter that heals damage or defects? and How mechanically strong can we make materials yet keep them light-weight?

Development of scientific principles of designing materials from the atomic scale for predictable performance at extreme conditions such as high stress, high radiation dose, etc also supports the mission of LANL's MARIE and DOE-NE.

Progress

The primary focus has been on the synthesis of metal-nonmetal nanocomposite systems following biologically-inspired design that would exhibit a considerably improved mechanical performance, beyond the limits imposed by traditional disciplines. To this end we have studied the synthesis parameters for Cu-TiN (copper-titanium nitride), with the goal of a strong yet ductile material system. The metal (Cu) in this system is soft and ductile, while the non-metal (ceramic TiN) is hard and brittle. Moreover unlike other metal-ceramic systems Cu has a low affinity towards nitrogen, and hence the Cu-TiN interface is expected to be chemically sharp and relatively weak in shear.

Nanolayered composites of Cu-TiN have been synthesized using physical vapor deposition (PVD). Most of the effort in this year till date has been concentrated on developing high quality Cu-TiN multilayer systems by adjusting the deposition parameters such as temperature, substrate bias, etc. Current results suggest that a combination of high temperature (300 C) and high bias on the TiN can generate low-porosity dense multilayer films. Testing of such miniaturized samples (thicknesses in the micrometer range) poses significant challenges. Among the experimental techniques available at these length scales, nanoindentation, with its high resolution load and depth sensing capabilities, shows the greatest promise due to its ease of experimentation and versatility. Towards this end we have utilized a novel spherical nanoindentation analysis technique which is able to transform the raw load-displacement data into meaningful indentation stress-strain curves (this technique was originally developed by the postdoc fellow as part of his

graduate work). More specifically, the use of these indentation stress-strain curves makes it possible to analyze the initial loading segments of spherical indentation (from shallow indentation depths of 50-100 nm). Thus the characterized property (e.g. indentation yield) corresponds to the intact material at the indentation site, and can be used to differentiate between inherent differences in the local material structure at the indentation site. This has enabled the measurement of local mechanical properties including the loading and unloading elastic moduli, the indentation yield points, as well as some of the post-yield characteristics. Work in the first year has been focused on validating this system on metal-metal (Cu-Nb) interfaces before proceeding to the more complex metal-nonmetal systems. Significant progress has also been made in designing another novel micro-mechanical testing system – that of compression testing of micro-pillars containing these multilayered nano-composites. Such micrometer sized pillars are typically produced by removing material around a selected region of interest using a focused-ion beam (FIB). However this technique typically requires tremendous resources in terms of sample preparation and operator time, due to the large amount of material that needs to be removed by FIB. Work in the first year has focused on reducing the sample preparation time needed for such an effort. This was achieved with the use of lithographic polymer photomasks during the PVD process. Etching off the polymer after the deposition process leaves only the multilayers deposited in a predetermined pattern. Since the amount of material needed to be removed by FIB is now significantly decreased, this reduces the sample preparation time by more than a third, and makes bulk production of micro-pillars possible.

Future Work

Using physical vapor deposition capabilities in the Center for Integrated Nanotechnologies (CINT) at LANL, nanocomposites foils of a metal such as copper and a non-metal such as carbon or carbide or metal nitride will be made. Deposition parameters such as deposition rate, temperature and relative thickness of the metal and non-metal layers will be controlled to produce either amorphous or crystalline form of carbon in the form of continuous or discontinuous layers in the copper matrix. The as-deposited foils will be vacuum annealed to further change the structure, e.g., crystallize the amorphous carbon or change morphology from continuous to island-like or grow the island-size or improve crystallinity for nitride layers. The as-deposited and annealed foils will be characterized using scanning and transmission electron microscopy to elucidate the morphology and crystallinity of the nano-phases. The initial nanomechanical characterization will include hardness, stiffness and compressive flow strengths using nanoindentation. The crack growth studies, including in situ experiments in a scanning electron microscope, will be the focus of the work in the second year.

Conclusion

The key expected results are (i) correlation between the synthesis parameters and the crystallinity, scale and morphology of the non-metallic phase in the metal matrix, and (ii) mechanical properties (strength, stiffness, toughness) for the different morphologies of the nanocomposites. Collectively, these results will provide the scientific principles to design metal / non-metal nanocomposites that possess unique combination of strength and toughness not achieved in any existing engineering material.

Nanoscopic Recrystalization Dynamics and Phase Behavior in Liquid Crystals and Polymers

Juan Duque
20120770PRD3

Introduction

In photothermal processes, photons of light are absorbed and transferred into thermal energy. This is an excellent technique for metallic nanoparticle detection, since it exploits the weaker size dependence on nanoparticle absorption over Rayleigh's scattering. A laser in resonance with the nanoparticle plasmons is used to obtain an optimal photothermal effect. An imaging technique that takes advantage of the photothermal effect is the photothermal heterodyne imaging (PHI) technique. A probe beam with minimal nanoparticle absorption is used to measure the induced change in the index of refraction by a modulated heating beam. This technique has been used to image extremely small nanoabsorbers, even single molecules, much smaller than the wavelength of light.

This unique effect offers the ability to heat the nanoparticle matrix at the nanoscale, which allows us the opportunity to answer some very interesting questions. The PHI technique is able to detect changes in refractive index and thus it was able to determine that at the nanoscale, the nematic-to-isotropic phase transition occurs at a lower temperature. The exact reason for this depression is due to a combination of interfacial tension and confinement. However, since this is a liquid crystalline system, the nanoparticles must be fixed to the surface, thus the transition is dependent on the interactions of the liquid crystal with the surface. A glass transition temperature can remove the surface effects. Nanoparticles can be suspended and fixed within a polymer at temperatures below the glass transition temperature and then heated to initiate the transition. Thin film work suggests there should be a large depression in this transition temperature; however, thin films have both a substrate and air interface. This information may lead to better theories and more accurate parameters for molecular interactions during a phase change.

Benefit to National Security Missions

These projects will introduce a new capability to the laboratory called photothermal heterodyne imaging technique. This technique is a highly sensitive method to probe temperature effects at the nanoscale to investigate the recrystallization dynamics and the glass transition temperature of different materials important in the developing of new meso-materials for energy conversion, photovoltaics, and sensing in relevance to the DOE, DOD, DHS, and NIH.

Progress

We are studying phase transitions at the nanoscale, focusing on transitions that can be probed through temperature changes, such as thermotropic liquid crystalline phase transitions, polymer glass transitions, and melting transitions. Originally, we planned to study these transitions only through a photothermal imaging technique that we brought to Los Alamos National Laboratory. In brief, photothermal imaging is a technique that allows nanoparticles to be visualized when they absorb photons and convert the energy to thermal energy. The thermal energy creates a scattering field that scatters a non-absorbing laser. This thermal energy is highly localized surrounding the nanoparticle, thus allowing a thermally induced phase transition to occur nanoscopically in the materials just surrounding the material. With this technique, we can monitor any changes in the critical temperature, or energy, needed to induce the phase transition and can imply as to the nature of the surrounding material, for example the local alignment and interactions with the nanoparticle. In the past twelve months, we have made headway in improving our ability to understand the nanoparticle interactions with the surrounding material by introducing two new characterization techniques that are superimposed on the same diffraction limited spot. Fluorescence is extremely sensitive to environmental changes, thus it will be used to probe fluorescent molecule near the surface of the

nanoparticles as the phase transition occurs. Lastly, Raman spectroscopy will be used to probe the local alignment as a function of temperature during the phase transition, which will give us better understanding of the recrystallization dynamics.

Future Work

- Development and optimization of a new experimental technique called photothermal heterodyne imaging (PHI) capable of imaging samples down to 1nm. frequency dependent experiment will be done at temperatures near the phase transition. Lower frequencies will allow more time for the liquid crystal to recrystallize and will result in greater signal. The multiple laser sources available at LANL (from 275 to 1000 nm) will increase the sensitivity of the measurement since the noise as a function of frequency is wavelength dependent.
- We will establish for the first time an approach to control/monitor the change of index of refraction with temperature, at the liquid crystalline phase transition, in order to enhance the PHI sensitivity. The high sensitivity of the PHI technique offers a low-powered method to probe the phase transition dynamics of nanomaterial with minimal external interactions. Preliminary results will provide information on the thermotropic liquid crystalline phase transition dynamics.

Conclusion

The photothermal heterodyne imaging technique is a very useful tool to visualize individual nanoabsorbers for a wide range of applications, such as protein tracking, nanopartical characterization, and nanoparticle localization in three-dimentional environments. We aim on determining the recrystallization characteristic time in liquid crystals as the temperature approaches the phase transition temperature and the role surface interactions play on the phase transition temperatures in liquid crystals and polymers.

The Fate of the Three Dimensional Electron Far Beyond the Quantum Limit

Ross D. Mcdonald
20120772PRD4

Introduction

We plan to carry out detailed study of magnetoresistance and/or magnetic susceptibility measurements on semimetal graphite and bismuth in a pulsed field magnetic field up to 100 T as the angle between applied field and the crystalline axis is varied. The high quality samples are commercially available. At low temperature, magnetoresistance and/or magnetic susceptibility easily track quantum oscillations when the Landau levels pass the Fermi level and abnormal transition. Single-particle theory without coulomb interaction will be utilized to compare with our results for two materials.

Benefit to National Security Missions

Exploration of low carrier density metals in extremely high (pulsed) magnetic fields and at low temperatures is directly relevant to MaRIE because of the need to develop and refine high-frequency conductivity probes at high data acquisition rates compatible with the sub-microsecond duration of transient events in these extreme environments.

Furthermore, investigating the novel states of three dimensional metals when extreme magnetic fields drive them beyond the quantum limit will increase our understanding of the fundamental interactions between electrons in metals, which may impact other lab missions who seek a more fundamental understanding of strategic metals (c.f. unknown band structure and Fermi surface of plutonium).

Progress

During the last year Zengwei has extended his proposed study of low carrier density three dimensional metals in pulsed magnetic fields to the topologically non-trivial metallic material bismuth tellurium. This material system is an important example of a topological insulator system that has been proposed to support two dimensional surface states. To date these surface states have been exceedingly hard to observe largely because of chemical stability and environmental exposure of the surface during measurement. Zengwei's high field measurements on sulphur doped bismuth tellurium reveal this to be a significantly more stable surface state with significantly higher electronic mobility than observed in other TI materials. Furthermore field orientation dependance reveals the quantization of the Hall voltage to originate from the 2D surface state. A high profile publication manuscript is in preparation. Further pulsed field measurements are underway aimed at employing a combination of electric and magnetic fields - i.e. using a gate voltage to tune the surface carrier density whilst probing the carrier density with the orbital quantizing effect of the magnetic field.

Zengwei has also undertaken pulsed magnetic field torque magnetometry measurements to investigate the physical properties of related strong spin-orbit materials that are too insulating for restively measurements in high magnetic fields. This is an on going activity in collaboration with the University of Cambridge that is yielding very interesting results.

Future Work

Apply existing measurement techniques (magnetization,magnetic torque,conductivity DC-rf frequencies) to the measurement of low carrier density metals in 65T (short) pulsed magnetic fields.
Refine these techniques for the particular challenges of measuring low carrier density samples e.g. high restivity and large magnetoresistance.

Implement these improvements in measuring the materials to the highest available non-destructive magnetic fields using the 100 T multi-shot magnet system.
Publish results in high impact journals.
Be invited to give high profile talks.

Conclusion

Within two years, we will finish detailed study of temperature- and angle-dependent phase diagram in bismuth and graphite up to 100T. We will uncover the nature of intriguing transitions from strongly correlated electrons far beyond QL. Our experimental results will contribute to better theoretical calculations. Collaboration between experiment and theory would significantly improve our understanding of the fate of the 3D electron gas beyond the QL. This research could shed light on how electrons interact. Based on this, we can extend comprehension to other more complicated strongly correlated systems such as heavy fermion systems, high Tc superconductors etc.

Publications

Lin, X., Z. W. Zhu, B. Fauque, and K. Behnia. Fermi Surface of the Most Dilute Superconductor. 2013. PHYSICAL REVIEW X. 3 (2): -.

Zhu, Z. W., A. Collaudin, B. Fauque, W. Kang, and K. Behnia. Field-induced polarization of Dirac valleys in bismuth. 2012. NATURE PHYSICS. 8 (1): 89.

Zhu, Z. W., B. Fauque, L. Malone, A. B. Antunes, Y. Fuseya, and K. Behnia. Landau spectrum and twin boundaries of bismuth in the extreme quantum limit. 2012. In PROCEEDINGS OF THE NATIONAL ACADEMY OF SCIENCES OF THE UNITED STATES OF AMERICA. Vol. 109, 37 Edition, p. 14813.

Access to Industrially Important Chemical Compounds by Direct Hydrogenation of Biomass Derived Molecules Containing Carbonyl Fragments

John C. Gordon
20120774PRD4

Introduction

The reduction of carboxylic acids has relied mostly on the (stoichiometric) use of reagents such as LiAlH4, NaBH4 and their derivatives (i.e. forcing conditions). Recent progress in the area of homogeneous, metal-catalyzed hydrogenations of carboxylic acids and their derivatives has been made however. Appropriately designed bifunctional catalysts have demonstrated utility in the area of polar functional group hydrogenations, as their metal-ligand cooperation effects promote mild activation of small molecules (in this case H2). Bifunctional catalyst promoted hydrogenations using H2 are now realized to be a practical tool in synthetic organic chemistry in both academia and industry. The industrial outlook for this approach to hydrogenation is bright because of its operational simplicity, scope, economic viability, and the growing awareness of the need for green chemistry approaches.

This research project will thus specifically target the rational design of new bifunctional metal complexes (M = Ru, Ir) capable of mild, selective and direct hydrogenation reactions of less electrophilic carbonyl groups. Particular emphasis will be placed on these molecules with respect to their ability to hydrogenate cheap, biomass-derived platform chemicals containing polar carbonyl moieties into more useful (and higher value) molecular building blocks. The hydrogenation of esters bearing alpha-fluorine atoms will also be pursued, as their hydrogenation products are of significant importance within the pharmaceutical industry.

Benefit to National Security Missions

The development of new methods for mild and selective hydrogenations of polar functionalities contained within cheap and widely available biomass derived compounds would provide routes to highly desirable building blocks for the pharmaceutical, polymer and optoelectronic industries. This area however remains a significant challenge. In particular, the hydrogenation of ureas, organic carbonates, carbamates and formates is of significant global interest since these classes of compounds can be produced from CO2 and CO. Milder hydrogenations applicable to CO2 and CO themselves could also provide alternative routes to methanol, an important fuel and synthetic building block in its own right. Success in this chemistry could therefore have significant positive impact for LANL, vis-à-vis the application of sustainable approaches to new polymers and materials synthesis, in energy applications, and in health related (pharmaceutical) R&D.

Progress

In the last few decades, bifunctional molecular catalysis based on metal–ligand cooperativity has been developed and has become a general strategy for effecting highly efficient molecular transformations in organic chemistry. Originally developed for the asymmetric transfer hydrogenation of ketones, metal–ligand bifunctional catalysts (in which non-innocent ligands directly participate in substrate activation) are also now applicable to the hydrogenation of less electrophilic polar functionalities. We are focusing on the synthesis and characterization of new earth abundant metal complexes supported by mixed donor (multidentate) ligands that are capable of promoting the hydrogenation of polar substrates. Although the project has just recently begun, we have already synthesized and characterized a series of ligands containing different phosphorus, nitrogen and sulfur donor arms. These ligands will now be used to construct catalysts containing metals such as iron, ruthenium, cobalt and copper. Catalysts will then be tested for their propensity to hydrogenate a variety of of carbonyl containing fragments, notably esters, carboxamides, ureas as well as potentially to less-electrophilic CO2 as a final target.

Future Work

We will utilize calculations to guide the design, synthesis and reactivity of various new bifunctional metal complexes (M = Ru, Ir) capable of mild, selective and direct hydrogenation reactions of polar carbonyl containing moieties such as esters, carboxamides, and carbonic acid derivatives. These are important classes of biomass derived compounds, often proving difficult to hydrogenate. Since biomass-based routes are expected to make a significant impact on the production of bulk chemicals within 10–30 years, these studies will provide us with a deeper understanding of the factors involved in hydrogenating these classes of compounds into other useful chemical building blocks.

Conclusion

The development of new methods for mild and selective hydrogenations of polar functionalities contained within cheap and widely available biomass derived compounds would provide routes to highly desirable building blocks for the pharmaceutical, polymer and optoelectronic industries. This area however remains a significant challenge. In particular, the hydrogenation of ureas, organic carbonates, carbamates and formates is of significant global interest since these classes of compounds can be produced from CO2 and CO. Milder hydrogenations applicable to CO2 and CO themselves could also provide alternative routes to methanol, an important fuel and synthetic building block in its own right.

Stimuli Responsive, Functional Biopolymers: Quinic Acid-based Polymers and Their Assemblies

Hsing-Lin Wang
20130778PRD1

Introduction

This project aims to develop functional biomolecules with emergent (mechanical, optical, and electronic) properties that are not accessible through conventional synthetic methods. The approach uses molecules that are known to form polymers compatible with biological systems with side chains that are active to which functional groups can be attached. Depending on the distribution and density of these functional groups on the side chains, a wide spectrum of mechanical and optical properties, and electronic structures can be accessed. Our goal is to exploit the emergent properties, and through the analysis of structure-property relationships, obtain valuable insight regarding the design of biopolymers with enhanced functionality that can be used toward sensing, bioimaging, drug delivery, optical, electronic and energy applications. Such an approach has not yet been studied in a systematic manner mainly because multidisciplinary knowledge ranging from organic synthesis to materials chemistry to biochemistry is needed.

The challenge is to develop synthetic chemistry routes that are facile and effective. Further, we must control the distribution of functional groups on the side chains in order to render desired properties. Dr. Pradeep Cheruku is a researcher who has the unique combination of skills and knowledge to execute the project and offers the best opportunity for success.

Benefit to National Security Missions

We expect that these new classes of biopolymers may exhibit high temperature thermal transitions and strong mechanical properties due to the high degree of hydrogen bonding and rigid carbocyclic backbone. We hope to show the correlation between nanoassembly structures and their associated properties to obtain valuable insights on the interplay between structure, dynamics and functions of the materials. We also expect to develop novel strategies for the design and synthesis of nanoassemblies with adaptive control to enable the materials with immense technological relevance in areas of optics, electronics, photovoltaic, and biomedical devices that impact our missions in energy security and threat reduction.

Progress

The Goal of this project is to investigate the development of functional biopolymers in which the existing functionalities can be coupled with oligomer, dye or other complex biomacromolecule for sensing and electronic applications. We chose to use quinic acid (QA) as a monomer to build the functional biopolymers due to its natural occurrence, chirality, poly functionality and well-established chemistry. In this project, we proposed the development of QA-based biopolymers to explore their properties/responses against various stimuli such as temperature, pH etc.

We synthesized the intermediates to obtain the polymerization precursors. It is a ten-step synthesis to prepare the polymerization precursor. We have completed 3 steps out of total 10steps. Each molecule is synthesized, purified using silica gel column chromatography and carefully characterized using NMR techniques to ensure that we have obtained the correct product with the desired purity.

Our plan is to conjugate these polymers with various fluorophores such as conjugated oligomers and other fluorescent dyes and follow their optical properties as we expect these optical properties are the function of the stimuli applied on these polymers. Toward this aim, we wanted to develop new fluorophores derived from biomolecules, amino acids, such as tyrosine and arginine. In this context, I have synthesized five analogs of tyrosine derived fluorescent conjugated oligomers and studied their optical properties. These molecules were

synthesized starting from the iodination of the natural amino acid tyrosine. Corresponding diiodo tyrosine was employed in palladium catalyzed Heck-coupling reactions with various electron – withdrawing and – donating groups at the para-position of the aryl ring. This allows us to fine tune the electronics and the dipoles of the molecules which play a crucial role in the formation of the aggregates which in turn directly impacts their optical properties. All products were purified using silica gel column chromatography. Characterizations and purity assessments were done by using NMR and HPLC (for water soluble molecules). These newly developed fluorophores bear amine (-NH2) and carboxylic acid (-COOH) functionalities as they are derived from natural amino acids. These functionalities will be used to conjugate to the polymers. Currently, my efforts are focused on the optimizing the bioconjugation using the model molecules before we actually couple them to the desired polymer. Interestingly, these newly developed fluorophores exhibit properties such as PH-sensitivity (shows different emission colors under acidic and basic environments), redox-sensitivity (fluoresense is quenched upon oxidation and regenerated upon reduction) and also solvatochromisam in different solvents. I am now compiling all these interesting properties and writing up a decent manuscript for the publication. We are to expecting submit our first manuscript in this project soon.

We have also synthesized one analog derived from amino acid arginine. This analog is structurally similar to the tyrosine derived molecules except the hetero atoms (nitrogen) with in the conjugated backbone. Due to the presence of the nitrogen atoms in the conjugated backbone, we are expecting these molecules to show different optical properties. These molecules are synthesized by following an entirely different synthetic route. Arginine is treated with the acetyl acetone to construct the core nitrogen-containing aromatic ring bearing activated methyl groups. Upon treating with a strong base, these methyl groups undergo aldol-type condensation with the benzaldehyde to give the corresponding conjugated fluorophore. Again, the aldehyde can be varied to obtain structurally different fluorescent molecules. We are currently exploring the synthesis of various analogs.

Future Work

We propose to investigate the development of functional biopolymers in which the existing functionalities can be coupled with oligomer, dye or other complex biomacromolecules for sensing and electronic applications.
We also propose the use of quinic acid (QA) as a monomer to build the functional biopolymers due to its natural occurrence, chirality, polyfunctionality and well-established chemistry. We plan to develop QA-based biopolymers and explore their properties against various stimuli such as temperature, pH etc.

The copolymer syntheses are carried out by copolymerization of methacrylate conjugates of QA (QA monomer and chromophore in the presence of a radical initiator like AIBN to synthesize QA-biopolymer on a poly(methacrylic acid) backbone). The FITC dye on the polymer acts as a spectroscopic reporter on the state of the polymer conformation. Conformational changes within the polymer trigger the arrangement/proximity of the fluorophores to put them in different environments and thus lead to a modulation of fluorescence. The hydroxyl groups on the QA of the polymer can be further functionalized to their corresponding carboxylic acid(anionic)/amine(cationic) groups. This may lead to pH responsive biopolymers which can shrink or swell at certain pHs.

Conclusion

We expect synthesis of a new class of biopolymers with thermal transitions and strong mechanical properties due to the high degree of hydrogen bonding and rigid carbocyclic backbone. We hope to show the correlation between nanoassembly structures and their associated properties to obtain valuable insights on the interplay between structure, dynamics and functions of the materials. We also expect to develop novel strategies for the design and synthesis of nanoassemblies with adaptive control to enable materials with immense technological relevance in areas of optics, electronics, photovoltaic, and biomedical devices that impact our missions in energy security and threat reduction.

NMR Study of Quantum States of Matter

Joe D. Thompson
20130780PRD1

Introduction

There are thousands of examples of a transition at finite temperature from a magnetically ordered state to a magnetically disordered state. At such a classical phase transition, thermal fluctuations due to the finite temperature environment drive the transition. But, it also is possible theoretically to have a transition from magnetically ordered to disordered states at absolute zero temperature where there are no thermal fluctuations. In this case the transition is driven solely by rules of quantum mechanics. Though theoretically possible, there are a growing number of experiments suggesting that such a quantum-driven transition exists, but none of these examples can be explained completely with existing theory. Further, experiments during the last decade have found that an unconventional form of superconductivity tends to appear in the vicinity of a quantum magnetic transition, but the possible relationship between quantum fluctuations at this zero-temperature transition and unconventional superconductivity remains an outstanding question.

Nuclear magnetic resonance (NMR) techniques are a particularly powerful probe of the nature of quantum fluctuations and their possible role in producing unconventional superconductivity and will be used to study a prototypical example CeRhIn5 whose magnetic transition can be tuned by applied pressure toward zero temperature where superconductivity emerges. The role of intentionally introduced disorder on the nature and effect of quantum fluctuations also is an important open question that will be addressed by systematically replacing Ce by La and In by Sn in CeRhIn5.

These experiments will provide critical tests of theoretical models of quantum phase transitions, which ultimately should enable a predictive methodology for the discovery of superconductors for energy conservation applications.

Benefit to National Security Missions

Unconventional superconductivity holds promise for exciting new energy and defense technologies, but how and where that superconductivity might appear cannot be predicted. Empirically, experiments have shown that this superconductivity frequently appears as a magnetic transition is tuned to zero temperature, but the nature of the quantum excitations and how they might induce superconductivity are major unanswered questions. Fundamentally new understanding of the mechanism of unconventional superconductivity and its possible relationship to quantum fluctuations is needed to be able to predict how and when superconductivity appears. Success in this project will provide basic new understanding of materials and how quantum fluctuations induce new quantum states of electrons. With unconventional superconductivity also found recently in plutonium-based materials, superconductivity itself can be used to inform a much clearer perspective of states of matter than can arise from the electronic complexity of Pu.

Progress

Postdoc hire-on date was delayed unexpectedly until July 1, 2013.

Future Work

Nuclear magnetic resonance (NMR) techniques will be used to explore and understand the nature of quantum fluctuations that evolve from a zero temperature magnetic transition. The compound CeRhIn5 is an excellent example of a system whose magnetic transition can be tuned by pressure to a zero temperature and will be used as a prototype for testing theoretical models of the signatures for and consequences of quantum fluctuations for the formation of electronic states from them.

Conclusion

This project addresses the fundamental, unanswered question of what happens when a magnetic transition

is tuned to absolute zero temperature. One possibility is that quantum fluctuations of the magnetic order at zero temperature produce an attractive interaction that creates an unconventional form of superconductivity or that these fluctuations induce some new, unanticipated quantum state. Success in this project will make significant strides in advancing our understanding of the consequences of quantum fluctuations that arise out of a zero-temperature magnetic transition..

Efficient Carbon Nanotube Growth on Graphene-metal Surfaces

Stephen K. Doorn
20130785PRD2

Introduction

The project goal is to optimize the synthesis conditions that promote the catalytic conversion of graphene into high yield few-walled (1-2 layers) carbon nanotubes (CNTs). The approach will overcome typical drawbacks of nanotube synthesis that include use of harsh chemical treatments of growth substrates and include the need for multi-step purification processes. These challenges will be overcome by using graphene sheets as an innovative new substrate for growth that allows one-step synthesis of composite materials. Growth can also be attained at low-temperatures (~200 degrees C vs the typical 800 degrees or higher) which is essential for enabling development of composites based on multiple materials with very different ranges of temperature compatibility.

Another innovative aspect is to use dip-pen lithography capability for fine-control over placement and morphologies of metallic nanoparticle growth catalysts. Optimization of our growth processes will require variation and study of the influence of multiple growth parameters. These will include modulation of catalyst particle size, composition, and placement.

We will also study the effects of variable temperatures and reactant gas composition and flow rates. The resultant synthesis will directly provide nanotube/graphene composites that will be studied for their energy harvesting and storage potential. Low temperature growth processes are anticipated to also allow the use of gold nanoparticles for growth as well, which will be the key to enabling development of nanotube-nanowire hybrids (not yet attained) of interest for optical and electronics needs.

The knowledge gained in these first synthesis directions will also allow us to taylor synthesis conditions to pursue growth of other novel composite materials including carbon nanotube hybrids with complex metal oxides. Such oxide thin films form the basis for superconducting and multi-ferroic materials of tecnological interest. Interactions with nanoelectronic materials such as nanotubes can introduce emergent electronic behaviors that may enhance the properties of interest.

Benefit to National Security Missions

The work is directly relevant to DOE Office of Science interests in the fundamental science of and development of multifunctional nanoscale materials. The work will also probe the fundamentals of carbon nanomaterial interactions with other materials, also of interest to DOE/SC. The nanotube/graphene materials are of significant interest for energy storage and energy harvesting, giving the work mission relevance for both energy security and the environment (climate and energy impacts). The effort is also directly related to development and basic understanding of nanomaterials with ultimate impact on electronics, sensing, and imaging needs as well.

Progress

To date limited progress is available as the postdoc has only been at Los Alamos for one month. However, significant progress has been made in preparing the laboratory space for both graphene and nanotube synthesis. A new IWD covering the expanded scope of the nanotube synthesis work is nearly in place. The growth furnaces have been put in place and Enkeleda has already generated some large area graphene films that will be used for generating multi-component hybrid structures.

Future Work

The goal is to identify the synthesis conditions required for high yield few-walled carbnon nanotube (CNT) growth on graphene-metal surfaces using a chemical vapor deposition approach. Few-layer and large area graphene sheets will be decorated with various types of metal nano-particles (nps) and their deposition will be accomplished using two different methods; dip pen nano-lithography (DPN) and a simple route involving a

mixture of the metal nanoparticle solution with graphene. Using DPN to precisely control the arrangement and the number of nps on the graphene sheet is very innovative and essential since the concentration of nps is known to affect the hydrogen/carbon ratio in the reaction mixture and nanotube formation. The influence of both techniques on the size and dispersion of nps, which are important factors in controlling the nanotube diameter, will also be investigated.

Given the complex nature of the growth kinetics of nanotubes with controlled wall numbers, the catalytic conversion of graphene into single-wall or double-wall CNTs will be a breakthrough in nature. Optimization of the synthesis conditions for few-walled CNT growth with controlled properties will be achieved by varying the following: catalyst size and composition (combination of two different metals at various loadings), reaction temperature, and type/flow rates of gases. To increase the single-wall nanotube yield, while preventing Ostwalt ripening, water vapor will be added in the CVD set up. Performing in-situ TEM experiments will be a crucial step towards understanding the complex role of graphene during the catalytic nanotube growth. Microscopy (TEM, SEM, AFM) and Raman spectroscopy analysis will be performed to study the morphological properties of nps and realize their interaction with the graphene surface during the nanotube formation.

Conclusion

The primary technical goal is to develop novel synthesis approaches to improve the optical and electronic properties of few-walled (targeting 1-2 layers) carbon nanotubes. The methods we anticipate using will also result in generation of functional hybrid carbon nanomaterials of interest for energy storage, electronic, and multi-ferroic applications. These may include hybrdi nanotube/graphen materials, nanotube/nanowire heterojunctions, and nanotube composites with complex oxide thin films.

Hybrid Nanostructures for Photoreduction of CO_2 to Hydrocarbons

Hongwu Xu
20130787PRD2

Introduction

The goal of this research is to develop novel hybrid nanostructures for photocatalytic conversion of carbon dioxide plus water into hydrocarbons. Semiconductor-based nanomaterials are promising materials that may enable this catalytic process, as they can couple single photon events with accumulation of multiple redox equivalents upon CO2 reduction. However, most of the nanomaterials studied are single-component systems, and their conversion efficiencies are too low for practical application. In addition, these nanoparticles often suffer from instability due to light-induced anodic oxidation in aqueous solutions. Hybrid nanostructures composed of core/shell nanoparticles may have effectively separated charges and catalytic sites for enhanced conversion and also possess good stability at relevant conditions.

The core/shell nanoparticles contain a semiconductor core and a metal oxide shell, linked to a nanoparticle catalyst. An example is ZnTe/ZnO core/shell linked to Pt. The core/shell nanostructure serves for initial photo-induced charge separation, while the metallic component provides catalytic sites for subsequent chemical conversion. We will take the advantage of high reducing ability of photo-generated electrons in the semiconductor core to produce high hydrocarbons (e.g., ethylene & propylene) in high yields. Coating the nanoparticle surface with a metal oxide shell not only protects the nanoparticle from dissolution during the photoreaction, but also facilitates charge separation by forming a barrier for controlled back electron transfer.

The project involves controllable synthesis of hybrid nanostructures with wet-chemical methods, followed by characterization of their structures, morphology and compositions using XRD, SEM, and TEM. The charge separation and transfer properties will be measured by transient visible-pump/visible probe and EPR spectroscopes, and photoreduction of CO2 with a photoelectrochemical system. Thermodynamic stability will be determined using high-temperature calorimetry. The goal is to determine the synthesis-structure-property-stability relations, which will then be fed back to the design of new nanostructures with enhanced properties and stability.

Benefit to National Security Missions

This project represents a research topic with great scientific value and tremendous potential for technological applications. Through controllable synthesis and systematic characterization of core/shell nanomaterials, the research is expected to lead to design and development of a novel class of hybrid nanostructures for efficient photocatalytic conversion of carbon dioxide plus water into hydrocarbon fuels and chemicals. The synthesis-structure-property-stability relationship to be determined in this research will lay the foundation for the ultimate development of solar-to-fuel conversion devices and have broad implications for rational design of functional materials in general. This project is tied to missions in DOE office of science, fossil energy and renewable energy as well as NSF, and to LANL's Materials Grand Challenge in the central themes of defects/interfaces and emergent phenomena.

Progress

No progress at the time of data sheet request. The postdoc is scheduled to hired on July 1, 2013.

Future Work

During the first year of this project, we will design, synthesize and characterize several hybrid nanostructures of photoactive materials that have both effective charge separation and high photo-driven reductive properties for efficient photocatalytic CO2-to-hydrocarbon conversion. Our synthesis includes three steps: 1) A wet-chemical synthetic approach will be employed to prepare ZnTe nanoparticles with various sizes, shapes and structures; 2) A layer of ZnO or TiO2 will be coated on the surface of

ZnTe nanoparticles to form core/shell structures through chemical methods; and 3) The core/shell nanostructures will be linked to Pt or RuOx catalytic nanoparticles through a successive growth approach. The structure, morphology and composition of the obtained nanostructures will be characterized using powder X-ray diffraction, scanning and transmission electron microscopy. Transient absorption spectroscopy will be used to measure their charge separation and transfer properties. Thermodynamic analysis will be conducted using high-temperature solution calorimetry and/or differential scanning calorimetry. The obtained results will allow revelation of the synthesis-structure-property-stability relationship, which will then be fed back to the design of new hybrid nanostructures with enhanced photocatalytic properties and stability.

Conclusion

Successful execution of this research will lead to design and development of a novel class of hybrid nanostructures for efficient photocatalytic conversion of carbon dioxide plus water into hydrocarbon fuels and chemicals. Through controllable synthesis and systematic characterization of the core/shell nanostructures, we will determine the synthesis-structure-property-stability relationship for this family of nanomaterials, which have implications for rational design of functional materials in general. The obtained results will lay the foundation for development of solar-to-fuel conversion devices and directly address LANL/DOE's grand challenges in energy and environmental materials research.

Alternating Positive-negative Charge Systems: New Compounds and Synthetic Routes

David E. Chavez
20130788PRD2

Introduction

This project will focus on the development of alternating charge molecules for energetic materials applications. These alternating charge molecules are predicted to have very promising energetic material performances properties, and may have very interesting safety properties. There exists a paucity of examples of these types of materials described in the literature, and therefore the basic scientific understanding and principles for synthesizing these materials required. The materials will be very challenging to construct, however, due to their predicted performance properties, there is high potential for opening up a new area of research in the area of energetic materials.

Benefit to National Security Missions

The project focuses on the development of novel energetic materials with unprecedented performance, and potentially, safety. This topic is directly relevant to NNSA defense programs, science campaign 2 and to the DoD. Because the project will develop a fundamental understanding of the proposed materials, it will have a direct impact on expanding fundamental chemistry concepts.

Progress

This project started in September 2013; therefore, there is no progress to date.

Future Work

The project will begin with the synthesis of novel tetrazine dioxides. The chemistry and synthetics routes to these materials will be the focus of the first year of the project. The tasks for the first fiscal year include:

- Propose two new tetrazine dioxide molecules for study
- Perform predictive modeling calculations on these materials
- Propose synthetic routes to the materials
- Attempt synthesis of compound 1
- If synthesis is successful, characterize compound 1
- Attempt synthesis of compound 2
- If synthesis is successful, characterize compound 2

Conclusion

While the high thermal stability of APNC systems is known, little is known about their mechanical sensitivities and the other molecular features affecting same. A fundamental understanding of these properties must be developed in order to design explosives of high performance and stability. The potentially unprecedented energetic performances of compounds of these types would lead to revolutionary effects in energetic systems as a result of higher energetic yields from smaller-sized devices, as well as new fundamental insights into factors affecting molecular stability.

Graphene Quantum Dots for Carrier-multiplication-enhanced Solar Cells

Victor I. Klimov
20130790PRD2

Introduction

Quantum dots (QDs) are nanometer-sized crystals of semiconductors that offer many unique optical and electronic properties of great interest to use in solar cells. One such property is high-efficiency carrier multiplication (CM) whereby absorption of a single photon produces multiple electron-hole pairs, potentially increasing the current produced in solar cells. To date, the measured efficiencies of CM in inorganic QDs are not high enough to impact the power output of real devices. In this project, we will explore the potential of graphene-based nanomaterials.

Graphene is a very strong absorber of light, and is highly conductive. Furthermore, recent theoretical calculations have shown that CM yields in graphene can greatly exceed those in inorganic solids. However, ordinary graphene cannot serve as an absorber in a solar cell, because it is a "semimetal" that has no band gap, which means it cannot produce a voltage in a device. However, it is possible to open the band gap by introducing confinement effects similar to those found in inorganic QDs, by making nanometer-sized graphene pieces, or graphene-QDs.

Although the production of ordinary graphene is a rapidly developing field, the exploration of graphene-QDs is in its relative infancy. Our effort will start with existing techniques for making graphene, and modify them for the production of graphene-QDs, which will allow us to perform the first high-level spectroscopic studies of these unique materials, including especially the first measurements of CM efficiencies. Correlating CM yields with the structure of the graphene-QDs will allow us to optimize the material by further modifying the growth conditions, with the goal of approaching the theoretically predicted record efficiencies.

Finally, we will explore the application of this material in proof-of-principle PV devices. By validating the promise of graphene-based nanostructures, this project may lead to a paradigm shift in research on advanced CM-based solar cells.

Benefit to National Security Missions

This work is a fundamental study of a relatively new material class that has been predicted to have properties of great relevance to optoelectronic devices in general, and solar cells in particular. Specifically, we will produce and study nanometer-sized pieces of graphene. Graphene is a form of carbon consisting of individual sheets of graphitic carbon. Interest in graphene for use in electronic devices has exploded over the past decade, but studies of nano-graphene pieces, or graphene quantum dots (in which the effects of quantum-confinement will produce very different properties) are still only at the starting point. Our focus will be on studying and optimizing those properties of nano-graphene of direct relevance to applications in solar energy capture and energy efficient solid-state lighting. In this way, our work is directly tied to the LANL Science Mission in the Basic Understanding of Materials, and in the process will involve exploration of Fundamental Chemistry. As the work progresses into producing graphene devices, it will directly add to progress in the LANL Energy Security Mission, particularly in the area of Renewable Energy. As such, it will be of primary interest to various offices within DOE, including especially the Office of Science. It can also be anticipated that research into combining nano-graphene with other types of quantum dots will lead to new phenomena of relevance to other types of devices, including in biosensing and radiation detection. Thus, there may be long-term benefits to LANL efforts and eventually to federal funding agencies in these areas.

Progress

This project will commence when the Oppenheimer Fellow, Dr. Shaojun Guo, is hired on July 15, 2013.

Future Work

This project will commence when the Oppenheimer Fellow, Dr. Shaojun Guo, is hired on July 15. The remaining three months of Fiscal Year 2013 will be devoted to establishing the grahene-production capability. This is a completely new activity for the Nanotechnology and Advanced Spectroscopy (NanoTech) Team, and thus will take some amount of time, and a great deal of Dr. Guo's effort and ingenuity to accomplish. It will involve Dr. Guo completing his relevant LANL training, working with Drs. Klimov and Pietryga (as mentors) to establish the proper Integrated Work Management (IWM) envelope for this work to proceed safely and securely, and constructing the necessary apparatus through leveraging of existing equipment and some small purchases. Project Year 1 will then also include the first three quarters of Fiscal Year 2014, during which Dr. Guo will optimize the graphene production apparatus to achieve materials with reproducibly high quality, and start to modify his techniques to produce nanometer-sized pieces of graphene (the graphene quantum dots, or graphene-QDs). At this point, he will begin to interact with spectroscopists on the Nanotech team to determine the most promising means for measuring the carrier dynamics in excited graphene-QDs, including for establishing the efficiency of carrier multiplication in these materials. As the materials production progresses, Dr. Guo will also keep all the members of the NanoTech Team apprised of developments through participation in weekly Team meetings, continuously looking for opportunities to use these materials in other studies.

Conclusion

We will adapt existing graphene fabrication techniques to produce high-quality graphene quantum dots. We will then perform high-level spectroscopic study of these materials, including the first measurements of graphene-based "carrier multiplication" (CM), a phenomenon known in other quantum dots in which a single photon produces more than one electron-hole pair. With spectroscopic feedback, we will optimize the fabrication techniques further to achieve materials with the highest CM efficiencies. Finally, we will fabricate "proof-of-principle" solar cells, based on graphene quantum dots, to demonstrate that CM can have a measureable impact on the power output of real devices, a potentially field-changing revelation.

Microstructured Biohybrid Synthesis of Photosynthetic Assemblies

Gabriel A. Montano
20130796PRD2

Introduction

Photosynthesis ubiquitously occurs in membranes. These lipid bilayers can be among the most crowded interfaces in nature with up to ~70% of the total available area occupied by proteins. Further, the effective concentration of photosynthetic pigments can be as high as 1 molar. Despite this, photosynthetic charge separation proceeds with unprecedented quantum efficiencies that approach unity due to a high level of two- and three-dimensional organization. The energetics of the reaction is sufficient to oxidize water and drive cellular processes that ultimately reduce CO2 into carbohydrates. How do these organisms capture the energy of light with such high efficiencies but more importantly, how can the design principles be exploited? While the former question has been investigated over the past decades, the latter has been relatively unexplored.

Utilizing soft materials capabilities developed by our team along with micro- and nano-patterning technologies at CINT we will investigate programmed organization of photosynthetic assemblies into two- and three-dimensional asssemblies. We will investigate parameters effecting biohybrid assembly such as packing density, distance and orientation of light-harvesting (LH) and reaction center (RC) complexes and optimize the biophysical phenomena of energy transfer and charge separation in robust, long-life assemblies.

The ability to intricately organize and design biohybrid photosynthetic systems would have transformative impact across multiple fields. In the proposed research, controlled assembly of photosynthetic complexes would allow for more efficient light harvesting into the system while also elucidating the spatial parameters required for optimal assembly functionality. Lastly, the approaches described here can be extended any variety of biomolecule (other proteins, DNA etc.) opening up additional applications in bio-sensors, -materials and research platforms.

Benefit to National Security Missions

The work to be performed directly addresses needs within DOE and energy-related efforts and fundamental biomaterials research design. Success of the proposed work will result in necessary information in order to develop a new class of energetic materials capable of achieving a long-standing goal: harnessing the energy of the sun with the efficiency of natural photosynthetic assemblies and the stability of standard photovoltaics. Secondarily, optimizing the bio/synthetic interface will have an impact far beyond energy science effecting arenas such as bio/chemical materials development and detection, sensor and prosthetic development and environmental remediation. Thus, the proposed research will generate opportunities within the confines of DOE as well as provide avenues for development within agencies such as DOD, IC, NIH and potentially more.

Progress

The project started in August 2013; therefore, there is no progress to date.

Future Work

Growth of green and purple bacteria for harvesting of individual photosynthetic components.

- Requires initial cell culture growth
- Requires isolation and purification of individual photosynthetic components
- Design of artificial LH/RC complexes using polymer/lipid and porphyrin based supramolecular assembly
- Development of initial 2D and 3D assemblies for characterization
- Requires demonstration of isolated photosynthetic assemblies and artificial photosynthetic assemblies into soft materials architectures
- Characterization of photosynthetic assemblies- i.e. stability, performance, communication (energy transfer, charge separation)

- Begin refinement of architectures to enhance stability/ performance
- Begin expression and growth of modified LH

Conclusion

The specific aims of this project are to: 1) Genetically engineer photosynthetic proteins and potentially bio-inspired artificial photosynthetic contructs for programmed assembly onto functionalized and patterned 2D and 3D architectures; 2) Investigate parameters effecting the optimization of biohybrid assembly e.g. packing density, distance and orientation of light-harvesting and reaction center photosynthetic complexes; 3) Systematically explore and optimize the biophysical phenomena of energy transfer/charge transfer in assemblies using an iterative design strategy. Results will have a tremendous impact in artificial photosynthesis, energy applications and biohybrid design.

Photoactive Energetic Materials for Quantum Optical Control

Sergei Tretiak
20130804PRD3

Introduction

The project will involve the development of a combined quantum mechanical and molecular mechanical (QM/MM) approach to characterize the dynamics of energy localization, chemical bond activation, and chemical reaction of photoactive energetic materials. Programmatic needs exist for the development of emergent technology that can address future requirements for enhanced safety and security of the nuclear stockpile. For example, laser-based ignition of insensitive explosive materials would provide tremendous improvements in detonator safety.

Benefit to National Security Missions

The proposed research aligns closely with national security missions of the Laboratory, in particular, high explosives science, detonator technologies, and Life Extension Programs (LEPs) addressing stockpile safety and security issues.

Progress

The project started July 2013; therefore, there is no progress to date.

Future Work

Methodology

I plan to develop a combined quantum mechanical and molecular mechanical (QM/MM) approach to treat large systems and include solvent and thermal bath effects. Our current NA-ESMD implementation only allows for phenomenological treatment of the thermal bath. QM/MM is a much more accurate approach in which a system is divided into a quantum mechanical region and a molecular mechanical region allowing realistic modeling of dielectric media. Depending on the molecular system, different force fields will be interfaced with our existing NA-ESMD code.

Applications

By concerted experimental and theoretical characterization of the dynamics of energy localization, chemical bond activation, and chemical reaction, insight can be gained on how to manipulate electronic structure through synthesis in order to design photoactive energetic materials with controllable optical functionality.

I plan to identify specific vibrational degrees of freedom responsible for bond breakage, rapid decomposition, and the onset of the exothermic chain reactions relevant to explosive initiation processes in the surrounding material. The developed methodology will be used to design and propose controllable materials. I will perform detailed numerical NA-ESMD simulations to investigate photoinduced pathways, timescales, branching effects, and multiple product formation, which can be experimentally validated by ultrafast spectroscopy capabilities in WX-9. I will assess possible photoinduced reaction coordinates and electron-vibrational relaxation pathways to elucidate mechanisms for optical initiation. I plan to use first principle electronic structure calculations to quantitatively evaluate the nonlinear optical responses to understand excited-state properties and to provide design strategy for new photoactive energetic materials.

Conclusion

The research will extend simulations of the excited state dynamics to the solid state using Quantum Mechanics/Molecular Mechanics (QM/MM) framework. In addition to the myriad of basic science applications, this approach will be used to model photoexcitation dynamics of energetic materials. This research will be tightly coupled with ongoing spectroscopic studies, aiming to establish a theory-guided strategy to design photoactive energetic materials with controllable optical functionality.

Poly-triphenylamine-functionalized Graphene Quantum Dots for Flexible High-Performance Polymeric Memory Devices

Hsing-Lin Wang
20130806PRD3

Introduction

The main focus of this project is to develop synthetic strategies for making graphene quantum dots (GQDs)- a small piece of grapheme with well defined molecular structure. These as-synthesized GQDs are highly processible and can be incorporated with poly(triphenyl amine), PTPA, to render memory and energy devices. The synthesis of PTPA-GQDs and their incorporation in memory and energy devices has never been attempted. The challenge of this project lies in the fact that the organic synthetic scheme for PTPA-GQD requires more than 20 steps. This is an extremely costly and time consuming process.

Although synthesis of simple GQDs have been demonstrated, synthesis of PTPA-GQD remains a challenge and the final yield of this compound may be low, which could impede us from developing application using this materials. Therefore, our challenges are not only in the synthesis of PTPA-GQDs, but also to find ways to increase the yield of the final product.

We expect the as-prepared PTPA-GQD will reveal excellent memory properties. In addition, polymer memory devices have potential to be flexible and easily integrated with conventional devices to show added value and complexity. The PTPA-GQD will also be tested as energy and sensing devices. Success in demonstrating derivatized GQD in the above devices could have intellectual property value and warrants publications in high impact journals.

Benefit to National Security Missions

Success of this project will lead to the development of one or several stable, high performance electronic, memory and energy devices. Success of this project will have immediate commercial application and add to the scientific knowledge of the interface between materials, and nanotechnology crucial to the lab mission for renewable energy and threat reduction. Unlocking the structural features and charge transfer mechanisms will allow design and synthesis of next generation memory and energy devices. The proposed work is in alignment with the central DOE missions and supports new program development in Office of Science, DTRA, and DARPA.

Progress

The project started August 2013; therefore, there is no progress to date.

Future Work

In the next fiscal year, we will focus on the synthesis of highly processible graphene quantum dots. Our design synthesis of graphene quantum dots employing multi-step organic synthesis using Suzuki coupling reactions will led to polyphenylene dendritic precursor containing triphenyl amine group, which will then be exposed to an excess of $FeCl_3$ in a dichloromethane/nitromethane mixture, yielding the polytriphenylamine-based graphene quantum dot (PTPA-GQD). The covalently bound TPA-GQD will be thoroughly characterized by X-ray photoelectron spectroscopy, MALDI-TOF MS, NMR, and IR spectroscopy.

Conclusion

We expect to achieve synthesis of processible grapheme quantum dots (GQDs). We expect the as-prepared PTPA-GQD will reveal excellent memory properties. In addition, polymer memory devices have the potential to be flexible and easily integrated with conventional devices to show added value and complexity. The PTPA-GQD will be used as a memory layer and fabricated on plastic poly(ethylene naphthalate) (PEN) substrates in a cross-point structure. We expect to demonstrate the reliable and reproducible performance of sandwiched PEN/Al/PTPA-GQD/Al memory devices; the performance characteristics will be analyzed statistically and under bending stress.

Publications

Chen, C., H. Yen, Y. Hu, and G. Liou. Novel Programmable Functional Polyimides: Preparation, Demonstrating Mechanism of CT Induced Memory, and Ambipolar Electrochromic Behavior. 2013. J. Mater. Chem. CJ. Mater. Chem. C.

Chou, Y., H. Yen, C. Tsai, W. Lee, G. Liou, and W. Chen. Nonvolatile transistor memory devices using high dielectric constant polyimide electrets. 2013. J. Mater. Chem. CJ. Mater. Chem. C. 1 (19): 3235.

Yen, H., J. Wu, W. Wang, and G. Liou. High-Efficiency Photoluminescence Wholly Aromatic Triarylamine-based Polyimide Nanofiber with Aggregation-Induced Emission Enhancement. 2013. Advanced Optical MaterialsAdvanced Optical Materials. 1 (9): 668–676.

Understanding and Controlling Magnetism in Multiferroics with THz Pulses

Rohit P. Prasankumar
20130812PRD3

Introduction

In ferromagnets, the magnetization can be controlled with an external magnetic field, an idea widely used, for example, in magnetic data storage. However, magnetic fields have some drawbacks: there are limitations to how fast they can be switched, they are inconvenient to use, and they consume extra energy. Much effort has thus been devoted to multiferroic materials, in which electric and magnetic polarizations exist simultaneously and can be coupled, enabling control of magnetism with an electric field.

Recently, there have been significant advances in the ability to synthesize these materials, which has led to much effort focused on increasing the magnetoelectric (ME) coupling, especially near room temperature. However, the microscopic origin of this coupling can vary across different classes of materials, and is not well understood. Low energy excitations (i.e. soft modes, magnons, etc.) are thought to play a key role in ME coupling, and therefore also offer a promising route to controlling it.

Here, we will use ultrashort optical and terahertz (THz) pulses to shed light on the microscopic origin of magnetoelectric coupling in different multiferroic materials (building on our previous work in this area). In these experiments, we will use these pulses to separately manipulate and probe the magnetic and electric orders in a given material, enabling us to, e.g., modify the magnetic order and probe the resulting changes in ferroelectric order, or vice versa. This will provide much insight into magnetoelectric coupling in multiferroics, which should extend our knowledge of their basic physics and also enable researchers to optimize them for applications.

Benefit to National Security Missions

The proposed experiments will provide LANL, as well as CINT, with the capability to investigate magnetoelectric coupling in multiferroic materials through selectively exciting the low-energy modes responsible for material functionality and probing their effects on this coupling. More generally, our effort to interface materials science with ultrafast terahertz (THz) and optical probes represents an essential element in the MaRIE strategy that connects the M4 facility to the Multi-Probe Diagnostic Hall. This work directly addresses the LDRD Grand Challenge in Materials, which underpins all three Laboratory mission areas. It also addresses several of the Grand Challenges for Basic Energy Sciences identified by the DOE Office of Science. We will work with the Program Director for Basic Energy Sciences to explore future funding opportunities within BES in the growing areas of ultrafast materials science.

Progress

Project started September 2013; therefore, there is no progress to date.

Future Work

Building on our previous work in this field, we will begin by optimizing our existing ultrafast optical and terahertz (THz) systems for the proposed experiments, with a particular focus on generating high energy mid-to-far-infrared pulses for photoexciting low energy modes in multiferroics. Our initial focus will be on the canonical multiferroic material, $BiFeO_3$ (BFO), which has attracted much interest due to its room temperature coexistence of magnetic and ferroelectric order, and the manganite $TbMnO_3$ (TMO), which is well known for its strong magnetoelectric (ME) coupling, albeit at low temperatures. We will also examine multiferroic heterostructures, consisting of thin ferroelectric and magnetic films grown on top of one another to maximize the coupling between them.

We will explore several experimental directions. In general, we will use these pulses to separately manipulate and probe the magnetic and electric orders in a given

material, enabling us to, e.g., modify the magnetic order and probe the resulting changes in ferroelectric order, or vice versa. This can shed light on ME coupling in the materials described above. For example, in BFO, an important unresolved question is whether the soft mode phonon drives the ferroelectric (FE) transition, and how this links to ME coupling. We can address this by photoexciting this mode and monitoring the resulting changes in the FE and magnetic order with an optical probe pulse. Similarly, in TMO, we can test a recent theoretical prediction by using intense THz pulses to photoexcite low energy modes, potentially enabling us to control magnetic order. Finally, in a multiferroic heterostructure, we can photoexcite low energy modes in a ferroelectric (FE) layer and examine the effect on ferromagnetic order in a proximal magnetic layer. These experiments should thus provide much insight into ME coupling in multiferroics, with wide ranging impact in physics and materials science.

Conclusion

Multiferroic materials, in which magnetic and ferroelectric order can be closely coupled, offer much promise for a variety of applications in data storage, novel logic elements, and sensing. However, the mechanisms underlying this coupling are not well understood, limiting the potential of these materials. Here, we will use ultrashort optical and terahertz (THz) pulses to shed light on the microscopic origin of magnetoelectric coupling in different multiferroic materials. This will provide much insight into magnetoelectric coupling in multiferroics, which should extend our knowledge of their basic physics and also enable researchers to optimize them for applications.

Environmental and Biological Sciences

Dynamic Earthquake Triggering, Granular Physics and Earthquake Forecasting: Determining the Physical Controls

Paul A. Johnson
20120007DR

Introduction

The March 11, 2011 M9.0 Tohoku-oki Earthquake, located ~100 km off the east cost of Honshu, was the fourth largest earthquake in recorded history, rupturing a 300 km segment of the plate boundary. The earthquake was due to ongoing subduction of oceanic crust beneath Japan. The slip magnitude between the two plates was 30-40 meters resulting in abrupt uplift of the seafloor, creating a tsunami that inundated port cities in eastern Honshu. A resultant nuclear disaster continues to unfold at nuclear power plants located in Fukushima. Despite the relatively sparse population in this region, the resulting economic losses are predicted to be about 4% of Japan's GDP.

An earthquake of M8-9 in a densely populated region such as Seattle could have catastrophic effects on the US. Prior warning of increased earthquake probability during a specific time interval could significantly mitigate the potential economic disaster.It has recently been postulated that a majority of earthquakes may be dynamically triggered. Our unique perspective is that characterizing triggering leads to fundamentally new means of earthquake forecasting of intervals of increased hazard. The Problem: Although earthquake forecasting is a highly complex, unsolved problem, significant advances may be possible in predicting time intervals of increased earthquake hazard. Institutes worldwide including the Working Group on California Earthquake Probabilities (WGCEP) currently do not include dynamic triggering in hazard estimates.

Our hypotheses are: a) Granular physics plays a key role in fault triggering in the laboratory and Earth. b) Isolating the triggering mechanism and characterizing its signatures will improve earthquake hazard analysis by determining the duration of enhanced earthquake probability from triggering.Our project goals are to: a) Characterize the granular physics that we posit enables triggering, b) apply novel statistical approaches to infer increased earthquake risk owing to triggering, and c) bridge laboratory scales to Earth scales.

Benefit to National Security Missions

Large earthquakes pose serious risks to national energy and economic security through their deleterious impacts on infrastructure, a stated LANL mission area. This work could have an enormous societal/infrastructure impact by forecasting times of increased earthquake hazard. Triggering may also have significant import to Ground Based Nuclear Explosion Monitoring (GNEM)—clandestine events could be better hidden in regions of triggered event clustering. Our work will improve understanding of seismic events as well as the exploitation, analysis, and interpretation of faint seismic signatures. The work may have broad application to vibration-induced failure in materials, including those relevant to the weapons program, aircraft, industrial machinery, and shaking of infrastructure from strong ground motion. This work will contribute to hazards analysis at LANL (CMRR). Moreover the work improves interdisciplinary capabilities at LANL by integrating efforts in seismology, geophysics, granular media, and continuum elastic-plastic deformation that are underpinning science for a diverse set of LANL priorities including MaRIE. We note the large costs to NNSA and nuclear power infrastructure that are driven by seismic requirements, particularly the largest credible events, which imply a need to quantify worst-case scenarios better than existing science can do.

Progress

We have made significant progress toward our stated goals of characterizing the effects of seismic waves on a fault system, with the ultimate goal of characterizing periods of increased earthquake hazard. We have placed significant effort into the question of whether or not large earthquakes cluster globally, meaning one earthquake may trigger another. In short, our work shows

tantalizing suggestion of clustering of large earthquakes; however, as the earthquake catalog of large events is so limited the statistical confidence in this result is limited. One paper has been published on our analysis and the other is in press. We are now considering other statistical means by which to test for global clustering, applying very small amounts of earthquake data.

We have also been developing the means to characterize hypothesized seismic-induced perturbation of the material in regions of active faulting. We believe that this perturbation leads to the periods of increased seismic hazard. Our work has been at the Parkfield segment of the San Andreas Fault, as stated in the proposed work, and also in Japan using their extremely good network of borehole stations. To date, we can state that there appears to be widespread changes in Japan seismicity due to the recent Indian Ocean earthquake of 2012, strongly suggesting earthquake triggering and long lasting elastic effects. Currently we are also, (i) looking at Global Positioning System (GPS) data that can be applied to see if there is associated earth surface displacement as we predict; (ii) looking for associated seismic wave velocity changes applying what is known as 'passive noise imaging' [the method employs use of ocean-generated noise that can be used for seismic imaging]; and (iii) beginning work on other potential triggering earthquakes such as the Great Chile earthquake (Maule) of 2010. At Parkfield we are developing other statistical methods that we will employ there and elsewhere, to determine if seismicity rates change due to potential triggering earthquakes.

Our supporting laboratory and numerical modeling work is advancing as well. The new shearing experiment meant to simulate earthquakes applying what is known as 'photoelasticity' is now operational and the first data sets are being collected. Photoelasticity allows one to visually observe and interpret changes in the stresses on and off the model fault. Model earthquake triggering studies will begin soon, and we intend to compare these to the numerical simulations that are well advanced. The other laboratory experiment is opaque but is three-dimensional, in contrast to the photoelastic experiment. This experiment is well advanced and we have a number of publications describing results. We are also comparing the results to three-dimensional simulations using the same numerical simulation method and a number of publications have resulted. In short the model and experimental methods are being used to develop methods to characterize shear along faults as well as the effects of earthquake triggering. We can statistically test whether or not the numerical simulations and experiments make sense in the context of real earthquakes, by looking at certain aspects of the laboratory and numerical simulation data that can be tested for scaling to the earth.

We are also studying the processes that lead to instability in the fault 'core' or fault 'gauge' (the ground-up material that lies between fault blocks) induced by seismic waves. These studies include both numerical simulation and laboratory studies as well. From these studies we hope to learn what the causes are for hypothesized long-lived changes in the earth that are due to seismic waves from other earthquakes. This long-lived behavior is responsible for the times of increased earthquake hazard.

We are working progressively more with external institutions that are intrigued by our unique vision and approach. These institutions include Pennsylvania State University, the United States Geological Survey, ETH Zurich (Switzerland), Bath University (UK), The 'Ecole Normal' and the Institute of Physics of the Globe in Paris (France), the University of Tokyo, Sendai University (Japan) and the University of Grenoble (France).

In summary, we are using a multi-pronged approach that includes seismic and other observations in the earth, laboratory and numerical modeling studies, to address the earthquake triggering/earthquake hazard problem. We are certain to make tremendous progress on this problem over the remaining period of time we have.

Future Work

Our goals for next year are, (1) to establish whether or not large earthquakes trigger large earthquakes worldwide (preliminary work suggests that the answer is yes) and if so, begin establishing a new model of how earthquakes occur globally; (2) to begin work on what the implications of such a conclusion may have on evaluating earthquake hazard; (3) to determine if mechanical property changes take place from seismic waves from distant earthquakes and to establish methods for monitoring such changes. A major task for the next fiscal year includes statistical analyses of earthquake catalogs to address the global triggering question. A second task is honing our skills at the Parkfield section of the San Andreas Fault (the Parkfield laboratory) in regards to determining if seismic waves from near and distant earthquakes perturb the mechanical properties of the fault region, and if so, for what time duration. Methods to be considered include using the interval between earthquakes in the perturbed region that should change in their frequency for a period of time after perturbation based on laboratory and simulation studies. A second method is monitoring velocity change in the perturbed region applying a number of approaches, including monitoring passive earth noise that can be applied to extract velocity changes

in the earth's crust. We will support the Parkfield studies with laboratory experiments and discrete element modeling.

Conclusion

Our goal is to determine intervals of increased earthquake hazard in regions of high earthquake risk. In particular, seismic considerations play large in the siting of energy and weapons complex infrastructure. By further delineating the time interval of increased hazard, local, regional and national hazard response officials could take appropriate precautions in order to mitigate casualties and to address pressing infrastructure issues. Further, our work will have an enormous impact on characterizing the physics of sheared granular media and how these materials transition from locked, or jammed, to fluidized via nonlinear dynamics, a topic that we are currently advancing.

Publications

Ben-Naim, E., E. G. Daub, and P. A. Johnson. Recurrence statistics of great earthquakes. 2013. GEOPHYSICAL RESEARCH LETTERS. 40 (12): 3021.

Ben-Naim, E., and P. L. Krapivsky. Statistics of superior records. 2013. PHYSICAL REVIEW E. 88 (2): -.

Daub, E., D. Shelly, R. Guyer, and P. Johnson. Brittle and ductile friction and the physics of tectonic tremor. 2011. Geophysical Research Letters. 38 (10): L10301.

Daub, E., E. Ben-Naim, R. Guyer, and P. Johnson. Are megaquakes clustered?. 2012. Geophysical Research Letters. 39 (6): L06308.

Elst, N. J. van der, E. E. Brodsky, P. Y. Le Bas, and P. A. Johnson. Auto-acoustic compaction in steady shear flows: Experimental evidence for suppression of shear dilatancy by internal acoustic vibration. 2012. JOURNAL OF GEOPHYSICAL RESEARCH-SOLID EARTH. 117: -.

Ferdowski, B., M. Griffa, R. A. Guyer, P. A. Johnson, C. Marone, and J. Carmeliet. Microslips as precursors of large slip events in the stick-slip dynamics of sheared granular layers: A discrete element model analysis. 2013. Geophysical Research Letters. 40 (16): 4194.

Ferdowski, B., M. Griffa, R. A. Guyer, P. A. Johnson, C. Marone, and J. Carmeliet. 3D Discrete Element Modeling of triggered slip in sheared granular media. Physical Review E.

Ferdowski, B., M. Griffa, R. A. Guyer, P. A. Johnson, and J. Carmeliet. Effect of boundary vibration on the frictional behavior of a dense granular layer. To appear in Acta Mechanica.

Gomberg, J.. Permanently enhanced dynamic triggering probabilities as evidenced by two M>7.5 earthquakes. 2013. Geophysical Research Letters. 40: L50933.

Gong, X., Q. Chen, Z. Peng, W. Wang, C. Wu, and J. Wu. Remotely triggered seismicity around the Fangshan Pluton near Beijing following the 2010 Mw 8.8 Chile earthquake. To appear in Chinese Journal of Geophysics.

Griffa, M., B. Ferdowsi, E. Daub, R. Guyer, P. A. Johnson, C. Marone, and J. Carmeliet. Meso-mechanical analysis of deformation characteristics for dynamically triggered slip in granular materials. 2012. Philosophical Magazine. : 1.

Griffa, M., B. Ferdowsi, R. A. Guyer, E. G. Daub, P. A. Johnson, C. Marone, and J. Carmeliet. Influence of vibration amplitude on dynamic triggering of slip in sheared granular layers. 2013. PHYSICAL REVIEW E. 87 (1): -.

Griffa, M., E. G. Daub, R. A. Guyer, P. A. Johnson, C. Marone, and J. Carmeliet. Vibration-induced slip in Sheared Granular Layers and the Micromechanics of Dynamic Earthquake Triggering. 2011. Europhysics Letters. 96 (1): 14001 (6 pp.).

Johnson, P.. Nonlinear acoustic/seismic waves in earthquake processes. 2012. In Nonlinear Acoustics State-of-the-art and Perspectives: 19th International Symposium on Nonlinear Acoustics ; 21-24 May 2012 ; Tokyo, Japan. Vol. 1474, p. 39.

Johnson, P. A., B. Carpenter, M. Knuth, B. M. Kaproth, P. -Y. Le Bas, E. G. Daub, and C. Marone. Nonlinear dynamical triggering of slow slip on simulated earthquake faults with implications to Earth. 2012. JOURNAL OF GEOPHYSICAL RESEARCH-SOLID EARTH. 117: B04310.

Johnson, P. A., B. Ferdowski, B. Kaproth, M. Scuderi, M. Griffa, J. Carmeliet, R. A. Guyer, P. Y. L. Bas, D. T. Trugman, and C. Marone. Acoustic emission and microslip precursors to stick-slip failure in sheared granular material. To appear in Geophysical Research Letters.

Miller, P. W., and E. Ben-Naim. Scaling exponent for incremental records. To appear in Journal of Statistical Mechanics.

Trugman, D. T., E. G. Daub, R. A. Guyer, and P. A. Johnson. Modeling dynamic triggering of tectonic tremor using a brittle-ductile friction model. 2013. Geophysical Research Letters. 40: L50981.

Wu, C. Q., D. R. Shelly, J. Gomberg, Z. G. Peng, and P. Johnson. Long-term changes of earthquake inter-event times and low-frequency earthquake recurrence in central California. 2013. EARTH AND PLANETARY SCIENCE LETTERS. 368: 144.

Wu, C., J. Gomberg, E. Ben-Naim, and P. Johnson. Testing

delayed triggering of repeating earthquakes in central California. Geophysical Research Letters.

Wu, C., X. Meng, Z. Peng, and Y. Ben-Zion. Lack of spatio-temporal localization of foreshocks before the 1999 Mw 7.1 Duzce, Turkey earthquake. To appear in Bulletin of the Seismological Society of America.

Wu, J., Z. G. Peng, W. J. Wang, X. Gong, Q. F. Chen, and C. Q. Wu. Comparisons of dynamic triggering near Beijing, China following recent large earthquakes in Sumatra. 2012. GEOPHYSICAL RESEARCH LETTERS. 39: -.

Predicting Climate Impacts and Feedbacks in the Terrestrial Arctic

Scott L. Painter
20120068DR

Introduction
We will address one of the most critical questions in contemporary climate science: will a warming terrestrial Arctic provide a net positive or negative feedback to the climate system? The Arctic region has been a global carbon sink for thousands of years and is currently the largest terrestrial store of carbon, but is now warming faster than the rest of the Earth. The scientific community cannot say how much Arctic carbon will thaw, decompose into greenhouse gases (GHG), and be released to the atmosphere or how fast it will happen because current modeling tools lack a critical process cascade: thaw-induced subsidence, reorganization of topography and drainage networks, and resulting redistribution of soil moisture. We propose to address this uncertainty by leveraging recent computational advances to develop a novel Arctic Terrestrial Simulator (ATS) that will incorporate for the first time the complex interactions among thermal, mechanical and hydrologic permafrost processes that control GHG production and sequestration in a thawing and topographically reorganizing landscape. Our overarching goals are to 1) provide the first reliable quantitative estimates of GHG releases and uptake from a warming Arctic landscape undergoing rapid topographic reorganization, and 2) provide critical new capabilities to further understand and refine predictions of GHG releases from the Arctic landscape.

Benefit to National Security Missions

Our work addresses one of the most significant gaps in the Nation's capability to understand and predict impacts of climate change. The LDRD investment in terrestrial Arctic prediction will fill the last gap in current high latitude high-performance modeling capability by providing high-resolution landscape modeling capability for the Arctic to complement existing ocean, sea ice, ice sheet and atmosphere predictive capability.

Progress

The Arctic Terrestrial Simulator (ATS) is being developed to provide Arctic process modeling capability within the framework of the highly parallel Amanzi code. Amanzi provides a number of important features for the ATS, including a very general parallel unstructured mesh capability, advanced discretization toolsets for these meshes, and parallel output for modern visualization tools. The hydrological, chemical, and ecological processes relevant to the Arctic tundra models are implemented in ATS in a series of Process Kernels (PKs). In FY2013, development of key PKs progressed significantly. In addition, computational strategies for developing terrain-following unstructured model grids based on available data sources were developed and successfully demonstrated.

A new constitutive model for water partitioning between ice and liquid phases in unsaturated frozen soils was developed and successfully compared to existing laboratory data. The new model forms the basis of the freezing soil hydrology PK, a key component of the permafrost model. A journal article on that work was submitted to the Vadose Zone Journal. A second journal article describing implementation of the freezing soil model was also prepared and submitted. Performance of the freezing soil hydrology PK was improved significantly through the use physics-based preconditioners, and is now sufficient for use in the fully coupled model.

A new and computationally tractable model for overland flow and heat transfer with freezing of ponded water was developed and implemented. Performance of that model was optimized and successfully coupled to the freezing soil model. The coupled model is the core component of a permafrost hydrology model.
Significant progress was made on implementing the computational infrastructure required for modeling deforming Arctic tundra topography.

Characterization of permafrost dominated landscapes is crucial for understanding and predicting the spatial and temporal distribution of climate change related impacts and feedbacks in the Arctic. We developed and evaluated an automated approach to identify and characterize Arctic ice-wedge polygonal tundra landscape components, such as troughs, ponds, river- and lake-like objects, which constitute drainage networks, using high spatial resolution satellite imagery. Identification and characterization of drainage network components is important for tracking Arctic tundra terrain evolution as well as for estimating water, heat and carbon fluxes for use in climate models. A journal article on the approach was prepared and submitted to Remote Sensing Letters.

Simulations to predict the future evolution of Arctic lowland tundra require high-resolution terrain-following computational grids. A computational workflow for generating such grids using available high-resolution digital elevation maps and remote sensing data was developed and successfully demonstrated using data from the Barrow Environmental Observatory.

A global sensitivity analysis for permafrost thawing simulations was conducted to help understand the relative importance of several physical parameters in controlling depth to permafrost. The thermal conductivity, porosity and vegetation characteristics were determined to be the three most important factors contributing to the active layer depth.

Future Work

Work on integrating newly developed thermal hydrologic process models in the Arctic Terrestrial Simulator (ATS) will continue in FY2014. Optimization and fine-tuning of the permafrost thermal hydrology model and the overland flow model, two of the four critical models, were completed in fiscal year 2013. FY2014 model development work will focus on a thaw-subsidence algorithm and a surface energy balance model that includes snow.

We plan to initiate the first fully coupled simulations of tundra evolution including evolving topography in early FY2014. Carbon cycle dynamics will then be added. Our goal is to have completed initial simulations of the future carbon releases from Arctic tundra including the effects of evolving topography by end of FY2014. In parallel with the ATS development and applications, we will continue developing journal articles on our process models and model applications.

Conclusion

Critical processes related to permafrost degradation are not represented explicitly in the current generation of climate models because they cannot be resolved on the scale of a grid cell. The new parallel simulation capability will enable mechanistic process understanding emerging from field studies to be used in a high-resolution predictive framework at appropriate temporal and spatial scales. The Arctic Terrestrial Simulator will be used to model large swaths of the Arctic landscape, resulting in the first projections of carbon release rates from the most vulnerable lowland tundra regions with high carbon stores, rapidly degrading permafrost and evolving landscape.

Publications

Coon, E., M. Berndt, J. D. Moulton, and S. Painter. The Arctic Terrestrial Simulator: Developing a flexible multiphysics simulator based on Amanzi. Presented at 2012 SIAM Annual Meeting . (Minneapolis, 9-13 July 2012).

Frampton, A., G. Destouni, Y. Sjoberg, and S. Painter. Transient modeling of permafrost dynamics in changing climate scenarios. Presented at 2011 Institute of Electrical and Electronics Engineers 7th International Conference on E-Science. (Stockholm, Sweden, 5-8 December).

Frampton, A., S. L. Painter, and G. Destouni. Permafrost degradation and subsurface-flow changes caused by surface warming trends. 2013. HYDROGEOLOGY JOURNAL. 21 (1): 271.

Frampton, A., S. L. Painter, and G. Destouni . Effects of hydrological inputs on the dynamics of permafrost system formation and degradation. Presented at European Geophysical Union General Assembly 2012. (Vienna, Austria , April 7-12, 2012).

Frampton, A., S. Painter, S. W. Lyon, Y. Sjoberg, and G. Destouni. Transient modeling of permafrost dynamics in a changing climate. Presented at American Geophysical Union Fall Meeting. (San Francisco , 5-9 Dec. 2011).

Lewis, K. C., G. A. Zyvoloski, B. Travis, C. Wilson, and J. Rowland. Drainage subsidence associated with Arctic permafrost degradation. 2012. JOURNAL OF GEOPHYSICAL RESEARCH-EARTH SURFACE. 117: -.

Painter, S. L., J. D. Moulton, and C. J. Wilson. Modeling challenges for predicting hydrologic response to degrading permafrost. 2013. HYDROGEOLOGY JOURNAL. 21 (1): 221.

Painter, S. L., S. Karra, and P. C. Lichtner. Three-phase numerical model for subsurface hydrology in permafrost-affected regions. The Cryosphere.

Skurikhin, A. N., C. Gangodagamage, J. C. Rowland, and C. J. Wilson. Arctic tundra ice-wedge landscape characterization by active contours without edges and structural analysis using high-resolution satellite imagery. 2013. Remote Sensing Letters. 4 (11): 1077.

Elucidating Humankind's Evolving Environment: From the Earth's Core to the Cosmos

Harald O. Dogliani
20120166DR

Introduction

This project combine tasks from geology, atmospheric sciences, space sciences, and astrophysics (normally very diverse fields) with the common theme that these fields have an effect on mankind. Earthquakes probably have the most obvious effect on mankind. We will study the acoustical properties of rocks to understand dynamic triggering of seismic slips along major earthquakes zones. To understand volcanoes better, we will model giant explosive eruptions, in particular, the interactions between gas-particulate mixtures and the surrounding rock. Climate change has many drivers and one of the most important is how sea ice in the Arctic interacts with the lower atmosphere. We will build computer models of that interaction to understand the impact of the diminishing southern ice cap. Our lives now depend on satellites and those satellites are susceptible to damage from space radiation. In particular, low earth orbit satellites are affected by the radiation that is determined by the ring current in Earth's magnetosphere. In turn, that ring current is affected by the upper atmosphere. We will produce the first upper atmosphere - ring current computer simulation to learn how to predict the levels of radiation that could affect our satellites. Astrophysics can be a laboratory that can teach us the fundamental nature of the universe. We will model dark energy in the sun to see if there is a way to directly detect it on Earth in laboratories. We will investigate how cosmic strings might be observable in large databases of variations that we see in the brightness of stars.

Benefit to National Security Missions

The basic science that we carry out has a breadth of mission impacts. Our work in climate and geology is related to energy production and understanding the impact of climate change. The research will connect University research in these areas to Los Alamos where they can be applied to our programmatic work. Ring currents in the magnetosphere will be studied under the space science focus and affects the particle background that is directly connected to understating the backgrounds in which non-proliferation measurements are made. The astrophysics research produce techniques to process large image-based data bases that build capability for space situational awareness.

Progress

We have described how pyrocumulus clouds form during intense fires and can lead to previously unexpected rapid spreading of fires. This occurred at a recent Los Alamos area fire.

An analytic program package was developed in support of HAWC, High Altitude Water Cherenkov Experiment, to measure and understand very high energy cosmic rays. Cosmic rays irradiate the earth with a stream of high energy nuclear particles that can effect communications and biological systems. The detector system located in Mexico has achieved initial operating capabilities and successfully mapped a portion of the sky, including where the earth's moon cast a shadow because it blocked cosmic rays from that direction. This is a first time event.

This project created a Web site to encourage the population at-large to report auroral observations, location, time and descriptions. These reports are then used as tip-off to the scientific community to make detailed observations of the phenomenology. Auroras are generally caused by streams of solar charged particles interacting with the earth's magnetic fields and reacting with the upper atmosphere where the tenuous and colorful glows are observed at night. Increased solar and hence auroral activity is relevant to understanding space weather that can have deleterious effects on satellite performance. Los Alamos scientists are studying the role of ocean eddy currents in the establishment of large-scale ocean circulation and climate. Indications are that such eddy

currents can play a significant role in how major currents flow and can have a significant effect on global climate dynamics.

In collaboration with New Mexico Tech, researchers are demonstrating that seismic data can be filtered and processed to detect and quantify the intensity of major oceanic storms by detecting the impact of waves on land-water boundaries. They have detected increased wave activity and storminess in the Southern Pacific North Atlantic. Decreasing secondary microseismic power trends in the Northern Europe and the Arctic may be the result of reduced large-scale storm activity in the Arctic Ocean.

Future Work

We continuously negotiate with researchers specific tasks to improve understanding of catastrophic events: global climate, geoscience, solar system, cosmology and relevant signatures. New task proposals are presently under evaluation for selection to begin in FY14. On going research includes: Descriptions of how rocks and hot gases result in an explosive volcanic events.

Collect data on the transition zone between arctic glacial fields and tundra to understand evolution of natural plant life, how it might survive or be replaced by other more temperate plants. Mathematically describe how ice ridges form on sea ice to improve sea ice/climate computer modeling programs.

Investigate how pyrocumulus clouds form and dissipate - this is a special situation that when it occurs forest fires expand much more rapidly and destroy vast areas well beyond conventional predictions.

Collect detailed data on glacial ice formation and evolution. The purpose is to improve glacial ice computer modeling programs to better predict how glacial warming is affecting global warming. Study Greenland ice core samples to better understand previous climate cycles and compare with main ocean current circulation; major changes of ocean circulation patterns have significant impact on global climate. For example Norway is relatively temperate because of a strong northward Atlantic current bringing warm water up from the more temperate south.

Conclusion

This project will bring together LANL staff with University researchers and students from around the nation to study the structure of the earth, space, and natural climate change. Our study of the underlying physics behind dynamic triggering of seismic and aseismic slip along major earthquakes zones on Earth helps prepare us for such handling events that would affect the entire country. Our modelling of interactions between the upper atmosphere and the Earth's magnetosphere will help predict how our assets in space will survive and function. Studying the possibilities of cosmic strings will probe at the fundamental nature of the Universe.

Publications

Abdo, A. A., A. U. Abeysekara, B. T. Allen, T. Aune, D. Berley, C. Chen, G. E. Christopher, T. DeYoung, B. L. Dingus, R. W. Ellsworth, M. M. Gonzalez, J. A. Goodman, J. Granot, E. Hays, C. M. Hoffman, P. H. Huntemeyer, B. E. Kolterman, J. T. Linnemann, J. E. McEnery, A. I. Mincer, T. Morgan, P. Nemethy, J. Pretz, E. Ramirez-Ruiz, J. M. Ryan, P. M. Parkinson, A. Shoup, G. Sinnis, A. J. Smith, V. Vasileiou, G. P. Walker, D. A. Williams, and G. B. Yodh. Constraints on the emission model of the “naked-eye burst” GRB 080319B. 2012. Astrophysical Journal, Letters. 753 (2): L31 (5 pp.).

Abdo, A. A., B. T. Allen, R. Atkins, T. Aune, W. Benbow, D. Berley, E. Blaufuss, E. Bonamente, J. Bussons, C. Chen, G. E. Christopher, D. G. Coyne, T. DeYoung, B. L. Dingus, D. E. Dorfan, R. W. Ellsworth, A. Falcone, L. Fleysher, R. Fleysher, J. Galbraith-Frew, M. M. Gonzalez, J. A. Goodman, T. J. Haines, E. Hays, C. M. Hoffman, P. H. Huntemeyer, L. A. Kelley, B. E. Kolterman, C. P. Lansdell, J. T. Linnemann, J. McCullough, J. E. McEnery, T. Morgan, A. I. Mincer, M. F. Morales, P. Nemethy, D. Noyes, J. Pretz, J. M. Ryan, F. W. Samuelson, P. M. Parkinson, A. Shoup, G. Sinnis, A. J. Smith, G. W. Sullivan, V. Vasileiou, G. P. Walker, M. Wascko, D. A. Williams, S. Westerhoff, and G. B. Yodh. OBSERVATION AND SPECTRAL MEASUREMENTS OF THE CRAB NEBULA WITH MILAGRO. 2012. ASTROPHYSICAL JOURNAL. 750 (1): 63.

Abdo, A. A., U. Abeysekara, B. T. Allen, T. Aune, D. Berley, E. Bonamente, G. E. Christopher, T. DeYoung, B. L. Dingus, R. W. Ellsworth, J. G. Galbraith-Frew, M. M. Gonzalez, J. A. Goodman, C. M. Hoffman, Hu&uml, C. M. Hui, B. E. Kolterman, J. T. Linnemann, J. E. McEnery, A. I. Mincer, T. Morgan, P. Nemethy, J. Pretz, J. M. Ryan, P. M. Parkinson, A. Shoup, G. Sinnis, A. J. Smith, V. Vasileiou, G. P. Walker, D. A. Williams, and G. B. Yodh. Spectrum and morphology of the two brightest Milagro sources in the Cygnus region: MGRO J2019+37 and MGRO J2031+41. 2012. Astrophysical Journal. 753 (2): 159 (8 pp.).

Abeysekara, A. U., J. A. Aguilar, S. Aguilar, R. Alfaro, E. Almaraz, C. Alvarez, J. de D. Alvarez-Romero, M. Alvarez, R. Arceo, J. C. Arteaga-Velazquez, C. Badillo, A. Barber, B. M. Baughman, N. Bautista-Elivar, E. Belmont, E. Benitez, S. Y. BenZvi, D. Berley, A. Bernal, E. Bonamente, J. Braun, R. Caballero-Lopez, I. Cabrera, A. Carraminana, L. Carrasco, M. Castillo, L. Cham-

bers, R. Conde, P. Condreay, U. Cotti, J. Cotzomi, J. C. D,ÄôOlivo, E. de la Fuente, C. De Leon, S. Delay, D. Delepine, T. DeYoung, L. Diaz, L. Diaz-Cruz, B. L. Dingus, M. A. Duvernois, D. Edmunds, R. W. Ellsworth, B. Fick, D. W. Florino, A. Flandes, N. I. Fraija, A. Galindo, J. L. Garcia-Luna, G. Garcia-Torales, F. Garfias, L. X. Gonzalez, M. M. Gonzalez, J. A. Goodman, V. Grabski, M. Gussert, C. Guzman-Ceron, Z. Hampel-Arias, T. Harris, E. Hays, L. Hernandez-Cervantes, P. H. Huntemeyer, A. Imran, A. Iriarte, J. J. Jimenez, P. Karn, N. Kelley-Hoskins, D. Kieda, R. Langarica, A. Lara, R. Lauer, W. H. Lee, E. C. Linares, J. T. Linnemann, M. Longo, R. Luna-Garcia, H. Martinez, J. Martinez, L. A. Martinez, O. Martinez, J. Martinez-Castro, M. Martos, J. Matthews, J. E. McEnery, G. Medina-Tanco, J. E. Mendoza-Torres, P. A. Miranda-Romagnoli, T. Montaruli, E. Moreno, M. Mostafa, M. Napsuciale, J. Nava, L. Nellen, M. Newbold, R. Noriega-Papaqui, T. Oceguera-Becerra, A. Tapia, V. Orozco, V. Perez, E. G. Perez-Perez, J. S. Perkins, J. Pretz, C. Ramirez, I. Ramirez, D. Rebello, A. Renteria, J. Reyes, D. Rosa-Gonzalez, A. Rosado, J. M. Ryan, J. R. Sacahui, H. Salazar, F. Salesa, A. Sandoval, E. Santos, M. Schneider, A. Shoup, S. Silich, G. Sinnis, A. J. Smith, K. Sparks, W. Springer, F. Suarez, N. Suarez, I. Taboada, A. F. Tellez, G. Tenorio-Tagle, A. Tepe, P. A. Toale, K. Tollefson, I. Torres, T. N. Ukwatta, J. Valdes-Galicia, P. Vanegas, V. Vasileiou, O. Vazquez, X. Vazquez, L. Villasenor, W. Wall, J. S. Walters, D. Warner, S. Westerhoff, I. G. Wisher, J. Wood, G. B. Yodh, D. Zaborov, and A. Zepeda. On the sensitivity of the HAWC observatory to gamma-ray bursts. 2012. ASTROPARTICLE PHYSICS. 35 (10): 641.

Baldridge, S. W., J. Valdes, O. Nedorub, B. Phrampus, M. Cording, L. W. Braile, J. F. Ferguson, and M. Benage. Seismic Investigations of an Accommodation Zone in the Northern Rio Grande Riff, New Mexico. Invited presentation at American Geophysical Conference. (San Francisco, CA, December 13-17, 2010).

Berryman, E. M., J. D. Marshall, T. Rahn, S. P. Cook, and M. Litvak. Adaptation of continuous-flow cavity ring-down spectroscopy for batch analysis of delta C-13 of CO2 and comparison with isotope ratio mass spectrometry. 2011. RAPID COMMUNICATIONS IN MASS SPECTROMETRY. 25 (16): 2355.

Chylek, P., C. Folland, G. Lesins, and M. Dubey. Twentieth century bipolar seesaw of the Arctic and Antarctic surface air temperatures. 2010. Geophysical Research Letters. 37 (8): L08703.

Chylek, P., C. Folland, H. Dijkstra, G. Lesins, and M. Dubey. Ice-core data evidence for a prominent near 20 year time-scale of the Atlantic Multidecadal Oscillation. 2011. GEOPHYSICAL RESEARCH LETTERS. 38: L13704.

Chylek, P., C. Folland, H. Dijkstra, G. Lesins, and M. Dubey. Ice-core data evidence for a prominent near 20 year time-scale of the Atlantic Multidecadal Oscillation. 2011. GEOPHYSICAL RESEARCH LETTERS. 38: L13704.

Chylek, P., C. Folland, L. Frankcombe, H. Dijkstra, G. Lesins, and M. Dubey. Greenland ice core evidence for spatial and temporal variability of the Atlantic Multidecadal Oscillation. 2012. Geophysical Research Letters. 39 (9): L09705.

Chylek, P., C. Folland, L. Frankcombe, H. Dijkstra, G. Lesins, and M. Dubey. Greenland ice core evidence for spatial and temporal variability of the Atlantic Multidecadal Oscillation. 2012. GEOPHYSICAL RESEARCH LETTERS. 39: L09705.

Cowee, M. M., S. P. Gary, H. Y. Wei, R. L. Tokar, and C. T. Russell. An explanation for the lack of ion cyclotron wave generation by pickup ions at Titan: 1-D hybrid simulation results. 2010. JOURNAL OF GEOPHYSICAL RESEARCH-SPACE PHYSICS. 115: A10224.

Cowee, M. M., S. P. Gary, H. Y. Wei, R. L. Tokar, and C. T. Russell. An explanation for the lack of ion cyclotron wave generation by pickup ions at Titan: 1-D hybrid simulation results. 2010. Journal of Geophysical Research - Part A - Space Physics. 115 (A10): A10224 (12 pp.).

Dentz, M., and D. Tartakovsky. Probability density functions for passive scalars dispersed in random velocity fields. 2010. Geophysical Research Letters. 37 (24): L24406.

Dentz, M., and D. Tartakovsky. Probability density functions for passive scalars dispersed in random velocity fields. 2010. GEOPHYSICAL RESEARCH LETTERS. 37: L24406.

English, N., N. McDowell, C. Allen, and C. Mora. The effects of alpha-cellulose extraction and blue-stain fungus on retrospective studies of carbon and oxygen isotope variation in live and dead trees. 2011. Rapid Communications in Mass Spectrometry. 25 (20): 3083.

English, N., N. McDowell, C. Allen, and C. Mora. The effects of alpha-cellulose extraction and blue-stain fungus on retrospective studies of carbon and oxygen isotope variation in live and dead trees. 2011. RAPID COMMUNICATIONS IN MASS SPECTROMETRY. 25 (20): 3083.

Flowers, B. A., H. H. Powers, M. K. Dubey, and N. G. McDowell. Inter-comparison of two high-accuracy fast-response spectroscopic sensors of carbon dioxide: a case study. 2012. ATMOSPHERIC MEASUREMENT TECHNIQUES. 5 (5): 991.

Keeling, R., A. Manning, and M. Dubey. The atmospheric signature of carbon capture and storage. 2011. PHILOSOPHICAL TRANSACTIONS OF THE ROYAL SOCIETY A-MATHEMATICAL PHYSICAL AND ENGINEERING SCIENCES. 369 (1943): 2113.

Levanic, T., M. Cater, and N. McDowell. Associations be-

tween growth, wood anatomy, carbon isotope discrimination and mortality in a Quercus robur forest. 2011. TREE PHYSIOLOGY. 31 (3): 298.

Likhachev, E. R.. Dependence of water viscosity on temperature and pressure. 2003. TECHNICAL PHYSICS. 48 (4): 514.

MacCarthy, J. K., B. Borchers, and R. C. Aster. Efficient stochastic estimation of the model resolution matrix diagonal and generalized cross-validation for large geophysical inverse problems. 2011. JOURNAL OF GEOPHYSICAL RESEARCH-SOLID EARTH. 116: B10304.

McCabe, M., P. Chylek, and M. Dubey. Detecting ice-sheet melt area over western Greenland using MODIS and AMSR-E data for the summer periods of 2002-2006. 2011. Remote Sensing Letters. 2 (2): 117.

Mesler, R., D. Whalen, N. Lloyd-Ronning, C. Fryer, and Pihlstro&uml. Gamma-ray Bursts in Circumstellar Shells: A Possible Explanation for Flares. 2012. Astrophysical Journal. 757 (2): 117 (11 pp.).

Reimus, P., G. Pohll, T. Mihevc, J. Chapman, M. Haga, B. Lyles, S. Kosinski, R. Niswonger, and P. Sanders. Testing and parameterizing a conceptual model for solute transport in a fractured granite using multiple tracers in a forced-gradient test. 2003. Water Resources Research. 39 (12): SBH141.

Reimus, null.. Laboratory testing and modeling to evaluate perfluorocarbon compounds as tracers in geothermal systems. 2011. DOE.

Russell, C. T., D. R. Weimer, N. Omidi, L. K. Jian, J. G. Luhmann, and R. J. Strangeway. Interplanetary field enhancements travel at the solar wind speed. 2010. GEOPHYSICAL RESEARCH LETTERS. 37: L07204.

Russell, C. T., D. R. Weimer, N. Omidi, L. K. Jian, J. G. Luhmann, and R. J. Strangeway. Interplanetary field enhancements travel at the solar wind speed. 2010. GEOPHYSICAL RESEARCH LETTERS. 37: L07204.

Severino, G., D. M. Tartakovsky, G. Srinivasan, and H. Viswanathan. Lagrangian models of reactive transport in heterogeneous porous media with uncertain properties. 2012. PROCEEDINGS OF THE ROYAL SOCIETY A-MATHEMATICAL PHYSICAL AND ENGINEERING SCIENCES. 468 (2140): 1154.

Severino, G., D. M. Tartakovsky, G. Srinivasan, and H. Viswanathan. Lagrangian models of reactive transport in heterogeneous porous media with uncertain properties. 2012. PROCEEDINGS OF THE ROYAL SOCIETY A-MATHEMATICAL PHYSICAL AND ENGINEERING SCIENCES. 468 (2140): 1154.

Sullivan, E., P. Reimus, and D. Counce. Transport of a reactive tracer in saturated alluvium described using a three-component cation-exchange model. 2003. Journal of Contaminant Hydrology. 62-63: 675.

Welling, D. T., V. K. Jordanova, S. G. Zaharia, A. Glocer, and G. Toth. The effects of dynamic ionospheric outflow on the ring current. 2011. JOURNAL OF GEOPHYSICAL RESEARCH-SPACE PHYSICS. 116: A00J19.

Welling, D. T., V. K. Jordanova, S. G. Zaharia, A. Glocer, and G. Toth. The effects of dynamic ionospheric outflow on the ring current. 2011. JOURNAL OF GEOPHYSICAL RESEARCH-SPACE PHYSICS. 116: A00J19.

Wiens, R. C.. A tale of 2 Missions ...and 2 Very Different Landings. Invited presentation at IGPP External Advisory Review Committee Dinner presentation. (Santa Fe, NM, July 17, 2012).

Maximizing Flux Through Engineered Metabolic Pathways

Clifford J. Unkefer
20130091DR

Introduction

The long-term goal of synthetic biology is to engineer microorganisms to produce high-value products for biotechnological applications like biofuels production, environmental remediation and biosynthesis of pharmaceuticals. To achieve this goal, it will be necessary to engineer functional multi step metabolic pathways in organisms, which will require a new approach to regulate the expression of each of the enzymes in a metabolic pathway in order to optimize the flux through the pathway.

We seek to develop a new paradigm in metabolic pathway engineering by creating a simple approach to optimize the expression of individual enzyme in a pathway to maximize flux through the pathway. Because previous attempts to improve metabolic flux by over-expressing individual enzymes have achieved only limited success, we will simultaneously optimize the expression of each of the enzymes in the pathway. This will be done using the novel strategy of directed evolution of riboregulators using in vivo selection. Riboregulators are recently discovered class of RNA molecules that can be used to control the translation of a gene and it is possible to design an ensemble of riboregulators so one can individually control the translation of each of the genes that encode for a metabolic pathway. Riboregulators make pathway optimization possible because: 1) they allow the expression of a particular gene to be tuned over a wide dynamic range; 2) a set of riboregulators can be readily designed to independently regulate the expression of multiple genes; and 3) they are very tractable for directed evolution, because they can be finely tuned by varying only a few nucleotides. Our riboregulators approach to synthetic biology will have wide applicability. We will demonstrate this novel approach by engineering a more carbon- and energy-efficient pathway for lipid biosynthesis in a photosynthetic organism, an essential goal of biofuel research.

Benefit to National Security Missions

Synthetic biology is on the verge of producing practical solutions in a wide variety of application areas (energy, sensing, medicine, materials). This DR will allow LANL to become a major contributor to this rapidly growing field. We will apply our new synthetic biology tool set to solve a key limitation in biofuel production. This project will help sustain LANL leadership in algal bioenergy and contribute directly to LANL's mission in Energy Security. At the same time there are many potential application of synthetic biology in health security. The riboregulators and synthetic biology tools developed here will provide underlying science and technology necessary to apply synthetic biology in LANL health security missions including developing countermeasures for emerging pathogens and biological weapons. This project will position LANL to compete as a strong science and technology player for new synthetic biology calls from DOE/EERE and DOE/BER in biofuels research, as well as DARPA and NIH funding for health security.

Progress

To optimize the expression of enzymes in a metabolic pathway, we are developing two-component riboregulators that will independently control the concentration of each enzyme in our engineered metabolic pathway. Our cis-repressor is designed to form a helix in the untranslated region of the messenger RNA, which occludes the ribosome-binding site, blocking translation. Thus, messenger RNAs for our target genes have the default state of gene expression turned off. Regulation of expression involves a second trans-activating RNA designed to hybridize with the messenger RNA in a way that frees the ribosome-binding site, allowing ribosome binding and protein synthesis. We have designed and tested the inherent dynamic range of our first generation of the two-component riboregulators. The cis-repressing sequence was designed to be universal with respect to the regulated gene. This was accomplished by utilizing

sequence only in the 5'-untranslated region to fold into a secondary structure (helices) having a predicted thermodynamic stability and blocking the ribosome-binding site. Two trans-activators were designed to modulate repression by the cis-acting elements. Each trans-activator was designed with sequence elements that afforded differential stability of inter-molecular helices vs. intra-molecular helices formed with the cis-repressor. When the thermodynamic stability of the intra-molecular helices is far greater than that of the productive inter-molecular helices, translation is all-off. The converse situation produces the all-on state. A single copy plasmid containing the trans-acting riboregulators and their target cis-repressed gene was constructed using the Gibson assembly method, which allows for the efficient, simultaneous insertion of multiple DNA fragments into a vector. The cis-repressed gene was the chloramphenicol acetyltransferase (CAT) gene, which imparts resistance to the antibiotic chloramphenicol. The plasmid was used to transform E. coli, and transformants were confirmed by DNA sequencing. Then individual colonies were plated on medium containing various concentrations of chloramphenicol. Growth differences between the all-off and all-on variants were apparent indicating that the trans-activators are able to increase the expression of the CAT imparting greater resistance to chloramphenicol. However, our analysis of the antibiotic resistance data indicated only ~2-fold increase in the expression of CAT in the presence of the all-on vs. the all-off trans-activators. We carried out other experiments that proved that while the basil level of expression of CAT was significant the trans-activator did indeed increase the expression. Overall these experiments were encouraging because we demonstrated that the two-component riboregulators could be used to control gene expression, but it is necessary to design the cis-repressor with greater thermodynamic stability to minimize expression in the absence of to trans-activator. As a result we have redesigned the cis-repressor and corresponding trans-activators, increasing the size of the helix-forming regions from 16 to 32 residues. We have just completed the construction of this second-generation two-component riboregulators. The dynamic range of this new system is now being evaluated using all-on and all-off trans-activators. We are confidant that we will soon have a library of selected riobregulators with an activity range spanning two orders of magnitude.

To evaluate our progress toward pathway optimization, we will develop a full kinetic model of our engineered pathway. Toward this end we have initiated a project to express, purify and characterize the kinetics of the enzymes in our pathway. Essential to our success was a phosphoenolpyruvate carboxylase (PEPC) that is not inhibited by metabolites in our pathway. We selected a PEPC gene from methanol utilizing bacterium in which PEPC also serves a central role in carbon assimilation. After expressing and purifying this PEPC, we developed an activity assay coupled to malate dehydrogenase and measured kinetic parameters. We demonstrated that indeed malate and aspartate do not inhibit the PEP carboxylase activity. Similar studies are near completion for glyoxylate carboligase, and 2-hydroxy-3-oxopropionate reductase, and we have constructed expression systems for all the other enzymes in our pathway.

In preparation for future engineering in a phototroph, we have established protocols for growth and transformation of the cyanobacterial strain, Synechococcus elongatus PCC7942. In addition, we have demonstrated lipid production from an engineered strain, provided by our collaborators, harboring two heterologous genes responsible for the biosynthesis of triacylglycerides (TAGs) using a neutral lipid dye with flow cytometry-based detection of the lipid droplets. Using flow cytometry to screen for lipid production will be essential for pathway optimization.

Future Work

We will continue to design and test a family of riboregulators that can be used for translational regulation of the expression of each of the enzymes in a complete metabolic pathway. In FY13, we will complete trans-activator library selection, verify and refine our ability to target multiple genes simultaneously and construct an initial four-gene pathway in E. coli. The final step of riboregulator construction will demonstrate our ability to selectively trans-activators to multiple genes, and our strategy of directed evolution of riboregulators through in vivo selection. To facilitate this process, we will use two orthogonal fluorescent reporters and two antibiotic reporters. As outlined in the proposal, the library of riboregulators will be composed of pools of randomized trans-activators driving the expression of the cis-repressed fluorescent and antibiotic marker genes. Targeting sequences will be tested simultaneously by incorporating two orthogonal trans-activators targeting two proteins at different locations in the vector. Two distinct targeting sequences will be combined with two regulatory structures from either the high activity pool or low activity pool. These trans-activators will allow us to verify our ability to target and differentially regulate two genes simultaneously. We will design and test 10 distinct targeting sequences that preserve dynamic range and minimize regulatory crosstalk for use in the construction of novel multigene pathways. Once we have finalized the design of the riboregulators, we will start assembling the large DNA necessary to encode the metabolic pathway in both E. coli and Synechococcus elongates. Initially we will focus on the first four enzymes in the pathway, which should recover

growth in mutants unable to express pyruvate dehydrogenase. Finally, to evaluate our progress toward pathway optimization, we will develop a full kinetic model of our engineered pathway. We will finish obtaining the necessary kinetic parameters for the enzymes in the pathway.

Conclusion

We will develop a family of riboregulators that can be used for translational regulation of the expression of each of the enzymes in a complete metabolic pathway. Demonstrate a strategy for the simultaneous directed evolution of riboregulators to optimize the expression of the enzymes to maximize flux through a metabolic pathway.
We will use known enzymes to engineer a more carbon- and energy-efficient pathway for lipid biosynthesis essential for biofuel production. In addition, we will use the directed evolution of riboregulators strategy developed above to optimize growth and lipid production in Synechococcus elongates, a cyanobacterium.

Publications

Hall, R. S., R. Martí-Arbona, S. P. Hennelly, T. S. Maity, F. Mu, J. M. Dunbar, C. J. Unkefer, and P. J. Unkefer. In-vitro Characterization of an L-Kynurenine-Responsive Transcription Regulator of the Oxidative Tryptophan Degradation Pathway in Burkholderia xenovorans. 2013. Journal of Molecular Biology Research. 3 (1): 55.

Hennelly, S. P., I. V. Novikova, and K. Y. Sanbonmatsu. The expression platform and the aptamer: cooperativity between Mg2+ and ligand in the SAM-I riboswitch. 2013. NUCLEIC ACIDS RESEARCH. 41 (3): 1922.

Hennelly, S. P., I. V. Novikova, and K. Y. Sanbonmatsu. The expression platform and the aptamer: cooperativity between Mg2+ and ligand in the SAM-I riboswitch. 2013. Nucleic Acids Research. 41 (3): 1922.

Jarchow-Choy, S., D. Fox, E. Schmidt, A. Koppisch, R. Marti-Arbona, and C. Unkefer. Monitoring the distribution of isoprenoid products from the MEP pathway in algae and cyanobacteria. 2013. ABSTRACTS OF PAPERS OF THE AMERICAN CHEMICAL SOCIETY. 245: -.

Martí-Arbona, R., T. S. Maity, J. M. Dunbar, C. J. Unkefer, and P. J. Unkefer. Discovery of a Choline-Responsive Transcriptional Regulator in Burkholderia xenovorans. 2013. Journal of Molecular Biology Research . 3 (1): 91.

Nguyen, T. T., R. Martí-Arbona, R. S. Hall, T. Maity, Y. E. Valdez, J. M. Dunbar, C. J. Unkefer, and P. J. Unkefer. Identification and In-vivo Characterization of a Novel OhrR Transcriptional Regulator in Burkholderia xenovorans LB400. 2013. Journal of Molecular Biology Research. 3 (1): 37.

Novikova, I. V., A. Dharap, S. P. Hennelly, and K. Y. Sanbonmatsu. Shotgun secondary structure determination of long non-coding RNAs. 2013. Methods. 63: 170.

Novikova, I. V., S. P. Hennelly, and K. Y. Sanbonmatsu. Sizing up long non-coding RNAs: Do lncRNAs have secondary and tertiary structure? . 2012. BioArchitecture. 2 (6): 189.

Novikova, I. V., S. P. Hennelly, and K. Y. Sanbonmatsu. . Experimentally determined secondary structures of cancer-related long non-coding RNAs. 013. In 245th ACS National Meeting & Exposition. (New Orleans, 7-11 April, 2013). , p. PHYS. Abstracts of Papers: ACS.

Novikova, I. V., S. P. Hennelly, and K. Y. Sanbonmatsu. Tackling structures of long noncoding RNAs. To appear in International Journal of Molecular Science.

Novikova, I. V., S. P. Hennely, C. S. Tung, and K. Y. Sanbonmatsu. Rise of the RNA machines: Exploring the structure of long non-coding RNAs. 2013. Journal of Molecular Biology. 425: 3731.

Sanbonmatsu, K. Y.. Rise of the RNA Machines: Long Non-Coding RNAs. Invited presentation at 10th Horizons in Molecular Biology Conference International . (Max Planck Institute, Gottingen, Germany, Sept 9-12 2013).

Sanbonmatsu, K. Y.. Integrating simulations and experiments of the SAM-I riboswitch. Invited presentation at RNA Dynamics. (Telluride, Colorado, 22-26 July, 2013).

Sanbonmatsu, K. Y.. Large-scale simulations of biomolecular machines. Invited presentation at Biosupercomputing Symposium. (Tokyo Japan, December 2012).

Sanbonmatsu, K. Y.. Understanding the atomistic mechanism of magnesium effects of RNA dynamics. Invited presentation at Mini-symposium on Modeling, Simulation and Function of Biomolecular Assemblies. (Tokyo University, Tokyo Japan, November 2012).

Terrestrial Vegetation, CO_2 Emissions, and Climate Dynamics

Nathan G. Mcdowell
20110014DR

Abstract

Vegetation mortality rates are increasing globally, appear to be driven by our changing climate, and are releasing large and sustained amounts of CO2 to the atmosphere. The critical urgency of forecasting climate impacts and feedbacks, coupled with the rising international focus on carbon management, make understanding, quantifying, and predicting terrestrial carbon balance and subsequent climate impacts one of the greatest science challenges currently facing America. We have built an extremely high resolution, highly accurate monitoring system for documenting forest mortality and for simulating the consequences of the mortality on climate forcing. Through this effort, we have generated three separate predictions of the future of forests in western USA. All results suggest that southwestern USA will be conifer-free due to chronic drought by 2050 AD, with the Pacific Northwestern forests lagging only slightly behind. Tests of this approach in other regions suggest it is robust to assumptions associated with variation in forest type. The monitoring and prediction system we have developed promises to continue yielding high impact, highly informative scientific results regarding the current and future changes to our global forests as climate continues to warm.

Background and Research Objectives

Terrestrial vegetation buffers fossil fuel emissions through storing CO2. Unfortunately, rapidly changing climate and accelerating vegetation mortality pose a threat to the long-term maintenance of the land CO2 sink. Predictions from dynamic global vegetation models suggest that despite enhanced photosynthesis due to elevated atmospheric CO2, increased temperature and reduced precipitation (drought) are expected to overwhelm this positive benefit and accelerate mortality, thus tipping the terrestrial system from a negative to a positive climate feedback in upcoming decades. The bulk of this response is due to drought-induced mortality. Alarmingly, emerging evidence of a global rise in widespread vegetation mortality strongly supports these predictions. However, we do not have a system for monitoring vegetation mortality remotely, which greatly limits our ability to evaluate models and predict future mortality.

Our objectives were to develop and evaluate a high precision, remotely sensed system for determining forest mortality, to improve models of vegetation mortality during drought, and to couple these to assess the climate forcing impacts of mortality.

Scientific Approach and Accomplishments

We had three key tasks: 1) remote sensing detection of vegetation stress and mortality, 2) estimating carbon storage and fluxes, and 3) assessing climate consequences based on results of (1) and (2). Our goal is to develop a globally comprehensive tool; however, because the computational requirements for complete global coverage are beyond the capacity of a DR, we tested our approach utilizing data sets of vegetation mortality and carbon storage, CO2 fluxes, and climate from multiple disparate locations.

Our accomplishments were many. Perhaps most importantly, we have three independent results (Jiang et al. 2013; Williams et al. 2013; McDowell et al. unpublished manuscript) showing that southwestern forests will be largely gone by 2050 AD. This shocking result has gained a lot of press (BBC, NPR, NY Times, for example). We have also presented this result to the UC-Board of Regents, to the LANS-Board of Governors, and to Energy Secretary Dr. Ernest Moniz. These results were the summation of many technical advances, including successful development of a high precision mortality monitoring system (Garrity et al. 2012; Mu et al. 2013; Skurikhin et al. 2013; Gangodoagamage et al. in review), and radical improvements to the mechanistic underpinnings of mortality simulations (Xu et al. 2012; 2013; McDowell et al. 2013). The science developed through this LDRD project

is ongoing through a recently held workshop where we brought together the world's experts in remote sensing of disturbance for a summary paper on the way forward, and through pending funding to DOE to continue the application of the integrated remote sensing and modeling.

Impact on National Missions

The impact is through allowing documentation of current and prediction of future vegetation consequences of climate change so that we can predict impacts on resources at home and globally. Furthermore, according to multiple New Mexico state senators and Secretary Moniz, we are doing the nation a favor by bringing these shocking results to the awareness of the public.

Publications

Allen, C., A. Macalady, H. Chenchouni, D. Bachelet, N. McDowell, M. Vennetier, T. Kitzberger, A. Rigling, D. Breshears, E. H. Hogg, P. Gonzalez, R. Fensham, Z. Zhang, J. Castro, N. Demidova, J. Lim, G. Allard, S. Running, A. Semerci, and N. Cobb. A global overview of drought and heat-induced tree mortality reveals emerging climate change risks for forests. 2010. In Conference on Adaptation of Forests and Forest Management to Changing Climate with Emphasis on Forest Health ; 20080825 - 20080828 ; Umea, SWEDEN. Vol. 259, 4, SI Edition, p. 660.

Craine, J., and N. McDowell. Resource limitation, tolerance, and the future of ecological plant classification. 2013. Frontiers in Functional Plant Biology. : fpls.2012.00246.

Franks, P., and N. McDowell. Forest sensitivity to CO2. . 2013. New Phytologist. : nph.12104.

Garrity, S., and e. al. Quantifying drought-induced tree mortality in a piñon-juniper woodland using multitemporal high spatial resolution satellite imagery. 2013. Remote sensing of Environment. 129: 54.

Jiang, X., S. Rauscher, T. Ringler, D. Lawrence, P. Williams, and M. Cai. Increasing risk of tree mortality in western North America towards the end of the 21st century. . 2013. J. of Climate. : JCLI.

McDowell, N.. Mechanisms Linking Drought, Hydraulics, Carbon Metabolism, and Vegetation Mortality. 2011. PLANT PHYSIOLOGY. 155 (3): 1051.

McDowell, N. G., M. G. Ryan, M. Zeppel, and D. Tissue. Improving our knowledge of drought-induced forest mortality through experiments, observations, and modeling. To appear in New Phytologist.

McDowell, N. G., and e. al. Evaluating theories of drought-induced vegetation mortality using a multi-model-experiment framework. To appear in New Phytologist.

McDowell, N., D. Beerling, D. Breshears, R. Fisher, K. Raffa, and M. Stitt. The interdependence of mechanisms underlying climate-driven vegetation mortality. 2011. TRENDS IN ECOLOGY & EVOLUTION. 26 (10): 523.

Mu, Q.. A remote sensed global terrestrial drought severity index. . 2013. Bulletin of the American Meteorological Society. 94: 83.

Williams, P., and e. al. Forest response to drought in the North American Southwest from 1000-2100 A.D. . 2012. Nature Climate Change. : 1.

Williams, P., and e. al. Who's the new sheriff in town regulating boreal forest growth?. 2012. Environmental Research Letters. : 041104.

Xu, C., C. Liang, S. Wullschleger, C. Wilson, and N. McDowell. Importance of feedback loops between soil inorganic nitrogen and microbial communities in the heterotrophic soil respiration response to global warming. 2011. NATURE REVIEWS MICROBIOLOGY. 9 (3).

Xu, C., N. G. McDowell, S. Sevanto, and R. Fisher. Our limited ability to predict vegetation responses to water stress. To appear in New Phytologist.

Xu, C., and e. al. Toward a better understanding of nitrogen-photosynthesis relationships based on nitrogen trade-offs among light absorption, electron transport, carboxylation, and carbon sinks. . 2012. Plos One. 7: e37914.

Advanced Metagenomic Analysis to Understand Dynamics of Soil Microbial Community under Conditions of Climate Change

Shunsheng Han
20110034DR

Abstract

Microbes form the majority biomass on earth and are related to almost all aspects of human life. The goal in this project was to develop tools and techniques to probe the dynamics of microbial communities of biological soil crusts in arid deserts and to document their response to various climate change related perturbations. Our technologies improved performance in two previous bottleneck areas. One is to sequence genomes of unculturable bacterial species, and another is the analysis of the huge amount of data from metagenomic sequencing in a timely fashion. We applied these technologies in analyzing soil microbiota in arid soils from Utah, one of our field sites for climate manipulation studies.

Background and Research Objectives

Microbial communities are complex 'supra-organisms' of bacteria, archaea, single-cell eukaryotes and viruses that function together as a whole in order to survive and thrive in their natural environmental niches. Microbes make up the majority of the living biomass on Earth and as such, are major contributors to carbon cycling and to the biogenic production and destruction of other greenhouse gases, including CO2, N2O and methane. Our present lack of understanding regarding the biochemical fluxes of C and N within these microbial communities constitutes a major source of uncertainty in our predictions of the consequences of climate change.

Characterizing the collective genomes of microbial communities, a nascent field known as metagenomics, can help bridge this information gap by revealing how climate change impacts the broad composition and function of members within environmental microbial communities, and by quantifying the net effect of these changes on both the C and N cycles. There are two ways to characterize metagenomes of microbial communities, sequencing the community collectively (shotgun metagenome) or each member separately. A combination of the two approaches, as proposed in Figure 1, will facilitate the analysis processes as the second approach will provide more reference genomes from the same sample for accurate and unbiased analysis of data from the first shotgun metagenomic approach. Recent developments in metagenomic sequencing make it possible to generate enough data for studying a relative complex community. However, as only a small fraction of all bacteria have been cultivated in isolation, a pre-requisite for standard genome sequencing efforts, it is very difficult to sequence each member of microbial community separately. This problem has been only partially addressed by DNA amplification of isolated genomes from a single cell (known as Single Cell Genomics, or SCG). Although sequences have been obtained from a number of different bacteria at the single cell level, the current SCG method results in hundreds to thousands of sequences for a genome with poor coverage, rendering it difficult to analyze. This speaks to the need for a more robust method to sequence genomes from single cells. Methods we developed are able to improve the coverage and to reduce the number of gaps to a near completion.

Existing methods for understanding uncultured microbial communities fall into three broad analysis techniques. None of these methods are adequate to fully analyze the huge amount of metagenomic data. Targeted metagenomics uses universal primers to preferentially sequence one particular gene (usually 16S rRNA). This method cannot provide functional profiles. Fragment recruitment (or nucleotide BLAST) is computationally expensive and requires closely related reference organisms. Protein-based BLAST is computationally expensive, fails with short reads (less than 100 bp) and confuses sequence similarities arising from inheritance with similarities arising from functional pressure (natural selection). Because the next generation of DNA sequencing technology generates gigabytes data in short sequences, new analysis techniques are needed.

Analysis methods based on local patterns offer enor-

mous advantages over methods based on global-similarity measures such as BLAST. We based our method around signatures of amino-acid 10-mers. Our signature-based method bypasses many paralog problems, uses signatures that persist across larger phylogenetic distances than do nucleic acids, produces matches that are highly significant, and is quite rapid to implement because patterns can be organized and searched via index structures. Some 20 million orthogenomic amino-acid 10-mer signatures are sufficient to cover all of current sequenced bacterial diversity down to the genus level while allowing detection of reads from never-before-sequenced phyla with reasonable likelihood.

Scientific Approach and Accomplishments

Artificial polyploidy

The typical genome recovery rate from SCG is generally less than 50% from environmental samples. The low recovery rate is related to amplification bias and DNA breakage due to only one copy of a genome. Artificial polyploidy is a technique that can be employed to increase the genome copy number in individual cells by blocking cell division while allowing for cell growth. The resulting cells are much larger with multiple genome copies. Sequencing from polyploid cells significantly increases the coverage of genomic sequence.

Gel microdroplet (GMD)

GMD allows us to perform DNA amplification on hundreds to thousands of copies of a bacterial genome. GMDs are small spheres composed of an agarose matrix in which one can grow colonies of bacteria starting from a single cell. They are very permeable and thus allow for communication among the microbial community members, which many bacteria require to complete some undetermined aspect of their life cycle. Critically, the reproducing cells remain spatially separate so individual colonies can be manipulated following group culture. In this study, we demonstrate its utility for producing near-complete genomes of environmental microorganisms by using human fecal and oral bacteria as a demonstration. We show that the resulting assemblies are vastly superior to those produced via single-cell sequencing and that GMDs also have the potential to produce genomic data for currently uncultured and unsequenced organisms. The near complete genomes in a single sample allow us to assess the genome diversity in environmental samples (Figure 2).

Phage antibody as tool for bacterial species isolation from environmental microbiota

Antibodies were selected using in vitro display libraries against two bacterial classes. In the first, proof of principle experiment, a highly specific antibody was selected against Lactobacillus acidophilus, a gut microbe that is also a significant constituent of yoghurt. This antibody was used to assess the abundance of L. acidophilus in a number of yoghurt samples, with the lowest being 0.3%. The genome of the amplified L. acidophilus purified from this yoghurt sample was then sequenced using Illumina sequencing, and the quality and extent of coverage, of a de novo assembly, was equivalent to that of a cultured organism. This work, which demonstrated the power of this approach on a true mixed-culture sample, has been submitted for publication. The second set of experiments were carried out on cultured soil bacteria. In this case two specific antibodies were selected against Streptomyces species cultured from soil. These antibodies were able to specifically stain the cultured Streptomyces, but not related species. Most significantly, as shown in Figure 3, these antibodies were also able to label a small number of bacteria in soil, demonstrating the power of the approach.

Sequedex – the bioinformatics tool for rapid analysis of metagenomic data

We developed a bio-informatics tool that leverages our understanding of evolution to identify local peptide signatures to classify phylogenetically and functionally raw sequence reads (4). An important feature of the algorithm is its ability to extrapolate to organisms not present in the database. That feature is essential when applied to soil metagenomes. Much of our effort focused in releasing software to the bio-informatics community that works on all platforms (www.sequedex.lanl.gov). The methodology offers unprecedented speed of analysis, and was awarded an R&D 100 award in 2012. The documentation of the released software is a substantial document that provides, in addition to guidance on how to install and run the Sequedex, various demonstration of how to use the output of our tool to answer various questions of interest. In a single step, the tool allows us to calculate phylogenetic and functional profiles of a metagenome. These profiles can be use to compare multiple samples, and to identify common determinants of an ecosystem (Figure 4, 5).

The usefulness of Sequedex goes well beyond the profiles. In particular, it provides a filter to classify raw sequence reads both in terms of phylogeny and functions. Once filtered, the reads can be assembled de novo, mapped to identified near neighbors, and placed into phylogenetic trees. As a result, Sequedex naturally fits into modern pipelines for analyzing reads from next generation sequencers.

Studies on soil microbiota under conditions of climate changes

Biological soil crusts (hereafter referred to as biocrusts, colonize the interspace soils between patchily distributed

plants in dryland ecosystems. Biocrusts have been identified in dryland ecosystems on every continent on Earth and function in retaining water, fixing soil particles, and fixing atmospheric nitrogen and carbon. Our first task in the project was to assess the ability of the current available sequencing technologies, using the available tools, in their ability to characterize microbial communities in a complex soil environment and document their response to climate change, such as elevated CO2.

We compared three different sequencing datasets, targeted amplification and sequencing of bacterial 16S rRNA genes, shotgun metagenome sequencing, and parsing rRNA genes out of the metagenomes. Our data indicated shotgun metagenomes were not able to discriminate ecological differences as well as targeted methods. This was apparently due to a lack of reference genomes and computational ability to process sequence datasets, a critical need being addressed in the other section of the project.

Our next objective was to assess the spatial heterogeneity of desert biocrust communities. Using a spatially nested sampling procedure we collected samples representing three different soil parent materials and different spatial scales, including a vertical dimension. We found that desert biocrusts were similar over large horizontal scales but differed significantly at small vertical scales.

We then wanted to study biological soil crusts at a continental scale to address whether soil crusts in different systems are unified by similar microbial populations. In this regard we collected soil crusts from Ward Hunt Island, Canada, the northern most terrestrial system on Earth . Soil crusts on Ward Hunt Island were similar in diversity and composition to crusts from more temperate latitudes, suggesting a biocrusts share similar structures even at great spatial scales.

Our final work involved documenting the response of soil communities to field manipulations simulating particular climate change and land use perturbations. In this vein we collected metagenomic samples to document changes in the microbial community structure and function as well as transcriptomes to characterize the specific functions microbes are employing under various climate change scenarios. We anticipate two to three more publications arising from this work in the near future.

Besides studies on soil microbiome, we also participated in analysis of human microbiomes associated with Human Microbiome Project and ocean microbiomes resulted in several publications in high-ranking scientific journals including Nature.

Impact on National Missions

The project falls in the scope of two grand challenges for science and engineering at Los Alamos: Complex Biological Systems and Information, Science and Technology. The scientific goal of deep understanding of microbial communities in arid lands will eventually facilitate the progress of another grand challenge, Energy and Earth Systems. It directly addresses key goals identified in the 2009 DOE report “Carbon Cycling and Biosequestration: Integrating Biology and Climate Through System Science.” Studying microbial community with LANL’s advantageous metagenomic technologies is one of the focuses of the grand challenge of Complex Biological Systems. These experimental and computational tools developed in the projects has put LANL at the forefront of metagenomics, and strengthened our leadership position in genomics and metagenomics.*Figure 1. Probing the dynamics of metagenome.*

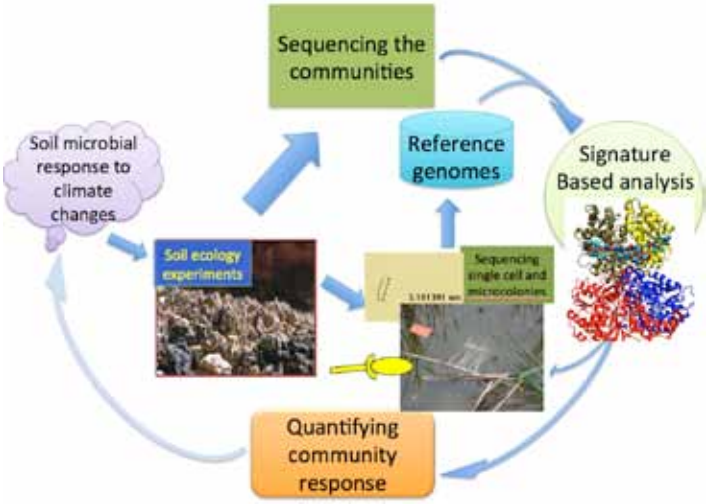

Microbiome in soil crust was sequenced as a community, metagenome, and individually as single cell or microcolonies propagated from individual cells. Then the two sets of data were analyzed together with Sequedex.

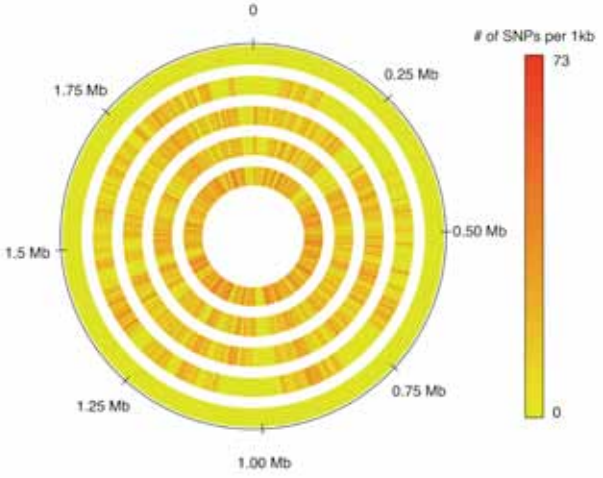

Figure 2. Genomes completed with GMD technology. The reddish color indicates the differences in these almost finished genomes comparing to a reference genome.

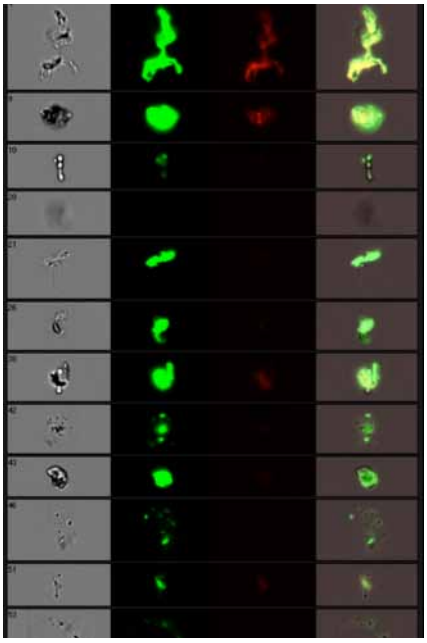

Figure 3. Labeling of bacterial cells from soil sample with phage antibody. Column 1 (left) phase contrast microscopy of individual soil bacteria; column 2: DNA stain; column 3: staining with antibodies; column 4: merging of column 2 and 3. The figure shows that a small number of soil bacteria were labeled with the specifically selected antibody.

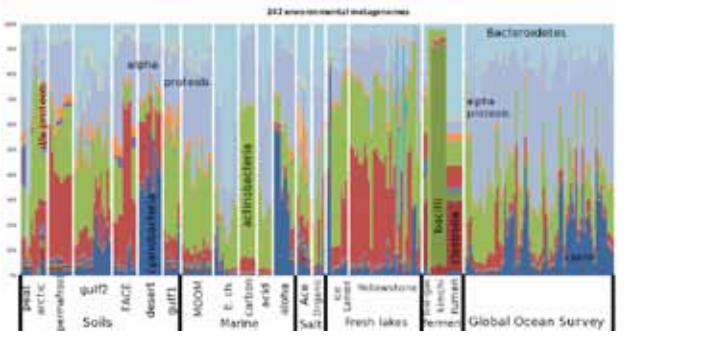

Figure 4. Phylogenetic profiles of 242 environmental metagenomes.

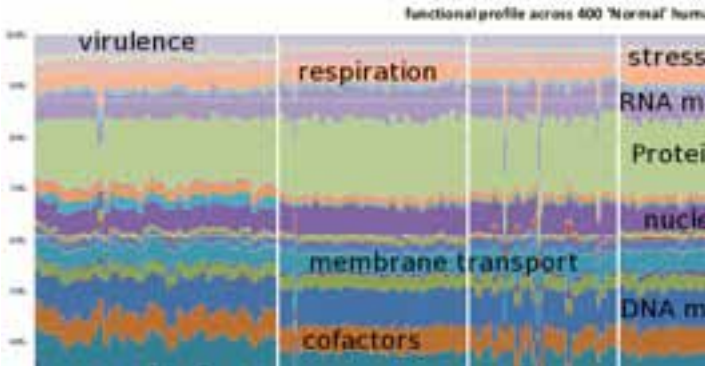

Figure 5. Functional profiles of 400 human microbiota metagenomes. Microbiota from different body sites had similar functional profiles when analyzed at top level of functional categories, though their phylogenetic profile were distinct.

Publications

A framework for human microbiome research. 2012. Nature. 486 (7402): 215.

Structure, function and diversity of the healthy human microbiome. 2012. Nature. 486 (7402): 207.

Beckloff, N., S. Starkenburg, and P. Chain. Bacterial genome annotation. 2012. Methods Mol Biol. 881: 471.

Berendzen, J., W. J. Bruno, J. D. Cohn, N. W. Hengartner, C. R. Kuske, B. H. McMahon, M. A. Wolinsky, and G. Xie. Accurate, sensitive, and rapid classification of short random fragments of bacterial DNA using phylogenetic signature peptide 10-mers. 2012. BMC Research Notes. 5: 460.

Close, D. W., F. Ferrara, A. E. K. Dichosa, A. R. Daughton, H. E. Daligault, K. G. Reitenga, N. Velappan, T. C. Sanchez, S. Iyer, C. S. Han, and A. R. M. Bradbury. Phage antibodies to dissect microbiomes for complete de novo genome sequencing of rare microbes. BMC Microbiology.

Dichosa, A. E K, M. Fitzsimons, L. L Weston1, L. G. Preteska, J. P. Snook, C. C. Lo, X. Zhang, W. Gu, K. McMurry, L. D. Green, P. S. Chain, J. C. Detter, and C. S. Han. Artificial polyploidy improves bacterial single cell genomics. 2012. PLOS One. 7 (5): e37387.

Dichosa, A. E., A. R. Daughton, K. G. Reitenga, M. S. Fitzsimons, and C. S. Han. Capturing and cultivating single cells in gel microdroplets (GMDs) to obtain near complete genomes. To appear in NATURE PROTOCOL.

Dunbar, J., S. Eichorst, L. Gallegos-Graves, G. Xie, N. Hengartner, R. Evans, B. Hungate, R. Jackson, J. Megonigal, C. Schadt, R. Vilgalys, D. Zak, and C. Kuske. Common bacterial responses in six ecosystems exposed to ten years of elevated atmospheric carbon dioxide. 2012. Environmental Microbiology 2012 May;14(5):1145-58. doi: 10.1111/j.1462-2920.2011.02695.x. Epub 2012 Jan 20. 14 (5): 1145.

Fitzsimons, M. S., M. Novotny, C. C. Lo, A. E. K. Dichosa, J. L. Yee-Greenbaum, J. P. Snook, W. Gu, O. Chertkov, K. W. Davenport, K. McMurry, K. G. Reitenga, A. R. Daughton, J. He, S. L. Johnson, C. D. Gleasner, P. L. Wills, B. Parson-Quintana, P. S. Chain, J. C. Detter, R. S. Lasken, and C. S. Han . Nearly finished genomes produced using gel microdroplet culturing reveals substantial intraspecies genomic diversity within the human microbiome. 2013. Genome Research. 23 (5): 878.

Hu, B., G. Xie, C. C. Lo, S. R. Starkenburg, and P. S. Chain. Pathogen comparative genomics in the next-generation sequencing era: genome alignments, pangenomics and metagenomics. 2011. Brief Funct Genomics. 10 (6): 322.

Martinez-Garcia, M., D. M. Brazel, D. M. Brazel, B. K. Swan, C. Arnosti, P. S. Chain, K. G. Reitenga, G. Xie, N. J. Poulton, M. Lluesma Gomez, D. E. Masland, B. Thompson, W. K. Bellows, K. Ziervogel, C. C. Lo, S. Ahmed, C. D. Gleasner, C. J. Detter, and S. Stepanauskas. Capturing single cell genomes of active polysaccharide degraders: an unexpected contribution of Verrucomicrobia. 2012. PLoS One. 7 (4): e35314.

Mason, O. U., T. C. Hazen, S. Borglin, P. S. Chain, E. A. Dubinsky, J. L. Fortney, J. Han, H. Y. Holman, J. Hultman, R. Lamendella, R. Mackelprang, S. Malfatti, L. M. Tom, S. G. Tringe, T. Woyke, J. Zhou, E. M. Rubin, and J. K. Jansson. Metagenome, metatranscriptome and single-cell sequencing reveal microbial response to Deepwater Horizon oil spill. 2012. ISME J. 6 (9): 1715.

Scholz, M. B., C. C. Lo, and P. S. Chain. Next generation sequencing and bioinformatic bottlenecks: the current state of metagenomic data analysis. 2012. Curr Opin Biotechnol. 23 (1): 9.

Steven, B., L. Gallegos-Graves, C. M. Yeager, D. Evans, J. Belnap, and C. R. Kuske. Dryland biological soil crust Cyanobacteria show unexpected decreases in abundance under long-term elevated CO2. . 2012. Environmental Microbiology. 14: 3247.

Steven, B., L. Gallegos-Graves, J. Belnap, and C. R. Kuske. Dryland soil bacterial communities display spatial biogeographic patterns associated with soil depth and soil parent material. 2013. FEMS Microbiology Ecology. 86 (1): 101.

Steven, B., L. Gallegos-Graves, S. R. Starkenburg, P. S. Chain, and C. R. Kuske. Targeted and shotgun metagenomic approaches provide different descriptions of dryland soil microbial communities in a manipulated field study. . 2012. Environmental Microbiology Reports. 4: 248.

Steven, B., M. Lionard, C. R. Kuske, and W. Vincent. High bacterial diversity of biological soil crusts in water tracks over permafrost in the high Arctic polar desert. 2011. PloS One. e71489: 10.1371/journal.pone.0071489.

Multi-scale Science Framework for Climate Treaty Verification: Attributing and Tracking Greenhouse Gas Fluxes Using Co-emitted Signatures

Manvendra K. Dubey
20110081DR

Abstract

As the consensus on the dangers of climate change and ocean acidification from uncontrolled anthropogenic fossil energy emissions strengthens, international agreements will demand stringent limits on greenhouse gas emissions. The Copenhagen negotiations underscored that a sound technical strategy to verify compliance with any such treaties is lacking, creating a major obstacle to meaningful agreements. Existing accords that stipulate concerted international action lack commitments to enforceable emissions reductions, primarily because of a failure to define verification protocols. Currently, carbon dioxide (CO2) emissions derived from energy consumption data are the basis of inventories, but these are uncertain and can be manipulated. Inventories must be verifiable, especially over denied territories such as China and India. Monitoring national CO2 emissions from afar is challenging because of CO2's large and variable background (390 ppm) and the dilution of anthropogenic sources by atmospheric mixing. Quantification of anthropogenic CO2 emissions that are 3% of natural CO2 fluxes globally and apportioning them among nations is a daunting task. We developed a calibrated scientific framework for climate treaty verification by reaching beyond isolated CO2 measurements to the monitoring of associated trace gases, in situ and remotely, to apportion and track emissions from distinct sources. We evaluated our method at Farmington, NM to verify the well calibrated in stack emissions reported by the Four Corners and San Juan power plants. We compared our regional scale remote sensing composition observations with forward model simulations to show that they can verify emissions with an accuracy of 2%. This finding will help design future verification satellites. Our remote observations can also discriminate the high NOx emitting Four Corners power plant from the low NOx emitting San Juan. In addition, we discovered large-scale enhancements of methane (CH4) a potent greenhouse gas that attributed to large fugitive leaks from coal and gas production that are missing in current inventories. Our project has integrated world-class LANL expertise in remote sensing, spectral inversion, in situ sensors and atmospheric models to develop sound and innovative monitoring strategies. We harnessed the unique breadth of Los Alamos expertise for an initial demonstration of verifying CO2 emissions over denied areas and quantifying CH4 fugitive leaks from oil and gas, both critical issues for energy security.

Background and Research Objectives

Trace gas pollutants (Nitrogen oxides (NOx), sulfur dioxide (SO2), and carbon monoxide (CO)) and carbon dioxide (CO2) emissions from anthropogenic fossil energy production cause air pollution and global warming, respectively. In the United States, pollutants (e.g. NOx, SO2, CO) and CO2 are considered a threat to public health and welfare under the Clean Air Act (CAA) and are regulated by the Environmental Protection Agency (EPA). While reporting requirements for air pollutants are mature, they are under development for CO2. Reported inventories convert the amount of fuel used in a specific activity to CO2 and pollutant gases produced, using emission factors that depend on fuel composition, combustion efficiency, and scrubbing methods. These bottom-up inventories are subject to significant uncertainties, manipulations, and also change with technology [1]. Atmospheric observations offer an independent top-down method to verify reported emissions. Pollutant trace gases have low atmospheric backgrounds and show large and distinct increases near various combustion sources. In fact, satellite observations of NO2 have been used to evaluate regional and local emissions [2,3]. While satellite NO2 observations are useful for trend analysis, they can underestimate the amount of NO2 because of their large observing footprint. In contrast, CO2 has a large background and variability. Consequently, source attribution and verification by direct CO2 measurements remains elusive [4], limiting our ability to develop an effective global climate treaty or carbon-trading scheme [5, 6, 7]. We postulated that measure-

ments of co-emitted trace gases and isotopic composition can be used to isolate anthropogenic CO2 emissions. Furthermore, contributions from specific sectors with distinct composition (trace gas to CO2 emission ratios, ERX = X/CO2, or isotopic ratio 13CO2/12CO2) can be delineated. We hypothesized that remote column trace gas measurements over large scales, which are less sensitive than in situ point surface measurements to small-scale variability from meteorology, can provide a more precise method to verify emissions [8, 9, 10]. We tested our hypothesis using ground based in situ and remote observations at a site with large power plant emissions of CO2 and pollutants, in the Four Corners, NM area.

The Four Corners region has also been a hub for conventional coal, oil and gas production and exploration for over half a century. It is currently undergoing a shift to non-conventional hydraulic fracturing. There is concern that this transition to non-conventional extraction of natural gas could lead to fugitive CH4 leaks that, if large enough, would offset the climate benefits of this clean and domestic fuel, since methane is 25 times more potent a greenhouse gas than CO2. Our project is the first to provide regional scale observations of fugitive leaks from conventional mining that are a needed baseline to quantify the changes from non- conventional extraction in these oil and gas plays.

Scientific Approach and Accomplishments

Our monitoring site is located in Farmington, NM (36.79°N 108.48°W, at 1643 m above sea level), an arid region with two large coal-fired power plants that emit approximately 30 Mton/year and 80Kton/year of CO2 and NOx, respectively. This region is the largest point source of pollution in North and South America. The Four Corners power plant has high ΔNOx/ΔCO2 emission ratio and is located ~12 km South of our site. The San Juan power plant, which has a low ΔNOx/ΔCO2 ratio due to environmental upgrades, is located about 3.7 km east of our site. LANL deployed a comprehensively instrumented automated observatory that monitors regional greenhouse (CO2, CH4, N2O) and pollutant gases (CO, NO2, O3, C2H6) retrieved from three solar spectrometers (Bruker 125 HR and Pandora), in situ measurements of CO2, CH4, CO, 13CH4, 13CO2, H2O and HOD made with Picarro laser cavity ring-down analyzer, in situ measurements of air pollutants NO2, NOx, SO2 and O3 using standardized EPA sensors (Figure 1). Our high frequency (seconds to minutes) measurements are continuous, with the solar spectrometers operating during daytime. The data collection began March of 2011 and ended in November 2013. We have assembled an exhaustive and unprecedented data on atmospheric composition at multiple scales that spans over 2.5 years to enable both CO2 emissions verification and fugitive CH4 leak detection [11]. To achieve this we also developed a customized atmospheric model that uses the nested grid Weather Forecast Model with chemistry (WRF-Chem). The model assimilates large-scale meteorological fields from satellites and balloon sondes (NCEP reanalysis) over the western US and downscales it to the Four Corners region. It simulates the power plant plume and its regional evolution at a very high resolution of 200m. LANL also used its specialized High GRADient (HIGRAD) model to simulate the buoyant rise and dispersion of the hot power plant plumes into the ambient atmosphere at an ultra-high resolution of 10 m. Real time in stack measurements of the CO2 and co-emitted pollutants made by Continuous Emission Monitoring System in the power plants (mandated by EPA in the US) were specified as input to the model. The results of these forward model simulations were then compared with our far field in-situ and remote atmospheric measurements to evaluate our top down CO2 and NO2 verification methods. Emission ratios (e.g. ΔNOx/ΔCO2) are easier to verify since the dispersion and dilution effects affect both species similarly- both are long-lived relative to the transport time. Finally, to evaluate the fugitive CH4 emissions we performed forward models with WRF-Chem using emissions from the global Edgar CH4 inventory in the Four Corners Region.

Fingerprinting power plant signals: The in situ and regional columnar chemical and isotopic composition of the atmosphere and its time evolution on a typical day when our instruments sampled the power plant is illustrated in Figure 2. It shows the comprehensive chemical detail with which we can quantify the plume [12]. We observe an early morning column XCO2 (mixing ratio of CO2) of 398 ppm that is 5 ppm higher than clean air background of 393 ppm. This indicates enhancements from the power plant from accumulation on the previous night. At 9:30 AM we see a clear rise in XCO2 that peaks at 407 ppm at 10:55 AM (Figure 2a) and then subsides by 11.30. This time evolution is closely tracked by all the other gases (Figures 2b-2e): X13CO2 increases by ~0.1 ppm, NO2 by 3.1 Dobson Units (DU), and XCO by ~30 ppb. The in situ measurements of CO2, 13CO2, NO2, and CO for June 6, 2012 also shown in Figure 3, indicate synchronous but much larger increases in all species at the surface that occurred between ~9 AM and 12 PM local time.

We have analyzed regional column ΔNO2/ΔCO2 ratios over a 6-month period and compared them to in situ plume ratios to show that a large and stable fraction of the regional atmosphere is polluted (70% to 75%) in the vicinity of large power plant sources in Four Corners [12]. We demonstrate that our remote column ΔNO2/ΔCO2 observations can resolve variations from regional sources with distinct

emission factors and apportion them using other signatures like SO2 and CO. Our findings offer promise for future satellite-based monitoring approaches that simultaneously measure column CO2 and NO2 at high spatial resolution and determine emission factors from space [13]. We also show the value of high frequency measurements that can be made from geostationary satellites and can better constrain effects of meteorological variability on the signals. Long-term observations of atmospheric ΔNO2/ΔCO2 above power plants would allow the verification of ΔNO2/ΔCO2 emission factor reductions from technology improvement and provide reliable constraints to estimate CO2 emission [e.g. Vulcan; 14]

Power plant signal and natural variability: Our data set, spanning 2 seasonal cycles, shows clearly the large-scale regional column increases in CO2 from the power plant emissions [Fig 3, 11]. We can use thresholds for co-emitted pollutants like CO to filter out these plumes. This filtering allows us to resolve the natural CO2 seasonal cycle in the US southwest - minima in summer due to photosynthetic sinks and maxima in winter from dormant vegetation. The seasonal amplitude of the natural CO2 cycle of about 5 ppm at Four Corners is consistent with published measurements in the region. The power plant signals we detect remotely in the column range from 2 to over 10 ppm are significant and frequent (Figure 3) with well-defined distributions that are controlled by the meteorology. Such large signals can be detected from space with ultra hyper-spectral sensors with sufficient spatial resolution for verification.

Verification of reported power plant emissions: We evaluate our hypothesis that regional-scale CO2 measurements are less sensitive than in situ point surface measurements to small-scale variability from meteorology, and better suited for emission verification. We also performed vertically resolved retrievals of CO2 from our solar spectrometer to use the much larger power plant signals in the bottom, well-mixed, boundary layer to constrain the reported emissions. Our observations are compared to forward model simulations for a particular period in Figure 4 [15]. Both models and observations reveal large CO2 (30-50ppm) increases above the background in the boundary layer (bottom to 3-km). The fluctuations in the observed CO2 are also very similar, although the model is unable to represent the high frequency features in the data. The linear regression of the observed boundary layer regional CO2 with the WRF-Chem simulated CO2 is extremely tight demonstrating that regional scale boundary layer CO2 measurements can be used to verify emissions. The observations show about 2 percent more CO2 than the model based on the in-stack emissions for this particular time (Figure 4). This demonstrates that remote sensing of regional CO2 can verify emission with an accuracy of about 2%, considerably greater than achievable by distributed in situ sensors [8, 9, 10, 15].

Fugitive Methane Leaks from Conventional Fossil Fuel Mining at Four Corners: A serendipitous discovery we made at our site was a pattern of large CH4 increases in the regional column in the morning, and the in situ data at night. We attributed this to fugitive emissions from fossil energy exploration, because ethane (C2H6) was also enhanced in the regional column at about 1-2% of CH4. This composition is consistent with the composition of thermogenic oil and gas reservoirs in the region [16]. We confirmed this with in situ analysis of the isotopic 13CH4 content of ambient air and found it to heavier than biogenic sources (e.g. landfills or ruminants) as well as the absence of co-emitted combustion signatures like CO from fires [17]. Our regional CH4 enhancements are large (20-50 ppb) in the morning and fall off in the afternoon. This behavior is consistent with the local meteorology, where the winds come from the SE in the morning bringing in air from the coal, oil and gas region, and shift to SW in the afternoon. To evaluate these "fugitive" CH4 emissions we performed model simulations using the Edgar CH4 inventory and compared it with our observations. The comparison of our data with archived satellite results over the last decade show a CH4 hot spot over the Four Corners region (Figure 5a). Furthermore, the morning enhancements in column CH4 we measure are much larger than the forward WRF model simulation, implying that observed leaks 3.3 times greater than in current Edgar emissions (Figure 5b) [18]. We find that missing fugitive CH4 leak in Four Corners could be contributing about 10% to the total national US emissions of CH4 from the natural gas sector. Furthermore, since current San Juan basin mining is dominated by coal, coal bed methane, and conventional oil and gas production, our finding demonstrates that the Edgar data are not suitable as a from which to assess changes from rising non-conventional fossil fuel extraction.

Impact on National Missions

In 2013, the President prioritized action on climate change. Recent extreme weather events like Sandy, Midwest tornadoes, and the California drought underscore the need to predict, prepare and mitigate their impacts. Extremes in weather exacerbate regional and local conflicts amongst peoples and nations and are projected to worsen with climate change. Verifying an enforceable future climate treaty will be an important global-scale US-led action, much like the nuclear test ban treaty, that would help mitigate these adverse climate change impacts on national security.

Our nation is also undergoing an energy revolution that promises energy independence by harvesting domestic oil and gas profitably using non-conventional method. However, gaps in our knowledge of fugitive CH4 leaks from such activities and a national distribution system poses unknown risks to the environment and is limiting its widespread use and public acceptance. Our work is one of the first nationwide to quantify fugitive CH4 leaks using regional scale observations and modeling and will help the nation achieve energy independence by extracting natural gas efficiently, profitably, and responsibly.

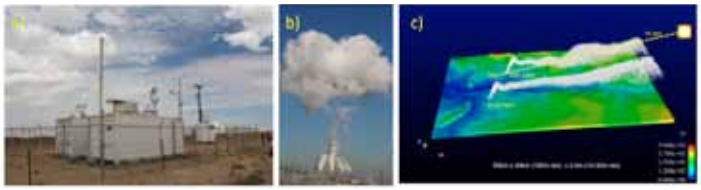

Figure 1. a) Picture of our Four Corners multi-scale monitoring site with remote and in situ instruments on 3 different sea-tainers, the site is robotic and instruments run automated, b) Picture of the San Juan power plant plume next our site and c) The LANL plume model simulates the dispersion of greenhouse gases and pollutants from the two power plants and results are compared with observations at our site to verify reported emissions from the in stack monitors.

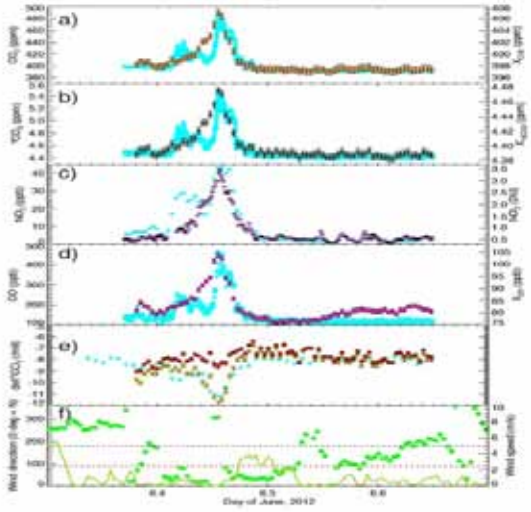

Figure 2. Example of the exquisite detail with which our multi-scale observations measure the plume on June 6, 2012 in panels a) through e) that note the specific gases and isotopes. The left scale is for the in situ sensors at the site that are sampling air at about 10m above the surface, and all the in situ data are in cyan. The right axis is for the regional scale column measurements made with our solar spectrometers. Panel f) displays the changes wind directions and speeds at our site for June 6, 2012 that explain with the time dependence of our plume observations.

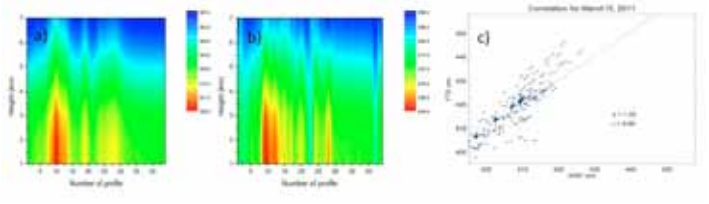

Figure 3. a) Observations of vertically resolved regional CO2 made with our solar spectrometer sequence by time (profile number) for March 15, 2011, b) Simulated regional CO2 profiles using in stack measured CO2 in the WRF model as a function of time (profile number(for the same day, c) Observed CO2 in the bottom layer versus simulated CO2 in the bottom layer show tight correlation and agree to within 2%.

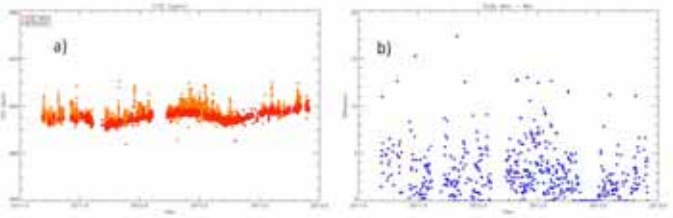

Figure 4. About 2.5 years of column regional CO2 data measured at 4 corners orange line is the data and red line is derived by filtering out the power plant signals using CO above background as a marker, b) Daily time series of the power plant signal estimated as the difference between the maximum and minimum observed for each day.

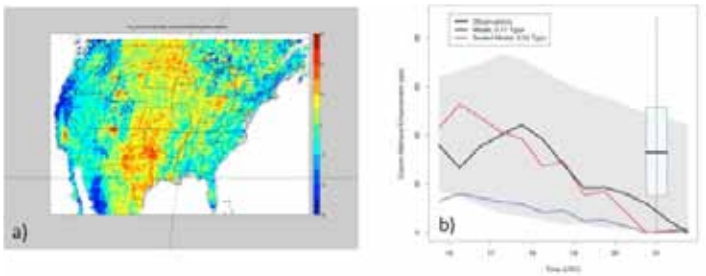

Figure 5. a) Satellite (European Space Agency, SCIAMACHY) observations of mean (2003-2009) excess column methane above background show very high (30 ppb) enhancements over Four Corners, b) Daily variation in column methane excess measured at our site (black) , simulated column methane excess using current Edgar emissions (blue) and the same scaled by 3.3 (red) that brings the mean model in line with the measurements. The shaded are is the variance in the observations and the box and whisker shows the mean and standard deviation for the observed column methane enhancement at our site.

References

1. Guan, D., Z. Liu, Y. Geng, S. Lindner, and K. Hubacek. The gigatonne gap in China's carbon dioxide inventories. 2012. Nature Climate Change. 2: 672.

2. Richter, A., J. P. Burrows, H. Nuss, C. Granier, and U. Niemeier. Increase in tropospheric nitrogen dioxide

over China observed from space. 2005. NATURE. 437 (7055): 129.

3. Kim, S. W., A. Heckel, G. J. Frost, A. Richter, J. Gleason, J. P. Burrows, S. McKeen, E. Y. Hsie, C. Granier, and M. Trainer. NO2 columns in the western United States observed from space and simulated by a regional chemistry model and their implications for NOx emissions. 2009. JOURNAL OF GEOPHYSICAL RESEARCH-ATMOSPHERES. 114: -.

4. Marquis, M., and P. Tans. Climate change - Carbon crucible. 2008. SCIENCE. 320 (5875): 460.

5. Dimotakis, P. E., B. Walker, K. K. Jonietz, and D. A. Rothman. A greenhouse gas information system: monitoring and validating emissions reporting and mitigation. 2011. A report prepared for the DOE Office of Science, , Sept. 26, 2011.

6. Pacala, S.. Verifying greenhouse gas emissions: methods to support international climate agreements. 2010. National Research Council. National Academies Press, Washington D.C., 2010.

7. Eggleston, H. S., L. Buendia, K. Miwa, T. Ngara, and K. Tanabe. 2006 IPCC Guidelines for National Greenhouse Gas Inventories. 2006. Institute for Global Environmental Strategies, Hayama, Japan. Prepared by the National Greenhouse Gas Inventories Program..

8. McKain, K., S. C. Wofsy, T. Nehrkorn, J. Eluszkiewicz, J. R. Ehleringer, and B. B. Stephens. Assessment of ground-based atmospheric observations for verification of greenhouse gas emissions from an urban region. 2012. In PROCEEDINGS OF THE NATIONAL ACADEMY OF SCIENCES OF THE UNITED STATES OF AMERICA. Vol. 109, 22 Edition, p. 8423.

9. Wunch, D., P. O. Wennberg, G. C. Toon, G. Keppel-Aleks, and Y. G. Yavin. Emissions of greenhouse gases from a North American megacity. 2009. GEOPHYSICAL RESEARCH LETTERS. 36: -.

10. Costigan, K. R., S. H. Lee, and M. K. Dubey. Simulated CO2 column concentrations of the Los Angeles Basin. Atmospheric Chemistry and Physics Discussions.

11. Dubey, M. K., R. Lindenmaier, B. Henderson, S. P. Love, J. R. Herman, Z. Butterfield, and T. A. Rahn. Multiscale Greenhouse Gas, Pollutant and Water Monitoring at Four Corners, NM: Emission Verification, Climate and Fugitive Leak Detection. Atmospheric Chemistry and Physics Discussions.

12. Lindemaier, R., M. K. Dubey, B. G. Henderson, Z. Butterfield, J. R. Herman, T. Rahn, and T. Hertel. Remote observations of power plant plume composition for emission factor verification. Atmospheric Chemistry and Physics Discussions.

13. Bovensmann, H., M. Buchwitz, J. P. Burrows, M. Reuter, T. Krings, K. Gerilowski, O. Schneising, J. Heymann, A. Tretner, and J. Erzinger. A remote sensing technique for global monitoring of power plant CO2 emissions from space and related applications. 2010. ATMOSPHERIC MEASUREMENT TECHNIQUES. 3 (4): 781.

14. Gurney, K. R., D. L. Mendoza, Y. Y. Zhou, M. L. Fischer, C. C. Miller, S. Geethakumar, and S. D. Du Can. High Resolution Fossil Fuel Combustion CO2 Emission Fluxes for the United States. 2009. ENVIRONMENTAL SCIENCE & TECHNOLOGY. 43 (14): 5535.

15. Lindenmaier, R., M. K. Dubey, F. Hase, S. H. Lee, K. R. Costigan, and B. G. Henderson. Vertical profile retrievals of CO2 from solar Fourier Transform Spectrometry: Top Down Verification of Power Plant Emissions at Four Corners, NM. Atmospheric Chemistry and Physics Discussions.

16. Lindenmaier, R., M. K. Dubey, D. Wunch, B. Henderson, and K. Costigan. Regional Column Methane and Ethane Measurements by Solar Fourier Transform Spectroscopy: Attributing Fugitive Leaks from Fossil Fuels at Four Corners, NM. Atmospheric Chemistry and Physics Discussions.

17. Arata, C., M. K. Dubey, and T. Rahn. Detection and attribution of methane sources in Four Corners, NM by a new 13CH4 cavity ring-down spectrometer. Atmospheric Chemistry and Physics Discussions.

18. Kort, E. A., C. Frankenberg, K. R. Costigan, R. Lindenmaier, and M. K. Dubey. Four Corners: North America's largest methane anomaly viewed from space. To appear in Nature.

Publications

Arata, C., M. K. Dubey, and T. Rahn. Detection and attribution of methane sources in Four Corners, NM by a new 13CH4 cavity ring-down spectrometer. Atmospheric Chemistry and Physics Discussions.

Chylek, P., M. K. Dubey, G. Lesins, J. Li, and N. Hengartner. Imprint of Atlantic multi-decadal oscillation and Pacific decadal oscillation on southwestern US Climate: Past, present and future . To appear in Climate Dynamics.

Costigan, K. R., M. K. Dubey, P. Chylek, B. Flowers, J. Reisner, A. Aiken, and L. Zhang. Combining Measurements

and Modeling to Quantify Power Plant Contributions to Atmospheric NO2 and CO2. 2011. In American Meteorological Society. (Seattle, WA, 22-27 Jan. 2011). , p. 250, 1. Seattle: AMS.

Costigan, K. R., M. K. Dubey, P. Chylek, S. P. Love, B. G. Henderson, B. A. Flowers, J. M. Reisner, T. Rahn, and C. R. Quick. Multi-Scale Science Framework for Attributing and Tracking Greenhouse Gas Fluxes at LANL's Four Corners New Mexico Test Bed. 2010. In American Geophysical Union Annual Meeting. (San Francisco, 0-13 Dec. 2010). , p. GC13D. San Francisco: AGU.

Costigan, K. R., S. H. Lee, M. K. Dubey, and D. Wunch. Simulated and observed CO2 column concentrations of the Los Angeles Basin. Atmospheric Chemistry and Physics Discussions.

Costigan, K. R., S. Lee, J. Reisner, M. K. Dubey, S. P. Love, B. G. Henderson, and P. Chylek. Muli-scale Modeling of Power Plant Plume Emissions and Comparisons with Observations. 2011. In American Geophysical Union Annual Meeting. (San Francisco, CA, 5-9 Dec. 2011). , p. A41B. San Francisco: AGU EOS.

Dubey, M. K.. Solar Fourier Transform Spectrometry in mid-near infrared and visible-ultraviolet to monitor greenhouse gas and co-emitted pollutant emissions from Four Corners, NM power plants. 2011. In European Geosciences Union General Assembly 2011. (Vienna, 3-8 April 2011). Vol. 13, p. EGU2011. Vienna: Geophysical Research Abstracts.

Dubey, M. K.. Multi-scale Measurements and Modeling to Verify CO2 and Pollutant Emissions from Four Corners, NM Power Plants. 2012. In Global Emissions Initiative: Emissions to Address Science Policy Needs . (Toulouse, France, 11-13 June 2012). , p. Web based. Boulder, CO: GEIA.

Dubey, M. K.. Multi-scale Measurements and Modeling to Verify Greenhouse Gas Emissions from Four Corners Power Plants. 2012. In 8th International Workshop on Greenhouse Gas Measurements from Space. (Pasadena, CA, 18-20 June 2012). , p. 1. Caltech: NASA-JPL.

Dubey, M. K., R. Lindenmaier, B. Henderson, S. P. Love, J. R. Herman, Z. Butterfield, and T. Rahn. Multiscale Greenhouse Gas, Pollutant and Water Monitoring at Four Corners, NM: Emission Verification, Climate and Fugitive Leak Detection. Atmospheric Chemistry and Physics Discussions.

Dubey, M. K., S. P. Love, B. G. Henderson, S. Lee, K. R. Costigan, J. Reisner, B. A. Flowers, and P. Chylek. Multi-scale Measurements and Modeling to Verify and Attribute Carbon Dioxide Emissions from Four Corners Power Plants. 2011. In American Geophysical Union Annual Meeting. (San Francisco, CA, 5-9 Dec 2011). , p. A41H. San Francisco: AGU, EOS.

Flowers, B. A., H. H. Powers, M. K. Dubey, and N. G. McDowell. Field inter-comparison of two high-accuracy fast-response spectroscopic sensors of carbon dioxide. 2011. Atmospheric Measurement Techniques Discussions. 4 (1): 5837.

Keeling, R., A. Manning, and M. Dubey. The atmospheric signature of carbon capture and storage. 2011. Philosophical Transactions of the Royal Society A - Mathematical, Physical, and Engineering Sciences. 369 (1943): 2113.

Kort, E. A., C. Frankenberg, K. R. Costigan, R. Lindenmaier, and M. K. Dubey. Four Corners: North America's largest methane anomaly viewed from space. To appear in Nature.

Lindenmaier, R., M. K. Dubey, B. G. Henderson, Z. Butterfield, J. R. Herman, T. Rahn, and T. Hertel. Remote observations of power plant plume composition for emission factor verification. Atmospheric Chemistry and Physics Discussions.

Lindenmaier, R., M. K. Dubey, F. Hase, S. H. Lee, K. R. Costigan, and B. Henderson. Vertical profile retrievals of CO2 from solar Fourier Transform Spectrometry: Top Down Verification of Power Plant Emissions at Four Corners, NM. Atmospheric Chemistry and Physics Discussions.

Pratola, M. T., J. Reisner, D. Higdon, and M. K. Dubey. Quantifying Uncertainty in CO2 Emissions with a Restricted Number of Remote Sensors: A Comparison of Model Calibration and Kalman Filtering Techniques. 2011. In American Geophysical Union Annual Meeting. (San Francisco, CA, 5-9 Dec. 2011). , p. A31B. San Francisco: AGU, EOS.

Multi-scale Dynamics of Biological Systems

Robert E. Ecke
20110435DR

Abstract

Biological systems involve dynamics in a fundamental way, spanning many orders-of-magnitude in time with corresponding multi-scale spatial structures. We helped elucidate the complex interactions of temporal and spatial degrees of freedom by using the modern tools of physical and mathematical sciences to make quantitative predictions about biological systems. Our work spans length scales from nanometers to millimeters, ranging from individual bio-molecules through complex phenomena within a single cell to the behavior of group of cells. At the molecular level, we contributed to the understanding of how the diversity of biological molecules such as DNA, RNA, or proteins arises from competing deterministic energy scales associated with chemical bonds, mechanical bending/breaking, and electromagnetic interactions and stochastic thermal energy. We have applied this insight to model proteins and membrane functions with applications to bio-fuel production. At the cellular level, we performed averaging over parts of the complex cellular bio-chemical kinetics to produce reduced models of gene regulation, expression and differentiation. We have also developed phenomenological models of cell regulatory processes that allow effective descriptions of cell functions without precise correspondence to microscopic detail.

Background and Research Objectives

Molecules consisting of many atomic units, i.e., polymers, proteins, DNA, RNA, are the building blocks of biological systems. Not only do the competing effects of chemical bond distortions, van der Waals interactions, and electrostatic interactions have approximately equal energies, these energies are comparable to the entropic free energies at biological temperatures. Thus, the molecules that define biological phenomena on the 1-100 nm scale are frustrated systems that live on a relatively shallow energy landscape. On the one hand, this shallow landscape makes individual bio-molecules relatively unstable. On the other hand, it makes them plastic and able to function as flexible and controllable nano-machines instead of as rigid particles with fixed chemical behavior. Natural bio-molecules evolve with small biases in the landscape that can make their thermodynamic behavior well defined while maintaining the functional benefits of plasticity. A grand challenge in molecular biology has been to characterize and predict structure-function relations for bio-molecules. Our goal is to address this challenge, but also to understand the role of dynamics in the control of bio-molecular function. Our specific goals at the macromolecular level were to characterize allosteric (non-local) regulation, multidimensionality and intrinsic disorder in proteins using networks models and to investigate protein-protein, protein-carbohydrate, protein/carbohydrate-membrane interactions.

Cells use networks of interacting bio-molecules to undergo differentiation, to maintain homeostasis, and to sense and respond to environmental conditions. Interactions in these networks span the 0.1-100 μm length scale, from local regions to the whole cell. The specific functions of cellular networks are diverse: metabolic networks control the transformation of molecular building blocks and energy storage/consumption; trafficking networks control the transport of bio-molecules across compartmental boundaries; cell signaling networks couple transient environmental and intracellular signals to longer-lasting covalent modifications of molecular targets; and genetic regulatory networks control production of mRNA and proteins using interactions among proteins, DNA, and the cell's transcriptional and translational machinery. Several large networks may be coupled together to give rise to quantifiable input-output behaviors. Compared to the complexity of the underlying networks, the input-output behaviors often have a simpler representation. Such cases motivate the development of accurate coarse-grained models that will be a major focus of our efforts. One of our goals represents a major challenge in modern biology: using a combination of quantitative experiments and theoretical/computational tools to

develop models of cellular networks that predict cellular behavior under new conditions. Specifically, our goals were to improve rule based bio-chemical reaction networks using novel methods and approaches from applied mathematics and statistical physics and to develop bio-informatic methods based on the physical sciences, e.g., prediction of promoters based on DNA melting properties or transcription factor binding sites.

Cells act collectively to realize macroscopic biological function. At this level of description and analysis, one needs to reduce microscopic detail and focus on cell models that incorporate the features necessary to characterize the cooperative behavior. In this area, our goals were to develop models that connect molecular states of cell signaling systems in cells to emergent cellular behavior, to model viral infection and evolution of multi-cellular complexes, and to investigate higher level motion driven by surface characteristics or asymmetries in individual bacterial movement.

Scientific Approach and Accomplishments

In the molecular area we considered the properties of disordered proteins. Many proteins fold to well-ordered structures that perform the intricate biological functions that make life possible. Some proteins, however, do not fold to an ordered state but instead are intrinsically disordered. These proteins are less well studied but important nevertheless. We developed an ideal chain model of intrinsically ordered proteins and demonstrated that one can divide the whole protein up into smaller peptides that can be independently investigated. This reduces the computational demands on creating an effective understanding of protein dynamics for disordered proteins (Sethi et al, Biophys. J. 2012). We also modeled and simulated using molecular dynamics the enzyme, organophosphorus anhydrase (OPAA), which is known to neutralize certain chemical nerve agents. The OPAA metalloprotein is a promising vehicle for therapeutic or sanitation purposes due to ease of production, but shows only limited activity to several V-type nerve agents. Molecular simulations of OPAA and several OPAA mutants could suggest mutations that would enhance activity for the V-type agents. We have developed all-atom models of OPAA using state-of-the-art parameterization approaches. The results suggest that the mutant OPAA protein shows enhanced activity to the V-type agents, a result that was confirmed by our experimental collaborators.

Using coarse-graining molecular dynamics, we extended this work to the molecular modeling of multi-protein complexes that confer antibiotic resistance in bacterial pathogens. Understanding the molecular basis of this drug resistance may help revitalize the effectiveness of our dwindling supply of antibiotics. Current work in this area is hindered by lack of a complete all-atom structure of the protein complexes that enable drug resistance in bacteria. We developed an experimental data-driven modeling pipeline which facilitates the construction of a wide range of these complexes, a first step in a broader multi-scale modeling of antibiotic drug resistance.

We explored antibody-viruses interactions. An effective vaccine for a virus such as HIV should generate antibodies that inactivate or neutralize the virus. Two major obstacles to vaccine development are immune evasion and extreme genetic diversity. By using network analysis we have identified pathways within the complicated antibody protein structures that may help understand how the virus can escape the immune response of the vaccine induced antibody proteins (Sethi et al, PLoS Comp. Bio. 2013). Also in the area of understanding HIV immune response, we performed theoretical calculations of the electrostatic surface potential (ESP) for HIV envelope (Env) proteins (Stieh, Retrovirology 2013). The Env proteins are responsible for initiating viral transmission by binding to T-cell surface proteins, and this process may be impacted by environmental factors such as salt concentration and pH. The impact of such factors is largely ignored in current HIV vaccine development efforts despite their potential significance. We performed ESP calculations that predict that binding would be enhanced or “primed” over a narrow range of pH, results that led us to hypothesize that virus transmitted from donors to recipients have more effectively primed ENV proteins (compared to the rest of the donor viral population).

We examined the conversion of biomass to a biofuel, a process that may provide an alternative and economical energy source. A challenge for this conversion is the degradation of the robust cellulose structures that give plants their structure. We have used multiple approaches to understand and improve this degradation process. In one approach, we used a coarse-grained hydrogen bound network model to study the stability of cellulose (Asztalos et al, Biotech. Biofuels 2012). We combined this with all-atom molecular dynamics simulations to develop a suite of tools to consider the multi-scale structural processes of cellulosic break down by both biochemical and thermochemical conversion (Bellesia et al, J. Phys. Chem 2011, 2012). Finally, we used comparative genomic analysis to detect and resolve inconsistencies in publicly available microbial genomes (Wall et al, PLoS Comp. Bio 2011). This approach may lead to better gene prediction by using multiple genomes for comparison.

In the area of cellular processes, we used single molecule experiments (Shepherd et al, SPIE Proc. 2012) and random-

process models (Munsky et al, Science 2012, Neuert et al, Science 2013) to characterize the gene regulation process whereby the proteins that are created from the DNA code act to regulate which further proteins are produced. This process is noisy, i.e., stochastic, and may involve small RNA as well as messenger RNA. The single molecule methods allow certain tagged molecules, illustrated in Figure 1, to be counted and their temporal variation to be determined. The models to account for these biological processes require this detailed data inputs but are already showing great promise as a tool for understanding biological function at the cellular level. We also developed a model that reproduces the temporal variation of certain types of cellular vesicles under a variety of conditions. Cells can form these vesicles to surround and degrade cellular intercellular components. The model describes accurately a mechanism of cell function that strongly impacts cell survival.

Hepatitis C viral (HCV) infection is a major cause of chronic liver disease and affects nearly 170 million people worldwide. In Figure 2, we show a schematic representation of the infection mechanism of HCV. Whereas the previous standard of care had modest effectiveness, the recent approval of two highly potent protease inhibitors and the ongoing development of dozens of direct-acting antiviral agents (DAAs) constitute a major milestone for HCV therapy. Mathematical modeling of viral kinetics under treatment has played an instrumental role in improving our understanding of virus pathogenesis and in guiding drug development. Viral kinetic models have proved useful to characterize treatment effectiveness during HCV therapy with interferon (IFN), but there are challenges associated with the standard model when fitting viral kinetic models to data. Understanding the combined effects of pharmacokinetic and viral kinetics on the performance of DAA's could provide valuable insights into its use of DAA's either individually or in combination with other DAAs in order to optimize future therapies. We developed a pharmacokinetic/viral kinetic (PK/VK) model to describe HCV RNA kinetics during treatment with DAAs. Additionally, we have developed intracellular models of HCV viral kinetics to further understand the effect of DAAs on HCV dynamics (Chatterjee et al, Antiviral Therapy 2012).

At the extracellular level that includes the behavior of populations, we developed a biogeochemical model of phytoplankton populations that leads to surprising nutrient- dependent food uptake. This model has important implications for carbon cycle models. We also created a model to investigate the influence of the environment on systems of flocking bacteria (Drocco et al, PNAS 2012) with potential application in disrupting biofilms and nanosorting devices. We discovered that barriers sort particles differentially depending on exclusion radius and on details of the flocking interaction. In particular, a model of flocking particles, it is possible to create a ratchet effect using a substrate in the form of an asymmetric barrier. In the ratchet effect, the particles preferentially translate in a particular direction even though the motive force of the individual particles has no net directionality as illustrated in Figure 3. We specifically demonstrated that for different species of flocking particles, it is possible to adjust the ratchet potential such that one species moves in one direction while the other species moves in the opposite direction. This could be a very powerful method for sorting different particle species, and could also lead to an understanding of how certain organisms can navigate complex environments. Finally, we investigated cell-to-cell communication between antiobiotic-resistant and antiobiotic sensitive cells. We learned that quorum signaling molecules control the dissemination of antibiotic resistance at the population scale, suggesting a mechanism for high antibiotic resistance of certain bacteria (Chatterjee et al, PNAS 2013).

In the area of evolutionary biology, we used mathematical models, particularly stochastic processes, to study multilevel selection. For example, a pathogen may be subject to selection within its host for faster replication. If faster replication is, however, associated with decreased host mobility and therefore lower transmission, it is unclear what the overall evolutionary trajectory of the pathogen would be. Using tools from stochastic processes and differential equations, we developed a mathematical formulation to understand the dynamics of such

Impact on National Missions

Our quantitative approach to biological dynamics at the molecular, cellular and systems level may have significant impact on applications in bio-security, energy, and health by ultimately allowing for cellular engineering, i.e., the manipulation of cellular behaviors for useful purposes. In bio-security, our work may contribute to the mitigation and detection of pathomic agents and infectious diseases. For example, such approaches may be key to the rapid development of drug therapies or vaccines against emerging bio-threats or pandemics. Another area of important impact is design of new bio-fuel processes for a sustainable energy economy. Our current work on theory and modeling of cellulosic degradation has made important contributions to this important national need. In the longer term, our multi-scale modeling from molecules to intercellular interactions may have far reaching impact on public health, bio-security, and fundamental understanding of biological systems at a quantitative and predictive level. Our approach and research efforts will contribute substantively

to that agenda in service of the LANL national security mission.

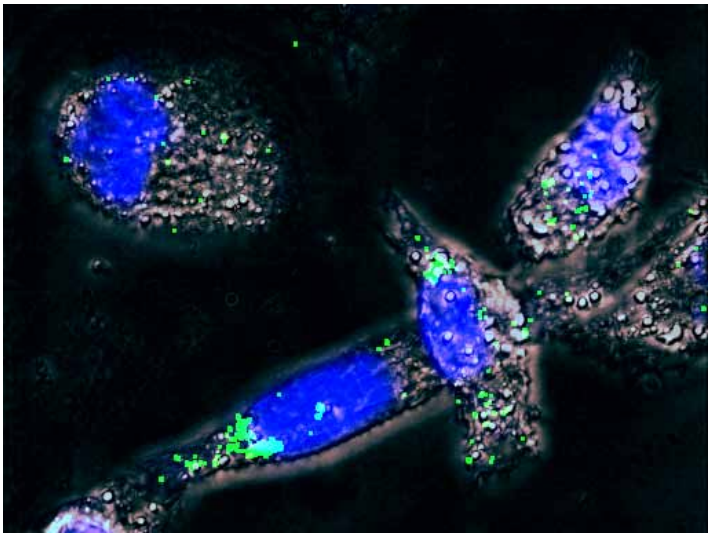

Figure 1. Fluorescent markers of biological expression of messenger RNA (mRNA) using single cell optical imaging. The green dots indicate the presence of mRNA in the cell - multiple cells are imaged.

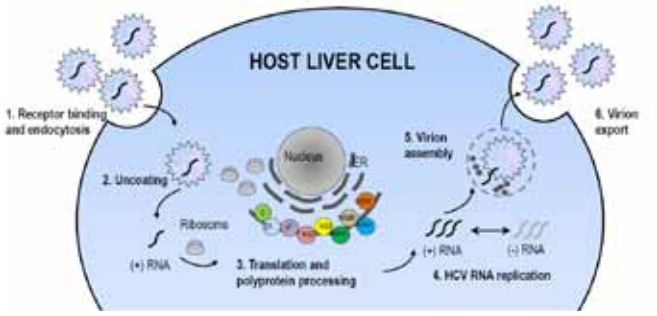

Figure 2. Schematic illustration of the life cycle of HCV in a host liver cell illustrating the mechanisms of viral infection and propagation.

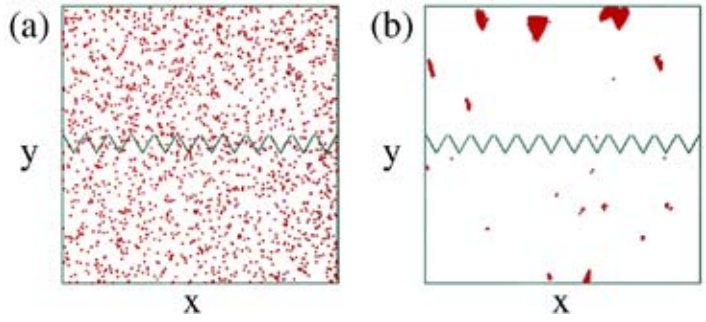

Figure 3. Images of flocking particles (bacteria) in a container with an array of funnel shapes. (a) Initial positions with an equal number of particles on either side of the barrier array. (b) After a period of time, flocking formations occur and the particles concentrate in the top chamber of the container. This results suggests that the controlled motion of certain types of active matter systems can be achieved with a fabricated substrate.

Publications

Akimov, A., and N. A. Sinitsyn. Sensitivity field for nonautonomous molecular rotor. 2011. Journal of Chemical Physics. 135 (22): 224105.

Alexandrov, B. S., V. Gelev, A. R. Bishop, A. Usheva, and K. O. Rasmussen. DNA breathing dynamics in the presence of a terahertz field. 2010. Physics Letters A. 374 (10): 1214.

Asztalos, A., M. Daniels, A. Sethi, T. Shen, P. Langan, A. Redondo, and S. Gnanakaran. A Coarse-grained Model for Synergistic Action of Multiple Enzymes on Cellulose. 2012. Biotechnology for Biofuels. 5 (1): 55.

Barua, D., W. S. Hlavacek, and T. Lipniacki. A computational model for early events in B cell antigen receptor signaling: analysis of the roles of Lyn and Fyn. 2012. Journal of Immunology. 189 (2): 646.

Barua, D., and B. Goldstein. A Mechanistic Model of Early Fc?RI Signaling: Lipid Rafts and the Question of Protection from Dephosphorylation. 2012. PLoS ONE. 7 (12).

Bellesia, G., A. Asztalos, T. Y. Shen, P. Langan, A. Redondo, and S. Gnanakaran. In silico studies of crystalline cellulose and its degredation by enzymes. 2011. Acta Crystallographica Section D-Biological Crystallography. 201 (66): 1184.

Bellesia, G., A. I. Jewett, and J. E. Shea. Relative stability of de novo four-helix bundle proteins: Insights from coarse grained molecular simulations. 2011. Protein Science. 20 (5): 818.

Bellesia, G., S. P. Chundawat, P. Langan, B. E. Dale, and S. Gnanakaran. Probing the Early Events Associated with Liquid Ammonia Pretreatment of Native Crystalline Cellulose. 2011. Journal of Physical Chemistry B. 115 (32): 9782.

Bellesia, G., S. P. S. Chundawat, P. Langan, A. Redondo, B. E. Dale, and S. Gnanakaran. Coarse-Grained Model for the Interconversion Between Native and Liquid Ammonia-Treated Crystalline Cellulose. 2012. Journal of Physical Chemistry B. 116 (28): 8031.

Chatterjee, A., J. Gudej, and A. S. Perelson. Mathematical Modeling of HCV Infection: What Can It Teach Us in the Direct Antiviral Agents Era?. 2012. Antiviral Therapy. 17: 1171.

Chatterjee, A., L. C. Cook, C. Shu, Y. Chen, D. Manias, D. Ramkrishna, G. Dunny, and W. Hu. Antagonistic self-sensing and mate-sensing signaling controls antibiotic-resistance transfer. 2013. Proceedings of the National Academy of Sciences. 110 (17): 7086.

Chatterjee, A., P. Smith, and A. Perelson. Hepatitis C Viral

Kinetics: The Past, Present, and Future. 2013. Clinics in Liver Disease. 17 (1): 13.

Chundawat, S. P., G. Bellesia, N. Uppugundla, L. D. Sousa, D. H. Gao, A. M. Cheh, U. P. Agarwal, C. M. Bianchetti, G. N. Phillips, P. Langan, V. Balan, S. Gnanakaran, and B. E. Dale. Restructuring the Crystalline Cellulose Hydrogen Bond Network Enhances Its Depolymerization Rate. 2011. Journal of the American Chemical Society. 133 (29): 11163.

Drocco, J. A., C. Reichhardt, C. J. Olson Reichhardt, and A. R. Bishop. Statics and Dynamics of Vortex Matter with Competing Repulsive and Attractive Interactions in the Presence of Periodic and Random Pinning. 2013. Journal of Physics: Condensed Matter. 25: 345703.

Drocco, J. A., E. F. Wieschaus, and D. W. Tank. The synthesis–diffusion–degradation model explains Bicoid gradient formation in unfertilized eggs. 2012. Physical Biology. 9 (5).

Drocco, J., C. J. Olson, and C. Reichhardt. Bidirectional sorting of flocking particles on asymmetric substrates. 2012. Proceedings of the National Academy of Sciences of the USA. 85 (5): 056102.

Drocco, J., C. Olson Reichhardt, and C. Reichhardt. Characterizing Plastic Depinning Dynamics with the Fluctuation Theorem. 2011. The European Physical Journal E: Soft Matter and Biological Physics. 34 (10): 1.

Drocco, J., C. Reichhardt, C. J. Olson Reichhardt, and A. R. Bishop. Statics and Dynamics of Wetting-Dewetting Transitions for Particles with Attractive Interactions on Periodic Substrates. 2012. In Optical Trapping and Optical Manipulation IX. , p. 84581j.

Drocco, J., L. M. Lopatina, C. Reichhardt, and C. J. Olson Reichhardt. Dynamics of Self-Driven and Flocking Particles on Periodic Arrays. 2012. In Optical Trapping and Optical Manupulation IX. , p. 84581i.

Dunbar, J., J. Cohn, and M. E. Wall. Consistency of Gene Starts Among Burkholderia Genomes. 2011. BMC Geonmics. 12 (1): 125.

Gao, D., S. S. Chundawat, A. Sethi, V. Balan, S. Gnanakaran, and B. Dale. Increased enzyme binding to substrate is not necessary for more efficient cellulose hydrolysis. 2013. Proceedings of the National Academy of Sciences. 110 (27): 10922.

Gnanakaran, G., J. Tian, and A. Sethi. Conformational study of quaternary epitope region of V1/V2 loop: influence of disulfide bonds and glycosylations. 2012. Retrovirology. 9 (Suppl 2).

Gnanakaran, S., M. G. Daniels, T. Bhattacharya, A. S. Lapedes, A. Sethi, M. Li, H. L. Tang, K. Greene, H. M. Gao, B. F. Haynes, M. S. Cohen, G. M. Shaw, M. S. Seaman, A. Kumar, F. Gao, D. C. Montefiori, and B. Korber. Genetic Signatures in the Envelope Glycoproteins of HIV-1 that Associate with Broadly Neutralizing Antibodies. 2010. PLoS Computational Biology. 6 (10): e1000955.

Gnanakaran, S., S. Bhattacharya, M. G. Daniels, B. F. Keele, P. T. Hraber, A. S. Lapedes, T. Y. Shen, B. Gaschen, M. Krishnamoorthy, H. Li, J. M. Decker, J. F. Salazar-Gonzalez, S. Wang, C. Jiang, F. Gao, R. Swanstrom, J. A. Anderson, L. H. Ping, M. S. Cohen, M. Markowitz, P. A. Goepfert, M. S. Saag, J. J. Eron, C. B. Hicks, W. A. Blattner, G. D. Tomaras, M. Asmal, N. L. Letvin, P. B. Gilbert, A. C. Decamp, C. A. Magaret, W. R. Schief, Y. E. Ban, M. Zhang, K. A. Soderberg, J. G. Sodroski, B. F. Haynes, G. M. Shaw, B. H. Hahn, and B. Korber. Recurrent signature patterns in HIV-1 B clade envelope glycoproteins associated with either early or chronic infections. 2011. PLoS Pathogens. 7 (9): e1002209.

Jin, M., J. Chen, X. - H. Zhang, M. Zhang, H. - Y. Li, W. - X. Cheng, N. Liu, M. Tan, T. Jiang, and Z. - J. Duan. Genetic Diversity of Noroviruses in Chinese Adults: Potential Recombination Hotspots and GII-4/Den Haag-specific Mutations at a Putative Epitope. 2011. Infection, Genetics and Evolution. 11 (7): 1716.

Jung, J., A. Sethi, T. Gaiotto, J. Han, T. Jeoh, S. Gnanakaran, and P. Goodwin. Binding and Movement of Individual Cel7A Cellobiohydrolases on Crystalline Cellulose Surfaces Revealed by Single-molecule Fluorescence Imaging. 2013. Journal of Biological Chemistry. 288 (33): 24164.

Kozer, N., D. Barua, S. Orchard, E. Nice, A. Burgess, W. Hlavacek, and A. A. Clayton. Exploring higher-order EGFR oligomerisation and phosphorylation—a combined experimental and theoretical approach. 2013. Molecular BioSystems. 9 (7): 1849.

Lemons, N. W., B. Hu, and W. S. Hlavacek. Hierarchical graphs for rule-based modeling of biochemical systems. 2011. BMC Bioinformatics. 12: 45.

Lou, C., B. Stanton, Y. C. Chen, B. Munsky, and C. A. Voigt. Ribozyme-based “insulator parts” buffer synthetic circuits from genetic context. 2012. Nature Biotechnology. 30 (11): 1137.

Lynch, R. M., R. Rong, S. Boliar, A. Sethi, B. Li, J. Mulenga, S. Allen, J. E. Robinson, S. Gnanakaran, and C. A. Derdeyn. The B Cell Response Is Redundant and Highly Focused on V1V2 during Early Subtype C Infection in a Zambian Seroconverter. 2011. Journal of Virology. 85 (2): 905.

Maienschein-Cline, M., A. R. Dinner, W. S. Hlavacek, and F. Mu. Improved Predictions of Transcription Factor Binding Sites Using Physicochemical Features of DNA. 2012. Nucleic Acids Research. : 771.

Martin, K., D. Barua, A. Kauffman, L. Westrate, R. Posner, W. Hlavacek, and J. MacKeigan. Computational model for autophagic vesicle dynamics in single cells. 2013. Autophagy. 9 (1): 70.

Morriss-Andrews, A., G. Bellesia, and J. -E. Shea. β-Sheet Propensity Controls the Kinetic Pathways and Morphologies of Seeded Peptide Aggregation. 2012. J Chemical Physics. 137 (145104).

Morriss-Andrews, A., G. Bellesia, and J. E. Shea. Effect of surface interactions on peptide aggregate morphology. 2011. Journal of Chemical Physics. 135 (8): 085102.

Munsky, B., G. Neuert, and A. van Oudenaarden. Using gene expression to understand gene regulation. 2012. Science. 336 (6078): 183.

Munsky, B., I. Nemenman, and G. Bel. Erratum: 'Specificity and Completion Time Distributions of Biochemical Processes' [J. Chem. Phys. 131, 235103 (2009)]. 2012. Journal of Chemical Physics. 136 (20): 209902.

Murphy, M. K., L. Yue, R. Pan, S. Boliar, A. Sethi, E. Karita, S. A. Allen, E. Cormier, J. E. Robinson, S. Gnanakaran, E. Hunter, X. Kong, and C. A. Derdeyn. Sequential exposure to specific antibody escape mutations may program neutralization breadth during subtype A HIV-1 infection. 2012. Retrovirology. 9 (Suppl 2).

Murphy, M., L. Yue, R. Pan, S. Boliar, A. Sethi, J. Tian, K. Pfafferot, E. Karita, S. Allen, E. Cormier, P. Goepfert, P. Borrow, J. Robinson, S. Gnanakaran, E. Hunter, X. Kong, and C. Derdeyn. Viral Escape from Neutralizing Antibodies in Early Subtype A HIV-1 Infection Drives an Increase in Autologous Neutralization Breadth. 2013. PLoS Pathogens. 9 (2).

Nemenman, I., J. R. Faeder, W. S. Hlavacek, Y. Jiang, M. E. Wall, and A. Zilman. Selected papers from the fourth annual q-bio conference on cellular information processing. 2011. Physical Biology. 8 (5): 050301.

Nemenman, I., S. Gnanakaran, W. S. Hlavacek, Y. Jiang, B. Munsky, M. E. Wall, and J. R. Faeder. The Fifth Annual q-bio Conference on Cellular Information Processing. 2012. Physical Biology. 9 (5).

Nemenman, I., W. S. Hlavacek, Y. Jiang, M. E. Wall, and A. Zilman. The third q-bio conference on cellular information processing. 2010. IET Systems Biology. 4 (6): 331.

Neuert, G., B. Munsky, R. Z. Tan, L. Teytelman, M. Khammash, and A. v. Oudenaarden. Systematic Identification of Signal-Activated Stochastic Gene Regulation. 2013. Science. 339 (6119): 584.

Olson, C. J., J. Drocco, T. Mai, M. B. Wan, and C. Reichhardt. Active matter on asymmetric substrates. 2011. Proceedings of the International Society for Optics and Photonics. 8907: 80970A.

Parthasarathi, R., G. Bellesia, S. P. Chundawat, P. Langan, B. E. Dale, and S. Gnanakaran. New insights into hydrogen bonding and stacking interactions in cellulose. 2011. Journal of Physical Chemistry A. 115 (49): 14191.

Sargsyan, O.. Analytical Framework for Identifying and Differentiating Recent Hitchhiking and Severe Bottleneck Effects from Multi-Locus DNA Sequence Data. 2012. PLoS ONE. 7 (5): e37588.

Sethi, A., B. Goldstein, and S. Gnanakaran. Quantifying Intramolecular Binding in Multivalent Interactions: A Structure-Based Synergistic Study on Grb2-Sos1 Complex. 2011. PLoS Computational Biology. 7 (10): e1002192.

Sethi, A., C. Deredyn, B. Korber, and S. Gnanakaran. Application of Molecular Dynamics and Network Analysis for Mechanistic Understanding of Allosteric Immune Escape Pathways in HIV-1. 2013. PLoS Computational Biology. : e1003046.

Sethi, A., D. Anunciado, J. Tian, D. Vu, and S. Gnanakaran. Deducing conformational variability of intrinsically disordered proteins from infrared spectroscopy with Bayesian statistics. 2013. Chemical Physics. 422: 143.

Sethi, A., D. Vu, and S. Gnanakaran. Conformational and Spectroscopic Characterization of Intrinsically Disordered Regions in Proteins. 2011. Biophysical Journal. 100 (3): 13a.

Sethi, A., J. Tian, D. Vu, and S. Gnanakaran. Identification of minimally interacting modules in an intrinsically disordered protein. 2012. Biophysical Journal. 103 (4): 748.

Shepherd, D. P., J. B. Sambur, Y. - Q. Liang, B. A. Parkinson, and A. Van Orden. In Situ Studies of Photoluminescence Quenching and Photocurrent Yield in Quantum Dot Sensitized Single Crystal TiO2 and ZnO Electrodes. 2012. Journal of Physical Chemistry C. 116 (39): 20169.

Shepherd, D. P., N. Li, E. Hong-Geller, B. Munsky, and J. H. Werner. New Tools for Discovering the Role sRNA Plays in Cellular Regulation. 2012. SPIE Proceedings. 8228: 822808.

Skar, H., R. N. Gutenkunst, K. Wilbe, A. Alaeus, J. Albert, and T. Leitner. Daily sampling of an HIV-1 patient with slowly progressing disease displays persistence of multiple env subpopulations consistent with neutrality. 2011. PLoS One. 6: e21747.

Stieh, D. J., J. L. Phillips, P. M. Rogers, D. F. King, G. C. Cianci, S. A. Jeffs, S. Gnanakaran, and R. J. Shattock. Dynamic electrophoretic fingerprinting of the HIV-1 envelope glycoprotein. 2013. Retrovirology. 10.

Tian, J., A. Sethi, B. Swanson, B. Goldstein, and S. Gnanakaran. Taste of Sugar at the Membrane: Thermodynamics and Kinetics of the Interaction of a Disaccharide with Lipid Bilayers. 2013. Biophysical Journal. 104 (3): 622.

Tian, J., A. Sethi, D. Anunciado, D. Vu, and S. Gnanakaran. A-Synuclein Interactions with Sodium Dodecyl Sulfates: A molecular dynamics study of the self-assembly system. 2012. Journal of Chemical Physics. 116 (15): 4417.

Wada, M., Y. Nishiyama, G. Bellesia, T. Forsyth, S. Gnanakaran, and P. Langan. Neutron crystallographic and molecular dynamics studies of the structure of ammonia-cellulose I: rearrangement of hydrogen bonding during the treatment of cellulose with ammonia. 2011. Cellulose. 18 (2): 191.

Wall, M. E.. Structure-function relations are subtle in genetic regulatory networks. 2011. Mathematical Biosciences. 231 (1): 61.

Wall, M. E., S. Raghavan, J. D. Cohn, and J. Dunbar. Genome majority vote improves gene predictions. 2011. PLoS Computational Biology. 7 (11): e1002284.

Whitney, J. B., P. T. Hraber, C. Ludemann, E. E. Giorgi, M. G. Daniels, T. Bhattacharya, and S. S. Rao. Genital Tract Sequestration of SIV Following Acute Infection. 2011. PLOS Pathology. 7 (2): e1001293.

Yang, J., X. Meng, and W. S. Hlavacek. Rule-based modelling and simulation of biochemical systems with molecular finite automata. 2010. IET Systems Biology. 4 (6): 453.

Yang, J., and W. S. Hlavacek. Scaffold-mediated nucleation of protein signaling complexes: Elementary principles. 2011. Mathematical Biosciences. 232 (2): 164.

Yang, J., and W. S. Hlavacek. Efficiency of reactant site sampling in network-free simulation of rule-based models for biochemical systems. 2011. Physical Biology. 8 (5): 055009.

Zhang, M., B. Foley, A. K. Schultz, J. P. Macke, I. Bulla, M. Stanke, B. Morgensterm, B. Korber, and T. Leitner. The role of recombination in the emergence of a complex and dynamic HIV epidemic. 2010. Retrovirology. 7: 25.

Zhuang, Z. Y., A. I. Jewett, S. Kuttimalai, G. Bellesia, S. Gnanakaran, and J. E. Shea. Assisted Peptide Folding by Surface Pattern Recognition. 2011. Biophysical Journal. 100 (5): 1306.

Zilman, A., V. V. Ganusov, and A. S. Perelson. Stochastic Models of Lymphocyte Proliferation and Death. 2010. PLoS One. 5 (9): e12775.

Discovery Science of Hydraulic-fracturing: Developing Innovative Concepts for Novel Working Fluids and Their Interactions with Rocks, Fractures, and High Value Hydrocarbons

Hari S. Viswanathan
20130150DR

Abstract

Shale gas is an unconventional fossil energy resource profoundly impacting US energy independence and is projected to last for at least 100 years. Production of methane and other hydrocarbons from low permeability shale involves hydrofracturing of rock, establishing fracture connectivity, and multiphase fluid-flow and reaction processes all of which are poorly understood. The result is inefficient extraction with many environmental concerns. These phenomena are part of a broader class of problems involving coupled fluid flow and fractures that are critical to other energy security areas such as shale oil, geothermal, carbon sequestration, and nuclear waste disposal as well as crack propagation in weapons applications. A science-based capability is required to quantify the governing mesoscale fluid-solid interactions, including microstructural control of fracture patterns and the interaction of engineered fluids with hydrocarbon flow. These interactions depend on coupled thermo-hydro-mechanical-chemical (THMC) processes over scales from microns to tens of meters. Determining the key mechanisms in subsurface THMC systems has been impeded due to the lack of sophisticated experimental methods to measure fracture aperture and connectivity, multiphase permeability, and chemical exchange capacities at the high temperature, pressure, and stresses present in the subsurface. In this feasibility study, we developed and prototyped the microfluidic and triaxial core flood experiments required to reveal the fundamental dynamics of fracture-fluid interactions. This will enable transformation of hydrofracturing from present ad hoc approaches to science-based strategies while safely enhancing production. Specifically, we have demonstrated an integrated experimental/modeling approach that allows for a comprehensive characterization of fluid-solid interactions and develop models that can be used to determine the reservoir operating conditions necessary to gain a degree of control over fracture generation, fluid flow, and interfacial processes over a range of subsurface conditions.

Background and Research Objectives

Shale gas is an unconventional fossil energy resource projected to last for nearly 100 years[1]. The increased availability of shale gas (i.e., methane), which produces 50% less carbon dioxide (CO2) than coal, is primarily responsible for US CO2 emissions in 2011 dropping to their lowest levels in 20 years. Production of methane and other hydrocarbons from low permeability shale involves hydrofracturing of rock, establishing fracture connectivity, and multiphase fluid-flow and reaction processes, all of which are poorly understood. The result is often inefficient extraction with many environmental concerns [1]. The fracking industry is motivated to reduce their 70 to 140 billion gallon per year water demand due to droughts in the west, a lack of deep wastewater disposal wells in the east, and possible forthcoming regulations[1]. Our objective was to demonstrate unique microfluidic and triaxial core flood experiments and integrate these with state-of-the-art numerical simulation. A secondary objective was to perform an initial evaluation of CO2-based fracturing fluids and techniques that could enhance production, greatly reduce water usage, and sequester CO2.

Fracking phenomena involve fluid-solid interactions embedded within coupled thermo-hydro-mechanical-chemical (THMC) processes over scales from microns to tens of meters [2]. Feedbacks between processes result in complex dynamics that must be unraveled if one is to predict and, in the case of unconventional resources, facilitate fracture propagation, fluid flow, and interfacial transport processes. These issues are part of a broader class of complex systems involving coupled fluid flow and fractures that are critical to energy security, such as shale oil, geothermal, carbon sequestration, and nuclear waste disposal, as well as, crack propagation in weapons and materials applications. In materials, suppressing crack propagation or limiting subsequent fluid flow may be the objective. However, while crack propagation in dry materials has been studied the role of fluids in

propagating fractures is not well understood. Predicting and controlling fracture propagation due to fluid-solid interaction would be transformative, with significant impact beyond just the hydraulic fracturing of rock.

Scientific Approach and Accomplishments

We experimentally measured and simulated a subset of the multi-scale, coupled processes from each of the research task areas described below. This involved experiments and models across the meso, core and reservoir scale. Specifically, capabilities developed and tested in this feasibility study include:

Mesoscale high-pressure microfluidics in geomaterial substrates etched at CINT: We have conducted high P microfluidics with standard silica wafers and demonstrated use of etched geomaterial (shale) at low P. Both capabilities are unique. Our experiment in Figure 1a shows super critical (sc) CO2 penetrating into a simple dead-end fracture to extract hydrocarbon at 1250 psi (water could not invade the dead-end fracture). Figure 1b shows penetration of oil (in red) in a complex fracture geometry following preferential pathways. We are now positioned to quantify benefits of scCO2 in extracting hydrocarbons from fracture-etched shale wafers (that will have realistic wetting, fracture and rock properties) at in situ pressure conditions.

Mesoscale Lattice Boltzmann modeling (LBM) of multiphase flow and particle transport: Our internationally recognized LBM code was enhanced to account for multiphase flow [3-5], multi-component chemistry [6], and phase transitions [7]. These unique LBM enhancements are required to interpret microfluidic experiments of multiphase flow, proppant transport [8], and chemical exchange kinetics [6] in mesoscale fracture systems. LBM will be further enhanced to simulate processes at the fracture-matrix interface and in nanoscale pores. The powerful combination of microfluidics and LBM sets the stage for transformative discoveries.

Core scale high-pressure tomographic triaxial coreflood experiments: We successfully demonstrated a unique apparatus for in situ generation and characterization of fractures. This allows direct measurement of fracture apertures, fluid distribution, and hydrocarbon extraction efficiency and involves a combination of x-ray (AET) and/or neutron tomography (LANSCE) and high-pressure fluid-flow experiments on shale cores subject to differential axial and confining pressure [9-10]. We have fractured dry and wet rocks under compressive loading during this feasibility study and conducted tomography ex-situ. We can now begin development of hydraulic fracturing experiments in the lab with measurement of stress, strain, and permeability while imaging 3D flow under in situ conditions.

Mesoscale simulation of crack-tip propagation dynamics: We identified how to extend our CartaBlanca [11-12] code (R&D100 winner) to resolve short timescale crack-growth dynamics due to fluid-structure interactions. We have demonstrated the capability of modeling water fracking through a simplified geomechanical model. We can now develop and calibrate models that consider rock heterogeneity and interactions among microcracks. We can also now study potential enhanced fracturing due to thermal stress at crack tips following rapid expansion of CO2. A well-calibrated physics-based geomechanical model capable of predicting scCO2 or water fracking will be a significant development in the energy industry. Several industrial collaborators have expressed strong interest in licensing such a capability.

Core scale finite-element/discrete-element modeling (FDEM) coupled with fluid flow: We have added the effect of instantaneous fluid pressure to FDEM for accurate simulation of how fluids and rock interact to generate fractures [13]. For follow-on work we can incorporate a fluid solver to characterize dynamic multiphase fluid effects. Current methods do not accurately propagate fractures across material interfaces or due to fluid pressure, so if successful, this will constitute the next generation fracture propagation model. These models will be validated using the tomography experiments.

Reservoir scale THMC fracture modeling of reservoir-scale hydrocarbon extraction: We have recently developed the capability to embed discrete fracture networks of arbitrary complexity into the massively parallel multiphase flow code PFLOTRAN [14]. Fracture networks based on upscaled FDEM results can now be used to investigate communication between generated and natural fractures linked to sweet spots in production. Through discussions with industry, we now have an extraordinary opportunity to use fracking data obtained from Apache Corp.'s science wells to benchmark our next generation models.

We have used these capabilities to define the type of studies we can now conduct at the pore, core and reservoir scales.

Pore scale: Lattice Boltzmann Models (LBM) are ideally suited to simulate pore-scale processes since they capture intra-pore geometries, complex flows, and all relevant physicochemical processes with high computational efficiency. Our models represent the state-of-the-art in existing mesoscale simulations by considering multiphase flow, multi-component chemistry, and phase transitions. In future research, LBM can be further enhanced and utilized to investigate the flow and phase behavior of natural gas within the matrix and at matrix-fracture interfaces. Fig-

ure 2a shows a microfluidic experiment in which a simple fishbone fracture pattern has been etched into Marcellus shale. A LBM of the experiment captures the fingering as the invading immiscible water displaces hydrocarbon, but bypassing the hydrocarbon in dead end fractures resulting in poor sweep (Figure 2b). At first glance, this example may appear simplistic. However, the finger width is controlled by flow rate and fluid viscosity ratios. Also, network geometry affects the finger width since fluid from the side channel narrows the finger. In proposed work, we will test the hypothesis that miscible scCO2 sweeps this network more efficiently (Figure 1a). This will require development of high-pressure geomaterial wafers that we will combine with our current high-pressure microfluidics capability. In addition, we will refine the etching process to create submicron (micron is the current limit) fracture apertures that will allow study of smaller scale interfacial dynamics. We can directly measure the interfacial area between phases that is critical to formulating relationships for multi-phase flow simulation. We can also observe phase transition behavior to benchmark EOS we will develop. Improved constitutive relationships and equations of state can also be tested at the continuum scale.

Core Scale: During this study, we have shown how fluids impact fracture patterns. In a triaxial experiment, dry anhydrite core fractured with multiple bifurcations (Figure 3a). A FDEM simulation of anhydrite results in qualitatively similar bifurcations (Figure 3b). When fluid pressure is used to initiate the fracture, enhanced propagation occurs highlighting the new ability of FDEM to capture fluid effects (Figure 3c). The simulations allow us to explore the impact of changing fluid properties and stress conditions on the same heterogeneous rock sample allowing analysis of the relation of particular fracture patterns to different working fluids. By integrating tomographic characterization of heterogeneities in the rock prior to fracturing with a detailed computational representation, we will develop more detailed and realistic FDEM results. For future work, we can further extend the FDEM to simulate multiphase fluids by coupling to a full fluid solver to create reservoir scale fracture networks.

Reservoir Scale: Figure 4 shows one workflow plan we developed in which FDEM will be validated at the core scale against triaxial experiments. The dominant fracture patterns from the FDEM technique will be used to determine the large fracture network at the reservoir scale. Micro-fracture data from FDEM will be used to obtain the effective matrix permeability at the reservoir scale.

We are unaware of any published codes or papers that present full THMC5 coupled simulations of shale gas with explicit resolution of discrete fractures and complex phase behavior. This capability is within reach through identified enhancements to PFLOTRAN: a competitive adsorption/desorption model of gas from shale; multicomponent, multiphase compositions of CO2/water/oil/gas; and coupling of flow equations with stress equations. PFLOTRAN could then be used to estimate the amount of hydrocarbon extracted using aqueous and CO2-based fracturing fluids over a wide range of T, P, stress, and fracture network properties. It will be used to optimize operating conditions that maximize hydrocarbon extraction rates, while minimizing water usage. Preliminary calculations also show that it should be possible to simultaneously enhance production and trap CO2.

Impact on National Missions

Natural gas from shale is a tremendous resource that has only recently been recognized and could lead to US energy independence3. The proposed work has the potential to reshape fracking processes of the future making them safer and more efficient. DOE is formulating calls for advanced fracking and companies such as Apache, Hess, Chesapeake and Chevron appear eager to collaborate. The Nation's fossil energy focus may soon transition from coal/CO2 sequestration to natural gas thus development and demonstration of new experimental and computational capabilities in this area, as was accomplished in this feasibility study will undoubtedly prove important in facilitating that transition.

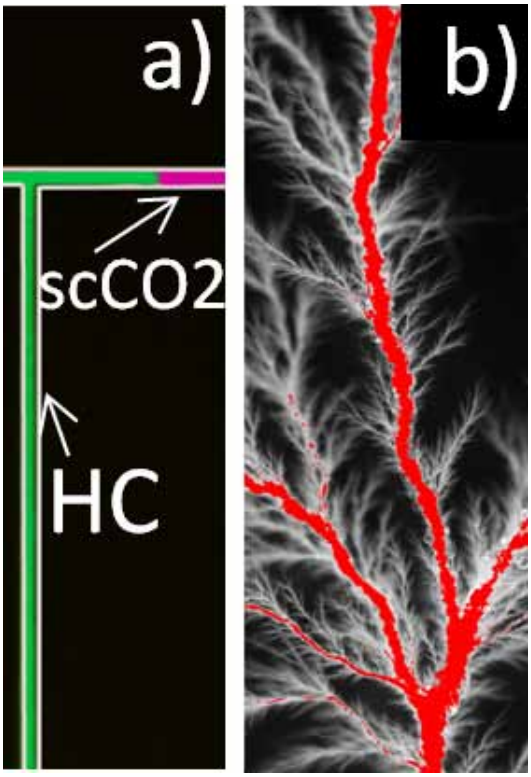

Figure 1. a) high pressure wafer, b) vascular network.

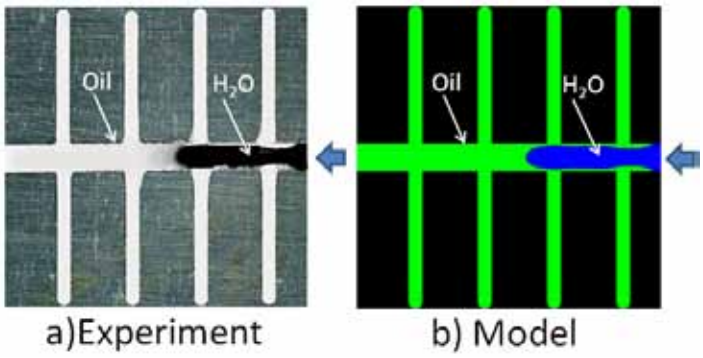

Figure 2. Displacement of hydrocarbon by water in a shale wafer.

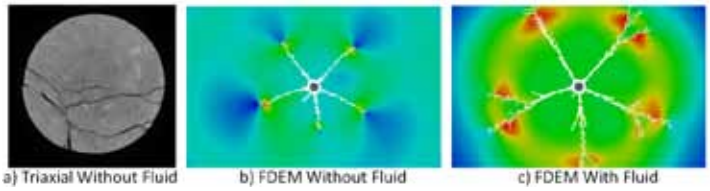

Figure 3. Triaxial experiments and FDEM models of fracture propagation in anhydrite. Colors show velocity of rock matrix movement (blue=low velocity and red=high velocity) due to fracture propagation.

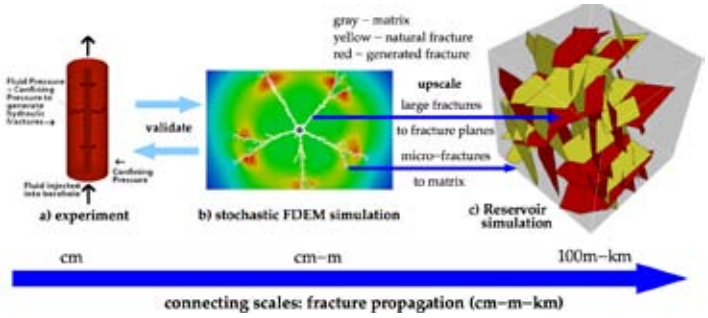

Figure 4. Work flow for benchmarking FDEM against triaxial experiment and then upscaling fracturing propagation statistics to planar discrete fracture networks and rock matrix at the reservoir scale.

References

1. Moniz, E. J., H. D. Jacoby, and A. J. Meggs. The future of natural gas. 2012. An Interdisciplinary MIT Study.

2. Study of the potential impacts of hydraulic fracturing on drinking water resources progress report. 2012. EPA 601/R.

3. Porter, M. L., E. T. Coon, Q. Kang, J. D. Moulton, and J. W. Carey. Multicomponent interparticle-potential lattice Boltzmann model for fluids with large viscosity ratios. 2012. Physical Review E.. 86: 1231.

4. Liu, H., A. J. Valocchi, and Q. Kang. A three-dimensional lattice Boltzmann model for immiscible two-phase flow simulations. 2012. Physical Review E. 85: 246.

5. Middleton, R., G. Keating, P. Stauffer, A. Jordan, H. Viswanathan, Q. Kang, and J. W. Carey. The cross-scale science of CO2 capture and storage: from pore scale to regional scale. 2012. Energy and Environmental Sciences. 5: 7328.

6. Kang, Q., P. C. Lichtner, H. Viswanathan, and A. I. Abdel-Fattah. Pore scale modeling of reactive transport involved in geologic CO2 sequestration. 2010. Transport in Porous Media. 82: 197.

7. Chen, L., and Q. Kang. Pore-scale modeling of multiphase reactive transport with phase transition and dissolution-precipitation in closed systems. . To appear in Physical Review E..

8. Connington, K., Q. Kang, H. S. Viswanathan, A. I. Abdel-Fattah, and S. Chen. Peristaltic particle transport using the lattice Boltzmann method. 2009. Physics of Fluids. 21: 301.

9. Carey, J. W., R. Svec, R. Grigg, J. Zhang, and W. Crow. Experimental investigation of wellbore integrity and CO2-brine flow along the casing-cement microannulus. 2010. International Journal of Greenhouse Gas Control. 4: 272.

10. Newell, D. L., and J. W. Carey. Experimental evaluation of wellbore integrity along the cement-rock boundary. 2013. Environmental Science and Technology. 47: 276.

11. Yang, D., R. Currier, and D. Z. Zhang. Ensemble phase averaged equations for multiphase flow in porous media, part 1: the bundle-of-tubes model. 2009. International Journal of Multiphase Flow. 35: 628.

12. Zhang, D. Z.. Ensemble phase averaged equations for multiphase flows in porous media, part 2: a general theory. 2009. International Journal of Multiphase Flow. 35: 640.

13. Zubelewicz, A.. Liquid-liquid-solid transitions in viscoelastic liquids. 2013. Sci. Reports. 3: 320.

14. Hammond, G. E., P. C. Lichtner, C. Lu, and R. T. Mills. PFLOTRAN: reactive flow and transport code for use on laptops to leadership-class supercomputers. 2012. In Groundwater reactive transport models. By Zhang, F., G. T. Yeh, and J. C. Parker. , p. 141. New York: Bentham Books.

Publications

Chaudhuri, A., H. Rajaram, and H. Viswanathan. Early-stage Hypogene Karstification in a Mountain Hydrologic System: A Coupled Thermo-Hydro-Chemical Model

Incorporating Buoyant Convection. To appear in Water Resources Research.

Zubelewicz, A.. Liquid-liquid-solid transitions in viscoelastic liquids. 2013. Scientific Reports. 3: 234.

Defeating Bacterial Multi-drug Resistance: An Experimentally Driven Multi-scale Study of Efflux Machinery

Sandrasegaram Gnanakaran
20130183DR

Abstract

Bacterial multi-drug resistance efflux pumps are complex molecular machines that expel multiple drugs and antibiotics. They also influence important genetic and cellular processes to confer additional drug resistance. We developed an initial mathematical framework to integrate structural, genetic, and cellular processes to understand how efflux pumps work. To test our model, we carried out measurements on the time-kill behavior of wild-type Pseudomonas aeruginosa as well a mutant strain lacking efflux pumps. The integrated model predicts the same quantitative behavior as the measurements and suggests specific experimentally testable mechanisms that are important for drug efflux. During this feasibility study, we have also determined the crystal structure of the inner membrane E. coli efflux protein and constructed a three-dimensional structural model of the entire efflux pump machinery of multiple organisms.

Background and Research Objectives

At present we rely heavily on antibiotics for the treatment of bacterial infections encountered in public health and bio-threat scenarios. However the rapid emergence of antibiotic-resistant bacteria poses a major hurdle in the treatment of such infections. Membrane protein complexes, called the multi-drug resistance (MDR) efflux pumps, are the most important machinery that bacteria utilize to pump out almost all types of antibiotics before they can act on their targets [1]. Although all bacteria express these MDR efflux pumps, very little is known about how they work. In this project, we develop a multi-scale model to integrate structural, genetic, and cellular processes that underlie the functions of MDR efflux pumps in antibiotic resistance (Figure 1). This knowledge will provide us with important clues for designing drugs that block the function of the MDR efflux pumps and rescue the activities of current drugs.

Bacteria utilize both genetic mechanisms and physical properties to resist the action of antibiotics. Genetic mechanisms include escape mutations on the target gene or acquisition of resistant genes by horizontal gene transfer. Physical processes include bacterial membrane structures or the impenetrable layer of biomolecules around a consortium of bacteria called biofilms. The MDR efflux pumps represent a special case in which physical processes and genetic mechanisms are coupled. It appears that the MDR efflux pumps not only pump out antibiotics but also genetically regulate the formation of biofilms. We will focus on a class of efflux pumps (the resistance nodulation cell division or RND pumps), which are primarily responsible for multidrug resistance in gram-negative bacteria. These tripartite efflux pumps are assembled from three proteins: an inner-membrane protein, an outer-membrane protein, and a periplasmic protein that connects the two. The three genes encoding these proteins form a cluster with an upstream switch acting as a regulator.

Bacteria detect the presence of an antibiotic inside the cell. Responding to this signal, they increase the production of efflux pumps that expel the drug [2] and decrease the production of porins that allow entry of the drug [3]. The production of efflux pumps is controlled both by local regulator proteins that turn on expression of the pump genes, and by global regulator proteins that affect expression of many genes including porins. The detailed mechanisms of how drugs interact with and control drug efflux systems will allow an understanding of how the bacteria respond to the threat of antibiotics. Efflux pumps can also transport quorum-sensing molecules which, when exported from one cell, induce neighboring cells to produce a new set of proteins for biofilm production allowing bacterial growth, virulence, and survival in the presence of antibiotics [5-6]. It is our hypothesis and the research objective that an experiment-based model that integrates structural, genetic, and cellular mechanisms to predict drug uptake and survival will provide a quantitative understanding of how efflux pumps and the associated genetic and cellular systems defend bacteria

against drugs and antibiotics. In this feasibility study, the research goal is to develop such a quantitative integrated framework for a model organism, Pseudomonas aeruginosa, based on published data and new measurements.

Scientific Approach and Accomplishments

We have developed a multi-scale model of a bacterial MDR efflux system using coupled ordinary differential equations that integrate structural, genetic, and cellular processes. The model describes the dynamics of cell state, growth, and death; antibiotic uptake; and efflux regulation. Each of these behaviors is precisely quantified using variables that correspond to experimental observables: live cells, dead cells, and antibiotic levels using fluorescence assays, and pump levels using mRNA sequencing and affinity reagents. In this way, the model is firmly grounded in the experimental data. Our model is a precise mathematical representation of a set of hypotheses or assumptions concerning the MexAB RND efflux system of P. aeruginosa. The model is designed to enable iterative refinement and may be adapted to predict any of the observed system behaviors for wild type or mutant cells.

To test our model, we carried out measurements on the death of wild-type Pseudomonas aeruginosa as well a mutant strain with a deficient efflux system, in the presence of an antibiotic (ciprofloxacin) that blocks a bacterial DNA gyrase during replication [6]. P. aeruginosa has several tripartite efflux pumps. Of particular interest is the MexAB-OprM pump because it has been shown to transport both ciprofloxacin and quorum sensing acetyl homoserine lactones [7]. Figures 2A and 2B show fits (lines) of our integrated model to the measurements of intracellular antibiotic (Figure 2A) and number of dead P. aeruginosa (Figure 2B) as a function of time. Figure 2A shows that the bacteria with an intact system (PAO1) took up antibiotic rapidly (red points) and then pumped it out rapidly. This is modeled with an intrinsic antibiotic uptake rate and an antibiotic-induced efflux rate that rapidly increases after antibiotic enters the cells (green curve). A mutant lacking the pumps (⍰MexAB-OprM) reveals two differences; a lower intrinsic uptake rate and much slower efflux of the antibiotic (blue points and purple curve). There is good agreement between model and experiment, indicating that our model provides insight into MDR efflux mechanisms involved in the dynamics of cell death and antibiotic uptake for P. aeruginosa.

Also as part of our feasibility project, we determined the crystal structure of the inner membrane E. coli efflux protein, AcrB, in complex with the antibiotic Linezolid (an inhibitor of bacterial protein synthesis) [8]. We found that three Linezolid molecules bind to the AcrB trimer in the periplasmic cavity. The residues 384-387 from each AcrB protomer are close to the bound Linezolid. The structure suggests that drug binding causes a conformational change in residues 670-675 (Figure 3). The drug binding and associated conformational changes we have identified will guide MD simulation studies for determining the mechanism of drug efflux through the tripartite complex. Preliminary MD simulations are underway that consider key mutations in this loop, seeking to find how they affect accessibility and binding.

We have constructed a structural model [9] of the P. aeruginosa tripartite MexAB-OprM complex based upon the crystal structures of the individual components MexA, MexB, and OprM, energetic calculations of the membrane-bound complex, and distance constraints between components derived from crosslinking studies. As shown in Figure 4, the three-dimensional structure of the complex spans the inner-membrane, periplasm, and outer-membrane of the bacteria. The three-dimensional structure of the tripartite complex sheds insight into molecular mechanisms of drug binding and export illustrated in Figure 1, and enables us to perform molecular dynamics simulations to quantify and develop more complex hypotheses.

Impact on National Missions

Multi-drug resistance poses a major hurdle in management of bacterial diseases encountered in both bio-threat and public health scenarios. Development of a capability in understanding and countering multi-drug resistance in bacteria will be directly relevant to the US and LANL missions in bio-security. This project is directed at the development of an integrated modeling capability that relies on appropriate and relevant experimental measurements to address multi-drug resistance. We have been able to measure and model the functional mechanism, genetic regulation, and cellular effects of the multi-drug resistance efflux pumps that offer resistance against all clinically approved antibiotics.

In this project, we developed an initial framework to couple processes at multiple length and time scales: the nanometer molecular machine that pumps out drugs in seconds to minutes; the induction of gene clusters of multiple genes spanning hundreds of nanometers and their induction occurring over hours; and the formation of biofilm covering several microns over days. Such a capability for integrated modeling of a complex adaptive molecular transport system will have broad applications in biosecurity, biofuel production, and clearance of toxic materials by both microbial and human cells.

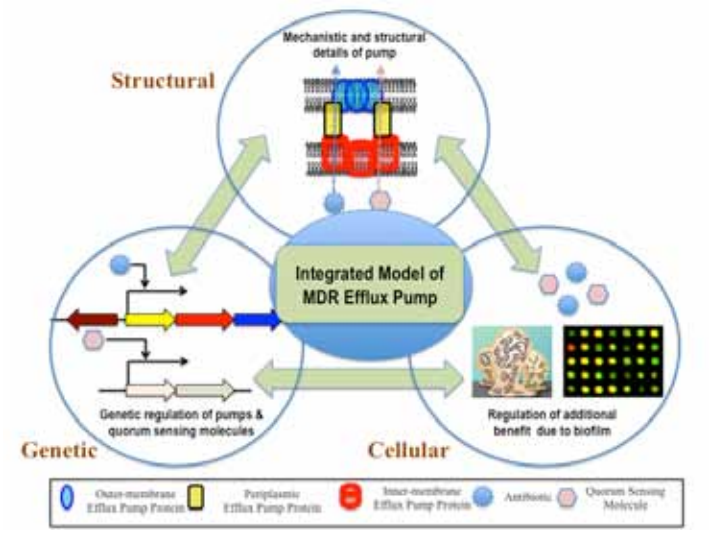

Figure 1. Schematic representation of the structural, genetic, and cellular processes associated with the MDR efflux pump

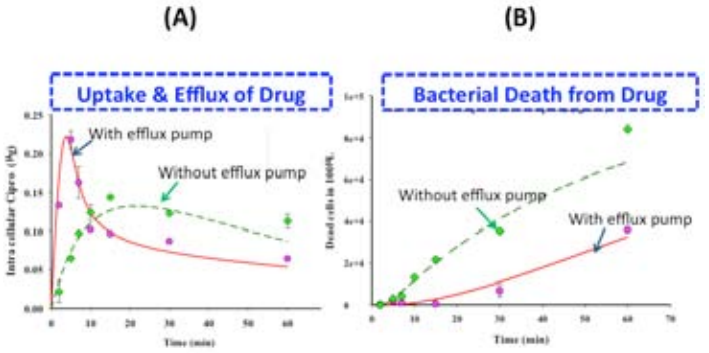

Figure 2. Fit of the theoretical curve with experimental data for normal P. aeruginosa and an efflux mutant: (A) intracellular level of ciprofloxacin; (B) mortality curve as a function of time

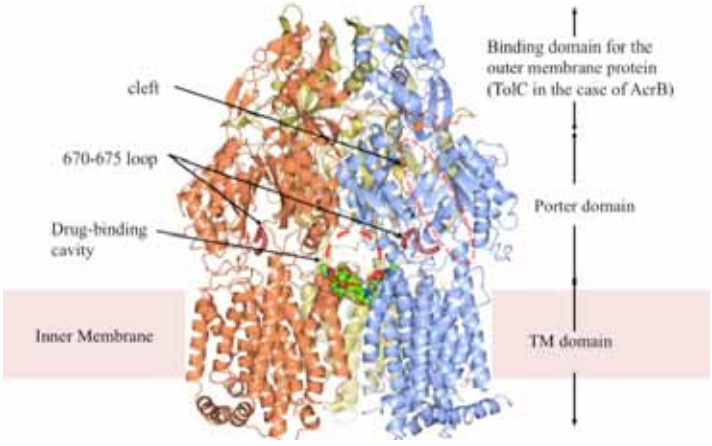

Figure 3. Crystal structure of the E. coli AcrB trimer bound to 3 molecules of Linezolid. The binding domain for the outer-membrane TolC is located at the top. The drug binding cavity is on the periplasmic side just at the end of the trans-membrane helices. The porter domain connects the TolC binding domain and the drug binding cavity. The location of the 670-675 \ loops that undergo conformation change is shown

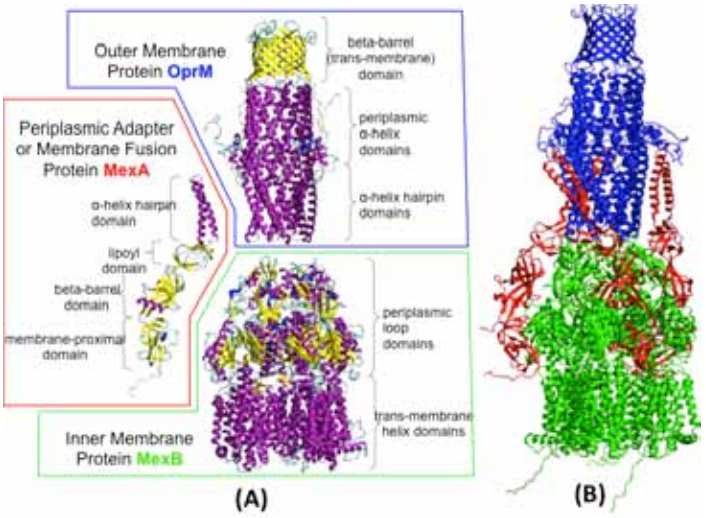

Figure 4. (A) Experimentally determined structures of different components of efflux pump. (B) The structure of the entire efflux pump machinery modeled using a geometry based computational method that takes into account known constraints from measurements.

References

1. Nikaido, H., and J. M. Pages. Broad-specificity efflux pumps and their role in multidrug resistance of Gram-negative bacteria. 2012. FEMS MICROBIOLOGY REVIEWS. 36 (2): 340.

2. Martins, A., C. Iversen, L. Rodrigues, G. Spengler, J. Ramos, W. V. Kern, I. Couto, M. Viveiros, S. Fanning, J. M. Pages, and L. Amaral. An AcrAB-mediated multidrug-resistant phenotype is maintained following restoration of wild-type activities by efflux pump genes and their regulators. 2009. INTERNATIONAL JOURNAL OF ANTIMICROBIAL AGENTS. 34 (6): 602.

3. Davin-Regli, A., J. M. Bolla, C. E. James, J. P. Lavigne, J. Chevalier, E. Garnotel, A. Molitor, and J. M. Pages. Membrane Permeability and Regulation of Drug "Influx and Efflux" in Enterobacterial Pathogens. 2008. CURRENT DRUG TARGETS. 9 (9): 750.

4. Hoiby, N., T. Bjarnsholt, M. Givskov, S. Molin, and O. Ciofu. Antibiotic resistance of bacterial biofilms. 2010. INTERNATIONAL JOURNAL OF ANTIMICROBIAL AGENTS. 35 (4): 322.

5. Minagawa, S., H. Inami, T. Kato, S. Sawada, T. Yasuki, S. Miyairi, M. Horikawa, J. Okuda, and N. Gotoh. RND type efflux pump system MexAB-OprM of pseudomonas aeruginosa selects bacterial languages, 3-oxo-acyl-homoserine lactones, for cell-to-cell communication. 2012. BMC MICROBIOLOGY. 12: -.

6. Bruchmann, S., A. Dotsch, B. Nouri, I. F. Chaberny, and

S. Haussler. Quantitative Contributions of Target Alteration and Decreased Drug Accumulation to Pseudomonas aeruginosa Fluoroquinolone Resistance. 2013. ANTIMICROBIAL AGENTS AND CHEMOTHERAPY. 57 (3): 1361.

7. Venturi, V.. Regulation of quorum sensing in Pseudomonas. 2006. FEMS MICROBIOLOGY REVIEWS. 30 (2): 274.

8. Hung, L. W., H. Kim, S. Murakami, G. G. Gupta, C. Y. Kim, and T. Terwilliger. Crystal structure of AcrB complexed with linezolid at 3.5 Å resolution . 2013. J. Struct. Funct. Genomics. 14 (2): 71.

9. Phillips, J., and G. S. Gnanakaran. Coarse-Grained Simulations of the MexAB-OprM Multidrug Resistance Efflux Pump. 2013. BIOPHYSICAL JOURNAL. 104 (2): 286A.

Publications

Hung, L. W., H. Kim, S. Murakami, G. G. Gupta, C. Y. Kim, and T. C. Terwilliger. Crystal structure of AcrB complexed with linezolid at 3.5 Å resolution . 2013. Journal of Structural and Functional Genomics . 14 (2): 71.

Phillips, J., and G. S. Gnanakaran. Coarse-Grained Simulations of the MexAB-OprM Multidrug Resistance Efflux Pump. 2013. BIOPHYSICAL JOURNAL. 104 (2): 286A.

Identifying, Creating, and Controlling Functional Hotspots in DNA

Boian Alexandrov
20110516ECR

Introduction

Transcription, i.e. the decryption of genetic code, is the biological function that governs the production of the biomolecules necessary to the cell. The ability to understand and control transcription yield: new biotechnological methods for pharmaceutical drugs, nutrients, bioenergy, biomaterials – in short, control over living matter. Transcription itself is controlled by various proteins (transcription factors), whose binding to the DNA double-helix enhance or suppress the process. Our prior work has already established that transcriptional start sites (TSSs) and transcription-factor-binding sites (TFBSs) possess enhanced local DNA breathing dynamics, where the two strands of DNA move back and forth, opening temporary gaps. When DNA local transient openings (bubbles) fall at the TSS or TFBS regions, we call them functional hotspots. Importantly, the patterns of the hotspots are strongly interconnected with the function of the TSS or TFBS. We have demonstrated this interconnection theoretically using computer simulations to identify hotspots for several TSSs and TFBSs, and experimentally by: i) designing DNA single-point mutations to silence TSS dynamics (i.e. by destroying functional hotspots), which led to suppressed transcription without affecting transcription-factor binding; ii) introducing an artificial mismatch opening at a TSS site (i.e. by creating functional hotspots), which led to bidirectional transcription initiation in the absence of basal transcription factors. Additionally, we have demonstrated theoretically that exposure to terahertz (THz) radiation can resonantly induce DNA hotspots, potentially enabling control of the local breathing dynamics, and hence control of gene expression.

Benefit to National Security Missions

Los Alamos National Laboratory has a large interest in genomic studies, development of modern statistical learning computational tools, and advanced knowledge on cell biological functions in connection with bioenergy, biomaterials of the future, and for environmental and safety concerns. Our tools for predicting promoters and transcription factor binding sites as well as for controlling genomic functional elements will be a timely and impactful contribution to the rapidly growing field of biotechnology and functional genomics. The capabilities provided by our project will provide unique assets and give LANL a significant advantage in genomic, biomaterials, and bioenergy science. This development will enhance LANL's capability to be at the forefront of these fields, and to harness vast databases of emerging genomic data, and gain control of biological function in the service of national missions in security, energy, and health.

Progress

We completed our transcription factors binding sites (TFBS) recognition protocol and developed a technology for transcription start sites (TSS) and TFBS modifications, based on modeling of DNA vibrational hotspots. The technology has a novel capability to predict effects of various DNA base modifications. We applied the recognition protocol and the modification technology to the genomic binding sites of two well-known transcription factors.

Specifically, we investigated in detail the relation between DNA breathing and the binding of Fis protein, which is known to bind at highly variable DNA sequences in Escherichia coli and Salmonella typhimurium. Leveraging our modification-prediction technology, we designed various Fis binding sites, using various nucleotide modifications, such as: mismatches; methylations; and substitutions in DNA segments with known interaction with Fis protein. In each case, our intention was to make the DNA hotspots either closer to or farther from the pattern of a typical hotspot of a "strong" Fis binding site, derived by our technology. Our predictions have been validated experimentally.

We applied our computational framework to recognize YY1 binding sites in vivo, by deriving a specific DNA breathing profile of the transcription factor YY1 binding sites. By computer simulations we indentified genomic YY1-binding sites and found that the genomic flanking sequence variations and single nucleotide polymorphisms, outside the YY1 binding motif, are capable of exerting long-range effects on DNA breathing and hence predetermine the YY1 binding. Our conclusions and predictions have been confirmed in the experiments reported in a joint-work with collaborators from Harvard Medical School. The research resulted in an article published in Nucleic Acid Research.

Led by our research on the interrelation between transcription factors binding and DNA dynamics, we prepared an Invention Disclosure in the LANL/IDEA. Our proposal was approved and an Invention Disclosure Record has been created in the laboratory docketing system.

We used our novel TSS and TFBS recognition protocol to annotate the regulatory sites in the whole genome of a novel phage, DANTE, sequenced by collaborators from Brown University. Our work was reported at, National scientific competition at HHMI.

We finished a detailed analysis of our second large set of terahertz (THz) irradiation experiments of mouse stem cells at MPA-CINT and NHMFL/LANL, and of the biological experiments conducted at Harvard Medical School and at UNMKUGR Genomic Center. Specifically we analyzed the gene expression data from 18 gene chip micro-assays, and additionally the RT-PCR data obtained for 23 selected genes, from the irradiation of cellular cultures of mouse mesenchymal stem cells irradiated by two different terahertz sources - one with single frequency and the other with broadband frequency, and with ultrafast pulses beam.

We demonstrated that the insignificant differential expression of heat shock and stress related genes as well as our temperature measurements implied a non-thermal response. The microarray survey and RT-PCR experiments demonstrate that at different irradiation conditions distinct groups of genes are activated. Stem cells irradiated for 12 hours with the broadband THz source exhibit an accelerated differentiation toward adipose phenotype, while the 2-hour (broadband or SF) irradiation affects genes transcriptionally active in pluripotent stem cells. Phenotypic and gene expression differences suggest that the THz effect depends on irradiation parameters such as duration, frequency, and type of THz source, and additionally on the level of stem cell differentiation. Computer simulations of the core promoters of two pluripotency markers reveal association between gene upregulation and propensity for DNA breathing. We propose that THz radiation has potential for non-contact control of cellular gene expression. The results were generalized in the Nature Magazine.

Future Work

We will finish our analysis of the annotation of the whole genome of the new phage DANTE, sequenced recently in Brown University. Next, with our collaborators from Harvard Medical School we will experimentally validate some of the annotations predicted by our simulations. The validation experiments will verify and establish our technology. Further, we plan to apply the developed genomic method for prediction of transcriptional start sites and transcription factor binding sites, to another whole genome of the phage SmallFry, recently sequenced in Brown University. The two whole phage genomes annotations will ascertain the ability of our method for functional phage predictions based on DNA hotspots dynamics calculations. Additionally, we will apply our new computational technology for design of transcription factor binding sites with various strengths, to another transcription factor, v-Myb, which is important in plants, algae, and mammalian gene expression. Specifically, we will design DNA segments with various modified binding affinities based on computer simulations. We will use base pairs substitutions and nucleotide methylations. Our new predictions will be verified by measuring the binding affinities to the designed DNA sequences via EMSA experiments in Hong-Geller laboratory at LANL. Additionally, we will perform statistical analysis of the available genomic data for Myb-DNA binding in order to verify the prediction of our simulations in vivo.

Conclusion

We expect to develop functional hotspot recognition protocols, which allow TSS and TFBS prediction significantly out-performing the available state-of-the-art tools, and thus help us understand how DNA does its job. Further, we expect to develop a methodology that will enable the design of hotspots so we can control gene expression. Finally, we expect to validate the hypothesis that THz irradiation has a frequency-specific effect on DNA functional hotspots that can be used for gene expression control.

Publications

Alexandrov, B. S., A. R. Bishop, L. Kalaydjieva, I. S. Kohane, K. O. Rasmussen, A. Usheva, and V. I. Valtchinov. DNA Conformation Dynamics and Human Diseases. 2012. LANL ADTSC Science Highlights 2012, LA-UR 12-20429.

Alexandrov, B. S., A. R. Bishop, N. Zahariev, and I. Kostadinov. Dispersed stable states spectrum of the wave equation with space-time periodic potential. 2013. Europhysics Letters. 103: 50001.

Alexandrov, B. S., K. O. Rasmussen, A. R. Bishop, A. Usheva, L. B. Alexandrov, S. Chong, Y. Dagon, L. G. Booshehri, C. H. Mielke, M. L. Phipps, J. S. Martinez, H. T. Chen, and G. Rodriguez. Non-thermal effects of terahertz radiation on gene expression in mouse stem cells. 2011. Biomedical Optics Express . 2 (9): 2679.

Alexandrov, B. S., K. O. Rasmussen, A. R. Bishop, and A. Usheva. Protein-DNA binding and breathing dynamics of DNA. 2013. JOURNAL OF BIOMOLECULAR STRUCTURE & DYNAMICS. 31: 49.

Alexandrov, B. S., M. L. Phipps, L. B. Alexandrov, L. G. Booshehri, A. Erat, J. Zabolotny, C. H. Mielke, H. T. Chen, G. Rodriguez, K. O. Rasmussen, J. S. Martinez, A. R. Bishop, and A. Usheva. Specificity and Heterogeneity of Terahertz Radiation Effect on Gene Expression in Mouse Mesenchymal Stem Cells. 2013. SCIENTIFIC REPORTS. 3: -.

Alexandrov, B. S., V. G. Stanev, A. R. Bishop, and K. O. Rasmussen. Anharmonic dynamics of intramolecular hydrogen bonds driven by DNA breathing. 2012. PHYSICAL REVIEW E. 86 (6): -.

Alexandrov, B. S., Y. Fukuyo, M. Lange, N. Horikoshi, V. Gelev, K. O. Rasmussen, and A. R. Bishop. DNA Breathing Dynamics Distinguish Binding from Nonbinding Consensus Sites for Transcription Factor YY1 in cells. 2012. Nucleic Acids Research. 40 (20): 10116.

Alexandrov, B., V. Valtchinov, L. Alexandrov, V. Gelev, Y. Dagon, J. Bock, I. Kohane, K. Rasmussen, A. Bishop, and A. Usheva. DNA Dynamics Is Likely to Be a Factor in the Genomic Nucleotide Repeats Expansions Related to Diseases. 2011. PLOS ONE. 6 (5): e19800.

Alexandrov, Boian S., Amy L. Bauer, Alan R. Bishop, F. Mu, E. Hong-Geller, K. Nowak-Lovato, Kim Ø. Rasmussen, and Ludmil B. Alexandrov. New Insights into Protein-DNA Binding from Simulations of DNA Breathing Dynamics. 2013. Los Alamos National Laboratory Associate Directorate for Theory, Simulation, and Computation (ADTSC) LA-UR 13-20839.

Bishop, A. R., K. O. Rasmussen, A. Usheva, and B. S. Alexandrov. Entropy–Driven Conformations Controlling DNA Functions. 2012. In Disorder and Strain-Induced Complexity in Functional Materials, Springer Series in Materials Science. Edited by Kakeshita, T., T. Fukuda, A. Saxena, and A. Planes. Vol. 148, 1 Edition, p. 273. Berlin: Springer.

Bock, J., Y. Fukuyo, S. Kang, M. Lisa. Phipps, L. Alexandrov, K. Rasmussen, A. Bishop, E. Rosen, J. Martinez, H. Chen, G. Rodriguez, B. Alexandrov, and A. Usheva. Mammalian Stem Cells Reprogramming in Response to Terahertz Radiation. 2010. PLoS One. 5 (12): Article No.: e15806.

Jablensky, A., D. Angelicheva, G. J. Donohoe, M. Cruickshank , D. N. Azmanov, W. D. Morris, C. S. Weickert, K. W. Carter, D. Chandler, B. S. Alexandrov, A. Usheva, B. Morar, P. L. Verbrugghe, A. Filipovska, O. Rackham, A. R. Bishop, K. O. Rasmussen, M. Dragovic, M. Cooper, M. Phillips, J. Badcock, E. Bramon-Bosch, O. P. Almeida, L. Flicker, M. Gill, A. Corvin, S. Macgregor, and L. Kalaydjieva. Promoter Polymorphisms in two Overlapping 6p25 Genes Implicate Mitochondrial Proteins in Cognitive Deficit in Schizophrenia. 2012. Mol Psychiatry. 17 (12): 1328.

Maniadis, P., B. S. Alexandrov, A. R. Bishop, and K. O. Rasmussen. Feigenbaum cascade of discrete breathers in a model of DNA. 2011. PHYSICAL REVIEW E. 83 (1, 1): 011904.

Nowak-Lovato, K., L. B. Alexandrov, A. Banisadr, A. L. Bauer, A. R. Bishop, A. Usheva, F. P. Mu, E. Hong-Geller, K. O. Rasmussen, W. S. Hlavacek, and B. S. Alexandrov. Binding of Nucleoid-Associated Protein Fis to DNA Is Regulated by DNA Breathing Dynamics. 2013. PLOS COMPUTATIONAL BIOLOGY. 9 (1): -.

Construction and Functionalization of Novel Biomimetic Human Liver

Jun Gao
20120716ECR

Introduction

The main objective of this project is to develop a fully functional in vitro human liver organ, as opposed to simple in vitro liver tissue, using cutting-edge advancements in tissue engineering and material technologies. In order to best replicate optimal liver organ performance and derive liver that can function normally, the liver tissue must contact essential body fluids, which transport immune cells and allow for nutrient and gas exchange, Thus, an ideal tissue would be permeated with structures that represent the vascular system to mimic such an exchange. Here, we propose to use the CellMax® Bioreactor coupled with a biocompatible hollow fiber network to grow an artificial liver organ while simulating the necessary vasculature and flow-through of immune cells. The internal lumen of hollow-fibers will be used as a scaffold to support vascular endothelial cell growth and will facilitate endothelium formation. The porosity of the hollow fibers can be engineered to allow for the diffusion of low molecular weight secretory factors while permitting exchange of nutrients and waste, but also preventing the cross-diffusion of immune/liver cells. The external space of the hollow fibers will provide a three-dimensional (3D) matrix for hepatic cell growth, while allowing for migration, organization, proliferation, and differentiation of hepatic cells resulting in fully developed, functional liver organ.

Benefit to National Security Missions

LANL has significant expertise in cutting edge Bioassessment development. This novel liver organ platform will be an important component in the arsenal of in vitro tissue/organ assessment platforms that already includes 3D in vitro skin and lung tissue systems. Success in developing the 3D in vitro liver organ will find immediate application to CBWA risk analysis and mitigation, supporting the LANL threat reduction mission and creating viable external funding opportunities, such as NIH and DTRA. Combining with our skin & lung tissue platform, we can use these complete in vitro 3D tissue/organs capabilities to develop proposals targeting environmental and workplace exposure paradigms.

Progress

The main objective of this project is to develop a fully functional in vitro human liver organ. Now we have successfully accomplished the specific aim I, and developed small-scale hepatic microvascular system in in vitro liver tissue (microfluidic platform). Different hollow fiber membranes (PP, ME, PVDF, PS, mPES and PES) were evaluated for vascular system development. We demonstrated that PP, ME and PVDF can be served as bio-compatible scaffolds for integral monolayer vascular endothelium development. The porosity of the hollow fiber membranes allowed the cross-diffusion of low molecular weight secretory factors for exchange of nutrients and biological signaling molecules. We observed that the hepatic vascular system was fully differentiated under biological relevant shear stress. The differentiation biomarkers were monitored by real-time PCR. Now we are reconstructing large-scale 3D liver system with functionalized vascular system as descried in Aim 2.

During this study, we developed both in vitro tissue engineering and microfluidic capabilities. The cutting-edge microfluidic capability facilitated the development of novel genetic analysis program. We developed one DR, 2 ERs and one DTRA proposals by using this microfluidic capability. This project also helped the development of some other novel ideas. We have submitted one IDEA (#13-00100 “Novel in vitro neuromuscular junction tissue platform on microfluidic for predictive toxicological study”).

We are in the process of preparing the manuscript for the small-scale liver tissue platform with functional vascular system. During the past one year project performance, we also hired one postdoc and one student,

and trained them on tissue engineering and microfluidic technologies. They have presented their studies on Post-doc Research Day and at the SULI student forum. This project provides me a great opportunity to collaborate with both internal (Chemistry, Material and Physics science) and external (UNM and Stanford University) senior scientists in this field. These collaborations will be extremely important for future career development.

Future Work

Construct bioreactor modular microsystems to represent complex physiology and biology of human liver. We will develop biologically relevant architectures of human liver and microvascular scaffolds using hollow fiber and microfluidic technology. We will integrate human primary liver cells and microvascular cells into the bioreactor modular, and develop a complete, surrogate small scale human liver organ. We will validate the system by identifying the liver specific development biomarkers. We will introduce hepatotoxic compounds into the small scale system and validate the toxicological responses.

Conclusion

We anticipate that we will successfully develop a complete, surrogate in vitro 3D human liver organ that will be implemented into diverse range of clinical, biomedical, pharmaceutical and toxicological applications. This platform can be used for long-term functional toxicological evaluation of chemical and biological warfare agents (CBWA). Further, this method of artificial organ construction can also be used to develop other human organs, such as kidney, pancreas and nerve tissue.

Publications

Gao, J., and S. Burchiel. Polycyclic Aromatic Hydrocarbons and the Immune System. Encyclopedic Reference of Immunotoxicology. Edited by Vohr, H..
Gao, J., and S. Burchiel. Genotoxic Mechanisms of PAH-induced Immunotixicity. Molecular Immunotocicology. Edited by Corsini, E..

The World's First Drought and Insect Caused Global Tree Mortality Monitoring System

Chonggang Xu
20130733ECR

Introduction

The critical urgency of forecasting climate impacts and feedbacks makes understanding, quantifying, and predicting terrestrial carbon balance and subsequent climate impacts one of the greatest science challenges currently facing the world. The real-time monitoring systems for dominant types of disturbances will provide a key foundation for our understanding of global carbon balance. We currently already have fire-burned area monitoring system and comprehensive land-use change database; however, there is no global monitoring system of drought/insect-caused vegetation mortality, which could be at similar magnitude of fire-caused tree mortality.

Armed with the world's leading capability in dynamic vegetation modeling and tree mortality research, we propose to develop the world's first automated global drought/insect-caused tree mortality monitoring system. The mortality monitoring system is developed based on the fusion of different sources of information including real-time mortality signal from remote sensing imagery, vegetation change information simulated from a vegetation dynamics model, radiative transfer and reflectance information from a forest reflectance model, and different sources of background information from forest inventory and remote sensing products. The fusion of different sources of information makes it feasible for the first time in the world to accurately quantify tree mortality using Moderate Resolution Imaging Spectroradiometer (MODIS) imagery from NASA, which is a common remote sensing tool for monitoring earth system processes globally. This detailed tree mortality quantification has never been possible by analyzing MODIS image alone. The successful development of our monitoring system will represent an enormous leap forward in our understanding of terrestrial carbon feedback to atmosphere, which is a key area of climatic change re-search in LANL's mission to understand and predict the impacts of global energy demand.

Benefit to National Security Missions

The development of the world's first insect-caused tree mortality monitoring system will represent an enormous step forward in our understanding of terrestrial carbon feedback to atmosphere, which is a key area of climatic change research in LANL's mission to mitigate the impacts of global energy demand. It can help DOE Office of Science build a global tree mortality database used for dynamic global vegetation model benchmarking, a key area that DOE Office of Science is developing through the International Land Model Benchmarking Project. The data generated through this project can be used to substantially improve tree mortality prediction in the DOE-sponsored Community Land Model (CLM) and thus improve global climate predictions.

Progress

We have made the following important progress that direct us favorably toward our final deliverable.
First, we have hired a new postdoc, Jordan Muss. He started on May 20th and he will be mainly responsible for data collection and implementation of our monitoring system in the SW.

Second, we have developed a make file so that the ED-FRT code is able to run on super computers. This is will be a great step toward our final delivery for the whole southwest.

Third, we have written a LANL high performance computing proposal for this project. We have been awarded with 50K CPU-hours under the project name of w13_ treemort.

Fourth, we have improved the ED model to explicit improve the water storage function, which helps ED to have an improved simulation of tree mortality under drought. This could potentially improve the ED-FRT performance under drought.

Fifth, we have compiled the benchmarking datasets for five sites in New Mexico, Colorado, Western Australia and Texas. This will provide the necessary data for our first methodology paper.

Sixth, we have purchased and installed necessary software to support this project including the remote sensing software (ENVI) and programming software (Intel Fortran Compiler).

Future Work

Our goal is to fully develop and test of the proposed tree mortality monitory system at fine scales. Specifically, we will refine and test the drought and insect caused tree mortality monitoring system for representative locations with high resolution images at Colorado, New Mexico and Western Australia. Each location is comprised of ~100 MODIS pixels. The goal includes the following tasks:

- Climate data, forest types, forest height and allometry information will be collected for different sites;
- Simulating a browning phase using foliar chlorophyll data collected from an experimental site provided by our collaborator Dr. Marcy Litvak at UNM (email: mlitvak@unm.edu; phone:505-277-5580), where piñon trees were girdled to mimic tree mortality
- At each site, proposed tree mortality monitory system will be applied to estimate amount of tree mortality, which is then evaluated against the classification results from the high-resolution images;
- A data assimilation approach will be developed to correct initial total plant density for a good fitting between simulated and observed reflectance signals from remote sensing imagery for the pre-mortality period

Conclusion

The success of the project will generate two critical products for global carbon cycle assessment and Earth system model simulation. First, we will fully develop and test world's first insect/drought-caused global tree mortality monitoring system through the coupling of a dynamic vegetation model, a light reflectance and transmittance model, and real-time remote sensing observations. Second, tree mortality database for build for New Mexico, Colorado and Western Australia with estimated carbon loss during the 2000-2012 period will be developed using the our developed monitoring system, which will be used for assessing regional simulations using the DOE-sponsored Community Land Model.

Publications

Adam, H., P. William, C. Xu, S. Rausher, and N. McDowell. Empirical and process-based approaches to climate-induced forest mortality models. To appear in Frontiers in Functional Plant Ecology.

Xu, C.. Decoupling correlated and uncorrelated uncertainty contributions for nonlinear models. To appear in Applied Mathematical Modelling.

Xu, C., R. Fisher, J. Muss, and N. McDowell. Uncertainty and Sensitivity Analysis for Process-based Tree Mortality Modelling. Invited presentation at ECOLOGICAL ASSOCIATION OF AMERICA 2013. (Minneapolis, 8-13 AGU 2013).

Xu, C., R. Fisher, N. McDowell, and S. Sevanto. Our Limited Ability to Predict Vegetation Responses to Water Stress. 2013. New Phytologist. 200 (2): 8.

Xu, C., and M. Chen. Application of Remote Sensing in Ecosystem and Landscape Modeling. To appear in Remote Sensing of Natural Resources. Edited by Wang, G..

From Troposphere to Ionosphere: How Much do Thunderstorms Disturb the Total Electron Distribution?

Erin H. Lay
20130737ECR

Introduction

The ionosphere is a high-density layer of plasma through which all satellite-detected natural and man-made electromagnetic signals from the Earth's surface must pass. Similar to dispersion of light by transparent solids, significant perturbations in the ionospheric plasma electrons disrupt electromagnetic signals. Variation in ionospheric plasma has traditionally been attributed to changes in geomagnetic activity (space weather). Only recently, the ionospheric community has begun to realize that tropospheric thunderstorms (below ~12 km) could have a significant effect on the ionospheric plasma by the following mechanism: when the updraft in a thunderstorm lifts the top of the cloud above the tropopause (altitude of a temperature inversion), the cloud can begin oscillating about that altitude for tens of minutes, producing a neutral pressure wave, called an atmospheric gravity wave (AGW), with periods of tens of minutes to hours.

The goal of this project is to quantify and characterize the ionospheric response to thunderstorm activity, and to determine the mechanisms and magnitude of such coupling. This study is the first empirical analysis comparing ionospheric fluctuations in the peak plasma layer to underlying thunderstorms. For the first time, we will be able to quantify and interpret the spatial extent and dynamic evolution F-layer ionospheric disturbances due to thunderstorm pressure waves. This is of extreme importance for understanding and predicting ionospheric disruption of satellite communications, GPS geolocation signals, and electromagnetic signals such as EMP that are an important part of the Lab's national security mission.

Benefit to National Security Missions

Contribution to Remote Sensing for Nuclear Nonproliferation and Counterproliferation: Significant perturbations in the ionospheric plasma electrons disrupt electromagnetic signals, such as electromagnetic pulses (EMP) that are a key signature of nuclear detonation. Better understanding of ionospheric disturbances near thunderstorms will improve EMP location accuracy and discrimination between various impulsive sources.

Contribution to Space Science: We will empirically study a new phenomenon for the first time in which atmospheric pressure waves from thunderstorms can significantly disturb the electron distribution in the ionosphere above the storms. Variation in ionospheric plasma has traditionally been attributed to changes in geomagnetic activity (space weather). Only recently, the ionospheric community has begun to realize that tropospheric thunderstorms (below ~12 km) could have a significant effect on ionospheric plasma. This study will provide basic scientific evidence of the relative importance of thunderstorm effects on the ionospheric behavior.

Other contributions: Understanding and predicting ionospheric variations is of importance in understanding disruption of satellite communications, GPS (Global Positioning System) geolocation signals, and electromagnetic signals such as EMP.

Progress

We have developed data analysis tools for freely-available measurements of total electron content made by Global Positioning System ground receivers. These can now be used to download and analyze many days of data at one time. Now that these tools are in place, we can begin a larger-scale data analysis project to observe total electron content (TEC) fluctuations near thunderstorms.

Our paper entitled "Variation in total electron content above large thunderstorms" by E.H. Lay, X-M. Shao, and C.S. Carrano was published in Geophysical Research Letters. This paper published the first account of TEC fluctuations observed corresponding to large mesoscale

thunderstorms in time and space. It also made note of a very high frequency perturbation (4 minute-period) associated with the thunderstorm.

Work has begun on identifying additional storms in the same region (United States Midwest) that also exhibit perturbations vs ones that do not, in order to begin determining the type of thunderstorm that contributes to these ionospheric fluctuations. To date, we have discovered one additional storm with high frequency fluctuations associated with another large mesoscale thunderstorm.

Future Work

Main task

Characterize and classify the upper ionospheric response to lower ionospheric disturbances detected using a regional lightning detection network.

Sub-tasks

- Develop data analysis tools for freely-available measurements of total electron content made by Global Positioning System ground receivers. These tools will be useful to the lab for any future ionospheric projects involving total electron content measurements.
- Identify storms in the Los Alamos Sferic Array lightning database with significant lower ionospheric perturbations. The technique to calculate perturbations already exists, but it must be applied to many storms to find which storms have significant perturbations.
- Determine the properties of the thunderstorms with significant lower ionospheric perturbations (i.e. spatial size, height, lightning activity).
- Perform correlational study between upper ionospheric fluctuations and lower ionospheric perturbations associated with thunderstorm activity.

Goals

- Begin to address thunderstorm/ionospheric coupling mechanisms.
- Submit 1-2 journal articles addressing the question of "What are the spatial size, magnitude, and temporal evolution of upper ionospheric perturbations related to nearby underlying thunderstorms on a regional scale, and how do they vary with thunderstorm properties (i.e. spatial size, height, lightning activity)?"

Conclusion

Goals

- Characterize spatial size, magnitude, and temporal evolution of ionospheric perturbations related to nearby thunderstorms on a regional scale, and how they vary with thunderstorm properties (i.e. size, height, lightning activity).
- Characterize the magnitude and spatial extent of troposphere/ionosphere coupling on a global scale as a function of geomagnetic latitude.

Impact

The findings from this study will be used to test and evaluate existing atmospheric gravity wave models, enabling us to distill and discover the physical processes responsible for energy and mass transport between the D-layer and F-layer, and to better now-cast and forecast ionospheric disturbances.

Publications

Lay, E. H., X. M. Shao, and C. S. Carrano. Variation in total electron content above large thunderstorms. 2013. Geophysical Research Letters. 40: 1945.

Mechanistic Studies Toward an Improved Carbonic Anhydrase for Biofuel Production

Suzanne Z. Fisher
20110535ECR

Abstract

Carbonic anhydrases (CA) are enzymes that can capture and regulate carbon dioxide by interconverting it with bicarbonate. These enzymes are stable and extremely fast, but work best over narrow ranges of pH and temperature. Our main goal was to characterize the structural and catalytic properties of CA and then to exploit that information to re-engineer CAs that can be used over the broad range of process conditions, specifically those relevant to algae growth. Obtaining the unique information about the structure-function of CA will require combining for the first time several different experimental techniques, some available only at LANL. We propose to combine static and dynamic information on hydrogen atom positions in the active site of CA by combining neutron crystallography and NMR spectroscopy. We will also co-optimize and select for interdependent catalytic and pH stability properties of CA. Using this approach we were able to construct a set of very interesting mutants with enhanced thermal stability and better kinetics compared to wild type CA.

Background and Research Objectives

Carbonic anhydrases are abundant enzymes, found in all organisms. Human CA II (which we refer to here as just CA) is one of the fastest known enzymes, is easy and cheap to produce, making it an attractive target for industrial development. Carbonic anhydrases activity has strong temperature and pH dependence with a peak at pH 7. Catalysis occurs in 2 steps: 1) hydration of CO2 bound at the active site to produce HCO3- and H+, and 2) rate limiting proton transfer away from the active site through a network of water molecules and amino acid residues out into bulk solvent, to regenerate the active site ready for the next reaction with CO2. The slower proton transfer step is the least understood part of the mechanism, mostly it has not been possible to visualize the location and movement of protons in CA using conventional X-ray and NMR structural measurement techniques. Figure 1 shows the differences in the active site water network of CA between different pH.

CO2 is the main source of carbon for most algae. A major problem for the DOE algal biofuels mission is the slow growth rate of algae (days or weeks). The uptake of CO2 into cells as bicarbonate is the rate-limiting step in biomass production while solubility of CO2 is also an issue. It has been shown that adding an efficient and stable CA to the algal growth medium can significantly increase and regulate the amount of bicarbonate available for uptake, thus improving the growth of algae for the production of biofuels and other value added products. Adding CA is an elegant and finely tunable way to deliver the right amount of dissolved CO2 or bicarbonate to the cells. Before CA can be effectively used in these areas, the strong pH-dependence of activity has to be altered, as many algae grow best at pH > 8.

Our approach led to many new insights into the CA active site and overall structure. We were able to make a background mutant with enhanced thermal stability and then used our explicit knowledge of the active to engineer a set of CAs with enhanced kinetics compared to wild type, no small feat when you consider that this is one of the fastest enzymes every characterized. Figure 2 shows a surface representation of the thermally stable CA and the mutations that confer stability.

Scientific Approach and Accomplishments

Neutron crystallography was used to locate protons along the CA proton pathway at several pHs, providing snapshots of water H-bonding networks and amino acid residue protonation states. We expect proton transport to depend crucially on the ability of key amino acids to bind and release protons i.e. their pKa. Although the presence of protons on amino acid residues at specific pH will be provided by our neutron studies, pKa (a dynamic measure of proton binding and release) can only be provided by NMR titration. We also labeled key amino acids with 13C so that their individual pKa values could

be determined. Combining static and dynamic information in this way will allow us to study the mechanism of proton transport and how it changes with pH. Site-directed mutagenesis allowed us to confirm the roles of specific amino acid residues. Our new mechanistic insights were used for rational site-directed mutagenesis to optimize fitness of CA for algal processes.

In summary, our new approach combines neutron crystallography, which reveals the location of protons in snap shots at different pH, with 13C-NMR titration, which can provide dynamic information about how the locations and accessibility of those protons change continuously with pH. Combining static and dynamic information on H movement in enzymes in this way is innovative and has broad applicability to many biological problems.

This work generated several high impact papers on the enhanced kinetics and thermal stabilization of CA (Fisher, S.Z et al. (2012) Kinetic and structural characterization of thermostabilized human carbonic anhydrase II, Prot. Eng. Des. Sel. 25, p.347-355). This work was selected to feature as a cover article. We also published the neutral pH structure by neutron diffraction of CA (Fisher et al. (2011) Neutron structure of human carbonic anhydrase II: A hydrogen bonded water network "switch" is observed between pH 7.8 and 10.0, Biochemistry 50, 9421-9423) and a few others, including a review and a JACS paper that was mentioned on over 240 news outlets (Fisher et al. (2012) Neutron diffraction of acetazolamide-bound human carbonic anhydrase II reveals atomic details of drug binding, J Am Chem Soc. 134, p.14726-9).

Impact on National Missions

This research directly supports LANL, DOE, and national missions in renewable energy, biofuels, and carbon management by providing a robust product that will enhance the production of renewable biofuels. Furthermore, the development of a new measurement capability based on combining dynamic and static information from neutrons and NMR, and a new engineering capability based on co-optimizing enzymes with complementary engineering steps, will be of broad significance for the study of a large range of biological problems.

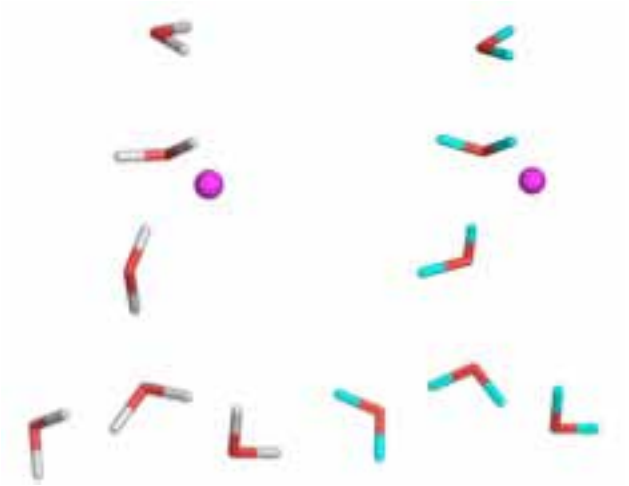

Figure 1. Active site water network hydrogen bond changes upon increasing pH. Left panel shows pH 7.8 and right panel shows pH 10.

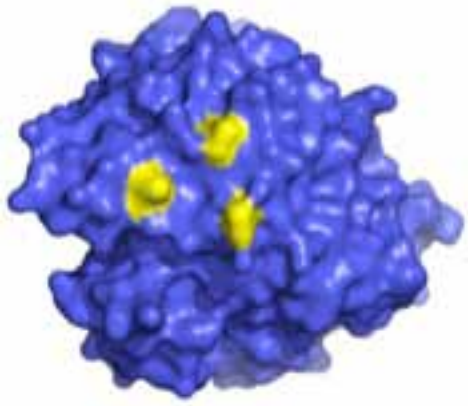

Figure 2. Surface representation of CA with the location of stabilizing mutations shown in yellow.

Publications

Fisher, Z., A. Kovalevsky, M. Mustyakimov, D. Silverman, R. McKenna, and P. Langan. Neutron structure of human carbonic anhydrase II: A hydrogen bonded water network "switch" is observed between pH 7.8 and 10.0. 2011. Biochemistry. : 1.

Fisher, Z., C. Boone, S. Biswas, B. Venkatakrishnan, M. Aggarwal, C. Tu, M. Agbandje-McKenna, D. Silverman, and R. McKenna. Kinetic and structural characterization of thermostabilized mutants of human carbonic anhydrase II . 2012. PROTEIN ENGINEERING DESIGN & SELECTION . 25 (7): 347.

Fisher, Z., M. Aggarwal, A. Kovalevsky, D. Silverman, and R. McKenna. Neutron diffraction of acetazolamide-bound human carbonic anhydrase II reveals atomic details of drug binding. 2012. JOURNAL OF THE AMERICAN CHEMICAL SOCIETY. 134 (36): 14726.

Low-Frequency Acoustic Interferometry for Probing the Stratosphere

Stephen J. Arrowsmith
20110556ECR

Abstract

This project has successfully demonstrated that passive acoustic sensors can be used to measure winds at high altitudes. The basis of our innovation is that the differences in arrival times of continuous ocean noise recorded by ground-based arrays separated by several 10s of kilometers are only sensitive to atmospheric effects between the arrays, thus it is not necessary to simulate the wave from source to receiver to image the local stratospheric atmosphere. Our novel approach has been accepted for publication in Geophysical Journal International and we are preparing on two additional publications based on this work. While other national and international groups working in this area have developed frameworks that require ground-truth (known) sources, our work provides the necessary framework for continuous measurement of winds at high altitudes using ocean noise. Continuous measurements of high altitude winds would provide a missing source of data for numerical weather and climate prediction models that has been identified as a major limitation in predicting the weather and climate [1,2,3]. Currently, winds in the middle and upper stratosphere are derived from the thermal wind equation, an equation that is known to fail in the tropics. There is also a range of defense applications from warfighter support, nuclear explosion monitoring, and predicting the dispersion of aerosols that would benefit from continuous wind measurements at high altitudes.

Background and Research Objectives

Atmospheric observations and modeling in the last decade have stressed the necessity of a better understanding of the stratosphere: 1) to improve weather forecast and climate prediction for short and seasonal time scales [1], and 2) to understand the dynamics of the troposphere. The challenge is that it is difficult to make direct measurements in this section of the atmosphere. The stratosphere lies between 10 and 50 km and features an increase in temperature due to the increase in concentration of ozone; this layer plays a crucial role for the interaction for mass and momentum with the troposphere. A series of recent papers have argued that future improvements in numerical weather and climate prediction lie in “raising the roof” of existing numerical models into the stratosphere [3,4]. Although the stratosphere is important, direct measurements of wind are limited to discrete sampling and/or very specialized instruments (Figure 1). Currently, winds in the middle and upper stratosphere are derived from the thermal wind equation, sporadic rocket soundings, and recently by quasi-continuous Doppler Rayleigh lidar. Doppler lidars are frequently used for remote sensing of wind in the aerosol loaded planetary boundary layer or parts of the troposphere. Due to the decreasing aerosol and molecular density, wind measurements by lidar in the stratosphere require a complicated setup of large aperture telescopes and powerful lasers. Such facilities are expensive to build and operate, and only provide wind profiles at a particular location. Aside from Doppler lidar facilities, our current best estimates of winds in the stratosphere are derived from satellite-based measurements of temperature. There are two fundamental limitations with deriving winds from temperature soundings in the stratosphere: (1) uncertainties in temperature measurements amplify when converted to wind [3], and (2) the thermal wind equation is known to be inadequate for estimating wind in the tropics [4].

Scientific Approach and Accomplishments

Research under this project has proved that it is theoretically possible to invert for winds in the stratosphere using low frequency acoustic background noise or microbaroms (acoustic energy from colliding ocean storms). The basis of our innovation is that the differences in arrival times of microbaroms recorded by ground-based arrays separated by several 10s km are only sensitive to atmospheric effects between the arrays, thus it is not necessary to simulate the wave from source to receiver to image the local stratospheric atmosphere (Figures 2 and 3). This work has been accepted for publication in

Geophysical Journal International [5]. Our method, which we have validated numerically, is unique because it does not require knowledge of the source location and can be applied to continuous infrasound from ocean storms. We applied our preliminary inversion framework to infrasound from a large bolide that was clearly detected by seven arrays in Utah. Our results [5] demonstrate that the observed data clearly favor a real-time model over a climatological averaged model for the time of arrival of infrasound at the Utah network. In particular, the results suggest that the zonal wind speed in the climatological averaged model is too weak, but that the zonal wind speed in the real-time model is more consistent with our observations, although still too weak. Following this research, we have identified three main shortcomings of existing infrasound networks, such as the Utah network in Figure 1, for measuring stratospheric winds using microbaroms: 1) the arrays typically target mining and other impulsive sources and are too small to properly measure microbaroms, 2) the sensors used for such arrays have peak sensitivity at frequencies higher than the microbarom spectrum (between 0.2 and 0.3 Hz), and 3) the distances between arrays in existing networks are too far to calculate stratospheric celerity. Within the past two months we have deployed infrasound instruments in New Mexico to determine the optimum configuration for obtaining time-delay measurements from microbarom signals. We found that an appropriately designed network of ~1 km aperture arrays, separated by distances of ~60 km, would provide the necessary dataset for an inversion using microbarom noise. We are finishing a second journal article detailing our New Mexico microbarom study.

Impact on National Missions

The ability to continuously measure winds at high altitudes using low-cost acoustic sensors has implications for a number of national missions in weather/climate prediction and defense. The joint DOE/NSF Community Earth System Model (CESM) is one of three US IPCC-class climate models in which LANL personnel in T-3 and CCS-2 currently play an active research role. The CESM model includes a whole atmosphere configuration that goes up to the thermosphere to account for mass and momentum coupling between different layers. Future work with existing personnel at LANL, including Phil Jones (T-3), should investigate how our measurements can be incorporated into such models. Joan Alexander at Northwest Research Associates in Boulder, Colorado has also expressed interest in collaborating with us on quantifying benefits to the weather/climate prediction community. Of particular interest for the stratosphere dynamics are effects on the ozone layer, which plays a key role in radiative interactions as well as gravity wave drag (a sub-grid scale phenomena that plays an important role in atmospheric dynamics). Furthermore, the opportunity of direct wind measurements in the tropics may be particularly important, where the thermal wind equation is known to work poorly. Our results also have implications for the NASA program and warfighter support and we have discussed with Reiner Friedel (ISR-1) how improved specifications of stratospheric winds has potential implication for improving GPS accuracy through improved correction for stratospheric effects. Improved specification of atmospheric winds also has an important implication for Global Security (LANL POC: Dale Anderson, EES-17): since knowledge of stratospheric winds affects the propagation of infrasound signals our results can improve infrasonic location and yield estimation of nuclear tests and improve the prediction of dispersion of radioactive aerosols, which can reach the stratosphere.

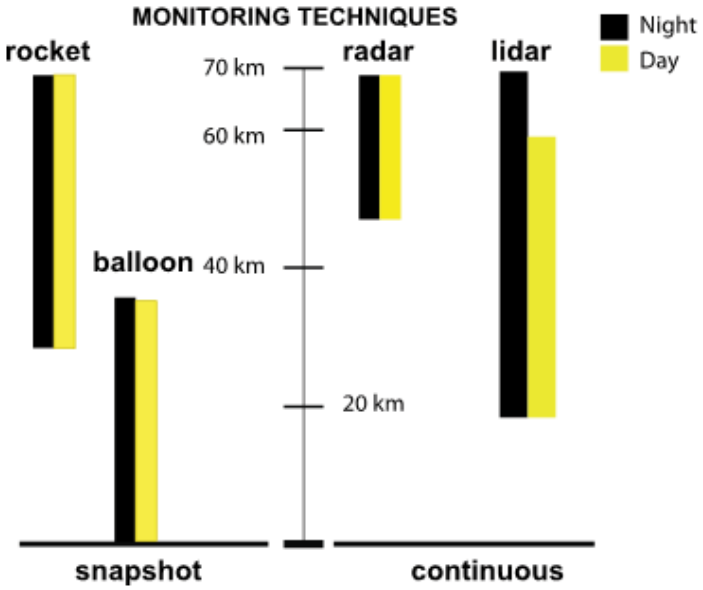

Figure 1. Direct measurements of wind at high altitudes is currently only possible with snapshot measurements and expensive LIDAR installations (limited to a handful of locations on Earth).

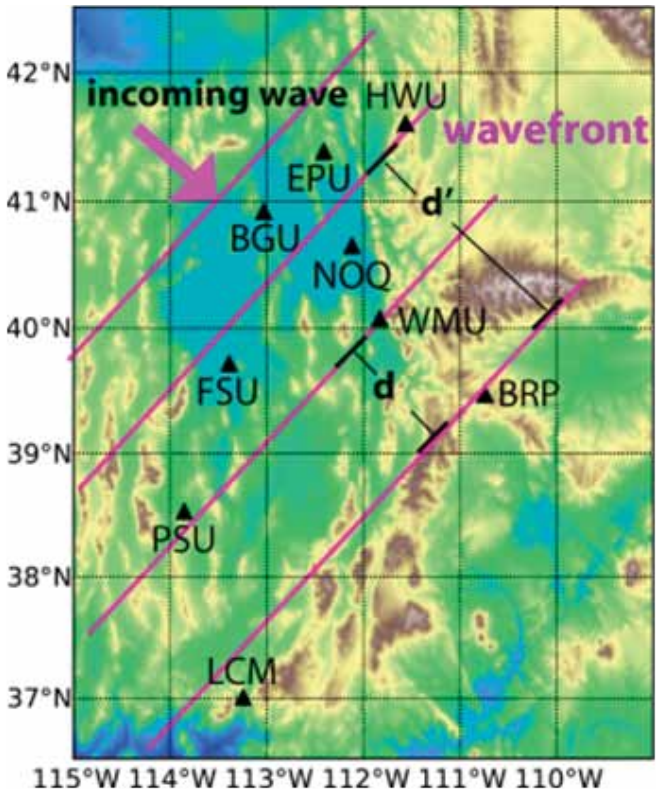

Figure 2. Using an acoustic sensor network in Utah, we written a paper, which is currently in review, that demonstrates how delay times between pairs of sensors can provide constraints on high-altitude winds.

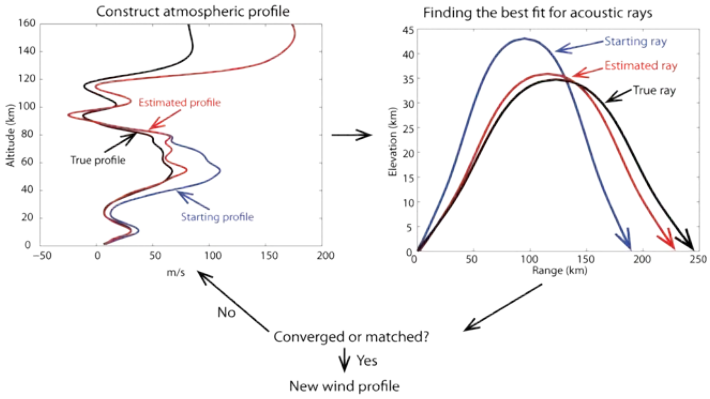

Figure 3. Our technique iteratively improves a starting model of the East-West wind component, obtained from state-of-the-art models, by modeling sound rays between sensors and minimizing the difference between the observed and predicted delay times.

References

1. Gerber, E. P.. Assessing and understanding the impact of stratospheric dynamics and variability on the earth system. 2012. Bulletin of the American Meteorological Society. 93 (6): 845.

2. Shaw, T. A., and T. G. Shepherd. Raising the roof. 2008. Nature Geoscience. 1: 12.

3. Kalnay, E., J. C. Jusem, and J. Pfaendtner. The relative importance of mass and wind data in the present observing system. Presented at NASA Symp. on Global Wind Measurements. (Columbia, MD, 1 Jan. 1985).

4. Zagar, N.. Assimilation of Equitorial Waves by Line-of-Sight Wind Observations. 2004. Journal of the Atmospheric Sciences. 61: 1877.

5. Arrowsmith, S. J., O. Marcillo, and D. P. Drob. A framework for estimating stratospheric wind Speeds from unknown sources and application to the December 25, 2010 bolide. To appear in Geophysical Journal International.

Publications

Arrowsmith, S. J., O. E. Marcillo, and D. P. Drob. A framework for estimating Stratospheric wind speeds from infrasound noise. Presented at Infrasound Technology Workshop 2012. (Daejeon, South Korea, 8-12 Aug. 2012).

Arrowsmith, S. J., O. Marcillo, and D. P. Drob. “A framework for estimating stratospheric wind speeds from unknown sources and application to the December 25, 2010 bolide. To appear in Geophysical Journal International.

Separation of Time Scales at High Latitudes: Fundamental Science and Numerical Method Development

Robert E. Ecke
20120206ER

Introduction

This project builds on a new, fundamental discovery -- a new regime in fluid dynamics, relevant to the high-latitude oceans (Wingate et al 2011) but with a broader impact on climate model development. The impact of this discovery can effect our understanding of important climate-related science questions such as: why are there columnar vortices propagating in the deep Arctic and do they contribute to the formation of deep water that can shut down the meridional overturning circulation?; and are there impacts due to oceanic heat transport related to in the reduction of Arctic sea ice? Further, the theoretical underpinnings of this work give us new insight into how to best solve the dynamical equations on new, heterogeneous computer architectures, which could lead to new numerical algorithms, the kind of algorithms that would allow climate models to possibly reach the human scale, rather than the global scale, in our lifetime. We therefore have two key objectives: 1) understand the fundamental fluid theory and its connection to new observations in the Arctic and 2) use the foundational principals in the theory to develop new, proof-of-principle, exascale-friendly, numerical methods for next generation ocean models.

Benefit to National Security Missions

This work directly impacts LANL's mission for Mitigating Impacts of Energy Demand Growth under the umbrella of the Energy and Climate Impacts (ECI) program development project. That work is focused on issues of high latitude climate interests. The first objective of this project brings capability in Arctic ocean science and fundamental fluids. It also directly impacts LANL's IS&T mission by bringing new applied mathematics and computing capabilities in the development of fast/slow time splitting for ocean models on heterogeneous architectures and will contribute toward the development of models that will one day reach the human scale.

Progress

ared Whitehead and Beth Wingate submitted the first paper on the emergence of slow dynamics in the limit of fast rotation to the Journal of Fluid Mechanics. He and Terry Haut have also made progress on understanding the mathematics of the 3 limit system. This will be a second paper. The implications of this work is a better, more general, understanding of time-scale-separated flows which are ubiquitous for climate models. These physical results are expected to impact our numerical results described in the next section. Jared's work has been so successful he has taken a faculty position at Brigham Young University where he'll begin as an Assistant Professor in December of 2013.

Terry Haut and Beth Wingate submitted the first paper on the asymptotic parallel-in-time (also called parareal) method. This new method could address important computation issues that will arise in exascale computing for climate models and have potential impact on other physics problem of interest to LANL. This is a very important paper that could not only be highly cited, but lead to greater understanding of how climate models will play out on new heterogeneous computing architectures. There is another paper in progress that describes a highly parallel technique for solving linear propgators, a necessary key to the asymptotic-parareal method that uses general methods for the horizontal discretization. This work is a high priority for LANL and the DOE. As a consequence of this work, and the paper, we have been invited to present a paper at the DOE ASCR Examath workshop, a workshop that will determine the content of next-generation DOE ASCR mathematics work. CCS2 is working on converting Terry Haut to staff.

Beth Wingate was the principle organizer of a major international conference -- the 2013 CNLS Annual Conference -- on Ocean Turbulence. This conference brought people in mathematics and ocean physics together to understand the major issues in ocean turbulence. Beth

Wingate and Geoffrey Vallis, the 2013 CNLS Ulam Scholar, were invited to write a 6 page paper for Nature by the Nature Editor for Climate, Michael White. Further, there is going to be a special issues of the Journal of Physical Oceanography on Ocean Turbulence for people to contribute papers to. And lastly, we believe we may have created a new community. The conference was so productive that I believe it will be reconvened in three years, perhaps in Santa Fe again.

Future Work

Study the relationship between the 3 known time-separated dynamical regimes in climate models

- Task 1: Finish the peer review process for the first paper
- Task 2: Complete a second paper on the mathematics of the 3 regimes
- Task 3: Use an experimental configuration to understand the relationship between the three limits

Continue working on the parallel-in-time method for exascale

- Task 1: Finish the peer review process for the first paper
- Task 2: Finish the second paper on linear propagators

Conclusion

We expect this work will lead to new understanding of the remarkable type of dynamics that happens in some areas of the world's oceans where there is weak stratification. We also expect this understanding to help in the development of proof-of-principle concepts for solving the dynamical equations used in the ocean on next generation computers, contributing to the ability to bring climate modeling to the human scale.

Publications

Haut, T. S., and B. A. Wingate. An asymptotic parallel-in-time method for highly oscillatory PDEs. To appear in SIAM Journal of Scientific Computing.

Whitehead, J. P., and B. A. Wingate. The influence of fast waves and fluctuations on the evolution of the 'slow manifold'. Journal of Fluid Mechanics.

Time-gated Super Resolution Imaging

James H. Werner
20120227ER

Introduction

We are building instrumentation that significantly advances the state of the art in optical microscopy. This new instrument design will have be approximately 50 times better than the state of the art in terms of resolution and functional working depth. Our first goal is to extend the effective Z-range of newly developed super-resolution methods to provide nanometer resolution throughout 3D volumes over ten microns cubed, at depths up to 100 microns. This represents an increase of better than an order of magnitude over the state of the art. This substantial increase in imaging depth will be enabled by two advanced optical methods (two-photon excitation and time-gated imaging). Our second research goal is to use these advances in the extension in Z-depth to examine structure and defects of important nano-structured materials and polymer scaffolds over functionally relevant length-scales. Our third research goal is to use these advances to image the cytoskeletal network throughout an entire mammalian cell.

Benefit to National Security Missions

Specifically, we will use this new instrumentation to image polymer materials and biological cells. The application of super-resolution methods to biological materials can lead to the preliminary data needed for competitive proposal submissions to DARPA, DTRA, or the NIH. The soft-materials science aspects of this project may be supported by DOE-BER or DOE-BES. We expect the results on the soft materials may affect laboratory programs in energy storage or light harvesting.

Progress

In the past year we have made substantial progress in both instrument hardware (design) and in writing control software for the new microscope. In particular, while we were making progress on point scanning by confocal excitation and detection, we decided this year to begin testing line-scanning (or selective plane illumination) methods to increase the speed of image acquisition and to reduce photo-damage to the material during excitation. We note that unlike confocal excitation/detection, only a single XY plane in the sample is illuminated at a time, with the spatial extent of the excitation light providing Z-sectioning.

The simplest method for excitation in selective plane illumination is to use a cylindrical lens to focus a standard Gaussian-shaped laser beam into a thin sheet of light. However, for tightly focused beams, the light rapidly diffracts/diverges. To overcome these problems, people have recently introduced Bessel beam excitation for selective plane illumination. Unlike a Gaussian laser focus (which diverges rapidly due to diffraction), Bessel beams can be collimated at very narrow beam waists (0.3 microns) for nearly 100 microns. While Bessel beams can have orders of magnitude larger Rayleigh ranges than Gaussian laser beams, a Bessel beam has side lobes/bands of intensity that can also excite the sample, leading to photo-damage or out-of focus fluorescence. Two photon excitation can be used to minimize the impact of these side-bands, but high-power two photon lasers are substantially more expensive than one-photon laser sources (e.g. a Ti:Saph laser used for two photon excitation is ~200K, whereas a diode laser used for 1 photon excitation is ~0.1 K). Spatially filtering the Bessel beam emission was demonstrated by one group, but the set-up required 3 synchronized galvo mirrors.

In the past year, our lab has recently developed a microscope design that can perform 1-photon Bessel beam scanning that only uses a single galvo mirror (hence lower cost, lower maintenance, and no synchronization issues.) In our design, the same galvo mirror (GM) that is used to scan the Bessel beam de-scans the fluorescence emission through a slit that acts as a spatial filter. A retro-reflection from a spherical conjugate mirror (CM) passes the spatially filtered light through the slit, with this spatially filtered light scanned across an imaging

CCD or CMOS camera by the same galvo mirror used to scan the excitation. While we are still optimizing parameters (including scan areas, optimal excitation powers), we have demonstrated proof of principle measurements on dye-filled beads adhered to a coverslip and we have characterized the Bessel beam shape used for fluorescence excitation. Future work includes combining this excitation method with single-molecule based super-resolution microscopy for rapid 3D volumetric imaging of whole cells and cell colonies at near 10 nm resolution. We submitted a LANL invention disclosure (S133062/L2013059) based upon this design.

Future Work

In the next fiscal year, we will have accomplished the following research goals:

- Fully automate data acquisition in the Bessel beam excitation geometry
- Demonstrate the advantages of Bessel beam excitation for test 3D systems (e.g. beads in polymer matrix)
- Fully characterize diblock copolymer samples by super-resolution imaging and AFM (separately)
- Acquire 3D images of diblock copolymer morphologies over functionally relevant length scales.
- Begin imaging 3D cell structures (in particular the actin cytoskeleton or mRNA spatial distributions)

Conclusion

We are building instrumentation that significantly advances the state of the art in optical microscopy. This new instrument design will have be approximately 50 times better than the state of the art in terms of resolution and functional working depth. These improvements in resolution and working depth will be then used to study defects and structures in important polymer materials. These materials are useful scaffolds for energy harvesting. In addition, we will study changes in cell structure that result from stimulation by external agents. This work will greatly impact material and biological research.

Publications

Han, J., A. Shreve, and J. Werner. Super-Resolution Optical Microscopy. 2012. In Characterization of Materials (Volume 2). Edited by Kaufmann, E.. , p. 1026. New York: Wiley.

Han, J., Y. Kunde, E. Hong-Geller, and J. Werner. Single Molecule Localization Microscopy of Actin Restructuring during Salmonella typhimurium Infection. Journal of Biomedical Optics.

Biofuel Enzymes by Design

William M. Challacombe
20120256ER

Introduction

The research will develop novel, rational design capabilities for multi-property optimization of biofuel enzymes, overcoming multi-scale challenges through integration of emergent theoretical and experimental technologies with complementary strengths: First, O(N) quantum chemical (QC) methods will be used to overcome length scale barriers with a cost that increases only linearly with number of atoms N in the QC model. Second, joint X-ray/neutron (XN) protein crystallography provides snapshots of stationary points along a com-plex reaction path, including the all important active site proton- and water-networks, guiding the reaction pathway between these experimental constraints. Innovation includes:(1) a unique combination of emergent technologies and (2) an unprecedented scale of thermo-chemical calculations (1000+ atoms). In addition to a more efficient XI, the proposed research will strongly impact the basic science backing DOE's biofuels mission, establishing rational design as a rigorous testbed for developing our understanding of enzyme biochemistry.

Benefit to National Security Missions

This project will enable program development broadly, from biofuels to health, materials and national security. We will target DOE-BER for program development and stand ready for opportunities to bring center level funding to LANL for biofuels research. Further opportunities will be sought under the NSF CBET program Catalysis and Biocatalysis and under DTRA and DHS for chemical warfare agent degrading enzymes.

Progress

- Entire five-step reaction mechanism of XI completed. Four of five transition state calculations have been completed. It will be possible to publish incrementally starting now, or soon after completion of fifth calculation. Novel results include: (a) The ring opening rather than the isomerization step appears to be rate limiting. This is the difficult step to finish; however, with the other steps in hand, we can draw this conclusion without completion of the last step. (b) Formation of the salt pair, LYS183-H+ and ASP287 -> LYS183 and ASP287H+. (c) This salt pair explains a conserved glycine residue, which mutant studies have incorrectly attributed to other factors. observation of an unproductive, non-Michaelis fork in the reaction path, corroborating an early conjecture of Petsko et al.
- Collaborator Kovalevsky has carried out kinetic mutant studies, publication pending.
- New work on Carbonic Anhydrase (as discussed with W. Priedhorsky and Fischer) has begun, examining the role of TYR7 in deprotinating the catalytic hydroxide anion.

Future Work

- Bonding and electrostatic analyses on the XI reaction mechanism
- Calculations on putative mutants, develop correlations between computed and observed reaction rates
- Calculations on Carbonic Anhydrase TYR7 pKa

Conclusion

The scientific effort will attempt to increase the efficiency of cellulosic biofuel production through the engineering of more efficient enzymes, in particular Xylose Isomerase (XI). Our goals are to (1) advance our understanding of the basic biological science that underpins the biofuels enzyme XI through the design of enhanced mutants, (2) establish technical leadership in rational biomolecular design, enabling LANL to attack a broad class of biofuel and energy security problems and, (3) explore the limits of this new capability through the stringent feedback between theory and experiment.

Publications

Kovalevsky, A. Y., B. L. Hanson, S. A. Mason, T. Yoshida, S. Z. Fisher, M. Mustyakimov, V. T. Forsyth, M. P. Blakeley, D. A. Keen, and P. Langan. Identification of the Elusive Hydronium Ion Exchanging Roles with a Proton in an Enzyme at Lower pH Values. 2011. Angewandte Chemie. 123 (33): 7662–7665.

Waltman, M. J., Z. K. Yang, P. Langan, D. Graham, and A. Kovalevsky. Engineering Acidic Streptomyces rubiginosus D-Xylose Isomerase by Rational Enzyme Design. Protein Engineering Design and Selection.

Metabolic Engineering of an Algal Lipid Bioswitch

Chris M. Yeager
20120400ER

Introduction

The ability to control or monitor gene expression in algae, via an engineered "bioswitch", would be a tremendous advance in the state of the science and aid in the development of engineered algal strains for large-scale biofuel production systems. In this project, we will develop a bioswitch/sensor for the unicellular model microalga, Chlamydomonas reinhardtii. We propose to: 1) develop a FadR-based biosensor for fatty acids in algae and 2) demonstrate a functional transcription factor-based bioswitch that can be used to control gene expression in algae. For goal #1, we will refine the FadR system to recognize different fatty acyl CoA species (different chain lengths, saturation) and possibly free fatty acids. Additionally, we will pursue the development of other transcription factor-based biosensors to measure free fatty acid and fatty acyl-ACP levels in algae. Bacterial and plant transcription factors that recognize these classes of fatty acids have been identified. For goal #2, we will develop a FadR bioswitch to control the expression of heterologous genes engineered into algae to reroute or fine-tune fatty acid metabolism. We will pursue the use of alternative transcription factors to act as a bioswitch, if FadR proves unsuccessful.

Benefit to National Security Missions

The project builds capability in engineering cellular factories and specifically aims to reduce the cost of biofuel production by simplifying oil extraction. Successful proof-of-principle demonstration in this project will position us to acquire external funding from the biofuels industry, from DOE EERE, or the DoD for further optimization, expansion, and commercialization of our concept.

Progress

Following the FY12 LDRD review, we were encouraged to confirm the effects of the predicted FadR mutations as outlined in the proposal, and to develop an alternative strategy move their bioswitch into bioenergy application in algae. Currently, we continue in to design and study the individual components that will allow the successful implementation of a lipid-responsive bioswitch in algae. Characterization of the FadR regulon in E. coli. During year one we discovered that the FadR regulon in E. coli likely consists of more many more genes/operons than has been reported. Since that time, we have discovered that the FadR consensus operon (ANTGGTCNGACCAG) is very similar to the operator consensus sequence (ATTG-GTAANACCAT) for another transcriptional regulator, PdhR. To our knowledge a single operator sequence that binds more than one transcription factor has not been reported; the paradigm is that transcriptional regulators recognize distinct operator sequences. Binding of FadR to PdhR operator sequences had been confirmed by gel shift assays. Reverse transcriptase qPCR assays have been developed for nine E. coli genes that we believe could be dually controlled by FadR and PdhR. Currently, we are comparing expression of these 9 target genes in wild type and fadR- and pdhR- E. coli.

FadR binding to FadO and the palmitoyl-CoA ligand

We have developed and optimized an experimental assay applying fluorescence anisotropy to measure the binding constant of GST-FadR for its palmitoyl-CoA ligand and DNA operator sequence (FadO). Under the experimental conditions we obtained a Kd value of 2 nM of FadR at 1 nM labeled-FadO and 600 nM for the palmitoyl-CoA ligand at 10 nM of FadR at 1 nM labeled-FadO.

Site Directed Mutagenesis of FadR

We have constructed the L102A, L165N, L102A/L165N, R213M, R213N and R213A mutants of FadR (target mutations based on computational analysis performed in year 1) using site directed mutagenesis. The mutants at the L102/L165 positions were constructed with the purpose of expanding the binding pocket of the lipid ligand to accommodate longer lipids. The A213 of FadR is directly involved in the binding of the CoA moiety of fatty acids; we have included mutations at this position

in an attempt to decrease FadR's affinity for the CoA moiety of the ligand. The mutant protein containing the R213A mutation was purified and exhibited drastically decreased binding for palmitoyl-CoA ligand (Kd >5 µM; wild type 600 nM). In contrast, the L102A mutant protein exhibited increased affinity for palmitoyl-CoA (Kd 390 nM). The mutant proteins have proven difficult to purify. Expression of the mutant L165A has proven challenging, and the R213M protein was not stable following purification. Ongoing efforts are yielding positive results, and analysis of R213N and the L102A/L165N double mutant should be accomplished in the coming weeks. The preliminary results from the characterization of the R213A mutant suggest that mutations at this position affect (decrease) the binding of the CoA-lipids (which is what we intended) while the L102A mutant increased the binding of the CoA-C12-lipid, which may be in line with our interest of improving the binding and of CoA-lipids with longer chains (C18).

Algae transformations

First, a bioswitch protein (engineered FadR) needs to be constructed and inserted into an algal host strain. We have obtained the chloroplast PB155 vector from Dr. Richards Sayre's laboratory for this task and have inserted the codon optimized E. coli FadR. Preliminary (two) attempts to transform the PB155/CO-FadR plasmid into Chlamydomonas reinhardtii have failed. Second, a reporter gene under the control of the bioswitch protein (i.e. FadR) needs to be inserted into an algal host strain. To achieve this we have obtained a vector (pSE 3HB Kan D2 gfp D1; from Dr. Stephen Mayfield, UCSD) that utilizes the psbD promoter to control the expression of algal-optimized GFP. We plan to achieve dual control and bioswitch activity of this GFP reporter by inserting FadO operator sequence within the psbD promoter, without disrupting its constitutive promoter function. Four variants of the psbD promoter containing the FadO operator sequence were constructed. The preliminary attempt (one) to transform these 4 constructs into C. reinhardtii resulted in the incorporation of one of them into the algae's chloroplast DNA. We are currently assessing GFP expression by this strain in the absence of the FadR bioswitch.

Future Work

The focus of our research for FY14 will be to: 1) complete testing of the binding affinity of the FadR variants that were computationally identified in year one of the project to the FadR operator and the response of the FadR variants different free fatty acids and fatty acyl-CoAs, 2) publish 2 manuscripts, one detailing the characterization of the FadR mutants discussed above, and a second describing the overlap between the FadR and PdhR regulons in E. coli, 3) successfully introduce a construct(s) into Chlamydomonas reinhardtii that expresses E. coli FadR (and select FadR variants identified in goal #1) and harbors a luciferase reporter under control of an algal promoter integrated with the FadR consensus operator sequence, 4) evaluate and publish the utility of the FadR construct (or related variants) to serve as a cellular sensor for fatty acyl-CoA levels in algae, 5) demonstrate the utility of the FadR construct as a bioswitch to control heterologous gene expression in C. reinhardtii.

Conclusion

Successful completion of the project will greatly advance our ability to manipulate and monitor gene expression in algae. The development and refinement of the FadR system as a biosensor to measure fatty acyl-CoA levels in bacterial or algal cells will be a significant technological advancement. Apart from its specific contribution to the algal biofuel field, the proposed research will develop capabilities to create novel bioswitches to manipulate cellular processes in other biotechnology applications.

A New Class of Antibody-like Molecules that Signal Upon Binding

Geoffrey S. Waldo
20120449ER

Introduction

Modern biology needs tools to specifically label target proteins in living cells so that their movements and activities can be watched and better understood. Our long-term objective is to make a new class of antibody-like proteins based on fluorescent proteins that become fluorescent when they bind to a specific peptide or protein surface. Unlike conventional antibodies, these reagents would be straightforward to make, and would be expressed functionally in living cells. They would give a signal only when they bound their intended target. The goals include: (1) making signaling antibodies that recognize linear epitopes by structural complementation with a peptide sequence, restoring folding and creating fluorescence; (2) making signaling antibodies that bind to surfaces of folded proteins, restoring fluorescence by shielding the chromophore of the fluorescent protein.

Benefit to National Security Missions

The capability established by the successful completion of this project will enable two major future mission areas, the first is the specific detection and monitoring of protein targets in living cells, and the second the detection and analysis of protein trafficking and expression during physiological processes including baselines and responses to environmental factors or disease states such as cancer. This also supports the high-content high-throughput cell assays needed for the DOE User Facility currently in project development with B Division. The live cell assays and signaling properties of these reagents support DOD and DHS interest in platform technologies for tracking physiological responses to chemical and biological agents in real time. New antibody-like technologies for cell biology are a priority in NIH, where it is recognized that current research in live-cell biology is limited by a lack of effective antibody reagents.

Progress

GFP (green fluorescent protein) 11-beta stranded protein

GFP strands 1 to 10 (GFP 1-10) can be engineered to bind and fold with a peptide corresponding to strand 11. Our goal is to create new GFP 1-10 capable of recognizing strand 11 sequences chosen to match disordered regions in antigens (pathogen, human, etc) so the new GFP 1-10 can act as a signaling antibody, turning green in the presence of the new target protein. The project has a computational part (in silico evaluation of effects of mutating strand 11 and the best mutations to place into GFP 1-10) and an experimental part (screening libraries of these mutations to find those that work in practice). Progress on Experimental Part: Our previous experiments on diversified libraries of every single residues of GFP 11 showed that changing residues pointing inside the barrel reduce folding of the GFP, those outside are more tolerant to mutations. A Goal was to evolve GFP 1-10 to recognize a disordered region of CFP-10 protein, a secreted antigen from TB. Mutating M218E, L220Q and E222Q to match CFP-10 mutations by themselves abolished complementation of GFP 1-10. Despite the enormous challenge, after several rounds of directed evolution and diversified libraries of GFP 1-10 we were able to select for GFP 1-10 recognizing a new GFP 11 sequence containing 7 residues similar to CFP-10 disordered tail. Importantly, we were able to include the two most disturbing mutations: M218E and L220Q in the new sequence of strand 11. Achieving this Goal scheduled for this FY13 was a key milestone. it indicates that even in this worst-case scenario, GFP 1-10 can be engineered to recognize very challenging GFP 11 proxy peptides. And it paves the way to developing GFP 1-10 as a signaling antibody for TB diagnostics and biological studies. We also completed our work on optimizing the CalGreen (a GFP from another species of jellyfish) and obtained crystal structures for Rosetta in silico modeling.

Our Computational goal is to predict which sequence variants of GFP 1-10 have the most stability with alternate sequences of S11 such as CFP-10 to reduce the number of clones to experimentally screen. To model and constrain the GFP chromophore to calculate reliable Rosetta energies, out Goal was to compare experimental data for the effects of single point mutations of S11, and the stability of the GFP 1-10 WT and GFP 1-10 mutants vs. the CFP-10 mutants. We hoped that the better-performing experimentally validated GFP 1-10 mutants would correspond to the better Rosetta energies.

Progress on Computational Part

GFP 1-10 and S11 sequences were modeled on crystal structure 2B3P. We developed controlled physically-model constraints on the GFP chromophore during the simulations, with small perturbation of the rigid body and sampling of side chain poses. We were able to calculate the difference between the binding energy of the GFP 1-10 and S11 mutants for all 240 possible 20 amino acid variants across the 12 amino acids of S11. Three methods of running simulations were developed (Packing and minimization at interface; including soft repulsion to model bulky residues; and packing and full backbone relaxation). We see similar trends in all three methods of computational predictions and are generally consistent with the experimental results. Importantly, we were able to accurately predict the experimental stability ranking of the various CalGreen protein mutants. This means we have a basis set of new scaffolds to make signaling antibodies from. We did discover that E222 is quite sensitive to side chain positioning, and our model based on static crystal structure 2B3P may not be flexible enough. We think determination of the crystal structures for some of the GFP 1-10 + S11 mutants can help us decide if our Rosetta simulation constraints need to be adjusted. Future Work. We will adapt GFP 1-10 to the fully mutated S11 so that it recognizes the CFP-10 disordered sequence, and to screen GFP 1-10 optima against the S11 single point libraries to test specificity and promiscuity of the GFP 1-10, and solve a crystal structure of the final complex. We will work with our GFP and CalGreen mutants too. We will refine our Rosetta methods using our experimentally-validated GFP and CalGreen structures and mutants.

Future Work

- Continue to work to establish a triage and ranking system for selecting disordered domains that are available for binding to GFP 1-10. Working with the Bradbury lab and members of B6 and the structural biology community on a national scale, we will annotate our list of disordered proteins for biological relevance in addition to experimental evidence of disorder. Where possible, we will identify targets that have conventional antibodies as controls.
- Engineer GFP 1-10 to recognize a subset (top 12) of these disordered tags.
- Generate GFP 1-10 capable of signaling binding to commonly used epitope tags (to help distribute the technology to research community).
- Experimentally determine the stability of specific S11 and GFP 1-10 mutants where they contact in the structure, and compare to Rosetta stability calculations.
- Generate stable versions of CalGrn 1-10 for in vitro and in vivo use as binders, that are more soluble that existing versions, to provide an orthogonal tag for multiplexing with GFP 1-10 binders.

Conclusion

Developing effective treatment modalities for cellular disorders requires understanding where and when proteins are expressed and their movements in living cells. Current antibodies used to study cell processes need labels, are hard to get into cells, and have high background. Our proposed ‘signaling’ antibodies work in living cells and light up when they bind to their targets. These signaling antibodies can take advantage of computer design to recognize new target molecules. With these tools researchers can speed translational medicine by spying on the movements of biological molecules in living cells under different conditions and during drug candidate screens.

Publications

Cabantous, S., H. B. Nguyen, J. D. Pedelacq, F. Koraichi, A. Chaudhary, K. Ganguly, M. A. Lockard, G. Favre, T. C. Terwilliger, and G. S. Waldo. A New Protein-Protein Interaction Sensor Based on Tripartite Split-GFP Association. 2013. Scientific Reports. : 1.

Energy Efficient, Inducible Harvesting of Microalgae for Biofuels Production

Richard T. Sayre
20120535ER

Introduction

A significant constraint for the large-scale commercialization of the emerging algal biofuels industry is the financially and energetically costly process of harvesting biomass from ponds. There are two constraints that limit the efficiency of microalgae harvesting. These include, the small size (2-10 um) of microalgal cells, and their very low densities in ponds ranging from 0.1-0.5% of the total mass. As much as 30% of the cost of producing algal biofuels is associated with the concentration of cells to a level that is workable for oil extraction (3, 4, 6). We propose to take advantage of the biology of the algae to facilitate harvesting by expressing surface-exposed, self-aggregating biomolecules under the control of inducible gene switches. These molecules were chosen for their ability to induce auto-flocculation of algae into macro-scale aggregates that can be cheaply harvested using low energy, high throughput, and commercially scalable technologies (acoustic focusing, straining, settling).
This work falls under the Designated Unclassified Subject Area of Biological Science. This work falls under the definition of applied research related to the function of biological systems and falls under the sub discipline of cellular, molecular and systems biology.

Benefit to National Security Missions

This project will address a critical national need and contribute directly to LANL's energy security mission in alternative energy. Lipid producing algae have the potential to displace petroleum for a large fraction of our transportation fuel needs. Economical methods for harvesting essential for implementation of algae for biofuel production. Our objective is to develop a low energy, low cost means to aggregate algal biomass that will also allow the culture media and water to be effectively recycled enhancing the sustainability of algal biofuel production systems. Controlled bioflocculation of algae will complement and enhance the existing and emerging algal biomass harvesting technologies being developed globally and at LANL.

Progress

Over the past year, we have successfully genetically engineered A. protothecoides with the hyaluronic synthase with and without UDP-glucose dehydrogenase expression, and we have shown sucessful mRNA expression of hyaluronic synthase in Auxenochlorella protothecoides with quantitative PCR. This project has also resulted in the creation of reliable molecular tools for the genetic engineering of A. protothecoides. After selecting 5 clones and development of a hyaluronic acid (HA) assay to visualize HA on the cell surface using fluorescence microscopy, we find few cells with surface-exposed HA. Based on recently published reports of HA expression in plants (Rakkhumkaew et al. Biotechnol Bioeng. 2013 Apr;110(4):1174-9), we believe HA may be building up within the algal cell and unable to exit the cell wall. We will examine this hypothesis by DEEM visualization with our collaborators and compound detection over the coming year.

Furthermore, we have successfully identified extended cell surface proteins and selected a candidate for tagging. By synchronizing cell cultures in photobioreactors, we were able to narrow the selection of candidate peptides. Based on BLAST comparison to Genbank proteins, A. protothecoides transcriptome and genomic data, amino acid content and hydropathy analysis, we identified a proline-rich protein (PRP) with an extended rod-like structure with homology to mammalian and plant cell wall proteins that was expressed in A. protothecoides. Due to the length of time for nanobody production, purification, and selection (>9 months), we utilized previous reports of the cell wall content of A. protothecoides (high in chitin), to develop a novel cell-cell binding system in which we tag the C-terminus (hydrophilic portion) of the PRP cell surface protein with a chitin-binding protein (CBP). In order to test the binding of CBP to cells, we expressed and purified a GFP-CBP fusion protein in E. coli (utilizing a His-tag and a Ni column) and confirmed the binding of this soluble protein to A. protothecoides.

As a negative control, we used C. reinhardtii (no chitin in the cell wall). We then created the PRP-CBP fusion in the A. protothecoides expression vectors we designed last year for microalgal protein expression. This vector has been transformed into A. protothecoides, and we will characterize mutants in the coming year.

Also, we have been identifying inducible systems of expression in order to "turn-on" gene expression in A. protothecoides. We tested the A. protothecoides promoter region of cyc6 (a Ni-induced system in C. reinhardtii) for Ni-induction, but this showed a low-level response to Ni, and the features responsible for Ni-induction in C. reinhardtii were not present in the promoter region. In the coming year, we will engineer the C. reinhardtii Ni-induced promoter in A. protothecoides and test expression, first using an antibiotic-resistance gene for proof-of-principle.

As of June, 2013, the work from this project will have been presented at two conferences and recognized by an a Los Alamos Outstanding Poster Award honorable mention.

Future Work

We have completed construction of transformation vectors to introduce critical genes involved in hyaluronic acid (HA) synthesis into the single-celled algae, Chlamydomonas and Chlorella. We will be expressing these genes and characterizing their phenotypes over the next year. In addition, we will build multi-gene constructs that we predict would enhance HA synthesis. In addition, we have identified cell surface proteins on Chlorella and their appropriate genes. We will be generating nanobodies against some of these peptide fragments and cloning the corresponding nanobody-encoding gene as a fusion to genes encoding other cell-surface displayed proteins with the objective of inducing autoflocculation. These constructs will be tested over the next year.

Conclusion

We expect to develop: 1) innovative technologies to control gene expression in Algae, 2) Expression of novel biomolecules that will efficiently flocculate algal biomass with virtually no energy costs. These results will lead to and energy efficient, economical methods for harvesting algae.

Publications

Subramanian, S., A. N. Barry, S. Pieris, and R. T. Sayre. Comparative energetics and kinetics of autotrophic lipid and starch metabolism in chlorophytic microalgae: implications for biomass and biofuel production. 2013. BIOTECHNOLOGY for BIOFUELS. 6 (1): 150.

Label-Free Measurement of Single Cells by Impedance Cytometry in a Microfluidic Device

Babetta L. Marrone
20130239ER

Introduction

Single cell analysis is needed for characterizing heterogeneous populations, which is not only important for most applications in the biosciences, but is particularly critical for emergent industries like algae biofuels and global public health. Single cell analysis systems require integration of technologies for counting, positioning, separating, sorting, characterizing, and identifying single cells in a high-throughput manner. Typically, these functions are accomplished using flow cytometry and sorting in a laboratory setting, which requires extensive sample preparation and fluorescent labeling for sensitive detection. Although very effective and highly specific, these approaches do not lend themselves to modern needs in bioenergy or global public health where cost, robustness, speed, and sample throughput are as important as the measurements being performed. Microfluidics "lab on a chip" technologies hold great promise for the future of single cell analysis in the field. However, as instruments "shrink" it will also be essential to simplify measurements.

We will develop a new approach for single cell analysis using impedance sensing on a microfluidic device. We will: 1) Design and construct a microfluidic-scale, impedance sensing device for detection and manipulation of large numbers of single biological particles based on intrinsic properties, without the use of specific labels. 2) Develop new signatures for distinguishing specific cells in context, based on intrinsic properties obtained by impedance sensing; and investigate the cellular sources of these responses. 3) Apply the new approach to solve real-world problems in biological detection using the model system of direct quantitation of biomass and lipid productivity during algae cultivation for biofuel production. The expected outcome of this project is a simplified measurement modality and new set of signatures for investigating and identifying biological particles in real time. High-impact applications include monitoring biofuel production, and other potential applications in medical diagnostics, biomedical research, pharmaceutical screening, toxicology, and environmental science.

Benefit to National Security Missions

We will develop a new measurement modality and new set of signatures for investigating and identifying biological particles in real time for high-impact applications in biofuel production, as well as medical diagnostics, drug discovery and screening, toxicology testing, and biomedical research. The greatest impact of this simple, label-free, nondestructive approach is that it can be implemented on small, low cost platforms, thus enabling introduction of real-time sensing and measurement technologies into new fields of bioenergy and health care. The work has immediate applications to DOE-EERE programs in renewable energy, replacing petroleum-based fuels with fuel made from algae feedstocks. The work will support automation of algae cultivation systems for biofuel production. Automation will save operating costs, optimizing growth and harvesting schedules to reduce the overall cost of biofuels production. The capability to design and test lab-on-chip devices directly addresses mission needs of the National Institutes of Health (NIH) and the Department of Defense. Both agencies are actively seeking to develop miniaturized sensor devices for biomedical and biosecurity applications in support of National and Global Security mission challenges. Specifically, the work directly addresses translational medicine and global public health missions of NIH by providing a new approach for disease diagnostics that is rapid, simple, and affordable.

Progress

This project has two main parts: Signature Development and Device Development. Our initial approach is to focus on extracting key intrinsic (unlabelled) features from cells that can be used as signatures. We will also build a device that can detect these signatures. Our hypothesis is that measurement of cell impedance will enable us to

distinguish key cell features that differ between populations of interest.

Signature Development
A primary goal is to develop precise new classifiers of complex cell populations based not on the properties of individual cells but on the multi-dimensional distributions of their collective statistics. Toward this end we have used the laboratory's Amnis ImageStreamX imaging flow cytometer. This instrument can detect twelve channels: two bright field, side scatter, and nine fluorescence wavelengths. For each channel an image of each particle in flow is obtained. The high information content that we can obtain on populations of single cells makes it ideal for identifying intrinsic properties of cells that could be used as classifiers and attributed to specific cell properties.

Initial experiments were focused on comparison of algae populations with low and high lipid content. Using several different combinations of laser excitations, fluorescence filters, and lipid staining protocols, we have collected a few hundred different features (related to cell fluorescence, size, shape, etc.) for each of approximately 10k cells in each of two replica populations of the high and low lipid populations. These data, as well as simulated mixtures of the data, are being used to train preliminary classifiers, based upon non-parametric mixture models. We have first considered classifiers based upon the distribution of each individual feature, and we are now extending to explore the classification of populations based upon several features at once. Our preliminary goal is to develop an approach to quantify a priori the accuracy with which we can identify the precise mixture of two different cellular populations (e.g., high and low lipid content), particularly when the heterogeneity within each population has the same or greater order of magnitude as the average difference between the two populations. To test each of our existing and future classification strategies, we intend to run a series of double blind tests in which one member of the team will prepare several unknown mixtures of cells and the algorithms will be asked to identify, and estimate uncertainty bounds for, the mixture. We envision that the computational classification tools being developed in this project (in Matlab and more recently in Python) will apply not only to the Amnis device but also to measurements taken through the acoustic focusing, impedance device under development as well as to other existing flow cytometry capabilities at the laboratory.

Device Development
Cell focusing is an essential feature of the impedance cytometer device that we plan to build as part of this project. Within the first quarter of FY13, we fabricated a first generation device with a Surface Acoustic Wave (SAW) cell-focusing feature. The device was constructed from silicone rubber on a lithium niobate substrate. SAW producing finger electrodes were electrodeposited onto the substrate at CINT. Microchannels were molded into PDMS rubber sheets, which were bonded onto the lithium niobate substrate. Feed and product flow occurred through holes drilled through the PDMS rubber sheets prior to assembly. Initial bulk impedance measurements of cellular solutions have been noisy, running into the detection limits of our Agilent impedance analyzer, a fact that confirms the need to measure cellular impedance on a microfluidic platform. The microfluidic platform with SAW focusing, gives us the ability to precisely align each cell in flow. This precise alignment and the comparatively high cell to orifice ratio allows for a high signal to noise ratio. Additionally, the mircofluidic platform allows for high throughput while still measuring on the single cell scale. First generation microfluidic SAW-impedance measurement devices have been designed, built and are in the initial testing stage.

After completing a literature search, the team reached a consensus on the best methodology to investigate novel impedance signatures of cells. The necessary equipment to implement this technology was researched and ordered. We purchased a digital microscope camera with analysis software and a National Instruments control system. This hardware is essential for development of the impedance cytometer system.

Future Work

- Build the next version of a microfluidic device combining SAW (for focusing) with impedance sensing of cell properties. Apply numerical modeling to guide and optimize the design of the device. The next version prototype will be built during the 2Q of FY14.
- Continue studies to identify intrinsic features of cells that can be used as candidate signatures in biological applications, using established methods (e.g. imaging flow cytometry). During FY14 we will focus on distinguishing cancer cells from non-cancer cells; and cancer cells from background blood.
- Use a special chamber for making single cell measurements of impedance responses off-line from the main microfluidic device to guide us in development of models needed to relate impedance responses to physical cell properties.
- Use the microfluidic device to study and validate the impedance sensing and develop signatures by attributing the measurements to specific cell properties. Apply computational approaches to model and predict the

effect of physical properties on measured impedance signals and verify the model by performing impedance measurements of cells with known physical properties.

- Develop the sorting feature of the microfluidic device, in 4Q of FY14. Sort cells based on size and another feature as measured by impedance analysis. Confirm the impedance measurements by comparison to established methods.
- Continue to demonstrate the general applicability of impedance sensing in new applications.

Conclusion

We will build a microfluidic device to measure and sort cells, based on impedance signals; and will demonstrate quantitative, measurement performance of this device to analyze cell size, lipid content, viability, and other intrinsic features. We will also determine the physical cell features that result in the impedance differences between single cells. The overall result of the project will pave the way for simple, label-free, single cell analysis devices that can be used for a variety of applications, e.g. to automate real-time cell analysis for algae biofuel production; or to bring cell diagnostic capabilities into resource-limited areas of the world.

Publications

Ai, Y., C. K. Sanders, and B. L. Marrone. Separation of Escherichia coli bacteria from Peripheral Blood Mononuclear Cells (PBMC) using Standing Surface Acoustic Waves (SSAW). 2013. Analytical Chemistry. 85 (19): 9126.

Multidisciplinary Studies of Long Non-coding RNAs: Towards a Structural Basis for RNA in Epigenetics

Karissa Y. Sanbonmatsu
20130319ER

Introduction

RNA (ribonucleic acid) is DNA's molecular cousin. RNA is similar to DNA in composition; however it often performs a function in the cell, unlike DNA, which is considered solely an information carrier. In all living systems, including humans and bacteria, the information for the blue print of the organism resides in DNA. The blue print is implemented by transferring the genetic information from DNA to RNA. Next, the genetic information is converted from the RNA into proteins, which make up the structures of the cells and perform the biochemistry. RNA has long been thought to mainly serve as a transferring medium, moving information from DNA to proteins. However, in the past five years, it has been found that the vast majority of the human genome (more than 90%) is converted into RNA, but never gets converted into proteins. In the past 2 years, it has been found that much of this RNA is in the form of long non-coding RNA (lncRNA, or 'link' RNA). These gigantic RNAs do not 'code' for protein, but instead are thought have a function themselves: turning on and off other genes. The RNAs are often associated with epigenetics. Epigenetics has exploded in the past 5 years and is closely related to stem cell programming. In epigenetics, Larmarkian-like effects occur, where the environment modifies, but does not mutate DNA. These modifications are passed down to future generations of organisms. For example, babies undergoing extreme stress shortly after birth have an altered stress response, which is passed down to the grandchildren. While many long RNAs have been found to be critical for cancer, hereditary disease, brain function and development, the mechanism of long RNA action is not understood. We will perform the first ever structural study of long RNAs to help determine their mechanism.

Benefit to National Security Missions

We will produce preliminary data for specific NIH calls in cancer-related non-coding RNAs and several calls for NIH's epigenomics program for epigenetic mark discover, including the role of noncoding RNAs in regulation of transcription (Jerome Garcia). The project is directly related to DARPAs CLIO Memory thrust, including "basic research towards use of epigenetic systems to report environmental events" (Cathy Cleland). It is indirectly related to DOE BER Biological Systems Science "Low dose radiobiology effects on epigenetic regulation."

Progress

In this fiscal year, we accomplished many of our goals and made tremendous progress. We were able to complete the first secondary structure of an intact long non-coding RNA, resulting in several publications and invited talks. We employed our novel shotgun secondary structure (3S) method, which did garner significant attention in the RNA community (especially at the recent RNA 2013 conference last week). In this method we perform several rounds of structural chemical probing. In chemical probing, a special reagent is added that only reacts with highly mobile nucleotides, allowing us to map which nucleotides are base paired in double helices and which nucleotides are single stranded. Thus, we perform 1 round of chemical probing on the entire long non-coding RNA. We then perform successive rounds on fragments of the RNA. If we obtain a match between signals for the full RNA and its fragments, this demonstrates that the fragments have a modular fold and comprise modular subdomains. By probing smaller and smaller fragments, we are able to determine the complete fold of the long non-coding RNAs, a hard problem, which has been long sought after. To verify the fold, we perform comparative species analysis, which enables us to identify conserved base pairs within the Watson-Crick double helices. Prior to our results, it was not known if long non-coding RNAs were completely disordered or if they were highly structured. Our study demonstrated that they can be highly structured, generating intense interest in the RNA structural biology community.

Future Work

In this fiscal year, we will apply our structure technique (shotgun secondary structure) to several more long non-coding RNA systems. The first system is COOLAIR, a canonical epigenetic switch in plants that allows plants to flower only after prolonged exposure to cold. The second system is Braveheart, a long non-coding RNA that plays a key role in heart cell development. The third system is Gas5, which is critical for hormone signaling. To accomplish this, we will transcribe the RNA for each system, denature the RNA, fold the RNA and chemically probe the RNA. In chemical probing, a special reagent is added that only reacts with highly mobile nucleotides, allowing us to map which nucleotides are base paired in double helices and which nucleotides are single stranded. In this way, we are able to determine the secondary structure of the long non-coding RNA.

Conclusion

Our goal is to perform the first structural study of long non-coding RNAs (ribonucleic acids). The only example of a large RNA complex whose 3-D structure has been solved is the ribosome, which took 3 decades of work. We will take the first step in structural studies of long non-coding RNAs by determining the 2-D structure. For large systems, 2-D structures are impossible to accurately determine computationally due to the large number of permutations and possible structures. We have devised a novel experimental technique called SHOT-GUN structure determination. We will use this to obtain the 2-D structure experimentally.

Publications

Hennelly, S. P., I. V. Novikova, and K. Y. Sanbonmatsu. The expression platform and the aptamer: cooperativity between Mg2+ and ligand in the SAM-I riboswitch. 2013. NUCLEIC ACIDS RESEARCH. 41 (3): 1922.

Novikova, I. V., A. Dharap, S. P. Hennelly, and K. Y. Sanbonmatsu. Shotgun secondary structure determination of long non-coding RNAs. 2013. Methods. 63 (170): 1.

Novikova, I. V., S. P. Hennelly, C. S. Tung, and K. Y. Sanbonmatsu. Rise of the RNA machines: Exploring the structure of long non-coding RNAs. 2013. Journal of Molecular Biology. 425 (19): 3731.

Novikova, I. V., S. P. Hennelly, and K. Y. Sanbonmatsu. Do lncRNAs have secondary and tertiary structure?. 2012. RNA BIOLOGY. 9 (12): 1398.

Novikova, I. V., S. P. Hennelly, and K. Y. Sanbonmatsu. Structural architecture of the human long non-coding RNA, steroid receptor RNA activator. 2012. NUCLEIC ACIDS RESEARCH. 40 (11): 5034.

Novikova, I. V., S. P. Hennelly, and K. Y. Sanbonmatsu. Sizing up long non-coding RNAs: Do lncRNAs have secondary and tertiary structure?. 2012. Bioarchitecture. 2 (6): 189.

Novikova, I. V., S. P. Hennelly, and K. Y. Sanbonmatsu. Tackling structures of long noncoding RNAs. To appear in International Journal of Molecular Science.

Novikova, I. V., S. P. Hennelly, and K. Y. Sanbonmatsu. Experimentally determined secondary structures of cancer-related long non-coding RNAs. Invited presentation at 245th ACS National Meeting & Exposition. (New Orleans, 7-11 April, 2013).

Sanbonmatsu, K. Y.. Rise of the RNA Machines: Long Non-Coding RNAs. Invited presentation at 10th Horizons in Molecular Biology Conference International. (Max Planck Institute, Gottingen, Germany, 9-12 Sept. 2013).

Sanbonmatsu, K. Y.. Integrating simulations and experiments of the SAM-I riboswitch. Invited presentation at RNA Dynamics. (Telluride, CO, 22-26, July 2013).

Sanbonmatsu, K. Y.. Large-scale simulations of biomolecular machines. Invited presentation at Biosupercomputing. (Tokyo, Japan, Dec. 2012).

Sanbonmatsu, K. Y.. Understanding the atomistic mechanism of magnesium effects of RNA dynamics. Invited presentation at Mini-symposium on Modeling, Simulation and Function of Biomolecular Assemblies.. (University of Tokyo, Tokyo, Japan, Nov. 2012).

How Trees Die: Multi-scale Studies of Carbon Starvation and Hydraulic Failure During Drought

Sanna A. Sevanto
20130442ER

Introduction

In this project we will develop Ultra Low Field (ULF) Nuclear Magnetic Resonance (NMR) and Magnetic Resonance Imaging (MRI) to simultaneously detect changes in both water and carbon use of trees and use this novel technique in targeted drought stress experiments for building a comprehensive multi-scale view of the role of carbon and water in plant mortality. NMR and MRI are ubiquitous tools for non-invasive studies of soft-tissue anatomy and function in medicine and biology and their suitability to studying water dynamics inside plants has been demonstrated. The traditional techniques, however are difficult to use in studies of trees because they require permanent magnets of high magnetic field that limit detectable sample size and shape restricting in vivo applications. The major challenge of studies of tree physiology and mortality is a lack non-invasive methods to detect water and carbon dynamics. These substances travel through the plant along pressure gradients and any invasive method will immediately change teh state of the system when applied. Therefore, development of non-invasive methods capable of in vivo measurements of plant function is essential for advancing our understanding of plant function and responses to climate.

ULF NMR/MRI uses simple pulsed electromagnets and optimized detection coils that operate in room temperature using very low magnetic fields; three orders of magnitude lower than traditional NMR/MRI making this technique adaptable to natural plant environment. The ULF NMR/MRI system is also very light (~10lb) and coil size is adaptable to tree size enabling measurements at several locations on a tree simultaneously.

Benefit to National Security Missions

Understanding global climate change impacts and feedbacks with terrestrial ecosystems is a critical mission for DOE-SC-BER. Climate change and weather will affect national security impacting also trade and transportantion as well as communication. Mechanistic understanding of vegetation function during drought and mortality is critical fundamental knowledge for prediction of progress of global climate change via the interactions of vegetation with climate.

Forests store ~30% of fossil fuel emissions, and forest mortality may release large amounts of carbon dioxide to the atmosphere affecting predictions of atmospheric carbon storage and effects of fossil fuel use. Forest mortality and increasing drought will also impact restoration of natural environments. Currently, understanding the mechanisms of vegetation mortality relies on unproven hypotheses because we lack non-invasive, in vivo methods to study plant water and carbon dynamics. The interaction of water and carbon transport in plants is one of the fundamental unresolved topics of plant biology. Improving our understanding of carbon-water interactions inside plants is critical for understanding controls of productivity (photosynthesis) and material allocation as well as plant water use. In addition to trees, the methods developed in this project will be applicable to other type of plants from crops to biofuel crops, and the fundamental science results can be applied to improve renewable food and energy resources.

Progress

Our goal for this year was to produce a robust Ultra Low Field (ULF) Nuclear Magnetic Resonance (NMR) system for measuring changes in water content inside living trees in greenhouse conditions, and evaluate whether carbon could be detected with this system as well. To achieve this we have performed temperature sensitivity tests with water bottles and tree branches and made substantial progress in understanding the temperature systematics. The error we currently expect from temperature variation is ~1-2%. We have standardized the measurement setup and were able to operate without a shield when using a slightly higher fixed magnetic field

instead of pre-polarization. This will enable multiple ULF NMR systems on one tree. We have run calibration measurements to determine the relationship between NMR signal and water content of different tree species and found out that NMR signal changes very linearly with water content in all species, but the overall signal strength depends on the species. To get a better understanding of the source of this variation we have conducted x-ray tomography and NMR measurements on the same branches and are analyzing the data for linking wood structure with NMR signal strength. We have also performed in vivo water content measurements on an apple tree. The results from that experiment show that we can detect long term changes in water content very reliably (drought and re-watering), but interpretation of the diurnal variations in the NMR signal require good understanding of the temperature effects.

We are currently repeating these measurements on an aspen tree with our improved coil temperature detection system which allows correction of the signal for temperature effects, and preparing a methods publication of our data. As of June 2013, we have not tested potential carbon injection methods for carbon detection, but theoretically we should be able to use either uptake of labeled carbon isotopes via photosynthetic pathway, spraying of labeled sugar water on the leaves or injection of sugar-solution into the conduits. The carbon signal should be high enough for detection with ULF NMR at least on the twigs close to the location of injection.

Future Work

The goal of the next fiscal year is to 1) perform first experiments on progress of hydraulic failure in trees using Ultra Low Field (ULF) Nuclear Magnetic Resonance (NMR) in a greenhouse environment, and 2) continue development of Magnetic Resonance Imaging (MRI) of water content changes and NMR detection of carbohydrates. In the experiments we will use manipulative methods to cause hydraulic failure in the conductive tissues and follow its progress with ULF-NMR. We will try to determine the link between hydraulic failure and carbohydrate availability by using surfactants (water loss -based hydraulic failure) and phloem girdling (carbohydrate loss -based hydraulic failure) as manipulations. The experiments will be supported by well-established plant physiological methods (gas exchange, sap flow, tissue water content).

Conclusion

Our technical goal is to develop Ultra Low Field (ULF) Nuclear Magnetic Resonance (NMR) and Magnetic Resonance Imaging (MRI) to accurately quantify water and carbon dynamics inside a tree in natural enviroments. Our science goal is to use ULF NMR/MRI to determine the roles and interactions of water and carbon cycling in tree drought mortality. Currently plant physiology and mortality studies lack non-invasive, in vivo methods. Our new technique will provide the key parameters and insights for mechanistic modeling of plant mortality, which is critical for understanding climate impacts and feedbacks on vegetation.

Publications

Cruz, N., J. Yoder, and M. Espy. Active Q-switching in NMR applications. Presented at 13th Annual Student Symposium, Los Alamos National Laboratory . (Los Alamos, NM, July 26-27).

Sevanto, S.. Phloem transport and drought. 2013. In 3rd International Conference on Plant Vascular Biology. (Helsinki, Finland, 26-30 Aug, 2013). , p. 56. Helsinki: Helsinki University Press.

Sevanto, S.. Phloem transport and drought. Journal of Experimental Botany.

Yoder, J.. Measuring absolute water content of trees in vivo with low field NMR. Invited presentation at Physics Division Summer Seminar PostDoc Series. (Los Alamos, NM, June 26, 2013).

Yoder, J., M. Espy, N. McDowell, J. Resnick, and S. Sevanto. Measuring absolute water content of trees in vivo by low field NMR in an uncontrolled environment. Presented at 54th Experimental Nuclear Magentic Resonance Conference. (Pacific Grove, CA, 14-19 April, 2013).

Pyrocumulus Collapse: Unpredicted Wildfire Dangers

Rodman R. Linn
20130487ER

Introduction

The Las Conchas wildfire surprised everyone when it unexpectedly burned over 35,000 acres in less than seven hours during its first night even though it was burning downhill in sparse vegetation and under mild wind conditions. One theory for this peculiar behavior is that a particulate-laden portion of the fire-induced pyrocumulus (pyro-cu) column collapsed, and unleashed a symbiotic density current/fire front that incinerated everything in its path. However the precipitating phenomenology of these events is not understood.

LANL's coupled fire/atmosphere model, FIRETEC, will be used in three tandem efforts and will focus on fundamental process and then merge these findings into combined analysis as the project progresses. These initial foci are: 1) assuring that the coupled fire/atmosphere code, HIGRAD/FIRETEC adequately captures the interaction between winds and plumes, 2) deciphering onset of a pyro-cu collapse and density current formation, and 3) understanding the interactions between a pyro-cu density current and a fire front.

The final goal is to reconstruct key aspects of the coupled fire/atmosphere interaction that occurred in the first night of the Las Conchas fire and identify if it was possible that the combined dynamics of the fire and ambient conditions could have lead to a partial pyro-cu collapse and whether such a collapse and resulting density current could have been responsible for the observed fire behavior. Such an effort has never before been possible due to computational cost and complexity of process interactions, but LANL's R&D 100 award-winning HIGRAD/FIRETEC is being reformulated to take advantage of LANL's new High Performance Computing (HPC) machines.

Benefit to National Security Missions

This work will establish the capability to perform much larger coupled wildfire simulations and enable wildfire risk assessment across the DOE complex. This work increases LANL's unique capacity to study coupled fire/atmosphere phenomena in realistically complex environments and supports the USDA Forest Service (USDA FS) wildfire research and management missions. This work will position LANL to serve a larger research role and to assume direct relevance to the fire management sector of the USDA FS. Pyro-cumulus columns inject significant amounts of particulate high in the atmosphere and thus have significant impacts on the atmosphere's radiation balance.

Understanding pyro-cumulus dynamics, conditions leading to collapse, and the effects of resulting density currents on fire behavior is crucial for elucidating the fire-related effects from an urban nuclear event (on US soil or elsewhere). In this setting, density currents would be channeled by street canyons, thereby focusing the kinetic and thermal energy and potentially increasing damage by an order of magnitude. LANL has ongoing activities in support of DHS, STRATCOM, and DTRA to understand damage and lives at risk from an urban conflagration that could likely result in a pyro-cumulus collapse.

Progress

A set of equations was derived to represent combustion products that could be tracked in the LANL-developed, atmospheric dynamics model HIGRAD/FIRETEC. The fundamental concept behind this model is to adjust the buoyancy term in the momentum equation to account for fire-produced particulate matter. When combustion products are injected into a volume of air, they increase its mass thereby reducing is buoyancy or even causing it to become negatively buoyant. This is analogous, but opposite to the way that water vapor loading in the atmosphere decreases the density of air and can causes a parcel to rise. Combustion-produced particulate mat-

ter results in more dense air than its surroundings and this products-laden air will have a tendency to descend. This model was a fairly simple representation of soot as Fullerene (C60). In a large, crowning wildfire, there is a range in the size of debris that is released. The size of these particulates can be small, such as molecular soot. But, it can range in size up to ash, pine needles and larger debris. The soot/water-vapor model consists of a new equation of state, including modified specific heats and gas constant. It also includes a source term to the mass conservation equation and requires additional conservation equations for soot and water vapor.

The theoretical soot/water vapor model described above has been incorporated into HIGRAD, in-order to test the plume collapse hypothesis. Indeed, preliminary results show that a soot-laden plume could collapse under its own weight under certain atmospheric and wildfire conditions. A second ongoing effort to study this phenomenon involves a simple analytical model that describes the fluid dynamics resulting from the presence of both a vertical temperature and a vertical soot gradient. Together, these gradients result in a vertical density gradient that could be stable or unstable. From this model, a parameter space can be extracted to quantify the effects of a large range of soot and temperature profiles within the confines of a wildfire plume. This parameter space can then be used to theoretically predict the collapse potential for plume and atmospheric conditions.

Additionally, initial-phase work efforts have been aimed at confirming HIGRAD/FIRETEC's ability to capture critical aspects of a cross flow interacting with a column of rising air. Thus far, we have focused on simulated results of the jet in a crossflow (JICF). The JICF has two sub-catagories, the non-bouyant JICF (NB-JICF) and the buoyant JICF (B-JICF). In the NB-JICF, mass and vertical momentum are injected from the bottom of a rectangular domain into a uniform crossflow, whereas the B-JICF involves a heated jet issuing from the surface. This work not only validates model accuracy, but has also yielded insightful results suggesting non-dimensional parameter regimes wherein plume collapse may be more or less likely.

To date we have performed numerous simulations and compared model results against experimental data and theoretical formulations for the NB-JICF jet-to-crossflow velocity ratios (Vr) and crossflow Reynolds number (Re) regimes as obtained through non-dimensionalisation of the governing equations. Similarly, it can be shown that the non-dimensional parameter Vr of the NB-JICF is analogous to a convective Froude number (Fr) obtained for the B-JICF governing equations. Armed with this new discovery we hope to show that salient characteristics of the less thoroughly studied B-JICF can be directly related to well known features of the more comprehensively studied NB-JICF. A publication on the relationship between these two scenarios will result pending simulations of the B-JICF that are currently underway.

Future Work

The research will continue along parallel foci that will coalesce into a combined study in later years: 1) coupled fire/plume/atmosphere/topography interactions leading to pyro-cu collapse; and 2) the interaction of the resulting density current with wildfire behavior.

In order to have confidence in the models ability to capture essential atmospheric processes, we will complete verification of FIRETEC's ability to capture critical plume interactions with shear environment.

To capture the coupled fire/atmosphere behavior at high resolution (2–5 m), represent realistic length-scales (100s of meters to km), and avoid adverse impacts of numerical boundaries, one of the initial tasks will be to reformulate the Monte Carlo radiation and parallel input/output data exchange so that fully coupled fire/atmosphere simulations can be performed on the large domains required for this study.

New models will continue to be implemented and evaluated in FIRETEC to include soot and water effects on buoyancy. This formulations are currently expected to include both Lagragian and Eulerian approaches.

The effects of a range of soot concentrations will continue to be evaluated in order to determine their implications and importance. In the event that plume dynamics are highly sensitive to soot concentration, this important finding would dictate a critical need for new instrumentation to accurately assess this hazard.

Initial wildfire acceleration and intensification as the leading edge of the density current reaches and passes through the fire will be studied over flat, sloping, and canyon topographies. These simulations will highlight the importance of: 1) the pressure gradient across the leading edge of the density current; 2) the uplift-ing vertical velocities ahead of the current; and 3) the sustained accelerated winds within the current.

Conclusion

Fire behavior experts have suggested one viable hypothesis for the fire behavior during the first night of the Las

Conchas fire: a partial collapse of the soot-laden pyrocumulus column (pyro-cu) that towered above the fire, causing a sustained density current carrying fire at high rates of speed. The proposed research will test this hypothesis, and decipher the combination of environmental conditions and fire behavior dynamics that enabled such an event. The insight provided by this research will help fire managers to identify pyro-cu collapse risk scenarios and to implement possible life-saving emergency actions if one occurs.

Biocatalysts for Remediation of Uranium Wastes

Francisca N. Rein
20130590ER

Introduction

A strategic priority of the U.S. Department of Energy is the cleanup of a multitude of sites across the Nation that contain subsurface contamination with radionuclides from legacy waste accumulated over five decades of nuclear activities during the Cold War. Given the daunting volume scales of soil and groundwater contamination with uranium and toxic heavy metals at low concentrations, in-situ bioremediation by microorganisms has been greatly regarded as a promising approach to cost-effective, viable technologies for environmental decontamination. This biological approach is based on the established fact that some bacteria contain specific multi-heme, c-type cytochromes that can catalyze the reduction of uranium from its soluble form in oxidation state U(VI) to its insoluble U(IV) state as uraninite (UO2). However, this reaction takes weeks to reach equilibrium and leads to incomplete reductions of uranium(VI) in contaminated sediments. Moreover, the use of sacrificial electron donors in bioremediation is impractical and promotes deactivation due to the competing re-oxidation by the reversible activity of sacrificial agents.

A major bottleneck for further advances in the derivation of effective technologies to address this grand challenge is the missing knowledge about the reaction mechanisms and their specific metal-binding interactions. Therefore, the overarching goal of our proposed research is the development of improved, bioengineered enzymes as biocatalysts toward the efficient and selective bioremediation of nuclear waste.

We will achieve this high-impact objective through an interdisciplinary application of our combined capabilities in biological and physicochemical sciences. Our research efforts were designed to address a critical environmental/health challenge of immediate national concern as well as to create new capabilities of relevance to current and emerging Laboratory missions in this direction.

Benefit to National Security Missions

This research supports the above missions by providing advancements toward the environmental decontamination and cleanup of nuclear waste. A key component of this research that underpins core missions in national security and stewardship is the development of new capabilities and knowledge about the physicochemical behavior of actinides/radionuclides. This project also ties directly into the LANL/LDRD Grand Challenge “Complex Biological Systems” (specifically “to resolve national challenges in energy, health and environment” as well as “biological interactions and metabolic patterns that control ecosystem functions”). The importance and urgent needs for basic science to enable bioremediation technologies have been recognized and stimulated by several DOE initiatives, especially through the Office of Biological and Environmental Research. In addition to DOE, this research has high relevance to NNSA, DoD, and DHHS (NIH) programs. With underlying themes related to (bio) sensing/detection of radionuclides or toxic substances, nuclear forensics, molecular bioelectronics, and bioenergy, the outcomes of our proposed R&D may naturally lead to ties into programs within DHS, Intelligence Agencies, DoD (DARPA, DTRA, ONR), and DOE (BES, ARPA-E) among some of the identified agencies/programs.

Progress

In these first nine months since the project start, our efforts have been primarily focused on establishing the preparative methodologies and (bio)analytical techniques for the isolation and characterization of our model biocatalyst for uranium electroreduction - the tetra-heme protein known as D. desulfuricans G20 cytochrome c3 (Cyt c3). From our initial approach, expressing this protein into Escherichia coli (E. coli) proved to be nontrivial. Multi-heme cytochromes are generally more difficult to express correctly because co-factors are needed to enable the proteins to obtain their native fold. In our case, Cyt c3 was no exception. Its four hemes

must be covalently attached (via thioether linkages) to the polypeptide chain at the CXX(XX)CH binding sites, and the correct distal axial ligands must be connected to the metal center (ferric ion) in the nascent protein. For these critical interactions to form properly during E. coli recombinant expression, specific molecular assembly proteins are needed. These helper proteins are collectively known as the Cyt c maturation proteins Ccm A-H (ccm cluster), which are responsible for the correct ligation of the hemes to the Cyt c3 apoprotein while it is translocated to the periplasmic space. To help promote the expression of Cyt c3, we therefore co-expressed the pC3 plasmid (which carries the Cyt c3 gene) with the pEC86 plasmid (a pACYC derivative carrying the ccm gene cluster).

Despite the significant improvements from the use of helper maturation proteins, the expression and growth of Cyt c3 required further optimizations due to our low yields obtained overall. To that end, we have incorporated several changes to our strategy. Various systematic attempts have led us to find that the most successful approaches involved auto-induction and temperature effects. After initially adopting methods that relied on using isopropylthio-β-galactoside (IPTG) to induce the expression of Cyt c3 under control of the T7 promoter, we have now found that auto-induction processes are superior because of control over amounts of media and supplements (e.g. glucose, lactose, phosphate, sulfate, and trace metals) to allow for bacteria growth to high densities prior to starting protein expression.

Another key finding was the reduction of the typical growth temperature from 37 °C to 30 °C. While reducing the temperature caused E. coli to grow slower, it presumably allowed the protein more time to properly fold into its native form. Following expression of Cyt c3, standard protocols have been successfully applied to its extraction, purification (ion-exchange chromatographic columns), and analysis (gel electrophoresis, absorption spectroscopy, and Coomassie/heme staining). Upon incorporating the above adaptations into the development of our methodology, we have now successfully obtained Cyt c3 with yield levels that are highly improved and viable to our project goals.

Parallel to our preparative emphasis of this initial phase of the project, our efforts have also involved implementing the approaches to electrode surface functionalizations as well as the analytical techniques needed for the bioelectrochemical and spectroscopic characterizations of the redox protein, both in aqueous solutions and immobilized as electrode films. Initial studies have already shown that our in-situ spectroelectrochemical techniques will be a particularly powerful approach not only to probe structure/function-property relationships as a function of the multiple oxidation states of Cyt c3 but also to investigate the mechanistic details of the reactions involving uranium electroreduction by the biocatalyst. In preparation for the next phase of our planned work, we have also developed and obtained approvals for all the required laboratory-related documentation (IWD, WPF, etc) to cover the radiological/chemical safety scope of our activities involving electrocatalytic testings with radionuclides (uranium-238) in our designated low-level rad laboratory.

Future Work

With the successful implementation of our preparative methods and analytical techniques for the expression, isolation, purification, and structural characterization of our model uranium-reductase in this initial phase (as described in the Progress section), we can next focus on 1) the structure/function-property relationships as a function of the multiple redox states of Cyt c3 in aqueous solutions and immobilized as electrode biofilms, and 2) the elucidation of reaction mechanisms for the multielectron uranium-reduction catalysis by Cyt c3. Of critical application into these tasks have been our capabilities developed for interfacial bioelectrochemistry, optical spectroscopies, and in-situ spectroelectrochemical methods.

Our next step will also require the generation of Cyt c3 mutants. Site-directed mutagenesis in association with structural and biochemical characterization of the protein and its mutants will lead to identification of structural features that are essential to U(VI)/U(IV) reduction. We plan to initially replace the axial His with Met to elucidate the role of bis-histidinyl axial ligation and cooperative redox behavior in the tetra-heme architecture. The cysteines from the CXXCH and CXXXXCH heme-binding motifs will also be replaced with alanines to perturb the binding of the porphyrin ring from the polypeptide chain. Because aromatic rings in the vicinity of porphyrin ring substituents may potentially play some role in electron transfer and redox regulation, we also plan to replace conserved aromatic residues with alanines (e.g. Phe19 and Tyr64). Replacement of Lys14 and Lys56 with alanine will also demonstrate whether these residues are essential to binding and reduction of uranium as predicted.

Combined with the synergistic tasks involving structure-function relationships and mechanistic redox characterization of Cyt c3 and its mutants, the ability to finely manipulate the protein environment at electrochemical interfaces will allow us not only to understand but also to re-design the protein with improved binding efficiency and redox reactivity toward multielectron uranium-reductase activity.

Conclusion

By seeking the understanding and application of chemical principles underlying the multi-electron reductase activity of cytochromes c3, our research can lead to high-impact contributions to the permanent environmental bioremediation of radionuclides and toxic metals. Through interdisciplinary application of biological and physicochemical capabilities, our work is aimed at advances of fundamental and practical importance for enabling the development of improved, bioengineered radionuclide-reducing systems to efficiently address the problem of incomplete reduction and recovery of uranium(VI) wastes. In addition to health/environment sciences and radionuclide (bio)chemistry, this project has a high potential for impact in areas such as nuclear forensics, (bio)sensing/detection, and bioenergy.

Publications

Rein, F. N., D. M. Vu, and R. C. Rocha. Multi-Electron Reductive Bioelectrocatalysis by a Tetraheme Cytochrome c3. .

Structure Determination of Large and Membrane-bound Proteins by Nuclear Magnetic Resonance (NMR) Spectroscopy

Ryszard Michalczyk
20130620ER

Introduction

This project addresses our current lack of knowledge of structure and function of membrane proteins and large protein assemblies by developing and applying novel Nuclear Magnetic Resonance (NMR) and stable isotope labeling methods to determine their solution structures. The limited spectral resolution of traditional multi-dimensional NMR experiments, coupled to magnetization losses due to fast relaxation in large proteins, presently limits the size of biomolecules suitable for NMR spectroscopy to <50 kDa for high resolution structures.

We will address these critical shortcomings by developing new solution NMR methods and isotope labeling schemes to produce the largest de novo NMR solution structures to date of a large, flexible protein complex (132 kDa) and a membrane-embedded system (74 kDa). The innovative aspect of this research lies in the interactive use of specific, site-selective isotope labeling and optimization of NMR methods for this specific labeling scheme. We will improve existing and develop new NMR methods applicable to solution structure determination of large protein complexes and membrane proteins by selective stable isotope labeling. We will design selective isotope labeling patterns and synthesize selectively labeled amino acids and metabolic precursors for protein labeling in vitro and in vivo. These methods will be applied to obtain the NMR solution structures of a 132 kDa protein complex and a membrane-inserted permease of 74 kDa. These will be the largest structures ever determined by NMR and will place LANL at the forefront of modern structural biology.

The results will provide new, unique, and exciting information about large, complex systems involved in synthesis of bioactive compounds (antibiotics, anti-cancer drugs, virulence factors, toxins, etc.) and development of antibiotic resistance, leading to their manipulation and subsequent production of new therapeutics and drugs. The potential impact of this research is vast.

Benefit to National Security Missions

Knowledge of the structures and mechanisms of both large proteins and their complexes and membrane-bound proteins is critical to our understanding of and intervention in processes as varied as antibiotic resistance and biosynthesis, biofuels production, and disease development (Parkinson's, Alzheimer's, diabetes, etc.). This project is directly related to LANL's missions in Global Security, Biothreat Reduction, and Energy Security and success of this project will open the structural biology field to the detailed mechanistic studies of large protein complexes and membrane-bound proteins involved in the above as well as many other processes placing LANL at the forefront of the field. Leveraging the results obtained here with LANL's synthetic stable isotope capabilities, will open funding areas from NIH, DTRA and DOE. Program managers in Global Security (Cathy Cleland) and DOE (BES/BER) will be informed of the results of our research so that future funding for these efforts can be developed.

Results obtained from this project will allow intervention into systems related to antibiotic resistance and toxin synthesis, leading to further research into development of new antimicrobials, inhibitors of efflux pumps and mechanism of membrane protein action relevant to multiple disease states. This relates directly to Biological Weapons and Defense and Pathogen Detection and Countermeasures. As such, this research is of potential high relevance to DOE, DOD and DHHS. It will also lead to discovery and innovation in Fundamental Chemistry (syntheses with stable isotopes) and Fundamental Bioscience.

Progress

During the first nine months of the project, we began work on development of new NMR (Nuclear Magnetic Resonance) pulse sequences and implementation of data handling protocols. We have created parameter

sets we expect to be optimal for specifically labeled proteins based on expected heteronuclear coupling constants in the NMR. Once specifically labeled amino acids are synthesized and incorporated into target proteins, these parameters will be further evaluated and optimized.
For data acquisition and handling we have imported and tested Non-Uniform Sampling (NUS) schemes based on maximum entropy and Iterative Soft Threshold (IST) reconstruction algorithms. We have initially tested both methods and found IST to be superior. The method will allow us to reduce number of spectra taken 4-fold for 3-dimensional NMR experiments and 10-20-fold for 4-dimensional experiments. Final tests will be performed on selectively labeled large proteins once they are produced from labeled amino acids.

We have also made significant progress towards selective amino acid labeling for large proteins. We have devised a pattern of selective isotopic substitutions for each of the twenty natural amino acids and identified required synthetic protocols based on literature data and previous developments at LANL's Stable Isotope Resource.
For optimal NMR performance, all amino acids will have amino nitrogens labeled with N-15 and α-carbons labeled with C-13 and duterated. The carbonyl carbons will be unlabeled and the side chains will have C-13 labeled and protonated carbons alternating with unlabeled deuterated carbons. A common precursors to these amino acids is [2-13C, 15N, 2H]-glycine attached to a chiral auxiliary synthon (2,10-camphorsultam). To this end, we have synthesized [2-13C, 15N]-glycine from 2-13C-bromoacetic acid (which we had available in the lab) and 15N-potasium succinimide. The reaction was performed on 0.5 mole scale and proceeded with good yield. The purified glycine was subsequently protected by esterification with methanol on the carboxyl group and with thiomethyl groups on the amino functionality.

Since all amino acids will be deuterated on C-alpha position, we attempted H/D exchange on glycine, protected glycine and glycinate sultam to establish the most efficient deuteration protocol. Deuteration attempt on glycinate sultam resulted in cleavage of glycine from the sultam and was abandoned. Deuteration of glycine proceeded very slowly at high temperatures (>160oC) in a microwave reactor and could only be performed on small scale (<2g at a time). However, deuteration of amino- and carboxyl-protected glycine proceeded at 25-40oC with catalytic amounts of sodium carbonate in D2O/methanol-d and resulted in 98%+ duteration and pure product with minimal workup (extraction). This procedure was followed for [2-13C, 15N]-labeled protected glycine to obtain 0.1 mole of the protected deuterated glycine. This was then attached to the sultam for further reactions.

We have also explored alternatives to thiomethyl protection of glycine. To this end, we have synthesized labeled glycine protected with diphenylmethylene group. Reaction was high yielding and resulted in a product that is stable, less volatile and, significantly, less pungent than the dimethylsulfide protected glycine. H/D exchange on this compound also proceeded well. This will be our new protection scheme for glycine.

Towards synthesis of amino acids with desired labeling patterns, we have reacted [2-13C, 15N, 2H]-glycinate sultam with bromoacetate, which after deprotection yielded 2g of [2-13C, 15N, 2H]-aspartic acid. Similarly, reaction of the glycinate sultam with 2H3-methyl iodide yielded [2-13C, 15N, 2H]-alanine. Thus we have fully synthesized three of the required amino acids and prepared an intermediate for syntheses of remaining compounds. We have also explored experimentally syntheses of phenylalanine and tyrosine side chains starting from pyranone and triethyl orthoformate for isotopic labeling. These syntheses are currently being optimized. Overall, chemical synthesis of amino acids is well on track.

For metabolic labeling of proteins, we have cloned the gene for the small protein, ubiquitin (76 amino acids) into E. coli hosts. Expression of this protein under various labeling conditions will allow us to monitor incorporation of isotopes at specific positions in amino acids, since NMR spectra for ubiquitin are well resolved and characterized. So far, we have performed growth in the presence of labeled glycerol and labeled pyruvate. Analysis of produced ubiquitin for isotope incorporation is in progress.

Future Work

During first year of the project, new NMR pulse sequences and data handling protocols will be developed and optimized; synthesis of labeled amino acids and precursors will begin with a target completion by the end of the first 18 months. Tasks to be completed include:

- Modify and optimize recently developed 3D TROSY-hNCAnH and Time-Shared 3D HSQC-NOESY NMR experiments by optimizing sequence pulses and delays for selectively labeled amino acids. To dramatically reduce acquisition time, we will incorporate non-uniform sampling (NUS) and a newly developed data reconstruction algorithms that only require a reduced number of data points to be recorded without loss of resolution and sensitivity. Experimental time will be reduced by an order of magnitude, with improved sensitivity.

The Time-Shared 3D-HSQC-NOESY will be extended to a 4D pulse sequence with 13C phase shifts allowing for unambiguous identification of cross-peaks and determination of distance constraints. Here too we will use and optimize the NUS scheme in combination with coupled read-out and excitation TROSY for maximum sensitivity and resolution. This will reduce the required experiment time, increase spectral resolution, and will also simplify resonance assignments and allow accurate determination of distance constraints for high-resolution structure determination.

- Devise new stable isotope labeling schemes for selected amino acids to simplify NMR studies of large and membrane inserted biomolecules. The isotopic labels will be incorporated at specific positions to optimize NMR signal and limit relaxation losses during experiments. Co-optimization of sample labeling and NMR methods development will improve the spectral resolution and signal quality allowing very large and membrane-inserted proteins to become accessible by NMR spectroscopy for the first time. The selectively labeled amino acids will be prepared by direct chemical synthesis and/or by using labeled metabolic precursors (glycerol, pyruvate) for in vivo protein production to allow very specific and selective isotopic enrichment.

Conclusion

We will improve existing and develop new NMR methods generally applicable to solution structure determination of large protein complexes and membrane proteins by selective stable isotope labeling. We will design selective isotope labeling patterns and synthesize selectively labeled amino acids and metabolic precursors for protein labeling in vitro and in vivo. These methods will be applied to obtain the solution structures of a 132 kDa protein complex and a membrane-inserted permease of 74 kDa. These will be the largest structures ever determined by NMR and will place LANL at the forefront of modern structural biology.

Integrated Biosurveillance

Benjamin H. Mcmahon
20130810ER

Introduction

Our pilot study will apply three state of the art diagnostic technologies to a high disease burden population in western Kenya. We will also perform the multiple types of epidemiological analyses necessary to derive understanding from the novel data. The samples are all derived from co-morbidities (tuberculosis, Salmonella, and Staphylococcus) associated with a 12 year longitudinal study performed in a pediatric malaria clinic in the Saiya District of Kenya by our collaborator, Prof. DJ Perkins of the University of New Mexico. The three diagnostic technologies are:

- Rapid Biomarker Detection: Approaches will be developed to detect proteins, lipids, and carbohydrates from human or animal samples. Reagents for tuberculosis, Staphylococcus, and Salmonella will be applied and assessed.
- Oligonucleotide-based diagnostics for pathogen characterization: This will include 48x or 96x multiplexed, PCR-based nucleic acid assays to species- strain- and antibiotic resistance- type for Salmonella and Staphylococcus.
- Sequencing of non-host RNA: Novel sample preparations will be developed and automated to provide 10 million pathogen RNA sequences from each sample. These data will be analyzed to observe unexpected pathogens, expression level of virulence factors, validity of nucleotide diagnostics from previous task, and strain-type relative database and other samples.

Our epidemiological model will predict outcomes for both individual patients and the population of Siaya (800,000 residents), as a function of investments, treatments, and mitigations. Our focus in the modeling will be to examine how the widespread co-morbidities of HIV, malaria, Salmonella, Staphylococcus, and tuberculosis combine to cause 1) poor outcome (30% mortality rate, at age 5), 2) emergence of antibiotic resistant forms and 3) presence of novel pathogens.

This project will lay the foundations to achieve our long-term technical goals of situational awareness for global pathogen circulation and emergence.

Benefit to National Security Missions

The primary relevance of this work to basic health research will be from improved diagnostic capabilities developed, as well as the direct understanding of specific co-morbidities to patient outcome in the Siaya District of Kenya.

The primary relevance of this work to Fundamental Bioscience will be from improved understanding of the evolution and emergence of pathogens from an immuno-compromised population the a high disease burden area - the Siaya District of Kenya.

The secondary relevance of this work to Information Science and Technology lies in the integration of disparate information types which will occur in the epidemiological modeling portion of this project.

Progress

This Integrated Biosurveillance project was a three month effort, designed to establish a collaboration and initiate a pilot study. A significant accomplishment of this effort was a series of presentations by the task leads to an external review on September 11 and 12, 2013, during the Biosurveillance Deep Dive, which was well received. The technical accomplishments of this work can be grouped into four LANL-funded portions and efforts of our UNM collaborator to produce project success. All five areas performed well against proposed tasks.

The sequencing task received 19 pure culture samples from DJ Perkins' culture collection, of known antibiotic resistance profiles and phenotypically identified as Salmonella and Staphylococcus species. They are currently (late September) being sequenced. For the RNA sequencing task a round of oligonucleotides have been designed, ordered, and received, and our DJ Perkins has identified a set of six whole-blood samples to be shipped to LANL according to protocols jointly designed and approved by both the Human Subjects Review Board and the Bio-safety committee. Extensive interactions with the other tasks has occurred to design the workflow downstream of this sequencing effort, to identify known virulence and antibiotic resistance markers.

The PCR diagnostics task has performed a literature search and an assay design calculation based on the contents of Genbank to design assays for genus and species identification of Salmonella and Staphylococcus isolates, and known drug-resistance markers of these species. Reagents emerging from this design were ordered and will be applied to the DNA extraction preparations used for sequencing described above, in the sequencing task.

The biomarkers task has performed a literature search and ordered antibodies to detect Salmonella and Staphylococcus directly from serum samples. This task also interacted with DJ Perkins to identify eight pediatric samples in the archive most-likely to test positive for tuberculosis, and they will be sent to LANL in the near future. Sources of biomarkers for testing the antibody assays were identified and ordered. Preliminary evaluation of Staphylococcus antibodies against a commercial lysate has occurred.
The Epidemiology task has created a baseline capability in the R programming language for both an agent-based model and a deterministic, compartmentalized model capable of modeling disease progression of co-morbidities, effectiveness of treatment both early and late in disease progression, and the competition between strains necessary for the emergence of drug-resistant strains. The land-use, roads, and rivers of the study area (Siaya District in Kenya) was abstracted into the geographically explicit model, and 1200 patients were mapped onto the study area with GoogleEarth.

Our UNM collaborator has provided extensive guidance to our effort in terms of formulating the scope, providing samples, and initiating activities necessary for the second portion of this project. In particular, he has expended significant effort into collating Cohort 2 of patients (n=850) with the already-published data from Cohort 2 (N=750).

Future Work

The overarching goal is to put us in a position to be in 'production mode' for National Security-driven biosurveillance of a high disease burden population.

Specifically, in this project, we will:

1. SRS-sequence RNA preps derived from human serum to (a) detection & ID bacterial and viral species, (b) identify genetic markers for drugs and mapping to assemblies in (1), (c) identifying phylogenetic markers and virulence factors of Staphylococcus and Salmonella.
2. Develop methods to substantially deplete samples of host and ribosomal RNA, to increase detection and characterization of pathogen RNA.
3. Apply and iteratively improve oligonucleotide designs to species- strain- and AB-resistance type Salmonella, Staph, and TB in pediatric blood and serum samples.
4. Use diagnostics deployed in (3) to constrain epidemiological model (see below).
5. Continue to validate and apply biomarker assays for Salmonella and Staphylococcus and test on pure culture and samples from (2). Assess sensitivity.
6. Benchmark Mass spec on samples from (1) and (2)
7. Demonstrate diagnosis of tuberculosis in pediatric blood samples with biomarker assay.
8. Develop statistical methods to constrain our baseline epidemiology model with patient data from Cohorts 1&2 (~1,500 patients, 10% positive for bacteremia).
9. Develop visualization and publication of epidemiology model of Saiya District, Kenya.

Conclusion

We will obtain draft genomes of twenty cultured samples of Staphylococcus and Salmonella obtained from the laboratory of DJ Perkins at UNM. We will obtain data from three types of diagnostics: sequencing of messenger RNA, a panel of either 48 or 96 nucleotide diagnostics, and a panel of biomarkers. For the information integration, we will extend the regression analysis to identify risk factors of clinical outcome for 1100 patients enrolled in Dr. Perkins' clinical trial, produce a baseline epidemiological model of co-morbidity in western Kenya, and develop the data structures to integrate information from our novel diagnostic data.

Grayscale Flow Cytometry - Multicoil NMR Sensors for Portable Flow Cytometry

Pulak Nath
20110166ER

Abstract

The long term research goal of this project was to develop a portable flow cytometer based on magnetic detection. The immediate goal was to conduct the proof of principle study for a novel NMR sensor applicable to flow cytometry. Several new capabilities were developed to address the immediate goal. Two unique permanent magnet designs were developed that simplify the fabrication of complex permanent magnet based circuits. New and flexible techniques to develop microfluidic platforms were developed that are low cost and compatible with mass-manufacturing methods. Preliminary data were obtained to detect Bacillus spores using NMR relaxometry - suggesting a novel method to spore detection without using conventional biochemical methods. A compact, multichannel, integrated circuit based NMR spectrometer console was also developed through collaboration with the Texas A&M University. Combination of these technologies has built the foundation to a new LANL capability: Compact, permanent magnet based NMR technology for portable applications. Using these capabilities, we have demonstrated the proof of principle which can lead to a portable flow cytometer based on magnetic detection. The current project supports several aspects of our national science initiatives including advanced manufacturing, bio threat reduction and public health.

Background and Research Objectives

Measuring cell specific information in high throughput platforms such as flow cytometers have found several clinical applications ranging from complete blood count to cancer diagnosis [1]. However, flow cytometers suffer from a fundamental limitation. They require significant, difficult-to-automate sample processing steps to analyze turbid samples like blood. They are also sensitive to cell autofluorescence – a common trait in cells that reduces sensitivity of measurements. These limitations are fundamental to the optical methods utilized in flow cytometry. Therefore, we will investigate and alternate method, namely NMR (Nuclear Magnetic Resonance) relaxometry, to develop capabilities for flow cytometry. We chose magnetic technology because of the recent popularity of magnetic separation in cell/molecular biology. Since most biological materials are diamagnetic or only weakly magnetic, labeling target cells with magnetic micro /nanoparticles makes them available to magnetic manipulation using simple permanent magnets. This method is very specific to the target cells or molecules. It is low cost, easy to operate and a large selection of magnetic micro/nanoparticles is commercially available. However, there are limited developments of magnetic sensors that are suitable for flow cytometry. Consequently, we will investigate NMR (Nuclear Magnetic Resonance) based detection of magnetically labeled cells (with magnetic nanoparticles) in a hydrodynamic configuration similar to flow cytometry. Furthermore, the NMR sensor proposed here will bear small footprints making it suitable for miniaturization and eventually, a portable platform for flow cytometry. Portable flow cytometers will make several medical diagnostics (e.g. Complete Blood Count tests, CD4 Testing for AIDS, Circulating Tumor Counts testing for cancer etc.) available at bed-side and in resource poor settings such as rural areas in the third world countries. Personalized diagnostics, such as measuring patient specific responses from antiviral therapy for HIV patients by counting CD4+ve cells or Chemotherapy for cancer patients by counting circulating tumor cells, will be available to patients at bed-side reaching far beyond the capabilities of sophisticated healthcare facilities. The device can also be useful for in-the-field ‘label-free’ detection of anthrax spores (magnetic due to accumulation of Manganese from the culture media) or malaria infected cells (magnetic due to the presence of paramagnetic crystals excreted by the malaria pathogen).

Although inspired by flow cytometry, this project does not aim to reinvent or replace current flow cytometers. Rather, we provide an innovative solution where the

conventional methods have struggled in spite of thirty years of research and development. The long term research goal of this project is to develop a portable flow cytometer based on magnetic detection. The immediate goal is to conduct the proof of principle study for a novel NMR sensor applicable to flow cytometry. This goal is divided into the two following specific aims:

Specific aim 1: To design and fabricate a magnetic sensor based on NMR microcoils for flow based measurements.

Specific aim 2: To demonstrate flow based measurements of cellular/molecular information of magnetically tagged cells in turbid samples.

Scientific Approach and Accomplishments

The principal objective of this project was to demonstrate the feasibility of measuring NMR relaxometry data from cells in flow. To enable the objective, our plan was to place multiple RF pickup coils in series along the flow path to pick up part of the signal at different time intervals and utilize the signal data points from each coil to extrapolate the Free Induction Decay. In order to achieve the goal, we have divided our approach into two main tasks: (1) Platform development; (2) Development and integration of NMR pulse sequences that can be applied in a multi-coil setting for flow based NMR relaxometry of cells.

Platform Development

There are three major components of a NMR spectrometer: (1) the magnet – which provides a magnetic field in which nuclear magnetic resonance takes place; (2) RF coil – which is used to manipulate proton spins of the liquid sample and collect signals emitted due to spin relaxation; and (3) a spectrometer – which is a hardware/software interface to control the RF pulses and data acquisition. Development of a NMR based sensor for flow cytometry can therefore be categorized in three different sections:

Magnet design and development: There are critical design requirements for any magnet to be used for NMR applications. A highly homogeneous field is required for successful NMR experiments. Homogeneity of a magnetic field is defined parts per million (ppm). 1 ppm means a millionth of the ratio (change in magnetic fields)/mean magnetic field over a given volume. Different types of measurements can be carried out using NMR phenomena. NMR relaxometry involves the measurement of spin-lattice relaxation (T1) and spin-spin relaxation (T2), which are physical characteristics of a given solution. NMR spectroscopy, on the other hand, can measure chemical shifts due to relaxation behavior of a given sample. The uniformity of the magnetic fields required to measure NMR relaxation parameters is moderate compared to measuring chemical shifts. For chemical shift measurement, the homogeneity required for magnet is <1 ppm.

In this work, our objective was to primarily design a magnet that is suitable for NMR relaxometry with a homogeneity <100 ppm over a microliter of sample. There are different ways to obtain the magnetic field required for NMR experiments. We chose permanent magnets due to their ability to obtain moderate fields with a compact, low cost, robust, and maintenance-free design. However, the static magnetic field from a single magnet depends on the shape of the magnet and offers minimal flexibility for configuration. Therefore, magnetic circuits containing multiple magnets and/or ferromagnetic components (e.g., flux guides, pole-pieces) are often utilized to configure a static magnetic field. However, the presence of strong magnetic force between magnets and/or ferromagnetic components leads to complicated fabrication methods for a given magnetic circuit. The majority of permanent magnet circuits are, therefore, fabricated manually requiring bonding materials, specialized equipment, and experience. We have developed two unique magnet designs that are capable of providing homogeneous magnetic fields for NMR relaxometry.

Shim-a-ring magnet: This design is termed as the 'Shim-a-ring' magnet. The design consists of a diametrically magnetized ring-shaped, cylindrical permanent magnet ('ring') placed inside a concentric ferromagnetic ring ('shim'). In addition to providing uniform field, the 'Shim-a-ring' design has several unique characteristics suitable for NMR and other applications. For example:

Ease of fabrication: 'Shim-a-ring' design is composed of only two components. The ring magnet and the shim self-assemble due to magnetic attraction between the two components when they are co-axially placed close to each other. This method eliminates the need for rigorous alignment of multiple components or the use of bonding materials to hold the different components in place.

Configurable magnetic fields: The field strength can be varied by changing the thickness of the shim, while the nature of the magnetic field can be varied (uniform and gradient field) by changing the shape of the bore hole of the ring magnet. By varying the shim diameter, the magnetic field can be tuned to high precision requirements typically required in NMR applications.

Higher uniform field: The uniform volume obtained from a 'Shim-a-ring' design has been found to be ~30 times greater than that of a comparable (with respect to magnet volume and mean magnetic flux densities) Halbach design. It should be noted that, Halbach designs are one of the

most prominent permanent magnet design used for NMR applications.

Ease of miniaturization: Since the 'Shim-a-ring' design is capable of self-aligning, it is also suitable for miniaturization. Miniaturization of other magnetic circuits (e.g. Halbach cylinders) can be complex since they require alignment of multiple magnets against their natural alignment tendency.

The uniformity obtained with a 'Shim-a-ring' magnet was in the order of 50 ppm over 1 microliter volume. The maximum magnetic field was ~0.54 Tesla. The magnet was a 50 mm in height and 80 mm diameter, and weight about 2.5 Kg. The design of a 'Shim-a-ring' magnet is presented in Figure 1(a).

Automated Halbach Assembly: The maximum field obtainable with the 'Shim-a-ring' design for any given configuration was in the order of 0.55 Tesla. Although, this was sufficient for NMR relaxometry applications – a higher magnetic field could provide higher signal to noise ratio. With Halbach designs, it is possible to obtain higher magnetic fields up to 2.0 Tesla. Therefore, we also investigated the fabrication of Halbach cylinders. Halbach cylinders are composed of multiple magnets (e.g. 8) and their fabrication requires the alignment of these components in specific orientations that are different form their natural alignment tendency. Typically, special tools and fixtures are utilized to align and fix one magnet at a time to obtain Halbach cylinders. In this part of the work, we have demonstrated a novel idea to align multiple magnets into a Halbach orientation. Our approach utilized the magnetic field form a larger magnet to automatically align multiple magnets into a Halbach assembly. Use of multiple Halbach rings assembled in this way could provide a higher magnetic flux density inside the bore. Pictures showing automatically aligned Halbach ring is presented in Figure 1(b).

RF coils and integrated microfluidic probe development: Solenoid shaped RF coils were utilized in conjunction with the Shim-a-ring magnet design to demonstrate NMR relaxometry. A single channel commercial NMR spectrometer (iSpin NMR console, Spincore technologies, Gainesville, FL) was utilized for data acquisition. RF microcoils were first fabricated by winding thin gauge wire around 3 mm diameter commercial NMR tubes. To develop NMR microcoils, thin gauge wires were wound around capillary tubing such that the sample volume was in the order of 1 microliter. Initial ability to obtain NMR Relaxometry data was carried out on common liquid samples such as DI water and DI water doped with CuSO4. Figure 2(a) shows a photograph our experimental setup and NMR relaxometry data.

In addition to using capillary tube based microfluidic platforms, planar microfluidic platforms were also investigated. The most common fabrication techniques of planar microfluidic platforms rely on photo-lithography and PDMS (Polydimethylsiloxane) based replication techniques. Although very popular at academic scale, PDMS based microfluidics techniques are usually not very suitable for mass production. To this end, we have chosen to investigate alternate methods to fabricate microfluidic channels. Our approach involved the use of off-the-shelf, finished or semi-finished materials (e.g. adhesive tapes, Kapton films, plastic sheets, etc.) and low cost readily available fabrication tools (e.g. laser cutters, lamination tools, press, etc.) to fabricate microfluidic platforms such that the fabrication method is easily transferrable to mass manufacturing. We have developed two types of fabrication. The first method was based on the lamination of CO2 laser patterned adhesive transfer tapes and plastic sheets. We have demonstrated excellent biocompatibility of these platforms by demonstrating Polymerase Chain Reaction (PCR). To further enable mass compatibility with mass manufacturing, we have developed a second technique that utilizes fabrications methods and materials common to the Flexible Circuit Industries. Due to recent progresses in the portable electronics, a wide range of films have become available. Some these films are based on Polyimide and Teflon – two materials well known for their temperature resistance, chemical compatibility, and biocompatibility. Functional microfluidic devices are often expected to be integrated with electrical components such as heaters, electrodes, coils etc. Since flexible circuits are designed to make multiple layers of electrical circuits, our objective was to investigate if it is possible to integrate microfluidic channels with the flexible circuit manufacturing methods. To this end, we have worked directly with a flexible circuit company, Rigid-Flex (Santa Ana, CA), and developed the ability to integrate microfluidic channels with the flexible circuit technology. It is possible to cut small channels (down to features with dimensions of 25 microns) using UV laser based laser cutters. However, a key challenge was to develop suitable bonding methods to form enclosed microchannels. Typical lamination techniques used in the flexible circuits industry rely on high pressure during bonding – such pressure caused the laminating films to bend into the channels resulting into deformation and sometimes, closing the entire channels restricting flow. Therefore, we have developed an innovative solution to attain bonding that can avoid bending of the laminating films into the channels. We investigated the use of thin films that are coated with thin heat sensitive adhesives on both sides. One side faced the laser cut channel and the other side was placed against a copper film – such that during the bonding process the laminating films (that form the top and bottom layer of the microchannels)

bonds with the copper. When the top/bottom laminating film bonds with the copper – the mechanical strength of the copper film limits the laminating films form deforming into the channel. After bonding, the copper layers can be completely removed by a commercial etchant. In case, it is desired to have electrical circuits integrated with the channel – the copper layer can be selectively removed by common flexible circuit fabrication methods (e.g. pattern exposure and etching). Figure 2(b) shows the difference in bonding outcome using conventional Flex Circuit fabrication method and the bonding methods developed at LANL.

Using these fabrication techniques we have developed microfluidic droplet generators that can be used to synchronously deliver samples into the NMR RF coil region for measurement in flow.

Multichannel NMR spectrometer development: Conventional NMR spectrometers are large and not suitable for portable applications. However, due to progress in microelectronics, new generations of spectrometers have been developed in recent years that are based on integrated circuits such as Field-programmable Gate Array (FPGA). FPGA based NMR spectrometers are sufficiently small to become portable. However, a multi-channel FPGA based spectrometer is not available commercially. In order to implement multiple RF coils in series along the flow path to perform NMR relaxometry in flow – we developed we developed an eight-channel FPGA based NMR spectrometer that is small enough to become portable. This part of the work was carried out in collaboration with Dr. Christian Hilty at the Texas A&M University. The relaxometry console was a NMR spectrometer for simultaneous acquisition of 8 signals after transmitting a common excitation pulse sequence. The console is intended for relaxometry, but can be used for other, general NMR spectroscopy applications as well. The console hardware is based on an Altera Cyclone IV FPGA with the DE0nano evaluation board, which interfaces to specific custom electronics. In addition to the hardware, a control software was developed for NMR data acquisition and processing.

Development and integration of NMR pulse sequences for flow based NMR

NMR pulse sequence for flow based NMR: In typical NMR relaxometry the sample sits under the RF coil while the RF coil is used to perform a series of operations, which involves the application of a series of polarization pulse followed by acquisition signals due to the electromagnetic radiation emitted by the spin decay. This is not practical for flow based NMR relaxometry. To enable detection in flow, first we will have to discretize the sample into small droplets and introduce them into a series of RF coils in a synchronous fashion. This capability was demonstrated by adopting droplet based microfluidics to our flow geometry. Each droplet flows past coils D1 … Dn. At each time samples are located below the coils, a NMR scan is triggered. The NMR scan is simultaneous for each coil. The NMR scan consists of application of a radio-frequency pulse with small flip-angle α (e.g. α=30-45˚), followed by data acquisition. The time between scans is tr. Therefore, it will be possible to find T1 by curve fitting the intensities from each coil.

Demonstration of T1 measurement using Biological samples: In order to demonstrate the ability obtain T1 form biological samples with our magnet assembly, we have chosen two types of biological samples. First we chose to measure sterilized sheep blood and serum samples. The presence of red blood cells in the serum can cause a reduction in the T1 relaxation time due to the effect of the iron laden protein hemoglobin in the red blood cell. We have prepared different concentrations of red blood cells by adding different volumes of sterilized sheep blood in serum and have measured the T1. The T1 increased with increasing dilution of the blood.

As a novel application of this technology we also investigated the effect of spore concentration of the T1 relaxation parameters. Bacillus spores are known to contain manganese oxides in their spore-coats [2]. Manganese oxides are known Magnetic Resonance Imaging (MRI) contrast agents that can reduce the T1 relaxation time of a sample. Therefore, we hypothesized that the T1 of a concentrated spore sample should increase with increasing dilution. We measured T1 relaxation parameters for different concentration of spores. Figure 3(a) shows a picture of the complete system developed under this project. The T1 dependence of blood cell concentration and spore concentrations are presented in Figure 3(b).

Impact on National Missions

This project supports Los Alamos National Laboratory's mission by developing science and engineering capabilities for the Science of signature pillar. Several unique capabilities have been developed to strengthen our core capabilities in Bioscience, Chemical Science, and Sensors, Instrumentation Systems. We have developed novel permanent magnet designs, new microfabrication methods for mass manufacturing of microfluidic platforms, demonstrated the feasibility of developing NMR relaxometry based flow cytometers, and have shown the novel ability to detect Bacillus spores using NMR relaxometry. These capabilities will support several applications beyond the scope of the current project. For example the simple fabrication of complex permanent magnet circuits and microfluidic platforms can support the national initiatives on advance manufac-

turing. The ability to detect spores with NMR can support our missions in biosecurity, public health and simplifies quality control in the sterilization industry. This work also fits the themes of the National Institutes of Health (NIH) roadmap. The DOD Congressionally Directed Medical Research Programs also seeks new technologies for medical diagnostics applications. Finally, this new capability can be the basis for seeking external funding from NIH or DOD to develop programs based on magnetic sensing for biological analysis.

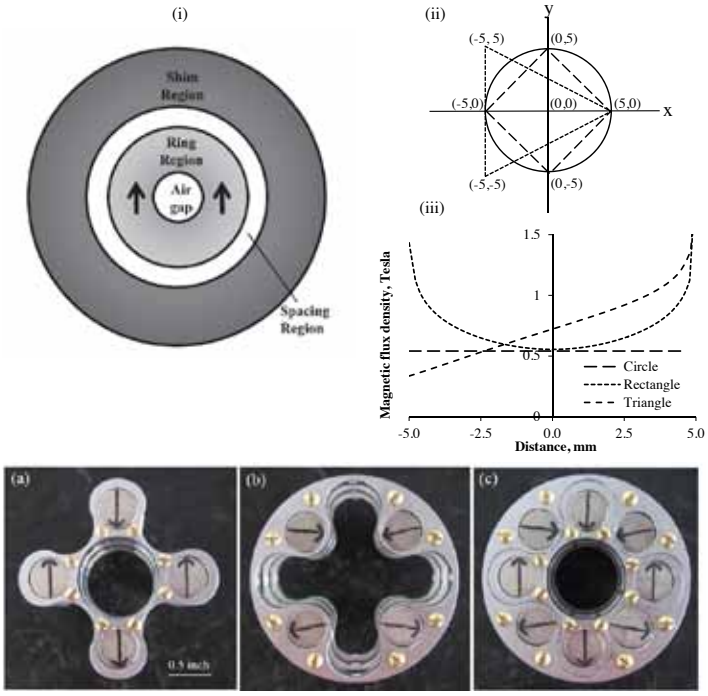

Figure 1. (a) (i) Schematic diagram showing the different regions of a "Shim-a-ring" magnet design. (ii) Geometric parameters of the different cross-section shape of the air gap; (iii) Graphs showing magnetic flux densities along x-axis for different cross-section shapes of the air gap. (b) Photograph showing the different stages of the 'two-step' automatic alignment: (a) in the first step interleaved sections were aligned and fixed in one holder (b) in the second step remaining sections were aligned and fixed in a different holder (c) The complete prototype after the two holders were assembled.

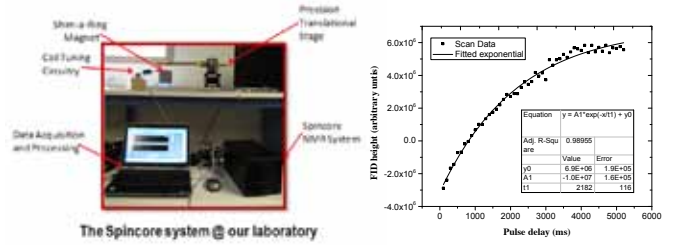

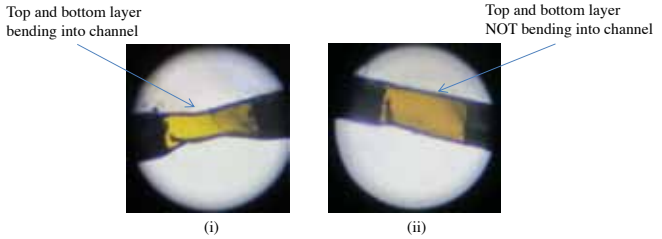

Figure 2. (a)(i) Experimental set up showing early single coil NMR relaxometry. (ii) T1 measurements of DI water averaged over 4 scans. (b) Microscope photograph showing the difference in bonding outcome using (i) conventional Flex Circuit fabrication method and (ii) the bonding methods developed at LANL.

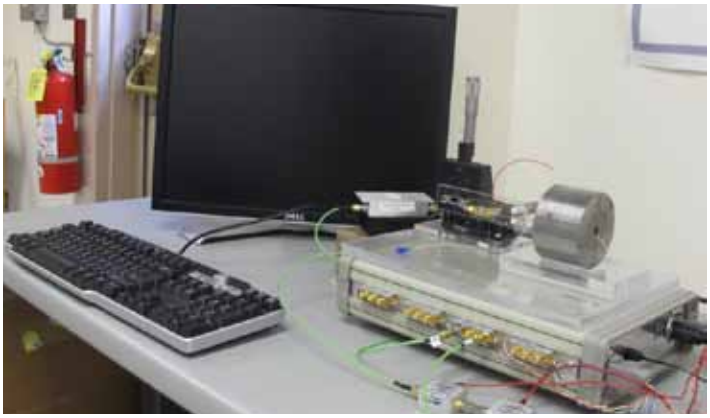

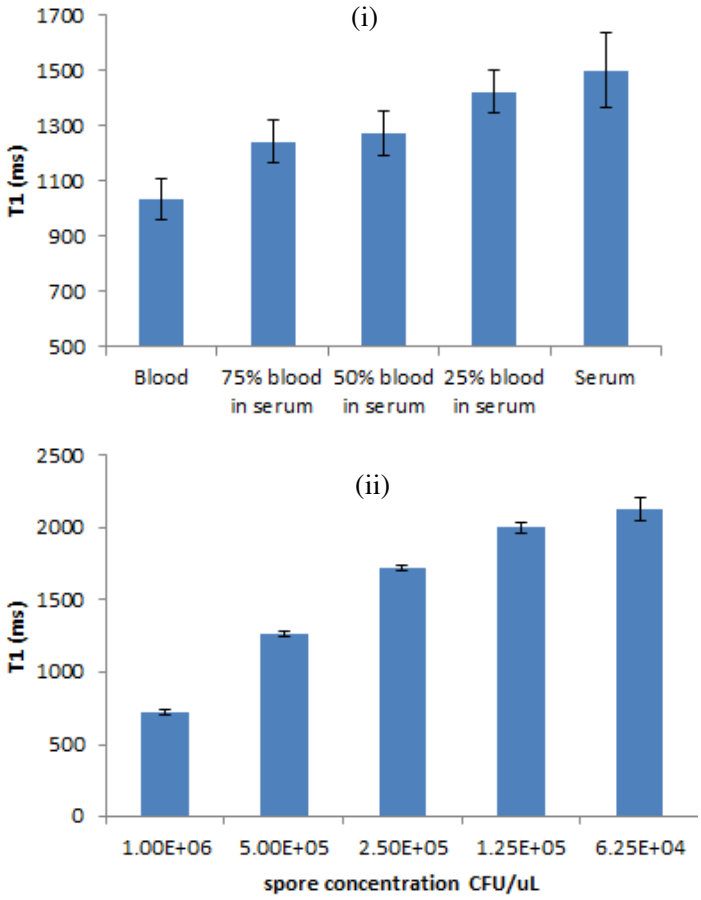

Figure 3. (a) Experimental set up showing the final device for flow based NMR Relaxometry (b) T1 relaxation data for different concentration of cells (i) Blood; (ii) Spore

References

1. Ling, J., U. Wiederkehr, S. Cabiness, K. R. Shroyer, and J. P. Robinson. Application of flow cytometry for biomarker-based cervical cancer cells detection. 2008. DIAGNOSTIC CYTOPATHOLOGY. 36 (2): 76.

2. MANN, S., N. H. C. SPARKS, G. H. E. SCOTT, and E. W. DEVRINDDEJONG. OXIDATION OF MANGANESE AND FORMATION OF MN3O4 (HAUSMANNITE) BY SPORE COATS OF A MARINE BACILLUS SP. 1988. APPLIED AND ENVIRONMENTAL MICROBIOLOGY. 54 (8): 2140.

Publications

Chandrana, C., D. Dunkerley, J. A. Neal, E. Eigenbrodt, B. Morgan, D. Platts, and P. Nath. Application of a simple, easy to fabricate, magnet for Nuclear Magnetic Resonance Relaxometry. Journal of Magnetism and Magnetic Materials.

Chandrana, C., J. Neal, B. Morgan, and P. Nath. Automated Fabrication of Halbach Rings for NMR Applications. 2013. In 54th ENC (Experimental Nuclear magnetic resonance Conference). (Monterey, 14-19 April, 2013). , p. 80. Monterey, CA: ENC.

Nath, P., C. Chandrana, J. A. Neal, B. Morgan, and D. Platts. Microfluidics integrated NMR coils on flexible circuits. 2013. In 54th ENC (Experimental Nuclear Magnetic Resonance Conference). (Monterey, 14-19 April, 2013). , p. 1. Monetery, CA: ENC.

Nath, P., C. K. Chandrana, D. Dunkerley, J. A. Neal, and D. Platts . The “Shim-a-ring” magnet: Configurable static magnetic fields using a ring magnet with a concentric ferromagnetic shim. 2013. Appl. Phys. Lett.. 102 (20): 202409 (4 pages).

Nath, P., T. S. Maity , F. Pettersson, J. Resnick, Y. Kunde, N. Kraus, and N. Castano. Polymerase chain reaction compatibility of adhesive transfer tape based microfluidic platforms. 2013. Microsystem Technologies. : 1.

Biofuel from Magnetic Algae

Pulak Nath
20110168ER

Abstract

The long term goal of this project is to develop cost effective and scalable technology to harvest biofuel from algae. In spite of significant research and developments, sustainable biofuel from algae remains elusive. According to the 2012 report on "Sustainable Development of Algal Biofuels in the United States" by the National Research Council (NRC), "Algal biofuels have the potential to contribute to improving the sustainability of the transportation sector, but the potential is not yet realized. Additional innovations that require research and development are needed to realize the full potential of algal biofuels". This project addresses this concern by providing innovative solutions such as 'magnetic algae'. Several new capabilities have been developed under this project. The ability to genetically engineer algae to produce algae that are susceptible to magnetic separation without the need for any labels is unique to LANL. Different types of continuous flow magnetic separators have been also developed which can find additional applications in bioscience and chemical science. There may also be opportunities to harness the potential of magnetic algae to make magnetic nano-particles, which can be a valuable co-product for the algal biofuel industry. This project supports Los Alamos National Laboratory's Energy security mission by developing science and engineering capabilities for the biofuel program and the science pillar on the experimental science focused on materials for the future.

Background and Research Objectives

The long term goal of this project is to develop cost effective and scalable technology to harvest biofuel from algae. High production costs limit algae based biofuel from becoming a viable replacement for fossil fuels. Current technologies for algae harvesting are either too expensive or only feasible at a laboratory scale. In this project, we will use magnetism to transform algal harvesting and oil extraction. A key challenge in using magnetics is that the object of interest needs to contain magnetic materials. There are bacteria and algae in the nature that can uptake iron from their habitat to form magnetite nanoparticles (known as magnetosomes) [1]. Several genes responsible for the formation of these particles have been identified. Our objective is to express one of these genes 'MagA' in algae to form biogenic nanoparticles that make the cells susceptible to magnetic separation. Following a recent precedent with human cells [2], we will introduce the MagA gene into algal cells enabling them to form intracellular magnetic nanoparticles from soluble iron. The presence of these nanoparticles will make them susceptible to low cost magnetic separation for harvesting. The performance of this technology in a continuous flow system will be quantified to assess feasibility and scaling requirements for technology transfer to industry.

Scientific Approach and Accomplishments

The principal objective of this project was to demonstrate the feasibility of genetically engineering algae such that they become susceptible to permanent magnet based separation. To enable the objective, our plan was to express an iron transporter gene from magnetotactic bacteria into a model algae system and investigate the ability to obtain 'magnetic' algae. In order to achieve this goal, we have divided our scientific approach into two main tasks: (1) Development of 'Magnetic' algae; (2) Development of flow-through, scalable magnetic separation techniques suitable for algae harvesting.

Development of 'Magnetic' algae

Genetic Transformation: We have investigated two genetic transformation methods to express MagA genes in Chlamydomonas reinhardtii: (i) Agrobacterium based transformation; and (ii) Bolistic gene gun based transformation. MagA was derived from Magnetospirillum magneticum (a magnetotactic bacterium). These bacteria are known to form magnetic nano-particles inside the cells. The gene sequence of MagA was optimized using codon equivalency to match the Chlamydomonas GC-rich

genome. Protocols have been developed to insert MagA into two different vectors: (i) pSL18 and (ii) PSAD. These transformation constructs contained the MagA sequence and a paramomycin resistance gene. The paramomycin resistance gene was inserted so that the transformed cells can be selected using their antibiotic resistance. Agrobacterium based transformation protocols were developed using the vector pSL18, whereas, Gene gun based transformation technique was developed using the vector PSAD. Figure 1 shows a schematic diagram of the steps involved for the PSAD based genetic transformation.

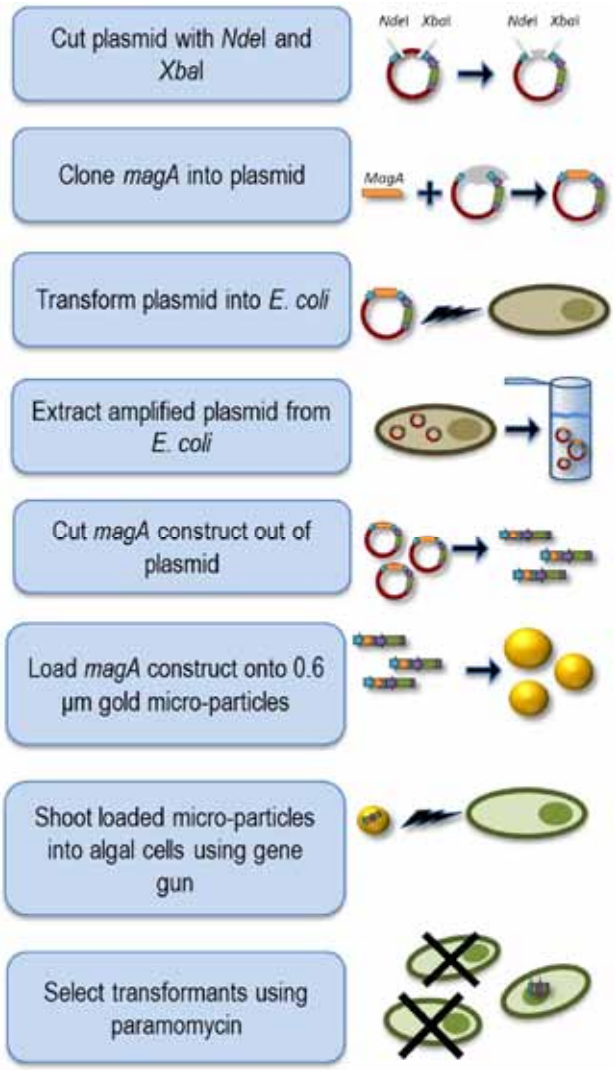

Figure 1. Schematic showing different steps involved in the genetic engineering of Chlamydomonas to obtain magnetic algae.

The Gene gun based transformation with PSAD vector was more successful than the agrobacterium based approach. Following transformation, the cells were grown in antibiotic solutions. Only the successfully transformed cells were able to grow in this medium. The colonies were then isolated and grown in iron rich medium. These cells were not susceptible to commercially available laboratory magnetic sorters. A special magnet with high gradient was developed to analyze whether the cells were becoming magnetic. The first generation of the magnet was analogous to commercially available laboratory magnetic sorters. A glass cuvette containing the cells was placed on the magnet such that the cuvette was positioned vertically. Due to gravity the algae are expected to settle to the bottom of the cuvette. However, if magnetic algae were present they would be attracted to the magnet and their deposition on the magnet will be visible through the naked eye (Figure 2(a)). Further detail on the magnet design will be discussed in a later section. Using this method, we were able to identify whether a transformation to obtain magnetic algae was successful.

(a)

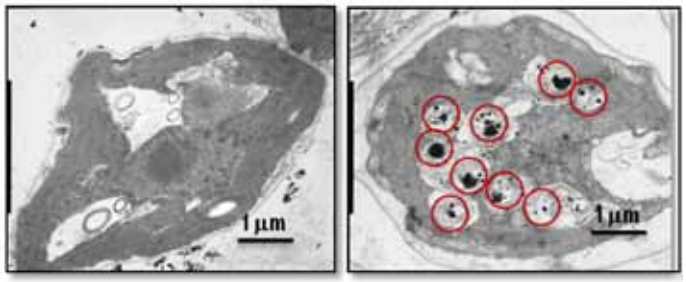

(b)

Figure 2. (a) Photograph showing the magnetic deposition platform for magnetic algae. The two dark green line inside the cuvette indicates the presence of magnetic algae. (b) TEM images showing magnetic nanoparticle formed in Magnetic algae.

The magnetic properties of the transformed Chlamydomonas were tested using our custom high gradient magnetic sorter within 24 hours of transformation and selection. Magnetic responses of the cells were qualitatively examined by observing the accumulation of the transformed Algae near the high gradient locations of the magnet. Wild type algae were used as positive controls for comparison. PSAD is a known strong, constitutive promoter native to Chlamydomonas [3]. Therefore, the Gene gun/PSAD based

transformed cells showed a stronger response to the external magnetic field. The effect of iron (Fe+2) concentration (10 micromols – 200 micromols) and the types of iron salts (Ferrous sulfate vs ferrous citrate) in the culture media was also investigated. Approximately 100 micromol of ferrous citrate was found to be optimum for the production of magnetotactic algae. The presence of MagA gene in the transformed population was confirmed by polymerase chain reactions. Positive response to magnetic fields indicated MagA gene expression/activity (i.e. magnetic nanoparticle production) in the transformed cells.

Electron microscopy analysis: While it was evident from the magnet test the transformed Chlamydomonas were indeed becoming magnetic, to ascertain the reason behind their acquired magnetism, we have chosen to investigate the presence of intracellular iron using Transmission Electron Microscopy (TEM). Cells were harvested, freeze-dried, and fixed on copper grids for transmission electron microscopy. However, it was not possible to obtain clear images of inside the intact cells. Therefore, sample preparation techniques were developed to enable TEM images of cellular cross-section. The freeze dried cells were stained with TEM sensitive dye, embedded in wax and sliced using an ultra-microtome. The sample preparation allowed us to successfully image the cell cross-section and investigate the presence of electron dense regions inside the cells. Electron dense regions will indicate the presence of metal nanoparticles inside the cells. Non-magnetic cells were compared to magnetic cells. Images revealed electron dense regions (Dark spots) only in the magnetic cells (Figure 2(b)). The dark sports were predominantly present inside the vacuoles of the cells. None of these dense spots were noted in the non-magnetic cells. The fact that the cells are magnetic and electron dense regions are seen in TEM images – we can assume that the presence of MagA causes increased influx of iron into the cells. The cells have found a mechanism to store the extra iron into the vacuoles to isolate the additional iron from potential active metabolic processes. Dark spots were in the size orders of 10 nm or less. The TEM images suggest that iron oxide nanoparticles are being formed inside the magnetic algae, which make them susceptible to permanent magnets.

Effect of Ferrous rich media on other algae: We have also investigated the effect of high iron concentration of other types of algae, namely Tetraselmis and Nannochloropsis. Interestingly, both the type of algae showed attraction towards permanent magnets – even without any genetic modification. Tetraselmis showed greater response to high concentration of iron than Nannochloropsis. Further investigation with Tetraselmis revealed that the cells were forming aggregated in the presence of high ferrous sulphate concentrations. These aggregates were susceptible to magnetic fields and therefore, were separable with a permanent magnet (Figure 3). These observations were probably not due to the formation of intracellular iron. The aggregates and magnetic susceptibility developed immediately after the addition of the ferrous salt (Figure 3). Microscopic investigation showed that the aggregates composed of the cells and other materials surrounding the cells. It is well known that ferrous sulphates exhibit paramagnetic properties and ferrous salts have the tendency to flocculate cells. Based on this observation, a new technique harvesting technique 'magnetic flocculation' may be developed which can be applied to non GMO (genetically modified organisms) Tetraselmis.

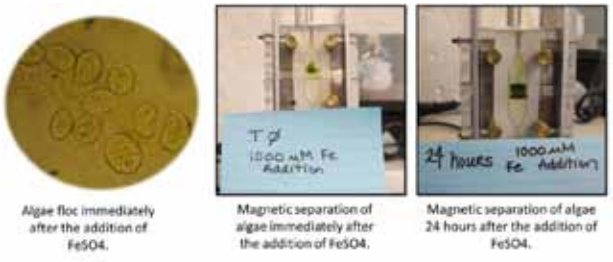

Figure 3. Pictures showing magnetic deposition of wild type Tetraselmis due to the addition of ferrous sulphate – a possible new technique to separate algae – magnetic flocculation.

Rapid/low cost analysis of algae growth: To determine the efficiency of magnetic harvesting and cell capture, we have identified a rapid method for determining cell concentrations and total cell numbers. The technique uses low cost, portable, off-the-shelf, automated cells counters. The cell counters offers very simple procedure compared to the use of flow cytometers. They were able to provide cell concentrations and cell size information. Cell size can change with each algal species dependent on physiological state. We have determined growth characteristics, average cell size, optical density, and cell numbers for the algal species Tetraselmis striata, Nannochloropsis salina, and Chlamydomonas reinhardtii. These techniques can be used to determine the efficiency of cell capture dependent on magnetic harvesting system design and algae cell magnetic potentials.

Development of flow-through, scalable magnetic separation

Magnetic deposition assay: Since the anticipated magnetic properties were unknown for the 'Magnetic' Algae – we have developed a permanent magnet circuit to obtain very high magnetic gradient. Several designs were considered. The optimized design was able to produce ~450T/m gradient over a desired thickness of the channel (Figure 4). This is an order of magnitude higher than common laboratory based magnetic separators. The magnet assembly

was built using block magnets such that the design can be scaled to obtain larger units for high throughput separation. However, the first objective was to design the magnet such that it can be used to determine whether the algae are magnetic or not. To this end, the design consisted of two very high gradient locations where the algae could deposit and form a band –visible to the naked eye. A cuvette filled with algae is placed next to the magnet. If the cells are magnetic, they accumulated in the high gradient location and thus, the magnetic deposition assay was developed to distinguish between magnetic and non-magnetic algae.

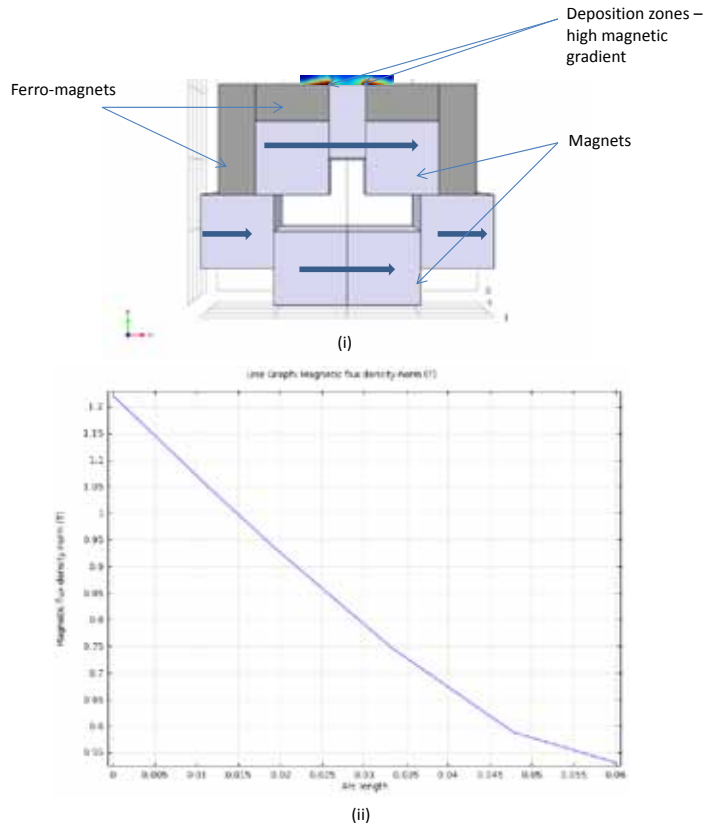

Figure 4. (i) Design of the high gradient deposition magnet; (ii) Magnetic flux densities in the one deposition zone.

2.2.2 Continuous Magnetic separation

While the magnetic deposition assay was useful to identify magnetic algae – it was not suitable for continuous collection of the separated algae. For algae harvesting application, it would be necessary to collect the algae in a continuous fashion. Therefore we have developed two new techniques for collecting weakly magnetic cells after separation in a high gradient magnetic separator. The first method is a semi-continuous process by which the deposited cells can be removed periodically by applying air bubbles. The surface tension arising from the gas liquid interface was stronger than the attraction of the magnet to the weakly magnetic cells. In this method, a flow through channel was designed that can be mounted on the deposition magnet. Algae solution is passed at a given flow rate over the high gradient zones of the magnet such that the cells can deposit due to magnetic attraction. When the zones are saturated with the magnetic cells, a bubble is introduced in the flow such that the bubble volume occupies the width and depth of the channel. As the bubble passes the high gradient zone the cells are scraped off from the deposited area (Figure 5(a)) and are carried to the outlet. The concentrated cells can then be collected by opening a valve at the outlet.

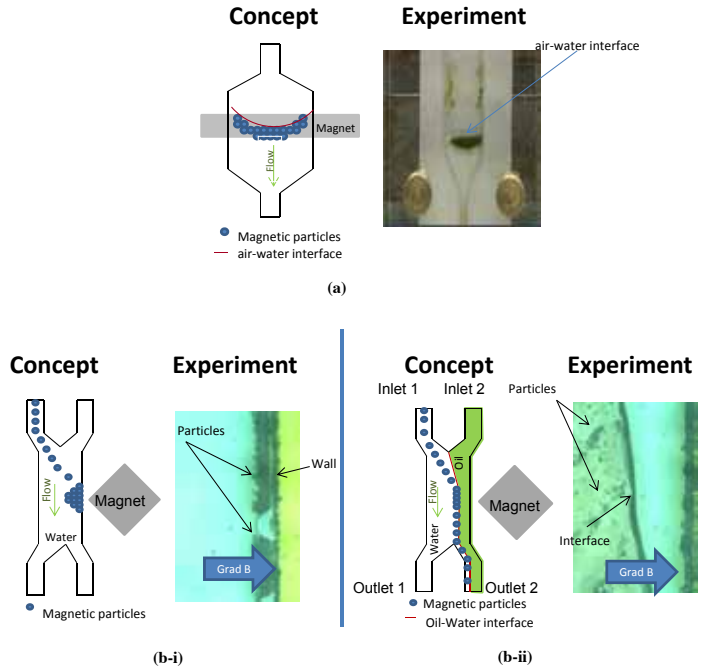

Figure 5. (a) Collection of deposited algae in a semi-continuous process using gas-liquid interface; (b-i) Conventional high gradient magnetic deposition; (b-ii) Use of oil-water interface to continuously recover magnetic particles in high gradient separation.

This method allowed us to collect concentrated algae by magnetic separation. However, this is a semi-continuous method. Therefore, we also investigated a continuous method of separation. Typically, continuous flow separation of magnetic cells can be achieved by deflecting the magnetic cells in flow with a carefully designed permanent magnet (Figure 5(b-i)). However, in this case magnetic algae are weakly magnetic and require very high gradient from separation. Therefore, we devised a new method that could allow continuous collection of magnetically separated cells. The proof of concept was demonstrated using magnetic particles and a fluidic channel. The fluidic channel consisted of two inlets and two outlets. High gradient magnet is placed on one side of the channel. If the channel was filled with flowing magnetic targets – the high gradient would cause the targets to accumulate on the wall

close to the magnet. However, we introduce a stream of immiscible fluid such that, under laminar flow condition, the two streams (oil phase and aqueous phase containing the magnetic targets) can proceed side by side (Figure 5(b-ii)). Due to the presence of the oil phase the magnetically separated targets cannot reach the wall. The surface tension between the oil and aqueous phase limits the magnetic particles to cross the interface and reach the wall. As a result, the separated particles proceed towards the outlets as a concentrated solution. The proof of this concept was demonstrated using magnetic microparticles.

A perspective on cost: Additional iron is needed to grow magnetic algae. However, the cost of ferrous salt addition will only be 0.0052 – 0.052$/gallon, if we add between 100 -1000 mol of ferrous salt.

Impact on National Missions

In spite of significant research and developments, sustainable biofuel from algae remains elusive. According to the 2012 report on "Sustainable Development of Algal Biofuels in the United States" by the National Research Council (NRC), "Algal biofuels have the potential to contribute to improving the sustainability of the transportation sector, but the potential is not yet realized. Additional innovations that require research and development are needed to realize the full potential of algal biofuels". This project addresses this concern by providing innovative solutions such as 'magnetic Algae'. We have demonstrated initial feasibility to address a major bottleneck in the Algal biofuel technology – microalgae harvesting. The Department of Energy plans to produce >1 billion gallons per year of cost-competitive algal biofuels by the year 2022. Significant challenge lies within the SCALE at which the algae would have be harvested. Permanent magnets for separation require no energy input for separation. Commercial permanent magnet based separators capable of processing up to 1000 liters/min (~250 gallons/min) are already available to deliver dry ferrous contaminants from fluids and coolants. Although at a nascent stage, this project's ability to produce 'magnetic' algae has the potential to support these initiatives by DOE. Furthermore, the 'magnetic' algae produce magnetic nanoparticles inside the cells – which may be utilized as a valuable co-product. The ability to produce magnetic nanoparticles in algae can also support other national initiatives such as the 'Living foundries' program at DARPA (Defense Advanced Research Projects Agency). This project supports Los Alamos National Laboratory's Energy security mission by developing science and engineering capabilities for the biofuel program and the science pillar on the experimental science focused on materials for the future. Several unique capabilities have been developed to strengthen our core capabilities in Bioscience, Chemical Science, and Sensors, Instrumentation Systems. Finally, this new capability can be the basis for seeking external funding from DOE or DOD to develop programs based on magnetic separation and biogenic materials production.

References

1. Komelli, A.. Molecular mechanisms of magnetosome formation. 2007. ANNUAL REVIEW OF BIOCHEMISTRY. 76: 351.

2. Zurkiya, O., A. W. S. Chan, and X. P. Hu. MagA is sufficient for producing magnetic nanoparticles in mammalian cells, making it an MRI reporter. 2008. MAGNETIC RESONANCE IN MEDICINE. 59 (6): 1225.

3. Fischer, N., and J. D. Rochaix. The flanking regions of PsaD drive efficient gene expression in the nucleus of the green alga Chlamydomonas reinhardtii. 2001. MOLECULAR GENETICS AND GENOMICS. 265 (5): 888.

Publications

Nath, P.. 'Magnetic' Algae. 2013. In ARPAe Innovation Summit. (Washington D.C., 25-27 february, 2013). , p. 126. Washington D.C.: ARPA-e.

Understanding Thunderstorm Effects on the Ionosphere: A New Approach to Investigate Possible Convective and Electrical Coupling Mechanisms

Xuan-Min Shao
20110184ER

Abstract

The goal of this project is to investigate and characterize the possible mechanical and electrical coupling mechanisms from thunderstorms to the ionospheric D-layer, and to quantify the magnitude of the electron density perturbations due to the various coupling mechanisms in space and time relative to the storm, by assimilating archived lightning observations and model simulations. Understanding how thunderstorms affect the D-layer is important in forecasting radio frequency (RF) communication and electromagnetic pulse (EMP) detection within the earth-ionosphere waveguide for ground-based systems, and in forecasting transionospheric communication and detection for satellite systems. Various thunderstorm-ionosphere coupling mechanisms have been proposed but very limited evidence has been obtained to quantify each of the theories. The unique approach of this project is to use lightning-produced EMPs captured from an array of receivers (LASA) to map the spatial and temporal perturbations of the D-layer electron density, and to compare the perturbations with existing and new electrical and convective models to understand the physical mechanisms.

Background and Research Objectives

D-layer disturbances over lightning storms have been sporadically reported and various thunder-storm-ionosphere coupling mechanisms have been proposed. But the nature of the disturbances in either time or space has been poorly understood due to the lack of proper observational methods. It is not uncommon that conflicting claims are reported in the scientific articles. By using the new technique further developed in this project, we have provided, for the first time, spatial and temporal information regarding ionospheric disturbances over and around the thunderstorms, and characterized the effects of the various proposed mechanisms.

Ionospheric variations recently have been hypothesized to relate to various convective and electrical coupling mechanisms of the troposphere storms. First, far-ultraviolet (FUV) observations onboard the IMAGE satellite discovered ionospheric variations that were closely coupled with tropospheric weather systems [1, 2]. Immel et al. [1, 2] suggested the variations were driven by atmospheric tidal waves. On the other hand the proposers of this project found a close correspondence between locations of peak FUV brightness with the global-scale lightning activity [http://wwlln.net], suggesting that thunderstorms and their lightning could be the origin of the variations. Second, VLF lightning observations made by a Duke University team have shown that intense lightning discharges enhanced the D-layer electron density by 108m-3 [6, 7, 8]. This VLF study was based on a single station measurement and used VLF waveguide propagation model for the data analysis, and therefore was only capable of providing a 1D, source-to-receiver path-averaged variation. It is very likely that the actual electron enhancement was substantially underestimated by this technique. The Duke team [6, 7] concluded that the observed enhancement was due to transient lightning EMP. Third, Inan et al., [9] measured narrowband VLF disturbances while storms were on the path from a CW transmitter to their receiver, found a fast VLF change followed by a long, 20-200s decay, and argued that the parent storms would continuously “heat” the ionosphere, as suggested by Pasko et al. [10]. However, the heating was not observed by Duke’s technique. Finally, Johnson and Davis [3, 4] monitored the sporadic E-layer with a localized ionosonde, and reported that AGWs and transient lightning EMP may both contribute to the variations. They derived their result from 5142 lightning events across several years by cumulatively averaging the possible variations, and it is not clear how reliable their claims are.

A critical component necessary to distinguish the different coupling mechanism hypotheses is the horizontal extent of the variation. The other equally important component is the temporal evolution of the variation,

which will show how the variation propagates to other regions of the ionosphere. Before this project, neither of these components had been available for the bottom of the ionosphere. With the unique LASA dataset and our recently developed full-wave VLF/LF propagation models [11, 12], these questions will be answered in this project. Unlike the waveguide model that includes all possible bounces between the ground and ionosphere along the entire path, this model only concerns the single, first-hop reflection off the ionosphere of the radiated lightning pulse, and therefore only probes a small region of the D-layer at the reflection point with each measurement. With waveforms from the distributed LASA sensors, a spatially-resolved (rather than a path-averaged) map can be generated.

Scientific Approach and Accomplishments

The research started with an analysis of the archived LASA data with an array of 6 sensors over the Great Plains. A LANL developed full-wave VLF/LF propagation model [11, 12], which simulates the time-domain ground and ionospheric waves, has been further developed and used to compare with the lightning waveforms to determine the D-layer height and electron density profile for each measurement. These parameters at the reflection region directly determine the received waveforms and can be conversely obtained by fitting the model with the measurement. A typical storm over the Great Plains lasts many hours and produces many thousands of lightning flashes over a range of hundreds of km. Together with the array of sensors, a time-evolving 2D map can be obtained.

The time-evolving 2D map will be examined against the different coupling mechanisms to understand their respective effects, based on their predicted different space/time natures. EMP coupling mechanism can be readily compared with the measurement. The theory for QE heating is based on the same physics as for EMP and its predicated effects have been reported in a series of research papers [9, 10]. Unrelated to the ionosphere community, AGW models for neutral atmosphere that simulate con-vective energy/moment transportations from troposphere to mesosphere have advanced significantly in recent years [13, 14]. And more importantly, OH airglow observations of AGW at the D-layer height that coincided in time and region with LASA data have been reported in recent months [15], and can be directly used for this study.

First year accomplishments

In the area of data analysis, we confirmed that our technique provides a much higher time and spatial resolution measurement of the D-layer fluctuation as compared to previously reported frequency domain techniques. As a result, a series of new D-layer phenomena have been discovered. In papers we reported the new techniques along with fluctuation observations from a single station measurement. It was clearly demonstrated that the apparent reflectivity and height exhibit significant variation on spatial scales of tens of kilometers and over time periods of hours. The range of the reflectivity variation was as large as 100% away from the averaged reflectivity, and the height varies by as much as 5% (4 km). The time scales and propagation velocities (50-100 m/s) of the fluctuations appear to be consistent with signatures of atmospheric gravity waves (AGW) at D-layer altitudes, and the direction of the fluctuation propagation suggests that the gravity waves were originated from the storm. In some localized ionosphere regions, we discovered some apparent splitting of the D-layer by 2 – 4 km that lasted a short time period of about 10 minutes.

Following the initial analysis, we extended the analysis to multiple-station measurement and to different storms. We confirmed that the AGW-like fluctuations were indeed originated from the storm, by looking the D-layer from three different directions. For the analysis, fluctuation maps in space and time were produced, and the movement of the fluctuations was examined based on the space-time maps. As proposed, we also examined the D-layer with two radio frequency bands (<30 kHz and 30-60 kHz) by digitally filtering the original waveforms and found that the high-band signal penetrated deeper into the ionosphere by 2-4 km, and produced more detailed features of the fluctuations.

In order to understand the D-layer properties behind the measurements, we improved the full wave, ground-ionosphere VLF/LF propagation model by increasing the frequency and incident angular resolutions in the model computation. For the specific purpose of this project, a new technique was developed to coherently combing the ground and ionospheric-reflected waves at the sensor locations. The output of the model predication was compared with the measurement, and some outstanding agreements on the time waveforms were obtained. In the paper, we showed that reliable lightning return stroke waveforms can be reproduced at different observing distances by the model simulation. Applying the model results to actual observations we found that additional and stationary ionization at the lower-boundary of the D-layer was introduced by the storm. This newly discovered phenomenon might be due to static electrical heating from the storm. We are in the process of further examining this new result.

The other new scientific result came out from this project in FY11 is a new understanding of the discharge physics of the lightning stroke to ground. In an attempt to obtain a "standard" return stroke time waveform from the observations for the VLF/LF propagation simulation, we found that

a statistically significant feature in the waveform after accumulated thousands of individual waveforms. Any existing return strokes models could not explain this small but persistent feature. Instead, the feature can only be explained by a dispersive discharge process along the lightning channel. This new result has a fundamental impact on the understanding of the dynamics of lightning discharge, and we are in the process of submitting the result for a publication.

During the first ten months of this project, one paper was published in JGR, two papers were presented in the XIV International Conference on Atmospheric Electricity, two papers to GRL and JGR are in the process of submission, and one presentation was given in the AGU fall meeting, as listed below.

Second year accomplishments
We discovered that the electron density in the nighttime lower ionosphere is reduced in response to a small thunderstorm, and the extent of the reduction is closely related in both time and space to the lightning activity of the underlying thunderstorm. This work has been published in Nature-Geoscience.

We found that thunderstorms produced wave-like fluctuations (atmospheric gravity wave, AGW) at the D-layer. From simultaneous multi-station observations, we determined the speed and direction of the AGW propagation and confirmed that these fluctuations are indeed originated from the underlying storm. This work has been published in Geophysical Research Letter.

A new lightning return stroke model has been developed to explain both the general and detailed electric radiation waveforms. Return stroked has been studied for decades, but our new model is the first to reveal the general behavior of electric current along the lightning channel. This work has been published in J. Geophysical Research.

Significant improvement on VLF/LF propagation model, that makes the accurate analysis possible, and leads to the discovery of the reduction of the electron density in the nighttime lower ionosphere. The improvement including the examinations of geomagnetic effects on VLF/LF propagation. This part of the work has been published in Radio Science.

Our VLF/LF propagation code has been delivered to AFTAC for programmatic missions.

Found evidence of thunderstorm effect on ionospheric F-layer by comparing thunderstorm activity with GPS-based TEC measurement. This work is still in progress.

Third year accomplishments
We realized that thunderstorms not only affects the ionosphere's lower boundary (D-layer) but also introduce fluctuations deep in the ionosphere's F-layer (300-400 km altitude). By examining the total electron content (TEC) observations with ground-based GPS receivers, we found that thunderstorms are responsible for AGW and infrasound fluctuations in the TEC measurement. This result has been published in J. Geophysics Res.

Following the Nature-Geoscience paper, we applied the advanced techniques to mesoscale storms, and find that static electrical field atop storms actually enhances the electron density as compared the EMP effects that reduces the electron density. This work has been submitted to J. Geophys. Res. For publication.

We further find that a specific infrasound signal at frequencies 3-5 mHz was sometimes related to thunderstorms. We have developed a new technique by using the phase information in the fluctuations to geolocate the sources of the signals. This work in still in its initial stage, but attracted attentions from multiple government agencies for programmatic applications.

An updated VLF/LF propagation code has been delivered to AFTAC.

Impact on National Missions

The proposed work has a direct impact on LANL's new thrust area of Space Situation Aware-ness (Jeffrey Bloch, jbloch@lanl.gov), which depends on understanding of space weather conditions for reliable space-ground communication and persistent and accurate global surveillance. The success of this project will form the foundation for a new LANL program supported by DOD. Through this project, our understanding on time-domain, long-distance VLF/LF propagation will be significantly improved, and this will be directly applied to a new Air Force mission that uses ground-based RF measurement for long-range nuclear explosion detection (Tomas Carey, tcarey@lanl.gov). In addition, the result of this project will be used to understand fundamental ionosphere anomalies, and will be used to improve the performance of LANL's space-based nuclear sensors (W, V sensors).

References

1. Immel, T. J., S. B. Mende, M. E. Hagan, P. M. Kintner, and S. L. England. Evi-dence if tropospheric effects on the ionosphere. 2009. Eos Trans. AGU. 90 (9): 69.

2. Immel, T. J., E. Sagawa, S. L. England, S. B. Henderson, M. E. Hagan, S. B. Mende, H. U. Frey, C. M. Swenson, and L. J. Paxton. Control of equatorial ionospheric

morphology by atmospheric tides. 2006. GEOPHYSICAL RESEARCH LETTERS. 33 (15): -.

3. Johnson, C. G., and C. J. Davis. The location of lightning affecting the ionospheric sporadic-E layer as evidence for multiple enhancement mechanisms. 2006. GEOPHYSICAL RESEARCH LETTERS. 33 (7): -.

4. Davis, C. J., and C. G. Johnson. Lightning-induced intensification of the ionospheric sporadic E layer. 2005. NATURE. 435 (7043): 799.

5. Shao, X. M., M. Stanley, A. Regan, J. Harlin, M. Pongratz, and M. Stock. Total lightning observations with the new and improved Los Alamos Sferic Array (LASA). 2006. JOURNAL OF ATMOSPHERIC AND OCEANIC TECHNOLOGY. 23 (10): 1273.

6. Cheng, Z., S. A. Cummer, H. T. Su, and R. R. Hsu. Broadband very low frequency measurement of D region ionospheric perturbations caused by lightning electromagnetic pulses. 2007. JOURNAL OF GEOPHYSICAL RESEARCH-SPACE PHYSICS. 112 (A6): -.

7. Cheng, Z., and S. A. Cummer. Broadband VLF measurements of lightning-induced ionospheric perturbations. 2004. GEOPHYSICAL RESEARCH LETTER . 32 (L08804): 1.

8. Cummer, S. A., U. S. Inan, and T. F. Bell. Ionospheric D region remote sensing using VLF radio atmospherics. 1998. RADIO SCIENCES. 33: 1781.

9. Inan, U. S., V. P. Pasko, and T. F. Bell. Sustained heating of the ionosphere above thunderstorms as evidenced in the early/fast VLF events. 1996. GEOPHYSICAL RESEARCH LETTER. 23: 1067.

10. Pasko, V. P., U. S. Inan, Y. N. Taranenko, and T. F. Bell. Heating, ionization and upward discharges in the mesosphere due to intense quasi-electrostatic thundercloud fields. 1995. GEOPHYSICAL RESEARCH LETTER. 22: 365.

11. Jacobson, A. R., X. M. Shao, and R. Holzworth. Full-wave reflection of lightning long-wave radio pulses from the ionospheric D region: Numerical model. 2009. JOURNAL OF GEOPHYSICAL RESEARCH-SPACE PHYSICS. 114: -.

12. Shao, X. M., and A. R. Jacobson. Model Simulation of Very Low-Frequency and Low-Frequency Lightning Signal Propagation Over Intermediate Ranges. 2009. IEEE TRANSACTIONS ON ELECTROMAGNETIC COMPATIBILITY. 51 (3): 519.

13. Vadas, S. L., and D. C. Fritts. Reconstruction of the gravity wave field from convective plumes via ray tracing. 2009. ANNALES GEOPHYSICAE. 27 (1): 147.

14. Yu, Y. H., M. P. Hickey, and Y. F. Liu. A numerical model characterizing internal gravity wave propagation into the upper atmosphere. 2009. ADVANCES IN SPACE RESEARCH. 44 (7): 836.

15. Yue, J., S. L. Vadas, C. Y. She, T. Nakamura, S. C. Reising, H. L. Liu, P. Stamus, D. A. Krueger, W. Lyons, and T. Li. Concentric gravity waves in the mesosphere generated by deep convective plumes in the lower atmosphere near Fort Collins, Colorado. 2009. JOURNAL OF GEOPHYSICAL RESEARCH-ATMOSPHERES. 114: -.

Publications

Jacobson, A. R., X. M. Shao, and E. H. Lay. Full--wave model of D-region upward VLF coupling to whistlers in the plasmasphere. Presented at AMERICAN GEOPHYSICAL UNION FALL MEETING. (San Francisco, CA, 3-7 Dec. 2012).

Jacobson, A. R., X. Shao, R. H. Holzworth, and E. H. Lay. Magnetic-azimuth dependence of D-layer radio reflectivity, using lightning sferics as radio transmitters. 2011. In AMERICAN GEOPHYSICAL UNION FALL MEETING . (San Francisco, CA, 5-9 Dec. 2011). , p. AE21B. Washington DC : AGU.

Jacobson, A., X. Shao, and E. Lay. Time domain waveform and azimuth variation of ionospherically reflected VLF/LF radio emissions from lightning. 2012. Radio Science. 47 (4): RS4001.

Lay, E. H., X. M. Shao, and A. R. Jacobson. High temporal and spatial-resolution detection of atmospheric gravity wave effects on D-layer electron density. 2012. In 2012 COUPLING, ENERGETICS, AND DYNAMICS OF ATMOSPHERIC REGIONS (CEDAR) WORKSHOP. (Santa Fe, New Mexico, 24-29 Jun. 2012). , p. MLTG. Boulder: UCAR.

Lay, E. H., X. M. Shao, and A. R. Jacobson. D-layer electron profiles observed with substantial spatial and temporal change near thunderstorms. JOURNAL OF GEOPHYSICAL RESEARCH.

Lay, E. H., X. M. Shao, and A. R. Jacobson. Electrical modification of D-layer electron distribution by local thunderstorm. Presented at AMERICAN GEOPHYSICAL UNION FALL MEETING. (San Francisco, CA, 3-7 Dec. 2012).

Lay, E. H., X. M. Shao, and C. S. Carrano . Variation in total electron content above large thunderstorms. 2013. GEOPHYSICAL RESEARCH LETTERS. 40: 1.

Lay, E. H., and X. -M. Shao. Multi-station probing of thunderstorm-generated D-layer fluctuations by using

time-domain lightning waveforms. 2011. Geophysical Research Letters. 38 (23): L23806.

Lay, E. H., and X. M. Shao. High temporal and spatial-resolution detection of D-layer fluctuations be using time-domain lightning waveforms. 2011. JOURNAL OF GEOPHYSICAL RESEARCH. 116 (A01317): doi:1029/2010A016018.

Lay, E. H., and X. M. Shao. High temporal and spatial-resolution detection of D-layer fluctuations by using time-domain lightning waveforms. 2010. In AMERICAN GEOPHYSICAL UNION 2010 FALL MEETING. (San Francisco, CA, 13-17 Dec. 2010). , p. AE21B. San Francisco, CA: American Geophysical Union.

Lay, E. H., and X. M. Shao. High temporal and spatial-resolution detection of D-layer fluctuations by using time-domain lightning waveforms. 2011. In XIV INTERNATIONAL CONFERENCE ON ATMOSPHERIC ELECTRICITY. (Rio de Janeiro, Brazil, 8-12 Aug. 2011). , p. 1. Rio de Janeiro, Brazil: International Commision on Atmospheric Electricity.

Lay, E. H., and X. M. Shao. Detection of D-layer perturbations with high time and spatial resolution. Invited presentation at CEDAR. (Boulder, CO, 1-2 JUN. 2010).

Lay, E. H., and X. Shao. D-layer fluctuations directly above a thunderstorm region detected by using time-domain LF/VLF waveforms. 2011. In AMERICAN GEOPHYSICAL UNION FALL MEETING. (San Francisco, CA, 5-9 Dec. 2011). , p. AE21A. Washington DC: AGU.

Shao, X. M., A. R. Jacobson, and E. H. Lay. On the behavior of return stroke current and the remotely detected electric field change waveform. 2012. JOURNAL OF GEOPHYSICAL RESEARCH. 117 (D07105): doi:10.1029/2011JD017210.

Shao, X. M., A. R. Jacobson, and E. H. Lay. Study of ionospheric D-layer fluctuation by comparing VLF/LF propagation model simulation with remotely detected lightning time waveforms. 2011. In XIV INTERNATIONAL CONFERENCE ON ATMOSPHERIC ELECTRICITY. (Rio de Janeiro, Brazil, 8-12 Aug. 2011). , p. 1. Rio de Janeiro, Brazil: International Commision on Atmospheric Electricity.

Shao, X. M., E. H. Lay, A. R. Jacobson, and C. S. Carrano. Changes of electron density in the ionosphere in response to lightning discharges and their parental thunderstorms. Invited presentation at AMERICAN GEOPHYSICAL UNION FALL MEETING. (San Francisco, CA, 9-13 Dec. 2013).

Shao, X. M., E. H. Lay, and A. R. Jacobson. Observations of electron density changes in ionospheric D-layer above tropospheric thunderstorms . 2012. In 2012 COUPLING, ENERGETICS, AND DYNAMICS OF ATMOSPHERIC REGIONS (CEDAR) WORKSHOP . (Santa Fe, New Mexico, 24-29 Jun. 2012). , p. SPRT. Boulder: UCAR.

Shao, X. M., E. H. Lay, and A. R. Jacobson. Using lightning waveforms to probe thunderstorm effects on the ionospheric D-layer . 2012. HIGH ENERGY DENSITY PLASMAS AND FLUIDS CAPABILITY REVIEW .

Shao, X. M., E. H. Lay, and A. R. Jacobson. Reduction of electron density in the night-time lower ionosphere in response to a thunderstorm. 2013. NATURE GEOSCIENCE. 6 (1): 29.

Shao, X. M., E. H. Lay, and A. R. Jacobson. Model simulation and remote electric field change measurement show return stroke current travels in a dispersive and lossy manner. Presented at AMERICAN GEOPHYSICAL UNION FALL MEETING. (San Francisco, CA, 3-7 Dec. 2012).

Shao, X., E. H. Lay, and A. R. Jacobson. Using lightning waveforms to probe thunderstorm's electromagnetic effects on the ionospheric d-layer. 2011. In AMERICAN GEOPHYSICAL UNION FALL MEETING. (San Francisco, CA, 5-9 Dec. 2011). , p. AE21A. Washington DC: AGU.

High Density Neuronal Recording Using Nanowire Capacitor Sensors

John S. George
20110264ER

Abstract

Understanding the neural basis of the processes of sensory perception, motor control, learning and memory, and even consciousness, is the final frontier of the biological sciences. This task requires us to measure and ultimately manipulate the dynamic function of large populations of individual neurons. We proposed and have demonstrated a novel scheme for in-vivo neuronal signal detection using semiconductor nanowire capacitor probes that operate by displacement currents, thus allowing the sensor to be completely encapsulated and eliminating problems associated with electrochemistry. Using our approach, sensors can be integrated and/or co-fabricated with active microelectronic devices, greatly increasing the feasible number of channels, which can be simultaneously recorded.

We developed nanowire capacitor devices, and optimized fabrication processes to achieve the desired probe resistance and capacitance. Biocompatible perfluoroalkane coatings for the 3D probes were developed, optimized, and tested for pin-hole free dielectric and saline-resistant films. We tested the functionality of probes by characterizing photoresponses of isolated retina. We compared capacitive measurements to conventional electrode arrays and intrinsic signal imaging techniques in order to validate the new technology and to assess the merits relative to competing techniques. We fabricated nanowire capacitor detectors on passive electrode arrays and characterized light responses in isolated retina with the new devices using capacitive detection (~60 channels). Future projects will develop arrays incorporating active readout circuitry (10,000-100,000 channels). The sensor array has the sensitivity, spatial resolution, and biocompatibility for basic studies of neural encoding and processing, as well as for high-density implantable electro-neural interface systems. Systems based on this technology will be used to explore emerging ideas about how information is encoded by synchronous firing or covariance within a local neuronal population. Capabilities developed and demonstrated by this work will support future external proposals to NIH, DARPA, DOD and other agencies, who all project increased and targeted investment in this area.

Background and Research Objectives

Understanding the neural basis of the processes of sensory perception, motor control, learning and memory, and even consciousness, is the final frontier of the biological sciences. This task requires us to measure and ultimately manipulate the dynamic function of large populations of neurons. Neural degenerative diseases and traumatic neurological injuries affect millions of people worldwide, motivating the development of neural prosthetic interfaces to restore sensory or motor function in affected individuals. Most existing interface systems for such applications are based on a relatively small number of relatively simple electrodes, but many applications require higher density arrays, able to selectively record from or stimulate individual neurons. Such systems will ultimately require incorporation of active circuitry into packages that can withstand chronic implantation. Advances in neural sensing and stimulation interface technology will lead to the development of hybrid biological-electronic sensor devices for robust, functioning neural prosthetic systems, and also provide a more comprehensive understanding of neural function.

In the past several decades, neural activity imaging and sensing techniques have been developed to record the activity of individual neurons and small networks. An emerging goal is to simultaneously measure the activity of all neurons in the retina or a limited region of brain tissue. Advances in sensing technology will allow a more comprehensive understanding of retinal processing and encoding leading to the development of hybrid biological-electronic sensor systems for robust, functioning prosthetic system. We anticipate that such knowledge will also serve as the foundation for more sophisticated machine vision systems that will ultimately emulate the

perceptual function of biological vision.

Both basic science and biomedical applications require electro-neural interface devices to withstand corrosion and induce minimal damage at the electrode/tissue interface. Current techniques of neural activity sensing employ multi-electrode arrays (MEAs) that are typically made of metal electrodes and utilize direct current measurement. Encapsulation of MEAs in a protective coating can eliminate corrosion and minimize electrochemical charge transfer across the electrode-tissue interface, which induce circuitry failure and neural damage through irreversible Faradic reactions.

To overcome the direct current limitations in existing MEA technology, capacitive charge transport between the electrodes and neural tissue might be employed. Capacitive sensing could alleviate most of the drawbacks of the Faradic current stimulation, including corrosion and evolution of chemically reactive species. Recent work has advanced the technology of capacitive stimulation of neurons and this method will likely prove important for designing future electroneural prosthetic systems. Capacitive coupling has been used for noninvasive measurements in a neuronal culture environment on a semiconductor chip, but the development of this technology has been limited, and present systems do not support implantation and chronic recording. Advances in the design and fabrication of systems for high-density capacitive coupling to neural tissue will advance prosthetic applications as well as our knowledge of systems neuroscience.

The principal objectives of the original project, as stated in the proposal include:

- Develop, design, and fabricate radial semiconductor nanowire capacitors for high density, three-dimensional implantable electroneural recording devices
- Develop prototype implantable devices with self-assembled, self-healing bio-compatible coatings for chronic applications.
- Study the dynamic function of a neural network by monitoring activity of every neuron in a patch of retina, using conventional electrode arrays. nanowire sensors and optical imaging techniques

In addition to these central aims we also described other potential applications of the technology. These include the use of capacitance-based sensors as non-contact pickups for electro-encephalography (EEG); and the possibility of stimulating neurons with capacitive currents.. We also discussed the development of hybrid bio-electronic sensors for chemical detection and neuromuscular interfaces to drive prosthetic devices for peripheral limb amputees. With support of the LDRD program office we have pursued these last two applications.

Scientific Approach and Accomplishments

During the first two years of the project we made very substantial progress on all of the original objectives of the project, as documented in previous progress reports and project appraisals. We have demonstrated the development of both micro- and nanoscale 3-D structures (arrays of silicon or metal pillars) and have manufactured these in sensor arrays that allow connection to the front-end active electronics used for conventional multi-electrode arrays. We have developed and characterized two classes of self-assembled organic coatings for micro-wire sensors. We have implemented capabilities for electrophysiological measurements with microelectrodes arrays, using a state of the art system acquired with LDRD funding. We have conducted multi-channel electrophysiological measurements in retina, combined with simultaneous high-resolution optical imaging measurements. Experiments have been conducted with both micro- and nanowire sensor arrays demonstrating the feasibility of physiological recordings in retina with LANL devices.

Major technological challenges of sensor development were addressed during the first two years, producing microstructured 3D sensor arrays that have been employed for electrophysiological measurements (Figure 1). The biggest remaining challenge for the third year was to improve the dielectric coating of the micro- and nanowire sensors, and to show that these devices enable capacitive sensing in the absence of galvanic connection to neuronal tissue. Both Huang and Branch worked on this problem, trying to achieve defect free dielectric coatings based on Halfnium oxide. Such devices could eventually incorporate an organic insulating layer.as demonstrated in previous work. As these devices were fabricated we characterized the resistance across the sensor dielectric coating using impedance measurements (Figure 2) before employing the sensor arrays for electrophysiological measurements (Figure 3).

We undertook an initial demonstration of the foundation technologies for construction of a hybrid sensor array incorporating cultured excitable cells (Figure 4). Because we did not have the required expertise for cultured cell work within the existing project team, we added Rashi Iyer, who in turn was able to recruit a postdoctoral fellow to participate in this work. We believe that the most feasible and useful approach will be to establish a neural interface for the peripheral nervous system be to culture muscle cells (myocytes) in contact with the sensor arrays. The

ultimate application would be to acquire control signals for prosthetic devices from the severed motor neurons of peripheral limb amputees. Such implantable interfaces are actively sought, again principally by NIH(NIBIB) and DARPA.

Because the development of techniques to encourage the regrowth and targeting of myocytes by motor nerve tracts was beyond the scope of the present project, we pursued the use of myocytes that have been transfected with channelrhodopsin, allowing their stimulation by light, closely analogous to our present work in retina.

Results

During the past year, we developed a three-dimensional micro pillar sensor array that utilizes capacitive coupling in order to sense electrical activity in excised retinal tissue. The device incorporates over 3600 capacitive probes organized into 60 independent sensor sites (for compatibility with existing electronics) spread over an area of 750 μm2. Each sensor site consists of an 8x8 array of Pt micropillars in order to maximize the capacitive response, interconnected by leads on the device.

The device is fully insulated by atomic layer deposition of hafnium oxide. Electrochemical impedance spectroscopy was used to study the oxide deposition on the 3D micro pillar sensor array to ensure a pinhole-free dielectric coating. The characteristic impedance magnitudes increased up to 3 orders of magnitude upon oxide deposition and phase measures indicate fully capacitive sensor sites.

The capacitive sensor was interfaced with retinal tissue and upon light stimulation electro-retinograms (ERG) were recorded. Our fabrication processes and electrochemical impedance measurements demonstrated the usefulness of such techniques for building high-density 3D arrays that were fully encapsulated with a protective dielectric coating. The work advances the technology towards capacitive sensing of neurons with a robust, non-invasive sensing device, providing a base for studying neural encoding and processing by networks of neurons and for the future development of neural prosthetics.

During the final year of the project, we requested and received permission to pursue a new direction in the project: developing hybrid sensors incorporating capacitive readout and/or stimulation of captive excitable cells (neurons and myocytes). The original motivation for this proposal by the project PI (George) was to develop a electroneural interface for the perpheral nervous system that would be suitable for neural control and feedback of a prosthetic limb. However, in early discussions with Iyer, we realized that such a system, allowing the activity of a neuromusclular junction formed in vitro to be controlled and monitors, would provide both an excellent model system for study of function, as well as a useful biosensor, e.g for detection of certain chemical warfare agents. In fact, a patent disclosure was developed for this idea.

The principal bioscience challenges in this work were to achieve sustainable culture of suitable populations of nerve and muscles cells, to achieve viable co culture of mixed populations of these cell types, to develop electrophysiological or other strategies for controlling and monitoring activity of these cells, and ultimately to develop integrated systems based on these capabilities.

Although this portion of the project only began in the last six months of the ER project, we nevertheless achieved substantial progress on these objectives.

We achieved viable primary cultures of both neurons and myocytes, and observed maturation of the immature cells into forms that appear morphologically to be functional, differentiated cells.

We developed several complementary strategies to allow co-culture of heterogenenous populations of neurons and myocytes.

We achieved transfection of cells with optogentic material that will ultimately allow the activity of these excitable cells to be stimulated and monitored by light.

With the demonstration of capacitive sensing of neurophysiological responses of retina, and the pilot work on development of cultures of excitable cells we have achieved all of the major technical objectives of the project, as originally proposed. However there are additional steps that we hope to pursue with follow-on, non-LDRD funding:

- Integrate the Hafnium insulated capacitive sensors with the self-assembled organic coatings previously developed.
- Build a version of the sensor arrays suitable for integration with commercially available read-out integrated circuits (ROICs) or with custom circuitry to allow sensor multiplexing for much higher density data acquisition over a serial interface. We anticipate the ability to record from hundreds of thousands of discrete sensor sites.
- Collaborate with others (e.g. Quan Qing at Arizona State University or Murat Okandan at Sandia) to develop ROICs incorporating front end Field effect transistors (FETs) for greater sensitivity readout of dense capacitive sensor arrays.
- Develop an implantable sensor for the peripheral nervous system incorporating captive neurons and

myocytes for bidirectional interface with motor/sensor nerve trunks.

Impact on National Missions

The project successfully developed and demonstrated a new technology for sensing of neural responses based on capacitive probes. The approach enables high density sensor arrays suitable for long-term studies of neural processing as well for chronic implantation for use as interfaces for electroneural prosthetic devices. Bio-hybrid devices based on such devices and incorporating cultured cells should find applications for sensing and monitoring applications as well as for model systems for biological studies. Development of advanced neural interfaces is a central focus of programs supported by DARPA and NIH/ NIBIB as well as previous programs supported by DOE and LANL LDRD. Development of artificial organ systems is a topic of interest to DTRA and NIH. High-density measurement of neural function is a principal focus of the multi-agency BRAIN initiative. Such studies also hold promise for elucidating mechanisms of information processing and encoding by the brain that are increasingly viewed as the basis of a new generation of neuromorphic computing systems that will be much smarter and more capable, with a fraction of the size, weight, and power requirements of conventional computing systems.

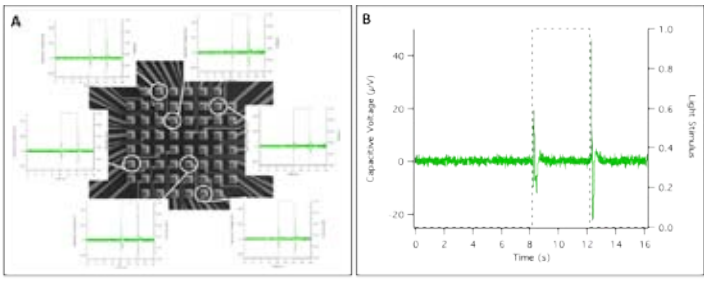

Figure 1. SEM images of the 60-electrode device with three-dimensional pillar electrodes (Inset A & B) connected by Pt metal traces terminating at bond pads on the outside edge of the device (Inset C).

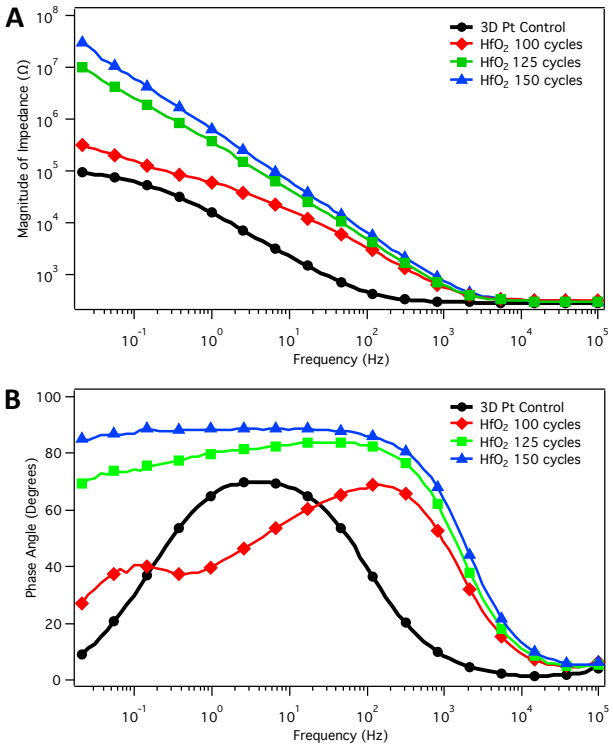

Figure 2. Interface impedance (A) and phase shift (B) vs. frequency of a 3D Pt electrode coated with 100-150 cycles of HfO2.

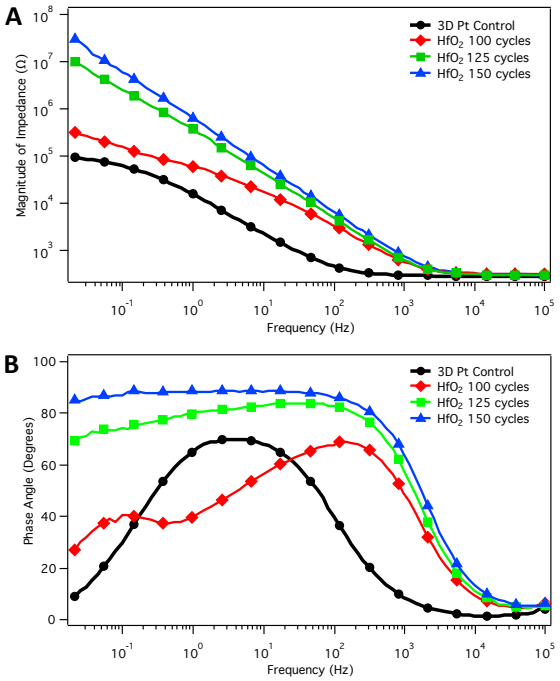

Figure 3. Responses (left axis) of isolated frog retina to light stimulation from 6 individual capacitive sensors with their respective location within the array (A) and a single capacitive sensor response (B). Stimulation (right axis) starts at 8 seconds and remains on for 4 seconds. Note that the retina characteristically responds to both the onset and offset of light stimulus.

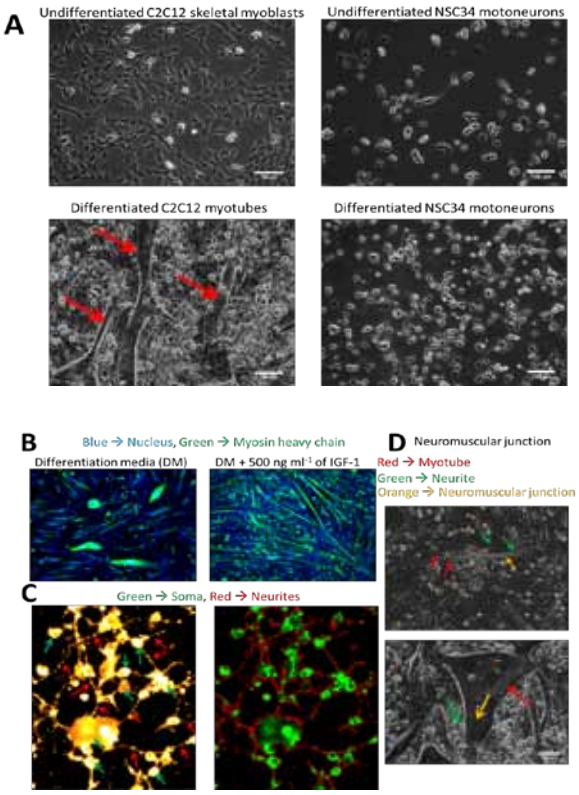

Figure 4. Formation of the neuromuscular junction (NMJ). (A) Differentiated and un-differentiated C212 (red) skeletal myoblasts and NSC34 motoneurons. (B) Fluorescent image showing myotubes (green) in differentiation media (DM) (C) Fluorescent image of neurites (red) sprouting from the cell body (green). (D) Phase contrast images of NMJ (orange) between C2C12 myotubes (red) and NSC 34 motoneurons (green).

Publications

Branch, B. A., Y. Hwang, J. L. Schei, A. M. Dattelbaum, D. Petsev, and J. S. George. Design and fabrication of a 3D pillar electrode array for transduction of retinal responses. 2013. ABSTRACTS OF PAPERS OF THE AMERICAN CHEMICAL SOCIETY. 245: -.

Branch, B., J. L. Schei, G. Gupta, A. Dattelbaum, D. Petsev, and J. S. George. Hafnium oxide encapsulated micropillar array for transduction of neural responses. IEEE Sensors.

Branch, B., J. L. Schei, K. Artyushkova, G. Gupta, A. M. Dattelbaum, D. N. Petsev, and J. S. George. 3D Capacitive sensor array for detection of neural responses . To appear in Journal of Solid State Science and Technology.

Branch, B., M. Dubey, A. S. Anderson, K. Artyushkova, J. K. Baldwin, D. Petsev, and A. M. Dattelbaum. Investigating phosphonate monolayer stability on ALD oxide surfaces. 2014. APPLIED SURFACE SCIENCE. 288: 98.

Branch, B., M. Dubey, A. S. Anderson, K. Artyushkova, J. K. Baldwin, D. Petsev, and A. M. Dattelbaum. Investigating phosphonate monolayer stability on ALD oxide surfaces. 2014. APPLIED SURFACE SCIENCE. 288: 98.

Dai, X., S. Dayeh, V. Veeramuthu, A. Larrue, J. Wang, H. Su, and C. Soci. Tailoring the Vapor-Liquid-Solid Growth toward the Self-Assembly of GaAs Nanowire Junctions. 2011. NANO LETTERS. 11 (11): 4947.

Dayeh, S. A.. One Dimensional Semiconductor Heterostructures: Potential and Implications for Advanced Technologies. Invited presentation at Nanovation: From Science to Startups. (UC Berkeley, 27 Oct 2012).

Dayeh, S. A., A. V. Gin, and S. T. Picraux. Advanced core/multishell germanium/silicon nanowire heterostructures: Morphology and transport. 2011. Applied Physics Letters. 98 (16): 163112 (3 pp.).

Dayeh, S. A., W. Tang, B. M. Nguyen, X. Dai, Y. Liu, Y. Hwang, X. H. Liu, and R. Chen. Nanoscale Heterogeneous Reactions and Interfaces in Ge/Si and for III-V on Si Integrated Devices. 2013. SEMICONDUCTORS, DIELECTRICS, AND METALS FOR NANOELECTRONICS 11. 58 (7): 115.

Dayeh, S. A., Y. Hwang, J. L. Disterhaupt, J. Yoo, I. H. Campbell, J. S. George, and S. T. Picraux. Nanostructures for solar energy and probing the brain. Invited presentation at NNSA LDRD 2012 Symposium. (Washington DC, 4 June 2012).

Dayeh, S. A., Y. T. Hwang, J. L. Disterhaupt, J. Yoo, I. H. Campbell, J. S. George, and S. T. Picraux. Nanostructures for solar energy and probing the brain. Invited presentation at 2012 LDRD Day. (Los Alamos, 23 Oct. 2012).

Dayeh, S., J. Wang, N. Li, J. Y. Huang, A. Gin, and S. Thomas. Picraux. Growth, defect formation, and morphology control of germanium-silicon semiconductor nanowire heterostructures. 2011. Nano Letters. 11 (10): 4200.

Dayeh, S., N. MacK, J. Y. Huang, and S. T. Picraux. Advanced core/multishell germanium/silicon nanowire heterostructures: The Au-diffusion bottleneck. 2011. Applied Physics Letters. 99 (2): 023102.

Dayeh, S., R. Dickerson, and S. Thomas. Picraux. Axial bandgap engineering in germanium-silicon heterostructured nanowires. 2011. APPLIED PHYSICS LETTERS. 99 (11): 113105.

Dayeh, S., X. H. Liu, X. Dai, J. Y. Huang, S. T. Picraux, and C. Soci. Rocking chair defect generation in nanowire growth. 2012. APPLIED PHYSICS LETTERS. 101 (5): 053121.

George, J.. Casting Light on Neural Function: A Subjective History. 2010. In Casting Light on Neural Function: A Subjective History. , p. 1.

Gintautas, V., M. Ham, B. Kunsberg, S. Barr, S. Brumby, C. Rasmussen, J. George, I. Nemenman, L. A. Bettencourt, and G. Kenyon. Model Cortical Association Fields Account for the Time Course and Dependence on Target Complexity of Human Contour Perception. 2011. PLOS COMPUTATIONAL BIOLOGY. 7 (10): e1002162.

Hwang, Y. T., J. Disterhaupt, J. S. George, S. T. Picraux, and S. A. Dayeh. High density capacitive pillar arrays for high fidelity neural sensors. Presented at 2012 MRS Fall Meeting. (Boston, 25-30 Nov. 2012).

Hwang, Y. T., J. L. Disterhaupt, J. S. George, S. T. Picraux, and S. A. Dayeh. High density electrically isolated capacitive pillar arrays for high fidelity neural sensors. Presented at Society for Neuroscience Meeting. (New Orleans, 13-17 Oct. 2012).

Hwang, Y., B. M. Nguyen, and S. A. Dayeh. Atomic layer deposition of platinum with enhanced nucleation and coalescence by trimethylaluminum pre-pulsing. 2013. APPLIED PHYSICS LETTERS. 103 (26): -.

Hwang, null., null. Dayeh, W. [. Tang, and null. Dai. All-solid state nickel silicide wafer bonding with wide thermal budget. 2012. LDRD.

Ji, Z., G. T. Kenyon, S. Brumby, L. M. Bettencourt, and J. S. George. Deep generative model of the where-what pathways in the primate visual cortex. 2011. In 41st Annual Meeting of the Society-for-Neuroscience ; November 12 -16, 2011 ; Washington, DC, USA. Vol. 41.

Kar, A., P. Upadhya, S. Dayeh, S. Tom. Picraux, A. Taylor, and R. Prasankumar. Probing Ultrafast Carrier Dynamics in Silicon Nanowires. 2011. IEEE JOURNAL OF SELECTED TOPICS IN QUANTUM ELECTRONICS. 17 (4): 889.

Li, Xianglong, Jeong-Hyun Cho, Nan Li, Yingying Zhang, D. Williams, S. Dayeh, and S. T. Picraux. Carbon Nanotube-Enhanced Growth of Silicon Nanowires as an Anode for High-Performance Lithium-Ion Batteries. 2012. Advanced Energy Materials. 2 (1): 87.

Liu, X. H., H. Zheng, L. Zhong, S. Huan, K. Karki, L. Q. Zhang, Y. Liu, A. Kushima, W. T. Liang, J. W. Wang, J. Cho, E. Epstein, S. Dayeh, S. Tom. Picraux, T. Zhu, J. Li, J. Sullivan, J. Cumings, C. Wang, S. Mao, Z. Z. Ye, S. Zhang, and J. Y. Huang. Anisotropic Swelling and Fracture of Silicon Nanowires during Lithiation. 2011. NANO LETTERS. 11 (8): 3312.

Liu, X. H., L. Q. Zhang, L. Zhong, Y. Liu, H. Zheng, J. W. Wang, J. Cho, S. Dayeh, S. Tom. Picraux, J. Sullivan, S. Mao, Z. Z. Ye, and J. Y. Huang. Ultrafast electrochemical lithiation of individual Si nanowire anodes. 2011. Nano Letters. 11 (6): 2251.

Mohite, A. D., D. E. Perea, S. Singh, S. A. Dayeh, I. H. Campbell, S. T. Picraux, and H. Htoon. Highly Efficient Charge Separation and Collection across in Situ Doped Axial VLS-Grown Si Nanowire p-n Junctions. 2012. NANO LETTERS. 12 (4): 1965.

Seo, M. A., S. A. Dayeh, P. C. Upadhya, J. A. Martinez, B. S. Swartzentruber, S. T. Picraux, A. J. Taylor, and R. P. Prasankumar. Understanding ultrafast carrier dynamics in single quasi-one-dimensional Si nanowires. 2012. Applied Physics Letters. 100 (7): 071104 (5 pp.).

Seo, M. A., S. A. Dayeh, P. C. Upadhya, S. T. Picraux, J. Martinez, B. S. Swartzentruber, A. J. Taylor, and R. P. Prasankumar. Polarization anisotropy of transient carrier dynamics in single Si nanowires. 2011. In 2011 Conference on Lasers and Electro-Optics, CLEO 2011 ; 20110501 - 20110506 ; Baltimore, MD, United States. , p. var.pagings.

Seo, M. A., S. A. Dayeh, P. C. Upadhya, S. T. Picraux, J. Martinez, B. S. Swartzentruber, A. J. Taylor, and R. P. Prasankumar. Polarization anisotropy of transient carrier dynamics in single Si nanowires. 2011. In CLEO: 2011 - Laser Science to Photonic Applications ; 1-6 May 2011 ; Baltimore, MD, USA. , p. 1.

Tang, W., S. Dayeh, S. Tom. Picraux, J. Y. Huang, and K. Tu. Ultrashort channel silicon nanowire transistors with nickel silicide source/drain contacts. 2012. Nano Letters. 12 (8): 3979.

Restoring Neurological Function with Self-assembled Lipid Bilayers

Srinivas Iyer
20110411ER

Abstract

Myelin is a complex tissue that covers nerves and permits electrical conduction through our bodies. The role of myelin is central to all neurological functions, thus perturbations of this tissue have devastating consequences to human health. These perturbations are typically manifested as "demyelination", a condition where segments of the nerve are left uncovered which then leads to a reduction in electrical conduction through the nerve. While conditions such as injury trauma and diabetes result in this condition, it is most prominent in the debilitating disease Multiple Sclerosis. The events surrounding myelin damage and repair has stayed at the forefront of neurochemical research, however insufficient information is available due to the lack of suitable experimental systems that reproduce the complexity of the natural tissue. The foremost goal of our effort is to generate an experimental system to investigate the role of specific structural features in myelin function. The complexity of natural myelin precludes such studies with tissue isolates, hence our assembly will enable mechanistic interrogations of structural events. The second and longer term direction is to establish self-assembly principles that will guide the ultimate development of artificial myelin tissue.

Background and Research Objectives

Nature has a huge repertoire of "smart" biomaterials that have evolved to satisfy physiological needs. Perhaps the most fascinating of these is the myelin sheath, an intricate nanoscale lipid-protein assembly. The easiest way to imagine myelin is as a stack of lipid bilayers held together by proteins. Myelin was defined by Ranvier in 1878 as a sheath that surrounds nerve fibers. Portions of the nerve are left uncovered at points called the nodes of Ranvier. It is at these nodes that the nervous impulse in the form of an action potential (voltage differential) is rejuvenated. The mechanism by which myelin exerts its function is its role as an insulator, preventing the dissipation of ionic gradients that are the basis of the action potential. Multiple disease states result in breakdown of myelin, consequently affecting even the most basic motor functions. Understanding these processes are thus at the very crux of therapeutic strategies for this important public health concern. The complexity of myelin structure precludes studies examining the effect of structural perturbations on function. Our overall objective is to create assemblies that mimic myelin that will enable systematic studies.

The main goals of the project included:

Aim 1: Use native myelin proteins to sequentially link several lipid bilayers.

Aim 2: Study size, integrity, fluidity and insulating capacity of the assembled structures.

Aim 3: Mimic known biochemical events surrounding demyelination and assess their contribution

Scientific Approach and Accomplishments

We have used nanoscale, controlled self-assembly method to create an architecture that closely mimics structural and functional aspects of the dense line of natural myelin. We have also performed electrical impedance measurements on these structures. This mimic will facilitate studies of the effect of myelin structure on its function and provide insights into hitherto unknown details of this very important tissue. These results will be used to design strategies for treating neurological disorders stemming from myelin damage. In this study, we examined fluidity and insulating capacity and describe the results below. We also addressed aim 3 by using myelin basic protein to stitch bilayers; however the results were not sufficiently conclusive to determine the effects of phosphorylation. We are developing a proposal to the NIH to investigate additional biochemical events as a follow-on project to this LDRD-ER.

Towards our overarching goal of developing

and understanding lipid systems that closely resemble myelin sheaths, we used two approaches:
(a) 1-step Approach: We document the synthesis and characterization of highly ordered and stable phospholipid-silica thin films that resemble multi-lamellar architectures present in nature such as the myelin sheath. We have used a near room temperature chemical vapor deposition method to synthesize these robust functional materials (Figure 1). Highly ordered lipid films are exposed to vapors of silica precursor resulting in the formation of nano-structured hybrid assemblies. This process is simple, scalable and offers advantages such as exclusion of ethanol and no (or minimal) need for exposure to mineral acids, which are generally required in conventional sol-gel synthetic strategies. The structure of the phospholipid-silica assemblies can be tuned to either lamellar or hexagonal organization depending on the synthesis conditions. The phospholipid-silica films exhibit long-term structural stability in air as well as when placed in aqueous solutions and maintain their fluidity under aqueous or humid conditions. This platform provides a model for robust implementation of phospholipid multilayers and a means toward future applications of functional phospholipid supramolecular assemblies in device integration. As an example, we used POPC lipid to construct our assemblies. Figures 2a and 2b show XRD patterns of lipid films before and after exposure to TMOS precursors at 37 °C. The patterns reflect the lamellar structure with a strong (001) diffraction peak at 50 Å for the control lipid assembly (no silica) and 55 Å for the hybrid lipid-silica film. Both the control and hybrid films exhibit higher order diffraction (002), (003), (004) peaks. A TEM micrograph of the surface region of a hybrid POPC-silica thin film after 1-hour exposure to TMOS vapor clearly indicates a lamellar structure (Figure 2c). No XRD peaks were observed after calcination, which suggests a collapse of the structure upon removal of the lamellar phospholipid assembly. Sequential fluorescence images of the silica-coated POPC multi-lamellar assemblies are shown in Figure 2e. FRAP measurements indicate that phospholipids in these multi-lamellar ultrathin films are diffusively mobile ($D = 0.1 \pm 0.04$ μm2/s) when placed in aqueous solution. It is interesting to note that these assemblies did not crack in aqueous conditions, possibly due to the low synthesis temperature.

In conclusion, we are able to easily fabricate tunable robust and fluid hybrid lipid-silica assemblies with various mesostructural features through minimal adjustments to the synthesis conditions. Our laboratories are currently optimizing reaction conditions for successful incorporation of relevant transmembrane peptides and proteins into the hybrid lipid-silica assemblies that resemble myelin.

(b) Layer-by Layer Approach: In parallel, we sequentially link several lipid bilayers in a controlled self-assembly process using vesicle fusion on conductive surfaces. The layer-by-layer approach enables an alternating structure with closer resemblance to the dense and Intra-period lines of myelin. Briefly, lipid vesicles (containing biotin) were infused on silicon wafers resulting in formation of first bilayer. Subsequently, streptavidin was added followed by fusion with another set of vesicles. This procedure was performed over and over again resulting in the formation of multi lamellar layer. Figure 3 shows the sequential images of the lipid layers on silicon substrates. As can be seen the lipid bilayers recover almost fully in 30-60 minutes. The diffusion constant estimated for these bilayers is in the range of 0.5-1.0 2/s.

Figure 4 shows the impedance spectra of the respective assemblies. An increase in impedance is observed after addition of each subsequent layer. Specifically, the appearance of a second capacitor is noticeable upon addition of each bilayer. These results clearly indicate that we can create layer-by-layer model systems that can be used to mimic and understand lipid multilayers. This is the first report on multi-lamellar assemblies that resemble myelin.

Impact on National Missions

Development of biomimetic models is an example of how molecules self-assembled at the nanometer length scale can improve our understanding of complex biological systems, a major area of interest of DOE BES. We have created a dynamic model system with which we can begin to understand processes critical to myelin sheath formation and degradation. This exploratory work has laid the groundwork for an increase in the scientific understanding of complicated myelin-associated diseases (DHHS interest, proposal under development for NIH). These efforts tie in with LANL's stated mission goals of being a premier materials laboratory with a focus on developing next-generation biomaterials. The health impacts fits into the Public Health mission of Bioscience Division and is of interest to certain agencies of the DoD especially in the area of treating warfighters after nerve trauma from battlefield injuries.

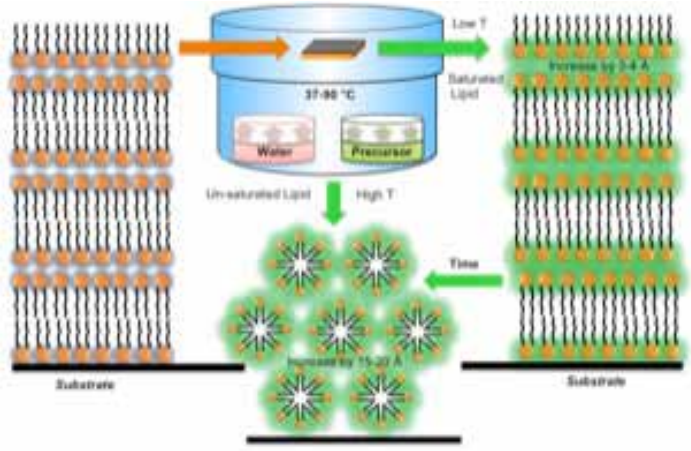

Figure 1. Schematic of the CVD process used to prepare silica encapsulated multilamellar lipid assemblies. Spin-coated multilamellar lipid stacks (left) are exposed to vapors of a silica precursor (TEOS or TMOS) and water. Silica forms selectively between the lipid head groups of the lamellar lipid assemblies. Increase in synthesis temperature, use of unsaturated lipid and long exposure times result in the formation of hexagonal phases.

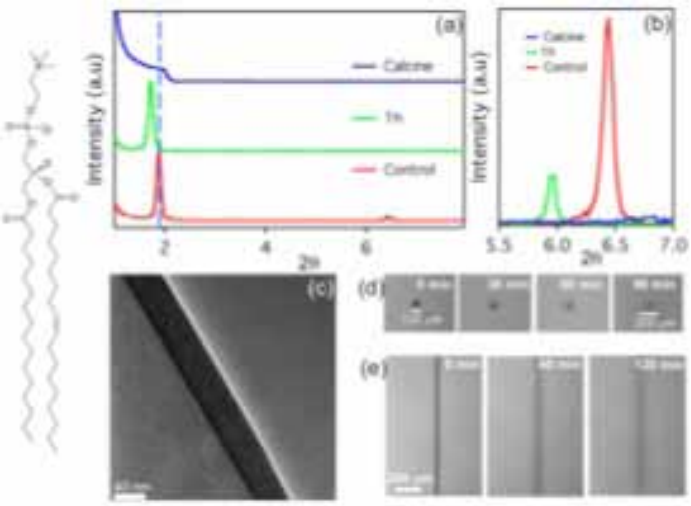

Figure 2. XRD, TEM and fluorescence images of POPC-silica assemblies prepared on silicon wafers. (a) XRD pattern before and after exposure to silica precursor vapors at 37°C, and after calcination. (b) XRD patterns of the 4th order diffraction peaks for the samples shown in (a). (c) TEM image of a POPC-silica assembly before calcination. (d) FRAP (luorescence recovery after photobleaching) of a lamellar POPC-NBD-PE silica film (synthesized at 60°C) performed in saturated water vapor. (e) FRAP of a lamellar POPC-NBDE-silica film under water (synthesized at 37°C). The dotted line in Fig. 5a was added to reference the (001) peak for all samples relative to the as-prepared spin-coated DMPC lipid assembly.

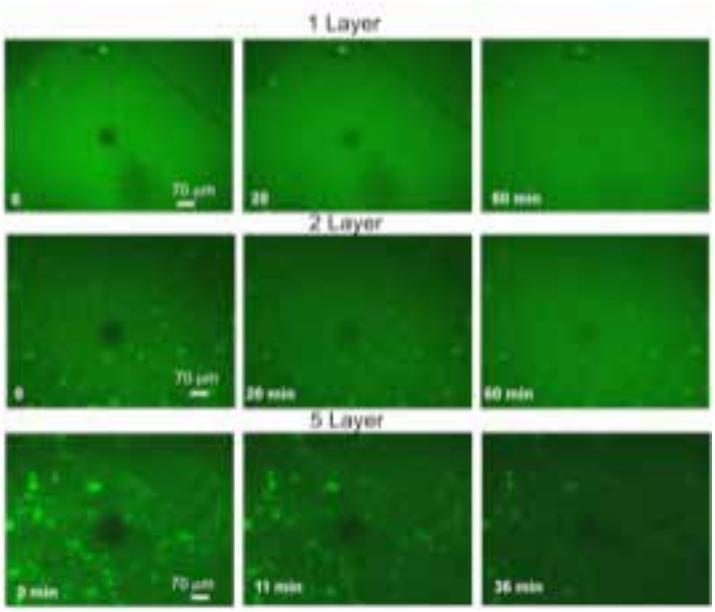

Figure 3. FRAP images of 1 Bilayer, 2 Bilayers and 5 Bilayers. After photobleaching, sequential images indicate the recovery of bilayer.

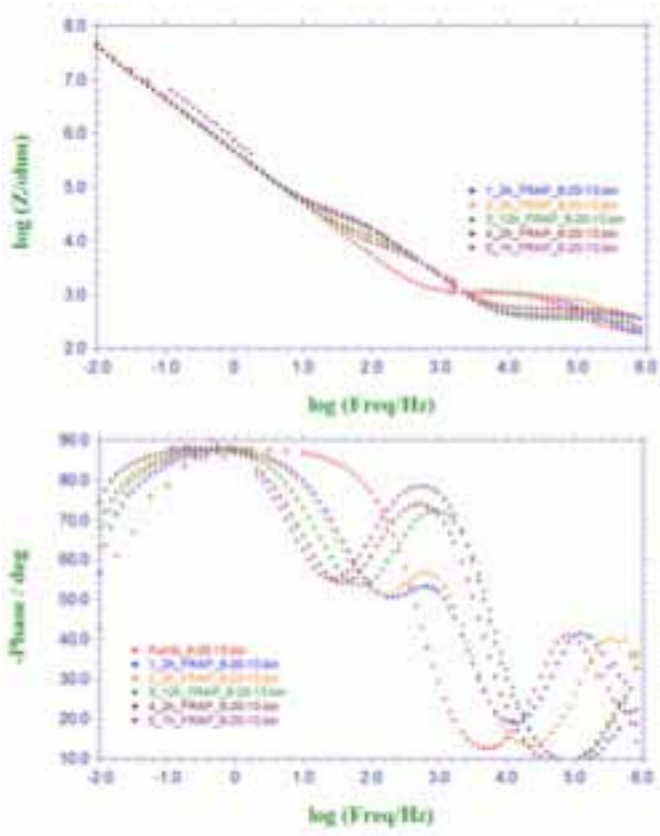

Figure 4. Bode plot of layer-by-layer lipid assemblies showing increase in impedance with size of assembly.

Publications

Gupta, G., S. Lyer, K. Leasure, N. Virdone, A. M. Dattelbaum, P. B. Atanassov, and G. P. Lopez. Stable and Fluid Multilayer Phospholipid-Silica Thin Films: Mimicking Active Multi-lamellar Biological Assemblies. 2013. ACS NANO. 7 (6): 5300.

Gupta, G., w. han, g. lopez, and l. ista. Silicieous nano-biomaterials. To appear in Handbook of nanobiomaterials. By r, .

Understanding the Mechanisms of Biological Transport for Nano-technology Applications

Sandrasegaram Gnanakaran
20110412ER

Abstract

The Nuclear Pore Complex (NPC) gates all the traffic between the cell nucleus and the cytoplasm in eukaryotic cells, and its transport mechanism is a subject of intense scientific debate. NPCs are remarkable biological machines that are directional and selective, but do not directly consume metabolic energy during the translocation process and seemingly do not undergo large-scale molecular transitions. We seek a mechanistic understanding of NPC transport and plan to leverage this understanding towards the design of bio-mimetic devices and sensors. In this project, we have developed several computational and theoretical tools that are appropriate to gain mechanistic understanding into both the equilibrium conformations of the system and its dynamic function. The project resulted in several multi-resolution techniques for a more detailed molecular understanding of the conformational dynamics of the channel. These tools have allowed us to develop conceptual models that capture the essentials of what is known about the transport mechanism and its selectivity, both for the NPC and for related nano-technological devices. With the approaches developed in this project, we can now show that NPC shares common mechanisms of transport selectivity and efficiency with many other biological and artificial nano-channels.

Background and Research Objectives

Proper functioning of living cells requires selective molecular transport into and out of the cell, and between different cell compartments. Many such channels carry selective transport without an input of metabolic energy and without large scale structural transitions from a 'closed' to an 'open' state; the transport is based on diffusion only. Understanding selective transport through such 'always open' channels is a fundamental biological problem, poses challenging physical questions, and has potentially far-reaching technological applications. The transport mechanisms of many of such channels, and in particular the selectivity mechanisms, are still subjects of intense scientific debate. This project focuses on transport through one particular channel of this kind, the Nuclear Pore Complex (NPC).

NPCs are large protein assemblies embedded in the nuclear envelope that gate all the molecular exchange between the nucleus and the cytoplasm in all eukaryotic cells (Figure 1). Transport through the NPC is a centerpiece of a large number of regulatory processes in the cell, and its overall structure and composition is highly conserved among species – from yeast to humans. The NPC is a remarkable biological machine that combines highly optimized and selective transport with speed, versatility, and robustness. It can selectively translocate thousands of molecules per second in both directions in the presence of vast amount of background molecular noise.

Transport through the NPC involves interactions of certain transport factors with the natively unfolded proteins lining the NPC channel. Understanding the conformational dynamics of these unfolded flexible proteins is a major challenge and requires development of new hybrid coarse-grained and atomistic simulation techniques. The research objective is to provide an integrated description of how conformational changes of the NPC constituents determine the dynamics of transport through it and, in particular, its selectivity. The conceptual understanding arising from the study of the NPC can be leveraged for design of artificial nano-sorting devices based on the same principles.

Scientific Approach and Accomplishments

The centerpiece of the transport mechanism is the layer of natively unfolded, unstructured, flexible proteins that are attached to the inner surface of the NPC passageway and protrude into its lumen, as well as from nuclear and cytoplasmic faces. These natively unfolded proteins have been shown to behave in many aspects as conventional polymers. The key element producing efficient and selec-

tive transport through the NPC is the transient binding of the transport proteins to specific binding sites on these polymers. Conformational changes of these polymers have been hypothesized to be involved in the gating and transport mechanisms, and several different models have been proposed [1]. However, many of these models rely on detailed assumptions about the features of the behavior of these polymers that are currently unknown.

We focused on coarse-grained modeling rooted in polymer physics and non-equilibrium statistical mechanics to elucidate the role of these conformational changes. As a first approximation, the models take into account only the most salient features or the polymers and their interactions with the transport proteins. Such models have an impressive record in explaining the properties of polymeric materials, even quite complicated ones. The folded structural proteins comprising the channel and other parts of the device are be modeled on the coarse grained level as smooth surfaces; their interactions with the chain monomers are chosen to represent the required surface interaction properties. The parameters of the coarse grained simulations are calibrated by comparison with available experimental data on conformations of unfolded proteins and, where necessary, informed by microscopic atomistic simulations on short time and length scales.

In this coarse-grained approach based on polymer physics and statistical mechanics, the unfolded proteins are represented as flexible polymeric chains and the models can be treated either by analytical methods or by computer simulations. The model has been so far realized in the planar geometry where the flexible chains are grafted to a flat surface and are in equilibrium with the solution of the transport factors. We have done this part in collaboration with Prof. Rob Coalson and Prof. David Jasnow and the graduate student Mr. Michael Opferman at the university of Pittsburgh [2, 3]. In parallel, we have developed simple approximate analytical models that capture the essential properties of the polymer-transport factor mixtures. Results of the models seem to explain the in vitro experiments on the nanomechanic behavior of the filaments with and without transport factors. The model has also uncovered hitherto unknown collective structural transitions in the assemblies of these polymers, induced by the presence of the transport factors [Figure 2]. These transitions seem to explain the experimental in vitro data (hitherto unexplained) and might be important in the gating and transport mechanisms of the NPC.

Together with the experimental collaborators at Texas A&M University, we have applied the previously developed diffusion type models of transport to the analysis of transport trajectories observed in the single molecule tracking experiments. We developed a theoretical model describing the energetics of the cargo complex's interactions with various parts of the NPC that allowed us to calculate the first passage transport times through the channel [4]. In this model, binding near the cytoplasmic and nucleoplasmic openings of the NPC (the "vestibules") is mediated by a low density of unfolded proteins. In contrast, the central permeability barrier is comprised of a substantially higher density of the unfolded proteins, which can only be overcome with a larger number of favorable interactions. Together, these features are described by a "double-well" shaped free energy landscape. The conclusion of this work is that the unfolded proteins are arranged in a non-uniform fashion such that multivalent interactions predominate in the center of the pore, but not at the periphery. The work emphasizes several important conclusions not addressed by previous models. In particular, transport protein interactions with individual binding sites on the unfolded proteins must be relatively weak, significantly weaker than the micromolar to nanomolar affinities reported by numerous in vitro studies. This is essential to obtain millisecond interaction times and is important for accounting for the apparent absence of multivalent interactions in the cytoplasmic and nucleoplasmic vestibules.

We have also provided evidence supporting the hypothesis that the layer of flexible polymers that forms a key component of biological and artificial channels presents a selective potential through which large molecules must diffuse. From this evidence, a recipe for optimizing the choice of the chemical constituents in these devices emerges in the case where the channel serves as a gateway separating two finite sized chambers. Using theoretical arguments augmented by Brownian dynamics simulations (Figure 3), we demonstrate that an optimal rate of translocation across these gateways may be engineered by systematically selecting the geometry as well as the synthetic or natural components of the polymer layer. The key to this optimization lies in tuning the local interactions between all of these constituents and the targeted cargo, striking a balance between the transit times and the probability of crossing the channel. The study reveals four findings significant to future artificial molecular sorter designs. First, increasing the local binding affinity between the transport moieties and the chain segments yields a non-monotonic variation in the rate of transit across the channel. Second, the time to travel across the channel increases as the binding affinity increases. Third, in accord with gene knockout experiments, reducing the number of chains within the channel changes the magnitude of the transit rates and times, but preserves the qualitative functionality for large cargos. Fourth, one may work within the practical constraints of synthetic chemistry and still reach a maximal

rate of translocation, as prescribed by a simple analytical treatment relating the effective potential to the binding strengths of a distribution of sites.

We have identified and addressed issues hampering the development of atomistic level description of about 30 different natively unfolded proteins known as nucleoporins or Nups that form the channel. The motivation for these studies is that an atomistic level description is required to refine the coarse-grained model to more faithfully reflect the geometry of the NPC and the sequence of the proteins. Multiple copies of Nups line the NPC, and their collective dynamics facilitates transport through NPC. The FG family of Nups (FG Nups) contains extensive regions of FG motifs (phenylalanine-glycine) that facilitate the passage of cargo complexes through the NPCs. However, the mechanism of the interaction of FG Nups with themselves or with cargo complexes is not clear.

We considered all-atom molecular dynamics (MD) simulations for two types of FG nups, non-cohesive Nsp1 and cohesive Nup116, in explicit water to study their conformational characteristics and intra-molecular interactions. These studies prompted us to reevaluate the applicability of commonly used biomolecular force fields towards modeling FG nups. We made extensive comparisons between different water models (Figure 4) and identified a better water model to use that properly solvated charged residues in FG nups [5]. We find that TIP4P-Ew water model provides hydrodynamic radius in agreement with experimental values and resulted in a more extended conformation (Figure 5). Also, we have proposed a network approach that can generally be applied to properly sample large natively unfolded proteins such as FG nups in all-atom simulations [6]. However, our work on this project and several of our other projects has suggested a better approach to deal with inaccuracies in the force field and the lack of sampling of FG nup-like proteins, as it remains practically impossible to generate ergodic ensembles for large natively unfolded proteins in MD simulations. The solution lies in using structure based measurements as constraints in simulations, Accordingly, we have proposed a novel Bayesian framework approach that can use secondary structure and solvation properties to obtain accurate thermodynamic weights of different conformations by quantitatively connecting simulations to infrared spectrum of a natively unfolded protein [7].

Additionally, MD simulations of multiple copies of FG nups show that interactions between FGnups are modulated by the anchoring distances within NPC. Also, these interactions between multiple FG nups promote formation of secondary structure. A manuscript summarizing the above findings is under preparation. The dynamics of FG nups in NPC has also been modulated by phosphorylation, glycosylation and di-sulfide bond formation. That has prompted us to explore the efforts of such post-translational modifications of FG-nups at atomistic scale. In that regard, we have been considering a natively unfolded peptide construct with two glycosylations and a disulfide bond. These all-atom MD simulations reveal that the size, secondary structure and folding of the peptide construct is impacted by glycosylation. Also, the disulfide bond between two unstructured peptides promotes beta strand formation (8).

In summary, mathematical modeling has proven to play an increasingly important role in the mechanistic understanding of the transport through the NPC in particular, because many of the details of in vivo transport are in accessible to direct experimental measurements at this point. In this project simplified models of diffusion through the NPC have provided important insights and the general framework for thinking about the transport through the NPC. The modeling of unfolded proteins is challenging both at coarse-grained and all-atom levels and requires new conceptual mathematical tools as we have implemented. Our coarse-grained approaches can capture the emergence of meso-scale order and function from underlying disorder. Importantly, the insights gained from these theoretical/computational studies on NPC can be applied to the design of bio-mimetic systems that can achieve highly regulated transport across biological or in vitro membranes.

Impact on National Missions

This project addresses basic questions about the mechanisms of intra-cellular transport as well as the technological and bio-medical applications, in an area where theoretical modeling is scarce and crucially needed. The research will provide a clear picture of the mechanisms of intracellular transport. This work supports missions of Threat Reduction by understanding the mechanisms of host-pathogen interactions. The principles of function of the NPC and similar biological channels can be used for novel applications such as design of novel vectors for delivery of materials into the cell nucleus and creation of artificial bio-mimetic nano-filtering devices. Thus, understanding the functioning of such biological and artificial channels poses fundamental biological and physical questions and has far-reaching applications in nano-technology and nano-medicine.

At LANL, this project has helped to develop the connection between protein biophysics and materials science, paving the way for creation of biosensors for detection of pathogens and chemical agents. Exquisite selectivity and robustness of biological channels provide inspiration for creation of artificial nano-molecular devices based on the

same principles. Such artificial devices are cutting-edge in the design of novel molecular sorters and sensors and can be used for single-mismatch DNA detection, protein sorting and pathogen detection; functional prototypes of such devices have been built.

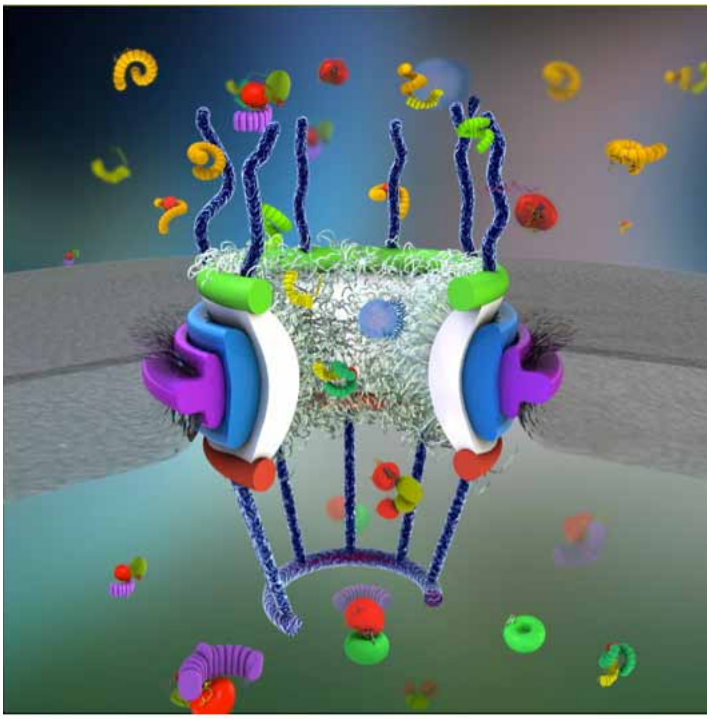

Figure 1. A schematic representation of the NPC structure with the cargo-complex indicated as a kap-beta-bound blue sphere inside the central channel. The NPC structure resembles an hourglass or donut. This channel is sandwiched between the cytoplasmic and nuclear rings. The molecules in different color are important molecules of nucleocytoplasmic transport: Impα, Impβ, Ran, CAS, Ran, RTF/P10, etc. Image from Int Rev Cell Mol Biol 28706: 233.

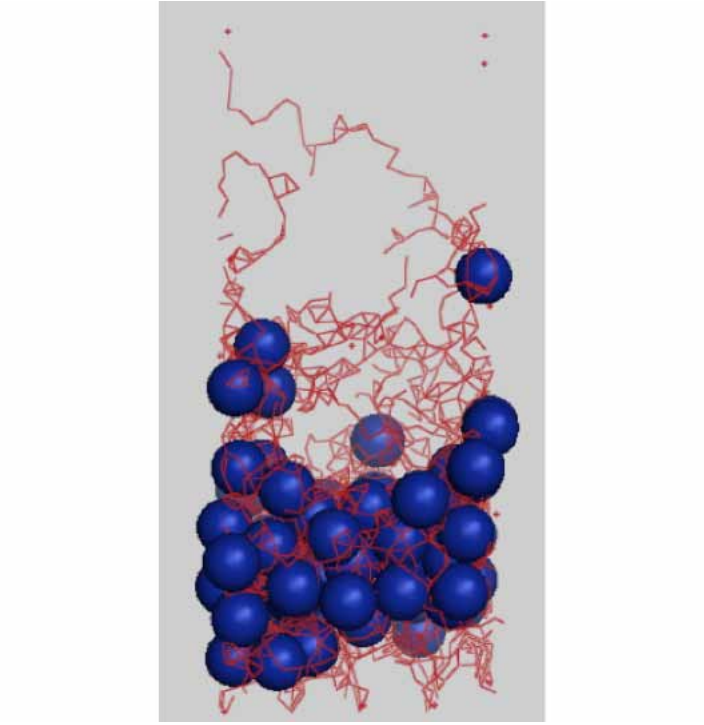

Figure 2. The morphologies of grafted polymer layers interacting attractively with nanoparticle inclusions, as a function of particle size and the interaction strength, using self-consistent field theory and Langevin dynamics simulations. We find that the addition of nanoparticles causes distinctive changes in the layer morphology.

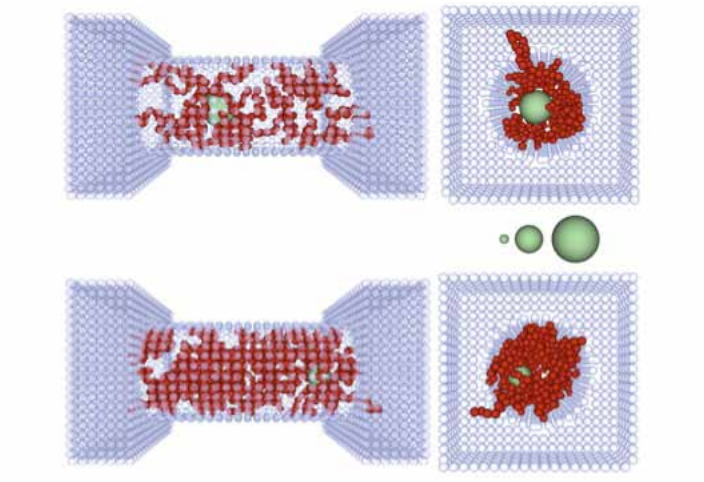

Figure 3. Snapshots from Brownian dynamics simulations of particle transit through a polymer-lined channel. The top image shows a large particle moving through a channel with moderate chain density. The bottom shows a medium-sized particle through a more densely filled channel. The three particles in between illustrate the three different sizes examined, all of which conform to the analytical theory.

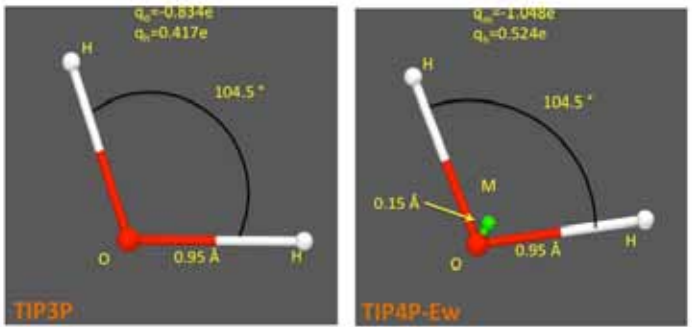

Figure 4. Two water models considered in the all-atom MD simulations.

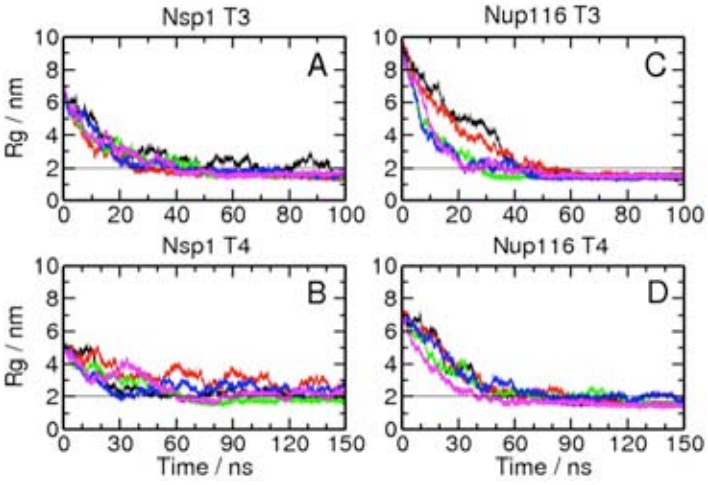

Figure 5. Radius of gyration for Nsp1/Nup116 as a function of time. (A) and (C) are the systems using TIP3P water model; (B) and (D) are the systems using TIP4P-Ew water model. Different colors in each plot correspond to different simulations with different random seeds in each system.

References

1. Jovanovic-Talisman, T., and A. Zilman. NANOBIOTECHNOLOGY Building a basic nanomachine. 2011. NATURE NANOTECHNOLOGY. 6 (7): 397.

2. Opferman, M. G., R. D. Coalson, D. Jasnow, and A. Zilman. Morphology of Polymer Brushes Infiltrated by Attractive Nanoinclusions of Various Sizes. 2013. LANGMUIR. 29 (27): 8584.

3. Opferman, M. G., R. D. Coalson, D. Jasnow, and A. Zilman. Morphological control of grafted polymer films via attraction to small nanoparticle inclusions. 2012. PHYSICAL REVIEW E. 86 (3): -.

4. Tu, L. C., G. Fu, A. Zilman, and S. M. Musser. Multivalent interactions are required for large cargo transport by nuclear pores: Implications for the spatial organization of the FG-nucleoporins . To appear in EMBO Journal.

5. Tian, J., A. Zilman, and S. Gnanakaran. Molecular Dynamics Simulation Studies of FG-repeat-containing Nucleoporins. J. Phys. Chem .

6. Sethi, A., J. H. Tian, D. M. Vu, and S. Gnanakaran. Identification of Minimally Interacting Modules in an Intrinsically Disordered Protein. 2012. BIOPHYSICAL JOURNAL. 103 (4): 748.

7. Sethi, A., D. Anunciado, J. Tian, D. M. Vu, and S. Gnanakaran. Deducing conformational variability of intrinsically disordered proteins from infrared spectroscopy with Bayesian statistics. 2013. Chemical Physics. 422: 155.

Publications

Gnanakaran, G., J. Tian, and A. Sethi. Conformational study of quaternary epitope region of V1/V2 loop: influence of disulfide bonds and glycosylations. 2012. RETROVIROLOGY. 9: -.

Jovanovic-Talisman, T., and A. Zilman. Nanobiotechnology: Building a basic nanomachine. 2011. Nature Nanotechnology. 6: 397.

Opferman, M. G., R. D. Coalson, D. Jasnow, and A. Zilman. Morphology of Polymer Brushes Infiltrated by Attractive Nanoinclusions of Various Sizes. 2013. LANGMUIR. 29 (27): 8584.

Opferman, M., R. Coalson, D. Jasnow, and A. Zilman. Morphological control of grafted polymer films via attraction to small nanoparticle inclusions. 2012. PHYSICAL REVIEW E. 86: 031806.

Sethi, A., D. Anunciado, J. Tian, D. Vu, and S. Gnanakaran. Deducing conformational variability of intrinsically disordered proteins from infrared spectroscopy with Bayesian statistics. 2013. Chemical Physics. 422: 143.

Singh, S., A. Junghans, J. H. Tian, M. Dubey, S. Gnanakaran, J. Chlistunoff, and J. Majewski. Polyelectrolyte multilayers as a platform for pH-responsive lipid bilayers. 2013. SOFT MATTER. 9 (37): 8938.

Tian, J. H., A. Zilman, and S. Gnanakaran. A Study of Intrinsically Disordered Proteins from Nuclear Pore Complex. 2013. BIOPHYSICAL JOURNAL. 104 (2): 55A.

Tian, J., A. Zilman, and S. Gnanakaran. Molecular Dynamics Simulation Studies of FG-repeat-containing Nucleoporins. J. Phys. Chem..

Tu, L. C., G. Fu, A. Zilman, and S. M. Musser. Multivalent interactions are required for large cargo transport by nuclear pores: Implications for the spatial organization of the FG-Nucleoporin . To appear in EMBO Journal.

Nonlinear Resonances between DNA and THz Radiation

Boian Alexandrov
20130765ER

Abstract

Recently, it was demonstrated that terahertz radiation (THz) can modify cellular gene expression and accelerate stem cells differentiation. The ability to selectively and remotely activate specific genes and reprogram cells has an incredible technological and economical potential. To be able to exploit this potential we need to understand the mechanism behind this complex phenomenon. Our mesoscopic modeling demonstrated a novel resonant mechanism of THz-DNA interaction. Our simulations showed that THz radiation can create unzipping or transient opening (bubbles) in the DNA molecule by interacting, in a novel nonlinear resonant manner, with the natural vibrations of the hydrogen bonds that stabilize the double helix. As a first step toward the understanding of this interaction we built a novel ultra-fast THz-UV pump-probe experimental setup and explored the existence of THz-induced DNA bubbles.

Background and Research Objectives

The emergence of reliable and powerful table-top terahertz (THz) radiation sources has triggered an avalanche of applications in security (e.g., airport screening), (bio) molecular spectroscopy, and medical imaging (cf. [1, 2]). As a consequence researchers across the world are beginning to explore the effects of THz irradiation on living matter. Thus, a range of non-thermal THz-induced biological effects have been observed, including: increased DNA production; changes in gene expression; genomic instability; changes in the cell-membrane potential; mitotic disturbances; acceleration of stem cell differentiation, and others (cf. [3, 4, 5]). The main question is: how the non-ionizing THz radiation can affect a biomolecule?

The structural integrity and flexibility of biomacromolecules is primarily governed by hydrogen bonds (H-bonds), whose natural vibration frequencies are in the THz range [6, 7]. Because the H-bonds are weak (only ~few kTs), many biomacromolecules experience relatively slow conformational motion resulting from the inherent thermal fluctuations at biological temperatures. The DNA molecule, for example, experiences thermal motions that induce spontaneous openings and reclosings of the double helix known as “DNA breathing [8],” or spontaneous “base flipping [9],” or “DNA bubbles [10],” whose frequencies are also in the THz range.

Our DNA simulations [11, 12] showed that THz radiation can interact with the natural vibrations of biomolecular H-bonds and change the local stability and flexibility of the biomolecule, and hence can interfere with biological function. We demonstrated that THz-DNA interac¬tion can pro¬duce unzipping or enhanced transients open-states in the double helix (THz-induced bubbles) [11, 12]. Our numerical data showed that the creation of these new open-states needs a strong assistance by the DNA breathing and hence this effect is advanced at the DNA vibrational hotspots, such as: gene promoters and protein-DNA binding sites (i.e., at locations that regulate gene expression). Further, led by our simulations we demonstrated that THz radiation can change gene expression and cell differentiation [13, 14, 15]. Our results also suggested that THz-induced bubbles depend on DNA sequence, THz-frequency, time of exposure, and amplitude of the field.

Scientific Approach and Accomplishments

The specific goal in this project was, in accordance with the suggestions and comments of the LANL Strategy and BIO SAP Teams to our 20130041DR full proposal, to demonstrate the existence of resonant THz-DNA interaction, or shortly, to demonstrate THz-induced DNA bubbles. To observe experimentally THz-induced transient bubbles in DNA, we performed ultrafast THz-UV time-resolved pump-probe spectroscopic experiments. Ultrafast (~40 fs) THz pulses, with broadband spectrum (0.1 - 12THz) and strong amplitude of the electric filed (~ 0.5- 1MV/cm) acted as pump, and, because the absorption of UV (at ~265nm) is sensitive to the openings of the double helix, variable time-delayed UV pulses were

used as probe.

The THz-UV pump-probe time-resolved spectroscopic setup was built at the MPA-CINT LUMOS facility. We gained multiple spectroscopic data showing THz-induced transient bubbles in DNA oligomers, selected by DNA dynamics simulations.

We conducted THz-UV pump-probe experiments with particular DNA oligomers, viz., wtP5: TGAGCACGCAGGGTCTCCATTTTGAAGCGGGAGG, and its modifications, selected via modeling of the DNA bubble activity. The PAGE purified, and at high concentration, wtP5 oligomers and their modifications consecutively were embedded in a temperature controlled 15µm thick water-sandwich holder (Figure 1 inset). This optical (liquid) cell was equipped with specific z-cut crystal quartz windows that are transparent to the THz and UV. The UV and THz pulses were positioned to hit the same spot of the cell.

We demonstrated that the THz and UV ultrafast pulses can be measured accurately through 15-30 µm thick water layer, as well as through 15-30 µm thick water-sandwich that contains sodium phosphate physiological buffer (pH 7.4) with various salt concentrations, Figure 1.

We validated our THz-UV pump-probe setup by measuring the differences in the absorption of UV ultrafast pulses by: i) double stranded DNA, ii) single stranded DNA, and iii) DNA with static bubbles created by insertion (in the wtP5) of 5 nucleotide mismatches (see the inset), Figure 2.

Finally, via consecutively changes of the delay between the THz-pump and the UV-probe pulses, we measured the differential transmitted UV probe signal through samples - with and without DNA, and observed THz-induced DNA bubbles. In Figure 3, we plot the time relaxation of THz-induced bubbles, registered by the change in the delayed UV-absorption. As it can be seen, the demonstrated relaxation time is ~36 ps. In the inset of the Figure 3, we represent the same process at a full scale. The first bump in the inset is the zero of the UV (the UV laser was switched off).

Impact on National Missions

Our data and computer simulations strongly suggest that THz radiation interacts (in a novel nonlinear resonant manner) with natural vibrations of biomolecular H-bonds, creating new conformational states that can change their stability and flexibility. These new open states, in turn, influence gene expression and stem cell differentiation and hence the THz radiation has the potential to be used as a remote regulator of various cellular functions. We observed directly THz-induced bubbles in DNA consistent with our modeling. Most importantly the retrieved experimental data shed light on the mechanism of THz-DNA interactions. Our observations can pave the way to a future mechanism for active remote control of cellular functions (NIH, DOE) and additionally offer a new method for THz spectroscopy of biological macromolecules (DoD). The project is closely aligned with the LANL's Focus Areas in Complex Systems, and it is in support of DOE's research strategies in System and Synthetic Biology.

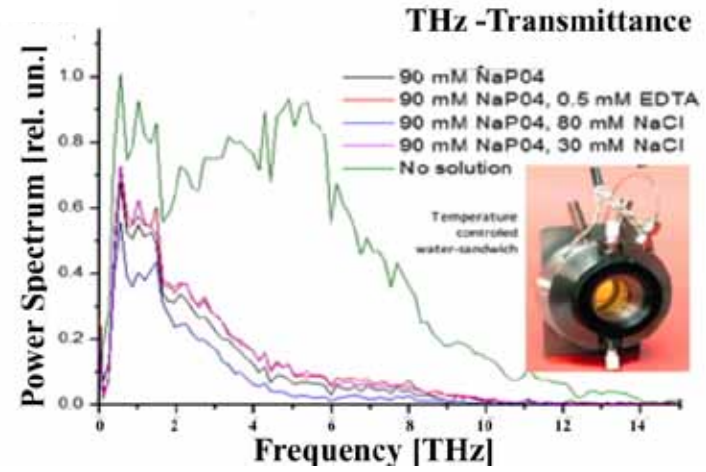

Figure 1. The ultrafast THz and UV pulses are successfully transmitted through DNA samples in a 15-30 µm water or physiological buffer with added salt.

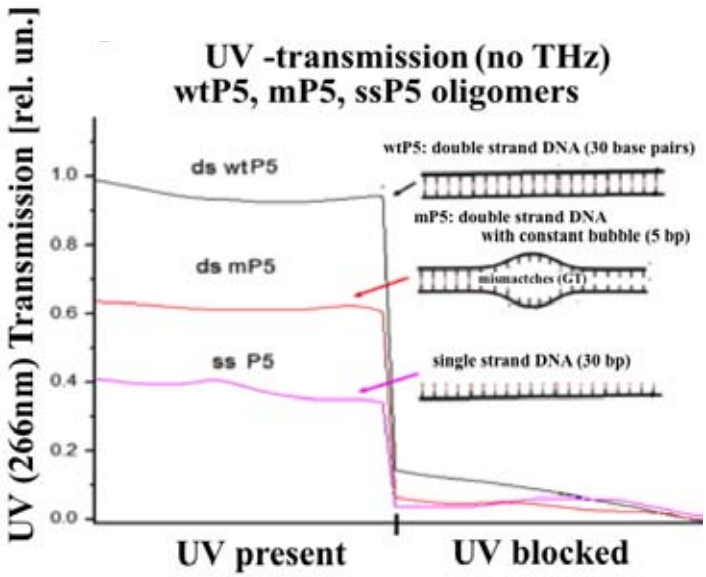

Figure 2. We can tell the difference between single stranded DNA and double stranded DNA. We can also register static DNA bubbles caused by artificially introduced mismatches (e.g., G/T pairing).

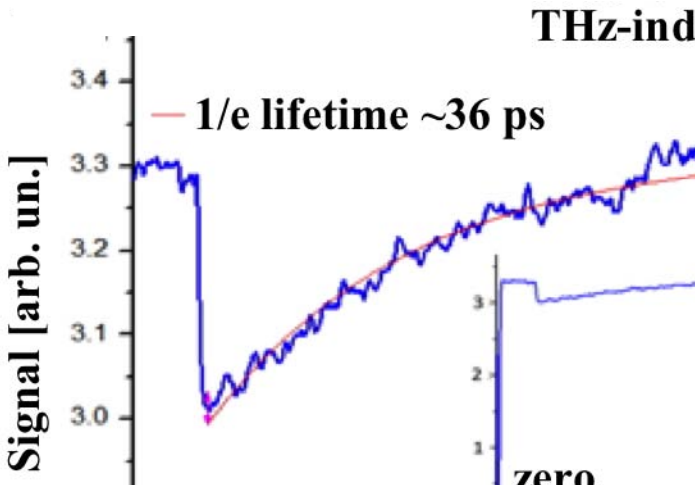

Figure 3. Observation of time-domain THz induced DNA dynamics, i.e. DNA bubbles induced by the THz-pump.

References

1. Tonouchi, M.. Cutting-edge terahertz technology. 2007. NATURE PHOTONICS. 1 (2): 97.

2. Brun, M. A., F. Formanek, A. Yasuda, M. Sekine, N. Ando, and Y. Eishii. Terahertz imaging applied to cancer diagnosis. 2010. PHYSICS IN MEDICINE AND BIOLOGY. 55 (16): 4615.

3. Alexandrov, B. S., M. L. Phipps, L. B. Alexandrov, L. G. Booshehri, A. Erat, J. Zabolotny, C. H. Mielke, H. T. Chen, G. Rodriguez, K. O. Rasmussen, J. S. Martinez, A. R. Bishop, and A. Usheva. Specificity and Heterogeneity of Terahertz Radiation Effect on Gene Expression in Mouse Mesenchymal Stem Cells. 2013. SCIENTIFIC REPORTS. 3: -.

4. Kim, K. T., J. Park, S. J. Jo, S. Jung, O. S. Kwon, G. P. Gallerano, W. Y. Park, and G. S. Park. High-power femtosecond-terahertz pulse induces a wound response in mouse skin. 2013. SCIENTIFIC REPORTS. 3: -.

5. Titova, L. V., A. K. Ayesheshim, A. Golubov, R. Rodriguez-Juarez, R. Woycicki, F. A. Hegmann, and O. Kovalchuk. Intense THz pulses down-regulate genes associated with skin cancer and psoriasis: a new therapeutic avenue?. 2013. SCIENTIFIC REPORTS. 3: -.

6. Fischer, B. M., M. Walther, and P. U. Jepsen. Far-infrared vibrational modes of DNA components studied by terahertz time-domain spectroscopy. 2002. PHYSICS IN MEDICINE AND BIOLOGY. 47 (21): 3807.

7. URABE, H., and Y. TOMINAGA. LOW-LYING COLLECTIVE MODES OF DNA DOUBLE HELIX BY RAMAN-SPECTROSCOPY. 1982. BIOPOLYMERS. 21 (12): 2477.

8. GUERON, M., M. KOCHOYAN, and J. L. LEROY. A SINGLE-MODE OF DNA BASE-PAIR OPENING DRIVES IMINO PROTON-EXCHANGE. 1987. NATURE. 328 (6125): 89.

9. ROBERTS, R. J.. ON BASE FLIPPING. 1995. CELL. 82 (1): 9.

10. ENGLANDER, S. W., N. R. KALLENBACH, A. J. HEEGER, J. A. KRUMHANSL, and S. LITWIN. NATURE OF THE OPEN STATE IN LONG POLYNUCLEOTIDE DOUBLE HELICES - POSSIBILITY OF SOLITON EXCITATIONS. 1980. In PROCEEDINGS OF THE NATIONAL ACADEMY OF SCIENCES OF THE UNITED STATES OF AMERICA-BIOLOGICAL SCIENCES. Vol. 77, 12 Edition, p. 7222.

11. Alexandrov, B. S., V. Gelev, A. R. Bishop, A. Usheva, and K. O. Rasmussen. DNA breathing dynamics in the presence of a terahertz field. 2010. PHYSICS LETTERS A. 374 (10): 1214.

12. Maniadis, P., B. S. Alexandrov, A. R. Bishop, and K. O. Rasmussen. Feigenbaum cascade of discrete breathers in a model of DNA. 2011. PHYSICAL REVIEW E. 83 (1): -.

13. Vafabakhsh, R., and T. Ha. Extreme Bendability of DNA Less than 100 Base Pairs Long Revealed by Single-Molecule Cyclization. 2012. SCIENCE. 337 (6098): 1097.

14. Bock, J., Y. Fukuyo, S. Kang, M. L. Phipps, L. B. Alexandrov, K. O. Rasmussen, A. R. Bishop, E. D. Rosen, J. S. Martinez, H. T. Chen, G. Rodriguez, B. S. Alexandrov, and A. Usheva. Mammalian Stem Cells Reprogramming in Response to Terahertz Radiation. 2010. PLOS ONE. 5 (12): -.

15. Alexandrov, B. S., K. O. Rasmussen, A. R. Bishop, A. Usheva, L. B. Alexandrov, S. Chong, Y. Dagon, L. G. Booshehri, C. H. Mielke, M. L. Phipps, J. S. Martinez, H. T. Chen, and G. Rodriguez. Non-thermal effects of terahertz radiation on gene expression in mouse stem cells. 2011. BIOMEDICAL OPTICS EXPRESS. 2 (9): 2679.

Publications

Alexandrov, B.. DNA Breathing Dynamics, Transcription, Protein-DNA Binding, and THz Radiation . Invited presentation at CINT User Conference, New Mexico, 2013. (Santa Fe, 24-26 September 2013).

Biomarkers for the 'Signature Wound' of Iraq and Afghanistan: Traumatic Brain Injury

Harshini Mukundan
20130802ER

Abstract

Traumatic Brain Injury (TBI) afflicts a significant percentage of US troops deployed in Iraq and Afghanistan, but is difficult to diagnose using current strategies. The ultimate goal of this project is to develop a rapid biomarker-based diagnostic for TBI in blood. However, this cannot be accomplished until a comprehensive repertoire of biomarkers secreted during brain injury if established. This requires an integrated biomarker discovery and detection approach, directly from human serum and cerebrospinal fluid. The 3-month project reported here is the first step in that direction wherein we aimed to develop two different methods for the discovery of novel biomarkers of TBI in blood and cerebrospinal fluid, as well as develop assays for two biomarkers on an ultra-sensitive waveguide-based platform that was developed at LANL. We were able to evaluate two different methods for biomarker discovery: MALDI mass spectrometry and 2 dimensional gel electrophoresis in serum samples. In addition to development of depletion protocols to remove abundant proteins in serum, we were also able to detect spiked TBI biomarkers using both methods. However, the results clearly show that for protein biomarkers, MALDI is much more sensitive than 2D gel electrophoresis. We also developed assays for two known biomarkers, procalcitonin and cardiolipin, using commercially available antibodies. Procalcitonin was detected using a sandwich immunoassay protocol. For detection of the amphiphilic cardiolipin that cannot be measured by conventional immunoassay strategies, we used the novel membrane insertion assay that was developed by our team. These assays demonstrate our ability to pull-down and detect biochemically diverse categories of biomarkers directly from human serum. Together, these studies have allowed us to garner significant preliminary data to demonstrate our capabilities to potential sponsors, to further build this project for real-world application.

Background and Research Objectives

TBI is the signature wound of U.S. soldiers deployed in Iraq and Afghanistan, and is broadly defined as any injury resulting from a blow to the head or penetrative insult capable of preventing brain function. While creation of mine-resistant ambush protected vehicles has definitely saved lives, incidence of TBI associated with rapid head movement and injury in the proximity of an explosion has greatly increased. The Pentagon estimates that 15,000 troops are afflicted with TBI, whereas the Brain Injury Association of America estimates the number at 360,0001. Part of the reason for this discrepancy is the lack of reliable diagnostics for TBI. TBI is a major concern for not just for deployed troops, but also children riding bicycles without head protection (~37,000/year), other accidents and injuries. Even as TBI affects ~ 2 million people/year in the U.S alone, there are no reliable tests for its diagnosis2. Indeed, the only tests used in the field are neuropsychological questionnaires such as the Automated Neuropsychological Assessment Metrics (ANAM)3. According to the congressional testimony of Lt. Gen. Dr. E. Schoomaker, results from ANAM are 'no better than a coin-flip', a clear testament to the need for better TBI diagnostics4,5. TBI causes a wide spectrum of pathological outcomes, potentially involving different forms of focal and/or diffuse damage, resulting from direct mechanical impacts to the brain parenchyma. In the human body, TBI induces a complex array of pathological conditions coupled with inflammatory responses. These responses result in the secretion of several biomarkers that can potentially provide a blood-based reproducible and quantitative diagnostic for TBI. Several potential biomarkers have been identified for TBI in blood: lactate dehydrogenase, neuron specific enolase, ubiquitin carboxyl terminal esterase-L1, Microtubule-associated protein-2, Tau protein, NR2 and GluR1 peptides, LRP1, vascular cellular adhesion molecule, IL-6, and cardiolipin. Inspired by the fundamental significance of lipids to the central nervous system, an oxidative lipidomics approach identified biomarkers like cardiolipin, F2-isoprostane,

thiobutyric acid and malondialdehyde as biomarkers of TBI. Despite this, there are no reliable biomarker-based approaches for the diagnosis of TBI. This is because of many reasons: 1) it is likely that no single biomarker can be a reliable diagnostic of brain injury in itself, and the use of a combination of biomarkers is necessary; 2) the timeline between the secretion of the biomarker in the cerebrospinal fluid (CSF) following brain injury and its appearance in blood has never been studied, 3) most studies have focused on one biochemical category of biomarkers, namely proteins, whereas it is likely that the magic bullet is completely varied in composition (sugar or lipid) and finally, 4) most of the work has focused on animal models of TBI (especially mice) whereas it is possible that biomarkers in humans are rather different than those in rodents.

Research Objectives: For these reasons, the quest for the biomarker(s) that can be the 'magic bullet' for diagnosis of TBI remains elusive. The ultimate goal of this proposal is to identify a comprehensive suite of biomarkers that can provide reliable diagnosis of mild to extreme TBI very shortly after infection. This reserve proposal is the first step towards achieving that ultimate goal, and the specific objectives of this reserve are:

Core Methodologies for Biomarker Discovery and Detection for TBI:

- Establish Institutional Biosafety committee and Institutional Review Board approvals to receive human cerebrospinal fluid (CSF) and serum (extension of existing protocol) form individuals with TBI. We already have a functional IBC and IRB for control human serum, and can commence that work from the initiation of the project.
- Establish best-practice method for sampling and storage of human CSF and sera to preserve the integrity of three potential biomarkers of TBI, namely cardiolipin, pro-calcitonin and microtubule-associated protein.
- Established methods and limit of detection for pull-down and detection of the three biomarkers mentioned above in control CSF and serum using 2D gel electrophoresis, membrane insertion (LANL strategy) and mass-spectrometry (DV, 3 months)6,7.

Detection of the Biomarkers in Serum and CSF:

- Establish multiplex assays (limit of detection, sensitivity and specificity) for the detection of the three biomarker on the waveguide-based biosensor platform developed at LANL.
- Validate assay performance in buffer vs. complex background.

Scientific Approach and Accomplishments

Our team has successfully completed and achieved almost all proposed objectives within a very short three month interval, as described here.

Documentation and Approvals

We have established all requisite approvals for doing this work (IWD, IBC and IRB). We also established contact with the University of California Brain Bank and requested CSF from 10 individuals (controls and concussion patients). However, this request takes 6-8 weeks to process and unfortunately, we were not able to receive CSF during the course of the reserve proposal. This is the only objective we were unable to address during this term. We performed all method and assay development on serum samples (Randox Laboratories).

Best practice methods for sample collection for cardiolipin and procalcitonin were established in serum. Four different methods: freeze thaw in liquid nitrogen, filtration, dialysis and protease inhibitor treatment were tried. Whereas the treatments did not affect the stability of procalcitonin positively or adversely, the recovery of cardiolipin was significantly decreased with filtration, dialysis and protease inhibitor treatment. Thus, rapid freeze thaw in liquid nitrogen was determined to be the best method to preserve the integrity of all biochemical categories of biomarkers.

Biomarker Discovery by 2D Gel Electrophoresis and Mass Spectrometry

Mass spectrometry and 2D gel electrophoresis methods were explored for biomarker discovery in serum. Cardiolipin and procalcitonin spiked serum samples were used to demonstrate the feasibility of these methods for biomarker discovery. Because of the abundance of several major proteins (e.g. albumin, -antitrypsin, transferrin, haptoglobulin) present in serum, these abundant proteins had to be depleted before any further analysis could be done. We used an ion-exchange based Abundant Serum Protein Depletion kit (Norgen Biotek, Ontario, Canada) to deplete these abundant proteins. The sera were first either spiked with cardiolipin and procalcitonin at various concentrations and then the spiked samples were processed for abundant protein removal. The samples were then acetone precipitated to concentrate the samples and to remove the eluted buffer. After that, the samples were analyzed by mass spectrometry and 2D gel electrophoresis (2DE) methods.

For 2DE method (Figure 1), the samples were rehydrated into the appropriate buffer, electro-focused on a 11 cm, pH 3-10 immobilized pH gradient strip (Protean IEF System, BioRad) to separate the molecules according to their isoelectric point, and then loaded onto 4-16% Tris-HCl SDS-PAGE gels to separate the molecules according to

their mass size (Criterion Cell, BioRad). The 2DE results are show in Figure 1. By comparing the 2DE images of the non-depleted human serum gel versus the depleted procalcitonin spiked human serum gel, we were able to detect the spiked procalcitonin (MW = 12,876 daltons, pI 5.31) at a concentration of 443 nM. We could not detect the spiked procalcitonin at lower concentration (87 nM) nor could we detect the spiked cardiolipin (23 M) in the serum samples. In addition, we were also able to observe the reduction of albumin, antitrypsin, transferrin, and haptoglobulin in all the depleted samples.

For the mass spectrometry method, the precipitated sample were re-suspended into the appropriate buffer, trypsin digested to generate small peptide fragments, ran through a C18 liquid chromatography column to do a broad separation of the fragments, and analyzed via a matrix-assisted laser desorption/ionization mass (MALDI) spectrometer. With this method we were able to detect the procalcitonin at the lower concentration (87 nM). As with the 2DE results, we also observed a reduction in the four abundant serum proteins in the depleted serum samples when compared with the non-depleted serum sample. Due to time constraints we were unable to test the spiked cardiolipin serum sample with this method.

Overall, we have demonstrated some promising results in using these two methods for biomarker discovery in sera. However, improvements can be made to increase the sensitivity of our methods. It appears that mass spectrometry is more sensitive for the detection of procalcitonin than 2D electrophoresis. However, this is a 'home-brewed' system that we generated with minimal resources, and we anticipate sensitivity enhancement with commercial systems for the full-fledged effort. Also, 2D is likely to be more efficient for proteins with different charge distribution, some of which have been suspected to be unregulated during TBI. Some of the things we can try in the future could be: 1) better depletion of abundant proteins with immune-affinity columns, 2) better protein separation by using narrower linear IPG strips (e.g. pH 4-7) or longer length IPG strips and larger SDS PAGE gels, 3) better staining methods (e.g. silver staining), and 4) labeling methods (e.g. iTRAQ) for the mass spectrometry and 5) enhancement of sensitivity of detection by pre-concentration methods.

Detection of the Biomarkers in Serum and CSF

For all waveguide-based assays, the waveguides and coverslips were freshly cleaned by sonication in chloroform, ethanol, and water (5 min in each solvent), drying under argon, and exposure to UV/ozone. A flow cell was constructed using a coverslip and waveguide sandwiching a 0.5 mm gasket with a flow channel cut into the center. A solution containing sonicated unilamellar vesicles of DOPC with 1% cap-biotinyl-DPPE was injected into this flow cell. After overnight incubation, the flow cell was washed to yield a supported lipid bilayer (SLB) membrane. The membrane was blocked for 1-4 h with 2% BSA/PBS, then rinsed with 0.5% BSA/PBS. Rinsing with 0.5% BSA occurred between all subsequent steps. The flow cell was assembled into the plastic holder of that we use to interrogate the assay, and the optical methodology was carried out as previously reported .

To analyze for procalcitonin, we utilized a sandwich immunoassay format on the waveguide-based optical biosensor8. AlexaFluor 647-labeled streptavidin (50 pM) was added to the flow cell to assess membrane/surface integrity; a strong signal (red trace) indicated that the surface was intact. This signal was photobleached, and streptavidin (10 nM, 5 min) and biotinyl-anti-procalcitonin monoclonal antibody (20 nM, 30 min) were added. Fluorescence was again recorded (green trace) to ensure no contamination with fluorescent species was present. Non-specific binding was assessed using AlexaFluor 647-labeled anti-procalcitonin polyclonal antibody (AF-pAb, 20 nM, 30 min, purple trace). The non-specific signal was photobleached, and procalcitonin (1 nM) was incubated at room temperature for 4 h. Another aliquot of the AF-pAb was added (30 min), and the signal was recorded (pale blue). We noted a ~20:1 specific/non-specific binding ratio, indicating successful detection of 1 nM procalcitonin, and possible detection of much less (Figure 2). The "corr" (corrected) values indicate that the spectra were recorded using a 300 ms integration time rather than the typical 3000 ms integration time due to the limited scale of the spectrometeter (4000 counts), and then corrected by excel. The sensitivity of this assay can be enhanced by longer incubation times and by using a combination of antibodies for the detection (preliminary data, not shown here) that exploit the surface avidity effect of the binding.

We also developed a membrane insertion assay for Cardiolipin, which is based on the direct integration of the molecule to the surface. Again, the sensitivity of this direct detection is poor but we suspect this is because the lipidic chain of cardiolipin is truncated in the commercially available materials, and this integral to membrane insertion. Cardiolipin is secreted fully in the host, and therefore, we suspect that assay sensitivity will be superior in real-world samples, and extracted cardiolipin.

Impact on National Missions

Traumatic brain injury is the signature wound of Iraq and Afghanistan. There are currently no reliable diagnostics for mild Traumatic Brain Injury, and it remains a very high priority for the Department of Defense, as is evidenced by

the congressional testimony of the Surgeon General of the USA in 2012. This work addresses this key gap and has developed key capabilities in this area, which are now being explored for further development using external sponsors.

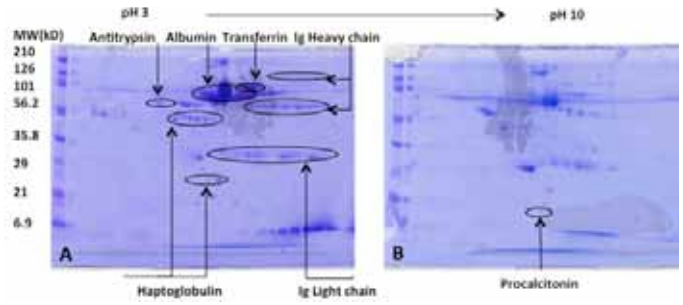

Figure 1. 2DE images of non-depleted human serum (A) and depleted and procalcitonin spiked human serum (B).

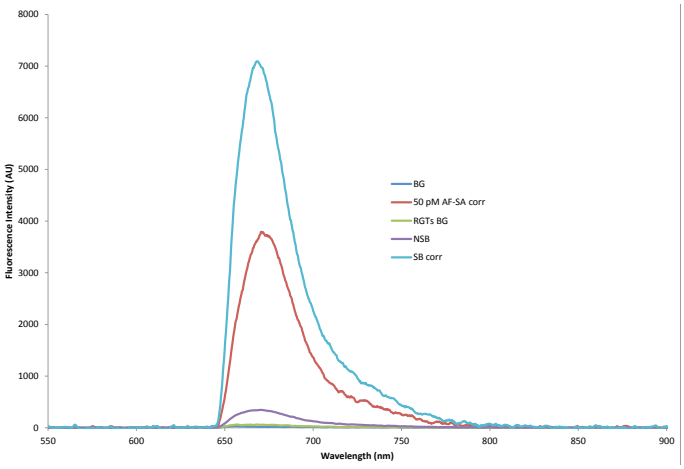

Figure 2. Detection of procalcitonin using the waveguide-based biosensor platform. The specific signal (pale blue) is 20X greater than the non-specific signal associated with the antibody (purple trace). The red line represents binding of AF647 labeled streptavidin to the biotinylated surface, proving membrane integrity. The green line is a measure of the waveguide-associated background. The data are corrected for use of a 10X attenuation filter (see text).

Publications

Anderson, A. S., D. Vu, and H. Mukundan. Biomarkers for Traumatic Brain Injury. To appear in Japan Society of Applied Physics and Materials Research Society, Joint Conference. (Kyoto, Japan, 17-20 Sep. 2013).

Determining Physiological Predictors of Climate-driven Forest Mortality

Nathan G. Mcdowell
20110756PRD4

Introduction

We propose to determine which, if any, common physiological responses during heat and drought-driven mortality exist at a global scale, and thus determine the simplest but strongest predictors of tree mortality across different species of trees. The experiments to determine these common predictors will be conducted on trees of multiple scales; from seedlings to >100 year old trees. Through the process, we will identify the final steps in mortality and survival, allowing modelers to simplify not only their prediction of stress but of the key aspects of plant physiology that partition plants between survival and death during drought. The final product(s) will identify the simplest, most common, and statistically strongest environmental and physiological predictors of mortality, and interpretation of their mechanisms.

Benefit to National Security Missions

The goal of this research will be to develop a bridge between physiology and modeling by identifying the simplest level of detail needed to predict tree drought mortality across multiple forest types. This work directly supports DOE's Climate and Environmental Science Division goals to understand the role of terrestrial ecosystems in a changing climate and is intended to promote long-term programmatic growth in this arena. Specifically the products of this research will be directly tailored for incorporation into DOE's Community Land Model. Addressing this key gap for coupled vegetation-climate models could lead to the rapid development of more accurate global change projections that are urgently needed to inform sound climate policy at a global level.

Progress

In the past 12 months Dr Adams has been amazingly productive. He has collected all of the data for at least two manuscripts from a field experiment at LANL examining forest mortality, which he is now putting together into manuscript format. He has also initiated data collection for a meta-analysis of forest mortality patterns. This collection is being done via networking with a large number of scientists. More than two-thirds of the data is now in Dr Adam's possession. Lastly, Dr Adams is working closely with our modelers to learn from them the key aspects for modeling mortality and to feed them information regarding how to model tree death. This is a component of a follow on paper that Dr Adams is working on. Dr. Adams is well on his way to a very productive career at Los Alamos.

Future Work

Dr. Adams will continue to collaborate with EES staff, post-docs, and students who are working on the Los Alamos Survival Mortality (SUMO) project to collect data on key physiological responses to drought through mortality in pinyon pine and juniper trees. Dr. Adams will continue to lead two sampling efforts at SUMO: 1.) to monitor stressed trees for insect attack and characterize tree defensive capabilities against insects at this experiment; 2.) repeated measurement of inherent hydraulic vulnerability to assess if functional tree water stress relationships change with drought and increased temperature. Dr. Adams will continue a SUMO supplemental experiment initiated in FY13 aimed at distinguishing the physiological threshold of survival and mortality using transplanted trees in the greenhouse at TA-51. The protocol of this experiment will be to drought stress sets of trees to hypothesized thresholds of survival, and then re-water these trees, measuring physiological responses and critically, whether the trees ultimately die or survive when re-watered. This experiment is aimed at elucidating the simplest key thresholds between tree mortality and survival that can be incorporated into mechanistic and predictive models of tree mortality. These data will inform ongoing modeling efforts by EES staff to address DOE's Climate and Environmental Science Division goals to understand the role of terrestrial ecosystems in a changing climate. Specifically, data from this experiment

will be used to parameterize tree mortality routines in DOE's Community Land Model.

Conclusion

Dr. Adams will develop a bridge between physiology and modeling by identifying the simplest level of detail needed to predict tree drought mortality across forest types. This work supports DOE's Climate and Environmental Science Division goals to understand the role of terrestrial ecosystems in a changing climate. Specifically the products of this research will be directly tailored for incorporation into DOE's Community Land Model. Addressing this key gap for coupled vegetation-climate models could lead to the rapid development of more accurate global change projections that are urgently needed to inform sound climate policy at a global level.

Publications

Adams, H., and e. al. Empirical and process-based approaches to climate-induced forest mortality models. To appear in Frontiers in Plant Science.

Adams, T., and e. al. Nonstructural leaf carbohydrate dynamics of Pinus edulis during drought-induced tree mortality reveal role for carbon metabolism in mortality mechanism. 2013. New Phytologist. : 1142.

Breshears, D., H. Adams, and e. al. The critical amplifying role of increasing atmospheric moisture demand on tree mortality and associated regional die-off. . 2013. Frontiers in Plant Science. 4: 266.

Franz, T., and e. al. Ecosystem-scale measurements of biomass water using cosmic ray neutrons. . 2013. Geophysical Research Letters. : 3929.

Zeppel, M., and e. al. Forest mortality due to drought: latest insights, evidence and unresolved questions on physiological pathways and consequences of tree death. 2013. New Phytologist. : 372.

Catalytic Mechanism and Inhibition of Metallo-beta-lactamases (MBL), the Ultimate Threat Against Antibiotics

Suzanne Z. Fisher
20120776PRD4

Introduction

The proposed work will utilize an innovative research strategy that is LANL-unique for novel antibiotics. We will combine neutron and X-ray diffraction to obtain high resolution structures and detailed information on how metallo beta-lactamases (MBLs) work to degrade clinically used antibiotics. Due to their readiness for horizontal transfer and evolution, MBLs entail a serious public health threat, with increasing antibiotic resistance found all over the world. Results will have direct implications for not only understanding how these enzymes work, but also to enable the design of clinically useful antibiotics not susceptible to breakdown by these harmful enzymes.

Benefit to National Security Missions

Metallo betal lactamases comprise a serious human health issue due to the innumerable complications associated with untreatable infections caused by some of the most dangerous bacteria present in clinical settings and intensive care units. This work, which can only be performed at LANL's world-class facilities, will provide the first neutron structures for antibiotic resistance enzymes found in multidrug resistant pathogens. This work will advance our basic understanding of enzyme mechanisms and drug binding. Neutron diffraction is underutilized for drug design and is the only technique that can give unique data on drug binding and degradation. This work may lead to novel compounds that will have an enormous impact on human health and disease.

We also envision a scenario where detection methods can be developed to find bacteria expressing resistance genes in the environment. This work directly addresses mission relevance in the fields of basic health research, bioscience, and pathogen detection.

Progress

Javier was able to obtain high quality clones of two different metallo-beta-lactamases, BcII and NDM. These seems to express well and having enough protein is the first crucial step for neutron studies. We were also able to crystallize one of these enzymes, BcII, at pH 7, which is more physiologically relevant than other reported structures at pH 4.5 and 6.

For NDM, the enzyme found in deleterious antibiotic-resistant pathogens, we designed and produced two double mutants that is unable to bind the second catalytic zinc in the active site. Instead we have populated these sites with alkaline earth metals magnesium and calcium. This allows us to bind antibiotics in the active site, but stops hydrolysis and allows us to study the binding mechanism. We are also optimizing conditions for large crystal growth for neutron studies of these variants.

To study the basic binding interactions and to investigate new possible lead compounds, we have co-crystallized sulfonamide drugs with both BcII and NDM. We are working on determining X-ray crystal structure to confirm binding. In progress also is co-crystal structures of BcII and NDM in complex with Aztreonam, the only known antibiotic that is still able to resist hydrolysis by these enzymes.

We are ready to progress to the next phase, the in vitro evolution of NDM to determine which active site mutations confers the ability to hydrolyze Aztreonam. This will deliver an early detection system for real world diagnostic application. We are working on permission and authorization to perform this work in a Biosafety Level 2 lab.

Future Work

For the second year, we are working towards determining X-ray and neutron structures of BcII and/or NDM-1 (wild type and mutants) with different active site metals. We have designed the appropriate expression plasmids

and have made enzymes with non-native metals in the active site. This will allow binding of antibiotics, but will prevent hydrolysis allowing us to study the binding interactions with the enzyme.

We will also pursue complexes with existing antibiotics to investigate binding and the enzyme residues that are involved with catalysis. Neutron crystallography, which will shed light on the H-bond networks in the active site, will facilitate this detailed investigation of drug binding and involvement of water activation.

We are pursuing sulfonamide-based drugs as lead compounds and are making complexes between these drugs and BcII and/or NDM-1. Sulfonamides are known to bind to other Zn-containing enzymes and we will pursue them here also.

Conclusion

We will characterize the enzyme NDM-1: (1) Water activation, (2) Substrate binding, (3) In vitro evolution. (1) we will solve the structure of NDM-1 through neutron crystallography, which will shed light on the H-bond networks in the active site. (2) we will engineer NDM-1 to enable binding alkali earth metals in the second Zn(II) site. This will eliminate enzyme activity while retaining substrate binding for structural analysis. (3) we will construct NDM-1 mutant libraries, which will be screened for resistance to monobactams. Mutants will be selected and analyzed to understand the structural traits of enzymes with broad substrate preferences.

Single Cell Genomics for Better Control of Plant Pathogens

Shunsheng Han
20130779PRD1

Introduction

The proposed research will use the rhizosphere-colonizing bacterium Pseudomonas chlororaphis strain 30-84. The strain is able to inhibit fungal pathogens and has become a model for a beneficial commensal bacterium. This strain demonstrates phenotypic variation resulting from spontaneous mutations. The goal of this research is to identify signature genomic and transcriptomic changes in response to environmental signals and investigate how these changes benefit the wild type populations using a plant associated bacterial as example.

Benefit to National Security Missions

The understanding of the relationship between plant and bacteria is directly linked to the DOE mission in the area of bioenergy. LANL, supported by DOE, has invested significantly in studying plant metabolism and algal biofuel. This work will enrich our portfolio in these areas and bridge the gaps between environmental microbiology and plant study.

Progress

The postdoc fellow Dongping Wang started on June 10, 2013. For the last 17 days, he has completed many required training courses including the General employee training. Many other trainings such as biosafety and laser training have been scheduled in July and August. Some experimental materials have arrived at the lab. Bacterial strains will be shipped from Texas A&M University once they are approved by the Institutional Biosafety Committee at Los Alamos National Laboratory.

We made an experimental plan for next fiscal year and will perform the following experiments to fulfill the aims of the proposed research:

- To identify mutational events during P. chlororaphis rhizosphere colonization, bacterial cells will be inoculated on plant roots. Bacterial spontaneous mutants will be isolated by both visual observation and flow cytometry sorting.
- Bacterial genome sequencing will be performed in Dr. Cliff Han's lab using the cutting edge sequencing platform and gel microdroplet culturing technology. Mutational events will be identified by comparing to a published wild type P. chlororaphis genome.
- To understand the roles of these genomic changes in bacterial persistence, mutant strains will be compared with the wild type to determine their ability to control fungal pathogens and form biofilms.
- We will also perform transcriptomic analysis to identify differentially regulated genes in the mutants compared with the wild type. Selected target genes will be further investigated using functional genomics tools such as gene deletion and over-expression.

These studies will provide a comprehensive view of bacterial genomic changes/cell differentiation during host association. The results will aid in designing new strategies in plant disease control.

Future Work

We will perform the following experiments to fulfill the aims of the proposed research:

- To identify mutational events during P. chlororaphis colonization, bacterial cells will be inoculated on plant roots. Flow cytometry will be used to determine the bacterial size and sort them into different groups.
- Single cell genome will be sequenced using gel microdroplet culturing in Dr. Cliff Han's group. Beneficial mutations will be identified by comparing with a published wild type genome sequence. These results will provide us with a complete set of mutations that are involved in host association.

- To study the role of these genomics changes in bacterial persistence, beneficial mutants will be compared with the wild type strain in their ability to produce fungal-inhibiting metabolites and form biofilms.
- Genomic mutations may lead to changes in gene expression. To understand the beneficial mutation at the transcriptome level, RNA sequencing will be conducted to identify differentially expressed genes between wild type and beneficial mutant strains. Together, these data will give us a comprehensive understanding of cell differentiations in response to environmental signals.
- The above analysis will identify candidate genes involved in disease control. Selected genes will be investigated using functional genomic approaches.

Conclusion

We expect to identify mutational events during P. chlororaphis colonization, to classify and identify the beneficial mutation that are involved in host association. We will also identify the role of these genomic changes in bacterial persistence. Understanding of molecular processes involved in bacterial adaptation could lead to better disease management strategies.

Publications

Wang, D., C. Han, C. Lo, A. Dichosa, P. Chain, J. M. Yu, L. S. Pierson, and E. A. Pierson. Genomic adaptations of a small colony variant (SCV) in the biofilm of Pseudomonas chlororaphis 30-84. Genome Biology and Evolution.

Joint Inversions of Seismic and Gravity Data in Volcanic Areas to Advance Hazards Assessment: A Focus on the Alaskan Subduction Zone and Kilauea, Hawaii

Monica Maceira
20130807PRD3

Introduction

Three-dimensional passive-source seismic velocity tomography is a powerful technique that utilizes energy produced by earthquakes to image potentially complex subsurface structures, such as magma distributions beneath volcanoes or subducting slabs. However, the resolution of these studies are generally limited by the natural distribution of earthquakes. While active sources can expand coverage, they are generally only used to image the upper crust and are costly. Gravity data, however, provide alternate sources of information regarding subsurface structures, and are available at a variety of scales. Due to the inherent relationship between density and seismic velocity, gravity and seismic data can be jointly inverted, providing an understanding of Earth structures that is not limited by the distributions of seismicity and has stronger constraints on the temperature, compositional, fluid, and magmatic distributions in a study area.

The current distribution of seismic stations in Alaska is focused near the relatively two-dimensional volcanic arc located above the subducting oceanic plate, limiting the ability to resolve its seismic structure. The inclusion of gravity data in a joint inversion will markedly increase the ability to resolve these features in three dimensions. I will address questions regarding the sources of volcanism in the Alaska subduction zone.

Kilauea Volcano presents a unique opportunity to study one of Earth's most active volcanoes, in a location that has produced historical tsunamigenic earthquakes. While previous seismic studies have focused on studying the near-surface beneath the summit caldera, portions of Kilauea's rift zones, or the seismically active tsunamigenic decollement fault beneath the volcanic material and the underlying oceanic crust, the extents of these studies are limited by the natural seismic distributions. By combining gravity and seismic data, I will address questions such as "Can the aseismic and seismic portions of the decollement be imaged, constraining the maximum magnitude of earthquake this fault can produce?"

Benefit to National Security Missions

The proposed research will enhance the capability of the Laboratory through unique expertise in imaging Earth structure. This expertise has applications to Nonproliferation R&D under Nuclear Nonproliferation, where accurate Earth models are needed to locate, identify and determine yield for seismic events of interest such as underground nuclear explosions. High-resolution Earth models are also required for characterization and monitoring within several other areas of LANL mission space including geothermal energy development (Applied Energy Programs Office) carbon sequestration (Fossil Energy, within the Office of Science Programs), and used fuel disposition and salt repository science (both within the office of Civilian Nuclear Programs).

Progress

This project had just started at the time of this report; therefore, there is no progress to date.

Future Work

I will simultaneously invert two different data types to derive the Earth's 3D velocity structure beneath the Alaska subduction zone and the Kilauea volcano, Hawaii. Seismic data will come from local, regional, and national networks and deployments, while gravity data will come from US satellite missions as well as in-land measurements. The research paths will be as follows: (1) develop code for efficient and robust multi-parameter inversion, (2) gather and pre-process the different data types, and (3) perform multi-parameter inversion to produce a validated high resolution high accuracy 3-D velocity image of the Alaska subduction zone and the Kilauea volcano, Hawaii.

The first year, focus will be on code development and

the Kilauea volcano, Hawaii, where seismic and gravity data are readily available. The expansion of USArray seismic stations to Alaska in the coming year will allow seismic models to be significantly improved during the second year of this project.

Conclusion

The expected results from the research are: I. Development of the next-generation method for imaging the 3-D structure of the Earth and, II. A high-resolution high-accuracy 3-D velocity im-age of the crust and upper mantle beneath the Alaska subduction zone and the Kilauea volcano. I expect to submit two papers to high-impact journals, one for each of the regions of interest, and addressing the scientific questions stated in the abstract.

Analysis of Protein Structure-Function Relations in Antibiotic Biosynthesis and Signal Transducing Receptors

Louis A. Silks III
20100603PRD2

Abstract

The vast majority of known antibiotic, chemotherapeutic, anti-viral, anti-inflammatory, analgesic, and immunosuppressant agents are natural products. However, only a marginal number of bioactive compounds from diverse sources of natural products have been explored even though they provide an incredible potential for the development of new drugs. Natural products or secondary metabolites are compounds with diverse bioactivity that are isolated from natural sources and are biosynthesized by large multi-functional enzymatic clusters in diverse bacteria, fungi and plants and represent the major source for all drugs and drug leads available to humans. Genetic and enzymatic studies provided insight of isolated enzymatic functions, but have not led to strategies for the discovery of novel natural products. Bioinformatics and structural biology studies are giving rise to three-dimensional folding and selective protein-protein recognition processes of key proteins involved in the biosynthesis of medically relevant natural products. This knowledge is the base to understand the spontaneous self-assembly of multifunctional protein clusters that biosynthesize natural products. Once understood, these biosynthetic complexes can then be engineered to give rise to produce new classes of highly specific and more potent drugs with fewer side effects or novel assembly lines can be efficiently identified in nature, their products predicted and novel drug leads identified.

To elucidate structures and structural complexes, Dr. Koglin spent part of his time making stable isotope-enriched proteins for structural studies. Expertise in biochemistry, synthetic chemistry and biophysics enables the design of labeled amino acids and to place them specifically into proteins improving the structural resolution of very large biological systems. Proteins of interest are studied by Nuclear Magnetic Resonance (NMR) spectroscopy, which is the only method to gain understanding of the structure and functional dynamic of these proteins. This gained knowledge translates to a detailed understanding of complex self-assemblies and the identification of novel drug leads.

Background and Research Objectives

The discovery and first direct correlation of antibacterial properties with a natural isolate from Penicillium chrysogenum in 1928 founded modern medicine. At the time of discovery, neither the chemical structure, biochemical process of activity or the biosynthetic route used by the producing fungus was understood. It took over 60 years to elucidate the biosynthesis of L-aminoadipyl-L-cysteinyl-D-valine (LLD-ACV), the penicillin and cephalosporin precursor. The basic genetic understanding of this biosynthetic system has been applied to discover many more antibacterial compounds. But reliance on similar biosynthetic mechanisms has resulted in the isolation of chemically similar compounds often as □-lactams and lactones or of other drugs with similar mechanisms of action and cellular targets. This similarity of current antibacterial compounds contributed to the recent, accelerating emergence of antibiotic resistance and significantly reduced the availability of effective antibiotic treatment options. Bacterial infections have once more become the third leading cause of death in United States, a major public health threats, and our ability to fight bacterial infections is increasingly problematic. Consequently, an in-depth understanding of the biosynthetic machineries and pathways that assemble chemical structural features in vivo are critical to the discovery of new biosynthetic clusters that may include not-yet described processing steps to produce novel secondary metabolites.

Biosynthetic processing by Non-Ribosomal Peptide Synthetase (NRPS) multi-functional enzymatic complexes is accomplished as a series of covalently tethered thioesters similar to fatty acid and polyketide biosynthesis. In each chain-elongating condensation, the growing NRP acyl chain participates as an electrophilic partner, undergoing attacks at the acyl thioester carbonyl while the monomer, to be incorporated, acts as a nucleophile.

For NRP chain elongation, the downstream nucleophile is the amine of an aminoacyl-S-peptidyl carrier protein (PCP) with which it forms amide or peptide backbone linkages. Carrier domains in general require post-translational modification with a phosphopantetheine (4'-PP) prosthetic group whose terminal thiol function (HS-4'-PP) becomes the site of covalent tethering of the growing acyl chains. They are often referred to as thiolation or T domains to emphasize that functionality. NRPS clusters occur either as distributed assemblies, each catalytic domain on a separate protein (Type II), or catalytic and carrier domains that are strung together into one or more functional modules within a single polypeptide chain. These multi-modular assembly lines are termed Type I. The most common organization of NRP synthetase assembly lines is the Type I pattern, exemplified by aminoadipyl-cysteinyl-valine (ACV) synthetase. The ACV assembly line contains a three-module, ten-domain, 480-KDa single subunit polypeptide and represents the first step in penicillin and cephalosporin biosyntheses. In Type I NRP synthetases, a T domain is embedded in each module, servicing in cis (domains of one protein) adjacent catalytic domains. The chemical logic and enzymatic activity of isolated functions of natural product assembly lines are now fairly well deciphered. This logic includes: (1) enzymatic priming of the apo form of a T domain by a phosphopantetheinyl transferase (PPTase) to install the active thiol function and the 4'-PP cofactor on a carrier protein so that covalent acyl/peptidyl chain growth can proceed; (2) selection and ATP-dependent activation of monomeric building blocks to allow chain initiation catalyzed by adenylation domains (A domains); (3) chain elongation that is mechanistically coupled to translocation of the activated substrates leading to amide or peptide bond condensation in the C domain; and finally, (4) termination of the process which is performed by a thioesterase (TE) domain as the most downstream enzymatic function. TE domains may be hydrolases, reductases, or regiospecific macrocycle-forming catalysts and they act to release the nascent product from the assembly line. A vast variety of tailoring enzymes can modify the peptide chain. By gaining insights into the genetic organization, biosynthetic logic, and structural recognition of these assembly lines, we can characterize the catalytic processes.

Still, very little is known about protein-protein interactions, substrate recognition processes, or the assembly order of isolated enzymes and modules that define the biosynthesis of secondary metabolites. This lack of fundamental knowledge makes it extremely difficult to predict the structure of secondary metabolites produced by large mega-enzyme clusters, such as antibiotics, solely based on their genetic encoding. The current development strategy needs to be re-imagined to identify new and effective drug candidates.

The aim of this project is (1) to develop methods that allow high-resolution structural studies on very large proteins and protein assemblies and (2) further the structural and functional elucidation of enzymes and assemblies of those biosynthetic systems as a crucial requirement for (3) the directed identification of novel drug leads. This research leads to understand the underlying logic of protein cluster assembly in general and to reveal the mechanism of natural product biosynthesis.

The overarching goal is to confront the accelerating development of antibiotic resistance. Dr. Koglin focuses on the biosynthesis of new natural products with novel chemical properties (chemotypes). Those have the potential to be developed into highly effective antibacterial treatments while being immune to current resistance mechanisms.

Scientific Approach and Accomplishments

Dr. Koglin has solved the largest protein structure in solution by NMR spectroscopy, using his own technologies. This record achievement has held for several years. Now, Dr. Koglin has applied novel methods of combining selective isotopic enrichment and NMR spectroscopy at Los Alamos National Laboratory to further push the current technology and enabled larger biological macromolecular assemblies to surrender their structures in high resolution. The results of the successfully completed project are now applied to build strong collaborations with Harvard Medical School and Massachusetts Institute of Technology at the Francis Bitter Magnet Laboratory. Scientists of Los Alamos National Laboratory are a key contributor in efforts to study large protein assemblies and membrane protein structures, dynamics and functions. Dr. Koglin has obtained the first structure of a C-domain by NMR spectroscopy (Figure 1). This is an important step to establish methods to study structures and dynamic of very large proteins and to gain insight into essential biosynthetic processes of bioactive compounds, which directly impacts the ability to identify effective antibiotics. So-called condensation (C) domains perform an essential and generally common step in natural product biosynthesis. They catalyze the peptide bond formation in all compounds that are derived from non-ribosomal peptides. The high-resolution NMR structure is again the largest structure of its kind and studies of enzymatic active protein complexes provide a detailed understanding of their function and substrate recognition processes for the first time. Despite a previously published complex enzymatic mechanism, we found that C domains are allosteric controlled and their structural dynamic limits space within the active site and the peptide bond is formed by chance between two activated amino acid residues. Since the peptide bond has a lower energy compared to thioester activated amino acid residues, this process

is not reversible. This finding is absolutely crucial for the biotechnological design of systems synthesizing novel engineered drug leads, since no complex catalytic cascade must be reconstructed for peptide bond biosynthetic steps. In addition this knowledge and methods enable (1) to block the biosynthesis of bacterial and fungal toxins, (2) to understand a family of proteins in the development of antibiotic resistance, (3) and to understand the drug niacin and its binding to what is called GPCR. This could give rise to alternative treatment of type II diabetes.

Dr. Koglin further applied the gained knowledge of structures and protein complexes to identify and initiated the characterization of a complete new class of natural products with antibacterial properties and developed a new approach to determine the cellular target of a novel compound or any given drug. Each of the identified novel natural products demonstrates confirmed broad-spectrum antibacterial activity and neither have been described in the literature or deposited in any database. These glycopeptides are produced by Non-Ribosomal Peptide Synthetase (NRPS) assembly lines from divergent species. However, they show structural similarity and possess a novel common chemotype. Preliminary antibacterial efficacy results and promising toxicology studies, validated externally, suggest that we have identified a new class of antibiotic compounds that act on an entirely new bacterial target. We further validated antibacterial efficacy, including against multi-drug resistant Staphylococcus aureus and Clostridium difficile. We initiated cytotoxic profiling on human cell-lines and small animals. The studied compounds show very low toxicity and single doses of up to 80mg/kg body weight are tolerated. This offers a wide therapeutic window. We elucidated the cellular target and currently establish the mechanism of action. As it turned out, these novel antibacterial drug candidates inhibit the assembly of the bacterial ribosome on mRNA and effectively prevent the biosynthesis of proteins in bacteria.

Initially, we have discovered a unique non-ribosomal peptide synthetase (NRPS) cluster for the biosynthesis of an unusual, novel secondary metabolite in the sequenced genome of a hyper-thermophile anaerobic bacterial strain. We purified the predicted secondary metabolite from the cultured producer strain and identified all the enzymatic functions of the proteins associated with this novel NRPS assembly line by in vitro assays. For this first example, we have identified the chemical structure as a glycopeptide and identified its biosynthetic pathway (Figure 2). This type of secondary metabolite is highly unusual. We have further linked the novel and unique enzymatic functions of the biosynthetic pathway to the structure of the isolated compound. In addition to a freestanding type II NRPS activation-and-carrier di-domain, this assembly line contains a short type I NRPS consistent with a second activation domain, one condensation domain for the synthesis of a cytosolic di-peptide, a thioesterase domain, and a C-terminal membrane-inserted export protein. An associated cytoplasmic glycosyl-transferase is responsible for decorating and bridging the short peptide during the precursor biosynthesis. After hydrolysis off the assembly due to the thioesterase and presumed N-C bond formation at the anomeric center of the first sugar moiety, the C-terminal membrane transport domain immediately exports the precursor. The precursor is never released into the cytoplasm and its processing is continued within the periplasmic space by a second glycosyl-transferase to form a disaccharide and a copper-amine-oxidase responsible for converting an amine into an aldehyde function. Both are membrane-bound and located in the periplasmic space, outside the cytoplasm. As a consequence, the functional organization of this assembly line spans the cytoplasm membrane and the biosynthesis of the identified compounds is subdivided. While precursors of the matured products are synthesized inside the cell, the final assembly of the bioactive secondary metabolites is located outside the cell. Since we could not identify an encoded resistance mechanism in the genome of the producing strain, this suggests that the bacterial toxicity profile of this secondary metabolite requires that the compound be not to be released inside the cell. We assume that the host itself is susceptible to its own metabolite based on the organization of the biosynthetic pathway that assembles cytoplasmic precursors in the periplasm. This also suggests that the evolution of antibiotic resistance against this compound may not be easily accomplished. We discovered the first and never before described split or fragmented biosynthesis of a secondary metabolite.

Based on our initial results, we identified a second example of a similar biosynthetic complex that incorporates a membrane-transport domain and extra-cellular maturation of a secondary metabolite. This second example is also involving a second glycosyl-transferase and an oxidative enzyme system to generate an aldehyde function. Compared to the identified first example, isolated from a hyper-thermophilic we found this second example in the genome of an aerobic cold lake bacterium. The living environments or ecological niches of both producer strains could not be more different. Recently, we identified and purified additional three and novel natural products, beside the two described examples. We elucidated their chemical structures by NMR spectroscopy and continue to develop purification methods to produce pure material for antibacterial efficacy and cytotoxic assays.

Impact on National Missions

This project supports the DOE mission in biological sciences and biosecurity by enhancing our understanding of how cellular processes work in tandem to form natural products of high biomedical value. We build capabilities for every agency that has a health mission, including HHS, DoD and DHS.

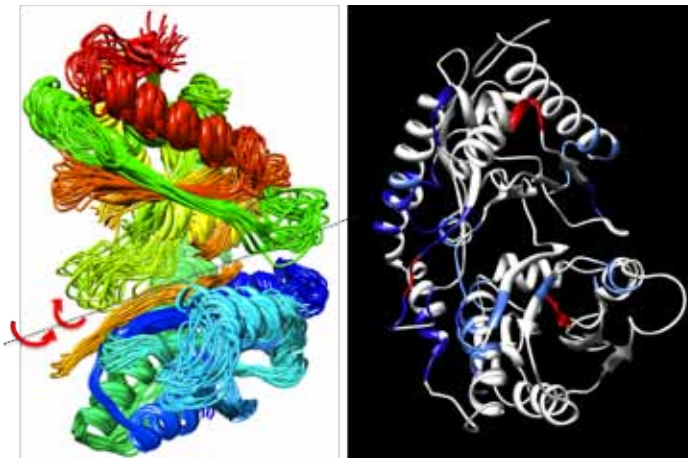

Figure 1. High-resolution structure of a condensation domain. The left image represents the structural bundle of the NMR structure calculation selected by lowest energy values. The RMSD is 1.2Angstrom and the structure is shown from N-terminus in blue to C-terminus colored red. At this resolution, dynamic and functional studies reveal the selective interaction and substrate recognition processes. The right panel shows the result of substrate recognition and binding shown in blue. Single amino acid residues responsible for the allosteric controlled structural dynamic causing the 'grinding' movement of the upper and lower half of the enzyme (red arrows in left panel) is shown in red.

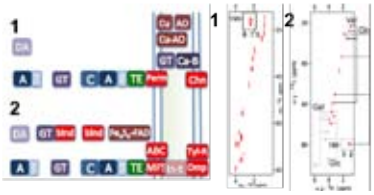

Species	ATCC	DMSO extract (µg/ml) #1	DMSO extract (µg/ml) #2	EtOAc extract (µg/ml) #1	EtOAc extract (µg/ml) #2
S. aureus	33591	>128	128	32	16
S. enterica	14028	128	128	32	16
K. pneumoniae	43816	N/A	N/A	16	8
H. influenzae	49247	2	1	0.5	<0.125
S. pneumoniae	49619	64	16	16	8
C. difficile	70057	64	16	32	16

Figure 2. Biosynthetic assemblies of novel natural products. The graphic presentation of first discovered split assembly line (labeled '1') that produces novel antibacterial compound reveals its uniqueness. While precursors are assembled in the cytoplasm, the final processing and maturation is located in the periplasm. Number '2' shows the graphic presentation of the biosynthetic cluster of the second identified and characterized natural product. Though the biosynthesis is entirely different, the produced compounds are chemically very similar as shown in the two 13C-HSQC NMR spectra. The table represents a summary of the antibacterial efficacy studies for both compounds. With increased purity, the efficacy improved dramatically including against human pathogenic bacteria.

Publications

Bowers, A. A., M. G. Acker, A. Koglin, and C. T. Walsh. Manipulation of thiocillin variants by prepeptide gene replacement: structure, conformation, and activity of heterocycle substitution mutants. 2010. Journal of the American Chemical Society. 132 (21): 7519.

Frueh, D. P., A. Leed, H. Arthanari, A. Koglin, C. T. Walsh, and G. Wagner. Time-shared HSQC-NOESY for accurate distance constraints measured at high-field in (15) N-(13)C-ILV methyl labeled proteins. 2009. Journal of Biomolecular NMR. 45 (3): 311.

Frueh, D. P., H. Arthanari, A. Koglin, C. T. Walsh, and G. Wagner. A double TROSY hNCAnH experiment for efficient assignment of large and challenging proteins. 2009. Journal of the American Chemical Society. 131 (36): 12880.

Frueh, D. P., S. Nichols, S. Mishra, H. Arthanari, A. Koglin, C. T. Walsh, and G. Wagner. Transient Domain Interactions in Non-Ribosomal Peptide Synthetases . 2011. BIOPHYSICAL JOURNAL. 100 (3): 17.

Frueh, D. P., S. Nichols, S. Mishra, H. Arthanari, A. Koglin, C. T. Walsh, and G. Wagner. Transient Domain Interactions in Non-Ribosomal Peptide Synthetases. 2011. Biophysical Journal. 100 (3): 17.

Koglin, A., V. Doetsch, and F. Bernhard. Molecular engineering aspects for the production of new and modified biosurfactants. 2010. Advances in Experimental Medicine and Biology. 672: 158.

Quantitative Modeling of Cellular Noise

Michael E. Wall
20100604PRD2

Abstract

We analyzed single-cell experimental data on various natural and synthetic gene regulatory systems. In bacteria we analyzed flow cytometry data to predict the behavior of genetic parts for synthetic biology applications such as biofuel production. In yeast we analyzed single molecule fluorescence in situ hybridization (smFISH) data to predict the response of cells to osmotic stress. In mammalian cell cultures we developed methods for measuring single-cell levels of small RNAs and used them to analyze the response of these cells to pathogen exposure. We gained important new insights into each of these systems and showed that distributions of single-cell behavior for diverse cell types can be quantitatively predicted with a very high level of accuracy. This work led to publication of a book chapter, an article in Nature Biotechnology, and two articles in Science on the identification of predictive models for gene regulation. The methods have been implemented in computer software that the community can use for similar studies. The results of this project will help to transform biology by enabling researchers to add an entirely new dimension to understanding predicting and controlling complex cellular behavior.

Background and Research Objectives

Even genetically identical cells in identical environments exhibit wildly different phenotypical behaviors due to cellular fluctuations known as gene expression 'noise'. Previously, such noise was considered a nuisance that compromised cellular responses, complicated modeling, and made predictive understanding all but impossible. Many past studies focused on how cellular processes remove or exploit noise to a cell's advantage. From these, it has become clear that different cellular mechanisms affect these cellular fluctuations in different ways. As a consequence, it is now clear that cellular fluctuations may actually contain valuable information about underlying cellular mechanisms. Finding and exploiting this information requires a strong integration of single-cell/single-molecule measurements with discrete stochastic analyses. The overall goal of this project has been to develop these tools in both the experimental and the computational realms and to define an integrated research strategy in which these tools can be systematically combined.

Analyzing Single-Cell Fluctuations. A system of ordinary differential equations, known as the master equation, is often used to describe the variability measured in biological systems at the level of single cells. Unfortunately, the master equation is difficult to solve for most systems. Prior to this project, Dr. Munsky invented a fast way of solving the master equation. His technique, known as the Finite State Projection (FSP) algorithm, enables computational researchers to ignore unimportant contributions to the master equation. By improving the efficiency and accuracy of stochastic analyses, his method set the stage for a large impact to the field. A sub-goal of this project was to further improve these tools for more efficient analysis of stochasticity in biological processes.

Integrating Experimental and Computational Analyses. Another goal of this project was to developed approaches to integrate computational FSP analyses with quantitative single-cell experimental analyses. Combining discrete stochastic analysis with single-cell/single-molecule measurements can reveal features of gene regulation that are hidden by bulk assays or deterministic analyses (Figure 1). To study single-cell responses, today's gold standards are flow cytometry, which enables researchers to quantify protein expression in thousands of cells per second, and single-molecule fluorescent in situ hybridization (smFISH), which enables direct counting of mRNA transcripts in individual cells. At the start of this project LANL had existing expertise in flow cytometry, led by Dr. Munsky's cosponsor (Babetta Marrone, B-DO). Expertise in smFISH has been developed at LANL during the course of this project through the recruitment of D. Shepherd, a postdoc co-advised by Drs. Munsky and Werner. Both flow cytometry and smFISH enables building distributions of cellular protein or RNA content, respectively (Figure. 1C) for different experimental conditions or at different times during a system response. In turn, these distributions can be computationally described by the master equation and analyzed using the tools devel-

oped by Dr. Munsky (see above). For relatively simple gene regulatory systems, temporally resolved mRNA or protein distributions have proved sufficient to constrain the model space to achieve understanding. Dr. Munsky reasoned that the systematic integration of single cell experiments and stochastic analyses would enable rapid quantitative hypothesis testing and the ability to identify system mechanism and/or parameters. The second sub-goal of this project was to combine data and stochastic modeling to enable this rapid hypothesis testing.

Developing Predictive Models for Complex Biological Systems. In the course of this research, Dr. Munsky recognized that and given complex biological behavior could be described at many different scales and at many different levels of abstraction. As a result, modeling of biological systems commonly faces a tradeoff between simple models that bear little resemblance to reality and detailed mechanistic models that are rife with unknown parameters. Although both approaches can improve conceptual understanding, neither is ideal to make quantitatively accurate predictions. Dr. Munsky then set a goal to develop a new approach to consider many different complexity levels and use uncertainty quantification methods to weigh tradeoffs between differing model complexities in the context of available data. By determining when models are too simple, when they are too complex, and then they are just right, it would become possible to acquire useful quantitative predictions.

Scientific Approach and Accomplishments

Dr. Munsky has made great progress on four tasks related to this project:

1) Identification of Gene Regulatory Networks Based Upon Stochastic Modeling and Flow Cytometry Measurements (with Chunbo Lou (MIT), Christopher Voigt (MIT)). Single-cell measurements using high throughput flow cytometry provide a wealth of information, which can reveal important aspects of genetic regulation. Dr Munsky used these measurements to identify the mechanisms and parameters of gene regulatory constructs, which may otherwise be difficult to measure. In this project, Dr. Munsky worked with collaborators Chunbo Lou and Christopher Voigt to identify predictive models that would guide the design of synthetic biological systems for eventual use in biofuel applications. Their results were published in a high impact journal: [Ribozyme-based “insulator parts” buffer synthetic circuits from genetic context, Nature Biotechnology, 30:11, 1137-1142, 2012].

Dr. Munsky has begun explorations in similar collaborations with LANL researchers to quantify cell-to-cell variability to identify predictive models that can guide the design of algae strains and harvesting technologies for biofuel applications in low quality water.

2) Systematic Identification of Signal-Activated Stochastic Gene Regulation (with Gregor Neuert (MIT/Vanderbily), Rui Zhen Tan (MIT), Leonid Teytelman (MIT), Alex van Oudenaarden (MIT/Hubrecht) and Mustafa Khammash (UCSB/ETH)). Single molecule fluorescence in situ hybridization (smFISH) allows researchers to count the number of mRNA molecules in individual cells. When combined with Dr. Munsky’s Finite State Projection method, these data help discriminate between vast numbers of quantitative model hypotheses. Dr. Munsky developed an iterative approach to (i) extract more quantitative information from single-cell experimental measurements and (ii) guide the design of subsequent experiments. He and his collaborators have identified and validated a stochastic model to accurately predict the time-varying behavior of three shock-response genes in yeast under the influence of multiple genetic mutations. This integration of experimental and computational methods represents a powerful new approach that can be applied to any gene, pathway, or organism. Dr Munsky and collaborators have published this work in two recent high-impact articles, both in Science: [Neuert, Munsky, et al, Systematic Identification of Signal-Activated Stochastic Gene Regulation, Science, 339:6119, 584-587, 2013], and [Munsky, Neuert, et al. Using Gene Expression Noise to Understand Gene Regulation, Science, 336(6078), 183–187, 2012]. Dr. Munsky and his experimentalist colleague Dr. Gregor Neuert (now assistant professor at Vanderbult University) share first authorship on both papers.

3) Identification of Transcriptional Regulation Dynamics During Host-Pathogen Interactions (with Elizabeth Hong-Geller (B7-LANL), Nan Li (B7-LANL), James Werner (MPA-CINT-LANL), Douglas Shepherd). As part of the project “Illuminating the Dark Matter of the Genome: Small RNAs as Novel Targets for Bioterrorism,” Dr. Munsky has been helping to apply his techniques to discover and characterize small, non-coding RNAs in biothreat agents. An overall goal is to characterize the dynamics by which small non-coding RNA affects gene regulation during host-pathogen interactions. Dr Munsky and colleagues seek to improve experimental approaches to count RNA copy numbers in single cells and computational/theoretical approaches to analyze these data. In this project, Dr. Munsky and Dr. Werner co-sponsored a postdoc (Dr. Douglas Shepherd), who started in May 2011. Preliminary work on this project was published at [Shepherd, et al., New tools for discovering the role sRNA plays in cellular regulation, Proc. SPIE 8228, 2012]. This work led to experimental and computational results that hint that spatial fluctuations provide a wealth of information about biological processes. As part of this work, Dr. Munsky and colleagues discovered a new technique to improve the single-to-noise ratio of individually labeled RNA molecules. This technique enables the reliable quantification of much smaller RNA molecules than were previously detectable. The results of this work are under review in the Annals of Chemistry, [D. Shepherd, et al, Counting small RNA in pathogenic bacteria. In revision for Analytical Chemistry, 2013].

4) Coarse graining strategies for transient analysis of stochastic gene regulation. At the 2011 q-bio Summer School (co-organized by Dr. Munsky), Dr. Munsky initiated collaboration with University of Pittsburgh researchers to develop efficient computational tools for stochastic processes. The resulting methods have been published in the proceedings of the 51st IEEE Conference on Decision and Control [J. Tapia, J. Faeder, B. Munsky, Adaptive Coarse-Graining for Transient and Quasi-Equilibrium Analyses of Stochastic Gene Regulation, Proc. of the 51st IEEE Conference on Decision and Control, 5361-5366, Maui, HI, Dec. 2012]. Dr. Munsky recently released stochastic analysis software as part of a review chapter that he published in 2012: [B. Munsky, Modeling Cellular Variability, in Quantitative Biology From Molecular to Cellular Systems, pp. 234-266, M. Wall, Ed., Taylor & Francis Group, New York, NY, 2012.].

Impact on National Missions

The work in this project addressed the problem of modeling stochastic systems in general and sought to validate methods using bacterial, yeast and mammalian gene regulation as test beds. The results have advanced several technical problems that involve modeling of stochastic behavior, which crosscuts the needs of many agencies and missions including DOE (biothreat reduction and using microbes for biofuel production), NIH (design of therapeutics for bacterial or viral infections), and broad problems in chem-bio, materials, chemistry, bioscience, health research, and bioenergy research.

Dr. Munsky's enthusiasm for the analysis of single-cell behavior has helped LANL to build a first-in-class team to integrate computational and experimental investigations of single-cell gene regulation. The team has developed the experience and experimental apparatus to take these investigations to the next level.

For the FY14 DR pre-proposal cycle, Dr. Munsky's stochastic modeling methods developed in this project are now also currently under consideration for use in several applications: (1) cyber security; (2) pathogenic bacterial resistance; (3) immune response; and (4) algal biofuels.

Dr. Munsky's work as the main organizer of the q-bio Summer School during the course of this project has helped LANL gain recognition in the global quantitative biology arena. Dr. Munsky, William Hlavacek (T6), Lev Tsimring (UC San Diego), and Jeff Hasty (UC San Diego) applied for an NIG R25 grant related to the summer school. This grant received a perfect score in review, and is currently pending funding of up to $1M over five years through the New Mexico Consortium.

Upon its conclusion, this project will lead to the conversion of Dr. Munsky to full time technical staff member in CCS-3. This project also led to the recruitment of a postdoctoral researcher, Dr. Douglas Shepherd (MPA-CINT), who is co-sponsored by Dr. Munsky.

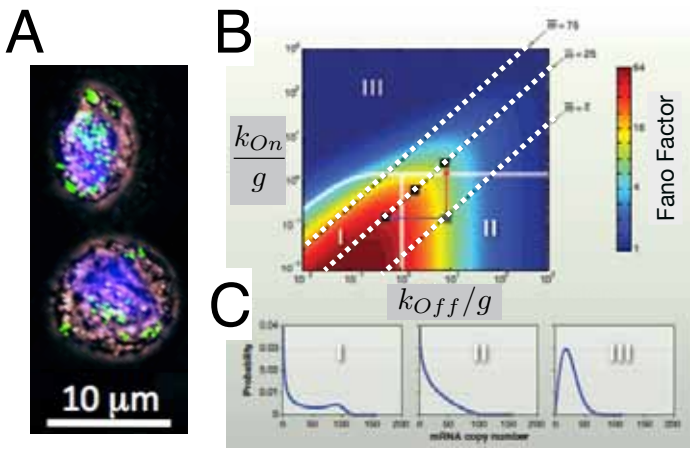

Figure 1. Single-molecule measurements. (A) Using smFISH, specific mRNAs appear as bright diffraction-limited spots, whose numbers and 3D locations can be quantified. (B) Measurements of the variances and full distributions are much more informative than average expression levels. Induction from one bulk expression level to another (i.e., from one dashed white line to the next) to another can be accomplished by different mechanisms (red or purple arrows). By keeping track of the corresponding change in variance, one can identify the hidden mechanism of induction (change in color). (C) These three distinctly different distributions all have the same mean but correspond to different classes of gene regulation—by measuring the shape of the distribution with smFISH, we can learn more about the underlying system, whereas qPCR would return only the less informative mean. (Images in panel A adapted from [Munsky, Science, 2012; panels B-C adapted from [Shepherd, SPIE, 2012]).

References

1. Neuert, G., B. Munsky, R. Z. Tan, L. Teytelman, M. Khammash, and A. van Oudenaarden. Systematic identification of signal-activated stochastic gene regulation. 2013. Science. 339: 584.

2. Munsky, B., G. Neuert, and A. van Oudenaarden. Using Gene Expression Noise to Understand Gene Regulation. 2012. Science. 336 (6078): 183.

3. Munsky, B.. Modeling Cellular Variability. 2012. In Quantitative Biology From Molecular to Cellular Systems. By Wall, M. E.. p. 233. Boca Raton, FL: Chapman and Hall.

4. Tapia, J., J. Faeder, and B. Munsky. Adaptive Coarse-Graining for Transient and Quasi-Equilibrium Analyses of Stochastic Gene Regulation. 2012. In 51st IEEE Conference on Decision and Control. (Maui, HI, December 10-13, 2012). , p. 5361. Maui, HI: IEEE.

5. Shepherd, D., N. Li, E. Hong-Geller, B. Munsky, and J. Werner. New tools for discovering the role sRNA plays in cellular regulation. 2012. (San Francisco, California, Jan. 2012). Vol. 8228p. . : .

6. Shepherd, D., N. Li, S. Micheva-Viteva, B. Munsky, E. Hong-Geller, and J. Werner. Counting small RNA in pathogenic bacteria. To appear in Analytical Chemistry.

7. Lou, C., B. Stanton, Y. Chen, B. Munsky, and C. A. Voigt. Ribozyme-based insulator parts buffer synthetic circuits from genetic context. 2012. Nature Biotechnology. 30 (11): 1137.

Publications

Lou, C., B. Stanton, Y. Chen, B. Munsky, and C. A. Voigt. Ribozyme-based insulator parts buffer synthetic circuits from genetic context. 2012. Nature Biotechnology. 30 (11): 1137.

Munsky, B.. Modeling Cellular Variability. 2012. In Quantitative Biology From Molecular to Cellular Systems. By Wall, M. E.. , p. 233. Boca Raton, FL: Chapman and Hall.

Munsky, B.. Integrated experimental and computational identification of stochastic gene regulation . Presented at Gordon Research Conference in Stochastic Physics in Biology. (Ventura, CA, 23-25 Jan. 2011).

Munsky, B., G. Neuert, and A. van Oudenaarden. Using Gene Expression Noise to Understand Gene Regulation. 2012. Science. 336 (6078): 183.

Munsky, B., S. Lampoudi, D. Thorsley, and A. Walczak. Conference Report. Presented at The 3rd workshop on stochasticity in biochemical reaction networks . (Banff, Canada, 12-16, Sept. 2011).

Munsky, B., and M. Khammash. Identification from stochastic cell-to-cell variation: A genetic switch case study. 2010. IET Systems Biology. 4: 356.

Nemenman, I., S. Gnanakaran, W. Hlavacek, Y. Jiang, B. Munsky, M. Wall, and J. Faeder. The Fifth Annual q-bio Conference on Cellular Information Processing. 2012. Physical Biology. 9: 050201.

Neuert, G., B. Munsky, R. Tan, L. Teytleman, M. Khammash, and A. van Oudenaarden. Systematic Identification of Signal-Activated Stochastic Gene Regulation. 2013. Science. 339 (6119): 584.

Shepherd, D., N. Li, E. Hong-Geller, B. Munsky, and J. Werner. New tools for discovering the role sRNA plays in cellular regulation. 2012. In Single Molecule Spectroscopy and Superresolution Imaging. (San Francisco, California, Jan. 2012). Vol. 8228, p. . : .

Shepherd, D., N. Li, E. Hong-Geller, B. Munsky, and J. Werner. Spatiotemporal Measurements and Modeling of Genetic Expression. Presented at Stochastic Physics in Biology. (Ventura, CA, 16-19, Jan. 2013).

Shepherd, D., N. Li, E. Hong-Geller, J. Werner, and B. Munsky. Spatiotemporal measurements and modeling of genetic expression . Presented at The Sixth Annual q-Bio Conference. (Santa Fe, NY, 8-12, Aug. 2012).

Shepherd, D., N. Li, S. Micheva-Viteva, B. Munsky, E. Hong-Geller, and J. Werner. Counting small RNA in pathogenic bacteria. To appear in Analytical Chemistry.

Tapia, J., J. Faeder, and B. Munsky. Adaptive Coarse-Graining for Transient and Quasi-Equilibrium Analyses of Stochastic Gene Regulation. 2012. In 51st IEEE Conference on Decision and Control. (Maui, HI, 10-13, Dec. 2012). , p. 5361. Maui, HI: IEEE.

Modeling the Surface Mass Balance and Freshwater Runoff from the Greenland Ice Sheet in a Changing Climate

Matthew W. Hecht
20100631PRD4

Abstract
This Final Report summarizes the very successful work of a Director's Postdoctoral Fellow on the surface mass balance and runoff from various glacial systems, including the Greenland Ice Sheet.

Background and Research Objectives
This project has focused on the hydrological cycle over Greenland, in particular on the balance between cold-season accumulation of snowpack and warm season runoff. The stated aim of the proposal was to predict local and regional changes in Greenland's surface mass balance and runoff in a changing climate based on computer modeling of the snowpack, with a dual approach of modeling the entire Greenland Ice Sheet while also applying more detailed study to two particularly well observed regions, the Kangerlussuaq and Sermilik Fjord drainage areas.

Dr. Mernild took good advantage of the opportunity provided by the Director's Fellowship. He not only met the objectives of our Proposal, but also found opportunities to make excellent use of a variety of observational sources, with a tremendously deep set of collaborators from the Laboratory and around the world, and has furthermore applied his analysis well beyond the boundaries of Greenland.

Scientific Approach and Accomplishments
One measure of accomplishment is the record of publications. In 2010, Dr. Mernild had six peer-reviewed publications, five of which were first-authored. In 2011 he had another three first-authored publications. As the LDRD-supported work has come to full fruition, Dr. Mernild has seen nine manuscripts appear in refereed journals already in 2012, and listed in the reference section, with another six in review. He has also had several invited presentations over the past year, including most notably at the annual meeting of the European Geophysical Union in Vienna. His EGU presentation, on Glaciers and Ice Caps: Contribution to sea level rise, also produced a press conference and wide coverage in the media, including an interview by the BBC.

Dr. Mernild continues to establish himself as an international expert on state of the World's glaciers and ice sheets. He has been asked to serve as a contributing author on the Sea Level Rise chapter of the upcoming Fifth Assessment Report of the International Panel on Climate Change. This is remarkable recognition for so young a scientist.

Impact on National Missions
LANL contributes to the US effort in climate modeling through the Community Earth System Model, in partnership with the NSF. The DOE has a particularly strong focus in high latitude climate, in part due to LANL's expertise in sea ice, and in the dynamical modeling of ice sheets. There had been no particular expertise in the DOE before Dr. Mernild's arrival in the study of year-to-year variations and trends in snowpack and runoff. This work has had a substantial impact on the national effort to monitor and understand trends in climate at the high latitudes.

References
1. Mernild, , and B. Hasholt. Climate-driven fluctuations in freshwater to Sermilik Fjord, East Greenland, during the last 4000 years. 2012. The Holocene. 22: 155–164.

2. Hanna, . Discerning the influence of North Atlantic atmospheric and oceanic forcing effects on 1900–2010 Greenland summer climate and melt. 2012. International Journal of Climatology.

3. Mernild, , and N. T. Knudsen. Multi-decadal marine and land-terminating glacier retreat in Ammassalik region, Southeast Greenland. 2012. The Cryosphere. 6: 625–639.

4. Mernild, S. H., and G. E. Liston. Greenland freshwater runoff. Part II: Distribution and trends, 1960–2010. 2012. Journal of Climate.

5. Liston, G. E., and S. H. Mernild. Greenland freshwater runoff. Part I: A runoff routing model for glaciated and non-glaciated landscapes (HydroFlow). 2012. Journal of Climate.

6. Hinzman, , and S. H. Mernild. Trajectory of the Arctic as an Integrated System. 2012. Ecological Applications.

7. Pedersen, , and C. S. Andersen. Sediment accumulation in a fjord in front of the Mittivakkat glacier delta, SE Greenland. 2012. The Holocene.

8. Hanna, , and K. Steffen. Recent warming in Greenland in a long-term instrumental (1881–2012) climatic context. Part 1: Evaluation of surface air temperature records. 2012. Environmental Research Letters. 7.

9. Mernild, , and M. van den Broeke. Simulated internal storage build-up, release, and runoff from Greenland Ice Sheet at Kangerlussuaq, West Greenland. 2012. Arctic, Antarctic, and Alpine Research. 44: 83.

10. Fausto, R. S., S.H. Mernild, B. Hasholt and A.P. Ahlstrom, and N.T. Knudsen. Modelling suspended sediment concentration and transport for the hydrological year 2004--2006. 2012. Arctic, Antarctic and Alpine Research. 44: 306.

11. Mernild, S. H., N. T. Knudsen, W. H. Lipscomb, J. C. Yde, J. K. Malmros, B. Hasholt, and B. H. Jakobsen. Increasing mass loss from Greenland's Mittivakkat Gletscher. 2011. The Cryosphere. 5: 341.

12. Mernild, S. H., T. L. Mote, and G. E. Liston. Greenland ice sheet surface melt extent and trends: 1960-2010. 2011. JOURNAL OF GLACIOLOGY. 57: 621.

13. Mernild, S. H., G. E. Liston, C. A. Hiemstra, J. H. Christensen, M. Stendel, and B. Hasholt. Surface mass-balance and runoff modeling using {HIRAM4} {RCM} at {K}angerlussuaq ({S}ondre {S}tromfjord), {W}est {G}reenland, 1950--2080. 2011. Journal of Climate. 24: 609.

Publications

Mernild, S. H., G. E. Liston, C. A. Hiemstra, J. H. Christensen, M. Stendel, and B. Hasholt. {Surface Mass Balance and Runoff Modeling Using HIRHAM4 RCM at Kangerlussuaq (Sondre Stromfjord), West Greenland, 1950-2080}. {201. {JOURNAL OF CLIMATE}. {24}: {609.

Mernild, S. H., M.-S. Seidenkrantz, P. Chylek, and and G. E. Liston. Climate-driven fluctuations in freshwater to {S}ermilik {F}jord, {E}ast {G}reenland. 2011. The Holocene. : in press.

Mernild, S. H., N. T. Knudsen, W. H. Lipscomb, J. C. Yde, J. K. Malmros, B. H. Jakobsen, and B. Hasholt. Record mass loss from Greenland's best-observed local glacier. 2011. The Cryosphere Discussions. 5: 461.

Mernild, S. H., N. T. Knudsen, W. H. Lipscomb, J. C. Yde, J. K. Malmros, B. Hasholt, and B. H. Jakobsen. Increasing mass loss from Greenland's Mittivakkat Gletscher. 2011. The Cryosphere. 5: 341.

Mernild, S. H., N. T. Knudsen, and E. Hanna. Mittivakkat {G} letscher, {SE} {G}reenland. 2011. In The Arctic Report Card, Greenland. Edited by J. E. Box et al.. NOAA Report.

Mernild, S. H., T. L. Mote, and G. E. Liston. {Greenland ice sheet surface melt extent and trends: 1960-2010}. {201. {JOURNAL OF GLACIOLOGY}. {57}: {621.

Mernild, S. H., and G. E. Liston. Greenland freshwater runoff. {P}art {II}: {D}istribution and trends, 1960–2010. 2011. J. Climate. : submitted.

Novel Laboratory and Field Observations to Model Climate Warming by Aged Absorbing Aerosols

Manvendra K. Dubey
20110751PRD3

Abstract

Climate forcing from absorbing aerosols such as black carbon (BC), a.k.a. "soot", emitted by the combustion of fossil fuels and wildfires are the most uncertain elements in terms of our ability to assess climate change, and currently BC is thought to be the second most important contributor to warming behind CO2. State-of-the-art techniques were applied to measure BC in the field and the laboratory for improved treatments in climate models. Aerosol optical and physical properties were measured in the ambient atmosphere in addition to the use of laboratory studies as a more controlled setting to study aerosol processing. This research is focused on the coupling of measurements made with a single particle BC-specific instrument that detects BC mass via laser-induced incandescence and photoacoustic spectrometers that measure the absorption and scattering due to particles, in addition to using various other supportive measurements to characterize the aerosol and gas-phase precursors. From the empirical measurements, simplified parameters are elucidated for application in climate models with the overall goal of reducing the uncertainty in the climactic impacts of aerosols, currently one of the largest uncertainties in global models today.

Background and Research Objectives

Gaps in our knowledge of emissions of absorbing aerosols like black carbon from fires and Aeolian dust that absorb sunlight to warm the climate are the largest source of uncertainty in climate model projections of climate change. We identified opportunities and used LANL state-of-the-art aerosol instruments in field and laboratory studies to understand how absorbing aerosols transformations influence their ability to absorb and scatter sunlight.

Wildfires: BC is not the only significant absorbing species in wildfire emissions. Tar balls, found to be present at 10x the amount of BC by number during New Mexico's Las Conchas wildfire in 2011 also contribute to absorption, and together lead to increased warming of the atmosphere. Further measurements are required, but it appears that with climate change leading to the presence of more and larger wildfires that this effect could compound global warming, and should not be overlooked in climate models. Additionally, single scatter albedo from fires correlates with combustion efficiency, and this relationship can be applied within models to constrain the radiative forcing from BB emissions.

BC Absorption Enhancement: Field measurements of BC in the United Kingdom indicate the first ambient measurements of an appreciable absorption enhancement (~30%) due to coatings on BC. This has been predicted based on laboratory work and modeling studies, but has not been confirmed in the field yet. Our measurements indicate that BC can have increased absorption due to coatings, and it should be noted that our numbers are a lower bound for this measurement so it is possible that the enhancement could be closer to the predicted factor of 2, which would have a large significance on the amount of warming due to BC. The methodology and key results are highlighted here.

BC Removal: A method was developed for the online removal of BC from mixed aerosol samples. Laboratory studies with a BC surrogate, Aquadag, indicate that laser-induced vaporization can be used to remove 90% on average of the original BC mass present. This technique could be applied to probe the optical properties of brown carbon from both laboratory and ambient samples, which would be of great interest to both the aerosol and climate community in general since these other absorbing aerosols are poorly characterized and could be significant contributors to the warming of the atmosphere, especially for locations with biomass burning. Other applications include removing BC to determine whether or not it has a significant role in both cloud and ice nucleation, which will also be very impor-

tant in determining both BC lifetime in the atmosphere and also its role in cloud processing and indirect effects on radiative forcing.

Improved Absorption Measurements: Direct online aerosol absorption measurements using photoacoustic spectroscopy are considered noisy in comparison to more traditional filter measurements. However, they are not subject to the biases that reduce accuracy of the filter measurements. From analyzing the aerosol absorption measurements at the stationary DOE ARM site at SGP, upgraded lasers and an external acoustic filter improve the data quality significantly, by factors of 1.3-5.8, depending on the wavelength of the measurement. Another technique was also explored that utilizes direct measurements, but from two different instruments. From this work, there will be an IOP next year at the SGP site to determine the best technique for measuring aerosol absorption in the field.

Transported BC: During the BEACHON field campaign in 2011 that was located in a remote forest in Colorado, BC dominantly originated from transported pollution from cities 20-50 miles away, Colorado Springs and Denver. More than half of the BC was thickly coated, consistent with aged BC, and was usually <5% of the total aerosol mass except during pollution events when it was ~10%. BC correlated with organic aerosols during the pollution periods, and there was also increased aerosol absorption indicating the presence of either external absorbing species, such as brown carbon, and/or enhanced absorption due to the BC mixing state.

Absorbing Dusts and Hematite: In addition to the major findings discussed here, we also performed laboratory experiments on size-selected absorbing dusts from different sites across the globe and on hematite, a dominant absorbing component in dusts. We measured the optical properties and determined a calibration for measuring hematite using laser-induced incandescence. We hope to continue this work and use the data to develop an optical model for dust that could be tested in the field.

Scientific Approach and Accomplishments

BC and Tar Balls in Wildfire Emissions

Biomass burning (BB) is one of the largest sources of carbonaceous aerosols in the atmosphere, significantly affecting earth's radiation budget and climate. Tar balls, abundant in biomass burning smoke, absorb sunlight and have highly variable optical properties, typically not accounted for in climate models. Individual biomass burning particles from the Las Conchas fire (New Mexico, 2011) were analyzed using electron microscopy. The relative abundance of tar balls (80%) was found to be 10 times greater than soot particles (8%). Soot, a.k.a. black carbon (BC) was quantified in terms of morphology and classified into four categories and are shown in Figure 1 below: ~50% are embedded (heavily coated), ~34% are partly coated, ~12% have inclusions, ~4% are bare. Tar balls were divided into two different classes, one being more oxidized than the other. Since the mixing of BC particles with other material affects their optical, chemical and physical properties inclusion of these observations should improve climate model performances.

Single scattering albedo (ω) from BB aerosols produced from ninety-nine experimental single source burns at the Missoula Fire Sciences Laboratory during FLAME-IV were compared with New Mexico's two largest wildfires, Las Conchas in 2011 and the Whitewater-Baldy Complex in 2012. Laboratory measured ω ranges from ~0.2 to 1, with the variation depending strongly on combustion conditions rather than fuel type. The flaming phase that precedes the smoldering phase has a lower ω due to a higher mass fraction of BC that increases as combustion efficiency decreases. During the later smoldering phase, ω remains relatively constant ~0.95 due to the largely scattering organics that are more dominant during this phase. ω is parameterized as a function of modified combustion efficiency using the laboratory data, which the field observations support, making it possible for use for evaluating the climate impacts of BB aerosols within radiative transfer models.

Absorption Enhancement Observed in the Field

Currently, absorption from BC is thought to be the second largest contribution to global warming after carbon dioxide, but with high uncertainty. Laboratory studies on the optical properties of BC and modeling studies indicate that BC could have up to a two-fold increase in absorption due to coatings on BC, which is not currently accounted for in most models. However, this kind of increase in absorption due to coatings on BC has yet to be measured in the field. As a matter of fact, the only study out currently indicates a very small increase in the absorption and considers coating BC to be a null effect. However, these are measurements from only one location, and the BC there was not well-aged nor did it have thick coatings present, therefore, supporting the published findings.

During the ClearfLo campaign in the UK, we denuded the BC up to 250 degrees C and measured the optical properties in order to determine whether or not there was an appreciable absorption enhancement due to the semi-volatile coatings found on BC. For two locations in the UK, we found ~30% absorption enhancement (see Figure 2) due to coatings on BC as determined by focusing on the longer wavelengths, 781 nm, where BC dominates the absorption spectrum. The absorption enhancement is also correlated with coating thickness and photochemical age, which supports theoretical predictions and laboratory simulations.

These results indicate that internally mixed BC can have increased absorption signals and that more studies need to be conducted to determine how often this is present in the atmosphere.

Removal of BC for Isolated Studies on Other Absorbing Aerosols

The ability to separate black carbon (BC) from organic carbon (OC) in an online aerosol sample would enable the physical processes and optical properties to be studied by carbon class. A novel method was developed to remove BC from an online aerosol sample with the soot surrogate Aquadag. This method can be applied to ambient and source aerosol samples to isolate the roles that different carbon classes have on climate, e.g. atmospheric warming, cloud formation and lifetime. Removal of BC from an ambient aerosol sample would allow for the isolated study of other absorbing aerosols such as dust and brown carbon.

Two Single-Particle Soot Photometers (SP2s) were used in series, along with a Three-Wavelength Photoacoustic Soot Spectrometer (PASS-3) for measuring optical properties. Polydisperse and monodisperse particles were sampled from 100 nm to 800 nm in diameter. For all monodisperse samples, the average percent remaining by mass and number of the original size selected are 11.1% ± 18.6% and 12.7% ± 21.9%, respectively. Figure 3 below shows an example of the particle mass size distribution before and after the removal of 500 nm diameter particles. The results are applicable to other instruments employing LII, e.g. the Soot Particle Aerosol Mass Spectrometer (SP-AMS), and could also potentially be used for the study of new and/or altered carbonaceous particles in a controlled environment.

Improved Absorption Measurements at an ARM Site

Direct aerosol absorption measurements using photoacoustic spectroscopy are considered "noisy." However, indirect measurements that have better precision use filters and as a result are subject to biases that significantly reduce their accuracy. Another proposed method has been to measure extinction and scattering and to calculate the absorption from the subtraction of the two measurements being made by two different instruments. There has been much debate within the last year about which technique is best suited for measuring aerosol absorption, especially in relatively clean areas with low signals. From our data and extensive experience with absorption measurements it was determined that the DOE would fund an Intensive Operating Period (IOP) that LANL would lead next year at the DOE Atmospheric Radiation Measurement's Aerosol Observing System (AOS) at the Southern Great Plains (SGP) Central Facility in Ponca City, OK to try to answer this question.

Aerosol absorption and scattering from the three-wavelength photoacoustic soot spectrometer (PASS3; Droplet Measurement Technologies) has been located in the DOE AOS at SGP since 2009. Approximately six months of measurements from January 2013 to July 2013 at 405 nm, 532 nm, and 781 nm with an upgraded instrument were analyzed. The uncertainty within the absorption measurement was improved by factors of 5.8, 3.8, and 1.3, respectively, for the three wavelengths with upgraded lasers and an external acoustic filter.

Direct absorption measurements from the PASS-3 are compared with two collocated filter measurements from the Continuous Light Absorption Photometer (CLAP, NOAA/GMD) at 467 nm, 528 nm, and 652 nm, and the Particle Soot Absorption Photometer (PSAP; Radiance Research) at 467 nm, 530 nm, and 660 nm in Figure 4. The CLAP appears to have less bias and better corrections for filter issues than the PSAP, and compares well with the direct PASS absorption measurements (Figure 4). Scattering measurements from the PASS-3 are compared with an integrating nephelometer (TSI) at 450 nm, 550 nm, and 700 nm. On average, the absorption and scattering signals indicate a generally clean location. The average absorption angstrom exponent at this site was determined to be 1.03, indicating minimal presence of absorbing species other than black carbon. The average single scatter albedo across all wavelengths and measurements is 0.8, showing a dominantly scattering aerosol at the site. Angstrom exponents are used to interpolate between the three different wavelength ranges, which are less than 20%.

During the ClearfLo campaign in 2012 we had both the extinction and scattering measurements, and attempted to perform resolving aerosol absorption via subtraction. Scattering and extinction from the two instruments compare well, however, the measured and calculated absorption have larger discrepancies and uncertainties as can be seen in the Figure below. This method will require careful calibration, collocation and any corrections for measurements at different wavelengths since it requires the subtraction of two large numbers (extinction and scattering) to determine a relatively small number (absorption).

Transported BC in a Remote Forest

BC and its optical properties were measured during the BEACHON campaign in 2011. The SP2 and 3 PASS instruments were deployed with complementary aerosol equipment to measure size-distributions and denude (heat the aerosol to remove semi-volatile components) the aerosol as were used during the sampling of the Las Conchas fire. We tried to conduct denuding studies to look for absorption enhancements due to coatings on BC, but the concentrations at this remote site were too small to achieve this.

BEACHON-RoMBAS was determined to be a "semi-clean" environment impacted by pollution transported from nearby cities (e.g., Colorado Springs, Denver). Average BC mass concentrations were ~ 50 ng m-3 with peak periods exceeding 500 ng m-3 due to transported pollution events. The BC mass concentration was <5% of the total PM1 mass on average during the campaign and is closer to ~10% during pollution events.

Most of the BC particles (55 ± 10%) were thickly coated, which is consistent to the sources being from transported/aged pollution. AAE's indicated aerosol absorption was dominantly from BC, indicating minimal presence of brown carbon or other absorbing organic species. This was also consistent with the mass absorption coefficients (MACs) that we measured at the site that were similar to measurements of pure BC. However, during periods of identified pollution plumes, there were elevated MACs, indicating possibly some transported absorbing organics unlike the organics present in the forest background. BC correlated with organics in the plumes, but none of the other measured aerosol chemical species (e.g., ammonium, chloride, nitrate, sulfate). It was also determined that BC was not significant in terms of aerosol hygroscopicity, the initial water uptake necessary for a particle to form a cloud droplet, at this site during the campaign (Ezra Levin, CSU, personal communication).

Participation in Large Interdisciplinary Field Campaigns
FLAME-IV: Fire Lab at Missoula Experiment-IV. Organized by Colorado State University, Carnegie Mellon University and the University of Montana, funded by NSF.

Publications

Aiken, A. C., B. A. Flowers, and M. K. Dubey. : Absorbing Aerosols: Field and Laboratory Studies of Black Carbon and Dust. 2011. In American Geophysical Union Annual Meeting. (San Francisco, 5-9 Dec. 2011). , p. : A53A. San Francisco: AGU, EOS.

China, S., C. Mazzoleni, K. Gorkowski, A. C. Aiken, and M. K. Dubey. Morphology and Mixing State of Individual Freshly Emitted Wildfire Carbonaceous Particles. 2013. Nature Communications. 4: 3122.

Docherty, K. S., A. C. Aiken, J. A. Huffman, I. M. Ulbrich, P. F. DeCarlo, D. Sueper, and D. R. Worsnop. The 2005 Study of Organic Aerosols at Riverside (SOAR-1): Instrumental Intercomparisons and Fine Particle composition. 2011. Atmospheric Chemistry and Physics. 11: 12387.

Duplissy, J., P. F. DeCarlo, J. Dommen, M. R. Alfarra, A. C. Aiken, and J. L. Jimenez. Relating Hygroscopicity and Composition of Organic Aerosol Particulate Matter. 2011. Atmospheric Chemistry and Physics. 11: 1155.

Gorkowski, K., M. K. Dubey, B. A. Flowers, A. C. Aiken, B. Z. Klein, C. Mazzoleni, N. Sharma, and S. China. Aerosol Optical Properties of Smoke from the Las Conchas Wildfire, Los Alamos, NM. 2011. In American Geophysical Union Annual Meeting. (San Francisco, 5-9 Dec. 2011). , p. A52A. San Francisco: AGU, EOS.

Mohr, C., F. D. Lopez-Hilfiker, P. Zotter, A. S. Prevot, S. C. Herndon, L. R. Williams, J. P. Franklin, M. S. Zahniser, D. R. Worsnop, W. B. Knighton, A. C. Aiken, K. J. Gorkowski, M. K. Dubey, and J. A. Thornton. Contribution of nitrated aromatics to wood burning brown carbon light absorption in Detling, UK during winter time. 2013. Environmental Science and Technology. 47 (12): 6316.

Ulbrich, I. M., M. R. Canagaratna, M. J. Cubison, Q. Zhang, N. L. Ng, A. C. Aiken, and J. L. Jimenez. Three-dimensional Factorization of Size-resolved Organic Aerosol Mass Spectra from Mexico City. 2012. Atmospheric Measurement Techniques. 5: 195.

Information Science and Technology

Optimization Principles for Co-design Applied to Molecular Dynamics

Stephan J. Eidenbenz
20110710DR

Introduction

Our goal is to develop a framework for hardware-software codesign as a formally-posed optimization problem. While the optimization framework will be applicable to multiple problem domains, for the target application we use molecular dynamics (MD), an exemplar for the need for computational scaling, and archetypal of the obstacles thereof. We view codesign as search and selection from a vast space of hardware and software designs that map to performance metrics. The objective function that we aim to optimize contains, as main components, run time (or computational rate), problem size, simulated time duration, energy use, and hardware cost. The framework will manifest itself in the form of (i) optimization software addressing hardware and software design space enumeration, and performance prediction methods at multiple scales, (ii) documented best practice insights, and (iii) theorems on upper and lower bounds on theoretically achievable performance for some algorithmic and hardware architecture combinations. On the application side, our goal is to enable the atomistic simulation tools that can probe the physics of processes such as ductile spall failure under shock conditions and the evolution of radiation damage. Achieving this requires two orders of magnitude increase in simulated time over current state-of-the-art petascale computing, and cannot be realized without this codesign approach, as direct implementation on an exascale platform would not achieve it. These two problems are of great intrinsic interest to the lab, addressing the response of materials in extreme conditions and enabling the design of more effective and safe fission power plants, respectively.

Benefit to National Security Missions

Successful implementation of our optimization framework will provide the unique capability of codesigning hardware and software on a sound semi-formal basis. It will enable effective implementation of physics simulations on future novel computer architectures, and provide a basis for more decisive influence on hardware design. For our molecular dynamics application domain, we will reach regimes that enable us to study a wealth of poorly understood phenomena of critical importance to the lab mission, including nuclear weapons, energy systems, and armor, to name but a few.

Progress

Along the two major tasks of building the Accelerated Molecular Dynamics (AMD) simulator AMDSim and developing a more detailed Profile-Parallelize-Predict (PPP) approach, we have made progress as follows.

We have developed the AMDSim code suite, so far consisting of TADSim to simulate temperature accelerated dynamics simulations, and ParRepSim to simulate parallel replica dynamics simulations. The codes have been thoroughly tested and validated against the real code using a metallic surface diffusion system. The validation process took longer than we had anticipated due to a few software errors but also due to the physics of the studied system, which turned out to be more complex than we expected. We developed a model for the escape rates (e.g., a diffusive jump of an atom on the surface) that includes an additional temperature dependence to account for anharmonicity. We also found it was important to include a temperature dependence in the number of steepest-descent iterations required to detect transitions. With this more refined model of the physics built into the TADSim code, a very satisfactory set of validation results was obtained. After the validation period, we have started large parameter scans, which constitute the first step in a process: first getting a global view of the multidimensional landscape, secondly using optimization to find local extrema in regions of interest. A new hurdle we are now facing is that the due to the large number of parameters that we test in our fully factorial design, a huge number (millions)

of simulated simulations must be performed. This leads to significant HPC cycle requirements as well as creating unusual challenges in effectively using the job queuing systems. We have been successful in our request for additional needed computing resources.

The PPP component has progressed most significantly in the automatic parallelization of serial programs via a multi-step tool chain. The tool chain itself consists of several discrete components, some freely available open-source software (most significantly the LLVM compiler infrastructure), and some developed by this project. In brief: a program in any language that LLVM or GCC can accept (C, C++, Fortran, etc.) is transformed to the LLVM intermediate representation, then transformed to introduce and maximize parallelism, essentially by respecting exactly the data dependencies, and otherwise ignoring the control dependencies that are often largely artifacts of the sequential programming language. In this form the program exhibits a theoretically maximal degree of parallelism. Subsequent analysis and transformation schedules the instructions with respect to a processor budget, memory access constraints, data transfer costs, etc., in other words, optimally or near-optimally on an arbitrary hypothetical computer architecture. Typically the goal is to minimize makespan--the time for all computations to complete, but other metrics are possible, such as total energy consumption. In this way we can answer such questions as "Given an architectural specification, what is fastest a given program could possibly run on it?" or "Given a program, what is the fastest it could run with current semiconductor technology but with unlimited budget?" In the context of the whole project, this gives us the automated performance prediction needed in the co-design optimization loop. Independently, we believe that the PPP capability has the potential to be a game-changer in automated program parallelization.

To validate our results we are currently targeting real extant hardware (Intel x86) on which to run the auto-parallelized code. This has proven to be rather more complicated than originally expected, mainly because the original nominal target of the transformed code was custom or simulated hardware. Nonetheless, we are on track to achieve this. A potential next step (next FY) would be to target a more exotic extant architecture such as the Intel MIC, which would be particularly appropriate because a) we have access to such hardware; and, b) a future version of the MIC may provide the bulk of the computational power of LANL's next capability machine.

Our work has resulted in a publication in the 2012 Winter Simulation Conference; three position papers for the DOE/ASCR Workshop on Modeling and Simulation of Exascale Systems and Applications are currently under review; and two more papers on AMDSim and PPP are in preparation.

Future Work

The goals and objectives for the optimization framework are structured along each major task as follows:

1. Complete the accelerated molecular dynamics simulation simulator (sic) to include all algorithmic variations for the temperature-accelerated dynamics (TAD) method, the parallel replica method (ParRep) and combinations of both. Variations include speculative execution of transition branches, alternate variations of checking for transitions, multiple high-temperature settings, etc. Our goal is to expand our current performance prediction method (AMDSim) to quickly adapt to algorithmic changes in terms of the ability to model them, which then can be fed into a set of optimization rules.
2. Complete the full optimization cycle for the hardware oriented PPP (Profile, Parallelize, Predict) approach, which aims to find shortcuts to optimal designs by exposing the inherent parallelism in a problem with near-optimum accuracy. A key challenge will be to find a balance between maximizing parallelism without losing performance to data movement. This task will build on the promising work of FY12 that included the development of a the ASET tool (for Architecture Space Exploration Tool).
3. Complete implementation of a suite of optimization rule sets, including genetic algorithms, simulated annealing, and other metaheuristics.
4. Integrate the optimization tools from (3) with the performance and algorithm-space exploration tools from (1) and (2) to run experiments at large scale. Our goal is to find novel architecture and software combinations that show promising performance in a simulated environment.

Conclusion

A successful codesign optimization framework will fundamentally change the way scientific applications are constructed: HW/SW codesign fundamentals will become an essential part of software engineering. The optimization framework will have manual and automated aspects. Similar to compiler optimization techniques used in classical compilers for the automated aspects, it will achieve peak performance when the human designer allows the optimizer to test a large set of potential solutions in a high-throughput optimization loop.

Publications

Optimization Principles for Hardware/Software Co-Design with Applications in Molecular Dynamics. 2012. In Poster at Supercomputing conference SC'11. (Seattle, WA, 12-18 Nov. 2011). , p. 1. Seattle, WA: ACM.

Delengov, V., Y. Li, J. Thompson, and L. Kroc. Hardware-Software Codesign. 2012. Claremont Graduate University Mathematics Clinic - Final Report.

Eidenbenz, S., A. Voter, K. Davis, S. Mniszewski, D. Perez, N. Santhi, S. Thulasidasan, H. Djidjev, L. Gurvits, and C. Junghans. Optimization Principles for Codesign applied to Molecular Dynamics: Design Space Exploration, Performance Prediction, and Optimization Strategies. 2012. In DOE ASCR/ASC Exascale Research Conference 2012. (Portland, NY, 16-18, April, 2012). , p. n.a.. Portland, OR: DOE.

Eidenbenz, S., A. Voter, K. Davis, S. Mniszewski, D. Perez, N. Santhi, S. Thulasidasan, H. Djidjev, L. Gurvits, and L. Kroc. Optimization Principles for Hardware/Software Co-Design with Applications in Molecular Dynamics. 2011. Los Alamos National Laboratory Unlimited Release.

Eidenbenz, S., K. Davis, A. Voter, S. Mniszewski, H. Djidjev, L. Gurvits, C. Junghans, D. Perez, N. Santhi, and S. Thulasidasan. Optimization Principles for Computational Co-Design with Applications to Molecular Dynamics . 2012. Poster at LANL Materials Capability Review.

Eidenbenz, S., N. Santhi, S. Mniszewski, and M. K. Davis. Performance modeling at Multiple Interacting Scales: hierarchical generalized instructions sets to move through different abstraction levels using stochastic substitution. 2013. LA-UR 13-24444.

Gurvits, L.. Simulating one Markov Process based on a Black Box for another: Rigorous Proofs. 2012. Draft version.

Kroc, L., N. Santhi, L. Kroc, V. Delengov, Y. Li, J. Thompson, and S. Eidenbenz. Optimization Principles for Arithmetic Functions in Hardware-Software Co-Design - Extended Abstract. 2012. In The Winter Simulation Conference. (Berlin, Germany, 9-12 December 2012). , p. 337. Berlin, Germany: SCS.

Mniszewski, S.. TADSim: Discrete Event Simulation of Temperature Accelerated Dynamics Performance. 2011. Los Alamos National Laboratory Unlimited Release Report.

Mniszewski, S., S. Eidenbenz, A. F. Voter, D. Perez, and C. Junghans. Parametrized discrete-event-based application simulators for performance modeling. 2013. LA-UR 13-24386.

Santhi, N., M. K. Davis, and S. Eidenbenz. Graphical models and a scalable methodology for exascale performance prediction. 2013. LA-UR 13-24435.

Williams, S., and S. Eidenbenz. Extensible design for multi-agent serial processes. 2013. LA-UR 13-27222 .

CoCoMANS: Computational Co-design for Multi-scale Applications in the Natural Sciences

Dana A. Knoll
20110737DR

Introduction

We will forge a qualitatively new predictive-science capability exploiting evolving high-performance computer architectures for multiple national-security-critical application areas—including materials, plasmas, and climate—by simultaneously evolving the four corners of science, methods, software, and hardware in an integrated computational co-design process. We will develop new "applications-based", self-consistent, two-way, scale-bridging methods that have broad applicability to the targeted science, will map well to emerging heterogeneous computing models (while concurrently guiding hardware and software to maturity), and provide the algorithmic acceleration necessary to probe new scientific challenges at unprecedented scales. Outcomes will 1) represent a paradigm shift in the pursuit of world-class science at LANL by bringing a wide spectrum of pertinent expertise in the computer and natural sciences in to play; 2) deliver a documented computational co-design knowledge-base, built upon an evolving software infrastructure; 3) foster broad, long-term research collaborations with appropriate hardware partners; and 4) deepen understanding of, and our experience-base with, consistent, two-way, scale-bridging algorithms.

Benefit to National Security Missions

The need for computational co-design and multiscale solution algorithms resides in almost every mission at LANL that involves computational science. Nowhere is the need greater than in the NNSA ASC program. We have carefully chosen two of our application areas, materials science and plasma physics, as these areas represent current and future multi-scale challenges to ASC. All three chosen application areas are relevant to the Office of Science mission. Most importantly, the research proposed here is a required investment to prepare for a LANL leadership role in the DoE Exascale Initiative. Mission applications for computing at this scale are legion, and include nuclear weapons, fusion and fission energy, explosives and armor, and climate/energy effects.

Progress

We have had two external reviews of the CoCoMANS project in FY-13. The first was the standard external review required by the LDRD office at roughly the mid-point of the project. This occurred at LANL on October 11, 2012. There were four external committee members (LLNL, MIT, Univ. of Utah, and Univ. of New Hampshire) and three internal committee members (XCP (2) and HPC). The second external review occurred on May 22, 2013 as part of the LANL Computational Physics and Applied Math (CPAM) capability review. This committee had seven external members. In both reviews the CoCoMANS project was rated overall as outstanding / excellent. Both committees see the project as making good progress, having the potential for significant long-term impact, and being in a leadership role.

The plasma application sub-area has made excellent progress in FY-13. A fundamental manuscript on the High-Order Low-Order (HO-LO) approach to electrostatic problems has been accepted for publication in the SIAM J. of Sci. Comput. The fundamental HO-LO electromagnetic algorithm has been developed and tested in prototype software. Two high profile paradigm shift physics problems have been defined and a paradigm shift report has been written. We have made good progress on mini-apps. Initial implementation of the HO-LO algorithm on multi-node many-core hardware has been successful and has clearly validated our "partial replication" implementation strategy. We have clearly demonstrated significant flops for minimal node-to-node communication. Initial HO solver implementation on GPUs has been successful and has clearly validated our "physics code abstraction" concept allowing for efficient implementation on multiple hardware types. We have submitted a manuscript on aspects of this success to the Supercomputing 2013 (SC13) conference in Denver CO (November

2013). Additionally, CoCoMANS plasma application talks where given at the APS Division of Plasma Physics meeting (Nov 2012) and the SIAM Computational Science and Engineering (CS&E) meeting (February 2013).

The ocean application sub-area has made excellent progress in FY-13. The HO-LO algorithmic approach to the free-surface ocean model has been solidified through prototype testing. We will proceed with an implicit LO solver and an explicit HO solver implemented utilizing the Jacobian-Free Newton-Krylov method and nonlinear elimination. We have defined a first level paradigm shift problem and vetted it with LANL ocean modeling experts. We have begun to write a paradigm shift document for the ocean application. We have a well define prototype / mini-app plan which will provide the required testing prior to compact application development. There has been initial progress on mini-app development and implementation on multi-node many-core hardware. We have executed initial on-node many-core parallel scaling studies and profiling studies. An initial HO-LO algorithm manuscript is in the review process. We have given talks on the ocean application at Frontiers in Computational Physics (Dec 2012), the SIAM Computational Science and Engineering (CS&E) meeting (February 2013), and the Copper Mountain Conference on Multigrid Methods (April, 2013).

During FY-13 we have had one PhD student (Jeff Willert, Applied math, NCSU) successfully defend his dissertation and accept a post doc position in T-3. We have converted a post masters student (Josh Payne, MS Nuc E, MIT) to a staff position in CCS-7. Finally, we began supporting a new PhD student (Chris Leibs, Applied Math, UC Boulder).

Future Work

In each application area, a large faction of initial algorithm development is done, significant prototyping software has been developed, and a first iteration idea of mapping these algorithms onto emerging architectures is in place. Our primary task for FY14 will be the development and implementation of mini-apps onto the Darwin cluster and gathering some profiling data from these mini-apps. Of course, this primary task will be executed with significant communication across the two application areas. The goal of this task will be to obtain the profiling data required to execute the first and second co-design iterations for each of the application areas.

To execute on our primary task we will need to execute on a number of sub-tasks in order. First, we must build adequate documentation of our prototype software to aid in the planning and development of the mini-apps. Next, some choices of language and programming models must be made in order to implement the mini-apps on the CCS-7 Darwin cluster. With the mini-apps implemented on Darwin, we must collect enough profiling data to isolate communication bottlenecks, determine the level of asynchronous computation, and to help understand where and how to overlap communication with computation.

With this profiling information in hand we can perform, and document, a co-design iteration. This will result in some level of refinement of the scale-bridging algorithms to account for the feedback from the initial mini-app work. At this point we will be able to add a level of detail to our compact-app plan in each application area. At this point we will also be able to define and develop specific software kernels, in support of each compact-app, which will be used in specific hardware vendor interactions.

Conclusion

The technical impact of this project will be a roadmap leading to a quantum leap forward in computational science for a variety of applications on modern architectures. No general scale-bridging algorithm of the type we propose has gone through a computational co-design activity. As a result of demonstrating a paradigm shift in specific application areas, we will define a computational co-design blue print for system-scale simulation with fine-scale physics fidelity for several applications. Furthermore, we will obtain a quantifiable understanding of the potential of various architectures to achieve such simulations resulting from our detailed interaction with vendors.

Publications

Chen, G., L. Chacon, C. A. Leibs, D. A. Knoll, and W. Taitano. Fluid preconditioning for Newton-Krylov-based, fully implicit, electrostatic particle-in-cell simulations. To appear in J. Comput. Phys..

Knoll, D. A.. Computational co-design of multi-scale-applications in the natural sciences: CoCoMANS. 2013. LANL Computational physics and applied math external capability review.

Knoll, D. A., L. Chacon, W. Daughton, and J. Payne. Plasma paradigm shift document for the CoCoMANS project. 2013. LA-UR-13-22126.

Newman, C., and D. A. Knoll. Physics-based preconditioners for ocean simulation. To appear in SIAM J. of Scientific Computing.

Payne, J., D. A. Knoll, A. McPherson, W. Taitano, L. Chacon, G. Chen, and S. Pakin. Computational co-design of a multiscale plasma application: a process and initial results. Presented at International Parallel and Distributed Processing Symposium. (Phoenix AZ, May 19-23,

2013).

Taitano, W., D. A. Knoll, L. Chacon, and G. Chen. Development of a consistent and stable fully implicit moment method for a Vlasov-Ampere particle-in-cell system. To appear in SIAM J. of Scientific Computing.

Willert, J., C. T. Kelley, D. A. Knoll, and H. Park. Hybrid deterministic / monte carlo neutronics. To appear in SIAM J. of Scientific Computing.

Hierarchical Sparse Models for Robust Analysis of Video Data

Steven P. Brumby
20120103DR

Introduction

Vision is one of the hardest and most intriguing problems in artificial intelligence and computer science. Advances in the field have hinged on three fundamental challenges: (1) how to create mathematical models of natural video sequences that can generate and interpret the visual scene; (2) how to learn image feature representations in such models across many spatial and temporal scales and for many object categories; and, (3) how to exploit the sheer size and richness of large-scale video datasets now becoming available. These three problems not only need to be solved together but are now within reach as a result of new theoretical, experimental and computational advances. Our project will create novel video analysis models and algorithms that we expect will approach human analyst performance and will surpass human speed.

Out team brings together world-class researchers in statistical modeling, computer vision, and high performance computing. We will pursue new research directions for three complementary areas of information science and technology: (1) develop semi-supervised learning algorithms to build multi-category deep probabilistic networks and study the performance of these models and algorithms on real-world data-sets with application to object detection, classification, and change/anomaly detection; (2) extend the theoretical framework of sparse representations and compressive sensing to learn hierarchical sparse representations that describe video data of natural scenes at many spatial/temporal scales and many levels of object complexity; and, (3) exploit many-core CPU and massively parallel GPU (graphical processing unit) computing technology for efficient training and fast execution of our models and algorithms, and explore size, weight and power (SWaP) constraints on algorithm and software design for next-generation smart sensors.

Benefit to National Security Missions

The theoretical framework, algorithms and codes proposed in this project will provide a solid basis for new information science and technology capability to support several of LANL's core mission areas. Robust, fast, automated understanding of video has the potential to revolutionize analysis of large-scale video data of experiments and simulations, global-scale environmental science, proliferation detection, and safety and security applications (perimeter security, workplace safety monitoring, remote hazardous inspections). This capability will also significantly impact DOE/NNSA and our USG partners by enabling: autonomous vehicles using passive video sensors, automated threat detection, forensic imagery and video analysis tools, persistent surveillance video tools for warfighter support, forest fire monitoring, border security, remote inspections of infrastructure, disaster response, and robotic space exploration. We will present our results at leading conferences, publish in high impact scientific journals, seek opportunities to brief potential sponsors, and develop white papers and proposals for demonstrations and follow-on projects.

Progress

Project is proceeding well, with progress on the core technical goals.

As planned, as of mid-FY13 we have now integrated the advanced sparse representation algorithms (non-convex basis pursuit denoising algorithms) into the high performance codes developed in FY13 (PANN), producing a new code we call VAST (Video Analysis and Search Technology). We were the highest-ranked Institutional Computing proposal for 2013, and have been awarded 1.5M core-hours/years for 2013 and 2014, which will cover all the key work and demonstrations planned. The team has now produced a total of 22 publications: 1 published Journal publication (IEEE Trans. Signal Processing), 14 refereed/published conference proceedings

papers (including high-impact ICASSP and IJCNN), 2 refereed published abstracts, and 5 unpublished conference papers (SIAM, DOE CoDA, invitation-only Snowbird Learning Workshop).

The team has identified and is collecting a new partially-labeled video dataset to support our core research, the Twitter Vine social media video dataset of public data, currently being posted worldwide at a rate of ~1M videos/day. We now have over 1 petapixel of video from this source, which has generated significant interest amongst sponsors and visitors. Social media video is an exciting new type of data, with many real-world applications ranging from epidemiology to facility security to intelligence, and the volume of social media video is expected to explode with the arrival of wearable networked video cameras (e.g., Google Glass). This data complements existing holdings of satellite imagery, aerial video, ground video, astronomical imagery, and social media (still) imagery that we continue to work on.

We are working with LANL Technology Transfer (TT) Division to support Intellectual Property (IP) protection and licensing of tools developed under our LDRD-DR. TT has contracted external counsel to support three patent filings based on our work.

This year we organized and co-sponsored a CNLS Workshop on Statistical Image Analysis in conjunction with our mid-project review. Feedback from our mid-project review was very encouraging.

The capability we are developing under this LDRD-DR has have brought in a number of DoD and USG Phase I demonstration projects and members of our team are supporting new projects won from DARPA (DARPA/MTO UPSIDE program) and NNSA+DTRA, with total funding exceeding 2M$. Several proposals for additional follow-on projects are in preparation, with Program Development funding from GS-PO. We have also started developing a collaboration with New York University (NYU) Polytechnic Center for Urban Science and Progress (CUSP), which grants us access to urban remote sensing video and social media datasets that directly support our core technical goals and position us for follow-on projects.

With regards to personnel changes, Post-Doc Zhengping Ji left LANL for a position at Samsung Research in Pasadena, CA. Graduate Student Dylan Paiton was accepted into the UC Berkeley Vision Science Ph.D. program as the student of Prof. Bruno Olshausen. Post-Masters student Scott Halverson from D-3 has joined the team, and we are currently interviewing potential Post-Docs to replace Zhengping. We are also supporting one of the student teams at this year's LANL Engineering Institute's Dynamics Summer School, which provides us with the opportunity to work with video data collected by a small remotely-piloted helicopter.

Future Work

As per our original project proposal, FY13 work will focus on the following tasks:

1. Semi-supervised multi-class learning - we will extend our models of sparse dictionary learning to greater numbers of object categories (i.e., ~1000 common object categories), using unsupervised learning to describe the unlabeled video frame backgrounds. Our goal is to compare our new algorithms to the state-of-the-art using the annual public ImageNet Large-Scale Visual Recognition Challenge (ILSVRC) as our benchmark.
2. Non-linear low dimensional + sparse models - we will extend our models of low rank + sparse frame decompositions to incorporate sensor platform motion and the non-linear video frame transformations induced by our multi-scale, multi-object learned dictionaries. This work will contribute to our ILSVRC benchmarking, and to analysis of video sequences.
3. MPI/GPU code development - we will implement the above novel algorithms for our supercomputing platforms, including LANL's new 200+ GPU "Moonlight" Institutional Computing resource.

Conclusion

We will develop a neuroscience-inspired computer vision system based on a hierarchical sparse generative model executing faster-than-real-time processing of natural video. This system will learn robust, multi-scale features for reliable data triage, and learn to reconstruct the relevant parts of the signal from a representation that serves as a basis for classification, segmentation, and change detection. This capability will support applications in proliferation detection, warfighter support, environmental science, and large-scale visualization of simulations. Our theoretical framework and high performance computing algorithms could also be applied to forensics, genomics, materials science, spectral analysis, and audio and text data-sets including web text.

Publications

Bachega, L., J. Theiler, and C. Bouman. Evaluating and improving local hyperspectral anomaly detectors. 2011. In 2011 IEEE Applied Imagery Pattern Recognition Workshop: Imaging for Decision Making, AIPR 2011 ; 20111011 - 20111013 ; Washington, DC, United States.

, p. var.pagings.

Brumby, S.. Image fusion for remote sensing using fast, large-scale neuroscience models. 2011. In Multisensor, Multisource Information Fusion: Architectures, Algorithms, and Applications 2011 ; 27-28 April 2011 ; Orlando, FL, USA. Vol. 8064, p. 806402 (8 pp.).

Brumby, S. P., M. I. Ham, and G. T. Kenyon. Semi-supervised learning of high-level representations of natural video sequences. Presented at Computational and Systems Neuroscience (COSYNE) . (Salt Lake City, UT, 23-26 Feb 2012).

Chartrand, R.. Nonconvex Splitting for Regularized Low-Rank plus Sparse Decomposition. Invited presentation at Joint Mathematics Meetings. (Boston, MA, 4-7 Jan. 2012).

Chartrand, R.. Nonconvex Splitting for Regularized Low-Rank + Sparse Decomposition. Invited presentation at Compressive Sensing Workshop: Leveraging Sparsity at UCLA & Beyond. (Los Angeles, CA, 6-8 March 2012).

Chartrand, R., and B. Wohlberg. A nonconvex ADMM algorithm for group sparsity with sparse groups . 2013. In IEEE International Conference on Acoustics, Speech, and Signal Processing . (Vancouver, BC, 26-31 May 2013). , p. ?. Vancouver: IEEE.

Chartrand, null.. Image processing and reconstruction. 2012. LDRD.

Galbraith, A. E., R. Chartrand, B. Wohlberg, and S. P. Brumby. Simulating vision through time: Hierarchical, sparse models of visual cortex for motion imagery. 2012. In IEEE Applied Imagery and Pattern Recognition (AIPR) 2012. (Washington, DC, 23-25 Oct, 2012). , p. 1. Washington, DC: IEEE.

Gunawardena, N., J. Heit, G. Lederman, A. Galbraith, D. Mascarenas, and S. P. Brumby. Remote placement of magnetically coupled ultrasonic sensors for structural health monitoring . Invited presentation at International Modal Analysis Conference. (Orlando, FL, 3-6 February, 2014).

Huang, W., Z. Ji, S. Brumby, G. Kenyon, and L. A. Bettencourt. Development of invariant feature maps via a computational model of simple and complex cells. 2012. In 2012 Annual International Joint Conference on Neural Networks, IJCNN 2012, Part of the 2012 IEEE World Congress on Computational Intelligence, WCCI 2012 ; 20120610 - 20120615 ; Brisbane, QLD, Australia. , p. var.pagings.

Ji, Z., J. Theiler, R. Chartrand, G. Kenyon, and S. P. Brumby. SIFT-based sparse coding for large-scale visual recognition. 2013. In SPIE Defense, Security, and Sensing. (Baltimore, MD, 29 April- 3 May 2013). , p. 87500K. Baltimore: SPIE.

Ji, Z., W. Huang, and S. Brumby. Learning sparse representation via a nonlinear shrinkage encoder and a linear sparse decoder. 2012. In 2012 Annual International Joint Conference on Neural Networks, IJCNN 2012, Part of the 2012 IEEE World Congress on Computational Intelligence, WCCI 2012 ; 20120610 - 20120615 ; Brisbane, QLD, Australia. , p. var.pagings.

Ji, Z., and S. P. Brumby. Integrating Bottom-up and Top-down Visual Attention for Object Segmentation. Presented at Vision Sciences Society (VSS) 2012 Annual Meeting. (Naples, FL, 11-16 May 2012).

Moody, D. I., S. P. Brumby, J. C. Rowland, and C. Gangodagamage. Learning sparse discriminative representations for land cover classification in the Arctic. 2012. In SPIE Optics + Photonics Annual Meeting 2012. (San Diego, CA, 11-16 Aug. 2012). , p. 85140Q. San Diego: SPIE.

Moody, D., S. Brumby, K. Myers, and N. Pawley. Sparse classification of rf transients using chirplets and learned dictionaries. 2011. In 45th Asilomar Conference on Signals, Systems and Computers, ASILOMAR 2011 ; 20111106 - 20111109 ; Pacific Grove, CA, United States. , p. 1888.

Paiton, D. M., S. P. Brumby, G. T. Kenyon, G. J. Kunde, K. D. Peterson, M. I. Ham, P. F. Schultz, and J. S. George. Combining Multiple Visual Processing Streams for Locating and Classifying Objects. Presented at IEEE Southwest Symposium on Image Analysis and Interpretation (SSIAI) 2012. (Santa Fe, NM, April 22-24, 2012).

Rodriguez, P., and B. Wohlberg. Iteratively Reweighted Least Squares for L1 Problems: Boring But Still Effective. Presented at 2012 SIAM Conference on Imaging Science. (Philadelphia, PA, May 20-22 2012).

Rodriguez, P., and B. Wohlberg. Fast principal component pursuit via alternating minimization . Invited presentation at IEEE International Conference on Image Processing . (Melbourne, AU, 15-18 Sept, 2013).

Rodriguez, P., and B. Wohlberg. A comparison of the computational performance of iteratively reweighted least squares and alternating minimization algorithms for l1 inverse problems . 2012. In IEEE International Conference on Image Processing. (Orlando, FL, 30 Sept- 3 Oct, 2012). , p. 3069. Orlando: IEEE.

Theiler, J., B. Wohlberg, and R. Chartrand. Local Robust Principal Components for Nonlinear Datasets,. Presented at 2012 SIAM Conference on Imaging Science. (Philadelphia, PA, May 20-22 2012).

Theiler, J., G. Cao, L. Bachega, and C. Bouman. Sparse Matrix Transform for Hyperspectral Image Processing. 2011. IEEE JOURNAL OF SELECTED TOPICS IN SIGNAL PROCESSING. 5 (3): 424.

Theiler, J., and B. Wohlberg. Detection of spectrally sparse anomalies in hyperspectral imagery. 2012. In 2012 IEEE Southwest Symposium on Image Analysis and Interpretation, SSIAI 2012 ; 20120422 - 20120424 ; Santa Fe, NM, United States. , p. 117.

Theiler, J., and B. Wohlberg. Regression framework for background estimation in remote sensing imagery. To appear in Institute of Electrical and Electronics Engineers (IEEE) Workshop on Hyperspectral Image and Signal Processing: Evolution in Remote Sensing (WHISPERS) . (Gainesville, FL, 25-28 June 2013).

Theiler, J., and B. Wohlberg. Detection of unknown gas-phase chemical plumes in hyperspectral imagery. 2013. In SPIE Defense, Security, and Sensing. (Baltimore, MD, 29 April- 3 May 2013). , p. 874315. Baltimore: SPIE.

Venkatakrishnan, S. V., C. A. Bouman, and B. Wohlberg. Plug-and-play priors for model based reconstruction. 2013. Purdue University, ECE Technical Reports.

Venkatakrishnan, S. V., C. A. Bouman, and B. Wohlberg. Plug-and-play priors for model based reconstruction. To appear in IEEE Global Conference on Signal and Information Processing . (Austin, TX, 3-5 Dec. 2013).

Wohlberg, B.. Inpainting by Joint Optimization of Linear Combinations of Exemplars. 2011. IEEE Signal Processing Letters. 18 (1): 75.

Wohlberg, B., R. Chartrand, and J. Theiler. A Robust Local Linear Data Decomposition. Presented at Learning Workshop. (Snowbird, UT, April 3-6, 2012).

Wohlberg, B., R. Chartrand, and J. Theiler. Local Principal Component Pursuit for Nonlinear Datasets. Presented at IEEE International Conference on Acoustics, Speech, and Signal Processing (ICASSP) (2012). (Kyoto, Japan, March 25-30, 2012).

Empowering the Expert: Machine Learning with User Intelligence

Reid B. Porter
20130013DR

Introduction

Scientists and intelligence analysts are very good at understanding and exploiting the specialized datasets with which they work; the problem is that there is too much of this data for them to look at. Data processing tools help to clean up, filter and identify the most relevant subsets of data, but recent developments in machine learning have indicated that there is a grand opportunity to dramatically enhance the efficiency and accuracy of this process, by involving the user in a more interactive dialog.

Traditional machine learning employs a fixed set of labels, supplied up-front by the user, to optimize data processing tools before they are applied to a larger dataset or data archive. This approach has proven successful both in theory (rigorous proofs) and in practice (commercial applications). Machine learning with user intelligence pushes the state of the art in two directions.

From up-front learning to interactive learning

Traditional machine learning tools stop when the human steps in. This means the expert is still the bottleneck in data exploitation: spending too much time in tedious and repetitive post-processing tasks and not enough time on validation and research. Machine learning with user intelligence starts when the human steps in, and tools are a force multiplier, where the user's intelligence is the force to be multiplied, not an expense to be minimized.

From label learning to relational learning

Machine learning with user intelligence formalizes the interactive dialog with relational objects, stated in terms of motifs, clusters, alignments, matches and other generalizations of standard labels. By providing additional interface "bandwidth" between the domain expert and the data processing tool (and thus creating a better expression of the dialog in terms of graphical models), higher quality associations are produced, and more effective tools can be built.

Benefit to National Security Missions

This project empowers scientists and defense analysts to exploit specialized data in less time, and with greater accuracy, both by automating tedious and repetitive tasks and by enabling them to focus on validation and higher-level objectives. This general capability will be valuable to a large number of government agencies and missions. This project will also develop specific tools for (at least) two LANL applications.

Nuclear Material Forensics

Experts draw upon a vast understanding of the nuclear fuel cycle to quantify spectroscopy images, but they spend weeks each year manually correcting tool estimates of particle and grain boundaries. This project's image quantification advances will be valuable to DOE, DHS, and DOD.

Cyber Security

Analysts draw upon a deep understanding of the computer network as well as attacker behavior to determine if anomalous network traffic requires further investigation. However there is simply too many anomalies for analysts to perform even the most cursory triage. This project's cyber-security tools will be valuable to DOE, DHS and DOD, in particular for the protection of the NNSA complex itself.

Progress

Within the first year we developed and submitted a comprehensive review article on 'Interactive Machine Learning.' This article provides a unified view of this emerging field and provides a road-map for both our project, and the larger community. Our team was invited to present this article at one of the first workshops on Interactive Machine Learning that was held in February 2013. The roadmap articulates the two main technical

thrusts in our project.

We call the first thrust the 'Training Dialog', and it moves us from up-front learning to interactive learning (as described in the project description). Progress included:

- We developed a number of experiments to quantify the benefit of having the 'user-in-the-loop' compared to traditional batch learning.
- We are also developing an Expectation Maximization based framework for interactive anomaly detection that can adapt to different types of user input. The approach starts with non-interactive machine learning tools (e.g. anomaly or change detection tools) and then incorporates increasingly complex user feedback (e.g. labels for one class, labels for multiple classes etc.).
- We developed a number of new machine learning methods that expand the range of tools and potential applications that we can use for interactive learning.
- We also collaborated with the Cyber-Security team at Los Alamos, to develop a prototype software interface for triage of network traffic anomalies. This prototype will enable us to test our methods on real network traffic data.

We call the second thrust the 'Training Vocabulary, and it moves us from label learning to relational learning (as described in the project description). Progress included:

- We developed new algorithms that learn from user examples to 'merge' segments of an image into larger (more meaningful) regions. These algorithms exploit 'connectivity' properties and provide a foundation for developing tools for image quantification applications in material science, bio-medical imaging and remote sensing.
- We developed a test and evaluation framework for 'learning to merge' and also developed a software prototype for demonstrating our tools. We also started to prototype a web interface for this application with the objective of hosting a crowd-sourced experiment. This experiment will provide a more extensive test and evaluation framework for 'learning to merge' and will help increase the profile of our project within the larger research community.
- The 'merge' problem is an example of a much larger (and fundamental) problem in machine learning known as structured output prediction, and this year our team has advanced the theoretical underpinnings for this problem. These advances make new connections between Belief Propagation and Perfect Matchings.

A number of proposals have been developed based on our work. These include:

- 'Millions of Spies, Millions of Eyes: Active Crowdsourcing for Nonproliferation', Christy Ruggiero, Reid Porter. This proposal builds on work with our collaborators at UCSC [10] and it proposes to develop a crowd-sourced interactive learning system for nonproliferation and arms control (submitted to DOE).
- 'Maximizing Relevance Feedback for Intelligence Message Traffic Analysis', David Izraelevitz, Reid Porter, submitted to DHS. This proposal builds on our advances in the 'Training Dialog' and proposes to integrate, test and deploy these advances to DHS tools and applications.

Future Work

Task: Develop methods for structured output prediction.
Goal: Efficient and general purpose learning algorithms to support increased user interaction.

Task: Develop interactive learning strategies for Graphical Models.
Goal: Algorithms that are robust to missing data and/or limited training examples.

Task: Identify and develop efficient strategies for combining inference and learning.
Goal: A better understanding of the accuracy and robustness of interactive learning with graphical models.

Task: Implement initial tools for image quantification and cyber-security applications.
Goal: Software that domain experts can use on practical datasets and an experimental platform for the project.

Task: Develop synthetic and benchmark experimental frameworks for interactive learning.
Goal: An ability to evaluate the accuracy and utility of tools for practical applications at various levels of interaction.

Conclusion

Our goal is to provide a general framework for data processing tools that directly targets the post-processing bottleneck. We emphasize graphical models in this development, as these provide a balance of rigor and flexibility on the learning front and domain adaptability on the interactivity front. An additional goal is to develop new

tools, optimized for specific applications in nuclear material forensics and cyber-security, where there is a critical need to make data exploitation more accurate and more efficient.

Publications

Chertkov, M., A. Gelfand, and J. Shin. Loop calculus and bootstrap-belief propagation for perfect matchings on arbitrary graphs. arXiv:1306.1267.

Gelfand, A., J. Shin, and M. Chertkov. Belief propagation for linear programming. CoRR, arXiv:1305.4130.

Harvey, N.. User driven sampling strategies in visual data exploitation. To appear in Visualization and Data Analysis, SPIE, 2014.. (San Franciso, 5-6 February, 2014).

Loxley, P.. Learning dictionary statistics from natural images. CoRR. abs/1304.0023.

Oyen, D., A. Niculescu-Mizil, R. Ostroff, A. Stewart, and V. P. Clark. Reliable differential dependency network analysis. Presented at International Conference on Machine Learning. (Beijing, China, 21-26 June).

Oyen, D., and T. Lane. Bayesian discovery of multiple Bayesian networks via transfer learning. To appear in IEEE International Conference on Data Mining. (Dallas, Texas, 7-10 Dec).

Porter, R. B., S. Lundquist, and C. Ruggiero. Learning to merge: a new tool for interactive mapping.

Porter, R., J. Theiler, and D. Hush. Interactive machine learning in data exploitation. To appear in IEEE Computers in Science and Engineering.

Shin, J., A. Gelfand, and M. Chertkov. A graphical transformation for belief propagation: maximum weight matchings and odd-sized cycles. CoRR, abs/1306.1167.

Theiler, J.. Spatio-spectral anomalous change detection in hyperspectral imagery. To appear in 1st IEEE Global Signal and Information Processing Conference. (Austin, Texas, 2-3 Dec).

Theiler, J.. Matched pair machine learning. To appear in Technometrics.

Vaish, R., S. Lundquist, R. Porter, and J. Davis. Crowd-sourcing bounding box annotations for computer vision. Presented at HCOM 2013: Human computation. (Palm Springs, California, 6-9 Nov).

Wolpert, D., and D. Rajnarayan. Using machine learning to improve stochastic optimization. 2013. In Twenty-Seventh AAAI Conference on Artificial Intelligence. (Bellevue, Washington, 14-15 July). , p. 146. Bellevue, Washington: AAAI.

Multi-perspective Network-scale Modeling and Detection for Cyber Systems

Michael E. Fisk
20110093DR

Abstract

Our work was at the intersection of "big data" or data-intensive computing, statistics, graph modeling, and graph algorithms. We established a new regime of cyber security detection and defense that uses whole-network traffic modeling and detection. In contrast, previous detection techniques were largely myopic and unable to detect the most subtle of contemporary attacks. In our approach, cyberspace activity from multiple observation perspectives is represented as a graph with edges (and nodes) described as a time-series measurements. We then build data-driven models of the localized dynamics in these graphs and use those models to detect anomalous change in the dynamics. In particular we focus on change that is consistent with attacker behavior. We use similar techniques to examine the dynamic execution of malicious software and to detect and cluster malicious software based on a combination of dynamic models and static features of the software. Finally, we developed predictive models that examine the resilience of command and control overlay networks (including botnets) to different strategies for detecting and disrupting those communications networks.

Background and Research Objectives

The field of computer intrusion detection is dominated by detection decisions that can be made form single observation points of activity from a single actor and/or against a single target. Further, most previous work is focused on signature-based techniques. Our objectives were to fuse different observational perspectives together in a single analytical context, to model the normal dynamics of these behaviors, to enable model-based detection of anomalous change that is consistent with malicious activity.

This work leveraged previous work at Los Alamos National Laboratory on computer misuse and anomalous change detection and to expand that work to the context of graphs where relationships between entities are as important as time-series observed at single points in the graph.

Scientific Approach and Accomplishments

Our accomplishments were in two major areas which are described in the following sections on subgraph modeling and detection and on whole-graph modeling to detect and cluster malware execution.

Model-Based Anomalous Subgraph Detection

For this work, we have developed a family of temporal graph models. The building blocks for those models are models for individual edges and nodes. To model activity time-series for each edge in a graph, we first developed two-state hidden Markov model that learns two different distributions of activity representing active and inactive (or high and low) levels of activity commonly seen in these edges. These models are then used to measure the likelihood of new events with respect to previous activity. Fitting these models to data is computationally intensive. For example, using our data-intensive computing framework, we modeled a month's worth of traffic on the LANL network (550,000 edges modeled). That computation required 1.5 CPU-years, but was completed in just over 2 days on a 256-core cluster. In subsequent work, we discovered that for some important real-world data sets, new edge formation is much more statistically significant than increased usage of previously existing edges. We developed and implemented models for the formation of new edges in the graph. We modeled the creation of new edges as a process that is dependent on the edge creation behavior of the two nodes participating in that edge.

We have examined multiple methods for identifying subgraphs which contain coincident anomalies. First, we developed a detection approach that enumerates every subgraph that contains a fixed shape (such as a 3-hop line or a star) and computes a joint likelihood of the time-series data observed across that entire graphlet.

By simple combinatorics, there are immense numbers of these graphlets in real-world graphs, but we have developed a hybrid parallel (both SMP and MPI) library for enumerating these graphlets and computing likelihood (or other arbitrary computation) on each. Using the LANL network data set again, we enumerated and measured the anomalousness of 300 million graphlets in 5 seconds on a 48-core computer. We have also scaled this anomalous graphlet detection work up to 1015 graphlets in less than 2 minutes of computation. We validated this techniques against well-understood data sets in LANL's own network data and demonstrated that actual intrusions were among the most anomalous events during those time periods.

We have also modeled the frequency at which graphlets occur in a given location in a graph in order to determine when anomalous structures exist and utilized additional criteria to reduce the search space to events that are consistent with certain malicious behaviors. For example, we developed the notion of telescoping subgraphs in which the duration of one edge encompasses the duration of subsequent edges in the subgraph. Finally, we performed some initial work to model attacker utility functions such that we can more generally restrict the search to anomalies that represent rational decision making by an adversary.

Much of our work was on network flow data, but we also developed models and associated detection results that incorporate observations of web requests, anomalous processes on nodes, and network traffic between nodes. We also developed techniques to register e-mail events on computer communication graphs by mapping users to computers based on e-mail authentication and data and where e-mail is sent.

We have also evaluated how well peer-to-peer botnet communications graphs can be detected when sensor coverage limits visibility to subsets of the communications graph and strategies that bot-herders could deploy to improve the resilience and robustness of peer-to-peer based botnet structures and possible countermeasures by the defender as a response. We have expanded this work, by allowing bots to use spoofing packets to hide their identities. The number of spoofing source IP addresses per bot is generated from high-variations distributions, so the sum over all observed bots converges slowly. Such behavior allows a bot-herder to obfuscate the size of a botnet. As a final part of our focus on botnets, we explored the idea of graph-based detection bots hidden in Twitter-like online social networks. Our key idea is to look for the core of large graphs, which remain relatively stable over its evolution. Botnets are more likely to stay in the periphery of such large graphs. We developed efficient algorithms to find such a core of a large graph, after removing which the remaining graph has only small strongly connected components; thus only a small number of nodes and messages need to be monitored. We worked on the Twitter dataset with more than 40 million nodes and 1.2 billion following relationships. We have modeled how malware spread in online social networks is affected by the structure and activity patterns of social network users.

Finally, we have also combined Bayesian networks and game theory to develop a comprehensive framework for evaluating consequences of DDoS attacks and effectiveness of multi-layer defense mechanisms. We have also developing graph similarity-based metrics and software to study evolution of Email communications. We also examined social networks, the spread of information in those networks, and how to detect malicious use of those networks. We developed graph-theoretic tools to identify suspicious nodes that can potentially pass C&C (command and control) information to a large number of individual bots using online social networks.

Malware Detection and Clustering

We developed a novel approach to malware detection based on the analysis of dynamic instruction traces from a large number of executable files. The base method can be trivially extended to an online procedure, provided the engineering hurdle of obtaining a sample of the instructions executed by a given process can be satisfactorily addressed. An execution trace collected from a running process is summarized by a state transition probability matrix, P, like that used to represent the probabilistic evolution of a Markov Chain. P is estimated by combining counts on all possible consecutive pairs of instructions with a prior model posing that the rows of P are independent Dirichlet vectors.

One binary classification approach that we developed is to model from estimated P matrices for a large number of known malicious and known benign software samples using nonparametric logistic regression on the elements of P. The elastic net technique is used to perform logistic regression with careful selection of useful variables from among the many thousands of predictors represented by the elements of P. We illustrate the utility of the method on a sample of malware, and compare the results favorably to other leading malware detection schemes (both signature and classification based). We also pursued a more classically statistical approach, using Dirichlet models to perform the classification. The false positive/true positive trade-off showed slightly better performance than the previous approach. In addition, these methods provide confidence intervals around the probability of maliciousness, providing analysts and automated methods with a quantification

of the uncertainty of the classification result. A top-tier statistics journal article on this work is in under review.

We have also pursued machine learning techniques on this same data. In this approach we use multiple graph kernels to provide distance metrics between pairs of Markov model graphs and use machine learning algorithms to build classifiers. We have developed a similar approach for anomalous change detection that identifies when a program's execution changes more than it usually does. We have developed new machine learning techniques, motivated by two goals. The first goal is to improve the classification of malware versus benign software. To this end, we have developed multi-view kernel methods, which combine various features of a given executable file. This approach is novel in the literature, and a paper has been submitted for review. The results are very promising, achieving far better performance than current state-of-the-art signature methods, as well as other statistical methods.

Second, we have developed methods for relating classes of malware to each other, with the ultimate goal of identifying families of malware and establishing a phylogenetic tree. Initial findings include good clustering of different types of malware. In addition, the malware which did not fall cleanly into a cluster, but was fairly close to two different clusters actually informed us on the content of those two clusters. It was discovered that in fact those two clusters tended to have some features which were common between them, and the malware which lay between the clusters were exemplified by these features. This is a promising aspect of this research, as it provides promise that research into phylogenetic trees is indeed tractable.

Impact on National Missions

This project will positively impact cyber security missions executed by both LANL's internal security program, essential to our DP mission, and Global Security programs, with secondary benefits on our commercial CRADAs (we are not funding any CRADAs, but technology developed under this LDRD may become background intellectual property that results in funding of subsequent work by an existing CRADA partner). Our advances have put us on a path to catch-up with and keep pace with contemporary, undetectable adversaries, and build a base for the future. Moving forward, we are also pursing ways to apply these dynamic graph modeling capabilities to other strategic analytical problems including biosurveillance and video analysis. Finally the data-intensive demands of this problem have led to insight on data-intensive computing, use of LANL's HPC platforms for data-intensive computing, and data management methodologies and abstraction layers for diverse, high-volume data.

Publications

Anderson, B., C. Storlie, and T. Lane. Multiple Kernel Learning Clustering with an Application to Malware. 2012. In Data Mining (ICDM), 2012 IEEE 12th International Conference on. , p. 804. IEEE.

Anderson, B., C. Storlie, and T. Lane. Improving malware classification: bridging the static/dynamic gap. 2012. In Proceedings of the 5th ACM workshop on Security and artificial intelligence. , p. 3. ACM.

Anderson, B., D. Quist, J. Neil, C. Storlie, and T. Lane. Graph-Based Malware Detection Using Dynamic Analysis. 2011. Journal in Computer Virology. 7 (4): 247.

Anderson, B., D. Quist, and T. Lane. Detecting Code Injection Attacks in Internet Explorer. 2011. In 35th Annual IEEE International Computer Software and Applications Conference STPSA workshop, 2011. (Saarbruecken, 6-10 June 2011). , p. 90. Saarbrucken: IEEE.

Arackaparambil, C., and G. Yan. Wiki-watchdog: Anomaly detection in wikipedia through a distributional lens. 2011. In Web Intelligence and Intelligent Agent Technology (WI-IAT), 2011 IEEE/WIC/ACM International Conference on. (Lyon, France, 22-27 August 2011). Vol. 1, p. 257. New York: IEEE.

Djidjev, H. N., and M. Onus. Scalable and Accurate Graph Clustering and Community Structure Detection. 2013. IEEE Trans. Parallel Distrib. Syst.. 24 (5): 1022.

Djidjev, H., G. Sandine, C. Storlie, and S. Vander Wiel. Graph Based Statistical Analysis of Network Traffic. 2011. In Ninth Workshop on Mining and Learning with Graphs. (San Diego, CA, 21-22 Aug. 2011). , p. 1. San Diego, CA: IEEE.

Djidjev, H., and G. Sandine. Graph-Based Traffic Analysis for Network Intrusion Detection. 2011. TSC Science Highlights, LA-UR 10-06320.

Djidjev, H., and G. Sandine. Graph-Based Traffic Analysis for Network Intrusion Detection. 2010. In 2010 Annual Computer Security Applications Conference (ACSAC). (Orlando, F, 5-9 December 2010). , p. 1. Orlando, FL: ACM.

Eidenbenz, S., M. Marathe, and A. Sen. Editorial for Computer Networks special issue on ''Towards a Science of Cyber Security''. 2013. Computer Networks. 57 (10): 2119.

Jin, D., D. Nicol, and G. Yan. An Event Buffer Flooding Attack against DNP3-Controlled SCADA Systems. 2011. In Proceedings of the 2011 Winter Simulation Conference (WSC'11). (Phoenix, AZ, 5-9 December, 2011). , p. 1. Phoenix, AZ: IEEE.

Kakumanu, S., S. Eidenbenz, and R. Sivakumar. Lattice routing: A 4D routing scheme for multiradio multichannel ad hoc networks. 2011. Ad Hoc Networks. 9 (1): 95.

Kent, , and L. M. Liebrock. Differentiating User Authentication Graphs. 2013. In Security and Privacy Workshops (SPW), 2013 IEEE. , p. 72. IEEE.

Liu, L., X. Zhang, G. Yan, and S. Chen. Chrome extensions: Threat analysis and countermeasures. 2012. Network and Distributed System Security Symposium (NDSS). : 1.

Neil, J. C., B. D. Uphoff, C. B. Storlie, and C. L. Hash. Towards Improved Detection of Attackers in Computer Networks: New Edges, Fast Updating, and Host Agents. 2013. In 1st International Symposium on Resilient Cyber Systems.

Neil, J., C. B. Storlie, C. Hash, Brugh, Alexander, and M. Fisk. Scan Statistics for the Online Detection of Locally Anomalous Subgraphs. 2013. Technometrics.

Nguyen, N. P., G. Yan, M. T. Thai, and S. Eidenbenz. Containment of Misinformation Spread in Online Social Networks. 2012. WebSci '12 Proceedings of the 3rd Annual ACM Web Science Conference . : 213.

Pelechrinis, K., G. Yan, S. Eidenbenz, and S. Krishnamurthy. Detection of Selfish Manipulation of Carrier Sensing in 802.11 Networks. 2011. Mobile Computing, IEEE Transactions . : 1.

Rahman, M., G. Yan, H. Madhyastha, M. Faloutsos, S. Eidenbenz, and M. Fisk. iDispatcher: A unified platform for secure planet-scale information dissemination. 2013. Peer-to-Peer Networking and Applications. 6 (1): 46.

Rahman, S., G. Yan, M. Faloutsos, H. Madhyashta, S. Eidenbenz, and M. Fisk. iDispatcher: A Unified Platform for Secure Planet-Scale Information Dissemination. 2011. Los Alamos Unlimited Release LA-UR 11-02386.

Yan, G.. Peri-Watchdog: Hunting for Hidden Botnets in the Periphery of Online Social Networks. 2011. Los Alamos Unlimited Release.

Yan, G.. Peri-Watchdog: Hunting for Hidden Botnets in The Periphery of Online Social Networks. 2012. Computer Networks. : 1.

Yan, G., C. Arackaparambil, S. Bratus, and A. Caglayan. On-Tuning the Knobs of Distribution-based Methods for Detecting VoIP Covert Channels. 2012. In Proceedings of Hawaii International Conference on System Sciences (HICSS-45). (Hawaii, 4-9 January, 2011). , p. 2431 . Hawaii: IEEE.

Yan, G., D. Ha, and S. Eidenbenz. AntBot: Anti-pollution peer-to-peer botnets. 2011. Computer Networks. 55 (8): 1941.

Yan, G., G. Chen, S. Eidenbenz, and N. Li. Malware propagation in online social networks: Nature, dynamics, and defense implications. 2011. In 6th International Symposium on Information, Computer and Communications Security, ASIACCS 2011 ; 20110322 - 20110324 ; Hong Kong, China. , p. 196.

Yan, G., S. Chen, and S. Eidenbenz. RatBot: Anti-Enumeration Peer-to-Peer Botnets. 2011. Information Security. 1 (1): 135.

Zeng, Yuanyuan, Guanhua Yan, S. Eidenbenz, and K. Shin. Measuring the Effectiveness of Infrastructure-level Detection of Large-scale Botnets. 2011. In 2011 IEEE Nineteenth IEEE International Workshop on Quality of Service (IWQoS 2011) ; 6-7 June 2011 ; San Jose, CA, USA. , p. 1.

Zhang, R., J. Sun, G. Yan, and S. Zhang. Fine-grained private matching for proximity-based mobile social networking. 2012. In INFOCOM, 2012 Proceedings IEEE. (Orlando, FL, Mrach 25 - 30). , p. 1969. Orlando, FL: IEEE.

Correlations and Dynamics in Information Science

Robert E. Ecke
20110434DR

Abstract
Information, and its processing, transport, and vulnerability, are matters of national security. The understanding and management of information systems in computer and communication networks, biological systems and social dynamics play a vital role in multiple national security challenges. With this project, the Center for Nonlinear Studies (CNLS) targeted fundamental science challenges that are central to long-term strategies for improving information management. The science efforts which focus on understanding the effects of "correlations and dynamics" in information systems explored the effects of random influences (stochasticity), the consequences and prospects of coordinating the action of pairs or higher numbers of units or 'nodes', the dynamics of timing and coordinating signals, and the accuracy of network models.

Background and Research Objectives
The science of this project focused on understanding the effects of "correlations and dynamics" in information systems. This project targeted fundamental science challenges that are central to long-term strategies in information processing systems.

Research was organized around three basic themes in information science:

Bioinformatics: Sensing and processing of information, bioinformatics, and bio-inspired methods of speeding searches and fast processing of information.

Complex Networks: Modeling and analysis of complex systems, applied mathematics analysis of tractable models, methods to develop real-world models, description of epidemics, and the development of fast, robust methods for real-time cyber security analysis.

Algorithms, Optimization, & Control: Inference and learning with stochastic information, and statistical mechanics techniques to understand information science questions in the large systems limit.

Within these themes we applied information processing tools to address the application areas of HIV and SIV transmission, cyberphysical security, electrical power systems (smart grids), computer vision, cybersecurity, transport networks, and epidemic spreading.

Scientific Approach and Accomplishments
Bioinformatics
We began a study of the genetic mutations of the Hepatitis C virus (HCV). The genetic diversity can be analyzed together with a model of random mutations to predict time since infection. Preliminary results show that the different mutation mechanisms in HCV will require modeling using multiple overlapping random processes [1].

We studied the spread and evolution of viruses. We traced the spread and dynamics of the Latvian HIV-1 epidemic using phylogenetic tools, finding an unexpected decrease in viral divergence due to the existence of a fast and slow rate of spread occurring simultaneously in this epidemic. We re-analyzed a previously described HIV-1 transmission chain in light of a phylogenetic model and found, contrary to previous thinking, that it might not be possible to extract a unique transmission history [2]. This work has implications for court cases that rely on sequencing data to support transmission claims.

Most notably embodied by Google Flu Trends, real-time estimates of the impact of disease based upon Internet data such as search queries and Twitter messages are emerging. These approaches use linear models of a single data source to measure a small number of diseases (influenza and dengue fever). Our current work extended this research direction by using non-linear models that include interaction features to measure a variety of diseases across the globe, using multiple publically available data sources (Twitter messages, Wikipedia

access logs, and Wikipedia edit logs). This work also seeks to provide short-term forecasts or identify fundamental limitations of the data streams that make such forecasting impossible.

We studied methods to improve and extend simulations of bio-chemical networks such as signal transduction networks. A better understanding of the dynamics of signaling pathways would have a significant impact on cancer research. Unfortunately, typical systems of interest are too large to model using ordinary differential equations and are currently only amenable to simulation that is often slow. We developed an approximate model reduction method that takes advantage of the modular character of most biochemical networks. The technique harnesses short bursts of simulation to approximate knowledge of the (unknown) underlying differential equations [3]. This can then be used to significantly speed up simulations and even fed back into standard numerical analysis tool-kits to do stability or bifurcation analysis of the system.

Algorithms, Optimization, and Control

We developed image processing algorithms to learn objects from images of natural scenes. A major achievement was made by showing how you can learn a sparse (small data) representation of images to create an algorithm that accurately categorizes objects. This algorithm performs well on for recognizing noisy handwritten numerals and beats existing algorithms on community standard image labeling tests. One of the main approaches [4], [5] is a deep generative model. The models are generative in that they postulate possible images that fit the data, and deep in that they fuse information at multiple semantic levels. The models also incorporate sparse coding, processing information by representing it with a sparse set of coefficients. The hierarchical sparse coding approach, which allowed information to flow both up and down the semantic hierarchy, won the best poster paper award at the 2011 IEEE International Joint Conference on Neural Networks. More recently, ideas from continuous optimization led to the development of surrogate functions that allow the computational learning tasks to be performed much more efficiently. This work has been applied to classification of images [5], [6], identification of objects within images [5], and identification of transient astronomical objects.

In general information science-related efforts, we analyzed and generalized the Belief Propagation (BP) approach to computing the permanent (a quantity much like the determinant, but harder to calculate) of a non-negative matrix [7]. Known bounds and conjectures were verified in experiments, and some new theoretical relations, bounds and conjectures were proposed. We developed a simple greedy algorithm for learning the best planar Ising model to approximate an arbitrary collection of binary random variables (possibly from sample data), and applied the algorithm to modeling voting [8].

We considered various important problems in communications, e.g., decoding of Low-Density Parity-Check codes, detection in two-dimensional intersymbol interference channels (magnetic and optical storage, cellular networks), etc., and modeled them as inference problems over graphs.

We used our information science capabilities to improve materials modeling. In a major advance, we developed a new algorithm to simulate fermions coupled to a classical field. By using the technique of "automatic differentiation" as the basis of a numerical method, our algorithm decreases the cost of a calculation significantly, enabling simulations of unprecedented system sizes, and revealing previously unknown quantum phases. We obtained coarse-grained dynamics of a quenched ferromagnet, generalizing conformal field theory results on a two-dimensional Ising model to higher dimensional, anisotropic systems.

In the area of energy distribution, we developed an algorithm for determining the optimal placement and timing of battery exchange and charging stations (for plugin hybrid electric vehicles – PHEV) [9]. This project produced a novel gradient descent algorithm for optimizing the placement of the stations that relied on continuous time optimization formulations. One of the more interesting aspects of the approach was the first-ever ability to model demand for PHEV charging as a function of the stations already built. In other words, we can model situations where technology availability increases technology adoption (i.e., the availability of stations increases the adoption of PHEVs). We developed a heuristic procedure for optimizing the placement and sizing of flexible energy storage in a grid that includes renewable energy sources, and studied a model of stochastic temporal fluctuations in a power grid.

Networks

We analyzed data integrity attacks for smart grid applications [10]. Real power injections at loads and generators, and real power flows on selected lines in a transmission network are monitored and transmitted to the system operator. These are used in state estimation algorithms to make dispatch, re-balance and other energy management system decisions. Coordinated cyber attacks on power meter readings can be designed to be undetectable by any bad data detection algorithm. These unobservable attacks present a serious threat to grid operations. In [11] we presented an efficient algorithm to find all unobservable attacks, involving the compromise of exactly two power injection meters and an arbitrary number of power meters

on lines. We characterized such attacks and studied countermeasures. This work continued with a better algorithm for detection and the study of consequence of any attack. We applied [12] the result from our study on attacks to power systems to develop a multi criteria decision making algorithm based on observability, cost importance and security.

We began working on issues related to state estimation of power systems. Power system operators rely critically on state estimation for verification, fault detection and localization, and redispatch under contingency operations. We explored techniques to accelerate state estimation by computing state estimates at a small subset of buses using limited measurements from the power subsystem of interest. These could be operator selected "important" buses, which connect to "important" lines with significant real power transfer. Our techniques are inspired by uncertainty quantification methods.

We developed several algorithms and techniques for power systems. We developed a technique to measure the vulnerability of power networks to generator failure that uses instanton techniques to estimate probabilities of unlikely events. This allows more accurate "N-1 contingency failure" analysis than the with the existing techniques. With a student we developed mathematically rigorous mapping from first-principles models of power generators to a coupled oscillator model. For that model, provably correct closed-form synchronization conditions were found that reveal the connection between synchronization in power networks and the network topology and parameters [13].

For random intersection graphs, which are models of social networks, we found conditions for model parameters that determine when the graph is mostly connected (has a "giant component") or not. These proofs are important for estimating, e.g. the extent of the spread of diseases in network models of social interactions [14], [15].

Impact on National Missions

This project supported and enhanced the fundamental science of Information Science and Technology, an area of strategic interest to the laboratory. The CNLS provided a basic science-oriented postdoc program in which the CNLS shared postdocs with staff involved in IS&T research in T, CCS, P and D-divisions.

By underpinning the fundamental part of the 'S' (Science) in IS&T, the project helped the laboratory fulfill its security mission, growing the area of Information Science. These efforts also increased LANL's presence in the academic world and helped with recruitment and retention. This project helped bring 16 postdocs and 15 students to LANL to work in the area of Information Science and Technology.

Two mission areas that will potential use output from this project are energy security with the Smart Grid efforts and bio-security with the quantitative biology, epidemiology and synthetic vision aspects of the IS&T work.

References

1. Giorgi, E. E., and T. Bhattacharya. A note on two-sample tests for comparing intra-individual genetic sequence diversity between populations. 2012. Biometrics. 68 (4): 1323.

2. Giorgi, E. E., B. T. Korber, A. S. Perelson, and T. Bhattacharya. Modeling sequence evolution in HIV-1 infection with recombination. 2013. Journal of Theoretical Biology. 329: 82.

3. Lemons, N., B. Hu, and W. Hlavacek. Hierarchical graphs for rule-based modeling of biochemical systems. 2011. BMC Bioinformatics. 12 (1).

4. Huang, W., Z. Ji, S. P. Brumby, G. Kenyon, and L. M. Bettencourt. Development of invariant feature maps via a computational model of simple and complex cells. 2012. p. 1.

5. Ji, Z., S. Brumby, G. Kenyon, and L. A. Bettencourt. Integrating Bottom-up and Top-down Visual Attention for Object Segmentation. 2012. Journal of Vision. 12 (9): 926.

6. Ji, Z., W. Huang, and S. P. Brumby. Learning sparse representation via a nonlinear shrinkage encoder and a linear sparse decoder. 2012. p. 1.

7. Chertkov, M., and A. B. Yedidia. Computing the Permanent with Belief Propagation. 2011. arXiv:1108.

8. Johnson, J., P. Netrapalli, and M. Chertkov. Learning Planar Ising Models. 2010. arXiv:1011.

9. Dvijotham, K., S. Backhaus, and M. Chertkov. Operations-Based Planning for Placement and Sizing of Energy Storage in a Grid With a High Penetration of Renewables. 2011. arXiv:1107.

10. Giani, A., and R. Bent. Addressing smart grid cyber security. 2013. p. 44:1–44:4. {ACM}.

11. Giani, A., R. Bent, M. Hinrichs, M. McQueen, and K. Poolla. Metrics for assessment of smart grid data integrity attacks. 2012. p. 1.

12. Linda, O., M. Manic, A. Giani, and M. McQueen. Multi-

criteria based staging of Optimal PMU Placement using Fuzzy Weighted Average. 2013. p. 1.

13. Dörfler, F., M. Chertkov, and F. Bullo. Synchronization in complex oscillator networks and smart grids. 2013. Proceedings of the National Academy of Sciences. 110 (6): 2005.

14. Bradonjić, M., A. Hagberg, N. Hengartner, N. Lemons, and A. Percus. The phase transition in inhomogeneous random intersection graphs. 2013. arXiv:1301.

15. Bradonjić, M., A. Hagberg, N. Hengartner, and A. Percus. Component Evolution in General Random Intersection Graphs. 2010. In Lecture Notes in Computer Science. Edited by Kumar, R., and D. Sivakumar. p. 36.

Publications

Backhaus, S., and M. Chertkov. Getting a grip on the electrical grid. 2013. Physics Today. 66 (5): 42.

Bienstock, D., M. Chertkov, and S. Harnett. Chance Constrained Optimal Power Flow: Risk-Aware Network Control under Uncertainty. 2012. arXiv:1209.

Boeras, D., P. Hraber, M. Hurlston, T. Evans-Strickfaden, T. Bhattacharya, E. Giorgi, J. Mulenga, E. Karita, B. Korber, S. Allen, C. Hart, C. Derdeyn, and E. Hunter. Role of donor genital tract HIV-1 diversity in the transmission bottleneck. 2011. Proceedings of the National Academy of Sciences. 108 (46): e1156.

Bonachela, J., M. Raghib, and S. Levin. Dynamic model of flexible phytoplankton nutrient uptake. 2011. Proceedings of the National Academy of Sciences. 108 (51): 20633.

Bradonjić, M., A. Hagberg, N. Hengartner, N. Lemons, and A. Percus. The phase transition in inhomogeneous random intersection graphs. 2013. arXiv:1301.

Bradonjić, M., A. Hagberg, N. Hengartner, and A. Percus. Component Evolution in General Random Intersection Graphs. 2010. In Lecture Notes in Computer Science. Edited by Kumar, R., and D. Sivakumar. , p. 36.

Bradonjić, M., and L. Lazos. Graph-based criteria for spectrum-aware clustering in cognitive radio networks. 2012. Ad Hoc Networks. 10 (1): 75.

Brandão, F. S., M. Christandl, and J. Yard. Erratum to: Faithful Squashed Entanglement. 2012. Communications in Mathematical Physics. 316 (1): 287.

Cale, E. M., P. Hraber, E. E. Giorgi, W. Fischer, T. Bhattacharya, T. Leitner, W. W. Yeh, C. Gleasner, L. D. Green, C. S. Han, B. Korber, and N. L. Letvin. Epitope-specific CD8+ T lymphocytes cross-recognize mutant simian immunodeficiency virus (SIV) sequences but fail to contain very early evolution and eventual fixation of epitope escape mutations during SIV infection. 2011. Journal of Virology. 85 (8): 3746.

Chandrasekaran, V., M. Chertkov, D. Gamarnik, D. Shah, and J. Shin. Counting Independent Sets Using the Bethe Approximation. 2011. SIAM Journal on Discrete Mathematics. 25 (2).

Chernyak, V. Y., and M. Chertkov. Planar graphical models which are easy. 2010. Journal of Statistical Mechanics: Theory and Experiment. 2010 (11).

Chertkov, M., I. Kolokolov, and V. Lebedev. Tail-constraining stochastic linear–quadratic control: a large deviation and statistical physics approach. 2012. Journal of Statistical Mechanics: Theory and Experiment. 2012 (08).

Chertkov, M., and A. B. Yedidia. Computing the Permanent with Belief Propagation. 2011. arXiv:1108.

Crespi, V., G. Cybenko, and A. Giani. Engineering Statistical Behaviors for Attacking and Defending Covert Channels. 2013. IEEE Journal of Selected Topics in Signal Processing. 7 (1): 124.

Duclut, C., S. Backhaus, and M. Chertkov. Hysteresis, Phase Transitions and Dangerous Transients in Electrical Power Distribution Systems. 2012. arXiv:1212.

Dvijotham, K., S. Backhaus, and M. Chertkov. Operations-Based Planning for Placement and Sizing of Energy Storage in a Grid With a High Penetration of Renewables. 2011. arXiv:1107.

Dörfler, F., M. Chertkov, and F. Bullo. Synchronization in complex oscillator networks and smart grids. 2013. Proceedings of the National Academy of Sciences. 110 (6): 2005.

Erdos, P., D. Gerbner, N. Lemons, D. Mubayi, C. Palmer, and B. Patkos. Two-Part Set Systems. 2012. Electronic Journal of Combinatorics. 19 (1).

Gerbner, D., N. Lemons, C. Palmer, B. Patkós, and V. Szécsi. Almost Intersecting Families of Sets. 2012. SIAM Journal on Discrete Mathematics. 26 (4): 1657.

Giani, A., E. Bitar, M. Garcia, M. McQueen, P. Khargonekar, and K. Poolla. Smart Grid Data Integrity Attacks. 2013. IEEE Transactions on Smart Grid. 4 (3): 1244.

Giani, A., E. Bitar, M. Garcia, M. McQueen, P. Khargonekar, and K. Poolla. Smart grid data integrity attacks: characterizations and countermeasures. 2011. In 2011 IEEE International Conference on Smart Grid Communications (SmartGridComm). , p. 232.

Giani, A., R. Bent, M. Hinrichs, M. McQueen, and K. Poolla.

Metrics for assessment of smart grid data integrity attacks. 2012. In 2012 IEEE Power and Energy Society General Meeting. , p. 1.

Giani, A., and R. Bent. Addressing smart grid cyber security. 2013. In Proceedings of the Eighth Annual Cyber Security and Information Intelligence Research Workshop. , p. 44:1–44:4. {ACM}.

Gintautas, V., B. Kunsberg, M. Ham, S. Barr, S. Zucker, S. Brumby, L. A. Bettencourt, and G. Kenyon. An improved model for contour completion in V1 using learned feature correlation statistics. 2010. Journal of Vision. 10 (7): 1162.

Gintautas, V., M. Ham, B. Kunsberg, S. Barr, S. Brumby, C. Rasmussen, J. George, I. Nemenman, L. A. Bettencourt, and G. Kenyon. Model Cortical Association Fields Account for the Time Course and Dependence on Target Complexity of Human Contour Perception. 2011. PLoS Computational Biology. 7 (10).

Giorgi, E. E., B. T. Korber, A. S. Perelson, and T. Bhattacharya. Modeling sequence evolution in HIV-1 infection with recombination. 2013. Journal of Theoretical Biology. 329: 82.

Giorgi, E. E., and T. Bhattacharya. A note on two-sample tests for comparing intra-individual genetic sequence diversity between populations. 2012. Biometrics. 68 (4): 1323.

Gutfraind, A.. Optimizing Topological Cascade Resilience Based on the Structure of Terrorist Networks. 2010. PLoS ONE. 5 (11).

Gutfraind, A., A. Hagberg, D. Izraelevitz, and F. Pan. Interdiction of a Markovian Evader. 2011. In Proceedings of the 12th INFORMS Computing Society Conference on OR, Computing, and Homeland Defense. , p. 3.

Huang, W., Z. Ji, S. P. Brumby, G. Kenyon, and L. M. Bettencourt. Development of invariant feature maps via a computational model of simple and complex cells. 2012. , p. 1.

Ji, Z., J. Theiler, R. Chartrand, G. Kenyon, and S. Brumby. Decoupling sparse coding of SIFT descriptors for large-scale visual recognition. 2013. Vol. 8750, p. 87500k.

Ji, Z., M. Luciw, J. Weng, and S. Zeng. Incremental Online Object Learning in a Vehicular Radar-Vision Fusion Framework. 2011. Intelligent Transportation Systems, IEEE Transactions on. 12 (2): 402.

Ji, Z., S. Brumby, G. Kenyon, and L. A. Bettencourt. Integrating Bottom-up and Top-down Visual Attention for Object Segmentation. 2012. Journal of Vision. 12 (9): 926.

Ji, Z., W. Huang, and S. P. Brumby. Learning sparse representation via a nonlinear shrinkage encoder and a linear sparse decoder. 2012. , p. 1.

Johnson, J., P. Netrapalli, and M. Chertkov. Learning Planar Ising Models. 2010. arXiv:1011.

Johnson, M., and A. Gutfraind. Evader interdiction and collateral damage. 2012. , p. 86.

Keszegh, B., N. Lemons, and D. Pálvölgyi. Online and quasi-online colorings of wedges and intervals. 2012. arXiv:1207.

Kudekar, S., J. Johnson, and M. Chertkov. Improved Linear Programming Decoding using Frustrated Cycles. 2011. arXiv:1105.

Kudekar, S., J. Johnson, and M. Chertkov. Linear Programming based Detectors for Two-Dimensional Intersymbol Interference Channels. 2011. arXiv:1102.

Kudekar, S., and N. Macris. Decay of Correlations for Sparse Graph Error Correcting Codes. 2011. SIAM Journal on Discrete Mathematics. 25 (2).

Lemons, N., B. Hu, and W. Hlavacek. Hierarchical graphs for rule-based modeling of biochemical systems. 2011. BMC Bioinformatics. 12 (1).

Li, H., M. Stoddard, S. Wang, L. Blair, E. Giorgi, E. Parrish, G. Learn, P. Hraber, P. Goepfert, M. Saag, T. Denny, B. Haynes, B. Hahn, R. Ribeiro, A. Perelson, B. Korber, T. Bhattacharya, and G. Shaw. Elucidation of Hepatitis C Virus Transmission and Early Diversification by Single Genome Sequencing. 2012. PLoS Pathogens. 8 (8).

Linda, O., M. Manic, A. Giani, and M. McQueen. Multi-criteria based staging of Optimal PMU Placement using Fuzzy Weighted Average. 2013. In 2013 IEEE International Symposium on Industrial Electronics (ISIE). , p. 1.

Liu, X. B., M. Wang, J. Meng, E. Ben-Naim, and Z. Y. Guo. Minimum Entransy Dissipation Principle for Optimization of Transport Networks. 2010. International Journal of Nonlinear Sciences and Numerical Simulation. 11 (2): 113.

Loxley, P. N., L. M. Bettencourt, and G. T. Kenyon. Ultra-fast detection of salient contours through horizontal connections in the primary visual cortex. 2011. EPL (Europhysics Letters). 93 (6).

Loxley, P. N., and L. M. Bettencourt. Visually-salient contour detection using a V1 neural model with horizontal connections. 2011. arXiv:1103.

Parrish, N., F. Gao, H. Li, E. Giorgi, H. Barbian, E. Parrish, L. Zajic, S. Iyer, J. Decker, A. Kumar, B. Hora, A. Berg, F. Cai, J. Hopper, T. Denny, H. Ding, C. Ochsenbauer, J. Kappes, R. Galimidi, A. West, P. Bjorkman, C. Wilen, R.

Doms, M. O'Brien, N. Bhardwaj, P. Borrow, B. Haynes, M. Muldoon, J. Theiler, B. Korber, G. Shaw, and B. Hahn. Phenotypic properties of transmitted founder HIV-1. 2013. Proceedings of the National Academy of Sciences. 110 (17): 6626.

Samaniego, H., G. Sérandour, and B. Milne. Analyzing Taylor's Scaling Law: qualitative differences of social and territorial behavior on colonization/extinction dynamics. 2012. Population Ecology. 54 (1): 213.

Silva, A., G. Jander, H. Samaniego, J. S. Ramsey, and C. Figueroa. Insecticide Resistance Mechanisms in the Green Peach Aphid Myzus persicae (Hemiptera: Aphidae) I: A Transcriptomic Survey. 2012. PLoS ONE. 7 (6).

Turitsyn, K., M. Chertkov, and M. Vucelja. Irreversible Monte Carlo algorithms for efficient sampling. 2011. Physica D: Nonlinear Phenomena. 240 (4–5): 410.

Whitney, J., P. Hraber, C. Luedemann, E. Giorgi, M. Daniels, T. Bhattacharya, S. Rao, J. Mascola, G. Nabel, B. Korber, and N. Letvin. Genital Tract Sequestration of SIV following Acute Infection. 2011. PLoS Pathogens. 7 (2).

Wolpert, D., M. Harré, E. Olbrich, N. Bertschinger, and J. Jost. Hysteresis effects of changing the parameters of noncooperative games. 2012. Physical Review E. 85 (3).

Wozniak, P., D. I. Moody, Z. Ji, S. P. Brumby, H. Brink, J. Richards, and J. S. Bloom. Automated Variability Selection in Time-domain Imaging Surveys Using Sparse Representations with Learned Dictionaries. 2013. In American Astronomical Society Meeting Abstracts. Vol. 221.

Yusim, K., R. Dilan, E. Borducchi, K. Stanley, E. Giorgi, W. Fischer, J. Theiler, J. Marcotrigiano, B. Korber, and D. Barouch. Hepatitis C Genotype 1 Mosaic Vaccines Are Immunogenic in Mice and Induce Stronger T-Cell Responses than Natural Strains. 2013. Clinical and Vaccine Immunology : CVI. 20 (2): 302.

Zdeborová, L., and F. Krzakala. Quiet Planting in the Locked Constraint Satisfaction Problems. 2011. SIAM Journal on Discrete Mathematics. 25 (2).

Gating and Emission Enhancement of Diamond Field-emitter Arrays

Heather L. Andrews
20120522ECR

Introduction

High-quality beams of electrons are critical to a wide array of ubiquitous devices. These devices range from microwave systems, electronic displays, and vacuum microelectronics to research equipment such as electron microscopes, terahertz sources, and free-electron lasers.

The quality of an electron beam can only degrade once the beam leaves its source, the cathode, so it is critical to develop cathodes that produce inherently high-quality beams. The broad goal of this research project is to further the development of a novel cathode called a diamond field-emitter array (DFEA) whose fundamental element produces nearly the highest quality electron beam allowed by the laws of physics. The specific objective for this project is to prove the relevance of DFEAs to high-power free-electron lasers (FELs) by demonstrating enhancement and control of emission and determining the limits of DFEA performance.

Benefit to National Security Missions

Cathodes that produce inherently high-quality electron beams are of key importance to many focus areas of global security including high-power free-electron lasers, directed energy sources and terahertz sources. The development of DFEAs could have a dramatic impact on the accelerator segment of LANL operations and assure LANL a place at the forefront of free-electron laser and high-power microwave source development.

Progress

Over the past year this project has accomplished a number of critical goals. First, the test chamber was fully assembled and pumped down to a very good vacuum. This is critical because one of the questions we need to address is Diamond Field-Emission Array (DFEA) performance under different vacuum levels. Next we received our first DFEA samples from our collaborators at Vanderbilt University. These will be tested in the very near future. The next set of samples are in preparation and will be delivered shortly. The pulsed power supply necessary to drive the cathodes up to their operational limit has been recommissioned and is being integrated into the experimental chamber. Finally, we have made significant progress testing the design of the cathode holder and anode. Each of these parts are custom, and critical to the experiment. They must withstand a very high electric field in order to test true DFEA performance. While they are designed to withstand the anticipated electric field, they must be tested because minor surface imperfections or even material defects can cause their behavior to deviate from that predicted by modeling.

Future Work

The main goals for the next fiscal year include testing the limits of DIamond Field-Emitter Array (DFEA) performance, and investigating whether laser light can be used to turn off and on DFEA emission. To accomplish the first goal we will progressively test larger and denser arrays to see how high current density can be achieved.

We will continue a small amount of modeling work to ensure the experimental set-up is sufficient to withstand the high-current density we expect to produce. Finally, we will investigate whether laser light can turn on and off the current emitted by DFEAs. We will do this by shining a laser on the front, side, and/or back surface of the DFEA, while the voltage used to produce emission is very low. If we observe emission in one of these configurations, we will make more thorough investigation to begin to determine the limits and conditions under which laser light gates DFEA cathodes.

Conclusion

This research is expected to produce experimental data describing the limits of operation of DFEAs. This data will inform the scope of potential applications of DFEAs as robust, high-quality cathodes. In the event DFEAs are

as widely applicable as they promise, this novel technology has the potential to greatly improve existing vacuum micro-electronic devices as well as allow new devices to be created.

Uncertainty Quantification for Networks

Earl C. Lawrence
20120123ER

Introduction

Dependence on network-delivered commodities, such as information and energy, places infrastructure networks in a prominent and growing role in national and global security. Because they have often grown incrementally and without comprehensive plans, these networks are complex, vulnerable, and incompletely known or described. Nevertheless, policy analysts need to make decisions about infrastructure resiliency and criticality. This research seeks to improve the decision-making process by providing methods for network uncertainty quantification (UQ): predicting unknown components and estimating uncertainty in these predictions. Specifically, our goal is topology, attribute, and flow inference in partially observed infrastructure networks using science-based simulation tools. Statistical methods exist for graph exploration and for incorporating complex simulators, but these two areas are separate and combining them requires advances in statistical methodology. These techniques will leverage the scientific knowledge built into a simulator for use with statistical methods for characterizing the space of graphs (topology) and attributes that describe networks.

Benefit to National Security Missions

This research will impact LANL programs in Global Security (PADGS) and Computer, Computational, and Statistics (CCS) Sciences and the missions of the Energy Security Institute and the Information Science and Technology Institute. PADGS will benefit from validated, science-based methodologies that estimate unobserved network features with known confidence. Many PADGS problems in homeland security and intelligence are currently intractable without the proposed capability. The core information science is also applicable to a wide variety of network domains including cyber, supply chains, natural gas, water, and oil, as well as social and biological networks. Possible applications include criticality, impact analysis, state estimation, event detection, effects-based operations, situational awareness after a disaster, cost estimation, and climate impact in future networks; influences between interconnected networks; and targeted data collection for uncertainty reduction.

Progress

This past fiscal year focused on two research directions. First, we have worked on expanding the network state under consideration. The first year focused on network topology. This past year, we have worked on adding other network quantities like loads and generations. These additions assume results from the topology estimation that gives a list of possible topologies with associated probabilities. For a given topology, we could use the power flow equations to see how settings of the unknown generations and loads produce lines flows and how those simulated line flows compare to measured data. Unfortunately, this is a very computationally intensive process. Thus, for each topology with significant probability, we build an approximation to the relationship between generations/loads and the line flows that correspond to measured data. This approximation allows us to quickly find the distribution of generations/loads that match observed data. Combined with earlier work, this will give us a fast way to estimate the general state of power grid based on a data measured at a few points in the network. This work is currently being written into a paper, with plans to submit to IEEE Transactions on Power Systems by the end of the summer.

The second direction we have pursued is to use the topology uncertainty quantification techniques from the first year in a network control application: optimal power flow (OPF). In the OPF problem, a grid operator determines the settings for generation capabilities based on the current state of the network (including demand, generation, and topology). When the state is precisely known, the generation settings can be determined using a fairly simple optimization routine. When the

estimated state is incorrect, the solution could lead to line overages and network failure, so incorporating uncertainty is important. Our work this year has been to expand the optimization framework to include the output of the topology estimation, a list of possible topologies with associated probabilities. This new chance-constrained OPF framework can be used to determine generation settings when the topology is not completely known, while minimizing the probability of line overloads. This work is also currently being written for IEEE Transactions on Power Systems with plans to submit by the end of summer.

In addition, a summary of the entire project so far was given in an invited talk at the 2013 Quality and Productivity Research Conference in the session Data-Driven Decisions in Smart City Infrastructure.

Future Work

We will shift our model development to use data from phasor measurement units (PMUs). A PMU is an example of the type of data collection device that so-called "smart grids" will use. They measure voltage and current information with high precision. This should position our work for use with newly developing technology.

We will continue to expand space of possibly network states, particularly for topology. We would like to move beyond the model bank formulation of year one and consider more general spaces of possible network topologies.

We will continue to expand the optimal power flow formulation to better account for sources of uncertainty. This will keep pace with our other work so that we can continue to demonstrate an end-to-end process for uncertainty quantification: take measurements, estimate uncertainty, and take uncertainty-aware actions in the grid.

Conclusion

The result of this research will be methodology for estimating, with uncertainty, the unobserved parts of infrastructure networks, such as electric power. This methodology will be a tool for better understanding how these networks perform, where and why they are vulnerable, and how to improve them. Some possible applications include criticality assessment of domestic and foreign networks, disaster recovery, and improving reliability and efficiency for the power grid.

Publications

Bent, R., D. Bienstock, E. Chertkov, E. Lawrence, and S. Vander Wiel. Chance constrained optimal power flow for topology uncertainty. Invited presentation at INFORMS Annual Meeting 2013. (Minneapolis, 6-9 Oct. 2013).

Garcia, M., A. Giani, and K. Poolla. Partial state estimation for Electricity Grids. To appear in 52nd IEEE Conference on Decision and Control. (Florence, Italy, 10-13 Dec. 2013).

Lawrence, E., S. Vander Wiel, and R. Bent. Model bank state estimation for power grids using importance sampling. 2013. Technometrics. 55 (4): ?.

Wiel, S. Vander, E. Lawrence, and R. Bent. Uncertainty quantification for networks with power distribution applications. Invited presentation at Conference on Data Analysis. (Santa Fe NM, 29 Feb - 2 Mar 2012).

Wiel, S. Vander, E. Lawrence, and R. Bent. Uncertainty quantification for power networks. Presented at Optimization and Control for Smart Grids. (Santa Fe NM, 21-25 May 2012).

Wiel, S. Vander, R. Bent, E. Casleton, and E. Lawrence. Identification of Downed Lines in Power Grids. Applied Stochastic Models in Business and Industry.

Wiel, S. Vander, R. Bent, E. Lawrence, and E. Casleton. Uncertainty quantification for networks with power distribution applications. Invited presentation at Quality and Productivity Research Conference 2013. (Niskayuna, NY, 5-7 June 2013).

Phylogenetic Classification and Analysis of Computer Malware

Guanhua Yan
20120443ER

Introduction

Computer malware have plagued the Internet for more than two decades and are now responsible for the majority of malicious activities in the cyber space. The two key challenges in defending against a malware attack are finding who originated this attack so that law enforcement can get involved (malware attribution), and identifying which family the malware belongs to so that effective mitigation techniques can be quickly deployed (malware classification). Addressing these issues demands in-depth analysis of malware code, which is currently done by either labor-intensive manual reverse engineering or error-prone signature-based schemes.

Against this backdrop, we propose methods to analyze malware programs efficiently and accurately using ideas from biological phylogenetics.We will develop malware phylogeny to organize previously observed malware instances into a structure that facilitates classification of new ones captured from the wild (e.g., email attachments). Moreover, malware phylogeny that accurately characterizes the evolution of malware instances sheds light on the originators of malware attacks.This project also concerns data-intensive phylogenetic inference, as it will be conducted on a large locally collected malware repository with millions of malware instances.

Benefit to National Security Missions

This projects meets two FY12 priorities of Information, Science and Technology. If we are successful in developing phylogenetic classification tools, we contribute to the Inference/Prediction priority by demonstrating statistical inference methods for the history of malware programs even though their evolution involves human intelligence. Even if we are ultimately unsuccessful in developing such tools, we advance the data intensive computing priority by developing efficient algorithms to extract representative features from a large malware database that contains millions of malware programs. Underlying these efforts is the realization that cyber-threat reduction is among the core missions of LANL. This project seeks to connect that capability with our leadership in the application of phylogenetics to biological (viral) systems and develop a novel capability within cyber security science.

Progress

In the past year, we finished these tasks under the auspices of this project. (1) We developed a principled solution to finding consensus in data clustering by multiple experts. Our project requires labeled data as ground truth to study malware evolution. As manually labeling a large number of malware samples is difficult, we rely on the classification results by multiple AV software to group malware samples. We formulate the problem rigorously and show that finding an optimal solution is computationally intractable. We further proposed a graph theory-based method to find sub-optimal solutions. (2) We developed a framework for automated malware classification. This framework can combine various types of malware features, some of which may have missing values, and use the Neyman-Pearson criterion to search optimal parameters of cost-sensitive classifiers. (3) We also developed a new transductive malware classification method to spread label information from labeled samples to unlabeled ones. (4) We have run phylogenetic software based on maximum-likelihood principles on the features we have collected from a few malware families to show their evolution. We are currently interpreting the results and evaluating how accurately the malware phylogeny reflects the realism. In the past year, we have three papers accepted for publication directly from the results of this project.

Future Work

The popularity of online social media networks has inspired researchers in diverse fields to mine events of interest (e.g., stock prices, epidemic disease, and earthquakes). These efforts, however, are mainly performed

in an offline fashion. Few efforts have been focused on the computational challenges involved in real-time event mining from streaming data sources. In this project, we will tackle two fundamental problems. (1) How to choose features that can be used to predict the events of interest?

In previous works, feature selection from streaming data sources is mainly done manually by domain experts. Such an approach does not scale well when we deal with large volumes of data. Based on the methods we have already developed, we will extend them to find features that are irrelevant to the events of interest. With a high-dimensional feature space, the combinatorial optimization problem may be computationally intractable. One possible solution is ranking features based on the distributional differences during the periods with and without events of interest and then applying a greedy approach to select relevant features. If we have a large number of features, this method may still be computationally expensive. An alternative method may be leveraging the structural information revealed by clusters of features to accelerate the process of feature selection. (2) Given a set of features, how to monitor events of interest? We will develop change-point detection algorithms that monitor the changes in the distributions of features (or combinations of features) that are indicative of occurrences of events of interest.

There are a broad spectrum of applications that can benefit from this project, including but not limited to bio-surveillence and logistics. The deliverables from this project will be effective and efficient algorithms for real-time monitoring of events of interest from streaming data sources such as Twitter tweets.

Conclusion

The end results of this project include (1) Fundamental understanding of evolution of computer malware based on a locally collected malware repository; (2) Classification of malware instances into different malware families using unsupervised machine learning techniques; (3) Malware phylogeny for each malware family that characterizes evolution of malware variants in the same malware family. Malware phylogeny will be used to find close ancestors when a new malware instance is spotted, and information about these ancestors will be used to both understand the origin of the new malware attack and estimate its behavior and potential damages.

Publications

Kong, D., and G. Yan. Poster: Discriminant Malware Distance Learning on Structural Information for Automated Malware Classication. 2013. In Proceedings of the ACM SIGMETRICS/international conference on Measurement and modeling of computer systems (SIGMETRICS'13). (Pittsburgh, PA, 17-21 June 2013). Vol. 41, 1 Edition, p. 347. New York: ACM.

Kong, D., and G. Yan. Discriminant malware distance learning on structural information for automated malware classification. 2013. In Proceedings of the 19th ACM SIGKDD international conference on Knowledge discovery and data mining (KDD'13). (Chicago, 11-14 Aug. 2013). , p. 1357. New York: ACM.

Kong, D., and G. Yan. Transductive malware classification: find your lineage from your neighbors. 2013. LA-UR 13-22771, Los Alamos National Laboratory..

Liu, L., X. Zhang, G. Yan, and S. Chen. Chrome Extensions: Threat Analysis and Countermeasures. 2012. In The 19th Annual Network & Distributed System Security Symposium (NDSS'2012). (San Diego, California, 5-8 Feb. 2012). , p. 1. Reston, VA, USA: Internet Society.

Yan, G.. Finding common ground among experts' opinions: conflict-free malware clustering for malware lineage analysis. 2013. LA-UR 13-22751, Los Alamos National Laboratory..

Yan, G., N. Brown, D. Kong, and M. Anghel. Towards a Comprehensive View of Feature Selection for Malware Classification. 2012. LA-UR 12-25308, Los Alamos National Laboratory.

Yan, G., N. Brown, and D. Kong. Exploring discriminatory features for automated malware classication. 2013. In Proceedings of the 10th Conference on Detection of Intrusions and Malware & Vulnerability Assessment (DIMVA'13). (Berlin, Germany, 17-19 July 2013). Vol. 7967, p. 41. Berlin Heidelberg: Springer.

Combinatorial Approaches To Graphical Models: Theory and Applications

Michael Chertkov
20120469ER

Introduction

In recent years, graphical models have come to play an important role in modern approaches to computer science and machine learning and have found many applications in various fields of science and engineering. In short, a graphical model is a statistical model for a collection of (possibly very many) random variables in which correlations among the variables are succinctly described by a sparse set of interactions or constraints among small subsets of variables. The conditional independence relations (Markov properties) satisfied by these variables are then summarized by a graph in which vertices represent random variables and edges denote interactions among the variables. Although graphical models provide a powerful and versatile modeling framework, they suffer from fundamental challenges in that inference in general graphical models is computationally intractable. This has motivated an extensive and on-going research effort to develop computationally-tractable, heuristic methods for approximate inference in graphical models.

We propose to pioneer advanced methods for graphical models derived from combinatorial methods of statistical physics. More specifically we intend to build on tractable methods developed for special classes of graphical models, namely Ising and dimer models defined on graphs of simple topology (planar and bounded-genus graphs). While inference is intractable for the Ising and dimer models on general graphs, it becomes tractable for planar graphs being equivalent to calculation of a matrix determinant or Pfaffian. These methods were originally developed to obtain estimates of lattice models in statistical physics and are little-known and underutilized in the machine learning community.

We believe that this research agenda will advance the field of graphical models in new directions and enhance LANL's presence and reputation in the domain of graphical models as well as cultivate fundamental capabilities to support DOE mission in the areas of information technology for very large-scale inference, estimation and optimization.

Benefit to National Security Missions

Our project will provide new powerful tools in learning of predictive statistical models from observations. Applications for these algorithmic and theoretical IT ``know how" tools are many, ranging from bio- and genetic networks, detection of anomalies in infrastructure networks, inverse problems in seismology, reservoir exploration and discovery in oil fields, to probabilistic co-design based on limited measurements. Our project primarily addresses Information Science & Technology Grand Challenge by providing data-driven algorithmic tool for ``Intelligent Data Acquisition, Management, And Analysis" (especially in what concerns Knowledge extraction, Automated discovery, Active learning, Anomaly detection, Data mining and Semi-supervised learning) and ``Computational Co-design" (in what concerns integration of domain expertise, e.g. in statistical modeling of observational data, and novel machine learning techniques the proposal develops. Consequently, proposed activities will help LANL to respond to incoming National Initiatives, DOE, DOD, DTRA, DARPA and DHS related to monitoring, detection, control and analysis of large data sets.

Progress

We developed a general purpose Belief Propagation (BP) algorithm for Linear Programming. BP is a popular, distributed heuristic for performing MAP computations in Graphical Models. BP can be interpreted, from a variational perspective, as minimizing the Bethe Free Energy (BFE). BP can also be used to solve a special class of Linear Programming (LP) problems. For this class of problems, MAP inference can be stated as an integer LP with an LP relaxation that coincides with minimization of the BFE at ``zero temperature". We generalized these

prior results and establish a tight characterization of the LP problems that can be formulated as an equivalent LP relaxation of MAP inference. Moreover, we suggest an efficient, iterative annealing BP algorithm for solving this broader class of LP problems. We demonstrated the algorithm's performance on a set of weighted matching problems by using it as a cutting plane method to solve a sequence of LPs tightened by adding ``blossom'' inequalities.

We have developed a Graphical Transformation for Belief Propagation: Maximum Weight Matchings and Odd-Sized Cycles approach. Max-product `belief propagation' (BP) is a popular distributed heuristic for finding the Maximum A Posteriori (MAP) assignment in a joint probability distribution represented by a Graphical Model (GM). It was recently shown that BP converges to the correct MAP assignment for a class of loopy GMs with the following common feature: the Linear Programming (LP) relaxation to the MAP problem is tight (has no integrality gap). Unfortunately, tightness of the LP relaxation does not, in general, guarantee convergence and correctness of the BP algorithm.

The failure of BP in such cases motivates reverse engineering a solution -- namely, given a tight LP, can we design a `good' BP algorithm. We have designed a BP algorithm for the Maximum Weight Matching (MWM) problem over general graphs. We prove that the algorithm converges to the correct optimum if the respective LP relaxation, which may include inequalities associated with non-intersecting odd-sized cycles, is tight. The most significant part of our approach is the introduction of a novel graph transformation designed to force convergence of BP. Our theoretical result suggests an efficient BP-based heuristic for the MWM problem, which consists of making sequential, ``cutting plane'', modifications to the underlying GM. Our experiments showed that this heuristic performs as well as traditional cutting-plane algorithms using LP solvers on MWM problems.

We also analyzed Loop Calculus and Bootstrap-Belief Propagation for Perfect Matchings on Arbitrary Graphs. In this sub-project we have discussed computation of the Partition Function (PF) and the Minimum Weight Perfect Matching (MWPM) on arbitrary, non-bipartite graphs.

We present two novel problem formulations - one for computing the PF of a Perfect Matching (PM) and one for finding MWPMs - that build upon the inter-related Bethe Free Energy, Belief Propagation (BP), Loop Calculus (LC), Integer Linear Programming (ILP) and Linear Programming (LP) frameworks. First, we described an extension of the LC framework to the PM problem. The resulting formulas, coined (fractional) Bootstrap-BP, express the PF of the original model via the BFE of an alternative PM problem. We then study the zero-temperature version of this Bootstrap-BP formula for approximately solving the MWPM problem. We did so by leveraging the Bootstrap-BP formula to construct a sequence of MWPM problems, where each new problem in the sequence is formed by contracting odd-sized cycles (or blossoms) from the previous problem. This Bootstrap-and-Contract procedure converges reliably and generates an empirically tight upper bound for the MWPM. We concluded this study by discussing the relationship between our iterative procedure and the famous Blossom Algorithm of Edmonds '65 and demonstrate the performance of the Bootstrap-and-Contract approach on a variety of weighted PM problems.

Future Work

We expect to continue our work on learning graphical models with the help of statistical physics models to develop computationally-tractable, heuristic methods for approximate inference. The focus next year will be two fold, first continuation of the work on inference algorithms and ideas, and second incorporating these ideas into learning, both of factor functions and of graphical relations.

On the first task, empowered by our recent progress in the field of counting perfect matchings over bipartite graphs, and developing fractal Belief Propagation (BP) and other related counting and reconstruction ideas for permanents, we plan to attack a more challenging problem of general matchings (not only perfect and defined beyond bipartite graphs). Maximum-A-Posteriori versions/formulations of the problems are known as allowing computationally sound solution, however these known algorithms are not of BP type. We will attempt to find the respective BP algorithms for MAP and then extend it to computing marginal probabilities and solving the counting problem. This research will also benefit from recently introduced Cumulant Expansion method for counting and related Loop Calculus approach developed at LANL.

Second, we will continue to work on learning, advancing learning of planar graphical models with the aforementioned cumulant expansion method and related Generalized BP approach. The main idea here is to develop an iterative process which first ignore part of correlations, reconstructing the best it can on a relatively small subgraph and then extend the structure sequentially to better fit the data. We will also explore very recent and promising ideas related to inference and learning of mixed problems defined over both discrete and continuous variables. These problems emerge naturally

in the context of optimization and control of infrastruc-

tures and are more challenging than either of the pure problems (discrete or continuous).

Conclusion

Our research goals can be broadly summarized as follows:

- Develop new methods for learning graphical models aimed at exploiting tractable computations on planar and bounded-genus graphs.
- Develop new combinatorial analysis of inference in graphical models and of some popular approximate inference methods such as belief propagation and its generalizations, providing improved convergence and error analysis of these methods
- Iinvent entirely new approaches to approximate inference for intractable graphs that leverage efficient computations for planar graphs (e.g., on planar subgraphs or planar covers of a non-planar graph) and demonstrate improvements over existing methods.

Publications

Chertkov, M., A. Gelfand, and J. Shin. Loop Calculus and Bootstrap-Belief Propagation for Perfect Matchings on Arbitrary Graphs. To appear in The Journal of Physics: Conference Series (JPCS).

Chertkov, M., and A. B. Yedidia. Approximating the Permanent with Fractional Belief Propagation. 2013. JOURNAL OF MACHINE LEARNING RESEARCH. 14: 2029.

Chertkov, M., and V. Chernyak. Statistical Inference in Structured Graphical Models: Gauge Transformations, Belief Propagation & Beyond. 2012. this is a big review -- still work in progress.

Gelfand, A., J. Shin, and M. Chertkov. Belief Propagation for Linear Programming. To appear in ISIT 2013. (Istanbul, Turkey, July 2013).

Shin, J., A. Gelfand, and M. Chertkov. A Graphical Transformation for Belief Propagation: Maximum Weight Matchings and Odd-Sized Cycles. To appear in NIPS 2013. (Lake Tahoe, CA, December 2013).

Combining Information Theory and Game Theory

David H. Wolpert
20120708ER

Introduction

Game theory is the formalism for analyzing how interacting, utility-maximizing agents (humans, organizations, firms) behave. Recent work has shown how to formulate game theory in terms of Bayes nets. Other recent work has shown how to analyze information flow across Bayes nets. In this project I will combine these two breakthroughs to analyze information "flow" among a set of interacting, agents and the effects of that flow on agent behavior.

Game theory analyzes the joint behavior of interacting agents when each agent predicts the behavior of the other agents, aware that those other agents are predicting their behavior. Any modification to the information flowing among such mutually predicting agents will affect their behavior. Conversely, any change in the behavior of an agent will affect the information flowing to the other agents. To understand this interplay between information flow and behavior, I integrate information theory into game theory. I will start by analyzing issues such as:

- Often reducing noise in the observations of an agent will increase their expected utility. Sometimes it will decrease the agent's expected utility. The reason is that in certain circumstances, if you reduce information flow to yourself - and your opponent knows that you now have less information - they will change their behavior accordingly, and that may end up benefiting you more than the loss of information hurts you. The first research issue is to characterize when it will benefit a player increase increase the noise in their observations.
- A related issue is understanding when an agent benefits if the noise level is reduced in the observations of the other agents. (In general, I may either be hurt or helped by a change in your noise level, independently of whether it helps or hurts you.)

Benefit to National Security Missions

This project will lay the foundation for quantitative LANL tools for the design of systems that gather and analyze intelligence in a broad range of scenarios, and how best to devote resources to impeding intelligence-gathering of potential adversaries. Those tools will complement LANL's strengths in measurement technology. As the work progresses, I will seek opportunities to contribute to LANL missions in Warfighter support and Global Security instrumentation. This work will build capabilities for D division, ISR, T division, CCS division, and ACS.

Progress

My first task is to construct a novel game theory representation, based on multi-agent influence diagrams, and establish the equivalence of this novel representation with the representations of conventional game theory. I have now completed this task, and am in the process of writing up the results for submission.

My second task is to complete a research project showing how to formalize such unawareness using the extension of multi-agent influence diagrams mentioned above. I have now completed this task, and am in the process of writing up the results for submission.
My third task was to complete the organizing of the joint LANL / Santa Fe Institute workshop on Combining Information Theory and Game Theory and run that workshop. I did this successfully.

Future Work

Conventional game theory uses two representations of games: "normal form", and "extensive form." Neither representation is amenable to Shannon information theory. Accordingly, one of the central features of my application of Shannon information theory to study games is by using a different representation, based on multi-agent influence diagrams. To relate this new work to the results in conventional game theory, I must estab-

lish the equivalence of this novel representation with the representations of conventional game theory. This is the first task for the coming year, which will result in a paper submission.

My second task is to complete the organizing of the joint LANL / Santa Fe Institute workshop on Combining Information Theory and Game Theory and run that workshop, and then publish a book of proceedings / classic papers.

Conventional game theory has considered two types of limitations on information: incomplete and imperfect information. However in many scenarios the limitation is due to inherent unawareness by a player of the form of the underlying game. For example, it may be that a player is not even aware of all the potential moves of their opponents, but then gains some information concerning those moves. The third task will be to complete a research project first showing how to formalize such unawareness using the extension of multi-agent influence diagrams mentioned and then analyzing the information theoretic aspects of such unawareness. This will be completed in FY14.

Conclusion

This project will create a new formalism for describing and analyzing how the interaction of multiple agents depends on and affects the information flow governing their interaction. This formalism will lay the groundwork for a range of applications including the design of large distributed systems for intelligence gathering and analysis.

Publications

Wolpert, D., M. Harre, E. Olbrich, N. Bertschinger, and J. Jost. Hysteresis effects of changing the parameters of noncooperative games. 2012. PHYSICAL REVIEW E. 85 (3, 2): 036102.

Wolpert, D., and D. Leslie. Information Theory and Observational Limitations in Decision Making. 2012. B E JOURNAL OF THEORETICAL ECONOMICS. 12 (1): 5.

Software/Hardware Mapping for Data Locality Optimization

Hristo N. Djidjev
20130252ER

Introduction

We consider the problem of mapping an existing sequential code onto a model of a multi-core high-performance computing (HPC) system so that the memory access/com-munication cost is minimized. This can be achieved by achieving high data access locality, one of the most important properties of efficient HPC codes. For instance, modern computer processors such as Graphics Processor Unit (GPU) and Cell have limited amount of local memory and the time of data transfer between that memory and the global memory is huge compared to the cost of computation or the cost of local access. Hence, it is important to have a method that maps the operations of a software code onto a hardware model in a way that maximizes locality and data reuse, i.e., such that as large as possible amount of computations are performed on the data in the local memory before that data is replaced with new data. Unfortunately, the corresponding mapping optimization problem is very difficult to solve efficiently as it is NP-hard. Hence, we will look at a subclass of all software codes, namely nested-loops, and at a subclass of all transformations, namely affine transformations. Previous research has shown that those subclasses capture the most relevant from practical point of view types of codes (as loops are usually responsible for most of the total computation time) and, on the other hand, result in optimization problems of manageable computational complexity. Our goal is to address the algorithmic challenges and to design mapping algorithms that are both accurate and scalable and to test their performance on a prototype mapping tool.

Benefit to National Security Missions

Co-design has been recognized as one of the high-priority areas of research for Information Science and Technology at LANL. This project focuses on a key step of the software/hardware co-design process – mapping the software representation onto the hardware model in order to maximize data reuse and locality and increase the amount of parallelism. The success of this project will advance the ability of LANL and DOE in solving the co-design problem and building competence for achieving exascale capabilities. This will lead to computers with improved performance and price parameters, improving the existing simulation capabilities. It will positively affect multiple application areas that rely on high performance computing and computational simulation for their data analysis and prediction.

Progress

Since the co-PI Leonid Gurvits left the lab in December 2012, we had to look for collaborators with experience in polyhedral optimization and high-performance computing, which was a difficult task given the small number of researchers working in both areas. We established cooperation with the group of Prof. Sanjay Rajopadhye from Colorado State University and created a joint research plan with him very closely tied to the ER. Also, one of his students, Vamsi Tandrapati, came in June 2013 for 3 months at LANL as a summer intern working on the project. Also, we are expecting Ramakrishna Upadrasta, who is very experienced in the above topics, to come as a postdoc in July 2013 for two years to also work on the project. With him and Vamsi on the team, the staffing problems have been successfully resolved.

The work so far has concentrated on developing the high-level optimization framework based on the polyhedral method. One of the important observations made is that the computational complexity of the optimization procedure can be significantly reduced, compared with the procedure originally described in the proposal, by eliminating the need to search the space of all hardware parameters for an optimal solution. Previously, for each set of hardware parameters (each point in the search space), one had to run a problem for optimally mapping the software representation onto the corresponding

hardware. The new approach directly finds the sets of the optimal hardware parameters by including them as variables in the mapping optimization problem. We are trying the new framework on simple algorithms with the purpose of computing the parameters of that optimization problem, using as input Jacobi-1D, Gauss-Siedel-1D and Smith-Watermann algorithms and as a software tools the Pluto polyhedral method tool.

Future Work

During the second year, we plan to complete the algorithm for codesign for a single algorithm and test it on a GPU-type architecture. We will start by choosing a codelet (a computationally intensive code snippet) from PolyBench or a "polyhedral" fragment from some code of interest. We will transform into Alpha polyhedral representation and pick a shape using the Pluto tool. Then we will choose a tile-parallelization strategy including schedule of tiles, allocation of tiles to processors, and inter-tile communication based on Pluto or similar tool. This will yield all parameters needed to formulate the constraints of the optimization problem. We will then try to solve that optimization problem for different meaningful objective functions. The next steps will be to generalize that framework for the case of an algorithm with multiple codelets.

Conclusion

We will formulate several versions of the optimization problem discussed above and develop efficient algorithms for their solutions. We will combine our new algorithms in a proof-of-principle tool and will test it on optimizing nested loops for GPU type architectures. The loops will be chosen both from simple linear algebra and numerical methods codes during the development phase, as well as on advanced codes used at LANL (e.g., in molecular dynamics simulations) for which GPU type implementations exist. The goal will be to compare the quality of our solution against hand-optimized GPU implementations in order to validate the results.

Publications

Aleksandrov, L., H. Djidjev, A. Maheshwari, and J. R. Sack. An Approximation Algorithm for Computing Shortest Paths in Weighted 3-d Domains. 2013. DISCRETE & COMPUTATIONAL GEOMETRY. 50 (1): 124.

Djidjev, H., and M. Onus. Using graph partitioning for efficient network modularity optimization. 2013. GRAPH PARTITIONING AND GRAPH CLUSTERING. 588: 103.

Djidjev, Hristo N.. Parallel seed-based approach to protein structure similarity detection. 2013. Los Alamos National Laboratory, LA-UR-13-27448.

Djidjev, Hristo N.. Efficient Shortest Path Computations on Multi-GPU Platforms. 2013. Los Alamos National Laboratory, LA-UR-13-26585.

Djidjev, Hristo N., Guillaume Chapuis, Sunil Thulasidasan, and Rumen Andonov. On Solving the Shortest Path Problem for Planar Graphs using Graphics Processors. 2012. Los Alamos National Laboratory, LA-UR-12-25700.

Djidjev, Hristo N., Rumen Andonov, Sanjay Rajopadhye, and Vamsi Tandrapati. Co-Design Optimization of Jacobi Kernel for GPU Architectures. 2013. Los Alamos National Laboratory, LA-UR-13-28110.

Djidjev, Hristo N., Sunil Thulasidasan, Rumen Andonov, Guillaume Chapuis, and Dominique Lavenier. Efficient Multi-GPU Computation of All-Pairs Shortest Paths. 2013. Los Alamos National Laboratory, LA-UR-13-28111.

Contextual Learning and Recognition

Alexei N. Skurikhin
20130265ER

Introduction

Event and object recognition requires analysis of massive quantities of data to detect and identify static or dynamic patterns of interest. One challenge for automated object recognition, and machine learning in general, arises from the fact that in spite of huge and growing quantities of data, complex event recognition often remains ill-posed. The object recognition ambiguity can be addressed by exploiting the fact that events rarely occur in isolation; they tend to co-occur and co-vary, and this correlation structure, known as context, provides important information for the disambiguation of the event. However, while being extremely useful for disambiguation of events and objects, such context-aware knowledge discovery typically leads to a significant increase in the number of features to be analyzed. Modeling contextual information and scaling machine learning methods for context aware object recognition to large problems are among the most challenging issues in developing the next generation of information extraction approaches.

We aim to develop novel efficient machine learning and inference methods for context aware probabilistic recognition of complex events and objects based on Markov and Conditional Random Fields. Development of scalable context learning and inference methods for probabilistic object recognition will have implications in many domains, such as computer vision, image interpretation, bioinformatics, text analytics, and web search. Furthermore, the problem of efficient learning and inference in general structure random fields is closely related to several important combinatorial optimization problems. Methods developed in this project will therefore facilitate progress in combinatorial optimization, probabilistic graphical modeling, and related areas.

Benefit to National Security Missions

This project contributes to addressing the Information Science and Technology Grand Challenge - the development of breakthrough mathematics and computer science required to extract knowledge from massive quantities of data. Current approaches to event and object recognition in imagery are overwhelmed by the number of images, the sizes of images (e.g., high-resolution satellite image can be up to 10^9 pixels and larger), and the diversity of visual features associated with objects of interest. Current approaches are also facing a need to deal with increasing use of signature suppression, camouflage, concealment, and deception. Context aware image data mining will provide an ability to focus human analysts on “hot spots” in such data.

The project is also related to the Threat Reduction mission. If successful, our methods will increase the productivity of human analysts, optimize the use of high-value sensors (which typically have a narrow field of view) for monitoring of wide areas, and improve the timeliness and accuracy of decision making.

Progress

Contextual learning is posed as a structured machine learning problem, which is about learning knowledge from data with internal structure in the form of one or more relations between co-occurring, co-located or co-varying objects, which are also known as inter-linked objects. Rather than recognizing each object independently, classification of such interlinked objects is done collectively by performing simultaneous classification of several objects, which act as context for each other. During the first year of the project, we made advancements in two areas. The first is the investigation and development of descriptors to characterize contextual cues. We focused on the computer vision area and developed algorithms to estimate similarities of image elements (such as image pixel patches) by considering longer range interactions between the elements across multiple spatial scales, using descriptors based on edge orientation histograms, phase congruency, differen-

tial invariants, and scale invariant interest points. These descriptors are used to characterize patches and their relationships (e.g., similarities), while patches themselves constitute complex objects which are modeled as flexible constellations of parts augmented with inter-part contextual relations. This provides a context modeling framework with statistical summary of the whole image, spatial layout properties within local image regions surrounding pixel patches, as well as reduces original image data size and thus learning and inference computational complexity due to the use of lower number of pixel patches instead of huge number of individual pixels constituting original image.

The second is an optimization approach for performing approximate probabilistic inference in contextual models of object recognition. The context framework based on graphical probabilistic models appears quite promising but faces a challenge of computational intractability of exact inference if underlying probabilistic graphical model contains cycles, which is the case in many real world cases, e.g. in computer vision where an image is modeled as grid structured pairwise Markov random field (MRF) and/or Conditional random field (CRF). To address the problem, we prototyped and investigated approximate inference based on pseudo-likelihood (PL) approach. Instead of calculating the probability of individual variables at sites in MRF/CRF given all other variables at different sites, the PL approach approximates the joint probability of the variables at nodes in MRF/CRF as a product of individual conditional probabilities over each variable, where the conditioning is on the neighbors of the variable. This property makes it a very efficient parameter learning method with some loss of accuracy, for it avoids exactly calculating the likelihood partition function. The PL-based approximation has been shown to produce consistent estimates in the large lattice limit. We investigated inference based on PL in "flat' and hierarchical CRF models.

Finally, when the data and/or parameter dimension is extremely large, particularly whenever the likelihood involves summing probabilities over many unobserved states such as genealogies in biology, and, for example, in applications in astronomy and cosmology, and corresponding models do not have an analytical likelihood function, we developed and investigated an approach to choose summary statistics for approximate Bayesian computation to enable inference without explicit likelihood.

Future Work

We plan to investigate and develop algorithms for approximate probabilistic inference to reduce computational complexity of the learning and recognition processes. We will investigate message scheduling schemes used during inference, as well as approaches to approximate inference in intractable graphs via ensembles of tractable sub-models.

For validation, we will utilize datasets used in the computer vision community, as well as seek for applications outside of computer vision area.

Conclusion

Our goal is to develop efficient machine learning and inference algorithms for probabilistic modeling of contextual information and context-aware object recognition based on Markov and Conditional Random Fields (M&CRFs). This will broadly entail investigating and developing algorithms for (1) multi-scale contextual modeling and (2) scaling an approximate probabilistic inference and M&CRF learning to large datasets. While developing these algorithms will have implications in many problem domains, we will focus on computer vision, on a challenging problem of object recognition in an unconstrained environment, for validating our algorithms.

Publications

Burr, T., and A. N. Skurikhin. Approximate inference options in data models for image analysis. 2013. presented at the Statistical Image Analysis Workshop, Santa Fe, NM, LAUR 13-21603.

Burr, T., and A. Skurikhin. Pseudo-likelihood inference for Gaussian Markov random fields. 2013. Statistics Research Letters. 2 (3): 63.

Burr, T., and A. Skurikhin. Selecting summary statistics in approximate Bayesian computation for calibrating stochastic models. 2013. BioMed Research International. 2013: 10 pages.

Skurikhin, A. N., S. R. Garrity, N. G. McDowell, and D. M. Cai. Automated tree crown detection and size estimation using multi-scale analysis of high resolution satellite imagery. 2013. Remote Sensing Letters. 4 (5): 465.

Physics-based Data Models and Architecture-optimized Backends for a Portable Data-parallel Computation Library

Christopher M. Sewell
20130418ER

Introduction

Portability is a major challenge for software developers due to the increasing heterogeneity of high-performance computing hardware. To address this issue, we have recently implemented several standard algorithms using NVIDIA's Thrust library. Thrust provides basic vector data types and implementations of a number of data-parallel primitives (such as scans, reductions, stream compactions, etc.) on these vectors in backends that target OpenMP and CUDA. While we believe that the data-parallel model embodied by Thrust is the right approach to achieve both portability and performance across a wide range of architectures, Thrust suffers from several major limitations that prevent its widespread use.

First, Thrust has an extremely simplistic data model, consisting only of one-dimensional vectors, which makes it difficult for a programmer to use with more complex data types commonly used in physics simulations, such as multidimensional and unstructured meshes.

Secondly, Thrust's OpenMP backend is not very efficient on many platforms, especially vector architectures, and devices which do not use CUDA or OpenMP are not supported. Thus, we propose to devise an abstract data model on top of Thrust which is co-designed with developers of a multimaterial hydrodynamics simulation. Furthermore, we intend to expand and improve the backends for Thrust to better target implementations of the data-parallel primitives to emerging technologies.

While we will target vendor technologies based on lab computing priorities, we expect to target the Intel MIC architecture and at least one additional platform, such as an IBM Power System or the ARM Architecture. Co-design will be integrated across all levels, from algorithm development to data model design to backend implementations to (on a limited scale) hardware vendor engagement.

This proposal is intended as a significant first step towards allowing scientists to easily map their simulations onto a Thrust-based data model and efficiently run their algorithms on emerging parallel technologies.

Benefit to National Security Missions

The deliverables and the experience resulting from the proposed work will build laboratory capabilities in programming models within the larger exascale computing co-design missions. The physics targeted by our front-end work has been chosen to support the type of simulations critical to the DOE Nuclear Energy Programs and other DOE agencies, while the architectures targeted by our back-end work are being chosen to support the specific hardware that will be likely to be used in the laboratory's next generation of supercomputers. The deliverables of this project, including interface reconstruction and advection operators for both structured and unstructured grids that can achieve good performance on several next-generation supercomputing architectures, could be used to interface with compressible multi-material hydro codes used extensively in the ASC program and in X Division. This work should also be complementary to other work on cross-platform high-performance computing at the laboratory. For example, the physics code resulting from this work could potentially be compiled by the compiler being developed by the Scout project, with this work providing a useful application and data abstraction for Scout, and the low-level compiler optimizations made by Scout providing an opportunity for further performance enhancement for this work.

Progress

We have implemented 1D, 2D, and 3D mesh data structures that allow physicists to easily map a structured grid to the 1D vectors used by Thrust. The design of the mesh data structures provides an interface familiar to computational physicists while introducing them to the concept of the data parallel programming model. This

enables them to take advantage of the available parallelism while still thinking in terms of familiar structures such as cells, vertices, and edges. This is the result of several iterations of tight and productive cooperation between the computational physicist and the computer scientists of the team. We have implemented volume fraction initialization using all three of these mesh data structures, and are currently implementing interface reconstruction for the 2D case.

We have purchased a small cluster of Intel Xeon Phi (MIC) nodes, which have been successfully installed within our group's Darwin cluster, and we have extensively studied this architecture (including attending several MIC programming workshops). We have run our PISTON isosurface operator, using the existing OpenMP backend, directly on an Intel Xeon Phi coprocessor (i.e., in "native" MIC mode), with good scaling results with the number of threads.

We then modified the OpenMP backend for selected data-parallel primitives in order to improve vectorization performance on the Xeon Phi. We have also started implementing backends for a small number of Thrust primitives using the "offload" mode (in which some processing is performed on the host and some on the coprocessor). In the near future, we plan to improve vectorization and support offload mode for additional Thrust primitives.

Furthermore, we have extended the Thrust library to support concurrency in distributed memory environments across multiple nodes. This enables the application developer to write data-parallel algorithms while viewing the data as single, long vectors, essentially without needing to explicitly take into consideration whether the values are actually distributed across nodes. Our distributed wrapper for Thrust handles the communication in the backend using MPI, while still using the standard Thrust library to take advantage of available on-node parallelism. We have written distributed implementations of several key data-parallel primitives, including scan, scatter/gather, sort, reduce, and upper/lower bound. In the near future, we expect to run algorithms using this distributed implementation on multiple Xeon Phi (MIC) coprocessors in our cluster.

We have submitted a paper about our distributed Thrust design to the Large Data Analysis and Visualization Symposium at the IEEE Visualization Conference. Marianne Francois gave an invited talk about the underlying physics for the interface reconstruction method entitled "Advances and Challenges in Modeling Interfacial Flows" at the March meeting of the American Physical Society. Infrastructure for project management has also been established, including a git repository on a shared network space and periodic project status update e-mails.

We believe that we are on track to meeting our two Year 1 milestones by the end of the fiscal year. Specifically, we expect to complete our implementations of interface reconstruction in 2D and in 3D using the structured mesh data structures that we have developed, and to be able to run our algorithms efficiently on a single Xeon Phi (MIC) coprocessor and on multiple Xeon Phi coprocessors.

Future Work

Second-year Physics Co-Design Milestone: Complete implementation of volume fraction initialization and interface reconstruction on unstructured meshes.
Second-year Backend Co-Design Milestone: Decide on additional target architecture(s), acquire access to necessary hardware, and learn how to use and understand the architecture(s).

Conclusion

We expect to deliver a fluid flow simulation of multiple materials that seamlessly maps its mesh data structures onto a new Thrust data model, enabling it to run key algorithms and operators with high parallel efficiency on multiple emerging supercomputing technologies. At a minimum, this would include visualization and analysis operators that compute information such as interface boundaries, taking advantage of cutting-edge parallel architectures such as Intel MIC. The data model developed should be applicable to a variety of other simulations, and the experience gained from optimizing for the targeted architectures should be applicable to a variety of additional platforms.

Publications

Sewell, C., L. Lo, and J. Ahrens. Portable data-parallel visualization and analysis in distributed memory environments. To appear in IEEE Symposium on Large-Scale Data Analysis and Visualization. (Atlanta, Georgia, 13-14 Oct. 2013).

Co-Design of Burst Buffer Hardware and Data Analysis/Visualization Software for Large-scale Simulations

Jonathan L. Woodring
20130457ER

Introduction

Burst buffers are new concepts for storage architectures that will enable larger supercomputers. A burst buffer can be thought of as a cache that sits between the high performance supercomputer and its file system. Its main purpose is to support high-speed checkpoint and restart for fault tolerance enabling larger supercomputers. The supercomputing communities are uncertain as to the burst buffers specifications and what they should be capable of performing. One extreme is that the burst buffer is no more than an extension of the file system acting as a buffer to the slower, larger, parallel file system. Another extreme for the burst buffer configuration is a robust data intensive parallel supercomputer.

The high potential of burst buffers starts with the fault tolerance enabling the next jump in scale of supercomputers. This potential is extended by this proposal: researching a burst buffer's ability to visualize, analyze, triage, and transform large-scale data while it is in transit (as the data are moving from compute to storage) or some combination thereof. This extended possible uses for the burst buffer will enable larger scale supercomputers and decrease time to results for users of supercomputers.

We propose to use the Parallel Ocean Program (POP) and possibly other simulation codes, the Darwin Cluster, and Burst Buffer prototype nodes to configure simulation-to-analysis data workflows. We will use combinations of different modes of analysis and burst buffer hardware configurations, such as in situ, in transit, and post-processing visualization and analysis. We will explore the hardware and software configuration space for these proposed burst buffer nodes ranging from simple cache appliances to a full-fledged data intensive system. Understanding what a burst buffer should be and what it is capable of, is a current barrier to designing and specifying the next generation of supercomputers.

Benefit to National Security Missions

The primary technical goal of this co-design effort is to provide specification documentation for burst buffers, large-scale simulations, and visualization and analysis workflows. Technical goals that must be achieved include building a software framework that enables post, in situ, in transit, and hybrid visualization and analysis processing, performance analysis of this software framework and building a prototype of a simulation working in this framework.

The impact of this work will influence the design of future supercomputers: both hardware and software. In addition, this work will influence computational science applications (across many disciplines) for large-scale design and analysis of results.

The A-relevant categories are sciences and programs that have a large simulation and/or supercomputing component to their research and programmatic needs. The results of this research will impact how future supercomputers, simulations, and analysis workflows are designed to work with burst buffer enabled supercomputing. To be able to run on the next-generation supercomputers, the science programs will need computational and large-scale data assistance to utilize the hardware (such as burst buffers) for the simulations and other computational components to scale up in size and complexity. Our research will be able to inform the simulation and computational scientists, analysts, and system designers the best practices for using burst buffers in visualization and analysis, in addition to checkpoint/restart.

Progress

The tasks for last year were:
1. Install and Configure Burst Buffer Hardware
2. Prototype of POP as a Benchmark
3. Generate Plots and Ratios of Data Production and

Ingestion Rates of each Component in the System Architecture while Running POP

We have successfully completed each of these tasks and created or finishing up the end of year deliverables for each task.

The burst buffer prototype hardware has been successfully deployed in the darwin research cluster. It is a small compute cluster consisting of compute nodes and solid state disk technology. In addition, we have set up a "scratch" parallel file system to model the typical parallel file systems used in HPC computing environments. The scratch parallel file system and burst buffers will be used to compare against in situ vs. in transit vs. post-processing analysis workloads, coexisting with checkpoint/restart.

The burst buffer prototype is flexible in that we can explore different hardware and software configurations, for experimenting with checkpoint/restart workloads and analysis configurations. We can reconfigure the burst buffers to act like traditional IO nodes (dumb buffers) compared to our desired usage of co-analysis and visualization offloaded from the compute, coexisting with compute heavy workloads and checkpoint/restart fault tolerance. Our experiments will be how we can optimize the time to results, while also providing fault tolerance services.

The current software stack under evaluation includes GPFS with file placement option (new beta software that was used in the IBM Watson system), JBOD (just a bunch of disks), PLFS, HPFS (Hadoop), existing POP analytic software, new POP analysis code, and software derived from ParaView/VTK. We will also be exploring other portions of the software stack in the next year, such as scheduling analysis with checkpoint/restart and how to perform migration of code to data (rather that data to code).

POP and a test input deck for simulation and analysis workloads has been successfully deployed on darwin and on the burst buffers as our test experiments. We are currently in the final stages of integration of parallel file system routines into POP and POP analysis code (this includes MPI-IO and PLFS file acceleration) for final benchmarking, listed in the next milestone. This will be useful to compare parallel writes to existing serial Fortran (POSIX) writes, and N-1 and N-N workloads.

Additionally, our current POP analysis work may have near future external impact, as it will be leveraged by the COSIM/CESM climate community. One of our benchmark analysis routines, developed for our experiements, is currently under evaluation by the COSIM team. It may be integrated into CESM (Community Earth Systems Model, a combined climate model used in the IPCC, Intergovernmental Panel on Climate), due to our acceleration of the MOC (Meridional Overturning Current), which will greatly accelerate the CESM/COSIM analysis workflow.

We are currently finishing the benchmark report for POP, POP analysis, and the prototype burst buffer itself. This report will be useful for us (as baseline numbers for future research in the second and third years), but for other researchers and engineers trying to evaluate burst buffer hardware and HPC environment configurations.

The base file system and hardware IO performance tests have been completed. We are currently in the phase such that we are tuning parameters and doing a further parameter sweeps to compare the IO performance improvements through tuning the IO system and different configurations. This parameter experimentation includes tuning the file system layers and hardware for optimization comparison and adds potential avenues for future experiments.

Additionally, we have benchmarked the MOC analysis operations for in transit mode and will be instrumenting POP itself with an in situ MOC calculation in the near future for direct comparison. After the parallel IO routines are finished this month, we will benchmark the checkpoint/restart capabilities on the burst buffer and baseline systems. This will include running the Lagrangian tracer analysis code and performance tests on in situ vs. in transit vs. post-processing tracers.

The expected rough draft of the report is due in July and the final benchmark report will be completed in August. These benchmark experimental numbers will give us the grounding to look for improvements in the analysis, computation, and scientific workflows in the next year and following year.

Future Work

Explore dynamic scheduling architecture for the burst buffer

Currently in HPC systems, resource provision is based around the batch queue model. If we assume that the burst buffers are part of the resource provisioning, this means in traditional HPC queues that burst buffers will be under utilized. For example, a simulation will only use a burst buffer temporarily, leaving it idle the rest of the time. To exploit the idle cycles, we will explore an IaaS model in an HPC environment. Other researchers have attempted this in the past, but with unsatisfactory results due to not fitting an HPC workload. We will configure our prototype

with HPC environments in mind, prioritizing checkpoint/restarts with an analysis (multi-user workload). This is unique outside of existing IaaS models and previous research.

Explore a programming model for applications, to move compute to data under distributed parallelism model (SPMD)

Currently, the models for moving computation to data or data to computation only exist in the loosely-coupled cloud computing environment (see Hadoop and map-reduce). In scientific computing, most researchers use the SPMD (single program, multiple data) programming paradigm, that is most personified by MPI and PGAS programming models.

We will look to extend the SPMD scientific programming model to account for data locality, which will be important for burst buffer analysis. If we assume that HPC data will be scattered across a burst buffer file system, especially without a global namespace, analysis applications need the capability to move computations to data, because data will not be able to be moved to computations. This programming model will allow scientific SPMD analysis adapt to "scattered data."

Explore advanced compiler technology

Advances in compilers (LLVM) will support scheduling, moving and executing analysis for automatic in situ, in transit, and post-processing placement for reduced time to results.

Conclusion

The primary technical goal of this co-design effort is to provide specifications for burst buffers and analysis workflows. Technical goals that must be achieved include building a software framework that enables post, in situ, in transit, and hybrid visualization and analysis processing, performance analysis of this software framework and building a prototype of Parallel Ocean Program working in this framework.

The impact of this work will influence the design of future supercomputers and simulations: both hardware and software. In addition, this work will influence computational science applications (across many disciplines) for large-scale design and analysis of results.

Publications

Mitchell, C., D. Bonnie, and R. Knight. Co-Design of Burst Buffer Hardware and Data Analysis/Visualization Software for Large-Scale Simulations: Burst Buffer Initial Test Report, August 2013. 2013. LA-UR-13-27974, Los Alamos National Laboratory.

Mitchell, C., and D. Bonnie. In-Transit Processing: Data Analysis using Burst Buffers. High Performance Parallel I/O. Edited by Prabhat, , and Q. Koziol.

Validating Near-ideal Data Throughput Using a Rate-compatible Protocol

Scott H. Robinson
20130504ER

Introduction

This project will demonstrate, both in the lab and under real world conditions, an advanced information coding technique, combined with a specialized transmission protocol, which will maintain near-ideal data throughput performance regardless of the noise present in a wireless (Radio Frequency or RF) communication channel. Working together, the coding technique and the transmission protocol dynamically tunes the throughput rate of each data packet to adjust to rapidly changing interference in the transmission channel. This is done automatically with a minimum amount of feedback and no specialized equipment to measure the quality of the channel. The result is a data transfer rate that approaches the theoretical maximum set by the Shannon limit.

Our technique maximizes data throughput capacity across a wide range of channel conditions; adjusts dynamically to changing conditions in the transmission channel without a priori knowledge; minimizes the amount of back channel communication required from the receiver; can be implemented using common communication hardware; and is compatible with existing modulation and channel bandwidths. Previous work included a detailed description of how data packets are constructed; how data packets are decoded; how handshaking is done between transmitter and receiver; and a computer simulation comparing expected performance of our technique to the performance of other existing techniques over a wide range of channel quality. The results of this simulation showed significant improvement over the other coding methods.

Our work will implement the coding algorithm and the transmission protocol in actual hardware and validate its data throughput performance under a wide range of interfering noise.

Benefit to National Security Missions

This project demonstrates technology that can significantly increase the data throughput capacity of existing wireless (RF) communication links. Any mission or agency concerned with the efficient and reliable delivery of digital information in the presence of dynamically changing interference could benefit from our work. NNSA is responsible for satellite instruments to meet national treaty monitoring requirements. This includes the delivery of sensor data to the ground during ionospheric disruptions due to a high altitude nuclear event. Our technology would ensure maximum data delivery under these dynamically changing conditions. Additionally, NNSA remote sensing missions also have the need to efficiently transmit data across a RF link and could benefit from our technology.

Agencies including the DOD, NASA and numerous Intelligence Agencies rely heavily on wireless communications to perform their missions. Often these RF links must operate when the condition of the communication channel is poor due to natural interference, weak transmission signals or intentional jamming. Our coding algorithm and transmission protocol can significantly improve the performance of these links.

In the world of commerce, the annual growth in wireless data traffic has been predicted at 74% over the next couple years. Much of this growth is driven by expanded use of smartphones. Due to the mobility of these devices, channel conditions constantly change due to their distance from a base station; intervening buildings or terrain; and noise present in the environment. Our technology can improve the performance under all these conditions while increasing the data carrying capacity of the RF spectrum.

Progress

Work this year has focused on three main areas: constructing a model of the information encoding technique and transmission protocol; implementing the design in logic compatible with hardware; and purchasing and gaining experience with the hardware and tools that will be used for building the prototype.

A variety of Low Density Parity Check (LDPC) codes were researched to identify the best form of a LDPC code that provides both good rate-compatible code performance and is well-matched to the prototype hardware. Through this research the Weight-3-Repeat-Accumulate (W3RA) code was selected. These codes have a simple encoder structure while still maintaining a lower bit-error-rate floor compared to other standard Repeat-Accumulate LDPC codes. Two methods to convert the W3RA code into a rate-compatible code were then explored. These techniques are check node splitting and check node puncturing. After evaluation, check node puncturing was selected due to the simplicity of its implementation.

High level simulation models of the encoder and decoder have been fully developed and tested. This work has included the creation of a unique algorithm that constructs a parity check matrix in a way that avoids a problem with decoding known as small Tanner graph cycles. If a check matrix has small Tanner graph cycles then the amount of redundant information in the code will be low and it will not operate well in the presence of noise. This algorithm is important to this effort so that the developed W3RA code will exhibit good decoding performance across a wide range of transmission channel conditions. Work continues on construction of a full end-to-end model that will use a Monte Carlo simulation to compare the bit-error-rate of the W3RA code when using different amounts of puncturing that provides the rate-compatible performance required.

Using the model of the encoder and decoder, logic has been developed to implement the design in a Field Programmable Gate Array (FPGA). This required the high level simulation model to be converted to a low level design using fixed point arithmetic and lookup tables to simplify hardware implementation. These designs are written in VHDL, a standard hardware description language used for FPGA design. Throughout the development process, simulation of the low level fixed point design and the VHDi design are performed and results are compared to the original design to ensure correct implementation.
A VHDL design of the W3RA code encoder has been completed. The encoder can handle permutation pattern sizes up to 65336 bits in length which is important to provide flexibility during future testing. The encoder uses block memory structures in the FPGA for storing message bits and parity check bits allowing it to support a variety of puncturing schemes. An initial VHDL design for the decoder has also been completed. This design uses a technique that allows the size of the decoder matrix and bit-widths to be adjusted to analyze performance trade-offs. A moderate sized version of the decoder was then synthesized into hardware so FPGA logic resources could be assessed including logic gate and block memory usage. Work continues to refine the design of the decoder to optimize the use of logic resources to allow larger versions to be efficiently realized.

Two wireless development kits have been purchased from Texas Instruments (part number CC1101DK) to provide the frontend radio component for the prototype. These units use the unlicensed instrumentation frequency band of 433 MHz. Initially, these radios will be connected together using a coax cable. Actual over-the-air transmission will be done during year two of the project and after permission to transmit is obtained from the laboratory. These radios will be connected to a FPGA Development board from Xilinx, the ML605. The FPGA on the ML605 will support the W3RA encoder, decoder and transmission protocol while the radio is used to physically transmit and receive the information.

Development is currently in progress to connect the various segments of the hardware design and create communication between the CC1101DK, the ML605 and a host PC. Once completed, the host PC will be used to configure the FPGA on the ML605 with the encoder, decoder and protocol design; adjust transmission parameters; send and receive messages; and monitor performance statistics.

Future Work

The goal during the first year of the effort has been to implement the information coding algorithm and transmission protocol in a prototype wireless device and perform initial data throughput testing in the lab.
The goal of the second year of the effort will be to demonstrate the ability of the design to maximize data throughput across a dynamically changing noisy channel. Initially work will be done in the lab to optimize the performance of the coding algorithm, the transmission protocol and its implementation in hardware. Additionally, tools will be developed to monitor, in real time, the throughput rate of the data being transferred by the devices and the signal to

noise ratio of the communication channel. The prototype devices will then be taken outside and tested wirelessly in an operational environment.

Major tasks for the second year of the effort are:

- Establish an experimental setup in the lab between two prototype devices communicating with each other using a coax cable. Use lab equipment to inject noise into the communication channel and monitor performance.
- Optimize performance of the information coding algorithm and transmission protocol in the hardware.
- Document the data throughput performance of the prototype devices across a wide range of simulated noise using the lab experimental setup.
- Move to wireless operations outside and document the data throughput performance of the prototype devices under operational conditions. These tests will include varying the power of the transmitter and monitoring performance while both devices are in motion.

Conclusion

At the completion of this project, a demonstration prototype will exist with sufficient quantitative test results to validate the data throughput performance of the information coding algorithm and transmission protocol across a wide range of channel conditions. These tests will be done both in the lab and over the air in an operational environment. These results will provide a solid foundation for future operational programs to evaluate the benefits and computational complexities of our technology.

Sparse, Distributed, and Robust Network Control

Marian Anghel
20130558ER

Introduction

The goal of this project is the design of distributed controllers for complex interconnected systems. Although emerging network control applications include large mechanical structures, distributed sensing, and interacting mobile robot agents, the focus of this project is the design of distributed controllers for large scale power grid systems.

This project aims to address two critical weaknesses of power grid systems. First, the current power grid has not yet fully embraced the most recent advances in distributed sensors, embedded computing systems, and advanced communication networks. Second, the power grid faces the simultaneous convergence of several emergent difficulties (intermittent renewable energy sources, frequent transmission congestions, relentless market pressure) which the existing centralized control infrastructure will not be able to solve.

In response to these challenges, this project seeks to construct an algorithmic synthesis of nonlinear and distributed control techniques for large networked power systems. More specifically, we propose a decentralized approach which exploits separability and decomposition of the corresponding control problem into nonlinear sub-problems which can be solved locally and efficiently. This project explores new ideas from compressed sensing, convex optimization, and algebraic geometry, that have the potential to radically change the ability to formulate the stability and control of the future Smart Grid (and in general large networked dynamical systems).

Success of this project will position LANL at the forefront of this research and enable engineering control systems to be developed that can operate at the global network scale.

Benefit to National Security Missions

Recent workshops organized by the Department of Energy (DOE) in partnership with Office of Electricity Delivery and Energy Reliability (OE) were focused on the challenges of grid modernization efforts (March 2009) and on the computational needs for the next generation electric grid (April 2011). The proposed research directly supports these program development directions.

More specifically, the report on "Advanced Control Methods" conducted by the National Energy Technology Laboratory for the DOE in 2007 has identified the need for the development of distributed intelligent agents that respond rapidly at the local level to unburden centralized control systems. Our project directly addresses this problem by developing a distributed control methodology which is robust with respect to system disturbances.

Furthermore, the Smart Grid Research and Development Program of the DOE/OE, identifies in its multi-year program plan the development of advanced control methods. As the smart grid evolves, this program notes that more complex automated control systems will be necessary to maintain optimum operation of the grid. The control algorithms that will be investigated in this project directly address the fundamental conceptual challenges posed by such automated control systems. Finally, the April 2011 DOE workshop, "Computational Needs for the Next Generation Electric Grid Proceedings," highlights a class of mathematical and computational problems relevant for potential power systems research. It identifies, in particular, the difficulties currently encountered by direct transient stability analysis methods. This project directly addresses this problem and our preliminary results have already offered significant breakthrough results based on novel algebraic control techniques.

Progress

We have built the software infrastructure needed to simulate the dynamics of classical power systems. We have also built the software framework needed to cast the power systems equations into a polynomial form that Sum of Squares (SOS) methods can use for system analysis and controller design. The SOS method is a recently developed algebraic framework for analysis of nonlinear systems, which uses the SOS decomposition of polynomials as a computational relaxation to polynomial non-negativity conditions. The algorithmic search for non-negative SOS polynomial enables the algorithmic construction of Lyapunov functions for nonlinear dynamical systems.

Moreover, we have implemented a decomposition technique that decomposes the power system into a number of smaller, weakly interacting subsystems. This algorithm was proposed by our collaborators at Oxford University and employs graph theoretic methods that takes into account both the strength of interactions and the energy flows between the generators in different subsystems. This algorithm generalizes early decomposition approaches that were based only on the magnitude of the elements of the system matrix - the strength of the interaction terms between the system generators. It was shown that this is not a good approach, as magnitude alone does not always provide a good indication of coupling strength between subsystems. The proposed algorithm takes both energy flow and dynamics into account whereas many other methods simply account for the system topology.

After we have performed a system decomposition into a number of dynamic subsystems specified a priori, we have computed Lyapunov functions for each subsystem and used them to estimate the region of attraction (ROA) pertaining to the equilibrium point of each isolated subsystem. We have used sparsity constraints to force a simple expression for these functions - minimize the number of monomials in our polynomial Lyapunov functions - and we have also computed sparsity free Lyapunov functions for which no sparsity constraints were imposed. We started to analyze how well these Lyapunov functions approximate the region of attraction of the stable operating point and how sparsity constraints affects the quality of these approximations.

Finally, after we have identified Lyapunov functions for each isolated subsystem, we started to aggregate together the subsystem Lyapunov functions in order to compute a composite Lyapunov function for the entire system. We note that using a good decomposition algorithm is critical for this approach to succeed. Indeed, the decomposition algorithm seeks a partition of the system with the objective of minimizing the effect that the neglected interaction dynamics between subsystems have on the subsystem drift dynamics. Hence, this decomposition will facilitate the construction of a composite Lyapunov function.

We have applied the combination of decomposition and SOS Lyapunov techniques to a 7 generator 26 bus power system model. We remark that this system is too big to be analyzed directly using SOS techniques.

The analysis has been described in a paper titled “Stability Analysis of Power Systems using Network Decomposition and Local Gain Analysis,” that was submitted and accepted to the 2013 IREP Symposium-Bulk Power System Dynamics and Control.

We have also significantly revised two papers that were submitted for publication before the start of this project and that were under review when this project started. The papers are highly relevant for this project. The first one titled “Algorithmic Construction of Lyapunov Functions for Power System Stability Analysis,” has been accepted for publication in IEEE TRANSACTIONS ON CIRCUITS AND SYSTEMS and is already published online. This paper describes a SOS based algorithm that is used for computing Lyapunov functions for each individual subsystem that results after the system decomposition algorithm is applied.

A second paper titled “Spontaneous synchrony in power-grid networks,” has been accepted and published by Nature Physics. This paper derives a condition under which the desired synchronous state of a power grid is stable, and use this condition to identify tunable parameters of the generators that are determinants of spontaneous synchronization. We intend to use this finding in the controller design phase of our project.

Future Work

In the first year of the project we have implemented a decomposition technique that seeks to decompose the system into a number of smaller, weakly interacting subsystems. This algorithm employs graph theoretic methods that takes into account both the strength of interactions and the energy flows between the generators in different subsystems.

We have also computed independent Lyapunov functions for each subsystem using a Sum of Squares (SOS) algorithm that we have recently introduced. We have used sparsity constraints to force a simple expression for these polynomial Lyapunov functions.

We have also computed estimates for the region of at-

traction (ROA) of each subsystem when its interactions with the rest of the system are neglected. These estimates provide a bound on the largest disturbance (angle and frequency deviations) that the subsystem can withstand without loosing its stability. We started to analyze the tradeoff between highly sparse (few monomial terms) polynomial Lyapunov function and the more complex functions that can be computed when no sparsity constraints are used in the SOS programming framework.

Furthermore, we started to implement SOS techniques to aggregate together these subsystem Lyapunov functions in order to compute a composite Lyapunov function for the entire system that takes into account the interactions between subsystems.

In the second year we will couple the decomposition approach with the SOS analysis framework to analyze power grid systems of increasing size. We will apply recursive decomposition techniques to larger power grid systems and we will compute the input-to-output stability properties of each stable subsystem using the SOS framework. By patching together the input-to-output response of each subsystem we will derive stability bounds for the large-scale complex system. We will improve the stability of each subsystem by designing local state and output feedback controllers and estimate their disturbance rejection performance.

Conclusion

This project will provide for the first time a methodology for the algorithmic construction of Lyapunov functions and for the design of distributed, nonlinear controllers for power grid systems.

The algorithm will use sparsity constraints to control the complexity of the controllers and a hierarchical decomposition methodology in order to extend modern nonlinear algebraic control techniques to large scale distributed systems.

The successful completion of this project will generate a renaissance of direct analysis methods based on Lyapunov techniques and will open new research directions in the distributed control of power grid systems.

Publications

Anghel, M., F. Milano, and A. Papachristodoulou. Algorithmic Construction of Lyapunov Functions for Power System Stability Analysis. 2013. IEEE Transactions on Circuits and Systems I: Regular Papers. 60 (9): 2533.

Anghel, M., J. Anderson, and A. Papachristodoulou. Stability Analysis of Power Systems using Network Decomposition and Local Gain Analysis. To appear in Bulk Power System Dynamics and Control Symposium.. (Crete, Greece, 25-30 Aug. 2013).

Motter, A. E., S. A. Myers, M. Anghel, and T. Nishikawa. Spontaneous synchrony in power-grid networks. 2013. NATURE PHYSICS. 9 (3): 191.

Rare Category Detection

James P. Theiler
20110126ER

Abstract

We investigated a new kind of anomaly detection, called Rare Category Detection, with the aim of more efficiently finding and more accurately identifying anomalies that are meaningful. We looked at this issue from a number of different angles, developing theoretical insights, practical implementations, and looking into a variety of potential applications, ranging from medical imagery to satellite state of health.

Background and Research Objectives

A seemingly impossible task in data mining is that of extracting meaningful rare-event data from massive data sets when we don't know what is meaningful until we see it. On the one hand, any credible solution, whatever its form, must incorporate a human expert to determine what is meaningful and what is not. On the other hand, human experts can directly examine only an infinitesimal fraction of the data, thus creating what appears to be a fundamentally intractable problem. To confront this intractability we must make prior assumptions, and hope that they capture some relevant characteristics of meaningful data. The most common prior assumption is that meaningful rare-event samples are unlike the rest of the data, that they are anomalous. And indeed, anomaly detection is an important component of the solution, though standard anomaly detection may by itself be inadequate. For example, in an astronomical image archive, we can identify the most anomalous 0.1% of the objects in the sky survey using standard anomaly detection, but only 1% of these anomalies (and only 0.001% of the full dataset) might actually be meaningful in the sense that they correspond to potential new discoveries by the astronomer. The goal is to identify these meaningful anomalies as efficiently as possible. Similar examples are can be found in the areas of network monitoring and file system forensics for cybersecurity, and nuclear forensics, scenario extraction, structural health monitoring, satellite health monitoring for the space nuclear detonation detection mission, remote sensing image analysis, and proliferation detection for national security. This project will develop theory, algorithms, and validation experiments for a new approach called rare category detection (RCD) that promises substantial improvements in our ability to detect meaningful anomalies.

Scientific Approach and Accomplishments

Rare Category Detection generally involves two stages: stage 1 identifies the initial regions of interest in the data (typically via more traditional anomaly detection) and stage 2 modifies and/or updates these regions after each user transaction.

In the first year, we developed a new kind of anomaly detection where instead of locating data from sparsely populated regions (as in standard anomaly detection) we locate data from regions with high concentration (so they are meaningful) but low probability mass (so they are still rare). We have discovered that the key to doing this efficiently is to synthesize a background data set and then solve a 2-class pattern recognition problem that discriminates between the observed data and the background. The utility of this method depends on how we synthesize the background. Instead of adopting a conventional approach that would synthesize the background from scratch using an artificial model, we have begun the development and testing of methods that produce a background by applying a special mapping to the observed data. This has numerous advantages for implementation, performance, and robustness.

In the first year, we also made progress on stage 2 with the development of "hemi-supervised" learning. This approach is effective in cases where the ground truth provided by the user is both one-sided and limited. In particular the user is only required to identify samples that are in a category (without needing to counterbalance those with samples that are "not" in a category). We have developed hemi-supervised methods that are effective for a wide range of situations that extend from

cases where the data can be described by simple Gaussian probability distributions to cases where the data distribution is arbitrarily complex. Furthermore, since the ground truth provided by the user is very limited we have begun to incorporate methods of "transfer learning" and "statistical relational learning" into our framework. Transfer learning is concerned with the storage of knowledge gained while solving one problem and then applying it to a different but related problem. This will allow us incorporate outside knowledge efficiently and effectively without burdening the user. Statistical relational learning is concerned with the discovery of relationships between different components of the data, and will be used to help us make connections between the small amount of ground truth data provided by the user and the other parts of the data.

A specific effort during the first year was the development of a new empirical error-minimizing algorithm for nearest-neighbor classifiers that reduces the number of exemplars (and hence the memory storage, and exploitation time) and obtains competitive performance to the conventional k-nearest-neighbor classifiers, which have significantly greater computational complexity. In addition, by directly minimizing error, our approach enables nearest-neighbor classifiers to be used for cost sensitive pattern recognition problems that arise in anomaly and rare category detection.

The second year pursued the further development of hemi-supervised detection methods for nonproliferation problems. In a typical nonproliferation problem, the proliferate activity produces a signal that is mostly known ahead of time, and the challenge is to detect this signal in a deployed environment where it is buried in significant amounts of broadband noise and narrowband clutter that are not known ahead of time. One aspect that makes this problem difficult is that the noise and clutter are not constant; they change from one deployment to the next, and they change from one time period to the next for a specific deployment. Existing detection methods assume a fixed model for the noise and clutter, and provide mixed results: they provide good performance when the model is approximately correct, and poor performance when it is not. On the other hand, the hemi-supervised detection methods developed in this project can adapt to the changes in noise and clutter, and can therefore provide good performance in all cases. The hemi-supervised approach requires that the detector be designed "on the fly" while the data is being collected in the field. As part of this effort, we successfully developed several components of the hemi-supervised detection algorithm, and worked on making these components efficient so that they can be used to design and implement the detector "on the fly".

An important step in the design of an optimal detector is to obtain a robust estimate of the broadband noise. This is a surprisingly difficult problem when the received signal contains a significant number of narrowband components, which is typical in a remote sensing environment. One of our second-year accomplishments was to develop a new method for estimating the broadband noise, and to prove that this method provides superior performance in these environments.

We also developed a new method for distinguishing between a proliferate signal and narrowband clutter. Many types of proliferate activities generate a harmonic series; i.e., a time series that consists an oscillatory signal plus its harmonics. However, a remotely sensed signal usually contains a large amount of sinusoidal clutter; i.e., a large number of arbitrarily spaced sinusoids. The difference between the proliferate harmonic series and the clutter sinusoids is that the clutter sinusoids are not harmonically aligned. Thus we can discriminate between the two by detecting the presence or absence of harmonic alignment. The usual solution to this problem is to identify all the sinusoidal components in the signal, and then to see how many of them are harmonically aligned. We have developed a simpler method that detects the presence of a harmonic signal more directly without having to identify all the sinusoidal components of the signal. This eliminates an intermediate step and improves detection performance.

The signal detection problem is one of a class of statistical problems called "composite hypothesis testing;" what's composite is that the signal of interest can take on multiple forms (for instance, signal strength is typically not known a priori, and one therefore wants to detect signals over a range of signal strengths). Although the simple hypothesis testing problem admits a well-known optimal solution – the likelihood ratio test – the composite hypothesis problem is more ambiguous. The standard solution is the generalized likelihood ratio test (GLRT), which involves replacing unknown "nuisance" parameters with their maximum likelihood estimates, and then following that up with a likelihood ratio test. Recently, a further generalization of the GLRT has been proposed which combines (or "fuses") what are known as "clairvoyant solutions" (these are the likelihood ratio solutions that would be obtained in the hypothetical situation that the nuisance parameters were known). We investigated these new clairvoyant fusion algorithms, and identified both efficient formulations and theoretical difficulties.

In the third year, we focused on an application in Space Nuclear Detonation Detection (SNDD), and in particular, investigated an archival dataset for the Space and Atmospheric Burst Reporting System Validation Experiment

(SAVE). This instrument was launched in November 2007, and began experiencing a series of unexpected events, starting in January of 2008, and culminating in a load bus glitch and instrument shut-down on March 12, 2008. Our interest was in identifying and characterizing anomalous behavior during the lifetime of the satellite. In the process of examining these data, we developed a further appreciation for the importance of feature selection, and some new tools and ideas. One new notion is the idea of "subtle anomalies" – these are data samples that are unusual in the context of a multidimensional distribution, but are not far from normal in the context of the individual features. Thus, if the temperature at a sensor is unusually high, then that is an anomaly; but if the temperature in one sensor is just slightly higher than average, while the voltage at an adjacent sensor is slightly lower than average, and if those sensors usually track each other, then that may be a subtle anomaly. These anomalies are interesting because they won't be found by simple "envelope based" anomaly detectors based on individual sensors.

The SNDD problem also forced us to confront the essentially non-Gaussian character of these data, and to address a distinction between outliers and anomalies. A few extreme outliers, due for instance to data drop-outs, might not themselves be very meaningful as anomalies, but can distort the covariance estimators that are central to the anomaly detection process. The Catch-22 is that covariance estimators are required for outlier detection, but the outliers need to be identified in order to obtain robust covariance estimates. Traditional algorithms approach this problem iteratively. But we can exploit the fundamentally heterogeneous nature of the features (some are temperatures, some are voltages, some are on/off, etc.) to our advantage, and identify outliers using individual envelope-based detectors. Removing those outliers, we then employ multivariate covariance-based methods for more meaningful anomaly detection.

Impact on National Missions

This project is directly linked to the core data analysis component of national security missions in cybersecurity and nonproliferation. It helps build a unique capability in machine learning that directly supports the future program development plans described by the LANL IS&T Center. Furthermore it provides capability that can be used to leverage program development in several key areas including: file system forensics and network monitoring for cybersecurity (DOE/NSA/CIA), satellite health monitoring (DOE/NNSA) and proliferation detection and monitoring (DOE/NNSA).

Publications

Kwon, H., X. Hu, J. Theiler, and A. Zare. Editorial: Algorithms for Multispectral and Hyperspectral Image Analysis. 2013. Journal of Electrical and Computer Engineering. 2013: 908906.

Mascarenas, D., A. Cattaneo, J. Theiler, and C. Farrar. Compressed sensing techniques for detecting damage in structures. 2013. Structural Health Monitoring. 12: 325.

Porter, R., D. Hush, and B. G. Zimmer. Error Minimizing Algorithms for Nearest Neighbor Classifiers. 2011. In Proceedings of the International Society for Optics and Photonics. (San Francisco, January 23-27, 2011). , p. 1. New York: SPIE.

Prasad, L., J. Theiler, M. Fair, and S. Swaminarayan. Feature Extraction, Anomaly, and Change Detection on WorldView 2 Imagery by Hierarchical Image Segmentation- a study. 2012. In Annual Conference on Algorithms and Technologies for Multispectral, Hyperspectral, and Ultraspectral Imagery XVIII ; 20120423 - 20120427 ; Baltimore, MD. Vol. 8390, p. 83901U.

Stearns, S. D., and D. R. Hush. Digital Signal Processing with Examples in MATLAB. 2011.

Theiler, J.. Confusion and clairvoyance: some remarks on the composite hypothesis testing problem. 2012. In Annual Conference on Algorithms and Technologies for Multispectral, Hyperspectral, and Ultraspectral Imagery XVIII ; 20120423 - 20120427 ; Baltimore, MD. Vol. 8390, p. 839003.

Theiler, J.. The incredible shrinking covariance estimator. 2012. In Automatic Target Recognition XXII ; 23-24 April 2012 ; Baltimore, MD, USA. Vol. 8391, p. 83910P (12 pp.).

Theiler, J.. Formulation for min-max clairvoyant fusion based on monotonic transformation of statistics. 2012. Optical Engineering. 51: 111714.

Theiler, J., and B. Wohlberg. Local coregistration adjustment for anomalous change detection. 2012. IEEE Transactions on Geoscience and Remote Sensing. 50 (8): 3107.

Zimmer, B. G., D. Hush, and R. Porter. Ordered Hypothesis Machines. 2011. Journal of Mathematical Imaging and Vision. : 1.

Zuluaga, M., D. Hush, E. F. Leyton, M. Hernandez Hoyos, and M. Orkisz. Learning from Only Positive and Unlabeled Data to Detect Lesions in Vascular CT Images ; pt.3. 2011. In Medical Image Computing and Computer-Assisted Intervention (MICCAI 2011). (14th International Conference ; 18-22 Sept. 2011). , p. 9.

Exact Renormalization Method for Frustrated Systems and Optimization

Cristian D. Batista
20110181ER

Abstract

We suggest a renormalization framework to study complex phenomena in interacting and frustrated systems, with additional applications in combinatorial optimization. Such phenomena are characterized by the competition and potential coexistence of various states of matter. Unveiling the organizing principles behind complex behavior in matter is a central problem in physics and other sciences. Our prime goal was to devise an exact and efficient computational method for understanding emergent behavior in physical systems with competing interactions. We applied recent and advanced results in information theory, mathematics, and quantum many-body physics, to construct a scale-renormalization algorithm that is exact under certain assumptions. Next, we used this algorithm to predict the low temperature physical properties of relevant models that remain unsolved. In addition, since combinatorial optimization problems can be reformulated in the physics language by associating a cost function with the energy of a physical system, we studied our method to solve spin glasses that encode the solution to these problems and devised a quantum algorithm that provides provable quantum speedups for these problems.

Background and Research Objectives

One of the most important challenges in materials science is to discover states of matter with novel responses and functionalities. The presence of strong competing interactions is the basic ingredient for achieving this goal. However, this characteristic also increases the complexity of these materials and challenges our ability of predicting their properties.

Frustrated systems give rise to rich and exotic phenomena that can lead to novel physical responses and functionalities. The variety of exotic states is due to the highly degenerate low-energy spectrum that results from the frustrated nature of the interactions. This property makes frustrated systems highly desirable for applications because small perturbations produce big changes in the response of the system. Frustrated systems are also at the root of Optimization: Certain instances of combinatorial optimization problems can be associated with frustrated systems whose ground states encode the solution to the problem.

Under this project we developed a code based on a novel algorithm for solving models that are relevant for describing such materials. We obtained all of the exact ground states under control and unraveled novel states of matter that are relevant for certain classes of frustrated materials. We also collaborated with our experimentalists from MPA-CMMS as some of the materials can be understood with our code.

Scientific Approach and Accomplishments

Code Development: We developed a code to efficiently solve a family of XXZ spin Hamiltonians on a ladder (1D) by using a new algorithm that was suggested in our proposal. The algorithm is an exact renormalization method that can be used to obtain all the ground states of the Hamiltonian. In particular, our code demonstrated to be very efficient for the problem under consideration: the memory requirements and CPU time scale with the square of the lattice size. This represents an exponential speedup with respect to other exact methods for the same problem, such as exact diagonalization (e.g., Lanczos). Remarkably, the numerical results played a crucial role in the determination of analytic solutions for this Hamiltonian family. Also, our algorithm was later generalized in order to solve other classes of highly frustrated spin models in D>1 dimensions (see below).

By running our code we were able to identify the exact ground state degeneracy as a function of the system or lattice size. This information was crucial for guiding the analytical efforts that we describe below. The results of our combined approach (numerical plus analytical) led us to the discovery of a new state of matter that consists of

an exact condensation of anyons [1]. Anyons are particles with fractional statistics, i.e., their statistics interpolates between bosons and fermions. Although anyons explain some aspects of the fractional Hall effect in two dimensions, they are not common in physics. In particular, there are very few one-dimensional models that contain anyonic solutions. Our method allowed us to identify the first exact solution of a very simple spin Hamiltonian that corresponds to a condensate of anyons (generalization to fractional statistics of the Bose-Einstein condensate). Although the notion of fractional statistics has been discussed in different contexts, we are not aware of any exact solution of a spin model that corresponds to an anyonic condensation. Therefore, we believe that our exact anyonic solutions are the first example of anyonic statistics in quantum magnets. We also computed relevant correlation functions that are necessary for characterizing these new states of matter. The results of this work were published in Phys. Rev. Lett. -Ref. [1], Figure 1.

In a second step of the project, we generalized our algorithm and developed a code for obtaining the entire set of ground states of two-dimensional (D=2) Hamiltonians that fulfill the hypothesis of applicability of our algorithm [2]. Such Hamiltonians do not need to be of the XXZ type. The tree structure of our novel renormalization algorithm is depicted in Figures 1 and 2.

By developing this code, we were able to demonstrate that it is possible to compute relevant correlation functions for the characterization of the zero temperature state of matter that is described by the Hamiltonians under consideration. In particular, we discovered a very unusual quantum critical point, which corresponds to the onset of antiferromagnetism-induced by an external magnetic field. Our results demonstrated that the novel numerical method developed under this project is extremely powerful, efficient and exact. These very unusual characteristics open the possibility of investigating new states of matter in highly frustrated materials. As we explain by the end of this document, during the last year of the project we started to consider materials problems, which are describable by Hamiltonians that fulfill the assumptions for applicability of our method.

Optimization: In optimization, the ground state of the Hamiltonian encodes the solution to the problem. Fast algorithms to prepare such ground states are thus desired. Typically, the time complexity of known algorithms for this problem depends strongly on the inverse of the spectral gaps to the next excited eigenstate; the smaller the gap, the larger the complexity. It is important then to devise other Hamiltonians that have the same ground states but a much larger spectral gap. These Hamiltonians can be used to solve the optimization problem more efficiently, Figure 2.

The family of Hamiltonians considered in the project satisfies certain interesting properties. One such property is that every ground state is also a ground state of local operators (projectors) that act trivially on it. We introduced the so called “spectral gap amplification problem” (GAP) for this family and showed that a quadratic amplification of the gap is possible and optimal. This allows for new quantum speedups for optimization and for the preparation of a large class of relevant quantum states (projected entangled pairs or PEPS). Our results were accepted for a presentation at QIP, the most important conference in quantum information, and published in SIAM J. Comp, a high-impact journal in computer science - Ref. [3].

The main difficulty for studying interacting systems is the exponential increase of the number of states with the system size. Renormalization approaches avoid this problem by retaining only the state-variables that play a significant role in the low-temperature properties. We remark that computing ground-state properties of frustrated models cannot be done via convex optimization: The cost function to minimize has a complex landscape with multiple minima, each associated with the corresponding ground state. Our method goes beyond convex optimization, and allows for attacking combinatorial optimization problems where the cost function is non-convex.

Applications to real materials: We also applied our algorithm to the computation of field-induced magnetization in a highly frustrated compound Ca3Co2O6 that consists of a triangular lattice of ferromagnetic Co chains [4]. The inter-chain coupling is antiferromagnetic leading to an enormous number of ground states. We applied our algorithm to the generation of all the possible ground states and subsequent computation of the magnetization vs. field curve starting from each of them. The output of this calculation was used to fit the experiments on compounds of the same family that were done at the National High Magnetic Field Laboratory of Los Alamos [5].

Our renormalization method allowed us to: a) Connect seemingly unrelated physical phenomena; b) Identify the general symmetry principles behind complex phase diagrams; Unveil new states of matter; c) Obtain exact solutions with complex ordering.

Impact on National Missions

We developed a novel scientific approach that created fundamentally new capabilities for bridging two LANL grand challenges: “Information, Science and Technology” (IS&T) and “Materials: Discovery Science to Strategic

Applications"(MDSSA). The research that we produced is a direct response to FY11 IS&T Grand Challenge priorities: development of methods for inference and prediction of large-scale complex systems and design of algorithms to efficiently ex-tract information from massive amounts of data. Our research is also a direct response to FY11 priorities of the Materials Grand Challenge and its three central themes: prediction and control, extreme environments, and emergent phenomena. Frustration is a challenging problem, identified in DOE's 'Directing Matter and Energy: Five Challenges for Science and the Imagination', that is exciting because of both, the scientific consequences of new states of matter and the technologically relevant multifunctional responses.

We received follow-up funds from the Air Force (AFOSR) for a grant on quantum methods for aerospace problems, where some of the techniques developed in this ER proposal (e.g., spectral gap amplification) will play a crucial role.

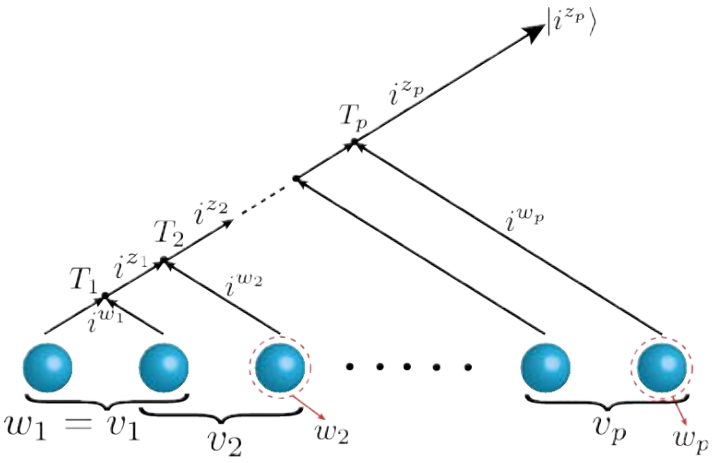

Figure 1. Representation of the tree-tensor network contraction for a system with p spins (blue circles). In this example, the sets vl refer to pairs of nearest-neighbor spins and each wl is a single spin. The tensors Tl live in the vertices of the tree and the contraction indices are in the edges. An arrow means a sum over the corresponding index.

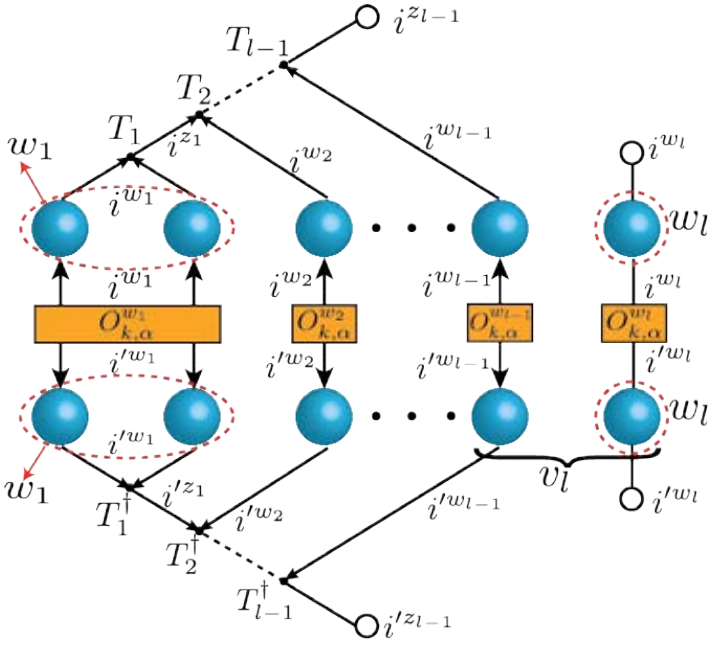

Figure 2. Representation of the network contraction for each matrix element for the same system of Fig. 1.

References

1. Batista, C. D., and R. D. Somma. Condensation of Anyons in Frustrated Quantum Magnets. 2012. PHYSICAL REVIEW LETTERS. 109 (22): -.

2. Feiguin, A., R. D. Somma, and C. D. Batista. Exact real-space renormalization method and applications. 2013. Physical Review B. 88: 075145.

3. Somma, R. D., and S. Boixo. Spectral Gap Amplification. 2013. SIAM Journal on Computing. 42 (2): 593–610.

4. Kamiya, Y., and C. D. Batista. Formation of Magnetic Microphases in Ca3Co2O6. 2012. Physical Review Letters. 109: 067204.

5. Kim, J., Y. Kamiya, E. D. Mun, M. Jaime, N. Harrison, J. D. Thompson, T. H. Yi, Y. S. Oh, S. W. Cheong, C. D. Batista, and V. S. Zapf. Multiferroicity with coexisting isotropic and anisotropic spins in Ca3Co{2-x}MnxO6. Physical Review Letters .

Publications

Altarawneh, M. M., G. W. Chern, N. Harrison, C. D. Batista, A. Uchida, M. Jaime, D. G. Rickel, S. A. Crooker, C. H. Mielke, J. B. Betts, J. F. Mitchell, and M. J. R. Hoch. Cascade of Magnetic Field Induced Spin Transitions in LaCoO3. 2012. PHYSICAL REVIEW LETTERS. 109 (3): -.

Batista, C. D., and R. D. Somma. Condensation of Anyons in Frustrated Quantum Magnets. 2012. PHYSICAL REVIEW LETTERS. 109 (22): -.

Delgado, F., C. D. Batista, and J. Fernandez-Rossier. Local probe of fractional edge states of S=1 Heisenberg spin chains. To appear in Physical Review Letters.

Feiguin, A., R. D. Somma, and C. D. Batista. An exact real-space renormalization method and applications. 2013. Physical Review B. 88 (7): 075145.

Kamiya, Y., and C. D. Batista. Formation of Magnetic Microphases in Ca3Co2O6. 2012. Physical Review Letters. 109: 067204.

Kamiya, Y., and C. D. Batista. Magnetic vortex crystals in frustrated Mott insulator . Physical Review X.

Kim, J., E. D. Mun, Y. Kamiya, M. Jaime, N. Harrison, J. Thompson, H. T. Yi, Y. S. Oh, S. W. Cheong, C. D. Batista, and V. Zapf. Multiferroicity with coexisting isotropic and anisotropic spins in Ca3Co{2-x}MnxO6. Physical Review Letters.

Koutroulakis, G., T. Zhou, C. D. Batista, Y. Kamiya, J. D. Thompson, S. E. Brown, and H. D. Zhou. Magnetic Phases of the Spin-1/2 Triangular-Lattice Antiferromagnet Ba3CoSb2O9 . Physical Review Letters.

Lin, S., and C. D. Batista. Orbital magnetism induced by heat currents in Mott insulators. Physical Review Letters.

Mun, E. D., G. Chern, V. Pardo, F. Rivadulla, V. Zapf, and C. D. Batista. Magnetic Field Induced Transition in the Multiferroic Spinel CdV2O4. Physical Review Letters.

Muniz, R., Y. Kato, and C. D. Batista. Generalized spin-wave theory: application to the bilinear-biquadratic model. Physical Review B.

Nishida, Y., Y. Kato, and C. D. Batista. Efimov effect in quantum magnets. 2013. NATURE PHYSICS. 9 (2): 93.

Somma, R. D., and S. Boixo. Spectral Gap Amplification. 2013. SIAM Journal on Computing. 42 (2): 593.

Wierschem, K., Y. Kato, Y. Nishida, C. D. Batista, and P. Sengupta. Magnetic and nematic orderings in spin-1 antiferromagnets with single-ion anisotropy. 2012. PHYSICAL REVIEW B. 86 (20): -.

Zhang, Z. F., K. Wierschem, I. Yap, Y. Kato, C. D. Batista, and P. Sengupta. Phase diagram and magnetic excitations of anisotropic spin-one magnets. 2013. PHYSICAL REVIEW B. 87 (17): -.

Computational Modeling of Topo-taxis: Directing the Motion of Bacteria and Cells with Microfabricated Topologies

Charles Reichhardt
20110189ER

Abstract

This project focused on computational modeling of nonequilibrium phenomena for particles undergoing motion on patterned substrates. Particular emphasis is on particles undergoing motion for different types of dynamics such as externally driven or self driven as well as understanding the effects of a substrate or a combination of a substrate and bulk driving on directed motion, aggregation, and functionality. These systems include externally driven particles such colloids, vortex and skyrmions as well as self-particles such as bacteria and artificial swimmers. We showed that these substrates can lead to directed motion is the a funnel like geometry is used as well as varies types of novel dynamics. We find that a strong substrate can arrest aggregation; however, under an applied drive the system with a substrate can aggregate much faster than systems without a substrate. This opens a new route for controlling pattern formation in aggregating materials. Additionally, we showed that aggregation can lead to enhanced diffusion or mobility in cases where there is an asymmetry in the substrate, which can be useful for particle separation. Our work also showed that skyrmions are very promising for possible applications of novel memory devices.

Background and Research Objectives

Equilibrium systems are systems that are not driven and examples include solids, liquid and gases. As external parameters such as presser, temperature or volume changes these system can exhibit transition such as from a liquid to a solid or a gas to a liquid. For solids there can also be transitions from one type of crystalline solid to another. Over the past 100 years withe developments in Statistical thermodynamics we now have considerable understanding of transitions in these systems and how to characterize transitions in them. Another class of systems is that of not in equlibrium or driven systems. A simple example of this is a continuously stirred liquids, which show a turbulent like motion. The open questions in this class of systems is there transitions from different types of non-equilibrium states. Are these transitions like a transition from a solid to liquid? Finley can we impose some kind of boundary conditions or a substrate to control the transition from the different states or control the motion of the microscopic degrees of freedom in these systems.

Although the non equilibrium system can include very complex systems even understanding some of the simplistic and looking for general principles could provide powerful tools for utilizing properties of non-equlibrum systems for applications. Some of the simplistic non-equlibrium systems with relatively few parameters are discrete particle bases systems. Examples include colloids or solid particles in solutions, electron crystals, vortices in superconductors, magnetic nano particles and so on. In these system an external force can be applied by the addition of electric field, magnetic field, or by having fluid flow through the systems. Another class of particle based non-equlibrium systems are self-driven particles or active matter. An example would be that of swimming bacteria, where the particles can be considered a self-driven elongated particles that swim according to some type of run and tumble dynamics and interact with other bacteria or obstacles. Other examples could be for pedestrian flow, vehicular flow, and crawling cells. More recently there have been several advances in artificial swimmers such as self-driven colloids. These system an exhibit a wealth of nonequlibrium type behaviors including pattern formation, chaotic type flows, and time dependent behaviors. Far less is known about what happens where these types of nonequilibrium systems are placed on some kind of topographic substrates. Such a substrates cane be create id my a micro fabricated surfaces, nanostructures and by optical means. The goal of the project was to understand how substrates with various typologies can change non-equilibrium behaviors, be useful for apparitions of these systems, and understand if universal principles apply to broad class of externally and self driven particle systems.

Scientific Approach and Accomplishments

Our approach has been to use a combination of large scale simulations and theory to model different aspects of particles externally driven and self particle assemblies. We first examined the effects of self-driven aggregating or flocking particles, and found that if the substrate is asymmetric, a novel ratchet effect occurs in which the aggregate exhibits a net dc motion even when there is no applied dc drive. We also showed that the size of the particles in the aggregate can lead to motion in different directions, so that a new type of particle separation can be achieved. We have also found that if the self driven particles are placed in between movable barriers that are very strong self-aggregation effect can occur in what we call an active matter Casimir which can be hundred of time stronger than for non active matter thermal particles. We also show that the for certain cases increasing the mobility of the individual self-driven particles will actually lead do a decreases mobility of the interacting particles of as a whole do to what is called an active matter jamming effect. This is particularity to understand when trying to use active matter systems to increase diffusion of mixing in certain systems where collective effects may work against certain desired effects. We have also been examining the kinds of patterns that can occur for externally driven particles on random and periodic substrates. Recently a new kind of magnetic defect called a skyrmion was found in certain chiral magnets however any piratical use of such objectives means we have to understand how they move and how to control the motion of such objects. We first developed a microscopic model for the motion of a single skyrrmion, which was varied in both continuum and molecular dynamics types simulations. We than found that by adding a random substrates that a pinning effect occurs leading to a critical value of the externally applied force being need to get the particles to move. We also found that if the particles are placed in a circular nanodiks that a novel rectifier should be possible and that they are indeed useful for applications. We have also been examine driving colloidal particles.

The last problem we address is that of particles with short range repulsion and longer range attraction. This interaction was modeled with two Bessel functions and compared to systems with only repulsion. Previous work showed that this model forms multiple clump and stripe phases; however, we demonstrated that these are not the true ground states, and that instead the system forms a single clump under long time thermal motion. The next question we addressed was to understand what happens to aggregation in the presence of quenched disorder. We model both random and periodic substrates and identify three regimes. (1) For weak substrates, the system completely phase separates. (2) For intermediate substrates, the substrate is effectively wetted by a portion of the particles while the remaining particles form a single clump. (3) For strong substrates, the substrate dominates the behavior and there is little or no aggregation. We next address the question of what happens under an applied drive. We found that even systems with strong substrates can exhibit dynamically induced aggregation when driven, and that the shape of the aggregation can be controlled and can take the form of stripe or labyrinth patterns. Applications for this system include a new dynamic method to create new kind of patterns. If such methods could be used on the nanoscale that having the ability to control the patterns would give us a way to tailor materials properties. Additionally there are examples of particles that can be toxic however when they aggregate they are actually less toxic so understanding to how to control aggregation on a substrate is also has applications in medical fields.

Over the three year time from of this project we have published over 25 papers. This includes publications in high impact journals such as Nature Materials, PNAS, Physical Review Letters, Applied Physics Letters, Physical Review B, Physical Review E, Soft Matter, and New Journal of physics. Additionally we have 5 more publications currently under review or to be submitted shortly. Additionally this work resulted in over 30 invited colloquial, and seminars at international conferences, universities and other national laboratories. The work partially supported two postdocs. One of them Jeff Drocco has now started as a permanent staff member at LLNL in the bio-threats division. The other is still at LANL. This work was also used to partially support two graduate students who will be getting there PhD's from Notre Dame in 2014.

Impact on National Missions

Particle separation. There are many examples of processes relevant to the mission where one would want to separate out different components of a mixture on the nanoscale. Our work suggests that the addition of active swimmers or active aggregating particles can be used to create a ratchet effect in which aggregates of one size move in one direction while aggregates of another size move in the opposite direction, leading to enhanced sorting. This could be used for a wealth of application for the lab mission of bio threat detection, bio fuels, new mineral extractions techniques, filtration, and environmental work.

Toxicology. Certain nanoparticles can have very toxic effects; however, the toxicity can be altered if the particles aggregate, and in certain cases the aggregates are nontoxic even though their component particles are toxic. This suggested that controlled aggregation could be used to reduce the toxicity of many types of materials that are byproducts

of missions relevant to the Nation. Our results suggest that the aggregation can be enhanced by moving nanoparticles over a substrate with a strong applied drive.

Novel non-volatile memory. Magnetic domain walls show considerable promise for applications in non volatile memory and novel logic devices, however there are several problems with these system in that domain walls are generally strongly pinned and hard to move, which means very high currents are needed. Recently a new type magnetic object called a skryrmion was found which is weakly pinned. We have shown how to create and destroy skrymoins in these systems and how to control there motion with external fields and substrates.

Publications

Chern, G. W., C. Reichhardt, and C. J. O. Reichhardt. Frustrated colloidal ordering and fully packed loops in arrays of optical traps. 2013. PHYSICAL REVIEW E. 87 (6): -.

Drocco, J. A., C. J. O. Reichhardt, C. Reichhardt, and A. R. Bishop. Static and dynamic phases for magnetic vortex matter with attractive and repulsive interactions. 2013. JOURNAL OF PHYSICS-CONDENSED MATTER. 25 (34): -.

Drocco, J. A., C. J. Reichhardt, and C. Reichhardt. Characterizing plastic depinning dynamics with the fluctuation theorem. 2011. European Physical Journal E. 34 (10): 117 (7 pp.).

Drocco, J., C. J. Olson Reichhardt, and C. Reichhardt. Bidirectional sorting of flocking particles in the presence of asymmetric barriers. 2012. Physical Review E - Statistical, Nonlinear, and Soft Matter Physics. 85 (5): 056102.

Drocco, J., C. Reichhardt, C. J. O. Reichhardt, and A. R. Bishop. Statics and dynamics of wetting-dewetting transitions for particles with attractive interactions on periodic substrates. 2012. OPTICAL TRAPPING AND OPTICAL MICROMANIPULATION IX. 8458: -.

Drocco, J., C. Reichhardt, and C. Reichhardt. Bidirectional Sorting of Self-Propelled Microswimmers in the Presence of Asymmetric Barriers. 2013. BIOPHYSICAL JOURNAL. 104 (2): 496A.

Drocco, J., L. M. Lopatina, C. Reichhardt, and C. J. O. Reichhardt. Dynamics of Self-Driven and Flocking Particles on Periodic Arrays. 2012. OPTICAL TRAPPING AND OPTICAL MICROMANIPULATION IX. 8458: -.

Libal, A., B. M. Csiki, C. J. O. Reichhardt, and C. Reichhardt. Colloidal lattice shearing and rupturing with a driven line of particles. 2013. PHYSICAL REVIEW E. 87 (2): -.

Libal, A., C. Reichhardt, and C. J. Reichhardt. Hysteresis and return-point memory in colloidal artificial spin ice systems. 2012. PHYSICAL REVIEW E. 86 (2, 1): 021406.

Lin, S. Z., C. Reichhardt, C. D. Batista, and A. Saxena. Particle model for skyrmions in metallic chiral magnets: Dynamics, pinning, and creep (vol 87, 214419, 2013). 2013. PHYSICAL REVIEW B. 88 (1): -.

Lin, S. Z., C. Reichhardt, C. D. Batista, and A. Saxena. Particle model for skyrmions in metallic chiral magnets: Dynamics, pinning, and creep. 2013. PHYSICAL REVIEW B. 87 (21): -.

Lin, S. Z., C. Reichhardt, C. D. Batista, and A. Saxena. Driven Skyrmions and Dynamical Transitions in Chiral Magnets. 2013. PHYSICAL REVIEW LETTERS. 110 (20): -.

Lin, S. Z., C. Reichhardt, and A. Saxena. Manipulation of skyrmions in nanodisks with a current pulse and skyrmion rectifier. 2013. APPLIED PHYSICS LETTERS. 102 (22): -.

Lin, S. Z., and C. Reichhardt. Stabilizing fractional vortices in multiband superconductors with periodic pinning arrays. 2013. PHYSICAL REVIEW B. 87 (10): -.

McDermott, D., J. Amelang, L. M. Lopatina, C. J. O. Reichhardt, and C. Reichhardt. Domain and stripe formation between hexagonal and square ordered fillings of colloidal particles on periodic pinning substrates. 2013. SOFT MATTER. 9 (18): 4607.

Ray, D., C. J. O. Reichhardt, B. Janko, and C. Reichhardt. Strongly Enhanced Pinning of Magnetic Vortices in Type-II Superconductors by Conformal Crystal Arrays. 2013. PHYSICAL REVIEW LETTERS. 110 (26): -.

Regev, I., and C. Reichhardt. Rheology and shear band suppression in particle and chain mixtures. 2013. PHYSICAL REVIEW E. 87 (2): -.

Reichhardt, C. J. O., E. Groopman, Z. Nussinov, and C. Reichhardt. Jamming in systems with quenched disorder. 2012. PHYSICAL REVIEW E. 86 (6): -.

Reichhardt, C. J. Olson, J. Drocco, T. Mai, M. B. Wan, and C. Reichhardt. Active matter on asymmetric substrates. 2011. In Optical Trapping and Optical Micromanipulation VIII ; 21-25 Aug. (2011 ; San Diego, CA, USA). Vol. 8097, p. 80970A (13 pp.).

Reichhardt, C. J. Olson, and C. Reichhardt. Vortex dynamics and symmetry locking on quasiperiodic and periodic substrates. 2012. Physica C: Superconductivity and its Applications. 479: 45.

Reichhardt, C. J., Liba&acute, and C. Reichhardt. Multi-step ordering in kagome and square artificial spin ice. 2012. New Journal of Physics. 14 (2): 025006 (15 pp.).

Reichhardt, C. J., and C. Reichhardt. Vortex dynamics and

symmetry locking on quasiperiodic and periodic substrates. 2012. PHYSICA C-SUPERCONDUCTIVITY AND ITS APPLICATIONS. 479: 45.

Reichhardt, C., J. Drocco, C. J. Reichhardt, and A. R. Bishop. The effect of pinning on vortex states with attractive and repulsive interactions. 2012. PHYSICA C-SUPERCONDUCTIVITY AND ITS APPLICATIONS. 479: 15.

Reichhardt, C., Z. Nussinov, and C. J. O. Reichhardt. Connecting Jamming and Depinning Transitions. 2013. SOLID STATE PHYSICS, VOL 57. 1512: 7.

Reichhardt, C., and C. J. Olson Reichhardt. Statics and dynamics of Yukawa cluster crystals on ordered substrates. 2012. Physical Review E (Statistical, Nonlinear, and Soft Matter Physics). 85 (5): 051401 (13 pp.).

Reichhardt, C., and C. J. Reichhardt. Dynamics and Directional Locking of Colloids on Quasicrystalline Substrates. 2011. In Optical Trapping and Optical Micromanipulation VIII ; 21-25 Aug. (2011 ; San Diego, CA, USA). Vol. 8097, p. 80970V (11 pp.).

Reichhardt, C., and C. J. Reichhardt. Structural transitions and dynamical regimes for directional locking of vortices and colloids driven over periodic substrates. 2012. Journal of Physics: Condensed Matter. 24 (22): 225702 (8 pp.).

Reichhardt, C., and C. J. Reichhardt. Dynamically induced locking and unlocking transitions in driven layered systems with quenched disorder. 2011. Physical Review B (Condensed Matter and Materials Physics). 84 (17): 174208 (16 pp.).

Reichhardt, C., and C. O. Reichhardt. Dynamical freezing of active matter. 2011. PROCEEDINGS OF THE NATIONAL ACADEMY OF SCIENCES OF THE UNITED STATES OF AMERICA. 108 (48): 19099.

Reichhardt, C., and C. O. Reichhardt. Dynamical freezing of active matter. 2011. PROCEEDINGS OF THE NATIONAL ACADEMY OF SCIENCES OF THE UNITED STATES OF AMERICA. 108 (48): 19099.

Reichhardt, C., and C. O. Reichhardt. DEFECT DYNAMICS Breaking up in a curved plane. 2012. NATURE MATERIALS. 11 (11): 912.

Zhou, C. Z., J. J. Su, M. J. Graf, C. Reichhardt, A. V. Balatsky, and I. J. Beyerlein. Plastic response of dislocation glide in solid helium under dc strain-rate loading. 2013. PHYSICAL REVIEW B. 88 (2): -.

Zhou, C. Z., J. J. Su, M. J. Graf, C. Reichhardt, A. V. Balatsky, and I. J. Beyerlein. Dislocation-induced anomalous softening of solid helium. 2012. PHILOSOPHICAL MAGAZINE LETTERS. 92 (11): 608.

Zhou, C., C. Reichhardt, M. Graf, J. Su, A. Balatsky, and I. Beyerlein. Comment on “Giant Plasticity of a Quantum Crystal”. 2013. Physical Review Letters . (111): 119601.

Algorithmic Co-design: Paradigms for Unstructured Problems on Accelerated Architectures

Sunil Thulasidasan
20110195ER

Abstract

This goal of this research effort was to develop algorithmic techniques to efficiently utilize the massive computing power afforded by today's parallel processors for solving problems that lack obvious data parallelism. Such problems are often characterized by irregular memory accesses and have traditionally been better suited for CPU architectures that are optimized for sequential and branch-heavy code.

The irregularity of these problems is a natural outcome of graph-based representations; graphs are mathematical objects that capture relationships between entities and many important scientific problems can be elegantly formulated in terms of graph-exploration and optimization. However, efficient graph representations, which are pointer-dense and unstructured, do not translate to efficient computations on parallel processors and many optimal graph algorithms do not lend themselves to easy parallelization. Nevertheless, it is becoming increasingly clear that massive on-chip parallelism will continue to be the architectural trend in the foreseeable future. The potential performance benefits in extracting parallelism on unstructured problems are thus too compelling to ignore.

The contributions in this project have had a common theme: namely providing algorithmic techniques and software implementations to exploit the massive parallelism for graph based problems using both shared and distributed memory designs. Specifically, for graph based problems, we attacked the classical shortest-path problem for planar graphs [3,5], and showed how reformulating the graph problem in terms of matrices and exploiting the resulting structured nature of matrix computations resulted in greatly improved speed-ups for path problems on certain kinds of real world graphs, such as those found in road networks. In addition, we also attacked the coverage problems in sensor network graphs by exploiting the spectral properties of the associated matrices and showed how such problems can be elegantly formulated for GPU architectures [2]. Further graph-based research included analysis and implementation of fast parallel algorithms for protein matching problems in computational biology [6], efficient algorithms for modularity-based graph clustering [7] and analysis of dynamics of influence on large-scale social networks [8]

On the software front, we developed and open sourced a library for easily prototyping simulations of large-scale complex networks on distributed memory parallel architectures. The library, named, SimX [3,15] is a general-purpose simulation library for rapidly developing parallel discrete-event simulation applications.

Our publication portfolio includes conferences and journals in the areas of algorithms, high performance computing, simulation tools and methodologies and data analytics. As part of this project, we also established successful collaborations with other researchers in the above fields, both domestically (MIT) and internationally (France, India and Turkey).

Background and Research Objectives

While GPUs and other stream processors were originally developed for numerically intensive media applications, advances in performances and programmability have resulted in these processors being successfully deployed for numerous computationally demanding scientific tasks. The impressive arithmetic power and massive parallelism of today's graphics processors is an outcome of the highly parallel and numerically intensive nature of computer graphics. Not surprisingly, the general purpose computing tasks that have been able to leverage the performance benefits of these processors exhibit many computational similarities to graphics applications, namely 1) high data parallelism, 2) high compute intensity, and 3) data locality which results in structured (or coalesced) memory accesses.

However, many problems do not readily exhibit the above properties. An important example of this is problems dealing with graph-based data structures, which are found in a variety of scientific domains. Graphs, which are essentially a representation of relationships between objects, find applications in such diverse domains as molecular biology epidemiology, transportation, social network analysis and data mining, to name a few. Efficient graph representations, (which store as little redundant information as possible) result in highly unstructured data; this makes them less than ideal candidates for streaming processor manipulations. Nevertheless, the massive parallelism afforded by today's graphics processors is too compelling to ignore. Current GPUs support hundreds of cores per chip and even future CPUs will be many cores. To harness this computing power for computing power for unstructured problems, we need a shift in algorithmic thinking since approaches that are theoretically non-optimal, but afford a greater degree of parallelism might actually be better suited to GPU-type architectures.

This has been confirmed by our research thus far into efficient computations for shortest-paths problems for certain kinds of graphs. By reformulating the graph problem in terms of matrix operations, and using matrix theoretic properties, we have been able to exploit the structured nature of matrix computations that are much more amenable to fine grained parallelization of GPUs. One of our research tasks focused on shortest-path (SP) problems in planar graphs; the SP problem is a fundamental one in computer science, while planar graphs (graphs that can be embedded in a plane such that no two edges cross each other) are found in diverse areas such as transportation, robotics, and chip design. The problem is to find paths of minimum cost between pairs of nodes in edge weighted-graphs, where the cost of a path p is defined as the sum of the cost of all edges that makeup p. The distance between two nodes v and w is defined as the minimum cost of a path between v and w.

Finding similarities between protein structures is a crucial task in molecular biology. Many tools exist for finding an optimal alignment between two proteins. These tools, however, only find one alignment, even when multiple similar regions exist. We propose a new parallel heuristic-based approach to structural similarity detection between proteins that discovers multiple pairs of similar regions using graph theoretic techniques. We prove that returned alignments have root-mean-square deviation lower than a given threshold. Computational complexity is addressed by taking advantage of both fine and coarse-grain parallelism.

In our work on modularity based graph clustering, we propose an approach for finding the communities of a network that is based on a reduction of the modularity optimization problem to the minimum weighted cut problem, We give an experimental evaluation of an implementation based on that approach on graphs from the 10th DIMACS Implementation Challenge Test bed [9].

Another graph-based problem we tackled was the coverage problem in sensor networks where we studied a distributed algorithm for coverage in mobile sensor when very little information is available regarding terrain topology. We use virtual forces based on potential fields to achieve coverage and obstacle avoidance. Additionally, a distributed dynamic relocation algorithm – triggered by event occurrences – is also simulated which achieves convergence to a formation that surrounds the event of interest, in the absence of prior information regarding formation geometry. Control laws are formulated based on potential fields; convergence to equilibrium, graph connectivity properties and sensitivity to parameters are simulated and analyzed using the spectral properties of the matrices associated with the sensor network graphs. [2] As part of this project, we also looked at graphs induced by large-scale real-world social networks. Specifically, we look at several graph-theory based heuristics for understanding the dynamics of influence and celebrity notion on Twitter [8].

On the software front, we were able to open source a library for easily prototyping simulations on distributed memory parallel architectures. The library, named, SimX [15] is a general-purpose simulation library for rapidly developing parallel discrete-event simulation applications. SimX provides the simulation developer with core functionality such as event queuing, entity management, time advancement, domain partitioning, synchronization and message passing. Parallel simulations are implemented using distributed memory and message passing. SimX has been written to be flexible enough to suit a variety of application domains that use discrete-event simulations for modeling, and has been designed to allow applications to scale from single processor workstations to high-performance clusters.

Scientific Approach and Accomplishments

Path problems on graphs: The algorithm we designed for the All-Pair Shortest Path problem (APSP) for planar graphs is based on a modification to the FW (FW) algorithm [10], exploiting the property of planarity. The complexity of our algorithm with respect to the number of nodes is close to quadratic (O(n2)), while its structure is regular enough to allow for an efficient parallel implementation, enabling us to exploit GPUs. Our algorithm decomposes the graph into p parts, solves the APSP problem for the sub-graph

induced by each part (in parallel, if the graph is too large to fit into memory and more than one GPU is available), and then uses that information to compute the distances between pairs. The details of the algorithm are given in [3].

The above algorithm was implemented on a GPU using CUDA, nVIDIA's parallel programming framework for the GPU. Modern GPUs are efficient at manipulating structured data like matrices, and their highly parallel architecture (a GPU trades the complicated cache and control logic in a CPU for a large number–often hundreds–of arithmetic units) makes them ideally suited for processing large blocks of data simultaneously (referred to as the SIMD–Single Instruction Multiple Data–paradigm).

In order to comply with the GPU paradigm, we define a computational kernel that implements Floyd-Warshall's algorithm and computes the APSP over a sub-matrix of the initial matrix. We then define computation grids, where blocks correspond to sub-matrices that can be computed simultaneously. Phase 1 of the algorithm consists of computing APSP in self-dependent (in terms of data dependencies) diagonal sub-matrices, using a block-parallel version of the Floyd-Warshall algorithm. Computations for these diagonal sub-matrices can be run in parallel in different GPU blocks. Phase 2 of the algorithm consists of computing APSP on a sub-graph of the initial graph solely comprised of boundary vertices. For this purpose, we implemented a GPU version of the blocked APSP algorithm described in [12], a variant of the Floyd-Warshall algorithm where computations are divided into groups that can be easily be mapped to GPU blocks. Phase 3 of the algorithm consists of computing APSP in the remaining non-diagonal sub-matrices, using the same parallel Floyd-Warshall algorithm. Since Phases 1 and 3 use the same data patterns we illustrate their data dependencies in Figure 1.

In order to test the efficiency of the algorithm, we compare two implementations of the partitioned APSP algorithm: (1) a single core CPU implementation of the partitioned all-pairs shortest-path algorithm (referred to as CPU version), and (2) a single GPU implementation of the partitioned all-pairs shortest-path algorithm (later referred to as GPU version).

The CPU version runs on an Intel(R) Xeon(R) CPU X5675 at 3.07GHz. The GPU version runs on an nVidia Tesla m2090 consisting of 512 cores at 1.3 GHz. The benchmark consists of random cost adjacency matrices, representing planar graphs with sizes ranging from 1024 vertices to 32,768 vertices. These graphs were generated using the LEDA graph generator [11]. Figure 2 shows the GPU versus CPU speed-up comparison for progressively larger graphs, with the GPU being up to 14 times faster than the GPU for larger graphs (32-k nodes). For the largest instance, the cost adjacency matrix requires about 4.2 GB of RAM. Instances larger than about 38,000 vertices would require more RAM than currently available on the GPU. One way around the memory size problem is to exploit the spatially constrained nature of paths in real-world graphs that will allow us to consider only a relatively small subset of the original graph [1]. We are also currently extending this work to tackle larger graph instances (up to one million nodes) by using LANL's new multi-GPU hybrid super computers.

Protein Similarity: Finding similarities between protein structures are a crucial task in molecular biology. Many tools exist for finding an optimal alignment between two proteins. These tools, however, only find one alignment, even when multiple similar regions exist. We propose a new parallel heuristic-based approach [6] to structural similarity detection between proteins that discovers multiple pairs of similar regions. We prove that returned alignments have root-mean-square deviations (RMSD) lower than a given threshold. Computational complexity is addressed by taking advantage of both fine and coarse-grain parallelism.

Our approach reduces the optimal alignment problem to the problem of finding a maximum clique in a graph called an alignment graph (Figure 3), where each edge corresponds to a matching of similar internal distances (up to a user-defined threshold T). Since the latter problem is an NP-hard problem, we relax this condition and accept cliques such that edges correspond to matching of similar internal distances up to 2T. For this relaxed problem we propose a polynomial algorithm and its efficient parallel implementation comparing two protein structures that guarantees to return alignments with RMSD less than a given threshold value, if such alignments exist.

In order to test our parallel implementation, we compare run times obtained with various numbers of threads on a single large instance. The input alignment graph for this instance contains 15024 vertices and about 9.5 million edges. Computations were run using a varying number of cores of an Intel(R) Xeon (R) CPU E5645 @ 2.40GHz. Figure 4 shows run times and speedups with respect to the number of CPU cores. The gain in terms of speedup becomes less significant beyond 12 cores. Note that similar results - both in terms of length and RMSD scores - can be obtained in less than 30 seconds with a sparser alignment graph.

Graph Modularity: For our graph modularity work [7], we designed an approach for finding the communities of a network that is based on a reduction of the modularity optimization problem to the minimum weighted cut problem, and we give an experimental evaluation of an implementation based on that approach on graphs from

the 10th DIMACS Implementation Challenge Test bed [9]. Specifically, we describe a reduction from the problem of finding a partition of the nodes of a graph G that maximizes the modularity to the problem of finding a partition that minimizes the weight of the cut in a complete graph on the same node set as G, and weights dependent on a random graph model associated with G. Modifying existing codes for graph partitioning can then solve the resulting minimum cut problem.

We have tested our algorithm against Ovelgonne and Geyer-Schulz's algorithm [14], which was ranked at the top in the DIMACS Challenge with respect to its accuracy. Figure 5 compares the performance of our algorithm with that algorithm. For each experiment, the table shows the average running time and modularity of the partition for each of the algorithms. The results show modularity of the clusters that our algorithm finds is 7% less on average, but our algorithm is 48 times faster on average. For one instance (kron-g500-logn16), our algorithm is 390 times faster.

SimX Parallel Simulation Library: The SimX library for developing parallel, discrete-event simulations in Python [3,15] of large-scale complex systems are written in C++ and Python. SimX APIs are exposed to Python, enabling rapid development and prototyping of a parallel simulation entirely in Python. SimX provides the simulation modeler with the core functionality needed in a parallel simulation library such as event queuing, process management, time advancement, domain partitioning, synchronization and message passing. Arbitrary Python objects can be sent and received between different simulation processes without having to write explicit serialization code. Further, the fast C++ core and distributed memory design of SimX makes the parallelization transparent to the user and allows applications to scale from multi-core user workstations to high performance clusters.

SimX is free software and has been open sourced under the GNU LGPL license. It is publicly available at http://github.com/sim-x. It has already been used in developing an agent-based simulation model of a monetary reserve system validated against real world data [13]. More SimX based applications are currently being developed at LANL and elsewhere.

Impact on National Missions

LANL is uniquely poised to make important contributions to the emerging field of heterogeneous computing. Our aim in this proposal was to take a significant step in that direction by exploring new algorithmic methods to enable us to unleash the potential of heterogeneous and accelerated computing on a lager variety of problems that are aligned with LANL and DOE missions. For example, the distributed memory GPGPU computing algorithms for path problems in graphs is relatively new territory and represents a significant opportunity for LANL to establish itself in this area.

Other specific examples of impact on national missions include: (a) Advances in parallel graph clustering and community detection algorithms will find numerous uses for analyzing signaling pathways and metabolic channels in biological networks (Grand Challenge: Complex Biological Systems), and network analysis in epidemiology (Bio-security Science) (b) Community detection algorithms can also be readily applied to detecting and characterizing terrorist networks and channels (Grand Challenge: Sensing and Measurement for Global Security) (c) Graph algorithms have also found numerous uses in LANLs efforts in infrastructure analysis (NISAC). The results of our effort can be used to vastly improve the scale and speed of current models and simulations. (d) LANL's efforts in data-intensive and exascale computing (Grand Challenge: IS&T) can directly leverage our work, since one of the major computational tasks in this domain will be inferring semantic relationships inside huge data sets that will necessarily involve massive amounts of unstructured computation.

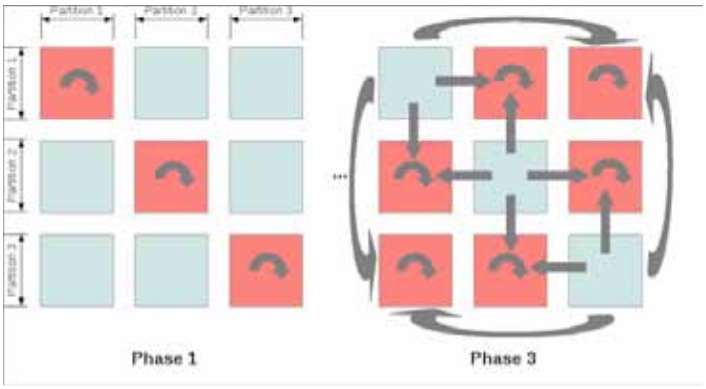

Figure 1. Block-level data parallelism and data dependencies in the adjacency matrix for phase 1 and phase 3 of the algorithm. Sub-matrices for which computations are required are shown in red. Arrows indicate data dependencies.

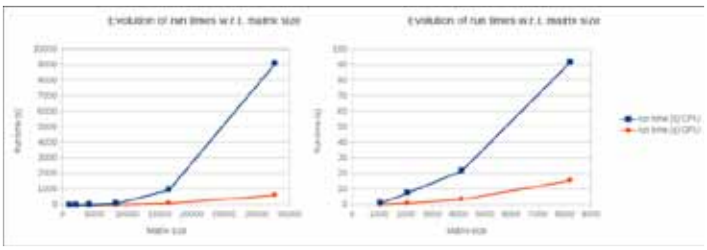

Figure 2. Run-times (left) with respect to input matrix size on the CPU and GPU versions. Figure on right shows first four data points zoomed in.

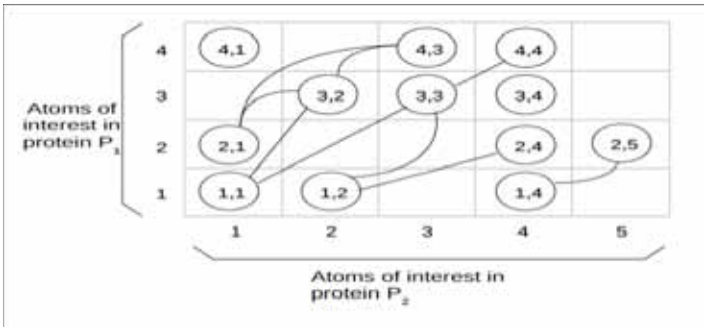

Figure 3. Example of an alignment graph used here to compare the structures of two proteins. The presence of an edge between vertex (1, 1) and vertex (3, 2) means that the distance between atoms 1 and 2 of protein 1 is similar to the distance between atoms 1 and 3 of protein 2.

# of cores	1	2	3	4	6	8	12	16	20	24
Run time (s)	6479	3696	2494	1932	1374	1072	781	723	676	643
Speedup	1	1.8	2.6	3.4	4.7	6.0	8.3	9.0	9.6	10.1

Figure 4. Dependence of the run times and speedups on the number of CPU cores.

Network	Modularity (Our Paper)	Modularity (OG)	Run Time (Our Paper)	Run Time (OG)
as-22july06	0.6338	0.6776	3.26	25.28
astro-ph	0.7162	0.7424	1.14	36.48
caidaRouterLevel	0.8421	0.8719	8.67	324.36
celegans-metabolic	0.4224	0.4490	0.03	0.22
citationCiteseer	0.7732	0.8228	12.17	579.16
coAuthorsCiteseer	0.8844	0.9051	18.97	618.75
cond-mat-2005	0.7187	0.7460	3.54	111.34
email	0.5654	0.5802	0.08	0.81
G-n-pin-pout	0.3829	0.4998	6.12	680.77
kron-g500-logn16	0.0402	0.0533	12.42	4682.84
memplus	0.5913	0.7000	0.53	20.47
PGPgiantcompo	0.8750	0.8862	0.64	8.45
polblogs	0.4260	0.4269	0.14	0.64
power	0.9329	0.9397	0.19	1.92
rgg-n-2-7-s0	0.9732	0.9780	6.55	174.76
smallworld	0.7455	0.7930	17.61	267.86
coPapersDBLP	0.8309	0.8666	142.91	6388.64
in-2004	0.9717	0.9806	1321.52	1717.6

Figure 5. Comparison of our algorithm with Ovelgonne and Geyer-Schulz's algorithm.

References

1. Thulasidasan, S.. Heuristic Acceleration of Routing in Transportation simulations using GPUs. 2011. (Barcelona, Spain, 21-5 March 2011). p. 90. Brussels, Belgium: ICST .

2. Thulasidasan, S.. A Simulation Based Analysis of Distributed Coverage and Dynamic Relocation for Mobile Sensor Networks Using Potential Fields. 2012. Los Alamos Technical Report LA-UR-12-25669.

3. Djidjev, H., G. Chapuis, S. Thulasidasan, and R. Andonov. On Solving the Shortest Path Problems for Planar Graphs Using Graphics Processors. 2012. LANL Technical Report LA-UR-12-25700.

4. Thulasidasan, S., L. Kroc, and S. Eidenbenz. Developing Parallel Discrete Event Simulations in Python: First Results and User Experiences with the SimX Library. 2012. LANL Technical Report, LA-UR-12-26739. Submitted to 6th International ICST Conference on Simulation Tools and Techniques (SimuTools 2013).

5. Djidjev, H., S. Thulasidasan, G. Chapuis, and R. Andonov. Accelerating Graph Algorithms Using Graphics Processors: Shortest Paths for Planar Graphs. 2013. ADTSC Science Highlights 2013: Information Science and Technology Section.

6. Chapuis, G., M. Le Boudic-Jamin, R. Andonov, H. Djidjev, and D. Lavenier. Parallel Seed-based Approach to Protein Structure Similarity Detection. (Warsaw, Poland, 8-11 Sep 2013).

7. Djidjev, H., and M. Onus. Using Graph Partitioning for Efficient Network Modularity Optimization. 2013. Graph Partitioning and Graph Clustering: Contemporary Mathematics. : 103.

8. Srinivasan, M. S., S. Srinivasa, and S. Thulasidasan. Exploring Celebrity Dynamics on Twitter. (New Delhi, India, 17-19 Oct 2013).

9. Tenth Dimacs Implementation Challenge. 2013. http://www.cc.gatech.edu/dimacs10/.

10. Cormen, T. H.. Introduction to Algorithms. 1990.

11. Melhorn, K. etal.. LEDA: A Platform for Combinatorial and Geometric Computing. 1999.

12. Venkatraman, G. etal.. A Blocked All-Pair Shortest-Paths Algorithm. 2003. Journal of Experimental Algorithmics. : 2.2.

13. Williams, S., and S. Eidenbenz. Themis-1: An Agent Based Model of a Modern Monetary Reserve System. Presented at Agent-Directed Simulation Symposium. (San Diego, 7-10 April 2013).

14. Ovelgonne, M., and A. Geyer-Schulz. An Ensemble Learning Strategy for Graph Clustering. To appear in Contemporary Mathematics 2010.

15. Thulasidasan, S.. simx 0.1. 2013. https://pypi.python.org/pypi/simx/0.1.

Publications

Chapuis, G., M. Le Boudic-Jamin, R. Andonov, H. Djidjev,

and D. Lavenier. Parallel Seed-based Approach to Protein Structure Similarity Detection. Presented at Tenth International Conference on Parallel Processing and Applied Mathematics (PPAM 2013). (Warsaw, Poland, 8-11 Sep 2013).

Djidjev, H., G. Chapuis, S. Thulasidasan, and R. Andonov. On Solving the Shortest Path Problems for Planar Graphs Using Graphics Processors. 2012. LANL Technical Report LA-UR-12-25700.

Djidjev, H., S. Thulasidasan, G. Chapuis, and R. Andonov. Accelerating Graph Algorithms Using Graphics Processors: Shortest Paths for Planar Graphs. 2013. ADTSC Science Highlights 2013: Information Science and Technology Section.

Djidjev, H., and C. Sommer. Approximate distance queries for weighted polyhedral surfaces. 2011. In Algorithms - ESA 2011. (19th Annual European Symposium ; 5-9 Sept. 2011 ;). , p. 579.

Djidjev, H., and M. Onus. Using Graph Partitioning for Efficient Network Modularity Optimization. 2013. Graph Partitioning and Graph Clustering: Contemporary Mathematics. : 103.

Srinivasan, M. S., S. Srinivasa, and S. Thulasidasan. Exploring Celebrity Dynamics on Twitter. Presented at 5th IBM Collaborative Academia Research Exchange Conference (I-CARE 2013). (New Delhi, India, 17-19 Oct 2013).

Thulasidasan, S.. Heuristic Acceleration of Routing in Transportation simulations using GPUs. 2011. In 4th International Conference on Simulation Tools and Techniques (SimuTools 2011). (Barcelona, Spain, 21-5 March 2011). , p. 90. Brussels, Belgium: ICST .

Thulasidasan, S.. The Graph Laplacian and the Dynamics of Complex Networks. 2012. Talk given at University of Washington, Department of Applied Mathematics [LA-UR-12-22065].

Thulasidasan, S.. A Simulation Based Analysis of Distributed Coverage and Dynamic Relocation for Mobile Sensor Networks Using Potential Fields. 2012. Los Alamos Technical Report LA-UR-12-25669.

Thulasidasan, S., L. Kroc, and S. Eidenbenz. Developing Parallel Discrete Event Simulations in Python: First Results and User Experiences with the SimX Library. 2012. LANL Technical Report, LA-UR-12-26739. Submitted to 6th International ICST Conference on Simulation Tools and Techniques (SimuTools 2013).

Extreme Quantum Simulation: Co-design from Desktop to Exascale

Nicolas Bock
20110230ER

Abstract

We present a novel approach to linear scaling matrix-matrix multiplication, the Sparse Approximate Matrix Multiply (SpAMM), a fast algorithm for matrices with decay that achieves a linear computational complexity with respect to matrix size. We find that the error achieved with SpAMM is lower than that of a conventional dense method (SGEMM) for small tolerances. In serial, SpAMM outperforms SGEMM with a cross-over already for small matrices and in parallel, we find near ideal scaling and load balancing on both shared and distributed memory systems, including modern accelerator architectures such as Intel's Xeon Phi.

Background and Research Objectives

Continued trends in computer architectures are transforming quantum simulations into an increasingly powerful, rigorous, predictive, and interpretive tool for chemistry, biology, and materials science. However, algorithms have not kept pace with the increasingly complex hardware. On the one hand, conventional algorithms for electronic structure are able to take full advantage of large parallel platforms through standard software libraries, but are throttled by a computational complexity that scales with system size cubed, i.e. a thousandfold increase in computational power translates only into a tenfold increase in the system size that can be computed in a given time. On the other hand, novel linear scaling algorithms, which exploit quantum locality of non-metallic quantum systems to achieve a sparse matrix representation and linear scaling through methods such as the Sparse Matrix-Multiply (SpMM) lead to irregular work and data and do not lend themselves to Cartesian domains or standard libraries. In addition, increasingly complex memory hierarchies and use of heterogeneous architectures through accelerator technologies such as GPUs only exacerbate this shortcoming on the path to the exa-scale. Despite the challenges facing linear scaling algorithms, the near exponential growth of computational power underscores the tremendous potential of these algorithms to take full advantage of the next generation of high performance computing platforms: A thousandfold increase in computational power translates into a thousandfold increase in system size while only into a tenfold increase in system size using conventional methods.

One of the first linear scaling approaches was Yang's "divide and conquer" (D&C) [1], an ad hoc scheme for patching together density matrices corresponding to fictitious quantum sub-domains. The appeal of D&C is that it is perfectly parallel, as troublesome off-diagonal information is ignored. However, it was found early that ignoring this off-diagonal information leads to uncontrolled errors and D&C was abandoned. More recently Wang et al. rediscovered D&C, however, this version of D&C is likewise unable to converge the total energy with increasing fragment size [2].

Over the past 12 years a rigorous alternative to linear scaling has been pioneered at LANL, demonstrating the ability to control the error in ground state, and static and dynamic response calculations [3-13]. Our early work to parallelize SpMM focused on spatial locality of the underlying physical system to maximize diagonal dominance, but did not address the spatial and temporal locality of work and data of the abstract convolution space of the multiply. Currently, a majority of work in electronic structure theory employs some version of SpMM, although no scalable algorithm for the general problem exists.

Scientific Approach and Accomplishments

The dominating obstacle towards a scalable high-performance SpMM is the irregular nature of data access, which cannot be predicted a priori. Costly latency and bandwidth barriers between memory hierarchies can quickly render an implementation I/O bound, and make data and load distribution challenging. A so-called cache-oblivious approach promises an elegant solution:

By ordering the abstract convolution along a space filling curve the spatial and temporal locality of data access is enhanced, which naturally leads to an algorithm that optimally overlaps I/O with computation, with potentially very competitive performance [14, 15]. We developed a serial, recursive version with encouraging results [16]. However, we found that convolution ordering effects applied to sparse matrices decrease with increasing matrix sparsity due to the increasingly irregular memory access and resulting lack of temporal locality and the inability of the CPU's hardware prefetch unit to hide memory access, ultimately rendering this cache-oblivious approach infeasible.

Keeping recursion, but dropping the ordering of the convolution, we refined our approach and introduced a new Sparse Approximate Matrix-Multiply (SpAMM) algorithm which multiplies potentially full matrices with decay and recursively eliminates insignificant contributions in the product space, leading to complexity reduction in the sparse product space [17], as opposed to truncation in the vector space and applying standard sparse matrix algebra (SpMM) [4]. The recursive approach is similar to Strassen's algorithm for fast dense matrix multiplication [18], and also to methods that improve locality across memory hierarchies (cache-oblivious approaches), pioneered by Wise and coworkers [19, 20]. SpAMM belongs to a broad class of generalized N-Body solvers, which are "fast" algorithms that achieve reduced complexity through hierarchical approximations, which can be found in high-performance implementations across a broad range of disciplines. Related solvers include the database join operation [21-23], gravitational force summation in astrophysics simulations [24, 25], the fast Gauß transform in machine learning [26, 27], and visualization applications [28, 29].

Despite the significant challenges due to irregular data access inherent in sparse solvers, it is possible to write high performance implementations of SpAMM. Our serial, single-precision implementation [30] employs a hand coded assembly kernel operating on 4 x 4 matrices and achieves around 70% performance compared to the SGEMM function of a vendor tuned library such as MKL or ACML, Figure 1. In combination with a linear tree to avoid explicit recursion and potentially costly branching in the code, we find an early cross-over to linear scaling for water clusters, and better performance than SGEMM between 50 and 90 water molecules, Figure 2. Eliminating insignificant contributions in product space achieves a smaller error compared to SGEMM for small SpAMM tolerances, which we attribute to differences in execution order; hierarchical vs. row-column, Figure 3.

Matrix-matrix multiplication is now aligned with the N-Body programming model employed by other quantum chemical solvers [31-33], which will lead to a quantum chemical solvers eco system based on a common framework and data structures, allowing for a significant reduction in code size and complexity of linear scaling quantum chemistry programs. In addition, the recursive approach employed by SpAMM allows for overdecomposition providing significant opportunities for parallelism. We are currently preparing a publication detailing our parallel SpAMM implementation on shared and distributed memory systems using advanced middle ware solutions to data distribution and load balancing. We find near ideal parallel scaling of SpAMM on shared memory architectures, including accelerator systems such as Intel's Xeon Phi, Figure 4, and are currently investigating scaling of SpAMM to thousands of nodes on a distributed computer platform, Figure 5. So far, results on scalability and load balancing are very promising, strongly indicating that the generalized N-Body framework with its potential for task overdecomposition presents a scalable, high-performance path towards large scale linear scaling electronic structure calculations.

Impact on National Missions

This research will deploy complimentary, LANL unique capabilities to establish a strategic thrust with broad Mission Relevance and a Program Development impact that is translational, providing coherence between basic research and engineering specifics. This work complements the developing SciDAC program Exascale for Energy, as well as DOE's Basic Research Needs: Catalysis for Energy, the BES grand challenge the ability to design and to implement new catalytic processes by design. More broadly, this project develops basic capabilities with broad laboratory mission relevance, including DARPA's Quantum Effects in Biological Environments (QuBE) and LANL's Matter-Radiation Interactions in Extremes (MaRIE). This project will also directly broadly impact the DOE and NNSA's push toward exascale computing, as well as BES and OBER missions in Energy and DHS Biothreat missions.

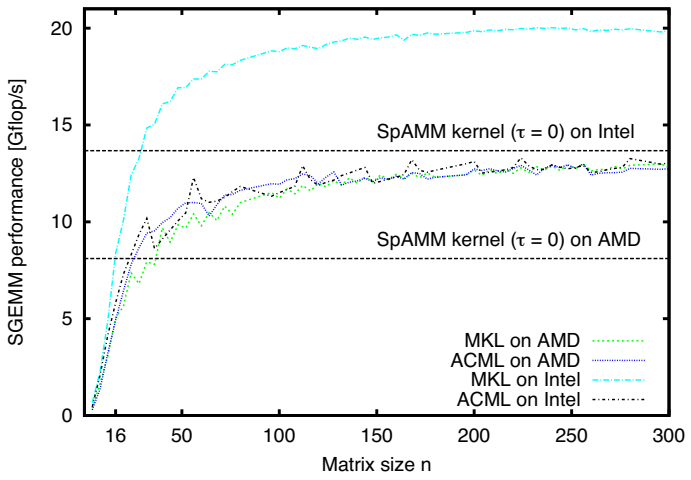

Figure 1. SpAMM kernel performance compared to library SGEMM. The horizontal lines indicate the SpAMM kernel performance, operating on fixed-size 4x4 matrices. The performance of SGEMM improves with increasing matrix size and levels off for larger matrices. The SpAMM kernel performs is about 70% of the large matrix performance of SGEMM.

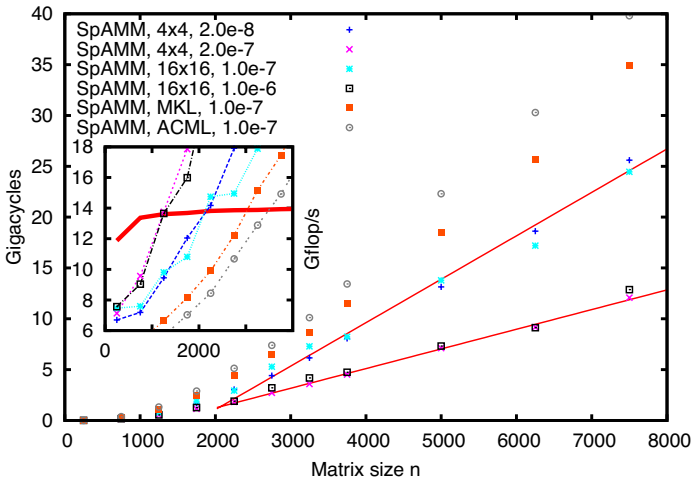

Figure 2. SpAMM serial performance on quantum chemical matrics of water clusters. The thick red line in the inset indicates SGEMM performance. SpAMM exhibits better performance than SGEMM already for small water clusters, and an early onset of linear scaling behavior.

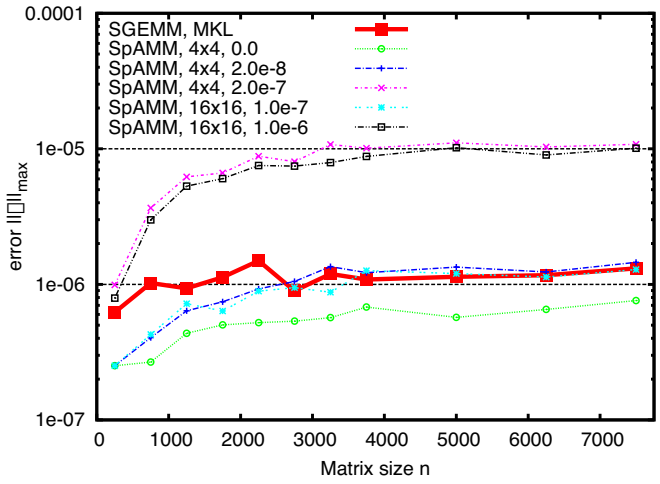

Figure 3. Error comparison of SpAMM and dense SGEMM. The thick red line indicates the SGEMM error with matrix size. Notice that SpAMM yields an error lower than SGEMM for small tolerances.

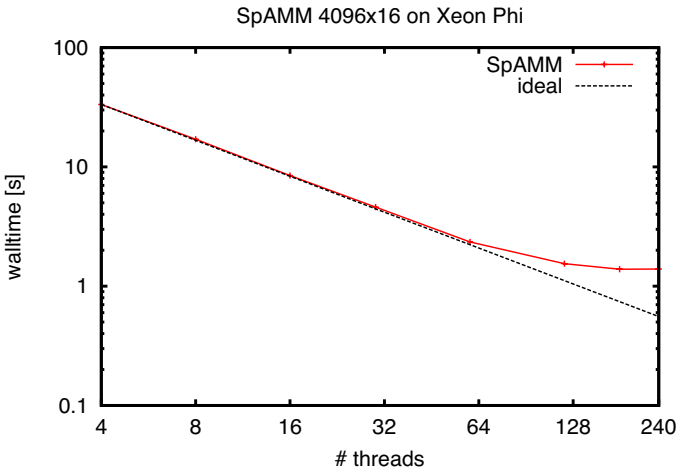

Figure 4. Parallel scaling of SpAMM on Intel Xeon Phi. Note that this version of the accelerator has 60 physical cores and can run up to 4 threads per core. We find continuing performance gains beyond 60 threads, however, parallel scaling slows from ideal.

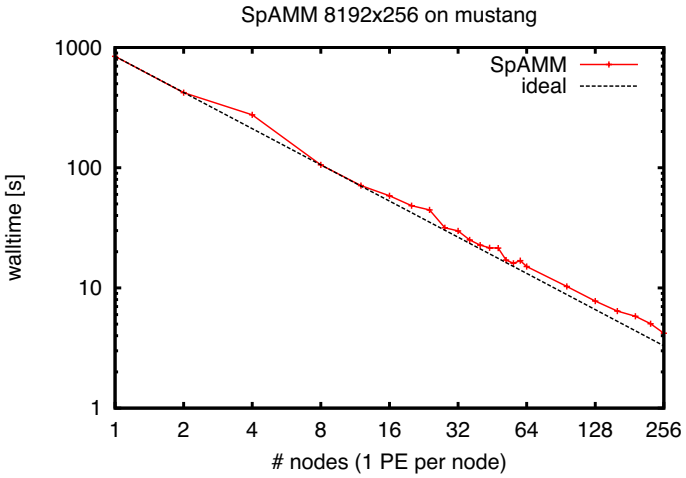

Figure 5. Parallel scaling of SpAMM on distributed memory computer cluster. We find near ideal parallel scaling up to 256 nodes.

References

1. Yang, W.. Direct Calculation of Electron Density in Density-Functional Theory. 1991. Phys. Rev. Lett.. 66: 1438.

2. Wang, Lin-Wang, Zhengji Zhao, and Juan Meza. Linear-scaling three-dimensional fragment method for large-scale electronic structure calculations. 2008. Phys. Rev. B. 77: 165113.

3. Challacombe, M., N. Bock, Chee Kwan Gan, Graeme Henkelman and Karoly Nemeth, Anders Niklasson, Anders Odell, Eric Schwegler, C.J. Tymczak, and Valery Weber. FreeON, a suite of linear scaling quantum chemistry programs, http://www.freeon.org/.

4. Challacombe, M.. A general parallel sparse-blocked matrix multiply for linear scaling. 2000. Comput. Phys. Commun.. 128: 93.

5. Németh, K., and M. Challacombe. The quasi-independent curvilinear coordinate approximation for geometry optimization. 2004. J. Chem. Phys.. 121: 2877.

6. Challacombe, M.. A simplified density matrix minimization for linear scaling self-consistent field theory. 1999. J. Chem. Phys.. 110: 2332.

7. Weber, V., A. M. N. Niklasson, and M. Challacombe. Higher-order response in O(N) by perturbed projection. 2005. J. Chem. Phys.. 123: 044106.

8. Niklasson, A., C. J. Tymcak, and M. Challacombe. Time-reversible ab initio molecular dynamics. 2007. J. Chem. Phys.. 126: 144103.

9. Weber, V., and M. Challacombe. Parallel algorithm for the computation of the Hartree-Fock exchange matrix: Gas phase and periodic parallel ONX. 2006. J. Chem. Phys.. 125: 104110.

10. Challacombe, M., and E. Schwegler. Linear scaling computation of the Fock matrix. 1997. J. Chem. Phys.. 106: 5526.

11. Niklasson, A. M. N., C. J. Tymczak, and M. Challacombe. Trace Re-Setting Density Matrix Purification in O(N) Self-Consistent Field Theory. 2003. J. Chem. Phys.. 118: 8611.

12. Gan, C. K., C. J. Tymczak, and M. Challacombe. Linear scaling computation of the Fock matrix. VII. Parallel computation of the Coulomb matrix. 2004. J. Chem. Phys.. 121: 6608.

13. Schwegler, E., M. Challacombe, and M. Head-Gordon. Linear scaling computation of the Fock matrix. II. Rigorous bounds on exchange integrals and incremental Fock build. 1997. J. Chem. Phys.. 106: 9708.

14. Bader, M., and C. Zenger. A Cache Oblivious Algorithm for Matrix Multiplication Based on Peano's Space Filling Curve. 2006. Lecture Notes in Computer Science. 3911: 1042.

15. Bader, M., S. Franz, and A. Heinecke. Hardware-Oriented Implementation of Cache Oblivious Matrix Operations Based on Space-Filling Curves. 2008. Lecture Notes in Computer Science. 4967: 628.

16. Bock, N., Emanuel H. Rubensson, Paweł Sałek, Anders M. N. Niklasson, and Matt Challacombe. Cache oblivious storage and access heuristics for blocked matrix-matrix multiplication. 2008. arXiv:0808.1108.

17. Challacombe, Matt, and Nicolas Bock. Fast Multiplication of Matrices with Decay. 2010. arXiv:1011.3534.

18. Strassen, Volker. Gaussian elimination is not optimal. 1969. Numer. Math.. 13: 354.

19. Frens, Jeremy D, and David S. Wise. Auto-Blocking Matrix-Multiplication or Tracking BLAS3 Performance from Source Code. 1997.

20. Wise, David S., Jeremy D. Frens, Yuhong Gu, and Gregory A. Alexander. Language support for Morton-order matrices. 2001.

21. Schneider, Donovan A., and David J. DeWitt. Tradeoffs in processing complex join queries via hashing in multiprocessor database machines. 1990.

22. Mishra, Priti, and Margaret H. Eich. Join processing in relational databases. 1992. ACM Comput. Surv.. 24: 63.

23. Chen, Shimin, Anastassia Ailamaki, Phillip B. Gibbons, and Todd C. Mowry. Improving hash join performance through prefetching. 2007. ACM Trans. Database Syst.. : 32.

24. Warren, Michael S., and John K. Salmon. A portable parallel particle program. 1995. Computer Physics Communications. 87: 266.

25. Warren, Michael S., and John K. Salmon. A parallel hashed Oct-Tree N-body algorithm. 1993. Proceedings of the 1993 ACM/IEEE conference on Supercomputing. : 12.

26. Gray, Alexander G., and Andrew W. Moore. N-Body Problems in Statistical Learning. 2001.

27. Greengard, Leslie, and John Strain. The fast Gauss transform. 1991. SIAM Journal on Scientific and Statistical Computing. 12: 79.

28. Choi, Myung Geol, Eunjung Ju, Jung-Woo Chang, and Jehee Lee and Young J. Kim. Linkless octree using multi-level perfect hashing. 2009. Computer Graphics Forum. 28: 1773.

29. Lewinger, Thomas, Vinicius Mello, Adelailson Peixoto, Sinesio Pesco, and Helio Lopes. Fast generation of pointerless octree duals. 2010. Computer Graphics Forum. 29: 1661.

30. Bock, N., and M. Challacombe. An Optimized Sparse Approximate Matrix Multiply for Matrices with Decay. 2013. SIAM J. Sci. Comput. 35 (1): C72.

31. Challacombe, Matt, Eric Schwegler, and Jan Almlöf. Fast assembly of the Coulomb matrix: A quantum chemical tree code. 1996. J. Chem. Phys.. 104: 4685.

32. Challacombe, Matt. Linear scaling computation of the Fock matrix. V. hierarchical cubature for numerical integration of the exchange-correlation matrix. 2000. J. Chem. Phys.. 113: 10037.

33. Challacombe, Matt, Eric Schwegler, and Jan Almlöf. Chemistry: Review of current trends. 1996.

Publications

Bock, N., and M. Challacombe. An Optimized Sparse Approximate Matrix Multiply for Matrices with Decay. 2012. arXiv:cs.NA. 1203.1692: 1.

Bock, N., and M. Challacombe. An Optimized Sparse Approximate Matrix Multiply for Matrices with Decay. 2013. SIAM Journal on Scientific Computing. 35 (1): C72.

Challacombe, M., and N. Bock. Fast Multiplication of Matrices with Decay. 2010. arXiv:cs.DS. 1011.3534: 1.

Smart Grid Control and Optimization

Michael Chertkov
20130766ER

Abstract

Over the three years preceding these efforts, a bigger (smart grid) DR team made significant progress towards developing an entirely new field of science consisting of a combination of Complex System Theory, Control Theory, and Computer Science and Optimization Theory. As is often the case, research generates new questions as well as answers. This one year reserve ER addressed questions in Grid Science that were opened by that work. We developed new approaches to modeling dynamical phenomena in power grids, such as electro-magnetic waves in transmission and dynamics of voltage drop in distribution. We also extend classic optimization and planning paradigms in power system with an innovative complex system approach, allowing a computationally advantageous way of dealing with uncertainties and fluctuations of renewable energy resources.

Background and Research Objectives

This one year reserve project has focused on extending our prior work on developing new optimization and control algorithm for operations and planning of modern power grids on both transmission and distribution levels.

The new research objectives of the project included – (a) focusing on dynamic phenomena in power grids, specifically on analysis of electro-mechanical waves in transmission systems and voltage dynamics in distribution systems; and (b) building the complex system approach, e.g. in modeling uncertainties in power grids, into more traditional optimization approaches.

Scientific Approach and Accomplishments

We extended our past work on modeling and simulation of electro-mechanical and voltage dynamics in distribution circuits, focusing on theoretical and intuitive understanding of the highly nonlinear and hysteretic phenomena that occur when voltage dynamics interact with large numbers of induction motors—phenomena that are becoming serious issues for local grid stability.

We combined (i.e. "reconstructed") our prior complex systems approach with control theory to incorporate our recently developed modeling of a feeder with large number of inductive motors for designing controls to maintain local grid stability.

Our past work on simulation-driven optimization methods for transmission expansion planning assumed that generator outputs are constant and well controlled, however, grid expansion that includes time-intermittent renewable generation breaks this assumption making optimal grid expansion planning far more difficult. We combined this optimization approach with a complex systems approach that will bring probabilistic measures of electrical grid failure into the simulation-driven optimization methods to create an entirely new network planning tool that balances probabilistic measure of risk against the costs of grid expansion.

Impact on National Missions

This project leverages LANL/DOE capabilities in information theory, infrastructure analysis, and complex networks for research in a national priority, the smart grid. The team's combined theoretical and applied expertise constitutes a forward-looking DOE capability in analysis of energy systems. Development of Information Science and Technology tools for smart grids contribute to energy security, and predictive science more broadly. Our research on optimization of renewable placement and the expansion of current laboratory infrastructure analysis tools to include intermittent renewables generation targets problems on the intersection of energy, climate, and infrastructure.

Our smart grid effort enables LANL/DOE to expand its infrastructure planning and analysis programs, initially focused mainly on infrastructure security and sponsored by the Department of Homeland Security, to a broader set of programs in energy infrastructure planning and efficiency analysis with the Department of Energy as pri-

mary sponsor. The project thereby positions LANL closer to the center of mass in energy research, a national and DOE priority area.

This project has led to programmatic funding from a range of federal agencies -- DTRA, NSF, and DOE/OE.

Publications

Backhaus, S., and M. Chertkov. Getting a Grip on the Electrical Grid. 2013. Physics Today. : 10.

Barrows, C., S. Blumsack, and R. Bent. Using Network Metrics to Achieve Computationally Efficient Optimal Transmission Switching. To appear in Proceedings of the 46th Hawaii International Conference on System Sciences (HICSS 2013). (Grand Wailea, Hawaii, Jan 2013).

Bienstock, D., M. Chertkov, and S. Harnett. Chance Constrained Optimal Power Flow: Risk-Aware Network Control Under Uncertainty. SIAM Review.

Bienstock, D., R. Bent, and S. Backhaus. Synchronization-Aware and Algorithm-Efficient Chance Constrained Optimal Power Flow. Presented at 2013 IREP Symposium-Bulk Power System Dynamics and Control. (Crete, Greece, 25-30 Aug, 2013).

Duclut, C., S. Backhaus, and M. Chertkov. Phase Transitions and Dangerous Transients in Power Distribution Systems. 2013. Physical Review E. 87: 062802.

Dvijotam, K., S. Backhaus, and M. Chertkov. Storage Sizing and Placement through Operational and Uncertainty-Aware Simulations. To appear in HICSS 2014. (Big Island, Hawaii, Jan 6-9, 2014).

dorfler, F., F. Bullo, and M. Chertkov. Synchronization in Complex Oscillator Networks and Smart Grids. 2013. PNAS. 110 (6): 2005.

Development of a Novel Algorithm to Generate User-defined Databases of Genomic Signatures

Patrick S. Chain
20130786ER

Abstract

We have implemented a novel algorithm that identifies nucleotide signatures – the unique genome – independent of functional annotation that is currently applicable to bacteria and viruses at any taxonomic rank. We have named it the GOTTCHA workflow for Genome Origins Through Taxonomic CHAllenge. Through many test cases, we have demonstrated its accuracy to be far superior to all other published tools available at the time of analysis. Specifically, we have examined in detail the performance of GOTTCHA versus other available tools on 24 synthetic metagenomes of varying complexity and read distribution, 4 mock metagenomes whose sequences were derived from actual sequencers and two real metagenomes. In addition we examined GOTTCHA's ability to successfully profile 2924 novel bacteria across all taxonomic ranks.

Background and Research Objectives

Read-based sequence identification is highly difficult, very computationally intensive given today's sequencer throughput capabilities, and particularly difficult when data is obtained from complex (metagenomic) samples (e.g. pathogens present during infection, in blood, sputum, feces, or organisms found in soil, water, etc.). While there are very rapid tools that provide a snapshot of possible taxonomic representation, there are no tools that rapidly examine all the data to identify even very rare members of natural or perturbed systems, primarily due to RAM and data throughput limitations as a result of extreme data redundancy. The database and tools proposed here will minimize the impact of data redundancy and strengthen our ability to detect and respond to biological outbreaks in a rapid, reliable, and tailored manner, by maximizing the specificity of biological knowledge one can obtain from a sample, as well as minimizing the time to acquire this knowledge, and to do so with as much sensitivity as possible.

This proposal will implement and deploy a novel algorithm to identify nucleotide signatures specific and unique to any organism or set of organisms. Although this algorithm conceptually has many uses, we will apply this method of generating ultra-specific databases to the problem of rapid and accurate organism identification based on sequence data. The database we initially propose constructing will contain all organism-specific (or clade-specific) signatures found anywhere in any genome, regardless of any predicted functions that may be associated with a given signature. The signatures can then be used to rapidly, accurately, and sensitively classify any sample based on sequence data and using open-source or proprietary tools. The proposed algorithm will be flexible and extensible, allowing end-users to generate specifically tailored databases for a multitude of purposes. Use of this database can be implemented to fortify current or future biosurveillance efforts, improve diagnostics in the public health or forensics fields, as well as providing and essential reference for fundamental science research in the fields of metagenomics and pathogen diagnostics.

Scientific Approach and Accomplishments

The GOTTCHA workflow consists of six tools: two pre-processing tools, the GOTTCHA generator, a read splitter-trimmer, the GOTTCHA profiler, and the GOTTCHA filter, which will be folded into the profiler at a later date. We used the Perl language to quickly implement the algorithm, though greater speed and memory efficiencies will be realized when this is ported to a compiled language. The two pre-processing tools written to prepare data for the GOTTCHA generator include mkSpeciesTree.pl and taxIndexer.pl. The first generates a single, universal taxonomic tree file using the GenBank files available to the user as well as a file containing all the genomic vitals of the bacteria to be analyzed (name, length, sequence type, TAXID, last update, etc.). The taxIndexer.pl tool uses the taxonomic tree file and the genomic vitals files to generate a single XML file for input into the GOTTCHA generator. It is at this level that the desired

taxonomic levels are specified. The GOTTCHA generator uses these data to compute the signatures, which currently takes approximately 12 days on a 2TB RAM 80-core server. Incrementally updating the database is a possibility given the intermediate files generated, but is not currently implemented.

Upon generation of the desired GOTTCHA database(s), three corresponding database statistics files are generated, organized according to the individual contigs, organisms or the database as a whole. Once these databases are generated, they are used as references to which metagenomic datasets are aligned and profiled. The read set is first trimmed with our split-trimming tool written in the D programming language, then mapped to the GOTTCHA database(s) with a read mapper. We assessed GOTTCHA's performance at the species level with the Burrows Wheeler Aligner (BWA) version 0.6.2-r126-tpx since it provides two important features: it allows local alignment and randomly assigns multiply-mapped reads. The GOTTCHA profiler then parses the resulting alignment file, assigns data to relevant taxonomies, and generates a preliminary result. The GOTTCHA filter is then applied on top of this to remove excess false positives due to read stacking, sequencing errors, and polymorphisms. Essential parameters of the filter were extracted from GOTTCHA's performance on 24 synthetic metagenomes ranging from 250k reads (25 organisms) to 1M reads (100 organisms), to 300M reads (>400 organisms). These were then applied to four mock metagenomes and two real metagenomes – one air filter and one clinical fecal sample – and GOTTCHA was shown to work well even for RNA samples. Our preliminary results of the clinical sample even showed that a linear relationship exists between recovered hits and the concentration of pathogen in the sample, though further testing is necessary to solidify this relationship under various conditions.

In order to assess GOTTCHA's performance on novel organisms, we attempted to classify almost 3000 novel draft genomes (not present in the GOTTCHA database) to their parent taxonomy. This included 1923 novel strains, 791 novel species, 175 novel genera, 26 novel families, 4 novel orders and 5 novel classes. GOTTCHA was able to identify many contaminated genome projects and even misnamed organisms, emphasizing GOTTCHA's success at organism classification.

With the funding provided by the LDRD reserve, we were able to meet our stated milestones. A draft manuscript of the application (intended for submission to Nature Methods) is available upon request, and the manuscript describing the generation algorithm is underway.

Impact on National Missions

This work ties directly to two LANL missions, the reduction of global threats and solving other emerging national security and energy challenges. The suite of tools and algorithms have been directly applied to the area of human pathogen (bacterial or viral) detection from within complex samples, primarily clinical. In addition, we propose to utilize these tools to identify emerging pathogens of importance to agriculture and food chain supply safety, as well as to understanding the interactions and impacts of various bacterial communities on algal biofuel production strains when grown in production pond environments.

Multi-Phenomenology Explosion Monitoring (MultiPEM)

Dale Anderson
20130798ER

Abstract

This research effort developed a general mathematical framework for two-phenomenology yield estimation for a single-point above-ground explosion, providing a mathematical pattern for multi-phenomenology yield estimation and error analysis. The development approach, construction of a statistical likelihood, embeds the mathematics of physical-basis into an error model for observed measurements that partitions total error into bias that can be calibrated, bias that is highly dynamic, and statistical error. Dynamic bias and statistical error are mathematically propagated to provide the error of a yield estimate. The mathematical theory of likelihood functions is mature. However, research to construct likelihood functions can be transformational, providing a very general research strategy for multi-phenomenology analysis in national security missions.

Background and Research Objectives

To estimate explosive yield, a variety of technologies could be used including, but not limited to, acoustic signatures, optical signatures, RF signatures, seismic signatures, craterology and various chemical signatures. Each technique has a different accuracy and precision and is subject to various errors that can affect the yield estimate. The Research challenge is how to mathematically combine these different data types into a single unified yield estimate that appropriately accounts for the uncertainties in each technology. Focusing on acoustic and optical signatures in this pilot project, our innovation is to separate the total error in the statistical likelihood into three components – source, path and sensor error. A multi-phenomenology yield estimate then derived as the value of yield that maximizes the likelihood. We can derive an expression for the uncertainty in a combined maximum likelihood yield estimate in terms of these error components.

Scientific Approach and Accomplishments

We have researched source models for the optical energy from either conventional explosions or nuclear explosions in the form of equations or representative data. For optical, we are working with some type of photo sensor with known sampling rate and detector efficiency such that we have some initial estimates of these uncertainties from careful calibrations. Whether the sensor is ground based or space based, the optical energy must pass through the atmosphere where, depending on timescales, two effects on the signal apply. For very early time features, atmospheric scattering may impose delays that distort the observed signal. The delay increases for longer paths. This can be modeled for various atmospheric conditions. The other effect is just that of absorption (attenuation) of the optical energy. This depends on the atmospheric path and can be modeled for different atmospheric conditions such as, look angle, absorption coefficient, aerosol content, cloud extent, etc.

It is assumed here that each phenomenology has associated models containing descriptions of how an event produces an observable signal and how that signal propagates from the event location to the receiver location. For the acoustic shockwave generated by the blast, a source model provides an estimate of the overpressure from explosive yield, ambient pressure, propagation range, and sound speed gradient. The optical signal of interest is the peak luminosity of the fireball that can be calculated from the explosive yield, conversion efficiency, event duration, and emission region size using an early time optical transient model. From these models, one can predict the details of a given observation by,

Source Model + Propagation Model = Prediction of Observation.

In actuality, models are imperfect and observations that provide values for the parameters in a model are imper-

$$Var(\bar{W}) = \frac{ln^2 10\left(\left(\tau_1^2 + \frac{\theta_1^2}{n_1} + \frac{\sigma_1^2}{m_1}\right)\left(\tau_2^2 + \frac{\theta_2^2}{n_2} + \frac{\sigma_2^2}{m_2}\right) - \tau_{12}\right)}{\left(\tau_1^2 + \frac{\theta_1^2}{n_1} + \frac{\sigma_1^2}{m_1}\right)S_1(W)^2 S_2'(W)^2 - 2\tau_{12}S_1(W)S_2(W)S_1'(W)S_2'(W) + \left(\tau_2^2 + \frac{\theta_2^2}{n_2} + \frac{\sigma_2^2}{m_2}\right)S_2(W)^2 S_1'(W)^2}.$$

Figure 1. Variance of two-phenomenology maximum likelihood yield estimate.

fect. The result is a prediction that doesn't match observation and a residual defined by the difference. One can separate the contributions to the residual by,

Source Error + Propagation Error + Receiver/Site Error = Total Error.

In the case that multiple observations of a single type are made, the different local and propagation errors from each unique observation provide a means to reduce their influence on the estimate of event characteristics. However, the source errors are common to all observations, and no number of extra observations from a single phenomenology will reduce the source errors in the residual. Multiple phenomenologies have the potential to reduce source error.

The residuals for each phenomenology can be expressed as a linear combination of random errors produced by the source with variance τ2, propagation effects with variance θ2, and local noise with variance σ2. The residual for a single measurement of a given type is then a multivariate normal distribution with zero mean and covariance matrix that includes tradeoff between source terms of the two phenomenologies, τ12.

The likelihood is the mathematical framework for combining observations and uncertainties from multi-phenomenology measurements, bound by a common source, towards estimating explosive yield and its error. For the two-phenomenology formulation, the variance of the maximum likelihood yield estimate is given in Figure 1.

This expression provides the capability to compute a confidence bound on a yield estimate that includes statistical and model error. The development properly weights measurements from two phenomenologies when estimating yield, and provides a mathematical pattern for multi-phenomenology yield estimation and error analysis. The error model formulation can be used to prioritize R&D resources towards the most significant reduction in estimation error (e. g., optimizing sensor network design to reduce local error, or quantifying source or path model improvement).

Impact on National Missions

Threats in national/homeland security and global explosion monitoring missions, such as the increasing threat of a terrorist event, require a multiple phenomenology approach for all four monitoring functions; source signal detection, source location, identification/discrimination, and yield estimation. For yield estimation, continuing with the single phenomenology approach has the unacceptable potential to give single phenomenology yield estimates with incongruous confidence bounds e.g., loosely overlapping bounds. As national missions transform to meet new requirements, developing capabilities that obviate potentially incongruous technical assessments, and potentially lead to enhanced results, is essential.

Climate Impacts Research through Large Remote-sensing Datasets

Timothy M. Kelley
20130800ER

Abstract

Understanding forest mortality—including mortality detection at pan-tropics and global scales—is crucial for accurate climate modeling. Los Alamos researchers recently developed a method, Regional Automated Disturbance Detection (RADD), for detecting changes in vegetation by using high-resolution remote-sensing data. The RADD method was implemented in a manner suitable for use on a regional scale; addressing the pan-tropics problem requires scaling up by six orders of magnitude. This brief LDRD Reserve project studied the feasibility of scaling up the RADD method, with the ultimate goal of tracking mortality at the pan-tropics scale. We identified two areas that hindered large-scale use: the rate at which secondary data products are derived, and the rate at which machine learning classification models are trained. By rethinking and re-implementing these parts of the RADD method, we have demonstrated speedups of two orders of magnitude on comparable hardware. Our study thus indicates that applying RADD at the pan-tropics scale is computationally feasible, following a straightforward path to scaling up to much larger hardware using techniques that are well understood in the high performance computing community. By initiating collaboration between ecologists and computer scientists; this project has presented the opportunity to consider the architectural requirements needed to build a scalable system usable by domain scientists. We identified the crucial computational elements for such a system, and illustrated some of these concepts with a simple domain specific language and execution environment.

Background and Research Objectives

Forest mortality is accelerating due to climate warming, with massive consequences on economics and climate. Modeling mortality within Earth System Models is critical to accurately predict future climate because changes in the vegetation can modify the global carbon cycle and land surface biogeophysical properties (e.g., albedo). However no globally comprehensive approach and datasets are available now to monitor vegetation dynamics. This lack of data precludes fundamental knowledge gathering about where, when, and why vegetation mortality occurs.

Techniques to quantify drought stress and canopy loss from remote-sensing data for 2000-present have been developed and tested at the global scale with Moderate-Resolution Imaging Spectrometer (MODIS); however, its spatial resolution of 1 km2 is too coarse to capture a large fraction of forest mortality. In contrast, Landsat provides 30 m resolution imagery at a similar frequency as MODIS (> monthly) since 1984. Unfortunately, no group in the world has yet considered it feasible to analyze and interpret global, high frequency Landsat data due to the storage and processing requirements.

Creating a global vegetation dynamics monitoring system requires answers to three challenges: (1) unsupervised vegetation dynamics algorithms in units relevant to the carbon cycle and Earth system models (kg carbon km2 yr-1), (2) the ability to attribute causes of changes found by (1), and (3) data handling and processing at very large scale. Solutions to (1-2) have been demonstrated for large areas of Southwestern USA. A solution to (3) has yet to be attempted. As a first step, we have studied the computational characteristics of the existing implementation of the RADD method. We have identified the key roadblocks to greater performance, and demonstrated methods to work around them. In particular, we set out to answer three key questions: (1) What rates of processing can we achieve with the RADD method? (2) What scales of storage and I/O bandwidth are required to realize our vision? (3) What architectures will best serve this mission?

Scientific Approach and Accomplishments

To answer these questions, we began with a careful study of the work of Garrity et al. The RADD method was

developed in MATLAB, a key tool used by domain scientists for prototyping new methods. It provides ready access to many algorithms, array manipulation, file I/O, and visualization in an environment that is easily manipulated by a lone researcher. The performance is not competitive, but the convenience makes up for that in the exploratory stages. Better performance is necessary, however, in order to work with datasets that are five to six orders of magnitude larger. Improved performance supports qualitatively better results at smaller scales, as well: the improvements from this study should permit the application of Gaussian mixture modeling with much greater frequency, enabling systematic studies for both validation and application of the method. From performance profiling, our study identified two aspects of Garrity's method that are key to performance: data preparation, and the training of machine learning models.

Data preparation includes the formation of secondary data products, such as the normalized difference vegetation index (NDVI) and the green red vegetation index (GRVI), requiring a balance of file I/O, compute throughput, and query handling. As with many existing packages, Garrity's MATLAB implementation loaded the multispectral data directly from discrete Landsat scenes—GEOTIFF encoded image files stored on a local file system. Typical Landsat-derived products are linear combinations of multiple spectral bands; reading the data dominates the computational cost. These derivations are highly parallelizable, per-pixel operations: the time to perform them can be greatly reduced by assigning the work to more processing cores. More complex operations that require some form of normalization procedure can still be parallelized across multiple scenes, a feature not typically exploited by existing methods. Reading large datasets from disk thus benefits from careful handling that balances I/O with processing.

To address this balance, we explored ways in which to understand and optimize the cost of I/O. In order to provide a consistent basis to compare different I/O approaches we developed a reasonably complex yet typical processing pipeline. A data view spanning multiple tiles was defined and a pipeline consisting of pan--sharpening, NDVI and GRVI calculation and a Sobel convolution kernel was applied.

We implemented this pipeline with four data storage and query structures using the Geospatial Data Abstraction Library (GDAL) to convert the Landsat-provided TIF files into numerical arrays. The first approach used flat files, closely emulating Garrity's MATLAB implementation with the notable addition of a lookup table to index and map input coordinates to physical files. The second implementation pre-converted Landsat data to binary blobs and stored them in an SQL database, along with metadata on per-scene basis. While this provided rapid metadata querying, this approach suffered when considering regions smaller than a 1 GB Landsat scene (e.g. subsampling). The third implementation addressed the granularity mismatch by storing the data through Pytables, a hierarchical database for managing large datasets. Data were pre-processed and stored in structured arrays, metadata stored on a per-pixel basis, and scenes eliminated altogether. The final implementation stored the data as extendable nodes within an HDF5 container. The scenes were mosaicked into contiguous data structures and were stored based on source, temporal, and spectral groups.

The performance of these approaches is compared in Figure 1. As expected, the HDF version had the best performance. By defining the computational workspace as a node within the HDF5 container, the output of an analysis operation was seamlessly buffered to disk allowing single pass analysis at very large scales. The SQL implementation had the second best performance. Given SQL's more powerful metadata querying capabilities, SQL could prove more useful depending on the balance between data granularity and query complexity. The use of a structured array with per--pixel attributes in the Pytables approach required strided data slicing such that operations on non-trivial regions were slightly slower than the loading the entire tile, but could be powerful in the context of sparse metadata driven operations.

The HDF5 backend was performance tested on various hardware, including RAIDed mechanical drives, solid-state hard-drives, and a 10 GigE network-attached storage (NAS) system. In order to remove the computational bottleneck and to provide a means to scale beyond the trial dataset, parallelization via spatial subdivision was implemented: our backend subdivided the domain and applied multithreaded operations. Despite sublinear scaling with thread count (Figure 2), the work quickly became I/O bound using either mechanical or solid-state drives. By 48 cores, this implementation had effectively saturated the underlying NAS file system; at this point, we were able to process scenes two orders of magnitude faster than Garrity's implementation. Extrapolating this performance, we believe that it would be possible to perform typical vegetative index preparation for the whole of North America in a matter of minutes.

The unsupervised classification method developed by Garrity et al. provides a powerful tool for identifying disturbances in vegetation indices. RADD identifies regions of space (pixels, effectively) whose classification changes over time and in ways consistent with vegetation mortality. Classification works by matching each pixel of the satel-

lite image with a vector ("observation"), finding a model that represents that vector data, and then applying that model to assign a likelihood of each observation belonging to each class. In this approach, clusters represent the classes in the vector space. The vector spaces are derived from the multiple bands of satellite imagery; for example, Garrity used a two--dimensional space spanned by ΔNDVI and ΔGRVI is used, where each Δ refers to the difference between measurements at two points in time of the NDVI and the GRVI indices, respectively. Later, Garrity experimented with much higher dimensional spaces—as high as 24 dimensions.

Garrity's RADD method used Gaussian mixture models (GMM) to perform clustering. In GMM, the probability of a vector belonging to a cluster (class) is represented by a multivariate Gaussian function. Training a model entails fitting the centroid, weights, and variance matrix of each Gaussian to a subset of the observations. Once trained, the model is applied to compute the probability of a given vector, and its corresponding pixel, belonging to a cluster. Our profiling revealed that almost all of the compute time is spent in the first step, training. For example, in a case in which training the model took 1195 seconds, applying it took 2.8 seconds.

GMM's are trained using the Expectation-Maximization (E-M) method. In the expectation step, the conditional probability of observing the present model given each training observation is computed. In the maximization step, the model is evolved in a way that increases the log-likelihood of the problem. Together, this algorithm is guaranteed to converge (perhaps slowly) to a solution (perhaps not globally optimal).

We profiled MATLAB using up to 7 seconds per iteration of the E-M algorithm on the hardest problem Garrity attempted—a 24 dimensional, 11-cluster model using about 250,000 training vectors. During profiling, we observed MATLAB using as many as 9 cores: it was already parallelized. Our modeling indicated that the work involved about 1010 floating point operations on about 48 MB of data. With well-written code, a single core should complete this within a few seconds. Our analysis determined that most of the work in the E-M algorithm could be performed in parallel. Little communication would be required—primarily, a reduction over training observations needs to be performed in the M-step.

We wrote a C++ code that trains and applies GMM's. The code was carefully written to permit use of fast Single Instruction Multiple Data features. We enabled multiple cores by threading the code with OpenMP. To compare the performance of this code with the original, we used three different GMM problems that Garrity et al. had worked with. The model parameters vary sufficiently that the three problems, considered together, span the performance space. Figure 3 shows the performance of the code on these problems compared the original MATLAB: our C++ implementation was up to 60 times faster. Figure 4 shows the absolute performance of the C++ implementation as a function of thread count. The scaling is reasonable for an OpenMP code. The code has further performance headroom via distributed parallelism. As noted, the only communication costs are reductions during the M-step, and scalable methods for performing such reductions are well known. Thus, we expect that application of GMM can scale out indefinitely.

Our brief study demonstrated that it is computationally feasible to create a system for applying the regional techniques of RADD to data at the pan-tropics scale. However, almost all of the work to achieve that lies ahead of us. As we look ahead, the guiding principle we propose is to harness the power of high performance computing and large scale data handling in a way that remains tractable and productive to scientists who are not programming specialists. This entails creating a system that responds to the needs of its users while making it possible to ignore as much of the implementation detail as often as possible. In carrying out this project, we have already identified some of the primary needs. From a computer science perspective, these needs include the following: select data according to moderately complex user queries at varying granularity; transform data between vector bases; form Cartesian products of vector bases; support a small set of vector and matrix operations; perform maps and reductions; iterate all of the above; visualize, monitor, and control these processes; define, partition, and schedule work onto available resources. These needs point toward a combination of a compact domain-specific language, and a runtime environment in which that language can execute.

Toward the end of the project, we developed a simple demonstration of these ideas. Exploiting the well-developed Google Maps API, we created a prototype interface and processing framework (Figure 5). Using this interface, the user is able to select a region upon which they wish to perform some form of analysis and by clicking VegeDyne, the analysis is executed and the product rendered above the map. (In this case, GRVI was calculated). In order to abstract the parallelization a prototype domain specific language was developed such that users could simply define the arithmetic operation between spectral bands, without specifying any geographical information. In the example shown in Figure 5, the GRVI operation is defined in our DSL as a JSON page attribute—the procedure is not

hardcoded into the back end. This is one quick example of how a domain specific language and accompanying runtime can present ecologists access to a computationally powerful environment with a simple interface.

Impact on National Missions

As discussed above, climate warming is accelerating forest mortality, with the prospect of participating in large, positive feedbacks. The capability to quantify and monitor vegetation dynamics would fill a crucial gap in the effort to accurately predict future climate. The present work has elucidated the requirements for building a system for the systematic, large--scale study of climate impacts on through remote--sensing data. The avenues explored here for improving data treatment and data analysis, together with our initial explorations of usability and extensibility, form part of a foundation on which such a system can be built.

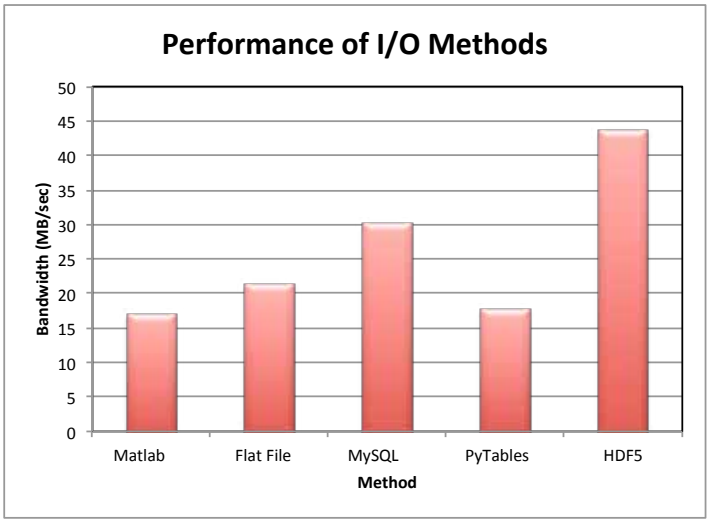

Figure 1. Comparing storage backend implementations with the reference Matlab implementation. As expected, the HDF5 implementation was the fastest. The MySQL implementation handled metadata queries better, but performance was hampered by inflexibility in data granularity.

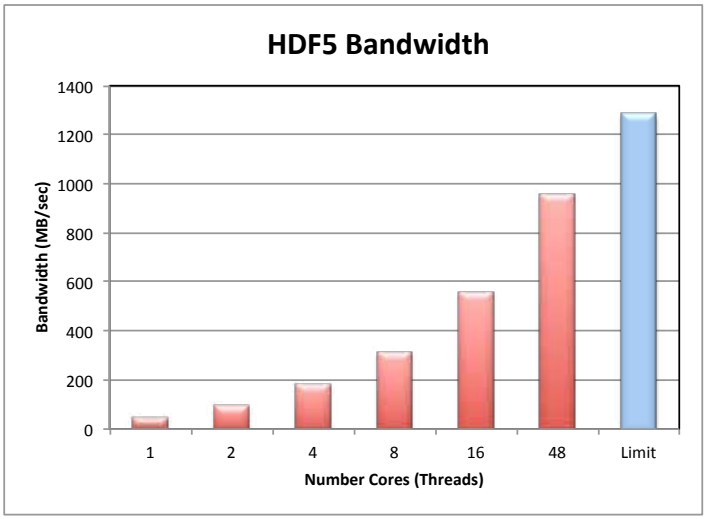

Figure 2. Total bandwidth as a function of the number of threads/cores for the HDF5 implementation. By 48 cores, performance approaches the hardware limit.

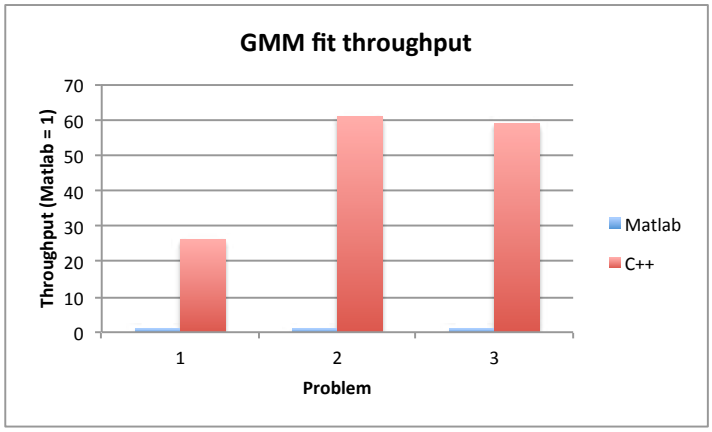

Figure 3. Throughput of the C++ Gaussian mixture model training code, normalized to the original MATLAB code, for three representative problems drawn from Garrity et al [10]. For the larger problems 2 and 3, performance is nearly 60 times faster on comparable hardware.

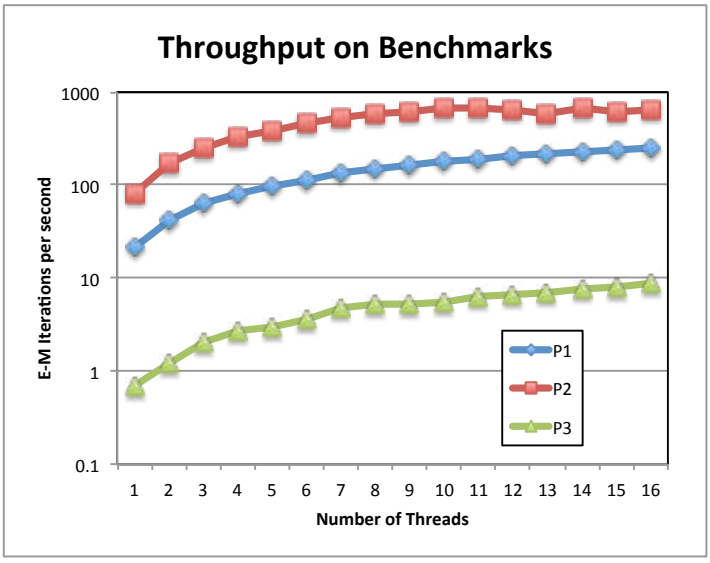

Figure 4. Absolute performance of the GMM training code, expressed as iterations per second. The code was threaded with OpenMP, and run up to 16 cores on a typical HPC cluster node. For the simplest problem, performance saturates at about 8 threads as absolute time approaches 1 millisecond per iteration. For the harder problems 2 and 3, performance increases up to 16 threads. These are reasonable results for OpenMP.

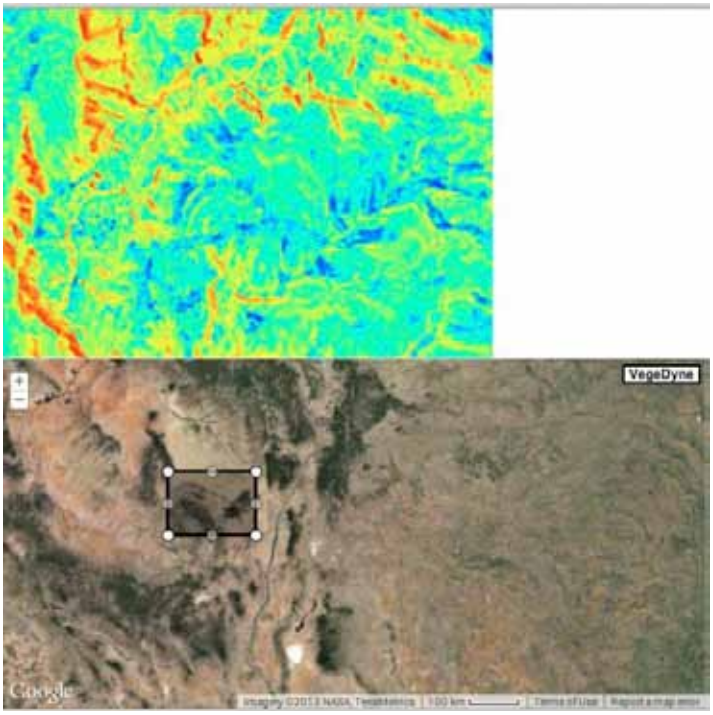

Figure 5. Screen capture from notional domain specific language.

Cyber Security of the Smart Grid

Russell W. Bent
20120752PRD2

Introduction

The national interest in a broad class of problems surrounding the cyber security of infrastructure systems is rapidly growing. Recent work has shown that it is possible for malicious entities to manipulate the data provided to control systems and cause operators to make bad decisions. To date, most research has focused on building better protection and/or detection schemes. This project focuses on the premise that malicious entities can gain access and developing techniques to mitigate the consequence of such access.

This project focuses on four directions to address these challenging information science questions: 1) Discovery, 2) Assessment, 3) Mitigation, and 4) Control. First, we will develop efficient algorithms for determining what combinations of control system sensors can be compromised without being detected by a security system. Second, we will develop metrics for assessing the possible consequences of a successful attack on the combinations discovered in 1). Third, we will develop strategies for combating the attacks, such as redundant sensor placement. Finally, we will develop new operations models that account for security concerns.

In order to solve these problems, we rely on interdisciplinary research at the intersection of power systems, operations, human factors, probability, networks, optimization, and control theory. The approaches will be tested on synthetic, academic benchmarks available in the open literature.

Benefit to National Security Missions

This project is directly connected to the Energy Security mission. Specifically, this project satisfies the mission's subtopic "Infrastructure reliability and security." As the demand for energy has grown in recent years, pressure has grown on critical infrastructure, in particular electric power grids, to operate more efficiently. This has led to a deployment of smart sensors and controls to achieve this goal. However, the deployment of these devices has made the power grid more vulnerable to malicious actors. A successful result on this project will allow for the satisfaction of the Energy Security Mission and ensure that nation's power systems are safe and reliable as instrumentation of the grid continues.

Second, there is strong connection to the information science mission as this proposal relies heavily on developing new advances in information science. In particular, this proposal relies on producing results in the fields of knowledge extraction, automated discovery, distributed computing, anomaly detection, and smart sensors, as outlined in the Information Science and Technology Grand Challenge.

Finally, this project is directly related to those federal organizations with missions related to cyber security including DOE, DHS, DOD, and NIST.

Progress

In FY13, the main task was the development of new approaches to mitigate the effect of data integrity attacks on power grids. To achieve this task there were three goals laid out to achieve 1) develop an optimization model for siting secure sensors to limit the consequence of data integrity attacks 2) develop a robust control scheme for responding to data integrity attacks and 3) produce a peer reviewed paper on the topic. Goals 1 and 3 have already been satisfied. For goal 1) Annarita Giani (the post doc funded by this project) developed an algorithm for determining the worst case consequence of a data integrity attack. Based on these consequences, a mixed-integer programming model was developed for optimal siting of mitigation devices to counter these attacks. Two types of siting models were developed. The first one determined the least number of mitigation devices required to counter all data integrity attacks of

concern. The second model determined the best locations to deploy a fixed set of mitigation devices so as to minimize the amount of unmitigated consequence. Goal 2 was satisfied in June 2013 with the submission of the paper entitled "Phasor Measurement Unit Placement for Unobservable Attack Detection" by Giani, Bent, Pan, and Poolla to the journal IEEE Transactions on Smart Grids.

This research was also the subject of an earlier workshop paper, "Addressing Smart Grid Cyber Security" by Giani and Bent. It was published in the proceedings of 8th Annual Cyber Secruity and Information Intelligence Research Workshop in Jan. 2013. This research has resulted in requests for invited talks by Annarita at Honeywell and United Technologies. Annarita was also asked to chair the 1st International Symposium on Resilient Cyber Systems to be held in August 2013 because of her contributions to the field. Research into Goal 2 is on track, and satisfaction of that goal is expected at the end of FY13.

Future Work

In FY14, the project will focus research efforts on the final task described in the proposal. Specifically, the main task of FY14 is the development of the science to understand physical consequence and cascading impacts from data integrity attacks. To achieve this task there are three goals we plan to achieve 1) develop a bi-level optimization model of physical consequences 2) develop a model of cascading impacts and 3) produce a peer reviewed paper on the topic.

Conclusion

This project is driven by emerging technologies in grid sensor and control devices and accordingly specifies the technical challenges in securing systems operated by these devices. We focus on a set of problems where we have well-developed Information Science & Technology (IS&T) capabilities, develop an end-to-end security assessment of cyber-physical systems, and thus make a significant impact. The new IS&T and energy security challenges require advances in applied math, algorithms, and system theory.

Publications

Crespi, V., G. Cybenko, and A. Giani. Attacking and Defending Behavioral Anomaly Detection Methods. 2013. IEEE Journal of Selected Topics in Signal Processing. 7 (1): .

Garcia, M., A. Giani, and K. Poolla. Uncertainty Quantification for Fast State Estimation. To appear in 52nd IEEE Conference on Decision and Control, CDC 2013. (Florence, Italy, December 10-13, 2013).

Giani, A., E. Bitar, M. Garcia, M. McQueen, P. Khargonekar, and K. Poolla. Smart Grid Data Integrity Attacks. 2013. IEEE Transaction on Smart Grid. 4 (3): 1244.

Giani, A., O. Linda, M. Manic, and M. McQueen. Known Secure Sensor Measurements Concept and Its Application for Critical Infrastructure Systems. 2013. In Systems and Optimization Aspects of Smart Grid Challenges. Edited by Marco, S., M. Carvalho, P. Pappu, and S. Vijay. Vol. IV, p. . New York: Springer.

Giani, A., R. Bent, F. Pan, and K. Poolla. Phasor Measurement Unit Placement for Unobservable Attack Detection. IEEE Transaction of Smart Grid.

Giani, A., R. Bent, M. Hinrichs, M. McQueen, and K. Poolla. Metrics for Assessment of Smart Grid Data Integrity Attacks. 2012. In 2012 Power And Energy Systems General Meeting. (San Diego, CA, July 2012). , p. 1. : IEEE.

Giani, A., and R. Bent. Challenges in Smart Grid Cyber Security. 2013. In 8th Annual Cyber Security and Information Intelligence Research Workshop. (Oak Rodge, TN, Jan. 2013). , p. 1. Oak Ridge, TM: ACM.

Linda, O., A. Giani, M. Manic, and M. McQueen. Multi-Criteria Based Staging of Optimal PMU Placement Using Fuzzy Weighted Average. 2012. to be submitted to 2013 Power And Energy Systems General Meeting.

Linda, O., A. Giani, M. Manic, and M. McQueen. Multi-Criteria Based Staging of Optimal PMU Placement Using Fuzzy Weighted Average. 2013. In 22nd IEEE International Symposium on Industrial Electronics. (Taipei, Taiwan, 28 May - 31 May 2013). , p. 1. Taipei, Taiwan: IEEE.

Wolpert, D., T. Bhattacharya, R. Bent, J. Neil, A. Kent, and A. Giani. Event-driven non-cooperative games. 2013. Los Alamos National Laboratory, LA-UR-13-22238.

Edge Traffic Monitoring in Computer Networks

Joshua C. Neil
20120767PRD3

Introduction

This research will simultaneously enhance two fields of interest to the laboratory and the nation as a whole. First, the work will result in improved computer network defense capability. The approach is to model edges (communications between pairs of computers in a network) using sophisticated statistical models. This edge modeling strategy will be combined with the PathScan methodology to serve as the basis for network monitoring at LANL. PathScan was developed at LANL, as part of the Network Scale Analysis and Defense for Cyber Systems LDRD, and has proven effective in detecting the lateral movement of hackers within the yellow network. While the base system is implemented, the improvements to the edge models as part of this project will significantly advance this important network security tool. This will benefit both LANL and other government and industry organizations seeking to better their network surveillance systems.

Second, the methods being researched have novel aspects in the field of statistical modeling. The technical challenges we face are also common to many other statistical applications (e.g., social, power grid, sensor networks, financial modeling, etc.) making this work potentially valuable across many disciplines.

Benefit to National Security Missions

This work is focused on cyber security. As such, it has broad relevance to many programs and agencies. The work has already attracted interest at other NNSA labs, as well as members of DOD and the intelligence community. Many of the categories marked A above were marked that way since they involve sensitive data which this project aims to protect through enhanced cyber security. Therefore, this work is relevant to the following missions: Nuclear Security and National Defense and Scientific Discovery and Innovation.

Progress

Criminal cyber activity is continously increasing. News media contain daily reports of government and corporate networks being compromised and valuable data being extracted. Detecting these attacks is clearly important. This project concerns anomaly based approaches to detecting such intrusions.

Anomaly based detection utilizes baseline models to identify abnormal activity. Motivating our approach is that compromised machines will typically share commonality in their anomalous activity, and leveraging this can increase the chance of detecting network intrusions, at the same time reducing the false alarms commonly associated with anomaly based intrusion detection.
So far, this project has considered two types of commonality across the compromised machines. The first is commonality in location, resulting in network localized anomalies. These come about when the compromised machines communicate over the network, such as when an attacker moves between machines in the network, or when multiple attackers are targeting the same set of computers. The second type concerns commonality in features, resulting in what we call host-similarity anomalies. These are motivated by the fact that compromised machines are likely to share a large number of characteristics, such as being recipients of the same phishing email, communicating with the same internet server from which the attack is orchestrated, sharing signs of the same malware being run on the computers, etc.

The project has developed two approaches to detecting network local anomalies. In the first, anomaly detection is viewed as a statisticial hypothesis testing problem. Each computer, and possibly each between computer communication, is associated with a hypothesis to be tested, for example: The computer is acting normally, versus The computer is acting abnormally. When viewed in relation to the network traffic, these computer-level hypotheses form a graphically struc-

tured hypothesis testing problem, where task is to decide between: The network is not under attack; versus: The network is under attack. By formulating models for how various attacks will perturb the data under attack, the approach allows for the construction of optimal tests for detecting network intrusions. Novel, and computationally efficient approaches for evaluating this overall hypothesis are developed.

In the second approach to detecting network local anomalies, a method based on scan-statistics for graphs is developed. In spatial data, a scan statistic is an anomaly score assigned to a local region in space, for instance for detecting local disease outbreaks. However, extending this idea to computer networks requires a notion of distance between computers. While the data can be viewed as producing a graph structure, the classical measure of graph distance does not work when applied to computer networks. The reason being the presence of highly connected servers, making most computers a most two or three network communications apart. To deal with this issue, we define locality based on proximity measures for graphically structured data. The approach is applied to a real network intrusion at LANL, clearly identifying the attack and uncovering interesting attack patterns.

Currently, work is in progress on identifying network intrusions via host-similarity anomalies. Much of the data logged concerning computers on a network is categorical, with a large and evolving pool of categories. Examples are visits to new web-pages, or new programs starting up on the machines. Individually, this new activity is typically not indicative of malicious activity, however, compromised machines are likely to have an unusually large number of such features in common. To utilize this we have developed an approach for scoring the commonality of computers based on their newly appearing features. These scores are then used to evaluate whether a given cluster of machines have an unexpectedly high degree of similarity, an evaluation which is then combined with computer-level anomaly scores to assess the overall indication of attack.

Future Work

In the coming year, investigations into multiple, isolated nodes who share common internet behavior will be investigated. Methods for detecting when this behavior indicates compromise or pending compromise will be developed, along with models for normal behavior, in order to detect statistically significant deviation.

Conclusion

Results include highly improved sensitivity to malicious activity within computer networks, through the use of advanced statistical models. These models will be entirely novel, and thus will also contribute to the general field of stochastic modeling technology.

Mixing and Diffusion in Granular Flows

Eli Ben-Naim
20130792PRD2

Introduction

This project aims to understand the complexity of force-carrying contacts in a granular medium, which can often lead to its destabilization (due to external forcing) along unexpected fault lines, as commonly observed in geophysical situations including earthquakes, mudslides, and avalanches. The approach will be twofold. First, a model of how granular materials flows will be developed for the types of conditions encountered in geophysical processes.

This is a high-potential scientific problem because, in over three decades of research, this most basic question regarding granular materials remains unsettled. Second, the force-chain network structure of granular materials will be obtained from model experiments, being conducted at Los Alamos, of a granular medium between sheared plates responding to the stimulus of their relative motion. The mathematical techniques of network analysis will be used to better understand the dynamic behavior of the medium under such loads.

This is a cutting-edge endeavor because few such laboratory scale experiments and analysis have been carried out previously. Additionally, new algorithms for simulating universal emergent behaviors (clustering, ordering, topology) arising from the interplay between discontinuous granular mixing dynamics and microscopic physics will be developed as part of this project. This is a high-risk undertaking because scaling dynamics of granular materials in geophysical situations to laboratory scale experiments has yet to be demonstrated. Success in the project would imply the ability to extend the scaling concepts that have been so successful in fluid dynamics and aerodynamics to a new area: solid mechanics.

Benefit to National Security Missions

Granular materials are ubiquitous and are found in a host of applied programs. Understanding mixing and flow of granular materials hence has impacts on many applied programs. This project aims at the development of a modeling and simulation capability for describing mixing and flow of granular materials. The ability to better model mixing of granular matter will impact energy applications such as storage and transportation of materials used in energy applications including coal and biofuels. Granular materials tend to segregate according to size, a property that can be an obstacle in manufacturing and transportation processes. This project addresses precisely mixing characteristics of granular materials and could lead to the design of optimized container design for improved mixing and more efficient transportation. The capabilities developed in this project will also be relevant for other DOE programs and needs including waste storage, waste handling and transportation, high explosives, and handling of materials produced in powder form.

Progress

This project is slated to start July 1, 2013. As such, no progress has been made to date.

Future Work

First, we will test the granular flow model of Jop et al. (Nature, 2006) against the experiments, being conducted at Los Alamos, of a sheared granular medium confined between two moving plates. We will determine the extent of applicability of this model, and we will establish the corrections that might be needed to capture the observations. Second, we will analyze the force-chain structure in this granular medium using techniques from network theory. In particular, we will aim to characterize the network structure and determine basic patterns and laws from the experiments. Our theoretical analysis will be compared with results of experiments on force chains in photoelastic granular materials.

Our theoretical models will be compared to empirical

laws and relations from geophysics, in order to establish the applicability of the model laboratory experiments to real-world geophysical granular flows.

Conclusion

The outcome of the first part of this work will be improved prediction of rare and destructive seismic events, which have significant implications for society at large. The outcome of the second part of this work will be improved understanding of how localized processes affect structure formation, which can lead to better prediction of dynamics as diverse as percolation in porous medium and spread of infections on networks.

Publications

Christov, I., R. Lupetow , J. Ottino , and R. turman . A Study in Three-Dimensional Chaotic Dynamics: Granular Flow and Transport in a Bi-Axial Spherical Tumbler. To appear in SIAM Journal on Applied Dynamical Systems.

Christov, I., and H. Stone. Shear dispersion in dense granular flows. Granular Matter.

Physics

TeV Jets: Nature's Particle Accelerators

Brenda L. Dingus
20120011DR

Introduction

Nature accelerates particles to energies exceeding 10 Joules—nearly a billion times higher than terrestrial accelerators—yet we do not know the origin of these particles or the mechanisms that produce them. The particles are produced outside our galaxy and they arrive at Earth from random directions due to their electrical charge and the long distances traveled through magnetic fields between galaxies and within our galaxy. However, these particles produce TeV gamma rays within their sources and these gamma rays travel straight to Earth to provide the most direct information about the physical mechanisms in these accelerators. The known extragalactic TeV gamma-ray sources are produced by jets of plasma accelerated to relativistic velocities and many exhibit rapid variability. The most advanced models of these jets suggest that magnetic fields play a critical role in extracting the gravitational energy from the black hole and accelerating particles to extreme energies. With this project, we will combine and extend LANL's observational, theoretical, and computational capabilities to study these extreme sources that test our under-standing of high-energy particle and plasma physics in an environment irreproducible on Earth.

New tools are required to understand Nature's highest energy particle accelerators. We propose to make new TeV gamma-ray observations to determine the properties of TeV jets and to make new models of the physical mechanisms occurring in TeV jets to compare with the observations.

Benefit to National Security Missions

Understanding cosmic accelerators is a major challenge in high-energy particle physics and plasma astrophysics, and gamma-ray observations provide some of the strongest constraints. The acceleration of cosmic particles is listed as one of the 11 key science questions in the National Academy of Sciences 2006 report "From Quarks to the Cosmos" and is further emphasized in the Astro2010 Decadal Survey in Astronomy and Astrophysics. This work is closely tied to the High Energy Physics program of the DOE Office of Science. In addition, the proposed work builds LANL's scientific capabilities in computational astrophysics, cosmology and time-domain astronomy. This project contributes strongly to NNSA national security programs by utilizing the state of the art simulation tools and tests petascale computing codes that could have major influences on the future of the ASC program.

Progress

The observational effort of this project has made great progress in this past year. The 300 photomultiplier tubes (PMTs) were delivered at the end of last fiscal year. Over 200 have been prepared with bases soldered and water proof encapsulation attached. Each of these 200 PMTs has been tested at multiple high voltages with light levels ranging from 0.1 to greater than 10,000 photoelectrons and an operating voltage selected. These 200 PMTs have been shipped to Mexico and almost 100 are installed in water Cherenkov detectors at the HAWC site. The installed PMTs are recording pulses at the expected rates and with the expected time resolution.

In addition, we have further developed the data acquisition system to handle these high rates so that all photoelectrons are recorded and then a software trigger is applied to find timing correlations associated with a gamma-ray event. When all 300 PMTs are installed, we will need to record 500 MB/sec. We are currently recording 151 MB/sec with 4 independent data systems. The final system will have 10 independent systems and we have performed tests with simulated data streams that confirm the 500 MB/sec is reasonable.

The other major part of the experimental effort is the incorporation of these PMTs into the reconstruction and analysis. This is proceeding well. We have detected the shadow of the moon made by cosmic rays and confirmed

our angular resolution. We are also studying a recent gamma-ray flare of the active galactic nuclei Mrk 421.

On the theoretical side of the project, we have performed many large-scale 3 dimensional special relativistic magnetohydrodynamic (MHD) simulations of jet formation and propagation. We have discovered that highly collimated magnetic structures can be formed from magnetic energy injection, demonstrating that Poynting dominated regime is essential for jet collimation. Furthermore, we found that the jet is subject to strong non-axisymmetric current-driven instabilities (CDI) which lead to substantial dissipation and jet speed is reduced. However, even with the presence of instabilities, the jet is not disrupted and will continue to propagate to large distances. We have analyzed the jet properties and shown that a substantial amount of magnetic energy has been transformed into kinetic energy. These 3-D MHD simulations have motivated kinetic energy dissipation studies that are being carried out in other parts of this project.

Specifically we have performed a series of fully kinetic simulations to study both the formation and dissipation dynamics of thin current sheets. Large-scale 3D simulations starting with a force-free current layer have revealed a number of new insights into the kinetic-scale dynamics of magnetic reconnection. In addition, we have discovered a new scaling for regimes with extremely strong magnetic fields, which predicts the dissipation rate may be slower than previously thought. To study the detailed acceleration mechanisms, we have implemented a particle tracking capability into our simulation code. Finally, we have started to perform a new type of 3D simulation initialized with a uniform plasma and finite amplitude Alfven waves, which interact nonlinearly and generate turbulence. One key feature is the spontaneous formation of kinetic-scale current sheets, which may be unstable to reconnection and thus give rise to a multitude of acceleration sites embedded in the turbulence. These new efforts may provide an important link between the kinetic and large-scale MHD studies, which also see evidence for these structures.

Future Work

This project has both an observational and a theoretical component. The observational work requires the construction of new hardware for detecting astrophysical sources of high energy gamma rays, and the theoretical work involves new computational modeling of the physics of particle acceleration and propagation in these gamma-ray sources.

In the next year, the new hardware procured by this project will be installed in the High Altitude Water Cherenkov (HAWC) observatory to lower its energy threshold and thus enable new observations of astrophysical particle accelerators. Continuous operations with 1/3 of the detector begin in August 2013 and the full detector will be operational by August 2014. With only one third of the detector, this observatory will be more than twice as sensitive as previous wide field of view, gamma-ray observatories and searches will begin for new sources as well as new flares of known sources. We will continue to develop the analysis tools to improve the background rejection and detect extragalactic sources. We are also creating collaborations to perform contemporaneous observations at multiple wavelengths that will be triggered by HAWC detections of flares.

Next year the theoretical modeling will also advance. We will continue with 3D MHD jet simulations and explore further the current driven instabilities and their impact on energy dissipation. These studies will yield important constraints on the rate of energy conversation from magnetic field to particles and the timescale of sudden events, both of which are being observed by TeV observatories, including HAWC. In addition, we have started the modeling of high energy radiation spectra using our 3-D MHD simulation results as inputs. This will eventually allow us to make comparison with multi-wavelength observations.

Conclusion

We will build an observatory to study the gamma-ray emission from transient extragalactic sources, such as black holes of mass exceeding a billion times our Sun's that eject plasmas in collimated jets. We also develop new computational tools on petascale computers to simulate the variability of the energy flowing in these jets and the mechanisms by which this energy can be used to efficiently accelerate particles. The observations will be compared to the output of the simulations to determine how Nature accelerates particles to energies that exceed those of man-made accelerators by factors of over many millions.

Publications

Abdo, A. A., A. U. Abeysekara, B. T. Allen, T. Aune, D. Berley, C. Chen, G. E. Christopher, T. DeYoung, B. L. Dingus, R. W. Ellsworth, M. M. Gonzalez, J. A. Goodman, J. Granot, E. Hays, C. M. Hoffman, P. H. Huntemeyer, B. E. Kolterman, J. T. Linnemann, J. E. McEnery, A. I. Mincer, T. Morgan, P. Nemethy, J. Pretz, E. Ramirez-Ruiz, J. M. Ryan, P. M. S. Parkinson, A. Shoup, G. Sinnis, A. J. Smith, V. Vasileiou, G. P. Walker, D. A. Williams, and G. B. Yodh. CONSTRAINTS ON THE EMISSION MODEL OF THE "NAKED-EYE BURST" GRB 080319B. 2012. ASTROPHYSICAL JOURNAL LETTERS. 753 (2): -.

Abdo, A. A., B. T. Allen, R. Atkins, T. Aune, W. Benbow, D. Berley, E. Blaufuss, E. Bonamente, J. Bussons, C. Chen, G. E. Christopher, D. G. Coyne, T. DeYoung, B. L. Dingus, D. E. Dorfan, R. W. Ellsworth, A. Falcone, L. Fleysher,

R. Fleysher, J. Galbraith-Frew, M. M. Gonzalez, J. A. Goodman, T. J. Haines, E. Hays, C. M. Hoffman, P. H. Huntemeyer, L. A. Kelley, B. E. Kolterman, C. P. Lansdell, J. T. Linnemann, J. McCullough, J. E. McEnery, T. Morgan, A. I. Mincer, M. F. Morales, P. Nemethy, D. Noyes, J. Pretz, J. M. Ryan, F. W. Samuelson, P. M. S. Parkinson, A. Shoup, G. Sinnis, A. J. Smith, G. W. Sullivan, V. Vasileiou, G. P. Walker, M. Wascko, D. A. Williams, S. Westerhoff, and G. B. Yodh. OBSERVATION AND SPECTRAL MEASUREMENTS OF THE CRAB NEBULA WITH MILAGRO. 2012. ASTROPHYSICAL JOURNAL. 750 (1): -.

Abdo, A. A., U. Abeysekara, B. T. Allen, T. Aune, D. Berley, E. Bonamente, G. E. Christopher, T. DeYoung, B. L. Dingus, R. W. Ellsworth, J. G. Galbraith-Frew, M. M. Gonzalez, J. A. Goodman, C. M. Hoffman, P. H. Huntemeyer, C. M. Hui, B. E. Kolterman, J. T. Linnemann, J. E. McEnery, A. I. Mincer, T. Morgan, P. Nemethy, J. Pretz, J. M. Ryan, P. M. S. Parkinson, A. Shoup, G. Sinnis, A. J. Smith, V. Vasileiou, G. P. Walker, D. A. Williams, and B. Yodh. SPECTRUM AND MORPHOLOGY OF THE TWO BRIGHTEST MILAGRO SOURCES IN THE CYGNUS REGION: MGRO J2019+37 AND MGRO J2031+41. 2012. ASTROPHYSICAL JOURNAL. 753 (2): -.

Abeysekara, A. U., J. A. Aguilar, S. Aguilar, R. Alfaro, E. Almaraz, C. Alvarez, J. D. Alvarez-Romero, M. Alvarez, R. Arceo, J. C. Arteaga-Velazquez, C. Badillo, A. Barber, B. M. Baughman, N. Bautista-Elivar, E. Belmont, E. Benitez, S. Y. BenZvi, D. Berley, A. Bernal, E. Bonamente, J. Braun, R. Caballero-Lopez, I. Cabrera, A. Carraminana, L. Carrasco, M. Castillo, L. Chambers, R. Conde, P. Condreay, U. Cotti, J. Cotzomi, J. C. D'Olivo, E. de la Fuente, C. De Leon, S. Delay, D. Delepine, T. DeYoung, L. Diaz, L. Diaz-Cruz, B. L. Dingus, M. A. Duvernois, D. Edmunds, R. W. Ellsworth, B. Fick, D. W. Florino, A. Flandes, N. I. Fraija, A. Galindo, J. L. Garcia-Luna, G. Garcia-Torales, F. Garfias, L. X. Gonzalez, M. M. Gonzalez, J. A. Goodman, V. Grabski, M. Gussert, C. Guzman-Ceron, Z. Hampel-Arias, T. Harris, E. Hays, L. Hernandez-Cervantes, P. H. Huntemeyer, A. Imran, A. Iriarte, J. J. Jimenez, P. Karn, N. Kelley-Hoskins, D. Kieda, R. Langarica, A. Lara, R. Lauer, W. H. Lee, E. C. Linares, J. T. Linnemann, M. Longo, R. Luna-Garcia, H. Martinez, J. Martinez, L. A. Martinez, O. Martinez, J. Martinez-Castro, M. Martos, J. Matthews, J. E. McEnery, G. Medina-Tanco, J. E. Mendoza-Torres, P. A. Miranda-Romagnoli, T. Montaruli, E. Moreno, M. Mostafa, M. Napsuciale, J. Nava, L. Nellen, M. Newbold, R. Noriega-Papaqui, T. Oceguera-Becerra, A. O. Tapia, V. Orozco, V. Perez, E. G. Perez-Perez, J. S. Perkins, J. Pretz, C. Ramirez, I. Ramirez, D. Rebello, A. Renteria, J. Reyes, D. Rosa-Gonzalez, A. Rosado, J. M. Ryan, J. R. Sacahui, H. Salazar, F. Salesa, A. Sandoval, E. Santos, M. Schneider, A. Shoup, S. Silich, G. Sinnis, A. J. Smith, K. Sparks, W. Springer, F. Suarez, N. Suarez, I. Taboada, A. F. Tellez, G. Tenorio-Tagle, A. Tepe, P. A. Toale, K. Tollefson, I. Torres, T. N. Ukwatta, J. Valdes-Galicia, P. Vanegas, V. Vasileiou, O. Vazquez, X. Vazquez, L. Villasenor, W. Wall, J. S. Walters, D. Warner, S. Westerhoff, I. G. Wisher, J. Wood, G. B. Yodh, D. Zaborov, and A. Zepeda. On the sensitivity of the HAWC observatory to gamma-ray bursts. 2012. ASTROPARTICLE PHYSICS. 35 (10): 641.

Aluie, H., Shengtai Li, and Hui Li. Conservative Cascade of Kinetic Energy in Compressible Turbulence. 2012. Astrophysical Journal, Letters. 751 (2): L29 (6 pp.).

Beresnyak, A., H. Xu, H. Li, and R. Schlickeiser. MHD Turbulence and Cosmic Ray Reacceleration in Galaxy Clusters. 2013. Astrophysical Journal. 771: 131.

Govoni, F., M. Murgia, H. Xu, H. Li, M. L. Norman, L. Feretti, G. Giovannini, and V. Vacca. Polarization of cluster radio halos with upcoming radio interferometers. 2013. ASTRONOMY & ASTROPHYSICS. 554: -.

Guan, X., H. Li, and S. Li. Relativistic MHD Simulations of Poynting Flux-Driven Jets. Astrophysical Journal.

Liu, Y. H., W. Daughton, H. Li, H. Karamabadi, and V. Roytershteyn. Bifurcated Structure of the Electron Diffusion Region in Three-Dimensional Magnetic Reconnection. 2013. Phys. Rev. Lett.. 110: 265004.

Liu, Y. H., W. Duaghton, H. Li, H. Karimabadi, and S. P. Gary. Do Dispersive Waves Play a Role in Collisionless Magnetic Reconnection?. Phys. Rev. Lett..

Si, J., S. A. Colgate, H. Li, J. Martinic, and D. Westpfahl. Data Acquisition in a High-Speed Rotating Frame for New Mexico Institute of Mining and Technology Liquid Sodium αω dynamo experiment. To appear in Review of Scientific Instruments.

Skillman, S., H. Xu, E. Hallman, B. O'Shea, J. Burns, H. Li, D. Collins, and M. Norman. Cosmological MHD Simulations of Galaxy Cluster Radio Relics: Insights and Warnings for Observations. 2013. Astrophysical Journal. 765: 765.

Xu, H., F. Govoni, M. Murgia, H. Li, D. Collins, M. Norman, and R. Cen. Evolution and Comparisons of Cosmological MHD Galaxy Cluster Simulations to Radio Observations. 2012. Astrophysical Journal. 759: 40.

IMPACT: Integrated Modeling of Perturbations in Atmospheres for Conjunction Tracking - A New Orbital Dynamics and Drag Model to Avoid Collisions in Space

Alexei V. Klimenko
20120036DR

Introduction

The goal of this project is to develop a new orbital dynamics and atmospheric drag model with accurate quantification of uncertainty. Objects in LEO (Low Earth Orbit) experience drag due to atmospheric friction, which makes it hard to predict their future paths. Current atmospheric density models used for orbital dynamics are all finely tuned to long-term averages. They show good statistical agreement with densities derived from actual spacecraft data during quiet times, but when the upper atmosphere starts changing, all bets are off. The models do not help use understand the physics going on in the upper atmosphere. Furthermore, orbital drag is averaged over a whole orbital period not accounting for local density variations, say from one side of the Earth to another. Current density model errors can lead to prediction errors of kilometers within a very short time. Our goal is to develop a new physics-based atmospheric density model by focusing on accurately describing the energy deposition and cooling during space weather events and updating this model to better account for observed changes in satellite tracks. This approach will enable us to answer important physics questions regarding the coupling between space weather, upper atmospheric density, and orbital drag.

Benefit to National Security Missions

Space Situational Awareness (SSA) is one of the core missions of Los Alamos as outlined in the Strategic Investment Plan. SSA is essential to ensuring stability in space and sustainability of our space activities and we will directly address this particular need with rigorous science and innovative technology. Our results will let SSA evolve from today's forensic operational mode to a predictive mode and transform it so that we will receive advanced warnings of possible collisions instead of being forced to investigate the cause in the aftermath (see Iridium-Cosmos collision). Specifically, our project is striving to advance the ability to monitor and track space objects by creating a new atmospheric drag model. This will allow us to provide accurate collision probabilities for avoidance maneuvers and the ability to track space objects during geomagnetic storms as well as better satellite lifetime and reentry estimates. Nuclear non-proliferation depends heavily on satellite observations. In addition, we will build underlying capability for understanding weapons effects on the upper atmosphere, with relevance to DP programs.

Progress

Density modeling and data assimilation with GITM

We have completed the data assimilation integration with the GITM model and have tested the sensitivity of model output to the model drivers. Currently the model is still using the solar radio flux parameter F10.7 as input but will upgrade the parameter input to EUV flux and assess the coupling function of EUV and heating/loss processes in the upper neutral atmosphere.

In parallel to the physics-based atmospheric density modeling, we are also exploring a non-linear regression type approach. We have tested a support-vector machine algorithm and found promising first results. We used solar wind and geomagnetic indices as input and are working on developing a predictive tool and comparing the results to the measured atmospheric densities from CHAMP and GRACE satellites.

Drag coefficient modeling

The use of fixed drag coefficients to infer atmospheric mass densities from the orbital decay of satellites has resulted in extensive biases in empirical atmospheric models. Physical drag coefficients can help reduce these biases by accurately modeling the interaction of gas particles with a satellite surface. We are using the NASA provided DAC code and our own test particle Monte Carlo code that are both validated with closed-form solutions for the drag coefficient in free molecular flow for simple geometries. Both the test particle Monte Carlo (TPMC) and the Direct Simulation Monte Carlo (DSMC) methods

accurately account for the changes in the incident velocity distribution function due to multiple reflections with the satellite surface. We have studied the sensitivity of the drag coefficient and orbit propagation due to changes in the atmospheric density, chemical composition, and temperature.

Observations
A problem at tube manufacturer for the camera has caused a significant delay in the procurement process. The tube has finally arrived (after a 1 year delay) and the camera team is currently testing the device and finishing the assembly of the camera. In the meantime, we have used a camera on loan to us and performed several observational campaigns. The data processing pipeline is now complete including detailed documentation. The camera and processing pipeline have been tested and validated against know objects with precision ephemeris including WAAS satellites. The accuracy of the camera has been quantified and data has been delivered to our collaborators at AFRL for testing and validation.

Collisions Statistics and UQ
We have completed the development and testing of full Monte Carlo modeling and importance sampling for collisional probabilities. The UQ framework improves on previous methods that focus on instantaneous collision probabilities based on Gaussian state assumptions. The new framework considers the distribution of the entire tracks for any pair of objects. The distribution for the relative distance between two objects over a fixed period of time is approximated with a distribution for functions. This approximation accounts for non-Gaussian state estimates and predictions from an orbital propagator. We have tested and validated the importance sampling method and studied the effect of atmospheric density model assumption on the collision probability.

Atmospheric Density Reconstruction using Satellite Orbit Tomography
We have developed a new method of estimating density using a tomography-based approach, inspired by X-ray computed tomography from the medical imaging field. The change in specific mechanical energy of the orbit is used as the measurement, which is related to the integrated density over the orbit. Using several such measurements from a number of satellites, one can estimate the density scale factor (i.e. a correction to an assumed density model).

Integration to End-to-End Model (E2E)
We have been working towards a first end-to-end model that incorporates all aspects of the IMPACT project. The integrated model will let us assess the uncertainty contribution of observations, density models, orbit propagation, drag coefficient, etc. It employs a light-weight service oriented architecture which lets the user enter and select parameters such time window, density model selections, subset of the satellite catalog. Data is then being processed on a high-performance computer and results are sent back to the browser.

Future Work

Observations
Before the end of this FY, we will have a fully automated data pipeline in place. More of our data will be delivered to our AFRL Kirtland collaborators for evaluation. In the coming FY, we will complete the dedicated IMPACT camera and continue the series of observational campaigns.

Density modeling and data assimilation with GITM
We will establish fine-tuning of solar/solar wind drivers of the GITM model to get a better forecast of neutral densities at high altitudes. We will include more appropriate EUV forecasting model replacing the F10.7 radio flux.

Collisional Probability and UQ
We will complete the uncertainty quantification of all modules in the integrated code. We will submit a paper on the collisional probabilities based on atmospheric densities with the GITM model.

Integration
We will complete the integration of our work into one single end-to-end model. This model will allow us to calculate collision probabilities using our physics-based atmospheric density model.

Technology Demonstrations
We will present our end-to-end model to potential stakeholders to validate mission relevance.

Conclusion

The results from this project will revolutionize the physical understanding of the upper atmosphere. We will build a new physics-based atmospheric density model that is tightly coupled to changing solar flux and space weather conditions. Our new physics-based atmospheric density model will describe the thermospheric response to energy input, recirculation, and cooling. By feeding back information from satellite tracking, it will provide both atmospheric density and relative velocity for orbital drag calculations. Results from our project will have a clear technical impact on understanding the upper atmosphere and transform the techniques of calculating drag and collision probabilities.

Publications

Elvidge, S., H. Godinez, M. Angling, and J. Koller. Improved

Mmodelling of Upper Atmospheric Densities Using Multi-model Ensembles. To appear in 3rd IMA Conference on Mathematics in Defence. (Malvern, UK, Oct 2013).

Godinez, H. C., B. Nadiga, A. Ridley, J. Koller, E. Lawrence, and D. Higdon. Atmospheric Density Specification with the Global Ionosphere-Thermosphere Model (GITM) using the Ensemble Kalman Filter. 2012. : 2012.

Godinez, H. C., J. Koller, and A. J. Ridley. Ensemble Data Assimilation for the Global Ionosphere-Thermosphe Model (GITM). 2013. J. Geophys. Res.. : in preparation.

Kelecy, T., M. Shoemaker, and M. Jah. Application of the Constrained Admissible Region Multiple Hypothesis Filter (CAR-MHF) to Initial Orbit Determination (IOD) of a Break-up. To appear in 6th European Conference on Space Debris. (Darmstadt, Germany, April 2013).

Klimenko, A., D. Palmer, D. Thompson, R. Linares, and E. Rabin. SSA Data Analysis Framework 1 Introduction 2 Fenton Hill Observatory Setup Overview 3 Input Data 4 Telescope Pointing. 2013. LANL Reports LACP-13-00008.

Lawrence, E., and D. Higdon. An Importance Sampling Method for Computing Collision Probabilities. 2013. Journal of Spacecraft and Rockets. : in preparation.

Linares, R.. Angles-Only Orbit Determination For Electro-Optical Sensors. 2012. SWX Reports.

Linares, R., J. L. Crassidis, C. Wetterer, K. A. Hill, and M. K. Jah. Astrometric and Photometric Data Fusion for Mass and Surface Material Estimation using Refined Bidirectional Reflectance Distribution Functions-Solar Radiation Pressure Model. To appear in Air Force Maui Optical and Supercomputing Site Conference. (Maui, HI, September 2013).

Linares, R., M. Shoemaker, A. Walker, P. Mehta, D. Palmer, D. Thompson, J. Koller, and J. L. Crassidis. Photometric Data from Non-Resolved Objects for Space Object Characterization and Improved Atmospheric Modeling. To appear in Air Force Maui Optical and Supercomputing Site . (Maui, HI, Sept 2013).

Linares, R., and J. L. Crassidis. Sigma Point Transformation for Gaussian Mixture Distributions Applied to Attitude Estimation. 2013. AIAA/AAS Space Flight Mechanics Conference.

Mehta, P. M., A. Walker, C. A. Mclaughlin, and J. Koller. Comparing Physical Drag Coefficients Computed with Direct Simulation Monte Carlo Using Different Gas-Surface Interaction Models. 2013. Journal of Spacecraft and Rockets. : submitted.

Mehta, P. M., and C. A. Mclaughlin. GRACE Drag Coefficient Model Developed using Direct Simulation Monte Carlo (DSMC) Method. 2013. AIAA/AAS Space Flight Mechanics Conference.

Mehta, P. M., and C. A. Mclaughlin. Drag Coefficient Modeling for GRACE using Direct Simulation Monte Carlo Drag Coefficient. 2013. AIAA/AAS Space Flight Mechanics Conference.

Mehta, P. M., and M. Shoemaker. Satellite Drag Coefficient Modeling. 2012. SWX Reports.

Mehta, P., and C. McLaughlin. Drag Coefficient Modeling for GRACE using Direct Simulation Monte Carlo. To appear in Advances in Space Research.

Shoemaker, M. A., B. Wohlberg, and J. Koller. Atmospheric Density Reconstruction using Satellite Orbit Tomography. To appear in Journal of Spacecraft and Rockets. : submitted.

Shoemaker, M. A., B. Wohlberg, and J. Koller. Atmospheric Density Reconstruction Using Tomography of Satellite Orbits. 2013. AAS/AIAA Space Flight Mechanics Meeting.

Walker, A.. Drag coefficients computed by the Direct Simulation Monte Carlo method. 2013. LANL Reports.

Walker, A., P. Mehta, and J. Koller. A Quasi-specular Drag Coefficient Model using the Cercignani-Lampis-Lord Gas-Surface Interaction Model. To appear in Journal of Spacecraft and Rockets.

Walker, A., P. Mehta, and J. Koller. Different Implementations of Diffuse Reflection with Incomplete Accommodation for Drag Coefficient Modeling. Journal of Spacecraft and Rockets.

Wetterer, C. J., R. Linares, J. Crassidis, T. Kelecy, M. Ziebart, P. Cefola, and M. Jah. Distribution Functions. 2013. AIAA/AAS Space Flight Mechanics Conference.

Hydrodynamical Mix Studies at the National Ignition Facility (U)

Michael J. Steinkamp
20120072DR

Introduction

The overarching goal of this project is the development and validation of computational sub-grid models, that capture the coupled physics of turbulent mix, Thermonuclear (TN) burn, and Charged Particle Transport (CPT), and will tightly couple many Inertial Confinement Fusion (ICF)-specific physics packages contained in the Eulerian Applications Project (EAP) code suite. This goal requires development of theoretical and experimental tools necessary for validation of our Eulerian computational sub-grid models. We must accurately capture the physics and mix morphology associated with TN burn in an ICF capsule. The experimental goals include the design of innovative NIF experiments and their associated diagnostics. Foremost among these are efforts to develop and improve Neutron Imaging (NI) and reaction-in-flight (RIF) neutron diagnostics. A more risky part of the experimental program is the development of prompt radiochemical diagnostics for use at NIF. New ideas for background mitigation and debris assay will be required and will be tested by a series of characterization and development experiments using the Omega Laser facility. These include a feasibility study for the tape transport system and gas jet transport system post-shot assay technique.

This project represents a completely new approach to the modeling of the way the physics of turbulent mix, TN burn and CPT are modeled. This approach has the potential to provide, for the first time, a physically self-consistent model of TN burn phenomena which has traditionally been treated in an ad-hoc and overly simplistic manner.

This project will utilize both OMEGA and NIF ICF capsule experiments to validate the modeling approach. As such this project represents a very aggressive comprehensive attempt at making ICF relevant to ASC code and model development in a generalized manner.

Benefit to National Security Missions

The products of this research would advance the state-of-the-art Inertial Confinemet Fusion (ICF) modeling capabilities in LANL's Eulerian ASC code suite. Both this new computational capability and the new diagnostics developed on the National Ignition Facility (NIF) would directly address NNSA's goal of fostering a scientific program at NIF that is both of broad scientific interest and of specific utility of the weapons program. Better understanding of turbulence has broad application to multiple missions including climate, energy (combusion), forensic particle transport, etc.

Progress

A sub-grid model that uniquely couples the BHR turbulent mix model and the thermonuclear burn package in a physical manner have completed and verified. Validation is currently in progress using a variety of available data sets. It has been determined that the most stringent test of this model is afforded by separated reactants experiments. In a separated reactant reactants experiment a deuterated (CD) capsule shell is utilized with a tritium fill. 14 MeV neutrons (D + T -> α + n (14 MeV)) will be generated only when the shell material intimately (atomically) mixes with the tritium fill. To this end, a collaboration with LLNL has been formed and personnel from this project have been integral participants in 4 NIF shots to date. Additional shots are planned and will be conducted during FY-13. In addition a dedicated shot on the OMEGA laser has been obtained for late FY-13 and the design of an OMEGA size capsule experiment was initiated. Validating the newest ICF relevant packages in the Eulerian code consumed a significant amount of effort during FY-12. These packages included the 3-T physics, charged particle transport, ion conduction and the PDF thermonuclear burn package.

Work that was initiated in FY-12 and continuing in FY-13 is centered on verifying and validating the knock-on physics in the charged particle transport package (neces-

sary to perform both RIF and CPT radchem calculations) implementing the necessary cross section data bases for CPT radchem, and completing the full implementation of the PDF burn model in the separated reactants portion of the code. Completion of these items is the necessary initial step in utilizing the separated reactants data along with the CPT radchem and RIF data along with the CPT and RIF data for validation of the PDF modeling approach.

The charged particle radchem development and the development of diagnostic techniques to measure high energy reaction in flight neutrons conducted during the last 12 months have proved successful. Both of these techniques provide independent measures of the amount and state (morphology and distribution) of shell mix into thermonuclear fuel.

In order to attain the high-fidelity experimental data required for TN burn model validation, the original and stretch experimental campaign goals, that we have accomplished thus far are:

- Executing more mix experiments with a deuterated (CD) capsule shell
- Simulating CD mix implosion experiments with the EAP code suite, and the turbulence transport model
- Experimentally observed RIF neutrons at the NIF
- Analyzed prompt assay detector development for Omega and are preparing presentations for summer conferences
- Presented prompt radchem concepts to the national ICF Diagnostics Working Group
- Through RIF neutron measurements, have shown quantum effects are important for charged particle stopping in a degenerate plasma. Publications on this work are in progress.

Future Work

The sub-grid modeling effort requires more work as we more fully integrate our current sub-grid thermonuclear (TN) burn model into other aspects of the Advanced Simulation and Computing (ASC) code's burn framework. To extend the Probability Distribution Function (PDF) approach, we are developing an approach that allows the fine-scales of turbulent motions to evolve in a natural fashion, rather than being simply slaved to the largest turbulent scales. This extension describes the evolution of the Kolmogorov dissipative scales and requires minimal changes to the code's mix model and provides spatial or scale information not predicted by either the BHR mix model or by the PDF alone. We are currently testing the new model on unstable flows. Successful implementation of this model will lead to the generation of a physical realization of sub-grid structure that is required for fully coupling to the charged particle transport and for future extensions to other aspects of sub-grid physics.

In order to attain the high-fidelity experimental data required to validate these computational sub-grid models, we are working towards both our original and our stretch experimental campaign goals, and they are to: (1) design and shoot separated reactant experiments at Omega, where we have obtained a dedicated shot day for late FY13, as well as separated reactants and Tritium filled capsules on the National Ignition Facility (NIF) in FY14 (in conjunction with the DIME project at LANL); also focusing on how to change the pressure and fill to influence capsule convergence; (2) develop a prompt radiochemical assay capability for the NIF; (3) develop concepts in NIF solid debris collection experiments; and (4) develop a reaction in flight (RIF) diagnostic capability in ignition capsules for better data collection and improved statistics for charged particle stopping.

Conclusion

Broadly, we identify two main technical products. The first will be the development of a new diagnostic suite for NIF, capable of addressing many issues in high-energy-density physics, but specifically targeting the physics of mixing at material interfaces in ICF capsules. Success of this diagnostic suite would enable the design and fielding of a full experimental mix program at NIF. The second technical product of our proposed research would be an experimentally validated computational subgrid model that couples the ICF-specific physics packages that model turbulence, mix, TN burn, and CPT, significantly advancing the capability of LANL's Eulerian ASC code.

Advancing the Fundamental Understanding of Fission (U)

Morgan C. White
20120077DR

Introduction

Nuclear fission is the energy source for both nuclear weapons and nuclear reactors. 73 years after the discovery of fission, it remains imperfectly understood. To improved that understanding, we will:

- Build a detector system to measure the velocity and total kinetic energy (TKE) of fission fragments as a function of incident neutron energy.
- Develop fission theory and modeling to enable the prediction of complete fission-fragment yields as a function of incident energy forming the basis of new evaluation tools for these data. Benchmark these tools based on the new experimental data.
- Evaluate the Pu239 fission-fragment yields based on the new theory and experimental data.

Recent inquiries into discrepancies between nuclear weapons yields reported by LANL and LLNL addressed fission-product yields. One conclusion was the "convincing experimental evidence for energy dependence" from 0.2 to 1.9 MeV of the Nd147 cumulative yield from Pu239 fission. This single finding brought the two labs into closer agreement. New experiments are necessary to confirm the energy dependence. There are no experimental data in the energy range from 2 to 14 MeV and a 25% discrepancy exists between measurements at 14 MeV. Confirming the low-energy yield findings, providing the missing data, and resolving the discrepancy are crucial issues within the Nuclear Performance grand challenge.

We will advance the state-of-the-art for fission science. This impacts defense programs, nuclear energy, and the science of signatures. We will push deeper into this frontier than previous studies, measuring more of the data than ever before, probing with theory why it happens this way, and gleaning knowledge that will help LANL and the nation stay at the forefront of this critical field.

Benefit to National Security Missions

An understanding of the fission process is critical to the Laboratory's national security missions. Assessment of fission yield from an NTS event or in a post-detonation situation depends on an accurate assessment of the fission-product yields. The accuracy and utility of simulations for device assessment, reactor design and safety, and SNM detection depend on the accuracy of the fission evaluations. An enhanced understanding of the fission process and the correlations in emissions will greatly enhance our ability to quantify the sources of uncertainty in our predictions. This project helps keep LANL and our nation at the forefront of fission science, further enhancing our reputation in this field, and strengthening the science-based deterrence provided by a strong national laboratory system.

Progress

The SPIDER project, LDRD 20120077DR, seeks to advance the fundamental understanding of fission through a better understanding of the moment of scission. We are seeking a new capability to measure the individual fragments as they are emitted at scission and will use these data to validated guide and validate advanced theories describing the same.

The theory portion of our project is making steady progress. We believe one of the strengths of this effort is its two pronged development. Our phenomenological model has been completed and used successfully to evaluate fission product yields and total kinetic energy as a function of incident neutron energy. This is a significant milestone completed within the project. While it is not predictive and must be tuned to experimental data, this tool provides a fallback that can be used to interpret the experimental data to be taken and provide the evaluated libraries, of the kind that will be used for applications and submitted to the US national ENDF/B repository, desired.

The advanced theory efforts have also made significant progress towards a more predictive evaluation capability. The LANL model describing the potential energy of the nuclear surface has been used in static analysis to predict the nuclear masses at the level of uncertainty in the experimental data. Our project seeks to add a capability to track the dynamic evolution of the nuclear potential such that one may follow the nucleus from its original excitation to the point of scission.

This year the code for the dynamic evolution has been developed to the point of tracking Monte Carlo samples of individual evolutions. Unfortunately, the use of the original grid designed for the static interpretation causes the model evolve into unphysical representations. Significant effort has been required to refine this grid to provide the smoothness necessary to allow for the dynamic evolution. These efforts are in the final stages and we expect to begin the last phase of this work by the end of the year. At that time, the tool can be used to compare against experimental data and tuning and validation efforts begin.

The experimental efforts have been more difficult than anticipated. Steady progress has been made developing and testing the individual components but putting together an instrument at the scale originally desired has proved impossible. As discussed with our appraisal panel in February, this has led to a reworking of the goals for the project. Our focus, as recommended by the committee, is now on proving the capability can be achieved and working to demonstrate that the final instrument can be built.

To this end, we are in progress to build a dual-arm, as opposed to the desired nine dual-arm pairs, instrument. Fabrication of all of the components is essentially complete and assembly is in progress to be ready to make measurements in this falls LANSCE beam cycle. To reach this point, significant research has been completed on many of the components that go into the overall system.

The instrument measures the velocity and energy of both fission fragments emitted. The velocity measurement uses a thin foil to produce electrons from the fragment passage and a fast timing plate to record that signal. Initial studies of carbon foils used for the electron production have shown them to be inadequate and mylar foils with sputtered metal coatings have been obtained and shown to produce better signals. We are now producing all of the subcomponents for the final dual-arm chamber.

The energy of the fragment is measured by an ionization chamber. These chambers are in wide spread use at LANL and we have successfully constructed a prototype. Testing indicates it is working as expected and optimization of this chamber continues including testing of new silicon nitride windows to reduce the energy loss of the fragment as it enters the detector. Use of accelerated radioactive beams at facilities like NCSL is being studied as a potential way to directly measure the pulse height defect identified as the largest source of uncertainty in this measurement.

Future Work

During the final year of the SPIDER LDRD project, we plan fulfill, in general, the original goals of our research plan. That is to take data on plutonium-239 fission fragments using a new 2V,2E detection system and to make evaluated data libraries for the fission fragment yields of the same. Unfortunately, we will be unable to build a full instrument and these measurements will not have the resolution to measure the distributions over the full range of incident neutron energies desired. However, they will demonstrate a capability that can be scaled to make these programatically desired measurements.

The experimental efforts will focus on completion of a dual-arm instrument that will be fielded on the LANSCE 1FP12 beam line. These measurements will focus on taking data on uranium-235 that can be compared to established standards. Data will also be taken on plutonium-239; these measurements will allow us to explore safety and measurement issues working with this more difficult isotope. During the year californium-252 measurements will also be made. The U235 and Cf252 measurements will be used to demonstrate the accuracy of the detector. The Pu239 measurements will prepare the way to make the final energy-dependent measurements of interest. The prototype chamber will also be used to investigate key challenges in scaling up to the final nine dual-arm pair instrument. The LANSCE Program Advisory Committee strongly endorsed this experimental plan.

The theory efforts will focus on finalizing the capability to perform advanced predictions. These can then be compared against the phenomenlogical model results that have already been produced. Eventually these will be tuned and validated with new data but in the meantime will still be the most accurate estimates of these key fission quantities and included in future application libraries.

Conclusion

The fission process plays a fundamental role in nuclear weapons and nuclear energy, and is therefore deeply tied to our national security and energy independence missions. We expect to improve our understanding of nuclear fission, which will support these important technologies and lead to important advances in basic science. The new experimental data and theoretical models will produce

evaluated nuclear data that feeds into the codes used for weapon simulations and nuclear reactors, and will thus improve technical design and performance predictions of these systems.

Publications

Arnold, C. W., F. K. Tovesson, K. C. Meierbachtol, A. B. Laptev, T. A. Bredeweg, M. Jandel, R. O. Nelson, and M. C. White . SPIDER: A Path to 1 AMU Resolution of Neutron-Induced Fission Fragments. Presented at Division of Nuclear Physics of the American Physical Society,. (Newport Beach, CA, 24-27 Oct. 2012).

Jandel, M.. Neutron-Induced Fission Measurements Using DANCE and LSDS Facilities at LANL. Presented at Dynamical Aspects of Nuclear Fission (DANF2011). (Smolenice, Slovakia, October 17, 2011).

Meierbachtol, K. C.. LDRD Review - SPIDER Detector Ionization Chamber Component. 2012. LA-UR-12-25207 Presentation to LDRD Review October 4, 2012.

Meierbachtol, K. C., F. K. Tovesson , C. W. Arnold , A. B. Laptev , T. A. Bredeweg , M. Jandel , R. O. Nelson , and M. C. White . A High Resolution Ionization Chamber for the SPIDER Fission Fragment Detector. Presented at 5th International Conference on Fission and Properties of Neutron-Rich Nuclei (ICFN5) [LA-UR-12-23824]. (Sanibel Island, FL, 04-10 Nov. 2012).

Meierbachtol, K., C. Arnold , A. Laptev, F. Tovesson, M. White, R. Blakeley , A. Hecht, and D. Mader. Development of an Ionization Chamber for the SPIDER Fission Fragment Detector. To appear in International Conference on Nuclear Data for Science and Technology. (New York, March 4, 2013).

Moller, P., J. Randrup, and A. J. Sierk. Calculated Fission Yields of Neutron-Deficient Mercury Isotopes. 2012. Physical Review C (Nuclear Physics). 85 (2): 024306 (6 pp.).

Sierk, A. J., J. P. Lestone, and P. Moller. Calculating Fission-Fragment Distributions. Invited presentation at 2012 Tri-Lab Nuclear Data Workshop. (Los Alamos, NM, 05-07 Mar. 2012).

Tovesson, F. K.. LDRD Review - SPIDER Detector Instrument Overview. 2012. LA-UR-12-25411 Presentation to LDRD Review October 4, 2012.

Tovesson, F. K., T. A. Bredeweg, A. B. Laptev, K. C. Meierbachtol, C. W. Arnold, M. C. White, A. Hecht, D. Mader, and R. Blakeley. SPIDER: A New Instrument For Fission Yield Measurement. Presented at 5th International Conference on Fission and Properties of Neutron-Rich Nuclei (ICFN5) [LA-UR-12-23883]. (Sanibel Island, FL, 04-10 Nov. 2012).

Tovesson, F., C. Arnold, A. Laptev, K. Meierbachtol, M. White, R. Blakeley, A. Hecht, D. Mader, and L. Snyder. SPIDER: a new instrument for fission fragment research at the Los Alamos Neutron Science Center. To appear in Fifth International Workshop on Nuclear fission and Fission-Product Spectroscopy. (Caen, France, May 28, 2013).

Tovesson, F., C. Arnold, A. Laptev, K. Meierbachtol, M. White, R. Blakeley, A. Hecht, D. Mader, and L. Snyder. SPIDER: A New Instrument for Fission Fragment Yield Measurements. To appear in International Conference on Nuclear Data for Science and Technology. (New York, March 4-8, 2013).

Physics Beyond the Standard Model with the Long-baseline Neutrino Experiment

Christopher M. Mauger
20120101DR

Introduction

The goal of this project is to enhance the physics reach of the Long-Baseline Neutrino Experiment (LBNE) by developing an integrated experimental, theoretical, modeling, and simulation capability at LANL that makes possible science beyond the LBNE baseline. We drawn on our extensive expertise in neutrino oscillations, nucleon decay, supernovae explosions, advanced detector development, and rare event searches. LANL also has a strong experimental history in near detector technology and large Cherenkov detectors, and we will field an integrated team capable of addressing the full range of physics available to LBNE. In this project, we explore novel methods at the near site to make higher precision measurements of the neutrino flux and cross sections than are possible with previous approaches. We will construct a liquid argon time-projection chamber and carry out measurements associated with improving LBNE's CP violation sensitivity and supernova neutrino program.

In addition, we carry out a theoretical program to enhance our understanding of neutrino-nucleus interactions. We optimize the performance of the far detector through a detailed simulation program relating calibration, light propagation and event signatures of both signal and background processes. Our theoretical studies of proton decay and supernova neutrino physics will also enhance the science that can be done with LBNE.

Benefit to National Security Missions

This project sits squarely in the LANL BSM Grand Challenge and strongly enhances the growing LANL-Fermilab strategic partnership. It enhances core capabilities of laboratory strength in several groups across two divisions. LANL has project, base and Early Career Award funding from DOE HEP to develop a conceptual design for a traditional near detector and project funding to lead the calibration effort of the far detector, but we lack a program to develop the physics reach of LBNE. With this proposal we build an integrated experimental and theoretical team at Los Alamos to tackle the large scope of BSM physics. This team will be unique within the LBNE collaboration and cement LANL's leadership role in both the technology and the physics of LBNE. It will simultaneously secure LANL's leadership in large-scale computing for nuclear and neutrino physics. Detector research at the cutting edge builds capability for national security nuclear sensing.

Progress

On the experimental side, we have done a detailed design of the liquid argon detector and begun the procurement process. The two key elements are the cryostat and the electronics. The cryostat is the largest expense and constitutes the box in which all of our experimental activity will have to be carried out. Extensive simulations were carried out to assure all scientific goals will be met. The electronics are custom devices that required extensive evaluation. Most are now in hand with the rest on order. The time-projections chamber is now fully designed. Additionally, significant scientific progress has been made on the planning for neutron beam running at LANSCE (Los Alamos Neutron Science Center). We now have two proposals in for engineering runs for the autumn run period at WNR (Weapons Neutron Research), the high-energy neutron beamlines of LANSCE. Also during this year, we have built an extensive and strong collaboration including many top institutions from outside of LANL.

Regarding neutrino flux measurements, we have taken data via the NA-61 experiment at CERN and begun the analysis. Due to a custom magnet configuration, this required thorough magnetic field simulations and study of the trigger configuration. Both of these are completed. The analysis will yield proton-carbon cross-sections with unprecedented sensitivity in one of the many regions of hadron production phase space important for understanding neutrino production in the Long-Baseline Neutrino Experiment (LBNE). These data will be ana-

lyzed and planning for future experiments carried out. The current work underway is an extensive calibration of the data from several detector systems.

In this time, extensive theoretical work has been carried out including advances in the study of supernova neutrinos, non-standard interactions (NSI), and neutrino scattering physics.

During the past year the theory effort has concentrated on calculations of inclusive electron and neutrino cross sections from Carbon-12. A preprint on the 12C electron scattering has been prepared, and a calculation of the sum rules relevant to neutrino scattering are underway. We find a significant enhancement of the transverse response, similar to previous calculations and experiments in 4He and also experimental results on 12C. Future calculations will help determine the impact of these calculations on neutrino scattering.

We have also worked on signals of supernovae neutrinos in liquid argon detectors. We are studying signals of various types of supernovae and in different epochs, now including initial estimates of coherent neutrino-nucleus scattering. We are examining potential signals in a variety of scenarios with different detector designs, and trying to understand the impact of eventual siting decisions on the LBNE far detector.

Future Work

In neutrino-nucleus scattering, we will work with the experimentalists to make the recent article on neutrino nucleus scattering as valuable as possible. We will also study continue to study uncertainties. The main work will be extend the present calculations of the deuteron to study light nuclei including 4He with the goal of eventually producing results on 12C.

In supernovae neutrinos, we will work to begin to implement calculations that include neutrino inelastic scattering (scattering from electrons, nuclei, etc.) as well as coherent forward scattering from neutrino-neutrino and neutrino-electron (MSW) effects. During the first year of the project we identified this is a potentially very important issue for supernovae neutrinos. We will continue to work with the experimentalists on issues related to the observation of supernovae neutrinos.

The focus of the experimental effort will be the construction and commissioning of a liquid argon time-projection chamber. The detector will have 5 tons of instrumented mass. The instrumentation will be a three-plane wire chamber with cold analog electronics. A YAG laser will be employed for detector calibration studies.

Neutrino flux-related measurements at NA-61 experiment at CERN will continue.

Conclusion

We will produce and publish new calculations for neutrino scattering on the deuteron, carbon, and oxygen, collect and publish data on novel H2O and D2O targets that include cross-section and absolute flux measurements, and produce and optimize the plan for analyzing the fundamental symmetries of nature with LBNE long-baseline neutrino data. Our calculations and simulations of nucleon decay modes and signatures will help improve the far detector for LBNE and squeeze additional scientific results from the currently running experiment, SuperKamiokande. Finally, our supernova neutrino studies will provide the path to extract fundamental physics from a galactic supernova burst.

Publications

Abazajian, K. N., E. Calabrese, A. Cooray, F. De Bernardis, S. Dodelson, A. Friedland, G. M. Fuller, S. Hannestad, B. G. Keating, E. V. Linder, C. Lunardini, A. Melchiorri, R. Miquel, E. Pierpaoli, J. Pritchard, P. Serra, M. Takada, and Y. Y. Wong. Cosmological and astrophysical neutrino mass measurements. 2011. ASTROPARTICLE PHYSICS. 35 (4): 177.

Akin, T., and A. Friedland. The 2010 Interim Report of the Long-Baseline Neutrino Experiment Collaboration Physics Working Groups. . 2011. e-Print: arXiv:1110.6249 .

Cherry, J., J. Carlson, A. Friedland, G. Fuller, and A. Vlasenko. Neutrino scattering and flavor transformation in supernovae. 2012. Physical Review Letters. 108 (26): 261104.

Mauger, C., G. Garvey, E. Guardincerri, D. Lee, Q. Liu, G. Mills, J. Mirabal-Martinez, J. Ramsey, K. Rielage, C. Sinnis, C. Taylor, R. Van de Water, and A. Yarritu. The CAPTAIN Detector and Physics Program . 2013. arxiv.org .

Shen, G., L. E. Marcucci, J. Carlson, S. Gandolfi, and R. Schiavilla. Inclusive neutrino scattering off the deuteron from threshold to GeV energies. 2012. Physical Review C (Nuclear Physics). 86 (3): 035503 (18 pp.).

Disruptive Innovation in Numerical Hydrodynamics

Jacob I. Waltz
20130005DR

Introduction

This project researches and develops innovative approaches for the numerical modeling of high-speed material flows that leverage emerging computer architectures and are applicable to a wide range of scientific and national security problems. The technologies under consideration are designed to enhance fidelity and computational efficiency relative to existing methods, especially in the areas of vorticity, time accuracy, and thermodynamic consistency. The specific focus is high-fidelity three-dimensional algorithms that have not been previously applied to LANL and NNSA problems but have significant potential should they be successfully developed.

In addition to the above this project is investigating approaches for emerging computer architectures such as the Graphics Processing Unit (GPU). Effective use of this computer hardware requires a large shift in both the design of numerical algorithms and the use of simulation tools. The research performed under this project is intended to address both issues and thereby create a path forward for emerging architectures and Exascale concepts, for example by emphasizing accuracy over memory.

The development of transformative numerical algorithms that are simultaneously optimized for new computer architectures carries significant technical risk, but if successful will enable a dramatic leap forward in predictive simulation capability.

Benefit to National Security Missions

We expect our research to lead to orders of magnitude improvements in fidelity and computational efficiency for work related to NNSA Defense Programs, Nonproliferation, and Science Campaigns. The impacts of these improvements will include faster responses to programmatic questions; increased population sizes for Uncertainty Quantification and other sensitivity studies; greater detail in discovery-scale simulations; and an enhanced ability to model realistic 3D features. Our work will also enable the use of commodity mesh generation software, which could lead to cost savings of several million dollars per year, and reduce problem setup time. Lastly, our work will allow future compute platforms to be used earlier and more effectively.

Future Mission

The jump in simulation capability that results from our research will enable the solution of entirely new classes of problems and therefore has the potential to significantly expand the scope of the Laboratory's simulation tools. New application areas might include design of blast mitigation structures for urban environments, energetic disablement calculations of Improvised Explosive Devices, anti-personnel and anti-structural analysis, and high-resolution studies of mix and ignition in Inertial Confinement Fusion targets.

Progress

In the past year the project has made significant technical progress in the following areas:

Hydrodynamic algorithms

A new class of hydrodynamic algorithm has been developed that significantly improves accuracy and fidelity particularly in the areas of vorticity and shock compression. This algorithm is in fact the first successful algorithm of its type to have ever been developed and therefore represents a significant research advance. Initial results with the algorithm are to be presented at a domestic conference in September 2013 (MULTI-MAT 2013), and a journal article describing the algorithm is in preparation.

Advanced architectures: The project has completed initial testing and implementation on Graphics Processing Units (GPUs). The project also has performed research on effective approaches for threading. The purpose of

these studies was to inform research and development choices for work that will take place in fiscal year 2014. Journal articles on these studies are in preparation.

Verification

The project has completed verification testing of an existing hydrodynamic algorithm which was considered a risk mitigation for the new algorithm but will serve as a complementary algorithm otherwise. Two journal articles were prepared. The first documented testing results on existing problems and was published in July (J. Waltz et al, `Verification of a three-dimensional unstructured finite element method using analytic and manufactured solutions', Computers & Fluids 81, 57-67 (2013)). The second article presented a novel set of test problems for the equations of fluid dynamics with specific relevance for Inertial Confinement Fusion. This article has been submitted to the Journal of Computational Physics and is under review. These test problems also were presented at a domestic conference (ASME V&V symposium) in May 2013.

Future Work

The major 2014 milestone for this project is to demonstrate multi-material simulations with a new hydrodynamic algorithm, including convergence analysis, accuracy measurements, comparison to experiment, and timing studies.

Additional tasks are to demonstrate and characterize initial performance on Many-Integrated-Core architectures, and to demonstrate and characterize initial distributed memory performance.

Each task will be documented with journal papers, internal reports, and/or presentations at technical conferences.

Conclusion

The goal of this project is to develop innovative approaches for the numerical modeling of high-speed material flows that leverage emerging computer architectures and will form the basis of next-generation simulation tools. The impacts of this work will include significant enhancements in simulation detail and accuracy; reduced uncertainty in simulation-based responses to programmatic issues; advances in scientific understanding in the broader numerical modeling community; and increased diversity in the suite of methods that are trusted for LANL and NNSA problems.

Publications

Canfield, T. R., M. R. J. Charest, N. R. Morgan, L. D. Risinger, J. Waltz, and J. G. Wohlbier. Simulation of multi-material flows using a finite element Riemann solver and adaptive unstructured grids. Presented at Conference on Numerical Methods for Multi-Material Flows. (San Francisco, CA, 2-6 Sep. 2013).

Canfield, T. R., N. R. Morgan, L. D. Risinger, J. Waltz, and J. G. Wohlbier. Manufactured solutions for the three-dimensional Euler equations with relevance to inertial confinement fusion. Presented at American Society of Mechanical Engineers Verification and Validation Symposium. (Las Vegas, NV, 22-24 May 2013).

Morgan, N. R., J. Waltz, D. E. Burton, T. R. Canfield, L. D. Risinger, J. G. Wohlbier, and M. R. J. Charest. A Godunov-like point-centered ALE finite element hydrodynamic approach. Presented at Conference on Numerical Methods for Multi-Material Fluid Flow. (San Francisco, CA, 2-6 Sep. 2013).

Waltz, J.. GPU and multicore acceleration of a 3D unstructured mesh Eulerian-AMR hydrocode. Presented at Nuclear Explosives Code Developers Conference. (Livermore, CA, 22-26 Oct. 2013).

Waltz, J., N. R. Morgan, T. R. Canfield, M. R. J. Charest, L. D. Risinger, and J. G. Wohlbier. A three-dimensional finite element arbitrary Lagrangian-Eulerian method for shock hydrodynamics on unstructured grids. 2013. Submitted to Computers & Fluids.

Waltz, J., T. R. Canfield, M. R. J. Charest, N. R. Morgan, L. D. Risinger, and J. G. Wohlbier. Operator splitting and time accuracy in Lagrange plus remap methods. Presented at Conference on Numerical Methods for Multi-Material Fluid Flow. (San Francisco, CA, 2-6 Sep. 2013).

Waltz, J., T. R. Canfield, N. R. Morgan, L. D. Risinger, and J. G. Wohlbier. Verification of a three-dimensional unstructured finite element method using analytic and manufactured solutions. 2013. COMPUTERS & FLUIDS. 81: 57.

Waltz, J., T. R. Canfield, N. R. Morgan, L. D. Risinger, and J. G. Wohlbier. Manufactured solutions for the three-dimensional Euler equations with relevance to inertial confinement fusion. 2013. Submitted to Journal of Computational Physics.

Wohlbier, J. G., L. D. Risinger, T. R. Canfield, M. R. J. Charest, N. R. Morgan, and J. Waltz. Programming for modern architectures in the CHICOMA hydrocode. Presented at Conference on Numerical Methods for Multi-Material Fluid Flow. (San Francisco, CA, 2-6 Sep. 2013).

Illuminating the Origin of the Nucleon Spin

Ivan M. Vitev
20130019DR

Introduction

Nucleons (protons and neutrons) are not fundamental constituents of matter, but are instead made up of quarks and gluons, the elementary particles of the strong interaction. There is compelling experimental evidence that the sum of the quark and gluon intrinsic angular momenta only contributes ~1/3 of the total proton spin. Thus, the majority of the proton spin is unaccounted for, which has been referred to as the "proton spin crisis". The missing fraction of the spin is likely carried by the orbital angular momentum of the quarks and gluons. The long-term goal of this project is to develop the experimental capability to measure the spin of the proton in terms of contributions from the spins of the quarks, gluons and their orbital angular momentum. An equally important goal is to understand the relative significance of these spin contributions in the theory of strong interactions, Quantum Chromodynamics (QCD), and how they manifest them-selves in reactions with polarized proton beams and/or targets. To this end, we will determine the momentum distribution of quarks inside the proton, transverse to the proton momentum, from which one can deduce whether quark orbital motion contributes significantly to the proton spin.

To determine the distribution of quarks and gluons within a nucleon, we will carry out the world's first measurement of the production of two simultaneous leptons (electrons or muons) from a polarized proton target bombarded by a high-energy proton beam. From a detailed analysis of the azimuthal distribution of such di-leptons, one can deduce properties of the polarized nucleon structure. In particular, we will measure both the sign and magnitude of the quark Sivers distribution, which is expected to be zero if the quarks have no orbital angular momentum.

Benefit to National Security Missions

This work is central to the FY13, FY14 LDRD Strategic Investment Plan of Nuclear and Particle Futures. Building upon our existing strategic partnership with Fermilab (E906, MiniBoone and LBNE), this project will strengthen our fundamental science capabilities, bring new high-luminosity polarized target technology to LANL and provide a "major physics thrust to follow current commitments to RHIC". This project will maintain LANL's leadership position in the field of spin physics and produce the world's most accurate polarized Drell-Yan measure-ment in proton-proton reactions. Our project is a timely and direct response to the DOE Mile-stone (HP13) to "test unique QCD predictions for relations between single-spin phenomena in p-p scattering and those observed in deep-inelastic scattering". We anticipate that this LDRD project will result in DOE Office of Science funding for a LANL-lead spin physics program at Fermilab. Our integrated experimental and theoretical program will allow us to lead in a major advance in understanding the polarized nucleon structure through the only U.S.-based dedicated polarized DY experiment. Providing a polarized target to FNAL will greatly enhance Fermilab's capabilities and provide a much needed user facility for spin physics. Our target will also be able to polarize ND3, thus enabling one to extend the spin physics to polarized neutrons. Furthermore, developing and testing particle detector technology at high luminosity will directly benefit MaRIE, a LANL institutional priority. This detector development is also of fundamental importance to nuclear detection for applied missions like nuclear nonproliferation. Such detectors often operate in a high background environment.

Progress

In the first fiscal year of this project, we carried out a feasibility study to reduce risk for FY14-16, in which the project will become a full-scale DR. The conclusions of this feasibility study will be validated by an independent peer review scheduled for Aug. 7.

Results on the polarized magnet: During the first week of January 2013, the LANL polarized target magnet was

crated and shipped to the University of Virginia for testing. This superconducting magnet has not been used since 1992, and one element of risk reduction was to demonstrate that the magnet is still functional. Kun Liu and Andi Klein flew out to UVa on 1/27 to perform several initial tests, including bringing the magnet up to full field (5.1 T.) In the first test, we performed a leak check of the whole magnet. Then, the magnet was first cooled with liquid nitrogen, verifying that the thermal insulation of the magnet was intact. Next, the superconducting coils were successfully cooled with liquid helium. Finally, the magnet current was slowly ramped up over 3 hours to achieve full field. We reached the design field of 5.1 T without a quench on Feb 5th. The magnet was left at full field for 24 hours. After 24 hours, the magnet was de-energized in order to perform a stringent final check. For this test, we chose a fast current ramp, such that the maximum field was reached in only 30 minutes. Again, the magnet behaved flawlessly. The magnet is at Oxford Instruments for superconducting coil re-orientation.

Results on the Letter of Intent: We have updated our physics performance plots, based on NLO Drell-Yan rates and realistic detector acceptance. The Drell-Yan cross section was taken from PYTHIA using the CTEQ5M parton distribution functions and verified against a modern NLO DY calculation from Vitev, et.al. Andi Klein, Patrick McGaughey and Xiaodong Jiang worked on the (LOI). We showed that approximately 110,000 reconstructed Drell-Yan pairs can be collected per year, after applying geometry cuts similar to that of E906. A strong sensitivity to the sign and magnitude of the Sivers asymmetry was demonstrated for non-zero values. The magnitude of the Sivers function can be determined to better than 4%. An international collaboration for experiment E1039 with more than 40 members was formed with LANL being the lead and Andi Klein and Xiaodong Jiang co-spokespersons. Member institutions include ANL, FNAL, U. Illinois, Academia Scinica Taiwan, KEK Japan, Ling-Tung U. Taiwan, LANL, U. Maryland, U. Michigan, U. New Hampshire, National Kaohuisung U. Taiwan, RIKEN Japan, Rutgers U., JLab, Tokyo Institute of Technology Japan, U. Virginia. The Letter of Intent was presented to the Fermilab Physics Advisory Committe on June 5th, 2013. We were given 30 min for presentation, which we consider quite encouraging. The PAC enthusiastically embraced our project and the Fermilab Director gave our project E1039 Stage 1 approval.

Results on theory: In lattice QCD, an international collaboration has been formed between LANL (Rajan Gupta, Tanmoy Bhattacharya, Boram Yoon), MIT (John Negele), NM State U. (Michael Engelhardt), Jefferson Lab (Alexei Prokudin) and U. Regensburg (Andreas Schafer) to study transverse momentum distributions (TMDs). A postdoctoral search was conducted and an offer made and accepted. Dr. Boram Yoon will join LANL on August 19, 2013. He is a young expert in lattice QCD. The collaboration has applied for time at Ntional centers through USQCD and received 3.83 million core hours for computing time. We started tuning and tests of the multigrid method for calculating the quark propagator. We now have the manpower and computing time in place to evaluate the contribution of disconnected diagrams to the TMDs. In perturbative QCD, we have studied the next-to-leading order pQCD corrections to the transverse momentum-weighted Sivers asymmetry for semi-inclusive hadron production in lepton-proton deep inelastic scattering (Zhonbo Kang, Ivan Vitev, Hongxi Xing). This is an important step toward the accurate extraction of the internal structure of the nucleon. Our paper was published Phys. Rev. D 87, 034024 (2013) and presented at the QCD Evolution Workshop, 2013. We have begun the analysis of the quark Sivers distribution (one TMD that is central to the goals of this project), using the world's polarized SIDIS data (Miguel Echevarria, Zhongbo Kang, Ivan Vitev).

Future Work

Experiment: In the next FY we will design and build a new Nuclear Magnetic Resonance system for the polarized target. Furthermore, we will setup a lab and test area in Area A of LANSCE, where we will setup and eventually test the magnet, when it comes back from Oxford. In collaboration with University of Virginia, we will modify the old refrigerator in such a way that it will fit into the new geometry, refurbish the sensors and He lines,test it at UVa and ship it to LANL. Once it is at LANL, the refrigerator will be mounted in the magnet.

Theory: In the next FY we will begin the investigation of the Sivers function evolution to leading logarithmic accuracy. We will also make progress in understanding the rapidity evolution technique. We will develop a global fitting package for the Sivers function in semi-inclusive deep inelastic scattering. We will extract the Sivers function and publish results. In Soft Collinear Effective Theory we will begin the application of the Rapidity Renormalization Group Technique to the polarized case, Drell-Yan in particular. We will initiate the derivation of the energy evolution equation for comparison to the ones obtained with the pQCD technique. In Lattice QCD we will incorporate a new multi-grid evaluation method in the suite of lattice codes. We will set up the production runs for disconnected diagrams at JLab and begin their evaluation. We will begin work on understanding the renormalization of lattice operators.

Conclusion

Through a synergy between theory and experiment, we will make a fundamental advance in our understanding of the origin of the nucleon spin. In a strategic partnership with Fermilab, we will carry out the world's most accurate measurement of di-lepton production from a polarized proton target bombarded by a high-energy proton beam. We will develop state-of-the-art theoretical and computational tools necessary to interpret the experimental results that will directly lead to a major breakthrough in our understanding of the structure of matter and the theory of strong interactions.

Publications

Kang, Z.. Single transverse spin asymmetries in polarized SIDIS and pp scattering. Invited presentation at The 5th Workshop of the APS Topical Group on Hadronic Physics. (Denver, 10-12 April 2013).

Kang, Z. B., I. Vitev, and H. X. Xing. Transverse momentum-weighted Sivers asymmetry in semi-inclusive deep inelastic scattering at next-to-leading order. 2013. PHYSICAL REVIEW D. 87 (3): -.

Klein, A., P. McGaughey, and I. Vitev. Letter of Intent for a Drell-Yan experiment with a polarized proton target. 2013. Fermilab PAC .

Vitev, I.. Transverse momentum-wighted Sivers asymmetry in semi-inclusive deep inelastic scattering at next-to-leading order . To appear in QCD Evolution Workshop 2013. (Newport News, 14-17 May 2013).

Peta-scale Studies of Cosmic Explosions and Supernova Shock Breakout with Palomar Transient Factory

Przemyslaw R. Wozniak
20130030DR

Introduction

The next generation Palomar Transient Factory (PTF-II) is poised to revolutionize the field of time-domain astrophysics with great potential for future discovery, especially in the area of explosive phenomena. This project will conduct the first systematic search for supernova shock breakout events and other explosive transients on time-scales of less than a day. In order to succeed, PTF-II must automatically identify actionable information from the torrent of imaging data, classify emerging events, and optimize the follow-up strategy. To address this challenge, we will develop an autonomous event broker that integrates cutting edge machine learning algorithms with high performance computing infrastructure. Our classification engine will be based on Bayesian belief networks and ensembles of decision trees. Follow-up optimization will employ mutual entropy minimization and dynamic scheduling of available instruments.

A major innovation of PTF-II is Spectral Energy Distribution Machine (SEDM), a low-resolution spectrograph that will enable rapid spectral classification of all interesting transients detected by the photometric pipeline. Our event broker will identify "young" supernovae and enable rapid follow-up observations with high-energy observatories in time to get a glimpse of the shock breakout.

We will also carry out extensive radiation hydrodynamics calculations of transient emission from hot shocks over a wide range of astrophysical scenarios to interpret PTF-II observations, inform transient classifiers, and test the performance of simulation codes in a critically important range of physical conditions. Our goals is to build and publish a suite of ~100 explosion models with time-resolved spectra and synthetic light curves at ~100 epochs. A detailed comparison of these models with observed light curves will provide valuable constraints on the structure of the supernova progenitor stars and lead to a better understanding of stellar deaths.

Benefit to National Security Missions

This project will build new Astro-informatics competency to address growing national needs in Space Situational Awareness (SSA), develop new capabilities for the Weapons Program, and test them using actual observations. We will combine observation, theory, and computation to explore the physics of cosmic explosions and contribute to a high-impact time-domain sky survey. This project will position us for a future role in the Large Synoptic Survey Telescope (LSST) survey and will open new opportunities for a major involvement in NASA missions and dark energy investigations identified in the strategic plan of the DOE Office of Science. We will develop novel algorithms for classification and tracking of celestial objects relevant to Space Situational Awareness programs aimed at sponsorship by NASA, Department of Defense, and other WFO organizations. Our models of supernova shock breakout and other explosive transients will test Advanced Simulation and Computing (ASC) capabilities in the critically important regime at the transition between diffusion and free streaming using both flux diffusion and implicit Monte Carlo codes. Ultimately, our nuclear nonproliferation efforts depend on satellite assets that are increasingly vulnerable, driving the need for Space Situational Awareness.

Progress

The work on transient classification and broker infrastructure development is progressing according to our original schedule. For our pixel level classification we constructed a large training data set with 78000 samples with known REAL/BOGUS labels based on the data from the PTF survey. Each sample is a vector of 40 features with additional 3*441 = 1323 features taken directly from new, reference, and subtracted images delivered by the image differencing pipeline. We evaluated the utility of Bayesian networks to classify this data using both structure and parameter learning. While the machine learned networks capture essential relationships considered by domain experts, their performance does not

match that of state of the art algorithms based on decision trees. We obtained a much more reliable pixel level classification using random forests, i.e. randomized collections of decision trees and voting. We also introduced a novel approach that draws on recent advances in computer vision. Using sparse representations with learned dictionaries (over-complete bases) we compute additional image based features. The addition of machine learned features to the baseline set of context features improves the figure of merit by a factor of 2x down to about 4.5% missed detection rate at 1% false positive rate.

We implemented a software package that performs this classification in real time using data from an online database. The current version of the software (RB3.x) has been installed at the NERSC super-computing center that hosts the iPTF database and is being configured for deployment. We launched a successful collaboration with UC Berkeley and JPL to further develop this system.

Our spectral classification effort focused on collecting suitable training data. We completed a preliminary classification run using Support Vector Machines (SVM) applied to several thousand time-resolved medium-resolution spectra of ~450 supernovae from the SNID database. The results are very encouraging with error rates below ~3% on data with high signal-to-noise ratio.

We began the work on event broker infrastructure. The prototype broker is implemented as a set of network servers communicating over TCP/IP sockets. Each stage of processing is encapsulated in a job queue that takes its input from the previous stage and submits jobs to the next one. We also implemented a basic event simulator that generates a stream of measurements from a simulated sky survey and submits this data to the broker using XML based VOEvent messages (a Virtual Observatory standard adopted by the community). Currently the broker performs basic spatio-temporal cross-correlation of measurements with multi-wavelength catalogs and context gathering using several external databases, some of which are replicated locally within the broker.

Since February 2013 the iPTF survey is back on sky and discovered more than 150 supernovae that account for most of the world supply. Using RAPTOR telescopes at LANL we collected multi-color follow-up observations of a nearby type II SN 13aaz discovered by iPTF in M65.

The light-curve simulation program is modeling a range of transient outbursts ranging from the “kilonova” produced in the merger of two neutron stars in a binary to standard models for type II supernovae. One of our key survey suites will focus on the role of circumstellar material (both winds and shell-like outbursts). We launched a web server and a public database supported under the TurboGears web framework that will export our models to researchers at LANL and the public using a sophisticated graphical interface.

As part of our data intensive computing effort we implemented a high-performance database for storing time-resolved imaging data based on advanced spherical indexing (Healpix). The database supports a wide range of spatial scales and pixel sizes suitable for a variety of telescopes and surveys. The system has been tested using ~1TB of images from RAPTOR telescopes.

Future Work

An iterative development schedule will be adopted to synchronize the project with the timetable for the Intermediate Palomar Transient Factory (iPTF). Our goal is to complete the second iteration of the event broker featuring initial versions of algorithms in the summer of 2014 when Spectral Energy Distribution (SED) Machine will be operating on the Palomar 60-inch telescope. We will further develop the data management infrastructure required to support a variety of automated machine learning classifiers and follow-up optimization algorithms that will be gradually integrated with the broker. The work on machine learning classification will focus on high level classification of astrophysical transients using survey data and any available external context data from cross-correlation analysis. An important objective is to implement reliable selection of very young supernovae using low-resolution spectra from SED Machine. We will continue to develop automated follow-up optimization algorithms for the event broker and implement first generation follow-up marshal toolbox to support PTF operations.

Theory and simulation effort will focus on running more supernova simulations that incorporate new atomic physics data and modelling capability. We will simulate and interpret existing PTF observations and generate light curves for available explosion models using our SPECTRUM tool chain. We will upload the first batch of supernova models into the online database that we developed and extend the web interface to this public archive to begin serving synthetic light curves of explosive transients. These light curves will be used to improve supernova selection algorithms.

Data intensive computing work will proceed in parallel. We will continue to integrate additional hierarchical partitioning and indexing schemes in spherical geometry (Hierarchical Triangular Mesh, pgSphere) with the existing framework for parallel hashed tree data structures. We will also create a new training data set using iPTF data collected

since February 2013 to support algorithm development and testing.

Conclusion

Time-domain astrophysics and the science of cosmic explosions are at the forefront of modern astrophysics. The Palomar Transient Factory (PTF) has emerged as the world leader in the exploration of cosmic explosions and the most successful precursor to multi-petabyte sky surveys of the future such as the Large Synoptic Survey Telescope (LSST). The main goal of this project is to develop information technology and data intensive computing infrastructure for the next generation PTF and open the domain of short time-scales (less than 1 day) for exploration by deep wide-area surveys.

Publications

Barth, A. J., A. Voevodkin, D. J. Carson, and P. Wozniak. A Search for Optical Variability of Type 2 Quasars in SDSS Stripe 82. To appear in The Astrophysical Journal.

Frey, L., C. Fryer, and P. Young. Can Stellar Mixing Explain the Lack of Type Ib Supernovae in Long-duration Gamma-Ray Bursts?. 2013. The Astrophysical Journal Letters. 773: L7.

Fryer, C.. Compact Object Formation and the Supernova Explosion Engine. To appear in Classical and Quantum Gravity.

Jin, Z. P., S. Covino, M. Della Valle, P. Ferrero, D. Fugazza, D. Malesani, A. Melandri, E. Pian, R. Salvaterra, D. Bersier, S. Campana, Z. Cano, A. J. Castro-Tirado, P. D'Avanzo, J. P. U. Fynbo, A. Gomboc, J. Gorosabel, C. Guidorzi, J. B. Haislip, J. Hjorth, S. Kobayashi, A. P. LaCluyze, G. Marconi, P. A. Mazzali, C. G. Mundell, S. Piranomonte, D. E. Reichart, R. Sanchez-Ramirez, R. J. Smith, I. A. Steele, G. Tagliaferri, N. R. Tanvir, S. Valenti, S. D. Vergani, T. Vestrand, E. S. Walker, and P. Wozniak. GRB 081007 and GRB 090424: The Surrounding Medium, Outflows, and Supernovae. 2013. The Astrophysical Journal. 774: 114.

Johnson, J., D. Whalen, W. Even, C. Fryer, A. Heger, J. Smidt, and K. J. Chen. The Biggest Explosions in the Universe. 2013. The Astrophysical Journal. 775: 107.

Ofek, E., A. Zoglauer, S. Boggs, N. Barriere, S. Reynolds, C. Fryer, F. Harrison, S. Cenko, S. Kulkarni, A. Gal-Yam, I. Arcavi, E. Bellm, J. Bloom, F. Christensen, W. Craig, W. Even, A. Filippenko, B. Grefenstette, C. Hailey, R. Laher, K. Madsen, E. Nakar, P. Nugent, D. Stern, M. Sullivan, J. Surace, and W. Zhang. SN 2010jl: Optical to hard X-ray observations reveal an explosion embedded in a ten solar mass cocoon. To appear in The Astrophysical Journal.

Palaversa, L., Z. Ivezic, L. Eyer, D. Ruzdjak, D. Sudar, M. Galin, A. Kroflin, M. Mesaric, P. Munk, D. Vrbanec, H. Bozic, S. Loebman, B. Sesar, L. Rimoldini, N. Hunt-Walker, J. VanderPlas, D. Westman, S. J. Stuart, A. Becker, G. Srdoc, P. Wozniak, and H. Olusei. Exploring the Variable Sky with LINEAR. III. Classification of Periodic Light Curves. 2013. The Astronomical Journal. 146: 101.

Sesar, B., Z. Ivezic, S. J. Stuart, D. M. Morgan, A. Becker, S. Sharma, L. Palaversa, M. Juric, P. Wozniak, and H. Olusei. Exploring the Variable Sky with LINEAR. II. Halo Structure and Substructure Traced by RR Lyrae Stars to 30 kpc. 2013. The Astronomical Journal. 146: 21.

Vreeswijk, P., A. Raassen, A. Smette, A. De Cia, P. Wozniak, A. Fox, W. Vestrand, and P. Jakobsson. Time-dependent excitation and ionization modelling of absorption-line variability due to GRB 080310. 2013. Astronomy and Astrophysics. 549: A22.

Whalen, D., J. Johnson, J. Smidt, A. Heger, W. Even, and C. Fryer. The Biggest Explosions in the Universe. II. To appear in The Astrophysical Journal.

Whalen, D., J. Johnson, J. Smidt, A. Meiksin, A. Heger, W. Even, and C. Fryer. The Supernova that Destroyed a Protogalaxy: Prompt Chemical Enrichment and Supermassive Black Hole Growth. 2013. The Astrophysical Journal. 774: 64.

Whalen, D., W. Even, C. Lovekin, C. Fryer, M. Stiavelli, P. Roming, J. Cooke, T. Pritchard, D. Holz, and C. Knight. Illuminating the Primeval Universe with Type IIn Supernovae. 2013. The Astrophysical Journal. 768: 195.

Wozniak, P. R., D. I. Moody, Z. Ji, S. P. Brumby, H. Brink, J. Richards, and J. S. Bloom. Automated Variability Selection in Time-domain Imaging Surveys Using Sparse Representations with Learned Dictionaries. 2013. In American Astronomical Society, AAS Meeting #221. (Long Beach, CA, 6-10 January 2013). , p. #431.05. Washington, DC: American Astronomical Society.

High Performance Atom-Based Sensors for Fields and Rotations

Malcolm G. Boshier
20130058DR

Introduction

The National Security community needs improved sensors for fields and rotations that advance the state of the art in performance, size/weight/power requirements, and ruggedness. We will respond to this challenge by developing new atom-based sensors for magnetic fields, for gravity, and for rotations.

Our approach harnesses unique LANL atomic physics capabilities - the "Painted Potential" for arbitrary manipulation of Bose-Einstein condensate (BEC) matter waves, and high sensitivity atomic magnetometers - in conjunction with the Laboratory's world-class quantum science expertise and its engineering capabilities. We will use the Painted Potential system to create a trapped BEC atom interferometer to measure gravity and (with different programming and detection) a rotation sensor based on an "Atom-SQUID." This new device is a matter wave analog of the well-known superconducting SQUID used for magnetic field sensing.

We will also advance the state of the art in magnetometry by pushing atomic magnetometers to their fundamental limits and by combining an atomic magnetometer with the Painted Potential to form a high resolution high sensitivity magnetic microscope. We will develop the theoretical description of these devices and also explore possibilities for quantum enhanced measurement, using quantum correlations to obtain measurement precision which beats the standard quantum limit (shot noise). Most of the size/weight/power requirements in these atom-based sensors are associated with optics and electronics, and so we will engineer those components to minimize their impact on the total sensor package. We will build a prototype atom magnetometer which can operate outside of the laboratory and beat the performance of the best commercial magnetometers by at least an order of magnitude.

The outcome of this project will be a new capability which can help meet Intelligence and Defense community needs for improved sensors.

Benefit to National Security Missions

Improved rotation sensors, gravity sensors and magnetometers are of broad interest to many agencies in the Intelligence and Defense Communities. Device applications include respectively inertial navigation, detection of underground structures and of oil or mineral deposits, and the use of power lines for communication and for characterization of activities in inaccessible facilities.

The devices based on quantum technologies that are the focus of this project offer potential gains in Size, Weight, and Power (SWaP) and in sensor performance. Theory predicts that the Atom-SQUID we will build should have state of the art rotation sensitivity, in a physics package which is much smaller than the Sagnac atom interferometers which currently have the best performance. A BEC waveguide atom interferometer would measure gravity precisely with a compact device that has no moving parts subject to wear. We will engineer atomic magnetometer technology into a portable device, taking atomic magnetometry from the laboratory to the field.

Finally, while our focus in this project is on applications to sensing, the BEC technologies that we are developing are also very relevant to quantum information processing and hence the Information Science and Technology Mission.

Progress

The magnetometer engineering team's task is to build a version of the laboratory Atomic Magnetometer (AM) lab instrument that can operate out in the field. Tasks partially or fully completed to date include the hardware circuit board and software interface to the laser diode controllers, a Helmholtz coil assembly and associated current drivers and low sensitivity magnetic field sensor all used to cancel the Earth's magnetic field, the stand-

alone power supply, the user interface, photodiode pre-amplifier and digitizer, and the enclosure. An isolated test bed has been identified, and initial baseline measurements have been made to characterize the location with commercial sensors. Signal sources to be used in the comparisons have also been identified.

The laboratory magnetometer team focused on improving AM performance in both low and high frequency regimes. A fiber-compatible polarization modulator is being investigated as a path to delivering low-frequency performance closer to fundamental limits. We also analyzed the performance of typical high frequency magnetometers and found significant discrepancies between measured performance and the fundamental limits expected from theory. We are now working on understanding these discrepancies and developing strategies to remove them.

The BEC team, having realized Josephson Junctions for a BEC in a toroidal trap, a so-called "Atom SQUID", began experiments to demonstrate rotation sensing with this device. There are two possible methods for the sensing of rotation by Atom SQUIDs. One is measuring the maximum velocity at which the BEC can flow around the torus without loss (the critical current) because that turns out to be a sinusoidal function of the rotation rate. The other examining which of the allowed quantized rotation states are chosen by the BEC when it is created in the torus, because if the experiment is rotating higher rotational states will be found more often. These two methods have now been tested and proof of principle results obtained for both approaches. At the same time we have been developing a theory of the Atom SQUID based on the well established theory of SQUIDs. This preliminary experimental and theoretical work so far supports our proposal that a compact highly sensitive rotation sensor may be built with Atom SQUIDs.

The quantum theory team has been studying the origin of interference in Bose-Einstein condensates. This is an important issue for the project because the gravity sensor to be constructed will be read out using the interference of matter waves. The usual experimental setup -- with two initially separated clouds of BEC -- precludes the existence of a preexisting phase as each cloud contains a fixed number of atoms (so, by Heisenberg's indeterminacy relations, its phase must be completely undefined). Yet, as a pioneering experiment showed, interference fringes do indeed form when the clouds are allowed to expand into each other. The standard explanation of this phenomenon attributes appearance of the interference pattern to the measurement carried out by photons that scatter from the atoms. We are considering a version of the experiment relevant to this project, where each cloud is split in two and these sub-clouds expand into each other in two arms of the interferometer. The question is whether the interference fringes that will presumably form within the two arms will be correlated, with peaks and troughs of the interference patterns aligned. The team has also investigated the maximum speed permitted by the laws of physics for manipulating matter waves, and how these limits might be reached in the laboratory. Finally the theory team has also been examining the static properties of a single impurity atom immersed in a BEC. We found that the state of the impurity atom can be extremely sensitive to the interactions with the BEC, which are themselves strongly affected by magnetic fields. We also discovered a deep and unexpected connection to polaron physics: a cold atom BEC can provide the first host medium to self-localize polarons both in a bubble state, analogous to electron bubbles in helium, as well as in a Landau-Pekar state, analogous to the self-localized electron in a dielectric crystal. We found that the system can be characterized by only two dimensionless coupling strengths and we showed that the system smoothly crosses over between the two states in the corresponding two-dimensional phase diagram.

Future Work

The project is developing three types of sensor, all based on atomic physics technologies. Two exploit our capability for manipulating Bose-Einstein condensates (BEC), a state of matter formed when atoms in a trapping potential (in our case the Painted Potential) are cooled to temperatures very close to absolute zero.

First, we will continue investigating the application of cold atoms to rotation sensing. Here we form a BEC in a toroidal trap with two thin potential barriers positioned diametrically opposite each other. Simple theory and our FY13 experiments imply that the maximum matter wave current able to flow without friction in this "Atom-SQUID" device is a sensitive function of the speed of rotation. In FY14 we will perform detailed experiments to investigate this property of the device. We will also continue developing a proper quantum theory for the Atom-SQUID, and begin to use it to devise optimum measurement strategies for the rotation measurement to be performed in FY14.

Second, in FY14 we will start investigating the performance of the Painted Potential as an atom interferometer to measure gravity. A single BEC will be divided into two pieces which sit at slightly different heights above the Earth. Releasing the two pieces of BEC allows them to overlap and form matter wave interference fringes which can be used to measure gravity. In FY14 we plan to begin construction of a second Painted Potential machine dedicated to these atom interferometry experiments. We will also begin

related theoretical investigations.

Third, we will continue development of atom magnetometers. The engineered atomic magnetometer instrument being designed in FY13 will be completed and tested in FY14. We will study the performance of laboratory atomic magnetometers with the goal of improving their performance towards the fundamental limits set by shot noise.

Conclusion

The overall goal of this project is to develop new atom-based sensors for magnetic fields, for gravity, and for rotations that advance the state of the art in performance, size/weight/power requirements, and ruggedness. We will move atomic magnetometers from the laboratory to the field, where they will advance applications ranging from to facility characterization via power line forensics to biophysics. We will start developing cold atom-based rotation sensors that would ultimately realize compact high-performance interial navigation systems. We will also build gravity sensors with the potential to out-perform current gravimeters, particularly in applications such as underground structure detection.

Publications

Blinova, A. A., M. G. Boshier, and E. Timmermans. Two polaron flavors of the Bose-Einstein condensate impurity. To appear in Physical Review A.

Campo, A. del. Shortcuts to adiabaticity by counter-diabatic driving. 2013. Physical Review Letters. 111: 100502.

Campo, A. del, I. L. Egusquiza, M. B. Plenio, and S. F. Huelga. Quantum Speed Limits in Open System Dynamics. 2013. Physical Review Letters. 110: 050403.

Ryu, C., P. W. Blackburn, A. A. Blinova, and M. G. Boshier. Experimental realization of Josephson junctions for an atom SQUID. To appear in Physical Review Letters.

Torrontegui, E., S. Ibanez, S. Martinez-Garaot, M. Modugno, A. del Campo, D. Guery-Odelin, A. Ruschhaupt, X. Chen, and J. G. Muga. Shortcuts to Adiabaticity. 2013. ADVANCES IN ATOMIC, MOLECULAR, AND OPTICAL PHYSICS, VOL 62. 62: 117.

Quantum Chemistry, Information, Materials and Metrology

Robert E. Ecke
20130727DR

Introduction

The goals of this project are to develop collaborative scientific progress at the interfaces of quantum chemistry and materials, quantum information and communication, and quantum optics. In particular, we will explore the intersection of quantum information, communication and computing with new materials functionality such as chiral superconductors and topological insulators and also with novel detection technology such as ultra-sensitive scanned probes. We will develop new computational approaches based on algorithms developed in quantum information science to more efficiently solve numerically quantum condensed matter models. We will explore the fascinating overlap between cold atom physics, with its pure systems and tunable properties, and technologically important materials systems such as superconductors and multiferroic materials. In this latter category, the interplay between electrons and the underlying field leads to exotic states of matter that can provide novel properties or functionalities such as magnetic control of transport properties (anomalous Hall effect), strong vortex pinning (high critical currents) in superconductors, and large magneto-electric effects in insulators. Through our theory and simulations we will identify classes of models and materials where this new functionality can be realized. We will use hybrid quantum chemistry and molecular mechanical methods to incorporate solvent and thermal fluctuation properties of real molecular systems and apply this new phenomenology to carbon nanotubes and biological light harvesting systems. We will investigate fluctuation induced quantum Casimir forces, and corresponding classical analogs, for equilibrium and nonequilibrium conditions. Our external collaborations will enable the use of opto-mechanical resonators for quantum communication, for fundamental studies of quantum friction, and for atomically-resolved spectroscopic scanned probe measurements of condensed matter systems such as quantum phase transitions occurring in novel systems of competing magnetic and superconducting order.

Benefit to National Security Missions

Novel applications of quantum science underpin numerous Laboratory efforts including quantum information that can enable secure data communication, new approaches to quantum devices such as a topological quantum memory, and improved algorithms for simulating scientific problems. Secure data communication has implications for classified environments and for the physical security of infrastructure systems such as the electrical power grid. Novel concepts in manipulating quantum systems will have impact on Laboratory materials strategy including under-standing the properties of actinides, in particular plutonium. Possible new quantum sensors could impact GS programs. We strongly impact DOE Office of Science mission in the fundamental understanding of electronic and magnetic materials with applications in energy, electronics, and computing. The ability to support both a robust fundamental science capability and nurture new applications will continue to drive our work in the quantum arena.

Progress

During FY13, we made the following progress:

- Demonstrated that magnetic vortex crystals are induced by magnetic field in certain classes of frustrated Mott insulators. Such materials, i.e. spontaneous crystals of topological spin structures, are attracting an enormous interest because they can provide new directions for future spin-electronic technology. We also showed how the magnetic excitations, i.e., “magnons”, of the fully polarized state a a quantum antiferromagnet in a a strong magnetic field form a diverse set of Bose-Einstein condensate states.

- Proposed a scheme using optimal control to achieve, in laser cooledatomic gases, temperatures closer to absolute zero than those currently possible - Phys. Rev. A 87, 043607 (2013).

- Developed a theory for the effects of time-dependent noise in thermally isolated systems - Phys. Rev. A 87, 043607 (2013).

- Predicted novel states of matter characterized by the coexistence of the integer quantum hall effect and spin ice and described the presence of novel anyonic excitations in metallic magnets.

- Developed an exciton scattering (ES) approach for efficient calculations of optical spectra in branched conjugated macromolecules, as an extension of reference quantum-chemical (QC) technique. We verified he applicability of the ES approach using the natural atomic orbital (NAO) analysis on ab initio QC computations. Excellent agreement for the absorption spectra between the ES approach and the direct quantum chemistry was achieved - J. Phys. Chem. Lett. 2012, 3 and other submitted papers.

- Began development of an extremely sensitive quantum magnetometer and applied it to the detection of ultrasmall magnetic fields originating from areas of only few square millimeters. The magnetometer is based on detecting the dynamics of atomic spins confined in a vapor cell kept at close to room temperature. This research lays the foundation for future exploration of cold atom magnetometers - Journal of Magnetic Resonance 231 (2013), p.39-45.

- Proposed a novel measurement approach that extends the domain of applications of the experimental technique (first developed at LANL) called spin noise spectroscopy - Appl. Phys. Lett. 102, 202405 (2013). In related work, we found a new capability of spin noise spectroscopy that allows characterization of semiconductor nanostructures.

Future Work

Overall, we will work at the interdisciplinary intersections of the fields of quantum science with an emphasis on Quantum Chemistry, Quantum Information and Communication, Atomic-Molecular-Optical (AMO) and Quantum Optics, and Quantum Materials. We will develop synergies among the topics but within each topic our set of goals is as follows:

Quantum Chemistry

We will 1) improve quantum chemical numerical approaches to incorporate non-adiabatic processes, solvent and thermal effects, and many atom simulations to better model complex quantum chemical processes; 2) Model ultrafast relaxation processes in carbon nanotubes which have important applications in electronics and optical materials; 3) Determine the role of long-lived electronic coherence in photosynthetic proteins that exhibit light-harvesting properties.

Quantum Information and Communication

We will 1) Develop applications of quantum channel capacity for quantum communication applications that provide secure communication; 2) Explore the intersection of quantum information algorithms and condensed matter systems to better compute the properties of magnetic spin systems; 3) Investigate utility of using topological entities for quantum computing applications such as computer memory.

AMO and Quantum Optics

We will 1) Develop theory and simulations for fluctuation-induced interactions in nanostructures, including Casimir forces, near-field heat transfer, patch effects, and quantum friction; 2) Explore the use of structuring for novel optical and acoustical phenomena in metamaterials, including sub-wavelength imaging, perfect absorbers; 3) Use cold atom methods as an ultra-sensitive magnetic field sensors.

Quantum Materials

We will 1) Exploit new efficient algorithms for treating quantum spins in classical fields to explore novel phases of fermionic matter that could lead to new functional materials; 2) Explore the use of topological entities for implementing quantum memory; 3) Investigate, using theory, simulation, and experiment, the properties of strongly correlated electron systems with novel magnetic, multi-ferroic and superconducting properties

Conclusion

Quantum science is an integrating centerpiece of numerous LANL strategic directions including information science, sensing, and materials. By supporting an interdisciplinary approach that ranges from fundamental science to applications, our work develops research collaborations among different quantum science areas, sustains and encourages broad scientific capability, and assists in identifying novel and transformational science frontiers at the interface of national security and discovery science.

Publications

Barros, K., and Y. Kato. Efficient Langevin Simulation of Coupled Classical Fields and Fermions. 2013. Arxiv.

Behunin, R. O., D. A. Dalvit, R. S. Decca, and C. C. Speake. Limits on the accuracy of isoelectronic gravity measurements at short separation due to patch potentials. 2013. Arxiv.

Campo, A. del. Shortcuts to Adiabaticity by Counterdiabatic Driving. 2013. Physical Review Letters. 111 (10):

100502.

Campo, A. del, I. L. Egusquiza, M. B. Plenio, and S. F. Huelga. Quantum Speed Limits in Open System Dynamics. 2013. Physical Review Letters. 110 (5): 050403.

Campo, A. del, J. Goold, and M. Paternostro. More bang for your buck: Towards super-adiabatic quantum engines. 2013. Arxiv.

Campo, A. del., T. W. Kibble, and W. H. Zurek. Causality and non-equilibrium second-order phase transitions in inhomogeneous systems. 2013. Journal of Physics: Condensed Matter. 25 (40): 325701.

Chern, G., A. Rahmani, I. Martin, and C. Batista. Quantum Hall ice. 2012. Arxiv.

D'Alessio, L., and A. Rahmani. Thermally isolated Luttinger liquids with noisy Hamiltonians. 2013. Physical Review B. 87 (17): 174301.

Impens, F., R. Behunin, C. C. Ttira, and P. Maia. Neto. Non-local double-path Casimir phase in atom interferometers. 2013. EPL (Europhysics Letters). 101 (6): 60006.

Intravaia, F., R. O. Behunin, and D. A. Dalvit. Quantum friction and non-equilibrium fluctuation theorems. 2013. Arxiv.

Kamiya, Y., and C. Batista. Magnetic vortex crystals in frustrated Mott insulator. 2013. Arxiv.

Kato, Y.. Multidiscontinuity algorithm for world-line Monte Carlo simulations. 2013. Physical Review E. 87 (1): 013310.

Kim, J. W., Y. Kamiya, E. D. Mun, M. Jaime, N. Harrison, J. D. Thompson, H. T. Yi, Y. S. Oh, S. -W. Cheong, C. D. Batista, and V. S. Zapf. Multiferroicity with coexisting isotropic and anisotropic spins in Ca$_{3}$Co$_ {2-x}$Mn$_{x}$O$_{6}$. 2013. Arxiv.

Koutroulakis, G., T. Zhou, C. D. Batista, Y. Kamiya, J. D. Thompson, S. E. Brown, and H. D. Zhou. Magnetic Phases of the Spin-1/2 Triangular-Lattice Antiferromagnet Ba3CoSb2O9. 2013. Arxiv .

Li, H., C. Wu, S. V. Malinin, S. Tretiak, and V. Y. Chernyak. Exciton Scattering Approach for Spectroscopic Calculation of Branched Conjugated Oligomers. Accounts of Chemical Research.

Li, H., S. Malinin, S. Tretiak, and V. Chernyak. Effective tight-binding models for excitons in branched conjugated molecules. 2013. The Journal of Chemical Physics. 139 (6): 064109.

Lin, S., and D. Roy. Role of kinetic inductance in transport properties of shunted superconducting nanowires. 2013. Journal of Physics: Condensed Matter. 25 (32): 325701.

Muniz, R., Y. Kato, and C. Batista. Generalized spin-wave theory: application to the bilinear-biquadratic model. 2013. Arxiv.

Pershin, Y., V. Slipko, D. Roy, and N. Sinitsyn. Two-beam spin noise spectroscopy. 2013. Applied Physics Letters. 102 (20): 202405.

Pyka, K., J. Keller, H. L. Partner, R. Nigmatullin, T. Burgermeister, D. M. Meier, K. Kuhlmann, A. Retzker, M. B. Plenio, W. H. Zurek, A. del Campo, and T. E. Mehlstäubler. Topological defect formation and spontaneous symmetry breaking in ion Coulomb crystals. 2013. Nature Communications. 4: 3291.

Rahmani, A., R. Muniz, and I. Martin. Anyons in Integer Quantum Hall Magnets. 2013. Physical Review X. 3 (3): 031008.

Rahmani, A., T. Kitagawa, E. Demler, and C. Chamon. Cooling through optimal control of quantum evolution. 2013. Physical Review A. 87 (4): 043607.

Rahmani, A., and G. Chern. Universal Rényi mutual information in classical systems: The case of kagome ice. 2013. Physical Review B. 88 (5): 054426.

Roy, D.. Cascaded two-photon nonlinearity in a one-dimensional waveguide with multiple two-level emitters. 2013. Scientific Reports. 3: 02337.

Roy, D.. Two-photon scattering of a tightly focused weak light beam from a small atomic ensemble: An optical probe to detect atomic level structures. 2013. Physical Review A. 87 (6): 063819.

Roy, D., C. J. Bolech, and N. Shah. Nature of the zero-bias conductance peak associated with Majorana bound states in topological phases of semiconductor-superconductor hybrid structures. 2013. Arxiv .

Roy, D., N. Bondyopadhaya, and S. Tewari. Topologically trivial zero-bias conductance peak in semiconductor Majorana wires from boundary effects. 2013. Physical Review B. 88 (2): 020502.

Roy, D., Y. Li, A. Greilich, Y. Pershin, A. Saxena, and N. Sinitsyn. Spin noise spectroscopy of quantum dot molecules. 2013. Physical Review B. 88 (4): 045320.

Savukov, I., and T. Karaulanov. Magnetic-resonance imaging of the human brain with an atomic magnetometer. 2013. Applied Physics Letters. 103 (4): 043703.

Savukov, I., and T. Karaulanov. Anatomical MRI with an

atomic magnetometer. 2013. Journal of Magnetic Resonance. 231: 39.

Shimada, H., J. L. Jacobsen, and Y. Kamiya. Phase diagram and the strong-coupling fixed point in the disordered O(n) loop model. 2013. Arxiv.

Torrontegui, E., S. Ibáñez, S. Martínez-Garaot, M. Modugno, A. del Campo, D. Guéry-Odelin, A. Ruschhaupt, X. Chen, and J. G. Muga. Chapter 2 - Shortcuts to Adiabaticity. 2013. In Advances in Atomic, Molecular, and Optical Physics. Edited by Arimondo, E., P. R. Berman, and C. C. Lin. Vol. Volume 62, p. 117. -: Elsevier.

Zhang, Z., K. Wierschem, I. Yap, Y. Kato, C. Batista, and P. Sengupta. Phase diagram and magnetic excitations of anisotropic spin-one magnets. 2013. Physical Review B. 87 (17): 174405.

Non-Equilibrium Phenomena in Materials, Fluids, and Climate

Robert E. Ecke
20130728DR

Introduction

This project develops collaborative scientific progress at the interfaces of hard materials, soft condensed matter physics, and fluid dynamics. In particular, we consider the structure and properties of disordered materials with emphasis on the role of topological defects, for example dislocations. We are exploring the connection between the behaviors of materials under shear with "universal" scenarios developed in the context of glasses and granular materials as well as more recently in the context of plastic flow via dislocations and thermally activated avalanches. We will measure the pair distribution function of geopolymers using neutron scattering and compare with molecular dynamics simulations. We will look for similarities between the transition from reversibility to irreversibility in materials under shear and soft condensed matter systems such as colloidal suspensions. Reversible and irreversible behavior and the associated kinetics are at the heart of the complex hysteresis and metastability governing the microstructure of materials that have been shocked. We are attempting to describe the universal behavior of phase transforming materials subjected to extremes by departing from the traditional approach of using equilibrium phase diagrams and notions and emphasize the importance of shear. We will understand and characterize how granular material properties can affect earthquake dynamics. We will relate laboratory experiments in rotating and/or stratified flows to asymptotically exact mathematical predictions and to applications in regional climate models such as heat transport in arctic oceans. Our external collaborations enable the cooperative study of porous media flows relevant to carbon sequestration, the exploration of turbulent mixing in the oceans, the description and characterization of radiation damage in materials, and the integration of perspectives on elastic-plastic deformation from both hard and soft matter points of view. These projects support LANL strategic goals in materials, in energy and climate, and in materials under extreme conditions.

Benefit to National Security Missions

The materials research that we propose is squarely in the mesoscopic regime where the discreteness of, for example, dislocations at atomistic scales encounters the elastic plastic continuum at macroscopic scales. This area is an important foundation for the MaRIE program and is applicable to recent DOE/BES priorities in fundamental materials research. Advances in this area would lead to better understanding and modeling of materials, allowing new applications. Improving our understanding of turbulence is relevant to the weapons program.

Progress

During FY13, we have made the following progress:

- Developed a careful mathematical analysis of scale decomposition and nonlinear dynamics in highly compressible turbulent flows. Our work provides a rigorous framework upon which earlier published work rests and shows how a proper density weighting allows the unravelling of an inertial scale-range over which viscous dynamics and external forcing are negligible. This gives a solid mathematical basis to attempts at extending Kolmogorov's potent ideas on a turbulent inertial range cascade to compressible turbulence. It shows that direct viscous effects on large-scale dynamics do not need to be modeled. It also shows that there is a new cascade mechanism that results intrinsically from compressibility effects of density fluctuations and pressure gradients that are not present in incompressible flows and needs to be modeled properly - Physica D: Nonlinear Phenomena 247 (1), 54–65 (2013)

- Showed that a key result by Hannes Alfven (Nobel Prize in Physics, 1970) can break down in the presence of strong nonlinear flow effects such as turbulence. Our work may answer a long-standing mystery in plasma physics and astrophysics on how magnetic reconnection takes place over fast time-

scales forbidden by Alfven's result yet manifested around us all the time in various forms such as solar flares and coronal mass ejections. The study combined interdisciplinary expertise in astrophysics, applied mathematics, fluid mechanics, data management, and computer science and adopted a fundamentally new approach to analyzing very large datasets. We conducted a state-of-the-art computer simulation, used novel ground-breaking database methods combined with high-performance computing techniques and original mathematical developments to make our compelling case that nonlinear flow interactions (or turbulence) alone can explain the phenomenon of fast magnetic reconnection - Nature 497, 466-469 (2013).

- Developed a novel experimental diagnostic capability to measure simultaneous temperature and velocity in rotating convection to characterize the heat transport efficiency of vortical structures. Such structures may be related to upwelling structures in the ocean that are important in heat transport efficiency that ultimately impact climate evolution. We use thermochromic liquid crystals to provide the dynamics of the overall temperature field of the vortex, use high precision thermal probes to measure vertical correlations associated with thermal vortical structures, and use particle tracking methods to determine the fluid velocity field.

- Characterized the onset of irreversibility in periodically sheared amorphous media. An important aspect of the physics of amorphous solids is the onset of irreversible behavior usually associated with yield. Using quasi-static molecular dynamics simulations, we observe a transition from reversible to irreversible deformation at a critical strain amplitude. For small strain amplitudes the system exhibits a noisy but repetitive limit-cycle. For large strain amplitudes, however, the behavior becomes chaotic (shows sensitivity to initial conditions) and thus irreversible. We suggest that the chaotic behavior is a result of the shear band instabilities that arise for large strains and the convective displacement fields they create.

Future Work

The overall structure of our work is in Structural Materials, Soft Condensed Matter Systems, and in Fluids and Climate. We seek synergistic efforts to emerge among topics but report our directed tasks in each area:

Structural Materials

We will 1) Explore complex hysteretic and metastable behavior in driven systems, including the role of topological defects in phase transformations and in elastic-plastic deformation; 2) Characterize glassy polymers using a combination of experimental neutron scattering PDF measurements and molecular dynamics simulations; and 3) Investigate novel properties and functions of geometrically frustrated materials.

Soft Condensed Matter Systems

We will 1) Develop models of the structural properties of bio-polymers such as DNA; 2) Explore sheared granular media and its relationship to earthquake dynamics; and 3) Investigate the reversibility transition, discovered in particle-fluid systems, for weakly sheared disordered materials.

Fluids and Climate

We will 1) Investigate mass transport properties of porous media flows, including differences between 2D and 3D geometries and comparisons with numerical simulations; 2) Measure heat transport, test asymptotic scaling in rotating Rayleigh-Bénard convection, and visualize vortical columns that transport heat; and 3) Explore how ocean phenomena at multiple length and time scales accumulate to produce the large-scale circulation responsible for the heat and tracer transport affecting the global climate.

Conclusion

The goals of this project are to develop collaborative scientific progress at the interfaces of hard materials, soft condensed matter physics, and fluid dynamics. We will develop models to connect to fundamental experiments, build theoretical frameworks, and perform mathematical analysis and computer simulations. We expect our results to impact applications such as geophysical fluid dynamics related to climate modeling.

Publications

Aluie, H.. Scale decomposition in compressible turbulence. 2013. Physica D: Nonlinear Phenomena. 247 (1): 54.

Ben-Naim, E., and P. L. Krapivsky. Discrete analogue of the Burgers equation. 2012. Journal of Physics A: Mathematical and Theoretical. 45 (45): 455003.

Chu, H., C. Zhou, J. Wang, and I. J. Beyerlein. An Analytical Model for the Critical Shell Thickness in Core/Shell Nanowires Based on Crystallographic Slip. 2013. J. 61 (11): 2147.

Ecke, R., and J. Niemela. Heat transport in the geostrophic regime of rotating Rayleigh-Bernard convection. Physics Review Letters.

Eyink, G., E. Vishniac, C. Lalescu, H. Aluie, K. Kanov, K. Bürger, R. Burns, C. Meneveau, and A. Szalay. Flux-freezing breakdown in high-conductivity magnetohydrodynamic turbulence. 2013. Nature. 497 (7450): 466.

Gupta, S., and A. Saxena. Negative Gaussian curvature distribution in physical and biophysical systems—Curved nanocarbons and ion-channel membrane proteins. 2012. Journal of Applied Physics. 112 (11): 114316.

Kent, J., J. P. Whitehead, C. Jablonowski, and R. B. Rood. Potential Vorticity: A diagnostic tool for general circulation models. Quarterly Journal of the Royal Meteorological Society.

Provis, J., A. Hajimohammadi, C. White, S. Bernal, R. Myers, R. Winarski, V. Rose, T. Proffen, A. Llobet, and J. J. van Deventer. Nanostructural characterization of geopolymers by advanced beamline techniques. 2013. Cement and Concrete Composites. 36: 56.

Regev, I., T. Lookman, and C. Reichhardt. Onset of Irreversibility and Chaos in Amorphous Solids Under Periodic Shear. 2013. arXiv.org.

Regev, I., and C. Reichhardt. Rheology and shear band suppression in particle and chain mixtures. 2013. Physical Review E. 87 (2): 201.

Reichhardt, C., J. Drocco, C. J. Reichhardt, and A. R. Bishop. Statics and Dynamics of Vortex Matter with Competing Repulsive and Attractive Interactions. 2013. Journal of Superconductivity and Novel Magnetism. : 1.

Rivera, M., H. Aluie, and R. Ecke. The direct enstrophy cascade of two-dimensional soap film flows. Physics of Fluids.

Wang, J., R. Zhang, C. Zhou, I. Beyerlein, and A. Misra. Characterizing interface dislocations by atomically informed Frank-Bilby theory. 2013. Journal of Materials Research. 28 (13): 1646.

Wang, X., and J. Whitehead. A bound on the vertical transport of heat in the 'ultimate' state of slippery convection at large Prandtl numbers. 2013. Journal of Fluid Mechanics. 729: 103.

White, C., G. Kearley, J. Provis, and D. Riley. Structure of kaolinite and influence of stacking faults: Reconciling theory and experiment using inelastic neutron scattering analysis. 2013. The Journal of Chemical Physics. 138 (19): 4501.

White, C., J. Provis, B. Bloomer, N. Henson, and K. Page. In situ X-ray pair distribution function analysis of geopolymer gel nanostructure formation kinetics. 2013. Physical Chemistry Chemical Physics. 15 (22): 8573.

White, C., K. Page, N. Henson, and J. Provis. In situ synchrotron X-ray pair distribution function analysis of the early stages of gel formation in metakaolin-based geopolymers. 2013. Applied Clay Science. 73: 17.

Zhou, C., J. Su, M. Graf, C. Reichhardt, A. Balatsky, and I. Beyerlein. Plastic response of dislocation glide in solid helium under dc strain-rate loading. 2013. Physical Review B. 88 (2): 4513.

CLEAN Detection and Identification of Dark Matter

Andrew Hime
20100063DR

Abstract

MiniCLEAN, a first-generation dark matter experiment with a target (fiducial) mass of 500 kg (150 kg), will be the first "single-phase" liquid argon detector including full 3-D event position reconstruction capability. The ability to inject a radioactive spike of 39Ar into the MiniCLEAN detector provides a unique opportunity to study background discrimination at the unprecedented level of parts in 1010. The data from MiniCLEAN will inform the ultimate background rejection capability of next generation experiments and provide the bedrock for design of a massive detector capable of extending the reach for WIMP dark matter by several orders of magnitude. Funding from this LDRD project has culminated in the concept, engineering design and fabrication of the MiniCLEAN detector. The detector is presently being assembled in the Cube-Hall at SNOLAB with collaborators from the United States, the United Kingdom and Canada.

Background and Research Objectives

It is now generally accepted in the scientific community that roughly 85% of the matter in the universe is in a form that neither emits nor absorbs electromagnetic radiation. Multiple lines of evidence from cosmic microwave background probes, measurements of galaxy cluster and galaxy rotation curves, strong and weak gravitational lensing and big bang nucleosynthesis all point toward a cosmological concordance model containing cold dark matter particles as the best explanation for the universe we see. Alternative theories involving modifications to Einstein's theory of gravity have not been able to explain the observations across all scales. A compelling candidate for dark matter is Weakly Interacting Massive Particles (WIMPs) that could be directly detected as they scatter from massive, ultra-pure detector targets operating deep beneath the Earth's surface.

The challenge to realizing sensitive dark matter detectors is in separating ubiquitous backgrounds from the nuclear-recoil events characteristic of the WIMP signature. Indeed, we face the daunting task of separating a single event in a tonne of target material or more following a year's exposure. Noble liquid detectors exploiting liquid xenon (LXe) or liquid argon (LAr) hold great promise in realizing this intimidating goal (Figure 1). LANL scientists co-invented and are spearheading a novel approach, dubbed CLEAN for Cryogenic Low-Energy Astrophysics with Noble Liquids, to the direct detection of dark matter using the unique capabilities of LAr for unprecedented discrimination between electromagnetic backgrounds (electrons and gamma rays) and nuclear-recoil events characteristic of the WIMP signature [1]. CLEAN is unique in its ability to exchange the LAr target with liquid neon (LNe) in the same detector, offering a means to further distinguish a potential WIMP signal from radioactive background and further expanding its scientific portfolio to the detection of low-energy neutrinos.

Our vision for a single-phase dark matter experiment has from the very beginning been focused on getting to very large-scale detectors. In this approach, a very large detector does not just have increased target mass for WIMP detection, it also has fewer sources of background, is easier to model precisely and understand, and in many ways is easier to build. The cost of increased size scales more slowly than the increase in surface area, hence far more slowly than the increase in target mass. We therefore believe the single-phase approach achieves the best WIMP sensitivity for the lowest cost. Figure 2 shows the basic design of a single-phase LAr detector, indicating the central LAr volume and the wavelength-shifting layer of tetra phenyl butadiene (TPB) used to convert the 128nm UV scintillation photons created in the argon to optical light detectable by the 4-π array of PMTs.

Scientific Approach and Accomplishments

As is the case for all of the noble liquids, LAr is naturally transparent to its own scintillation light and can be made very pure, leading to long attenuation lengths for the UV

photons. Most critically, the time profile of the scintillation light created by the nuclear recoil signal is dramatically different than that for electron-like backgrounds. Ionizing radiation passing through a noble liquid leads to the formation of dimers in both singlet and triplet states. When these states decay, they create ultraviolet scintillation light. LAr is special in that the lifetimes of these states are vastly different---6 ns for the singlet and 1.6 μs for the triplet---and the relative amplitudes of these states depend on the type of ionizing radiation. Boulay and Hime recognized in ref.[1] this utility for dark matter detection in LAr. The rejection made possible by this timing difference is crucial because beta decays of intrinsic ("internal") 39Ar are the only background that large size cannot mitigate.

A significant effort has gone into the design, engineering and evaluation of the MiniCLEAN detector [2]. The central detector, shown in Figure 3, is composed of three major elements, an Inner Vessel (IV) that contains the liquid cryogen, an array of 92 Optical Cassettes that are inserted into the IV and define the inner target region, and an Outer Vessel (OV) that provides secondary containment and the necessary thermal insulation of the inner cryostat. The detector will be shielded by 150 cm of water with an active muon veto and operated 6800 feet underground in the Cube Hall at SNOLAB.

With a team of engineers, designers and safety experts at LANL, the collaboration has ensured that all of the MiniCLEAN detector components can meet the physics goals of the experiment through a safe design. Finite element analyses, calculations of loads and pressures, thermal stresses, and evaluation of fault conditions have been performed for each component. Experts in cryogenic and pressure vessels have performed calculations to determine the necessary relief systems needed on the OV and IV to safely contain any system failures that would lead to boil-off of the cryogen. In addition, a full hazard analysis plan has been developed to mitigate all possible hazards: seismic, fire, fall, cryogenic and oxygen deficiency, pressure, chemical, electrical, radiation, lifting, and drowning. Figure 4 indicates some of the major elements of fabrication and construction made possible with funding from this LDRD project.

The primary risks to the viability of the single-phase approach are associated with the expected light yield (which affects energy threshold, position reconstruction, and particle identification), the efficacy of neutron tagging, and the development and measurement of 39Ar background rejection using pulse-shape discrimination (PSD). The upcoming MiniCLEAN run, which is funded in FY14 through the DOE Office of High Energy Physics, provides us with an excellent opportunity to demonstrate all salient technical capabilities of the single-phase approach. MiniCLEAN is large enough that it allows us to test our entire suite of background rejection tools with 3-D event reconstruction, and we will deploy the requisite calibration sources to test our detector model in detail.

Establishing a high statistics measure of the PSD capability in LAr that is meaningful for a large dark matter experiment (~1010 events) is challenging, to say the least. This will be possible in the MiniCLEAN detector where 1010 decays will be recorded during a dedicated run with a 39Ar spike for a period of ~100 days. The 39Ar radioactivity has been available through LANL's radioisotope program and will be extracted and purified in Nuclear Chemistry Division's "hot-cell". When injected into MiniCLEAN, the acquired data sample will have utility in informing the capabilities and limitations of multi-tonne, second generation detectors such as DEAP-3600 and DarkSide and a potential third generation detector using a target mass ~100x larger than MiniCLEAN. Ultimately, we want to be able to generate an understanding of the PSD capability in LAr as a function of energy threshold and target mass and at what point it becomes necessary to consider the added expense and complexity of using argon depleted of 39Ar.

The PSD calibration using the 39Ar spike in MinCLEAN will improve our knowledge of the capabilities of LAr by about two orders of magnitude beyond that demonstrated in our smaller prototype detectors. It is pertinent to emphasize that MiniCLEAN is the only experiment advertised to perform dedicated measurements of 39Ar PSD capability with adequate statistics using a radioactive spike. While our aim is to inform the design of the much larger, third generation LAr detector, such measurements will have immediate utility for next generation experiments like DEAP-3600, which will utilize a 3600 kg target of LAr and operate adjacent to MiniCLEAN in the Cube-Hall at SNOLAB. If DEAP-3600 should see events in the nuclear recoil region-of-interest, it will not be possible to know, a priori, that it isn't background leakage from 39Ar apart from extrapolation from a model for PSD. MiniCLEAN will allow a direct prediction of the background expected in these second generation experiments and will provide a critical element in the discovery of WIMP dark matter should an experiment like DEAP-3600 claim observation of a signal.

More broadly, this research will also inform the "dual-phase" detector program of DarkSide. Dual-phase detectors rely on PSD using the primary scintillation light (S1) and the ratio of the secondary and primary light (S2/S1). The secondary signal is acquired by drifting the electrons produced in the primary ionization component of the WIMP interaction. An overarching goal of the PI has been to develop a model for scintillation and charge yield for LAr

as a function of drift field. In this way, a complete and general model of PSD in LAr can be attacked as a function of electric field --- zero field for single-phase versus optimized field for dual-phase --- and thus assess in a quantitative manner the most promising route to a large LAr dark matter experiment. Already, preliminary studies indicate some interesting results (Figure 5).

It has been assumed, quite generally for dual-phase detectors, that the scintillation yield does not depend in any significant way on the applied drift field. The model under development by the PI, however, predicts a rather significant dependence in LAr and this dependence has been observed recently in LAr (left panel of Figure 5). Furthermore, it is generally claimed that the discrimination power of S1/S2 that is afforded in a dual-phase detector in addition to the S1 signal used alone in a single-phase detector puts the dual-phase technique at an advantage. As it concerns the overall ability for rejecting electron backgrounds, however, this conclusion is incorrect (right panel of Figure 5). Since the scintillation yield (S1) becomes reduced in an electric field and since the PSD capability is such a strong function of this yield, the added power of S1/S2 can never compensate for that which is lost due to the lower S1 yield. Indeed, it appears to be the case that the optimum electric field w.r.t. electron background discrimination in LAr is the case of zero-field. This is a profound realization and one that deserves further study.

The ability to reject electron backgrounds in LAr has significant impact on the design and scientific reach of next generation experiments. On the one hand the results indicate that PSD, and thus the low-energy threshold achievable, in LAr is optimized at zero-field (i.e. using the single-phase approach). On the other hand, a dual-phase detector affords superior position reconstruction resolution that might prove necessary to better reject external backgrounds such as fast neutrons or radon daughter decay from detector surfaces. It therefore begs the question: Is it possible to conceive of a hybrid design wherein the virtues of both the single-phase and dual-phase capabilities can be realized in the same experiment? It may be possible, for example, to consider a detector that has full, 4-pi photomultiplier coverage to maximize light yield as in MiniCLEAN while maintaining the better position reconstruction of a time-projection-chamber using an optimized and “minimal” applied drift field.

Unique to CLEAN is the possibility to exchange the LAr target with liquid neon (LNe). LNe has the advantage that it can be made extremely clean and free of internal radioactivity. Owing to its smaller atomic number, however, the predicted WIMP-nucleus interaction rate is about eight times smaller than in LAr for the equivalent target mass and energy threshold. Nonetheless, at the CLEAN scale, a LNe target could cover the minimal theoretical phase space of interest (Fig.1). Moreover, with LNe in place of LAr, the number of detected WIMP events would drop by a factor of ~8, much like a “beam off” measurement, while the number of external backgrounds will remain the same, apart from predictable differences in detector response between the two targets.

The ability to swap targets in the same detector and to test directly a possible signal is a powerful capability of the CLEAN approach. It may be the only way in a massive dark matter detector to verify a signal, and thus WIMP discovery, without simply relying on an independent experiment for confirmation. While our immediate priority is to carry out the LAr program described above, we will seek funds in FY15 in order to carry out a similar demonstration of the CLEAN approach using a LNe target.

Finally, other fundamental applications of the CLEAN approach have come to bare. In particular, it has been recognized that a single-phase LAr detector at the tonne-scale is ideal for detecting, for the first time, the Coherent Elastic Neutrino-Nucleus Scattering (CENNS) predicted by the standard model. This prediction, made over 35 years ago, has so far eluded detection for lack of a detector technology, like CLEAN, capable of achieving the necessary target mass and low-energy threshold. LANL scientists are now collaborating with FermiLab to propose such an experiment using the “off-axis” neutrinos produced at the Booster-Neutrino-Beam.

Impact on National Missions

The direct detection and identification of dark matter is one of the most compelling problems facing modern science and constitutes a top priority within the DOE Office of Science for High Energy Physics through its Cosmic Frontier Program. It bears repeating that the existence of dark matter reflects one of few instances where there is direct evidence for physics beyond the Standard Model.

The development of ultra-sensitive, rare event detectors such as MiniCLEAN requires the combined efforts and skills of a scientific and engineering team afforded by a National Laboratory. Developing these novel radiation detectors can have direct impact on the non-proliferation program owing to the capability for distinguishing a weak neutron signal in the presence of an intense gamma-ray background. Initial research into this application has been supported by an NA22 grant to pursue this possibility.

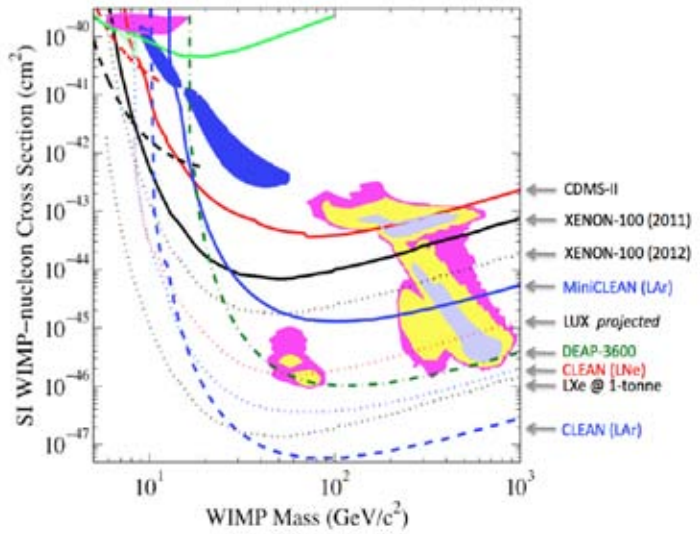

Figure 1. Recent upper limits and projected sensitivities for the spin-independent WIMP-nucleon cross-section as a function of WIMP mass. Allowed regions reported by DAMA (magenta), CoGeNT (light green), and CRESST-II (blue), are under tension from the bounds from CDMS-II and XENON-100. Parameter space corresponding to constrained SUSY models with recent LHC and Higgs constraints is shown as the shaded regions at 68%, 95%, and 99% confidence intervals. A (45-tonne) CLEAN experiment would provide excellent coverage of the most interesting regions of parameter space and would be capable of both LAr and LNe targets. The projected sensitivity for DEAP-3600, LUX and a generic LXe experiment at the 1-tonne scale are shown for comparison.

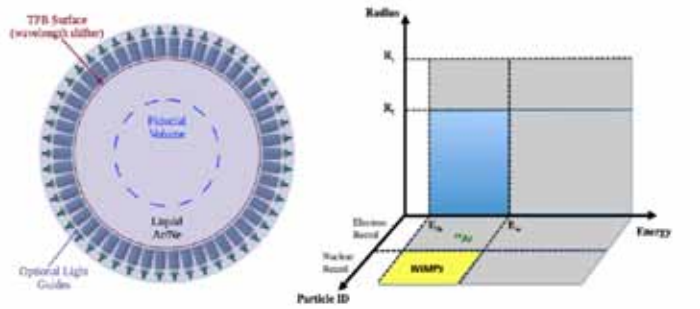

Figure 2. (left) Schematic version of a single-phase cryogenic liquid scintillation detector. The UV scintillation light (128 nm) is converted to detectable optical light by a wavelength-shifting layer viewed in 4-pi by a PMT array. (right) Rejection of internal (39Ar beta decay) is via Particle-ID using pulse-shape discrimination of the triplet-to-singlet light ratio. External backgrounds (surface radon progeny and fast neutrons) are rejected by self-shielding and fiducialization. MiniCLEAN will be the first single-phase LAr detector with 3D event reconstruction.

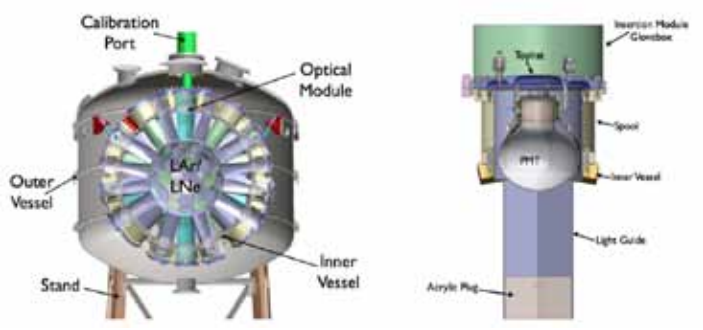

Figure 3. (Left) Model of the MiniCLEAN central detector with its 4π target viewed by 92 optical cassettes. (Right) The optical cassettes are 30 cm long and consist of a 10 cm thick acrylic plug, the front surface of which is coated with a wavelength-shifting fluor (TPB), and 30 cm light guide leading to the PMT. The inner target defined by the TPB surface contains 500 kg of LAr within a nominal radius of 44 cm.

Figure 4. A collage of MiniCLEAN detector components under assembly at SNOLAB: (top left) the Outer Vessel on its stand and inside the water shield tank in the Cube-Hall; (top right) a view of light-guides as they are pre-fit into the Inner Vessel; (bottom left) a PMT assembled in its holder along with the light-guide and acrylic plug with wavelength shifter; (bottom right) the Inner Vessel that serves to hold the cryogenic target and 92 optical cassettes.

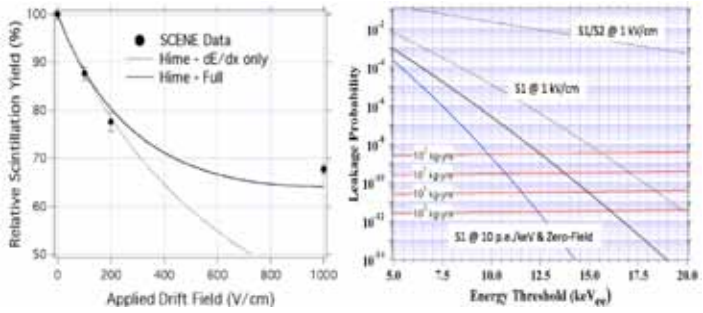

Figure 5. The data points are recent measurements by the SCENE collaboration for the relative scintillation yield in LAr as a

function of applied electric field. The curves are generated from a model, under development by the PI. Right: The solid blue curve indicates a projection of electron background leakage from 39Ar beta decay in zero field when the light yield is 10 p.e./keV. The corresponding prediction for dual-phase operation using a drift field of 1 kV/cm is shown as the solid black curve and is a product of discrimination factors from S1 and S1/S2.

References

1. Boulay, M. G., and A. Hime. A Technique for the Direct Detection of Weakly Interacting Massive Particles using the Scintillation Time Dependence in Liquid Argon. 2006. Astroparticle Physics. 25: 179.

2. Hime, A.. The MiniCLEAN Dark Matter Experiment. Invited presentation at proceedings of the DPF-2011 Conference. (Providence, RI, 2011-arXiv:1110.1005).

Publications

Bodmer, M., F. Giuliani, M. Gold, A. Christou, and M. Batygov. Design of an active magnetic field compensation system for MiniCLEAN. 2013. NUCLEAR INSTRUMENTS & METHODS IN PHYSICS RESEARCH SECTION A-ACCELERATORS SPECTROMETERS DETECTORS AND ASSOCIATED EQUIPMENT. 697: 99.

Caldwell, T.. Characterization of the R5912-02 MOD Photomultiplier Tube at Cryogenic Temperatures. To appear in LIDINE 2013. (Fermilab, 29-31 May 2013).

Gastler, D., E. Kearns, A. Hime, L. C. Stonehill, S. Seibert, J. Klein, W. H. Lippincott, D. N. McKinsey, and J. A. Nikkel. Measurement of scintillation efficiency for nuclear recoils in liquid argon. 2012. PHYSICAL REVIEW C. 85 (6): -.

Gehman, V. M.. Fluorescence efficiency and visible reemission spectrum of tetraphenyl butadiene films at extreme ultraviolet wavelengths. 2011. Nuclear Instruments and Methods. A654: 116.

Graesser, M. L., I. M. Shoemaker, and L. Vecchi. Asymmetric WIMP dark matter. 2011. Journal of High Energy Physics. 10: 110.

Guiseppe, V., K. Rielage, S. Westerdale, S. Elliott, and A. Hime. Radon Progeny Deposition Model. 2011. In 3rd Topical Workshop in Low Radioactivity Techniques. (Sudbury, Canada, 28-29 August 2010). Vol. 1338, p. 95. AIP Conference Proc.: AIP.

Hime, A.. The MiniCLEAN Dark Matter Experiment. 2011. In DPF-2011 Conference. (Providence, RI, 8-13, Aug. 2011). , p. 1. DPF Conference Proceedings: arXiv:1110:1005v1.

Hime, A.. CLEAN Detection of Dark Matter. Presented at UCLA Dark Matter 2012. (Marina Del Rey, CA, 22-24 Feb. 2012).

Hime, A.. CLEAN Detection of Dark Matter. Presented at CIPANP 2012. (St. Petersburg, FL, 29 May-4 July, 2012).

Hime, A.. CLEAN Detection of Dark Matter. Invited presentation at Identification od Dark Matter 2012. (Chicago, IL, 23-27 July, 2012).

MacMullin, S., M. Boswell, M. Devlin, S. R. Elliott, N. Fotiades, V. E. Guiseppe, R. Henning, T. Kawano, B. H. LaRoque, R. O. Nelson, and J. M. O'Donnell. Partial gamma-ray production cross sections for (n, xn gamma) reactions in natural argon at 1-30 MeV. 2012. PHYSICAL REVIEW C. 85 (6): -.

Rielage, K.. Status and Prospects of the MiniCLEAN Dark Matter Experiment. 2012. In 19TH PARTICLES AND NUCLEI INTERNATIONAL CONFERENCE (PANIC11). Vol. 1441, p. 518.

Seibert, S.. Status of the MiniCLEAN Dark Matter Experiment. To appear in LIDINE 2013. (Fermilab, 29-31 May 2013).

Shoemaker, I. M.. Indirect and direct detection of dark matter. Invited presentation at Aspen Center for Physics. (Aspen, CO, 6-12 Feb. 2011).

macmullin, s., M. Boswell, M. Devlin, S. Elliott, N. Fotiades, V. Guiseppe, R. Henning, T. Kawano, B. LaRoque, and R. Nelson. Neutron-induced gamma-ray production cross sections for the first excited-state transitions in Ne-20 and Ne-22 . 2012. Phys. Rev. C. 86: 067601.

Multi-Messenger Signals from Low-mass Supernovae

Christopher L. Fryer
20110032DR

Abstract
This project focused on modeling all the observational diagnostics of core-collapse supernovae, from probes of circumstellar medium (supernova light-curves and spectra) to probes of the explosion mechanism (nucleosynthetic yields and compact remnant masses) to the inner core (neutrinos and gravitational waves).

Background and Research Objectives
Supernovae are one of the ideal physics laboratories for matter in extreme conditions produced in nature. This project focused on modeling the diagnostics of these experiments, from probes of circumstellar medium (supernova light-curves and spectra) to probes of the explosion mechanism (nucleosynthetic yields and compact remnant masses) to the inner core (neutrinos and gravitational waves). This work led to collaborations between a broad set of scientists both within the laboratory (T, CCS, LANSCE, P, XTD, XCP, ISR) and the international community (we are now collaborating with over 100 scientists world-wide). Over the course of the 3 years, the publication rate of the team skyrocketed and in the final year over 40 papers were submitted to refereed journals (with a total of 80 papers over the course of the DR). A large fraction of these papers were high impact for LANL; 20% of these papers have each garnered over 15-20 citations per year. During this project, we instigated collaborations with Southwest Research Institute, the Argentina-led Transient Optical Robotic Observatory of the South (TOROS), the Palomar Transient Factory (PTF) and expanded our collaborations with the Nucleosynthesis Grid (NuGrid) collaboration and the Joint Institute for Nuclear Astrophysics (JINA). Below we highlight a few of the specific results from this project, spanning the 3 different diagnostic categories at LANL.

Scientific Approach and Accomplishments
Circumstellar Medium: Most of our work probing the circumstellar medium focused on supernova light-curves. During the course of this project, our supernova light-curve code moved from the first calculations to truly a production-level capability, with a fast-growing user base. This past year alone, we submitted 7 papers studying supernova light-curves. Many of these studies focused on understanding better the mass loss from stars and, in doing so, we moved to the latest progenitor models. One of our biggest discoveries with these models is the fact that the stellar structure changes significantly with newer algorithms for stellar convection. For the models produced by the Tycho code with their new mixing algorithm based on multi-dimensional simulations (e.g. Viallet et al. 2013), we found that above 20 solar masses, most of the helium is burned into carbon and oxygen (Frey et al. 2013). This expansive burning provides a natural explanation for the high fraction of type Ic supernovae as well as the lack of type Ib supernovae associated with gamma-ray bursts.

Explosion Mechanism: A main thrust of the project has been to better understand the nucleosynthetic yields of core-collapse supernovae. Nucleosynthetic yields have the potential to probe the strength and asymmetry of the supernova engine. For example, the high 44Ti yield in the Casioppeia A remnant. We published over 30 refereed papers during this project improving our theoretical rates for core-collapse nucleosynthesis. A further 6 papers were published (most in the last year) using modern rates to calculate nucleosynthetic yields from massive stars. Our project combined development of new experimental tools to calculate nuclear cross-sections with new theories to calculate these cross-sections. LANL's expertise in fission products is ideally suited to calculating r-process yields and we have focused a lot of our effort on this important piece of nucleosynthesis. However, the picture of two extreme processes, the r- and s-processes, to explain all the heavy elements has been significantly muddied in the past few years. It is now believed that intermediate processes (neutron capture that is not so fast that elements are pushed to

the drip line, but not so slow that elements are limited to being only one or two neutrons beyond the valley of stability) can dominate the nucleosynthetic yields that we see. The LANL-founded NuGrid collaboration has been at the forefront of this new paradigm. The first NuGrid paper summarizing the range of nucleosynthesis processes was submitted this year (Pignatari et al. 2013, astro-ph/1307.6961). We have integrated LANL rates into the NuGrid network framework, tying our experimental and theoretical work firmly into the recent work in the astrophysics community.

Another probe of the supernova explosion is the mass of the compact remnants formed during the stellar collapse. We led a series of papers tying the explosion energy and stellar progenitor to the expected remnant mass. Fryer et al. (2012) completed a detailed survey of these ties, providing a new set of remnant mass predictions (based on the explosion mechanism). This high impact paper has, a year and a half after publication, received nearly 40 citations and will in, just a few years, become another high impact (>100 citation) paper for Fryer (according to LANL's experts database, Fryer has more first-author high-impact papers than anyone at LANL – including such superstars as John Sarrao, Bette Korber, Alan Bishop, …) The high impact again illustrates the broad application and cutting edge research led in this DR project.

Explosion Engine: The final focus of the project was to study the details of the supernova engine itself. Gravitational waves and neutrinos are the only direct probes of the explosive engine. We carried out a number of projects studying the role of neutrino oscillations (working with experts like George Fuller for which we successfully proposed a collaborative grant during this project) and neutrino cross-sections. Our neutrino cross-section work ties well with the focus of the Institute for Nuclear Theory in Seattle and we are closely collaborating with this community. Similarly, we revived the LANL effort in gravitational waves, organizing a 3 month long workshop on gravitational waves at the Kavli Institute for Theoretical Physics at Santa Barbara, taking part (and leading in some cases: Andersson et al. 2013 – CQG, 2013, Fryer & New 201) several reviews in this field (including invited reviews at the American Physical Society Meeting). Finally, LANL joined the TOROS collaboration to better tie our work to the gravitational wave community.

This project made great strides in all of these fields, each a full discipline in itself. This project places LANL as a firm leader in integrating all these disciplines under a single roof and represents a breadth not seen at universities or national laboratories for that matter. But this is a strength of the national laboratories and LANL in particular, the ability to bring together a broad set of disciplines to study an applied problem (and indication of the breadth is the fact that over 40 academy of scientists work in this field and scientists from our project personally interacted with over 15 of these academy of scientists during the course of the project). Unfortunately, this project opened up many new questions for every one we answered, and this field is, if anything, more wide open than when we started. But we do understand the multi-messenger signals much better now and have established LANL as a leader in this broad, but integratable, topic.

Impact on National Missions

These projects had a lot of synergy with the ASC and Campaign programs within LANL. The multi-physics nature of the supernova problem is akin to the multi-physics problems in these programs and most (7 of 10) of the post-docs in this program were converted into staff in the last 2 years of this project. Software developed for the astrophysics light-curve program is now used in a wide variety of mission science. Finally, the nuclear physics techniques developed in this project facilitate better uncertainty quantification (UQ) and we are actively engaged in this UQ analysis in a follow-on project.

References

1. Viallet, M., C. Meakin, D. Arnett, and M. Mocak. TURBULENT CONVECTION IN STELLAR INTERIORS. III. MEAN-FIELD ANALYSIS AND STRATIFICATION EFFECTS. 2013. ASTROPHYSICAL JOURNAL. 769 (1): -.

2. Frey, L. H., C. L. Fryer, and P. A. Young. CAN STELLAR MIXING EXPLAIN THE LACK OF TYPE Ib SUPERNOVAE IN LONG-DURATION GAMMA-RAY BURSTS?. 2013. ASTROPHYSICAL JOURNAL LETTERS. 773 (1): -.

3. Fryer, C. L., and K. C. B. New. Gravitational Waves from Gravitational Collapse. 2011. LIVING REVIEWS IN RELATIVITY. 14: -.

Publications

Belczynski, K., G. Wiktorowicz, C. L. Fryer, D. E. Holz, and V. Kalogera. MISSING BLACK HOLES UNVEIL THE SUPERNOVA EXPLOSION MECHANISM. 2012. ASTROPHYSICAL JOURNAL. 757 (1): -.

Belczynski, K., T. Bulik, C. L. Fryer, A. Ruiter, F. Valsecchi, J. S. Vink, and J. R. Hurley. On the maximum mass of stellar black holes. 2010. Astrophysical Journal. 714 (2): 1217.

Bennett, M. E., R. Hirschi, M. Pignatari, S. Diehl, C. Fryer, F. Herwig, A. Hungerford, G. Magkotsios, G. Rockefeller, F. Timmes, M. Wiescher, and P. Young. The effect of ¹²C + ¹²C rate uncertainties

on s-process yields. 2010. In Nuclear Physics in Astrophysics IV ; 8-12 June 2009 ; Frascati, Italy. Vol. 202, 1 Edition, p. 012023 (4 pp.).

Bennett, M. E., R. Hirschi, M. Pignatari, S. Diehl, C. Fryer, F. Herwig, A. Hungerford, G. Magkotsios, G. Rockefeller, F. Timmes, M. Wiescher, and P. Young. The effect of C-12+C-12 rate uncertainties on s-process yields. 2010. NUCLEAR PHYSICS IN ASTROPHYSICS IV (NPAIV 2009). 202: -.

Bennett, M. E., R. Hirschi, M. Pignatari, S. Diehl, C. Fryer, F. Herwig, A. Hungerford, K. Nomoto, G. Rockefeller, F. X. Timmes, and M. Wiescher. The effect of C-12+C-12 rate uncertainties on the evolution and nucleosynthesis of massive stars. 2012. MONTHLY NOTICES OF THE ROYAL ASTRONOMICAL SOCIETY. 420 (4): 3047.

Dominik, M., K. Belczynski, C. Fryer, D. E. Holz, E. Berti, T. Bulik, I. Mandel, and R. O'Shaughnessy. DOUBLE COMPACT OBJECTS. I. THE SIGNIFICANCE OF THE COMMON ENVELOPE ON MERGER RATES. 2012. ASTROPHYSICAL JOURNAL. 759 (1): -.

Dominik, M., K. Belczynski, C. Fryer, D. E. Holz, E. Berti, T. Bulik, I. Mandel, and R. O'Shaughnessy. DOUBLE COMPACT OBJECTS. I. THE SIGNIFICANCE OF THE COMMON ENVELOPE ON MERGER RATES. 2012. ASTROPHYSICAL JOURNAL. 759 (1): -.

Ellinger, C. I., P. A. Young, C. L. Fryer, and G. Rockefeller. A CASE STUDY OF SMALL-SCALE STRUCTURE FORMATION IN THREE-DIMENSIONAL SUPERNOVA SIMULATIONS. 2012. ASTROPHYSICAL JOURNAL. 755 (2): -.

Ellinger, C., P. Young, C. Fryer, and G. Rockefeller. A case study of small-scale structure formation in three-dimensional supernova simulations. 2012. Astrophysical Journal. 755 (2): 160 (34 pp.).

Eriksen, K. [Los Alamos National Laboratory]., C. [Los Alamos National Laboratory]. Fontes, J. [Los Alamos National Laboratory]. Colgan, null. Zhang, A. [Los Alamos National Laboratory]. Hungerford, C. [Los Alamos National Laboratory]. Fryer, J. [Rutgers University]. Hughes, R. [Smithsonian Astrophysical Observatory]. Smith, and null. Badenes. Fe Atomic Data for Non-equilibrium Ionization Plasmas. 2012. DOE/LANL.

Fryer, C. L., A. J. Ruiter, K. Belczynski, P. J. Brown, F. Bufano, S. Diehl, C. J. Fontes, L. H. Frey, S. T. Holland, A. L. Hungerford, S. Immler, P. Mazzali, C. Meakin, P. A. Milne, C. Raskin, and F. X. Timmes. Spectra of type Ia Supernovae from Double Degenerate Mergers. 2010. Astrophysical Journal. 725 (1): 296.

Fryer, C. L., D. J. Whalen, and L. Frey. Modeling Emission from the First Explosions: Pitfalls and Problems. 2010. In First Stars and Galaxies: Challenges for the next Decade ; 8-11 March 2010 ; Austin, TX, USA. Vol. 1294, p. 70.

Fryer, C. L., K. Belczynski, E. Berger, C. Thone, C. Ellinger, and T. Bulik. THE POPULATION OF HELIUM-MERGER PROGENITORS: OBSERVATIONAL PREDICTIONS. 2013. ASTROPHYSICAL JOURNAL. 764 (2): -.

Fryer, C. L., K. Belczynski, G. Wiktorowicz, M. Dominik, V. Kalogera, and D. E. Holz. COMPACT REMNANT MASS FUNCTION: DEPENDENCE ON THE EXPLOSION MECHANISM AND METALLICITY. 2012. ASTROPHYSICAL JOURNAL. 749 (1): -.

Fryer, C. L., and A. Heger. Forming massive black holes through stellar collapse: Observational diagnostics. 2011. Astronomische Nachrichten. 332 (4): 408.

Fryer, C., K. Belczynski, G. Wiktorowicz, M. Dominik, V. Kalogera, and D. Holz. COMPACT REMNANT MASS FUNCTION: DEPENDENCE ON THE EXPLOSION MECHANISM AND METALLICITY. 2012. ASTROPHYSICAL JOURNAL. 749 (1): 91.

Fryer, C., and K. B. New. Gravitational Waves from Gravitational Collapse. 2011. Living Reviews in Relativity. 14: 1.

Fryer, null.. Mixing in astrophysics. 2011. DOE.

Herwig, F., M. Pignatari, P. R. Woodward, D. H. Porter, G. Rockefeller, C. L. Fryer, M. Bennett, and R. Hirschi. Convective-reactive Proton-¹²C combustion IN Sakurai's object (V4334 Sagittarii) and implications for the evolution and yields from the first generations of stars. 2011. Astrophysical Journal. 727 (2): 89 (15 pp.).

Herwig, F., M. Pignatari, P. R. Woodward, D. H. Porter, G. Rockefeller, C. L. Fryer, M. Bennett, and R. Hirschi. Convective-reactive Proton-¹²C combustion IN Sakurai's object (V4334 Sagittarii) and implications for the evolution and yields from the first generations of stars. 2011. Astrophysical Journal. 727 (2): 89 (15 pp.).

Herwig, F., M. Pignatari, P. Woodward, D. Porter, G. Rockefeller, C. Fryer, M. Bennett, and R. Hirschi. CONVECTIVE-REACTIVE PROTON-C-12 COMBUSTION IN SAKURAI,ÄôS OBJECT (V4334 SAGITTARII) AND IMPLICATIONS FOR THE EVOLUTION AND YIELDS FROM THE FIRST GENERATIONS OF STARS. 2011. ASTROPHYSICAL JOURNAL. 727 (2): 89.

Herwig, F., null. Pignatari, P. [LCSE and Department of Astronomy. Woodward, D. [Minnesota Supercomputing Institute. Porter, G. Rockefeller, C. [Computational Computer Science Division. Fryer, M. Bennett, and R. Hirschi. CONVECTIVE-REACTIVE PROTON-{sup 12}

C COMBUSTION IN SAKURAI'S OBJECT (V4334 SAGITTARII) AND IMPLICATIONS FOR THE EVOLUTION AND YIELDS FROM THE FIRST GENERATIONS OF STARS. 2011. Journal Name: Astrophysical Journal. 727 (2): Medium: X; Size: 15 pages.

Holloway, S. T., T. Kawano, and P. Moller. Time Dependent Particle Emission from Fission Products. 2011. Journal of the Korean Physical Society. 59 (2): 875.

Ichikawa, T., A. Iwamoto, Mo&uml, and A. Sierk. Contrasting fission potential-energy structure of actinides and mercury isotopes. 2012. Physical Review C (Nuclear Physics). 86 (2): 024610 (8 pp.).

Ichikawa, T., A. Iwamoto, P. Moller, and A. Sierk. Contrasting fission potential-energy structure of actinides and mercury isotopes. 2012. PHYSICAL REVIEW C. 86 (2): 024610.

Ichikawa, T., Y. Kanada-En'yo, and Mo&uml. Cluster formations in deformed states for ²⁸Si and ³²S. 2011. Physical Review C (Nuclear Physics). 83 (5): 054319 (7 pp.).

Ichikawa, T., Y. Kanada-En,Äôyo, and P. Moller. Cluster formations in deformed states for Si-28 and S-32. 2011. PHYSICAL REVIEW C. 83 (5): 054319.

Johnson, J. L., D. J. Whalen, C. L. Fryer, and H. Li. THE GROWTH OF THE STELLAR SEEDS OF SUPERMASSIVE BLACK HOLES. 2012. ASTROPHYSICAL JOURNAL. 750 (1): -.

Kawano, T., P. Talou, M. B. Chadwick, S. Holloway, P. Moller, and T. Watanabe. Applications of the Hauser-Feshbach Theory to Advanced Nuclear Sciences. 2011. JOURNAL OF THE KOREAN PHYSICAL SOCIETY. 59 (2, 3, SI): 785.

Magkotsios, G., F. X. Timmes, A. L. Hungerford, C. L. Fryer, P. A. Young, and M. Wiescher. Trends in ⁴⁴Ti and ⁵⁶Ni from core-collapse supernovae. 2010. Astrophysical Journal Supplement Series. 191 (1): 66.

Mesler, R., D. Whalen, N. Lloyd-Ronning, C. Fryer, and Pihlstro&uml. Gamma-ray Bursts in Circumstellar Shells: A Possible Explanation for Flares. 2012. Astrophysical Journal. 757 (2): 117 (11 pp.).

Mo&uml, , J. &. Randrup, and A. Sierk. Calculated fission yields of neutron-deficient mercury isotopes. 2012. Physical Review C (Nuclear Physics). 85 (2): 024306 (6 pp.).

Mo&uml, , W. Myers, H. Sagawa, and S. Yoshida. New Finite-Range Droplet Mass Model and Equation-of-State Parameters. 2012. Physical Review Letters. 108 (5): 052501 (4 pp.).

Moller, P., A. J. Sierk, R. Bengtsson, H. Sagawa, and T. Ichikawa. Nuclear shape isomers. 2012. ATOMIC DATA AND NUCLEAR DATA TABLES. 98 (2): 149.

Moller, P., W. Myers, H. Sagawa, and S. Yoshida. New Finite-Range Droplet Mass Model and Equation-of-State Parameters. 2012. PHYSICAL REVIEW LETTERS. 108 (5): 052501.

Passy, J., O. De Marco, C. Fryer, F. Herwig, S. Diehl, J. Oishi, M. Mac Low, G. Bryan, and G. Rockefeller. SIMULATING THE COMMON ENVELOPE PHASE OF A RED GIANT USING SMOOTHED-PARTICLE HYDRODYNAMICS AND UNIFORM-GRID CODES. 2012. ASTROPHYSICAL JOURNAL. 744 (1): 52.

Pignatari, M., E. Zinner, M. G. Bertolli, R. Trappitsch, P. Hoppe, T. Rauscher, C. Fryer, F. Herwig, R. Hirschi, F. X. Timmes, and F. K. Thielemann. SILICON CARBIDE GRAINS OF TYPE C PROVIDE EVIDENCE FOR THE PRODUCTION OF THE UNSTABLE ISOTOPE Si-32 IN SUPERNOVAE. 2013. ASTROPHYSICAL JOURNAL LETTERS. 771 (1): -.

Pignatari, M., M. Wiescher, F. X. Timmes, R. J. de Boer, F. K. Thielemann, C. Fryer, A. Heger, F. Herwig, and R. Hirschi. PRODUCTION OF CARBON-RICH PRESOLAR GRAINS FROM MASSIVE STARS. 2013. ASTROPHYSICAL JOURNAL LETTERS. 767 (2): -.

Pignatari, M., R. Hirschi, M. Wiescher, R. Gallino, M. Bennett, M. Beard, C. Fryer, F. Herwig, G. Rockefeller, and F. X. Timmes. THE C-12+C-12 REACTION AND THE IMPACT ON NUCLEOSYNTHESIS IN MASSIVE STARS. 2013. ASTROPHYSICAL JOURNAL. 762 (1): -.

Pignatari, M., R. Hirschi, M. Wiescher, R. Gallino, M. Bennett, M. Beard, C. Fryer, F. Herwig, G. Rockefeller, and F. X. Timmes. THE C-12+C-12 REACTION AND THE IMPACT ON NUCLEOSYNTHESIS IN MASSIVE STARS. 2013. ASTROPHYSICAL JOURNAL. 762 (1): -.

Qiang, Yuan, null. Bi Xiaojun [Key Laboratory of Particle Astro, null. Liu Siming [Department of Physics and Astron, Y. U. Fan Zhonghui [Department of Physics, and C. [Los Alamos National Laboratories. Fryer. MODELING THE MULTI-WAVELENGTH EMISSION OF THE SHELL-TYPE SUPERNOVA REMNANT RX J1713.7-3946. 2011. Journal Name: Astrophysical Journal. 735 (2): Medium: X; Size: 9 pages.

Ramaprabhu, P., G. Dimonte, P. Woodward, C. Fryer, G. Rockefeller, K. Muthuraman, P. -H. Lin, and J. Jayaraj. The late-time dynamics of the single-mode Rayleigh-Taylor instability. 2012. Physics of Fluids. 24 (7): 074107 (21 pp.).

Randrup, J., Mo&uml, and A. J. Sierk. Fission-fragment mass distributions from strongly damped shape evolu-

tion. 2011. Physical Review C (Nuclear Physics). 84 (3): 034613 (15 pp.).

Randrup, J., P. Moller, and A. J. Sierk. Fission-fragment mass distributions from strongly damped shape evolution. 2011. PHYSICAL REVIEW C. 84 (3): 034613.

Randrup, J., P. Moller, and A. Sierk. Brownian shape motion: Fission fragment mass distributions. 2012. In CNR*11 - Third International Workshop on Compound Nuclear Reactions and Related Topics ; 19-23 Sept. (2011 ; Prague, Czech Republic). Vol. 21, p. 08006 (8 pp.).

Randrup, J., and P. Moller. Brownian Shape Motion on Five-Dimensional Potential-Energy Surfaces: Nuclear Fission-Fragment Mass Distributions. 2011. PHYSICAL REVIEW LETTERS. 106 (13): 132503.

Raskin, C., E. Scannapieco, C. Fryer, G. Rockefeller, and F. X. Timmes. Remnants of Binary White Dwarf Mergers. 2012. Astrophysical Journal. 746 (1): 62 (10 pp.).

Raskin, C., E. Scannapieco, C. Fryer, G. Rockefeller, and F. X. Timmes. REMNANTS OF BINARY WHITE DWARF MERGERS. 2012. ASTROPHYSICAL JOURNAL. 746 (1): 62.

Raskin, C., E. Scannapieco, C. Fryer, G. Rockefeller, and F. X. Timmes. REMNANTS OF BINARY WHITE DWARF MERGERS. 2012. ASTROPHYSICAL JOURNAL. 746 (1): -.

Raskin, C., E. Scannapieco, C. Fryer, G. Rockefeller, and F. X. Timmes. REMNANTS OF BINARY WHITE DWARF MERGERS. 2012. ASTROPHYSICAL JOURNAL. 746 (1): -.

Raskin, C., E. Scannapieco, G. Rockefeller, C. Fryer, S. Diehl, and F. X. Timmes. Astrophysical Journal. 2010. Astrophysical Journal. 724 (1): 111.

Roming, P. W. A., T. A. Pritchard, J. L. Prieto, C. S. Kochanek, C. L. Fryer, K. Davidson, R. M. Humphreys, A. J. Bayless, J. F. Beacom, P. J. Brown, S. T. Holland, S. Immler, N. P. M. Kuin, S. R. Oates, R. W. Pogge, G. Pojmanski, R. Stoll, B. J. Shappee, K. Z. Stanek, and D. M. Szczygiel. THE UNUSUAL TEMPORAL AND SPECTRAL EVOLUTION OF THE TYPE IIn SUPERNOVA 2011ht (vol 92, pg 751, 2012). 2013. ASTROPHYSICAL JOURNAL. 762 (2): -.

Roming, P. W. A., T. A. Pritchard, J. L. Prieto, C. S. Kochanek, C. L. Fryer, K. Davidson, R. M. Humphreys, A. J. Bayless, J. F. Beacom, P. J. Brown, S. T. Holland, S. Immler, N. P. M. Kuin, S. R. Oates, R. W. Pogge, G. Pojmanski, R. Stoll, B. J. Shappee, K. Z. Stanek, and D. M. Szczygiel. THE UNUSUAL TEMPORAL AND SPECTRAL EVOLUTION OF THE TYPE IIn SUPERNOVA 2011ht. 2012. ASTROPHYSICAL JOURNAL. 751 (2): -.

Roming, P. W., T. A. Pritchard, J. L. Prieto, C. S. Kochanek, C. L. Fryer, K. Davidson, R. M. Humphreys, A. J. Bayless, J. F. Beacom, P. J. Brown, S. T. Holland, S. Immler, N. P. Kuin, S. R. Oates, R. W. Pogge, G. Pojmanski, R. Stoll, B. J. Shappee, K. Z. Stanek, and D. M. Szczygiel. The Unusual Temporal and Spectral Evolution of the Type IIn Supernova 2011ht. 2012. Astrophysical Journal. 751 (2): 92 (16 pp.).

Ruiter, A. J., K. Belczynski, S. A. Sim, W. Hillebrandt, C. L. Fryer, M. Fink, and M. Kromer. Delay times and rates for Type Ia supernovae and thermonuclear explosions from double-detonation sub-Chandrasekhar mass models. 2011. MONTHLY NOTICES OF THE ROYAL ASTRONOMICAL SOCIETY. 417 (1): 408.

Ruiter, A. J., K. Belczynski, S. A. Sim, W. Hillebrandt, C. L. Fryer, M. Fink, and M. Kromer. Delay times and rates for Type Ia supernovae and thermonuclear explosions from double-detonation sub-Chandrasekhar mass models. 2011. MONTHLY NOTICES OF THE ROYAL ASTRONOMICAL SOCIETY. 417 (1): 408.

Scannapieco, E., C. Raskin, M. Della Valle, C. Fryer, J. Rhoads, G. Rockefeller, and F. X. Timmes. Constraining Type Ia Supernova Progenitors. 2013. BINARY PATHS TO TYPE IA SUPERNOVAE EXPLOSIONS. 281: 275.

Staff, J. E., A. Menon, F. Herwig, W. Even, C. L. Fryer, P. M. Motl, T. Geballe, M. Pignatari, G. C. Clayton, and J. E. Tohline. DO R CORONAE BOREALIS STARS FORM FROM DOUBLE WHITE DWARF MERGERS?. 2012. ASTROPHYSICAL JOURNAL. 757 (1): -.

Staff, J., A. Menon, F. Herwig, W. Even, C. Fryer, P. Motl, T. Geballe, M. Pignatari, G. Clayton, and J. Tohline. Do R Coronae Borealis Stars form from Double White Dwarf Mergers?. 2012. Astrophysical Journal. 757 (1): 76 (17 pp.).

Talou, P., T. Kawano, J. E. Lynn, P. Moller, O. Bouland, and M. B. Chadwick. Recent Advances in Nuclear Fission Theory: Pre- and Post-scission Physics. 2011. JOURNAL OF THE KOREAN PHYSICAL SOCIETY. 59 (2, 3, SI): 797.

Talou, P., T. Kawano, J. E. Lynn, P. Moller, O. Bouland, and M. B. Chadwick. Recent Advances in Nuclear Fission Theory: Pre- and Post-scission Physics. 2011. JOURNAL OF THE KOREAN PHYSICAL SOCIETY. 59 (2): 797.

Tho&uml, , A. de Ugarte Postigo, C. L. Fryer, K. L. Page, J. Gorosabel, M. A. Aloy, D. A. Perley, C. Kouveliotou, H. T. Janka, P. Mimica, J. L. Racusin, H. Krimm, J. Cummings, S. R. Oates, S. T. Holland, M. H. Siegel, M. De Pasquale, E. Sonbas, M. Im, W. -K. Park, D. A. Kann, S. Guziy, Herna&acute, A. Llorente, K. Bundy, C. Choi, H. Jeong, H. Korhonen, Kuba&grave, J. Lim, A. Moskvitin, Mu&ntilde, S. Pak, and I. Parrish. The unusual γ-ray burst GRB 101225A from a helium star/neutron star merger at redshift 0.33. 2011. Nature. 480 (7375): 72.

Tsang, M. B., J. R. Stone, F. Camera, P. Danielewicz, S. Gandolfi, K. Hebeler, C. J. Horowitz, J. Lee, W. G. Lynch, Z. Kohley, R. Lemmon, P. Moller, T. Murakami, S. Riordan, X. Roca-Maza, F. Sammarruca, A. W. Steiner, I. Vidana, and S. J. Yennello. Constraints on the symmetry energy and neutron skins from experiments and theory. 2012. PHYSICAL REVIEW C. 86 (1): -.

Veselsky&acute, , A. N. Andreyev, S. Antalic, M. Huyse, Mo&uml, K. Nishio, A. J. Sierk, P. Van Duppen, and M. Venhart. Fission-barrier heights of neutron-deficient mercury nuclei. 2012. Physical Review C (Nuclear Physics). 86 (2): 024308 (8 pp.).

Whalen, D. J., C. C. Joggerst, C. L. Fryer, M. Stiavelli, A. Heger, and D. E. Holz. FINDING THE FIRST COSMIC EXPLOSIONS. II. CORE-COLLAPSE SUPERNOVAE. 2013. ASTROPHYSICAL JOURNAL. 768 (1): -.

Whalen, D. J., W. Even, C. C. Lovekin, C. L. Fryer, M. Stiavelli, P. W. A. Roming, J. Cooke, T. A. Pritchard, D. E. Holz, and C. Knight. ILLUMINATING THE PRIMEVAL UNIVERSE WITH TYPE IIn SUPERNOVAE. 2013. ASTROPHYSICAL JOURNAL. 768 (2): -.

Whalen, D. J., and C. Fryer. The Observational Signatures of Primordial Pair-instability Supernovae. 2010. In Deciphering the Ancient Universe with Gamma-ray Bursts ; 19-23 April 2010 ; Terrsa, Kyoto, Japan. Vol. 1279, p. 116.

Whalen, D. J., and C. Fryer. The Observational Signatures of Primordial Pair-Instability Supernovae. 2010. DECIPHERING THE ANCIENT UNIVERSE WITH GAMMA-RAY BURSTS. 1279: 116.

Woodward, null., null. Dimonte, null. Rockefeller, null. Fryer, null. Dimonte, null. Dai, and R. J. Kares. Simulating Rayleigh-Taylor (RT) instability using PPM hydrodynamics @scale on Roadrunner (u). 2011. DOE.

Yuan, Q., S. Liu, Z. Fan, X. Bi, and C. Fryer. MODELING THE MULTI-WAVELENGTH EMISSION OF THE SHELL-TYPE SUPERNOVA REMNANT RX J1713.7-3946. 2011. ASTROPHYSICAL JOURNAL. 735 (2): 120.

Yuan, Qiang, Siming Liu, Zhonghui Fan, Xiaojun Bi, and C. Fryer. Modeling the multi-wavelength emission of the shell-type supernova remnant RX J1713.7-3946. 2011. Astrophysical Journal. 735 (2): 120 (9 pp.).

Yuan, Qiang, Siming Liu, Zhonghui Fan, Xiaojun Bi, and C. Fryer. Modeling the multi-wavelength emission of the shell-type supernova remnant RX J1713.7-3946. 2011. Astrophysical Journal. 735 (2): 120 (9 pp.).

Network-centric Quantum Communications

Richard J. Hughes
20110046DR

Abstract

Trends in communications networks are presenting new cyber security concerns that are challenging to meet with conventional cryptography. In principle, quantum cryptography using single-photon communications, with its security rooted in inviolable laws of quantum physics, could meet these challenges, provided it could evolve from the current point-to-point instantiations to a form compatible with multi-node networks. Previous approaches to quantum communications (QC) networks based on a mesh of point-to-point links lack scalability, require dedicated optical fiber, are expensive and not amenable to mass production, only provide one of the cryptographic functions (key distribution) needed for secure communications, and so have elicited limited practical interest. We have invented and experimentally demonstrated a new approach to information assurance called network-centric quantum communications (NQC), achieving at least a three-year lead over the state-of-the art in QC research internationally. NQC is scalable, resilient, deployable, amenable to mass production, and ultimately affordable. We have shown that NQC can solve new network security challenges in the critical infrastructure control sector, in particular. Long-duration/high-value network security environments within the NNSA and certain DoD complexes, and hand-held device security are other NQC application areas that are being explored. We have protected the NQC intellectual property with twenty nine US and foreign patent applications, and joint development opportunities with US industry are under discussion.

Background and Research Objectives

Communications networks have revolutionized the way we work, live, operate computer systems and run our national infrastructure. But hardly a day goes by without a report highlighting the pressing need for improved cyber security technologies to protect our economic and National security. Cryptography provides security for the protection of data in motion and in storage, as well as ensuring that control, access and network management can only be performed by authorized parties. Critical to these functions is the secure distribution of the secret random number sequences known as cryptographic keys to authorized users: secret keys are used as parameters within algorithms to encrypt, authenticate or sign data that must be secure. Protocols to generate a shared secret key between two parties are therefore of fundamental importance to network communications. Many of today's widely-used protocols base their security on assumptions about the computational power of an adversary, such as the difficulty of factoring large integers. Such classical schemes lack "forward security" –an attacker could record the protocol execution steps, break the security on faster computers in the future, and compromise past protocol sessions and the communications they had secured. Protocols with information-theoretic (forward) security, are therefore highly desirable. This is possible with quantum communications (QC) [1, 2], which requires a channel that transmits quantum states of single-photons (polarization for example), with negligible loss of quantum coherence. Eavesdropping on QC can be detected, because of the inevitable disturbance of quantum states caused by measurements, and attackers cannot passively monitor the quantum signals owing to the indivisibility of elementary particles, or faithfully copy them because of the quantum "no cloning" theorem.

QC protocols combine single-photon transmissions with non-secret conventional communications to accomplish specific cryptographic tasks. (Figure 1) The state-of-the art in QC is a specific protocol known as quantum key distribution (QKD) [1] for establishing a shared secret key between two mutually trusting parties. In optical fiber QKD transmission ranges of more than 200km have been achieved [3]; our team has previously achieved a record 144km with the strongest security assurances [4]. Small companies in the US and Europe sell point-to-point QKD products [5, 6] for applications such as secure

off-site back-up. Research groups in the US [7], Europe [8], China [9] and Japan [10] have explored "trusted QKD networks", formed from a mesh of trusted nodes between which two-party QKD is performed on dedicated optical fibers, distinct from the data network being secured. A user can establish a secret key with a distant node by transporting it, encrypted using QKD, through intermediate nodes. Because the key exists "in the clear" within each intermediate node, these nodes must be physically secure and trusted. This approach is expensive and does not scale well: adding users requires additional physically-secure trusted nodes; and a duplication of network infrastructure. Furthermore, it is incompatible with existing network architectures. Underlying these shortcomings is the absence of a method for establishing trust between users. Our NQC invention [11, 12, 13] overcomes these limitations to bring the unrivalled forward security of QC to networks in scalable, deployable, robust form and includes advances in key management that bring new capabilities that take QC beyond key distribution.

Scientific Approach and Accomplishments

In NQC, quantum communications between each of N client nodes and a central server node at the physical layer support a quantum key management (QKM) layer [14], which in turn enables secure communications functions (confidentiality, authentication and non-repudiation) at the application layer between N2 client pairs [11]. (Figure 2) The NQC "hub-and-spoke" topology is widely encountered in optical fiber networks, and permits a hierarchical trust architecture that allows the server (the "hub") to act as the trusted authority (TA, "Trent") in cryptographic protocols for authenticated key establishment. (This avoids the poor scaling of previous approaches that require a pre-existing trust relationship between every pair of nodes.) By making Trent a single multiplexed QC receiver, and the client nodes (Alice, Bob, Charlie, etc.) QC transmitters, NQC amortizes the cost and complexity of one of the most demanding QC components – the single-photon detectors – across multiple network nodes [12]. In this way the NQC architecture is scalable in terms of both quantum-physical resources and trust.

In previous optical fiber QC instantiations information bits (quantum bits or "qubits") have been encoded in the optical phase of single-photon states. This has required interferometric stability and inevitably necessitates bulky and expensive hardware. Instead, for NQC we encode information bits in photon polarization states, allowing the QC transmitters – referred to as QKarDs - to be miniaturized and fabricated using integrated photonics methods [15]. This opens the door to a manufacturing process with its attendant economy of scale, and ultimately much lower-cost QC hardware. Our first-generation, modularly-integrated QKarD is a fiber-coupled device, which incorporates a distributed feedback laser and modulator, that produces short (< 1ns), single-photon (mean-photon number < 1), polarized light pulses at telecom wavelengths (1,550nm), at a 10 MHz repetition rate in our NQC test bed. (Figure 3) This device is produced by a small-scale manufacturing process and could be incorporated into end devices. We are designing a next-generation, monolithically-integrated QKarD, which will be an order of magnitude smaller in each linear dimension, and amenable to much lower cost mass production. In our test bed the QC data processing is handled by PCs at each node, with Trent's software architecture capable of accommodating up to 100 client QKarDs on that platform, and more than 1,000 with server-class hardware [16]. But we have also demonstrated that the processing software in each client can be transitioned to a field-programmable gate array (FPGA), providing further miniaturization for use cases such as hand-held device security.

Trent, the NQC receiver, incorporates passive polarization analysis with single-photon detectors, operated at a typical detection efficiency of ~ 15%. In our NQC test bed, which we have operated continuously for 3 years, we have time-multiplexed Trent with three QKarD transmitters, Alice, Bob and Charlie, over 50 km of single-mode fiber; larger numbers of clients could be accommodated with a combination of temporal and wavelength multiplexing. Fiber birefringence necessitates polarization tracking and compensation [17], which in our test bed is performed in-band at Trent, temporally multiplexed with the QC signals, resulting in a QC duty cycle of 20%. (When implemented out-of-band we expect our novel tracking scheme [18] will compensate even the much higher polarization rates that will be encountered in challenging environments such as optical fibers strung on telephone poles.)

We operate several QC protocols on each client-Trent link in our test bed. We have implemented quantum secret sharing (QSS) [19] over fiber spans as large as 50km between a client and a single, logical Trent node. The vital trusted authority, Trent, is comprised of two physical nodes: an intermediate, integrated-photonics modulation node and a QC receiver node [20]. With QSS a client's key is split between the two physical parts of Trent, both of which would be required to cooperate to reconstruct the key. In this way compromise of either one of the two parts of Trent would not compromise the client's key [14]; an attacker would have to successfully compromise both nodes. (Splitting of the key into additional shares would be possible with more intermediate nodes.)While other researchers have previously demonstrated some elements of a QSS

protocol, our implementation is the first that is complete, correct, verifiable and secure. However, for brevity we will describe a simpler test bed configuration in which a QKD protocol is performed on the client-Trent links.

In other advances we have implemented a quantum identification protocol, QID [21], between each client and Trent, providing a mechanism for client device enrollment and revocation [14, 21] on the NQC network. Following successful completion by the client of the QID challenge-response with Trent, a short authentication key is generated enabling client-Trent QKD protocols to be performed. These protocols allow users anywhere on the network to share keys and perform all of the standard cryptographic functions we use on a network such as digitally signing documents and authenticating messages or software packages with the security guarantees of quantum keys. We have developed and performed analysis of a new type of potential security issue in the implementation of the basic QKD protocol, extending the security guarantees in the face of a new, general class of adaptive attacks [22].

Following the generation of shared secret keys between each client and Trent using QKD (or QSS), NQC protocols at the QKM layer provide keys for client-to-client secure communications at the application layer [14]. For example, suppose Alice requires a secret key to encrypt a message to Bob using the AES algorithm [23], and/or authenticate the message using the HMAC algorithm [24]. (Other symmetric key encryption/authentication algorithms could be used instead.) For definiteness, we assume that this will be a 256-bit key. First, Alice and Trent parse the results of their QKD session into a 256-bit key, KA. Similarly, Bob and Trent parse the results of their QKD session into a distinct 256-bit key KB. Trent knows both keys and can provide non-secret, classical information to Alice, namely a list of the bit positions in KA where her key bits need to be flipped to match Bob's key. This information, which we call a pair key, enables Alice to securely transform her key, KA, into the key KB that she needs for communications with Bob. Important security advantages of this QKM protocol are that: it does not require pre-placement of long-term secret keys shared by a client and Trent; and each new client-to-client key has no algorithmic heritage in any previous key. Trent could even go offline after publishing a look-up table of clients' pair keys, and the clients would still be able to execute the above key agreement protocol using previously-generated, and securely-stored quantum keys.

We have also invented a quantum digital signature (QDS) protocol [14] that allows Alice to sign messages to Bob. Alice requires a secret signing key, S, to calculate her signature, and Bob requires Alice's non-secret signature verification key, V. In QDS Alice's S key is one of the keys she shares with Trent through QKD. Trent can calculate V from S, and provide it to Bob, authenticated with one of the Bob-Trent QKD keys. When Bob receives the signed message from Alice he can then verify her signature using V. With the inclusion of the digital signature capability, NQC can provide the full functionality of a public key infrastructure [14].

Impact on National Missions

By transferring key management functions to the quantum-physical from the computation realm, NQC protocols have intrinsically much lower latencies than their conventional counterparts. This attribute is of high significance as a solution to the hard cyber security challenges of critical infrastructure protection, which are a top national security concern. The NQC project has already led to a follow-on project with DOE's Cyber Security for Energy Delivery Systems (CEDS) program. Energy delivery systems such as the SmartGrid have requirements for the secure, low-latency (~ few ms) delivery of data from, and commands to, Internet-connected control devices. In the electricity transmission sector, for example, phasor measurement units (PMU) provide information 30 times per second to control centers (phasor data concentrators, PDC) on the phase of the electricity at locations throughout the grid. There is a low-latency data origin authentication requirement for the multicast of this PMU data to PDCs. These requirements are very challenging with present-day cryptography on standard processors, without compromising either the security assurances or the quality-of-service: public key signatures are too slow, for example; while message authentication codes using a common group key are vulnerable to compromise of a single node. (Similar security/latency requirement mismatches exist throughout the electric grid, as well as in Supervisory Control and Data Acquisition (SCADA) systems generally.) Newer, lightweight cryptography could meet the requirement, but with conventional approaches the key management would be impractical. However, optical fiber is widely-deployed throughout the electric grid, and so NQC with its essentially unconstrained ability to supply fresh, forward-secure keys on-demand is capable of supporting lightweight cryptography for these applications. In December 2012 at the US Department of Energy's Trustworthy Cyber Infrastructure for the Power Grid (TCIPG) test bed at the University of Illinois Urbana-Champaign (UIUC) we demonstrated that our NQC technology could provide the necessary security, well within the required latency, for PMU communications.

NQC can address long-duration/high-value security needs within many network environments, such as: certain DoD and DOE/NNSA complexes; between government agencies in the Washington, DC area; financial networks; and for

secure cloud computing. NQC can also provide multi-level security within optical network environments. Other examples include: IAEA treaty monitoring; within a US Embassy compound; or on board a military or commercial aircraft. NQC could as well enable a hand-held QC device to be used for identification, authentication, access control and secure telephone calls. NQC is extensible to other types of networks: an aircraft or satellite acting as a trusted node could establish ad hoc secure networks of ground, sea and air-based users on a continental or even a global scale.

Throughout the NQC project we have been mindful that our inventions will only have practical value as cyber security solutions if they can ultimately be transitioned to the private sector. We have been diligent in protecting the intellectual property that we have created, filing twenty nine US and foreign patent applications. NQC technology transfer discussions with several major US corporations are already well-advanced.

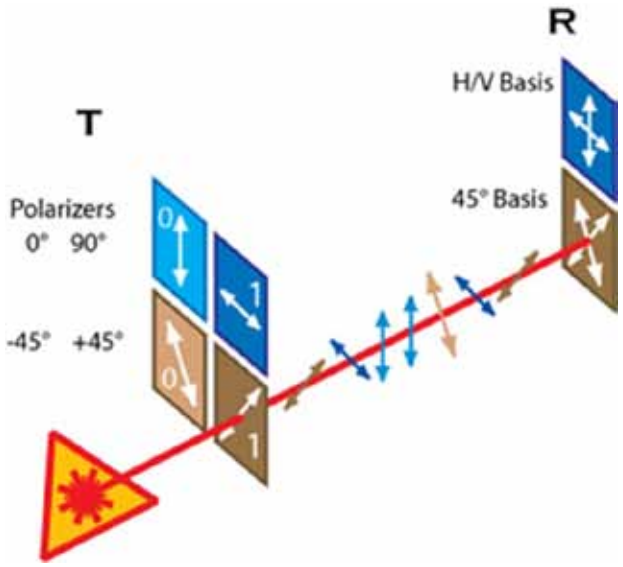

Figure 1. In a QC protocol random bits are encoded at transmit node ("T") in orthogonal photon states (linear polarization in this case), using either the rectilinear basis (0° or 90°), or the diagonal basis (-45° or +45°). For each photon receive node ("R") makes a random choice of decoding basis, either rectilinear or diagonal. The detected bits are post-processed with conventional communications.

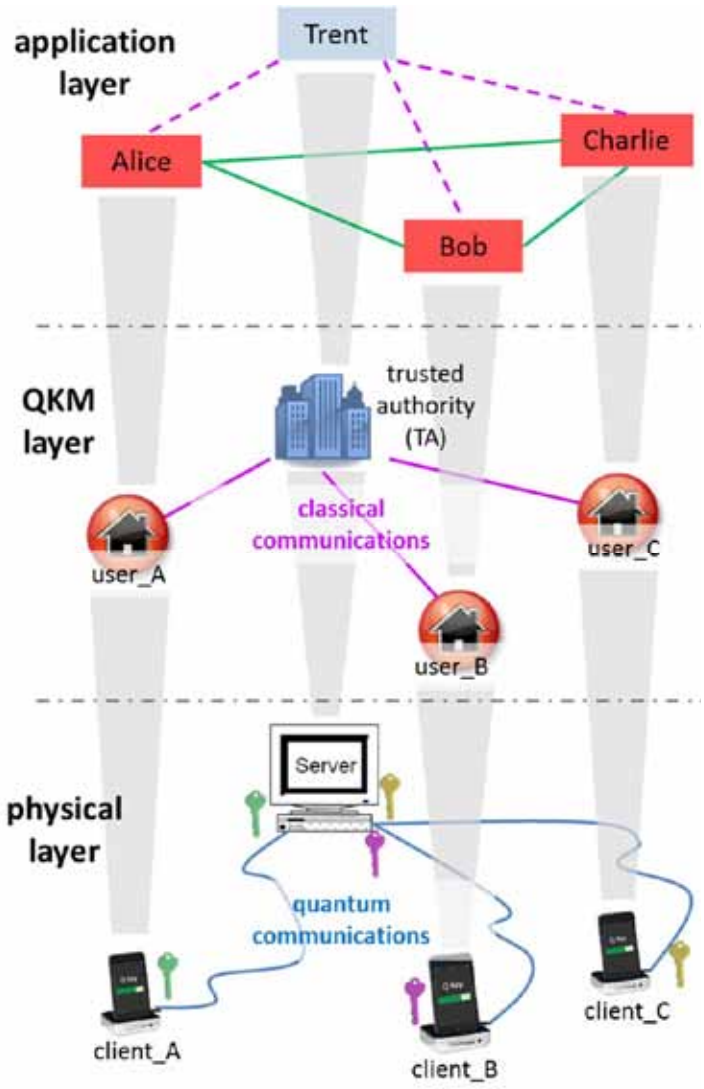

Figure 2. Network-centric quantum communications (NQC) architecture. (See text for details.)

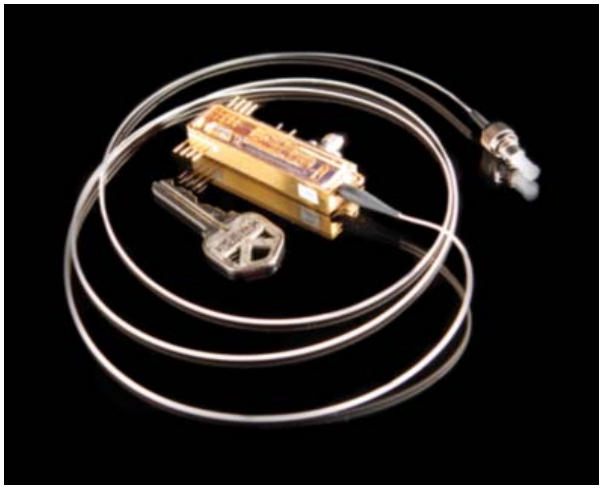

Figure 3. Generation 1 quantum smartcard or QKarD. (See text for details.)

References

1. Bennett, C. H., and G. Brassard. Quantum cryptography: public key distribution and coin tossing. 1984. In Proceedings of the IEEE International Conference on Computers, Systems and Signal Processing. (Bangalore, India, 1984). , p. 175. Piscataway, NJ: IEEE.

2. Stucki, D., N. Walenta, F. Vannel, R. T. Thew, N. Gisin, H. Zbinden, S. Gray, C. R. Towery, and S. Ten. High rate, long-distance quantum key distribution over 250 km of ultra low loss fibres. 2009. New Journal of Physics. 11: 075003.

3. Rosenberg, D., C. G. Peterson, J. W. Harrington, P. R. Rice, N. Dallmann, K. T. Tyagi, K. P. McCabe, S. Nam, B. Baek, R. H. Hadfield, R. J. Hughes, and J. E. Nordholt. Practical long-distance quantum key distribution system using decoy levels. 2009. New Journal of Physics. 11: 045009.

4. MagiQ Technologies. 2013. MagiQ home page.

5. idQuantique, SA. 2013. idQuantique home page.

6. Elliot, C.. Building the quantum network. 2002. New Journal of Physics. 4: 46.

7. Peev, M.. The SECOQC quantum key distribution network in Vienna. 2009. New Journal of Physics. 11: 075001.

8. Wang, S.. Field test of wavelength-saving quantum key distribution network. 2010. Optics Letters. 35: 2454.

9. Sasaki, M.. Field test of quantum key distribution in the Tokyo QKD Network. 2011. Optics Express. 19: 10387.

10. Hughes, R. J., J. E. Nordholt, and C. G. Peterson. Secure multi-party communication with quantum key distribution managed by trusted authority. 2013. US Patent 8,483,394 awarded July 9, 2013.

11. Nordholt, J. E., R. J. Hughes, R. T. Newell, C. G. Peterson, D. Rosenberg, K. P. McCabe, K. T. Tyagi, and N. Dallmann. Quantum key distribution using card, base station and trusted authority. 2013. US Patent Application US20130101119 A1 published April 25, 2013..

12. Hughes, R. J., J. E. Nordholt, K. P. McCabe, R. T. Newell, C. G. Peterson, and R. D. Somma. Network-centric quantum communications with application to critical infrastructure protection. 2013. ArXiV.

13. Hughes, R. J., J. E. Nordholt, and J. T. Thrasher. Quantum key management. 2013. US patent application US 20130083926 A1.

14. Nordholt, J. E., C. G. Peterson, R. T. Newell, and R. J. Hughes. Quantum communications system with integrated photonics devices. 2013. US patent application US2013/055430.

15. Nordholt, J. E., R. J. Hughes, J. M. Riese, C. M. Ahrens, C. G. Peterson, and J. W. Harrington. Scalable software architecture for quantum cryptographic key management. 2013. US patent application US2013/055356.

16. Nordholt, J. E., C. G. Peterson, R. T. Newell, and R. J. Hughes. Polarization tracking system for free-space optical communication, including quantum communication. 2013. US Patent application US20130083925 A1.

17. Nordholt, J. E., C. G. Peterson, R. T. Newell, and R. J. Hughes. Great circle solution to polarization-based quantum communication (QC) in optical fiber. 2013. US patent application US 20130084079 A1.

18. Hillery, M., V. Buszek, and A. Berthiaume. Quantum Secret Sharing. 1999. Physical Review A. 59: 1829.

19. Schmidt, C.. Experimental single qubit quantum secret sharing. 2005. Physical Review Letters. 95: 230505.

20. Hughes, R. J., J. E. Nordholt, C. G. Peterson, J. T. Thrasher, R. T. Newell, J. T. Yard, and R. D. Somma. Multi-factor authentication using quantum communication. 2013. US patent application US2013/055410.

21. Somma, R. D., and R. J. Hughes. Security of decoy-state protocols for general photon-number-splitting attacks. 2013. Physical Review A. 87: 062330.

22. Announcing the Advanced Encryption Standard (AES). 2001. National Institute of Standards and Technology (NIST) FIPS-197.

23. The keyed-Hash Message Authentication Code (HMAC). 2002. National Institute of Standards and Technology (NIST) FIPS 198.

Publications

Hughes, R. J., J. E. Nordholt, K. P. McCabe, R. T. Newell, C. G. Peterson, and R. D. Somma. Network-centric quantum communications with application to critical infrastructure protection. 2013. ArXiV.

Hughes, R. J., J. E. Nordholt, and C. G. Peterson. Secure multi-party communication with quantum key distribution managed by trusted authority. 2013. US Patent 8,483,394 awarded July 9, 2013.

Hughes, R. J., J. E. Nordholt, and J. T. Thrasher. Quantum key management. 2013. US patent application US 20130083926 A1.

Hughes, R. J., and J. E. Nordholt. Refining quantum cryptography. 2011. Science. 333: 1584.

Nordholt, J. E., C. G. Peterson, R. T. Newell, and R. J. Hughes. Great circle solution to polarization-based quantum communication (QC) in optical fiber. 2013. US patent application US 20130084079 A1.

Nordholt, J. E., C. G. Peterson, R. T. Newell, and R. J. Hughes. Polarization tracking system for free-space optical communication, including quantum communication. 2013. US Patent application US20130083925 A1.

Nordholt, J. E., R. J. Hughes, R. T. Newell, C. G. Peterson, D. Rosenberg, K. P. McCabe, K. T. Tyagi, and N. Dallmann. Quantum key distribution using card, base station and trusted authority. 2013. US Patent Application US20130101119 A1 published April 25, 2013..

Smith, G., J. Smolin, and J. Yard. Quantum communication with Gaussian channels of zero quantum capacity. 2011. Nature Photonics. 5: 624.

Somma, R. D., and R. J. Hughes. Security of decoy-state protocols for general photon-number-splitting attacks. 2013. Physical Review A. 87: 062330.

Ursin, R., and R. J. Hughes. Sharing quantum secrets. 2013. Nature. 501: 37.

First Direct Measurement of Particulate Evolution in Isochorically Heated Dense Plasma (U)

Brian J. Albright
20130082DR

Abstract

This one-year project was intended to determine the feasibility of a completely new class of high-energy-density-physics (HEDP) experiments using laser-based, very rapid (i.e., over time scales of trillionths of seconds) heating of matter. The primary objective of this work was to see whether we could study plasma-phase "electrostatically enhanced mix" (EEM) at material interfaces, a problem of both widespread application and a great unsolved scientific problem in its own right. The work involved both a theoretical/modeling and experimental study. Both were highly successful, enough so that this work motivated an LDRD new start in FY14 to extend our pilot experiments and, we hope, lead to the resolution of whether and for how long EEM dominates the evolution of plasma. Proof-of-principle integrated experiments were conducted which involved both creation of multi-species plasma and the x-ray imaging of an evolving plasma interface. Also, radiation hydrodynamics and plasma kinetic simulations were used to design relevant follow-on experiments that extend this proof of principle.

Background and Research Objectives

One of the biggest challenges to doing controlled HEDP experiments on facilities such as the National Ignition Facility at Lawrence Livermore National Laboratory, the Z Machine at Sandia National Laboratory is that the time scale over which plasma can be made (of order ten billionths of a second) is the same time scale over which the matter evolves. As a result, what plasma one makes often has large variations in density and temperature, making it very difficult to design controlled, "unit-physics" experiments that rigorously test one's physics hypotheses. This is an endemic problem with the use of such facilities.

However, if we could somehow create dense plasma on far shorter time scales—trillionths instead of tens of billionths of seconds—then we could design experiments where the plasma has no time to expand and where we know to good accuracy what state the plasma is in. Such experiments are possible on the LANL Trident laser, thanks to innovations in recent years (supported by LDRD) in laser-generated ion beam technology. The Trident short-pulse beam, of order 80 Joules in energy and 0.5 trillionths of a second pulse duration, when focused onto a very thin (of order 100 nanometers thickness), planar target, can create an exotic type of plasma within the target where the electrons are highly relativistic, with energies of order 100 times their rest mass, and the plasma within the target can enter the "relativistically induced transparency" (RIT). RIT enables very efficient coupling between laser and plasma and enables the formation of large electric fields with amplitudes of up to 100 trillion volts/m. These fields can accelerate ions and make collimated ion beams of MeV to GeV ions over time scales shorter than a trillionth of a second.

These ion beams can be used to rapidly heat target matter into the plasma state, enabling a brand-new, heretofore unexplored class of plasma experiments with unprecedented control over the initial conditions. The purpose of our project was to assess the feasibility of such an experiment, using the Trident short pulse laser to create matter and one of the long-pulse beams to make x-rays to be used to image the evolving plasma. A major objective was to test whether the key diagnostic, the x-ray backlighting and gated x-ray imager, was capable of operating in the high electromotive pulse (EMP) environment of a Trident short-pulse experiment and if so, whether it could indeed image the evolving plasma. Additionally, kinetic simulations using the LANL VPIC particle-in-cell code and radiation-hydrodynamics simulations using the LASNEX code were used to design and refine follow-on experiments to extend this "proof-of-principle."

The overarching objective was to demonstrate the real potential to solve one of the great problems in our

understanding of plasma-phase mix: namely, the role of large, electrostatic fields at material interfaces in driving the mix process. This is the biggest difference between plasma-phase mix and fluid-phase mix, one that has not been explored previously. As indicated below, this objective was met.

Scientific Approach and Accomplishments

Our experimental accomplishments (Figure 1 for a schematic of the apparatus):

We designed and fielded an integrated target holder (Figure 1) capable of housing the three key components of our experiment: the thin foil target that interacts with the incident short pulse beam to create the ion source, the solid-density sample of material to be heated by the ion beam, and the x-ray source foil that is irradiated by the incident long-pulse beam. Key access ports in this mount were also designed to allow diagnostic lines of sight for the Thompson parabola (to measure ion energy loss in the target) and the gated x-ray imaging (GXI) diagnostic.

We demonstrated that the GXI diagnostic is capable of operating in the high EMP environment of a Trident short-pulse experiment and that the photon counts in our experiment would be adequate to image the target. This was a nontrivial accomplishment, and in doing this work we discovered a minor parallax issue that will need to be resolved in future experiments of this type. We also identified an x-ray fiducial from the relativistic electron background that we will exploit in future experiments for timing.

We performed initial design of an optical/UV pyrometer (for making temperature measurements of our heated plasma) to be used in follow-on experiments. While preliminary, this allowed us to make a down-selection of different approaches to pyrometry.

We fielded an integrated proof-of-principle experiment that demonstrated all of the essential features of a follow-on experiment. This experiment employed the use of a thin tungsten wire surrounded by a plastic foam. Both were irradiated by an laser generated ion beam (carbon and protons) and the evolution of the foam was captured using an x-ray backlighter and the GXI diagnostic. This experiment demonstrated conclusively the feasibility of experiments of this type in resolving the question of the role of EEM in plasma-phase mix (Figure 1).

We serendipitously uncovered a new means of improving our ion heater beam and allowing for access of a wider range of plasma temperatures in our sample. This work is being prepared for publication.

Our theoretical/modeling accomplishments:

We performed a suite of collisional kinetic simulations of high-Z/low-Z interface evolution in plasma. These simulations (Figure 2) support the hypothesis that EEM can be a dominant actor in governing plasma-phase mix at interfaces.

We have begun a radiation-hydrodynamics design of experiments to ensure that our follow-on experiments can indeed sample relevant plasma conditions for addressing these problems (Figure 2). Work is underway to understand the implications of the use of the novel ion beams discovered above in place of our carbon and proton beams.

Impact on National Missions

This work has three key areas of impact on missions:

Establishing the feasibility of using short-pulse laser-driven particle beams for the creation of HEDP plasma in mission-relevant conditions. Every major HEDP facility in the DOE complex has (or has planned) a co-located short-pulse laser, so this pilot work may open up a brand new set of experiments and vastly expand the utility of these facilities.

Demonstration of “proof of principle” experiments that get at one of the most important problems in our understanding of mix behavior in plasma media. Indeed, the physics of plasma-phase mix undergirds much of our uncertainty of nuclear performance, both in inertial confinement fusion and other applications, and thus the design of controlled, unit-physics experiments in these areas is vital.

If successful, follow-on experiments will be used to extend the NNSA Advanced Simulation and Computing (ASC) common mix framework in the LANL multi-physics codes to incorporate plasma-phase dynamics.

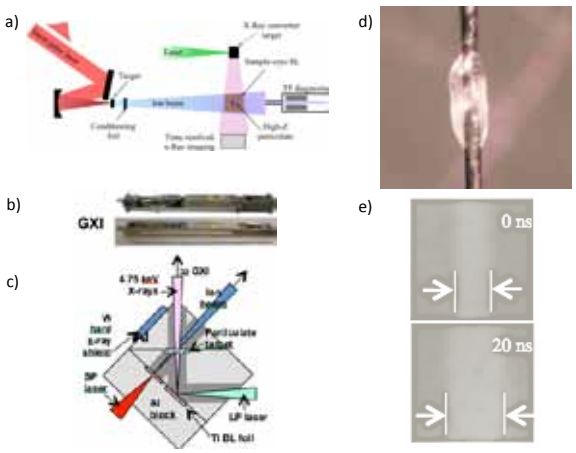

Figure 1. Experimental apparatus and data. Shown are: a) a schematic of the experiment, including key diagnostics; b) the GXI diagnostic used to measure the expanding plasma; c) a schematic of the target mount; d) multi-component target used in pilot experiments (tungsten wire surrounded by plastic foam); e) x-ray images of the evolving multi-component plasma target, showing position of the plasma interface initially and at 20 ns after heating.

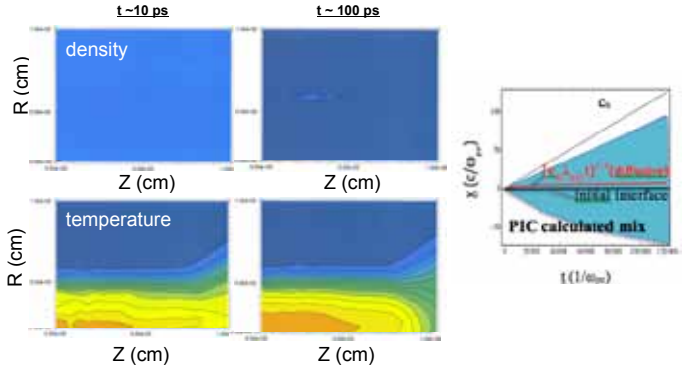

Figure 2. Simulation data. The four left panels are from Lasnex radhydro modeling of a future experiment, indicating the remarkable plasma uniformity made possible by laser-ion-beam-based isochoric heating. The rightmost panel is from a VPIC (collisional) kinetic plasma simulation of the evolution of the "mix layer" near a plasma interface. The presence of large electrostatic fields (i.e., the EEM process) enhances the rate of atomic mixing compared with that of simple diffusive mixing (shown in red).

Publications

Fernández, J. C., B. J. Albright, F. N. Beg, M. E. Foord, B. M. Hegelich, J. J. Honrubia, M. Roth, R. B. Stephens, and L. Yin. Fast ignition with laser-driven proton and ion beams. To appear in Nuclear Fusion.

Hegelich, B. M., I. Pomerantz, L. Yin, H. C. Wu, D. Jung, B. J. Albright, D. C. Gautier, S. Letzring, S. Palaniyappan, R. Shah, K. Allinger, R. Horlein, J. Schreiber, D. Habs, J. Blakeney, G. Dyer, L. Fuller, E. Gaul, E. Mccary, A. R. Meadows, C. Wang, T. Ditmire, and J. C. Fernandez. Laser-driven ion acceleration from relativistically transparent nanotargets. 2013. NEW JOURNAL OF PHYSICS. 15: -.

Jung, D., L. Yin, B. J. Albright, D. C. Gautier, S. Letzring, B. Dromey, M. Yeung, R. Horlein, R. Shah, S. Palaniyappan, K. Allinger, J. Schreiber, K. J. Bowers, H. C. Wu, J. C. Fernandez, D. Habs, and B. M. Hegelich. Efficient carbon ion beam generation from laser-driven volume acceleration. 2013. NEW JOURNAL OF PHYSICS. 15: -.

Jung, D., L. Yin, D. C. Gautier, S. Letzring, B. Dromey, R. Shah, S. Palaniyappan, T. Shimada, R. P. Johnson, J. Schreiber, D. Habs, J. C. Fernández, B. M. Hegelich, and B. J. Albright. Laser-driven 1 GeV carbon ions from preheated diamond targets in the Break-Out Afterburner regime. 2013. Physics of Plasmas. 20: 083103.

Understanding Energetic Ion Transport and Loss in Natural and Artificial Radiation Belts at Low Altitudes

Misa Cowee
20120715ECR

Introduction

Energetic particles in natural and artificial radiation belts can cause damage to the civilian and military assets whose orbits intersect those belts. To better predict the threat posed to satellites, we must understand the physical processes which govern the formation and loss of these radiation belts. Observations indicate that geomagnetic storms can cause energetic (MeV) protons trapped in the natural inner radiation belt to become de-trapped and lost on timescales faster than any known physical processes associated with the Earth's radiation belts. Recent analytic studies indicate that these protons may be rapidly de-trapped because their motion is modified by sudden changes in the magnetic field during magnetic storms, in a process called magnetic "field line curvature" (FLC) scattering. Our goal is to carry out particle simulation tests for FLC scattering to better understand the physics of this loss mechanism and the magnetospheric conditions which cause it. Additionally, we will use the simulation to investigate the role of FLC scattering in the formation of artificial radiation belts produced after a High Altitude Nuclear Explosion (HANE). Observations of the Starfish nuclear test of 1962 indicated that its artificial radiation belt extended above 10,000 km and persisted for several years, damaging a large fraction of the existing space infrastructure. The extent of this artificial belt was not predicted at the time and has not been explained since. We will test a new hypothesis that the ionized fission fragments became de-trapped due to FLC scattering in the HANE-perturbed magnetic fields, allowing them to travel to higher altitudes where they subsequently populated the artificial radiation belt. Thus the results of this study can be applied towards greater understanding of both natural and artificial radiation belt dynamics and will also quantify the FLC scattering process for use in space weather models for the first time.

Benefit to National Security Missions

This research directly supports the DOE/NNSA/Nuclear Nonproliferation, DOC/NOAA and NASA missions because its results will fill a gap in our space weather modeling effort. Energetic protons in the inner radiation belt are not currently included in such models, but pose a significant hazard to spacecraft in orbit. Space weather effects on sensors can compromise our Nuclear Detonation Detection (NDD) remote sensing program, so understanding the potential hazard from natural or artificial radiation belts from a High Altitude Nuclear Explosion (HANE) is critical. NOAA provides space weather forecasts, so improved modeling capability in the inner belts would increase the accuracy of such predictions. NASA's goal of advancing space science and our understanding the near-Earth space environment is directly supported by this research. Predicting natural or man-made space weather hazards are also important for commercial satellites, whose damage could results in severe economic losses.

Progress

In the last year, we have continued development and validation of our particle tracing simulation code. We have expanded the code to include several magnetic field models and created new diagnostics. We have carried out an initial study for the de-trapping of inner belt protons particles due to magnetic "field line curvature" (FLC) scattering, and compared results to previously published observations and analytic models. Our simulation results have shown that FLC scattering is a viable mechanism to explain the loss of inner belt protons after a geomagnetic storm, which had been previously hypothesized. The results have helped us to identify possible explanations for the discrepancies between the current analytic model predictions and the observations of the inner belt proton structure after geomagnetic storms.

Our simulation results have shown that the inner belt protons which are transported radially in the system due to FLC scattering are not always lost to the atmosphere (de-trapped), instead many of them become trapped but at a different radial distance from where they started.

Such transport effects are not included in current analytic models, which assume that all such particles are de-trapped. Compared to the observations, the analytic models predict a much steeper gradient in the proton fluxes with radial distance, and they predict that the de-trapping extends to much lower radial distances. Our simulations, therefore, can partially explain these discrepancies, and yield results in better agreement with observations than the analytic models.

Another important result we have found is that the analytic models incorrectly assume that there is an easily identified "trapping limit" which clearly defines which proton populations will be de-trapped by FLC scattering during a geomagnetic storm and which will not. Our simulations show the very concept of a trapping limit may not apply for particles with chaotic trajectories, and the values of the trapping limits given by the analytic models do not even accurately predict the de-trapping behavior in the simulation.

Based on our results thus far, we suggest that any predictive model of the de-trapping of the inner proton belt due to FLC scattering during geomagnetic storms must account for the relocation of trapped protons across the belt in addition to their loss. We have presented this research at two conferences, the American Geophysical Union meeting in December 2012 and the Geospace Environment Modeling workshop in June 2013. A manuscript describing the first results is in preparation and we expect to submit it for publication by the mid-summer 2013.

Future Work

Our goal is to test the hypothesis that magnetic "field line curvature" (FLC) scattering is the mechanism responsible for both the recent observations of sudden de-trapping of inner radiation belt energetic protons during geomagnetic storms as well as the outward transport of ionized fission fragments after a High Altitude Nuclear Explosion (HANE) which explains the fifty year-old mystery of why the artificial radiation belts produced by the HANE test shots extended to such high altitudes. During FY14, we will use the simulation code we built in FY12 and FY13 to follow the gyromotion of energetic ions and apply it to quiescent and disturbed magnetospheric configurations to understand how de-trapping is sensitive to perturbations in the magnetic field. During FY14, we will continue to quantify how FLC scattering and de-trapping of natural inner radiation belt proton depends on geomagnetic storm strength and proton energy and pitch angle and compare our simulation results with observations from the HEO, SAMPEX and POES spacecraft to quantify the de-trapping conditions and effect on the proton fluxes so that this loss mechanism can be included in space weather models. In FY14 we will also determine if FLC scattering of HANE ionized fission fragments is a viable mechanism to transport of these fragments beyond the burst region. We will investigate how this process depends on the burst location (altitude, latitude, longitude), magnetic cavity configuration, fission fragment spatial and velocity distribution, and fission fragment mass and charge state. We will compare our simulation results to the spacecraft and sounding rocket observations of the artificial radiation belts taken after the HANE tests of 1958 to 1962 to quantify this effect so that it can be included in artificial radiation belt models.

Conclusion

Our first objective is to understand the loss of energetic protons in the natural radiation belts due to magnetic "field line curvature" (FLC) scattering and identify what conditions cause it. Understanding this mechanism allows us to include it in radiation belt models, to better predict the hazard posed to satellites. Our second objective is to understand how FLC scattering of fission fragments produced by a High Altitude Nuclear Explosion (HANE) affects artificial radiation belt formation. With proliferation of nuclear weapon and missile technologies, it is important to be able to predict the potential impact on our space infrastructure from HANEs.

Publications

Cowee, M. M., K. Liu, W. Tu, R. H. Friedel, and G. D. Reeves. "Test Particle Simulations of mu-Scattering in the Inner Proton Belt". Presented at American Geophysical Union Fall Meeting 2012. (San Francisco, CA, Dec 3-7, 2012).

Tu, W., M. M. Cowee, and K. Liu. "Test particle simulations of field-line-curvature scattering in the inner proton belt". Presented at Geospace Environment Modeling Workshop. (Snowmass, Co, June 16-23, 2013).

Enabling Temporal and Spatial Shaping of Ultra-intense Laser Pulses for Next-generation, Compact Particle and Radiation Sources

Rahul C. Shah
20120721ECR

Introduction

Intense laser pulses are being studied for application to next generation compact particle sources. At current, these pulses have smooth Gaussian envelopes, which in time have duration and rise determined by laser physics, and in space have dimension limited by classical focusing optics. In this project we seek to explore possibilities enabled by new means of temporally and spatially concentrating the light and develop the avenues by which to achieve them. At the onset, we had hypothesized that plasma shuttering, a highly non-linear process, might be optimized by means of a spatially flat-top focus. While we have preliminarily devised techniques for flattop focusing, our particle-in-cell simulation (for Trident type parameters) shows that the plasma and laser ripple, resulting in laser filamentation. With respect to Trident experiments, we are instead turning to the use of a low density plasma (realized with nano-pore foams developed thru this project) to controllably focus and shutter the light and enhance accelerated particle spectra. Separately, we are also studying a means to manage impact of the plasma rippling by use of a multiple layered target in which one material buffers these effects to the benefit of a second layer.

Benefit to National Security Missions

A new level of spatial and temporal control over ultra-intense laser pulses is needed to advance our development of next generation accelerators for laboratory applications. The proposed work investigates how sharp rise and flat top spatial laser pulses can be generated by a unique combination of relativistic plasma physics and optical engineering. In doing so, this project opens up a rich, first-of-its-kind technological tool which will yield large scientific possibilities for laser-particle acceleration, laser-x-ray generation, and their applications. We envision follow-on support from MARIE, Office of Fusion Science (OFS), and the Domestic Nuclear Detection Office (DNDO).

Progress

The most significant outcome of the first year has been the preliminary work, both calculation and experimental, on a multitude of topics allowing us to evaluate and adapt the original ideas described in the proposal.

The calculation work began with a post-undergraduate summer student's efforts to develop a basis for focusing an intense laser pulse to a near diffraction-limited spatial flattop. To avoid non-linear effects we were most interested in an approach to spatial shaping based on wave-front modification, which previously had been studied only in the geometric limit applicable for much larger focal dimensions. Because of the intractability of the diffractive case, we turned to a genetic algorithm based approach. The technique proved successful in finding super-Gaussian type foci of the same dimension as the diffraction limited spot. Furthermore, we found that a single wave-front solution applied for all focusing speeds.

While we seem to have initiated a promising approach to flat-top focusing, our work in simulating the laser-plasma interaction using two-dimensional particle-in-cell shows that, for our conditions, the spatial flat-top does not create the hypothesized planar interaction. Instead, the plasma ripples and the laser filaments. Given the tendency for the plasma to render a planar interaction unstable, we began exploring the use of thin plasma slabs of nearly transparent density so as to optimize the self-focusing and temporal transmission of the light pulse. As our simulations show that electric fields are strongly driven on the rear side of the plasma slab, we extended our design to that of an integrated target, as opposed to the concept of a component "plasma optic." Even with only a small effort towards this optimization to date, we have designed two targets with ion spectra significantly improved (flat and peaked in energy) over typical exponential distributions. Study of the detailed underlying mechanisms of the ion spectral improvement

remains as a task for the coming year.

To achieve such targets we have engaged LANL's MST for development of nano-pore foam and aero-gels. While similar nano-pore targets have been used elsewhere, to our knowledge we are the first to have obtained the ~10 micron thicknesses necessary for the optimized particle spectra obtained in our simulations. Our up-coming experiments will diagnose hole-boring velocity, transparency time, transmitted energy, beam foot-print, and ion-spectra. Last year, in lieu of these targets, we explored the use of stacked nm foils in which the first foil shaped the light pulse for the second, "primary" target. By means of the instantaneous Doppler shift recorded with reflected light field measurements we observed the un-mistakable signature of a cleaner temporal rise on the second "primary" target foil. (An interferometric technique to measure this rise was also developed but was not yet fielded on light transmitted thru an actual target). The reflected light, however, also indicated that the intensity focused on the secondary target was reduced over the nominal levels. Such a combination of nm targets is difficult to optimize since the actual experimentally achieved laser rise can create hydrodynamic expansion many times greater in scale than the thickness of the nm shaping foil. The near-critical density targets, which our simulations already suggest enable a richer ability to optimize the ion spectra than the nm foils, ought also prove far more robust given their much larger scale length of microns.

Future Work

In the first set of experiments we are examining the concept of plasma lensing, or the use of low density plasma slabs to control self-focusing and transmission time for optimization of accelerated ion spectra. These experiments are based on our own 2D VPIC simulations indicating plateau spectra (in lieu of typical exponential drop-off) and quasi-mono-energetic spectra could be achieved with ~10 micron thickness and plasma densities about 10-30-fold less than typical solid density films. To implement such targets we have worked extensively with LANL's MST who have fabricated 7-12 micrometer thick slabs of nano-pore SiO_2 aero-gels fabricated at densities of ~100 mg/cc. To our knowledge we are the only researchers in the world with access to such targets. Preliminary results show that the targets can indeed be fielded and are producing flatter ion spectra. Along with ion measurements, we will measure hole-boring velocity via the instantaneous Doppler shift of reflected light and the transmitted laser foot-print as well as temporal field.

A second set of experiments has been inspired by recent suggestions in the literature that multiple species of different charge-to-mass ratio will act to buffer rippling Rayleigh-Taylor like instabilities between the laser and plasma. In our own simulations we have observed that such instabilities rapidly develop with a single species. The published experiments lacked our ability to directly diagnose transparency by means of the reflected light temporal phase and envelope. Using our unique diagnostic, we will examine if transparency time changes as we add an additional 10 nm C layer to Al and Cu targets of 10-100 nm thicknesses.

Following the experiments we will conduct 2D simulations to aid in our interpretation of the physics and publication. If time permits we will revisit the work on spatial flattop focusing.

Conclusion

We will use the temporal and spatial shaping of Trident laser pulses in near critical density plasma to optimize accelerated particle spectra. In addition to experimentally measuring the spectra using state-of-the-art nano-pore foam targets, we will use reflected and transmitted light diagnostics to characterize the dynamics of the interaction for detailed comparison with simulation. We will also study, in both simulation and experiment, how multiple ion species in the target allow control over transparency time. Outcomes are revised from original (electric field measurements in both transverse dimensions and test-bed flat-top focusing) so as to support the evolved direction.

Investigating the Itinerant to Localized Crossover of the 5f Electrons in Plutonium Alloys and Compounds

Paul H. Tobash
20120736ECR

Introduction

Now more than ever, it is apparent that the 94th element in the periodic table, plutonium, offers challenges in the areas of metallurgy and physics. Perhaps the biggest question that needs to be answered is how to understand the true nature of the 5f electrons of Pu which have been shown to exhibit both itinerant (delocalized) and localized behavior. The controversy on explaining the absence of local magnetism in elemental Pu is the ultimate issue this work addresses. Electronic structure calculations have suggested the ~20% volume change from δ-Pu to α-Pu can only arise from the formation of magnetic moments (e.g. increase in lattice spacing). The experimental evidence however is not consistent with this picture where no magnetism is detected. Thus, we propose to synthesize Pu binary alloys that can be directly compared to elemental delta-Pu. Ultimately, we will be able to determine the critical compositions for a number of LANL mission-relevant binary alloys where magnetism emerges and eventually vanishes, as one moves closer to "delta-Pu"–like compositions. After preparing these alloys, we will probe this crossover behavior by measuring their physical properties, which include magnetic susceptibility, heat capacity, and electrical resistivity. The ability to "freeze out" the complicated physics using low temperatures will be necessary in order to study electronic correlations and detect the presence of magnetism. Thermal expansion measurements will be utilized via a new low temperature dilatometry setup in order to gain insight on volume changes resulting from the presence of magnetic moments. This allows for a link into the expected pressure dependence of the materials using the Ehrenfest relationship. This would be a significant part for the synergy of the experiment/theory framework of fundamental Pu physics because the invaluable input parameters for first principle band structure calculations based on Density Functional Theory (DFT) methods.

Benefit to National Security Missions

The information gained from the project directly addresses the emergent phenomena present in Pu materials. These are applicable to the goals outlined in the Pu science strategy that are of interest to DOE and the Office of Basic Energy Science (BES). These include first understanding the electronic structure in Pu materials and secondly, the dynamic behavior of these materials in extreme environments such as temperature, magnetic field, and pressure. With clean electro-refined Pu readily available, this project will allow for a systematic approach to incorporate materials synthesis, analysis, and characterization to probe the evolution of magnetism in mission-related alloy materials and ultimately lead to a more fundamental understanding of the 5f electrons in Pu. This is a novel targeted approach to tracking the crossover with compositions close to δ-Pu to address the Pu grand challenge for the dual nature of the 5f electrons.

Progress

To date the project is halfway finished and at this point at least on track to gain the desired results by April 2014. The significant and most noteworthy work will be completed in the second half of this project where the Pu-rich materials that were spelled out in the proposal will be synthesized and fully characterized. The importance of these compounds is recognized from their close relation to delta-Pu and other LANL mission related work in general. A new capability is also on track to come online in the next few months and also to be used to measure many of these newly prepared compounds. These results will allow us to better probe the interesting behavior of the actinide containing materials.

The current status of our synthetic efforts is halfway through the targeted compositions with all of the Pu-lean compounds being made and measured. These compounds include PuGa3, PuSn3, and PuIn3. We have secured additional Pu starting material that will be used

to prepare the rest of the compositions. We have also synthesized a Pu6Fe compound which has a close relationship to the Pu-rich materials. The final compounds will be completed in the newly installed induction furnace at the CMR facility. As a comparison for the delta-like compositions we are targeting, we have measured the specific heat and electrical resistivity on a newly cast delta-Pu sample. This will serve as a baseline for later doping studies in the system as a function of the stabilizing element such as In, Sn, and Ga.

For the new measurement capability, we have finished assembling the dilatometry probe that will be used to measure thermal expansion of the alloys and compounds. The original designer of the cell has been invited to visit LANL in late August and run calibration tests and also to look at a new encapsulation setup for running Pu on the probe itself. We will be testing the measurement setup in a cold Quantum Design PPMS and then will be introducing this setup to CMR to ultimately measure the Pu materials. A number of collaborations have also been established early on in this project. We have prepared samples of PuSn3 to look at the valence of Pu and the effects of the ligand atoms around Pu. These measurements were completed through a postdoc working in the chemistry division. We also have plans to run some high pressure work on these compounds in the future that would require the successful funding of a possible ER proposal for this work. The theorist that is working on the project has completed much of his band structure calculations on the compounds we wanted to look at. We have also performed first-principles electronic structure calculations on the family of intermetallic Pu3X compounds (including Pu3Ga, Pu3In, and Pu3Sn). These compounds are isostructural to each other, which enables us to understand systematically the nature of Pu 5f localization and delocalization. We have established a connection between the lattice parameter and the degrees of 5f electron localization and identified Pu 5f electrons are most localized in Pu3Sn in all three compounds based on the effective band width of Pu 5f orbital as estimated from the partial density of states. As a future plan, we will carefully analyze the relative strength of Pu 5f hybridization with Pu 6d (which is major source for delocalization in elemental Pu solids) and further extend our theory capability to tackle the most challenge problem of elemental Pu solid doped with Ga, In, Sn impurities for the understanding of phase stability.

A paper on the new '115' compounds and their relation to these compounds is in preparation. This will serve as a nice comparison to the binary alloys of this project and the ternary intermetallic compounds which were recently synthesized in the last few months at CMR. I am planning to attend 3 upcoming conferences where I will present some of this new work outlined above. Pu Futures 2014, MRS2014, and the US/Russia Workshop are all important venues to showcase this new work and possibly establish additional external collaborations for LANL.

Future Work

Many of the goals which were outlined are currently being worked on. The PI is building and testing the induction furnace melter which will be utilized to synthesize the mission relevant alloys that were outlined in the proposal. Once the furnace is in place, the desired alloys will be prepared and then their physical properties will be characterized. These measurements will include magnetic susceptibility, heat capacity, and electrical resistivity. Thermal expansion measurements will also be completed using the low temperature capacitance dilatometer which the PI is assembling and later calibrating. This dilatometer is expected to be up and running in the next couple of months if testing is carried out with satisfaction. The PI expects to obtain preliminary results by December 2013 with a majority of the alloys being synthesized and characterized. These results will indicate if the technique proposed is showing a measure of success. The alloys which are expected to be made along with the temperature profile to be used (which is unique to each one) has been outlined and discussed with other individuals on the project. The PI also expects to obtain electronic structure data on many of these alloys from the theorist who is staffed on the project. These calculations will be completed once the samples are synthesized and the needed properties are measured experimentally.

The tasks for next fiscal year include:Synthesize all alloys and compositions to be studied (Pu-rich line compounds and delta-like alloys). Characterize these materials using powder X-ray diffraction, heat capacity and magnetic susceptibility. Move the tested thermal expansion setup over to CMR and begin to measure Pu materials once encapsulation setup has been sufficient to measure radioactive materials. Begin to compile preliminary results in order to find missing compositions to target magnetism.

Conclusion

Once the targeted compounds are made, the subsequent measurements to probe the crossover of the 5f electrons are relatively straightforward and are sufficient enough to make conclusions for the critical point of where magnetism disappears as we approach δ-Pu. We expect to:

1) Find magnetism in the Pu3X compounds based on the previous hypothesis for the expansion of the unit cell volume leading to a stronger coupling of the magnetic moments (more in the localized regime).

2) Track the emergence of magnetism in the thermal expansion measurements.

Publications

Bauer, E., P. Tobash, J. Mitchell, and J. Sarrao. Single crystal growth of plutonium compounds from molten metal fluxes. 2012. Philosophical Magazine. 92 (19-21): 2466.

Deterministically Enhanced Monte Carlo for Radiative Transfer

Allan B. Wollaber
20120738ECR

Introduction

Hot problems (supernovae, inertial confinement fusion, oxy-coal combustion) can require an accurate simulation of radiative heat transfer, but modeling the nonlinear exchange of energy between matter and photon radiation is a considerable algorithmic and computational challenge. The Implicit Monte Carlo (IMC) method has emerged as the preferred approach for high-fidelity radiation simulations, but its underlying equations can produce nonphysical solutions for large time steps, and its stochastic implementation leads to statistical noise, particularly in "cold" problem regions. We propose a novel way to use a low-order linear algebra (deterministic) calculation to simultaneously (1) enhance the temporal accuracy of the IMC solution, (2) reduce its statistical uncertainty, and (3) accelerate the overall calculation. Specifically, averaged interaction coefficients are generated during the high order calculation and provided to a dimensionally reduced deterministic solver that then calculates an estimate of the upcoming radiation and material temperature solutions. The approximate material temperature is then exploited to provide time-centered (instead of time-explicit) interaction coefficients and a physics-based time-step controller for the upcoming IMC cycle. The approximate radiation temperature is utilized to reduce the statistical uncertainty in the IMC solution, to reduce the time to solution, and to identify important problem regions to further accelerate the calculation. Thus primed, the IMC calculation is carried out and supersedes the approximate solution. We intend to deploy this approach in production software to enable first-ever, high-fidelity comparisons between telescopic observations of type IA supernovae and simulations of their radiation-hydrodynamical evolution, which should help solidify our current understanding of the history and structure of the observable universe.

Benefit to National Security Missions

The essential goal of this work is to accelerate and enhance the accuracy of high-fidelity radiative transfer simulations. The challenge goal of this work is to enable first-ever high-fidelity radiation simulations of type 1a supernovae that are of direct relevance to cosmologists, astrophysicists, and work supported by DOE's Office of Science (both in HEP and ASCR). This work is also applicable to the simulation of inertial confinement fusion experiments performed at the National Ignition Facility for DOE's NSSA. Finally, the hybrid deterministic-Monte Carlo approach for radiation transport is relevant to other instances of neutral particle transport, such as occurs in the simulation of nuclear reactors or of oxy-coal combustion.

Progress

We implemented several solver and temperature-coupling capabilities into Albireo (a standalone executable in Asterisk).

- Solver options: "only IMC", "only low order", or "IMC and low order"
- Temperature coupling options: "just follow IMC" or "use temperature guess"
- Provided a fixed point iteration option to nonlinearly converge the low order temperature
- These features have been tested and reported

Presented the accuracy-enhancing temperature coupling methodology at the biennial American Nuclear Society's Mathematics and Computation Division meeting (this is the premier conference for researchers in my field).

After initially running into a setback regarding the accuracy and positivity of the low order, tensor diffusion solution using the standard continuous finite element methodology (CFEM), we implemented a custom finite volume (FV) spatial discretization. The FV discretization produces better results, although this unplanned effort took about a month to implement.

Implemented an initial variance reduction capability

- Alex Long was hired on as a summer student in May. He has already modified Asterisk and Jayenne project software to implement variance reduction (particle splitting and a lower weight window cutoff to control particle weights based on the deterministic, tensor-diffusion solution). Testing is now underway.

Future Work

During the remaining 10 months of this project (ending April 2014), we intend to:

implement a wavefront-detection type algorithm to limit particle splitting:

- A naive application of the deterministic solution as the weight-window center can lead to large particle splitting ratios that decreased the overall efficiency in preliminary work for multifrequency problems (see A.B. Wollaber, "Advanced Monte Carlo Methods for Thermal Radiative Transfer" PhD Thesis, The University of Michigan, 2008).

Test the methodology on a supernova simulation:

- Expose an interface that makes this methodology callable from a host application
- Work with Chris Fryer et. al. to deploy this methodology on a "real" supernova light curve simulation

Conclusion

The anticipated result is production software that automatically enhances the accuracy and efficiency of high-fidelity radiation-hydrodynamics simulations with respect to current software.

Publications

Wollaber, A. B., and J. S. Warsa. A New, Coupled Transport-Diffusion Method for Radiative Transfer Calculations. 2013. In International Conference on Mathematics and Computational Methods Applied to Nuclear Science and Engineering (M&C 2013). (Sun Valley, ID, 5-9 May 2013). , p. 7293. La Grange Park, IL: American Nuclear Society.

Large-scale Simulations for Nuclei and Strongly-correlated Matter

Stefano Gandolfi
20120758ECR

Introduction

The goal of this project is to calculate properties of nucleonic matter and neutron stars that are of great relevance for nuclear astrophysics. The equation of state and related properties including the spin- and neutrino- response are critical to understand current observations of the mass-radius relationship, and the cooling and X-ray emission of neutron stars. The inhomogeneous neutron matter in the crust can be modeled by neutrons interacting via nuclear forces confined in external traps, and the higher-density homogeneous matter can also be studied through large-scale Quantum Monte Carlo simulations.

A quantitative understanding of homogeneous and inhomogeneous matter from first principles is an essential first step towards building an energy density functional for nuclei, as properly calibrated nuclear energy density functionals must capture the effects of the interaction and reproduce experimental results for any nuclear system. The characterization of nuclear energy density functionals is of high impact to study properties of neutron-rich nuclei that will be realized in several current and upcoming DOE experimental facilities including CARIBU and FRIB.

We will simultaneously study related strongly-correlated ultracold Fermi gases. In the dilute regime where the density is low enough, properties of neutron matter are very similar to those of ultra-cold Fermi gases near infinite scattering length. This limit of cold Fermi atoms is the most strongly-coupled system known, as its scattering cross-section diverges. These systems are realized in experiments through the use of the Feshbach resonances; their properties are independent of the microscopic details of the interaction and are thus universal. Because of their universality, ultra-cold Fermi gases are an ideal system to test microscopic many-body theories and compare to nuclei and other strongly-correlated systems.

Benefit to National Security Missions

This project ties to the basic research mission of LANL's nuclear theory program, sponsored by the DOE Office of Science. Calculations of nuclear properties and those of nucleonic matter are relevant to DOE facilities including CARIBU at ANL and the upcoming FRIB facility at Michigan State University. It is also of direct relevance to DOE nuclear physics priorities in nucleonic matter and nuclear astrophysics.

The work is also related to an underlying capability in nuclear structure and reactions at LANL, e.g. in support of the weapons program. It is relevant to theories of nuclear structure and reactions, particularly light-ion reactions.

Progress

In the last year we have finished and published several results related to this project.

We have successfully studied the neutrino- and anti-neutrino-deuteron interaction. We have calculated the dynamic response function for neutrino energies up to a GeV, and addressed the role of two-body processes in the nuclear currents. We have derived the corresponding cross-sections. The results have been published in Phys. Rev. C.

The energy of the unitary gas in a trap for different number of atoms has been calculated using Quantum Monte Carlo methods. The results have been compared to the case of trapped neutrons, and have been published in Prog. Theor. Exp. Phys.

In addition, we have calculated the energy-dependence of the unitary Fermi gas to the effective range of the potential. This calculation is important to understand the difference between low-energy neutron matter and the unitary Fermi gas. The results have been published in Prog. Theor. Exp. Phys. and in Phys. Rev. A.

We have calculated the structure factor and the contact parameter of the unitary Fermi gas. The accurate predictions obtained from Quantum Monte Carlo simulations have been compared to new experimental measurements of the same quantities. The new theoretical/experimental results have been published in Phys. Rev. Lett.

We have finished and published in Phys. Rev. C the calculation of the spin response of neutron matter. Using Quantum Monte Carlo methods we have calculated selected sum-rules that we have used to constrain the spin-response function. This is relates to the neutrino interaction with neutron matter as a function of the neutrino energy. The results have been used to calculate the neutrino emissivity that is directly related to the cooling of neutron stars.

We have calculated the binding energy of a Lambda particle in selected hyper-nuclei from A=5 to 91. Our calculation showed that the three-body force, i.e. the Lamda-nucleon-nucleon interaction, are dramatically important in these systems. The results have been published in Phys. Rev. C.

We have calculated the energy of neutrons confined in external traps using different nuclear Hamiltonians. This work is important to constrain nuclear energy density functionals, but also to understand the effect of using different Nuclear Hamiltonians to study neutron-rich systems.

We have also compared other properties of these systems, i.e. densities, radii, pairing gap and spin-orbit splittings. The results have been published in Phys. Rev. C.

Future Work

In the next fiscal year we expect to produce new calculation of trapped Fermions (cold atoms) and neutrons. We will study the role of pairing correlations in these systems that are important to calculate the pairing gap. The neutron pairing in confined geometries will be important to constrain the pairing term in density functional theories for finite nuclear systems. The study of properties of confined unitary Fermi gases is important to fit density functionals and test their quality to deal with small systems and/or in the presence of external potentials modelling optical lattices.

We will calculate the sum-rules of electromagnetic and weak interactions in light nuclei. The results will allow us to fit the neutrino-nucleus response for selected nuclei, and to calculate the cross-section. We first will perform the calculation for very light nuclei, like the alpha particles, and then will try to address nuclei up to the carbon. We expect these results to be important in understanding the contribution of one and two body currents in the neutrino-nucleus interaction.

Conclusion

Our results will have important impacts in several communities. The calculation of nucleonic matter will provide a strong support to experimental data to fit energy density functionals used to describe stable and unstable neutron-rich nuclei, and of the crust of neutron stars. Also, ultracold Fermi gas experiments are also beginning to probe inhomogeneous systems in external potentials. We will also calculate dynamic properties of these strongly-coupled systems. The calculation of the spin-response allows us to estimate the neutrinos mean free path in dense neutron star matter, and to study the cooling rate of neutron stars observed by modern X-ray telescopes.

Publications

Bogner, S., A. Bulgac, J. A. Carlson, J. Engel, G. Fann, and others. Comput.Phys.Commun.. 2013. Comput.Phys. Commun.. 184: 2235.

Carlson, J., S. Gandolfi, and A. Gezerlis. Quantum Monte Carlo approaches to nuclear and atomic physics. 2012. PROGRESS OF THEORETICAL AND EXPERIMENTAL PHYSICS. (1): -.

Forbes, M. M., S. Gandolfi, and A. Gezerlis. Effective-range dependence of resonantly interacting fermions. 2012. PHYSICAL REVIEW A. 86 (5): -.

Gandolfi, S.. The equation of state of neutron star matter and the symmetry energy. 2013. In 11TH INTERNATIONAL CONFERENCE ON NUCLEUS-NUCLEUS COLLISIONS (NN2012). Vol. 420, p. -.

Gandolfi, S.. Quantum Monte Carlo study of inhomogeneous neutron matter. 2012. HITES 2012: HORIZONS OF INNOVATIVE THEORIES, EXPERIMENTS, AND SUPERCOMPUTING IN NUCLEAR PHYSICS. 403: -.

Gandolfi, S., J. Carlson, and S. Reddy. Maximum mass and radius of neutron stars, and the nuclear symmetry energy. 2012. PHYSICAL REVIEW C. 85 (3): -.

Gezerlis, A., I. Tews, E. Epelbaum, S. Gandolfi, K. Hebeler, A. Nogga, and A. Schwenk. Quantum Monte Carlo Calculations with Chiral Effective Field Theory Interactions. 2013. PHYSICAL REVIEW LETTERS. 111 (3): -.

Hoinka, S., M. Lingham, K. Fenech, H. Hu, C. J. Vale, J. E. Drut, and S. Gandolfi. Precise Determination of the Structure Factor and Contact in a Unitary Fermi Gas. 2013. PHYSICAL REVIEW LETTERS. 110 (5): -.

Illarionov, A. Y., S. Fantoni, F. Pederiva, S. Gandolfi, and K. E. Schmidt. Determination of the finite temperature equation of state of dense matter. 2012. PHYSICS OF ATOMIC NUCLEI. 75 (7): 866.

Lonardoni, D., S. Gandolfi, and F. Pederiva. Effects of the

two-body and three-body hyperon-nucleon interactions in Lambda hypernuclei. 2013. PHYSICAL REVIEW C. 87 (4): -.

Lovato, A., S. Gandolfi, R. Butler, J. Carlson, E. Lusk, S. C. Pieper, and R. Schiavilla. Charge Form Factor and Sum Rules of Electromagnetic Response Functions in C-12. 2013. PHYSICAL REVIEW LETTERS. 111 (9): -.

Maris, P., J. P. Vary, S. Gandolfi, J. Carlson, and S. C. Pieper. Properties of trapped neutrons interacting with realistic nuclear Hamiltonians. 2013. PHYSICAL REVIEW C. 87 (5): -.

Shen, G., L. E. Marcucci, J. Carlson, S. Gandolfi, and R. Schiavilla. Inclusive neutrino scattering off the deuteron from threshold to GeV energies. 2012. PHYSICAL REVIEW C. 86 (3): -.

Shen, G., S. Gandolfi, S. Reddy, and J. Carlson. Spin response and neutrino emissivity of dense neutron matter. 2013. PHYSICAL REVIEW C. 87 (2): -.

Steiner, A. W., and S. Gandolfi. Connecting Neutron Star Observations to Three-Body Forces in Neutron Matter and to the Nuclear Symmetry Energy. 2012. PHYSICAL REVIEW LETTERS. 108 (8): -.

Tsang, M. B., J. R. Stone, F. Camera, P. Danielewicz, S. Gandolfi, K. Hebeler, C. J. Horowitz, J. Lee, W. G. Lynch, Z. Kohley, R. Lemmon, P. Moller, T. Murakami, S. Riordan, X. Roca-Maza, F. Sammarruca, A. W. Steiner, I. Vidana, and S. J. Yennello. Constraints on the symmetry energy and neutron skins from experiments and theory. 2012. PHYSICAL REVIEW C. 86 (1): -.

Precision Predictions for Jet Cross Sections

Christopher Lee
20120759ECR

Introduction

The Large Hadron Collider (LHC) is now colliding protons at the highest-ever energies to search for new particles beyond the Standard Model of particle physics. New particles and forces may explain the origin of all matter and mass in the Universe. Many possible new particles are expected to decay quickly to "jets" of hadrons, energetic sprays of bound states of quarks and gluons like those that make up ordinary matter. But purely Standard Model processes already produce jets ubiquitously. Modern strategies to search for new physics have made it a key priority to identify and precisely predict differences in the substructure of jets produced by new or Standard Model particles.

This project will predict Standard Model jet cross sections (probabilities to produce jets as a function of their energies, shapes, sizes, and substructure) to unprecedented precision in order to discern signatures of new physics over background in jets. We will first tackle two unsolved problems in Quantum Chromodynamics (QCD), the theory of interactions between quarks and gluons. These problems limit the precision currently attainable in predicting jet cross sections. Accurate predictions for jet cross sections require summing the probabilities of emitting arbitrarily many soft (low-energy) or collinear (parallel) gluons or quarks in or from jets. Summing only a finite number of emissions yields inaccurate results---"resummation" of infinitely-many emissions is crucial. Techniques for resummation exist for relatively simple cross sections, but not for the more intricate cross sections used in jet substructure-based strategies to search for new physics. We will solve the long-standing problems of resumming gluons that split and cross jet boundaries, and of resumming emissions confined within very small jet cones. We will use our solutions to predict to high precision the cross sections used to search for signatures of new physics in the detailed structure of jets.

Benefit to National Security Missions

Two key missions of the DOE Office of Science in High-Energy Physics are 1) to improve our understanding of Quantum Chromodynamics (QCD), the theory of the strong interactions between quarks and gluons, constituents of all ordinary matter; and 2) to search for new particles and forces beyond the Standard Model that will explain the origin of matter, dark matter, and masses of elementary particles. In Nuclear Physics, a key DOE mission is to use heavy ion collisions to understand the nature of the quark-gluon plasma and extreme states of QCD matter which pervaded the very early Universe.

Jets of hadrons produced by energetic quarks and gluons are key to achieving these objectives. They reveal the behavior of QCD itself, contain evidence of new particles that decay to jets, and probe properties of dense QCD matter through which they pass.

We tackle problems at the forefront of QCD perturbation theory. Physically accurate predictions of jet cross sections require resumming arbitrarily many soft and collinear quark and gluon emissions in and from jets. We will resum correlated emissions of gluons and quarks across jet boundaries and within very small jet cones, both unsolved problems in QCD. Our new tools will allow unprecedented precision in predicting jet cross sections for probing QCD, new physics, and dense matter at the Large Hadron Collider (LHC).

Historically, individuals hired for their expertise in this area have gone on to address a range of Laboratory challenges, including bio and energy security, thanks to their broad analytical skills.

Progress

In the last year, we have explored several candidates for effective field theories to resum non-global logarithms (NGLs) and logs of jet radii R. We have evaluated the

theoretical promise of each and identified two promising candidate theoretical frameworks we will fully implement in the next year to achieve the logarithmic resummations.

A key step has been to separate the steps of resumming NGLs and logs of R. Previously we believed they should be done together, that is, by first using ordinary soft-collinear effective theory (SCET) to separate hard, hard-collinear, and soft degrees of freedom from one another to sum logs of R, and then to further factorize the soft sector using a second effective theory to resum the NGLs. However, now we understand that it is more promising to reverse this order. First, we separate the modes of full QCD (Quantum Chromodynamics) into hard and soft degrees of freedom to sum the NGLs. Only then do we separately factorize these hard and soft sectors into hard/hard-collinear and soft/soft-collinear modes. The soft/soft-collinear factorization is also a step we have proposed for the first time. We are in the midst of completing the theoretical formulation of this doubly-factorized effective field theory and implementing it to resum logs of R and NGLs.

In summary, in the past year we have tested and identified the most promising avenues for constructing effective theories that will achieve resummation of NGLs and logs of R, preparing us well to achieve these goals in concrete predictive calculations in the upcoming year.

Also in the past year, we have found a new area of application of the effective field theory methods upon which this LDRD is building to resum perturbative expansions of jet cross sections in deep inelastic scattering (DIS) of electrons and protons. While the methods of SCET had previously been applied to electron-positron and proton-proton jet cross sections, we realized they had never been fully implemented in electron-proton collisions. We predicted jet cross sections in DIS using a variable “1-jettiness” that measures how jet-like the final state of a DIS event is, but without using measures like jet radii or NGLs. This type of “global” measurement is a precursor to accurately predicting jet cross sections using the more non-global or exclusive measures that use jet radii and contain NGLs. We predicted 1-jettiness cross sections in DIS to next-to-next-to-leading logarithmic (NNLL) accuracy in resummed perturbation theory for the first time, one order beyond any previous work on DIS jet cross sections. We also discovered the universality of nonperturbative corrections to several different types of 1-jettiness cross sections. This discovery and the NNLL perturbative resummation exhibit the power of the effective theory approach to jet physics. We completed a paper on this work (arXiv:1303.6952) which has been accepted by Phys. Rev. D for publication. This work advances the precision with which the strong coupling alpha_s or the internal structure of the proton can be measured using jets in DIS.

Future Work

In the next fiscal year we will implement the new effective theory frameworks we have conceived of to resum logarithms of jet radii and of non-global logarithms. We will calculate predictions to at least next-to-leading-logarithmic (NLL) accuracy in resummed perturbation theory. We will demonstrate that our resummed predictions match the predictions of fixed-order Quantum Chromodynamics (QCD) calculations from numerical programs to second-order (alpha_s^2) in the strong coupling.

We will also continue the new direction of research into high-precision resummed predictions for jet cross sections in deep inelastic scattering (DIS) of electrons and protons. We will perform calculations of the fixed-order QCD cross sections to next-to-leading order (NLO) and of the soft function in the soft-collinear effective theory (SCET) factorization theorem to O(alpha_s^2), both of which way lay necessary groundwork to extend the precision of these predictions to NNLL+NLO accuracy, allowing for higher-precision extractions of the strong coupling alpha_s from DIS jet data.

Conclusion

First, we will create new theoretical tools in QCD that make possible the resummation of quark and gluon emissions from jets in in two unsolved scenarios: correlated emissions splitting across jet boundaries and emissions confined to very small jet cones. These tools will solve long-standing problems at the forefront of QCD perturbation theory and make possible precise predictions of many more observables than at present. Second, with these tools we will achieve the level of precision in predicting jet cross sections required to use jets and their substructure to distinguish signals of new physics from Standard Model background.

Publications

Kang, D., C. Lee, and I. W. Stewart. Using 1-jettiness to measure 2 jets in DIS 3 ways. 2013. PHYSICAL REVIEW D. 88 (5): -.

First Principle Study of Relativistic Beam and Plasma Physics Enabled by Enhanced Particle-In-Cell Capability

Chengkun Huang
20130744ECR

Introduction

The Particle-In-Cell (PIC) method is a fully kinetic ab-initio method widely used in plasma and particle beam modeling. Although the standard PIC method with the second order accurate numerical algorithm is well suited for the study of beam and plasma dynamics at low speed, its application to relativistic phenomena is severely limited. The major limitations come from the dispersive and anisotropic propagation properties of the electromagnetic (EM) wave on the grid, the numerical instability associated with the unphysical Cherenkov radiation, the inaccuracy in the relativistic particle kinematics and the undesirable noise from under-resolved dynamics. In this work we will develop, validate and apply a new computational framework so as to be able to compute and understand cutting-edge problems involving highly relativistic charged particles. Our approach is to address the deficiencies of the standard PIC method and include enhancements with carefully designed high order particle shapes/digital filters, a relativistically accurate particle pusher and most importantly a 4th-order accurate and tunable EM field solver developed recently. This enhanced PIC capability will provide, for the first time, accurate and self-consistent modeling for many relativistic beam/plasma problems of importance to LANL's mission and to the broader scientific community. Specifically, we will focus on (1) understanding how the microbunching instability can arise from the interactions between a highly relativistic beam and its radiation in a Free Electron Laser (FEL) bunch compressor and how it affects the beam quality and FEL performance; (2) investigation of the collisionless particle acceleration process in astrophysical shock and the deceleration process related to the collective wave-particle interaction in high-energy-density plasmas. The former application is directly relevant to the success of the MaRIE X-ray FEL signature facility while the latter addresses fundamental science questions in both astrophysics and a high-risk yet high-potential fast-ignition technology for inertial fusion energy.

Benefit to National Security Missions

The proposed work will establish a high-fidelity first-principle predictive modeling capability and improve the understanding of high current beams interaction with its coherent radiation and the kinetic plasma behavior under extreme conditions. We are pushing the envelope of the PIC method which is widely used in the lab for various DOE/NNSA projects in high energy density plasma, accelerator beam dynamics, astrophysics and space applications, thus yielding many scientific possibilities for LANL. The improved modeling capability and the new insights into the XFEL microbunching instability and particle acceleration/deceleration mechanisms link directly into LANL's missions of (1) Matter-Radiation Interactions in Extremes (MaRIE) Signature Facility, (2) Nuclear, Particle, Cosmology, and Astrophysics and (3) Nuclear Energy.

Progress

The project started in July 2013; therefore, there is no progress to date.

Future Work

The project has a start date of July 1 in FY13. In the rest of FY13, we expect to characterize the new high order field solver and identify the optimal tuning parameters and the strategy of noise control for the micro-bunching instability, collisionless shock and fast ignition study. We will derive the full dispersion relation of the new solver to guide our tuning process. Then at the end of FY13 or the beginning of FY14, we will begin the study of the micro-bunching instability by first benchmarking with our 2D coherent synchrotron radiation model for a non-evolving beam. For collisionless shock and fast ignition study, we will begin by investigating the wake of a single relativistic particle both in free space and in a plasma. After these benchmarking, we will proceed to the study of the relevant physics in FY14. In particular, by the end of FY14, we expect to conduct detail validated simula-

tion study of (1) micro-bunching instability relevant to X-ray free electron design design, (2) relativistic collisionless shock for astrophysics and (3) fast ignition concept.

Conclusion

The technical goal of our work will be a validated new PIC capability that can be effectively applied to relativistic beam and plasma problems with superior accuracy and stability for a wide range of parameters. The scientific goal is a detailed understanding that bridges the gap between present simulations and theories/models for the micro-bunching instability and collisionless particle acceleration/deceleration processes. Our results will impact the design of the MaRIE X-ray free electron laser, fast ignition inertial fusion experiments and help elucidate the origin of energetic particle in the cosmos.

Publications

Huang, C., T. J. T. Kwan, and B. E. Carlsten. Synchrotron Radiation Near Field In 3D. To appear in 25th Particle Accelerator Conference. (Pasadena, 30 Sept. - 4 Oct. 2013).

Stochastic Modeling of Phase Transitions in Strongly Interacting Quantum Systems

Christopher Ticknor
20130749ECR

Introduction

This research explores thermal phase transitions in quantum systems. Two sets of codes will be developed, the first is a static, perturbative treatment. This will extend a standard treatment for quantum gases at finite temperature to study multicomponent, dipolar quantum gases. The second set of codes, is a stochastic method, this theory will more fully account for the fluctuating nature of quantum systems. Both codes will be used to study intriguing quantum behavior near thermal phase transitions. Completely developing the SPGP method in 2 years will be a challenge - there are many technical challenges to be met. These codes will tackle an interesting problem: thermal phase transitions. Understanding such complex systems is a significant challenge, with substantial payoff.

Benefit to National Security Missions

The numerical methods studied here are an important step in developing hybrid quantum/classical codes that can treat fundamental quantum behavior in high temperature regimes. Solving a full quantum treatment at high temperatures is simply not possible, and therefore an alternate method needs to be developed which retains aspects of quantum behavior. That is exactly what this work does. This work additionally looks at phase transitions of quantum systems. This will help understand the behavior of finite quantum systems beyond ideal settings and conditions.

Progress

Since this project started in Jan 2013, I have implemented the first part of the research. I have produced a multicomponent, linear excitation theory including non-local interactions. Furthermore, I have produced a paper with these codes, currently under review of PRA Rapid.

This work was not even for the full system (dipolar gas) because there is so much to understand about mixture systems. This will lead to a slight diversion in the plan. There are more simple studies to be done on phase transitions in this system. So I will further the research on mixtures and produce research articles of high quality.

This work has been extended for the local version to the full finite temperature theory. I have added another basis set to better handle the non-local interactions. This will greatly enhance my ability to study the strongly interacting quantum limit.

Future Work

In the next year, I will fully develop a perturbative and static treatment known as: Hartree-Fock Bogoliubov Popov (HFBP). With this code, I will study the thermal phase transition of a two component immiscible, dipolar quantum gas.

Next, I will start the development of a dynamic method known as the Projected Gross Pitaevskii (PGP) method. This method will study two thermal phase transitions: the miscible/immiscible character of the quantum gas and the phase coherence as temperatures is changed. This method will be able to go the strongly interacting regime, unlike the first method (HFBP).

Conclusion

The goal of this project is twofold: first, develop two flavors of codes to study finite temperature quantum gases. Second, study thermal phase transitions of quantum gases. It is unknown how temperature alters the miscible/immiscible character of ultracold quantum gases. Additionally, study the thermal phase transitions which dictates the coherence of the quantum gas. This work will influence how experiments are run and how finite quantum systems are understood.

Publications

Ticknor, C.. Excitations of a trapped two-component Bose-Einstein condensate. 2013. PHYSICAL REVIEW A. 88 (1): -.

Answer to Heavy Element Production Puzzle by Measuring Neutron-induced Charged Particles at LANSCE

Hye Young Lee
20130758ECR

Introduction

This project is to build a new capability of measuring neutron-induced charged particle reactions at Los Alamos Neutron Science Center (LANSCE). Neutron-induced charged-particle reactions are critical to understand the currently unsolved heavy-element production puzzle, since these reactions in stars compete with neutron capture reactions, a main process to produce heavy elements. Of importance, the Ne-22(a,n)Mg-25 reaction has been studied for decades to provide a key answer to how the neutron source was generated for successive captures in heavy element production. However, the direct measurements contain large uncertainty due to the technical difficulties in detecting low cross-section reactions and large background. Using this new capability, a time-reversed Mg-25(n,a) measurement at LANSCE will shed a new light on the critical region of interest to help astrophysics modelers explain how heavy elements are produced.

Developing the efficient detection system, waveform digitizers, and low background environment is the integral part of this project. Along the experimental effort, it is planned to study reaction processes using the Monte Carlo Hauser-Feshbach method, which was developed by the T-2 group. We have been collaborating to improve the theoretical prediction power by comparing the calculations with the experimental data, and this new capability will certainly enhance the reliability of theoretical predictions for currently unavailable reactions-impossible to measure in laboratories due to very short lifetime of nuclei.

Benefit to National Security Missions

Neutron-induced charged particle reactions are important to the Weapons Program for the interpretation of radiochemical diagnostics, nuclear forensics, and other applications. Scientifically, this project is well-matched to ongoing Los Alamos Neutron Science Center (LANSCE) efforts to increase our portfolio and capabilities in nuclear astrophysics, while developing instrumentation that can address outstanding problems for multiple sponsors. This combination of world-class basic science while simultaneously solving problems for the nation in multiple nuclear science thrusts makes this truly a LANL-appropriate endeavor.

Progress

The conceptual design of the low energy ionization chamber was determined to use a Frisch grid and segmented anodes. Multiple design considerations were put into the process of optimizing in low-energy alpha particle detection for nuclear astrophysics interest and also with the flexibility of converting this ionization volume into one of delta-E detectors for high energy charged particle detections, which is planned to be completed in the next year.

The conceptual design of the high energy charged-particle detection system is to use a stack of silicon strip detectors to increase detection solid angle coverage and improve angular resolutions. The choice of most advanced silicon strip detectors were under discussion with the company for the feasibility of development and a delivery time for next fiscal year.

Upon completion of design parameters in the ionization chamber, hardware procurements were progressed in deciding the specifications of electronics. For the best results in reducing the background in signals and improving particle identification capability, I chose two different types of digitizers. VX1720 from CAEN has a sampling rate of 250 Mega-samples/second with 12-bit digitization resolution, and VX1724 from CAEN has a sampling rate of 100 Mega-samples/second with 14-bit digitization resolution. A 9-slot VME crate from Wiener and optical link communication are chosen for the application. All these electronics are expected to be delivered by the end of July. At the moment, procurement for the gas handling system is underway.

A Monte Carlo code was developed to simulate the signal strength in different geometry of a cathode and anodes, the detection thresholds, and the detection efficiency. The code written in C++ runs in the platform of the ROOT package. One student from the SARA (Service Academy Research Associates) program has worked for 6 weeks to develop this Monte Carlo code.

Based on the characterization of the ionization chamber in Monte Carlo simulations, I have discussed with the engineer for the general vacuum chamber design. I have contacted a mechanical engineer to work on machine drawings for manufacturing, which is scheduled for this summer. I am also working on the materials to be used in the ionization chamber and I contacted the providers for the details. All the procurements went reasonably well and I am still working on hardware manufacturing.

I have submitted a beam time request proposal to the Weapons Neutron Research (WNR) Program Advisory Committee in April 2013 and a 10-day beam time will be awarded sometime during the upcoming beam cycle (Aug. 13 through Dec. 21, 2013).

Future Work

For the second fiscal year, the project is planned to commission the newly developed low-energy detection system and complete the development of high-energy detection system.

First, assemble all the components with proper small element procurements to build an low-energy ionization chamber. Once all the hardware is installed, test signals with a calibration source at the TA53-Building 17, which is our group's lab space. I also expect to start a paper work to place proper safety concerns like an IWD. With the requested beam time, 10 days will be awarded to test in-beam background and all the functions.

Second, for the high-energy detection system, silicon strip detectors with proper preamplifiers will be purchased and additional digitizers. The full system will be commissioned with alpha source. For the in-beam test, another beam time request proposal will be submitted to the WNR Program Advisory Committee.

Conclusion

We expect to produce reliable neutron-induced charged-particle reaction data by developing the experimental capability at LANSCE. The new detection system consists of highly segmented silicon detectors for a large detection coverage with good angular information and waveform digitizers with improved timing resolution. Implementing software filters in digitized waveforms, which is traditional, can provide additional information for improving resolution and performance of detectors. The combination of two techniques allows us to improve the signal-to-background ratio, pushing the current limitation on detecting low energy charged particles to lower energy than the previously achieved.

The Dynamic Environment of Iron Core Formation and Collapse

Casey A. Meakin
20120530ECR

Abstract

This project has sought to advance our understanding of how turbulent flow shapes the evolution of stars, and in particular those stars thought to end their lives in supernova explosions. Towards this end we have carried out new multi-dimensional simulations of turbulent convection and nuclear burning in stellar interiors and have undertaken the most detailed analysis of this type of numerical data yet, with the following main results. Our analysis has clarified the important role played by several previously ignored physical processes in the dynamics of turbulent stellar flow including pressure-dilatation, pressure-flux, and kinetic energy dissipation. This work has also clarified the shortcomings of modern turbulence models for treating stellar flow; in particular the so-called "down-gradient" and "return-to-isotropy" closure relationships are shown invalid. Our work provides a framework for assessing future turbulence models against multi-dimensional simulation data. Finally, this work has resulted in several follow on projects, including both interfacing our results with core-collapse supernova modeling efforts as well as more detailed statistical turbulence analysis work including evolution equations for higher order statistical moments (e.g., for turbulent fluxes), a scale-by-scale analysis of the simulated flows, and extensions to treat rotating and magnetized systems.

Background and Research Objectives

Massive stars end their lives after they have completed successive stages of nuclear burning in their cores, ultimately converting their initial hydrogen and helium composition into a dense central core composed of primarily iron-peak elements. Iron peak material reside at the peak of the nuclear binding energy curve, which means that additional energy cannot be liberated through continued nuclear burning. This circumstance, together with a gravitational instability, eventually results in the collapse of the iron core thus formed. The ensuing collapse of the core to nuclear densities is thought to be responsible for producing a shock wave, which eventually tears the entire star apart in a supernova explosion.

Despite decades of intensive theory, however, we still do not have a robust or detailed understanding of how this iron-core collapse event results in a supernova explosion. While we have identified the source of energy needed to power such an explosion (the gravitational potential energy liberated during the collapse), we do not yet understand how this energy is harnessed. Stellar evolution, which encompasses the details of iron core formation and collapse, is a strongly turbulent, highly non-linear phenomenon, which is not directly amenable to paper and pencil theory and therefore depends on simulation for progress. The first simulations of stellar core collapse, produced in the late 1960s, were successful, but were calculated entirely in 1D, from star birth, to iron core formation, to iron core collapse and explosion. However, as the input physics used in these simulations improved (e.g., better equation of state, better transport physics), 1D models began to fail to explode. Subsequent generations of multi-dimensional models of the core collapse event, which continued to use iron cores evolved in 1D as initial conditions, were begun, and despite initial successes, these too were eventually found to fail to produce explosions naturally and robustly. This remains the current state of the research.

There are two strongly favored candidate solutions to this problem, either (1) researchers hope that further refinement in simulating iron core collapse will lead to successful explosions, which would therefore indicate an incredible sensitivity to the finest details of the problem, or (2) finally examining the highly uncertain initial conditions, currently based on 1D models of stellar evolution, will provide the missing link in our understanding of this "supernova problem".

The present work pursues this second avenue, for the following reasons. First, if refined simulations of core collapse do result in robust explosions, these results will

remain contingent upon the uncertain initial conditions of 1D stellar evolution. Second, we now have very strong evidence that the 1D initial conditions used for core collapse modeling are in fact flawed [1,5-7].

Objectives

We believe the above background motivates the need for a better understanding of stellar evolution, which is tantamount to better understanding the details of turbulent convection. Therefore, we pursue this goal in the present work through multi-dimensional simulation of stellar interiors combined with an appropriate analysis framework to interpret the resulting very large data sets.

Scientific Approach and Accomplishments

Our scientific approach has been three pronged, including new large-scale computations, the mathematical development of an analysis framework, and data reduction of numerical results within this framework. In the following subsections we provide a summary of our approach and accomplishments in these three areas, and then conclude with a list of the follow-on work that has resulted from this project.

Computations

On the computational side, we have developed new simulation models and have acquired significant compute resources to carry these out (over 10 million CPU-hours on competitive national facilities, including XSEDE and DOE platforms). Additionally, our codes have been optimized to perform efficiently in parallel on over 100 thousand cores on both Cray and IBM platforms (currently tested up to ~130k cores with nearly perfect scaling, and limited to this number of cores only due to system availability).

All of our simulations have been conducted with the PROMPI code [5-7], an Eulerian, Godunov-based finite-volume hydrodynamics code outfitted with physics appropriate for modeling stellar interiors, including a realistic equation of state, multi-species advection, nuclear reaction rates and network evolution code, thermal (radiative) conduction and realistic opacities, and gravity. Our simulations are conducted within the implicit large-eddy simulation (ILES) framework [4], wherein molecular dissipative processes and sub-grid scale physics are relegated to the inherent dissipation of the hydrodynamics algorithm. An assessment of the behavior of this sub-grid physics is part of the subject of our analysis (discussed more in the following sections).

The new simulations undertaken for this project can be categorized as follows:

1. We have extended and built upon earlier generation simulations of oxygen shell burning [1,5-7], a phase of stellar evolution preceding core collapse in massive stars. In particular, we have conducted a resolution study up to 200 million zones for a 25 species reactive flow in order to assess the dependence of various statistical properties on spatial zoning. These new calculations have also included larger computational domains and longer run times than earlier work [4]. These calculations cost ~4.5 Million CPU-hours and were conducted entirely on the NICS Kraken Cray XT5 at the University of Tennessee. Additionally, each of these calculations were instrumented with code to produce running averages needed to best sample the mean-fields described in the next two sections (published in [12]).

2. We have developed new simulation setups to directly model the final burning stage prior to core collapse, which is silicon burning. This involved extending our nuclear reaction physics and redesigning our computational domain configuration to include full shell and full core calculations [8]. This latter aspect of development involved implementing a “star-in-box” setup, wherein spherical objects are embedded in a Cartesian box of zone with boundary effects ameliorated through “sponge-layer” damping [13]. Finally, an important part of this new set was the calculation of initial conditions for simulation. These were drawn from a new library of 1D stellar evolution calculations produced with the MESA code [11]. As of the termination of this project, we have begun a series of 2D simulations with 3D simulations imminent. We have ported this new setup to the NICS Kraken and ANL Vesta/Mira IBM BG/Q computing platforms. Our intentions are to complete our 2D survey and perform a capstone 3D simulation by early Fall 2013 and submit this work for publication at that time.

RANS Framework

We have developed the statistical moment equations, often referred to as Reynolds Averaged Navier-Stokes (RANS) equations [2-3], for the fully compressible, multi-species equations of hydrodynamics relevant for stellar modeling in spherical coordinates. The end result is a set of mean-field equations describing the statistical behavior of the mean flow, thus providing a framework to analyze the importance of various distinct physical processes.

This framework lends itself to the following: (1) it provides a means to assess the applicability of a broad range of turbulence closure models in the literature, (2) it allows the analysis and comparison of heterogeneous sets of turbulence data in a unified way, and (3) it provides a means to asses the behavior of sub-grid scale behavior inherent in

our numerical simulation scheme, including but not limited to turbulent dissipation and material mixing, offering further insight into the ILES approach.

Our development of the first order moment equations, and a second order moment equation for turbulent kinetic energy are published in [12]. Additional moment evolution equations, including variances for all relevant thermodynamic quantities and fluxes have also been developed and are in preparation [9]. The latter work also includes a (Fourier mode) scale-by-scale decomposition for each moment, thus providing a means to quantify the contribution to each physical process by either large-scale coherent flow components and/or the smaller scale statistically steady components.

Data Analysis

Much of the value of a three-dimensional simulation of turbulent flow resides in the ability to perform detailed analysis and calculate statistics from the numerical data. This is in sharp contrast to current experimental work which is still hampered by generally poor resolution, dimensionality (sometimes only 2D slices of 3D fields are possible), and limited access to physical fields (often limited to only kinematic quantities, such as the velocity field). Numerical simulation provides access to the complete system data for analysis. Towards this end, we have extracted mean fields for all of the terms constituting the RANS moment equations discussed above. In order to achieve the highest fidelity statistics we have instrumented our simulation code to calculate running averages which sample each numerical time step thus providing data that would have been impossible to produce as a post-process due to the data storage requirements.

Our primary results from this effort include:

1. We have identified and characterized the main physical processes responsible for the evolution. Of most interest is our identification of the work done by turbulent pressure fluctuations (pressure-dilatation) in a subset of our models. This process has not been included in any model of stellar convection known to this author, yet contributes ~40% of the total turbulent kinetic energy production in our models. Other noteworthy processes identified in our simulations include pressure-flux and turbulent kinetic energy flux as important process, particularly at convective boundaries where these processes mediate the interaction between the convection zone and the stably stratified layers that confine the turbulent motions.

2. Our work has provided insight into the behavior of the simulation method and the ILES paradigm. We have concluded the following. First, turbulent dissipation is well behaved in our models implying that relegating the action of viscosity to the numerical algorithm (and not treating it explicitly as in a direct numerical simulation (DNS) is justified. In particular, our resolution study demonstrates that our results are consistent with the presence of an inertial range and statistical behavior that is independent of dissipation-scale (i.e., grid-scale) behavior. Second, we have shown that mixing behavior at convective boundaries (analogous to the "entrainment" phenomena in geophysics) requires further study and does not show as good convergence as the dissipative phenomena in the bulk of the convective layer: some length scale of importance is not resolved. This motivates a controlled, systematic follow up work, possibly with DNS.

3. We have compared the statistical properties of our 3D simulation results with modern closure relationships, typified by those discussed in Besnard et al. [2] and find poor agreement. The core features of these relations, i.e, "down-gradient" for fluxes and "return-to-isotropy" for Reynolds-stress, match the data poorly (including sign errors). Preliminary analysis [9] indicates this is due to violation of the "scale-separation" hypothesis, whereby fluxes are governed on scales much smaller than the integral scale. We find transport dominated by the largest scales, those produced by global scale Rayleigh-Taylor instability [12]. We are following with a scale-by-scale budget analysis in an effort to construct hybrid closure models that combine large-scale transport with small-scale dissipation.

Follow-on Projects

Follow-on work that has been initiated by this project include:

1. Core collapse simulations of 2D and 3D progenitor structures with Fryer (LANL: using the SN-SPH Code), Ott (Caltech: using the Zelmani/Einstein Toolkit Code), and Adam Burrows (Princeton: using the Castro Code): We are providing each of these teams the results of our 2D/3D silicon-burning calculations, to use as initial conditions fir core-collapse simulations to assess the role of multi-dimensional effects in shaping the supernova explosion mechanism (some preliminary work published in [10]).

2. Continued effort on 3D progenitor modeling: we are extending simulation and analysis work to look at more complex phenomena, including magneto-hydrodynamics and angular momentum (rotation).

3. We have developed a strong collaboration between

Maxime Viallet (Munich), Miroslav Mocak (LANL), and David Arnett (Arizona) on turbulence analysis, which is expected to continue into the upcoming years.

Impact on National Missions

Our work deepens our understanding of the astrophysical sites (massive stars) hosting supernovae and gamma-ray bursts, which have broad implications for NASA funded astronomical observatories, including potential impact on mission design. DOE/SC is impacted by our work through basic studies of turbulent reactive fluids, and mixing and transport modeling, as well as through the exercise of large scale computing facilities and the development of new techniques required to execute our proposed simulation work. Our reactive hydrodynamics work builds capability for new approaches to weapons modeling.

References

1. Arnett & Meakin, "Toward Realistic Progenitors of Core-collapse Supernovae", 2011, The Astrophysical Journal, 733, 78

2. Besnard, D., Harlow, F., Rauenzahn, R. & Zemach, C., "Turbulence Transport Equations for Variable-Density Turbulence and Their Relationship to Two-Field Models", 1992, LANL LA--12303-MS

3. Chassaing, P., "Variable Density Fluid Turbulence", 2003, Applied Mechanics Reviews, vol. 56, issue 5, p. B72

4. Grinstein, F.F, Margolin, L.G., Rider, W.J., Editors, "Implicit Large Eddy Simulation: Computing Turbulent Fluid Dynamics", Cambridge UP, 2007, 2nd printing 2010.

5. Meakin & Arnett, "Active Carbon and Oxygen Shell Burning", 2006, The Astrophysical Journal Letters, 637, 53

6. Meakin & Arnett, "Anelastic and Compressible Simulations of Stellar Oxygen Burning", 2007, The Astrophysical Journal, 665, 690

7. Meakin & Arnett, "Turbulence Convection in Stellar Interiors. I. Hydrodynamic Simulation", 2007, The Astrophysical Journal, 667, 448

8. Meakin, C. & Arnett, D., "Core-Collapse Progenitor Evolution. I. Silicon-shell Burning Hydrodynamics", The Astrophysical Journal, in preparation

9. Mocak, M., Meakin, C., Viallet, M., & Arnett, D., "Turbulent Convection in Stellar Interiors. IV. Scale-by-Scale Budget Equations for Turbulent Fluctuations and Transport", The Astrophysical Journal, in preparation

10. Ott. C. et al., "General-relativistic Simulations of Three-dimensional Core-collapse Supernovae", 2013, The Astrophysical Journal, 768, 115

11. Paxton, B., et al., "Modules for Experiments in Stellar Astrophysics (MESA)", 2011, The Astrophysical Journal Supplement, 192, 3

12. Viallet, M., Meakin, C., Arnett, D., & Mocak, M., "Turbulent Convection in Stellar Interiors. III. Moment Equations and Stratification Effects", 2013, The Astrophysical Journal, 769, 1

13. Zingale, M. , et al., "Low Mach Number Modeling of Type Ia Supernovae. IV. White Dwarf Convection", 2009, The Astrophysical Journal, 704, 196

Publications

Meakin, C., and D. Arnett. Core-collapse supernova progenitor evolution. I. Silicon-shell burning hydrodynamics. 2013. The Astrophysical Journal, in preparation..

Meakin, C., and D. Arnett. Core-collapse supernova progenitor evolution. II. Iron-core formation hydrodynamics. 2013. The Astrophysical Journal, in preparation..

Mocak, M., C. Meakin, M. Viallet, and D. Arnett. Turbulent convection in stellar interiors. IV. Scale-by-scale budget equations for turbulent fluctuations and transport. 2013. The Astrophysical Journal, in preparation..

Ott, C., E. Abdikamalov, P. Moesta, R. Haas, S. Drasco, E. O'Connor, C. Reisswig, C. Meakin, and E. Schnetter. General-relativistic simulations of three-dimensional core-collapse supernovae. 2013. The Astrophysical Journal. 768 (2): 115.

Viallet, M., C. Meakin, D. Arnett, and M. Mocak. Turbulent convection in stellar interiors. III. Mean-field analysis and stratification effects. 2013. The Astrophysical Journal. 769: 1.

Foundational Methods and Experiments in Ultracold Molecular Physics

Michael D. Di Rosa
20110356ER

Introduction

We will investigate a novel experimental approach to cooling and storing stable molecules at ultracold temperatures and high densities. Our method of cooling molecules involves lasers as established by us in 2004, adopted recently by a pre-eminent research group for a prefatory experiment, and featured in the Search & Discovery column of the January 2010 issue of Physics Today. That column highlighted the work of DeMille and colleagues at Yale in deflecting a molecular beam by a transversely directed laser beam—a precursor to laser cooling—by combining the type of diatomic molecule and the laser-induced electronic transitions we had prescribed. More importantly, the article heralded that laser cooling of molecules was perhaps not "impossible" and anticipated far-reaching consequences in quantum and chemical sciences once molecules were laser- cooled to <1 mK and collected. Molecules have not been laser cooled, however, let alone concentrated in the ultracold, dense ensembles needed for experiments. Our project aims to remedy these fundamental needs of cooling and storage so that molecular physics may enter the same ultracold conditions that reinvented atomic physics.

Our two major experimental goals are the laser cooling of molecules in their lowest-energy internal state and the demonstration of an accumulator that is based on principles of high-energy physics and suitable for collecting successive injections of high-density packets of laser-cooled (paramagnetic) molecules or atoms. The two achievements are each noteworthy, laser cooling for its precedence and the accumulator as a new platform for experiments in ultracold physics and chemistry. In our research, these two elements will be demonstrated separately, with the accumulator proved for the case of laser-cooled atoms as proxies for laser-cooled molecules. Time permitting, we will inject laser-cooled molecules into the accumulator to further reinforce this accumulator's capacity to serve future and first experiments in ultracold molecular physics and chemistry.

Benefit to National Security Missions

The principles and techniques introduced by this research will have a malleable applicability to fundamental and applied science. In the latter vein, outlets for the work are conceivable in areas of national security, homeland security, remote sensing, secure communication, and information analysis. Regarding fundamental science, ultracold molecular matter is rife with research opportunities that will help us understand and control the quantum mechanics of reactions and collective phenomena, thus providing another window into the details of curious material behaviors we wish to exploit or invent. The development of this promising, nascent field will be challenging and will take the combined expertise and resources such as the Laboratory possesses by virtue of its missions. Its influence on Laboratory programs would then come naturally, and most effectively, by our firsthand knowledge and practice.

Progress

Our progress to date was summarized by the poster "Developing Density of Laser-Cooled Neutral Atoms and Molecules in a Linear Magnetic Trap," authors J. Velasquez, III, P. L. Walstrom, and M. D. Di Rosa, presented by postdoc Joe Velasquez at the 44th Annual Meeting of the DAMOP Division of the American Physical Society (held 3-7 June, 2013). Joe drew a crowd intrigued by our inventive research.

The poster reviewed our proposed approach (with supporting numerical studies) for accumulating and storing cold (millikelvin) molecules at high densities, featured our working molecular/atomic beam machine, and highlighted some first results we obtained with our "test particle" of lithium. Our concept for an accumulator attracted attention as did our variation of a standard chemical-physics technique for creating monoenergetic beams of atoms and molecules. In our beam machine, we seed by laser ablation from a solid target the atoms or molecules of interest directly into the dense part of

a supersonic expansion of a carrier gas. Collisions would ideally force the seeded particles, initially at some tens of thousands of kelvin (the sun, for comparison, shines at 5,980 K) in the bright plasma plume of laser ablation, to adopt the translational characteristics of the carrier gas, though we have not found evidence for this in the literature. The many chemists using these sources, dubbed "Smalley" sources after their Nobel-prize-winning originator, are usually unconcerned with the translational energy. We showed that Li atoms seeded by laser-ablation of a lithium rod into a (heavier) supersonic carrier do indeed equilibrate to the cold, moving-frame translational temperature of the carrier following its expansion to a collisionless beam. Interestingly, the Li beam turned out to be colder than expected. Where the argon carrier of the experiment has a temperature of 5 K in the moving frame, lithium had a measured temperature of 3 K. We expect to see similar results when we seed laser-ablated CaH into the expansion. This result announced that (1) the cryogenic systems favored today by the cold-molecule contingent are unnecessary for delivering cold molecules to experiments and/or laser manipulations and (2) seeded supersonic expansions might deliver atoms to any of the favored styles of traps at greater instantaneous and average fluxes than that possible by the conventional choice of an effusive source.

A third of the poster reviewed the maturing accumulator concept. When the project began, our model accumulator was a "racetrack" with two straightaways connected by 180-degree turns. Injection took place along one of the straightaways. A simple analysis showed the racetrack was perfect for our purposes, holding the injected particles and those already stored for an indefinite number of laps. Our recent simulations, however, showed that a racetrack would not in practice be able to hold our magnetic particles in stable orbits. The earlier, simple model assumed the magnetic field defined by the racetrack would be a sort of smooth tube within which the particles would be guided. Barring no expense, this could be created by using superconducting current loops. Practically, however, the track is more easily and cheaply constructed by piecing together magnetic segments. Unfortunately, the inevitable gaps between segments leads to ripples along the guiding magnetic tube, appearing to the particles like a badly wash-boarded road. The cumulative effect of all the corrugations bounced particles out of the simulated racetrack within a lap or two (Walstrom and Di Rosa, IPAC Conference Proceedings, pp. 1281-1283, May 2012). We are a unique group in atomic/molecular physics group to have at our disposal for the design of traps the sophisticated particle-tracking codes developed for high-energy physics; anything short of this misrepresents reality.

We then developed the idea of a linear trap and accumulator, which we introduced in the poster. So far, our simulations indicate that particles will be absolutely confined in this style of trap, even in its practical construction. It is also far simpler to make than a racetrack. While we thought this to be an original idea for a trap, we found assuring precedence of its use (in 2009) in trapping ultracold neutrons. The additional use of the trap as an accumulator remains unique, however. Modeling the efficiency of injection into the accumulator is underway.

Future Work

Laser cooling of the paramagnetic CaH is a primary goal and will be a highlight of international recognition. Our other goal, that of introducing techniques for magnetic-particle accumulation, is however more expediently proved through use of a surrogate that is more easily laser cooled. In our case, that surrogate—that test particle—is lithium, partly because the lasers we use to cool CaH can be tuned to cool Li. We then make the connection that the accumulator demonstrated for a paramagnetic atom such as lithium is applicable to laser-cooled paramagnetic molecules such as CaH. Though developed with molecules in mind, the accumulator is a general device that could very well benefit the field of atomic physics. The accumulator can then be used to build sufficient densities of cold molecules or cold atoms or both for experiments that require collisions, whether for studies in chemistry or quantum-state scattering, or as a start toward creating a quantum-degenerate molecular gas.

The following four major goals are set for next fiscal year, with note that we have built our atomic/molecular beam machine and have demonstrated its performance by sending bursts of lithium atoms traveling at ~540 m/s along its axis.

1. Using standard laser-based techniques, slow and cool the atomic-beam packets of Li to 30 m/s and 1 mK, conditions that mimic what we expect to obtain when cooling packets of laser-cooled CaH.

2. Demonstrate (with the slow and cooled Li beam) the state-switching concept for injection into an accumulator.

3. Switch the machine's source to CaH, optimize that source, and then demonstrate the laser-slowing and cooling of CaH.

4. Install the linear accumulator (having designed and built it during the FY), and demonstrate its operation with Li atoms.

Accompanying these goals will be the equally important task of preparing manuscripts for professional publication.

Conclusion

Materials are extraordinarily different at ultracold temperatures. Kamerlingh Onnes, who in 1911 discovered superconductivity, remarked that his finding of a new state of matter through his work in gas liquefaction surpassed his wildest anticipation. A century later, superconductivity underlies multi-billion dollar industries such as medical imaging. We are mindful of applications our research has in new types of sensors. More generally, however, the dense samples of ultracold molecules we seek to generate will give us and others a new view to the inner workings of matter for both discovery and exploitation, of which superconductivity is but one storied example.

Publications

Ferguson, S., P. Walstrom, J. Velasquez, III, and M. Di Rosa. Design of a magnetic trap and accumulator for laser-cooled atoms and molecules (LA-UR-13-25214). Presented at LANL Student Symposium. (Los Alamos, NM, 26-27 July 2013).

Velasquez, J., P. L. Walstrom, and M. D. Di Rosa. Developing density of laser-cooled neutral atoms and molecules in a linear magnetic trap. Presented at 2013 Meeting of the Division of Atomic, Molecular, and Optical Physics of the American Physical Society. (Quebec City, Quebec, Canada, 3-7 June 2013).

Walstrom, P. L., and M. D. Di Rosa. Beam transport and storage with cold neutral atoms and molecules. 2012. In International Particle Accelerator Conference 2012. (New Orleans, 20-25 May 2012). , p. 1281. New York: IPAC'12 OC / IEEE.

Next Generation Earth Models

Monica Maceira
20120047ER

Introduction

The main goal of this project is to develop a fast and robust method to derive pictures of the Earth's structure from a combination of four geophysical data sets. Our multi-parameter inversion will produce more accurate Earth models than currently available and will form the basis for the next generation of Earth models.The specific elements of the proposal are to 1) develop an efficient and robust multi-parameter inversion scheme, 2) develop the methodology for pre-processing and weighting the data sets to produce the best image, and 3) develop a detailed, validated model of the Earth's crust beneath the western United States.This project addresses the fundamental problem of creating an accurate image of the Earth, currently a barrier to deeper understanding of the Earth's current state and evolution.

Benefit to National Security Missions

The research will create unique expertise at the Laboratory and will enhance the Laboratory's capability to address core missions in Ground-based Nuclear Detonation Detection within Nuclear Nonproliferation, as well as missions in geothermal energy, geological carbon sequestration, used fuel disposition, and repository science under Applied Energy Programs, Fossil Energy, and Civilian Nuclear Programs. All of these efforts rely on accurate determination and monitoring of Earth structure for success. We also foresee a follow-on LDRD DR aimed at extending this modeling to the global scale using High Performance Computing. The end result would be a world-wide map of strain perturbations for the purpose of earthquake prediction.

Progress

The key accomplishments this year have been:

- Gathering and processing and incorporation of all receiver function data into the inversion. We have also tested the prospect of low pass filtering of the receiver functions to eliminate excessive noise in some of the receiver functions. While this helps, and allows for inclusion of some additional data constraints, the bulk of the noisy receiver functions are not improved through this approach. This suggests that these data are intrinsically bad and should not be used in the inversion.
- The thorough implementation and testing of the gravity element of our tripartite inversion for crust and upper mantle structure of the western US. I have implemented two types of filtering for the gravity partials, and tested three different velocity/density relationships. So far, shear velocity results from these efforts are very similar, indicating that the inversion scheme is robust and not sensitive to starting models or velocity/density relationships.
- Presentation of our latest results at the American Geophysical Union meeting, 12/2012, in San Francisco
- Preparation of a journal article showing our joint inversion results using two data types: surface waves and receiver functions. This paper is approximately half completed as of 6/6/13. Below is the abstract for our paper, outlining our results.

As datasets for studies of Earth's crust and mantle become more extensive, we have the unique opportunity to test comprehensive analysis methods not previously possible. The western United States is an ideal test bed for such research due to the extensive geophysical data now available. Utilizing these data resources we have implemented a joint, simultaneous inversion of receiver functions and surface wave dispersion to produce an image of the shear wave velocity structure beneath the western U.S. to depths of about 200 km. We use a standard Least Squares inversion method optimized for sparse large sparse matrices with simple parallelization. Our results are largely consistent with previous work for the area, but with increased vertical resolution due

to methodology. Surface wave dispersion measurements come from analysis of regional earthquakes using multiple filter analysis, with good geographic coverage from periods of 8 s to 130 s. Receiver functions are downloaded from the Earthscope Automated Receiver Survey and we compare results using both high and low frequency receiver functions. Overall, structure beneath the western United States is lower velocity than that for the continental craton to the east of the Rocky Mountains. In particular, low velocities are seen in the mid-crust under Yellowstone, as well as beneath northern coastal California and coastal Oregon. In the middle to lower crust we see low velocities beneath the Aspen Anomaly, the San Francisco Peaks, the Cascade Range and the western Basin and Range. At "typical" Moho depths of 35 km. we see low velocities beneath the Colorado Plateau and the Snake River Plain indicating thicker crust for those provinces, while low velocities beneath western Washington likely reflect subduction of ocean crust in that location and resultant thickening of the crustal stack. To the south of the Colorado Plateau, beneath the southern Basin and Range, we see higher than average velocities. Broad low velocities are observed under California and Oregon at depths of 80 km, tapering through the Snake River Plain to a terminus at Yellowstone. At this depth velocities are also lower under the Rio Grande Rift. Broad but less pronounced low velocities are observed continuing to depths of 200km where they then increase to more significant levels."

Future Work

The rest of this fiscal year and the next fiscal year will be spent acquiring and processing the body wave data (the last of the four data types), and performing inversions of all combinations of data types. For the body wave data we will draw on data holdings from our LANL seismic research database. Results will be presented at the annual meeting of the American Geophysical Union and/or the Seismological Society of America meeting. We anticipate finishing and submitting our first paper on joint inversion of surface waves and receiver functions by the end of this fiscal year. We then will write and submit a manuscript on the joint inversion of gravity, receiver functions and surface wave data for the western United States. Following the incorporation of body wave data into the inversion, we will write and submit a paper on that topic. All papers will be submitted to high profile earth science journals.

Conclusion

The expected results include a fast multi-parameter inversion code for determining high resolution Earth models, a detailed model of the crust and upper mantle of the western US available, and several publications in high impact Earth science journals. The code will be state of the art for several years and will be used throughout the scientific community for understanding the structure of the Earth's crust and mantle. These models will reveal insights into how the Earth's lithosphere is formed and how it evolves over time, with impacts on geothermal resources, disposition of nuclear waste, and global nuclear explosion monitoring.

Publications

Modrak, R., M. Maceira, J. van Wijk, and D. Coblentz. Joint inversion of group velocity dispersion estimates and gravity data: Implications for the East Africa rift structure. Earth and Planetary Science Letters.

Steck, L., M. Begnaud, S. Phillips, and R. Stead. Tomography of crustal P and S travel times across the western United States. 2011. JOURNAL OF GEOPHYSICAL RESEARCH-SOLID EARTH. 116: B11304.

Steck, L., M. Maceira, and C. Ammon. Crust and Upper Mantle Structure of the Western US from Simultaneous Inversion of Surface Wave Dispersion, Gravity, and Receiver Functions. 2012. In Seismological Society of America Annual Meeting. (San Diego, 17-19 April). Vol. 83, p. 357. Albany: BSSA.

Zhang, H., C. Thurber, M. Maceira, and P. Roux. Joint inversion of body-wave arrival times and surface-wave dispersion for three-dimensional seismic structure around SAFOD. Pure and Applied Geophysics.

Non-Equilibrium Fluctuation-induced Interactions

Diego A. Dalvit
20120149ER

Introduction

Fluctuation-induced interactions are ubiquitous inphysics. Relevant examples are forces between nanostructures due to quantum fluctuations of the electromagnetic field (EM Casimir interactions), andforces oncolloidal particles due to density fluctuations of binary fluid mixtures (critical Casimir interactions). Although much of the equilibrium aspects of these interactions are understood and confirmed by experiment, non-equilibrium is still an open territory. The goal of this proposal is to carry out a consorted theoretical and experimental effort to investigate non-equilibrium quantum and thermal fluctuation-induced electromagnetic interactions at the nano-scale, using state-of-the-art analytical, numerical, nanofabrication, and measurement tools.

Our approach will enable the understanding of, and ultimately controlover fluctuation-induced interactions in dynamical and thermal non-equilibrium systems, such as: (i) non-contact forces and friction between patterned surfaces and atoms in relative motion, induced by quantum EM fluctuations; and (ii)nano-scale radiative heat transfer between complex nanostructures, induced by thermal EM fluctuations. We plan to formulate the first principles, microscopic theory of non-equilibrium EM fluctuation interactions using the open quantum systems paradigm, and to develop numerical methods to compute them exactly for complex nanostructures out of dynamic and/or thermal equilibrium. We will verify the stationary thermal non-equilibrium aspects by demonstrating, for the first time, tailored nano-scale radiativeheat transfer between structured surfaces. To this aim we will fabricate dielectric and metallic patterned nanostructures,and measure heat transfer between them using scanning thermal microscopy.

Our end result will be a suite of theoretical and experimental tools designed to explore non-equilibrium aspects offluctuation-induced interactions. This novel capability will enable the rational design of nanostructures with desired nano-electromechanical functionalities (e.g. systems with reduced friction), and enhanced near-field thermophotovoltaic energy conversion efficiencies.

Benefit to National Security Missions

This project ties to LANL missions on quantum science and nanotechnology. It leverages existing capabilities across the laboratory, both in the T and MPA divisions. We expect to produce new ideas that will help consolidate LANL as a world leader in fluctuation-induced interactions. The new capabilities that we will build, including analytical tools, numerical algorithms, nanofabricated surfaces,and scanning thermal microscopy techniques for engineered heat transfer, will enable LANL to pursue future missions in nanotechnology, nanophotonics, and quantum physics. One of the possible external agencies that we believe may be potentially interested in our R&D is DARPA, with which we have worked in the past on equilibrium Casimir physics.

Progress

We have performed theory and numerical studies of non-equilibrium fluctuation-induced phenomena, both in radiative heat transfer and quantum friction. On the first topic, we have computed the radiative heat transfer between nanostructured gold plates in the framework of the scattering theory, and predicted an enhancement of the heat transfer as one increases the depth of the corrugations while keeping the distance of closest approach fixed. This effect was interpreted in terms of the evolution of plasmonic and guided modes as a function of the grating's geometry. This work was published in Physical Review B as a Rapid Communications. In quantum friction, we have studied the non-contact drag force between a moving atom and a surface arising from the exchange of energy and momentum mediated by quantum and thermal fluctuating photons. Using fundamental theorems of quantum statistical mechanics, such as the fluctuation-dissipation theorem, we have obtained how the quantum frictional force depends on the atom's

velocity and the atom-surface separation, and have clarified some controversies in the literature about the correct calculation of this effect. We are currently writing up a manuscript to submit to Physical Review. In addition, we have developed a quasi-analytical approach to computing fluctuation-induced interactions (such as Casimir forces and radiative heat transfer) in nanosctructured surfaces based on a modal approach. Our method is based on the exact analytical form of the eigenvectors of such structures and the numerical computation of the eigenvalues from a simple transcendental equation. This was was published in Physical Review A.

We have designed and fabricated submicron scale gratings for experimental study of radiating heat transfer between grating-plane and sphere. Our theoretical study shows that rate of radiative heat transfer increases with the grating's corrugation depth. A grating design with a periodicity of 1 μm and 50% filling fraction shows an order of radiation enhancement as the grating aspect (depth/width) ratio approaches to 10. We fabricated a set of gratings using standard nano-lithography, etching, and metallization techniques. At this point, theses gratings are fabricated on silicon substrates which are subsequently metalized with a film thickness greater than the skin depth. The fabrications starts with e-beam lithography on a silicon substrate, next a dry RIE etching is used to obtain desired corrugation depth, and finally, the gratings are metalized using a sputtering system. We optimized the recipe for highly anisotropic silicon etching and also optimized metallization parameters for uniform metal thickness around the grating structure. After metallization of 60 nm of silver, which is thicker than the skin depth, our gratings have 50% filling fraction. We vary the grating depth from 1.5 μm to 4.5 μm which gives a range of aspect ratio from 3 to 9. Further design modification of gratings will commensurate with measurement of current samples.

We have tested the performance of our newly developed variable-temperature UHV scanning thermal microscope by measuring the temperature distribution on gold/silicon gratings. When such heterogeneous samples are heated using electron bombardment in vacuum, inhomogeneity in material properties lead to nonuniform temperature distribution on the surface. We have shown that our thermal microscope is capable of detecting these variations with better then 15 mK resolution. To measure nanoscale heat transfer between the tip and a flat gold surface, we have used the same instrument in thermal conductivity detection regime. In these studies, commercially available RTD tips are heated using AC currents and heat dissipation due to thermal conduction through the vacuum gap leads to tip temperature variations as a function of the tip-sample separation. Even though we were not able to detect variations of the heat transfer with sub-micron tip-sample separation, we could detect lateral variations of thermal conductivity between tip and sample which would be applicable to studies of wide range of nanostructured thermoelectric materials available at CINT. To improve the resolution and detect near-field effects in heat transport dependence on sub-micron tip-sample separation, we have established collaboration with PicoCal personnel who will provide novel 4-probe RTD tips that will allow at least an order of magnitude enhancement in the microscope sensitivity to thermal conductivity changes. The improved measurements resolution will enable reliable quantification of tip-sample separation dependence of the heat transfer between plane and heterostructured metal surfaces. in the plane sample geometry.

Future Work

We will study nanoscale radiative heat transfer between metallic and dielectric nanostructures, including gratings, multilayered materials, and metamaterials. Along this line of research we will design, fabricate, and characterize structures in the micron to nano scale size that will be used in our experiments on radiative heat transfer. We will perform the calibration of the experimental set up using the sphere-plane configuration and compare results with theory.

Along the other thread of the quantum friction, we will study non-contact forces and friction between patterned surfaces and atoms in relative motion, induced by quantum EM fluctuations. We will finish our ongoing work on quantum friction between atoms and surfaces in relative motion, and then generalize our results to the case of quantum friction between two surfaces in relative motion.

Conclusion

The main expected result of this project is a complete physical description of non-equilibrium fluctuation-induced interactions. Our two main deliverables will be: 1) a predictive theoretical/numerical framework for non-equilibrium fluctuation-induced interactions, and 2) the first experimental demonstration of engineered radiative heat transfer with fabricated nanostructures. We will perform theory, numerics, and experimental validation.

Publications

Behunin, R. O., F. Intravaia, D. A. Dalvit, P. A. Neto, and S. Reynaud. Modeling electrostatic patch effects in Casimir force measurements. 2012. Physical Review A (Atomic, Molecular, and Optical Physics). 85 (1): 012504 (9 pp.).

Behunin, R. O., Y. Zeng, D. A. R. Dalvit, and S. Reynaud.

Electrostatic patch effects in Casimir force experiments performed in the sphere-plane geometry . 2012. Physical Review A. 86: 052509.

Behunin, R., D. Dalvit, R. Decca, and C. Speake. Limits on the accuracy of isoelectronic gravity measurements at short separation due to patch effects. Physical Review D.

Guerout, R., J. Lussange, F. S. Rosa, J. -. Hugonin, D. A. Dalvit, J. -. Greffet, A. Lambrecht, and S. Reynaud. Enhanced radiative heat transfer between nanostructured gold plates. 2012. PHYSICAL REVIEW B. 85 (18): 180301.

Intravaia, F., P. S. Davids, R. S. Decca, V. A. Aksyuk, D. Lopez, and D. A. R. Dalvit. A quasi-analytical modal approach for computing Casimir interactions in periodic nanostructures . 2012. Physical Review A. 86: 042101.

Intravaia, F., R. Behunin, and D. Dalvit. Quantum friction and non-equilibrium fluctuation theorems. Physical Review Letters.

Intravaia, F., S. Koev, I. Jung, A. Talin, P. Davids, R. Decca, V. Aksyuk, D. Dalvit, and D. Lopez. Strong Casimir force reduction through metallic surface nanostructuring. 2013. Nature Communications. 4: 2515.

Rodriguez, A., M. Homer Reid, A. Woolf, D. Dalvit, F. Capasso, S. Johnson, and F. Intravaia. Geometry-induced Casimir suspension of oblate bodies in fluids. Physical Review Letters.

Rosa, F. S., D. A. Dalvit, and P. W. Milonni. Electromagnetic energy, absorption, and Casimir forces. II. Inhomogeneous dielectric media. 2011. PHYSICAL REVIEW A. 84 (5): 053813.

Sushkov, A. O., W. J. Kim, D. A. Dalvit, and S. K. Lamoreaux. New Experimental Limits on Non-Newtonian Forces in the Micrometer Range. 2011. Physical Review Letters. 107 (17): 171101 (4 pp.).

Petascale Kinetic Plasma Simulation of the Interaction Among Laser Speckles in Nonlinear Optical Systems

Lin Yin
20120153ER

Introduction

Understanding nonlinear optics of plasmas is a high energy density physics grand challenge. Decades of research has shown that this problem plays host to a wide range of complex physics. This problem is ideal for advancing fundamental, discovery-class science in part because supercomputing power and simulation codes have co-evolved to the point where ab initio exploration of the underlying physics is now possible.

With Petaflop-class supercomputers, the investigators have advanced the understanding of the basic physics of stimulated Raman scattering in solitary laser speckles, the irreducible "building blocks" of intensity structures found in laser beams. If laser speckles do not meaningfully interact with one another, then a knowledge of single-speckle behavior and the statistics of speckle intensities would be all that's needed to craft a macroscopic model of plasma behavior: a large laser beam with hundreds of thousands of speckles would act merely as the simple sum of the many constituent speckles plus a relatively tame background contribution.

However, since laser speckles interact nonlinearly with one another, "meso-scale" modeling becomes essential because small aggregates of laser speckles may exhibit emergent behavior. One way that this could happen is through the exchange of particles and seed wave energy among laser speckles. An intense speckle in an environment with other speckles nearby could "destabilize" those neighbors, resulting in enhanced emission of particles and transmission of wave energy from those speckles back to the original speckle, thus affecting its behavior nonlinearly and nonlocally.

In our research, we will study LPI in first-principles computer simulations of both modest- and large-sized ensembles of laser speckles. We will employ the LANL VPIC particlein-cell code to perform simulations in various plasma conditions in order to identify when and how emergent phenomena may take place.

Benefit to National Security Missions

Our project engages in high-risk/high-payoff scientific R&D that has the potential to enable inertial confinement fusion experiments to achieve ignition, justifying the first element in Agency Relevance. There is also an effort in the DOE SC Office of Fusion Energy to consider inertial fusion energy in various IFE approaches, including conventional ICF and fast ignition ICF; our work also supports that primary mission, so the DOE/SC "A" is appropriate.

Ignition experiments on the NIF have been identified as vital for SSP and other defense programs missions. Mission relevance "A" should be checked for "Nuclear Weapons: Safety, Security, and Reliability of the Nuclear Stockpile" under "Mission Relevance".

The DOE/SC energy mission driver makes fusion nuclear energy an appropriate energy security mission; hence, "A" was checked for Nuclear Energy in this category.

HEDP is a priority of the Laboratory that is closely aligned with its nuclear security and energy independence goals; this work underpins the use of leading HEDP experimental facilities. A natural customer for this work would be the Science Campaigns, specifically C10 (LANL Program Manager: Steve Batha); this work would also be applicable to ongoing C4 projects. LANL is likely to play a leading role in any prospective national inertial fusion energy program, a topic presently being assessed by a National Research Council panel (whose final report will be submitted in two years). LPI is a natural problem area and test bed for improvements to our VPIC codebase, which is being further adapted for GPU multi-core and Exascale supercomputers.

Progress

In laser-driven fusion experiments, stimulated Raman

scattering (SRS) occurs when electron density fluctuations are amplified resonantly by the incident laser beams and scattered light. These laser beams comprise several thousands of individual laser speckles. In this project, we employ the VPIC particle-in-cell (PIC) code to perform simulations of SRS to study how laser speckles interact through the exchange of particles and seed waves. During the second year of the project, the nonlinear physics governing the kinetic behavior of stimulated Raman scattering (SRS) in large networks of speckles has been identified in the trapping regime at $k\lambda D \sim 0.3$ (here k is the wave number of the electron plasma waves and λD is the Debye length) in homogeneous and inhomogeneous plasmas. Hot electrons from intense speckles, both forward and side-loss hot electrons produced during SRS daughter electron plasma wave bowing and filamentation, seed and enhance the growth of SRS in neighboring speckles by reducing Landau damping. Trapping-enhanced speckle interaction through transport of hot electrons, backscatter, and sidescatter SRS light waves enable the system of speckles to self-organize and exhibit coherent, sub-ps SRS bursts with more than 100% instantaneous reflectivity, resulting in an SRS transverse coherence width much larger than a speckle width and a SRS spectrum that peaks outside the incident laser cone.

Future Work

In laser-driven fusion experiments, stimulated Raman scattering (SRS) occurs when electron density fluctuations are amplified resonantly by the incident laser beams and scattered light. These laser beams comprise several thousands of individual laser speckles. In this project, we employ the VPIC particle-in-cell (PIC) code to perform simulations of SRS to study how laser speckles interact through the exchange of particles and seed waves. The primary objective of the work we proposed is to use petascale kinetic plasma simulations to examine the interaction among laser speckles in nonlinear optical systems.

With the additional diagnostic, algorithm development, and new boundary conditions for laser injection implemented during the first year, we will study SRS in VPIC simulations of large-sized ensembles of laser speckles in the second year of our project. We will perform two-dimensional simulations in various plasma conditions in order to identify when and how speckle interaction may take place in large networks of speckles. These “capability-class” simulations of large networks of laser speckles to will validate our understanding of the basic phenomena discovered so far.

Conclusion

Through the use of 2D and 3D kinetic simulations at modest and large scale, along with theory of reduced model including the trapped electron effects, we expect to understand how the intensity thresholds are lowered through longitudinal and transverse coupling among speckles via hot electron exchange and scattered light, to predict the threshold for linear to nonlinear transition, and to obtain the conditions for emergent phenomena in speckled laser beams.

Publications

Yin, L., B. J. Albright, H. A. Rose, K. J. Bowers, B. Bergen, and R. K. Kirkwood. Selforganized bursts of coherent stimulated Raman scattering and hot electron transport in speckled laser plasma media. 2012. Physical Review Letters. 108: 245004.

Yin, L., B. J. Albright, H. A. Rose, K. J. Bowers, B. Bergen, R. K. Kirkwood, D. E. Hinkel, A. B. Langdon, P. Michel, D. S. Montgomery, and J. L. Kline. Trapping induced nonlinear behavior of backward stimulated Raman scattering in multispeckled laser beams. 2012. Physics of Plasmas. 19: 056304.

Yin, L., B. J. Albright, H. A. Rose, D. S. Montgomery, J. L. Kline, R. K. Kirkwood, P. Michel, K. J. Bowers, and B. Bergen. Self-organized coherent bursts of stimulated Raman scattering and speckle interaction in multi-speckled laser beams. 2013. PHYSICS OF PLASMAS. 20 (1): -.

Multiscale Spacecraft Charging Simulations in Support of New Space Missions

Gian L. Delzanno
20120190ER

Introduction

This project is aimed to open up a new field of experimental space plasma physics. The space experiment will connect the Earth magnetosphere and ionosphere by emitting an energetic beam of electrons from a magnetospheric spacecraft and detecting the beam optically in the ionosphere. Thus, for the first time, dynamic magnetospheric processes will be probed directly by magnetic field line mapping over vast regions (thousands of kilometers) of near Earth space.

The major obstacle to this experimental technique is how to emit enough electrons from the spacecraft to permit ionospheric imaging without deleteriously charging the spacecraft or, in other words, how to control the charging of the spacecraft to benign levels which will allow the electron beam to be emitted. This is the goal of this LDRD project.

The spacecraft charging problems considered here are extremely difficult to solve computationally, since they involve spatial scales from mm to 10's of km and time scales from microseconds to seconds. To solve this multiscale problem, we will model the interaction of the beam-emitting spacecraft with the surrounding magnetospheric plasma using a state-of-the-art 3d PIC code. The micro and macro scale physics will be simulated for realistic geometries and conditions.

This work will result in a thorough and hitherto unknown understanding of the magnetospheric conditions in which it is possible to stably emit a beam of electrons. This understanding will enable LANL to proceed with plans to propose a NASA Explorer mission ($200M - $500M, named ConnEx) to experimentally study magnetic field line connectivity. Ultimately, this LDRD project may facilitate a paradigm shift in space plasma physics from using static magnetic field models to using dynamic probing of the magnetic field configuration of the Earth magnetosphere.

Benefit to National Security Missions

This project represents an opportunity for LANL to lead the NASA community into new exciting science, enabled by new, pioneering experimental techniques. In addition, this work involves unique computational capabilities which, together with the significant experimental capabilities available at LANL, could be united for future missions. This will allow unprecedented leverage between scientific and programmatic pursuits. In this regard, we have already identified program development opportunities with the NASA Explorer program or the Innovative Advanced Concepts Office. A program development plan is ready (the ConnEx proposal to trace magnetic field lines from the magnetosphere to the ionosphere) and a successful outcome of this LDRD proposal would enable its pursuit. We also emphasize that the computational tools available, which will be further developed in this project, could have an impact in other fields where kinetic plasma simulations are important such as, for instance, magnetic fusion energy.

Progress

We have submitted two papers, one to Journal of Computational Physics on numerical methods for calculating particle trajectories in a given electromagnetic field in cylindrical geometry and one to IEEE Transaction on Plasma Science on an overview of the CPIC code with application examples on the charging and shielding of an object in a plasma.

We are working on the parallelization of CPIC, performing domain decomposition of the computational domain and using the MPI library to handle the communication among different processors. The code has been parallelized in two dimensions, while the work on the three dimensional version is ongoing. We have successfully benchmarked the parallel code against the examples that are presented in the paper above. With this upgrade CPIC is significantly further ahead of its competitors in terms of flexibility, performance and the ability to

handle larger and more challenging problems.

We have continued the work to obtain a static solution for the plume near the spacecraft. We have studied the most popular plume models (Korsum and Tverdokhlebova, Parks and Katz, Ashkenazy and Fruchtman) and discovered that they are intrinsically inconsistent and can produce unphysical solutions. Notably the first model is used to obtain the plasma contactor plume in studies relevant to the International Space Station. These models are based on a macroscopic description of the plasma and the choice of a self-similar solution, but do not fully satisfy the original model equations. We have developed a new self-similar model that mitigates these drawbacks by adding degrees of freedom to the solution. In addition, we have developed a numerical code that solves the full set of model equations (without self-similarity) and used it to calculate the accuracy of the self-similar models. Our new model has the following advantages: does not produce unphysical solutions; produces a broader family of static plume models; and the accuracy of such model (relative to the full numerical solution) is at least an order of magnitude better and in some cases the error is just a few percent. A manuscript is in preparation on these results. The model is currently being extended to include a magnetic field parallel to the plume injection.

We have performed microscopic (Particle-In-Cell) simulations of the plume injection. We have studied the case where the plasma injection is perpendicular to the magnetic field and found that while the plume expands several instabilities develop. These are (1) the deformation of the head of the plume with the formation and detachment of large plasma vortices, (2) the development of large amplitude surface waves on the plume flanks and (3) the overall kinking of the plume at later times. These results are important as they indicate that, for plume injection perpendicular to the magnetic field, static models are inadequate. In order to interpret the results concerning the flank instability, we have developed a simple linear theory model. The theory reproduces qualitatively some aspects of the simulations, namely the development of two modes with different wavelengths localized at the top and bottom flanks. It also characterizes the instability as a Kelvin-Helmoltz instability, driven by the velocity shear that develops due to charge separation (induced by the magnetic field) in small layers on the plume flanks. A manuscript is in preparation on these results.

We have continued efforts with the NSF Geospace Environmental Modeling program's focus group on Scientific Magnetic Mapping and Techniques. This raises the international magnetospheric community's awareness of mapping issues, and understanding of the scientific gaps, which contributes to increasing the importance of ConnEx mission goals. The focus group meets twice yearly, with three sessions at the upcoming summer meeting. New this year is the utilization of data from the new NASA Van Allen Probes. These data can be used to provide more realistic parameters for the ConnEx mission. A manuscript is in preparation which tests the mapping during an active geomagnetic storm time and other researchers are actively using the new dual probe data for other mapping questions.

Future Work

We plan to continue the characterization of the contactor plume with PIC simulations in a rescaled parameter regime, focusing on (1) plume injection parallel to the magnetic field, and (2) plume injection perpendicular to the magnetic field.

With the new plume model developed for the injection parallel to the magnetic field, we will continue performing PIC simulations of the spacecraft charging in presence of electron beam emission. The goal is to characterize (1) the physics of spacecraft charging in presence of plume and electron beam, (2) the scaling laws that govern the amount of current that can be drawn from the spacecraft, (3) the neutralization of the contactor cloud from the surrounding environment.

We plan to perform studies similar to those in (2) but for an injection perpendicular to the magnetic field. These simulations are significantly more challenging since the development of the plume is affected by plasma instabilities. We will therefore rescale the simulation parameters to keep the cost of the simulation manageable, and extract relevant scaling laws.

We will continue work with the Magnetospheric Mapping NSF focus group. Activities for the next year will include facilitating a mapping challenge, likely using new Van Allen Probes data, and summarizing current mapping techniques and their uncertainties into a review paper.

We note that the results from these studies will extend beyond this project, since contactor plasmas are used in various space applications and spacecraft charging is a fundamental process that plagues every spacecraft.

Conclusion

First, this project will provide a thorough understanding of the key physical processes that govern the neutralization of charged bodies (such as a spacecraft) in space. Second, it will quantify the maximum amount of electrons that can be emitted from a magnetospheric spacecraft. Both goals will provide the foundation for a new experimental tech-

nique aimed at dynamic probing of the Earth magnetosphere, which will shed new light on some of the processes that govern the Earth magnetosphere-ionosphere. This project can also have significant impact on how to protect satellites and spacecrafts from the nearby environment and on future space missions.

Publications

Boella, E., M. Giraudo, and G. L. Delzanno. Numerical investigation of the oscillations in a virtual cathode. Presented at 40th European Physical Society Conference on Plasma Physics. (Aalto, Finland, 1-5 Jul 2013).

Camporeale, E.. CPIC: a curvilinear Particle-In-Cell code for plasma-material interaction studies. Presented at American Physical Society April meeting (International Sherwood Fusion theory conference. (Atlanta, GA, 31 Mar - 3 Apr 2012).

Camporeale, E., G. L. Delzanno, J. E. Borovsky, E. A. MacDonald, and M. F. Thomsen. The expansion of plasma in a transverse magnetic field. Presented at 2013 International Sherwood Fusion Theory Conference. (Santa Fe, NM, 15-17 April 2013).

Camporeale, E., G. L. Delzanno, J. E. Borovsky, E. A. MacDonald, and M. F. Thomsen. The expansion of a plasma in a transverse magnetic field. Presented at 40th European Physical Society Conference on Plasma Physics. (Aalto, Finland, 1-5 Jul 2013).

Delzanno, G. L., E. Camporeale, E. Hogan, J. D. Moulton, J. E. Borovsky, E. A. MacDonald, and M. F. Thomsen. Probing the Earth's magnetosphere with an electron gun. Presented at 55th Annual Meeting of the APS Division of Plasma Physics . (Denver, CO, 11-15).

Delzanno, G. L., E. Camporeale, J. D. Moulton, J. E. Borosvky, E. A. MacDonald, and M. F. Thomsen. CPIC: a curvilinear Particle-In-Cell code for plasma-material interaction studies. Presented at American Geophysical Union fall meeting. (San Francisco, CA, 3-7 Dec 2012).

Delzanno, G. L., E. Camporeale, J. D. Moulton, J. E. Borovsky, E. A. MacDonald, and M. F. Thomsen. CPIC: a curvilinear Particle-In-Cell code for spacecraft-plasma interaction studies. Invited presentation at 12th Spacecraft Charging and Technology conference. (Kitakyushu, Japan, 14-18 May 2012).

Delzanno, G. L., E. Camporeale, J. D. Moulton, J. E. Borovsky, E. A. MacDonald, and M. F. Thomsen. CPIC: a curvilinear Particle-In-Cell codes for dusty plasma studies. Invited presentation at 13th Workshop on the Physics of Dusty Plasma. (Waco, TX, 20-23 May).

Delzanno, G. L., E. Camporeale, J. D. Moulton, J. E. Borovsky, E. A. MacDonald, and M. F. Thomsen. CPIC: a curvilinear Particle-In-Cell code for plasma-material interaction studies. Presented at American Physical Society Division of Plasma Physics meeting. (Providence, RI, 29 Oct -2 Nov 2012).

Delzanno, G. L., E. Camporeale, J. D. Moulton, J. E. Borovsky, E. A. MacDonald, and M. F. Thomsen. CPIC: a Curvilinear Particle-In-Cell code for plasma-material interaction studies. To appear in IEEE Transactions on Plasma Science.

Delzanno, G. L., E. Camporeale, J. E. Borovsky, E. A. MacDonald, M. F. Thomsen, and E. A. Hogan. Probing the Earth's magnetosphere with an electron gun. Presented at 40th European Physical Society Conference on Plasma Physics. (Aalto, Finland, 1-5 Jul 2013).

Delzanno, G. L., E. Camporeale, J. E. Borovsky, E. A. MacDonald, M. F. Thomsen, and S. Markidis. Instabilities during the expansion of a plasma in a transverse magnetic field. Presented at AGU Fall meeting. (San Francisco, CA, 9-13 Dec 2013).

Delzanno, G. L., E. Camporeale, and J. D. Moulton. Adaptive Particle-In-Cell methods. Invited presentation at 40th European Physical Society Conference on Plasma Physics. (Aalto, Finalnd, 1-5 Jul 2013).

Delzanno, G. L., and E. Camporeale. On particle movers in cylindrical geometry for Particle-In-Cell simulations. 2013. Journal of Computational Physics. 253: 259.

Giraudo, M., G. L. Delzanno, and E. Camporeale. Theoretical and computational studies of the sheath of a planar, electron emitting wall. Presented at American Physical Society Division of Plasma Physics. (Providence, RI, 29 Oct - 2 Nov 2012).

Hogan, E. A., G. L. Delzanno, E. Camporeale, J. E. Borovsky, E. A. MacDonald, and M. F. Thomsen. Modeling the expansion of a contactor plasma. Presented at American Geophysical Union fall meeting. (San Francisco, CA, 3-7 Dec 2012).

Hogan, E. A., G. L. Delzanno, E. Camporeale, J. E. Borovsky, E. A. Macdonald, and M. F. Thomsen. Modeling the expansion of a contactor plasma. Presented at American Physical Society Division of Plasma Physics meeting. (Providence, RI, 29 Oct- 2 Nov 2012).

Zhao, L., and G. L. Delzanno. Charging and shielding of a non-spherical object in a plasma. Presented at 55th Annual Meeting of the APS Division of Plasma Physics . (Denver, CO, 11-15 Nov 2013).

Zhao, L., and G. L. Delzanno. Charging and shielding of a non-spherical dust grain in a plasma. Presented at AGU Fall meeting. (San Francisco, CA, 9-13 Dec 2013).

Laboratory Study of Cosmically-relevant Collisionless Shocks

Scott C. Hsu
20120200ER

Introduction

This project will generate/diagnose collisionless shocks and diagnose/characterize shock-particle interactions in an existing laboratory plasma facility in P-24. Although collisionless shocks in plasmas were first predicted in the 1950's and discovered in the 1960's, many research questions relating to the microscopic physics of collisionless shock formation, evolution, and shock acceleration of particles to very high energies remain unanswered. The proposed experiments will emphasize the ability to (1) to control and scan physics parameters over a range of values and across physics regimes in order to validate physics models, and (2) obtain far more measurements in both space and time compared to either in situ space satellite measurements or astronomical observations. The collisionless shocks will be created via the head-on collision of two oppositely directed high velocity plasma jets launched by pulsed-power driven plasma rail-guns. A magnetic field will be applied via coils at the jet interaction region to access magnetized regimes which are essential for cosmic-relevance. The scale sizes of the jets and shock thickness will be 30 cm and 1 cm, respectively, enabling detailed characterization of shock structure and evolution via relatively simple diagnostics. As described in the proposal, key dimensionless parameters in the experiments will satisfy quantitative physics criteria for the collisionless shocks to be of cosmic relevance. The objectives of this work are to develop insights into collisionless shocks not obtainable via satellite measurements or astronomical observations alone, and to un-fold the specific physics mechanisms underlying collisionless shock formation and shock-particle interactions.

Benefit to National Security Missions

The recent LANL NPAC Strategic Capability Planning exercise (April, 2010) recognizes that the depth/breadth of theory, experimental, and computational capability for the study of extreme astrophysical environments is a LANL scientific "crown jewel." This project will add a unique laboratory component to that capability while providing a recruiting portal for students and postdocs. In addition, this project leverages existing DOE/SC investment in the experimental facility, which supports another NPAC recommendation to promote LANL's astrophysics/cosmology portfolio to DOE/SC. Fundamental research in plasma turbulence builds capability for some of the toughest questions in weapons physics.

Progress

Thus far in FY13, the project has fired more than 1000 experimental plasma shots of head-on collisions of supersonic plasma jets, and we have pushed into collisionless parameter regimes that are the focus of the project. We have also completed, and submitted for publication, an extensive set of electromagnetic particle-in-cell (PIC) numerical simulations to guide the experiments, including simulations of jet propagation and both unmagnetized and magnetized jet merging. Finally, we are working on adding additional diagnostic instruments for characterizing the shock structure and evolution, as well as a pulsed magnetic coil set for doing magnetized shock experiments in the third and final year of the project.

The experiments are showing the formation of a dynamic interaction region between the two merging jets. We are still in the process of obtaining better experimental measurements, but we believe that the lower-density leading edges of the jets are interpenetrating at early times, and then when the higher-density bulks of the jets meet, a more shock-like interaction initiates and proceeds. The scale size of the interaction region is ~10 cm, which is smaller than the collision mean-free-path between counter-propagating jet ions. Thus, this is already strong evidence of a collisionless interaction (despite the lack of such an interaction in the unmagnetized simulation results).

We are in the process of writing up the unmagnetized jet-collision results for publication; also, the results will be presented by postdoc Auna Moser at the internation-

al conference Interrelationship between Plasma Experiments in the Laboratory and Space (IPELS) in Japan (July, 2013).

The simulations have investigated jet propagation over the 1 m distance before they collide, as well as show what jet parameters are needed to give rise to the collisionless shock interactions we seek to study experimentally. In highly resolved 1D and 2D simulations, we have shown that collisionless shocks are generated using our measured jet parameters and when immersed in ~1 kG magnetic fields. The magnetic field orientation, as well as jet density gradients, are shown to have a strong effect on the nature of the jet interaction.

We have built and installed probe diagnostics to measure local magnetic field, electron temperature/density, and plasma electric potential. We are presently troubleshooting the probes as they are being affected by pulsed power electrical noise pickup. We have also built and operated a schlieren system to provide 2D time-resolved images of shock formation/evolution. We wrote and had accepted an operational IWD for the schlieren system. Right now, the schlieren system optics is being improved to maximize the sensitivity, and thus we have not yet obtained a shock image using the schlieren. We have an independently funded DOE undergraduate student joining us for the summer to build another probe to measure ion particle energies, to diagnose shock-particle interactions in our experiment. Finally, we will modify an existing capacitor bank and design/fabricate magnetic coils to add up to a several-kG magnetic field for experiments in the third year.

Future Work

Tasks for FY14 will focus on executing magnetized shock experiments using newly installed magnetic coils (to be completed in FY13) and based on numerical simulation work completed in FY13. In particular, we will diagnose the interaction region of two hydrogen plasma jets using newly implemented diagnostics (schlieren, interferometry, magnetic and electrostatic probes, and gridded ion energy analyzers) to provided new data on shock structure, evolution, and shock-particle interactions.

Conclusion

Expected results are fundamental experimental data that will improve our understanding of cosmically-relevant collisionless shocks. In particular, the data will (1) demonstrate the formation/existence of collisionless shocks in a laboratory experiment, (2) provide characterization of shock structure and evolution as a function of plasma parameters, and (3) provide insight into the important mechanism of shock acceleration of particles.

Publications

Merritt, E. C., A. L. Moser, S. C. Hsu, J. Loverich, and M. Gilmore. Experimental Characterization of the Stagnation Layer between Two Obliquely Merging Supersonic Plasma Jets. 2013. PHYSICAL REVIEW LETTERS. 111 (8): -.

Thoma, C., D. R. Welch, and S. C. Hsu. Particle-in-cell simulations of collisionless shock formation via head-on merging of two laboratory supersonic plasma jets. 2013. PHYSICS OF PLASMAS. 20 (8): -.

Nuclear Quadrupole Resonance: From No Field to Ultra-low Field

Michelle A. Espy
20120218ER

Introduction

The ability to non-invasively determine chemical composition is a significant problem for both medical, industrial and security screening. For example, the ability to ascertain what a material is or whether it is counterfeit without opening a package. Methods based in magnetic resonance, nuclear magnetic resonance (NMR) or nuclear quadrupole resonance (NQR) are very appealing because they provide a clear path to chemical information that does not require ionizing radiation and can penetrate material. Our goals for this proposal are to leverage existing LANL expertise in magnetic resonance at low magnetic fields (< 100 mT) for NQR-based non-invasive screening of materials. Our focus is to develop methods to enhance NQR sensitivity, and demonstrate applicability to stand-off detection of contraband (explosives and drugs).

We will demonstrate an NQR capability that can be combined with our present ultra-low field (ULF) NMR systems. We will show nearly simultaneous (interleaved) NMR/NQR.

We will enhance the sensitivity of NQR by use of pre-polarization, in which spin polarized protons are recruited in an external pulsed magnetic field an transfer their polarization to the 14N nuclei when ramped down past the NQR frequency. We will then study the use of magnetic field gradients and/or radiation damping to reduce the T1 (spin-lattice relaxation) time of the material which would speed up the polarization process.

Finally, we will investigate the use of cross-relaxation again, this time using the NMR to read out the NQR. This approach allows for low-frequency readout of the NQR signal, enhanced signal strength for low NQR frequency materials (like TNT) and the combination with T1 dispersion contrast from the NMR which could greatly enhance medical imaging applications.

Benefit to National Security Missions

NQR is a powerful method to detect interesting 14N containing substances (e.g. proteins in the human body, melamine in food, numerous explosives, and illicit drugs). NQR can provide highly specific chemical information, is not a trace method, and can be measured from a distance (~ 10-20 cm). LANL already possesses many of the tools required to develop NQR into a powerful approach. We propose to develop and extend NQR by use of pre-polarization and combination with ULF NMR readout. We will develop sensitive NQR that can penetrate through metals but does not require uniform or sophisticated magnetic fields (suitable for fielding). We will work closely with existing sponsors (NIH, DHS, OBER) to extend ongoing applications from ULF NMR to NQR. But the numerous new applications enabled will provide significant program development opportunities in global security ranging from stand-off detection of explosives within IEDs or the human body to transformational medicine.

Progress

We have constructed a fully homemade portable NQR spectrometer designed to measure NQR modes from 400 kHz to 5 MHz in a 100 ml sample volume. The spectrometer is composed of a transmit/receive solenoid coil, variable tuning and matching capacitors, and supporting circuitry. An induced NQR signal is so tiny (nV – μV), thus it is amplified by a gain of ~ 60 dB in last stage. Initially, we tested a sodium nitrite powder sample because of its relatively high NQR frequency at 4.64 MHz (thus is easier to detect). We have successfully observed first NQR signal from the sample. 50 data sets were averaged to give an SNR of roughly 40. The spectrometer was also used to measure relaxation times (T1 and T2) of the sample with standard pulse sequences. To improve the SNR, we employed a pre-polarization field applied to the proton subsystem in order to enhance the NQR signal by up to one-order of magnitude by using the mechanism of cross-polarization. To demonstrate the polarization

enhanced NQR, we tested ammonium nitrate because it is of significant interest, it has NQR modes at frequencies less than 500 kHz (thus is difficult to detect), and it has both 14N and 1H nuclei. Because the Q factor of the spectrometer was measured to be low at such a low NQR frequency, we replaced the T/R solenoid coil with another one with a higher inductance. The improvement gives higher Q factor of ~ 100 (thus the NQR signal is increased). In addition, we improved a pulse by delivering more power to the system at the start of the pulse, so that the pulse rises to a desired voltage in a shorter time. That results in making the pulse closer to ideal rectangular shape. Protons in ammonium nitrate are pre-polarized by an electromagnet placed 1 m away from the NQR spectrometer. After demagnetization, the ammonium nitrate sample is quickly moved into the solenoid coil in the spectrometer. We have successfully detected a polarization enhanced NQR signal from ammonium nitrate with a multipulse sequence. The calculated SNR was roughly 30 at a polarization field of 280 mT and a polarization time of 30 s. The enhancement factor was measured to be 13. We also confirmed temperature dependence of NQR frequency, polarization time dependence of the NQR signal, and polarization field dependence of the NQR signal. In conclusion, we demonstrated the polarization enhancement technique in ammonium nitrate. The results above have been presented at the 54th ENC conference in April and the postdoc research day in June this year. In the near future, we will publish the results.

We were also able to demonstrate acquisition of the NQR signal from ammonium nitrate via proton read-out. We saw very interesting behavior in the spectra for T1 vs. magnetic field, as measured by a field-cycling relaxometer. This behavior included the expected “dips” in T1 which have been reported in the literature to occur when the fast relaxing 14N interacts with the protons in hydrogen and shortens T1. However, we also observed peaks in T1 vs. magnetic field, indicating regions where the 14N was actually relaxing slower and lengthening the T1 relaxation. To our knowledge, this effect is predicted but has not been published via proton NMR measurements. We then cross-validated this against compounds where the 14N had been replaced by 15N (no NQR) .

For the remainder of the project we will focus on demonstration of single-sided detection, demonstration of combined NMR and NQR, and demonstration of T1 shortening.

Future Work

Our project goals are to demonstrate 1) a portable NQR system with sensitivity to small quantities of nitrogen containing materials of interest such as explosives or explosive surrogate materials; 2) demonstrate polarization enhanced NQR and 3) demonstrate NQR in combination with ultra-low field NMR.

In the past year we were able to achieve Goal #1 showing a fieldable system for NQR detection of materials of significant interest to potential customers such as ammonium nitrate and surrogates for contraband. We deliberately chosematerials that were at low NQR frequencies because they are the most challenging. Our success has demonstrated that we have mastered the technique. In the next year we will continue to refine this technique - and a specific aim will be the ability to accommodate larger sample sizes, and attain single sided detection that is a more practical geometry for medical and screening applications.

The second goal has been partially achieved by showing that we can use NMR-like pre-polarization methods to cause signal enhancement of the NQR via cross relaxation. We have now demonstrated this for ammonium nitrate and achieved a > 10X enhancement. We have also demonstrated read-out of the NQR signal through traditional NMR methods via cross-relaxation. A manuscript on these accomplishments is in preparation and the work will be presented as an invited talk at an upcoming conference on magnetic resonance based methods for explosives detection.

The third goal for the coming year will involve demonstration of interleaved NMR and NQR and follows naturally from the second goal. We intend to leverage an existing ultra-low field NMR system based on inductive coil detection for the NMR portion. We will also investigate methods to shorten the effect of long T1 times on the measurements.

Conclusion

We will develop a non invasive technique to characterize nitrogen content of materials. Nitrogen content in tissue is an indicator of the presence of proteins and can be used to study diseases in which protein concentrations are affected such as de mylenation of neuronal tissues associated with multiple sclerosis, ALS, and other neurological conditions.

This approach is also useful for the stand off detection of energetic materials, contraband, land mines and improvised explosive devices.

Publications

Kim, Y., T. Karaulanov, J. Yoder, A. Matlashov, S. Newman, A. Urbaitis, P. Volegov, and M. Espy. Development of a Pulsed 14N Quadrupole Resonance Technique for Solid Explosives Detection. Presented at Experimental Nuclear Physics Conference. (Asilomar, CA, April 14-19, 2013).

Kim, Y., T. Karaulanov, M. Espy, A. Matlashov, S. Newman,

A. Urbaitis, P. Volegov, and J. Yoder. Nuclear Quadrupole Resonance Technique for Solid Explosive Detection. To appear in Journal of Magnetic Resonance.

Laser-driven Relativistic Mechanics, Radiation, and Ion Acceleration

James A. Cobble
20120259ER

Introduction

It is well known that relativistic-electron jets stream from targets illuminated by extremely high-intensity lasers (I > 10^18 W/cm^2). However, little detailed information is available concerning jet properties, and all lasers are different. The LANL Trident Laser is among the best in the world in beam contrast, energy content, and focusability. It is the proper tool to use to fulfill our first goal: to diagnose the relativistic electron jets for various laser conditions with a suite of new diagnostics to remove the present ambiguity related to jet geometry, the current carried by the jet, and jet stability. Our second goal is to model jet behavior through mature particle-in-cell numerical simulations that will ultimately be transferable to an advanced computer platform. Because the unique physics environment created by a relativistic plasma jet produces intense radiation sources – both particles and x rays, one may envision several applications that could benefit human kind. Our third goal is to manipulate the jet with modifications of the laser drive to establish scaling laws for the applications for laser- accelerated protons (upwards of 100 MeV) and laser-produced, multi-tens-of-keV x-ray bursts. This leads to the ability to design appropriately-sized larger facilities in the future that may implement useful robust sources of both particle and x-ray energy for diverse applications: fusion, cancer treatments, ion acceleration, and flash x-ray radiography.

Benefit to National Security Missions

The inherent relativistic electron jet dominates radiation processes for electrons, ions, and x rays in ps-laser interactions. Once jet manipulation is understood and scaling laws are determined, managers have a decision point for capability building. We will know: 1) how big and what quality of laser is necessary to pump electron (or ion) fast ignition at the National Ignition Facility, 2) what is required to accelerate ions to greater than 1-GeV energy for cancer or other uses, whether for medical or national security purposes, 3) the feasibility of focusing other energetic ions, and 4) what laser to build for MaRIE for shock physics and materials research utilizing 20 – 100-keV x rays. Successful development of high-energy backlighters opens doors, for example, the possibility of phase-contrast imaging with x rays, a possible result of this project.

Progress

In the last 12 months, we validated the ability to attain phase-contrast images of the electron debris ejected from the rear of targets irradiated by lasers at intensities exceeding 3x10^20 W/cm^2. We have catalogued time-lapse PCI images of the expanding plasma from ~0.5 – 70 ps after the start of the laser pulse. The imaging probe laser, wavelength 527 nm, has captured wave-front distortions due to the integrated plasma density, not only the relativistic electron jets, sometimes with apparent filamentation, but also of thermal electrons accompanying protons accelerated to tens of MeV by the departure of the relativistic electrons from the target vicinity. We have solved the problem of electron spectroscopy with a magnetic field to reveal the electron energy distribution as a function of laser irradiance and the divergence (emittance) of each band of the measured energy spectrum. We have made current density measurements, which coupled with the divergence measurement, lead to an estimate of integrated electron current. As a stretch goal for this project, we have fulfilled laboratory safety requirements to deploy a gas-Cherenkov detector to monitor gamma-ray production both from prompt laser-target interactions and from the impact of accelerated protons that convert to gammas in a 'proton catcher' downstream one meter. Either of these features could lead to a laser-produced 'dial-a-gamma-energy' source for national security programs. The time-resolving GCD is on loan from the ICF program. Particle-in-cell codes are presently being deployed to model the early-time behavior of the relativistic mechanics. As simulations become more mature and analysis of the PCI images produces projected electron density maps, we will compare

code predictions to experimental measurements. So far, all targets have been synthetic diamond or carbon-based plastics. Finally, we have obtained a set of thin-film metal targets – 50 – 500-nm thickness – to measure ionic line emission for so-called 'hollow atoms' – atoms in the vicinity of the electron channel through the target where the spectator atoms have been preferentially stripped of their K-shell electrons. We plan to monitor spectral content as a function of target thickness to observe possible amplified spontaneous emission – laser-like radiation – from the target plasmas.

Future Work

The high-power laser creates a relativistic, multi-MA electron jet through its interaction with a thin-film target. The jet will be resolved with temporally gated phase-contrast imaging using a ps UV laser probe. The jet's length, diameter, duration, and stability will be determined. The beam current will be measured by charge collection; hence, the current density may be calculated. In like manner, the development of the virtual cathode sheath is diagnosed both geometrically and temporally. Proton-beam geometry and energy and x-ray yield will be measured with radiochromic film and calibrated x-ray detectors respectively. The scaling of radiation with laser focal properties, particularly pulse duration and focal-spot quality, and with target configuration will be measured with these detectors. Thus, we determine the laser's effect on the relativistic jet for process optimization whether the desired property is electron beam current, ion current or acceleration, or x-ray production. Matching simulations with real experimental data, we may predict plasma behavior and radiation efficiencies at even higher laser operating conditions.

We are presently in the middle of our 4-wk experimental run for FY13, and results are very promising. We have measured current density, electron-beam divergence and energy distribution, and have obtained phase-contrast images of the electron beam as it emerges from the target. Simulation platforms are being developed for use in FY14, during which we shall press forward with investigations of gamma-ray emission and 'hollow-atom' spectra -- relevant for homeland security, among other things, and novel soft-x-ray laser action.

Conclusion

Characterization of the laser-driven relativistic electron jets (evidence of their instantaneous current and their geometry – their divergence and whether or not they filament) is important to the physics of their applications, e.g., electron fast ignition, ion fast ignition, high x-ray flux for radiography, and general steep-gradient, high-flux ion acceleration. Results will therefore help determine our control of the jets and the how useful they may be for fusion ignition, for flash radiography of dynamic shock experiments, and for ion-beam treatment of tumors.

Publications

Cobble, J. A.. Trident shot 23858 –electron and proton energies & Dexter calibration. 2013. P-24:2013-038, LA-UR-13-26309.

Cobble, J. A.. Proton converter for GCD on Trident. 2013. P-24:2013-022.

Cobble, J. A.. SUBJECT: Divergence of E beam in 100-TW Trident Experiments. 2013. P-24:2013-070, LA_UR-13:27148.

Cobble, J. A., S. Palaniyappan, D. C. Gautier, Y. H. Kim, D. D. Clark, R. P. Johnson, T. Shimada, J. C. Fernandez, and H. W. Herrmann. Relativistic transparency experiments at the Trident Laser. 2013. In 55th Annual Meeting of the APS Division of Plasma Physics. (Denver, Colorado, 11-15 November 2013). Vol. 58, No. 16 Edition, p. PO6.00009. Bulletin of the American Physical Society: American Physical Society.

Monte Carlo for Quantum Transport

James E. Gubernatis
20120266ER

Introduction

We propose to develop the first significant Monte Carlo tool to simulate transport in an extended quantum system. To do so, we need to remove a computational bottleneck present in the current approach. We will do this in an insightful fashion and thereby generate a new computational capability, posed for widespread application. Simulating non-equilibrium phenomena, such as transport, is difficult whether the system is quantum or classical. For classical systems, Boltzmann equation and molecular dynamic methods are ubiquitous. These approaches however are not applicable to quantum problems. While a Monte Carlo method, called wave function Monte Carlo, works well for quantum systems with small size, for example, quantum dots and qubits, its computational cost scales exponentially with size. We argue that this difficultly is not with the core strategy of the method but with the way Monte Carlo is being used in it. We observe the bottleneck is a step analogous to one appearing in other quantum Monte Carlo methods. Thus, by adapting one of these techniques to a new context, we argue that we can eliminate this bottleneck and do so in a novel manner. For concreteness, we will target transport in nanoscale materials. Our intent is to provide theorists with a tool to model these materials and to benchmark approximate theories of the behavior of these models. The new simulation capability will also provide experimentalists with a tool to reduce the trial and error in the design of transport devices and to aid in the interpretation and design of their experiments.

Benefit to National Security Missions

The objective of this project is the development of a new computational capability. We emphasize that it has a broader range of applications than nanotechnology. This range umbrellas the same range of activities as the Laboratory's proposed material flagship, MaRIE, and will provide useful tools for researchers engaged in this project. While the focus of this project is on transport, the seminal ideas came from quantum optics where the focus is the interaction of a few cold atoms with electrostatic traps and the interaction of an atom with a laser. Accordingly, the new computational tool has multiprobe utility. Quantum optics and MaRIE share the same goal of prediction and control. In fact, the integration of the proposed research with MaRIE would give MaRIEa distinctive look. Additionally, the new computational capability will create new opportunities for high performance computing. The Monte Carlo method is a natural for exascale computing.

Progress

We completed the wavefunction Monte Carlo code development started last year, succeeded in understanding when the steady-state of the simulation should be independent of the initial conditions, and began to benchmark the code against published results. We also resolved the questions we had about how we should calculate one-dimensional transport.

The code that was under development uses a Monte Carlo method instead of a more costly and memory intensive deterministic method to solve the master equation for an open quantum system interacting with its environment. Our ultimate objective is replacing current Monte Carlo techniques with ones that execute even faster.

Of interest is the long-time solution of the master equation, the steady state. In most cases we want the steady state to be independent of the initial state as being so is more indicative of the general character of the problem. For the models we are considering, we established the independence of their steady states from the initial conditions. That they are independent is something simply assumed in the literature.

We want in particular to calculate the heat current generated in an open quantum system that is in contact with heat baths of two different temperatures. Published

is a variety of definitions for the current. We decided to use one that gave for a one-dimensional current going left to right the sign opposite to the current going right to left. This definition fits the physics. Most others did not or else were unclear about what was actually being calculated.

In benchmarking the code against published one-dimensional simulations using the wavefunction Monte Carlo method, we experienced significant disagreements between what was published and what we were calculating. In particular, predictions of the Monte Carlo code with the new and the previous definitions of the current did not agree with published results.

To resolve this disagreement, we developed a code to solve the master equation deterministically. Having this code enables us to compare two quite different calculations of the same thing. We focused on comparing the density matrices as all measurements derive from it. The deterministic time-dependent results for the density matrix should agree with the Monte Carlo's ensemble averages as a function of time and the deterministic steady-state results should agree with the long-time average of the Monte Carlo results. Developing this code took considerable effort because we could not use any portion of the wavefunction Monte Carlo code.

We found that only the Monte Carlo ensemble averages for short times agreed with the deterministic predictions. Further, the differences did not, as they should, become smaller as the Monte Carlo ensemble size, the length of integration time, or the accuracy of the differential solvers were increased. When we turn off the interaction between the heat baths and the open system, which removes the Monte Carlo from the problem, the two approaches agree perfectly which implies the problem is not with the way we calculate our measurements. If we look at the currents produced in the open systems by just the consequences of the heat bath, which emphasizes the Monte Carlo portion of the calculation, we see the disagreements. The bias, of the order of a few tenths of a percent, appears caused by the off-diagonal elements of the density matrix becoming small and exhibiting large statistical errors. Common measures of comparing density matrices, such as the trace norm and the entropy, imply a much better agreement between the two approaches; however, they are insensitive to these matrix elements being small. We are using a root mean-square measure which is more common to Monte Carlo simulations. We are still working on understanding the problem. It appears that the statistical error generated by this particular Monte Carlo method might just be something that is naturally large so reducing it it takes a lot of computer time.

We discovered a way to compute the spectral function of the open system with the wavefunction Monte Carlo method. The ability to do so enables a direct comparisons of our simulations with spectroscopic experiments. If we have time, we plan to implement this method.

Future Work

We will focus on making the wavefunction Monte Carlo method more efficient. Currently, we are using the standard drift-jump algorithm. A variety of options exists. Because of the stochastic jumps that occur in the wavefunction as a function time, we propose to implement a version of what is called the worm algorighm. In it, a random walker (the worm) moves between different space-time points and at each point changes its directions or changes its quantum state. With it we hope to eliminate the need in the present method of compiling statistical information by multiple restarts of the simulation. With the worm algorithm, it appears possible to simulate to a fixed time once and use the stochastic movement of the worm to sample statistical information from this solution.

With more efficiency, we will then perform an extensive set of one-dimensional transport simulations. By the end of the year, we intend to move the simulations and code development to two-dimensions. In higher dimensions, the quantum transport theorems for our master equations suggest establishing independence of the steady state from the initial state will be easier to achieve.

Towards the end of the year we will move towards two-dimensions in steps, that is, moving from one chain, to two coupled chains, to three coupled-chains, etc., to study the crossover in dimensional behavior. This sequencing will be important because many low-dimensional quantum systems, often called one-dimensional, are actually quasi-one-dimensional, with the length in one dimension greatly exceeding that in the other. We propose to do the first such study of this physics. More efficient Monte Carlo methods are needed to make this type of study possible.

Conclusion

Without doubt our new Monte Carlo method will be more efficient than the present one. The main question is, "By how much more?" Unfortunately, the field has few exactly solvable problems that provide benchmarks. It does though have a few published results for smaller lattices with related models against which we can benchmark the methods. We will execute these benchmarks and then push the simulation to larger systems,

Publications

Berry, D., R. Cleve, and R. Somma. Exponential improvement in precision for Hamiltonain-evolution simula-

tion. Physical Review Letters.

Gubernatis, J. E.. Sign and Phase Problems: Monte Carlo for the unsampleable. Invited presentation at Monte Carlo Methods in the Physical and Biological Sciences. (Providence, RI, 29 Oct - Nov 2, 2012).

Gubernatis, J. E.. Wavefunction Mote carlo for transport in open quantum systems. Presented at March Meeting 2013, American Physical Society. (Baltimore, 18-22 Mar. 2013).

Hu, F. M., T. O. Wehling, J. E. Gubernatis, T. Frauenhein, and R. M. Nieminen. Magnetic impurity affected by spin-orbit cou[ling: behavior near a topologival phase transitions. 2013. Physical Review B. 88: 045106.

Ren, J., J. X. Zhu, J. E. Gubernatis, C. Wang, and B. Li. Thermoelectric transport with electron-phonon coupling and electron-electron interacion in molecular junctions. 2012. Physical Review B. 85: 155443.

Somma, R. D., D. Nagaj, and M. Kieferova. Quantum Speed-up by Quantum Annealing. 2012. Physical Review Letters. 109: 050501.

Nonequilibrium Spin Noise in Semiconductors: Physics and Applications

Nikolai Sinitsyn
20120340ER

Introduction

We develop a novel approach for probing material characteristics and new functionalities in commercially important semiconductors. The novelty of our approach is in the observation that a recently developed spin noise spectroscopy technique can probe essentially new physical phenomena in the non-equilibrium regime. To study this regime we will develop the theory that will interpret our observations of out-of-equilibrium electron spin noise in semiconductors. Our preliminary theoretical studies predict new effects that we will verify. Each effect reveals physics that is either difficult or impossible to study with other competing techniques. If demonstrated, these effects will open up the path for further applications, including high precision measurements of a spin-orbit coupling, obtaining properties of an electron liquid near the metal-insulator transition, characterizing electron transport at extreme conditions of electric breakdown, discovering new types of quantum phase transitions, measuring entanglement entropy and many other effects of importance for the future of several fields.

Benefit to National Security Missions

This project will build Laboratory capabilities in the development of novel measurement methods that enable new scientific discovery at LANL. Our project is enabled by recent technological advancements that use the very large data storage and manipulation capabilities. The project will advance new Laboratory capabilities that underpin a wide variety of Laboratory missions including Nanotechnology and Quantum Information Science. Demonstration of new effects by the nonequilibrium spin noise spectroscopy measurements will generate worldwide attention and will form a robust platform for a nanoscale spintronics program at LANL. The present project will lay the groundwork for future proposals for external funding to address national problems, including new functional materials capabilities for MaRIE and energy efficient applications (DOE, DARPA).

Progress

We wrote a manuscript called “Nonequilibrium spin noise spectroscopy” (available as LANL internal publication and submitted to Phys.Rev.Lett). It targets the very basic effects suggested in the early proposal of this LDRD ER. In this work we discuss advantages of measuring spin noise in nonequilibrium regime and estimate several effects to be experimentally verified. We also discuss applications for precise measurements of spin orbit coupling anisotropy and exploring physics of spin noise.

We have submitted an extended article with a proposal to apply spin noise spectroscopy for characterization of nanostructures. We already received positive reviews of Phys. Rev. B referees. The work shows that spin noise spectroscopy method, developed at LANL, has particular advantages for nanostructure characterization.

We published an article in Applied Physics Letters with proposal of new measurement strategy, which we call “Two beam spin noise spectroscopy”. We showed that by measuring spin noise by two spatially separated beams it is possible to obtain new information about spin dynamics in semiconducting materials and nanowires.

On experimental side, first, one article called “Optical Spectroscopy of Spin Noise” was published in Phys. Rev. Lett. 10, 176601 (2013) by the experimental team in which the fact that measuring beam is selectively coupled to different quantum dots is clearly exposed.

Several other experiments were performed, which require additional theoretical studies and experiments. We measured spin noise at high intensities of a measurement beam and observed new phenomena, such as anomalous peaks in the noise power, which are currently not explained but the team has developed working hypothesis for their understanding. We also observed features of noise power spectrum that suggest the appearance of purely quantum effects such as the quan-

tum Zeno effect in GaAs. Our current goal is to produce better arguments for a decisive conclusions about these observations.

Future Work

We will explore the effects of spin-orbit coupling, and interactions on spin correlators in GaAs semiconductors, and obtain specific properties of materials and information that can be extracted from such measurements. Spin noise in electric fields will be studied theoretically by Green function techniques, which can be considered as a high order Kubo formula and by methods of the quantum counting statistics. Some of the previous insight about nonequilibrum noise in electric cur-rents will be translated into a theory of spin noise. A complementary theoretical approach, which already allowed us to gain an important insight, is based on the kinetic equation for hydrodynamic evolution of charge and spin density where interactions are included in the collision term. In 2014, we will concentrate on developing theory of high order correlators in spin noise spectroscopy and effects of many-body interactions. The latter will be based on theory of Luttinger liquids supplemented by our methods that we already developed for characterizing spin noise in quasi-1D geometry. Experiments will be focused on verification of our recent prediction of the peak shift effect in electric field and on studies of spin noise at high intensity, where we observe unexpected phenomena that we are just starting to explore.

Conclusion

We will develop the technique that we call the nonequilibrium noise spectroscopy. It will allow us to look at material properties that simply could not be probed directly by any other approach and it will enable design of new materials for efficient energy transport and electronic devices. Specifically, we will demonstrate high precision measurements of spin orbit anisotropy and the first studies of the metal-insulator transition in GaAs semiconductors. Higher order spin correlations will reveal the fundamental statistical physics of nonequilibrium spin dynamics and will constitute a significant a-vance in the field of quantum measurement science.

Publications

Chaudhury, S., J. Cao, and N. A. Sinitsyn. Universality of Poisson Indicator and Fano Factor of Transport Event Statistics in Ion Channels and Enzyme Kinetics. 2013. Journal of Physical Chemistry B . 117: 503.

Chernyak, V. Y., J. Klein, and N. A. Sinitsyn. Algebraic topology and the quantization of fluctuating currents. 2013. Advances in Mathematics. 244: 791.

Ganeshan, S., and N. A. Sinitsyn. Fluctuation Relations for Current Components in Mesoscopic Electric Circuits. 2011. Physical Review B. 84: 245405.

Li, Y., N. A. Sinitsyn, D. Smith, D. Reuter, A. Wieck, D. Yakovlev, M. Bayer, and S. Crooker. Intrinsic spin fluctuations reveal the dynamical response function of holes coupled to nuclear spin baths in (In,Ga)As quantum dots. 2012. Physical Review Letters. 108: 186603 .

Pershin, Y. V., V. A. Slipko, D. Roy, and N. A. Sinitsyn. Two-beam spin noise spectroscopy. 2013. Applied Physics Letters . 102: 202405.

Roy, D., Y. Li, A. Greilich, Y. V. Pershin, A. Saxena, and N. A. Sinitsyn. Spin noise spectroscopy of quantum dot molecules. 2013. Physical Review B. 88: 045320.

Sinitsyn, N. A., Y. Li, S. A. Crooker, A. Saxena, and D. L. Smith. Role of Nuclear Quadrupole Coupling on Decoherence and Relaxation of Central Spins in Quantum Dots. 2012. Physical Review Letters. 109: 166605 .

Sinitsyn, N. A., Yuriy V. Pershin, Valeriy A. Slipko, and N. A. Sinitsyn. Nonequilibrium spin noise spectroscopy. 2013. Physical Review Letters. 111: 067201.

Sykes, A., D. Solenov, and D. Mozyrsky. Bloch-Redfield theory of high-temperature magnetic fluctuations in interacting spin systems. 2012. Physical Review B. 85: 174419.

Zapasskii, V. S., A. Greilich, S. A. Crooker, Y. Li, G. G. Kozlov, D. R. Yakovlev, D. Reuter, A. D. Wieck, and M. Bayer. Optical Spectroscopy of Spin Noise. 2013. Physical Review Letters. 110: 176601.

Flipping the (Light) Switch on Nano-magnetism: Emergent Photomagnetization in Quantum-confined Semiconductors

Scott A. Crooker
20120374ER

Introduction

Manipulation of magnetic metals forms the cornerstone of today's vast information-storage industry, while in parallel, semiconductors provide the basis for current microprocessor technologies. It is therefore not surprising that the marriage of magnetism and semiconductors – as typified in today's magnetic semiconductors -- is a thriving research area (briefly, these materials achieve new functionality by coupling, via spin-exchange interactions, the semiconductor's electrons and holes with embedded magnetic dopants). As fundamental research in both magnetism and semiconductors continues its focus on miniaturization, magnetic semiconductors are also now pushing the limits of quantum confinement. Recent work at LANL and elsewhere have demonstrated the synthesis of truly "0-dimensional" magnetic semiconductors in the limit of extreme quantum confinement: these new materials are semiconductor nanocrystals (of, e.g., ZnSe or CdSe) containing small numbers (<5) of magnetic atoms (Mn, Co, Fe). Remarkably, these novel nanoscale materials exhibit unexpected and new emergent properties that simply do not (or cannot) exist in their more conventional 3-D or 2-D forms. New properties include the ability to tune magnetic exchange interactions via quantum confinement and wavefunction engineering at the nanometer scale, magnetic polaron formation at high temperatures, and – especially -- a recently-discovered photo-induced magnetism in a new magnetic semiconductor system based on copper-doped nanocrystals.

Our scientific goal is to investigate these new families of nanometer-scale magnetic semiconductors, with an emphasis on wavefunction engineering and controlled placement of magnetic dopants within core-shell nanocrystals to achieve new functionality. The work will focus on emergent optically-controlled magnetization, tunable spin-exchange interactions, and ultrafast spin dynamics. Colloidal synthesis and time-resolved magneto-optical studies form the essential components of this proposal. Preliminary growth and measurements of these new materials (described below) indicate that all aspects of this project are achievable within 3 years.

Benefit to National Security Missions

This project will build Laboratory capabilities in the development of novel materials-synthesis and experimental techniques that enable new scientific discovery at LANL. It is based on recent advances in colloidal growth and tunable magnetic doping of nanocrystals that have already demonstrated new emergent functionality. Our approach goes well beyond this specific example photo-induced magnetization in doped nanocrystals: long-term advantages and applicability of nano-scale heterostructures and time-resolved magnetization dynamics are very general.

Progress

In the last year we have published a high-profile paper in Nature Nanotechnology that describes the main findings of the first stage of this ER -- namely, establishing the existence of optically-induced magnetism in these copper-doped ZnSe nanocrystals.

We have also been focusing on new copper indium sulphide nanocrystals (CIS), a new materials systems that has been attracting much attention for solar energy light harvesting. Our recent preliminary data suggests that the light emission mechanism in these new CIS materials is quite similar to that from copper doped ZnSe (despite the completely different stoichiometry), and likely has to do with copper defects. We have measured magneto-PL as well as magnetic circular dichroism on these CIS materials, and they definitely show a slight paramagnetic behavior, indicative of paramagnetic copper atoms. This work is currently being written up.

Concurrently, our ultrafast OPO laser system is up and running; this will very soon be sapplied to copper-doped nanocrystals in order to study their magnetization dynamics.

Future Work

We will be focusing in the next year on both copper-doped ZnSe nanocrystals as well as new copper indium sulphide nanocrystals (CIS), a new materials systems that has been attracting much attention for solar energy applications. Our recent preliminary data suggests that the light emission mechanism in these new CIS materials is quite similar ot hat from copper doped ZnSe (despite the completely different stoichiometry). In the next year we anticipate that time resolved magneto-optical measurements of these CIS materials will also be performed. The next main steps are to i) study the *dynamic* magnetization of these particles by using ultrafast optical techniques such as time-resolved Faraday rotation, and ii) to measure the optical properties of individual nanoparticles by using a single-quantum-dot microscope. Equipment infrastructure for both of these measurements is already in place.

Conclusion

Using our spectroscopic methods, we expect to have direct access to the as-yet-unknown dynamics of photo-induced magnetization in engineered nanocrystals. We expect to observe ultrafast spin precession frequencies of electrons and holes (enhanced by sp-d exchange), and picosecond/nanosecond timescales for collective magnetization alignment (and much longer timescales for eventual spin-lattice relaxation). Any demonstration of engineered sp-d coupling and its associated dynamics will represent totally new data that will be found of significant interest to researchers working in all areas of nanoscale magnetism, magnetic semiconductors, and spin interactions.

Publications

Pandey, A., S. Brovelli, R. Viswanatha, L. Li, J. M. Pietryga, V. I. Klimov, and S. A. Crooker. Long-lived photo-induced magnetization in copper-doped ZnSe/CdSe core/shell nanocrystals . 2012. Nature Nanotechnology. 7: 792.

A Novel Exploration of Nature's Largest Explosions

W T. Vestrand
20120375ER

Introduction

We propose to deploy an integrated suite of autonomous robotic optical instruments, with capability unmatched anywhere in the world, to measure the properties of prompt optical flashes generated by Gamma-Ray Burst (GRB) explosions. The novelty of our approach lies in the use of simultaneous multi-color measurements, polarimetry, and high cadence photometry of the prompt optical flash--each for the first time. Used with gamma-ray measurements from NASA's Swift and Fermi missions, these multi-wavelength observations will probe the physics of gamma-ray bursts to an unprecedented level of detail, both temporal and spectral. To interpret these measurements, and explore their implications, our observational effort will be complemented by a theory effort, culminating in a generic numerical model for the synchrotron and inverse-Compton emissions from relativistic outflows, with the end goal of understanding the extreme physics present during nature's largest explosions. Some of the key science questions about GRBs that we will answer are: What are the physical conditions in GRB jets and the radiation mechanisms that produce the prompt optical and gamma-ray emission?; Is the prompt emission highly polarized, as some models predict?; What is the precise temporal relation between the prompt optical and gamma-ray emission components? The simultaneous observations made by our ground-based optical instruments and NASA satellites will provide previously impossible measurements of the relativistic jet and central engine.

Benefit to National Security Missions

The ability we develop to identify, follow-up, and interrogate rapid astrophysical explosions will have significant impact for NASA's goal of Understanding the Origin and Evolution of the Universe and will provide important context information for NASA's Swift and Fermi Missions. The persistent monitoring and real-time robotic techniques we refine on this exploratory scientific investigation will have important applications in Space Situational Awareness and can address the declared needs of some of our programmatic customers. The principal investigator is a member of the Space Systems Program Office at LANL and with be working directly with external customers to transition this work to new Work For Others (WFO) programs.

Progress

The optical light that is generated simultaneously with the x-rays and gamma-rays during a gamma-ray burst (GRB) provides important clues about the extreme nature of the explosions that occur as massive stars collapse to form black holes. This year we detected a bright optical flash (7th magnitude) and fading afterglow from a powerful burst, GRB 130427A, that set new records for gamma-ray brightness and duration. Bright optical flashes are rare, and this flash, the second brightest ever detected, is the first to allow detailed comparison with the properties of the gamma-ray emission at very high energies. We found a striking similarities between the optical light curve and >100 MeV photon flux light curve during the first 7,000 seconds. We attribute this link to co-generation in an external shock. The simultaneous, multi-color, optical observations are best explained at early times by reverse shock emission generated in the relativistic burst ejecta as it collides with surrounding material and at late times by a forward shock traversing the circumburst environment.

We examined the peaks of 30 optical GRB afterglows and 14 X-ray light curves that display a good anticorrelation of the peak flux with the peak epoch. We investigated the ability of two forward-shock models for afterglow light-curve peaks - an observer location outside the initial jet aperture and the onset of the forward-shock deceleration - to account for those peak correlations. For both models, the slope of the Fp-tp relation depends only on the slope of the afterglow spectrum. We found that only a conical jet seen off-aperture and interacting with a wind-like medium can account both for the X-ray

peak relation, given the average X-ray spectral slope βX = 1.0, and for the larger slope of the optical peak relation. However, any conclusion about the origin of the peak flux-peak epoch correlation is, at best, tentative, because the current sample of X-ray peaks is too small to allow a reliable measurement of the Fp-tp relation slope and because more than one mechanism and/or one afterglow parameter may be driving that correlation.

Future Work

Our GRB observational program will continue to focus on the observations that our RAPTOR telescopes our uniquely capable of providing. The RAPTOR-Z high cadence imager and multi-color follow-up telescopes—RAPTOR-T and RAPTOR-S—will be used to make observations of Swift localized GRBs. We plan to expand our GRB observational campaign on two fronts: (1) Deploy real-time localization software on our hybrid search/follow-up array (RAPTOR-W) to search for counterparts to Fermi Gamma-Ray Burst Monitor (GBM) triggers; and (2) search for GRB prompt/precursor emission with our full sky persistent monitors in Hawaii and New Mexico.

In the coming year our theory effort will concentrate on candidate GRB models and their predicted polarization signatures. We goal is to conduct a more comprehensive study of the range of possibilities than has been conducted to date and prepare for interpretation of the GRB polarization we expect to conduct during the second half of our program.

New instrument development will be focused on the construction of the polarimeter. The polarimeter will employ a rapidly spinning Polaroid that is synchronized with a fast frame rate (~9 Hz) electron multiplication CCD camera. Our schedule aims for final integration of the hardware in September 2013 and first light for the polarimeter in November 2013.

We will also make routine, densely sampled (twice per night), multi-color optical observations of the bright gamma-ray emitting blazars. And, as the polarimeter is brought on line, we will begin collecting nightly polarimetry measurements of 12 optical bright (mv<15) GeV gamma-ray emitting blazars (3C 273, Mrk 421, Mrk 501, CTA 102, etc.). A related goal is the construction of a photometry database that allows access to the large sample of measurements that we are collecting for bright blazars.

Conclusion

We will provide a better understanding of the most extreme explosions known in the Universe. These so-called Gamma-Ray Bursts are bright flashes of gamma-ray emission---arriving at Earth today--that were generated in the early Universe, when a class of very massive stars collapsed to form the first black holes. We will use the spectral, temporal, and polarization properties of these black hole birth announcements to decipher the extreme explosion physics and collect new clues about the origin of our Universe. Building this technical capability will also enable new approaches to National Security problems related to Space Situational Awareness.

Publications

Ackermann, M., R. Kiziah, P. Zimmer, J. D. Beason, E. Spillar, W. T. Vestrand, and M. Weeks. Alternatives for Ground-Based, Large-Aperture Optical Space Surveillance Systems. To appear in 2013 AMOS Technical Conference. (Maui, 10-12 Sept. 2013).

Bode, M., and W. T. Vestrand. Small and robotic telescopes in the era of massive time-domain surveys. 2012. In New Horizons in Time-Domain Astronomy, International Astronomical Union Symposium 285. (Oxford, England, 19-23 September 2011). Vol. 285, p. 235. Cambridge, England: Cambridge University Press.

Jin, Z., S. Covino, and M. Della Valle et al. GRB 081007 and GRB 090424: The surrounding medium, outflows, and supernovae. 2013. Astrophysical Journal. 774 (2): 114.

Panaitescu, A., W. T. Vestrand, and P. R. Wozniak. Peaks of optical and X-ray afterglow light curves. 2013. Monthly Notices Royal Astronomical Society. 433: 759.

Panaitescu, A., W. T. Vestrand, and P. Wozniak. The effect of photon-photon absorption on Fermi-LAT light-curves of GRB afterglows. Astrophysical Journal.

Panaitescu, A., W. T. Vestrand, and P. Wozniak. An external-shock model for GRB afterglow 130427A. Monthly Notices Royal Astronomical Society.

Panaitescu, A., and W. T. Vestrand. The possible ubiquity of energy injection in gamma-ray burst afterglows. 2012. Monthly Notices of the Royal Astronomical Society. 425 (3): 1669.

Vestrand, W. T., J. Wren, A. Panaitescu, P. Wozniak, H. Davis, D. Palmer, G. Vianello, N. Omodei, S. Xiong, M. S. Briggs, M. Elphick, W. Paciesas, and W. Rosing. The bright optical flash and afterglow from the gamma-ray burst GRB130427A. To appear in Science.

Vreeswijk, P., C. Ledoux, A. Raassen, A. Smette, P. Wozniak, W. T. Vestrand, and P. Jakobsson. Time-dependent excitation and ionization modelling of absorption-line variability due to GRB 080310. 2013. Astronomy and Astrophysics. 549: 22.

Transport by Thermodynamic Cross-terms in ICF Capsule Plasmas

Xianzhu Tang
20120395ER

Introduction

Recent proton radiography measurements reveal that electric fields of ~10^9V/m are self-generated during inertial confinement fusion (ICF) implosions. The impact of such enormous fields on the capsule performance cannot be fully accounted for by radiation-hydrodynamic codes that are mainly used to simulate ICF implosions. In particular, it has been claimed that the factor of two discrepancy between these codes' predictions and experimentally observed neutron yield is due to the electric field enhanced barodiffusion at the front of the rebounding shock wave, an effect that cannot be straightforwardly captured within the hydrodynamic approach.This observation raises several important research questions. First, the above-mentioned qualitative analysis discusses the effect of barodiffusion in the absence of thermodiffusion, as well as viscous effects. The two latter phenomena may affect the capsule performance as much as the former one and therefore need to be properly evaluated. Second, baro- and thermo-diffusion are among a subset of plasma transport driven by thermodynamic cross-terms. A comprehensive physics understanding of all thermodynamic cross-terms in ICF plasmas where strong electric field exists must be developed. Third,a new computational approach, capable of capturing the relevant physics with reasonable computational effort, needs to be developed. To address these issues this project will develop a consistent analytical theory of ion diffusion in the front of a shock wave propagating over a binary mix of plasmas. Insights into the effect of baro- as well as thermo-diffusion will be obtained. The next-step goal is to develop a comprehensive transport theory for ICF shock front plasma taking into account all thermodynamic cross terms. The final goal of the proposal is to verify analytical theory with two-fluid plasma simulations solving the Braginskii equations. In such a code, electron and ion fluids are treated separately, thereby allowing evaluating the electric field and the associated diffusive fluxes.

Benefit to National Security Missions

In an Inertial Confinement Fusion capsule under spherical implosion, the fusion yield is critically dependent on the relative concentration of the D and T fuel ions, which have different mass and charge ratio. The projects aims to develop a fundamental understanding and modeling tool for the shock-enhanced relative ion transport. This will have direct impact the NNSA's ICF program and SC's Inertial Fusion Energy program. The capability developed will be transferred to both the ICF and IFE program in three years. We will work with LANL's program managers in ICF, ASC, and SC/OFES to ensure this transition.

Progress

In a comment to PHYSICAL REVIEW LETTERS Volume: 109 Issue: 26 Article Number: 269501 DOI: 10.1103/PhysRevLett.109.269501 published DEC 27 2012, Kagan and Tang identified a discrepancy between Peter Amendt's formulation of inter-species ion diffusion and ours, which was published in Physics of Plasmas Vol. 19, Issue: 8, Article Number: 082709, DOI: 10.1063/1.4745869 in AUG 2012, and resolved it by correctly applying the thermodynamic approach of Landau and Lifshitz. In a reply, Amendt et al. consented to our correction.

In a preprint to be submitted to Physics of Plasmas, we gave an exposition of how to correctly apply the thermodynamic approach of Landau and Lifshitz to the inter-species ion diffusion problem.

In a preprint to be submitted to Physical Review Letters, Kagan and Tang performed first-principles calculation of thermo-diffusion in a multi-species plasma, and found that contrary to the neutral gas case, thermo-diffusion can become dominant in a plasma due to the long range nature of Coulomb interaction. This contrasts with previous findings from LLNL by Amendt and his collaborators that thermo-diffusion can vanish. We also identified the cause of their error.

In a set of three preprints to be submitted to Physical Review Letters and Physics of Plasmas, we laid down the theoretical formulation of reduced Fokker-Planck models for high energy ion distribution in an ICF hot spot, computed the tail ion distribution, and discovered the so-called inverse Knudsen layer effect on fusion reactivity. This work lead to an innovative experimental design and interpretation framework to separate the effects of ion diffusion and Kundsen-layer reactivity reduction on total fusion yield in ICF expriments, which provided the scientific foundation for a DR full proposal on "Plasma Physics Effects on Fusion Yield in Inertially confined systems."

A student, Francesco Boffa, has further developed a 2D implosion module within LAPS which uses spectral volume discretization. This sets up the implementation of the ion diffusion calculation.

Future Work

The following tasks/goals are planned for the next fiscal year:

- Complete the theory of inter-species ion diffusion flux in terms of all thermodynamic forces
- Carry out simulation and theoretical studies of the weak shock structure
- Implementing inter-species ion diffusion flux in a 1D implosion code

Conclusion

The scientific effort aims to produce three primary outcome. The first is a comprehensive plasma transport theory taking into account all thermodynamic cross terms in spherical implosion with multiple ion species. The second is a spherically symmetric two-fluid plasma simulation code that captures the multiple ion species dynamics and transport in an imploded target. The third is the application of simulation code to validate the theoretical model and explore ways to improve the neutral fluid hydrodynamic model for capturing transport physics such as baro- and thermo-diffusion.

Publications

Hsu, S. C., T. J. Awe, S. Brockington, A. Case, J. T. Cassibry, G. Kagan, S. J. Messer, M. Stanic, X. Tang, D. R. Welch, and F. D. Witherspoon. Spherically imploding plasma liners as a standoff driver for magnetoinertial fusion. 2012. IEEE Transactions on Plasma Science. 40 (5): 1287.

Kagan, G., X. Tang, S. Hsu, and T. Awe. Bounce-free spherical hydrodynamic implosion. 2011. Physics of Plasmas. 18 (12): 120702.

Kagan, G., and X. Tang. Electro-diffusion in a plasma with two ion species. 2012. Physics of Plasmas. 19 (8): 082709.

Kagan, G., and X. Z. Tang. Comment on "Plasma Adiabatic Lapse Rate". 2012. Physical Review Letters. 109: 269501.

Kagan, G., and X. Z. Tang. Thermo-diffusion in inertially confined plasmas. Physical Review Letters.

McDevitt, C., X. Z. Tang, Z. Guo, and H. L. Berk. A comparative study of tail ion distribution with reduced Fokker-Planck models. Physics of Plasmas.

Srinivasan, B., and X. Z. Tang. The mitigating effect of magnetic fields on Rayleigh-Taylor unstable inertial confinement fusion plasmas. 2013. PHYSICS OF PLASMAS. 20 (5): -.

Tang, X. Z., C. McDevitt, Z. Guo, and H. L. Berk. Fusion yield recovery by escaping hot-spot fast ions in the neighboring fuel layer. Physical Review Letters.

Tang, X. Z., H. L. Berk, Z. Guo, and H. L. Berk. Reduced Fokker-Planck models for fast particle distribution across a transition layer of disparate plasma temperature. Physics of Plasmas.

Tang, X. Z., Z. Guo, G. Kagan, C. McDevitt, and B. Srinivasan. Plasma effects on thermonuclear yield rate in the presence of hydrodynamic mix. Journal of Physics: Conference Series.

Co-Evolution of Protoplanets and Transitional Protoplanetary Disks: Pathway to Giant Exoplanet Formation

Hui Li
20120399ER

Introduction

The past 15 years have witnessed the astonishing discoveries of 40 exoplanets and they have stimulated an explosive growth in studying the basic processes that regulate the planet formation (e.g., Papaloizou & Terquem 2006; Lubow & Ida 2010). Giant planets (e.g., ?Jupiter mass) are believed to form farther out in protoplanetary disks where there is enough gas and dust for theirformation. An equally dramatic discovery is that some protoplanetary disks show large (tens of astronomical unit) gaps and holes that are believed to be caused by the forming giant planets (e.g., Williams & Cieza 2011). The study of the co-evolution of protoplanets and their nascent disks is believed to hold the key to understanding the planet formation. The primary objectives of this project are two-fold. First, how do the forming giant planets create gaps and holesin transitional protoplanetary disks that are consistent with observations? And second,what are the key physical processes that govern the gas accretion through the circumplanetary disk around the giant planet that leads to planet formation? The proposed work is computationally intensive and it builds upon the unique strength at LANL where we have developed advanced disk+planet simulation tools. With the adaptive mesh refinement capability especially, we will be able to simultaneously capture the global protoplanetary disk dynamics together with resolving the accretion through a much smaller circumplanetary disk around the planet. Utilizing LANL's advanced capabilities in theory and computing, we expect that the proposed research will enable us to make a critical impact now, especially when a new era is anticipated with the advent of ALMA and EVLA observations with unprecedented sensitivity and spatial resolution.

Benefit to National Security Missions

Understanding the formation of exoplanets is one of the grandest challenges for the coming decade in astronomy and astrophysics, as evidenced by the recent Decadal Survey (Astro2010): "New Worlds, New Horizons in Astronomy and Astrophysics"("New Worlds" refers specifically to exoplanet research). The critical physics that underpins this field include high Reynolds number turbulence and shear flow instabilities,all of which match with LANL's strength, both in theory and large-scale computing. With the advent of ALMA and EVLA, LANL can make a critical impact now, building on our existing expertise in disk+planet computational studies.

Progress

We have developed and implemented a new bi-fluid model for dusty protoplanetary disks for both our 2D and 3D codes. The dust particles are treated as a pressureless fluid and evolved according to the hydrodynamic equations. The coupling between the gas and dust in a disk is through the drag force, which causes the dust particles to drift inward in the radial direction. We have performed extensive tests of our model and code using the theoretical results in the literature and our numerical results are in good agreement with the theoretical prediction.

In addition, we have implemented dust diffusion due to the turbulent motion of the gas in a disk. We have modified the dynamic equations of the dust so that they are consistent with the dust diffusion. This procedure removes the possible instability caused by the dust diffusion. We have performed simulations to study the dust settling in the vertical direction of 3D disk due to the dust diffusion and obtained similar results to the theoretical prediction.

We have performed many simulations to study the asymmetric dust distribution observed by ALMA and other telescopes. In particular, we have studied how the banana-shaped dust distribution can be formed via the interaction among dust, gas, and the planet. We have found the Rossby wave instability (RWI) is a robust mechanism to form banana-shaped gas blobs in a disk. Furthermore, we have investigated two mechanisms

to generate the RWI. Both of them require relatively low viscosity. One mechanism is using large planets to induce the RWI around the planet. We use Saturn-, Jupiter-, and two-Jupiter-mass planet in our simulations. In 2D simulations, we clearly see the banana-shaped distribution of the gas and dust. The banana-shaped density blob can be maintained for hundreds of orbits. In 3D simulations, however, we find that the evolution of RWI and banana-shaped density blobs are short-lived and quickly become ring-shaped distribution.

We have performed simulations to study the RWI in a disk without planets. The RWI can be produced with an initial density bump. We study how the vortices are generated via RWI and how they are merged and combined into one big vortex. We also study the RWI dependence on the disk self-gravity. The RWI caused by the initial density bump is short-lived and quickly disappear due to migration or diffusion. To have a long-lived RWI vortex, we set up a disk with non-uniform disk viscosity, where a region of disk has very low viscosity, similar to the dead-zone configuration. Even without initial density bump, the non-uniform viscosity can produce a density bump near the low viscosity region in a few hundreds of orbits. With small perturbation, the RWI can be produced and vortices can be generated. We can see the banana-shaped density distribution generated and maintained for a long time.

These studies are helping us to make direct comparisons between our simulations and the new observations. This allows us to constrain the disk properties and provides more detailed understanding on how the planet + disk interactions evolve in a dusty protoplanetary disks.

Future Work

We will continue the development of our new 3-D hydrodynamic code, now including the both the gas and dust dynamics. Modeling the dust evolution is a new feature of this code and it will allow us to make more direct comparisons with observations.

We will collaborate with other teams to model the radiation intensity and spectra from dusty protoplanetary disks, esp. those from ALMA and other infrared telescopes.

We will investigate how the non-axisymmetric features can be produced by various

disk properties and/or from disk+planet interactions.

Conclusion

Understanding the origin of exoplanets is an exciting new frontier in astronomy and astrophysics. It will have profound impact on understanding the formation process of solar system. New observations by the new generation of astronomical observatories will enable us to constrain current models or lead us to new scenarios of planet-disk interaction with unprecedented sensitivity. Applying the state-of-the-art theory and simulation techniques developed at LANL, we will be able to make a timely impact in this important, thriving field.

Publications

Aluie, H., Shengtai Li, and Hui Li. Conservative Cascade of Kinetic Energy in Compressible Turbulence. 2012. Astrophysical Journal, Letters. 751 (2): L29 (6 pp.).

Collins, D., A. Kritsuk, P. Padoan, H. Li, H. Xu, S. Ustyugov, and M. Norman. THE TWO STATES OF STAR-FORMING CLOUDS. 2012. ASTROPHYSICAL JOURNAL. 750 (1): 13.

Johnson, J. L., and H. Li. Constraints on planet formation via gravitational instability across cosmic time. 2013. Monthly Notices of Royal Astronomical Society. 431: 972.

Johnson, J., and H. Li. THE FIRST PLANETS: THE CRITICAL METALLICITY FOR PLANET FORMATION. 2012. ASTROPHYSICAL JOURNAL. 751 (2): 81.

Li, H., and S. Li. 3D Simulations of Type-I Migration in Nearly Laminar Disks. 2013. European Physical Journal. 46: 05003.

A Computationally Efficient Model for Warm Dense Mixtures

Didier Saumon
20130244ER

Introduction

This research will create the theoretical and computational framework to model mixtures of two (or more) materials in the "warm dense matter" regime. This will be a new, state-of-the-art capability to model extreme states of matter that will support future experiments at high-energy-density-physics facilities (e.g., the National Ignition Facility) and numerous fundamental and programmatic applications involving the hydrodynamics of dense plasma mixtures.

Warm dense matter (WDM) conditions typically occur at temperatures of 5000 to 10,000,000 degrees and densities from a tenth to fifty times normal solid densities. WDM is too hot to be treated by the standard methods of condensed-matter and liquid-state physics, but too cool to be modeled as a weakly coupled plasma; it is too dense to be treated as an ionized gas, but not dense enough to approach simplifying asymptotic limits. It lies in an intermediate region where all the physics matters and simplifying approximations are elusive. It is a frontier of high energy density physics of great practical importance.

WDM mixtures lie at the heart of unsolved problems in planetary science and stellar astrophysics. Examples include the phase behavior of hydrogen and helium in Jupiter and Saturn and gravitational stratification of elements in white dwarf stars. WDM mixtures also occur during the implosion phase of inertial confinement fusion capsules and in nuclear explosions.

Our proposed work lies at the forefront of this exciting and rapidly growing field. While large-scale simulations, such as quantum molecular dynamics, are currently the favored approach to study WDM, they are computationally very expensive – requiring hundreds or thousands of computing hours for a single result. By contrast, our model, based on a modern variant of the "quantum hypernetted chain" theory, holds the promise of being a hundred to a thousand times faster, comparably accurate, and tractable for mixtures.

Benefit to National Security Missions

NASA: The primary applications thrust of our research is astrophysical – with an initial focus on examining hydrogen and helium phase behavior in Jupiter and Saturn, and understanding heavy-element diffusion in DZ white dwarf stars. In a broader sense, this research will create a robust capability for scientists to develop accurate equations of state and transport coefficients for wide varieties of astrophysical phenomena.

Understanding of Materials: Warm dense matter is a frontier of materials physics. Because it describes a region of temperature and density space devoid of simplifying approximations, all of the physics matters. It is also a region difficult to probe experimentally. The capability to model mixtures in this regime will advance our basic knowledge of materials behavior in extremes.

MaRIE: One of the objectives of MaRIE is to probe experimentally the same regions of temperature and density that we are describing theoretically, so the two programs are wonderfully complementary. Our theoretical model could be used to design and guide MaRIE experiments, and the experimental results could be used to validate and improve our model.

NNSA/DP & Nuclear Weapons: During a nuclear explosion, and in inertial confinement fusion, mixtures of warm dense matter can be created. This research potentially enhances our capability of modeling materials as they pass though this regime.

NNSA/Non-proliferation: The ability to make accurate equations of state for a wide variety of warm, dense, mixed materials lends itself to better anticipating and ameliorating the effects of rogue WMDs.

Progress

In the eight months since the start of this project, we accomplished the following:

Task one is complete. We formulated the multiple-component mixture theory by expanding that of our single-component microscopic model. We arrived at a simpler form than we originally anticipated. This set of equations is not only valid for binary mixtures but is readily extended to mixtures of an arbitrary number of (classical) ionic species and (quantum mechanical) electrons.

This mathematical formalism has been implemented in a computer code that solves the system of non-linear, coupled equations for mixtures. Substantial progress has been achieved as our success in Task #1 led to writing a computer code for a mixture of any number of elements (not just two). This code has excellent convergence properties and we have demonstrated its ability to solve the system of equations for ternary mixtures. Thus, we have already overcome one of the main technical difficulties in Year 1. Our proposed incremental numerical approach is no longer necessary as we now have a numerical capability that we did not expect to develop until year 3.

We have initiated the validation of the results for mixtures of carbon and hydrogen ("plastic") against published quantum molecular dynamics computer simulations based on a more fundamental theory but computationally very costly. Initial results are encouraging and show good agreement at high densities (>7 g/cm3) and high temperatures (>80000K).

Task two is nearly completed. In a very significant way we have surpassed our original goal for Year 1.

Furthermore, two new ideas developed under our equation of state and plasma physics projects have flowed into our LDRD work. The microscopic model for the electronic structure of the plasma ions, the electronic screening, and the fluid structure of the plasma is no longer the quantum hypernetted-chain (QHNC) model (our initial proposed approach), but an original and important variation that has proved far superior for modeling warm dense matter of one-component systems. This improves the fidelity of the microscopic physics of our mixture model.

We have also developed a new formulation of transport theory valid for weak to moderately strong interacting systems that allows very fast calculation of diffusion coefficients. This will result in a significant economy of computer time by limiting the need for expensive molecular dynamics computer simulations to the cases where the interactions are very strong. We anticipate a much higher output of results for our first application.

We are on track to achieve our science goals for FY13 and have made headway in

solving problems that we had originally planned to address in Years 2 and 3.

Future Work

Building on our accomplishments during Year 1, we will address the following tasks in year 2:

1. Complete the calculation (started in year 1) of a table of diffusion coefficients of relevance to white dwarf stars with helium-rich outer layers with traces of heavier elements (the so-called DZ stars). We will first look at the diffusion of silicon in helium. If such a table can be generated in a reasonable amount of time, we will also study the diffusion of carbon in helium. The diffusion coefficients will be calculated with our new theory for the calculation of diffusion coefficients, complemented with classical Molecular Dynamics simulations.

2. Formulate the thermodynamics (pressure, internal energy, entropy, etc) of mixtures within our model to develop the capability to compute equations of state of binary mixtures directly.

3. Write / test / validate a computer code to calculate the thermodynamics of mixtures based on the results of task #2.

4. After the completion of task #3, we will turn to applications: a) Calculation of an equation of state table for C/He mixtures in white dwarf stars; b) Calculation of the diffusion coefficients in H/He mixtures in giant planets such as Jupiter and Saturn. This application will push our model in a new physical regime where we do not know how well (or how poorly) it will perform.

5. We anticipate the publication of the work completed during year 1 in peer-reviewed journals. A first publication will describe our model for mixtures and a second will present the results of the calculation of diffusion coefficients in DZ white dwarf stars.

Conclusion

The primary result will be a robust capability to calculate the equation of state and transport coefficients of warm dense mixtures using a single, unified approach with no adjustable parameters. We will develop the theoretical framework, implement the model in codes, validate the model through comparisons with experimental data and quantum molecular dynamics simulations, apply the model

to study high-impact astrophysical problems related to planetary luminosity and white-dwarf stars, and advance the model to the point where it can be broadly used to generate a variety of equations of state for mixtures relevant to astrophysical, fusion, and national security research.

A New Hypothesis to Explain the Variability of the Outer Radiation Belt: Can we Predict Post-storm Fluxes of Energetic Electrons Based only on Pre-storm Fluxes of the Lower-energy Population?

Gregory S. Cunningham
20130297ER

Introduction

The primary goal of the proposed work is to test the hypothesis that flux levels of mega-electronvolt (MeV) electrons in the outer belt can be predicted on an event-by-event basis solely as a consequence of electromagnetic waves accelerating low-energy particles that are convected in from the outer magnetosphere. In order to conduct a test of this hypothesis, we need a category of events for which fluxes of MeV electrons in the outer belt are highly depleted so that we can predict their buildup over time due to acceleration of a low-energy source population. We have identified High-Speed Streams (HSS) as meeting this need. Assuming we have an initially-depleted state of the MeV electron population in the outer belt, we must be able to predict the time-evolving distribution of low-energy electrons convected into the outer belt, since the low-energy electrons are the source that will be accelerated to higher energies through diffusion. The Ring-Current Atmosphere interactions (RAM) code will be used for this purpose, first for HSS events and then for geomagnetic storms. It must be demonstrated that RAM is predictive for HSS events, since RAM has been primarily applied to storms. Finally, given the time-dependent population of low-energy electrons, which acts as a boundary condition for the 3D diffusion code, we must be able to predict event-specific distributions of the amplitude of the electromagnetic waves responsible for diffusing the low-energy particles up to higher energy. We will build an event-specific empirical wave amplitude database using data from the soon-to-be-launched Radiation Belt Storm Probes (RBSP) mission that will, in its own right, result in considerable utility to the magnetospheric science community.

Benefit to National Security Missions

This project will test the hypothesis that fluxes of outer belt energetic electrons after geomagnetic events can be predicted from knowledge of the low-energy source population prior to the event and electromagnetic wave distributions during the event. In order to test the hypothesis, we will create a new modeling capability that couples a low-energy code that predicts the source population to a code that predicts the evolution of the high-energy fluxes. Such a capability, though highly desirable, does not exist in the magnetospheric science community, making it nationally competitive. The hypothesis, if proved true, will enable forecasting of space hazards due to energetic electrons in the outer radiation belt hours to days in advance. Such a capability would directly impact NASA's goal to improve our understanding of how the sun impacts the environment in which satellites operate, e.g. the 'Living With a Star' program. The DOD, specifically the Air Force Weather Agency, is tasked with alerting owners of national security assets in space of impending hazards, and so DOD will directly benefit. NOAA, specifically the Space Weather Prediction Center, is tasked with alerting owners of commercial space-based assets of impending hazards in space, and so it will also directly benefit. Finally, the DOE builds satellite instrumentation that is hosted on satellites owned and/or operated by the DOD and Intelligence Community. The owners/operators of these satellites rely on predictions from AFWA/SWPC, and hence will also benefit from such a capability .

Progress

The 3D diffusion code has been extended to permit the use of time-varying boundary conditions using in-situ data from the Combined Release and Radiation Effects Satellite (CRRES) or an initial condition from the Van Allen Probes (formerly called the Radiation Belt Storm Probes. or RBSP) mission. The model uses a wave amplitude database conditioned on geomagnetic activity that was constructed prior to the start of the LDRD project. The prediction efficiency of the model was quantified during a training interval specified by the Radiation Belts and Waves (RBW) focus group of the National Science Foundation's Geospace Environment Modeling (NSF-GEM) program. The sensitivity of the prediction

efficiency to various model parameters, including radial diffusion coefficient, location of the boundary condition, and amplitude of the waves inside the plasmasphere, were all computed in an effort to tune the model to perform as well as possible during the challenge interval also specified by the RBW focus group. The performance of the tuned model was then computed for the challenge interval. The results from this study were submitted to the Journal of Geophysical Research In May 2013, and are under review. The results will also be presented at the NSF-GEM RBW focus group meeting in June 2013 and compared to the performance of other models.

The need for an outer boundary condition in the 3D model was removed by implementing a time-varying magnetopause location that depends on solar wind driving. For particles outside the magnetopause, the lifetime is computed as a fraction of their drift period around earth, which is energy-dependent (lower energies have a longer lifetime). Eliminating the boundary condition in the 3D model means that a source for new particles must be incorporated into the model. This source will come from a low-energy boundary condition from the Ring-current Atmosphere Model (RAM) or from data. We have received an example output of the RAM code from Vania Jordanova and are working to include it as a low-energy boundary condition in our 3D diffusion code. We will also be working this summer to include data from the Van Allen Probes and/or the Time History of Events and Macroscale Interactions during Substorms (THEMIS) mission as a low-energy boundary condition. Our goal is to present this work at the American Geophysical Union meeting in December 2013 and prepare articles for inclusion in a special issue of Geophysical Research Letters on early innovative results from the Van Allen Probes.

Finally, a new approach to constructing event-specific wave models for chorus has been investigated. The basic idea behind this approach is to observe the precipitation of mid-energy electrons whose anisotropic pitch-angle distributions are unstable to the growth of chorus waves. When the wave amplitudes are high, then precipitation fluxes will also be high, and so one can infer the wave amplitudes from observations of the precipitation fluxes, which are monitored by a relatively dense network of low-earth orbiting satellites (the National Oceanic and Atmospheric Administration's Polar-Orbiting Earth Satellite, or NOAA POES). The NOAA POES satellites provide excellent coverage in magnetic local time (MLT) and adequate temporal resolution (due to their 90-minute orbit). The idea is to use POES observations from specific events to estimate the wave amplitudes for those events rather than relying on databases that are binned by magnetic activity as we are currently doing. Because the NOAA POES satellites offer excellent coverage in MLT and good time resolution, we do not have to construct spatiotemporal correlations of the waves in order to produce global maps of wave intensity using point observations from the Van Allen Probes. This work is in the process of being written up and will be submitted to Geophysical Research Letters.

Future Work

Quantify spatiotemporal correlations in the waves using RBSP data and use them to compute uncertainties on diffusion coefficients.

Run the modified diffusion code for HSS events using RAM output as boundary condition.

Predict event-specific energization of MeV electrons, and compute prediction efficiencies by comparing to data.

Incorporate a substorm injection model to capture the transport of low-energy electrons into the inner magnetosphere during substorms.

Conclusion

We expect to prove, or disprove, the hypothesis that it is the variability of the low-energy electron source population which, when combined with geomagnetic event-specific wave distributions, is responsible for the variability of post-event high-energy electron fluxes. If proven true, this hypothesis will lay the foundation for predicting post-event high-energy electron fluxes hours to days in advance, an important capability for protecting space-based assets. If proven false, intermediate objectives like producing an event-specific empirical wave database and coupling a low-energy Ring-Current Atmosphere interactions code to a high-energy 3D diffusion code will be of value to the scientific community.

Publications

Chen, Y., G. Reeves, R. Friedel, and G. S. Cunningham. Remote sensing whistler-mode waves from low-Earth-orbit electron observations: Statistical and case study results. To appear in Geophysical Research Letters.

Tu, W., G. S. Cunningham, Y. Chen, M. G. Henderson, E. Camporeale, and G. D. Reeves. Modeling radiation belt electron dynamics during GEM challenge intervals with the DREAM3D diffusion model. To appear in Journal of Geophysical Research-Space Physics.

A New Approach to Multiscale Plasma Physics Simulations

Gian L. Delzanno
20130334ER

Introduction

Plasmas are characterized by a wide range of spatial and temporal scales, and pose a formidable challenge to the numerical modeling and to our ability to perform predictive simulations. This project focuses on a new method that promises to solve some longstanding issues in computational plasma physics and, in particular, of Particle-In-Cell (PIC) approaches (which are commonly used to model microscopic plasma phenomena). Ours is essentially a spectral approach, where the distribution function in velocity space is not handled by superparticles as in PIC, but by an expansion in a suitable basis. The method is then cast as a series of partial differential equations for the coefficients of the expansion. First, our preliminary results indicate that this approach can achieve machine precision accuracy with a relatively low number of basis functions and at a small fraction of the computational cost incurred to obtain a (much less accurate) solution with a PIC code. Second, since the low order terms of the expansion correspond to the typical macroscopic moments (density, mean velocity and energy), the microscopic/macroscopic coupling critical to multiscale plasma physics is naturally built-in. We have successfully demonstrated on a test case that we could use very few basis functions in certain regions of the computational domain (where the plasma behaves as a macroscopic fluid) while retaining many more basis functions in other areas (where the microscopic details of the plasma are important). Third, the algorithm can make effective use of emerging architectures, such as GPUs, for the optimization of the basis functions. The goal of this project is to develop the spectral capability just described for general multiscale plasma physics problems. As a case study, we target an application relevant to space weather, an important area for LANL mission in threat reduction and global security.

Benefit to National Security Missions

The capability focus of this project could be a game-changer in the field of computational multiscale plasma physics since (1) the problematic coupling of macroscopic and microscopic scales needed in many problems of interest is naturally handled by the method and (2) it offers the possibility for much more accurate results at a fraction of the computational cost obtained by conventional approaches. As such, any application where plasmas are important will benefit from this capability. It is immediately relevant to the DOE/NNSA nuclear weapons mission, but it also includes agencies such as DOE (office of science), NASA (space science) and DOC (NIST and NOAA). It will also impact many areas of LANL mission, including nuclear weapons, energy security and global security/space situational awareness.

Progress

In the first eight months of this project, we have developed a code to study the evolution of a collisionless plasma in the electrostatic limit, based on an expansion in Hermite polynomials.

We formulated a second order accurate, semi-implicit time discretization, where some of the operators are treated with an explicit time discretization and the others are treated with an implicit time discretization. The semi-implicit code conserves the total mass and momentum (but not energy) of the system exactly. The advantage of a semi-implicit method relative to a conventional fully explicit method is that it features a much larger stability domain at the same computational cost. In the examples considered we have proved that the largest time step in the explicit method is at least 400 times smaller than the time step that can be used in the semi-implicit method.

We compared the semi-implicit method against explicit PIC simulations for standard test problems (plasma waves, Landau damping, two-stream instability, ion acoustic wave) and found that the Hermite code is a couple of orders of magnitude more accurate and faster. On a Landau damping study, the Hermite code results

to be about 180 times more accurate than the PIC code, and 14 times faster. A manuscript is in preparation on the results of 1) and 2).

We developed a fully implicit formulation for the Hermite code. By using an implicit second order accurate Crank-Nicholson time discretization and a spectral (Fourier) spatial discretization, we have proved that the resulting numerical model conserves the total mass, momentum and energy of the system exactly. This is a major result considering that PIC algorithms that conserve mass, momentum and energy exactly do not exist. Exact conservation properties, however, are related to the choice of the temporal and spatial discretization and we are now trying to extend it to other popular discretizations schemes like finite differences or h-p finite elements. Another important advantage of the implicit formulation is that the stability domain of the method further increases relative to the semi-implicit case discussed above.

We developed an energy-conserving Hermite code based on the implicit formulation. At each time step the resulting nonlinear equations are solved with an unpreconditioned Jacobian Free Newton-Krylov solver. We have successfully applied the implicit Hermite code to the same test cases described in 2). A comparison with a recently developed implicit PIC code [Markidis and Lapenta, Journal of Computational Physics 2010] is underway. A manuscript is in preparation on the results of 3) and 4).

We developed a C++ project, called Space Weather Simulation Framework (SWSF), that has support for launching and controlling processes across multiple OpenCL (CPUs or GPUs) devices. Additionally, SWSF provides low-level data structures for representing fields on structured or unstructured meshes using a general mesh specification file. We have also developed a C++ design pattern that allows asynchronous task launch to a user-defined “event” handler. This feature is necessary for us to schedule the update of the basic solver concurrently with the solution of the optimization parameters. As part of this design pattern, we have also added an integrated communication manager that utilizes MPI to allow the high-level parallelization of various solver events. This model allows serial execution for our early development plan, but also supports the full distributed-memory parallelization needed that we aim for. Finally, in order to support flexible problem definition, SWSF utilizes an XML input format that allows parameter specification using several basic types. This approach will allow us to adapt our input deck format to support new solver features and characteristics as they become relevant.

While we have established the strength of the method in terms of accuracy and computational efficiency on examples that test the disparity of scales typically associated with plasmas, we are focusing on other examples where the plasma behaves macroscopically (requiring a low number of polynoms) in some parts of the domain, whereas it requires microscopic physics (high number of polynoms) elsewhere. We are exploring techniques to handle the microscopic/macroscopic coupling by adapting the local number of polynoms automatically (instead of in a predefined way) to increase the robustness of the code.

Future Work

The proposed work will continue to build on the working version of the Hermite spectral capability that we developed.

- We will continue the extension of the code from one to two dimensions, in order to apply it to more complex problems. This is a milestone for the project.
- We will begin the extension to the electromagnetic case.
- We will explore preconditioning techniques for the linear iterations of the Newton-Krylov solver to speed-up the convergence of the method.
- We will exploit the CPU/GPU infrastructure that we have built to study the choice of the optimal base for the Hermite expansion. This technique relies on the assumption that the plasma does not change much during few time steps of the simulation so that the optimization can be performed asynchronously. Therefore we will quantify the level of asynchronism that can be exploited, the code speed-up and the accuracy of the resulting technique. This is another milestone for the project.
- The code will be verified against standard test cases. We will also continue benchmarking against PIC codes since our metric for success is to prove that our new technique can be much more accurate and faster than PIC, which is the community standard.

Conclusion

This project will deliver an electromagnetic, parallelized code that models a collisionless magnetized plasma. The code will be compared against available PIC codes (the dominant method in the community) and our metric for success will be based on the comparison in terms of accuracy, efficiency and code speed-up. We expect that our tool will outperform PIC codes, as our preliminary results indicate. If we can indeed confirm the huge savings factors of our approach relative to PIC, it will be a breakthrough

in computational plasma physics that can impact many plasma applications, such as space weather or magnetic fusion energy.

Publications

Camporeale, E., G. L. Delzanno, B. Bergen, and J. D. Moulton. Fourier-Hermite spectral method for the Vlasov equation. Presented at 55th Annual Meeting of the APS Division of Plasma Physics. (Denver, 11-15 Nov 2013).

Camporeale, E., G. L. Delzanno, B. Bergen, and J. D. Moulton. On the velocity space discretization for the Vlasov-Poisson system: comparison between Hermite spectral and Particle-in-Cell methods. Part 1: semi-implicit scheme. 2013. To be submitted to Journal of Computational Physics.

Camporeale, E., G. L. Delzanno, B. Bergen, and J. D. Moulton. On the velocity space discretization for the Vlasov-Poisson system: comparison between Hermite spectral and Particle-in-Cell methods. Part 2: fully-implicit scheme. 2013. To be submitted to Journal of Computational Physics.

Delzanno, G. L., E. Camporeale, B. Bergen, and J. D. Moulton. Fully-implicit Fourier-Hermite spectral method for the Vlasov equation. Presented at Vlasovia 2013. (Nancy, France, 25-28 Nov 2013).

Enhancing Thermoelectric Properties of Topological Insulators through Nanostructuring

Nikolai Sinitsyn
20130348ER

Introduction

This project is motivated by the recent discovery of new materials, called Topological Insulators (TI) which demonstrate a new state of electrons that is topologically distinct from the conventional band insulators or metals. One of the manifestations of the topological properties is appearance of conducting electron states, on the surface of material, which propagate throughout the sample without elastic scatterings. Our idea is that nanostructuring of TIs can substantially increase the role of these states in charge and thermal transport to the level of obtaining a device structure with record high thermoelectric characteristics.

Benefit to National Security Missions

Major applications of thermoelectrics is to (i) create efficient silent and compact solid state refrigerators, that one day will replace noisy and spacious spinning components of home fridges. (ii) various technologies to recover heat energy, e.g. from car engines and microprocessors and convert it back to useful electricity.

(i) and (ii) correspond to DOE goals. Climate impact is positive because substances used in modern refrigerators are harmful for atmosphere, e.g. they destroy the ozone layer. Replacing them by thermoelectric cooling will solve the problem.

(iii) NASA application is due to new energy sources for satellites that can be built from thermoelectrics.

Progress

By collaborating with Prof. Shixiong Zhang of Indiana Univerity, we have successfully synthesized nanowires/nanoribbons of Telluride-based topological insulators such as Bi2Te3 and Ag2Te. We have utilized thermal vapor transport method to fabricate nanowires and nano ribbons of diameter: 50~300 nm and width 500nm respectively. A student of Prof. Zhang, Enzhi Xu will visit CINT (both LANL gate way and Sandia Core facility) to perform device fabrication and characterization of Te based nanowires under the guidance of Han Htoon and Jennifer Hollingsworth.

As a complementary approach to the top-down synthesis methods provided to the project by our collaborators, we are also pursuing novel solution-phase syntheses for Bi2Te3 nanoparticles. The colloidal methods afford access to ultra-confined sizes beyond the reach of the vapor-phase methods. Thus far, we have successfully replicated a literature approach for synthesizing sub-10 nm Bi2Te3 spherical nanocrystals (Scheele et al. Adv. Funct. Mater. 2009, 19, 3476–3483). This approach requires first synthesizing Bi nanoparticles that are then converted to a Bi-Te alloy and, finally, into Bi2Te3 nanocrystals. Our goal, however, is to synthesize ultra-small-diameter nanowires using the metal-catalyzed solution-liquid-solid (SLS) method. To this end, we are attempting to modify the literature synthetic method for nanocrystals to be amenable to adaptation to SLS growth. Specifically, SLS will require that Bi2Te3 is formed by direct reaction of Bi and Te molecular precursors, rather than reaction through a Bi (or Te) crystalline intermediate. We have to date performed numerous reactions between different Bi and Te molecular precursors in a range of solvents and mediated by a range of different surfactants. These have been characterized by powder x-ray diffraction (XRD) and transmission electron microscopy (TEM). While XRD shows that we are creating crystalline Bi2Te3, the morphology remains non-optimal and/or the nanoparticles are aggregating. We will continue optimization of the procedure and, once obtained, will extend growth to nanowires via SLS, which can afford sub-10 nm diameter 1-dimensional structures.

On the theoretical side, we developed a completely new approach for classification of topological phase transitions, which can be encountered in topological insulators. Such a classification is an important question that should help to identify distinct phases of new materials.

We noticed that arbitrary dissipation effects make the effective Hamiltonian of a Bloch band system non-Hermitian. We then showed that the classification of distinct phases of a non-Hermitian Hamiltonian follows almost trivially by identifying a pattern of Bloch band structure with a topologically equivalent element of the Braid group.

It has been discussed recently that topological properties of transport can be broken by the inter-band transitions, so called Zener tunneling, near the interface of topological material. Importantly, Zener tunneling in topological insulators cannot be described by a standard Landau-Zener formula. This motivated us to explore Landau-Zener transitions in more relevant to topological insulators multi-channel scatterings framework. We uncovered an unexpected phenomenon of exponentially strong suppression of Landau-Zener transition amplitudes even in the limit at which standard Zener tunneling would be strong. Results were published in Phys. Rev. Lett. A side result of this research was an application in a different field – dynamic quantum phase transition, in which we predicted unusual distribution of defects produced during multi-channel Landau-Zener scattering in Bose condensates.

Future Work

We will develop a theory of thermoelectric effects in thin films and nanowires made of TIs. This goal will require an understanding the role of disorder and quantum confinement and electron/phonon interactions on the topologically protected surface states. Our preliminary studies showed complexity of the disorder effects on transport whose understanding promises to reveal unusual properties. Complimentary experimental efforts will be focused on measurements of thermal transport in topological insulator nanowires using state of the art CINT Discovery platform. This will provide a selective probe for conflicting processes determining the figure of merit. Theoretical results will be benchmarked against experimental data and used to provide a guideline for subsequent experimental studies.

Conclusion

We will develop a theory of thermoelectric effects in thin films and nanowires made of TIs. This goal will require an understanding the role of disorder and quantum confinement on the topologically protected surface states. Developing a theory of thermoelectric effects and its application for optimizing the sample parameters to increase the figure of merit is the main theoretical goals of this project. Complimentary experimental efforts will be focused on measurements of thermal transport in topological insulator nanowires using state of the art CINT Discovery platform.

Publications

Ren, J., and N. A. Sinitsyn. Braid Group and Topological Phase Transitions in Nonequilibrium Stochastic Dynamics. 2013. Physical Review E. 87: 050101(R) .

Roslyak, O., and A. Piryatisnki. Sonoluminescence of carbon nanotubes. 2013. Unpublished Document.

Sinitsyn, N. A.. Landau-Zener Transitions in Chains. 2013. Physical Review A. 87: 032701.

Sinitsyn, N. A.. Nonadiabatic transitions in exactly solvable quantum mechanical multi-channel model: role of level curvature and counterintuitive behavior. 2013. Physical Review Letters. 110: 150603.

Giving Cold Atoms Weight: creating Heavy Fermions in Optical Lattices

Cristian D. Batista
20130385ER

Introduction

Lanthanide and actinide based compounds belong to the family of strongly correlated ma-terials. The coexistence of localized f-electrons with itinerant s, p or d electrons that interact via the so-called Kondo exchange, leads to very unusual phenomena such as exotic magnetic order-ings, unconventional superconductivity and heavy fermion behavior. One of the most intriguing phenomena is the non-Fermi liquid ("strange metal") behavior that arises near the quantum phase transition or quantum critical point (QCP) that separates the magnetically ordered and the Heavy fermion sates. This "strange metallic state" originated by the fluctuations of a QCP usually appears in the proximity of unconventional superconducting states. Unfortunately, the experimental characterization of this fascinating state of matter is limited by many factors that we discuss below. Consequently, there is a need for finding controllable realizations of this physics that can shed light on the basic properties of the strange metallic state that arises near the QCP. We will address this need by modeling a class of atomic gases known as Bose-Fermi resonant systems in an optical lattice, and identifying regimes of parameters for which the atomic system can be mapped into a lattice of local moments (localized f-electrons) that interact via ex-change with itinerant electrons. Describing and testing this non-trivial mapping requires a description that bridges the Angstrom-sized atomic physics scale with the micron-sized optical lattice physics.

Benefit to National Security Missions

We argue that the closed channel amplitude physics of the Fesh-bach resonance give access to the Kondo physics responsible for heavy fermion behavior in traditional strongly correlated materials. Narrow Feshbach resonances, which are beginning to be explored experimentally, give large closed channel amplitudes near resonance. We will describe the narrow resonance properties and we will explore the validity of the effective Hamiltonian that can be mapped onto the Kondo Lattice Hamiltonian. We will explore the phase diagram and dynamics. By guiding cold atom physics towards a first realization of heavy fermion physics, this project will establish the first one-to-one strongly correlated physics connection for cold atom physics. Moreover, our studies of the dynamics will feed back onto the heavy fermion physics and we will suggest heavy fermion experiments that can explore the boson-fermion and Kondo physics mapping. This research is very relevant for uncovering the origin of the complex properties of rare lanthanide and actinide based materials which are relevant for the nuclear energy security mission.

Progress

In the cold atom toolkit, Feshbach resonances have played a unique role in boosting the cold atom capability of simulating quantum many-body physics: no other quantum many-body system has had a knob available to tune the particle-particle interactions at will. Recently, the increased control and accuracy of external magnetic fields has opened up a new class of Feshbach resonances: narrow Feshbach resonances, width that is typically less than 10 mG (10 milliGauss). While these resonances are more difficult to control experimentally, these resonant interactions also open up new avenues. The effective range of the narrow resonant binary atom interactions can be comparable to or exceed the average inter-particle distance, the closed channel amplitude dominates the coupled channel interaction physics and the energy dependence of the scattering physics can select a slice of phase space that is much less than the many-body-relevant phase space volume. These aspects directly affect the physics of atoms in an optical lattice and may allow the simulation of Heavy-fermion like Kondo physics, the topic of this project.

On the atomic side of the project, we have accomplished the following steps in our investigations: (i) We have derived the energy-dependent binary atom scattering length for narrow resonances and we have shown that

its energy scaling depends on only three parameters. We have shown that it is the slowness of the interaction that characterizes the narrow resonant interactions. (ii) We have solved the problem of two harmonically confined atoms near a narrow Feshbach resonance (providing a model of the on-site interactions in an optical lattice). (iii) We have derived the fraction of the collision time that the interacting atoms spend in the closed channel state. As this fraction is sensitive to the energy of the collision complex and as the closed channel state is unstable with respect to three-body loss processes, narrow Feshbach resonances can select the energy of atoms that are preferentially removed, introducing a new method for magnetic field steered evaporative cooling or heating. (iv) We have tested the exact eigenstates of the harmonically confined binary atom system against a two-state model and we found that the two-state model, which is at the heart of the Kondo-Hamiltonian, describes the harmonically confined narrow resonance well near resonance if the frequency of the width is comparable to or less than the trapping frequency.

We are in the process of writing up these results. We have also wrote a Density Matrix renormalization group code for simulating the Kondo Lattice model. We are currently analyzing the results for different types of correlation functions.

Future Work

- Develop the Density Matrix Renormalization Group codes for the Kondo Lattice Model described in our project.
- Derive the Kondo Lattice model from first principles in the context of atomic gases and express the Hamiltonian parameters, t, ε, and g as a function of more fundamental parameters of the atomic gas.
- Explore closed channel amplitude in narrow Feshbach resonance interactions in scat-tering and in on-site interactions. Test validity of effective g/ε model interactions in predicting static properties.
- Explore tuning options of effective model.

Conclusion

The successful accomplishment of this project will guide the realization of heavy fermion phases with atomic gases near Feshbach resonances. This extraordinary achievement will open an intriguing new avenue: controlled experimental explorations of the critical regime near the fermionic quantum critical point that separates the magnetically ordered state from the heavy fermion phase. This breakthrough would have a profound impact on our understanding of actinide and lanthanide based compounds that are of strategic relevance to LANL's mission.

Publications

Rahmani, A., T. Kitagawa, E. Demler, and C. Chamon. Cooling through optimal control of quantum evolution. 2013. PHYSICAL REVIEW A. 87 (4): -.

Topology in Superposition: Quantum Decoherence in Many-body Systems

Wojciech H. Zurek
20130409ER

Introduction

We will investigate decoherence of quantum systems in realistic models, where the environment causing decoherence is a many-body system (i.e., a system composed of interacting subsystems). In particular, we shall study decoherence caused by environments driven through a critical point of a quantum phase transition.

We will also study superpositions of collective states of many-body systems. Both spin and field theoretic models of phase transitions exhibit stable topological defects (monopoles, vortex lines, domain walls, etc.) as well as non-topological but relatively stable configurations such as solitons. These objects are the epitome of locality. Yet, the underlying many-body system is quantum and, thus, abides by the quantum principle of superposition. Therefore, it should be possible to construct superpositions where a topological defect is in a non-local "Schrödinger cat" state, with a vortex or soliton simultaneously in two places. Such situations are difficult to even imagine or represent in terms of effective, mean-field "order parameter" theories. However, there are solvable models that should allow us to study how manifestations of non-locality and other explicitly quantum behaviors (present at the microscopic level) get eliminated from collective many-body states on the macroscopic level.

All along we will explore possibilities of experimental testing of our predictions in cold atom and condensed matter systems with an eye towards applications in materials science and metrology.

Benefit to National Security Missions

This research will contribute to condensed matter science at Los Alamos, providing critical insights into quantum technological applications. These are diverse, including superconductors, metrology, etc. Computing may be most significant and urgent. There is the dream of quantum information processing, but even if it turns out to be more distant than some hope, the fundamental elements of computers will reach single atom size this decade ("Moore's law"). Understanding what happens to superpositions of collective degrees of freedom and of relevant sources of decoherence is indispensable in these (and similar) applications of interest to LANL. Moreover, quantum superpositions in cold atom systems that we plan to study can be used to enhance sensitivity of measuring devices. Capabilities foreseen for MaRIE seem well suited for condensed matter studies related to this project (dynamics of phase transitions).

Progress

In the past year, we have proceeded towards the goal of understanding decoherence on several fronts:

We have studied conditions that allow a quantum state of a macroscopic system to produce many imprints (e.g., on its environment; this is the main process behind decoherence). The question is technically challenging, as macroscopic systems are generally in mixed states, and interact with other systems. We have established that – even in such circumstances – the condition for the states of the system to be reproducible (i.e., to act as viable "originals" for copies) they must be distinguishable. (Technical requirement for this is that they must have support in distinct – orthogonal – subspaces of the Hilbert space.) A paper that describes this result has been just published in Physical Review A.

We have also studied production of multiple (even if imperfect) copies is central to realistic models of decoherence (that extend the original idea of a monolithic environment to a collection of its natural subsystems – e.g., photons in a photon environment). This leads to the so-called "quantum Darwinism". With Michael Zwolak, Zurek has studied the nature of such an information flow between the system and the environment. The conclusion is that in this case the environment acts as a communication channel – a quantum communication channel that transmits multiple copies of the (effectively

classical) information about the preferred basis that is singled out by decoherence. This analogy is reflected in the appearance of the Holevo quantity (that bounds the capacity of quantum channels to transmit classical information). Holevo quantity is maximized for the preferred, effectively classical states of the system. Moreover, depending on the choice of the observable of interest, classical information available from the environment fragments (given by the Holevo quantity) decreases while quantum information (quantified by the quantum discord) increases. The sum of these two – Holevo quantity plus quantum discord – turns out to be the von Neumann mutual information which is independent of the choice of the observable. This is a de facto conservation law that expresses complementarity which has profound consequences for the emergence of preferred effectively classical observables, as well as for the loss of quantumness. Our paper on this subject has been just published in Scientific Reports.

With Alexander Streltsov we were able to provide an attractive view of quantum discord while shedding a new light on quantum measurements. The motivation goes back to the forefathers of quantum theory: Niels Bohr proposed that the outcome of the measurement becomes objective and real, and, hence, classical, when its results can be communicated by classical means. In this work we revisited Bohr's postulate using quantum discord -- one of the modern tools from the quantum information theory arsenal. We find a full confirmation of Bohr's idea: if a measurement device is in a nonclassical state, the measurement results cannot be communicated perfectly by classical means. In this case some part of information in the measurement apparatus is lost in the process of communication: the amount of this lost information turns out to be the quantum discord. The information loss occurs even when the apparatus is not entangled with the system of interest. The tools presented in this work allow to generalize Bohr's postulate: we show that for pure system-apparatus states quantum communication does not provide any advantage when measurement results are communicated to more than one recipient. We further demonstrate the superiority of quantum communication to two recipients on a mixed system-apparatus state and show that this effect is fundamentally different from quantum state cloning. The paper has been just accepted in Physical Review Letters.

Last not least, we have studied appearance of topological defects in phase transitions in an ion trap. This work with Adolfo del Campo is (so far) confined to classical regime, but ion traps are perhaps the best candidate to study superpositions of topological defects that are of interest for the proposal.

Future Work

Our goals for the second year of this project include study of the dynamics of many-body systems suitable for investigation of the dynamics of phase transitions and its relation to decoherence. Bose - Hubbard model (which has a reasonable chance of experimental implementation in the not too distant future) will be amongst these studied. Study of various models with the relevance for the forthcoming experiments in Bose-Einstein condensates will be also undertaken.

Investigation of information propagation throughout the many-body environments will continue to the second year of the project. We have already made significant progress by establishing complementarity between quantum discord (measure of quantumness of correlations) and Holevo quantity (that characterizes capacity of quantum channels for classical information transfer). Moreover, we have characterized constrains imposed by repeatability of measurements on the states of macroscopic quantum systems that allow them to be read off many times and/or by many observers. This is of importance to quantum Darwinism.

The work on the Chernoff information and its relation to quantum Darwinism will be pursued.

Study of the imprinting of "histories" on the many-body environment will be the new focus of our research on quantum Darwinism. Exploration of the suitability of objects such as solitons for the the study of superpositions in Bose-Einstein condensates will be also pursued.

In the first year we have (with colleagues in Germany) published (Nature Communications, to appear) a joint paper on the formation of topological defects in "ion crystals" -- regular formations of ions that are investigated for the purpose of quantum emulation and quantum computing. While the experimental results were obtained in the regime where the ion chain was effectively classical, we shall pursue the research into the quantum regime (with the hope that experiments shall eventually follow).

Conclusion

We will characterize decoherence of topological defects in different theoretical models describing both magnetic and cold atom systems. In both cases, we will quantify how a many-body quantum environment interacting with a topological defect leads to the destruction of a coherent quantum superposition state in which a topological defect was initially prepared. This work will significantly advance fundamental understanding of the role of many-body effects in the ubiquitous decoherence process responsible for the emergence of the classical "everyday" world out of the quantum substrate.

Publications

Pyka, K., J. Keller, H. L. Partner, R. Nigmatullin, T. Burgermeister, D. M. Meier, K. Kuhlmann, A. Retzker, M. B. Plenio, W. H. Zurek, A. del Campo, and T. E. Mehlstaubler. Topological defect formation and spontaneous symmetry breaking in ion Coulomb crystals. 2013. NATURE COMMUNICATIONS. 4: -.

Riedel, C. J., W. H. Zurek, and M. Zwolak. The rise and fall of redundancy in decoherence and quantum Darwinism (vol 14, 083010, 2012). 2013. NEW JOURNAL OF PHYSICS. 15: -.

Streltsov, A., and W. H. Zurek. Quantum Discord Cannot Be Shared. 2013. PHYSICAL REVIEW LETTERS. 111 (4): -.

Tylutki, M., J. Dziarmaga, and W. H. Zurek. Dynamics of the Mott Insulator to Superfluid quantum phase transition in the truncated Wigner approximation. 2013. 21ST INTERNATIONAL LASER PHYSICS WORKSHOP. 414: -.

Zurek, W. H.. Wave-packet collapse and the core quantum postulates: Discreteness of quantum jumps from unitarity, repeatability, and actionable information. 2013. PHYSICAL REVIEW A. 87 (5): -.

Zwolak, M., and W. H. Zurek. Complementarity of quantum discord and classically accessible information. 2013. SCIENTIFIC REPORTS. 3: -.

Ultra-bright Electron Beam Acceleration in Dielectric Wake Accelerators

Evgenya I. Simakov
20130463ER

Introduction

The goal of this project is to demonstrate operation of a high-brightness Dielectric Wakefield Accelerator (DWA) with an acceleration gradient above 100 MV/m and less than 0.1% induced energy spread in the accelerated beam. We currently project the DWA concept as a performance upgrade for the future LANL signature facility MaRIE. The pre-conceptual design for MaRIE is underway at LANL, with the design of the electron linear accelerator being one of the main re-search goals. The cost of the linac is significant and the TA-53 space constraints dictate that the final energy of the electron beam for the X-ray Free-Electron Laser (XFEL) is no higher than 12 GeV. The number and the energy of photons produced by the XFEL is however strongly de-pendent on the electron beam's energy with the more energetic beam delivering more energetic photons to the user. Although generally the baseline design needs to be conservative and rely on existing technology, any future upgrade would immediately call for looking into the advanced accelerator concepts capable of boosting the electron beam energy up by a few GeV in a very short distance without degrading the beam's quality. This work has the potential to advance the DWA technology to a level that would make it suitable for MaRIE and also for a number of oth-er national security applications.

Benefit to National Security Missions

The proposed work has the potential to advance DWA technology to a level to make it suitable for a number of national security applications, including compact accelerators for warfighter support (e.g. small weaponized free-electron lasers) and active interrogation (e.g. small and in-expensive electron accelerators as compact front ends for muon active interrogation sources or alternatively to generate bremsstrahlung radiation). Additionally, this technology may be appli-cable for the future upgrades to increase the energy and luminosity of the MaRIE XFEL.

Considering the long time scale associated with the MaRIE project, this technology, if demon-strated now, may provide an approach to boost the energy of the electron beam feeding the Ma-RIE XFEL from the nominal 12 GeV up to 20.8 GeV with a very low cost upgrade. This up-grade would allow a much greater production of 126-keV photons, now at the third harmonic of 42 keV. With the current 12 GeV MaRIE linac design, generation of the third harmonic photons is suppressed in the wiggler. However, photon energy above 120 keV is required for the K-shell ionization of uranium and other actinides, an important MaRIE mission and part of its funding justification. An 8.8-GeV DWA afterburner would lead to over an order of magnitude greater production of these high energy photons.

Progress

There were two the most significant outcomes of the first year of this project. First, our team have completed the preliminary design of the Emittance Exchanger (EEX) for shaping the electron beam and started to plan for an experiment. Second, we have established all the necessary collaborations to jump start the experiments in Year 2.

We used the Elegant matrix code developed and distributed by the Argonne National Laboratory to design the electron beam optics for the EEX which would convert the Gaussian electron beam at the input into two bunches at the output: the drive bunch with a double-triangular current distribution and the witness bunch with the trapezoidal current distribution. The EEX optics consists of two dipole doglegs and a tuned pair of a deflecting cavity and a fundamental mode cavity in between. A number of quadruple magnets precedes the doglegs, and a number of sextupoles may be used in the system to compensate for non-linear effects. The role of each element in the beamline is evaluated. The non-linear beam shaping mask is designed to produce the desired current distributions out of a given Gaussian

bunch. The Gaussian bunch under consideration is the one that is being produced at ASTA user accelerating facility at Fermilab.

Our T and XCP divisions part of the team successfully conducted particle-in-cell (PIC) simulations of propagation of realistic distributions of electrons in a dielectric fibers. PIC simulations were found to be in good agreement with theory with respect to frequency, amplitudes and transformer ratio of the excited electomagnetic signal. Resolution of PIC simulations was studied and adequate resolution was found to ensure accurate results. It was confirmed that the wakefield excited by the drive beam is largely insensitive to the beam's emittance, radial profile and energy. Simulations were conducted with the two codes, MERLIN and LSP-3D, which perfectly agreed with each other.

With regards to the planned experiment, we have initiated collaborations with the Argonne National Laboratory (ANL) and the Fermilab (FNAL). We have participated in dielectric wakefield accelerations experiments, that are being conducted by the ANL and Euclid Techlab's personnel at Brookhaven National Laboratory. The Accelerator Test Facility (ATF) at BNL uses a simple dispersive dogleg to shape electron bunches before passing them through dielectric fibers. We have built several masks and installed them on the ATF beamline to observe bunch shaping. We have conducted simultaneous modeling of the ATF beamline with Elegant to understand the observed results. Bunch shaping in a dogleg has been confirmed in an experiment. We also passed a shaped electron bunch through a dielectric fiber and observed energy modulation in the drive bunch and energy change in a witness bunch.

We currently participate in a bi-weekly teleconference with ANL and FNAL, at which different research group discuss their near-term plans and experiments on dielectric wakefield acceleration. ANL is planning to put and Emittance Exchanger at their APS facility and conduct some beam shaping experiments. LANL has provided input for their design of the experiment. LANL personnel is planning to travel to the ANL and participate in the APS experiment.

LANL has shipped a 1.3 GHz deflecting cavity to FNAL to construct the EEX experiment at their ASTA beamline. ASTA user facility is coming to operation this summer. The PI is planning to travel to the first ASTA user workshop in July, 2013 to learn more about the timeline of the EEX experiment. Right now, all the experimental components for the EEX experiment are available at ASTA. Once the facility itself is operational, the assembly of the EEX beamline is going to start.

LANL is putting together a mini-workshop on dielectric wakefield accelerators for FELs in December 2013. The main goal of the workshop is to attract the attention of the DWA community towards the specific needs of LANL's MaRIE FEL.

LANL team is planning to present a poster at the International Conference on Plasma Science in June, 2013 and has submitted 3 abstracts to the US Particle Accelerator Conference in October 2013.

Future Work

In FY13 we will initiate the project and conduct the numerical and theoretical analysis of the coupled wakefield interaction (shaping both the drive bunch and the main beam). Preliminary optimized shapes will be determined. Detailed particle-in-cell (PIC) simulations of the preliminary optimized shapes and geometry will be conducted. Emittance exchanger (EEX) and mask optics will be preliminary designed and verified with PIC simulations. Once the simulations are complete, we will start ordering experimental hardware, which includes the dielectric loaded waveguide, support hardware and the mask.

Conclusion

The most important outcome of the proposed research will be the experimental demonstration of a high-brightness dielectric wakefield accelerator with an accelerating gradient well above 100 MV/m and less than 0.1% induced energy spread in the accelerated beam. It is very likely that we will be able to demonstrate the following secondary outcomes: (1) simultaneous generation of a drive bunch and main beam for the first time, (2) significant increases in a DWA transformer ratio, and (3) significant decreases in the measured energy spread from a main beam accelerated through a wakefield process.

Publications

Huang, C., T. Kwan, D. Shchegolkov, and E. Simakov. Particle-In-Cell Modeling of Dielectric Wakefield Accelerator. To appear in 2013 North American Particle Accelerator Conference. (Pasadena, CA, Sept. 29 - Oct. 4th, 2013).

Shchegolkov, D., E. Simakov, S. Antipov, M. Fedurin, and C. Swinson. Beam Pulse Shaping Experiments for Uniform High Gradient Dielectric Wakefield Acceleration. To appear in 2013th North American Particle Accelerator Conference. (Pasadena, CA, Sept.29-Oct.4th, 2013).

Shchegolkov, D., and E. Simakov. Design of an emittance exchanger for producing arbitrary shapes of the electron beam current. Physical Review Special Topics - Accelerators and Beams.

Simakov, E., C. Huang, T. Kwan, and D. Shchegolkov. Shap-

ing Electron Bunches for Ultra-bright Electron Beam Acceleration in Dielectric Loaded Waveguides. To appear in 2013 North American Particle Accelerator Conference. (Pasadena, CA, Sept. 29 – Oct. 4th, 2013).

Wide Field-of-View Plasma Spectrometer

Ruth M. Skoug
20130564ER

Introduction

Through this LDRD-ER project, we will develop and demonstrate a fundamentally new type of space plasma spectrometer (named the "2PS" Spectrometer for 2π-sr) whose field-of-view is nearly 2π-sr using fewer resources than traditional methods. The enabling component is analogous to a pinhole camera having an electrostatic energy-angle filter at the image plane. At the end of this project, we will have an optimized design and thorough understanding of the measurement concept as well as demonstration of the electrostatic energy-angle filter and its performance. The 2PS Spectrometer represents a revolutionary advance for measurement of space plasmas and will realize improved performance with a reduction in required size, mass, and power resources. The concept and operation are intrinsically simple, and enable ultrafast (<0.1 s) measurement of plasma distribution functions to understand, for the first time, the physical processes that drive the complex plasma dynamics of the solar wind and the terrestrial magnetosphere. This breakthrough additionally enables robust plasma measurements on 3-axis stabilized spacecraft and smallsats, which is critical for the Lab's future national security payloads as well as future scientific missions.

For 50 years, Los Alamos has flown plasma spectrometers for national security payloads as well as NASA scientific missions to study solar wind and planetary magnetospheres such as Earth and Saturn. The Lab has expanded its national security mission into space situational awareness, which entails understanding and predicting the space environment and its impact on the national space infrastructure. The 2PS Spectrometer will enable Los Alamos to continue to lead studies of space plasmas and the space environment, and will position the Lab as an even stronger "go-to" institution for such measurements. We anticipate that this concept may also be the foundation for future generations of national security payloads.

Benefit to National Security Missions

The 2PS Spectrometer represents a revolutionary advance for measurement of space plasmas and will realize improved performance with a reduction in required size, mass, and power resources. It will also, for the first time, enable ultra-fast measurements of plasmas to discover and test hypotheses about physical processes that induce dynamic plasma variations on short time scales. By allowing investigation of processes at short time scales (<0.1 s) this work is thus directly relevant to a number of NASA space science goals, including studies of turbulence and reconnection in space plasmas.

For 50 years, Los Alamos has flown plasma spectrometers for national security payloads as well as NASA scientific missions to study solar wind and planetary magnetospheres such as Earth and Saturn. Monitoring and understanding of the space plasma environment is a critical component of the LANL nuclear detonation detection nonproliferation mission. LANL has expanded its national security mission into space situational awareness, which entails understanding and predicting the space environment and its impact on the national space infrastructure. We anticipate that the 2PS instrument concept may also form the foundation for future generations of national security payloads.

The low-resource 2PS spectrometer could also form the basis of a solar wind monitoring instrument for space weather forecasting purposes. While space weather monitoring falls under the purview of NOAA, it is of interest to many agencies (e.g. DOC, NASA, NSF, DoD, DOE, etc.) who together have formed the National Space Weather Program (NSWP) to coordinate efforts in this area.

Progress

Work on the 2-pi Plasma Spectrometer (2PS) project in FY2013 involved two components: simulation of the instrument concept, and development and testing of

prototype hardware in the laboratory.

Experimental work began by investigating round holes drilled in a prototype filter plate. The use of round holes rather than stacked plates with cylindrically symmetric slits is significantly easier to fabricate, and thus allows us to more quickly validate the instrument concept. We tested both drilled holes and tapped holes, where the tapped holes are intended to prevent particles from specular reflection into the detector. Results of these studies using H, He, and O ions showed that tapping the holes does in fact reduce scattering by nearly two orders of magnitude.

In a parallel effort, we investigated suitable detectors for the 2PS spectrometer. For our initial prototype tests, we determined that we could use the existing imaging microchannel plate (MCP) system in our test laboratory. While this MCP is too small for a full 2PS instrument, it is suitable for the initial prototype testing. Our research this year shows that 10x10 cm MCPs are available, and that existing electronics could be modified to use these MCPs with a crossed-delay-line (XDL) anode. In addition, collaborator Eberhard Moebius has MCPs from a previous project that may be suitable for a next-generation prototype instrument. As the existing XDL sensors exceed 2PS requirements, no technology development is required for this subsystem. We anticipate using this more sophisticated detectors in future prototype development.

We ran extensive simulations using the SIMION software package in preparation for building a prototype detector. These simulations included modeling of the original symmetric instrument concept, as well as simulations of a simplified model based on round holes rather than cylindrically symmetric slits. Simulation of the hole-based instrument required a 3D SIMION model, as this instrument lacks the cylindrical symmetry of the original. Modeling showed that the energy and angle response of the hole-based instrument is very similar to the full instrument concept, and thus that this simplified design is suitable for proof-of-concept experiments. Further modeling efforts focused on simulating details of the prototype design to allow the instrument to be more easily fabricated.

We then constructed and began testing an initial prototype instrument based on round holes. This instrument includes 11 holes, for detection of particles at 11 different entrance angles. As drilling holes at angles is difficult, the design uses appropriately sized counter-sunk holes at the entrance and exit of the filter plate, with a larger straight hole connecting these. The instrument was fabricated and installed in a vacuum chamber for testing with an ion beam source. As noted above, an existing imaging MCP system is being used as a detector. The ion beam source can generate particles from ~1-60 keV, an appropriate range for this instrument.

Initial test results do indeed validate the instrument concept, with particles for a given hole observed at the expected central energy and incoming angle. However, there are interesting differences between the prototype instrument and the simulated design, in particular in the energy resolution of the instrument, where the laboratory prototype shows significantly better results than predicted. With the instrument tuned for detection of 10 keV ions, we have input ions over a range of 5-60 keV, and find an energy response $\Delta E/E$ that is factor of 2 better than predicted. We are investigating whether this is due to fringing fields, construction tolerances, limitations of the model, or some other cause. Results of these studies will inform the second-generation prototype instrument, to be constructed during the second year of this project. In particular, we are very interested in determining the reasons why the laboratory prototype has a better energy response than predicted by the model so that we can exploit these features in future versions of the instrument.

Future Work

Work during the first year has validated the 2-pi Plasma Spectrometer (2PS) instrument concept. During the second year of this three-year project, we will continue optimization of the 2PS spectrometer. We will begin by completing our studies of the initial prototype, and understanding the differences between this design and the simulations. As fringing fields may be (positively) affecting the prototype response, we will analyze the effects of fringe fields around the aperture and filter plate channel openings. We will perform further simulations to optimize the instrument performance, including variation of the filter plate channel length-to-width ratios, ratio of channel diameters to the distance from the entrance aperture, and entrance aperture diameter. The results of these laboratory and simulation studies will inform further development of the 2PS instrument. We expect to fabricate and test a second preliminary prototype instrument during year two. It is likely that this instrument can also use laboratory detectors, but we will evaluate the need for XDL hardware at this stage. In addition, we will begin design work for a final prototype instrument. We will ramp up efforts to design a stacked-grid filter plate, including simulations and preliminary studies. This work will be led by collaborator Eberhard Moebius from the University of New Hampshire, and is expected to involve a student participant. We will determine detector and electronics needs for this complete prototype, and then determine available and lead times for acquisition of these parts. We expect that by the end of the second year we will be ready to begin final

design fabrication of a full prototype instrument.

Conclusion

The 2PS plasma spectrometer acquires a complete measurement with a single high voltage sweep, allowing measurement of a complete distribution function in less than 0.1 sec. These fast measurements will enable study of ultrafast dynamic processes in the solar wind and magneto-spheric plasma environments. The unique design enables a dramatic reduction of resources (mass, power, size, and cost) compared to existing designs. We expect that the mass and power resources will be less than 1 kg and 2 W for one instrument, suitable for use in either cubesat or traditional satellite applications, as well as on 3-axis stabilized spacecraft.

Magnetic Nanomarker Detection and Imaging with SQUIDs

Andrei N. Matlashov
20130624ER

Introduction

We propose a revolutionary new technology and instruments for ultra-sensitive magnetic detection and imaging of tissue cells with a detection limit of below 10^4. By comparison, conventional x-ray mammography requires over 10^8 cancerous cells for detection. Our method will consist of targeting cells using antibody labeled single-core superparamagnetic nanoparticles, followed by detection and imaging of the targeted area using high-resolution Superconducting Quantum Interference Device (SQUID) gradiometers. Superparamagnetic relaxometry (SPMR) is used for detection of targeted cells with very high specificity: Only bonded (immobilized) nanoparticles will be detected via their Néel relaxation. The bonding will occur only with cancer cells because of specific antibodies conjugated to the nanoparticle surface. Unbound nanoparticles will not contribute in the SPMR decay signal. By combining SPMR with ultra-low field magnetic resonance imaging (ULF MRI), using the same instrument, the targeted area will be imaged to provide anatomical information. The same magnetic particles will also work as MRI contrast agents, as they can be detected due to their influence on the relaxation rates of 1H nuclear spins, which are an abundant signal source due to the high water content of soft tissue. The combination of ULF MRI and SPMR will provide both accurate localization and cell count of the targeted tissue. SQUIDs enable detection via gradiometers with unprecedented sensitivity. This approach will provide a robust diagnostic tool for detection and localization of diseased (e.g., cancerous) tissue targeted with magnetic markers at a very early disease stage. This technique can be used as an in vivo (inside body) diagnostic. ULF MRI and SPMR measurements have never before been combined in a single device.

Benefit to National Security Missions

We propose here a revolutionary advance in the ability to detect and image very small numbers of labeled cells or other microscopic objects, with the resolution at least one order of magnitude better than any presently available methods suitable for routine and/or repetitive use. This project illustrates LANL's unique inter-disciplinary ability to develop new instrumentation and measurement technologies.

Two key components are present at LANL – 1) Ultra-high resolution SQUID instrumentation; and 2) Magnetic nanoparticle synthesis and purification, surface modification, and specific bioconjugation.

The combination with imaging provides a truly unique approach to address both the presence and location of labels. The long-term relevance to national security science is both in global health (as an early cancer diagnostic), but also global security (the ability to rapidly detect exposure to pathogens for example, or small quantities of molecules in the environment) and in the capability to provide rare-molecule detection. Success of this project will lead to further development of the method using funds from different agencies such as NIH or, for instance, from DoD Congressionally Directed Medical Research Programs such as Breast Cancer Research Program.

Progress

During the current financial year the project development moved in three parallel directions. First, the existing 7-channel SQUID-based system had been modified and upgraded. It allowed use for both ultra-low field magnetic resonance imaging (ULF MRI) and superparamagnetic relaxation (SPMR) measurements using same phantoms. Second, 25-30 nm diameter super-paramagnetic nano-particles immobilized in agarose have been used to make phantoms with different shapes and particles concentration. Third, a new 7-channel system with three additional reference channels was designed and currently is about 75% complete. This system will be used for combined ULF MRI and SPMR measurements in unshielded environment using phantoms. Potentially

this system can be also used with small animal models or human tissue samples in medical research facilities.

The existing 7-channel system consists of axial second-order gradiometers 37 mm diameter and 60 mm baseline. They are positioned in parallel one in the middle and six others surrounding it in a hexagonal pattern with 45 mm separation between the axes. ULF MRI was performed using field-cycling and spin-echo protocol. A 2D Fourier imaging protocol was used with a frequency and phase encoding gradients. The resulting voxel size was 3×3 sq. mm with 160 mm diameter field of view. The 400-turn pre-polarization coil was cooled by liquid nitrogen. It was placed co-axial with the central gradiometer about 100 mm below its bottom pick-up coil. This coil generated a 50 mT pre-polarization field for MRI measurements and 5.5 mT magnetizing field for SPMR measurements.

Recording of the magnetic field relaxation signal started about 12 ms after the magnetizing field was zeroed. The relaxation signal from nanoparticles was masked by large transient signal. It was possible to suppress the transient by factor about 5 using a compensation coil. After that a baseline was recorded without a phantom and subtracted from the signal recorded with a phantom in place. This difference reveals the relaxation signal primarily from the nanoparticles. Raw relaxation signals were fitted using a logarithmic function in the area of slow signal decay and a 5th-order polynomial fit of the early relaxation curve for extrapolation to time zero. A dipole approximation was used for single vial localization and the magnetic moment was estimated using an inverse problem solution.

The phantoms were prepared using vials (with nano-particles inside) placed in a large dish of water. Agarose with uniformly embedded iron oxide nanoparticles at about 7×10E+11 per 1 ml was used to fill the vials. Such amount of nano-particles corresponds to about one million of tagged cells or 1 mm size tumor. We assumed that agarose keeps some fraction of nanoparticles immobilized allowing only Néel relaxation in the case of magnetic relaxometry. In the case of ULF MRI, the same nanoparticles work as a contrast agent.

We performed the first ever combined ULF MRI and SPMR measurements. Nanoparticles efficacy as a contrast agent was clearly demonstrated. Small vial with 1 ml nanoparticles was used for SPMR measurements. It was successfully localized using an inverse problem solution and a single dipole approximation. These preliminary results have been submitted to International Superconducting Electronics Conference (ISEC 2013) and chosen as an invited oral presentation. It was also invited as a peer-reviewed publication in IEEE Xplore.

We demonstrated the first time ever the possibility of combining magnetic relaxometry and ULF MRI in a single instrument. An image showing the influence of the nanoparticles as a contrast agent was obtained, and a plausible fit for the location and strength of a magnetic dipole was obtained by magnetic relaxometry. Future work will focus on using the MRI to constrain multiple dipole fitting. The combination of MRI with magnetic relaxometry will clearly improve our ability to accurately estimate and localize dipoles, with direct impact on the efficacy of the technique as a sensitive cancer diagnostic tool.

Future Work

During the first year of the project we decided to forgo ULF MRI experiments using a single channel system and use a modified 7-channel system. This approach allowed us to demonstrate the first time ever the possibility of combining magnetic relaxometry and ULF MRI in a single instrument. This system shows about 3 mm MRI spatial resolution with 160 mm field of view. In the next fiscal year we will improve its spatial resolution by a factor of 2 and also improve its signal-to-noise ratio by upgrading the fields generation coil system. This system will be used inside a magnetically shielded room (MSR).

We will demonstrate interleaved ULF MRI and SPMR using a single-dipole phantom that will allow us to compare the accuracy of an inverse problem solution with and without MRI data. We will then do localization procedures using multi-dipole phantoms and distributed source phantoms to solve an inverse problem that would be impossible without MRI data. We will investigate resolution limits for both SPMR and ULF MRI measurements.

Different type of phantoms will be made. For biomarker development we will otimize the multifunctional coating, functionalize the surface with amines or carboxylic acids and attach antibodies to the surfaces using one of several robust and well-known techniques, such as EDC/NHS coupling.

Unshielded measurements: a new multi-channel system will be built and tested for experiments in unshielded environment.

Conclusion

We will build instruments and demonstrate a proof of principle that magnetic nanomarker detection and imaging with SQUID-based gradiometers can lead to a creation of revolutionary new cancer diagnostic methods at a very early disease stage. We will 1) demonstrate interleaved ULF MRI and SPMR measurements using a single device; 2) reach 2×2×4 mm3 ULF MRI system spatial resolution; 3) reach SPMR detection limit of below 10,000 cells; 4)

design and build a multichannel system capable of doing measurements in unshielded environment; 5) develop desired optimized superparamagnetic nano-markers; and 6) experimentally demonstrate performance of the method using phantoms and mice.

Publications

Magnelind, P., Y. J. Kim, A. Matlashov, S. Newman, P. Volegov, and M. Espy. Superparamagnetic relaxometry for early cancer detection using a low-Tc SQUID-gradiometer array. To appear in Eleventh European Conference on Applied Superconductivity. (Genova, Italy, 15 - 19 Sep. 2013).

Matlashov, A., P. Magnelind , H. Sandin, M. Espy , A. Anderson , and H. Mukundan. SQUID instrumentation for early cancer diagnostics: combining SQUID-based ultra-low field MRI and superparamagnetic relaxation . 2013. In Fourteenth International Superconducting Electronics Conference . (Cambridge, 7 - 11 July 2013). , p. 231 . Cambridge: IEEE Xplore.

Matlashov, A., P. Magnelind, Y. J. Kim, H. Sandin, M. Espy, A. Anderson , and H. Mukundan. SQUID-based ULF MRI and superparamagnetic relaxometry for early cancer diagnostics. 2013. Superconductivity News Forum (Global Edition). (25): ST 342.

Beyond the Standard Halo

Michael S. Warren
20130626ER

Introduction

It is widely anticipated that dark matter will be detected in the upcoming generation of solid state and noble liquid direct recoil experiments. To correctly interpret these results -- whether positive or negative -- and to compare them to other indirect searches (e.g., with cosmic rays or LHC), it is crucial that the theoretical uncertainties entering into the predicted scattering rates be reduced as much as possible. The dominant uncertainty in this calculation is the small-scale distribution of dark matter. Predictions for direct detection experiments are often computed with the assumption that our local dark matter distribution can be treated as a "standard halo,'' a smooth isothermal sphere. However, observations and numerical simulations suggest that this assumption is invalid.

Although we have compelling measurements of the large-scale properties of our galaxy's dark matter halo, we have no direct information on how this dark matter is distributed on small scales. The goal of our research is to understand the small-scale distribution of dark matter within halos, and apply this knowledge to the interpretation of experimental and observational results. To achieve this, we will perform the world's highest-resolution N-body simulations using our 40M CPU-hour per year allocation on the new LANL Mustang supercomputer. This combination of observations, theoretical advances, and numerical simulations provides an exciting opportunity to identify dark matter, with implications for some of the most important questions in science, such as how galaxies form and what determines the properties of fundamental particles.

Benefit to National Security Missions

Understanding the nature of the dark matter is among the most important unsolved problems in physics. An immense amount of theoretical, observational, and experimental activity is underway in anticipation of the dark matter particle being unveiled. Such a discovery would have profound consequences. To correctly interpret these results, it is crucial that the theoretical uncertainties be well understood.

Modern N-body simulation codes provide the theoretical basis for our present understanding of the mass distribution in the Universe, and are an essential link in the chain which connects particle physics to cosmology. The aim of our research is to understand in exquisite detail the distribution of dark matter within halos, and to connect this knowledge with the growing suite of astrophysical and particle physics observations. To achieve this, we will perform the world's highest-resolution N-body simulations with our Hashed Oct-tree (HOT) N-body code and our recent 40M CPU-hour per year allocation on the new 38,000 processor LANL Mustang supercomputer.

The software developed to perform the simulations and analyze the data during this project will enhance our capability for modeling and high-performance computing, as well as serve as a proving ground for high-performance computers and data-mining technology. The project will demonstrate advanced computational techniques which are applicable to a variety of difficult fundamental problems in hydrodynamics, materials science, biology and chemistry.

Progress

The number of dark matter halos in the Universe of a given mass is a fundamental statistic called the mass function. The mass function is sensitive to cosmological parameters such as the matter density, the initial power spectrum of density fluctuations, and the dark energy equation of state. For these reasons, the mass function is a major target of current observational programs, and provides a basic constraint on the properties of individual halos. Precisely modeling the mass function is an enormous challenge for numerical simulations, since both statistical and systematic errors conspire to prevent the emergence of an accurate theoretical model. The

dynamic range in mass and convergence tests necessary to model systematic errors require multiple simulations at different resolutions, since even a very large simulation does not have sufficient statistical power by itself.

We provide the first mass function calculated from a simulation using the new standard Planck 2013 cosmology, with a 4096^3 particle simulation and six 2048^3 simulations completed and shared with our collaborators within 30 days of the publication of the Planck 2013 results. Changes in the parameters from the previous WMAP7 model are large enough that extrapolations from the other cosmologies are likely subject to systematic errors which are large compared to the statistical precision of our results.

We find that Tinker (2008) underestimates the mass function at scales of 10^15 solar masses by about 5% when compared with the older cosmological model it was calibrated against. For the Planck 2013 cosmology, the Tinker08 mass function is 10% low at large scales, due to the added systematic effect of non-universality in the underlying theoretical model.

We identify a previously unidentified systematic error stemming from the improper growth of modes near the Nyquist frequency, due to the discrete representation of the continuous Fourier modes in the ideal input power spectrum with a fixed number of particles. This is a resolution-dependent effect which is most apparent when using particle masses larger than 10^11 solar masses(corresponding to using less than 1 particle per cubic Mpc/h). Uncertainty in the appropriate correction and consequences of this effect appear to be the dominant source of systematic error in our results. If uncontrolled, this discretization error confounds convergence tests which attempt to isolate the effects of the starting redshift of the simulation, since the error becomes larger at higher starting redshifts.

We are in direct conflict with recent results (Watson, 2012) which find the spherical overdensity mass function to be lower than the the Tinker08 result at high masses. Potential explanations would be insufficient force accuracy of the CUBEP3M code, with a secondary contribution from initial conditions that did not use 2LPT corrections.

The standard practice in cosmological N-body simulations is to smooth the forces at small scales, usually with a Plummer or spline kernel. We have implemented these smoothing kernels in our code as well as the additional kernels described by Dehnen (2001). Dehnen concludes that the optimal softening method uses a compensating kernel, with forces that are higher than the Newtonian force at the outer edge of the smoothing kernel, which compensates for the lower forces in the interior and serves to reduce the bias in the force calculation. Our tests confirm these conclusions, and we use Dehnen's K1 compensating kernel for our simulations.

We published a paper in the Proceedings of Supercomputing '13 where we report on improvements made over the past two decades to our adaptive treecode N-body method (HOT). A mathematical and computational approach to the cosmological N-body problem is described, with performance and scalability measured up to 256k (2^18) processors. We present error analysis and scientific application results from a series of more than ten 69 billion (4096^3) particle cosmological simulations, accounting for 4 x 10^20 floating point operations. These results include the first simulations using the new constraints on the standard model of cosmology from the Planck satellite. Our simulations set a new standard for accuracy and scientific throughput, while meeting or exceeding the computational efficiency of the latest generation of hybrid TreePM N-body methods.

Future Work

Our simulation campaign is enabled by our large allocation of Institutional Computing time, and the extraordinary performance of our N-body code. In the past, numerical cosmology groups have performed a single world-class simulation (in the range of 1-5M CPU hours) every few years. With our present resources, we can perform a world-class simulation every month. Multiple simulations provide an invaluable check on the statistical and convergence properties of our simulations.

We have previously explored cosmologically relevant volumes (300 Mpc or more with particle masses greater than 10^8 solar masses. In FY2014 we will progress to higher resolution using a combination of re-simulations at higher resolution of interesting objects we have identified in current simulations, as well as performing new simulations with hierarchical initial conditions (where boundary conditions are provided by more massive particles, concentrating the computational effort on high-resolution sub-regions). Our work in this area will be further enabled through the use of PANPHASIA initial conditions based on the work of Jenkins (2013). We expect to perform 6-10 simulations with ~ 100 billion particles and mass resolution between 10^4 and 10^8 solar masses during FY2014. We submitted an INCITE computing proposal during the summer, which if successful will allow us to capstone our simulations with a trillion particle run using the Titan supercomputer at ORNL during calendar year 2014.

We will address what our simulation results imply for the sensitivity of the experiments. The vast majority of sensi-

tivity projections are currently performed with extremely restrictive simplifying assumptions. We will avoid these assumptions, and translate the results of current experiments into specific predictions.

Conclusion

We intend to simulate the evolution of matter and to resolve dark matter structures over a spatial range of a million. We will pursue both the dissipationless aspects of structure formation (i.e. dark matter only') and consider baryons -- the gas which can shock and dissipate energy, form stars, and generally modify the dynamical evolution of the dark matter on small scales -- with improvements to the smoothed particle hydrodynamic (SPH) component of our code. Connecting fundamental cosmological theories with observational dark matter data can only be accomplished with numerical experiments such as those we propose here.

Publications

Hamaus, N., B. D. Wandelt, P. Sutter, G. Lavaux, and M. S. Warren. Cosmology with Void-Galaxy Correlations. 2013. arXiv preprint arXiv:1307.2571.

Song, J., J. J. Mohr, W. A. Barkhouse, M. S. Warren, K. Dolag, and C. Rude. A Parameterized Galaxy Catalog Simulator for Testing Cluster Finding, Mass Estimation, and Photometric Redshift Estimation in Optical and Near-infrared Surveys. 2012. The Astrophysical Journal. 747 (1): 58.

Sutter, P., G. Lavaux, B. D. Wandelt, N. Hamaus, D. H. Weinberg, and M. S. Warren. Sparse sampling, galaxy bias, and voids. 2013. arXiv preprint arXiv:1309.5087.

Warren, M. S.. 2HOT: An Improved Parallel Hashed Oct-Tree N-Body Algorithm for Cosmological Simulation. 2013. arXiv preprint arXiv:1310.4502.

Warren, M. S., and B. Bergen. Poster: The Hashed Oct-Tree N-Body Algorithm at a Petaflop. 2012. In High Performance Computing, Networking, Storage and Analysis (SCC), 2012 SC Companion:. , p. 1442.

Coherent Diffractive Imaging of Ultrafast Ejecta Processes

Cynthia A. Bolme
20130632ER

Introduction

This project will use an ultrafast laser to create a shock wave at a metal sample surface. The metal sample will have a periodically roughened surface, and the interaction of the shock wave with the structured surface will create instabilities in the material that will evolve in small jets of ejecta particles. This process will be imaged using ultrafast soft x-rays that are created by the same laser system that drives the shock. Using coherent soft x-rays, we will provide resolution of the ejecta formation process that is 20 times better than has been previously performed.

We will also perform molecular dynamic simulations of this ejecta forming process that are perfectly matched in length and time scales to the experiments. By comparing the simulation with the experiments, we will gain new insight into instability formation and evolution. By comparison of these results with previous results of larger scale ejecta formation, we will learn about the importance of time and length scales on instability growth.

Benefit to National Security Missions

The development of this tabletop source will immediately address core mission problems and provide important validation of physics-based material models as the spatial and temporal resolutions achievable with this imaging diagnostic will be orders of magnitude better than current dynamic diagnostic alternatives. This diagnostic ability was specific called out in the report from the Research Needs for Material Mixing at Extremes workshop stating, “developing diagnostics for HED flows that will allow us to penetrate the mixing regions with greater resolution than ever before achieved.” This project will also greatly advance the state-of-the-art in dynamic materials imaging using coherent x-ray diffractive imaging, a key diagnostic proposed in the Matter-Radiation Interactions in Extremes (MaRIE) signature facility.

Progress

Efforts in FY13 have included experimental design, lab setup, equipment procurement, and code development. We reiterate here that only a few similar systems exist in the world (none to our knowledge in the western hemisphere) that can produce enough coherent, soft x-ray flux for single shot coherent diffractive imaging (CDI). At the time of writing this proposal, about half way through the fiscal year, we feel we are on track to make our milestone for this FY of having the soft x-ray source up and running and initial attempts at static single shot imaging.

This FY, we have focused our efforts on setting up the tabletop, single shot high harmonic generation system. The laboratory that housed the laser system proposed for this project had not been used in many years, so much of our effort in the first months has been to get the lab ready, update the laser interlocks, and upgrade the laser system. LUMOS team postdocs and students from WX-9 and LUMOS also played valuable contributions in these efforts. This effort also included a full upgrade of the first stage laser amplifier.

Concurrently with these efforts, we have performed a thorough design of the optical relay system, soft x-ray generation, and experimental geometry. These efforts have included conducting literature searches for similar laser development and soft x-ray generation efforts. Additionally, numerical calculations and optical modeling were performed to try to reduce risk and ensure a successful experimental design. Two specific design challenges that were overcome had to do with the optical design. First, there was a challenge in properly designing the up to 7 meter long focus of the intense (up to 100 mJ per pulse, 45 fs) near-infrafred (IR) laser pulses into a long, low pressure gas cell for optimal phase matching conditions. This design included folding the beam back on itself inside an evacuated chamber to avoid nonlinear effects in air such as self focusing. Achieving this phase matching condition is critical in order to ensure

the brightest and most coherent beam for CDI. A second design aspect that was challenging given somewhat limited space in the laboratory was in separating the collinear soft x-ray and mid-IR light. Our design incorporates a beam splitter that will allow us to remove most of the unwanted IR light that needed to be placed sufficiently downstream that the IR pump light would not damage it.

In addition to experimental design and cleaning, we also performed an IWM safety review and wrote and reviewed the IWD documentation including laser safety. We are currently beginning to set up the coherent soft x-ray generation system and vacuum chamber and are planning the soft x-ray optical we will perform static imaging experiments of surfaces in vacuum. Another large effort in these first months has been the identification and purchasing of necessary equipment including vacuum components, optics, soft x-ray detectors, and in vacuum motion control. We have currently received several vacuum components and the soft x-ray detector and have purchases in the works for in vacuum motion controllers and optics.

This FY, we have also been further developing and refining our 2-dimensional molecular dynamics simulations of ejecta in Al, with a specific focus on the process of evolution of the instability and break up of the material into particulates. MD simulations of ejecta formation have been performed on solid state copper looking at the effect of surface morphology in a quasi-2D sense. Additional work has been done in the selection of an Al potential. We have observed that the surface morphology plays a significant role in the resulting structures formed. As an example a pure sinusoidal wave with a kh0=1.0, we observe in copper a spike height of 57.3 nm whereas other surfaces with the same kh0 range from 151 nm to 15 nm. Analysis is underway to determine how well equation (3) of Ref [Dimonte, et. al. PRL, 107, 264502 (2011)] holds or if it needs to be modified to capture the surface morphology effect.

Future Work

After successful setup of the tabletop soft x-ray system and initially performing single shot coherent diffractive imaging (CDI) of static objects if FY13, efforts in FY14 will focus on moving towards actually performing the pump-probe dynamical imaging of the shock breakout on the roughened metal surface. We will optimize static imaging with the coherent soft x-ray source for brightness, stability, and image resolution, and we will incorporate the single shot imaging with ultrafast laser shocked samples. Samples for these studies will be lithographically patterned samples for resolution determination and in order to determine the beam characteristics on a shot to shot basis. Further efforts will include optimizing the laser shock drive and characterizing the shock properties. These efforts may include performing diagnostics studies on the shock drive beam and on shock breakout on the metal surface. The modeling effort will attempt to secure computational resources to begin the simulation of 3-dimensional surfaces, i.e. sinusoidal pits or wells. These structures will attempt to replicate the surface conditions present on the experimental set-up that we propose. Additional analysis of the simulations performed in FY13 will be done to correlate with the existing solid and liquid break-up models. The experimental dynamic images will allow us a direct comparison with the 3D MD models and will allow us to refine them.

Conclusion

This project's goals are to image ultrafast laser shock driven ejecta particles and to compare the imaging data with molecular dynamics simulations. This project will demonstrate the first single shot coherent x-ray diffraction imaging of a dynamic process and will validate molecular dynamics simulations. Additionally, we will provide an important new experimental capability, x-ray imaging of dynamic events, and will create data on instability formation with unprecedented time and length scales.

In Search of Light WIMPs

Alexander Friedland
20130637ER

Introduction

Astrophysical and cosmological observations over the last two decades have proven that ordinary matter constitutes only a few percent of the energy density of our Universe. Most of the energy density is contained in dark matter and dark energy. While the dark matter is know to hold the galaxies together, its physical nature remains a mystery. Laboratory experiments aiming to detect the dark matter particle form one of the cornerstones of the worldwide campaign to discover new physics beyond the Standard Model. The search for dark matter is one of the stated priorities of the DOE Office of Science.

Traditionally, direct detection experiments have been guided by the so-called WIMP (Weakly Interacting Massive Particle) paradigm. In this paradigm, one expects the dark matter particle to be in the mass range of 100-1000 times the mass of the proton. Yet, in the past few years, a contradictory picture has emerged that appears incompatible with the minimal WIMP framework. Several experiments, specifically CoGeNT, CRESST-II, and DAMA, have claimed evidence for dark matter, whereas CDMS, XENON10, and XENON100 have reported null results. To untangle this paradox urgently requires simultaneous advances in both theory and experiment.

We will attack the physics of dark matter on two fronts: by scrutinizing theoretical models that go beyond the minimal WIMP framework and by performing a low-threshold search for dark matter using the Majorana Demonstrator experiment. The experiment will be carried out in the timeframe of this proposal and will result in the world's best sensitivity in the light dark matter window. The theory effort will analyze the experimental results in the broad context of existing searches and will translate them into the physical properties of dark matter in various scenarios of new physics.

Benefit to National Security Missions

The search for dark matter is one of the leading priorities of the DOE Office of Science. The aim of this project is to enhance the capabilities of the Majorana detector to make it into the world's best probe of dark matter in the light mass window. Additional strategic impact derives form the capability of the Majorana detector in low-background counting. Improving this capability by going to lower energies will enable to us to study a wider range of samples. We presently count samples for programs in HEP and NP that require fabrication of experimental apparatus from radio-pure parts. We have also counted a sample for NIF-related efforts.

Progress

We have carried out our first study of the capabilities of the Majorana Demonstrator as a light WIMP detector. We have shown that, for a cross section near the current experimental bound, the Majorana Demonstrator should collect hundreds or even thousands of recoil events. This opens up the possibility of simultaneously determining the physical properties of the dark matter and its local velocity distribution, directly from the data. We have further investigated this possibility and found that allowing the dark matter velocity distribution to float considerably worsens the WIMP mass determination. We have traced this result to a previously unexplored degeneracy between the WIMP mass and the velocity dispersion. This establishes that knowledge of the dark matter velocity distribution through numerical simulations is essential for the mass and cross section determination of a light WIMP.

The paper with these results has just been accepted to Physics Letters B (vol 724, pp 183-191, 2013).

Future Work

The prototype module for the MAJORANA DEMONSTRATOR is presently (July 2013) being populated with detectors in our underground laboratory at Sanford Underground Research Facility (SURF). This module should be commissioned within a couple months and will then

operated for science runs. Data from the runs of that module will form the basis for determining the sensitivity of the DEMONSTRATOR to dark matter signals. We will be analyzing data with that question in mind. The LANL team will also be looking at data from a test bed in our laboratory at WIPP to develop analysis tools for studying the low energy spectrum. The detectors have been running there for many months and have provided that opportunity.

On the theoretical side, we will build on our initial study (carried out and published in FY13) of the dependence of the Majorana sensitivity on the dark matter velocity distribution. We will incorporate the results of the numerical N-body simulations to obtain the physical uncertainty on the mass and cross section determination. We will also explore models in which the mediator particle generating the WIMP-quark interactions is heavier than 1 GeV, but leads to momentum and velocity-dependent WIMP-quark interactions. Separately, we will study dark matter a mass in the ~10 MeV to 100 MeV range. We will also analyze the expected data from the running direct and indirect detection experiments and from the Large Hadron Collider. Lastly, we will study the reach of the IceCUBE experiment, with special attention paid to the oft-neglected prompt two-neutrino dark matter annihilation mode.

Conclusion

The project aims to carry out the world's most sensitive search for dark matter in the mass window of 5-100 proton masses, using the Majorana detector. It also plans to develop a theoretical framework for understanding the particle physics nature of dark matter, given the latest data from other direct detection experiments, LHC, IceCUBE, Fermi, and other relevant searches. The experimental and theoretical parts will be tightly integrated and the analysis of data will be done jointly.

Publications

Friedland, A., and M. Shoemaker. Integrating In Dark Matter Astrophysics at Direct Detection Experiments. 2013. Physics Letters B. 724: 183.

Giovanetti, G. K.. A Dark Matter Search with The MAJORANA Low-Background Broad Energy Germanium Detector. Invited presentation at TAUP 2013. (Asilomar, CA, USA, 9 Sep. 2013).

Electron Capture Spectroscopy for Neutrino Mass: Isotopes, Science, and Technology Development

Michael W. Rabin
20130679ER

Introduction

Measuring neutrino mass is an extremely challenging major science goal with intense current interest. Laboratory measurements of the electron energy spectrum from tritium beta decay set an upper bound for the electron antineutrino mass of ~2.2 eV (95% CL), which is only about four parts-per-million of the electron mass. This conventional measurement method will soon reach its technological zenith in the enormous KATRIN experiment with a mass sensitivity of ~0.2 eV (by about 2019), but with no hope of significant improvement. Alternative methods are therefore necessary to confirm, refute, refine, or surpass the expected results of this ultimate Goliath of electromagnetic spectrometers. But no known method can do the job today; there are no other sufficiently sensitive, technologically mature methods for laboratory-based, model-independent neutrino mass measurement. Our goal is to develop specific, key science capabilities central and necessary for one of the proposed methods: electron capture spectroscopy (ECS) of the unusual, rare and low decay-energy isotope 163Ho. To determine the neutrino mass, the ECS method requires rare isotope production, radiochemical purification, encapsulation of the Ho inside ultra high resolution cryogenic microcalorimeters (with Delta(E)~1-2 eV at E~3 keV), and spectral analysis near the reaction endpoint. To achieve ~0.1 eV mass sensitivity, a large-scale, highly demanding ECS experiment will need significant method development, sensor arrays with ~10,000 pixels, array-compatible readout, and years of operation. Though ~0.1 eV mass sensitivity is our long-term ambition, it is well beyond the scope of the present project, and we will limit ourselves to developing key methods necessary for ECS success.

Benefit to National Security Missions

The development of these techniques is directly applicable to basic nuclear physics and nuclear forensics. For basic nuclear physics, the key goal will be to build consensus within DOE OOS for this work electron capture spectroscopy technique as a route to determining neutrino mass. As the techniques and capabilities improve, we anticipate this effort will be highly competitive for a major initiative for a large scale experiment for neutrino mass measurement. For nuclear forensics, we are already fully engaged with US government and international community. The encapsulation of radionuclides directly into our sensors is a potential new technique for these nuclear materials analysis with special advantages.

Progress

We have made progress in three specific areas: isotope production, chemical purification, and measurement with microcalorimeter sensors. Isotope production for this project is done through nuclear transmutation. We have investigated the production based on multiple methods of nuclear transmutation, principally neutron and proton irradiation. Preliminary modeling and calculation in this area has been completed. Analysis suggests that neutron irradiation of enriched erbium has a higher production rate, though at cost in isotopic purity of the intermediate product. A manuscript covering this area has been prepared and recently accepted for publication in Nuclear Instruments and Methods. Related material was presented at the NuMass workshop where key representatives of each of the significant research programs working on Ho-163 isotope production participated. This work has also addressed the purity requirements relative to both short-term method and measurement technique development and long-term neutrino mass measurement. Chemical purification based on high-pressure (or high-performance) liquid chromatography has also made progress. The development of HPLC has focused on the chemical separation of target holmium from proton-irradiated dysprosium parent material. Small scale HPLC using milligram quantities of material has shown the first successful results with nonradioactive materials. The key result is temporal separation between holmium and dysprosium in HPLC chromatograms, an essential first step. Subsequent work is expected to demonstrate scaling up

of this process and assessment of feasibility within a fume hood. Related work on chemical separation has considered potential for HPLC separation from neutron-irradiated erbium, but this path is not currently emphasized in the laboratory due to time order of element elution. The third area of progress is in measurement with surrogate isotope Fe-55. We have successfully gone from having zero sensors in this category to a series of progressively more successful experiments. The key objective is to demonstrate successful electron capture spectroscopy with an easily available material during the period when we have no purified Ho-163. We have conducted a new sensor microfabrication and introduced Fe-55 into this new sensor type. Resolution-limiting factors are being assessed now. Multiple methods for the incorporation of the electron-capture-decaying species have been investigated.

Future Work

We plan to produce high specific activity 163Ho utilizing the IPF at LANSCE. The Ho will be chemically recovered from the target material matrix, leveraging the extensive team expertise at the TA-48 hot cell facility. Purified Ho product will subsequently be converted into aqueous samples suitable for incorporation into microcalorimeters. Detector design, fabrication and testing will begin with our successful TESs, but with intent to optimize for the encapsulation of radioactive materials into very low heat capacity structures. For detector development in year 1, objectives will be demonstrate that we can achieve high resolution spectra and develop the chemical purification process under cold (nonradioactive) conditions. This will allow us to confidently execute a single proton irradiation and a single round of hot cell chemistry in year two.

Conclusion

We have three specific project goals. Make 163Ho at high rate with high isotopic and chemical purity. Encapsulate radionuclides, measure ECS with □elta(E)~1-2 eV, at target rate 1000 cps. Use high resolution ECS to measure 163Ho decay energy (Q). An important feature of each of these goals is method scalability, which is what makes sub-eV mass sensitivity possible. A definitive measurement of Q directly addresses ultimate scale required. Combining these results creates an integrated 163Ho ECS capability directly useable with any thermal-type cryogenic detector, independent of thermometer choice, readout method, or multiplexing scheme.

Publications

Engle, J. W., E. R. Birnbaum, H. R. Trellue, K. D. John, M. W. Rabin, and F. M. Nortier. Evaluation of Ho-163 production options for neutrino mass measurements with microcalorimeter detectors. 2013. NUCLEAR INSTRUMENTS & METHODS IN PHYSICS RESEARCH SECTION B-BEAM INTERACTIONS WITH MATERIALS AND ATOMS. 311: 131.

Jet Probes of New Physics at RHIC and at the LHC

Ivan M. Vitev
20110098ER

Abstract

High-energy colliders today test not only theories of particle and nuclear physics, but indeed, of the very first moments of the evolution of our Universe itself. Experiments at the Large Hadron Collider (LHC) advance both of these frontiers by colliding protons and nuclei at unprecedentedly high energies and thereby explore the origin of mass, possibly the nature of dark matter, and the unexpected properties of new phases of matter, such as the strongly interacting quark-gluon plasma (QGP). The Relativistic Heavy Ion Collider (RHIC) continues to probe the properties of the QGP at lower energies, complementing the LHC heavy-ion effort. This project developed novel quantitative theoretical tools that bridge the gap between particle and nuclear science and help decipher the flood of experimental data for signatures of new physics. It addressed the topmost priority for both the particle and nuclear physics communities by developing and advancing the theory of jets (collimated showers of energetic subatomic particles) in reactions with protons and nuclei to a new level of precision and used them as probes of new physics at RHIC and at the LHC. The team published 6 refereed journal articles (including 4 Physical Review Letters and Physics Letters B) and two more are in preparation. Results from this work was presented in 9 invited conference and workshop talks and summarized in 3 refereed conference proceedings. The start-up of the LHC, the rapidly growing interest in jet physics, and the expertise of the research team has ensured a significant scientific impact of this project. This work supported the Laboratory Mission to enhance the nation's scientific capabilities, as defined by the DOE Office of Science. Within LANL, our project was well-aligned with the Beyond the Standard Model (BSM) Grand Challenge.

Background and Research Objectives

The overarching goal of this project was to develop modern theoretical and computational tools to identify and characterize new physics at the Relativistic Heavy Ion Collider (RHIC) and at the Large Hadron Collider (LHC). To this end, we proposed to advance the theory of jets - collimated showers of energetic subatomic particles that are abundantly produced at these facilities when particle beams collide. RHIC and LHC explore a broad spectrum of exciting novel phenomena that range from the formation of the quark-gluon plasma to the creation of new forms of matter that are believed to make up the fabric of our Universe. Understanding the Quantum Chromodynamics (QCD) theory of jet production and propagation in the vacuum and in matter having extremely high energy density is essential to elucidating both the unexpected properties of the QGP and the TeV-scale physics that is Beyond the Standard Model (BSM). We proposed to identify experimental jet observables of new physics in proton-proton (p+p) and nucleus-nucleus (A+A) reactions and evaluate them using modern techniques, such as effective field theory. Our goal was to incorporate the theoretical advances in jet simulation packages and employ the resulting tools to interpret the anticipated copious data from RHIC and the LHC. We expected that our project would establish the correct physics mechanisms of jet-plasma interactions and help eliminate the vast model dependence that currently hinders the precise determination of the plasma properties. We would identify search strategies for and/or place constraints on the Standard Model Higgs boson, as well as on models of supersymmetry, which predict massive new particles that decay into jets. The start-up of the LHC and the rapidly growing interest in jet physics would make it timely for this project to have a significant impact.

Scientific Approach and Accomplishments

One of the main tasks of the LHC is to discover the Higgs boson and complete the Standard Model of particle physics. In 2012 the ATLAS and CMS experimental collaborations announced the discovery of a Higgs-like particle with a mass around 125 GeV. The evidence for this particle was found in two final states, namely di-photons and di-bosons. Since the time of the discovery these

experiments have gathered more data and confirmed that the couplings of this particle to photons and di-bosons are in good agreement with the predictions of the Standard Model. But in the Standard Model the Higgs boson is also predicted to decay into pairs of fermions, such as a tau lepton pair or a pair of b-quarks. Here the evidence for the Higgs boson decaying into these final states is weak, though still not in disagreement with the Standard Model predictions. The reason for the disparity is that the discovery channels for the Higgs boson – di-photons and di-bosons decaying to leptons – are experimentally extremely clean. In contrast, the b-quark or tau-lepton final states are messy due to the hadronic nature of their decays and large Standard Model backgrounds. In fact, it turns out that if the mass of the Higgs boson is below O(135 GeV), then large statistics are required to discover the Higgs particle in the b-quark or tau-lepton final states when conventional analyses are applied.

New jet physics techniques to discover the Higgs boson decaying to fermion pairs, using less statistics and having different systematics, are therefore highly desired. Currently M. Graesser, along with LANL post-doc G. Ovanesyan and external collaborators J. Thaler and T. Chan (MIT) are finishing a paper that proposes a new method of analyzing the Higgs boson data to do just that [1]. Specifically, we are investigating the so-called ``tauN subjettiness", which was originally introduced to study boosted top quarks or boosted W bosons. The idea is to look for specific number of subjets in a big protojet and track back this number to a characteristic Higgs boson decay channel. In our forthcoming paper we are investigating applications of tauN for discovering a boosted SM Higgs boson in its decay mode to b-quark jets. The main new result of our work is that the tauN method and previous analyses have comparable efficiencies for retaining the Higgs mass peak. We find however that the best discriminating observable is the ratio tau2/tau1, which provides higher efficiency – of order 30% - than the currently best method, called the BDRS algorithm. This is illustrated in Figure 1, where the Higgs and vector boson signals stand out above the QCD background.

The remaining outstanding work to be done before publishing our results is the following. A larger sample of Standard Model backgrounds must be simulated to ensure our results are not biased by the statistical fluctuations of our Monte Carlo samples. We also have to include pile-up in our event generation (pile-up refers to multiple proton-proton collisions within a single bunch crossing) and pass all events through a detector simulation. Simulating pile-up and detector effects are particularly important in order to further establish confidence in our findings. The big protojet used in our analysis is pretty fat, and therefore can easily be contaminated by pile-up - debris produced from other proton-proton collisions (i.e., not from the one producing the Higgs boson). While our analyses currently include methods to filter or prune away the particles produced from pile-up, we still need to simulate the pile-up in order to establish that our methods are robust against such effects. Pile-up can also affect other important observables, such as the missing energy (MET) of the event and whether a lepton is isolated. A detector simulation is primarily needed to model the effects of energy mismeasurement on the jet mass, jet pT and MET of the event.

Another major component of the LHC program is to carry out ultra-high energy heavy ion reactions. Better understanding the physics of jets in these reactions requires the construction of a modern effective theory for jet propagation in matter. As a part of this project, I. Vitev and G. Ovanesyan constructed the Lagrangian for such theory, which we called Soft Collinear Effective Theory with Glauber gluons (SCETG). We derived the Feynman rules for this Lagrangian for different types of scattering centers in the medium, with which an energetic jet may interact, and for different choices for the degrees of freedom of the gluons (the mediators of the strong force) that enter our calculations. We presented the first proof that the jet broadening and energy loss results do not depend on this artificial choice of "gauge". This fact, known as "gauge invariance", allows us to put calculations of jets in heavy ion reaction on firm theoretical footing. By virtue of SCETG, we extended the evaluation of medium-induced radiation beyond the soft gluon approximation. We also showed how the process-dependent medium-induced radiative corrections factorize from the jet production cross section. Our paper "An effective theory for jet propagation in dense QCD matter: jet broadening and medium-induced bremsstrahlung" is published in the Journal of High Energy Physics [2]. We have given several invited talks on the subject at major conferences. In our second publication we applied this new effective theory SCETG to calculate all the remaining quark and gluon splitting probabilities in the medium [3], for the first time without assumption that either of the split partons is soft (published in Physics Letters B).

In a third publication [4] I. Vitev and external collaborators B.W. Zhang and Y. He presented first results of high accuracy (known as next-to-leading order) for jet production in the recent LHC lead-lead run. Specifically, we focused on the suppression for the single and double inclusive jet cross sections in heavy ion collisions. Our analysis included not only final-state inelastic jet interactions in the quark-gluon plasma created in such collisions, but also initial-state cold nuclear matter effects. We demonstrated how an enhanced di-jet asymmetry in central Pb+Pb reac-

tions at the LHC, recently measured by the ATLAS and CMS experiments, can be derived from these results. We showed quantitatively that a significant fraction of this enhancement may be related to the collisional interactions between the quarks and gluons in the jet and the strongly-interacting medium and pointed to a suite of measurements that can help build a consistent picture of parton shower modification in heavy ion collisions at the LHC. (Such stopping power calculations are also of interest to traditional plasma physics and Warm Dense Matter). Figure 2 shows the comparison of the di-jet imbalance measured by ATLAS and CMS to our calculations. Our paper "Next-to-leading order analysis of inclusive jet and di-jet production in heavy ion reactions at the Large Hadron Collider" is published in Physics Letters B. We have given one invited talk on the subject and published refereed conference proceedings.

To gain further insight into the mechanisms that control the modification of jets in strongly-coupled plasmas, Vitev and collaborators (LANL post-doc and Director's Fellow B. Neufeld and external collaborators B.W. Zhang and W. Dai) made predictions for the momentum imbalance distributions of photon-tagged and Z0-tagged jets at the LHC. The advantage of these channels is that the photon and the Z0 boson do not interact strongly with the quark-gluon plasma. Consequently, they escape the region of hot dense matter unscathed and their experimentally measured momentum can serve as a benchmark with respect to which the momentum degradation of the away-side jet can be evaluated. The net observable effect is a modification of the away-side jet distribution, as illustrated in Figure 3, where theoretical simulations are compared to the CMS experimental results. The exact shape of the medium-modified momentum imbalance distribution depends on the details of the experimental measurements (known as experimental cuts). Theoretical simulations were solicited by the ATLAS collaboration and an excellent agreement between our theory and the LHC results was shown at the Quark Matter 2012 conference in Washington DC. Our theoretical predictions have been published in two high-impact Physical Review Letters [5,6]. We have delivered 3 invited talks on our results at major international conferences in the field. Our work was selected as a jet physics highlight of Quark Matter 2012, the most recent biggest conference in the field of heavy ion physics.

Last but not least, we (I. Vitev, LANL post-doc G. Ovanesyan and external collaborator M. Fickinger) worked toward achieving an even higher accuracy in the calculations of jet production in heavy ion reactions. For this purpose, one needs to evaluate the processes where a quark or a gluon evolves into a 3-parton final state. The central question in this case is whether these final-state particles follow a particular angular ordering pattern. For example, if the angle of each subsequent branching is smaller than the angle of the previous one, the phenomenon is called angular ordering. If the angle of each subsequent branching is larger than the angle of the previous one, the phenomenon is called angular anti-ordering. We found that in all cases the amount of radiation that leaks out of angular ordered cones corresponds to no angular ordering. In fact, standard parton cascade based on simple superposition of binary branchings reproduces very well the distribution of the final-state partons. This work is published in the Journal of High Energy Physics [7]. Or results have been presented in two invited talks.

Impact on National Missions

This project supports the Laboratory Mission to enhance the nation's scientific capabilities, as defined by the Department of Energy (DOE) Office of Science. Within LANL, this project is well-aligned with the Beyond the Standard Model (BSM) Grand Challenge and responds directly to the LDRD Program Office call to "develop new theory to search for BSM physics" and to "further our understanding of quantum chromodynamics" at the Large Hadron Collider and the Relativistic Heavy Ion Collider. Research along these lines is now part of the Nuclear & Particle Futures pillar. Within the scientific community at large, this project addresses top priorities established by the DOE and the National Science Foundation Offices of High Energy Physics and Nuclear Physics in the 2008 High Energy Physics Advisory Panel P5 and the 2007 Nuclear Science Advisory Committee reports, respectively. There is significant interest in the stopping power of strongly-coupled plasmas for charged particles in the DOE Office of Fusion Energy Sciences, especially in the area of Warm Dense Matter. Physics at the nuclear scale and below is an underlying capability for the weapons program.

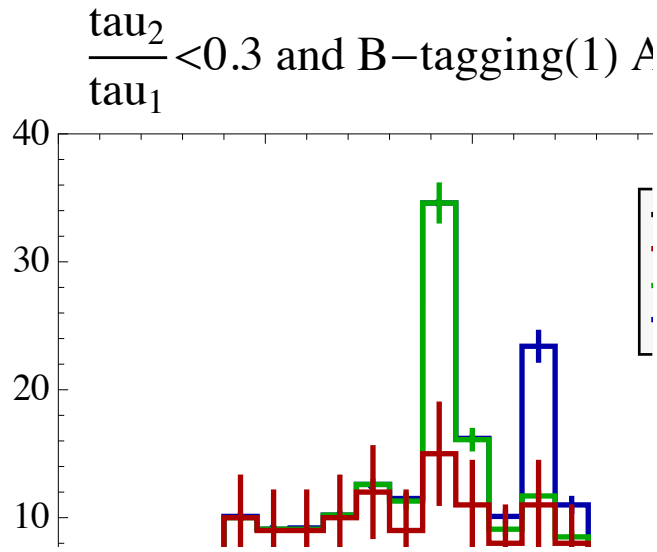

Figure 1. Example of how N-subjettiness techniques help isolate the Higgs and vector boson signals at the LHC above the QCD background (jets).

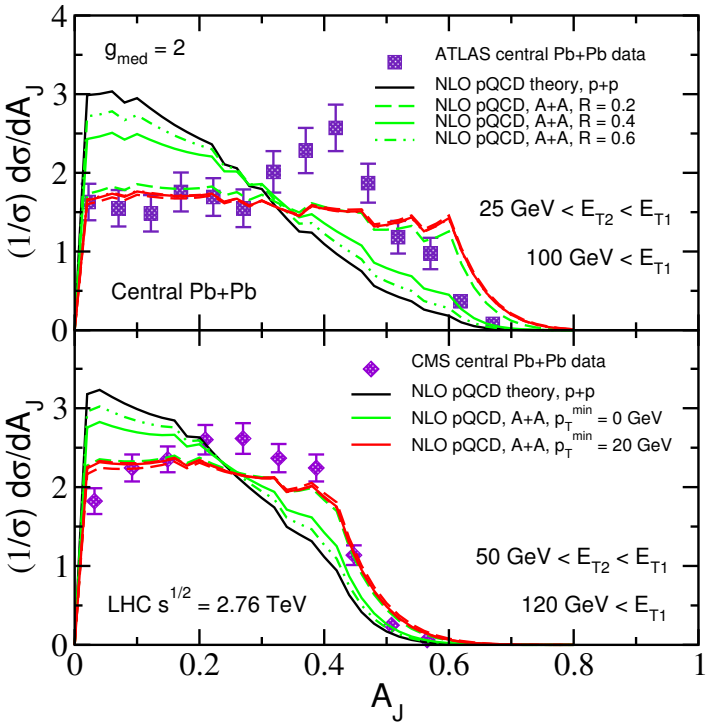

Figure 2. Comparison of theoretical simulations with collisional and radiative energy losses to the ATLAS and CMS dijet asymmetry results in lead-lead collisions at the LHC.

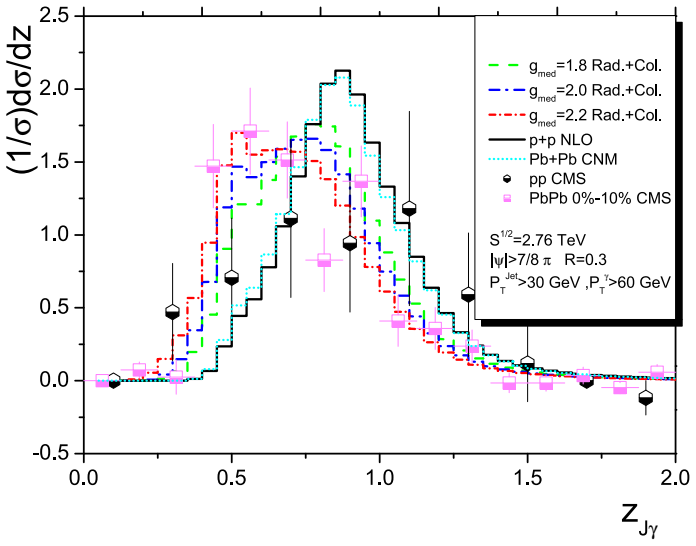

Figure 3. Comparison of the theoretically predicted photon-tagged jet momentum imbalance distribution to CMS data in lead-lead collisions at the LHC.

References

1. Ovanesyan, G., M. Graesser, T. Chan, and J. Thaler. Tau_N subjettiness methods for Higgs discovery. 2013. Manuscript in Preparation.

2. Ovanesyan, G., and I. Vitev. An effective theory for jet propagation in dense QCD matter: jet broadening and medium-induced bremsstrahlung. . 2011. Journal of high energy physics. 2011 (6): 80.

3. Ovanesyan, G., and I. Vitev. Medium-induced parton splitting functions from Soft Collinear Effective Theory with Glauber gluons. 2011. Physics Letters B. 706: 371.

4. He, Y., I. Vitev, and B. Zhang. Next-to-leading order analysis of inclusive jet and di-jet production in heavy ion reactions at the Large Hadron Collider. 2012. Physics letters B. 713: 224.

5. Vitev, I., and R. B. Neufeld. The Z0-tagged jet event asymmetry in heavy-ion collisions at the CERN Large Hadron Collider. . 2012. Physical Review Letters. 108: 242001.

6. Dai, W., I. Vitev, and B. W. Zhang. Momentum imbalance of isolated photon-tagged jet production at RHIC and LHC. 2013. Physical Review Letters. 110: 142001.

7. Fickinger, M., G. Ovanesyan, and I. Vitev. Angular distributions of higher order splitting functions in the vacuum and in dense QCD matter. 2013. Journal of High Energy Physics. 1307: 039.

Publications

Dai, W., I. Vitev, and B. W. Zhang. Momentum imbalance of isolated photon-tagged jet production at RHIC and LHC. 2013. Physical Review Letters. 110: 142001.

Fickinger, M., G. Ovanesyan, and I. Vitev. Angular distributions of higher order splitting functions in the vacuum and in dense QCD matter. 2013. Journal of High Energy Physics. 1307: 039.

He, Y., I. Vitev, and B. Zhang. Next-to-leading order analysis of inclusive jet and di-jet production in heavy ion reactions at the Large Hadron Collider. 2012. Physics letters B. 713: 224.

Huang, J., Z. Kang, and I. Vitev. Inclusive b-jet production in heavy ion collisions at the LHC. To appear in Physics Letters B.

Ovanesyan, G.. An effective theory for jet propagation in dense QCD matter: jet broadening, radiative energy loss and LHC phenomenology. 2011. Poster for Quark Matter 2011, Annecy, France.

Ovanesyan, G.. Effective theory approach to jet propagation in dense QCD matter. Invited presentation at Boston jet physics workshop, Harvard University, Cambridge, January 2011. (Cambridge, January 11-14. 2011).

Ovanesyan, G.. Effective theory description of jets in dense QCD matter. Invited presentation at Winter Workshop on Nuclear Dynamics 2011. (Winter Park, February 6-13).

Ovanesyan, G.. Effective theory approach to jet propagation in dense QCD matter. Invited presentation at SCET workshop 2011. (Pittsburg, 6-8 March, 2011).

Ovanesyan, G.. Effective theory for jets in medium. Invited presentation at Department of particles and fields meeting. (Providence, RI, 9-13 August, 2011).

Ovanesyan, G.. Medium-induced Splitting kernels from SCETG . 2013. In Quark Matter 2012. (Washington, August 2012). , p. 981c. Ridge, NY: Nuclear Physics A.

Ovanesyan, G., M. Graesser, T. Chan, and J. Thaler. Tau_N subjettiness methods for Higgs discovery. 2013. Manuscript in Preparation.

Ovanesyan, G., and I. Vitev. An effective theory for jet propagation in dense QCD matter: jet broadening and medium-induced bremsstrahlung. . 2011. Journal of high energy physics. 2011 (6): 80.

Ovanesyan, G., and I. Vitev. Medium-induced parton splitting functions from Soft Collinear Effective Theory with Glauber gluons. 2011. Physics Letters B. 706: 371.

Vitev, I.. NLO analysis of inclusive jet, tagged jet and di-jet production in Pb+Pb collisions at the LHC. 2011. Journal of Physics G. 38: 124087.

Vitev, I.. Electroweak boson-tagged jet event asymmetries at the LHC. 2013. In Quark Matter 2012 . (Washington, August 2012). , p. 701c. Ridge, NY: Nuclear Physics A.

Vitev, I.. Jet quenching . Invited presentation at QCD Structure I. (Wuhan, China, October 2012).

Vitev, I.. Hadron, photon, and jet production at the LHC. Invited presentation at High pT at he LHC . (Wuhan, China, October 2012).

Vitev, I., and R. B. Neufeld. The Z0-tagged jet event asymmetry in heavy-ion collisions at the CERN Large Hadron Collider. . 2012. Physical Review Letters. 108: 242001.

Daylight Imaging with Seismic Noise

Xiaoning Yang
20110108ER

Abstract

In this project, we developed a new methodology to extract the Earth's attenuation property from seismic noise. In recent years, seismic background noise has been increasingly exploited to glean useful information about the Earth. Most of the research, however, is directed at getting the seismic velocity property, i.e., how fast a seismic wave travels, of the Earth. Our research represents a breakthrough in that the new method allows us to obtain the seismic attenuation property of the Earth, i.e., how the Earth absorbs seismic-wave energy, from seismic background noise. This is a far more difficult problem.

In addition to developing the new method, we constructed a tomographic attenuation map of the western U.S. using the method. The map correlates well with the geology and with other published results. We also developed a new theoretical formula linking the noise measurement with properties of the noise field and those of the Earth. This permits a straightforward mapping between observations and their underlying causes. The new formula has been tested with numerical simulations.

The new methodology that we developed has direct applications to problems in global security and energy security missions of the Laboratory. The new capabilities acquired during this project advanced the standing of the Laboratory in this field and have attracted new funding to the Laboratory.

Background and Research Objectives

Seismic background noise is usually treated as a nuisance that is either ignored or suppressed. In recent years, however, studies have revealed that there is a wealth of information contained in seismic noise that we can extract. By processing the noise using the cross-correlation method, we can bring out useful signals that are buried in the noise. The signal that emerges from the noise cross-correlation (NCC) is related to what we call the Green's function. It is the seismic signal generated by an impulsive source at one location inside the Earth, and recorded by a seismic sensor at another location. The Green's function between the two locations contains information about the strength of the source and properties of the Earth medium in which the signal propagates. Specifically, it contains, in its travel time between the two locations, information about the seismic velocity of the Earth, and in its amplitude, information about the Earth's attenuation. It can then be used to probe these properties and develop velocity or attenuation images of the Earth through tomography. The technique to image the Earth using noise is known as "daylight imaging", in analogy to the illumination of shaded areas by scattered daylight.

Traditionally, we obtain the Green's function by recording the signal from an energetic seismic source such as an earthquake. Using NCC, we cross-correlate noise recorded by two seismic sensors at two different locations to obtain an approximation of the Green's function between the two locations without a source. The approximation is called the empirical Green's function (EGF). This gives us a new tool to investigate the Earth since we do not rely on when and where earthquakes occur and we can design our sensor deployment to suite our specific needs. It is particularly important for regions where earthquakes are scarce. In addition, by investigating how and why we can extract the Green's function from NCC, we have a better understanding of seismic noise generation and propagation within the Earth, which is a basic science question.

In the last decade, the science to derive the velocity property of the Earth from the travel time of EGF has been relatively well developed theoretically [1-3] as well as in laboratory experiments [4, 5] and in field applications [6-8]. To obtain the attenuation property from EGF amplitude, which dictates how seismic energy decays

with distance and in different directions, however, remained a challenge. This is because the amplitude of the EGF is affected not only by the Earth medium, but also by the locations and strengths of noise sources, which are not very well known. To date, most of the studies using seismic noise to extract EGF deal with velocity measurements. Very few studies tried to extract attenuation from noise. Our research is the first attempt to make accurate attenuation measurements from NCC and to develop a tomographic attenuation map from the measurements.

In this research, our objectives are to 1) develop new theory and methodology to accurately measure Earth's attenuation from EGF and 2) construct a two-dimensional (2D) attenuation map of the western U.S. using noise data recorded by the USArray, which is a dense and regularly spaced seismic sensor array deployed throughout the continental U.S. including Alaska. Through these objectives, we advance the Earth science by achieving better understanding and utilization of seismic noise.

We have accomplished both of these objectives during the course of this project. We have developed a novel methodology to accurately measure Earth attenuation from noise cross-correlation. We have also made theoretical developments to characterize the behavior of seismic noise field. Using the new method we developed, we constructed a tomographic attenuation map for the western U.S. In addition, we also conducted numerical simulations to confirm our theory.

Scientific Approach and Accomplishments

Lobkis and Weaver [1] first put forward a theory in 2001 stating that the signal from cross-correlating noise generated by a diffuse noise field, meaning that noise sources are uniformly distributed in space, and recorded by two sensors A and B at different locations is equivalent to the Green's function between the two locations. The onset time of the Green's function is the signal travel-time from sensor A to sensor B, which can be used to measure the wave velocity of the medium between A and B. The amplitude of the Green's function is a product of the noise-field intensity and the medium-attenuation effect between A and B. If the noise field is fully diffused, noise-field intensity is a constant and can easily be removed from the amplitude. The corrected amplitude can then be used to measure the medium attenuation.

When seismologists applied this theory to seismic noise, they discovered that the seismic noise field is not fully diffused. Instead, the seismic noise-field intensity changes with location, direction and time. Nevertheless, scientists obtain reliable velocity measurements from NCC that are as accurate as those measured from earthquake signals. This, however, is not the case for attenuation measurements from NCC. Because the noise-field intensity mainly affects the amplitude of EGF, attenuation measurements from these amplitudes are biased from the true values. This poses a major obstacle to reliably measuring attenuation from EGF.

In this research, we attack the problem from two directions. We investigate novel NCC calculation methods that minimize the variation of noise-field intensity. We also conduct numerical and theoretical analysis to characterize how the noise field behaves.

Since the theory requires a perfect diffuse noise field for NCC to work, any attempt to make the seismic noise field more diffuse should help with reducing the bias caused by the noise-field variation. To accomplish this, we turn our attention to the coda wave of the EGF. In general, the Green's function in the real Earth is not just a single pulse representing the signal traveling from A to B. It is usually composed of a long wave train, whose amplitude tapers off with increasing time. The later part of this wave train is called coda. It is made up of waves that are reflected off of heterogeneities – small-scale material elastic and anelastic property variations that exist throughout the Earth. Because these heterogeneities as sources of the coda wave are more diffused spatially than the source for the direct signal of EGF, we should be able to take advantage of this and create a smoother effective noise-field intensity. To do this, we use the coda wave of EGF in a second iteration of NCC calculation. We call the new technique the correlation of coda of correlation, or C-cubed (C3).

Figure 1 is an illustration showing how C3 works. To calculate C3 between a pair of seismic sensors R1 and R2, we select another group of sensors surrounding R1 and R2. We call these sensors coda sensors. We first calculate NCC between each of these coda sensors S and R1, and between S and R2. We then calculate C3 between R1 and R2 by cross-correlating the coda waves of NCC previously calculated between S and R1, and S and R2. C3 from all coda sensors are then added together to further improve the noise-field diffusivity and to improve the signal-to-noise ratio.

Figure 2 gives an example comparing EGF amplitude decay as a function of inter-station distance with that of signals from an earthquake. The map on the left shows the locations of seismic sensors (circles) used to calculate the cross-correlation and an earthquake (red star). NCC is calculated between the first sensor (black circle) and other sensors (yellow circles) in a linear array to obtain EGF between the sensors. EGF amplitudes are then compared with signal amplitudes from the earthquake in the plot

on the right. Green-circle sensors are coda sensors used to calculate C3. The amplitude decay of the earthquake signal is due to the Earth attenuation and amplitudes of EGF should follow the same decay rate if there is no bias. Apparently amplitudes from simple NCC calculations decay slower. Amplitudes obtained using the C3 technique, on the other hand, have a decay rate similar to that of the earthquake signal.

To establish the statistical significance of our comparison, we select a suite of linear sensor arrays at different locations and in different directions from among USArray sensors for further testing. Based on the slope of the straight lines shown in Figure 2, we estimate a parameter called attenuation coefficient that reflects how strongly the Earth attenuates the energy of waves propagating through it. The larger the value is, the more strongly the Earth attenuates the wave energy. Figure 3 compares the attenuation coefficients estimated from earthquake signals with those estimated from noise, using the suite of sensor arrays and selected earthquakes. It is apparent that using C3, we significantly reduce the bias (average difference) of traditional NCC estimates (from -5.5×10-4 km-1 to -0.8×10-4 km-1). The variation of the difference (spread) is also reduced (from 3.2×10-4 km-1 to 1.2×10-4 km-1).

After developing the C3 method, we use the method to construct an attenuation map of the western U.S. as the second objective of our project. We select crisscrossing arrays of seismic sensors from among the USArray sensors to calculate C3 EGF. Amplitudes measured from these EGF are then used in a tomographic inversion procedure to produce a 2D map of attenuation variations. Figure 4 shows the map from the inversion. Attenuation patterns correlate well with known geological features, both large and small. Examples include strong attenuation in Columbia Plateau, along the Sierra Nevada mountain range and in Yellowstone area, and weak attenuation in Colorado Plateau. The whole Basin and Range province has generally strong attenuation except for some small areas such as its northern end. The map also compares favorably with other published attenuation information for the western U.S. [9].

In addition to developing a new NCC processing method and constructing an attenuation map for the western U.S., we also conduct theoretical and numerical investigations to constrain the behavior of seismic noise field. Based on the theory that elastic-wave fields, including seismic noise field, should obey the so-called radiative transfer equation, we develop a new relationship that links the EGF amplitude with the Earth's attenuation and a specific form of noise-field representation. With this new formula, both the Earth's attenuation and the noise-field intensity can be teased out of EGF amplitudes through a tomographic inversion. Our numerical simulations confirm the feasibility of this approach.

So far, we have published four peer-reviewed papers documenting our accomplishments. The first three papers, published in the Comptes Rendus Geoscience, in the Journal of Acoustical Society of America and in the Geophysical Journal International respectively, describe our theoretical development and our numerical simulation results. We report the development of the C3 method in a paper published in the Journal of Geophysical Research: Solid Earth. Our tomography results will be published in another paper in the near future.

Impact on National Missions

Our research has important implications to multiple national missions of the Laboratory. One of those missions is global nuclear security. As a critical component of the mission, we monitor the world for (potentially clandestine) nuclear-explosion tests using seismology. To do a good job using the seismic method, we need to know the detailed property of the Earth in which seismic waves propagate. Traditionally, we obtain this information using seismic waves generated by earthquakes or man-made sources such as underground explosions. The technique of using seismic noise to image the Earth allows us to create better images of the Earth, which in turn improves our capability to monitor the globe for potential nuclear explosions. This is particularly important for regions where we do not have many earthquakes, and for cases in which we need specific sensor configurations to obtain good images of the Earth.

Another important application of daylight imaging is in natural-resources exploration, which is part of the energy security mission. As the technology advances, dense, large-scale, 2D seismic sensor arrays are deployed in many exploration campaigns. Seismic noise recorded by these sensors can be used to construct detailed images of the Earth on reservoir scales. It eliminates the need to use active explosion sources, which is extremely expensive. Since the sensor arrays can be put in place for a long period of time, noise signals from these sensors can also be used to monitor the changes of Earth medium properties over time. This is important for fluid-migration monitoring as well as carbon-sequestration monitoring.

Our achievement in this area puts the Laboratory at the forefront of the field. Our work has attracted the attention of Department of Energy/National Nuclear Security Agency funding officials. They have awarded a Broad Area Announcement contract to us in collaboration with University of Illinois at Urbana Champaign to continue the development of the methodology and to apply the method to other regions of interest. The new capability that we de-

veloped in this project will allow us to open new research areas in the Nuclear Detonation Detection program at the Laboratory. We are also actively pursuing the opportunity to apply the new methodology to energy security problems such as reservoir and carbon-sequestration monitoring and geothermal exploration.

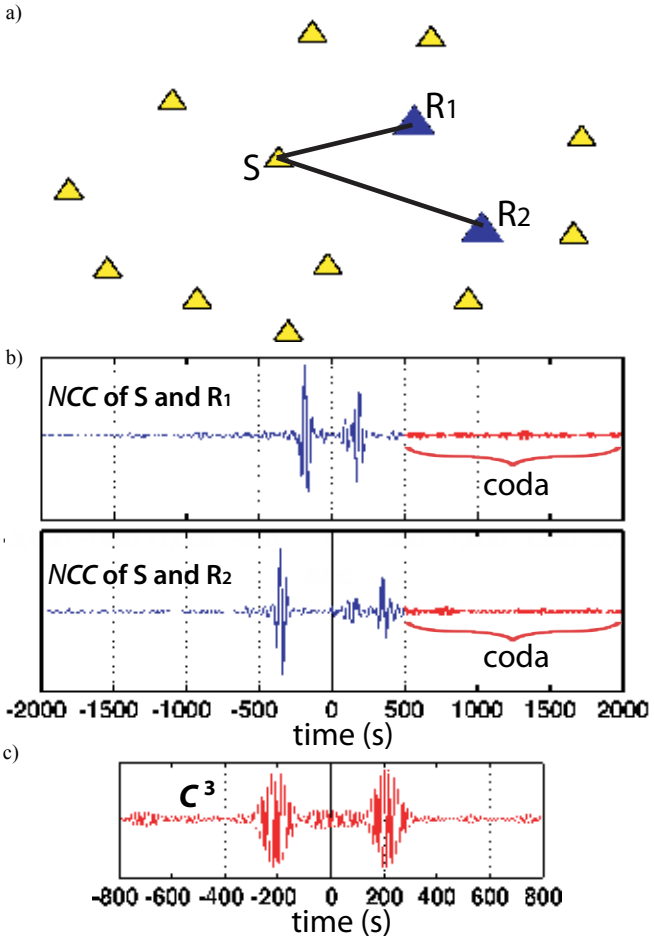

Figure 1. An illustration showing the correlation of coda of correlation (C3) calculation. a) Schematic locations of sensor pair R1 and R2, and coda sensors S (yellow triangles). b) Noise cross-correlation (NCC) signal (empirical Green's function, or EGF) between S and R1, and between S and R2. Coda waves, which are highlighted in red, are used to do another correlation calculation to obtain C3 EGF shown in c). EGF signal shows up in both positive and negative times due to noises that propagate in opposite directions. The more symmetric appearance of C3 EGF indicates that the noise field is made more diffuse through the C3 procedure.

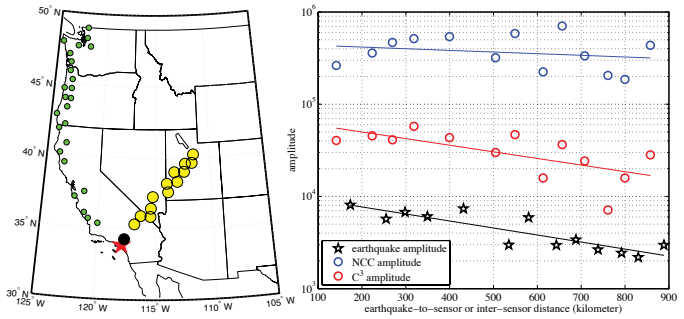

Figure 2. A comparison between earthquake amplitude decay, amplitude decay from traditional NCC, and C3 amplitude decay. The map on the left shows the locations of seismic sensors (circles) used to record the earthquake (red star) and to calculate the noise cross-correlation (NCC and C3). NCC and C3 are calculated between the black sensor and yellow sensors. Green circles are coda sensors. We use sensors along the coast as coda sensors because they generate C3 with better signal-to-noise ratios. The plot on the right shows the amplitude-decay comparison. Straight lines are best linear fits to the data.

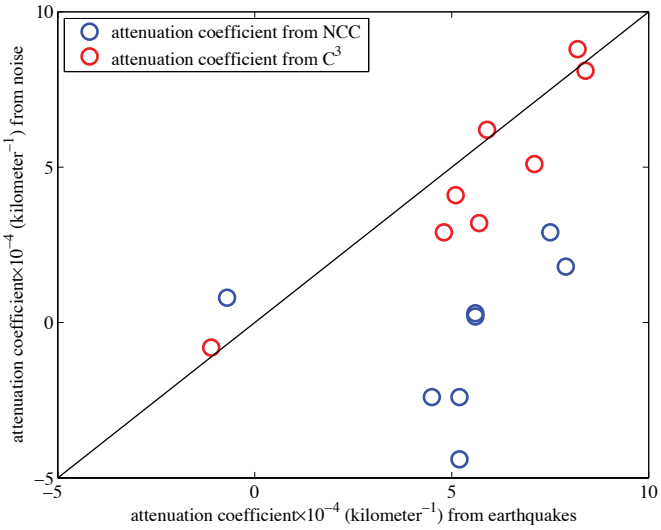

Figure 3. Attenuation coefficients estimated from noise versus attenuation coefficient estimated from earthquake signals. The average difference between C3 estimates and earthquake estimates is -0.8×10-4 km-1 with a spread of 1.2×10-4 km-1. The average difference between traditional NCC estimates and earthquake estimates is -5.5×10-4 km-1 with a spread of 3.2×10-4 km-1.

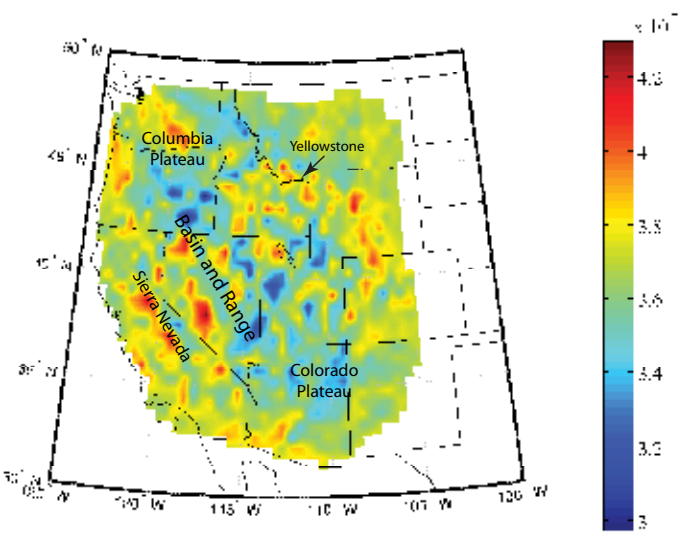

Figure 4. Attenuation-coefficient map of the western U.S. from the tomographic inversion of EGF amplitudes measured using the C3 method. Warm color indicates stonger attenuation compared with cool color.

References

1. Lobkis, O. I., and R. L. Weaver. On the emergence of the Green's function in the correlations of a diffuse field. 2001. JOURNAL OF THE ACOUSTICAL SOCIETY OF AMERICA. 110 (6): 3011.

2. Snieder, R.. Extracting the Green's function from the correlation of coda waves: A derivation based on stationary phase. 2004. PHYSICAL REVIEW E. 69 (4): -.

3. Roux, P., K. G. Sabra, W. A. Kuperman, and A. Roux. Ambient noise cross correlation in free space: Theoretical approach. 2005. JOURNAL OF THE ACOUSTICAL SOCIETY OF AMERICA. 117 (1): 79.

4. Weaver, R. L., and O. I. Lobkis. Ultrasonics without a source: Thermal fluctuation correlations at MHz frequencies. 2001. PHYSICAL REVIEW LETTERS. 87 (13): -.

5. Larose, E., P. Roux, and M. Campillo. Reconstruction of Rayleigh-Lamb dispersion spectrum based on noise obtained from an air-jet forcing. 2007. JOURNAL OF THE ACOUSTICAL SOCIETY OF AMERICA. 122 (6): 3437.

6. Campillo, M., and A. Paul. Long-range correlations in the diffuse seismic coda. 2003. SCIENCE. 299 (5606): 547.

7. Bensen, G. D., M. H. Ritzwoller, and N. M. Shapiro. Broadband ambient noise surface wave tomography across the United States. 2008. JOURNAL OF GEOPHYSICAL RESEARCH-SOLID EARTH. 113 (B5): -.

8. Prieto, G. A., and G. C. Beroza. Earthquake ground motion prediction using the ambient seismic field. 2008. GEOPHYSICAL RESEARCH LETTERS. 35 (14): -.

9. Phillips, W. S., and R. J. Stead. Attenuation of Lg in the western US using the USArray. 2008. GEOPHYSICAL RESEARCH LETTERS. 35 (7): -.

Publications

Weaver, R. L.. On the amplitudes of correlations and the inference of attenuations, specific intensities and site factors from ambient noise. 2011. Comptes Rendus Geoscience. 343: 615.

Weaver, R. L.. On the retrieval of attenuation and site amplifications from ambient noise on linear arrays: further numerical simulations. 2013. GEOPHYSICAL JOURNAL INTERNATIONAL. 193 (3): 1644.

Weaver, R. L.. Retrieval of Green's function in the radiative transfer regime. 2013. JOURNAL OF THE ACOUSTICAL SOCIETY OF AMERICA. 133 (2): 792.

Zhang, J., and X. Yang. Extracting surface wave attenuation from seismic noise using correlation of the coda of correlation. 2013. Journal of Geophysical Research: Solid Earth. 118: 2191.

Balanced and Unbalanced Turbulent Cascades

Balasubramanya T. Nadiga
20110150ER

Abstract

Despite its importance in the understanding and modeling of climate variability, the energetics of ocean circulation is still not well understood. After identifying gaps in current understanding in the field, we focus our research efforts on the movement of energy across scales in two fundamental and prototypical, but distinct oceanographic contexts: a) Effects of basin geometry on geostrophic turbulence and b) The interaction of balanced and unbalanced motions in the interior ocean. Our findings lead us to propose fundamental modifications to the state-of-the-art understanding of how energy moves across scales in ocean circulation in a series of articles in leading journals in the field. In the context of the DOE and LANL mission to model terrestrial climate, the improved understanding of energy pathways in ocean circulation achieved under this LDRD project is expected to lead to improvements in predictive modeling of climate variability.

Background and Research Objectives

Differential solar heating of the atmosphere-ocean system between the tropical and polar latitudes is the ultimate driver of climate on earth. In particular differential heating of the atmosphere sets up large scale wind patterns and latitudinal temperature gradients that then drive the general circulation of the world oceans (Figure 1). The latter in turn crucially controls the variability of climate on the interannual and longer timescales.

The large-scale ocean circulation that results from the large-scale atmospheric forcing itself develops instabilities and gives rise to intermediate-scale eddies. The large-scale circulation and the resultant eddies are both, however, in approximate geostrophic balance---a balance between pressure gradients and rotational effects. An important aspect of turbulence in the context of such balanced dynamics (called geostrophic turbulence) is an inverse cascade of energy. Such an inverse cascade of energy leads to a confinement of energy to large scales, a side effect of which is to render small scale dissipation ineffective in directly dissipating balanced mesoscale and large-scale energy. Thus a fundamental question regarding the energetics of ocean circulation is as to how the ocean equilibrates in the presence of continuous large-scale forcing and an inverse cascade back to large scales at intermediate scales. An analysis of the problem points to the need for better understanding how energy moves across scales and reservoirs in the multiscale system that constitutes ocean circulation.

Scientific Approach and Accomplishments

Our research focuses on the movement of energy across scales in two prototypical, but distinct oceanographic contexts: a) Effects of basin geometry on geostrophic turbulence and b) The interaction of balanced and unbalanced motions in the interior ocean.

Effects of basin geometry on geostrophic turbulence

We first point out that even in the classical regime of geostrophic turbulence, the question of energy transfer across scales is not well understood in oceanographically relevant settings. This is because much of the theory of geostrophic turbulence has been worked out assuming zonally or doubly periodic geometries that are relevant in the atmospheric context.

Accomplishments: In geometries of relevance to the atmosphere, energy transfers between scales occur solely in association with nonlinearity. In a basin setting that is the primary geometry of relevance to the oceans, this is not the case; meridional boundaries allow for the linear beta-term to also transfer energy across scales (see [4,5]). (Note that meridional boundaries play an important role in the dynamics in each of the oceans including the Antarctic.)

We find the classic picture of energy cascades in geostrophic turbulence to be an oversimplification in the basin setting ([6]): Unlike in the classic picture of inverse

cascade of energy---a crucial aspect of geostrophic turbulence, the scale at which the vertically-uniform mode receives energy (from vertically-varying modes) is not fixed at the deformation scale. Instead it is variable and is related to the scale at which bottom drag removes energy from the vertically-uniform mode (Figure 2).

Unlike in the classic picture of geostrophic turbulence, we find that the nonlinear inverse energy cascade does not extend between a deformation scale source and a larger scale sink (see [6]). Instead, it is part of a robust double cascade of energy. This newly identified mechanism results from a self-organization of the flow and leads to a local recycling of energy in scale space. In physical space, this mechanism is related to multiple, alternatingzonal-jet structures can develop in the ocean (in addition to the usual gyre circulation and mesoscale eddies) in responseto purely large-scale and steady-wind forcing (Figure 3).

Balance-imbalance interactions in the interior ocean
The inverse energy cascade of large-scale, quasi-two dimensional (anisotropic) rotating, stratified turbulence is in contrast to the forward energy cascade of small-scale, three dimensional, isotropic turbulence. The scales and phenomena that span these two asymptotic regimes of turbulence and the interactions of the flow with boundaries are then expected to hold, in part, the answer to the ocean-equilibration question above. The range of such processes include submesoscale and inertia-gravity wave processes and they are further broadly categorized into boundary and surface related processes, inertia-gravity wave processes, and other instability processes (e.g., see [2] and references therein). A great amount of research effort in the recent past has focused on surface and bottom boundary related processes (e.g., see [3] and references therein). Since atmospheric forcing of ocean circulation is mediated by the top surface, the importance of understanding the dynamics of this region cannot be over-emphasized. Nevertheless, a fundamental question remains as to whether surface-related processes are necessary to the activate pathways that lead to a forward cascade of balanced energy. Indeed, the bulk of the balanced energy resides in the vertical interior and there is the alternative (spatially) more local route to dissipation directly through the interior turbulent cascade. It is research into this latter alternative route to dissipation that led us to significant breakthroughs.

Accomplishments: We consider the nonlinear evolution of an interior baroclinic front in a regime of rotating stratified flow that is of direct relevance to circulation in the oceans---a regime characterized by small large-scale Rossby and Froude numbers and a small vertical to horizontal aspect ratio (see [7, 8]). Using high-resolution simulations of the non-hydrostatic Boussinesq equations and companion balanced integrations of the quasi-geostrophic equations, we find evidence for a local route to dissipation of balanced energy directly through interior turbulent cascades as opposed to boundary and surface related processes. In particular, we identify two phases of imbalance. Energetic consequences of the initial phase are minimal and characteristics of this phase of imbalance are similar to those of the kind of imbalance considered in previous studies. The second phase of imbalance has larger energetic consequences and evidence, including the robust formation of cyclonic spiral structures (Figure 4, left panel), suggests that ageostrophic baroclinic instabilities play an important role in setting up this interior dissipation route. Finally, we demonstrate, for the first time, an exponential scaling of interior dissipation with Rossby number (Figure 4, right panel).

Related work on parameterizations and statistical mechanical approaches resulted in two other publications [9, 10].

Impact on National Missions

This research directly supports one of the aims of the Biological and Environmental Research arm of the DOE Office of Science as relates to understanding of complex environmental systems across many spatial and temporal scales by coupling theory, model, and simulations. In particular, DOE seeks the ability to model climate variability towards providing environmental sustainability and stewardship. Proper representation of energy budget in the ocean model component will lead to a more realistic representation of ocean circulation and thus enhance its predictive capabilities.

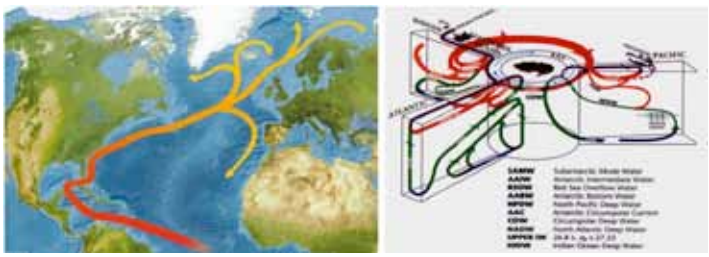

Figure 1. Global ocean circulation is forced at the large scales and controls climate variability. It is a combination of a) surface-intensified wind-driven circulation, as exemplified by the Gulf Stream and the subtropical gyre of the North Atlantic (shown on the left), and b) large-scale overturning circulation that is buoyancy- driven and popularly called the ``conveyor-belt'' circulation (schematic on right from Wood Hole Oceanographic Institution).

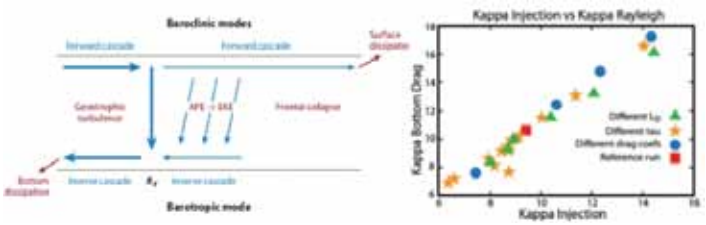

Figure 2. Schematic on left shows currently accepted phenomenology of geostrophic turbulence. In particular injection to vertically-uniform (barotropic) mode is at a fixed scale. Figure on the right shows our finding that this injection scale varies with the bottom drag scale showing that energy is injected into the vertically-uniform mode at the horizontal scale that is most energetic.

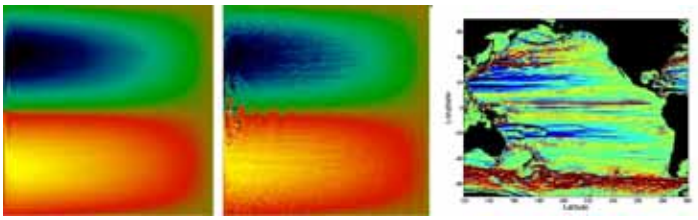

Figure 3. In an idealized setting of the wind-driven circulation, broad, sweeping flow in the interiors accompanied by swift return western boundary currents are expected (as on the left). Instability of such a circulation gives rise to mesoscale eddies (as seen in the western central region in the picture on the right). But we find for the first time that even with steady and large- scale winds alone, distinct multiple zonal jets—jets that are narrow in the latitudinal direction and elongated in the zonal direction—can appear (center). These jets are an explanation of recently observed alternating jets in the world oceans. For example, the right panel (from [1]), shows zonal velocity at 400 m. This study used POP, developed at LANL (http://climate.lanl.gov), and is forced by unsteady winds and buoyancy.

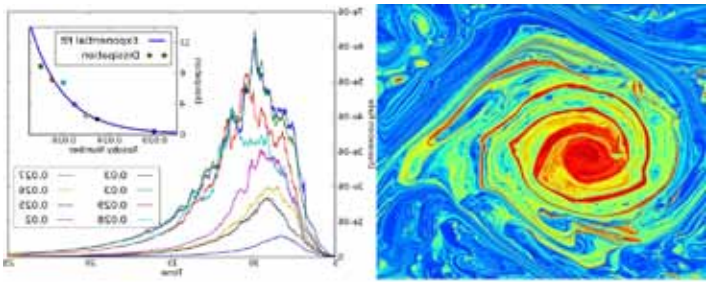

Figure 4. Snapshot of potential vorticity on a horizontal surface (left) from one of the high resolution runs that uses the most accurate description of dynamics. State-of-the-art ocean modelling studies are conducted at far coarser resolutions and using various other approximations. Imbalanced instabilities in this highly accurate simulation give rise to a spiral eddy. These eddies are ubiquitous in space imagery of the world oceans, but are not captured in state-of-the-art ocean models because of computational limitations. Right: Energetic consequences of the imbalanced instabilities as a function of Rossby number. As Rossby number increases, these instabilities become very important.

However, since they cannot be captured by state-of-the-art ocean models, our results suggest a parameterization of the effects of these instabilities. Such a parameterization will lead to improvements in predictive modeling of earth's climate.

References

1. Richards, K. J., N. A. Maximenko, F. O. Bryan, and H. Sasaki. Zonal jets in the Pacific Ocean. 2006. GEOPHYSICAL RESEARCH LETTERS. 33 (3): -.

2. Molemaker, M. J., J. C. McWilliams, and I. Yavneh. Baroclinic instability and loss of balance. 2005. JOURNAL OF PHYSICAL OCEANOGRAPHY. 35 (9): 1505.

3. Thomas, L. N., A. Tandon, and A. Mahadevan. Submesoscale processes and dynamics. 2008. In Ocean modeling in an eddying regime . , p. 17. Online: Wiley.

4. Nadiga, B. T.. On zonal jets in oceans. 2006. GEOPHYSICAL RESEARCH LETTERS. 33 (10): -.

5. Nadiga, B. T., and D. N. Straub. Alternating zonal jets and energy fluxes in barotropic wind-driven gyres. 2010. OCEAN MODELLING. 33 (3-4): 257.

6. Straub, D. N., and B. T. Nadiga. Energy fluxes in the quasigeostrophic double gyre problem . Journal of Physical Oceanography.

7. Nadiga, B. T.. Imbalance on a baroclinically unstable interior front . Journal of Fluid Mechanics.

8. Simon, G., and B. T. Nadiga. Instability of a periodic flow in geostrophic and hydrostatic balance . Physics of Fluids.

9. Nadiga, B., and F. Bouchet. The equivalence of the Lagrangian-averaged Navier-Stokes-Œ± model and the rational large eddy simulation model in two dimensions. 2011. Physics of Fluids. 23 (9): 095105.

10. Loxley, P., and B. Nadiga. Bistability and hysteresis of maximum-entropy states in decaying two-dimensional turbulence. 2013. Physics of Fluids. 25: 015113.

Publications

Connaughton, C., B. Nadiga, S. Nazarenko, and B. Quinn. Modulational instability of Rossby and drift waves and generation of zonal jets. 2010. JOURNAL OF FLUID MECHANICS. 654: 207.

Godinez, H., and B. T. Nadiga. Effects of coupling strength and stochastic parameterizations on data assimilation. 2012. In EGU General Assembly Conference Abstracts. (Vienna, 22-27 Apr. 2012). Vol. 14, p. 3413. Munich: EGU.

Loxley, P., and B. Nadiga. Bistability and hysteresis of maximum-entropy states in decaying two-dimensional turbulence. 2013. Physics of Fluids. 25: 015113.

Nadiga, B. T.. Stochastic approaches for multiscale modelling in geosciences. 2011. In European Geophysical Union, General Assembly 2011. (Vienna, Austria, 3-8 Apr. 2011). Vol. 13, p. 13064. Munich: European Geophysical Union.

Nadiga, B. T.. Flux of energy across scales in two oceanographic flows. 2011. In Balance, Boundaries, and Mixing in the Climate Problem. (Montreal, 28-30 Sep. 2011). , p. --. Montreal: Centre de Recherches Mathematiques.

Nadiga, B. T.. Imbalance on a baroclinically unstable interior front . Journal of Fluid Mechanics.

Nadiga, B. T., and D. N. Straub. Alternating zonal jets and energy fluxes in barotropic wind-driven gyres. 2010. OCEAN MODELLING. 33 (3-4): 257.

Nadiga, B. T., and D. N. Straub. Zonal jets and energy cascades in the baroclinic ocean double gyre problem. 2011. In American Geophysical Union Fall Meeting. (San Francisco, CA, 5-9 Dec. 2011). , p. OS41A. Washington D.C: AGU.

Nadiga, B. T., and F. Bouchet. When can we expect statistical mechanics to help predict large scale atmospheric and oceanic features?. 2010. In American Geophysical Union, Fall Meeting 2010. (San Fransico, 13-17 Dec. 2010). , p. B1209+. Washington D.C.: American Geophysical Union.

Nadiga, B. T., and T. J. O'Kane. Predictability of Low-Frequency Regime Transitions in the Barotropic Vorticity Equation Driven by Weak Stochastic Forcing. 2011. AGU Fall Meeting Abstracts. : B1487.

Nadiga, B. T., and W. R. Casper. Energy cascade in the regime of realistic ocean circulation. 2011. In Annual Meeting of the American Physical Society Division of Fluid Dynamics . (Baltimore, MD, 20-22 Nov. 2011). Vol. Bulletin of the APS, 56, p. L1.008. New York: American Physical Society.

Nadiga, B., and F. Bouchet. The equivalence of the Lagrangian-averaged Navier-Stokes-Œ± model and the rational large eddy simulation model in two dimensions. 2011. Physics of Fluids. 23 (9): 095105.

Simon, G., and B. T. Nadiga. Instability of a periodic flow in geostrophic and hydrostatic balance . Physics of Fluids.

Straub, D. N., and B. T. Nadiga. Energy fluxes in the quasi-geostrophic double gyre problem . Journal of Physical Oceanography.

Time-dependent Quantum Molecular Dynamic Simulations of Dense Plasmas Supporting Thomson X-ray Scattering Experiments

Jerome O. Daligault
20110228ER

Abstract

We have developed a computational capability that solves the real-time dynamics of strongly interacting quantum electrons and classical ions in dense plasmas. This capability allows the calculations of truly dynamical and non-equilibrium properties that are inaccessible to state-of-the-art quantum molecular dynamics approaches. We have begun to use this unique tool to develop a fundamental physics understanding of correlation and quantum effects on the properties of dense plasmas, to foster and validate better models of dynamical processes in dense plasmas, and to assist and motivate experiments.

Background and Research Objectives

The understanding of strongly coupled quantum plasmas is an important challenge in modern physics. The new generation of X-ray light sources, such as the Linac Coherent Light Source at Stanford, holds the promise to profoundly advance our fundamental understanding of dense plasmas. X-ray scattering experiments will be performed with far greater spatial and energy resolution, and will provide access to measurements that have so far been impossible. As suggested by early experimental efforts, the ability to model dynamical and non-equilibrium systems must be developed if we are to maximize the scientific impact of the wealth of data from those experiments. Indeed, in addition to the in-situ measurements, the coming experiments will make it possible to measure genuine dynamical properties of dense plasmas. Moreover, by their nature dense plasma experiments generally produce highly time-dependent (i.e. non- equilibrium) situations. Finally, time-dependent simulations are required to support application-driven experiments, e.g. to assess the effectiveness of energy deposition by charged projectiles in fast ignition physics.

The main goal of this project is to enable first-principle simulations of dense plasmas both in and out of equilibrium. To this end, we have developed a new modeling capability that solves the real- time dynamics of strongly interacting quantum electrons and classical ions in warm dense matter and dense plasmas. The capability enables the calculation of truly dynamical and non-equilibrium properties that are so far inaccessible with state-of-the-art quantum molecular dynamics (QMD) approaches.

Scientific Approach and Accomplishments

Simulation capability

As described in the proposal, we briefly recall that the new simulation tool solves a mixed quantum-classical dynamics that involves an approximation of the time-dependent DFT (TDDFT) equations for the electrons and the classical equations of motion for the ions; TDDFT extends the basic ideas of equilibrium DFT implemented in the state-of-the-art simulation codes to the treatment of time-dependent phenomena. It allows for a truly dynamical treatment of the electrons, with no reliance on the Born-Oppenheimer approximation. While the high computational cost of TDDFT has so far limited its application to small atomic systems (e.g. molecules in intense laser fields), we believe that the next generation computational resources will bring its application to bulk systems within reach.

We refer to our approach as the Time-Dependent Thomas-Fermi approximation (TDTF) since it can indeed be regarded as the extension to time dependent phenomena of the popular Thomas-Fermi model used to model the equilibrium properties (e.g., equations of state) of dense plasmas. The electrons are described as a (quantum) distribution function f(r,p,t) in phase-space, which contains not only information on the electron particle density but also on its dynamics, e.g. the electronic current. The distribution function evolves according to a Vlasov-like kinetic equation that is coupled to the classical ion dynamics RJ(t). This traditional structure of the kinetic equation is very advantageous since it allows using the numerical methods of traditional plasma physics. Accordingly, the numerical methods that we have been

implementing make use of ideas of the particle-in-cell (PIC) and molecular dynamics (MD) methods, combining particle-particle and particle-mesh calculations. To solve the Vlasov-like equation, we thus decided to use a so-called "test particles method", where the distribution function f (r, p, t) is sampled with a swarm of Ntp test particles centered at rk(t) and momentum pk(t) By direct substitution, the solution of (1) amounts to the solution of coupled Newton's equations, which lies in the realm of classical molecular dynamics simulations. Because it involves the dynamics of long-range interacting particles, the problem is particularly adapted to the molecular dynamics capability previously developed by the PI Daligault especially for this type of interactions. The latter uses the state-of- the-art Particle-Particle-Particle-Mesh (P3M) algorithm, which combines high-resolution of close encounters (PP) and mesh-based long-range force calculation (PM), and the particle dynamics are resolved using the Verlet algorithm in periodic boundary conditions. In its current version, the code allows the simulation of large, complex purely classical Coulomb systems, including mixtures, Coulomb and screened Coulomb systems containing up to several millions of particles, and over long time scales; in the past, the code was successfully used to address investigate key microphysical properties of dense plasmas of importance to laser-produced high-energy-density plasmas and astrophysical plasmas.

A flowchart of the algorithm is shown in Figure 1. The algorithm combines both molecular dynamics techniques (as used in material sciences) and particle-in-cell (PIC) simulation techniques (as used in traditional plasma physics). We note the interesting fact that the test-particle method is a particle-mesh approach similar to the standard PIC, except that in traditional applications of PIC each test particle represents many real particles whereas here each test particle represents a fraction of a physical electron. The code is written in Fortran 95 and implemented in parallel using Message Passing Interface (MPI)). We are currently testing the performances of the algorithm as a function of the various purely numerical parameters (> 10 parameters), including the number of numerical particles, the mesh size and various parameters involved in the P3M method. We have determined the domain of stability of the code as a function of the numerical parameters, where stability is measured by the time over which a simulation conserves energy, entropy and fermionic character.

A salient development in this year (that we had not initially envisioned) has been the implementation of the delta-f method, a state-of-the-art method developed in plasma physics to accurately solve the gyro-kinetic equations. In the delta-f method, the distribution function f=f0+delta f, where f0 is known (either analytically or numerically) and "delta f" represents the part of the distribution that is being calculated with test particles. This greatly reduces the noise inherent to P3M simulations. We have developed a version of the delta-f method that is suitable to our problem and have successfully implemented it. The number of numerical particles needed is reduced by at least one order of magnitude from that needed by the brute-force implementation that we had originally envisioned.

We have also developed a separate code to construct the initial conditions of the main capability. Given an ionic configuration at initial time t0, one needs to know the initial electron distribution function f(r,p,t0), which is strongly spatially inhomogeneous. While testing the main code with fixed ionic impurities as originally planned in the proposal, we realized that our original scheme for the initial conditions was not accurate enough, and therefore we decided to implement an alternative, but much more complicated method. The development of this auxiliary code called for significantly more time and efforts that we had anticipated. It uses an approach recently presented in Phys. Rev. E 73, 016403 (2006) and solves the equilibrium Thomas-Fermi equations using techniques developed in density functional theory (including Car-Parrinello, Fourier transform based field solver...) We have successfully implemented this approach and validated it by comparison with results in the literature. As a by-product, this code gives us access to equilibrium properties of dense plasmas. We have made contact with equation-of-state experts at Los Alamos (D. Saumon, XCP-5), who have shown great interest in our new numerical capability. Together with the main code, both equilibrium and nonequilibrium properties will be accessible within the same simulation capability (e.g. calculate self-consistently the equation of state, electron conductivity and ion viscosity of a dense plasma).

Finally, we have developed our own average-atom code in order to build various electron-ion interaction potentials needed in the main code. In the average atom model, the plasma surrounding an atom is smeared out and replaced by a boundary condition; the model amounts to considering a neutral atom of finite size a, where a is the interionic distance. There are two main kinds of potentials depending on whether one considers all the electrons in the plasma on the same footing or whether one discards the tightly bound electrons. In all electron calculations, which are required when dealing with fully ionized plasmas, the electron-ion potential should in principle be the bare Coulomb potential shown in blue. However, it is well known that the TF density is ill behaved and diverges at the ionic position. This is illustrated in Figure 2 by the blue line that shows the TF electron density as a function of the

distance from a nucleus. To deal with this we regularize the electronic density below some cutoff radius rc, and use this density to get a regularized potential by inverting the TF equation, which is illustrated here by the red line. In the second case, a nucleus and its cloud of tightly bound electrons are described by an effective, pseudopotential.

Simulation results

1) Conservation of fermionic character: a very strong constraint on the numerical scheme is that it must conserve the quantum fermionic character of the distribution function f used to describe the electrons. The evolution equation that is being solved is a Liouville equation: it preserves the phase-space volume and therefore preserves the number of electrons per unit of phase-space volumes imposed by the Pauli principle. Another way of saying the same thing is to say that the evolution equation solved by the new code does not create entropy. However, numerically, due to the discretization of the equations, one actually solves the latter approximately only. One solves an equation that contains a spurious collision term due to all the glitches caused by the numerical approximations. This collision term irreversibly lead to the ”Boltzmannization” of the distribution function. It is important that this Boltzmannization occur as late as possible. We have tested the numerical scheme on the jellium model, where a uniform background that neutralizes the electron system replaces ions. Figure 3 shows the occupation number, i.e. the distribution of energy states, for a partially degenerate electron gas at three different times in units of inverse plasma frequency. Over this time scale, the quantum statistics is well conserved and spurious collisions have not ruined the dynamics yet.

2) Landau Damping and the Onset of Particle Trapping in Quantum Plasmas. The notion of wave-particle interactions, the coupling between collective and individual particle behaviors, plays a fundamental role in modern plasma physics. Landau damping, the collisionless damping of an electron plasma (Langmuir) wave, is a paradigmatic illustration of the effectiveness of wave-particle couplings in plasmas. Resonant electrons with velocities sufficiently close to the wave phase velocity experience a nearly constant force and so can efficiently exchange energy with the wave. For Langmuir waves of vanishing amplitude about a uniform equilibrium, the energy exchanges overall result in the exponential damping of the wave amplitude in time at a rate g(k) (k is the wave number). In general, this linear theory prediction breaks down after a time O(1/\w(k)) beyond which particles can get trapped and oscillate at a bounce frequency wB(k) in the potential troughs of the electrostatic wave. Landau damping is effective provided g(k)<< w_B$, while when g(k)<< wB(k), the damping saturates and the wave amplitude remains finite (neglecting collisions). The question arises as to how these classical wave-particle couplings are modified in quantum plasmas, as occurs when the electron Fermi energy EF(n and m are the electron density and mass) exceeds the thermal energy kBT. Here, the Fermi-Dirac (FD) statistics should substitute the Maxwell-Boltzmann (MB) statistics and one should ascribe wave-like attributes to the electrons. Understanding the properties of quantum plasmas (e.g., warm dense matter) is a frontier of high-energy density physics with relevance to laboratory experiments and astrophysics, which has recently been emboldened by new experimental facilities and high-performance computing.

Until now, most theoretical and numerical studies have relied on linear response theory, whereby the fluctuation-dissipation theorem connects equilibrium properties to transport properties such as electrical conductivities or Thomson scattering cross sections. Nonlinear effects such as trapping have been ignored, although laboratory experiments often create non-equilibrium conditions. With our new tool, we have investigated the onset on electron trapping in quantum plasmas across the degeneracy regimes, from fully-degenerate, zero temperature to classical, high-temperature plasmas. We assessed for the first time the onset of particle trapping in electron plasma waves in quantum plasmas. In addition to the characteristic classical time scales, namely the plasmon frequency, linear Landau damping rate and bounce frequency in the electrostatic wave trough, quantum trapping depends on an additional time scale related to the recoil of electrons after absorption/emission of plasmons.

Figure 4 shows the results of simulations for the time evolution of the Fourier component of the electric field E(k,t) as obtained with an initial standing wave of (dimensionless) amplitude epsilon=0.005 for a number of initial wavevectors k around the trapping threshold value k* discussed before for reduced densities rs=1 and degeneracy parameters EF/kBT = 0.1 (degenerate) and 7.5 (classical regime); Here rs=n-1/3/aB is the reduced density, EF is the Fermi energy, T the temperature . In both cases, for wavevectors k>k*, we observe that, after a fast transient time due to phase mixing, the electric field oscillates and its amplitude envelope decays exponentially in time with frequency and damping time in excellent agreement with linear theory (see blue crosses in the figure). For long-wavelengths k< k*, while the wave amplitude display a preliminary exponential Landau decay (again in remarkable accordance with linear theory as shown in Figure 4) then the latter saturates: the amplitude starts oscillating on a small frequency time scale, the amplitude of which increases with decreasing k. For k<< k*, in the time asymptotic limit, the

trapping oscillation in the electric field envelope disappear and the wave goes on propagating at constant amplitude. These are signatures of trapping: nonlinear effects stop the damping at a threshold in agreement with the theory, even for small amplitude waves, chance that trapped particle dynamics play an important role in the evolution of the system long before the wave has had a chance to damp by a substantial amount according to linear theory.

Impact on National Missions

A new and unique simulation capability in modeling extreme states of matter at LANL has been developed. The capability will allow significant scope for exploration of non-equilibrium conditions in dense plasmas and materials under extreme conditions (e,g, radiation damage, ion slowing-down, non-equilibrium phase transitions). This work enhanced our basic science capabilities, enabling LANL to better meet its mission challenges, including the science campaigns, Advanced Scientific Computing (ASC) and national High Energy Density Laboratory Plasma (HEDLP) programs. This exploratory research has strong ties to two LANL grand challenges, namely “Materials: Discovery Science to Strategic Applications” and “Nuclear Performance”, and to the areas that will be explored in the future MaRie facility at LANL. We are exploring potential funding opportunities with the interested program managers.

Overall, this project advances methods and predictive power for the burgeoning area of warm dense matter, with potentially significant impact on high-energy density physics modeling, including inertial-confinement fusion physics. Those applications aside, the theoretical understanding of and tools for simulation of dense plasma physics are highly cross-disciplinary as dense plasmas are exactly where the methods of condensed matter physics and plasma physics each lose traction.

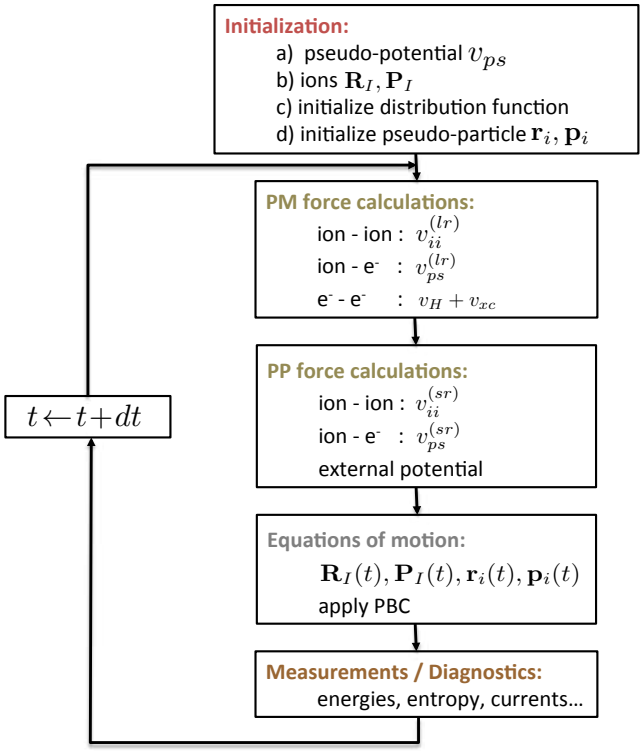

Figure 1. Flowchart of the algorithm implemented. Here are the salient characteristics of the numerical scheme. We consider periodic boundary conditions so that the main simulation cell represents a small but representative chunck of a plasma. First a few words about the ions. They interact through the bare, long- range Coulomb interaction and require an Ewald summation to account for the interaction with periodic replicas. A very good algorithm to deal with this is the so-called particle-particle particle-mesh or P3M algorithm, which is a sophisticated way of dealing with Ewald summation. It combines high-resolution of individual encounters and rapid, mesh-based, long-range force calculation. Briefly, the Coulomb potential is split into two part, for instance with the help of an error function: a short-range part that contains the singularity at the origin, and the remaining part that is long-range and is smooth enough so that its Fourier transform vanishes very rapidly with increasing wavevector. The resulting short-range forces are treated using traditional molecular dynamics techniques such as nearest-neighbor lists and constitute the PP part of the P3M algorithm. As for the long-range forces, they are calculated on a mesh in a way that is not unlike what is done in particle-in-cell code. First the particles are assigned on the mesh, and the force field is calculated on a mesh by solving a Poisson equation using fast-fourier transforms. The force field is interpolated back onto the particles.

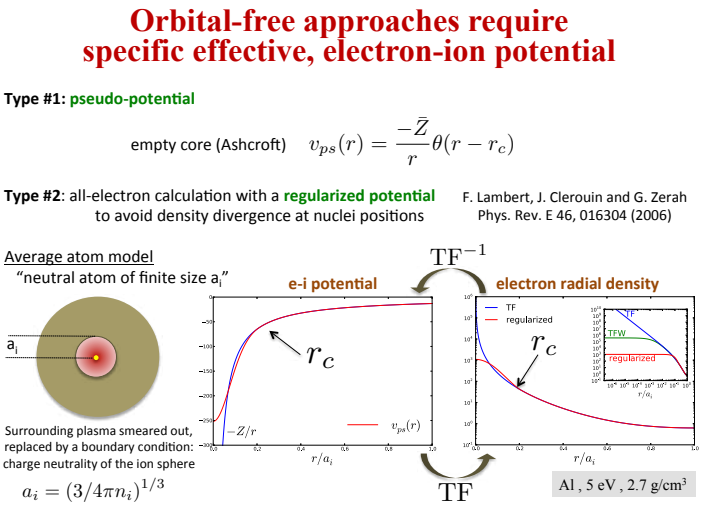

Figure 2. Electron-ion pseudo-potential calculation using the Thomas-Fermi average atom model.

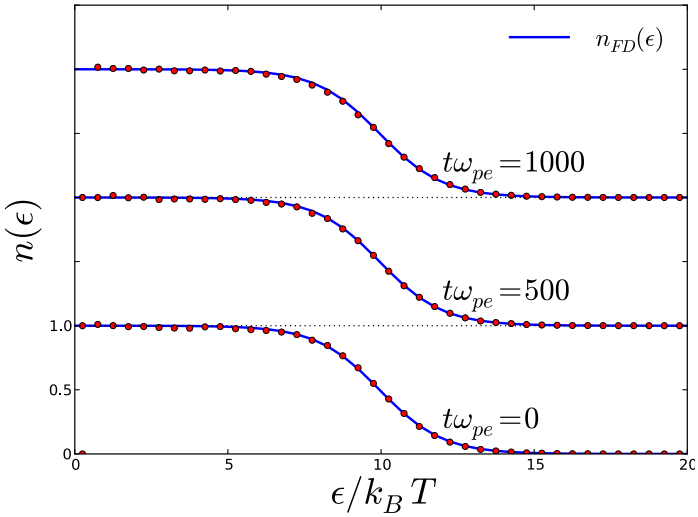

Figure 3. Distribution of energy states, for a partially degenerate quantum electron plasma at three different times in units of inverse plasma frequency (conditions: rs=a/aB=0.1, degeneracy EF/kBT =0.1, where a is the inter-particle distance, aB the Bohr radius, kBT the temperature, and EF the Fermi energy.) The blue line is the exact Fermi-Dirac distribution function for these conditions, and the red dots show the occupation number extracted from the code at different times.

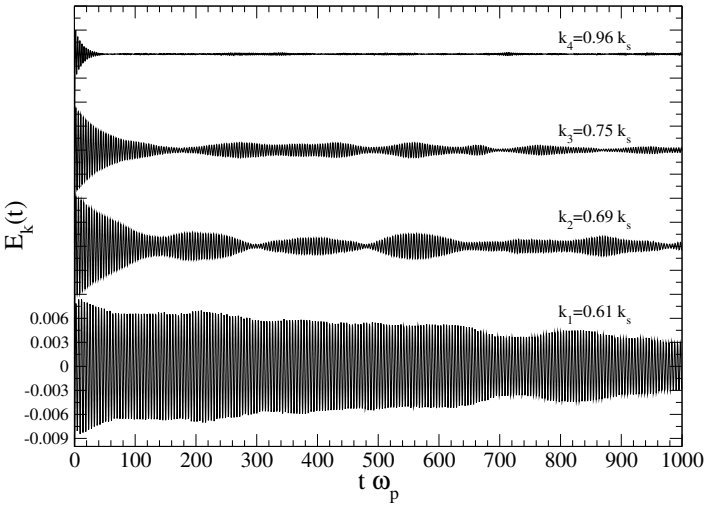

Figure 4. Damping of electrostatic plasma wave in a quantum plasma.

References

1. Daligault, J.. Nonlocal orbital-free noninteracting free-energy functional for warm-dense matter. To appear in Physical Review B.

2. Daligault, J.. Time-Dependent Thomas-Fermi Simulations of Dense Plasmas. Invited presentation at international meeting "Orbital-Free Density Functional Methods. (Paris, Sept. 2012).

3. Daligault, J.. Non-Adiabatic Electron-Ion Coupling in Quantum Molecular Dynamic Simulations. Invited presentation at Workshop on "Nonequilibrium Phenomena, Nonadiabatic Dynamics and Spectroscopy". (Tellurides, CO, July, 2013).

Publications

Daligault, J.. Time-Dependent Thomas-Fermi Molecular Dynamics Simulations of Dense Plasmas. Invited presentation at Computational Challenges in Warm Dense Matter, long program Computational Methods in High Energy Density Plasmas held at the Institute for Pure and Applied Mathematics (IPAM). (Los Angeles, 21-25, 2012).

Daligault, J.. Orbital-Free Molecular Dynamics Simulations of Dense Plasmas. Invited presentation at CECAM workshop on "Orbital-free approach for high energy density physics". (Paris, France, 5-7 Sept. 2012).

Mithen, J. P., G. Gregori, and J. Daligault. Comparative merits of the memory function and dynamic local field correction of the classical one-component plasma. 2011. Physical Review E. 85 (5): 056407.

Mithen, J. P., J. Daligault, B. J. B. Crowley , and G. Gregori. Density fluctuations in the Yukawa one-component

plasma: an accurate model for the dynamical structure factor. 2011. Physical Review E. 84: 046401.

Mithen, J. P., J. Daligault, and G. Gregori. Applicability of the hydrodynamic description of classical fluids. 2011. Physical Review E. 83: 015401(R).

Mithen, J. P., J. Daligault, and G. Gregori. Molecular Dynamics Simulations for the Shear Viscosity of the One-Component Plasma. 2012. Contributions to Plasma Physics. 52 (1): 58.

Mithen, J. P., J. Daligault, and G. Gregori. Onset of negative dispersion in the one-component plasma. 2012. Proceedings of the Strongly Coupled Ultra Cold and Quantum Plasmas conference in Lisbon, held in Lisbon in September 2011.. 2012 (1421): 68.

Precision Measurement of Atomic Parity Violation in Trapped Yb+

Martin M. Schauer
20110258ER

Abstract
Atomic parity non-conservation (PNC) experiments have provided constraints on physics beyond the standard model that rival those of accelerator-based experiments such as the LHC but in a very different energy regime. PNC measurements in trapped ions have the potential to improve the sensitivity of such experiments by an order of magnitude or more. We have developed an experiment based on single, trapped, Ytterbium ions with demonstrated sensitivity sufficient to begin to search for PNC effects.

Background and Research Objectives
A single trapped ion provides a superior system for studying all aspects of atomic structure and numerous fundamental questions about quantum mechanics, but it has yet to be fully exploited for studying nuclear structure, the Weak interaction, or extensions to the Standard Model. Parity non-conservation is uniquely sensitive to the relatively small signals due to the weak interaction, since all other known interactions conserve parity. A measurement of atomic PNC to 0.1% would be sensitive to new heavy gauge bosons with masses up to about 2.5 TeV [1][2].

PNC has been measured in atomic system with precisions of about 1% [3], but these measurements are currently limited by sensitivity, systematic effects, and atomic structure unknowns. A trapped ion provides a system for making the same measurement with the possibility of more than an order of magnitude improvement in sensitivity and more easily understood systematic uncertainties. In addition, using an ion trap allows identical measurements of a number of nuclear isotopes of the same atom which would dramatically improve interpretation of the results by factoring out difficult-to-calculate aspects of atomic structure.

Measurements on Ba+ ions based on a method proposed by Fortson [4] did not reach the necessary sensitivity due technical issues revolving around laser development and certain systematic effects. Later work by Schacht showed how to address the most troublesome systematic effects [5]. This development along with the more easily accessible laser wavelengths for Ytterbium ions led to the proposed work discussed here. The goal of this research was to demonstrate the viability of this approach in Yb+ ions.

Scientific Approach and Accomplishments
The largest effect of the weak interaction in atomic systems is the mixing of certain atomic states. In the case of Yb+ the effected states are the 2S1/2 and 2P1/2. The result of the weak interaction is that the ground state no longer has completely well-defined parity. Hence the transition amplitude for the 2S1/2 to 2D3/2 state now has a small dipole component in addition to electromagnetically-allowed quadrupole component. These components will have different spin dependences, and this will result in different AC Stark shifts, or light shifts, for transitions between different mj magnetic sublevels of the atomic states. We seek to measure the size of this spin-dependent shift, since it can provide constraints on physics beyond the standard model of particle physics.

Broadly speaking, there are two key areas which will determine our ability to make this measurement: the accuracy with which we can measure the frequency of the hyperfine transitions and the size of the laser-induced AC Stark shift. We are now able to measure the 12.6 GHz center frequency of the magnetic-field-insensitive F=0, mf=0 to F=1, mf=0 transition with a precision of 0.05 Hz/hr1/2 and the F=0, mf=0 to F=1, mf=±1 transitions with a precision of better than 10 Hz/hr1/2.

We have developed a laser source to drive the 436 nm S-D transition, thereby providing the necessary light shift, which regularly operates at 70 mW of laser power. A 100 mW laser beam focused to a 10 µm spot will produce a 1 GHz spin-independent quadrupole shift and a 1

Hz spin-dependent, PNC-induced dipole shift when on resonance. Given this laser power, the 10 Hz/hr1/2 sensitivity we have achieved is therefore sufficient to distinguish the PNC-induced shift from the quadrupole shift within about 100 hours of observation time, well within the capabilities of our apparatus.

We have measured light shifts of several Hz with the 436 nm laser detuned from resonance. With these relatively small shift,s we are only sensitive to the quadrupole-induced component of the light shift. In order to increase the magnitude of the light shift, the laser must be brought closer to resonance with the S-D transition frequency. This is in itself not difficult, but must be done in a deliberate way to understand systematic effects such as laser polarization and frequency stability. It is possible that additional frequency stabilization of the laser will be required, and although this is not trivial, such stabilization is a well established technique.

The above-mentioned precision was achieved with no magnetic shielding. This is quite remarkable, since the $\Delta mF=\pm1$ transitions suffer from linear Zeeman shifts. This precision was achieved through careful attention to the trap environment, but more importantly, by rigorous statistical analysis of the pump-probe process that lies at the heart of these measurements. We are not aware of any other ion trap experiments that have incorporated such an analysis, and this may prove to be a valuable technique for numerous other experiments. Several manuscripts describing this work are under preparation. Furthermore, a measurement of the lifetime of the D-state, which is important for the eventual interpretation of any PNC measurements, was made using these methods, and a manuscript describing this work is under review.

Some increased precision can be achieved by shielding the trapped ion from ambient magnetic fields. We have constructed and started to test a new trap that has magnetic shielding incorporated into the vacuum system. This should provide magnetic field suppression at the location of the trapped ion by a factor of at least 1000 over the unshielded trap. However, this would only result in about a factor of two improvement in the linewidth, since fluctuations in the intensity of the 436 nm laser presently contribute a roughly equal amount to the linewidth as magnetic foiled noise does in the unshielded trap. Further improvement in the sensitivity would require intensity stabilization of the laser or the use of a standing wave at the ion location. Full implementation of the new trap has not been achieved as of this writing.

Impact on National Missions

The tools and infrastructure developed in the course of this experiment are directly applicable to other LANL efforts, most notably the recently approved work on Thorium metastable nuclear states. This work, if successful, could lead to clocks and sensors of unprecedented sensitivity.

Development of the high power 436 nm laser involved doubling of an 871 nm Ti::Sapphire laser through the use of nonlinear crystals in a high finesse resonant cavity. The thorium work requires the generation of vacuum ultraviolet (VUV) light (<200nm) to drive atomic transitions, as well as the nuclear transition, through the same sort of techniques albeit in a much more challenging regime. The experience gained on the 436nm laser will be directly applicable to the VUV system.

Identification of the Thorium nuclear state will be done through pump/probe experiments, the same technique used to measure the transition frequencies of the atomic levels in Ytterbium mentioned above. Hence, the optimization techniques developed here will be indispensable to extracting the small signals one can expect to encounter in the Thorium work. More generally, interpreting those signals will require a thorough understanding of the atomic physics at play, just as in the Ytterbium experiments.

At a wider level, the techniques developed to deal with systematic effects and the surprisingly high sensitivity should reinvigorate the PNC experiment community. It is interesting to note that there are a large number of experiments that fall into the pump/probe class and that the statistical techniques developed here may be of interest to this broader national community.

Finally, our techniques are potentially applicable to the analysis of picoscale samples for forensics and non-proliferation missions.

References

1. Rosner, J. L.. Atomic p[arity violation and precision electroweak physics. 1999. Physical review D. 61 (1): 016006.

2. Rosner, J. L.. Atomic parity violation as a probe of new physics. 1990. Physical Review Letters. 65 (24): 10.

3. Wood, C. S., S. C. Bennet, D. Cho, B. P. Masterson, J. L. Roberts, C. E. Tanner, and C. E. Weiman. Measurement of parity nonconservation and an anapole moment in cesium. 1997. Science. 275 (5307): 1759.

4. Fortson, N.. Possibility of measurinr parity nonconservation with a single trapped atomic ion. 1993. Physical Review Letters. 70 (16): 2383.

5. Schacht, M.. Precision measurement of p-odd neutral

currents in trapped ions. 2011. LDRD ER proposal.

Publications

Schacht, M., J. R. Danielson, S. Rahaman, J. R. Torgerson, J. Zhang, and M. M. Schauer. 171Yb+ 5D3/2 hyperfine state detection and F=2 lifetime. Physical Review A.

Schacht, M., and M. M. Schauer. Shelving and probe efficiency in trapped ion experiments. Physical Review A.

The Largest Cosmic Implosions: Formation of Supermassive Black Holes

Hui Li
20110300ER

Abstract

The past decade has witnessed the astonishing discovery that supermassive black holes (SMBHs) reside in the centers of nearly all galaxies exist at redshift z ~6.5, less than one billion years after the Big Bang. To understand the formation of supermassive black holes in the early universe, we have performed extensive numerical simulations to understand the formation of massive stars in the early universe and their impact on their surroundings. We showed that, at a high accretion rate, massive stars could be turned into massive seeds for SMBH formation. Various SMBH growth history and models are calculated and compared with available observational constraints. In addition, we have investigated the processes of angular momentum transport in the formation processes. These studies have provided critical information for future strategies of major observatories such as WFIRST. Capabilities built through this project (including postdoc training) have contributed well to programmatic research and recruiting.

Background and Research Objectives

To form SMBHs so early in the Universe, the center of a galaxy must accumulate about 1065 baryons in a region the size of our solar system on a short timescale. The physics of the SMBH formation has become an important mystery, given the important roles of SMBHs in cosmology, in cosmic re-ionization, and in shaping the subsequent cosmic structure formation. Understanding such systems thus poses one of the most exciting challenges in modern astrophysics where gravity, magneto-hydrodynamics and radiation-hydrodynamics of baryons must work collectively to accommodate such an extreme outcome.

The primary scenario we studied in this project is that the gravity of matter in a high density region of the primordial background plasma will eventually lead to the formation of a massive “seed” at the center of baryon and dark matter halo. This seed then grows its mass by accretion, though its strong radiation will tend to regulate how much material can accrete and how fast material can accrete. The more massive the seed is, the more likely it can reach supermassive black hole early in the universe, as indicated by the observations.

During the past several years, we have made important progress in addressing the black hole formation problem. Some critical questions we investigated include: 1) what is the likely mass of the “seeds” of SMBHs? 2) Will the formation of massive “seeds” eventually overcome the radiation feedback to form SMBHs? 3) What regulates the angular momentum transport during the collapse leading to compact object formation? LANL has the unique advantage of being able to model the collapse of cosmological halos together with the central object’s implosion and explosion. The results obtained thus far have placed LANL at a strong position for the up-coming revolution in astronomy to be initiated by the James Webb Space Telescope and WFIRST in the coming decade.

Scientific Approach and Accomplishments

We have completed one major study on understanding the formation and growth of massive “seeds”. We investigated the collapse of baryons into extremely massive stars (with masses higher than 10,000 solar masses) in a small fraction of proto-galaxies. We have determined the maximum masses such stars can attain by accreting primordial gas, which depends on how fast material can accrete. We find that, at relatively low accretion rates, the strong ionizing radiation of these stars will limit the growth of these seeds. On the other hand, our extensive numerical simulations of protogalactic collapse have shown that the accretion rates unto these primordial stars can be quite high. In fact, under these high rates, the massive star mass can reach even about 1,000,000 solar masses, almost 1% of a SMBHs. This is because the radiation produced by the forming massive star is confined deep within the protogalaxy so its feedback is

limited and de-coupled from the rest of host galaxy. In addition, our detailed analyses led us to conclude that initial BH seeds may have been as massive as 100,000 solar masses. This conclusion is strongly in favor of the direct collapse scenario of SMBH seed formation, in which a supermassive primordial star forms in a region of the universe with a high molecule-dissociating background radiation field, and collapses directly into a 10,000 – 1,000,000 solar mass seed BH. These results corroborate recent cosmological simulations and observational campaigns that suggest that these massive BHs were the seeds of a large fraction of the SMBHs residing in the centers of galaxies today.

Next, we have completed a large number of simulations to understand the impact of the birth and death of massive stars that provide insights into the early stages of the SMBH growth. The numerical studies were carried on several fronts: First, we simulated the effects of the explosion of one such massive star, to understand whether it helps fuel the rapid growth of a massive black hole by changing the cooling processes in the surrounding gas. Second, we investigated the blast wave from these explosions in terms of how it can deposit dense metal-enriched material into the surroundings. We have modeled the light curves and spectra of the first supernovae in the universe with the radiation hydrodynamics code RAGE with various types of explosions: core-collapse, pair-instability, Type IIn and supermassive thermonuclear events.

Overall, our extensive theoretical and numerical studies have not only enabled a deeper understanding of the formation processes of SMBHs, but also produced several testable predictions. In fact, because the radiations from the growing star are trapped, they are likely to be reprocessed into strong Balmer series emissions, which may be observable by the James Webb Space Telescope. This, strong He II with wavelength at 1640 λm, and continuum emission are likely to be the key observational signatures of the progenitors of SMBHs at high redshift. Furthermore, we have discovered that these ancient explosions will be detectable by the James Webb Space Telescope (JWST) and the Wide-Field Infrared Survey Telescope (WFIRST) at the earliest epochs in the universe. These simulations are also having a real science impact on the astronomy community. Lead scientists who are leading the development of NASA's next major observatory WFIRST have consulted us on filter designs for WFIRST to detect these ancient events in the near infrared, and have solicited contributions from LANL on the science case for WFIRST to be submitted to NASA. We have also been contacted by several independent groups of astronomers for assistance in devising searches for the earliest supernovae in the universe, Population III SNe. Reporters have also contacted us about our work, which has appeared in the June 12, 2013 issue of New Scientist (The Supernova that Blew up a Galaxy). Our numerical models have culminated in a number of Journal publications.

Impact on National Missions

The work has addressed one of the most exciting and fundamental questions in modern astrophysics and cosmology, namely how the supermassive black holes (SMBHs) form at the centers of galaxies in the early Universe. The project has also advanced LANL's capabilities in: a) large-scale computational astrophysics by studying multi-dimensional gas collapse physics, b) cosmology by simulating the formation of SMBH from galaxy scale to black-hole scale, nuclear and particle physics by investigating the neutrino cooling signatures during the SMBH formation. Through making important contributions in this forefront scientific challenge, we have enhanced LANL's scientific reputation and attracted top scientists to the Laboratory. One postdoc has been converted to be a staff member, working in a programmatic area. The other postdoc has also gotten involved in programmatic research as well, supporting the nuclear security mission.

Publications

Fryer, C. L., and A. Heger. Forming massive black holes through stellar collapse: Observational diagnostics. 2011. Astronomische Nachrichten. 332: 408.

Guo, F., S. Li, H. Li, J. Giacalone, J. R. Jokipii, and D. Li. ON THE AMPLIFICATION OF MAGNETIC FIELD BY A SUPERNOVA BLAST SHOCK WAVE IN A TURBULENT MEDIUM. 2012. ASTROPHYSICAL JOURNAL. 747 (2): 98.

Johnson, J. L., H. Li, D. J. Whalen, and D. E. Holz. Supermassive Seeds for Supermassive Black Holes. 2013. Astrophysical Journal. 771: 116.

Johnson, J., D. J. Whalen, W. Evan, C. L. Fryer, J. Smidt, A. Heger, and K. Chen. The Biggest Explosions in the Universe. To appear in Astrophysical Journal.

Johnson, J., D. J. Whalen, W. Even, C. L. Fryer, A. Heger, J. Smidt, and K. Chen. The Biggest Explosions in the Universe. To appear in Astrophysical Journal.

Johnson, J., D. Whalen, C. Fryer, and H. Li. THE GROWTH OF THE STELLAR SEEDS OF SUPERMASSIVE BLACK HOLES. 2012. ASTROPHYSICAL JOURNAL. 750 (1): 66.

Li, S.. High-order time integration with local Lax-Wendroff procedure for central scheme on overlapping grid. 2012. Journal of Computational and Applied Math. 236: 4756.

Li, S.. Code comparison on MHD wave propagation problems. 2012. In Numerical Modeling of Space Plasma

Flows: ASTRONUM2011. (Valencia, Spain, 13-17 June, 2011). Vol. 459, p. 353. Valencia, Spain: ASP Conference Series.

Si, J., S. Colgate, H. Li, J. Martinic, D. Westpfahl, J. Slutz, B. Klein, P. Schendel, C. Scharle, T. McKinney, R. Ginanni, I. Bentley, T. Mickey, and J. Lacy. Data Acquisition in a High-Speed Rotating Frame for New Mexico Institute of Mining and Technology Liquid Sodium αω dynamo experiment. To appear in Review of Scientific Instrument.

Whalen, D., A. Heger, K. Chen, W. Even, J. Smidt, C. Fryer, M. Stiavelli, H. Xu, and C. C. Joggerst. Supermassive Population III Supernovae and the Birth of the First Quasars. To appear in Astrophysical Journal.

Whalen, D., J. Johnson, J. Smidt, A. Heger, W. Evan, and C. Fryer. The Supernova that Destroyed a Protogalaxy: Prompt Chemical Enrichment and Supermassive Black Hole Growth. 2013. Astrophysical Journal. 774: 64.

Whalen, D., L. Frey, W. Even , J. Smidt, C. Fryer, M. Stiavelli, D. Holz, A. Heger, S. E. Woosley, C. Lovekin, and A. Hungerfort. Finding the First Cosmic Explosions I: Pair-Instability Supernovae. To appear in Astrophysical Journal.

"Listening" to the Noise of a Single Electron Spin: Methods for Fast, Ultra-sensitive, Non-perturbative Noise Spectroscopy

Scott A. Crooker
20110306ER

Abstract

Measurement of electron and nuclear spins forms the basis of modern magnetic resonance technologies such as NMR, MRI, and electron spin resonance. Driven by the desire and need for ever-increasing sensitivity and resolution (e.g., for MRI), the number of detected spins necessarily decreases. The goal of this project is to reach the limit of *single* quantum-mechanical spins – that is, a single electron -- and to measure the intrinsic fluctuations of that single spin. At present, however, the direct magnetization measurement of a single spin is a tremendously difficult proposition, due to the extreme sensitivity required (conventional NMR or MRI lacks the sensitivity by about a factor of a trillion!). Nonetheless, from viewpoints of both fundamental measurement and basic science, single-spin detection represents a truly landmark achievement in measurement science. Exploiting recent advances in optical detection and efficient digital signal processing, coupled with alternative measurement approaches based on passive spin noise detection (rather than conventional perturbative studies), we have demonstrated a viable route for measurements of a single quantum-mechanical entity – a single electron spin.

Background and Research Objectives

Not all noise in experimental measurements is unwelcome. Certain fundamental noise sources contain extremely valuable information about the system itself – a classic example being the inherent voltage fluctuations that exist across any resistor (Johnson noise), from which temperature can be determined. In magnetic systems, fundamental noise exists in the form of small, random spin fluctuations.

For example, statistical fluctuations of N paramagnetic spins should generate "spin noise" of order sqrt(N), even in zero magnetic field. Crucially, the frequency spectra of these tiny fluctuations - if measurable - reveal the important dynamic properties of the spins (such as spin precession frequencies, decoherence times, and interparticle couplings), without ever having to excite, pump, or drive the spin ensemble away from thermal equilibrium. Such a noise-based approach to spin resonance is in marked contrast to conventional nuclear- or electron-spin resonance measurements, which necessarily perturb the spins. Nevertheless, this approach is guaranteed by the Fluctuation-Dissipation Theorem. Importantly, noise-based measurements become viable alternatives to conventional (dissipative) methods as the few-particle limit is approached (N→1), since noise signals fall only as sqrt(N) rather than as N.

The goal of this project is therefore to measure the random spin fluctuations of electron and hole spins that are trapped in semiconductor quantum dots, with an aim to eventually reach the truly quantum-mechanical limit of a single electron (or hole) spin. Measuring spin dynamics via intrinsic noise signatures (rather than via perturbative pump-probe techniques) provides a completely alternative and arguably more meaningful approach to ascertain intrinsic spin dynamics. We therefore develop an ultra-sensitive magnetometer capable of "listening" to the tiny spin fluctuations of truly quantum-mechanical objects: single electron spins trapped in semiconductor quantum dots. New instrumentation for efficient digital signal processing based on configurable hardware (FPGAs) formed an essential component of this work.

Scientific Approach and Accomplishments

We demonstrated that our scheme for using lasers to sensitively measure spin fluctuations works -- and works very well -- for electrons trapped in semiconductor quantum dots. We completed our first set of measurements, wherein we showed that not only are spin fluctuation signals measurable using the optical techniques that we proposed, but that the data are of sufficient quality to achieve a detailed understanding of spin relaxation and coherence for the case of electron spins in semiconductor quantum dots. This initial work was written up

and published in the high-profile journal Physical Review Letters, and the paper was especially highlighted by the journal Editors.

Based on this work, we received numerous invitations to present invited talks at international conferences. For example, we presented an invited talk at the SPIE meeting in August 2012 (San Diego), the 4th Nano-MRI conference (Switzerland, July 2012), the 2012 Quantum Dot conference (May 2012). We have also been invited to give seminars/colloquia at Rice University, Texas A&M, Ohio State, U. Oregon, and Argonne Nat'l Lab. Also, our postdoc Yan Li has landed a prestigious faculty job as an assistant professor at the University of Utah (Dept. of Physics), which she started in July 2013.

As a result of our data, our theoretical component has made significant advances in our understanding of how single electron spins couple to a bath of nuclear spins (directly addressing the "central spin problem" -- a topic of hot theoretical interest). This work was also published in Physical Review Letters.

Again, as a result of our data, our close collaboration with the Dortmund and Bochum University groups of Professor Manfred Bayer and Dirk Reuter continue. We have just published a joint theoretical/experimental paper on the use of these new experimental techniques as a high-resolution spectroscopic tool. Again, this paper was accepted at the prestigious journal Physical Review Letters.

In the last year we finished construction of the new ultra-stable single-quantum dot microscope, which works very well. Yan has shown that we can measure the absorption from a single quantum dot, which is a remarkable achievement. We have measured noise signals from this quantum dot – thereby achieving our goals. We are currently writing up these results for publication.

Impact on National Missions

This project has built Laboratory capabilities in the development of novel measurement methods that enable new scientific discovery at Los Alamos National Laboratory. It is based on recent technological advancements that enable the use of FPGAs and on the very large data storage and manipulation capabilities that have now become available. Our basic approach to noise spectroscopy goes well beyond the specific example of electron spin noise that will be investigated here and the advantages of noise spectroscopy as an experimental probe are very general. The project advances new Laboratory capabilities that underpin a wide variety of Laboratory missions. Demonstration of single spin noise spectroscopy measurements has generated worldwide attention and has formed a robust platform for nanoscale spintronics at LANL.

Publications

Cooper, F., B. Mihaila, J. F. Dawson, C. Chien, and E. Timmermans. Auxiliary-field approach to dilute Bose gases with tunable interactions. 2011. Physical Review A (Atomic, Molecular, and Optical Physics). 83 (5): 053622 (15 pp.).

Cooper, F., Chih-Chun Chien, B. Mihaila, J. Dawson, and E. Timmermans. Composite-field Goldstone states and Higgs mechanism in dilute Bose gases. 2012. Physical Review A (Atomic, Molecular, and Optical Physics). 85 (2): 023631 (5 pp.).

Dawson, J., B. Mihaila, and F. Cooper. Josephson relation for the superfluid density and the connection to the Goldstone theorem in dilute Bose atomic gases. 2012. PHYSICAL REVIEW A. 86 (1): 013603.

Li, Y., N. Sinitsyn, D. L. Smith, D. Reuter, A. D. Wieck, D. R. Yakovlev, M. Bayer, and S. A. Crooker. Intrinsic Spin Fluctuations Reveal the Dynamical Response Function of Holes Coupled to Nuclear Spin Baths in (In,Ga)As Quantum Dots. 2012. PHYSICAL REVIEW LETTERS. 108 (18): 186603.

Mihaila, B., F. Cooper, J. Dawson, C. Chien, and E. Timmermans. Analytical limits for cold-atom Bose gases with tunable interactions. 2011. Physical Review A - Atomic, Molecular, and Optical Physics. 84 (2): 023603.

Mihaila, B., J. Dawson, F. Cooper, C. Chien, and E. Timmermans. Auxiliary field formalism for dilute fermionic atom gases with tunable interactions. 2011. PHYSICAL REVIEW A. 83 (5): 053637.

Roy, D., Y. Li, A. Greilich, Y. Pershin, A. Saxena, and N. Sinitsyn. Spin noise spectroscopy of quantum dot molecules. 2013. Physical Review B. 88: 045320.

Sinitsyn, N., Y. Li, S. A. Crooker, A. Saxena, and D. L. Smith. Role of Nuclear Quadrupole Coupling on Decoherence and Relaxation of Central Spins in Quantum Dots . 2012. Physical Review Letters. 109: 166605.

Zapasskii, V. S., A. Greilich, S. A. Crooker, Y. Li, G. G. Kozlov, D. R. Yakovlev, D. Reuter, A. D. Wieck, and M. Bayer. Optical Spectroscopy of Spin Noise. 2013. Physical Review Letters. 110 (17): 176601.

The Terahertz Quantum Hall Effect

Rohit P. Prasankumar
20110311ER

Abstract

Two-dimensional electron gases (2DEGs) in semiconductor heterostructures are a widely used platform for modern electronics. However, at very low temperatures (T<4 K) and high magnetic fields (B>>1 T), they evolve into a new frontier for quantum processes and a testing ground for novel theoretical predictions. This is arguably best exemplified by the quantum Hall effect (QHE), which has been the subject of intense research worldwide (and four Nobel Prizes) since its discovery in 1980. Despite the many publications devoted to elucidating different aspects of the static properties of the QHE, there remain several unanswered questions regarding the underlying physics of this unique phenomenon. For example, the precise nature of the quantum phase transitions between conductivity plateaus as a function of B field is unclear, particularly in understanding the importance of electron-electron interactions. This could be revealed by measuring the conductivity over a broad bandwidth (several terahertz (THz)), which should be possible since researchers have recently predicted that the optical Hall conductivity will have a plateau structure that persists even in the AC regime (at terahertz (THz) frequencies),1, 2 which we refer to as the "Terahertz Quantum Hall Effect (THz-QHE)". Experimental characterization of the THz Hall conductivity could thus conclusively resolve a host of anomalies regarding the existence of a quantum phase transition in quantum Hall systems, while also having wide ranging implications across many areas of physics.

The goal of this project was to use ultrafast THz spectroscopy to gain new insight into the quantum Hall effect by probing regimes inaccessible to conventional electrical measurement techniques. To accomplish this, we developed an innovative experimental technique, THz quantum Hall spectroscopy (TQHS), which would allow us to make non-contact measurements of the complex conductivity tensor as a function of magnetic (B) field and temperature (T) over a broad frequency (ω) range, and apply it to probe QHE physics in novel regimes. Through comparison to theoretical models, we could then shed new light on the nature of the quantum phase transitions in the QHE, with the potential to conclusively determine the physics behind this phenomenon. Furthermore, the ability to perform THz spectroscopy in a magnetic field would also impact the study of many other phenomena, ranging from the QHE in graphene to electromagnons in multiferroics. Here, we will describe our efforts in these directions, and show that this project has resulted in capabilities that will continue to impact LANL research.

Background and Research Objectives

The discovery of the integer QHE by von Klitzing, et al1 opened a rich field of research, spurring breakthrough innovations in many areas of physics. The most remarkable characteristic of the integer QHE is a quantized Hall conductivity (σxy), which takes exact integer multiples (ν) of e2/h, leading to its use as a resistance standard.3 Experimental observations of the QHE employ the same geometry used to measure the classical Hall effect, in which a magnetic field B is applied perpendicular to the direction of current flow in a sample and a voltage is induced orthogonal to both B and the current, from which one can then obtain the Hall conductivity. To measure the QHE, a similar experiment is performed on a high mobility 2DEG under much higher magnetic fields and lower temperatures (T), which cause the density of states to clump into a series of discrete Landau levels separated by the cyclotron energy (typically in the THz range). As the magnetic field is swept, the longitudinal conductivity (σxx) oscillates between zero and non-zero values depending on the relative position of the Fermi energy EF with respect to Landau level positions for a given magnetic field (Fig. 1).4

Although the physical reasons for the quantization of conductivity are relatively well understood,5 the nature of the quantum phase transitions between conductivity

plateaus as a function of B (RH in Fig. 1) is not yet clear. Existing scaling theories of the integer QHE have assumed the interactions between electrons to be irrelevant6; however, in reality the electrons interact and move in a finite magnetic field, which can cause deviations from existing theories. Therefore, despite decades of research, the correct theoretical description of quantum phase transitions in the QHE is still unresolved.

The most critical piece of data for testing the validity of different scaling theories is a measurement of the complex conductivity tensor, $\sigma_{\mu,\upsilon}(\omega,T,B)$ (where the use of the indices μ and υ includes both the diagonal and the Hall conductivity), over a broad bandwidth of several THz,6, 7 which is impossible to perform with existing electrical techniques. Measurements of the THz Hall conductivity would therefore offer much insight on QHE physics but have not yet been performed, impeding progress in this field and motivating this work. The use of ultrafast THz spectroscopy to study the quantum Hall effect in the AC regime could conclusively determine the underlying physics behind this unique phenomenon, with significant ramifications for applications of the QHE. In addition, non-contact THz measurements would provide the ability to both spatially resolve the contributions of edge states to the conductivity and temporally resolve carrier relaxation back to equilibrium after ultrafast photoexcitation, pushing our understanding of quantum Hall physics to new frontiers.

Therefore, in this project, our original objectives were to employ THz spectroscopy to demonstrate the existence of Hall plateaus in the THz-QHE in 2DEGs embedded within GaAs/AlGaAs heterostructures, and to study:

- The validity of different scaling theories of quantum phase transitions between Landau levels in the QHE, explored through measurements of frequency-temperature conductivity scaling over a broad frequency range (0.1–7 THz) and comparisons to theoretical models
- Spatially-resolved mapping of the complex conductivity tensor to compare electron properties at the edges of the system with the properties within the bulk material
- The influence of femtosecond optical excitation on the THz response of a 2DEG in the quantum Hall regime

These experiments would be free from many of the artifacts, such as spatial inhomogeneity and sample geometry, which complicate electrical measurements of the QHE. Perhaps more importantly, THz spectroscopy allows us to test and extend different theories of the QHE that cannot be studied by any other existing technique.

Scientific Approach and Accomplishments

The scientific directions described above depend on the design and development of our THz quantum Hall spectroscopy system, which made this the primary initial focus of our project. The essence of this technique is its ability to generate linearly polarized THz radiation and coherently detect orthogonal components of the radiation transmitted through a sample while varying the magnetic field. This facilitates characterization of the THz Hall conductivity in a 2DEG sample by measuring the orthogonal components of the transmitted THz radiation, one polarized in the direction of the incident radiation and the other in the perpendicular direction. The orthogonal component results from B-field induced THz emission and exhibits the characteristics of quantum Hall transitions (THz-QHE). These experiments would thus allow us to measure the frequency and temperature dependent complex Hall conductivity tensor, $\sigma_{\mu,\upsilon}(\omega,T,B)$ over a bandwidth of several THz, allowing us to explore the directions described above. We note that there are fewer than ten systems of this kind in the world, to the best of our knowledge.

In the first year of this project, our efforts thus focused on designing and building the novel setup required for measuring the THz-QHE, as well as on hiring a new postdoc to replace the project co-PI, Prashanth Upadhya, who left LANL in 2011 for a professorship at IISER-Kolkata, in India. We spent a significant amount of initial time planning and designing this system, in which the major components are a femtosecond Ti:sapphire oscillator (already installed in our laboratory) and a superconducting magnet. The superconducting magnet, which was custom designed to our specifications for these experiments by Oxford Instruments, was delivered (after a lead time of ~9 months) in late 2011 and installed in early 2012. Simultaneously, we hired a new postdoc, Stephane Boubanga Tombet, to work on this project; he experienced some unexpected visa issues, delaying his arrival at LANL until February 2012. These delays in receiving the superconducting magnet and hiring a new postdoc to work on the project set us back significantly as compared to our original timeline, but once Dr. Boubanga-Tombet arrived we were able to make substantial progress. He spent the next year building the TQHS system, which was completed in the spring of 2013.

Our first data was taken in April of 2013 on a topological insulator sample provided by our collaborator, Professor Benjamin Williams at UCLA, who had submitted a CINT user proposal to perform THz-TDS measurements in a B field on his samples, since this capability was not readily available elsewhere. We measured the transmission of the THz electric field through this sample at a temperature of 2.4 K as a function of the magnetic field (Fig. 3).

These results demonstrated the capability of our TQHS system to perform THz experiments under an applied B field, which was quite exciting. We then planned to spend the last part of the project exploring the scientific directions described above, particularly exploring the THz-QHE in 2DEGs and in graphene, while also working with Prof. Williams and his postdoc Zhijun Liu (who visited CINT) to obtain a full set of data on his samples. Unfortunately, we suffered some additional setbacks that prevented us from doing this. Soon after acquiring the data shown in Fig. 3, the photoconductive antenna used to generate THz radiation burned out (a commonly encountered problem). We had alternate antennas available, but unanticipated technical issues prevented us from performing B-field-dependent experiments (although we were able to acquire data with no B field). This problem in itself could be overcome by ordering new antennas, which was done. However, more importantly, Dr. Boubanga-Tombet accepted an associate professorship at Tohuku University in Japan, leaving LANL in June of 2013. This limited our progress in the last few months of this project and prevented us from directly measuring the THz-QHE.

It is important to note, however, that our TQHS system is a capability that very few other groups in the world possess, and it will allow LANL to perform a wide variety of experiments in the future. For example, our group at LANL has pioneered the study of ultrafast phenomena in multiferroics8; our TQHS system will enable us to study elementary excitations in these materials, known as "electromagnons"9, providing more insight on magnetoelectric coupling in these systems. Overall, the development of our TQHS system is an important addition to LANL's suite of ultrafast optical and THz capabilities.

In addition, it is worth noting that during the first year of this project, when waiting for the magnet to arrive, we initiated a collaboration with David Hilton's group at the University of Alabama-Birmingham (UAB) and Steve McGill at the NHMFL in Tallahassee to perform THz cyclotron resonance experiments on 2DEGs. Prashanth Upadhya visited the NHMFL and helped construct an ultrafast THz magnetospectrometer that is based on an Oxford Instruments split coil magnet (similar to the system we built at the CINT Core Facility). This system allows the measurement of the conductivity tensor in a quantum confined semiconducting system at THz frequencies as a function of temperature (down to 0.4 K) and magnetic field (0–7 T). Experiments were then performed to test and study the behavior of the 2DEG sample that will be used for our THz QHE experiments at LANL. Under a perpendicular magnetic field, the density of states in 2DEGs clump into discrete Landau levels separated by the cyclotron energy (which is typically in the THz frequency range). Characterization of the cyclotron resonance in the time domain has revealed useful information on the carrier scattering dynamics and dephasing mechanisms in the high mobility samples that we tested. This understanding is essential for the experimental realization of the THz QHE. This collaboration enabled us to be scientifically productive while waiting for different components of our setup to arrive, and a publication on our results is in preparation.

Furthermore, this collaboration also extended to ultrafast optical and infrared measurements on the canonical metal-insulator transition material vanadium dioxide (VO2), in which we were able to study the effects of strain-induced domain formation from growing VO2 films on different substrates on carrier dynamics across the metal-insulator transition. This work has been presented at several conferences (APS, Ultrafast Phenomena, and the Gordon Conference on Ultrafast Phenomena in Cooperative Systems) and is being prepared for publication. In addition, we also examined plasmonic carrier injection in Au nanomesh/VO2 hybrid samples, which has been submitted to Nano Letters10.

Finally, our theoretical efforts throughout the project duration focused on expanding upon the novel directions that we planned to pursue once our experimental setup was built. These include the study of percolation clusters in quantum Hall systems through the power law scaling of the THz conductivity, as well as the use of THz spectroscopy to study edge states of the QHE through a high frequency tail in the THz spectrum.

Impact on National Missions

This project directly addresses several challenges described in the 2007 BES report "Directing Matter and Energy: Five Challenges for Science and the Imagination," including controlling material processes at the level of electrons (which could potentially be done with shaped THz pulses), understanding how the properties of matter emerge from correlations of the electronic constituents (which is the basis of the QHE), and how we characterize and control matter far away from equilibrium (which can be done by photoexciting a material with a femtosecond optical pulse and using a THz pulse to observe the associated changes in the time-dependent conductivity as a function of B field). It also addresses the new BES initiative in Mesoscale Science, particularly in the dependence of the QHE on electron-electron interactions. In addition, the TQHS system developed in this project addresses the Materials Grand Challenge at LANL while bringing a new capability to LANL that has already been utilized in experiments by CINT users and been leveraged in support of other LDRD projects.

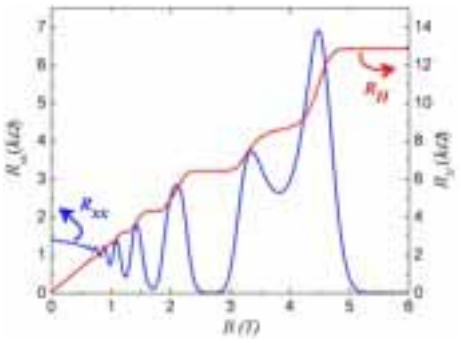

Figure 1. (from ref. 4). Shubnikov-de Haas oscillations (Rxx) and Hall resistance (RH) of a GaAs/AlGaAs 2DEG heterostructure measured electrically on a Hall bar at T=1.5 K.

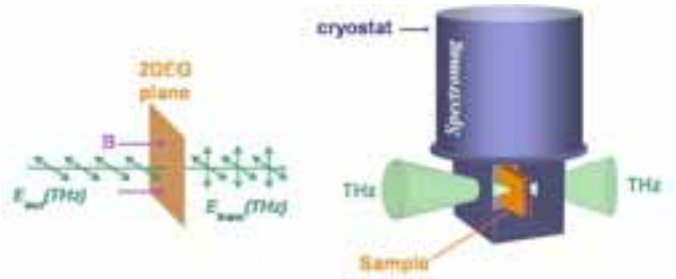

Figure 2. Setup for TQHS measurements.

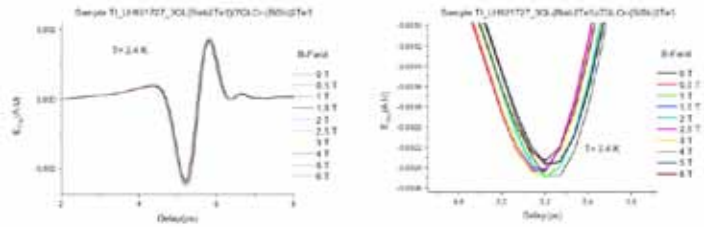

Figure 3. Time-dependent transmission of the THz electric field through a (BiSb)2Te3 topological insulator film as a function of applied B field. Left panel: THz signal over the full temporal range. Right panel: B-field-dependent changes at the negative peak of the THz signal, near a time delay of 5.2 picoseconds (ps).

References

1. VONKLITZING, K., G. DORDA, and M. PEPPER. NEW METHOD FOR HIGH-ACCURACY DETERMINATION OF THE FINE-STRUCTURE CONSTANT BASED ON QUANTIZED HALL RESISTANCE. 1980. PHYSICAL REVIEW LETTERS. 45 (6): 494.

2. TSUI, D. C., H. L. STORMER, and A. C. GOSSARD. TWO-DIMENSIONAL MAGNETOTRANSPORT IN THE EXTREME QUANTUM LIMIT. 1982. PHYSICAL REVIEW LETTERS. 48 (22): 1559.

3. Jeckelmann, B., and B. Jeanneret. The quantum Hall effect as an electrical resistance standard. 2003. MEASUREMENT SCIENCE & TECHNOLOGY. 14 (8): 1229.

4. Upadhya, P. C., J. E. Cunninaam, C. K. Tiang, M. Lachab, S. P. Khanna, E. H. Linfield, and A. G. Davies. Cyclotron absorption in two-dimensional electron systems monitored by terahertz time-domain spectroscopy. 2007. In 2007 JOINT 32ND INTERNATIONAL CONFERENCE ON INFRARED AND MILLIMETER WAVES AND 15TH INTERNATIONAL CONFERENCE ON TERAHERTZ ELECTRONICS, VOLS 1 AND 2. , p. 481.

5. Yoshioka, D.. The Quantum Hall Effect. 2002.

6. HUCKESTEIN, B.. SCALING THEORY OF THE INTEGER QUANTUM HALL-EFFECT. 1995. REVIEWS OF MODERN PHYSICS. 67 (2): 357.

7. Damle, K., and S. Sachdev. Nonzero-temperature transport near quantum critical points. 1997. PHYSICAL REVIEW B. 56 (14): 8714.

8. Qi, J., L. Yan, H. D. Zhou, J. X. Zhu, S. A. Trugman, A. J. Taylor, Q. X. Jia, and R. P. Prasankumar. Coexistence of coupled magnetic phases in epitaxial TbMnO3 films revealed by ultrafast optical spectroscopy. 2012. APPLIED PHYSICS LETTERS. 101 (12): -.

9. Sheu, Y. M., S. A. Trugman, Y. S. Park, S. Lee, H. T. Yi, S. W. Cheong, Q. X. Jia, A. J. Taylor, and R. P. Prasankumar. Ultrafast carrier dynamics and radiative recombination in multiferroic BiFeO3. 2012. APPLIED PHYSICS LETTERS. 100 (24): -.

10. Pimenov, A., A. M. Shuvaev, A. A. Mukhin, and A. Loidl. Electromagnons in multiferroic manganites. 2008. JOURNAL OF PHYSICS-CONDENSED MATTER. 20 (43): -.

11. Kida, N., Y. Takahashi, J. S. Lee, R. Shimano, Y. Yamasaki, Y. Kaneko, S. Miyahara, N. Furukawa, T. Arima, and Y. Tokura. Terahertz time-domain spectroscopy of electromagnons in multiferroic perovskite manganites [Invited]. 2009. JOURNAL OF THE OPTICAL SOCIETY OF AMERICA B-OPTICAL PHYSICS. 26 (9): A35.

12. Sushkov, A. B., M. Mostovoy, R. V. Aguilar, S. W. Cheong, and H. D. Drew. Electromagnons in multiferroic RMn2O5 compounds and their microscopic origin. 2008. JOURNAL OF PHYSICS-CONDENSED MATTER. 20 (43): -.

Publications

Appavoo, K., N. F. Brady, B. Wang, M. A. Seo, J. Nag, R. P. Prasankumar, S. T. Pantelides, D. J. Hilton, and R. F. Haglund. Plasmonic electron injection drives ultrafast phase transition by ultrafast phonon collapse I: experiment. Presented at March Meeting of the American Physical Society. (Baltimore, MD, 18-22 March, 2013).

Appavoo, K., N. F. Brady, B. Wang, M. A. Seo, J. Nag, R. P. Prasankumar, S. T. Pantelides, D. J. Hilton, and R. F. Haglund. Ultrafast phase transition driven by plasmonic electron injection. Nano Lett..

Appavoo, K., N. F. Brady, M. A. Seo, J. Nag, R. P. Prasankumar, D. J. Hilton, and R. F. Haglund, Jr.. Ultrafast metal-insulator transition in VO2 driven by electron injection. Presented at Conference on Lasers and Electro-Optics. (San Jose, CA, 6-11 May, 2012).

Appavoo, K., N. F. Brady, M. A. Seo, J. Nag, R. P. Prasankumar, D. J. Hilton, and R. F. Haglund, Jr.. Dynamics of ultrafast interfacial electron injection on phase-transition mechanism. 2013. In 18th International Conference on Ultrafast Phenomena. (Lausanne, Switzerland, 8-13 July, 2012). , p. 03026. London: Oxford University Press.

Brady, N. F., K. Appavoo, M. A. Seo, J. Nag, R. P. Prasankumar, D. J. Hilton, and R. F. Haglund, Jr.. Dynamics of ultrafast electron injection in phase-changing vanadium dioxide. Presented at Ultrafast Phenomena in Cooperative Systems. (Galveston, TX, 19-24 Feb., 2012).

Brady, N. F., K. Appavoo, M. A. Seo, J. Nag, R. P. Prasankumar, D. J. Hilton, and R. F. Haglund, Jr.. Ultrafast dynamics of VO2 grown on different substrates with non-degenerate pump-probe spectroscopy. Presented at Ultrafast Phenomena in Cooperative Systems. (Galveston, TX, 19-24 Feb., 2012).

Brady, N. F., K. Appavoo, M. A. Seo, J. Nag, R. P. Prasankumar, R. F. Haglund, Jr., and D. J. Hilton. Ultrafast dynamics of the VO2 insulator-to-metal transition observed by nondegenerate pump-probe spectroscopy. 2013. In 18th International Conference on Ultrafast Phenomena. (Lausanne, Switzerland, 8-13 July, 2012). , p. 3006. London: Oxford University Press.

Brady, N. F., K. Appavoo, M. A. Seo, J. Nag, R. P. Prasankumar, R. F. Haglund, Jr., and D. J. Hilton. Substrate effects on the ultrafast dynamics of the VO2 insulator-to-metal transition observed by nondegenerate pump-probe spectroscopy. Presented at Frontiers in Optics. (San Jose, CA, 17-18 October, 2011).

Brady, N., K. Appavoo, P. Upadhya, M. A. Seo, J. Nag, R. P. Prasankumar, R. F. Haglund, Jr., and D. J. Hilton. Ultrafast pump probe transmission spectroscopy of VO2. Presented at March Meeting of the American Physical Society. (Boston, MA, 27 Feb.-2 March, 2012).

Wang, B., K. Appavoo, N. F. Brady, M. A. Seo, J. Nag, R. P. Prasankumar, D. J. Hilton, R. F. Haglund, and S. T. Pantelides. Plasmonic electron injection drives ultrafast phase transition by ultrafast phonon collapse II: theory. Presented at March Meeting of the American Physical Society. (Baltimore, MD, 18-22 March 2013).

A Compact, Brilliant, Coherent X-ray Source Based on a Dense Relativistic Electron Mirror

Juan C. Fernandez
20110341ER

Abstract

World-wide, scientists are searching for the next generation of coherent X-ray sources. Free-electron lasers (FELs) supply powerful coherent X-ray beams. However, X-ray FELs are extremely expensive and available in only a few institutions. With comparable power output, the microscale X-ray source based on relativistic electron mirror (REM) may revolutionize X-ray generation by providing such capability driven by a relatively compact high-intensity laser. The same is true of a recently discovered relativistic laser-plasma process known as Coherent Synchrotron Emission (CSE), which generates coherent laser-frequency harmonics all the way up to x-ray energies. In this LDRD project, although the original scope was to examine the former, both mechanisms have been researched. For the former, the research has centered on testing a scheme, developed via simulations, to overcome the known limitations of the REM. The final experiments on this project on this topic are proceeding at this moment. Regarding the latter, the CSE mechanism has been established on experiments at the LANL Trident laser facility, explained theoretically, successfully reproduced on simulations, and reported in a journal publication. This part of the research has been achieved as part of an international collaboration. These experiments have demonstrated CSE generation of x-rays extending to the keV range.

Background and Research Objectives

In this project, two mechanisms for laser-driven generation of coherent x-rays have been studied. The first, the original aim of this project, was light generation based on the so-called relativistic electron mirror (REM) [1]. The second, pursued subsequently, is based on Coherent Synchrotron Emission (CSE) [2].

REM

Ultra-intense lasers are now strong enough to push all electrons out of a nanometer foil and accelerate them to relativistic energy during a period of a few-light-cycles. Under the right conditions, such electrons can preserve their ultrathin character (thickness ~ nm) and form a relativistic forward-propagating electron sheet, i.e., a REM, moving with a relativistic factor γ. When a second, counter-propagating, lower intensity probe laser collides with this REM, a coherent and powerful X-ray pulse can be produced through coherent Thomson scattering (CTS). The ratio of X-ray photon energy to laser photon energy is called as Doppler shift factor, ideally 4γ2. To date, the technique has been developed extensively in a regime in which the x-ray contributions from each electron sum linearly, i.e., incoherent scattering. In contrast, coherent scattering, in which the output goes with the square of the number of participating electrons, will occur if the electrons are bunched with a layer thickness less than that of the output x-ray wavelength. Remarkably, this bunch layer requirement can be achieved by using a fast-rising intense laser pulse to rip an entire relativistic electron population from an ultra-thin foil target. The laser subsequently traverses plasma and continues to propagate forward. There is evidence [2,3] that such thin electron sheets are generated in Trident-laser experiments with nanofoil diamond or diamond-like (DLC) targets. Such experiments have operated in a novel laser-plasma regime, the relativistically-induced transparency (RIT) regime. In this regime, the laser drives all the target electrons to relativistic energies. Then, the electron mass in the laboratory frame greatly increases, and therefore the effective plasma frequency decreases, at some point dipping below the laser frequency. At that point, the laser drives the electrons volumetrically (not just at the "critical" density surface), and traverses forward beyond the target. For reasons that are explained in the next Section, the onset of RIT is relatively sudden, occurring in less than the 50 fs time resolution of our diagnostic. That raises the possibility of using RIT as a switch to produce a fast rising laser pulse, which is useful for the aims of this project, as explained below.

However, as shown in earlier theoretical investigations,

the laser plasma interaction not only imparts forward momentum to the electrons, but finite transverse momentum as well. As a result, the actual upshift factor is degraded to ~ 2γ, and coherence is spoiled, even for an otherwise sufficiently thin REM.

In this project, we have studied the novel double-foil REM-CTS scheme [1], illustrated in Figure 1, to overcome these problems with the REM concept. It combines the well known approach to up-shift optical frequencies via relativistic Doppler shifting from energetic electrons, with a scheme to recover coherence and the ideal upshift, 4γ2 by eliminating the transverse electron momentum that would otherwise spoil both in a short-pulse laser interacting with a nanofoil target. This is done with a secondary thick foil that reflects back the transmitted laser. That second interaction cannot impart any net directed momentum to an electron sheet (a well known result that rules out direct electron acceleration by a laser), but it can cancel transverse momentum imparted earlier by the same laser to those electrons. It is intuitively clear that implementing this scheme would work best with a laser pulse with a rise time of a few cycles (~ 1 – 10 fs), rather than the > 500 fs Trident pulse. The use of a pre-foil target to steepen the Trident pulse by exploiting RIT is a possible and attractive practical alternative to a native ultrafast-rising laser pulse.

The objectives of this project can be summarized as: 1) extending the theory for this improved double-foil REM-CTS concept with a more proper nonlinear relativistic treatment, 2) exploring improvements to the original scheme, 3) validating experimentally the RIT regime where Trident experiments operate, 4) exploring whether an RIT pre-foil target could be used to decrease the rise time of the Trident laser pulse, and 5) testing experimentally the ability of the double-foil REM-CTS scheme to reduce (or eliminate) the transverse momentum from an REM.

CSE

This part of the project relates to the fact that, in the process of characterizing and validating the modeling results for the Trident laser plasmas in the RIT regime intended for the REM-CTS experiments, the generation of laser harmonics are expected via the well-known process of relativistic oscillating mirror (ROM) prior to the onset of RIT. Basically, the electrons at the critical surface oscillate in response to the laser field. However, even if the laser field oscillates harmonically, relativistic effects make the electron oscillatory response anharmonic, generating copious amounts of light at upshifted frequencies. Although these harmonics are normally seen only in the backwards direction with thin targets, the questions of whether there is forward ROM emission, and whether this source could be another viable coherent x-ray source, became convenient subjects of further investigation in this project. The experiments instead uncovered a novel mechanism for the generation of forward directed harmonics: coherent synchrotron emission (CSE). The accomplishments of the elucidation of the CSE mechanism and its demonstration of in Trident experiments [2] are summarized in the next Section, and may be found in the journal article.

Scientific Approach and Accomplishments

REM

The first accomplishment of this project (goal REM-1 above) has been to improve the original theoretical treatment of the double-foil REM-CTS scheme [1] with a relativistic treatment extended into the non-linear regime, i.e., a02 > 1 [4], where a0 is the normalized laser electric field of the probe laser to be backscattered and upshifted (not the one that makes the REM). In this treatment, it is shown that the CTS process saturates when a0 exceeds ~ 1, as shown in Figure 2(a), by nonlinear effects such as pulse contraction and steepening. The second theoretical accomplishment relates to goal REM-2 above. Although a uniform and stable relativistic electron sheet can be generated by the double-foil target scheme with a linearly polarized drive laser, the energy and density of the electron layer are found to be sensitive to the carrier-envelope phases of few-cycle laser pulses. To circumvent this problem, it has been shown in a separate article [5] that by utilizing a circularly polarized laser, the electron layer becomes completely independent of the phase of the laser, avoiding the rigorous requirement for phase stabilization in an ultra-intense few-cycle laser system, making the double-foil REM-CTS scheme for coherent x-ray sources more attainable. This result is shown in Figure 2b.

The third goal, REM-3 above, has also been richly fulfilled. We have utilized the superior complement of optical diagnostics on Trident, especially our single-shot diagnostics implementing the well-known Frequency Resolved Optical Gating (FROG) scheme, which are capable of measuring fast optical signals with 50 fs resolution in a single high-energy shot, which is unique. These have been applied to measure the incoming laser, the reflected laser light, and the transmitted laser light after the onset of RIT. The outcome of these measurements include the first demonstration of relativistic transparency , enabled by ultrahigh contrast laser pulses interacting with diamond nanofoils, as well as the first demonstration and characterization of the RIT regime and unprecedented validation of the simulation accuracy [6]. The dynamics are illustrated in Figure 3a. It also shows the rationale for the possibility of exploiting RIT as a rectifying light switch. Figure 3b and 3c show representative traces of the measured reflected and transmitted laser light. Figure 3b shows the reflected laser pulse

(3b), which goes down abruptly when RIT is established across the target thickness. Figure 3c shows the onset of a transmitted laser pulse (which is normally absent in thick targets), shown to be much shorter than the reference laser pulse. The evaluation of a laser pulse shaped (optically rectified) by RIT (goal REM-4) was inconclusive. Although Figure 3c may suggest a slower rise time than expected, the measurement is contaminated by diffracted light from the whole radial extent of the laser spot. Since the radial laser-intensity profile is approximately Gaussian, the RIT onset varies with radius, which smears out the measured rise time. A later implementation of the diagnostic implementing image relay has solved that problem, and the true rise time of the transmitted pulse will be determined in the future.

The initial plans for utilizing current sheets generated with Trident using nanofoils has been ruled out by more detailed simulations with the VPIC code. The simulations indicate that the Trident pulse with 200 cycles gives not one but many mirrors. This is shown in Figure 4a. A first measurement of this has been done utilizing the setup illustrated in Figure 4b. It is consistent with the predicted electron-sheet bunching at twice the laser frequency. An integrated double-foil REM-CTS test with such a multiplicity of REMs would be very difficult to interpret. It shows that a much shorter laser pulse is preferable.

To that end, we have established a collaboration with UT Austin, where much shorter, high-energy laser pulses are available. A subcontract to UT in this 3rd and final year of the project has been setup to enable the collaboration using these systems for these final experiments. Our initial plan was to use a 35fs, 3J laser. Simulations for such a laser are shown in Figure 5, showing the effect of the reflected laser from the secondary foil in decreasing electron transverse momentum, as evidence by a change in the electron beam divergence. That initial plan was foiled by a breakage of key components that disabled the system. The experiment has been redeployed in the GHOST laser system, which features similar energy and a 150fs pulse length, still much shorter than Trident. Those experiments are ongoing at the time of this writing.

CSE

As part of this project, strongly beamed XUV/X-ray harmonic emission with scaling consistent with the CSE mechanism has been observed in transmission from ultrathin solid foils, as seen in experiments at the LANL Trident facility with diamond nanofoil targets [2]. The fundamental mechanism for coherent XUV/X-ray generation in this geometry has been studied using particle-in-cell (PIC) codes. Dense nanobunches of electrons are formed at the front surface of the target and accelerated into the transmitted direction owing to the relativistic ponderomotive force of the laser. These nanobunches undergo rapid elliptical trajectories across the plasma-vacuum boundary before being emitted through the rear of the foil in the transmitted laser direction. Examining the temporal evolution of radiation emitted from a given trajectory reveals an intense, ultrafast (<0.1 laser cycle duration) XUV pulse emitted in the transmitted direction just as the bunch reverses its direction towards the target. The nanobunches are observed to have a spatial extent at the resolution limit of the simulation of ~10nm. In the experiment, strong suppression of lower-order harmonics (n<26) is observed with a 200nm-thick diamond target, implying a maximum target density of >252 Nc = 625 Nc at the time of generation, where Nc = 1 × 1021 cm-3, the critical density for 1054 nm laser light. The observed absolute energy in a single harmonic can be estimated as 200 ±50 μJ at 20nm (58th harmonic) for a 200nm DLC foil target and can be considered a lower bound due to the limited detection aperture in our experiment. The on-axis cone angle of ~1 keV emission (n ~ 1,000) is observed to be 10 ± 1 mrad at full-width at half maximum. The significantly slower decay of CSE spectra (n-4/3) when compared with those produced by the ROM mechanism (n-8/3) indicates the potential for substantial increases in peak intensity, well beyond those predicted under idealized conditions for the ROM mechanism. The ability to generate CSE extending to the X-ray regime in transmission is enabled by the unique electron dynamics driven by the intense laser field at the front surface of the relativistic plasma. These dynamics allow for dense nanobunches (that is, 10-9 m scale) to be formed and accelerated on ultrafast timescales (<< 10-15 s). The observation of harmonic spectra in transmission from ultrathin foils with characteristic CSE scaling is clear evidence that the unique dynamics provided during relativistic laser plasma interactions can produce and rapidly accelerate dense attosecond electron bunches suitable for the emission of bright, coherent XUV/X-ray radiation in a convenient, practical geometry.

Impact on National Missions

The pursuit of coherent x-ray sources impacts the ability to execute the science, defense and global security missions of the DOE and the NNSA. This project supports the LANL Materials Research Pillar, one of the identified broad range of activities needed to succeed in these missions. A brilliant X-ray source enables to study the properties and structure of materials under extreme conditions of pressure and temperature in dynamic experiments. Investigating the potentially transformational technologies within this project has the potential of fundamentally shaping the future signature facility (MaRIE) and improving LANL's capabilities and scientific outlook for years to come.

Figure 1. Schematic depiction of laser-based coherent x-ray generation by coherent Thomson backscatter from a relativistic electron mirror. Left: The intense laser incident on an nanofoil target makes an electron sheet moving forward with a relativistic factor γ, and traverses the target. That sheet would not support coherent scattering due to finite lateral momentum imparted by the laser on first passage. The laser, upon reflection and traversal through the sheet in the opposite direction, nearly cancels the transverse momentum on the sheet, leaving only longitudinal momentum, making it capable of coherent scattering. Right: A relatively weak backward propagating laser is upshifted to a frequency 4γ2, i.e., a coherent x-ray pulse.

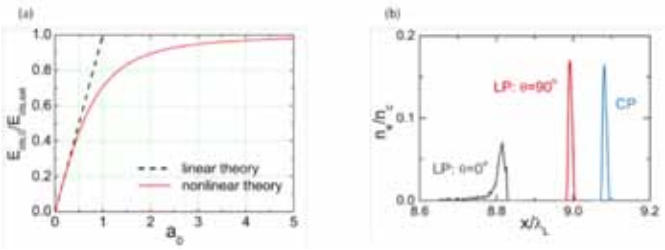

Figure 2. (a) Saturation of nonlinear scattering. a0 is the normalized electric field strength. (b) Relativistic electron mirror density profile snapshots as a function of polarization and carrier-phase relationship for linear polarization (black, linear polarization with phase =0 deg; red, linear polarization with phase of 90 deg.; and blue, circular polarization). There is no dependence of carrier phase for circular polarization.

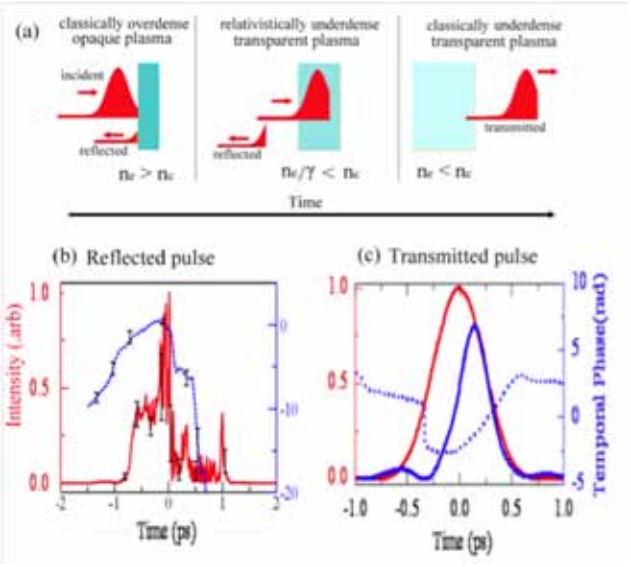

Figure 3. (a) Laser plasma interaction leading to transmitted laser pulse shaping via relativistic transparency. (b) Laser pulse shape (red solid line) and its temporal phase (blue dotted line) reflected from a 100 nm diamond foil. The reflected light intensity drops abruptly when the plasma becomes relativistically transparent. (c) Incident laser pulse (red solid line) and the laser pulse transmitted through a 10 nm DLC foil (blue solid line) and its temporal phase (blue dotted line). The sharp rise time in the transmitted laser pulse is degraded due to initial self-focusing and diffraction.

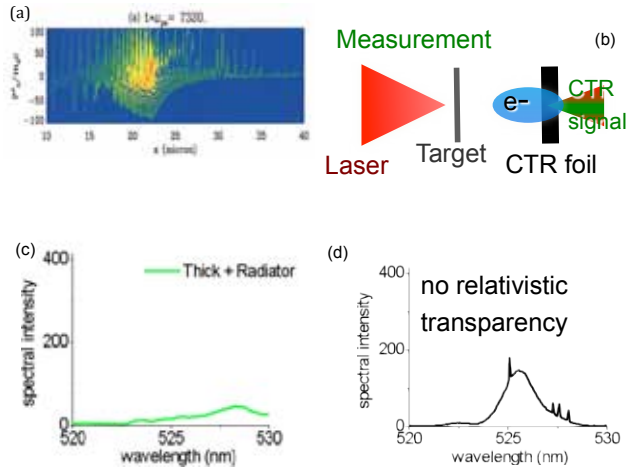

Figure 4. (a) Theoretical prediction with a sub-ps Trident pulse interacting with a nanofoil, showing the generation of multiple current sheets every half cycle. (b) Experimental setup to characterize the laser-driven electron sheets with Coherent Transition radiation (CTR). (c) CTR spectrum from a thick target, which does not undergo RIT, showing a broad electron spectrum, as predicted by simulations (not shown). (d) CTR spectrum from a nanofoil, which undergoes RIT, consistent with the simulation prediction of multiple electron sheets.

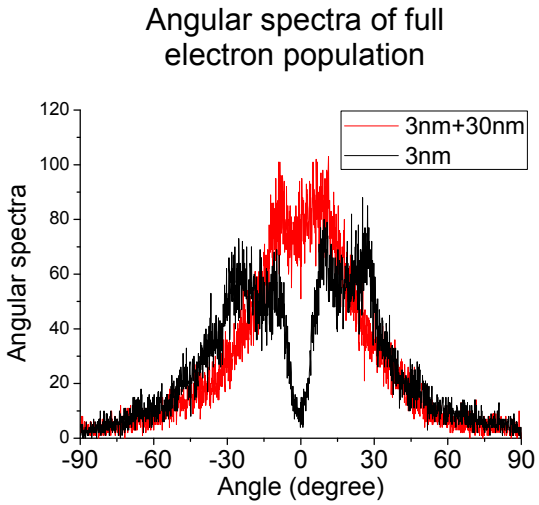

Figure 5. Predicted angular electron spectrum resulting from the interaction of a 3 nm DLC foil with a 35fs, 3J laser pulse (black), and from a 3 nm + 30 nm double-foil target. The two simulations show the collimating effect on the electron sheets of the laser-pulse reflected from the 30 nm foil.

References

1. Wu, H. C., J. Meyer-ter-Vehn, J. Fernandez, and B. M. Hegelich. Uniform Laser-Driven Relativistic Electron Layer for Coherent Thomson Scattering. 2010. PHYSICAL REVIEW LETTERS. 104 (23): -.

2. Dromey, B., S. Rykovanov, M. Yeung, R. Horlein, D. Jung, D. C. Gautier, T. Dzelzainis, D. Kiefer, S. Palaniyppan, R. Shah, J. Schreiber, H. Ruhl, J. C. Fernandez, C. L. S. Lewis, M. Zepf, and B. M. Hegelich. Coherent synchrotron emission from electron nanobunches formed in relativistic laser-plasma interactions. 2012. NATURE PHYSICS. 8 (11): 804.

3. Kiefer, D., A. Henig, D. Jung, D. C. Gautier, K. A. Flippo, S. A. Gaillard, S. Letzring, R. P. Johnson, R. C. Shah, T. Shimada, J. C. Fernandez, V. K. Liechtenstein, J. Schreiber, B. M. Hegelich, and D. Habs. First observation of quasi-monoenergetic electron bunches driven out of ultra-thin diamond-like carbon (DLC) foils. 2009. EUROPEAN PHYSICAL JOURNAL D. 55 (2): 427.

4. Wu, H. C., J. Meyer-ter-Vehn, B. M. Hegelich, and J. C. Fernandez. Nonlinear coherent Thomson scattering from relativistic electron sheets as a means to produce isolated ultrabright attosecond x-ray pulses. 2011. PHYSICAL REVIEW SPECIAL TOPICS-ACCELERATORS AND BEAMS. 14 (7): -.

5. Wu, H. C.. Phase-independent generation of relativistic electron sheets. 2011. APPLIED PHYSICS LETTERS. 99 (2): -.

6. Palaniyappan, S., B. M. Hegelich, H. C. Wu, D. Jung, D. C. Gautier, L. Yin, B. J. Albright, R. P. Johnson, T. Shimada, S. Letzring, D. T. Offermann, J. Ren, C. K. Huang, R. Horlein, B. Dromey, J. C. Fernandez, and R. C. Shah. Dynamics of relativistic transparency and optical shuttering in expanding overdense plasmas. 2012. NATURE PHYSICS. 8 (10): 763.

Publications

Dromey, B., S. Rykovanov, M. Yeung, R. Horlein, D. Jung, D. C. Gautier, T. Dzelzainis, D. Kiefer, S. Palaniyppan, R. Shah, J. Schreiber, H. Ruhl, J. C. Fernandez, C. L. S. Lewis, M. Zepf, and B. M. Hegelich. Coherent synchrotron emission from electron nanobunches formed in relativistic laser-plasma interactions. 2012. NATURE PHYSICS. 8 (11): 804.

Jung, D., R. Hoerline, D. C. Gautier, S. Letzring, D. Kiefer, K. Allinger, B. J. Albright, R. Shah, S. Palaniyappan, L. Yin, J. C. Fern·ndez, D. Habs, and B. M. Hegelich. A novel high resolution ion wide angle spectrometer. 2011. Review of Scientific Instruments. 82 (4): 043301.

Palaniyappan, S., B. M. Hegelich, H. C. Wu, D. Jung, D. C. Gautier, L. Yin, B. J. Albright, R. P. Johnson, T. Shimada, S. Letzring, D. T. Offermann, J. Ren, C. K. Huang, R. Horlein, B. Dromey, J. C. Fernandez, and R. C. Shah. Dynamics of relativistic transparency and optical shuttering in expanding overdense plasmas. 2012. Nature Physics. 8: 763.

Palaniyappan, S., R. C. Shah, R. Johnson, T. Shimada, D. C. Gautier, S. Letzring, D. Jung, R. Hoerlein, D. T. Offermann, J. C. Fernandez, and B. M. Hegelich. Pulse shape measurements using single shot-frequency resolved optical gating for high energy (80 J) short pulse (600 fs) laser. 2010. Review of Scientific Instruments. 81 (10): 10E103.

Palaniyappan, S., R. C. Shah, R. Johnson, T. Shimada, D. C. Gautier, S. Letzring, D. Jung, R. HoÃàrlein, D. T. Offermann, J. C. FernaÃÅndez, and B. M. Hegelich. Pulse shape measurements using single shot-frequency resolved optical gating for high energy (80 J) short pulse (600 fs) laser. 2010. Review of Scientific Instruments. 81 (10): 10E103.

Wu, H. C.. Phase-independent generation of relativistic electron sheets. 2011. Applied Physics Letters. 99 (2).

Wu, H. C., J. Meyer-ter-Vehn, B. M. Hegelich, and J. C. Fernandez. Nonlinear coherent Thomson scattering from relativistic electron sheets as a means to produce isolated ultrabright attosecond x-ray pulses. 2011. Physical Review Special Topics-Accelerators and Beams. 14 (7).

Majorana Neutrinos

Steven R. Elliott
20120293ER

Abstract
The Majorana nature of the neutrino (whether or not it is its own antiparticle) is a key question that impacts the fields of particle physics, nuclear physics, cosmology, and astrophysics. In particular this issue is extremely important in understanding the matter/ antimatter asymmetry of the Universe. The process of neutrinoless double beta decay can only exist if neutrinos are Majorana particles. Furthermore, searches for double beta decay are the only practical way to seek an answer to this question. Our project was aimed at demonstrating a prototype module of a new experimental approach to the search for double beta decay.

Background and Research Objectives
The Majorana nature of the neutrino (whether or not it is its own antiparticle) is a key question that impacts the fields of particle physics, nuclear physics, cosmology, and astrophysics. In particular this issue is extremely important in understanding the matter/ antimatter asymmetry of the Universe. The process of neutrinoless double beta decay can only exist if neutrinos are Majorana particles. Furthermore, searches for double beta decay are the only practical way to seek an answer to this question. Our plan to address this question is to look for neutrinoless double beta decay in the isotope 76Ge. High purity Ge detectors fabricated with material enriched in 76Ge provide an excellent opportunity for these experiments because the detector material can also play the role of the source.

The MAJORANA Project, will use detectors fabricated from enriched Ge to search for double beta decay. These detectors are very expensive and it is necessary to test the planned deployment of those detectors.

As a project aimed at a proof-of-principle, we developed a prototype cryostat filled with non-enriched Ge detectors. This work is a separate activity from MAJORANA and has its own technical goals. The results from this work will ensure that follow-on cryostats containing Ge detectors fabricated from enriched Ge will be successful.

Scientific Approach and Accomplishments
We obtained all of the equipment and supplies to assemble the prototype cryostat. We obtained beneficial occupancy of our underground laboratory and installed apparatus, including the shield for the detector. Because of various timing issues and the availability of the underground lab, we decided to assemble the prototype there. This permits a more sensitive understanding of the performance of the prototype module. We have assembled the prototype module and performed a number of tests that resulted in changes to the electronics and vacuum design.

The specific scope of this project was to test a string of detectors prior to enriched detectors being deployed in MAJORANA. The string is a group of Ge detectors held together in a linear arrangement. The string design for MAJORANA was tested with this so-called prototype cryostat. Strings will be deployed within the prototype module for testing, and the performance of these strings is critical to the success of detectors made from very expensive enriched material. For this string test within the prototype module, all parts were bought by LDRD. These parts include all the detectors, the data acquisition system, vacuum system and shielding. Software development was done by a university partner (UNC). Both the fabrication and test was supported by LDRD. Figure 1 shows a photograph of the prototype module soon after assembly and just before insertion into a glove box and the installation of a detector string. The work was done at the Sanford Underground Research Facility in Lead, SD.

The primary goal of this project was to bring a prototype cryostat filled with natural Ge detectors to fully operational status. The results from this prototype led to improvements in the design of cryostats that will house

Ge detectors fabricated from enriched Ge. This included aspects of the vacuum and wiring of the string. We identified and have designed fixes for several internal electronic and cryogenic issues. Our results allow the MAJORANA project to proceed with construction of the first cryostat that will house enriched Ge detectors. The analysis of the data from these enriched detectors will lead to much needed improved constraints on neutrino properties, in particular, whether the neutrino is its own antiparticle (a so-called Majorana neutrino).

Impact on National Missions

The work has developed science and technology underpinnings for new program areas. In particular, the path for impact on LANL programs are indicated by the Community support of this science as described by NRC committees and the DOE NP/HEP NuSAG review committee. The 2007 Nuclear Physics Long Range Plan strongly endorses research in this area. The DOE Office of Nuclear Physics and the NSF have been very supportive and therefore the future funding potential is strong. The similarity in requirements means that the R&D for neutrinoless double beta decay will be applicable to certain environmental monitoring applications. The low-background and detector expertise capabilities developed by this project have been applied externally-supported projects in homeland security.

Figure 1. The prototype module just before a detector string was inserted. The large Cu cylinder to the right is the vacuum cryostat that contains the detectors.

References

1. Elliott, Steven R.. Recent progress in double beta decay. 2012. Modern Physics Letters. A27: 1230009.

2. Elliott, Steven R.. The Majorana Demonstrator neutrinoless double-beta decay experiment. To appear in Advances in High Energy Physics.

Publications

Elliott, S. R.. The MAJORANA DEMONSTRATOR Neutrinoless Double-Beta Decay Experiment. To appear in Advances in High Energy Physics.

Elliott, Steven R.. Recent Progress in Double Beta Decay. 2012. Modern Physics Letters A. 27: 1230009.

Quantum Hydrodynamics Approach to Non-equilibrium Modeling of Compressed Plasmas

Michael S. Murillo
20130242ER

Abstract
Experiments in the high energy-density physics regime are notoriously challenging to perform and diagnose; and, such experiments require very large and expensive facilities. For all of these reasons it is prudent that we rely on simulations to the largest possible degree. In many cases, the simulations are quite challenging because the matter has complicated properties, which makes the subject itself interesting and useful. We have proposed a hybrid method of performing microscopic simulations of warm dense matter in which very strong interactions between the nuclei and quantum mechanical properties of the electrons are both accounted for. Our goal is to understand those subtle physics issues associated with inertial confinement fusion experiments.

Background and Research Objectives
Billions of dollars have been invested in the National Ignition Facility. The campaign to achieve ignition ended about a year ago – without achieving ignition. While the reasons are unknown, and are likely to be complex, one potential error was missing physics in the simulations used to design the experiments. Our objective was to build a new simulation capability that could address physics that is known to not be in the simulations used to design last year's experiments.

Our main objective was to combine a molecular dynamics approach, which naturally handles strong interactions between nuclei, with a dynamical quantum description of the electrons, including important electric fields that arise form charge separation. The most challenging portion is the description of the dynamical quantum electrons.

Scientific Approach and Accomplishments
Our approach was to begin with the electron description. In general, computing the time evolution of a quantum many-body system is extremely difficult. However, for high energy-density matter one can make some simplifying assumptions due to the disorder caused by higher temperatures. Two theoretical approaches were considered and initial coding was completed. One potential description is through a quantum hydrodynamics approach, which has computational advantages, but could be lacking in physics fidelity. We explored how such an approach could be made computationally attractive through a smoothed-particle hydrodynamics approach. Second, a potentially more refined approach uses quantum kinetic theory, which retains much more information than does hydrodynamics. We also developed a test code for solving such kinetic equations.

Impact on National Missions
The impact on core nuclear weapons missions and inertial confinement fusion campaigns could be large. Such a code capability would allow one to compute various physics processes to very high fidelity in the absence of experimental data.

Toward Laser Manipulation and Quantum Control of Th-229 Nuclei Embedded in a Solid

Xinxin Zhao
20130503ER

Abstract
The thorium-229 (t1/2 =7340 yr) nucleus possesses the lowest-energy nuclear isomeric state [1-3] in nature. This LDRD reserve project aims to preserve the momentum of LANL's recent breakthrough in 229Th isomer research [4] and work towards the first direct optical spectroscopic measurement of the 229Th isomeric nuclear transition using a monochromator. Such an optical spectroscopy measurement will greatly reduce the search range required to directly excite the nuclear isomeric transition with a laser. The successes of this project would lead to exciting new developments such as a solid-state nuclear clock that will have a transforming impact in quantum optical science, precision measurements, navigation, cosmology, and threat reduction.

Background and Research Objectives
It has been known for decades that the 229Th nucleus possesses the lowest-energy nuclear isomeric state [1-3] in nature. Two widely accepted indirect measurements of the transition energy [2, 3] place it within reach of existing laser capabilities notwithstanding a huge uncertainty in the transition wavelength. There is now a growing interest in 229Th isomer research because of its potential application in nuclear, atomic, condensed matter and optical physics, quantum information, and metrology, including the development of an optical clock based on this nuclear transition. The laser-accessible energy and the long lifetime of the isomeric state results in an exploitable Q = f/ δf of up to 1020 for this nuclear transition, which combined with the well isolated environment of the nucleus provides a nuclear probe of unprecedented precision, and would lead to a nuclear frequency standard with a stability 100 times better than the best atomic clocks.

The project aims to eventually pin down the wavelength of the nuclear transition to a level that is ~2 orders of magnitude better than the current published result, which is a prerequisite for the laser search to succeed. The success of this measurement would quickly establish LANL as a leader in the field.

Scientific Approach and Accomplishments
The challenges for optical spectroscopy of the isomeric transition are very low signal count rate and many co-existing "dirty effects" that are much larger than the signal. We have overcome all these difficulties but need to perform the measurements at higher resolution over the expected wavelength range that is very time-consuming because of the low signal count rate and high background from the dirty effect. In the past year, great progresses have been made in preparation for such a measurement.

(1) We have perfected the system and completed the tests of the spectrometer that couples an MgF2 plate to a monochromator for such a measurement. The system collect 229g, 229mTh recoil ions from alpha-decay of 233U into a MgF2 plate (233U à 229g, 229mTh + α), and measure the emission spectrum using a vacuum UV monochromator with an estimated isomer signal to noise ratio of more than 10. Tests show that our system has an accuracy of 0.25 nm and sufficient sensitivity to see the transition, as shown in Figure 1. Determining the isomeric emission wavelength to this accuracy would be a very important scientific result.

(2) Because the MgF2 phosphorescence and scintillation backgrounds depends on the temperature, we have stabilized the temperature of the MgF2 plate holder to 23.6±0.3 °C year round, despite a very large room temperature fluctuation due to aging facilities (air condition doesn't work in the summer, not enough heating in the winter).

(3) We have obtained 0.95g of pure 233U material from ORNL, which contains only 3ppb of the 232U contaminant. The 233U will be used for making recoil sources as soon as funding is available. The 233U material is more

than 2600 times purer than what we have been using, and will last for years without the problems caused by the in-growth of 233, 232U decay daughters. This will greatly simplify and speed up the measurement.

(4) We have built a larger collaboration across the lab with scientists in T, P and MST divisions for an ambitious ER project.

(5) Technical spin-off of the thorium research has already led to an idea approved by LANL for patent application market survey.

Impact on National Missions

Success of the optical spectroscopy measurement would clear the path for laser excitation of the nuclear isomeric transition that lays the foundation for a nuclear clock. This would result in a wide range of enabling capabilities such as an improved Global Positioning System (GPS), detection of underground structures, or the rise of the sea level through its sensitivity to gravitational red-shifts. LANL is one of only a few institutions that can assemble a tightly-coupled effort combining experimental capabilities in actinides nuclear chemistry, atomic, nuclear and material sciences.

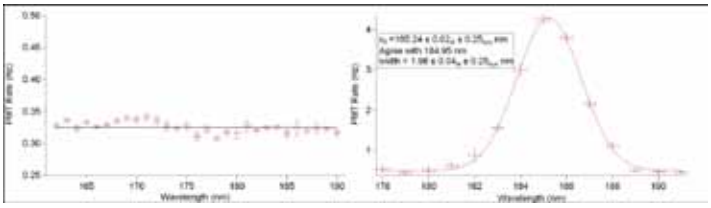

Figure 1. Tests of spectrometer system. Plot on the left: Dark counts of our monochromator system as a function of the wavelength. Plot on the right: The 184.95 nm line of a Hg pencil lamp (running at 10 mA) observed from the indirect scattered light through a 20 micron pinhole located one foot away from the monochromator entrance slit.

References

1. Kroger, L. A., and C. W. Reich. Features of the low-energy level scheme of 229Th as observed in the gamma-decay of 233U. 1976. Nuclear Physics A. 259: 29.

2. Helmer, R. G., and C. W. Rewich. An excited state of 229Th at 3.5 eV. 1994. Physical Review C. 49: 1845.

3. Beck, B. R.. Energy splitting of the ground-state doublet in the nucleus 229Th. 2007. Physical Review Letter. 98: 142501.

4. Zhao, X.. Observation of the deexcitation of 229mTh nuclear isomerPhysica. 2012. Physical Review Letters. 109: 160801.

Materials Study for Small Self-regulating Fission Reactor System for Space Applications

Patrick R. McClure
20130767ER

Abstract

Historically NASA has relied on 238Pu-based power systems for space exploration. Diminishing global supply of 238Pu has reached a critical point and is adversely impacting future NASA deep space science missions. LANL is proposing a very simple reactor concept as an alternative to 238Pu power sources. This simple reactor concept is a fast spectrum reactor that incorporates a solid uranium core that is highly reflected and has heat pipes as a means of heat extraction from the reactor core to the power conversion system. Unique features include low thermal power and self-regulation.

This research investigates two issues that require further investigation to advance this reactor concept. The first is selection of the appropriate materials and the second is the physics of self-regulation with emphasis on accident conditions.

In the materials portion of the project, we investigated the alternatives materials configurations for the reactor. This research included selection of the uranium alloy and its casting; selection of the reflector material; and the methods used to achieve thermal bonding between the heat pipes and the reactor. The materials selected have huge impacts on the overall performance of the reactor system.

In the self-regulation portion of the project, we investigated the physics of fast reactors in more detail. A unique feature of highly reflected fast reactors is the large percentage (up to 50%) of fissions caused by neutrons that return from the reflector. An important feature of these reflected neutrons is their long average lifetime, which can be two to four orders of magnitude longer than in-core neutrons. As a result, a substantial fraction of the reactivity "worth" (neutron multiplication) is delayed as the core waits for these very-long-lifetime reflected neutrons to return. These "geometric delayed" neutrons therefore can have a major influence on the overall neutronic response of the reactor.

Background and Research Objectives

LANL is proposing a reactor for space applications that is based on the physics of a fast reactor with heat pipes to transfer heat from the nuclear fuel to Stirling engines as a means of power conversion.

Heat pipe/Stirling engine reactors have been proposed because of their inherent simplicity. The simplicity of these reactor argues for a reliable, safe, easy to operate and easy to manufacture reactor. One of the key features of these types of reactors is the reactivity feedback mechanism that allows for the reactor to be self-controlling. Fast reactors in this size range are controlled by thermal expansion and subsequent negative reactivity feedback. Thermal feedback lowers reactor power if less heat is extracted by the power conversion. In self-regulating cores, therefore, a narrow temperature region exists over which design power can be delivered to the power converter; any change in one parameter will necessarily change the other. Precise understanding of coupled core and heat conversion system physics is essential to accurately designing and/or predicting the operating envelope of self-regulating nuclear reactors. This means that design selections such as the type of uranium alloy and engineering details such as the fabrication methods used to achieve thermal bonding between the heat pipes and reactor core can have huge impacts on the overall performance of the reactor system. The purpose on the first phase of this research was to investigate a matrix of materials and bonding techniques for the fuel/heat pipe to optimize the choice of materials.

Another unique feature of highly reflected fast spectrum reactor is that very large percentage (over 50%) of the fissions is caused by neutrons that return from the reflector. The result is very long lifetimes of reflected neutrons as compared to those that stay within the core. The average lifetime of neutrons in the core is on the

order of 10-8 s, while the average lifetime of neutrons returned from the reflector is on the order of 10-6 s to 10-4 s. In effect, this lifetime increase creates additional delayed neutron groups, referred to as "geometric delayed" neutron groups. Although the fraction of decay-based delayed neutrons is <1%, they are absolutely essential to the controllability of a nuclear reactor. "Geometric delayed" neutron groups are on a shorter time scale but can be significant because they provide a much larger fraction of the flux. Previous studies of "geometric delayed" neutrons have shown that for large insertions of reactivity, the delayed neutron groups have a pronounced effect on the ability of the reactor to handle transient events and could potentially reduce peak power by several multiples lower than when "geometric delayed" neutrons are ignored. The purpose of the second phase of this project was to modify the LANL system code, FRINK to handle geometric delayed neutrons automatically based on data derived from MCNP6. This would allow for the effect of geometric delayed neutrons to be accounted for in the safety assessment of these reactor types, where ability of the reactor to survive rapid insertions of reactivity during an accident are of a concern.

Scientific Approach

The research was performed with the two principle LANL reactor design tools. The first design tool is the radiation transport code, MCNP61. MCNP6 (Monte Carlo Neutron Photon) is the LANL Monte Carlo code for radiation transport. The MCNP6 code is widely used in studies of advanced reactor concepts.

The second design tool is the systems modeling code FRINK2. The systems model is a point kinetics neutronics model coupled to a two-dimensional heat transfer model. The model also includes a heat pipe model and a representation of the energy removed by the operation of the Stirling engine.

The process for the materials study included the selection of candidate fuel and reflector materials and a method for bonding the heat pipes to the reactor core. The process is described in more detail in the following paragraphs.

A high-uranium density fuel is needed to design a system that is attractive. The ideal fuel candidate from a mass perspective is pure uranium HEU; however, pure uranium metal becomes very soft at high temperature (>800°C). The following materials were examined in this study as candidates for the fuel:

- Pure Uranium
- U doped with small quantities of Fe or Si
- Uranium with 2.5% Vanadium
- Uranium with 1.5%, 7% and 10% Molybdenum
- Addition of a can (stainless-steel) around the fuel

Material properties for pure Uranium were provided by MST-6. Material properties with the additive materials were provided courtesy of staff at the Y-12 plant.

There are only two candidate reflector materials that could meet the anticipated requirements: Beryllium (Be) and Beryllium Oxide (BeO). Other materials will not have sufficient neutron reflection to meet launch criticality safety requirements. The material properties for Be and BeO were provided by MST-6.

The final issue was how to create an acceptable thermal-structural bond between the core and the heat pipes. The first concept examined was to embed the heat pipes in the reflector, because this simplifies system development. The second option was to bond the heat pipes to the outside of the fuel because this lowers the temperature gradient.

In order to measure of success from modeling, criteria were needed to score each design configuration. The criteria are presented below. The criteria are all weighted equally:

- Lowest system mass
- Smallest size
- Smallest delta temperature across reactor fuel and heat pipe
- Least Impact on reactor neutronic performance
- Least impact from off normal performance
- Least potential for long-term material interactions
- Least impact to launch safety accidents

The choices of materials and bonding techniques formed a "matrix of calculations" to against the success criteria. The results were used to down-select to the appropriate design for the reactor concept.

For the second portion of this project, the systems code FRINK was modified to allow the prompt neutrons to be parsed into geometrically delayed neutron groups. This involves multiple runs of MCNP to obtain the reactivity coefficients of each subdivision of the reactor (e.g. the reactor is broken into fuel region, several regions for the reflector, etc.) and the average lifetime of neutrons for that component. Once the reactivity coefficients and neutron lifetimes are calculated, they and the geometry of the model are input to FRINK. The reactivity coefficients determine the reactivity worth of each component based on

temperature. The neutron lifetime determines magnitude of reactivity worth on neutron multiplication and hence the power in a time-step. Once known, the power in a region is used to advance the thermal solution to the next time step. To provide an example of the impact of "geometrically delayed" neutrons, transient calculations were performed on the proposed reactor concept.

Accomplishments

For the first phase of this project the materials study evaluated the proposed combinations of materials and bonding techniques. The "matrix of calculations" consisted of a set of 23 calculations done with MCNP and the systems model, FRINK. The results of these calculations gave the following insights:

Vanadium performed slightly worse than Molybdenum in impacting neutronics for similar material qualities. Also the data set for Vanadium was less robust than for Molybdenum (potential for adverse thermal issues.) Vanadium was then dropped from further consideration.

Heat pipes in the reflector did not perform as well as heat pipes at the edge of the fuel. The heat pipes in the reflector produced too large of a delta temperature for the power level of the reactor. By placing the heat pipes at the edge of the fuel the delta temperature was lower. Also, a mechanical press fit of the heat pipes to the fuel is possible in this location. Finally, if a gap was introduced between the fuel and the reflector the reflector ran cooler and thus less excess reactivity was needed in the system. For these reasons, the heat pipes at the edge of the fuel were selected for the design.

Beryllium Oxide and Beryllium both performed well for the system neutronically. BeO has better high temperature properties and was selected as the reflector material.

Configurations with a higher length to diameter ratio were favored over small ratios for launch safety considerations. This was a discriminator for some of the Molybdenum plus U systems.

Doped U systems behaved neutronically and thermally identical to pure Uranium systems. It is believed that the dopents will assist in grain refinement, yield strength and ultimate strength. Creep strength was believed to be unaffected. However, both U and doped U have a low creep strength at the desired operating temperature. This issue introduces uncertainty into the performance of the system, as discussed in the next bullet.

Uranium versus Uranium plus Molybdenum was a hard decision. So, difficult that a sub-matrix of these two options was done that included an additional 22 calculations on small variations within this sub-matrix. Both Uranium fuel and a Molybdenum alloy had positives and negatives. U and doped U make for a smaller, lighter core that has the best neutronics (they have the highest density of uranium.) However, material properties are pushed to their limit and the probability of failure is higher than desired, (this uncertainty in strength at high temperatures was described in the previous bullet.) Molybdenum added to Uranium was acceptable for size, weight and neutronics and eliminates most material limits issues. However, the size and mass was less than ideal for shipping and manufacture. The final selection a 7% Molybdenum added to Uranium because the material properties removed the issue of phase change, low melting temperature and issues with creep strength at high temperature. Mass estimates for 7% Moly ranged from a low of 258 kg to over 300 kg, which was competitive to the pure Uranium systems with a mass range of 226 kg to 255 kg. For this reason, the7% Moly alloy was chosen as the final material for the reactor design.

The results of the material study produced a reference preliminary reactor design. This reactor concept is shown in Figures 1 to 3. The core is a casting of HEU with 7% Molybdenum as an alloy, with an OD of 11 cm and a length of 25 cm. There is a 3.7 cm B4C control rod that inserts into a hole along the axial core centerline. The reference heat pipes have a super-alloy steel wick and shell. The peak fuel temperature is limited to 1200 K, which limits the core power to ~4 kWt. Each heat pipe is 1.27 cm in diameter and ~4 m long. The baseline reflector material is BeO. The reference power conversion system configuration uses multiple Stirling engines to produce 800 to 1000 Watts of electricity.

For the second phase of this project, a series of calculations were performed to show the importance of "geometrically delayed" neutrons to safety calculations performed for a highly reflected fast reactor. A series of reactivity insertion events ranging from $0.25 to $3.00 were performed for the aforementioned reactor over a range of reactivity insertion timing that ranged from instantaneous to 500 seconds. The results of these calculations are shown in Figure 4 to 5.

The modeling of "geometric delayed" neutron groups has a significant impact on reactivity insertions of greater than $1 ($1 is a reactivity insertion that causes a prompt supercritical condition and is a part of the accident set run for reactor safety calculations.) Figure 4 shows the difference in energy inserted into the reactor accounting for geometrically delayed neutrons and without their inclusion. Note the two orders of magnitude difference in the results. For reactivity insertion accidents, correctly modeling these

accidents is paramount to the development of the reactor concept. In most cases these reactor concepts will start with several dollars of excess reactivity at startup temperature. Reactivity will be inserted slowly to allow the reactor core to establish thermal equilibrium during startup. Precise understanding of how a sudden reactivity insertion would impact reactor startup is a necessary licensing step. Figure 5 shows the results of reactivity insertions for a range of times and the predicted peak fuel temperatures. The results provide information of the necessary reactivity insertion rate to prevent the melting of the reactor fuel during startup.

Impact on National Missions

NASA uses deep space science missions to explore the underlying fabric of the universe. Deep space missions have relied on radioisotope power systems for energy. The nuclear isotope that powers these systems is Plutonium 238. Currently, the United States has a dwindling supply of Plutonium 238 putting NASA deep space missions at risk.

The small reactor system proposed by Los Alamos would have many advantages. The design is simple and relies on existing technologies. The use of uranium fuel and the low power of the reactor mean that safety and regulatory issues are greatly reduced or eliminated. The great potential of this reactor concept was recently recognized when it received a 2013 R&D 100 award.

Los Alamos sees this small nuclear reactor as a stepping-stone to a reinvigoration of nuclear reactors for space applications. Currently NASA is attempting to fund the technology development of this reactor concept. Cut backs in NASA funding are making this difficult, but all indications point to this technology going forward.

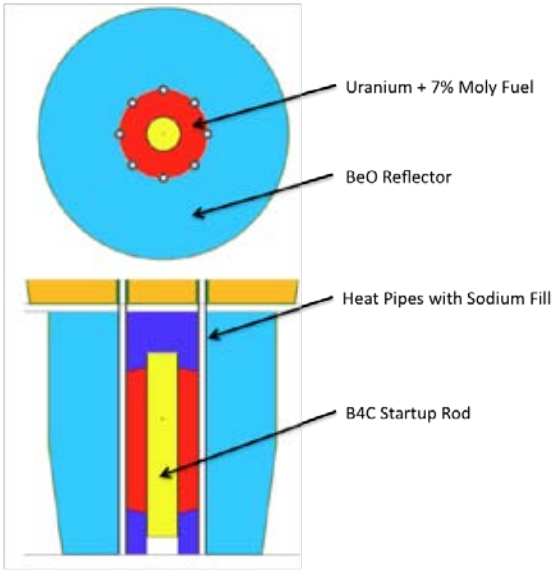

Figure 1. Reference Reactor Concept

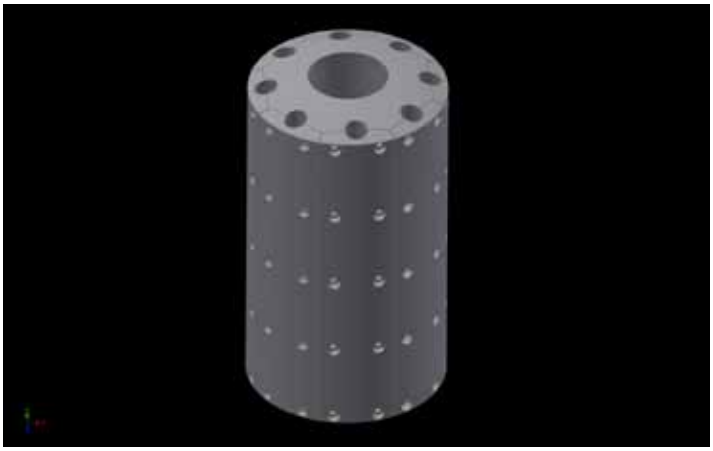

Figure 2. Example Heat Pipe Bonding Technique

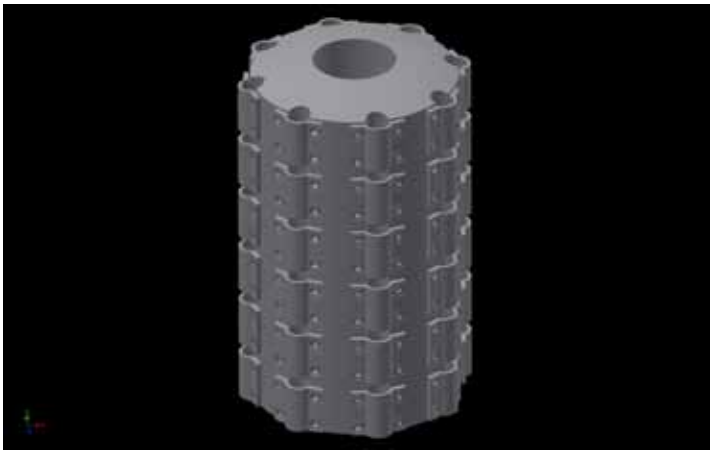

Figure 3. Example Heat Pipe Bonding Technique

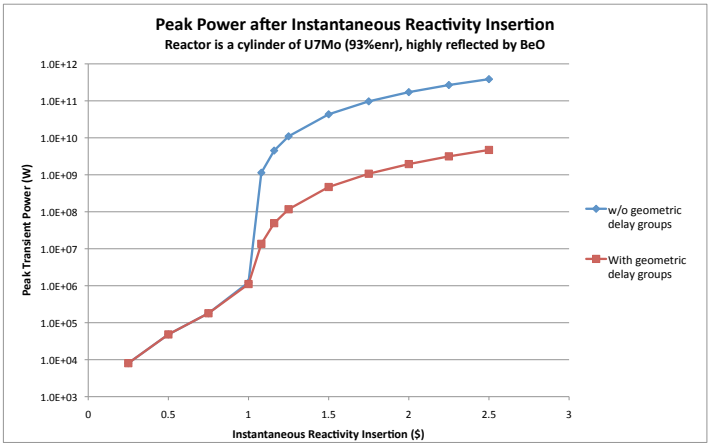

Figure 4. Peak Power After Reactivity Insertion

Figure 5. Peak Fuel Temperature vs Reactivity Insertion Rate

References

1. Pelowitz, D. B.. MCNP6 User's Manual. 2005. Los Alamos National Laboratory Report LA-CP-05-0137 .

2. Poston, D. I., D. D. Dixon, T. F. Marcille, and B. W. Amiri.

FRINK – A Code to Evaluate Small Reactor Transients. 2007. In Proceedings of Space Technology and Applications International Forum (STAIF-2007). (Albuquerque, NM, 2007). Vol. #800, p. 50. Melville, New York: AIP Conf. Proc..

Publications

McClrue, P. R., D. I. Poston, and D. D. Dixon. EXPERIMENTAL DEMONSTRATION OF A HEAT PIPE/STIRLING ENGINE NUCLEAR REACTOR. 2013. In American Nuclear Society Annual Meeting. (Atlanta, GA, 10-15 June 2013). , p. 1020. La Grange Park, Il: ANS.

Poston, D. I.. CRITICALITY AND DYNAMIC BENCHMARKING OF THE DUFF REACTOR TEST. 2013. In American Nuclear Society Annual Meeting. (Atlanta, GA, 10-15 June 2013). , p. 1015. La Grange Park, Il: ANS.

Poston, D. I., D. D. Dixon, P. R. McClure, and M. A. Gibson. A Simple, Low-Power Fission Reactor for Space Exploration Power Systems. 2013. In Proceedings of Nuclear and Emerging Technologies for Space 2013. (Albuquerque, NM, 25-28 Feb. 2013). , p. 15. Albuquerque: American Nuclear Society.

Poston, D. I., P. R. McClure, D. D. Dixon, and M. A. Gibson. Experimental Demonstration of a Heat Pipe/Stirling Engine Nuclear Reactor. To appear in Journal of Nuclear Technology.

Poston, D. I., P. R. McClure, and D. D. Dixon. The DUFF Experiment – What Was Learned?. 2013. In Proceedings of Nuclear and Emerging Technologies for Space 2013. (Albuquerque, NM, 25-28, Feb. 2013). , p. 20. Albuquerque: ANS.

pRad Measurements of Meteorites

Chad T. Olinger
20130811ER

Abstract

Nondestructively exploring three-dimensional density structure of meteorites establishes new signatures associated with meteorite structure, providing new opportunities to investigate metamorphic relationships such as aqueous alteration veins, chondrule size and shape distributions as well as identification of xenoliths for subsequent isotopic and elemental analyses. This LDRD reserve proposal continues to develop capabilities using Proton Radiography (p-Rad) to nondestructively obtain meteorite structural information, a capability demonstrated for the first time in December 2012. In addition, we use p-rad density signatures to guide sectioning for complementary study using the Cameca IMS 1280 Large Geomoetry Secondary Ion Mass Spectrometer (LG SIMS) and scanning electron microscopy (SEM). In addition to these two activities, this project also took advantage of a target of opportunity using the Lujan Center's neutron tomography capability. Very preliminary analysis suggests the ability to nondestructively identify the size and location of specific mineral phases through neutron resonance spectroscopy using pixelated time-of-flight measurements.

Background and Research Objectives

A one day target of opportunity was exploited in December of 2012 radiographing an H chondrite meteoritic sample know as Abbott, which represents material that was processed on the surface of a planetessimal and a pallasite meteorite named Milton, which represents a rock formed near the core of a highly differentiated parent body. These samples provided challenges for developmental p-Rad tomography techniques. Significant internal structure could be identified in both of these quick turn-around samples, demonstrating the power of p-Rad for geologic/planetary science studies and motivating the current LDRD reserve proposal.

We had the initial goals of 1) expanding on the number and types of meteorite samples analyzed with p-Rad and 2) selecting features identified through non-destructive p-Rad tomography for subsequent LG SIMS measurements. Collaborators from the University of New Mexico Institute of Meteoritics Carl Agee and Rhian Jones were instrumental in quickly providing samples for the preliminary study in December as well as a sample of the 2013 Chelyabinsk meteorite fall for p-Rad in this 3-month reserve effort. In addition, we procured two samples of the Murchison meteorite, with the intent that measurements of this relatively abundant sample will eventually motivate future P-Rad of the similar Sutter's Mill meteorite, which, similar to the Chelyabinsk meteorite, represents a bolide event equivalent to a 4kT explosion over California on April 22, 2012.

Scientific Approach and Accomplishments

Due to activation of short-lived radionuclides from proton radiography and the short (3-month) time frame of this study, we were unable to perform fresh P-Rad measurements on the same samples we used for SEM and LG-SIMS measurements. Our strategy therefore evolved to performing SEM and LG SIMS measurements on the Abbott and Milton samples radiographed in December 2012, and obtaining new P-Rad measurements on one of the Chelyabinsk meteorite samples provided by UNM.

Programmatic efforts had priority on P-Rad beam time, and uncertainties associated with this encouraged us to also pursue a parallel path of neutron tomography at the Lujan center. We had sufficient samples to provide each of these three measurement pathways separate samples, with the goal of performing complementary measurements where possible. The Chelyabinsk sample that had p-Rad tomography performed is awaiting neutron tomography later this week.

To date, we have obtained bulk elemental compositional maps on cross-sections obtained on the Milton (Figure 1) and Abbott (Figure 2) meteorites. The December 2012 P-Rad tomographs of Abbott demonstrated a significant

rind around the entire perimeter, which we conjectured might represent fusion crust or desert varnish. However, SEM elemental maps did not reflect any systematic change in elemental abundance across this zone. We now believe it is possible that this apparent rind was an artifact of the computed tomographic inversion, where limbing (reduced energy attenuation where the proton path length is reduced) can be an issue. These SEM images also reveal that what we believed to be chondrules within the meteorite are, at least in many cases, silicates enclosed by metal inclusions, but not necessarily individual chondrules with rims. The SEM maps do reveal a highly heterogeneous structure that can now be correlated with the original P-Rad tomographs. These SEM maps also transect veining features that show enhanced concentrations in Al and Fe. Plans were to obtain oxygen isotope transects with the LG SIMS on the Milton sample in mid-September at the time of the writing of this report, those values have not yet been reported.

A ~1 cm diameter sample of the Chelyabinsk meteorite was radiographed at P-Rad under this effort, and can now be used to inform subsequent sampling. We have a movie of the 720 ½ degree steps of the P-Rad of this sample, as well as a computed tomograph movie of virtual slices moving up through this sample (Figure 3 is a representative image from the raw radiograph).

We also acquired spatially resolved neutron time-of-flight spectral transmission images of a ~ 3 cm sample of the Chelyabinsk meteorite (Figure 4). Spectral features in Figure 4 reflect a clear neutron absorption feature at 129 eV. At the time of the writing of this report, the data are less than 24 hours old; the neutron resonance feature is consistent with 59Co absorption feature. This would identify the mineral phase to be most likely kamacite; having identified this feature, the entire sample can now be reanalyzed to nondestructively identify those phases in 3D.

Our plan moving forward is to publish these results and develop LDRD and NASA cosmochemistry proposals that build on these preliminary results.

Impact on National Missions

Nuclear forensics is a significant direction for part of the global security mission of LANL. While these measurements are not specifically directed at nuclear forensics, they do exercise capabilities relevant to nuclear forensics and have generated results that are publishable in the open literature and demonstrate the value of coordinated nondestructive radiography techniques with sectioning and subsequent elemental and isotopic mapping of samples. These correlated measurements informed the p-Rad computed tomographic analysis resulting in improvements to the analysis algorithm. These improvements prevented the computational artifact of the thick "rind" observed in the original Abbott tomograph in December from being repeated in the more recent computed tomograph image of the Chelyabinsk meteorite. Moreover, spatial resolution has improved from ~100 microns in December 2012 to ~20 – 40 microns in the September 2013 radiograph of Chelyabinsk. Each of these tools individually establishes capabilities for nuclear forensics and potentially nuclear archeology. Combined, they provide the opportunity for targeted destructive analyses, further advancing these fields while also advancing the state of the art for geologic and planetary science studies, all of which support the nation's leadership in science.

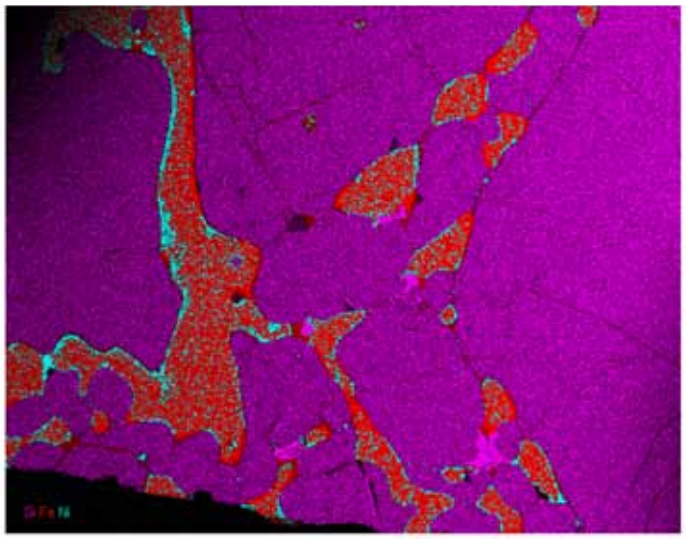

Figure 1. Milton SEM Elemental Map

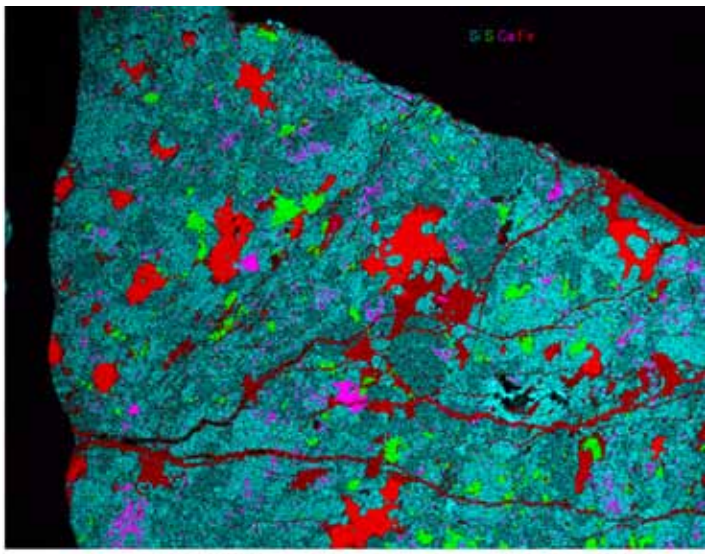

Figure 2. Abbott SEM Elemental Map

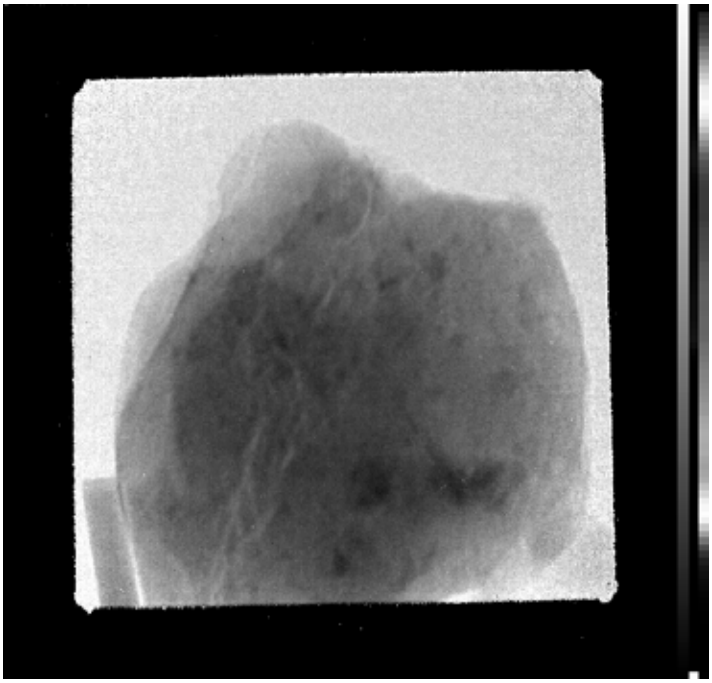

Figure 3. Proton Radiograph of Chelyabinsk Meteorite

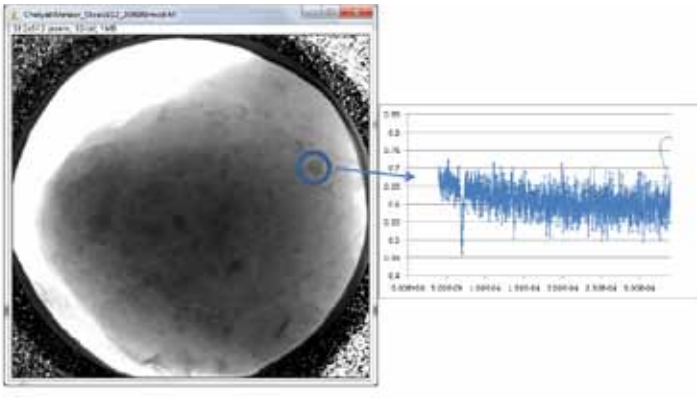

Figure 4. Neutron Radiograph of Chelyabinsk Meteorite with time-of-flight spectrum showing a Co-59 absorption feature.

Publications

Olinger, C. T.. Proton radiography of meteorite samples. 2013. Presentation to The Albuquerque Astronomical Society.

Quantum Simulations: From Superconductivity to Nanoscale Electronics

Eddy M. Timmermans
20110711PRD2

Introduction

We study cold atom systems and their use as quantum simulators of superconductors and many-body effects in nanoscale transport. This is a competitive field with broad implications, e.g., in condensed matter physics, nanoscale science, and quantum information. Quantum simulation uses the highly controllable nature of one quantum system (here, a cold atom cloud) to create simplified analogs of complex materials and devices in order to gain direct theoretical and experimental insight into the underlying physical phenomenon. We develop, theoretically, a scheme for emulation of various superconductors in cold atom setups to address problems inaccessible in traditional condensed matter settings. In particular, we develop a unified theory of spectroscopic measurements on cold atom and superconducting systems in order to help understand the mechanisms of high-Tc superconductivity as revealed by cold-atom simulations. From here, more complex systems will be studied to understand quantum and nonequilibrium effects in nanoscale electronic systems, as well as to provide additional measurement techniques capable of probing the cold atom systems. This will elucidate the role of electron-electron interactions and dissipation in electronic transport – effects that are difficult to capture in traditional theoretical approaches to transport.

The postdoc's (PD) work characterizes the promising methods for extracting information from cold atom systems that may reveal the main phenomena that underpin high-Tc superconductivity. Superconducting materials have the potential to revolutionize power distribution, i.e., create more efficient means of distributing electricity that will be helpful in moving to green sources of energy among other things. Also, the PD investigates nonequilibrium and inhomogeneous cold atom systems in order to understand quantum effects in electronic transport, which is crucial in designing functional nanoscale devices.

Benefit to National Security Missions

This work may bring better understanding of high-Tc superconductors: materials with zero electrical resistance. These materials have important applications like, e.g., they can eliminate virtually all the loss of energy that goes into resistive heating in the lines transmitting electricity. This research will also advance fundamental understanding of materials on the basic quantum level. Both goals are becoming focus areas for numerous sponsors including DOE and BES, for example, for both applied and basic aspects of energy research.

Progress

The PD searched the literature on the response of superconductors and superfluids to external perturbations. Surprisingly, most authors did not notice that their results violate the important conservation law of particle numbers. We found that this inconsistency is due to the neglect of collective excitations associated with the coherent state of superconductor and superfluids. We successfully developed a consistent description of the response of superconductors and superfluids that satisfies the conservation law. Also we addressed useful criteria for checking whether a theory respects the conservation law and point out some pitfalls if one tries to fix the problem naively. Importantly, the PD's theory provides better estimations of the excitation spectrum and compressibility.

The PD has developed codes for studying quantum dynamics of atoms and applied them to new designs of devices using atoms and engineered optical trapping potentials. Since atoms are charge-neutral, connecting the system to a battery cannot drive an atomic current. However, a recently developed technique let atoms exchange momentum and energy with photons and we developed a method for driving atoms based on this scheme. We found that the current of a fully quantum system exhibits very different behavior from what one

may expect by treating the atoms as classical objects. We also propose new designs of devices that allow one to control the direction and magnitude of the atomic current by tuning the external photon source. This level of control had not been possible in the literature prior to the PD's work.

Experimentally one can mix two species of atoms together. To elucidate the physics of such systems, the PD developed a theoretical framework for describing such a mixture. Since the inter-species repulsive interactions are tunable, the system can either be a homogeneous mixture or it can separate into two parts with different species avoiding each other (phase separation). At extremely low temperature, there has been an effective description of this system. However, at finite temperature there are many thermal excitations and a more sophisticated treatment is needed. Using advanced quantum-mechanical methods the PD successfully included the interactions among those thermal excitations and found that the two possible states at low temperature continue to exist at higher temperatures. Moreover, the inter-species interactions can be controlled by an external magnetic field. The PD thus generalized our theory to include dynamical effects when the interaction is changed suddenly. From the PD's simulations we observed that the system develops interesting patterns reflecting the stable state after the change. Our work provides more insight into multi-species superconductors and superfluids and the results have been published.

In previous work the PD found that the heat transport properties of DNA molecules can change dramatically when DNA dissociates from its double-helix structure to two single strands due to high temperature. The PD successfully designed a device utilizing this property of DNA. This device has a piece of DNA clamped by two metallic leads with different temperatures. By choosing different sequences or length of DNA, this device has thermal switching behavior at different temperatures. Immediately after his publication, a European and a US group performed experiments and demonstrated novel devices inspired by our work.

Future Work

This project addresses three major challenges:

Recent experiments have demonstrated the ability to mix atoms in different quantum states/species. We plan to extend our theoretical study of atomic systems to those multi-component systems. One major challenge is to include inter-species interactions while respecting the number conservation of each species. We derive the corresponding equations describing physical quantities that can be measured in experiments. By comparing our results with experimental data, we may explore novel quantum phases and understand interplays among different species.

When two systems exchange particles, correlations start to build up. A quantity called entanglement entropy describes how correlated the two systems are and it is of broad interest ranging from black-hole physics to quantum information. We will study the dynamics of the entanglement entropy when atoms are driven by a bias and flow across an artificial lattice generated by laser light. There have been theoretical predictions based on modeling atoms as billiards moving in the lattice. However, atoms should be modeled as quantum waves and we can study them using our quantum description. We run simulations and investigate how important quantum effects are in the entanglement entropy.

We continue our study on energy transport in complex molecules using both analytical calculations and molecular-dynamics simulations to investigate how to control the thermal conductance of a given material. We found that by increasing the binding energy on each atomic site of a molecular chain, the molecule conducts less heat. We aim to study how the thermal conductance changes if local structures of a molecule are altered as scientists do regularly nowadays. Sorting out what kinds of local structures can help increase or decrease the heat conductance could lead us to better designs of thermally controlled devices.

Conclusion

The results from quantum simulations may provide more insight into the parallels between cold atom and high-Tc superconducting systems, which represents a unique opportunity in the field of physics. The analogies may, eventually, lead to the discovery of novel superconductors of higher transition temperatures. Superconductivity is one of the most significant discoveries in the 20th century and has important applications in dissipationless power transmission and advanced medical instruments. The unified theory, which we will develop for quantum transport in nanoscale will lead to new design of nano devices. These new nano devices will play a crucial role in next-generation electronics.

Publications

Chern, G. W., C. C. Chien, and M. Di Ventra. Dynamically generated flat-band phases in optical kagome lattices. Physical Review Letters.

Chien, C. C.. Spatially varying interactions induced in atomic gases by optical Feshbach resonance . 2012. Physics Letters A. 376: 729.

Chien, C. C., D. Gruss, M. Di Ventra, and M. Zwolak. Interaction-induced conducting-nonconducting transition of ultra-cold atoms in 1D optical lattices . 2013. New

Journal of Physics. 15: 063026.

Chien, C. C., F. Cooper, and E. Timmermans. Large-N approximation for single- and two-component dilute Bose gases . 2012. Physical Review A. 86: 023634.

Chien, C. C., H. Guo, and K. Levin. Comment on "Density and spin response of a strongly-interacting Fermi gas in the attractive and quasi-repulsive regime". 2012. Physical Review Letters. 109: 118901.

Chien, C. C., J. She, and F. Cooper. Mean-field description of pairing effects, BKT physics, and superfluidity in 2D Bose gases. Annals of Physics.

Chien, C. C., K. A. Velizhenin, Y. Dubi, and M. Zwolak. Tunable thermal switching via DNA-based nano devices. 2013. Nanotechnology. 24: 095704.

Chien, C. C., M. Zwolak, and M. Di Ventra. Bosonic and fermionic transport phenomena of ultra-cold atoms in 1D optical lattices . 2012. Physical Review A. 85: 041601.

Chien, C. C., and F. Cooper. Quench dynamics and emergence of phase separation in two-component atomic Bose gases at zero temperature and above the BEC critical temperature. 2013. Physical Review A. 87: 045602.

Chien, C. C., and M. Di Ventra. Dynamical crossover between the infinite-volume and empty-lattice limits of ultra-cold fermions in 1D optical lattices . 2012. Europhysics Letters. 99: 40003.

Chien, C. C., and M. Di Ventra. Controlling transport of ultra-cold atoms in 1D optical lattices with artificial gauge fields. 2013. Physical Review A. 87: 023609.

Cooper, F., B. Mihaila, J. F. Dawson, C. C. Chien, and E. Timmermans. Auxiliary field approach to dilute Bose gases with tunable interactions . 2011. Physical Review A. 83: 053622.

Cooper, F., C. C. Chien, B. Mihaila, J. F. Dawson, and E. Timmermans. Composite-field Goldstone states and Higgs mechanism in dilute Bose gases . 2012. Physical Review A. 85: 023631.

Dawson, J. F., F. Cooper, C. C. Chien, and B. Mihaila. Leading-order auxiliary field theory of the Bose-Hubbard model. 2013. Physical Review A. 88: 023607.

Doi, K., M. Tsutsui, T. Ohshiro, C. C. Chien, M. Zwolak, M. Taniguchi, T. Kawai, S. Kawano, and M. Di Ventra. Electrochemical response of biased nanoelectrodes in solution. Journal of Physical Chemistry C.

Guo, H., C. C. Chien, Y. He, and K. Levin. Fundamental constraints on linear response theories of Fermi superfluids above and below Tc. 2013. International Journal of Modern Physics B. 27: 1330010.

Guo, H., C. C. Chien, and Y. He. Gauge invariant linear response theory of relativistic BCS superfluids . 2012. Physical Review D. 85: 074025.

Guo, H., C. C. Chien, and Y. He. Theories of linear response in BCS superfluids and how they meet fundamental constraints. 2013. Journal of Low Temperature Physics. 172: 5.

Guo, H., Y. He, C. C. Chien, and K. Levin. The compressibility in strongly correlated superconductors and superfluids: from BCS to BEC. To appear in Physical Review A.

Guo, H., Y. Li, Y. He, and C. C. Chien. Density and spin linear response of atomic Fermi superfluids with population imbalance in BCS-BEC crossover. Physical Review A.

Mihaila, B., F. Cooper, J. F. Dawson, C. C. Chien, and E. Timmermans. Analytical limits for cold-atom Bose gases with tunable interactions. 2011. Physical Review A. 84: 023603.

Mihaila, B., J. F. Dawson, F. Cooper, C. C. Chien, and E. Timmermans. Auxiliary field formalism for dilute fermionic atom gases with tunable interactions. 2011. Physical Review A. 83: 053637.

Velizhanin, K. A., C. C. Chien, Y. Dubi, and M. Zwolak. Driving denaturation: Nanoscale thermal transport as a probe of DNA melting. 2011. Physical Review E. 83: 050906.

Wulin, D., B. M. Fregoso, H. Guo, C. C. Chien, and K. Levin. Conductivity in Pseudogapped Superconductors: The Role of the Fermi Arcs. 2011. Physical Review B. 84: 140509.

Wulin, D., H. Guo, C. C. Chien, and K. Levin. Spin Transport in Cold Fermi gases: A Pseudogap Interpretation of Spin Diffusion Experiments at Unitarity . 2011. Physical Review A. 83: 061601.

Wulin, D., H. Guo, C. C. Chien, and K. Levin. Two-component optical conductivity in the cuprates: A necessary consequence of preformed pairs . 2012. Physical Review B. 86: 134518.

Shortcuts to Adiabaticity in Quantum Devices

Wojciech H. Zurek
20110736PRD2

Introduction

The concept "Fast Good" pushed forward by the world-leading chef F. Adria might be a motto born in modern cuisine, but it actually applies to many areas of the day-to-day life. When it comes to technology there is certainly no doubt that shortening production processes pays great dividends, and the quest for faster and more powerful devices such as computers has been running for decades as dramatically illustrated by Moore's law.

But all quantum technologies crash with the Fast Good trend at a fundamental level. At a microscopic scale, higher performance of a quantum device comes generally at the price of slowing down its running time, as dictated by text-book theorems in quantum theory. The focus of this research project is to spur quantum technologies by changing this state of affairs and finding ways out to fulfill both sides of the Fast-Good dichotomy. It will deepen the current understanding of dynamical process, put forward new schemes in the state-of-the-art experimental control of quantum devices, and accelerate the development of new benchmarks in quantum metrology, simulation and computation.

Benefit to National Security Missions

This project will allow for a better control of quantum systems. This has broad applications, that cut across many areas of interest to DOE and LANL. This includes nanoscience, quantum sensitive measurement, information processing, and related areas. While this is admittedly long-term research, the measurement tools that may develop could impact any national security mission that depends on sensing technology.

Progress

In the last 12 months, Adolfo del Campo has submitted 7 publications to peer-review journals including two Physical Review Letters, a third paper under consideration in this journal, two manuscripts under consideration in Nature Communications, a review accepted in Advances in Atomic, Molecular, and Optical Physics, an other review accepted in Journal of Physics: Condensed Matter. This work has been devoted to the following accomplishments.

Prior to his arrival to LANL, the JRO fellow Adolfo del Campo proposed theoretically an experimental test of the Kibble-Zurek mechanism, the paradigmatic theory for defect formation across a phase transition. After starting a collaboration with the experimental group at PTB led by Tanja Mehlstaubler, the first experimental results on the universal defect formation dynamics in inhomogeneous systems have been reported jointly. The results are currently under consideration in Nature Communications for publication.

The understanding of inhomogeneous phase transitions was reviewed and extended in collaboration with the PI (Wojciech Zurek) and Tom Kibble, the founding fathers of the paradigmatic model to describe the universal dynamics of defect formation across phase transitions (the Kibble-Zurek mechanism). It has been shown that in inhomogeneous systems defect formation can be controlled, a possibility of great interest in material science.

The first review on the field of shortcuts to adiabaticity was also coauthored by the Adolfo del Campo.

New shortcuts to adiabaticity have been developed, generalizing the counter-diabatic driving technique which allows one to drive a system quickly mimicking adiabaticity. The new approach is extremely powerful since it applies to many-body interacting systems as well as non-linear systems where the old theory was not applicable. Experimental tests of this technique have been designed and proposed.

Further, shortcuts to adiabaticity have been applied to finite-time thermodynamics, leading to an experimentally realizable scheme to engineer with trapped ions a superadiabatic engine which operates at maximum

efficiency and with tunable output power.

Future Work

In quantum technologies, when implementing in the laboratory a given process or operation, one faces a trade-off between the accuracy and speed of implementation. This is dictated by the quantum adiabatic theorem. Its breakdown leads inevitably to formation of excitation, which is undesirable for a wide range of applications, such as the preparation of novel quantum phases in quantum simulation, and adiabatic quantum computation. Suppressing excitations is also of interest to a variety of operations in the laboratory, like entangling strings of atom.

The goal is to propose methods to mimic adiabaticity, even when the dynamics is ultrafast and adiabaticity breaks down. In other words, the project aims at preparing the same target state that would result in a truly adiabatic (slow) process, but imposing simultaneously a fast implementation. The JRO fellow will continue developing new techniques in the field of shortcuts to adiabaticity and explore their applications.

This will include the design of of a superadiabatic engine based on the counter-diabatic driving of particles undergoing Brownian dynamics, operating at maximum efficiency, and the design of a new experiment to test the Kibble-Zurek mechanism in colloids.

With respect to the trapped ions which were used in the experimental results reported in FY13, colloids allow to access large system sizes, can be easily imaged, and are greatly overdamped. All this features will allow us dto overcome the main drawbacks of ion traps, and generate a new set of experiments on the universal dynamics of defect formation.

Finally, Adolfo del Campo will study the fundamental limits to the speed of evolution which constitutes ultimate limits to quantum computing and information processing.

Conclusion

Though quantum technologies such as atomic clocks have been benefiting society since the fifties, it is clear that they are playing and ever increasing role. They have the potential to do better and completely outperform conventional electronics. The exploitation of quantum laws in metrology, shows how the race for ever better clocks have brought technological advances such as the GPS required for satellite navigation, ultimately transforming society in a global scale through new communication and business models. Other quantum technologies in a nascent stage, might revolutionize the fields of simulation, computation and communication.

Publications

Campo, A. del. Shortcuts to Adiabaticity by Counterdiabatic Driving. 2013. PHYSICAL REVIEW LETTERS. 111 (10): -.

Campo, A. del, I. L. Egusquiza, M. B. Plenio, and S. F. Huelga. Quantum speed limits in open system dynamics . 2013. Physical Review Letters. 110: 050403.

Campo, A. del, M. M. Rams, and W. H. Zurek. Assisted finite-rate adiabatic passage across a quantum critical point: Exact solution for the quantum Ising model. 2012. Physical Review Letters, 109, 115703 (2012) . 109: 115703.

Campo, A. del, T. W. B. Kibble, and W. H. Zurek. Causality and non-equilibrium second-order phase transitions in inhomogeneous systems. 2013. J. Phys.: Condens. Matter. 25: 404210.

Campo, A. del, and M. G. Boshier. Shortcuts to adiabaticity in a time-dependent box . 2012. Scientific Reports. 2: 648.

Campo, A. del, and W. H. Zurek. Universality of phase transition dynamics: topological defects from symmetry breaking. Professor Tom Kibble's 80th birthday's Symposium. Edited by Gauntlett, J. P..

Nigmatullin, R., A. del Campo, G. De Chiara, G. Morigi, M. B. Plenio, and A. Retzker. Formation of helical ion chains . 2011. LA-UR 11-06244.

Pyka, K., J. Keller, H. L. Partner, R. Nigmatullin, T. Burgermeister, D. M. Meier, K. Kuhlmann, A. Retzker, M. B. Plenio, W. H. Zurek, A. del Campo, and T. E. Mehlstaubler. Topological defect formation and spontaneous symmetry breaking in ion Coulomb crystals. 2013. NATURE COMMUNICATIONS. 4: -.

Torrontegui, E., S. Ibanez, S. Martinez-Garaot, M. Modugno, A. del Campo, D. Guery-Odelin, A. Ruschhaupt, X. Chen, and J. G. Muga. Shortcuts to Adiabaticity. 2013. ADVANCES IN ATOMIC, MOLECULAR, AND OPTICAL PHYSICS, VOL 62. 62: 117.

Influence of Velocity Shear on Turbulent Magnetic Reconnection at the Earth's Magnetopause

William S. Daughton
20110750PRD3

Introduction

Magnetic reconnection is a basic process that occurs in hot ionized gases known as plasmas. As this process develops, magnetic field energy is rapidly converted into particle kinetic energy. This process plays an important role in a wide variety of problems in space, laboratory and astrophysical plasmas. The focus of this project is on the dynamics of magnetic reconnection within the Earth's magnetosphere – a protective magnetic bubble that partially shields our planet from energetic particles. In this environment, magnetic reconnection often occurs in the presence of intense velocity shear, which can drive the formation of large-scale flow vortices, in much the same way as in ordinary fluids. However, in high-temperature plasmas, these vortices are closely coupled to the evolution of the magnetic field lines, which can then trigger the process of magnetic reconnection. Thus in reality, these two processes can interact in a complex manner, which can only be fully described with three-dimensional computer simulations. This project will lead to a new understanding regarding how velocity shear influences reconnection by employing some of the world's fastest supercomputers such as the Kraken and Jaguar machines. The research will involve a combination of basic theory and large-scale kinetic simulations that describe the temperature plasma at the most fundamental level. The project will utilize the plasma simulation code VPIC, which has been carefully optimized to take full advantage of these new computers. In order to intelligently setup and interpret these simulations, some basic theoretical approaches will also be utilized.

Benefit to National Security Missions

This research will exploit the newest generation of petascale supercomputers using a kinetic simulation code (VPIC) specially optimized for these machines. Some of these calculations will be performed locally at Los Alamos using NNSA computers, while other calculations will be performed on flagship DOE supercomputers such as Jaguar at Oak Ridge. These efforts are at the very forefront of high performance computing, both for scaling the calculations to large numbers of cores (~200,000) and in remote visualization and analysis of the results. We thus build capability for hydrodynamic simulations of nuclear weapons. Scientific results from this research will benefit NASA missions focused on understanding the near-Earth space environment. In particular, the upcoming Magnetospheric MultiScale (MMS) mission will focus on the kinetic physics of magnetic reconnection with the Earth's magnetosphere. The same science is essential to understanding the environment for satellites that support nuclear nonproliferation and other national security missions.

Progress

Ionized gas (or plasma) is continually streaming outward from the Sun. When this stream of plasma interacts with the magnetic field of the Earth, it produces the magnetosphere – a protective magnetic bubble that partially shields our planet from energetic particles. The dynamics of the magnetosphere has long been of interest both scientifically and for practical impacts to modern infrastructure, including damage to satellites, interruption of GPS service, and power grid failures. The focus of this Director's fellowship project is to examine several natural processes that can give rise to leaks in this shield. These leaks typically occur within a thin boundary layer in which both the magnetic field and plasma velocity change rapidly. The rapid change in the magnetic field drives a process known as magnetic reconnection, which can change how field lines are connected in the plasma and release energy stored in these fields. On the other hand, the strong velocity shear in these boundary layers can drive an instability known as Kelvin-Helmholtz, which leads to swirls and vortices in the flow. While both of these processes are interesting and important, they are usually studied separately. However, in the real magnetosphere they may often occur together and influence each other in complex ways. We are addressing this possibility by performing large-scale computer simula-

tions using the LANL developed VPIC code which describes the physics of these processes in a rigorous manner. During the past fiscal year, we have completed the first 3D simulations of this process using 100,000 cores on the Jaguar computer at Oak Ridge National Laboratory. Many additional smaller scale simulations were also performed on the Mustang machine at LANL. As described in a new paper, these 3D simulations feature the development of magnetic flux rope structures around the periphery of the vortex, leading to a complex tangled magnetic field and fully turbulent layers. These 3D features lead to enhanced mixing of particles across the boundary layer, which may be important for modeling the low-latitude magnetopause boundary layer. While the paper describing these results is still in review, the preliminary results have attracted considerable attention at the Fall AGU meeting and Takuma Nakamura was asked to give an invited talk at the upcoming IAGA meeting, one of the largest international conferences in geophysics.

During the final months of this project, we will work towards analyzing existing simulations and performing a few additional simulations with more realistic initial conditions. We expect to finish several additional journal articles from this work.

Future Work

This Director's funded fellowship will reach completion in November, 2013. As described in our new JGR paper, the results from this project are leading to a new understanding of vortex-induced reconnection at the Earth's magnetopause. These are the first fully kinetic 3D simulations of this process, and the results have raised a number of new questions as well as testable predictions for future spacecraft observations. During the remainder of this project, we will perform a few additional simulations and work towards finishing the analysis of the existing 3D results. Our goal is to develop a better understanding of how the mixing across the layer is influenced by the initial conditions. We will document these results in additional journal articles, and present our findings at both domestic and international meetings.

Conclusion

Scientists believe that magnetic reconnection plays a central role in a wide variety of applications such as geomagnetic substorms, solar flares and laboratory fusion machines. The ability to predict the complex nonlinear behavior of high temperature plasma is of great practical importance for these applications. For example, the results of this project may have direct application to modeling the plasma environment surrounding the Earth where communication satellites play a crucial role in modern society.

Publications

Karimabadi, H., V. Roytershteyn, M. Wan, W. H. Matthaeus, W. Daughton, P. Wu, M. Shay, B. Loring, J. Borovsky, E. Leonardis, S. C. Chapman, and T. K. M. Nakamura. Coherent structures, intermittent turbulence, and dissipation in high-temperature plasmas. 2013. PHYSICS OF PLASMAS. 20 (1): -.

Nakamura, T. K. M., R. Nakamura, A. Alexandrova, Y. Kubota, and T. Nagai. Hall magnetohydrodynamic effects for three-dimensional magnetic reconnection with finite width along the direction of the current. 2012. JOURNAL OF GEOPHYSICAL RESEARCH-SPACE PHYSICS. 117: -.

Nakamura, T., W. Daughton, H. Karimabadi, and S. Eriksson. Three-Dimensional Dynamics of Vortex-Induced Reconnection and Comparison with THEMIS Observations. 2013. Journal of Geophysical Research. 118: doi:10.1002/jgra.50547.

Non-equilibrium Transport in Nanoscale Thermal Energy Harvesting

Jianxin Zhu
20120737PRD1

Introduction

Energy harvesting and waste is a great bottleneck in the supply of energy resources to a sustainable economy. In addition to developing carbon-free green energy sources, it is also beneficial to enhance the efficiency of energy utilization. On this aspect, control of energy at the nanoscale creates unprecedented opportunities for directing and conversion of energy. Among various forms of energy, heat, electricity, and light are three of the most familiar. Future generations of multimode energy harvester rests with the integration of electronics, photonics, and phononics (carrying heat). Therefore, it is critical to gain a fundamental understanding of non-equilibrium transport of electrons/phonons (vibrational thermal energy) at the nanoscale, the interplay between them as well as their coupling to photons.

In this project, we will achieve this goal by considering out-of-equilibrium transport through open quantum nanoscale systems in contact with electrical and/or thermal reservoirs. We will develop new theoretical approaches to tackle the problem in a wide range of parameter space, like the strength of electron-electron interaction and electron-phonon coupling. Scientifically, we will address the effects of these interactions on thermoelectricity, and pay special attention to the conditions for optimal thermoelectric figure of merit value. Furthermore, we will consider the coupling of local vibration modes and electrons in these nanoscale systems to a coherent optical field, and investigate the optical control of thermoelectric transport out of equilibrium.

Benefit to National Security Missions

The development of a fundamental understanding of non-equilibrium transport of electrons/phonons (vibrational thermal energy) at nanoscale will have an immediate impact to energy generation and harvesting. It will support and guide experimental effort on energy research at LANL. Once the effects of electron-electron and electron-lattice vibration mode coupling on the non-equilibrium thermoelectric transport is understood, the efficiency of thermoelectricity at the nanoscale can be optimized.

Furthermore, by coupling these electronic and local vibrational degrees of freedom to photons (light), the thermoelectric transport out of equilibrium can be controlled. The research is aligned with the Energy Frontier Research Centers Program established by Department of Energy on the aspect of energy efficiency.

Progress

We have developed a thermal transport theory based on the scattering wave approach for various interface systems, including normal metal or topological insulator and superconductor interface. By applying the interfacial heat transfer formula, we have uncovered several anomalous thermal properties, such as thermal energy's Klein tunneling, asymmetric Kapitza resistance and negative differential thermal resistance. We have also discovered a new class of Hall-like effects, that is, the asymmetric Andreev reflection is able to induce the electric and thermal Hall-like effects in metal/anisotropic superconductor junctions. These findings could have potential applications for the smart energy control in various hybridized mesoscopic systems.

We have uncovered the fundamental effects of geometric phase and topological bands in several scenarios of energy transport. Our main results include: Geometric phase effect can provide additional channel for energy transfer, thus enhances the transfer efficiency; Topological bands of magnon can transfer the energy and spin information robustly and non-dissipatively; The complex bands of nonequilibrium open systems can be clarified by the braid groups and process topological phase transitions: the braid phase transition. These uncovered fundamental effects have potential applications for efficient energy transport and harvesting.

Spin Seebeck effect is a new phenomenon that temperature bias can produce a pure spin (without electric) current and an associated spin voltage. We have uncovered the intriguing rectification effect and negative different conductance for spin Seebeck effect, so that spin Seebeck diode and transistor are now within our grasp. We expect our findings will act as new methods facilitating the functional use of heat and opens a new possibility of spintronics and spin caloritronics.

Future Work

We will expand our present focus to include more many-body degrees of freedom and extend the thermal energy harvesting to the spintronics and spin caloritronics. By integrating electron-phonon, electron-spin (magnon), magnon-phonon, electron-photon interactions in the non-equilibrium transport study of hybrid condensed matters and nano-devices with interfaces, we expect to integrate the thermoelectricity, optomechanics, photovoltaics to achieve the multi-mode efficient energy harvesting.

Upon gaining the knowledge of functional thermal devices, such as thermal diode, transistor, switch, memory, we are going to explore the design principle of "thermal metamaterials". We will spend time on developing the special conformal field theory to the thermodynamics and heat transfer in various materials with possible hybrid interfaces. Heat flux cloaking and concentrating in designed solid states would be the first attempt to achieve the goal of "thermal metamaterials."

Conclusion

This project will develop a theoretical understanding of non-equilibrium transport of electrons and phonons (carrying thermal energy) at the nanoscale. It will investigate the effects of electron-electron interaction and electron-local vibration mode coupling on the non-equilibrium transport at the nanoscale. The study will address the optimization of the thermoelectric energy conversion. Finally, we will explore how thermoelectric transport out of equilibrium through the nanoscale systems will be affected by the coupling of electronic and local vibrational degrees of freedom to a coherent optical field, leading to the possibility of optical control of energy conversion efficiency.

Publications

Chen, T., X. Wang, and J. Ren. Dynamic control of quantum geometric heat flux in a nonequilibrium spin-boson model. 2013. Physical Review B. 87: 144303.

Li, N., J. Ren, L. Wang, G. Zhang, P. Hanggi, and B. Li. Phononics: manipulating heat flow with electronic analogs and beyond. 2012. Reviews of Modern Physics. 84: 1045.

Ren, J.. Predicted rectification and negative differential spin Seebeck effect at magnetic interfaces. 2013. arXiv.org.

Ren, J., J. Zhu, J. E. Gubernatis, C. Wang, and B. Li. Thermoelectric transport with electron-phonpn coupling and electron-electron interaction in molecular junctions. 2012. Physical Review B. 85: 155443.

Ren, J., S. Liu, and B. Li. Geometric heat flux for classical thermal transport in interacting open systems. 2012. Physical Review Letters. 108: 210603.

Ren, J., and J. Zhu. Heat diode effect and negative differential thermal conductance across nanoscale metal-dielectric interfaces. 2013. Physical Review B. 87: 241412(R) .

Ren, J., and J. Zhu. Anomalous energy transport across topological insulator superconductor junctions. 2013. Physical Review B. 87: 165121.

Ren, J., and J. Zhu. Theory of asymmetric and negative differential magnon tunneling under temperature bias: Towards a spin Seebeck diode and transistor. 2013. Physical Review B. 88: 094427.

Ren, J., and J. Zhu. Asymmetric Andreev reflection induces electric and thermal Hall-like effects in anisotropic superconductors. 2013. arXiv.org.

Ren, J., and N. A. Sinitsyn. Braid group and topological phase transitions in nonequilibrium stochastic dynamics. 2013. Physical Review E. 87: 050101(R).

Yan, G., J. Ren, Y. Lai, C. Lai, and B. Li. Controlling complex networks: how much energy is needed?. 2012. Physical Review Letters. 108: 218703.

Zhang, L., J. Ren, J. S. Wang, and B. Li. Topological magnon insulator in insulating ferromagnet. 2013. Physical Review B. 87: 144101.

High Efficiency Upconversion of Infrared Radiation in Semiconductor-metal Nanostructures for Applications in Solar Energy

Victor I. Klimov
20120746PRD1

Introduction

One factor that limits a power output of traditional solar cells is an inefficient use of the infrared (IR) portion of the solar spectrum leaking through a transparency window of a semiconductor defined by its bandgap. This problem can potentially be resolved by "upconverting" IR photons via the process of two-photon absorption (2PA). In a 2PA material, an electron is promoted across the bandgap by absorbing simultaneously two low-energy photons, which generates a higher energy exciton. For current state-of-the art 2PA materials the "threshold" light intensity, above which 2PA becomes significant, is considerably higher than the solar flux. The situation can be improved using light concentration. However, even for a concentration factor of 1000, the solar light intensity is still lower than the 2PA activation threshold. This implies that the utilization of 2PA ideas in solar energy conversion requires new types of 2PA chromophores with cross-sections that are orders of magnitude higher than in existing materials. The purpose of this project is to explore two effects for a dramatic increase of 2PA of semiconductors. One is a "giant" field enhancement in the presence of nanoscale metals and the other – 2PA through intra-gap states introduced by surface treatment of nanoscale semiconductors.

Benefit to National Security Missions

This project is relevant to LANL and DOE interests in both world-class fundamental science and strategic applications. Successful implementation of new strategies for capturing infrared light can yield solar-energy-conversion technologies relevant to DOE and LANL missions in Energy Security. At the recent DOE workshop on Basic Research Needs for Solar Energy Utilization, it was recognized that while solar photovoltaics is an important clean energy source, the practical large-scale applications of solar cells would require new concepts and novel materials for solar energy conversion. Novel concepts of enhanced two-photon absorption in hybrid semiconductor/metal structures that are explored in this project can potentially help in the realization of such breakthrough technologies that combine low fabrication costs with high power conversion efficiencies.

Progress

During the past year, we have investigated PbSe/CdSe core-shell colloidal quantum dots (QDs) prepared by the cation-exchange method. First, large monocomponent PbSe QDs are fabricated (radius R of ca. 4 nm), and then a CdSe shell of a controlled thickness (H) is prepared by exchanging Pb for Cd in the near-surface layer of the dots. This procedure maintains the total size of the structure, therefore, the increase in the thickness of the CdSe shell is accompanied by the reduction of the core size. In addition to core infrared (IR) emission, the thin-shell QDs exhibit broad and structureless visible photoluminescence (PL), originating, most probably, from the surface defect states. As the shell thickness increases, the visible emission gets stronger and narrower. It also progressively redshifts until it reaches ~650-680 nm for the 2.8-nm-thick shell samples. Performing an effective mass modeling of the structures, we assign the IR band to the 1Se-1Sh transition while the visible band to the 1Se-2Sh transition. The energy of the 2Sh state is above the valence band edge of CdSe, and therefore, the corresponding hole wavefunction extends across the entire volume of the core-shell QD. This is in contrast to the 1Sh state, which is tightly confined to the core.

We have studied nonlinear absorption properties of the QDs described above by monitoring visible up-converted emission, excited with the IR fs laser pulses that are in the range of optical absorption of the PbSe core. Quadratic dependence of the visible emission intensity on excitation power confirms a two-photon excitation mechanism. The measured two-photon absorption cross sections are about one order of magnitude larger than those of core-only CdSe QDs and reach values up to ~3×107 GM. We explain such an increase in the cross sections by resonance enhancement effect due to core

absorption, which is further enhanced by Auger-assisted upconversion. The latter effect is activated when two or more holes are excited in the core. In this case, the energy released during Auger recombination of one of the holes with a conduction-band electron is transferred to another core-localized hole. In our specially designed structures, this energy is sufficient to promote a hole to the shell region where it can recombine radiatively with an electron, producing visible PL. The quantum yield of this emission is directly proportional to the time of hole re-capture by the core. To evaluate this time we have conducted time-resolved, streak-camera studies of visible emission using 400 nm excitation with 100 fs pulses.

We observe that the dynamics of the initial IR peak does not change with the excitation fluence, while the dynamics of the 600 nm peak is fluence-dependent. Both can be characterized by a biexponential decay with the time constants of ~20-30 ps and ~300 ps. As the excitation fluence is increased the ratio of the amplitudes of the two components (fast-to-slow) remains constant (~10) for the 650-nm peak and decreases from ~40 to ~5 for the 600-nm peak. We attribute the initial fast component to hole capture by the core, while the slower component to radiative decay of shell localized holes. Based on these measurements, the hole capture time is around 20-30 ps. This time constant is significantly longer than characteristic times of intraband relaxation in standard monocomponent PbSe QDs (~0.3 – 1 ps), which leads to a great enhancement of “hot” visible PL in our core/shell structures.

These preliminary studies of novel core-shell PbSe/CdSe QDs indicate that they have a number of unusual and potentially useful properties. One such property is dual-color emission, which is characterized by two bands, one located in the IR and the other in the visible spectral range. These new dots also demonstrate a more than ten-fold enhancement of a two-photon absorption cross section, which is contributed by both resonant core-mediated transitions and Auger-assisted upconversion. These QDs are promising for various applications, and can be used, for example, as dual-color probes in two-photon bioimaging or “up-converters” of low-energy solar photons in IR-enhanced photovoltaics.

Future Work

As was demonstrated previously, enhancement of the nonlinear response can be achieved via utilization of plasmonic resonances in hybrid semiconductor-metal nanostructures. For example, Raman scattering, which is a third-order nonlinear process (same as 2PA) could be enhanced by up to ~10^10 times in the presence of nanoscale metals. This effect has been explained by field enhancement due to excitation of coherent oscillations of the electron gas known as surface plasmons (SPs). To study the effect of SPs on 2PA, we will use well-defined semiconductor-metal systems recently developed by LANL researchers . These structures comprise a metal gold or silver core over-coated with a thin layer of a dielectric (silica), followed by a layer of nanocrystal quantum dots (NQDs). These hybrid materials offer an unprecedented level of control of SP interactions with NQD excitons that can be tuned by adjusting the thickness of the silica spacer as well as the positions of both excitonic and plasmonic resonances. Experimental studies of the 2PA properties of NQDs combined with theoretical calculations will provide directions for the synthesis of optimized structures with large 2PA cross sections. The experimental studies will be done using a state-of-the-art 2PA spectrometer, similar to one recently developed by the applicant and implemented in studies of organic 2PA chromophores. A further increase in 2PA, if needed, will be achieved by introducing “engineered” states within the band-gap region. As was recently demonstrated by LANL researchers, by treating PbS NQDs with thiol-based ligands it is possible to introduce mid-gap states that served as charge conduit in dark. Additionally, these states were optically active and participated in optical transition with sub-gap energies. These observations indicate that the surface related mid-gap states can also serve as intermediate levels facilitating the 2PA process.

Conclusion

Utilization of infrared solar photons (IR) can significantly enhance the efficiency of photovoltaic cells. The goal of this project is to explore the utility of plasmon-enhanced two-photon absorption (2PA) for conversion of IR photons into larger-energy excitations in semiconductor nanocrystals. To accomplish this goal, we will conduct studies of 2PA as a function of nanocrystal size, shape, and composition. We will further investigate the influence of plasmonic field enhancement of 2PA cross-sections. Based on these studies we will identify optimal nanostructure designs that can allow for capturing a significant fraction of solar IR radiation at moderate concentration factors of ~1000.

Publications

Makarov, N. S., H. McDaniel, N. Fuke, I. Robel, and V. I. Klimov. Photocharging artifacts in measuremens of electron transfer in quantum-dot-sensitized mesoporous titania films. J. Phys. Chem. Lett..

Makarov, N. S., Q. Lin, K. Velizhanin, and V. I. Klimov. PbSe/CdSe core/shell colloidal quantum dots with enhanced optical nonlinearities and dual-band infrared/visible emission. 013. In Conference on Nonlinear Optics. (Kohala Cost, HI, USA, July 21-26, 2013). , p. NTh1A.3. Washington: Optical Society of America.

Minority Carrier Devices Based on Concentric Nanowires: Theory and Experiment

Quanxi Jia
20120747PRD1

Introduction

The goal of this work is to achieve a comprehensive understanding on minority carrier dynamics at nanoscale, and identify novel physics intrinsically related to small dimensions, in order to provide insights for nano-device design and optimization. This work will provide a robust assessment of the fundamental limits and potential of nanowire devices operating with minority carriers, complement current nanowire activities at CINT, and may inspire new research directions in the area of photovoltaics at LANL. The work will focus on Si photovoltaics and SiGe heterostructured tandem solar cells to maximize potential solar cell performance from these devices. A considerable effort will be paid on heterostructure transistor devices where the standby power and active power can be reduced with tailoring the composition and contact engineering to these structures thereby addressing an increasingly important area of semiconductor technology, green-electronics.

Benefit to National Security Missions

This work lies at the heart of solar cell technology and low power transistor devices, both of which tie well with the DOE and DOD energy agenda. These devices operate on minority carrier transport in semiconductors, and the goal of this work is to achieve a comprehensive understanding on minority carrier dynamics at nanoscale, and identify novel physics intrinsically related to small dimensions, in order to provide insights for nano-device design and optimization. This work will provide a robust assessment of the fundamental limits and potential of nanowire devices operating with minority carriers, complement current nanowire activities at CINT, and may inspire new research directions in the area of photovoltaics at LANL.

Progress

We continued to make excellent progress in all areas relevant to this research project including growth, device modeling and fabrication as well as characterization. Using high resolution transmission electron microscopy (HRTEM), we have advanced in materials synthesis of Si/Ge NWs using vapor-liquid-solid (VLS) growth mechanism. High quality Ge/Si NW with various designs have been grown and characterized. The main research focuses entail fabrication of novel NW devices based on Ge/Si heterostructures. This work is being conducted using a large combination of tools and systems at CINT such as HRTEM and in-situ thermal annealing under TEM, e-beam/photo lithography, Scanning electron microscopy/Focused Ion Beam (SEM/FIB), metal deposition by e-beam evaporation and sputtering, plasma-enhanced chemical vapor deposition (PECVD) and atomic layer deposition (ALD) of high-k dielectrics, inductively coupled plasma (ICP) dry etchings of Si, Ge and dielectrics, and thermal oxidation furnaces. The combination of high quality materials and advanced fabrication techniques has resulted in great accomplishments, currently being wrapped up for publication.

Device physics of NW FETs

NW has been being considered as an attractive candidate for new generation material due to its unique configuration that allows effective electrostatic coupling between gate control voltage and carrier conduction channel. High performance Si/Ge NW FETs have been demonstrated, but so far, little work has been reported on the device physics and experimental proof for the advantages of the Ge/Si core/shell structure over standard Si or Ge NWs. A large number of Ge/Si core/shell NWs with different diameters were processed into FETs and characterized to extract the size-dependence of FET performance. Our findings are experimental evidence for the linear dependence of device's on-current on diameter, which signify confinement of carriers near the NWs' perimeter in the on-state. In the off-state, it is more difficult to turn off larger diameter device (higher required gate voltage, and slower current drop) due to larger volume of carriers to be depleted. Comparison between Ge/Si core/shell and Ge NWs exhibited a factor of 3-fold

increase of device on-current, which is shown to be due to mobility enhancement in core/shell NWs.

Ultra-short metal/semiconductor/metal heterostructures for ultra-short channel length FETs

Aiming to create ultra-short (<10 nm) channel length FETs, solid-state-reaction between Ni and Ge/Si core/shell NWs is utilized to create a NiGe(or Si) / Ge(Si)/ NiGe(Si) meta/ semiconductor/metal with controlled size. Thermal annealing provides kinetic energy to Ni atoms to penetrate into Ge/Si semiconductors and create metallic NiGe/NiSi layers with high electrical conductivity, which can serve as drain and source for the un-reacted Ge/Si semiconductor channel in FETs. Developments in device fabrication allow us to integrate FET device structures on a 50 nm thick Si3N4 membrane in order to monitor and control reaction mechanism in-situ with HRTEM. Reaction between Ni with Ge/Si heterostructure exhibited completely difference reaction behaviors/mechanisms that haven't been observed in Ni-Ge or Ni-Si reactions. In-situ HRTEM revealed atomically smooth layer-by-layer propagation of Ni into the Ge/ Si semiconductors, allowing for precise control of channel length and junction abruptness. The achieved channel length of 5 nm is the shortest channel length in Ge/Si NW FETs up to date.

Advances in growth and processing developed this year will enable novel materials and device configurations that can open new frontiers for NW research (as described in proposed work for next fiscal year).

Future Work

In the next fiscal year, we will concentrate on the materials synthesis and device fabrication of Si/Ge heterostructured nanowires (NWs) for energy applications. The following specific tasks will target on developing low power consumption high performance electronics (1 and 2) and high performance thermoelectric materials (3).

1. Ultra-short channel length field effect transistors (FETs): We have successful realized a NiGe (or Si)/ Ge(Si)/NiGe(Si) NW heterostructre with the Ge(or Si) semiconductor segment as short as 5 nm. The next step is to fabricate FETs from such ultra-short channel lengths. Devices with <10 nm channel length are highly desirable as it requires much lower power consumption for the same performance as longer channel length ones. Reducing the channel length is also a path way for miniaturization, an industrial strategy to integrate more devices on the same area, hence increasing performance and reducing fabrication cost.

2. Novel design of NWFETs: On-going work has identified a fundamental drawback in current design of Ge/Si core/shell NWFETs: standard NWFETs require large diameter to be able to drive large current, but such large diameters make it hard to turn off the device. We have developed a new device concept using Si/Ge/Si core/ multiple-shell structure that is theoretically proven to overcome this fundamental drawback. We will address experimental challenges (growth, processing and measurement) to demonstrate a device prototype.

3. Thermoelectric materials: Nanowires have been proven excellent thermoelectric materials with low thermal conductivity due to their size in the nano range. With state-of-the-art device fabrication capability developed this year, we plan to further improve thermoelectric performance of the NWs system by creating nanowire superlattice: a complex repetitive …NiGe(Si)/Ge(Si)/ NiGe(Si)/Ge(Si)/… heterostructure from the building block NiGe(Si)/Ge(Si)/NiGe(Si) developed this year. Multiple heterointerfaces between NiGe(Si) and Ge(Si) is predicted to enhance phonon scattering for reduced thermal conductivity, while maintaining high electrical conductivity.

Conclusion

We expect to be able to model and realize Ge, Si, and Ge/Si heterostructured nanowire solar cell arrays with fab-compatible processes that can outperform their bulk counterparts. We also plan to reduce breakdown voltages in avalanche photodiodes and in impact ionization field-effect transistors by proper band-edge engineering available in our heterostructures wires. We will also work on tunnel field-effect transistors in the III-V material system where steep turn-on characteristics, similar to impact ionization FETs, are feasible targeting low power operation.

Publications

Dayeh, S. A., W. Tang, B. M. Nguyen, X. Dai, Y. Liu, Y. Hwang, X. H. Liu, and R. Chen. Nanoscale Heterogeneous Reactions and Interfaces in Ge/Si and for III-V on Si Integrated Devices. Invited presentation at ECS Meeting. (San Francisco, CA, 27 Oct - 1 Nov. 2013).

Liu, Y., X. H. Liu, B. M. Nguyen, J. Yoo, J. P. Sullivan, S. T. Picraux, J. Y. Huang, and S. A. Dayeh. Tailoring Lithiation Behavior by Interface and Bandgap Engineering at the Nanoscale. To appear in Nano Letters.

Nguyen, B. M., J. Yoo, S. A. Dayeh, P. Schuele, D. Evans, and S. T. Picraux. Design of Radial p–i–n Silicon Nanowires for High-Performance Solar Cells. 013. In The Wonder of Nanotechnology: Quantum Optoelectronic Devices and Applications. Edited by Razegh, M., I. L. Esaki, and K. von Klitzing. , p. 823. Bellingham, WA: SPIE Press.

Nguyen, B. M., J. Yoo, S. A. Dayeh, and S. T. Picraux. Design

of radial p-i-n Si nanowires for high performance solar cells. Presented at 11th international conference on infrared Optoelectronics: Materials and Devices (MIOMD XI). (Evanston, IL, Sep. 2012).

Nguyen, B. M., W. Tang, S. T. Picraux, and S. A. Dayeh. One dimensional transport in Ge/Si core/shell nanowires: physics and devices applications. Presented at CINT User Conference. (Albuquerque, 19-20 Sept.).

Nguyen, B. M., W. Tang, and S. A. Dayeh. Ultra-short channel field effect transistors based on Ge/Si core/shell nanowires. Invited presentation at SPIE Photonics West. (San Francisco, 2-7 Feb.).

Nguyen, B. M., W. Tang, and S. A. Dayeh. Ultra-short channel field effect transistors based on Ge/Si core/shell nanowires. Invited presentation at SPIE Photonic West. (San Francisco, CA, Feb. 2013).

Nguyen, B. M., Y. Liu, W. Tang, S. T. Picraux, and S. Dayeh. Ultra-short channel field effect transistors based on Ge/Si core/shell nanowires. Invited presentation at SPIE Photonic West. (San Francisco, CA, Feb. 2013).

Nguyen, B. M., Y. Liu, W. Tang, and S. Dayeh. Tailoring Ni-Ge/Si core/shell reaction rates through in-situ microscopy for ultra-short channel nanowire field effect transistors. Presented at MRS Spring Meeting . (San Francisco, CA, April 2013).

Frustrated Materials

Cristian D. Batista
20120751PRD2

Introduction

One of the most spectacular manifestations of geometrical frustration is the presence of the novel states of matter and associated phase transitions. These novel phases arise as a compromise between the opposite tendencies that are inherent to frustrated geometries. A triangular plaquette is an archetypal building block for lattices with geometrical frustration. Many unusual magnetic and orbital orderings in frustrated magnets are best understood from the viewpoint that the system is in the vicinity of a metal-insulator transition. It is a challenging theoretical task to model these systems which lie in the intermediate-coupling regime between deep Mott insulator and the metallic phase. To carry out such studies, we will employ a combination of analytical and numerical techniques. We will use mean field and semi-classical techniques for computing thermodynamic properties. For the numerical approach we will implement a Mote Carlo algorithm for solving the problem of itinerant electrons interacting with localized classical spins. Since the action is quadratic in the fermion operators, the itinerant electrons can be integrated out exactly, leading to an effective non-local classical action for the local moments that will be solved by applying the Metropolis algorithm. All the thermodynamic properties will be computed under control because the statistical error can be made arbitrarily small by increasing the sample size. The temperature dependence of the thermodynamic quantities will be directly compared against the experiments.

Benefit to National Security Missions

Given the complexity of correlated materials and the unlimited number of compounds, the discovery of new states of matter and functionalities must be organized around simple guiding principles. Our basic principle for discovering complex and collective forms of matter that exhibit novel properties and respond in new ways to environmental conditions is to make, characterize and model classes of materials with controllable degree of electronic localization. These classes can either be Mott semiconductors or intermetallic compounds. By modeling of bulk materials and films, we will establish guiding principles for finding novel states with optimized functionalities. This is a necessary step towards the dream of "materials by design."

Progress

The research of Dr. Gia-Wei Chern at LANL is focused on the general area of frustrated materials. The main goal is to understand and control the fundamental properties of these complex systems with applications to magnetic storage, computing, and sensing. In particular, his main effort in the past months has been devoted to understanding the novel transport properties in metallic frustrated magnets. By considering Kondo-lattice models in frustrated lattices, e.g. pyrochlore or kagome lattices, Dr. Chern and his collaborators have uncovered a novel mechanism for resistivity minimum, which does not originate from the conventional Kondo-screening, in some metallic pyrochlore magnets. By establishing the connection between electronic transport and the spin-spin correlations in the highly constrained cooperative paramagnetic regime, the proposed mechanism can explain similar resistivity minimum phenomena in frustrated magnets in general.

In addition, Dr Chern and his collaborators have also discovered a novel phase exhibiting a quantized Hall effect in a highly degenerate ice manifold. A similar phase, dubbed chiral spin liquid, has recently been reported in pyrochlore irradiates. Their result thus provides a proof of principle for the existence of such novel state of matter.

Another main area of his research is the study of artificially created frustrated systems, in particular the so-called artificial spin ice. One of the key advantages of these systems is that they allow direct experimental access to the microscopic degrees of freedom. With other collaborators in LANL, Dr. Chern has proposed a

realization of the famous 3-coloring problem in systems of colloidal particles interacting with an array of optical traps. Experimental realization of such systems will allow us to study the dynamics of defects in this highly degenerate critical phase. Artificial spin ice is a booming field in condensed matter physics. Among the most exciting recent developments is the emergence of magnetic monopoles in these materials. Emergent phenomena, which until now have only been accessible at low-T, will then be tailor-designed to manifest at room temperature. In particular, the existence of mobile magnetic monopoles coupled to magnetic fields provides a promising approach to realize magnetricity, the control and manipulation of magnetic currents. With the rapid progress in nano-fabrications, it is now possible to realize artificial spin ice in various lattice geometries. Working with collaborators both in LANL and other institutes, Dr. Chern has explored novel phenomena of monopoles in different geometries. One of the major findings along this direction is the phenomenon of monopole screening in lattices with mixed coordination numbers.

Future Work

- Compute the magnetic phase diagram of double-exchange system on the frustrated lattices: The interplay of magnetic frustration and the nonlocal nature of electron-mediated spin interaction gives rise to unusual magnetic orders and exotic phases. There are a growing number of compounds that are described by such models. We will develop sophisticated and efficient Monte Carlo algorithms for computing the phase diagram of these models.

- Compute thermodynamic and transport properties of metallic spin ices: A similar study for the metallic spin-ice systems will shed some light on the strange chiral phase with disordered spins recently observed in pyrochlore Pr2Ir2O7. We will examine the dynamics of monopoles induced by the electron-mediated RKKY interactions.

- Metal-insulator transitions in frustrated magnets: Many of the unusual magnetic and orbital orderingin pyrochlore magnets are best understood from the viewpoint that the system is close to a metal-insulator transition. Indeed, some of them also exhibit a room-temperature metal-insulator transition that is accompanied by magnetic ordering. We will explore the role of orbital degrees of freedom in such transitions for multiband Hubbard models.

- Mott transitions and physics in strongly coupled spin-orbital systems: Strong spin-orbit coupling candramatically change the band structure of weakly interacting solids, leading to band insulator with a nontrivialtopology. It has been shown recently that the Kitaev model can be realized in iridium oxides A2IrO3 that areMott insulators with strong spin-orbit coupling. We will investigate the general properties of topological Mottinsulators, their experimental characterization, and their connection with topological band insulators when thesystem undergoes a Mott transition.(5) Quasiparticles of orbital ice: recently, we have uncovered a nontrivial many-body ground-state solution forthis system. We will study the elementary excitations in orbital ice and to pursue an algebraic approach forexactly solving the quantum orbital model.

Conclusion

- Find novel magnetic orderings in double-exchange models and spin-density wave instability of Hubbard model on frustrated lattices.

- Understand the thermodynamic properties of metallic spin ice, particularly the exotic chiral spin-liquid phase in pyrochlore compound Pr2Ir2O7.

- Develop theoretical models for electron transport in the emergent Coulomb phase in metallic spin ice systems.

- Develop numerical algorithms for studying the order-by-disorder phenomenon in frustrated magnets

- Provide a theoretical modeling of magnetic and orbital ordering in vanadium spinels.

Publications

Chern, G. W., A. Rahmani, and I. Martin. Quantum Hall ice. Physical Review Letters.

Chern, G. W., C. C. Chien, and M. Di Ventra. Dynamically generated flat band phases in optical kagome lattice. Physical Review Letters.

Chern, G. W., C. Reichhardt, and C. J. O. Reichhardt. Frustrated colloidal ordering and fully packed loops in arrays of optical traps. 2013. PHYSICAL REVIEW E. 87 (6): -.

Chern, G. W., M. Morrison, and C. Nisoli. Degeneracy and criticality from emergent frustration in artificial spin ice. To appear in Physical Review Letters.

Chern, G. W., R. M. Fernandes, R. Nandkishore, and A. V. Chubukov. Broken translational symmetry in an emergent paramagnetic phase of graphene. 2012. PHYSICAL REVIEW B. 86 (11): -.

Chern, G. W., S. Maiti, R. M. Fernandes, and P. Wolfle. Electronic Transport in the Coulomb Phase of the Pyro-

chlore Spin Ice. 2013. PHYSICAL REVIEW LETTERS. 110 (14): -.

Chern, G. W., and C. D. Batista. Spontaneous quantum Hall effect via a thermally induced quadratic Fermi point . 2012. Physical Review Letters. 109: 156801.

Chern, G. W., and O. Tchernyshyov. Magnetic charge and ordering in kagome spin ice. 2012. PHILOSOPHICAL TRANSACTIONS OF THE ROYAL SOCIETY A-MATHEMATICAL PHYSICAL AND ENGINEERING SCIENCES. 370 (1981): 5718.

Chern, G. W., and P. Mellado. Magnetic monopole polarons in spin ices with mixed coordination numbers. Physical Review Letters.

Chern, G. W., and R. Moessner. Dipolar Order by Disorder in the Classical Heisenberg Antiferromagnet on the Kagome Lattice. 2013. PHYSICAL REVIEW LETTERS. 110 (7): -.

Choi, E. S., G. W. Chern, and N. B. Perkins. Chiral magnetism and helimagnons in a pyrochlore antiferromagnet. 2013. PHYSICAL REVIEW B. 87 (5): -.

Choi, E., G. W. Chern, and N. B. Perkins. Helimagnons in a chiral ground state of the pyrochlore antiferromagnets. 2013. EPL. 101 (3): -.

Lin, S. Z., Y. Kamiya, G. W. Chern, and C. D. Batista. Reentrant Berezinskii-Kosterlitz-Thouless Transition in a Triangular Ising Thin Film. Physical Review Letters.

Mun, E. D., G. W. Chern, V. Pardo, F. Rivadulla, V. S. Zapf, and C. D. Batista. Magnetic field induced transition in multiferroic spinel CdV2O4. Physical Review Letters.

Perkins, N. B., G. W. Chern, and W. Brenig. Raman scattering in a Heisenberg S=1/2 antiferromagnet on the anisotropic triangular lattice. 2013. PHYSICAL REVIEW B. 87 (17): -.

Rahmani, A., and G. W. Chern. Universal Renyi mutual information in classical systems: The case of kagome ice. 2013. PHYSICAL REVIEW B. 88 (5): -.

Zhang, S., I. Gilbert, C. Nisoli, G. W. Chern, M. J. Erickson, L. O'Brien, C. Leighton, P. E. Lammert, V. H. Crespi, and P. Schiffer. Crystallites of magnetic charges in artificial spin ice. 2013. NATURE. 500 (7464): 553.

Atomic Coherence with X-Ray Free-electron Lasers

Bruce E. Carlsten
20120754PRD2

Introduction

Atomic coherence with intense visible and infrared lasers is an exciting emerging field, which allows exploration of strange atomic behavior though controlling recombination rates and suppressing absorption. These effects include such as slowing down or speeding up light, efficient frequency up-conversion, and more efficient photocells. Additional new phenomena may be possible by using intense X-ray lasers, such as the one proposed for the LANL MaRIE facility. The purpose of this project is to extend this new field to the X-ray regime. Currently, X-ray lasers based on self-amplified spontaneous emission do not provide spectral brightness necessary to excite atomic coherence properties and novel designs for X-ray free electron lasers are needed. We will first look at the generation of an optical comb with train of electron bunches prepared via laser modulation technique. As an alternative approach, we will study parametric interaction of fundamental and sub-harmonic in bi-energetic electron beam in order to imprint longitudinal coherence of the sub-harmonic onto the fundamental. We will then consider how electron wave function spreading will affect the performance of a hard X-ray free electron laser operating at lower electron energies for cost reduction. We have three major focus areas: start-up noise, gain reduction, and saturation process. We will model operation of these X-ray free electron lasers and apply the generated electric fields to modeling the excitation of atomic transitions. This will allow us to quantify the amount of atomic coherence one could generate using these new X-ray free electron lasers.

Benefit to National Security Missions

This research may lead to enhanced materials performance and devices relying on atomic technologies, such as higher efficient photocells and smaller and more controllable devices based on quantum heat engines, quantum information storage and processing, atomic clocks, magnetometers, interferometers, and novel laser systems.

Progress

During FY13 we have examined several experiments done at LCLS where atomic coherence was used to modify transition rates of Neon. These experiments have shown that spectral brightness of self-amplified spontaneous emission based X-ray free electron lasers is not sufficient to provide noticeable coherent effects. It has also indicated that novel designs for future X-ray free electron lasers are required in order to make them suitable for fundamental atomic and quantum research.

Search for the novel designs have required us to re-examine the basics of X-ray free electron laser theory. Our analysis showed that the quantum mechanical nature of electrons manifested as the spread of their wave packets becomes significant in hard X-ray free electron lasers such as SACLA in Japan and LANL proposed MaRIE. This is a 10% effect in the case of lasing at the fundamental and increases to 30% for the third harmonic generation. It is a collective effect.

We have developed a novel X-ray free electron laser design that was inspired by the concept of optical frequency combs. Starting with a train of electron bunches that generates a single coherent X-ray pulse per bunch, one generates a periodic train of X-ray pulses. In this regime, the radiation spectrum becomes discrete with spectral brightness being increased by at least an order of magnitude. We did numerical simulations and confirmed the predictions. It has been also discovered that such an electron beam is easier to prepare so that it has improved gain. Furthermore, the propagation of a long train of short electron bunches in metal pipes is advantageous since it does not suffer from resistive wall wake effects that introduce inhomogeneous energy loss on the beam. This work was presented at the LANL postdoc competition and won an outstanding poster award.

Future Work

We expect progress will be made in three areas in FY14.

First, quantum effects of electron wave function on start-up noise, gain reduction, and saturation regime in the case of hard X-ray free electron laser operating at lower energies will be evaluated. Second, novel X-ray free electron laser designs with higher spectral brightness will be studied. Finally, quantum atomic effects that can be induced by this novel X-ray free electron lasers will be identified. In the first area, future hard X-ray free electron lasers, such as the one proposed for MaRIE, are proposed to operate at lower electron energies to reduce construction and operation cost. In this new regime the quantum effects on the electron beam and the X-ray generation mechanism may become significant. Specific examples may include start-up noise modifications, gain reduction due to phase uncertainty, and quantum saturation regime where due to the spread of an electron wave function electrons are trapped and untrapped at the same time. In the second area, we will first look at optical comb generation in the X-ray domain where a train of electron bunches is used to excite a train of optical pulses; we will then look at parametric generation of coherent X-ray radiation in bi-energetic electron beam. We will finally use modeled electric field to drive atomic coherences in simple atomic systems in order to validate X-ray free electron laser applicability for fundamental atomic and quantum research.

Conclusion

The goal of this project is to investigate novel designs of X-ray free electron lasers that offer improved spectral brightness needed to excite atomic coherence. The expected results are: optical comb generation with train of electron bunches as well as the parametric generation in a bi-energetic electron beam; effects of an electron wave function on start-up noise, gain reduction, and saturation regime in the case of hard X-ray free electron laser operating at lower energies; validation of X-ray free electron lasers for fundamental atomic and quantum research by apply generated electric fields to excite atomic coherence in simple atomic systems.

Precision Fission Cross Section Measurements with a Time Projection Chamber

Fredrik K. Tovesson
20120755PRD2

Introduction

We intend to study nuclear reactions, particular fission, with a newly developed instrument (a Time Projection Chamber) at the Los Alamos Neutron Science Center (LANSCE). This goal is to measure these reactions with unprecedented accuracy in order to meet needs for the nuclear energy and weapons programs. This is the first time ever that a Time Projection Chamber (TPC) is applied to this type of research, and if successful this could have major impact on the field. The experiments will be carried out at LANSCE, which is a world class facility for nuclear research and one of only two places where this work could be performed. There are major difficulties in reaching the goal of this project, as a completely new technique is being developed. Particle tracking of fission fragments, neutron beam characterization and radioactive sample handling all poses challenging problems to solve. However, if these challenging problems are solve a major improvement in the accuracy that can be reached in fission cross section measurements will be achieved. The data than can be measured with this approach will have far reaching implications for nuclear energy research, the weapons program, and basic science.

Benefit to National Security Missions

The results that will come out of this work build capability for high level milestones for the weapons program. The data will help better understand the performance of nuclear weapons, improve predictive capabilities, and support the science-based approach to the stockpile stewardship mission.

It will also support the nuclear data effort of the DOE nuclear energy programs such as the Advance Reactor Campaign and Fuel Cycle Technologies. The cross sections that will be measured were identified within the nuclear data effort as being in need of improvement, and will be used to improve simulations of new advanced reactor and fuel concepts.

The new technique for nuclear physics that is developed within this project will also provide new advanced capabilities for nuclear science research at LANCSE and other facilities in the US and world wide. We will also advance our understanding of the nuclear fission process within the scope of the project.

Progress

The main accomplishment this year was completing the analysis of the experimental data collected during the 2011-2012 LANSCE run cycle. This was a major achievement on the path to getting to the final nuclear data measurement completed.

There was also significant progress made in terms of coordinating the in-beam data collection efforts for the TPC project, which involved:

- Supervising two undergraduate and two graduate summer students
- Preparing and submitting safety documentation
- Setting up the experimental area, detector system, and auxiliary equipment
- Troubleshooting and maintaining experimental equipment during the run

A number of presentations were made through the year:

- Delivered an invited talk at an international conference - Collective Motion in Nuclei under Extreme Conditions (COMEX4), Hayama, Japan, October 2012
- Cross-Section Evaluation Working Group Meeting – Brookhaven National Laboratory, November 2012
- International Conference on Nuclear Data for Science and Technology – New York NY, March 2013 (Featured Talk, refereed conference proceedings to be published January 2014)

- Gordon Research Conference on Nuclear Chemistry – New London NH, June 2013

- Submitted and defended a proposal to the LANSCE Program Advisory Committee to measure the U-238/U-235 (n,f) cross-section ratio using the TPC

Future Work

One task for FY14 is to collect more beam data at the Los Alamos Neutron Science Center (LANSCE) on nuclear fission of Uranium-238 and Uranium-235 using a Time Projection Chamber (TPC). This measurement will be performed in the 2013 LANSCE run cycle, which ends in December 2013.

The second task is to analyze the data collected with the TPC in order to determine the probability for nuclear fission to occur in Uranium-238 when bombarded with neutrons of different energies. This is a complex analysis that involves the study of tracks made by fission fragments in the detector, as well as determining the kinetic energy of the incident neutrons that induced the reaction.

The overall goal for this fiscal year will be to produce a preliminary fission probability (a so-called reaction cross section) as a function on incident neutron energy for Uranium-238 relative to Uranium-235.

Conclusion

Within this project we expect to demonstrate that the TPC can reach the expected accuracy of approximately 1% in fission cross section measurements. We will deliver the U-238/U-235 fission ratio, and develop all the necessary procedures to run beam experiments for Pu-239. We will also develop a an expanded research program for the TPC, which will include more detailed studies of the nuclear fission process.

Publications

Meharchand, R., F. Tovesson, A. B. Laptev, and K. Meierbachtol. TPC measurement support. 2012. LANL internal report LA-UR-12-25409.

Meharchand, R., T. Hill, and L. Snyder. Analysis of TPC Single Sextant U-238/U-235 Engineering In-Beam Data. 2012. LANL Internal Report LA-UR-12-25452.

The Assembly of Primeval Galaxies and the Birth of the First Quasars

Hui Li
20120756PRD2

Introduction

Soon after the Big Bang, gravity caused dark matter and primordial gas to collapse into a vast cosmic network of filaments and halos (roughly spheroidal clumps of dark matter and gas). These halos congregated into the first primitive galaxies 400-600 million years after the Big Bang. Protogalaxies were also the first great nucleosynthetic engines in the universe, polluting the intergalactic medium (IGM) with heavy elements from intense winds and radically transforming generations of stars after them and making planets and life possible. Such galaxies are also believed to be the birthplaces of the seeds of the supermassive black holes (SMBH) residing at the centers of most massive galaxies today. Because they lie at the edge of the observable universe, these galaxies are beyond the realm of current instruments but will soon be detected by the James Webb Space Telescope (JWST) and the Thirty-Meter Telescope (TMT). State-of-the-art protogalaxy simulations fail to resolve the cycle of primordial star formation and explosion in each halo as they are assembled into the first galaxies. We will develop a new generation of protogalaxy simulations that will bridge all spatial scales relevant to their formation. We will also build the first numerical models ever of the birth of the first quasars.

Benefit to National Security Missions

This research addresses the fundamental question on how the primeval galaxies and black holes in the early universe. The results from this study will provide first-principle physical understanding of the formation of first objects under extreme conditions. They will also prepare us for the upcoming new observations by the nation's leading telescopes, both ground-based and space-borne. This research contributes to the basic science capabilities at the Laboratory. It also provides the necessary physics basis for many challenging problems associated with the Beyond the Standard Model Grand Challenge at LANL.

Progress

Primordial supernova explosions are key to the formation of the first galaxies (and hence the science objectives of my Director's Fellowship) because they chemically enrich them with the first heavy elements and may trigger second-generation star formation in them. They will also be important to detecting such galaxies, since some of these primitive structures would otherwise be too dim to be detected in wide-field surveys. In the first year of my Fellowship we have modeled the light curves and spectra of the first SNe in the universe with the radiation hydrodynamics code RAGE: core-collapse, pair-instability, Type IIn and supermassive thermonuclear events. We have discovered that these ancient explosions will be detectable by the James Webb Space Telescope (JWST) and the Wide-Field Infrared Survey Telescope (WFIRST) at the earliest epochs in the universe.

These simulations are having a real science impact on the astronomy community. David Spergel and Jason Kaliari from Princeton and STScI have consulted us on filter designs for WFIRST (which is now in its planning stages) to detect these ancient events in the near infrared (NIR) and have solicited contributions from LANL on the science case for WFIRST to be submitted to NASA. We have also been contacted by several independent groups of astronomers for assistance in devising searches for Pop III SNe. Reporters have also contacted us about our work, which now appears in the June 12, 2013 issue of New Scientist (The Supernova that Blew up a Galaxy). My numerical models will culminate in the publication of 6 Astrophysical Journal publications.

We have also begun to simulate the formation of the first quasars in the universe 500 Myr after the big bang and their evolution down through cosmic time in large simulation boxes with the cosmology code Enzo. The births of these quasars will soon be discovered by successors to the Swift mission such as JANUS or LOBSTER. If we find that such black holes can reach a billion solar

masses by redshift z = 7, we will have explained one of the outstanding problems in cosmology today: the appearance of supermassive quasars less than a billion years after the big bang.

Future Work

We will perform cosmological simulations to study the formation of primeval galaxies and investigate how they will contribute to future structure formation. Our simulation campaign will unveil not only the nature of primeval galaxies but also how they began early chemical enrichment and reionization of the universe. Our models will also determine the initial conditions of massive galaxy formation down through cosmic time. These simulations will leverage LANL's expertise in radiation transport, explosions and turbulent subgrid mixing and have the potential to transform their subject, putting LANL at the forefront of high-redshift cosmological structure formation.

Conclusion

Our simulation campaign will unveil not only the nature of primeval galaxies but also how they began early chemical enrichment and reionization of the universe. Our models will also determine the initial conditions of massive galaxy formation down through cosmic time. These simulations will leverage LANL's expertise in radiation transport, explosions and turbulent subgrid mixing and have the potential to transform their subject, putting LANL at the forefront of high-redshift cosmological structure formation.

Publications

Johnson, J., D. Whalen, W. Even, C. Fryer, A. Heger, J. Smidt, and K. Chen. The biggest explosions in the universe. 2013. The Astrophysical Journal. 775 (2): 8.

Whalen, D., A. Heger, K. Chen, W. Even, J. Smidt, C. Fryer, M. Stiavelli, and H. Xu. Supermassive population III supernovae and the birth of the first quasars. To appear in The Astrophysical Journal.

Whalen, D., J. Johnson, J. Smidt, A. Heger, W. Even, and C. Fryer. The supernova that destroyed a protogalaxy: prompt chemical enrichment and supermassive black hole growth. 2013. The Astrophysical Journal. 774 (1): 10.

Whalen, D., J. Johnson, W. Even, C. Fryer, A. Heger, J. Smidt, and K. Chen. The biggest explosions in the universe. II. To appear in The Astrophysical Journal.

Whalen, D., L. Frey, W. Even, J. Smidt, C. Fryer, M. Stiavelli, D. Holz, A. Heger, S. Woosley, C. Lovekin, and A. Hungerford. Finding the first cosmic explosions I: pair-instability supernovae. To appear in The Astrophysical Journal.

Searching for Sterile Neutrinos with MircoBooNE

Richard G. Van De Water
20120757PRD2

Introduction

The project is to work on the next generation large scale neutrino experiment (MircoBoone) at Fermi National Accelerator Lab (FNAL contact person: Sam Zeller, 630-840-6879, gzeller@fnal.gov). The experiment plans to follow up on the recent tantalizing neutrino oscillation measurements from LSND and MiniBooNE that are hinting at the possibility of a new fundamental particle called sterile neutrinos. Such a discovery would have profound effects ranging from fundamental properties of the Standard Model, to the origin and evolution of the Universe and Cosmology. MicroBoone will search for neutrino oscillations using a new neutrino detection technology involving a Time Projection Chamber in liquid Argon. This spatially high resolution detector can separate many classes of events, allowing a rejection of background photons from signal electrons. This capability will allow a definite determination of the origin of the LSND/MiniBooNE signals. There will be many technical challenges in making this new technology work as planned.

Benefit to National Security Missions

MicroBooNE will be testing a new technology of time projection chamber in liquid Argon. This new technology will require much research to understand and make work as expected. We will be contributing directly to the work to readout the detector and also reconstruct the events that will allow us to make physics measurements of Argon neutrino nuclear cross sections and neutrino oscillations. Also, if the oscillation measurements reveal the existence of sterile neutrinos, then a re-evaluation of the standard model of particle physics and evolution of the Universe is required to accommodate this new particle/state of matter. Fundamental work of this sort builds capability for sensitive nuclear detection, of interest to nuclear security programs.

Progress

Wesley has been a major player in the development of the data acquisition system (DAQ). This complex system is now reading out test electronics and is operating at the required speed to run the entire system.

He has also begun development of neutrino reconstruction algorithms and has made significant progress in developing techniques to determine the vertex position of neutrino events.

Lastly, Wesley has been asked by the collaboration (over 100 scientists) to lead the reconstruction algorithm group. This is in recognition of his outstanding scientific talents.

Future Work

The goal in the next year is to complete and commission work on the Data Acquisition System (DAQ) that reads out the time projection chamber in the liquid Argon. Computers are used to read out the 10,000 channels of electrons that record the signals. The DAQ code must constantly monitor the electronics and read out the channels when data is available. The data are then assembled into events to be permanently recorded on disk for subsequent analysis. The trigger information and detector status most constantly be monitored and recorded by the DAQ. The goal in the first year was to develop the low level drivers that read out individual channels. This forms the basic building block of the DAQ. Also, minimal DAQ code will be developed to help debug and characterize the electronics during the assembly and installation of the electronics in the detector hall.

Conclusion

In the next two year period we expect to build the detector, commission, and begin taking data. If the new technology works as planned, then we can determine if the MiniBooNE signal is due to electrons, as opposed to photons, which is expect if the origin of the signal is neutrino oscillations. A paper will be published on these results.

3D Turbulent Magnetic Reconnection Experiments and Simulations

Thomas P. Intrator
20120768PRD3

Introduction

Background: The plasma universe including our solar system is threaded with magnetic fields. These magnetic fields are typically "frozen" into the magnetohydrodynamic (MHD) plasma fluid frame, and in many cases of interest play an essential role in organizing the plasma. The twisting, folding, and annihilation of magnetic field can energize particles. Our knowledge of fundamental principles underlying local magnetic structure allows us to extend understanding to remote stars and galaxies, solar system space weather, and magnetic fusion energy devices.

Magnetic reconnection is a general category of important plasma physics processes in which magnetic field lines reorganize, and usually change their topology while annihilating the associated magnetic flux. The typical two-dimensional (2D) Sweet-Parker physics picture invokes oppositely directed magnetic fields that are advected by plasma fluid motion towards each other, where they collide and form a thin discontinuity and an induced current sheet. Magnetic flux diffuses into the thin "diffusion" region, and plasma jets are flung out in slingshot fashion sideways as reconnecting magnetic fields first bend, reconnect to other field lines, and finally straighten out. However it is becoming increasingly apparent that these thin current sheets are inherently unstable to the formation of islands or plasmoids, each of which has a current rope threading the O-point of each island. The necessity of including the magnetic flux rope dynamics forces us to confront the 3D nature of the problem. Any useful reconnection theory should account for the 3D features.

Proposed work: The reconnection scaling experiment (RSX) system at LANL provides diagnostics to observe reconnection in the full three dimensions from macro to micro length scales. We will measure 3D interactions of reconnecting current sheets, as they shred into islands (which are current ropes in 3D) that cascade down to kinetic scales, and display sporadic, bursty, and turbulent dynamics.

Benefit to National Security Missions

One of the missions undertaken by DOE Office of Science is Fusion Energy Sciences. Plasma science forms the basis for research that is needed to establish our ability to harness the power of the stars in order to generate fusion energy on earth. The research required for fusion energy's success is intimately tied to rich scientific questions about some of nature's most extreme environments, inside and outside of stars, and has practical implications to industry beyond energy as well. The impact of a fusion energy source will be huge, as energy drives much of our domestic and foreign policies. A major fusion energy scenario requires magnetized plasmas, and the situation in real life is fully 3D. Our proposed research speaks directly to the fundamental science of magnetized plasmas.

NASA also has a mission of Science, as we explore the Earth, solar system and universe beyond, to reap the benefits of Earth and space exploration for society. Our research project aims to unravel some fundamental questions about how magnetic structure "works" in three dimensions.

Progress

The reconnection scaling experiment (RSX) at LANL provides diagnostics to observe reconnection in the full three dimensions from macro to micro length scales. We will measure 3D interactions of reconnecting current sheets, as they shred into islands (which are current ropes in 3D) that cascade down to kinetic scales, and display sporadic, bursty, and turbulent dynamics.

During the past 7 months (2012Nov-2013May) since Dr. Feng arrived at LANL, we have been characterizing the 3D behavior of a single flux rope. The behavior of a single flux rope allows us to understand key and simpli-

fied features of this complicated 3D, two flux rope problem. Two post docs (J. Sears and Y. Feng) have measured the non linear dynamics of plasma magnetic fields, plasma pressure, and flows. We have amassed a huge 3D dataset (> 2000 shots, 25000 probe locations) for a single Reconnection Scaling Experiment (RSX) flux rope. The 3D analysis shows unexpected behaviors.

We are in the process of intpreting the experimental results, and already have a story that seems destined for Physical Review Letters.

Future Work

A large array of multiple plasma guns will be fabricated and installed on the Reconnection Scaling Experiment. This will allow us to create flux ropes of varying sizes and shapes by merging, 1,2,3,4 or more plasma gun jets into single streams of plasma. Current sheets will then be created from rows of plasma guns and we will experimentally characterize their interactions. In parallel, we will start to set up the input parameters for the VPIC particle in cell code, so that we can simulate the RSX experiment computationally.

Conclusion

Magnetic reconnection plays a crucial role in many different astrophysical and laboratory plasma phenomena, which are all intrinsically 3D. Recent theories and simulations implicate generic current sheet instabilities that generate islands. Cascades of plasmoids down to kinetic spatial scales naturally link reconnection, turbulence, cascades, and dissipation. We propose the first experiments to verify the 3D dynamics of magnetic field annihilation and reconnection. We will carry out 3D computational simulations and benchmark them to experimental data to better understand the formation and interaction of flux ropes within the Earth's magnetosphere, and the basic physics of laboratory, space and astrophysical plasmas.

Publications

Feng, Y., J. Goree, and B. Liu. Longitudinal viscosity of two-dimensional Yukawa liquids. 2013. PHYSICAL REVIEW E. 87 (1): -.

Goree, J., B. Liu, and Y. Feng. Diagnostics for transport phenomena in strongly coupled dusty plasmas. To appear in Plasma Physics and Controlled Fusion.

Intrator, T. P., X. Sun, L. Dorf, J. A. Sears, Y. Feng, T. E. Weber, and H. O. Swan. Flux ropes and 3D dynamics in the Relaxation Scaling Experiment. To appear in Plasma Physics and Controlled Fusion.

Measurement of Orthogonal Velocity Components Using Photon Doppler Velocimetry

Matthew E. Briggs
20120771PRD4

Introduction

The primary research will be experiments using PDV in laboratory and gun shots and the addition of the reference electric field to the scattered electric field in the theoretical analysis. This could demonstrate the extent to which PDV with dynamic speckle analysis can simultaneously measure axial and lateral target surface velocities, using existing test setups. This capability would provide a detailed view of a structure's response to excitation, thereby lifting a fundamental limitation on currently deployed velocimetry techniques.

The theoretical development of dynamic speckle measurements for extracting lateral motion from PDV data records, along with any corresponding experimental investigations are unique and appropriate for publishing in a journal that covers optical sensor research.

Benefit to National Security Missions

Velocimetry is used widely across many applications. By giving insight into the lateral velocity (new) simultaneously to longitudinal velocity (existing), our understanding of material responses to driving forces will be qualitatively advanced. This will provide significant additional constraints on the physics and modelling of systems important to a broad range of federal missions. In particular, velocity measurements are primary or secondary on many of our most important nuclear weapon safety, security, reliability & non-proliferation measurements. These measurements are also primary on many material response to shock experiments.

Progress

We have accomplished the work as planned: We have completed 3 rounds of laboratory tests that have demonstrated that we can indeed measure the phenomenon as intended, and elucidated the physical principles underlying the phenomenon. Erik has published his first paper on the topic and is now preparing a 2nd paper on the topic. The first paper was a note that showed we could indeed observe the phenomenon as proposed. The second is a much longer paper laying out the details of how to apply our analysis and comparing to data. In addition, Erik has laid out a program for the Los Alamos Dynamics Summer School that will engage a team of undergraduates in exploring aspects of his research. The students are arriving next week. He has also prepared a paper for the post-doc poster day.

Future Work

During the first year we will complete a literature survey on the topic, and present a research plan at the annual Photon Doppler Velocimetry Workshop. We will decide which of the various analysis tools in the literature for extracting lateral velocity from dynamic speckle to use first, test it with existing laboratory experimental velocimetry apparatus, and then develop a plan for the second year.

We have accomplished the above as planned, and Erik is now preparing a 2nd paper on the topic (his first has already been published.) Our plan for next year is to expand the testing of the speckle analysis on experiments involving straining and non-straining surfaces in order to see if we can distinguish between the two.

Conclusion

To demonstrate the extent to which PDV with dynamic speckle analysis can simultaneously measure axial and lateral target surface velocities, using existing test setups. This research will be of broad interest to the velocimetry community, and to the larger community of material and weapons scientists. Even qualitative information about lateral motion fills a limitation on velocimetry measurements that has been present since the start of the field. If quantitative analysis of lateral motion turns out to be robust, then the applications will become much more wide ranging, as PDV is now being used around the world.

Publications

Briggs, M., D. Knierim, E. Moro, and S. McGrane. Optical distance measurements to recover the material approach missed by optical velocimetry. To appear in Shock Compression of Condensed Matter. (Seattle, July 2013).

Hull, L. M., M. E. Briggs, and E. A. Moro. The effect of tangential velocity components and surface evolution on photon Doppler velocimetry measurements. 2013. Los Alamos National Laboratory Report.

MOro, E. A.. New Developments in photon Doppler velocimetry. To appear in Shock Compression of Condensed Matter. (Seattle, July, 2013).

Moro, E. A.. Extracting transverse motion from speckle dynamics in photon Doppler Velocimetry. Presented at Postdoc Research Day at Los Alamos National Laboratory. (Los Alamos, 2013).

Moro, E. A., M. E. Briggs, and L. H. Hull. Point-measurement of strain-induced speckle dynamics, observed with photon Doppler velocimetry. To appear in 15th International Detonation Symposium. (San Fransisco, 2014).

Moro, E. A., M. E. Briggs, and L. M. Hull. A comparison of techniques for extracting transverse speed from photon Doppler velocimetry signal content. To appear in IEEE Sensors. (Baltimore, 2013).

Moro, E. A., M. E. Briggs, and L. M. Hull. “H4442, H4442 Test Report: Surface evolution of radially expanding cylinders and the measured response in photon Doppler velocimetry. 2013. Los Alamos National Laboratory.

Moro, E. A., and M. E. Briggs. Note: Simultaneous measurement of transverse speed and axial velocity from a single optical beam. 2013. Review of Scientific Instruments. 84: 016110.

Moro, E. A., and M. E. Briggs. Defining parametric-dependencies for the correct interpretation of speckle dynamics in photon Doppler Velocimetry. Applied Optics.

Moro, E. A., and M. E. Briggs. Extracting transverse motion from speckle dynamics in photon Doppler velocimetry. Presented at 2013 Nuclear Explosives Design Physics Conference. (Livermore, January, 2014).

Moro, E. A., and M. E. Briggs. Extracting lateral motion from the dynamic amplitude modulations-the dynamic speckle-of a PDV signal. 2012. In 2012 PDV Workshop at Sandia National Laboratory. (Albuquerque, 2012). , p. 1. Columbus: Ohio State University.

Warren, W. J., L. Ott, E. Elmore, E. A. Moro, and M. E. Briggs. Laser speckle dynamics sensing applications. To appear in IMAC-XXXII. (Orlando, 2014).

The Role of Microscopic Eye Movements in Visual Perception

John S. George
20120773PRD4

Introduction

Eye movements are fundamental for processing and perceiving visual information about the surrounding world. Large-scale eye movements, called saccades, facilitate exploration of the visual environment by successively positioning the fovea (the region of retina that provides greatest visual acuity) on areas of interest in the visual field. During periods of eye "fixation," microscopic eye movements–shifts on the order of a photoreceptor cell–are observed in all vertebrate animals. Due to complex experimental requirements, the role of these movements, called ocular tremor, is not well understood. We hypothesize that ocular tremor contributes to low-level visual processing by generating patterns of synchronous firing between neighboring retinal neurons, and that correlated firing encodes unique spatiotemporal visual information, improving signal-to-noise ratios and visual acuity. I will study neural firing in response to visual stimulation of isolated retina, and characterize the perceptual consequences of eye movements in human subjects. These experiments are inspired by LANL computational models that simulate retinal and neural consequences of ocular tremor. The work exploits laboratory technologies for high spatial/temporal resolution measurement of neuronal function in order to provide further insight into visual signal encoding and processing.

Benefit to National Security Missions

The objective of the work is to better understand the mechanism that supports the encoding and processing of visual information by the retina and cortical visual systems of the brain. This work will enable better interpretation of neural signals for diagnostics of pathology, and facilitate treatment of retinal degeneration or neural injury via neural prosthetic devices such as those developed with DOE support in the Artificial Retina project and by NIH. The work will also enhance our understanding of neural mechanisms of visual cognition, supporting the development of neural-inspired computation systems for image processing and interpretation. Such efforts have been supported by recent and ongoing LDRD projects and are highly relevant for missions in DOE, DoD, and the intelligence community.

Progress

During the first 8 months of this project, Dr. Schei and collaborators have made significant progress on all of the key scientific and technological objectives outlined in the research proposal and initial datasheet.

Electrophysiological studies of isolated retina from tiger salamander have produced robust recordings of the population electroretinogram (an integrated response over a large population of retinal neurons) as well as reliable recordings of neural spiking (action potentials produced by individual neurons) generated by controlled light stimuli. A series of experiments were conducted to simulate biological eye movements by mechanically jittering a small light source, which was projected through the microscope optics onto the retina. We observed a strong correlation between neural oscillations apparent in the electrophysiological response (a time histogram of recorded spikes) and the frequency of stimulus jitter.

Experimental results were compared to the results and predictions of neural simulations, and a poster was presented at the Vision Sciences Society meeting in May of 2013.

Combined electrophysiological and optical recordings of retinal responses have been obtained. This should help identify the specific cellular sources of dynamic electrical responses.

A new video-based stimulation system is being assembled which can be used for both in vitro retinal physiology and for human perceptual and physiological experiments.

Basic setup of a fundus camera suitable for noninvasive imaging in situ of the human retina has been completed,

except for coupling the optical system to an electronic imager, and integrating the video stimulation system. (These components are presently being used for tissue physiology experiments.)

Basic setup has been completed of an adaptive optics system intended to allow imaging of individual photoreceptors in the human retina through fundus camera optics. This should allow us to track microscopic eye movements noninvasively with human subjects in perceptual experiments, as well as to characterize intrinsic eye movements in salamanders.

Enhancements to the high-speed camera system (firmware upgrades to the camera, and replacement of the computer based data acquisition system) have been completed.

Schei is mentoring a Los Alamos Scholarship Fund student intern during the summer of 2013. This student is designing and implementing human perceptual experiments (employing fast video presentations with or without simulated eye movements) that will be used to characterize perceptual performance in preparation for future experiments that will additionally collect noninvasive optical and electrophysiological measures.

Schei has continued to contribute to an ongoing LDRD ER project on Advanced Neural Interfaces, assisting with measurements of retinal electrophysiology used to validate and characterize performance of novel devices produced by the project.

In addition to the VSS presentation, this work was presented at Los Alamos Postdoc Research Day and was awarded honorable mention. Another publication based on Schei's graduate work has recently been accepted for publication in the disciplinary journal Sleep.

Future Work

Specific Aim 1: Simulate ocular tremor in an isolated amphibian retina by jittering a visual stimulus, while measuring electrophysiological activity of retinal neural populations. I will use commercial microelectrode arrays, as well as high-density nano-pillar arrays developed and fabricated at CINT, for high fidelity neural measurements of neural ensemble firing patterns. The objective is to characterize neural firing patterns in response to moving stimulation patterns, and to confirm the proposed physiological foundation of perceptual enhancement.

Specific Aim 2: Correlate neural spiking activity to intrinsic optical responses of isolated retina. Electrophysiological activity alters the optical properties of neurons and can be used to measure subthreshold activity and responses of specialized "analog" neurons of retina, as well as the spiking activity of the retinal ganglion cells that constitute the optic nerve. I will combine high- speed video microscopy with high-density electrophysiological measurements to investigate the relationship between neural firing patterns and optical responses imaged in retina.

Specific Aim 3: Characterize and simulate ocular tremor in the human eye. I will use high-speed optical imaging techniques with an ophthalmoscope camera employing adaptive optics to correct aberrations in eye's optics. This instrument will allow us to characterize optical tremor in an intact human eye, and to measure neural responses to tremor or to synthetic motion of a visual stimulus. The objective is to assess the role of physiological encoding in perceptual judgment.

Conclusion

Physiological measures of natural or simulated ocular tremor will enhance our understanding about retinal processing and encoding visual information, by testing and improving current computational models of retinal function. A deeper understanding of neural encoding and processing will enable better interpretation of neural signals for diagnostics of pathology, prosthetics to treat neural injury, and neural-inspired computation systems. Furthermore, these experiments will provide tools to define the role of ocular tremor in human visual perception by combining physiological and psychophysical measurement techniques.

Publications

George, J., J. L. Schei, P. Schultz, and G. Kenyon. Implications of microscopic eye movements for retinal encoding. 2013. In Vision Sciences Society. (Naples, Fl, 10-15 May 2013). Vol. 13, 9 Edition, p. 1341. New York: Journal of Vision.

Schei, J. L., G. Kenyon, and J. George. Contributions of microscopic eye movements to retinal encoding. To appear in Optical Society of America Vision Meeting. (Houston, 4-6 Oct. 2013).

Using Jet Production to Investigate quark-Gluon Plasma at RHIC

Xiaodong Jiang
20120775PRD4

Introduction

With the PHENIX experiment at Relativistic Heavy Ion Collider (RHIC) of DOE's Brookhaven National Laboratory (BNL), this research is in part a study of two-particle correlations demonstrating how the path-length through the Quark-Gluon Plasma (QGP) affects the fast moving particles to a degree beyond that expected within many theoretical expectations. Since then he have been helping the PHENIX experiment, in which LANL participates heavily, extend the current suite of measurements by separating out fast moving charm and bottom quarks. One major goal of this project is to use the fact that heavy quarks traverse the QGP differently depending on the mass of the quasi-particle excitations to study the properties of Quark-Gluon Plasma. Experimentally, this approach requires excellent particle tracking near the collision point and to that end PHENIX has installed a new set of vertex tracking detectors, the Vertex Detector (VTX) and the Forward Vertex Detector (FVTX), the latter a $5 million DOE project led by the LANL P-25 group. Specifically the postdoc fellow will continue to contribute to the data acquisition system of the PHENIX experiment, of which he is already a well-respected expert, and working on the reconstruction algorithms of the VTX detector. He is also expected to participate deeply in the next decadal plan to upgrade the PHENIX detector (the sPHENIX proposal, and the forward-sPHENIX proposal) to fully reconstruct jets and thereby better characterize the quasi-particle description of the Quark-Gluon Plasma.

This project expands the study of physics of Quark Gluon Plasma into using particle-jets to investigate the properties of quark gluon plasma. This topic and the research method proposed is a brand new direction in the field of High Energy Nuclear Physics. Therefore, this project is not improperly augmenting the existing P25 research program current funded by DOE.

Benefit to National Security Missions

This project is at the very frontier of High-Energy Nuclear and Particle physics research. The project, using a new experimental probe of particle jet production, is aimed at answering the question of "what are the properties and the behaviors of the extremely hot an dense Quark-Gluon Plasma formed within the first few seconds right after BigBang, the start of our Universe ? ". This project is aligned with the Nation's Nuclear Physics Long Range Plan (DOE Office of Science), advancing our basic knowledge of fundamental nuclear physics. The hardware and software tools developed through this project and the technical expertise gained through this project will also benefit LANL's mission on energy security, national security and nuclear non-proliferation.

This project expand the study of physics of Quark Gluon Plasma into using particle-jets to investigate the properties of quark gluon plasma. This topic and the research method proposed is a brand new direction in the field of High Energy Nuclear Physics. Therefore, this project is not improperly augmenting the existing P25 research program currently funded by DOE.

With the PHENIX experiment at Relativistic Heavy Ion Collider (RHIC) of DOE's Brookhaven National Laboratory (BNL), LANL team at BNL contact: Dr. Xiadong Jiang and Dr. Ming Liu 505 606 0437.

Progress

Over the last six months significant progresses and accomplishments have been made on the following fronts:

- RHIC PHENIX Heavy Ion physics analysis using Run-2012 data and information from Vertex Detector (VTX) and forward Vertex Detector (FVTX). Particle tracking codes, with a brand new tracking algorithm has been developed and tested. Raw data processing of U+U, Cu+Au, Au+Au collisions have been completed with the new package of tracking code, physics analysis have made good progresses, and various PHENIX "preliminary-results" have been reported in

international conferences. Mike continue sto lead the Heavy Flavor Physics working group within the PHENIX Collaboration.

- A new run (RHIC Run-2013, with the FVTX detector fully functional) was completed Jan-June 2013, with 510 GeV proton+proton collisions. Mike's efforts on supporting FVTX day-to-day operation, calibrations and online detector performance checks have earned him a high respect within the Collaboration. Physics analysis process is well underway, with Mike leading the efforts of FVTX tracking. Mike has been selected to give invited PHENIX presentations at international conferences such as HardProb2013, Physics-In-Collision-2013.

- On the future PHENIX upgrades, Mike has the lead in jet production simulations for sPHENIX and Forward-sPHENIX, defined physics requirements for building new spectrometer/detectors. Several progress reports have been made by Mike to the PHENIX Collaboration on jet shape, jet-identification and jet-reconstruction during Collaboration meetings, leading to major technical decisions by the Collaboration towards the future construction of sPHENIX and forward-sPHENIX detectors.

Future Work

With the PHENIX experiment at Relativistic Heavy Ion Collider (RHIC) of DOE's Brookhaven National Laboratory (BNL), LANL team at BNL contact: Dr. Xiadong Jiang and Dr. Ming Liu 505 606 0437.

The Postdoc Fellow is expected to work very closely with P-25 group members on the PHENIX experiment focusing on heavy ion physics with the Vertex Tracker (VTX) and the Forward Vertex Tracker (FVTX) as well as preparing for future upgrades. As such, the technical responsibilities of his research include:

- PHENIX experiment at RHIC: heavy quark energy loss and flow, large -gap two-particle correlations

- sPHENIX upgrade at RHIC: jet physics in both heavy ion collisions and polarized protons

Specific items include:

- Hardware responsibilities for the FVTX project: DAQ and detector operations in Run13 and Run14.

- Software responsibilities for the FVTX and VTX projects: FVTX track reconstruction, integration of VTX and FVTX algorithms, physics analysis

- sPHENIX physics and detector design: Simulations of key measurements and design parameters of the central barrel and the forward sPHENIX detectors.

- Physics analysis of jet observables in heavy-ion and p+p collisions.

This project expands the study of physics of Quark Gluon Plasma into using particle-jets to investigate the properties of quark gluon plasma. This topic and the research method proposed is a brand new direction in the field of High Energy Nuclear Physics. Therefore, this project is not improperly augmenting the existing P25 research program current funded by DOE.

Conclusion

With the PHENIX experiment at Relativistic Heavy Ion Collider (RHIC) of DOE's Brookhaven National Laboratory (BNL), LANL team at BNL contact: Dr. Xiadong Jiang and Dr. Ming Liu 505 606 0437.

- Combined tracking analysis code of Phenix VTX and FVTX detector.

- Data quality control during the operation in run-2013 and run-2013 for VTX and FVTX detectors,

- Preliminary analysis results of PHENIX run-2012 data on heavy flavor quark, and "jet-like" observables in Heavy-Ion collisions.

- Preliminary design report of sPHENIX and forward-sPHENIX upgrades, using jet observable to probe QGP in Heavy Ion Collision.

Publications

Adare, A., C. Aidala, N. N. Ajitanand, Y. Akiba, H. Al-Bataineh, et.al. Cold-Nuclear-Matter Effects on Heavy-Quark Production in d+Au Collisions at root S-NN=200 GeV. 2012. PHYSICAL REVIEW LETTERS. 109 (24): -.

Adare, A., C. Aidala, N. N. Ajitanand, Y. Akiba, R. Akimoto, H. Al-Ta'ani, et.al. J/psi suppression at forward rapidity in Au plus Au collisions at root s(NN)=39 and 62.4 GeV. 2012. PHYSICAL REVIEW C. 86 (6): -.

Adare, A., S. Afanasiev, C. Aidala, N. N. Ajitanand, Y. Akiba, H. Al-Bataineh, et.al. Spectra and ratios of identified particles in Au plus Au and d plus Au collisions at root s(NN)=200 GeV. 2013. PHYSICAL REVIEW C. 88 (2): -.

Adare, A., S. Afanasiev, C. Aidala, N. N. Ajitanand, Y. Akiba, H. Al-Bataineh, et.al. Transverse-momentum dependence of the J/psi nuclear modification in d+Au collisions at root s(NN)=200 GeV. 2013. PHYSICAL REVIEW C. 87 (3): -.

Adare, A., S. Afanasiev, C. Aidala, N. N. Ajitanand, Y. Akiba,

H. Al-Bataineh, et.al. Measurement of transverse single-spin asymmetries for J/psi production in polarized p + p collisions at root s = 200 GeV (vol 82, 112008, 2010). 2012. PHYSICAL REVIEW D. 86 (9): -.

Adare, A., S. Afanasiev, C. Aidala, N. N. Ajitanand, Y. Akiba, H. Al-Bataineh, et.al. Inclusive cross section and single transverse spin asymmetry for very forward neutron production in polarized p plus p collisions at root s=200 GeV. 2013. PHYSICAL REVIEW D. 88 (3): -.

Adare, A., S. Afanasiev, C. Aidala, N. N. Ajitanand, Y. Akiba, H. Al-Bataineh, et.al. Neutral pion production with respect to centrality and reaction plane in Au plus Au collisions at root S-NN=200 GeV. 2013. PHYSICAL REVIEW C. 87 (3): -.

Adare, A., S. Afanasiev, C. Aidala, N. N. Ajitanand, Y. Akiba, et.al. Medium Modification of Jet Fragmentation in Au plus Au Collisions at root S-NN=200 GeV Measured in Direct Photon-Hadron Correlations. 2013. PHYSICAL REVIEW LETTERS. 111 (3): -.

Adare, A., S. Afanasiev, C. Aidala, N. N. Ajitanand, Y. Akiba, et.al. gamma (1S+2S+3S) production in d plus Au and p plus p collisions at root s(NN)=200 GeV and cold-nuclear-matter effects. 2013. PHYSICAL REVIEW C. 87 (4): -.

Adare, A., S. Afanasiev, C. Aidala, N. N. Ajitanand, Y. Akiba, et.al. Double-spin asymmetry of electrons from heavy-flavor decays in p plus p collisions at root s=200 GeV. 2013. PHYSICAL REVIEW D. 87 (1): -.

Extending the Time-scale of Protein Simulations Using Accelerated Molecular Dynamics Techniques

Arthur F. Voter
20130777PRD1

Introduction

The goal of this project is to apply the parallel replica dynamics (ParRep) method to the dynamics of protein folding. ParRep advances an infrequent-event system rapidly from state to state by parallelizing time over many replicas of the system in each state. A recent advance in the understanding of the generality of ParRep, allowing for more general state definitions, opens the possibility of effective application to complex systems such as proteins, something that was previously thought to be impossible in most cases. This new approach will be developed and tested on a small model peptide system such as alanine dipeptide, for which the exact dynamics are known, and then extended to more complicated systems such as Met-enkephalin, verifying the folding characteristics against existing data. If this new methodology can be developed to be effective for accurate protein folding, the potential payoff is substantial, as most protein folding and function takes place on time scales longer than are accessible with direct molecular dynamics. Moreover, this methodology should transfer well for study of dynamics in other complex and soft-matter systems important in nanotechnology, energy conversion and alternative energy generation.

Benefit to National Security Missions

The accurate description of processes such as protein folding, protein function, drug function, etc., on biologically relevant timescales is a long-standing problem. This project aims to develop a methodology to extend the accessible simulation time scale for these types of processes. If this project succeeds, it will impact not only bioscience, but other areas where complex or soft-matter dynamics are important. Such a capability could be extremely useful to understand active site protein chemistry, which could lead to the design of bio-inspired catalysts with high efficiency and selectivity. This specifically addresses a key mission of the Physical Biosciences program of the Chemical Sciences, Geosciences, & Biosciences (CSGB) Division of the Basic Energy Science Office. This work could also lead to improved understanding of bio-chemical reactions inside the cell that could be used for energy-related applications, also an area of interest to the CSGB.

Progress

This project began just a few months ago. Exploratory simulations have been performed using the GROMACS code on the alanine dipeptide system. Tens of thousands of trajectories were initiated from a single geometry, and the escape time distribution was determined for various definitions of the state boundary, as defined by rectangular regions in the phi-psi (Ramachandran) plot. As predicted by the quasi-stationary distribution theory, after a suitable dephasing time, the decay of the population from the defined state becomes cleanly exponential. Thus, as anticipated, this system and this type of state-boundary definition would allow treatment with parallel replica dynamics to accelerated the rate of state-to-state transitions. However, one aspect that is less than satisfactory for using this as a model system is that the average escape time from the deepest state is not long enough to get significant parallelization gain. Thus, we are now in the process of choosing a second system to continue our study, one that has deeper states that give less frequent events.

Future Work

In the first year, the parallel-replica dynamics method will be implemented into the GROMACS bio-simulation package. We will then begin developing the new, generalized methodology on a small model peptide system such as alanine dipeptide, where the dynamics will be compared to the known exact dynamics for that same model system. We will investigate definitions for the states of the system, with the goal of finding the largest separation of time scales between the dephasing time (the time to settle into the equilibrium or steady-state distribution) and the average escape time from the state. We will also begin investigating how to determine, in

general, the length of this dephasing time. This is the most challenging part of the project.

Conclusion

The overall goal of this project is to develop a viable methodology for application of the parallel-replica dynamics method to protein folding. Success in this project will impact biochemistry, as time scales for important protein dynamics, DNA dynamics, membrane function, etc., are beyond the reach of standard molecular dynamics. Success will also impact other fields where soft-matter or complex dynamics are important, as accurate atomistic evolution of these systems on long time scales beyond about one microsecond is currently impossible. Examples include heterogeneous catalysis and processing steps in surface coatings for solar cells or semiconductors.

Electronic and Photonic Transport in Chiral Materials and Nanostructures

Diego A. Dalvit
20130781PRD1

Introduction

Graphene and topological insulators are the most recent discoveries in material science, and represent the cutting edge of condensed matter physics. Among many applications, these materials are the most promising candidates to replace semiconductors in commercial electronics. They will make possible, for example, to create a microprocessor with orders of magnitude higher speed and almost no energy losses. Spin-orbit coupling in these systems represent a form of chirality, which is a property prevalent in Nature. The study of the electronic and photonic chiral materials offers exciting opportunities for discovering interesting new physics and technologically important applications, including spintronics-based information processing, new material probe techniques, and Casimir force repulsion.

Benefit to National Security Missions

This project will impact LANL/DOE mission on basic energy sciences, materials, and nanotechnology, as it will develop new theoretical and numerical tools to describe some of the most exciting materials in condensed matter physics, including graphene, topological insulators, and topological superconductors. It also has the potential of attracting interest from external agencies, such as DARPA, that have shown recent interest in controlling Casimir forces and in energy harvesting.

Progress

The postdoc arrived July 2013; therefore, there is no progress to date.

Future Work

The tasks to be performed are:

- Study of charge/spin density response functions in chiral materials, that give important information about the charge/spin quantum fluctuations and their collective modes that can be measured by electron energy loss spectroscopy and spin-noise Faraday rotation experiments ongoing at LANL.
- Study of how chiral materials, including graphene and topological insulators and superconductors, influence Casimir interactions at the nanoscale.

Conclusion

The expected results of this project is a comprehensive study of the transport properties of strongly spin-orbit coupled materials including topological insulators and superconductors, as well as nanostructures built from chiral materials such as graphene superlattices. Specifically, we will study how density-density and current-current correlation functions depends on the spin-orbit coupling, external magnetic fields, and electron-electron interactions. We will also perform research on the optical properties of chiral materials with the intention to elucidate how electromagnetic fluctuation-induced (Casimir) forces depend on the physical parameters of such systems, with the ultimate goal of determining optimal strategies for controlling the Casimir effect.

Exploring Doubly Parasitic Radioisotope Production Via Secondary Neutron Fluence From the 100 MeV IPF Irradiations

Eva R. Birnbaum
20130782PRD2

Introduction

The Isotope Production Facility (IPF) at Los Alamos National Laboratory (LANL) produces the radioactive isotopes strontium-82 and germanium-68 for use in medical imaging. The IPF's high proton beam current and lengthy irradiations produce a secondary neutron field with a utilitarian scale that is beyond the reach of medical cyclotrons and energetically distinct from reactor neutron fluences. There are currently no large facilities in the United States with access to such a significant, high-energy neutron flux, yet IPF secondary neutrons' potential for research in novel methods of isotope production and materials science remains unexploited. These radioisotopes are necessary to a variety of scientific and medical fields, and in many cases the stability of future uninterrupted supply is uncertain. Additionally, LANL's globally recognized expertise in the characterization and handling of radioisotopically and chemically diverse products of fast neutron irradiations is uniquely capable of facilitating such an exploration.

Current two week irradiations produce several tera-neutrons per second, approaching the scale of medium-sized research reactors. The Monte Carlo N-Particle eXtended (MCNPX) code, developed at LANL, has been used to simulate the secondary neutron field and optimize the design of research targets that can confirm predictions about the size and charter of this neutron flux. Using these simulations, special activation foils have been introduced into the neutron field and the radioisotope products of neutron-initiated reactions. Once computational predictions have been confirmed by experiment, MCNPX codes will be further used to design future experiments in materials science development and to produce radioisotopes in the service of the larger scientific community. Delivery of these and other isotopes whose study is proposed makes possible targeted radiotherapy for cancer patients, experiments in solid-state physics, diagnosis of a wide range of pathologies, and the development of improved materials for civil and scientific purposes.

Benefit to National Security Missions

A comprehensive understanding of the secondary neutron flux at the Isotope Production Facility will expand the capabilities of the Isotope Program to study and produce a broader suite of isotopes for medical, national security, and basic science applications. Studies will also improve nuclear models and provide an avenue for study of materials under extreme environments.

Progress

Dr. Engle has made good progress in his primary proposal area to fully characterize the secondary neutron flux at the Isotope Production Facility. Based on simulations calculated with MCNPX code, a series of materials were chosen to experimentally probe this neutron flux. A set of special activation foils were introduced into the neutron field during the last IPF run cycle and brought to the TA-48 count room for measurement. The radioisotope products in these foils yield information on neutron-initiated reactions. Measurements using these foils have characterized these neutrons' flux energy distribution, and efforts are now underway to investigate the production of 47Sc for medical radiotherapy, and to characterize the products from high energy neutron irradiation of thorium targets for the production of alpha emitting actinide isotopes. A second generation neutron target is being developed which will enable longer-term, production scale irradiations of chosen targets in a safe environment tailored for downstream radiochemical isolation of desired radioactive products.

Concurrently, Dr. Engle has benefitted from the proton irradiation capabilities of the LANSCE and IPF facilities, which have been used to initiate nuclear formation cross section measurements for several radioisotopes of interest to medical and basic science research. Cross section measurements are in progress for a number of isotopes with potential medical application. Isotopes under

investigation include: the lanthanide isotope 153Gd, which is useful as a flood source for instrument calibration and imaging; the 165Tm/165Er parent/daughter pair, considered as novel approaches to targeted radioimmunotherapy of malignant and viral diseases; and a comprehensive understanding of radioactive impurities co-produced during proton irradiations of thorium to produce 225Ac for alpha therapy of disease. Two publications have been submitted on these works and an additional two manuscripts are in preparation.

Dr. Engle has also been engaged by the ongoing LDRD-ER funded effort to measure neutrino mass via calorimetric electron capture spectroscopy of the rare-earth isotope 163Ho. The collaborative effort within C-IIAC, ISR-2, and NEN-5 to investigate potential routes to production of large quantities of this isotope has resulted in an invited talk at the NuMass 2013 meeting in Milan and in the submission of an additional manuscript since the Reines fellowship was awarded.

The Isotope Program has recently been directed by the Office of Science to pursue the development of metallic rubidium targets, to replace RbCl as the material of choice for irradiations to produce 82Sr for cardiac positron emission tomography. Dr. Engle contributes to this project in collaboration with several LANL experts in accelerator targetry and separations chemistry.

Since receiving the Reines award, Dr. Engle has also presented nuclear data at the 2013 International Nuclear Data Meeting in New York and at the 8th Targeted Alpha Therapy Meeting at ORNL, and has consented to serve on the scientific committee of the 15th semi-annual Workshop on Targetry and Target Chemistry in Prague, scheduled for the summer of 2014.

Future Work

- Finish computational modeling of the Isotope Production Facility neutron flux using LANL-developed state-of-the-art computational tools like MCNPX/MCNP6 and CINDER90. Work with Mike James (NEN-5), Stepan Mashnik (XCP-3), and others to investigate accuracy of evaluated data libraries and MCNP-implemented physics models, which are applied to the problem of computational predictions of isotope production using the IPF secondary neutron flux.
- Continue investigation of IPF's potential for contribution to fusion energy research program through testing of tritium breeding, chemical speciation and migration through test materials.
- Tailor the predictions of these models to experimental measurements of activation experiments using test foils and quantification of radioisotopes produced in the foils by neutron-initiated reactions.
- Use the validated codes to design a series of test irradiations and radiochemical separations to produce scandium-47 using enriched titanium (Ti) and vanadium (V) targets.
- Irradiate these test materials (Ti and V) at IPF and use gamma spectroscopy to quantify radioactive products and possible impurities.
- Conduct 200 and 100 MeV incident proton energy irradiations of thulium targets to complement 800 MeV irradiations completed in December 2012 and oversee assay of these irradiated samples using the C-NR countroom and TA-48 Hot Cell Wing facilities.
- Analyze spectroscopy of 800 MeV p + Tm irradiation foils to calculate nuclear formation cross sections. Apply these cross sections to the evaluation of spallation-regime isotope production schemes.
- Finalize analysis of 40 – 200 MeV p + Tb residual cross sections to evaluate the potential for Gd-153 production at IPF. Make determination regarding securing IP or publication of results.
- Complete publication of 40 – 800 MeV p + Th target residual cross sections.
- Continue contributions Rb metal targetry and production of Ho-163 for neutrino mass measurement.

Conclusion

The goal of this project is to elucidate a more complete understanding of the secondary neutron flux at the Isotope Production Facility. These experiments will define production methodologies that will supply radioisotopes on the cutting edge of research in several fields. Production of isotopes including scandium-47, actinium-225, and radium-225 for medical radioimmunotherapy will be investigated. The neutron flux can also be used to study the effects of high radiation environments and thus fuel development of materials and devices that can withstand the extreme conditions in space or power production devices such as fusion reactors.

Publications

Engle, J. W., E. R. Birnbaum, F. M. Nortier, J. A. Rau, K. D. John, and H. R. Trellue. Purification of (PU)-P-242 by irradiation with thermal neutrons. 2013. NUCLEAR INSTRUMENTS & METHODS IN PHYSICS RESEARCH SECTION B-BEAM INTERACTIONS WITH MATERIALS AND

ATOMS. 298: 70.

Engle, J. W., E. R. Birnbaum, H. R. Trellue, K. D. John, M. W. Rabin, and F. M. Nortier. Evaluation of Ho-163 production options for neutrino mass measurements with microcalorimeter detectors. 2013. NUCLEAR INSTRUMENTS & METHODS IN PHYSICS RESEARCH SECTION B-BEAM INTERACTIONS WITH MATERIALS AND ATOMS. 311: 131.

Engle, J. W., S. G. Mashnik, J. W. Weidner, L. E. Wolfsberg, M. E. Fassbender, K. Jackman, A. Couture, L. J. Bitteker, J. L. Ullmann, M. S. Gulley, C. Pillai, K. D. John, E. R. Birnbaum, and F. M. Nortier. Cross sections from proton irradiation of thorium at 800 MeV. 2013. PHYSICAL REVIEW C. 88 (1): -.

Theoretical Investigation of Nucleon and Nuclear Structure at Very High Energies

Ivan M. Vitev
20130783PRD2

Introduction

The theoretical study and experimental exploration of the internal structure of nucleons (protons and neutrons) and nuclei are of fundamental importance to science and have recently entered a new exciting phase. In the past decades an understanding of nucleons in terms of quarks and gluons (partons) has successfully emerged. Progress has been made in constructing a "one-dimensional" picture of the nucleon, in the sense that we "only" know about the longitudinal motion of partons in fast moving protons and neutrons. However, the parton's motion that is perpendicular (transverse) to the proton momentum is still largely unknown and urgently needed in order to construct the 3-dimensional image of the proton. Since the transverse momentum component is usually much smaller than parton's longitudinal component, it is critical to develop accurate theoretical tools to extract this information. We propose two unique ways to attach this problem. One is through the transverse spin dependence of experimental observables, as transverse spin can correlate with the parton transverse momentum. The other way is through a discovery of a novel nuclear dependence, as the small transverse motion can be amplified by the nuclear size. We will develop the first solid theoretical framework that can utilize both methods to pinpoint the partons' transverse motion in both the proton and the big nucleus.

Benefit to National Security Missions

This project ties directly into the Laboratory mission in scientific innovation and discovery. Understanding the structure of the nucleon is central to the nuclear physics component of the National Science Foundation (NSF) and Department of Energy (DOE) Office of Science portfolios. Specifically, this project will provide new and unique 3 dimensional imaging information for the nucleon structure at the ~20% level. It will also give essential insights into how the quark and gluon dynamics are modified in a large nucleus. It will produce theoretical tools for the community to accurately and reliably extract such information from data collected in the US and abroad. It also provides much-needed theoretical guidance for and interpretation of the experimental results from the flagship nuclear physics program in US and abroad. This project will also help firm the scientific case for a future Electron Ion Collider.

Progress

Since the beginning of fiscal year 2013, we have made significant progress toward the ultimate goal of this project. We have published 4 papers: two in Physical Review D, one in Physics Letters B, and one in Physical Review Letters. We are also actively involved in preparing a white paper on the future experimental direction on spin physics. This white paper discusses future critical measurements and theoretical advances in spin physics for the upgraded Relativistic Heavy Ion Collider (RHIC) at Brookhaven National Laboratory. In particular, our proposed observables and simulations are essential for understanding the transverse spin dependent observables.

Two highlights of our work concern the evolution and universality properties of the so-called Sivers effect. The Sivers function represents the probability to find unpolarized patrons inside a transversely polarized proton. It contains both the longitudinal and transverse motion of the partons. Understanding how the Sivers function changes with energy and in different processes is critical to extract the information on the Sivers function consistently from the world-wide experimental data.

In a recent paper published in Physical Review D, we computed the next-to-leading order contribution to the transverse momentum weighted Sivers asymmetry in semi-inclusive hadron production in deep inelastic scattering (SIDIS). From this calculation, we were able to extract the momentum scale evolution of the relevant parton correlation function. This parton correlation function allows us to pin down the averaged parton

transverse motion inside the transversely polarized proton. Our calculation also demonstrates how this averaged transverse motion changes when one probes it at different momentum scales.

In another paper, published in Physical Review Letters, we studied how the Sivers effect changes when going from SIDIS to single inclusive jet production in proton-proton collisions. In particular, we evaluated the initial-state and final-state interactions between the active parton and the remnants of the proton, which are responsible for the difference of the observed Sivers effect in different processes. By doing so, we found the relation between the Sivers function in these two different processes. We first performed a global fitting of the existing SIDIS experimental data to extract the Sivers function. We then started with this Sivers function, properly took into account the differences in the Sivers function in single inclusive jet production, and made a prediction for the spin asymmetry for the jet production. We compared our prediction to the recent available experimental data from AnDY collaboration at RHIC at Brookhaven National Laboratory and found reasonable agreement. This provides a first indication on the process-dependence of the Sivers effect in different processes.

Future Work

As emphasized in our project description, we will take two complementary approaches to pin down the parton's transverse motion in nucleons and nuclei. Focusing on the spin dependence, in the next fiscal year we will derive energy evolution equations for the parton momentum distribution inside the proton. This will allow for a direct comparison between theory and experimental data taken at very different center of mass energies. We will then implement these evolution equations in the description of the experimental data on semi-inclusive hadron production in deep inelastic scattering (SIDIS) processes. Using a global fitting procedure, we will extract for the first time the parton transverse momentum distributions with much better accuracy. On the nuclear dependence side, we will focus on the multiple quark and gluon scattering in a big nucleus that generates transverse motion. In particular, we will perform the first calculation of the multi-parton interaction contributions to the same SIDIS process with full next-to-leading order accuracy. This will enable us to gain experience and apply the same method to other experimental processes.

Conclusion

We will develop a new consistent theoretical formalism for evaluating the cross sections in polarized reactions with protons and nuclei. We will also investigate the novel nuclear dependence of experimental spin observables in both electron-nucleus and proton-nucleus collisions. We will use these theoretical formalisms to interpret the experimental data collected at the major experimental facilities in the US and abroad and extract the valuable information on the parton's transverse motion. This will provide unique 3-dimensional imaging information for the proton and nuclear structure at high energies.

Publications

Aschenauer, E. C., A. Bazilevsky, K. Boyle , R. Fatemi , C. Gagliardi, M. Grosse-Perdekamp, Z. B. Kang, Y. Kovchegov, and J. Lajoie. The RHIC Spin Program: Achievements and Future Opportunities . 2013. White Paper on RHIC spin physics to the Tribble Panel and Nuclear Science Advisory Committee.

Gamberg, L., Z. B. Kang, and A. Prokudin. Indication on the process-dependence of the Sivers effect. 2013. Physical Review Letters. 110 (23): 232301.

Gamberg, L., and Z. B. Kang. Single transverse spin asymmetry of prompt photon production. 2012. Physics Letters B. 718 (1): 181.

Kang, Z. B.. QCD and RHIC spin physics. Invited presentation at 2012 Fall Meeting of the APS Division of Nuclear Physics. (Newport Beach, CA, 24-27 Oct. 2012).

Kang, Z. B.. Polarized p+A, single spin asymmetries. Invited presentation at BNL-LANL-RBRC Joint Workshop on The Physics of p+A Collisions at RHIC. (Upton, NY, 7-9 Jan. 2013).

Kang, Z. B.. Single transverse spin asymmetries in polarized SIDIS and pp scattering. Invited presentation at The 5th Workshop of the APS Topical Group on Hadronic Physics. (Denver, CO, 10-12 Apr. 2013).

Kang, Z. B.. Forward physics from a theoretical perspective. Invited presentation at STAR Meeting on eSTAR Letter of Intent, Forward-Upgrades and Results from U+U Collisions. (Los Angeles, CA, 28-30 Aug. 2013).

Kang, Z. B., I. Vitev, and H. Xing. Transverse momentum-weighted Sivers asymmetry in semi-inclusive deep inelastic scattering at next-to-leading order. 2013. Physical Review D. 87 (3): 034024.

Kang, Z. B., and B. Xiao. Sivers asymmetry of Drell-Yan production in the small-x regime. 2013. Physical Review D. 87 (3): 034038.

Vitev, I.. Transv. Invited presentation at Transverse momentum-weighted Sivers asymmetry in semi-inclusive deep inelastic scattering at next-to-leading order. (Newport News, VA, 6-10 May 2013).

The Intersection of the Energy, the Intensity, and the Cosmic Frontiers in the Era of the Large Hadron Collider and XENON experiments

Michael L. Graesser
20130789PRD2

Introduction

The overall goal of the project is to develop new methods and theories that may deepen our understanding of particle physics in two areas. One area is at distances 100-1000 times smaller than a proton, where we think the physics "responsible" for giving mass to fundamental particles is occurring. The other is during epochs of the very early universe, when the abundance of dark matter was being set and when the excess of matter over anti-matter occurred.

To do that, the project will develop new models for dark matter interacting with the Higgs boson, and simultaneously, develop new experimental tools that will improve the ongoing searches at the Large Hadron Collider (LHC) for new particles.

The proposed research to look for connections between dark matter and the Higgs boson may provide us with a new framework for understanding why the Universe has more particles than anti-particles. The proposed work will either discover such a new framework, or provide us with a deeper understanding of the limitations of new interactions between the Higgs boson and dark matter.

An important research tool for understanding the implications of particle theories in a collider environment is the use of jets. Jets are energetic sprays of particles that are detected at collider experiments. Jet substructure refers to the physical properties of the particles inside the jet. The substructure of a jet depends on the physics that produced it.

The proposed research in jet substructure physics will generate important tools that will: improve the potential for the LHC to discover new particles; and improve the ability of the LHC to perform more accurate measurements. Applied to the Higgs boson, these methods may be quite rewarding, since they may enable experimentalists at the LHC to discover and measure various decay modes of this particle.

Benefit to National Security Missions

One of the central goals of particle physics and the DOE Office of Science High Energy Physics is to understand the physics of matter at very short distances - 1000 times smaller than the size of a proton - and at energies 100-1000 times higher than the energy in a proton. Currently the main experimental facility to achieve that goal is the Large Hadron Collider (LHC) located outside of Geneva, Switzerland. This experiment recently discovered a new particle that has the physical features of the so-called "Higgs boson".

Another important thrust of particle physics and the DOE Office of Science High Energy Physics is to understand the physical properties of dark matter.

The discovery of the Higgs boson brings into sharp focus two important scientific questions: how does matter - such as quarks and the electron - gain inertial mass has become acute; and why does the Universe appear to have more particles than anti-particles?

The discovery of additional new particles at the LHC will provide more information that may help address the first question. To that end, while at Los Alamos Tuhin Roy will develop new search strategies to improve the experimental reach of the LHC.

Tuhin will also develop new models of dark matter interacting with the Higgs boson, which may address the second question. The properties of such theories may be tested at the LHC and/or future dark matter direct detection experiments.

Progress

This project started September 2013; therefore, there is no progress to date.

Future Work

In the first year the proposed work will:

Develop tools for separating jets produced by the strong force, from those produced by the decay of a new particle
As described under "Project Description", "jets" are an important research tool for understanding the implications of particle theories in a collider environment. Jets are energetic sprays of particles, such as of protons, neutrons, pions, kaons,..., that are produced from the collision of two protons at a collider, and then detected inside the experiment. Jets are produced from Standard Model (SM) processes - specifically the strong force - but can also be produced in the decay of a new particle.

The first step in achieving this goal is to identify specific classes of models of Beyond-the-Standard Model (BSM) physics that will be the target for discovery. Then a new idea for jet substructure will be applied to these classes of BSM models and SM backgrounds. The significance of the new idea(s) will be evaluated through computer simulations.

Propose new interactions between dark matter and Higgs boson; then identify regions of the parameter space that allows for the Higgs boson to undergo a "first order" phase transition
A phase transition refers to the transition of matter from one phase to another, such as water boiling to form water vapor or water cooling to form ice. A "first order" phase transition refers to a phase transition in which the transition occurs through the formation of bubbles. An example of a first order phase transition is water boiling. A first order phase transition is one of the conditions that more or less must occur in the early universe in order for more baryons to be produced than anti-baryons. (Protons and neutrons are baryons.)

Conclusion
The overall goal is to advance our understanding of particle physics at distances much smaller than a proton and during epochs in the early universe.

New methods are needed to improve the potential for the Large Hadron Collider (LHC) to discover new particles and to improve accuracy. The results of this proposal may be quite rewarding, since, for example, they may enable the LHC to discover and measure various decay modes of the Higgs boson.

Formulating new interactions between dark matter and the Higgs boson may lead to a new understanding for why the universe has more particles than anti-particles.

Boosting New Physics Discoveries with Jet Substructure

Christopher Lee
20130794PRD2

Introduction

The Standard Model (SM) of particle physics is the most precise and successful theory in the history of science, but it still cannot explain dark matter or the huge hierarchy of energy scales (from nuclear forces to gravity) found in nature. Much excitement today comes from predictions of new models of elementary particles that could help solve these mysteries and be detected at the Large Hadron Collider (LHC).

The LHC collides protons at high energies and records the resulting particles that are produced. The most common type of SM final state contains collimated streams of hadrons called jets, produced by radiation from high-energy quarks or gluons. On occasion, new, non-SM particles may be produced and also decay into jets. Finding them is a very difficult needle-in-the-haystack problem to distinguish jets produced by new particles from the vastly larger number of jets produced by ordinary SM processes. This makes high-precision predictions of the SM jet background essential. Unfortunately, jet cross sections are among the least precisely understood due to the often prohibitively difficult nature of the calculations.

This research aims to vastly increase the precision of theoretical jet cross section predictions. We will develop strategies to characterize and probe the substructure of jets, which can serve as a discriminant between signal and background jets. We will apply our expertise in theoretical methods to resum the effects of infinitely many quarks and gluons radiated from jets to predict jet cross sections to high precision and accuracy. We will develop new methods to predict cross sections dependent on subjet measures. We will thereby improve the theoretical input into Monte Carlo event generators that simulate large numbers of particles in high-energy collisions. All of these tools together will greatly advance our ability to find evidence of new physics at the LHC inside hadronic jets.

Benefit to National Security Missions

Two key missions of the DOE Office of Science in High-Energy and Nuclear Physics are 1) to improve our understanding of Quantum Chromodynamics (QCD), the theory of the strong interactions between quarks and gluons, constituents of all ordinary matter; and 2) to search for new particles and forces beyond the Standard Model that will explain the origin of matter, dark matter, and masses of elementary particles.

Understanding properties of jets of hadrons produced by energetic quarks and gluons are key to achieving these objectives. They reveal the behavior of QCD itself and contain evidence of new particles that decay to jets.

This project tackles problems at the forefront of QCD perturbation theory and strategies to search for signatures of new physics in the substructure of jets. Physically accurate predictions of jet cross sections require resumming arbitrarily many soft and collinear quark and gluon emissions in and from jets. We will develop and apply tools for resummation to achieve unprecedented precision in predicting jet cross sections for probing QCD and new physics at the Large Hadron Collider (LHC). In concert we will invent and develop new strategies for finding and characterizing jet substructure and interpreting those characteristics as signatures for new physics.

Historically, individuals hired for their expertise in this area have gone on to address a range of Laboratory challenges, including bio and energy security, thanks to their broad analytical skills.

Progress

This project started September 2013; therefore, there is no progress to date.

Future Work

In the first year of this project, we will:

- Evaluate previously proposed measures of jet substructure for their amenability to precise theoretical calculation, and if necessary improve them or invent new measures that are better suited to precise predictions.
- Develop theoretical tools to predict subjet cross sections, by extending the tools of soft collinear effective theory (SCET) to handle multiple jet directions contained within a single, larger jet.
- Apply the new theoretical tools to predict signal and background cross sections for searches for heavy particles such as top quarks, Higgs bosons, or beyond-the-Standard-Model particles that decay to hadronic jets.

Conclusion

In this new, exciting era in particle physics, this project will play a crucial role in guiding what observables to measure at the Large Hadron Collider and how to interpret such measurements for signals of new physics. We focus on probing the substructure of jets of hadrons to which new physics particles decay and which can be used to distinguish jets produced by known and by new physics. We will make simultaneous advances in search algorithms, theoretical predictions, and computational programs for jet cross sections that are all part of a comprehensive strategy for finding new physics using hadronic jets.

Physics of Cosmic Ray Shocks and the High Energy Universe

Hui Li
20100611PRD2

Abstract

Astrophysical plasmas are magnetized and well-described on large scales by Magnetohydrodynamics or MHD. Their dynamics are affected by turbulence, which is observed in the Sun, solar and stellar winds, accretion disks and spiral galaxies, violent outflows from active galactic nuclei, supernova explosions and so on. Another basic component of magnetized astrophysical plasmas is so-called cosmic rays (CRs), charged relativistic particles, mostly protons, with energies from 10^8 to 10^21 eV. The mysterious property of CRs is that they have an energy density comparable to that of kinetic motions and magnetic fields, e.g., around 1 eV/cm^3 in our Galaxy, which is likely related to the interaction between CRs and MHD plasmas, the process which is still poorly understood. The physics of CR acceleration in shocks, where CRs have a pressure comparable to gas pressure and strongly modify the shocks, is dominated by the mutual interaction of CRs and turbulence.

Background and Research Objectives

Magnetohydrodynamic turbulence is a complex nonlinear problem. It is multidisciplinary in nature, as highly conductive plasmas are found not only in astrophysical objects, but in our own solar system, in the solar wind, and also in laboratory plasma experiments. MHD turbulence is ubiquitous in these environments. Turbulence must be considered to understand large-scale flows. This was realized a long time ago, making turbulence a major theme in hydrodynamics for the past century. MHD turbulence and its applications for astrophysics are much younger, but even now it is clear that there is a wealth of phenomena to study. The next degree of complexity in astrophysical plasmas arises when one considers cosmic rays – highly energetic particles, which interact with MHD fluid and which are dynamically important in many astrophysical environments, such as galactic disks and supernova remnants. MHD turbulence and its interaction with cosmic rays is an interesting problem, but hard. Cosmic rays are dynamically important: processes as galactic dynamo or star formation could only be fully understood if cosmic rays are included in the dynamics the interstellar medium (ISM) and molecular clouds. Another classic example of the importance of the mutual interaction between cosmic rays and MHD fluid is the problem of cosmic ray acceleration in supernova remnants, i.e. the problem of the origin of the Galactic cosmic rays themselves. We know that cosmic rays are present in supernova remnants in large amounts but we are not sure why their acceleration is efficient. It has become clear that ambient scattering of cosmic rays is grossly insufficient to provide sizable acceleration; to get around this, it was proposed that astrophysical shocks are strongly modified by cosmic rays and become turbulent. The reason why this problem has been around for more than thirty years is that in order to be efficient, diffusive shock acceleration must involve interaction of cosmic rays streaming in front of the shock with the undisturbed ISM plasma, creating a precursor turbulence, which in turn reduces the cosmic ray mean free path, making acceleration more efficient. Without this back-reaction the acceleration in supernova remnants should be negligible, contrary to observations. Despite this problem having attracted a lot of attention, most existing approaches to it are as yet heuristic. Full understanding is complicated by the strongly nonlinear supersonic dynamics of the precursor MHD turbulence interacting with collisionless particles via magnetic field.

A number of widely different approaches have been used to tackle the cosmic ray acceleration problem. For example, PIC simulations are the most first-principle-based and used to solve particle dynamics in self-consistently evolved electromagnetic fields. Unfortunately, PIC simulations in three dimensions will always be limited in the range of scales they cover. Only a few hundred, or at best, a few thousand plasma skin depths can be reached by three-dimensional PIC. Although this is tiny compared to astrophysical scales, some ideas in diffusive shock acceleration (DSA) can be checked by PIC. Monte Carlo

simulations assume certain diffusive properties and can, indeed, cover a wide range in cosmic ray energies but, unfortunately, require a priori knowledge of particle scattering. Important advances in the particle acceleration theory were made by realizing that the precursor magnetic fields have to be significantly amplified. In this respect important progress has been made in the studies of cosmic ray current instability. Another mechanism is the small-scale dynamo excited by the baroclinic term in strongly modified shocks. Although we would like to know the outcome of the full kinetic streaming instability in the precursor, this is hard due to the tangled nature of the magnetic field generated by small-scale dynamo.

Scientific Approach and Accomplishments

MHD turbulence is essentially nonlinear and cannot be treated perturbatively. In this situation it is especially important to use direct numerical simulations as a guide to theoretical understanding. We used numerics to understand basic physical processes, rather than trying to simulate a real astrophysical object and obtain a final answer. We studied supersonic, weakly compressible and incompressible MHD turbulence and developed novel methods of data analysis, and in so doing executed some of the highest resolution numerical experiments ever performed. In 2013, we were awarded DOE INCITE allocation of 35 million CPU hours to study MHD turbulence. Our versatile MHD code that solves MHD, hydro and reduced MHD equations are currently the fastest available. Not only do we run MHD simulations, but also as a step towards understanding MHD-particle interaction we developed a particle tracing code that was used for calculating scattering and diffusion of fast particles in magnetic fields, generated in MHD simulations. Later, we started using PIC and relativistic MHD codes. Careful application of numerics to theory, and, likewise, clear formulation of the theoretical problem to resolve it with numerics, have resulted in several key findings in the MHD theory and cosmic ray scattering outlined below. We have proposed that the process of magnetic energy generation in turbulent conductive medium is universal in large Reynolds number flows, and supported this by analytical arguments and high resolution numerical simulations. We measured the efficiency of small-scale dynamo, which is the fraction of the supplied energy that goes to magnetic energy. Our study addressed a long-standing puzzle: why almost all media in astrophysical environments are magnetized, even in situations where turbulence exists for only a few dynamical times or where the large-scale dynamo is absent. We were able to resolve a long-standing debate between a -5/3 and -3/2 spectral slope of MHD turbulence. By running the highest resolution MHD simulations ever performed, we found that the process of so-called scale dependent dynamic alignment, deemed universal by some researchers, actually saturates at high Reynolds numbers. Our claim on alignment and spectral slope was based on a rigorous numerical argument called resolution study, in contrast with previous claims based on subjective criteria. We also measured the Kolmogorov constant of MHD turbulence and anisotropy constant of MHD turbulence. This was the first and till now the only conclusion of this kind. Spectral and anisotropy properties that we obtained have applications in all areas of astrophysics, plasma physics and solar and heliospheric physics. In our view, our most important achievement to-date is a model for so-called imbalanced MHD turbulence. While the Goldreich-Sridhar model has become a standard description of MHD turbulence, it only considered purely balanced (zero cross-helicity) case, which is rarely seen in nature. Imbalanced turbulence appears whenever there is a strong source of perturbations such as the Sun in the solar wind or the central engine in AGN. Also, the stochastic nature of turbulence requires knowledge of the general imbalanced case to fully understand globally balanced turbulence. Our model has been successful in describing the anisotropy difference observed in the imbalanced case. Driven by the interest in ISM turbulence, which is both strongly magnetized and supersonic, we and our collaborators discovered anisotropy in density perturbations. It turns out that despite density perturbations being initially created by random shocks, the structure of these perturbations, which are revealed by second-order structure function of log-density, is primarily created by Alfvenic shearing and has a scale-dependent anisotropy similar to Goldreich-Sridhar anisotropy. As a first step to the cosmic ray acceleration problem, we proposed a model of diffusive shock acceleration (DSA) where the magnetic field in the precursor is amplified due to turbulence excited by the baroclinic term. It turns out that this mechanism is rather efficient in generating large-scale magnetic fields. We also studied cosmic ray scattering in MHD turbulence by both numerical and analytical means. We showed that for low energy cosmic rays existing in turbulent MHD environment particle instabilities play a key role, dominating scattering, as long as compressive MHD modes are present. More recently, we used numerical simulations with particle tracing to directly evaluate CR scattering frequencies and diffusion tensor in MHD turbulence. An important recent development is the discovery of asymmetric diffusion of magnetic field lines. Stochasticity of magnetic field lines is important for particle transport properties. Magnetic field lines separate faster than diffusively in turbulent plasma, which is called superdiffusion. We discovered that this superdiffusion is pronouncedly asymmetric, so that the separation of field lines along the magnetic field direction is different from the separation in the opposite direction. While the symmetry of the flow is broken by the so-called

imbalance or cross-helicity, the difference between forward and backward diffusion is not directly due to imbalance, but a non-trivial consequence of both imbalance and non-reversibility of turbulence. The asymmetric diffusion perpendicular to the mean magnetic field entails a variety of new physical phenomena, such as the production of parallel particle streaming in the presence of perpendicular particle gradients. Such streaming and associated instabilities could be significant for particle transport in laboratory, space, and astrophysical plasmas. We were also interested in reconnection and associated release of energy. Magnetic reconnection is a topological rearrangement of the magnetic field lines, leading to the release of magnetic energy, which is associated with solar X-ray flares. Magnetic field lines are supposed to be frozen into the well-conducting plasma; so quiet laminar reconnection is extremely slow and cannot explain observed phenomena. This prompted research into collisionless reconnection. The stochasticity of magnetic field lines due to ambient turbulence leads to fast reconnection, also the tearing instability of the thin current sheet was proposed as a driver of resistivity-independent reconnection, which was shown to be consistent with two-dimensional simulations. By doing three-dimensional high-resolution simulations of nonlinear evolution of the thin current sheet we found that it spontaneously evolves into a turbulent current layer and shows a constant reconnection rate of 0.015 of Alfven speed and the dissipation rate per unit area which is independent of resistivity. This demonstrates that nearly ideally conductive fluids can be fairly resistive in presence of magnetic discontinuities. The significant fraction, 40%, of magnetic energy is dissipated inside of the current layer, which, at the early stages of reconnection process, can result in huge dissipation per unit volume and explain electron acceleration and X-ray flares.

Impact on National Missions

One of the missions of NNSA is to achieve inertial confinement fusion (ICF). This requires not only technical work, but also theoretical understanding of fundamentals of plasma physics. Recently, several authors have brought up the spontaneous generation of magnetic fields in ICF and its importance for plasma and fluid instabilities in the target. There have been several proposals to impose external magnetic fields to the target to study its influence on the instabilities and confinement. Our work on universal nonlinear small-scale dynamo places a lower limit on magnetic energy growth in well-conducting plasmas, and is, therefore, important for ICF.

Another challenge on a national level is predicting space weather. My work on MHD turbulence, applied to the solar wind is helping to better understand heliosphere and ultimately better predict space weather.

Publications

Beresnyak, A.. Spectral Slope and Kolmogorov Constant of MHD Turbulence. 2011. Physical Review Letter. 106: 5001.

Beresnyak, A.. Universal Nonlinear Small-Scale Dynamo. 2012. Physical Review Letters. 108 (3): 035002 (4 pp.).

Beresnyak, A.. Asymmetric Diffusion of Magnetic Field Lines. 2013. Astrophysical Journal Letter. 767: 39.

Beresnyak, A.. On the Rate of Spontaneous Magnetic Reconnection. Nature.

Beresnyak, A.. Basic Properties of MHD Turbulence in the Inertial Range . 2012. MNRAS. 422 (4): 3495.

Beresnyak, A., H. Xu, H. Li, and R. Schlickeiser. MHD Turbulence and cosmic ray reacceleration in Galaxy Cluster. To appear in Astrophysical Journal.

Beresnyak, A., H. Yan, and A. Lazarian. Numerical Study of Cosmic Ray Diffusion in Magnetohydrodynamic Turbulence. 2011. Astrophysical Journal. 728: 60.

Beresnyak, A., and A. Lazarian. Scaling laws and diffuse locality of balanced and imbalanced magnetohydrodynamic turbulence. 2010. Astrophysical Journal Letters. 722 (1): L110.

Non-Condon and State Interaction Effects in Carbon Nanotubes

Stephen K. Doorn
20100629PRD3

Abstract

This project focused on probing electron-phonon coupling behaviors in carbon nanotubes by employing resonance Raman spectroscopy of pure chirality samples. The results have overturned a number of long held assumptions in nanotube science and have generated several important first-time observations. The results appear or will appear in a number of high-profile publications. Briefly, we have demonstrated for the first time quantum interference effects in the nanotube Raman response. We have also shown the breakdown of the Condon approximation in metallic and semiconducting nanotubes. We have for the first time also probed in detail the double resonance Raman process of the 2D mode and shown novel behaviors of the LO and TO phonon modes in both metallic and semiconducting nanotubes.

Background and Research Objectives

Our goal is to understand the interaction of carbon nanotubes and light. Recent results [1] from the carbon nanotube effort at LANL suggest that molecular vibrations and electronic states are connected. More technically, the transition moment dipole, which determines strength of electronic excitations, depends on the vibrational coordinate, indicating a breakdown in the fundamental Condon approximation for understanding spectroscopic quantum behavior. The approximation states that electronic excitations occur on a fast timescale relative to vibrational motion. This project aims to probe this violation of the Condon approximation using Raman spectroscopy. The goal is to probe the structural and energy dependence of this behavior. To do this requires access to high purity single-structure samples, which are only available at LANL through a collaboration with colleagues at NIST [2]. Measurements on such samples are also allowing us to probe quantum interference phenomena and fundamental electron-phonon coupling behaviors in carbon nanotubes, all of which ultimately relate back to optical behaviors of interest for applications.

Scientific Approach and Accomplishments

1) Studies of non-Condon behavior: Earlier work at LANL demonstrated that the non-Condon behaviors manifest themselves as a strong asymmetry in plots (excitation profiles) of how Raman intensity changes with excitation energy for a specific vibrational mode. One of the project goals was to determine how this asymmetry depends on vibrational mode and on specific optical transition that is probed.

Asymmetry has already been demonstrated for high frequency (so-called G-modes near 1600 cm-1in frequency) modes [1]. Its presence for the important low-frequency (near 200-300 cm-1) radial breathing mode (RBM) had not yet been established. To resolve the asymmetry for the RBM required optical excitation into the lowest-energy nanotube transitions (E11). The result showed the RBM displays no non-Condon effect (Figure 1a). Impact of excitation into different Eii was probed using the higher frequency G-modes. Excitation into the lowest energy E11 transitions were found to give smaller asymmetries than displayed for excitation into the next higher energy E22 transition (see Figures 2 and 3). Higher energy excitations (E33 and E44) were also probed, with similar results found as for E22. The results of these Eii and vibrational mode dependence studies are currently being written up for submission as an article to Physical Review B.

Results on the semiconducting structures described above suggested that specific symmetry tubes (called near-armchair structures) will have more pronounced non-Condon effects. To test this, excitation profiles were also obtained on (6,6) and (7,7) species of nanotubes—true armchair structures. The result showed an increased asymmetry compared to other structures studied to date. The armchair results are currently being written up as a paper to be submitted to Physical Review Letters. The results are translating into follow on theory work aimed at understanding the symmetry impacts on the non-Condon behavior.

2) Studies of Quantum Interference Behavior: We have successfully demonstrated for the first time unambiguous signatures of quantum interference in the Raman response of carbon nanotubes. The result also led to an understanding of the relative behavior of the signs of matrix elements defining how electrons and phonons interact in nanotubes, which underlie a number of other important optical behaviors. Non-Condon effects were demonstrated to also occur for high energy transitions and interference effects were demonstrated to be a sensitive probe of energy separation of electronic states that are near each other in energy. As one specific example, in the (10,5) structure the G-plus and G-minus phonon intensities were found to reverse (Figure 2) from what is normally. This behavior is a direct consequence of strong destructive interference occurring for the G-plus mode while the G-minus experiences strong constructive interference. This behavior only occurs as a result of the E33 and E44 interfering transitions having zero energy separation. The results were published in Physical Review Letters, 108, 117404, (2012).

3) Analysis of the 2D Mode in Pure Chirality Samples: Probing of the 2D (near 2600 cm-1) vibrational mode behavior is only possible in pure chirality samples and is important for probing phonon structure in tubes and how it couples to various momentum regions of the electronic structure. Analysis of the 2D data requires modeling of electronic and phonon densities of states and how they interact under particular optical excitations. The software to do this analysis has been completed and evaluated with several test case systems. The program has also now been applied to particular nanotube structures for which we have good experimental data. The 2D phonon band is related to a double resonant Raman process. The two phonons involved in the process scatter an excited electron in a way that the intermediate states are real, which leads to an enhancement of the Raman signal. The exciting aspect about this process is that the involved phonons have non-zero momentum and that the momentum varies with the initial electronic state thus with the excitation energy. This mode is therefore suitable to experimentally map the phonon dispersion of the particular carbon based macro molecule. As an example of our modeling capability, iIn Figure 3 we simulated the 2D mode Raman spectrum as a function of excitation energy for a (9,1) nanotube. Initial experimental results show a good agreement with this simulation. The results are currently being written up for submission to Physical Review B.

4) Electronic doping of “armchair” metallic nanotubes: Electrostatic doping of films of armchair metallic tubes have been carried out with an eye towards evaluating the doping effect on phonon frequencies. The result will settle existing debate on how dopants interact with metallic nanotube electronic structure. Specifically, the Kohn anomaly and its effect on the LO phonon in carbon nanotubes is a well known and studied phenomenon in nanotube research. The Kohn anomaly induces a strong electron-phonon coupling of the LO phonon to electrons at the Fermi-level which leads to a broadening and down shift of the phonon frequency. At the same time the TO phonon is predicted to up-shift. It is possible to “switch off” the Kohn anomaly by changing the Fermi energy, which can be achieved by gating or doping. The top of Figure 4 shows the G-mode (LO and TO phonons) Raman spectra of armchair carbon nanotubes [(8,8), (7,7), and (6,6)], which we electro-chemically doped, from -1.2 to 1.2 V (bottom to top). The bottom spectra nicely show the down shifted and broadened features, which are related to the LO-phonon. The two narrow features at ~1580 and ~1590 cm^-1 are related to the TO phonon. As predicted by theory they have higher frequencies compared to semiconducting nanotubes, which are not effected by the Kohn anomaly. When we dope the sample by increasing the potential we are able to “switch off” the Kohn anomaly, as is apparent from the up-shift and narrowing of the LO-phonon related peaks. However, the peaks which are related to the TO phonons are not showing any significant shift (bottom plot in Figure 4). If the unusually high frequencies of the TO-phonon would be related to the Kohn anomaly the “switch off” should result in a down-shift of up to 60 cm-1. Therefore we conclude that the increase of the TO-phonon frequencies is related to a screening of the phonon by free carriers in metallic tubes rather than the Kohn-anomaly. These results overturn a long-held assumption in nanotube electron-phonon coupling behavior and are currently being written up for submission to Physical Review Letters.

5) Chirality dependence of the LO and TO phonons in Semiconducting Carbon Nanotubes: Raman spectroscopy of the G-band frequencies in pure chirality semiconducting nanotube samples has allowed us to accurately determine the structural dependence of both the G-plus and G-minus (LO and TO) phonon modes. The result opens up the TO mode as a new route to structural identification of tubes. Additionally, the results allow us to determine the origins of structural dependences based on rehybridization, confinement, and electron-electron interaction effects. The work is published in ACS Nano, 6, 904 (2012).

Impact on National Missions

Results of this project will have a direct bearing on developing optical and electronic properties of carbon nanotubes for photonic and energy harvesting applications and may also contribute to sensing and spectral tagging applications. As a result this work will have direct relevance to

the mission of the DOE-BES funded Center for Integrated Nanotechnologies and the potential applications will be of interest to agencies including NIH, DOE, DHS, and DOD with potential impact on threat reduction and renewable energy missions.

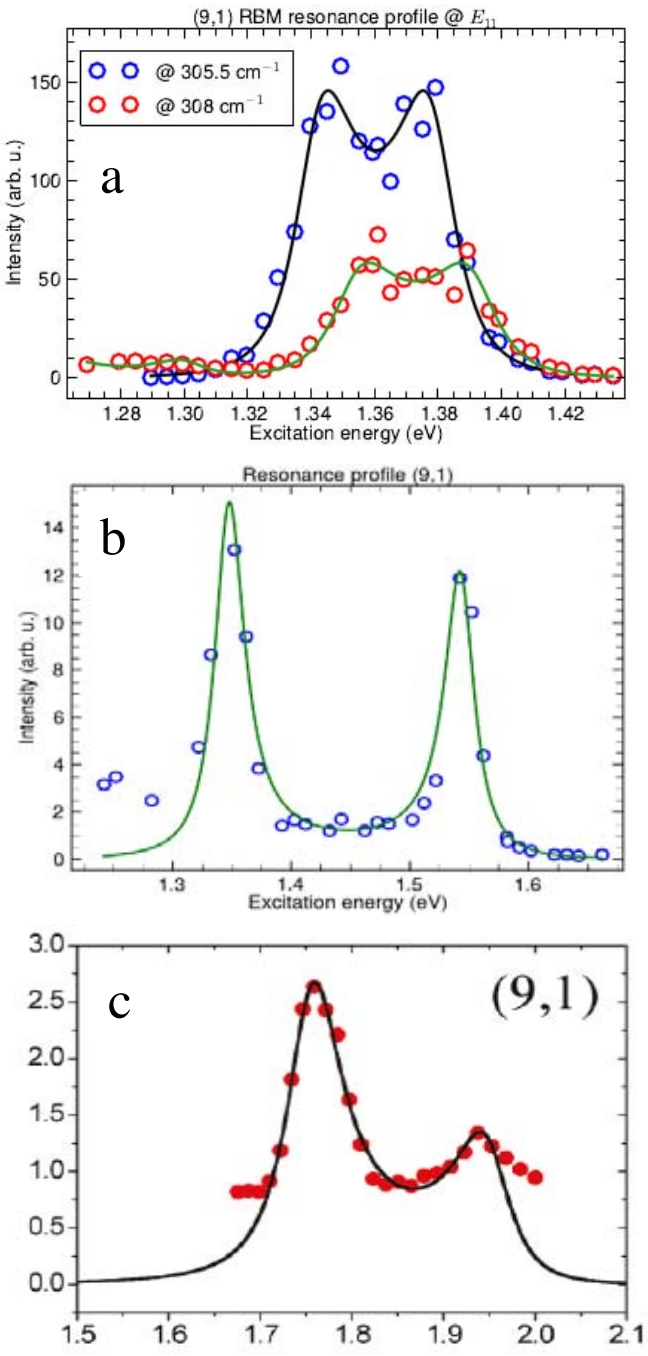

Figure 1. a) RBM resonance Raman excitation profile for (9,1) tube in E11 excitation. b) G-band resonance Raman excitation profile for (9,1) tube in E11 excitation. c) G-band resonance Raman excitation profile for (9,1) tube in E22 excitation.

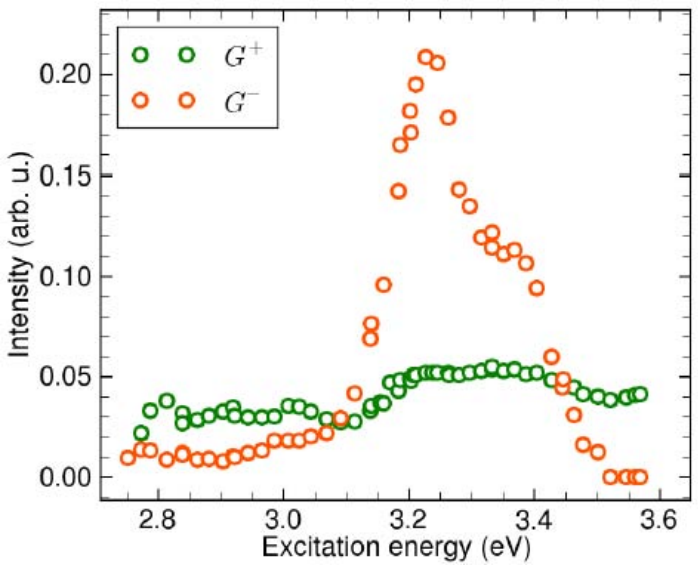

Figure 2. Resonance Raman G-plus (green circles) and G-minus (orange circles) band resonance Raman excitation profiles for the (10,5) tube in E33/E44 excitation.

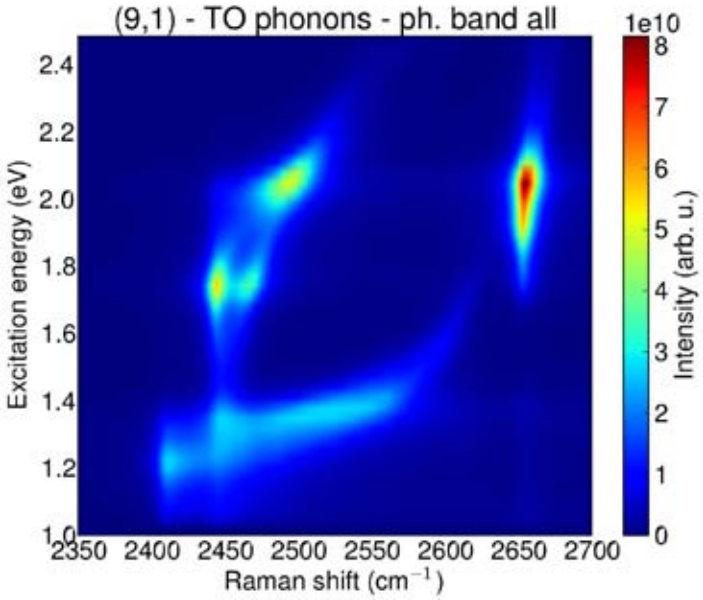

Figure 3. Plot of calculated 2D double resonance Raman intensity as a function of excitation energy and phonon frequency as modeled for the (9,1) tube.

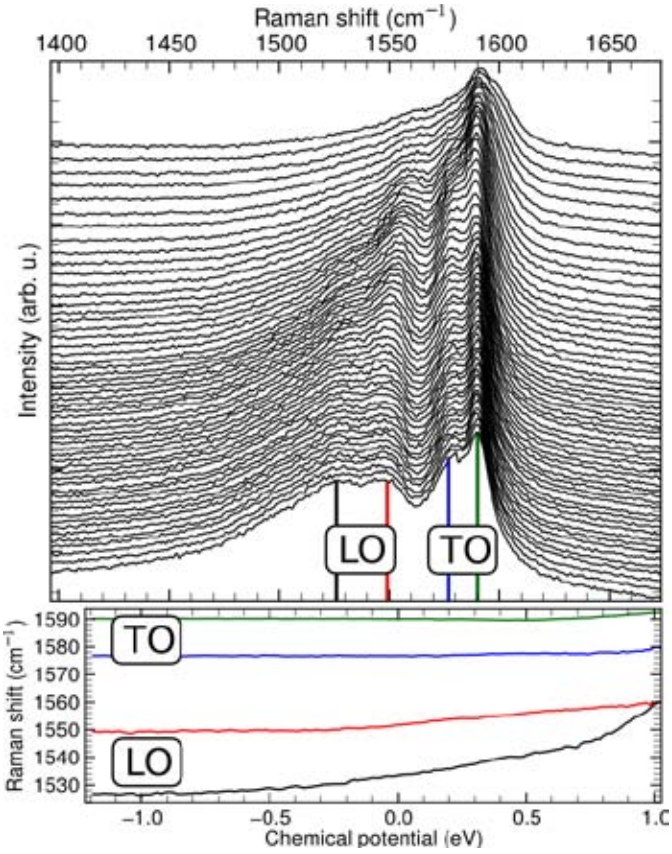

Figure 4. Top Panel: Plot of LO and TO Raman spectrum for an armchair-enriched sample of carbon nanotubes as doping potential is varied from +1.2 V (top spectrum) to -1.2 V (bottom spectrum. Bottom panel: Plot of LO and TO frequencies as doping potential is changed.

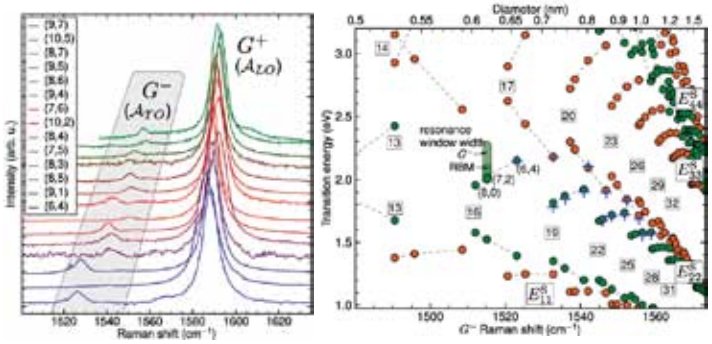

Figure 5. Left Panel: Plot of LO and TO Raman spectra for a range of nanotube chiralities as labeled. Right Panel: Plot of TO frequency as a function of nanotube transition energy and tube diameter for E11 through E44 excitations and demonstrating the ability to now use the TO band as a means for identifying nanotube structure.

References

1. Duque, J. G., H. Chen, A. K. Swan, A. P. Shreve, S. Kilina, S. Tretiak, X. Tu, M. Zheng, and S. K. Doorn. Violation of the Condon approximation in semiconducting carbon nanotubes. 2011. ACS Nano. 5 (6): 5233.
2. Tu, X., S. Manohar, A. Jagota, and M. Zheng. DNA sequence motifs for structure-specific recognition and separation of carbon nanotubes. 2009. Nature. 460: 250.

Publications

Duque, J. G., H. Telg, H. Chen, A. K. Swan, A. P. Shreve, X. Tu, M. Zheng, and S. K. Doorn. Quantum interference between the third and fourth excitonic states in semiconducting carbon nanotubes. 2012. Physical Review Letters. 108: 117404.

Telg, H., J. G. Duque, M. Steiger, X. Tu, F. Hennrich, M. M. Kappes, M. Zheng, J. Maultzsch, C. Thomsen, and S. K. Doorn. Chiral index deendence of the G+ and G- Raman modes in semiconducting carbon nanotubes. 2012. ACS Nano. 6 (1): 904.

A New Regime of Carrier Multiplication Using Intraband Re-excitation of Nanocrystals

Victor I. Klimov
20100632PRD4

Abstract

This project's goal has been to answer the question: What are the dominant decay mechanisms that compete with carrier multiplication in semiconductor nanocrystals? Carrier multiplication (CM) is a process whereby absorption of a single photon results in multiple electron-hole (e-h) pairs (excitons). This process could benefit a number of solar-energy conversion technologies, most notably photocatalysis and photovoltaics (PVs). The work in this project was primarily motivated by an outstanding challenge in this field, which has been the lack of capability to quickly discern between candidate materials for enhanced CM in nanocrystals (NCs). By studying materials of a variety of compounds and shapes we have been able to rationalize relative changes in CM yields of these materials and ascribe these changes to known physical processes. In fact, as our understanding has grown, we have developed an ever more sophisticated phenomenological model which accurately describes the observed trends. This has resulted in the first ever prediction and realization of increased CM efficiency in a material, suggesting our approach will be useful for a more rational search of future materials with higher CM.

Background and Research Objectives

The realization of low-threshold carrier multiplication (CM) in semiconductor nanocrystals (NCs) is a promising step toward realization of next generation solar cells – low cost photovoltaics (PVs) with efficiencies beyond the Shockley-Queisser limit. CM or multiexciton generation (MEG) is a process whereby multiple electron-hole (e-h) pairs (excitons) are generated via absorption of a single photon. In bulk semiconductors, CM occurs via impact ionization where a valence band electron is promoted to the conduction band via a collision with a high-energy charge carrier. In this traditional picture, the efficiency of CM is set by the competition between impact ionization and phonon emission. Understanding what sets the limits of CM efficiency is an important challenge due to its direct impact on solar-energy conversion technologies. For example, a single-junction PV with an ideal CM yield can produce a power conversion efficiency exceeding 40%, which is a considerable improvement over the traditional Shockley-Queisser limit of ~31%; the ideal CM yield is described by a staircase function in which each increment of the incident photon energy by the band-gap results in a new e-h pair, corresponding to an increase of quantum efficiency (QE) by 100%.

In bulk semiconductors, CM has been observed since the 1950's and the underlying mechanism is typically attributed to impact ionization. Two important parameters of this process are the activation threshold and the e-h pair creation energy, which is the energy lost by the ionizing particle in a single impact ionization event. In the ideal case, energy conservation dictates that the minimal values of the threshold and e-h pair creation energy are Eg and 2Eg, respectively. However, in bulk semiconductors, because of the additional restrictions imposed by momentum conservation and fast intraband energy losses due to phonon emission, both of these quantities are considerably higher than the ideal limit. In wide-gap semiconductors, typical values are ~4Eg for the threshold and ~3Eg for the e-h pair creation energy, becoming even greater for narrow-gap materials. As a result, the benefits of CM in PVs based on traditional bulk solids are negligible; specifically, the CM-induced enhancement in the power conversion efficiency expected for an optimized SiGe alloy is less than 1%.

Quantum confined semiconductor particles or quantum dots (QDs), on the other hand, have been expected to increase CM yields due to their discrete structure of electronic states. Firstly, a wide separation between NC discrete states has been expected to suppress phonon emission due to a phonon bottleneck and thus favor CM, as was first pointed out by Nozik in 2002. Secondly, three-dimensional (3D) spatial confinement leads to relaxation of translational momentum conservation, which should reduce the threshold for CM as well as the

e-h pair creation energy. These considerations motivated a renewed interest in CM with a focus on quantum-confined nanomaterials.

The first experimental observation of enhanced CM in quantum dots as compared to bulk material was reported for PbSe NCs by the Klimov group in 2004, where CM was detected using the fast Auger decay signatures of multiexcitons in transient absorption (TA). Following this initial report, CM in NCs has become a subject of intense experimental and theoretical investigations. By now, measurements show excellent agreement between data sets obtained by different groups and/or different spectroscopic techniques. Furthermore, the results of spectroscopic studies of CM have recently been validated by direct photocurrent measurements in photovoltaic devices, demonstrating that CM can be useful in real devices.

The outstanding challenge, however, has been the lack of an established theory which would allow for direction on how to further increase CM efficiencies. This research has successfully addressed this lack of direction in the form of well thought out experiments which delineate between the potential physical properties that set CM yields.

Scientific Approach and Accomplishments

To address the decay mechanisms available to a photogenerated charge and how these mechanisms set the CM yield, we have studied the influence that size, shape and composition have on the CM process in semiconductor nanocrystals. Using measured biexciton Auger lifetimes and intraband relaxation rates, we have rationalized relative changes in CM yields as a function of composition. Indeed, by studying PbS, PbSe, and PbTe NCs for a variety of sizes we determine that the significant difference in the CM yields in these compounds comes from the dissimilarities on their non-CM relaxation channels, i.e., the processes that compete with CM. We further explored the role of nanostructure shape in the CM process. We observe in PbSe that via a moderate NC elongation (aspect ratio of ~7) we can obtain a 50-to-80% increase in the multiexciton yield compared to spherical nanoparticles. Together, these studies demonstrate that CM can be understood within the framework of competing mechanisms and provide a prescription for how to increase CM yields.

The important result of this project has been the formulation and then experimental proof that the e-h pair creation energy can be represented in terms of two timescales: the timescale which characterizes CM; and, the competing cooling rate, which we assume to be dominated by phonon emission. As we will show below, this resulted in the first ever predictive prescription on how to choose a material with increased CM yields. The original insight that allowed us to come to this formulation came from considering the decay processes available to a photogenerated exciton as an effective time window in which CM can occur. Then, expressing the CM yield for excitation energies just above the threshold energy for CM to occur, we were able to express the CM yield directly as the product of the two timescales above [1]. The demonstration that this is more generally true requires significantly more calculation but nevertheless arrives at exactly the same formulation, as reported in [2]. What is most significant, however, is the experimental proof which validates this approach.

Naively, based on the approach outlined above, one needs only to measure the CM timescale and cooling rate (kcool) of the competing process to predict the CM performance. Unfortunately, while kcool can be at least inferred from analyzing intraband relaxation below the threshold for CM, direct measurements of the CM timescale are not so straightforward and have not yet been carried out. To overcome this problem, we infer the CM timescale from measurements of the inverse process – biexciton Auger recombination. During this process, one exciton recombines by transferring the recombination energy to an electron or a hole of the second exciton, producing a hot exciton. This is precisely the inverse of CM, where a hot exciton relaxes by creating a new e-h pair. Thus, CM and Auger decay are described by the same interaction Hamiltonian and are therefore interconnected.

Another important simplifying feature of CM rates is the observation of universal scaling of Auger lifetimes with the NC volume, termed volume-scaling. Volume-scaling was originally discovered in studies of CdSe NCs, and subsequently the universality of this feature was established for many other compositions, including the lead chalcogenides studied here. While the exact physical mechanism underlying these universal trends is not fully understood, it likely relates to the relaxation of momentum conservation, which diminishes the role of the exact band structure in Auger recombination. The consequence is that universal volume-scaling of Auger lifetimes suggests that CM rates in NCs are also likely to be dominated by NC size and not by composition. This would further suggest that the observed differences in e-h pair creation energy and CM yield for similarly sized NCs of different compositions is mostly due to the differences in intraband cooling rates. To test the validity of these conclusions we have conducted side-by-side studies of CM yields, intraband cooling, and Auger rates, in NCs of our three different lead chalcogenides: PbSe, PbS, and PbTe.

In Figure 1 we show all of the data required to make a qualitative prediction of the relative CM yields for these three materials based on Auger timescales and phonon

cooling rates. In Figure 1a, we show biexciton Auger lifetimes as a function of confinement energy (Ec): Ec = Eg - Eg0, where Eg0 is the bulk energy gap. Consistent with volume scaling, NCs of all three compositions show a similar dependence of Auger lifetime on Ec and similar density of states further imply similar CM time constants.

In Figure 1b, we show a representative data set which we use to extract the intraband cooling rate near the band edge in PbSe NCs. Specifically, we measure the time required to populate the ground state after excitation. We calculate the energy loss rate from the ratio of the 1P-1S energy spacing to the time required to populate the 1S state. Conducting these measurements for all three materials we find the energy loss rates are related by (PbTe):(PbSe):(PbS) ≈ 1:2:4. Then, we assume that a similar ratio between cooling rates also holds at energies relevant to CM. Given this comparison of relaxation rates and the similarity in CM time constants expected for these three compounds, we would expect CM yields to increase going from PbS to PbSe and then to PbTe.

The test of our prediction is shown in Figure 2 for which we see that we clearly confirm the predicted trend. CM yields in PbSe NCs are systematically higher than in PbS NCs and then further increased in PbTe NCs. For example, for at excitation of 4.3Eg, the CM yield is 15%, 35%, and 65% in PbS, PbSe, and PbTe NCs, respectively. Interestingly, the ratio between these yields (1:2.3:4.3) is close to the relative ratios of the cooling rates. This effort represents the first ever confirmation of a predicted increase in CM yields as a function of nanocrystal composition and should provide for a more rational search of NC materials with even higher CM efficiencies.

One potential critique of the above approach is that the CM timescales were essentially the same for all three compounds. One could argue that this approach only establishes the importance of competing decay mechanisms such as phonon emission and in fact does not establish the importance of the CM time constant in setting the CM efficiency. To address this issue, we designed and completed a series of experiments on the same compound but of different shapes [3, 4]. Because all shapes are composed of the same material we ensure that the competing mechanism (phonon cooling) is the same for all samples; this allows us to attribute any changes in the Auger rate and CM yield to changes in the carrier-carrier interaction responsible for these two processes.

We examine CM yields and Auger recombination in PbSe for both spherical NCs (quantum dots) and NRs. The measurements indicate that the Auger time constant tends to be longer in NRs than in spherical nanoparticles and increases approximately linearly with the NR volume (Figure 3a). On the other hand, CM measurements shown in Figure 3b (excitation at 3.1 eV), show that NRs are either similar or more efficient than quantum dots. We see, however, that for a given excitation energy, the NR data show a significant spread in CM values indicating that some other parameter(s) play an important role in determining the overall CM yield. A significant discovery that we made [3] is that CM performance depends strongly on the degree of elongation, i.e. the aspect ratio (L/d), as shown in Figure 3c. These data show a progressive increase in the multiexciton yield NRs up to an aspect ratio of ~5-7 and then a decrease for larger aspect ratios. Repeating this measurement for various diameters indicates that this aspect-ratio dependence is band-gap independent. The universality of this "optimal aspect ratio" may greatly help ongoing theory work to understand the underlying physics of CM in nanocrystals. Importantly for this work, however, is the clear demonstration that CM rates play just as vital a role in the CM process as competing mechanisms such as phonon emission.

The content of this report has been borrowed heavily from the project publications on these subjects. The references include [1-5].

Impact on National Missions

This work has directly addressed many FY13 grand challenges related to energy generation; these include: "Materials Discovery Science to Strategic Applications" and "Energy and Earth Systems." This work has provided vital direction toward the practical use of carrier multiplication to enhance photon-to-charge conversion in real devices. For an example, the results in [1] directly influenced the decision to use PbSe as the nanocrystal material composition in a recent paper published in Science Magazine which for the first time observed external quantum efficiency greater than unity within the solar spectrum. Finally, the results here provided first ever confirmed prediction of enhanced carrier multiplication in a material (PbTe) and have provided a prescription for how to increase CM efficiency in future materials.

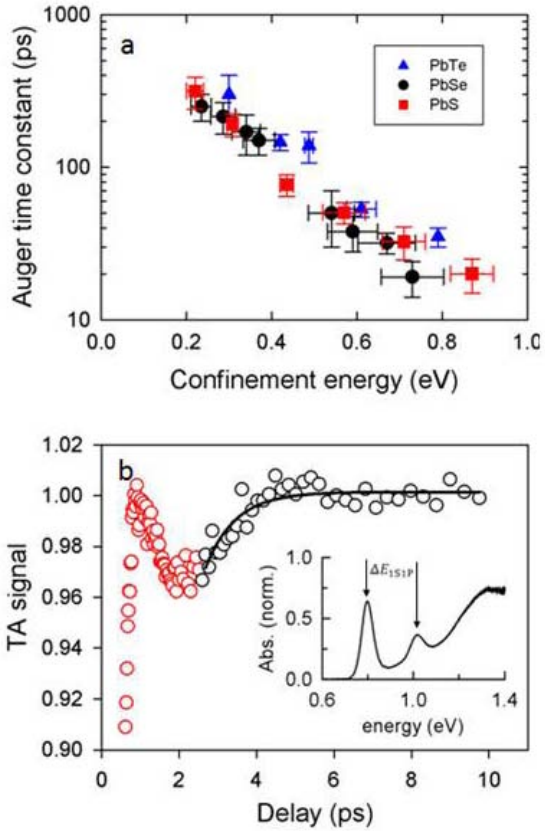

Figure 1. Quantitative studies of Auger lifetimes and 1P-1S energy loss rate used as "surrogates" for CM time constants and kcool, respectively. (a) Biexciton Auger lifetimes for PbS, PbSe, and PbTe NCs plotted as a function of confinement energy demonstrate a universal trend seen previously for NCs of a variety of compositions. (b) The buildup of 1S bleaching for PbSe NCs measured by TA is used to estimate the intraband cooling rate. The red data points represent the instantaneous Coulomb shift due to hot carriers; it is followed by slower growth due to population transfer from the 1P to the 1S state. The 1S-1P energy separation is derived from the absorption spectrum (inset).

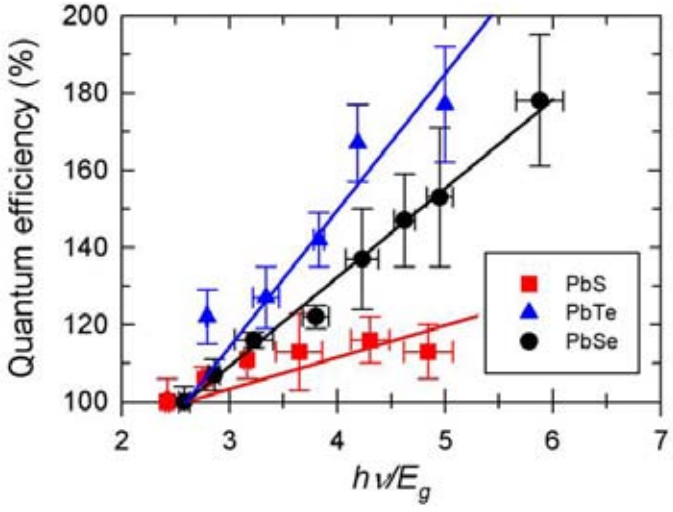

Figure 2. Quantum efficiencies (QEs) for PbTe (blue triangles), PbSe (black circles) and PbS (red squares) as a function of normalized photon energy; measurements were made using a fixed excitation energy (3.1 eV) and differently sized NCs. Despite their similar Auger time constants (see Figure 1a), these materials show strikingly different CM yields, indicative of different e-h pair creation energies. These trends are consistent with the trends in competing cooling rates (kcoolPbS>kcoolPbSe>kcoolPbTe)

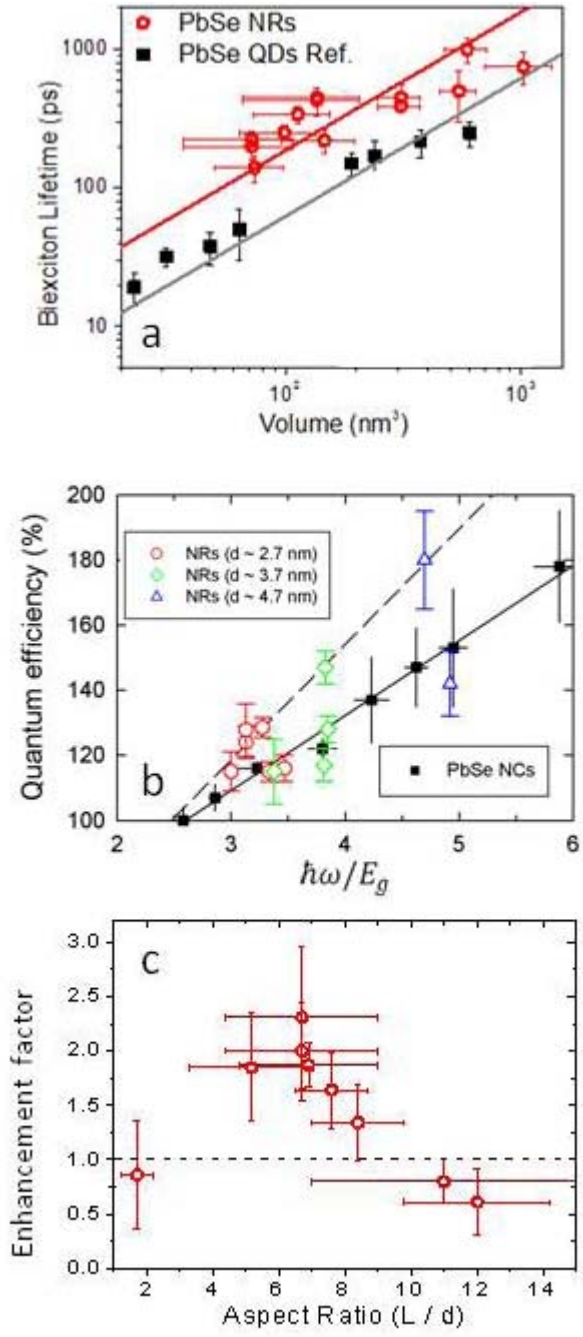

Figure 3. Auger time constants and carrier multiplication (CM) quantum efficiency for PbSe nanorods (NRs). (a) NRs (red circles) appear to demonstrate similar, although systematically higher, size dependence of Auger time constants as spherical particles (black squares). (b) Quantum efficiency of CM measured for various diameters and aspect ratios plotted as function of normalized photon energy; the measurements were conducted at 3.1 eV excitation (red and green symbols) and 4.65 eV excitation (blue

triangles). The NR results are compared to our measurements on PbSe quantum dots (QDs) (black solid squares), sometimes showing enhancement but not always. (c) Upon plotting the enhancement factor of NRs to QDs we see a clear aspect ratio dependence that does not depend on the initial band gap. This feature hints at universal shape dependence of CM in NRs.

References

1. Stewart, J., L. Padilha, M. Mumtaz. Qazilbash, J. Pietryga, A. Midgett, J. Luther, M. Beard, A. Nozik, and V. Klimov. Comparison of Carrier Multiplication Yields in PbS and PbSe Nanocrystals: The Role of Competing Energy-Loss Processes. 2012. NANO LETTERS. 12 (2): 622.

2. Stewart, J. T., L. A. Padilha, W. K. Bae, W. K. Koh, L. Li, A. Pandey, J. M. Pietryga, and V. I. Klimov. Carrier multiplication in PbTe, PbSe, and PbS quantum dots within the framework of two competing energy relaxation mechanisms. Nature Physics.

3. Padilha, L. A., J. T. Stewart, R. L. Sandberg, W. K. Bae, W. K. Koh, J. M. Pietryga, and V. I. Klimov. Aspect ratio dependence of Auger recombination and carrier multiplication in PbSe nanorods. Nano Letters.

4. Padilha, L. A., J. T. Stewart, R. L. Sandberg, W. K. Bae, W. K. Koh, J. M. Pietryga, and V. I. Klimov. Carrier multiplication in semiconductor nanocrystals: Influence of size, shape and composition. To appear in Accounts of Chemical Research.

5. Koh, W. K., A. Y. Koposov, J. T. Stewart, I. Robel, J. M. Pietryga, and V. I. Klimov. Heavily doped n-type PbSe and PbS nanocrystals using ground-state charge transfer from cobaltocene. Nature Materials.

Publications

Koh, W. K., A. Y. Koposov, J. T. Stewart, I. Robel, J. M. Pietryga, and V. I. Klimov. Heavily doped n-type PbSe and PbS nanocrystals using ground-state charge transfer from cobaltocene. Nature Materials.

Padilha, L. A., J. T. Stewart, R. L. Sandberg, W. K. Bae, W. K. Koh, J. M. Pietryga, and V. I. Klimov. Aspect ratio dependence of Auger recombination and carrier multiplication in PbSe nanorods. Nano Letters.

Padilha, L. A., J. T. Stewart, R. L. Sandberg, W. K. Bae, W. K. Koh, J. M. Pietryga, and V. I. Klimov. Carrier multiplication in semiconductor nanocrystals: Influence of size, shape and composition. To appear in Accounts of Chemical Research.

Stewart, J. T., L. A. Padilha, W. K. Bae, W. K. Koh, L. Li, A. Pandey, J. M. Pietryga, and V. I. Klimov. Carrier multiplication in PbTe, PbSe, and PbS quantum dots within the framework of two competing energy relaxation mechanisms. Nature Physics.

Stewart, J., L. Padilha, M. Mumtaz. Qazilbash, J. Pietryga, A. Midgett, J. Luther, M. Beard, A. Nozik, and V. Klimov. Comparison of Carrier Multiplication Yields in PbS and PbSe Nanocrystals: The Role of Competing Energy-Loss Processes. 2012. NANO LETTERS. 12 (2): 622.

Heavy quarks in Cold Nuclear Matter and in the Quark Gluon Plasma

Ming X. Liu
20100635PRD4

Abstract

In this project, we study the properties of a new state of matter that may have been absent from the Universe since a first few milliseconds after the Big Bang. To probe this hot dense state we use heavy quarks, with whimsical names like “charm” and “beauty”. These quarks are distinct from the up and down quarks of normal matter. This hot dense matter, called a Quark Gluon Plasma (QGP), is created in high-energy heavy-ion collisions at the Relativistic Heavy Ion Collider (RHIC) at Brookhaven National Laboratory. A new silicon vertex detector (FVTX), developed under LANL leadership, identifies heavy quarks. These quarks travel only a short distance before decaying into muons. Although the distance is short, it can be measured by this new FVTX detector, thereby detecting the ephemeral life of a heavy quark. Bound states of two heavy quarks are also detectable. The quarks experience the effect of the QGP as they travel through it on the way to our detectors.

The new FVTX detector was built and added to the existing PHENIX detector at RHIC at the end of 2011. The new detector has been commissioned early this year 2012 when it saw its first colliding beams. Collisions with various types of high-energy beams including gold and cooper nuclei, and polarized protons were collected in 2012 and delivered the data required to obtain a complete picture of the heavy quark physics; and to extract properties of the QGP. Analysis for physics results is in progress now and preliminary results show that we can clearly identify muon tracks with the new FVTX detectors. Our final data analysis will deliver scientific results that are not possible within the baseline project.

Background and Research Objectives

Collisions of heavy ions at center-of-mass energies of 200 GeV performed at the Relativistic Heavy Ion Collider (RHIC) at Brookhaven National Lab have shown that a new form of matter has been formed where quarks and gluons (partons) are not confined in individual nucleons as they normally are in nature. The effects on particle production of this de-confined medium can reveal how this novel medium behaves. The two large experiments at RHIC have both measured electron decay of D mesons containing a charm quark with mass around 1.8 GeV/c2 and of B mesons containing a beauty quark with mass around 5.3 GeV/c2. The high transverse momentum electrons from these heavy-quark mesons are suppressed by the same amount as mesons containing light quarks when compared to their production on free nucleons. This surprising observation suggests that the effect of the medium on meson production is more complex than first thought. To gain a full understanding of the phenomena, more precise measurements of the heavy quark mesons for a variety of different collision systems and over a broad kinematic range are needed. Another interesting related effect is the dissociation of heavy quarkonia (pairs of charm or beauty quarks; J/ψ, ψ’ and ϒs) because of color screening in the deconfined medium. This dissociation is supposed to happen at a certain density or temperature of the medium for each quarkonium state. The observation of heavy quarkonia such J/ψ, ψ’ and ϒ dissociation in heavy ion collisions, along with lattice QCD estimates of their dissociation temperatures, can reduce the current uncertainty in the temperature achieved in the hot-dense medium.

Initial-state effects also influence the production of these heavy-quark objects, such as the modification of the initial parton distribution in nuclei compared to those in a free nucleon. These effects are not well understood and are largest in the forward direction.

The goal of this project was to identify the heavy quark (charm or bottom) and study the quark-mass and momentum dependency of the heavy-quark suppression as well as to search for angular asymmetries relative to the reaction plane of the collision. These measurements have been made for particles scattered in angles around 90 degrees relative to the beam (mid-rapidity). The FVTX

will allow the study of heavy quarks in smaller angles (forward rapidity) exploring regions where the initial state effects are more pronounced. This information will be important as an input to the models, which describe the hydrodinamical behavior of the QGP.

Scientific Approach and Accomplishments

The PHENIX forward detectors can track and identify muons with a set of trackers and absorbers (where only muons can penetrate). The heavy quarks we want to measure are included in the sample of muons detected by the forward detectors. Despite the large rejection of other particles that are not muons in the absorbers, there are too many pions produced in the collisions and many of then can penetrate them and be detected as a muon. Besides, pions also decay in muons and if that happen before they reach the absorber they can also contribute to the background in our muon sample from heavy-quarks.

We have built and installed a new Forward Silicon Vertex Detector (FVTX), which consists of four silicon mini-strip stations in front of each of the two PHENIX muon detectors. The two FVTX detectors can perform tracking of particles going in the direction of the forward detectors before reach any absorber material. These tracks indicate how far the particle was produced from the collision point. Pions that could cross the absorber material usually have their direction modified inside the absorbers, so a track from these pions seen before (in FVTX) and after (in MuTr) the absorber will not match. Muons from pion decays are mostly created far from the collision point allowing their rejection using FVTX. Muons from heavy quarkonia (J/ψ, ψ' and Υ1S+2S+3S), Drell-Yan and W decays are produced at the collision point. Open heavy-quark mesons D (B), containing a charm(bottom) valence quark, typically travel a distance of 123-312 (460-500) m before decay. Therefore, the displacement-vertex measurement of the particles crossing the FVTX will help in the identification of muons and they sources.

We successfully commissioned and took p+p, U+U and Cu+Au collisions data in 2012 using FVTX. Through this project, Cesar has continued to establish himself as a leading international expert in the field of heavy-ion physics and has positioned himself to play a lead role in the new physics that will be enabled by the new LANL-led Forward Silicon Vertex Detector (FVTX).

He was nominated to represent the PHENIX collaboration and gave plenary invited talks about heavy quark and quarkonia at the Quark Matter Conference in 2011, this year's Nuclear Dynamics Winter Workshop and two talks in the International Workshop on Heavy Quark Production in Heavy-Ion Collisions. As a leading expert on heavy-quarks (charm and beauty) within the PHENIX experiment and in the world, he represented all latest results from the Relativistic Heavy Ion Collider (RHIC) at the Brookhaven National Laboratory.

The LANL group has been leading the construction and installation of the FVTX upgrade detectors in the PHENIX experiment at RHIC. This new detector was successfully installed at the end of 2011 and participated in the data taking during 2012 run. Cesar has played a major role during this commissioning preparing the integration of the FVTX electronics with the complicated data acquisition system of PHENIX and debugging it during installation and during the U+U run.

With the arrival of 2012 physics data, Cesar worked on physics analysis of the new FVTX muon data, including developing of the tracking code to match FVTX track with Muon track in p+p and A+A collisions, analysis of high mass dimuon pairs from J/Psi decays and simulations that provide direct preparation for using the new FVTX detector. Improvements on the J/psi mass peak resolution were already achieved when using FVTX hit information to reconstruct dimuons in p+p collisions. With additional dimuon counts we hope to start to see a second peak from ψ' with a mass slightly larger than the J/ψ. He is well positioned to lead the first analysis using the new FVTX from this year's data as soon as the data reconstruction is finish by the end of this year.

Pre-FVTX analysis are also being completed by Cesar. A list of final and preliminary results are:

Final analysis of quarkonia (J/psi, Psi', Chi_c) in 200 GeV p+p collisions, which result in, a long paper [PRD85,092004(2012)], which is the reference for all quarkonia measurements, made by PHENIX. Preliminary result of the asymmetry of J/ψ angle detection relative to the collision reaction plane. This measurement can indicate if the J/ψ suppression observed in Au+Au collisions depends on the path length in Au+Au or if J/ψ yields also contain coalescence or regeneration of open charms in the QGP. The result are 5 times more precise than the original one obtained in 2007 due to enhanced statistics and careful handling of the backgrounds. However, even with the precision we have we can't still claim any asymmetry or distinguish for different theoretical scenarios. The addition of the data set taken in 2011 can further reduce the uncertainties on this measurement.

Work on determining the nuclear modification of Upsilons in Au+Au collisions. A clear Upsilon peak in the invariant mass distribution of dimuons was found for the first time in such collisions in the forward rapidity at RHIC.

5. Cesar is the leader of the Quarkonia Topical Group, chair of the Muon Software meetings, first contact person for all issues involving the forward detectors software and extended member of the PHENIX Speakers Bureau.

Impact on National Missions

This work addressed the fundamental study of de-confined quark-gluon matter created in very high-energy heavy-ion collisions, which mimic the first few milliseconds of the universe. These studies are the primary goal of the forefront Relativistic Heavy Ion Collider facility that is the leading U.S. Nuclear Physics facility. It also addressed a U.S. Nuclear Science Advisory Committee (NSAC) Goal that deals with the structure of nuclei at a very small momentum scale where gluons in those nuclei become saturated and alter their structure, compared with their normal structure in free protons.

Publications

Adare, A., S. Afanasiev, C. Aidala, Ajitanand, N.N., Y. Akiba, and others. {Production of omega mesons in p+p, d+Au, Cu+Cu, and Au+Au collisions at sqrt(s_NN)=200 GeV}. 2011.

Adare, A., S. Afanasiev, C. Aidala, Ajitanand, N.N., Y. Akiba, and others. {J/psi suppression at forward rapidity in Au+Au collisions at sqrt(s_NN)=200 GeV}. 2011.

Adare, A., S. Afanasiev, C. Aidala, Ajitanand, N.N., Y. Akiba, and others. {Cold Nuclear Matter Effects on J/psi Yields as a Function of Rapidity and Nuclear Geometry in Deuteron-Gold Collisions at sqrt(s_NN) = 200 GeV}. 2010. Phys.Rev.Lett..

Adare, A., and others. {Suppression of back-to-back hadron pairs at forward rapidity in d+Au Collisions at sqrt(s_NN)=200 GeV}. 2011.

Adare, A., and others. {Observation of direct-photon collective flow in sqrt(s_NN)=200 GeV Au+Au collisions}. 2011.

Adare, A., and others. {Measurements of Higher-Order Flow Harmonics in Au+Au Collisions at sqrt(s_NN) = 200 GeV}. 2011.

Adare, A., and others. {Ground and excited charmonium state production in $p+p$ collisions at $\sqrt{s}=200$ GeV}. 2011.

Adare, A., and others. {Heavy Quark Production in p+p and Energy Loss and Flow of Heavy Quarks in Au+Au Collisions at sqrt(s_NN)=200 GeV}. 2010.

Adare, A., and others. {Suppression of away-side jet fragments with respect to the reaction plane in Au+Au collisions at sqrt(s_NN) = 200 GeV}. 2011. Phys.Rev.. C84: 024904.

Adare, A., and others. {Event Structure and Double Helicity Asymmetry in Jet Production from Polarized $p+p$ Collisions at $\sqrt{s} = 200$~GeV}. 2011. Phys.Rev.. D84: 012006.

Adare, A., and others. {Identified charged hadron production in $p+p$ collisions at $\sqrt{s}=200$ and 62.4 GeV}. 2011. Phys.Rev.. C83: 064903.

Adare, A., and others. {Azimuthal correlations of electrons from heavy-flavor decay with hadrons in p+p and Au+Au collisions at sqrt(s_NN)=200 GeV}. 2011. Phys.Rev.. C83: 044912.

Adare, A., and others. {Measurement of neutral mesons in p+p collisions at $\sqrt(s)$= 200 GeV and scaling properties of hadron production}. 2011. Phys.Rev.. D83: 052004.

Adare, A., and others. {Nuclear modification factors of phi mesons in d+Au, Cu+Cu and Au+Au collisions at sqrt(S_NN)=200 GeV}. 2011. Phys.Rev.. C83: 024909.

Adare, A., and others. {Cross Section and Parity Violating Spin Asymmetries of W+/- Boson Production in Polarized p+p Collisions at sqrt{s}=500 GeV}. 2011. Phys.Rev.Lett.. 106: 062001.

Adare, A., and others. {Cross section and double helicity asymmetry for Eta mesons and their comparison to neutral pion production in p+p collisions at sqrt(s)=200 GeV}. 2011. Phys.Rev.. D83: 032001.

Adare, A., and others. {Measurement of Transverse Single-Spin Asymmetries for J/psi Production in Polarized p+p Collisions at sqrt(s) = 200 GeV}. 2010. Phys.Rev.. D82: 112008.

Adare, A., and others. {High pT direct photon and pi0 triggered azimuthal jet correlations and measurement of kT for isolated direct photons in p+p collisions at sqrt{s}=200 GeV}. 2010. Phys.Rev.. D82: 072001.

Adare, A., and others. {Azimuthal anisotropy of neutral pion production in Au+Au collisions at sqrt(s_NN) = 200 GeV: Path-length dependence of jet quenching and the role of initial geometry}. 2010. Phys.Rev.Lett.. 105: 142301.

Adare, A., and others. {Elliptic and hexadecapole flow of charged hadrons in Au+Au collisions at sqrt(s_NN) = 200 GeV}. 2010. Phys.Rev.Lett.. 105: 062301.

Adare, A., and others. {Transverse momentum dependence of meson suppression Eta suppression in Au+Au collisions at sqrt{sNN} = 200 GeV}. 2010. Phys.Rev.. C82: 011902.

Adare, A., and others. {Transverse momentum dependence of J/psi polarization at midrapidity in p+p collisions at sqrt(s) = 200-GeV}. 2010. Phys.Rev.. D82: 012001.

Adare, A., and others. {Trends in Yield and Azimuthal Shape Modification in Dihadron Correlations in Relativistic Heavy Ion Collisions}. 2010. Phys.Rev.Lett.. 104: 252301.

Adare, A., and others. {Detailed measurement of the e+ e- pair continuum in p+p and Au+Au collisions at sqrt{sNN} = 200 GeV and implications for direct photon production}. 2010. Phys.Rev.. C81: 034911.

Adare, A., and others. {Enhanced production of direct photons in Au+Au collisions at sqrt(sNN)=200 GeV and implications for the initial temperature}. 2010. Phys.Rev.Lett.. 104: 132301.

Adare, A., and others. {Double-Helicity Dependence of Jet Properties from Dihadrons in Longitudinally Polarized p+p Collisions at sqrt{s}=200 GeV}. 2010. Phys.Rev.. D81: 012002.

Afanasiev, S., and others. {Enhancement of the dielectron continuum in s(NN)**(1/2) = 200-geV Au+Au collisions}. 2007. Phys.Rev.Lett..

Silva, C. da, and others. {Recent Heavy Flavor and Quarkonia Measurements from the PHENIX Experiment}. 2011.

Silva, C. da, and others. {Decay Angular Distributions for the J/Psi Measured by PHENIX}. 2011.

The Formation and Evolution of Black Holes in the Universe

Christopher L. Fryer
20100636PRD4

Abstract

Many questions at the forefront of modern astrophysics and cosmology pertain to the formation and growth of the first black holes in the universe. Here we describe our work studying these questions over the past months, with particular attention to one of the main models for early black hole formation via the collapse of supermassive stars. We made considerable progress in understanding the formation and fate of these objects, and our research into this and related topics has resulted in 13 successful publications. Our work has shed light not only on the origin of the first black holes, but also on the first planets and powerful early supernovae, and overall on how the first galaxies in the universe came to be.

Background and Research Objectives

It is now well established that most massive galaxies, including our Milky Way, harbor supermassive black holes at their centers. There are a variety of correlations between the observed properties of galaxies and the masses of their central black holes, and this point to an interwoven evolution of galaxies and black holes going back to the formation of the first such objects in the early universe. One of the principal questions challenging astrophysicists and cosmologists today is how the first supermassive black holes formed and evolved. In particular, there have now been detected numerous black holes with masses exceeding a billion times that of our Sun, already in place less than one billion years after the Big Bang, when the universe was less than ten percent of its present age.

One of the most promising and fascinating explanations for these early behemoths is that they initially formed from the collapse of supermassive stars that formed from the primordial gas. In this scenario, the primordial gas is prevented from forming hydrogen molecules that allow it to cool and form typical primordial stars. Instead, the gas remains hot until it collapses under its own gravity and forms a star with a mass in excess of 10,000 times that of our sun. Such stars are generally thought to collapse to black holes. Since they start out very massive, it is possible for them to grow to become the supermassive black holes, which have been detected at very early cosmic times.

One of the main aims of our research was to gain a better understanding of how such black holes formed, and we were largely focused on how and where their supermassive star progenitors formed. The sites of their formation are the cores of the earliest nascent galaxies, and the formation and evolution of each depends in crucial ways on the other. Therefore, we studied a number of aspects of galaxy and black hole formation, using a variety of techniques, in hopes of understanding the whole picture.

We carried many projects from conception to publication, resulting in a total of 13 publications during the duration of the project. These included the first analytical modeling of the growth of radiating supermassive stars; some of the most realistic large-scale cosmological simulations to date, which allowed to pin down the formation sites of supermassive black holes in the early universe; and utilization of the available observational data on the nature of black hole growth, in order to show that supermassive stars, while exotic, are indeed the strongest candidates for the seeds of the largest supermassive black holes. These works have helped to propel forward the study of supermassive star and black hole formation, with numerous international groups now engaging in related research that builds upon, and is motivated by, our own.

In addition, we have pursued other questions with bearing on the formation of the first galaxies and which help to get at the question of how we can verify our theories for how and where the first black holes formed. Among the other projects that we have carried through publication are studies of the explosions of supermassive stars,

which were among the most energetic thermonuclear events in the history of the universe; studies and simulations of bright supernovae and gamma-ray bursts which could have originated in the first galaxies; and two investigations into how the first planets in the universe formed around the stars inhabiting the first galaxies.

Scientific Approach and Accomplishments

We adopted various technical approaches to the questions we addressed. For some of the more exploratory projects, many addressing questions that had not previously been considered in much detail, we used analytical techniques. In this way, we estimated the masses to which primordial stars can grow, in the face of the high-energy radiation that they emit, as shown in Figure 1. This work helped to support the idea that supermassive stars could actually be assembled in the early universe. The maximum mass to which stars can grow by accreting gas at a constant rate. As shown by the blue line, the radiation emitted by the star will stop accretion only after it has grown to a high mass, if it accretes gas at a sufficiently high rate, as expected for supermassive stars in the early universe.

We also made the first estimate of the amount of heavy elements required to form the first planets in the universe, as shown in Figure 2. We found that our theory, which was built from the main, overarching theory for planet formation, was consistent with the growing amount of data on exoplanetary systems. This work received a surprising amount of coverage in the popular press, being covered on msnbc.com, space.com and Astrobiology magazine.

The colored lines show the minimum heavy element abundance, here shown as the iron abundance ([Fe/H]) as a proxy, for planet formation. The black points show the heavy element abundances of known planets, none of which exhibit heavy element abundances below the minimum we estimated (from Johnson & Li 2012).

Other projects demanded much more complex approaches, and for some of these we carried out sophisticated, large-scale cosmological simulations in which we modeled in detail the formation of galaxies and the emergence supermassive stars. In one such simulation, we included the build-up of the early stellar radiation field, which is expected to lead to supermassive star formation (due to the photodissociation of hydrogen molecules), as shown in Figure 3. This simulation, which included star formation and heavy element enrichment, in addition to radiation from stars, was arguably the most realistic and complete simulation of the formation of the first galaxies ever done, Figure 3.

The build-up of the radiation field produced by the light emitted form stars in the first galaxies, from early to later times (left to right). The intensity of the molecule-dissociating radiation field increases steadily, and this eventually leads to the assembly of hot primordial gas from which supermassive stars form (from Johnson, Dalla Vecchia & Khochfar 2013).

Another example of a cosmological simulation is shown in Figure 4, which shows the blast wave created by the explosion of a supermassive star in one of the most energetic explosions in the universe. This work showed how such enormous explosions, expected to be as powerful as 10,000 typical supernova, impacted their host galaxies and highlighted how the heavy elements they produced may be found in ancient stars still inhabiting our galaxy today. While the cosmological simulation was needed to capture the large-scale evolution of the blast wave, we simulated the small-scale evolution is great detail as well, using the Los Alamos RAGE code. The combination of these two calculations made this most detailed cosmological supernova calculation ever carried out, Figure 4.

Impact on National Missions

Among the simulations we carried out in the course of our research were some of supernovae run with the Los Alamos RAGE radiation hydrodynamics code. We were able to uncover problems with the implementation of gravity in this code, and since then significant progress has been made in correcting these problems. Indeed, our supernova simulations have been an influential utilization of radiation transport codes developed at Los Alamos.

In addition, as regards new staff, the postdoc funded for this research, Jarrett Johnson, has subsequently joined the scientific staff of the Lab in XTD-6. Wes Even, a postdoc collaborator on our research, has also joined the Lab as staff in CCS-2.

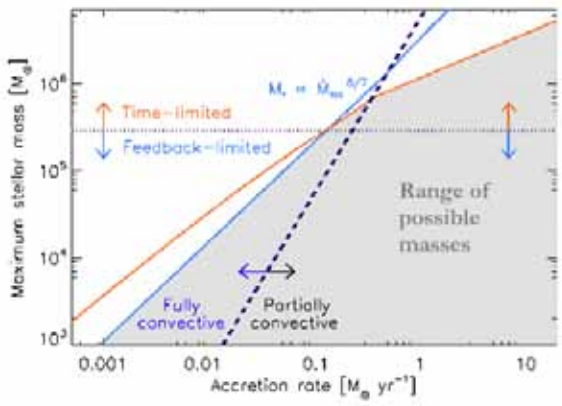

Figure 1. The maximum mass to which stars can grow by accreting gas at a constant rate. As shown by the blue line, the radiation emitted by the star will stop accretion only after it has grown to a high mass, if it accretes gas at a sufficiently high rate,

as expected for supermassive stars in the early universe (from Johnson et al. 2012).

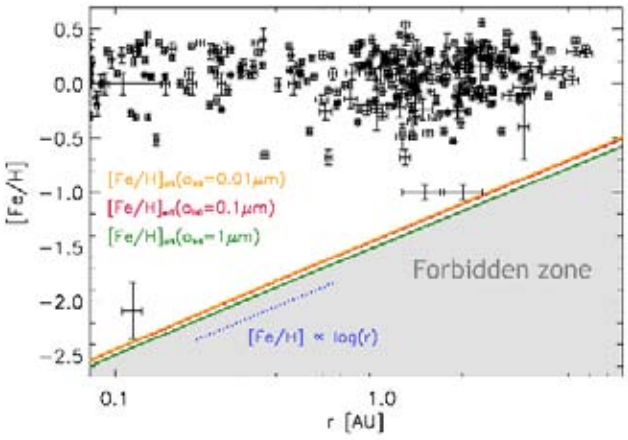

Figure 2. The colored lines show the minimum heavy element abundance, here shown as the iron abundance ([Fe/H]) as a proxy, for planet formation. The black points show the heavy element abundances of known planets, none of which exhibit heavy element abundances below the minimum we estimated (from Johnson & Li 2012).

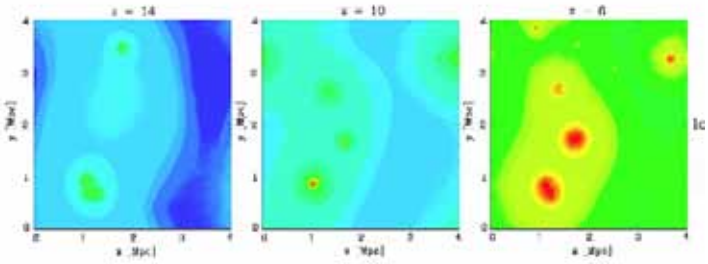

Figure 3. The build-up of the radiation field produced by the light emitted form stars in the first galaxies, from early to later times (left to right). The intensity of the molecule-dissociating radiation field increases steadily, and this eventually leads to the assembly of hot primordial gas from which supermassive stars form (from Johnson, Dalla Vecchia & Khochfar 2013).

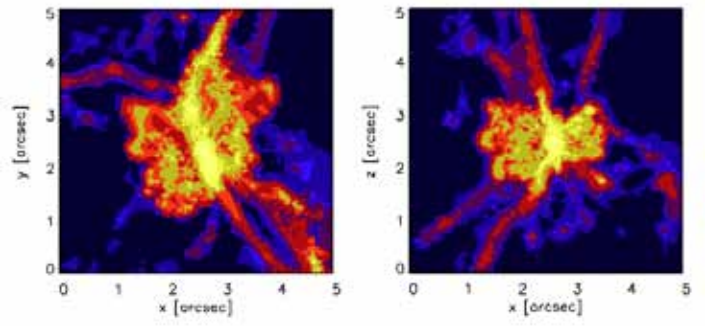

Figure 4. Two views of the blast wave produced by the explosion of a supermassive star in the early universe, as seen on the sky (in units of seconds of degrees). Such supernova explosions would have been among the most energetic thermonuclear events in the history of the universe (from Johnson, Whalen, Even, Fryer, et al. 2013).

Publications

Agarwal, B., S. Khochfar, J. L. Johnson, E. Neistein, C. Dalla Vechia, and M. Livio. Ubiquitous seeding of supermassive black holes by direct collapse. 2012. Monthly Notices of the Royal Astronomical Society. 425 (4): 2854.

Elliott, J., J. Greiner, S. Khochfar, P. Schady, J. L. Johnson, and A. Rau. The long gamma-ray burst rate and the correlation with host galaxy properties. 2012. ASTRONOMY & ASTROPHYSICS. 539: A113.

Johnson, J. L.. Angular momentum transport by thermal emission in black hole accretion disks. 2011. Astronomische Nachrichten. 332 (8): 841.

Johnson, J. L.. The First Galaxies: Theory and Simulations. 2013. In The First Galaxies: Theoretical Predictions and Observational Clues. Edited by Wiklind, T., B. Mobasher, and V. Bromm. Vol. 396, p. 177. Berlin: Springer-Verlag.

Johnson, J. L., C. Dalla Vecchia, and S. Khochfar. The First Billion Years project: the impact of stellar radiation on the co-evolution of Populations II and III. 2013. Monthly Notices of the Royal Astronomical Society. 428: 1857.

Johnson, J. L., D. J. Whalen, H. Li, and D. Holz. Supermassive Seeds for Supermassive Black Holes. To appear in The Astrophysical Journal.

Johnson, J. L., D. J. Whalen, W. Even, C. L. Fryer, A. Heger, J. Smidt, and K. Chen. The Biggest Explosions in the Universe. The Astrophysical Journal.

Johnson, J. L., and H. Li. Constraints on planet formation via gravitaional instability across cosmic time. 2013. Monthly Notices of the Royal Astronomical Society. 431: 972.

Johnson, J. L., and S. Khochfar. The Contribution of Supernovae to Cosmic Reionization. 2011. Astrophysical Journal. 743: 126.

Johnson, J., B. Agarwal, D. Whalen, C. Dalla Vecchia, C. Fryer, S. Khochfar, Hui Li, and M. Livio. The growth of the stellar seeds of supermassive black holes. 2012. In First Stars IV - from Hayashi to the Future ; 21-25 May 2012 ; Kyoto, Japan. Vol. 1480, p. 313.

Johnson, J., D. Whalen, C. Fryer, and Hui Li. The growth of the stellar seeds of supermassive black holes. 2012. Astrophysical Journal. 750 (1): 66 (12 pp.).

Johnson, J., and Hui Li. The First Planets: the Critical Metallicity for Planet Formation. 2012. Astrophysical Journal. 751 (2): 81 (11 pp.).

Whalen, D. J., W. Even, L. H. Frey, J. L. Johnson, C. C. Lovekin, C. L. Fryer, M. Stiavelli, D. E. Holz, A. Heger, S. E.

Woosley, and A. L. Hungerford. Finding the First Cosmic Explosions I: Pair-Instability Supernovae. To appear in The Astrophysical Journal.

Auger-recombination-free Nanocrystals by Rational Design of Confinement Potential

Victor I. Klimov
20110544PRD1

Abstract

The goal of this project has been to achieve fundamental understanding of the interplay between structural characteristics and photophysical properties of colloidal core/shell nanocrystals (NCs) with designed interfacial composition. The main aim of these studies has been the development of NCs, which would allow us to achieve lasing in the regime of electrical injection. New light-emitting and especially lasing structures based on low-cost, chemically synthesized materials would benefit numerous technologies from solid-state lighting and displays to optical telecommunication and quantum cryptography. NCs are particularly attractive for these applications due to their efficient and size-tunable emission. A significant impediment to applications of NCs in lasers is fast nonradiative Auger recombination (AR), which limits optical gain lifetimes to sub-ns timescales. Recent studies of LANL researchers have demonstrated that AR is significantly reduced in so-called "giant" NCs (g-NCs) comprising a small CdSe core overcoated with a thick CdS shell (Garcia-Santamaria et al., Nano Lett. 2009). The goal of this project has been to elucidate the reasons underlying the suppression of AR in these NCs by conducting direct measurements of multiexciton dynamics in conjunction with studies of NC structure/composition via analytical spectroscopic methods such as Raman scattering and fluorescence line narrowing (FNL). The insights gained from these studies have been used to design novel structures in which AR is efficiently suppressed which have allowed us to extend the optical gain lifetime and increase its magnitude and also boost the efficiency of NC-based light emitting diodes (LEDs).

Background and Research Objectives

Colloidal semiconductor nanocrystals (NCs) have been considered as promising materials for optoelectronic applications because they exhibit particle-size-tunable emission color and high (>90%) intrinsic quantum yields in emission. Furthermore, NCs are produced through inexpensive, scalable solution-based synthesis amenable to simple fabrication processes such as spin-coating, ink-jet and roll-to-roll printing. Over the last few years, several examples of LEDs based on nanostructured materials have been reported by different groups, and have shown a remarkable tunability across the entire visible spectrum.

The performance of NC-LEDs is greatly limited by fast nonradiative AR. In conventional 'single-component' NCs, Auger lifetimes are proportional to NC volume, a seemingly universal trend that has been observed for many different semiconductors. The development of approaches for reducing AR rates, while still preserving a significant degree of spatial confinement, is a long-standing goal in the field of NCs. Recently, core-shell nanostructures of CdTe/CdSe, CdZnSe/ZnSe, and CdSe/CdS (thick-shell samples) as well as CdSe/CdS quantum-dot/quantum-rod structures have been shown to exhibit a significant suppression of AR as assessed from single-NC data or time-resolved ensemble studies. The reasons for this dramatic suppression of AR in thick-shell CdSe/CdS NCs (as well as in other reported nanostructures) are still not understood. Recent theoretical calculation by Cragg and Efros demonstrated that AR can be reduced by several orders of magnitude by replacing the sharp step-like potential with smooth profile. In core-shell NCs, this is achievable by promoting a gradual transition of the compositional profile between the core and the shell domains, which yields an alloyed region of mixed composition. The goal of this project has been to achieve optimized NCs with suppressed Auger recombination through engineering of the confinement potential.

Scientific Approach and Accomplishments

The first part of this Project consisted of an experimental investigation of the fine structure of the excitonic states in CdSe/CdS heterostructures where spatial separation between electrons and holes can be tuned by controlling shell thickness (Fig. 1). This study has allowed us to gain deeper understanding of the photophysics of this

class of nanomaterials and to formulate a new paradigm for controlling exciton dynamics via engineered electron-hole exchange interaction. Specifically, we showed that the splitting energy between dark and bright excitonic states in core/shell CdSe/CdS NCs can be tuned externally by controlling the degree of delocalization of the electron wavefunction in the CdS shell (Fig. 2). By applying this new strategy, we were able to fabricate NCs with light-emission properties, which are independent of magnetic field up to 7 Tesla and of temperature from 300 K to 1.5 K. Because of its fundamental and technological importance, this study, published Nature Communications, has been highly cited (23 citations in one year) and has already resulted in several follow-up publications from other groups.

Based on this newly acquired knowledge of excitonic fine structure, we have able to use CdSe/CdS NCs as a model system to investigate the role of interfacial alloying on AR in the light of a recent theoretical paper by Cragg & Efros (Nano Letters, 2009) that predicted orders of magnitude suppression of AR in NCs where the abrupt potential step is substituted by a smooth potential gradient. Studying thick shell CdSe/CdS NCs through ultrafast optical spectroscopy we observed a very significant suppression of AR that greatly exceeded expectations based on established arguments, such as volume scaling (Fig. 3).

This observation suggested a dominant role of the interfacial composition, which defines the shape of the confinement potential, in AR suppression. Probing elusive sub-nanometer variations in the NC composition constituted a significant experimental challenge. To this end, we have developed a new experimental method based on fluorescence line narrowing spectroscopy (FLN, Fig. 4). In this method, NCs are excited with a cw laser on the red side of the BE absorption feature, which effectively selects a sub-ensemble of the largest NCs in the sample. As a result, the low-temperature FLN spectra typically exhibit narrow emission peaks due to zero-phonon and phonon-assisted excitonic transitions. As a result of this spectroscopic selection, using FLN we can clearly resolve features due to phonon-assisted transitions involving various longitudinal optical (LO) modes; based on the intensity of these modes we can analyze the composition of the NC within the volume sampled by a photoexcited exciton.

Figure 4a shows the 1.55 K FLN spectra of CdSe core-only NCs and a few CdSe/CdS NC samples with increasing shell thicknesses. The spectrum of core-only NCs exhibits a feature due to exciton recombination assisted by the LO phonon of CdSe (LO1; 25 meV), with overtones at 2LO1 (50 meV) and 3LO1 (75 meV). The growth of the CdS shell results in additional peaks due to phonon-assisted transitions involving a CdS LO phonon (LO2 at 35 meV and 2LO2 at 70 meV). Remarkably, with increasing H, we also observe the emergence of a new FLN feature at LO12 = 60 meV (see, e.g., the spectrum of the 7 ML-shell sample), which is due to the combination of LO1 and LO2 modes. Such a "combinatory" mode is a signature of the CdSeS alloy and is indicative of the development of an interfacial "graded" region where the mismatch between CdSe and CdS lattice is gradually recovered. The increases in the amplitude of the LO12 feature correlates with the reduction in the intensity of the CdSe-related phonon replica, indicating progressive consumption of the core material, which accompanies the formation of the alloy layer.

We quantify these observations by plotting relative intensities of the signals related to three different components of the NCs as a function of R (Fig. 5): the interfacial alloy region [Aalloy; triangles in (a)], the CdSe core [ACdSe; solid circles in (b)], and the CdS shell [ACdS; open circles in (b)]. In these plots, the signal related to a certain NC region (e.g., the integral intensity of the LO1 and the 2LO1 features in the case of the CdSe core) is normalized by the total area of all phonon replicas in the FLN spectrum. The data presented in this way clearly indicate that most of the interfacial alloying occurs until the shell thickness reaches ~9 MLs, while further shell growth is not accompanied by any significant expansion of the alloy region. Interestingly, the largest change in the Auger decay time also occurs in the same range of shell thicknesses for which we observe the formation of the alloyed interface. Specifically, τ_{2A} changes by more than two orders of magnitude (from 250 ps to 31 ns; the latter value corresponds to $\beta = 4$), when H increases from 0 to 11 ML. This increase is about ten times larger than that predicted based on changes in the effective exciton volume and e-h spatial overlap.

At larger values of H, the Auger time increases more slowly and can be ascribed to the reduction in the e-h overlap integral. For example, when H grows from 9 to 14 ML, which corresponds to the range where the alloy thickness is essentially constant, we observe a three-fold increase in τ_{2A} (from 31 ns to 90 ns). This correlates well with an approximately three-fold reduction in Θ_{eh} (from 0.24 to 0.09) as derived from changes in single exciton dynamics (τ_x increases from 45 ns to 115 ns, Fig. 3a). These results strongly suggest that the major contribution to the observed suppression of AR arises from the softening or smoothing of the confining potential due to formation of an alloyed layer at the CdSe/CdS interface. Through this novel approach, we provided the first experimental verification of Efros's theory, which we published in a highly cited article in Nano Letters (34 citations; highlighted in Chemical & Engineering News).

One important consequence of suppressed AR is a sig-

nificant increase in emission efficiencies of multiexciton states. For example, in the core-only samples studied in this work, the emission quantum yield of biexcitons is ~1%. However, it reaches 40 – 50% in CdSe/CdS structures with shell thickness of 9 ML and is as high as 60 – 80% in samples with a 19 ML shell (Fig. 5b, inset). This increase in PL yields of multiexciton states can greatly benefit applications of NCs in technologies involving light emission such as lasing, optical amplification and solid-state lighting. To explore the applicability of CdSe/CdS NCs to LEDs, we conducted a detailed systematic study of the effect of shell thickness on device performances, showing a tenfold increase of LED efficiency for thick shell NCs. We explained this increase by greatly reduced rates of AR and strongly suppressed NC-to-NC energy transfer with respect to conventional systems for which these parasitic non-radiative processes severely reduce the electroluminescence efficiency. This study has been published in Nano Letters.

As demonstrated above, core/shell NC in which a CdSe core is overcoated by a thick CdS shell show dramatically suppressed AR and are therefore interesting candidates for efficient NC-LEDs. In addition, optical characteristics of these systems (including PL QY and long-term optical stability) were observed to be largely independent of the ligand coating. However, there are several potential issues that could make these systems unsuitable for LED applications. Currently, solution-phase QYs are at most ~50%, compared to near-unity in the case of optimized thin-shell NCs. In addition, the density of NCs in the LED active layer is effectively reduced due to the much larger size of a thick shell NC compared to a conventional system. Together, these features could render an active layer less emissive compared to a standard NC film. Furthermore, the thick shell comprising the relatively wide band-gap semiconductor, CdS, could inhibit charge injection and raise the LED turn-on voltage. To investigate these issues, we utilize a simple LED device architecture for comparing g-NCs to conventional thinner-shell systems.

In our experiments (Fig. 5), we have used a simple device architecture, which comprises a NC active layer in between a PEDOT:PSS-coated indium-tin oxide (ITO) anode and a LiF/Al cathode. The LEDs were fabricated on ITO-coated glass substrates. The PEDOT:PSS layer (~30 nm) was spin-coated onto the substrate and annealed at 250 °C for 20 min inside an inert-atmosphere (UHP Ar) glovebox. The high-temperature annealing yields a compact hole-conducting layer. The NC active layer was then spin-coated (~2500 rpm) from a 10 mg/ml NC octane solution. Finally, 2 nm of LiF and 100 nm of aluminum were thermally evaporated onto the NC layer through a shadow mask to form the top electrode.

The EL response of a representative LED comprising an active layer made from 4-nm diameter core, 16-monolayer shell CdSe/CdS NCs is reported in Fig. 5a. A plot of luminance versus voltage reveals a clear EL 'turn-on' at a bias of 3.0 V. The LED reaches a maximum luminance of 2000 Cd/m2 at a current density (J) of 1200 mA/cm2 and voltage of 11 V (Fig. 5a). The EL spectrum overlaps almost precisely with the PL spectrum (Fig. 5b), where the latter was obtained from a solution of the NCs prior to device fabrication. Interestingly, at higher current densities, we do observe a weak, high-energy band that we tentatively attribute to emission from higher order excited states (inset of Fig. 5b). Such emission from charged or multiexciton states becomes possible in the case of efficient suppression of nonradiative Auger recombination, as shown in the previous section. Significantly, the luminance level for 'standard video brightness' (200 Cd/m2) arises in this device at 6.5 V and 180 mA/cm2. EQE reaches a maximum of 0.17% at 100 mA/cm2 (7.0 V) with a peak luminance efficiency of 0.36 Cd/A. A photograph of the device (Fig. 5c, inset) reveals uniform pixel brightness over the relatively large area of the device (0.03 cm2) at a bias of 9 V. The device shows no sign of degrading when tested repeatedly after storage in air for more than a month. Importantly, earlier reports using similar architectures and conventional CdSe/ZnS core/shell NCs resulted in an EL efficiency less than ~6x10-3 Cd/A, which is nearly two orders of magnitude lower than that of our 16-ML-shell CdSe/CdS device.

Impact on National Missions

As mentioned above, NCs are appealing candidates for efficient solid state lighting technologies. Given the size of the already existing market, applied research in this field and efficient transfer of knowledge to the industrial entities opens new opportunities for economic growth. In addition, there is a chance that new governmental regulations will further push for this paradigm shift thereby providing an additional stimulus or the development of the solid state lighting industry, with obvious increase of its economic relevance. Clearly, companies with privileged access to technical expertise will be in a leading position within the industry and will benefit of an important time advantage that could allow them to establish themselves on the market before other players become competitive. Although the fundamental knowledge of the physical processes underpinning the operation of efficient NC-based devices is not trivial, their production, once properly understood and optimized, is relatively inexpensive compared to other materials such as epitaxial semiconductor structures, which instead require expensive facilities typical of microelectronic industry. In addition, the technical entry barrier is low, which makes it particularly easy to be transferred to companies.

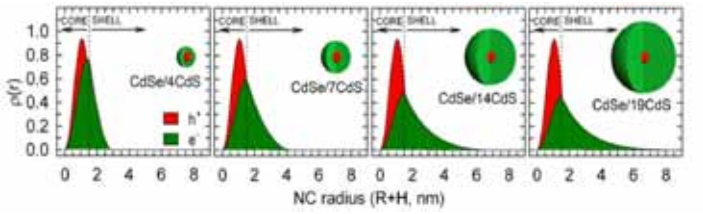

Figure 1. Spatial probability distribution of the hole (red area) and electron (green areas) for R = 1.5 nm and H = 1.6 nm, H = 2.8 nm and H = 7.6 nm.

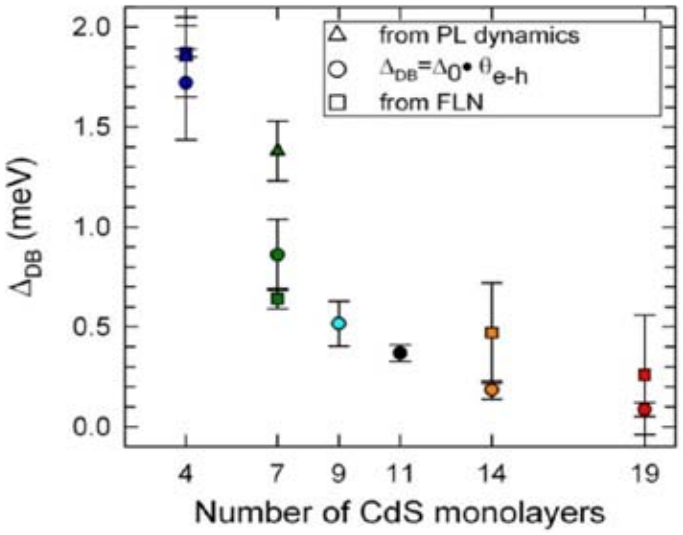

Figure 2. Dark-bright splitting energy as a function of the CdS shell thickness (in monolayers) for core/shell CdSe/CdS NCs.

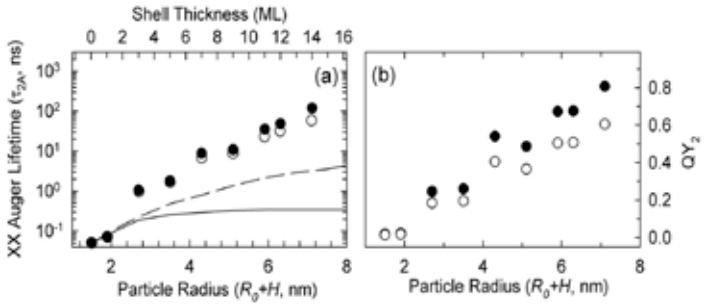

Figure 3. (a) Biexciton AR lifetimes. Lines show AR lifetimes expected for the cases of linear scaling with effective exciton volume and the volume-scaling corrected for e-h spatial separation (dashed line). (b) "Intrinsic" biexciton emission quantum yield; this expression does not account for "extrinsic" carrier losses due, e.g., to trapping at surface defects.

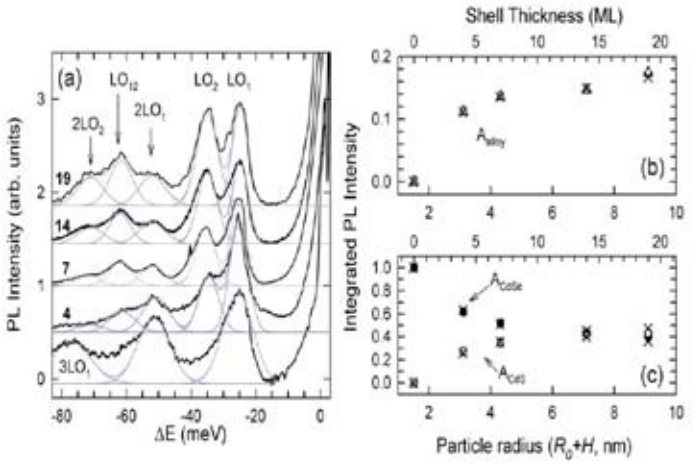

Figure 4. Compositional analysis of CdSe/CdS NCs based on the intensities of phonon replica in FLN spectra. (a) The 1.55 K FLN spectra (black lines) of core-only CdSe NCs (bottom curve) and four CdSe/CdS NC samples with R0 = 1.5 nm and different shell thicknesses (H = 1.6, 2.8, 5.6, and 7.6 nm, corresponding values in ML are reported next to each curve); the horizontal-axis zero corresponds to the excitation energy. Gray lines show Gaussian fits of the FLN spectra that account for contributions of phonon replicas associated with LO modes of CdSe (LO1), CdS (LO2), and CdSeS (LO12); surface phonons were not included in the fitting procedure. (b, c) Spectrally integrated intensity of the FLN features due to the alloy mode (triangles in (b)), the CdSe mode (solid circles in (c)) and the CdS mode (open circles in (c)) plotted as a function the nanoparticle radius. Crosses are the calculations.

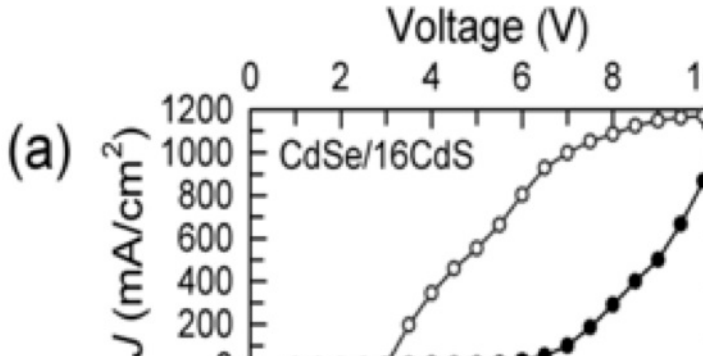

Figure 5. a) Top panel: Current density (full black circles) and luminance (empty circles) characteristics of a NC-LED incorporating a monolayer of CdSe/16CdS NCs. Lower panel: PL of the active layer compared to the EL spectrum of the same NC-LED as in the top panel at increasing working voltage (namely, 5, 6, 7, 8 V). The inset shows a detail of the high-energy portion of the EL spectra at increasing driving voltage (as indicated by the arrow). b) External quantum efficiency of the same device as a function of current density. Inset: Photograph of a working LED at driving voltage of 9V (J = 450 mA/cm2) showing uniform EL emission from several LEDs on the same substrate.

Publications

Brovelli, S., C. Galland, R. Viswanatha, and V. Klimov. Tuning radiative recombination in cu-doped nanocrystals via electrochemical control of surface trapping. 2012. Nano Letters. 12 (8): 4372.

Brovelli, S., R. D. Schaller, S. A. Crooker, Garci&acute, Y. Chen, R. Viswanatha, J. A. Hollingsworth, H. Htoon, and V. I. Klimov. Nano-engineered electron-hole exchange interaction controls exciton dynamics in core-shell semiconductor nanocrystals. 2011. Nature Communications. 2: 280 (8 pp.).

Galland, C., S. Brovelli, W. K. Bae, L. A. Padilha, F. Meinardi, and V. I. Klimov. Dynamic hole blockade yields two-color quantum and classical light from dot-in-bulk nanocrystals. 2013. Nano Letters. 13: 321.

GarciÃÅa-SantamariÃÅa, F., S. Brovelli, R. Viswanatha, J. Hollingsworth, H. Htoon, S. Crooker, and V. Klimov. Breakdown of volume scaling in auger recombination in CdSe/CdS heteronanocrystals: The role of the core-shell interface. 2011. Nano Letters. 11 (2): 687.

Pal, B., Y. Ghosh, S. Brovelli, R. Laocharoensuk, V. Klimov, J. Hollingsworth, and H. Htoon. 'Giant' CdSe/CdS core/shell nanocrystal quantum dots as efficient electroluminescent materials: Strong influence of shell thickness on light-emitting diode performance. 2012. Nano Letters. 12 (1): 331.

Pandey, A., S. Brovelli, R. Viswanatha, J. M. Petryga, V. I. Klimov, and S. A. Crooker. Long-lived photoinduced magnetization in copperdoped ZnSe–CdSe core–shell nanocrystals. 2012. Nature Nanotechnology. 7: 792.

Viswanatha, R., S. Brovelli, A. Pandey, S. A. Crooker, and V. I. Klimov. Copper-doped inverted core/shell nanocrystals with "permanent" optically active holes . 2011. Nano Letters. 11: 4753.

Universal Physics with Ultracold Atoms

Joseph A. Carlson
20110633PRD2

Abstract

This project was directed at studies of universal physics in cold atom systems. The goal is to elucidate the properties of these systems, allowing insight from one field to strengthen our understanding across several fields. Topics that were studied included new types of crossover physics in multicomponent Fermi gases, Efimov effects in quantum magnets and in two-dimensional systems. These topics have applications in cold atoms, nuclear physics, and condensed matter.

Background and Research Objectives

Strongly-interacting Fermi systems appear in many subfields in physics and their understanding is important but often challenging. Ultracold atoms are ideal to tackle such problems because of the prominent advantage of the ability to control the atom-atom interaction. In particular, the limit of strongest interaction (unitarity limit) has attracted considerable attention because of the universality meaning that its properties are independent of details of the interaction potential. Physics in the unitarity limit can shed light on various strongly interacting systems ranged from high-Tc superconductors to neutron stars and is thus an important interdisciplinary field. The goal of my research is to take the advantage of ultracold atoms to deepen and enlarge our understanding of the universal few-body and many-body physics that are relevant beyond ultracold atoms and to explore new frontiers across traditional disciplines in physics.

Scientific Approach and Accomplishments

Dr. Nishida obtained several important physics results during his Oppenheimer Fellowship at Los Alamos. Dr. Nishida first studied a new type of crossover physics in three-component Fermi gases.[1] The standard two component system (e.g. spin up and spin down) has a smooth crossover from the BCS (weak pairing) regime to the BEC (strong pairing into bosons) regime as the strength of the coupling is increased. The three-component system has a richer structure, with different 'phases' of atoms, dimers, and trimers connected by crossovers and phase transitions. The phase diagram is shown in Figure 1.

The weak coupling regime is shown on the left of the diagram. In this regime two species form a standard superfluid with the remaining species unpaired. The coupling increases toward the right of the diagram. At the bottom of the figure the effective range is nearly zero and three atoms of each species can collapse to a deeply bound state. The three-component system has a transition from a system with an unpaired species to one without – an 'atom-trimer continuity' transition analogous to the quark-hadron duality that exists in nuclear matter at zero temperature with increasing density. This work was published in Physical Review Letters and is the subject of much new theoretical and experimental investigation. Extensions of this work are likely to be important in nuclear physics where alpha particle clustering is important.

Dr. Nishida then worked with Christian Batista (T-4) and Yasuku Kato on the Efimov effect in quantum magnets.[2] The Efimov effect is a discrete scaling symmetry in few-body systems that relate few-body states at definite ratios of binding energies. It is typically thought of as a continuum few-body effect. Nishida and collaborators discovered that the Efimov also exists in quantum magnets, many-body systems typically defined on a lattice. This novel understanding has led to new searches for Efimov effects in a variety of systems. This paper was published in Physical Review Letters.

Another important area of investigation Dr. Nishida conducted was developing a 'super'-Efimov effect in two-dimensional systems.[3] The Efimov effect has traditionally been studied in normal three-dimensional systems. Many condensed matter systems have reduced dimesionality induced by anisotropies in the background structure of the material. Dr Nishida and collaborators

found that spinless fermions in two-dimensions fine-tuned to a p-wave resonance can form an infinite tower of bound states with a univeral doubly-exponential scaling pattern. This states could be observed in cold-atom experiments. This paper was published in Physical Review Letters.

Dr. Nishida published several other papers as part of this project, including studies of electron spin resonance ina dilute magnon gas,[4] and magnetic and nematic orderings in spin-1 antiferromagnets with single-ion anisotropy. The latter was published in collaboration with scientists in T-4.

Impact on National Missions

This project made a significant impact on our understanding of strongly-correlated systems in condensed matter and nuclear physics. In particular the work on multicomponent Fermi systems is influencing studies of nuclear physics, where four species (spin up and spin down neutrons and protons) can cluster into alpha-particle like states. Similar investigations are being pursued in condensed matter and cold atoms. This work will help break the standard two-component paradigm (neutrons or protons paired) used to study large nuclei. These examinations are critical to the study of neutron-rich matter and nuclei at FRIB (the Facility for Rare Isotope Beams) at MSU.

Dr. Nishida's work will also be critical for understanding novel states of matter theoretically and experimentally, including studies conducted at LANL.

Figure 1. Phase Diagram of Three Species of Fermions versus coupling strength (horizontal axis) and effective range (vertical axis).

References

1. Nishida, Y.. New Type of Crossover Physics in Three-Component Fermi Gases. 2012. PHYSICAL REVIEW LETTERS. 109 (24): -.

2. Nishida, Y., Y. Kato, and C. D. Batista. Efimov effect in quantum magnets. 2013. NATURE PHYSICS. 9 (2): 93.

3. Nishida, Y., S. Moroz, and D. T. Son. Super Efimov Effect of Resonantly Interacting Fermions in Two Dimensions. 2013. PHYSICAL REVIEW LETTERS. 110 (23): -.

4. Wierschem, K., Y. Kato, Y. Nishida, C. D. Batista, and P. Sengupta. Magnetic and nematic orderings in spin-1 antiferromagnets with single-ion anisotropy. 2012. PHYSICAL REVIEW B. 86 (20): -.

Publications

Knap, M., A. Shashi, Y. Nishida, A. Imambekov, D. A. Abanin, and E. Demler. Time-Dependent Impurity in Ultracold Fermions: Orthogonality Catastrophe and Beyond. 2012. PHYSICAL REVIEW X. 2 (4): -.

Nishida, Y.. Impossibility of the Efimov effect for p-wave interactions. 2012. PHYSICAL REVIEW A. 86 (1): 012710.

Nishida, Y.. Probing strongly interacting atomic gases with energetic atoms. 2012. PHYSICAL REVIEW A. 85 (5): 053643.

Nishida, Y.. Probing strongly interacting atomic gases with energetic atoms. 2012. PHYSICAL REVIEW A. 85 (5): 053643.

Nishida, Y.. New Type of Crossover Physics in Three-Component Fermi Gases. 2012. PHYSICAL REVIEW LETTERS. 109 (24): -.

Nishida, Y.. Impossibility of the Efimov effect for p-wave interactions. 2012. PHYSICAL REVIEW A. 86 (1): -.

Nishida, Y.. Probing strongly interacting atomic gases with energetic atoms. 2012. PHYSICAL REVIEW A. 85 (5): -.

Nishida, Y., S. Moroz, and D. T. Son. Super Efimov Effect of Resonantly Interacting Fermions in Two Dimensions. 2013. PHYSICAL REVIEW LETTERS. 110 (23): -.

Nishida, Y., Y. Kato, and C. D. Batista. Efimov effect in quantum magnets. 2013. NATURE PHYSICS. 9 (2): 93.

Nishida, Y., and D. Lee. Weakly bound molecules trapped with discrete scaling symmetries. 2012. PHYSICAL REVIEW A. 86 (3): 032706.

Nishida, Y., and D. Lee. Weakly bound molecules trapped with discrete scaling symmetries. 2012. PHYSICAL REVIEW A. 86 (3): -.

Wierschem, K., Y. Kato, Y. Nishida, C. D. Batista, and P. Sengupta. Magnetic and nematic orderings in spin-1 antiferromagnets with single-ion anisotropy. 2012. PHYSICAL REVIEW B. 86

A New Drift Shell Integration Technique for Inner Magnetospheric Space Weather Models

Josef Koller
20110735PRD2

Abstract

Energetic particles within the magnetosphere undergo three periodic motions including the gyration, bounce, and drift with associated adiabatic time scales and invariants. The particle drift shell L*, the third adiabatic invariant, is computationally demanding from the standard method because the global magnetic field lines need to be traced and integrated. This project developed a new tool using the novel neural network technique to efficiently calculate the drift shell L* in microseconds instead of seconds without losing accuracy. Furthermore, since a global magnetic field configuration is the essential element in obtaining the drift shell, this project uses the magnetospheric configuration form a first-principle inner magnetosphere model LANL RAM-SCB, rather than the commonly employed empirical magnetic field model. The newly developed L* neural network is capable of removing the computational bottleneck and hence allows for real-time radiation belt modeling and space weather forecasting.

Background and Research Objectives

During geomagnetic storms triggered by abrupt solar activities, the severely enhanced energetic electron flux and radiations in the Van Allen radiation belts will pose threats to both spacecraft and astronauts. The understanding and modeling of the radiation belt are therefore of great importance both practically and scientifically. The overarching goal of this project is to investigate the physical processes that are responsible for the radiation belt dynamics, such as transport, loss, and energization. The dynamics of energetic particles can be conveniently expressed and visualized by three adiabatic invariants. While the first two are relatively easy to be computed provided with the magnetic field information locally or along a field line, the third invariant, i.e., the particle drift shell L*, is computational expensive since numerical tracing of the global magnetic field lines is needed in the standard approach described in Roederer (1970).

This project aims to develop a drift shell model using a novel technique to efficiently calculate the drift shell L* while preserving a high fidelity of accuracy as the standard method. Instead of using the common empirical magnetic field model, which can reasonably represent a statistical, average magnetosphere, a magnetically self-consistent inner magnetosphere model LANL RAM-SCB, which solves the magnetic field from fundamental equations of plasma physics, is employed for the determination of the drift shell. This project will not only evaluate the applicability of the newly developed neural network in predicting the L* and its accuracy, but also demonstrate the application in addressing the physical processes in the radiation belt dynamics. The L* neural network approach will remove the computational bottleneck in the accurate radiation belt modeling or data assimilation, therefore allowing for real-time space weather forecasting.

Scientific Approach and Accomplishments

A modern machine learning technique (i.e., feed-forward artificial neural network) allows one to establish the complicated relationship between the external solar wind driving and responses within a complex nonlinear system like the terrestrial magnetosphere system. The artificial neural network, inspired from the biological neuron system that is typically composed of the stimulation and the response, consists of one input layer, one hidden layer, and one output layer (Figure 1). In this study, the input parameters on the neurons, include time, location, solar wind and interplanetary magnetic field conditions, and magnetospheric disturbance index, and the output layer is the particle drift shell L*. The input parameters are multiplied by weights w and then modified by an activation function f, producing the output at each neuron to be inter-connected to the neurons in the next layer. The output L* therefore can be described by:

Training a neural network refers to a process that

generalize the relationship between the input and the prescribed target. The training begins with an initial guess of the weights in the network and then iteratively adjusts them through an optimization algorithm until the error between the target and the network output is minimized or reaches a tolerance. Once the training is completed (i.e., the weights and bias are determined), given any input, the drift shell L* can be easily computed.

One important component in the training data is the desired output, that is, the drift shell L*, which is used for supervising the learning/training process. This prescribed L* is obtained from numerical tracing of global field lines, the traditional standard approach, within a global magnetospheric magnetic field model by means of the IRBEM Fortran library (http://sourceforge.net/projects/irbem). The commonly used global magnetic field model is Tsyganenko empirical model, such as T89, T96, T01Storm, T01Quiet, and TS05. While these empirical models represent a statistical, average magnetosphere, a first-principle magnetic field model RAM-SCB self-consistently solves the global magnetic field configuration based on plasma physics. In this study, the RAM-SCB magnetic field configuration is employed to produce the L* for the learning of the neural network.

In order to achieve a trustworthy neural network, sufficient training data is required to avoid issues like over-fitting and memorization of the input-output pattern. The training patterns are generated with random input. The location, one of the input parameters, is randomly selected within the domain (r: [1.03, 11.5] RE, θ: [-90°, 90°], φ: [0, 360°] in spherical coordinates). Each location corresponds to a random time from 01/01/1994 to 01/01/2005 (for empirical magnetic field models) or from 01/01/2001 to 01/01/2007 (for the RAM-SCB model) and a random pitch angel from 0 to 90°.

Validation of the self-consistent inner magnetosphere model RAM-SCB

This physics-based model couples the ring current-atmosphere interaction model (RAM), which solves the bounce-averaged ring current particle phase space distribution function [Jordanova et al. 2006] in a non-dipole magnetic field, with a 3-D Euler potential based plasma equilibrium magnetic field code (SCB) [Zaharia et al. 2004; 2008] that calculates the magnetic field self-consistently in force balance with the anisotropic ring current distributions. We carried out validation study of this self-consistent inner magnetosphere model by simulating several geomagnetic storms with different activity levels and by comparing against a variety of in-situ satellite measurements including magnetic fields from POLAR and Cluster spacecraft, energy differential ion (H+, O+, and He+) flux from Cluster/CODIF instrument and found reasonably good agreements during storm times.

L* neural network with Tsyganenko empirical magnetic field models and the physics-based LANL RAM-SCB model

We developed the L* neural networks trained from seven different empirical magnetospheric field models and one first-principle inner magnetosphere model RAM-SCB using the traditional integration technique. Their applicability under different geomagnetic activity conditions is also evaluated. These neural networks are found to be highly reliable with the prediction efficiency (PE) about 0.98, expect for extreme conditions when the magnetosphere is largely disturbed. These L* neural networks have been released on the website: http://lanlstar.net, implemented to the python-based tool SpacePy developed at LANL, and delivered to the Coordinated Community Modeling Center (CCMC) at NASA for public application.

Quantify the effect of the magnetopause shadowing on radiation belts dropouts

Radiation belts changes dramatically during geomagnetic storm times. Sudden dropouts of electron flux are common phenomena. However, the relative contribution of different loss mechanisms remains far from well understood. We use the 1D radiation belt diffusion code to study the effect of the magnetopause shadowing on the dropouts. The initial condition is obtained by averaging over quiet time results from DREAM for different (u, K) combinations. The magnetopause in the model is represented by the last closed drift shell L* which is K-dependent. The loss process in the simulation includes the drift loss out of the magnetopause that is coupled with outward radial diffusion. The resulting PSD is converting to omni-directional flux, which is compared to GPS flux observations to quantify the effect of the loss process on the main phase electron dropout. The results indicate that the magnetopause shadowing together with the outward radial diffusion can account for 67-88% of the total electron loss in the high-speed solar wind stream (HSS) events.

On the L* accuracy and its effect on the PSD radial profile

We utilizes the phase space density (PSD) matching technique developed by Chen, et al. [2005] to estimate the L* accuracy during quiet time. This technique compares two PSD values at the same Phase Space Coordinates (i.e., the same adiabatic invariants u, K, L*)), using a matching ratio which is usually deviates from unity due to errors mainly from the L* calculation from the underlying global magnetospheric model. The PSD data from three LANL-GEO satellites is used to measure the L* error. Results indicate that the neural network L* with different underlying magnetospheric models has uncertainties statistically below 0.4, implying that these neural networks can be reliably

used to calculate the drift shell L* during geomagnetically quiet time. However, the neural network with the underlying T01Storm model is found to have the most accurate L* among all the Tsyganenko empirical models.

To investigate how the L* uncertainty affects the PSD estimation, 100 magnetosphere configurations is created using solar wind input parameters randomly disturbed based on their measurement uncertainties. These 100 global magnetospheric configurations are then used for the L* calculation at a fixed location. These L* values and the corresponding PSD consequently form a pseudo-Gaussian distribution. A change of 0.2 in the L* can vary the PSD by 30%. By taking L* and PSD at different locations from the above magnetospheres, the PSD radial profile is found to be shift but with its shape retained.

Radiation belt data assimilation using RAM-SB magnetospheric field configuration

The LANL-GEO and POLAR spacecraft flux measurements are converted to PSD data for assimilation of the radiation belt electron distribution during a moderate geomagnetic storm event in Dec 19-22, 2002. While he "flux-to-PSD' conversion is highly dependent on interpolation method along the process, the cubic-spline interpolation method is found to be sufficiently more accurate than linear interpolation method in producing reliable PSD input data. Using localized adaptive inflation (LAI) technique in the ensemble Kalman filter enables successful data assimilation by appropriately accounting for model errors. Since the L* is highly dependent on the magnetic field model utilized, we compared above assimilated results with that using an empirical model Tsyganenko 2001 magnetic field configuration in converting the PSD data. The two assimilated radiation belts show similarities in terms of capturing dynamic features in the storm, including the peak location, dropout, and recovery of the phase space density. By comparing the predicted flux from the data assimilation with flux observation from an independent satellite, we found that using the RAM-SCB magnetic field configuration for obtaining PSD data for the data assimilation provides better estimation of the radiation environment, implying that the RAM-SCB models a more realistic representation of the global magnetospheric configuration.

Impact on National Missions

This program has built a tool to calculate particle drift shells in the inner magnetosphere. The computational speed is at least six orders of magnitudes faster than standard integration techniques. The tool has enabled us, for the first time, to develop high precision space weather data assimilation and forecasting models, which are an important component to NOAA Space Weather Prediction Center and DoD Air Force Research Lab and Space Command. Understanding the space environment is critical to fielding the satellite systems that are needed to monitor nuclear nonproliferation. The underlying space physics builds capability to understand the effects of nuclear detonations in space, supporting stockpile stewardship.

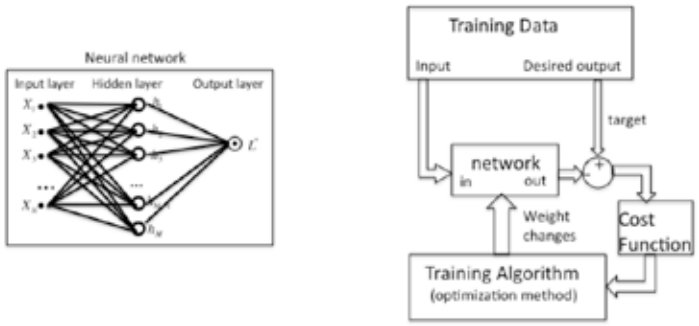

Figure 1. Left: The architecture of a multi-layer neural network. Right: The learning/training procedure of a neural network.

References

1. Yu, Y., J. Koller, S. Zaharia, and V. Jordanova. L* Neural Network from Different Magnetospheric Field Models. 2012. Space Weather. : S02014.

2. Yu, Y., V. Jordanova, S. Zaharia, J. Koller, J. Zhang, and L. Kistler. Validation Study of the Magnetically Self-Consistent Inner Magnetosphere Model RAMS-SCB. 2012. Journal of Geophysical Research - Space Physics. 117 (A03222): 1.

3. Yu, Y., and A. Ridley. Exploring the influence of ionospheric heavy ion outflow on magnetospheric dynamics: dependence on the source location. To appear in Journal of Geophysical Reserach.

4. Yu, Y., J. Koller, and S. Morley. Quantifying the effect of magnetopause shadowing on radiation belt electron dropout. To appear in Journal of Geophysical Research.

5. Rastaetter, L., and Y. Yu. Geospace Environment Modeling 2008-2009 Challenge: Dst Index. To appear in Space Weather.

6. Yu, Y., J. Koller, V. Jordanova, and S. Zaharia. On the L* neural network and its accuracy. Journal of Geophysical Research.

7. Yu, Y., J. Koller, V. Jordanova, S. Zaharia, and H. Godinez. Radiation Belt Data Assimilation using RAM-SCB Magnetic Field Configuration. Journal of Geophysical Research.

Publications

Rastaetter, L., and Y. Yu. Geospace Environment Modeling 2008-2009 Challenge: Dst index. To appear in Journal of Geophysical Research.

Yu, Y., J. Koller, S. Zaharia, and V. Jordanova. L* Neural Network from Different Magnetospheric Field Models. 2012. Space Weather. : S02014.

Yu, Y., J. Koller, V. Jordanova, S. Zaharia, and H. Godinez. Radiation belt data assimilation using RAM-SCB magnetic field configuration. Journal of Geophysical Research.

Yu, Y., J. Koller, V. Jordanova, and S. Zaharia. On the L* neural network and its accuracy. Journal of Geophysical Research.

Yu, Y., J. Koller, and S. Morley. Quantifying the Effect of Magnetopause Shadowing on Radiation Belt Electron Dropout. Journal of Geophysical Research.

Yu, Y., V. Jordanova, S. Zaharia, J. Koller, J. Zhang, and L. Kistler. Validation Study of the Magnetically Self-Consistent Inner Magnetosphere Model RAMS-SCB. 2012. Journal of Geophysical Research - Space Physics. 117 (A03222): 1.

Yu, Y., and A. Ridley. Exploring the Influence of Ionospheric Heavy Ion Outflow on Magnetospheric Dynamics: Dependence on the Source Location. To appear in Journal of Geophysical Research.

"Listening" to the Noise of a Single Electron Spin: Ultra-sensitive, Non-perturbative Spin Noise Spectroscopy

Scott A. Crooker
20110747PRD3

Abstract

Measurement of electron and nuclear spins forms the basis of modern magnetic resonance technologies such as NMR, MRI, and electron spin resonance. Driven by the desire and need for ever-increasing sensitivity and resolution (e.g., for MRI), the number of detected spins necessarily decreases. The goal of this project is to reach the limit of *single* quantum-mechanical spins – that is, a single electron -- and to measure the intrinsic fluctuations of that single spin. At present, however, the direct magnetization measurement of a single spin is a tremendously difficult proposition, due to the extreme sensitivity required (conventional NMR or MRI lacks the sensitivity by about a factor of a trillion!). Nonetheless, from viewpoints of both fundamental measurement and basic science, single-spin detection represents a truly landmark achievement in measurement science. Recent advances in optical detection and efficient digital signal processing, coupled with alternative measurement approaches based on passive spin noise detection (rather than conventional perturbative studies), suggest a viable route that forms the basis of this work.

Background and Research Objectives

Not all noise in experimental measurements is unwelcome. Certain fundamental noise sources contain extremely valuable information about the system itself – a classic example being the inherent voltage fluctuations that exist across any resistor (Johnson noise), from which temperature can be determined. In magnetic systems, fundamental noise exists in the form of small, random spin fluctuations. For example, statistical fluctuations of N paramagnetic spins should generate "spin noise" of order sqrt(N), even in zero magnetic fields. Crucially, the frequency spectra of these tiny fluctuations - if measurable - reveal the important dynamic properties of the spins (such as spin precession frequencies, decoherence times, and interparticle couplings), without ever having to excite, pump, or drive the spin ensemble away from thermal equilibrium. Such a noise-based approach to spin resonance is in marked contrast to conventional nuclear- or electron-spin resonance measurements, which necessarily perturb the spins. Nevertheless, this approach is guaranteed by the Fluctuation-Dissipation Theorem. Importantly, noise-based measurements become viable alternatives to conventional (dissipative) methods as the few-particle limit is approached (N→1), since noise signals fall only as sqrt(N) rather than as N.

Our scientific goal was therefore to develop an ultra-sensitive magnetometer capable of "listening" to the tiny spin fluctuations of truly quantum-mechanical objects: single electron spins trapped in semiconductor quantum dots. New instrumentation for efficient digital signal processing based on configurable hardware (FPGAs) are essential to this work.

Scientific Approach and Accomplishments

Yan Li, the postdoc supported by the project, has successfully demonstrated that our scheme for using lasers to sensitively measure spin fluctuations works -- and works very well -- for electrons trapped in semiconductor quantum dots. We completed our first set of measurements, wherein we showed that not only are spin fluctuation signals measurable using the optical techniques that we proposed, but that the data are of sufficient quality to achieve a detailed understanding of spin relaxation and coherence for the case of electron spins in semiconductor quantum dots. This initial work was written up and published in the high-profile journal Physical Review Letters (Yan Li et al), and the paper was especially highlighted by the journal Editors. The reference can be found in the reference section below.

As a result of her data, our theoretical component has made significant advances in our understanding of how single electron spins couple to a bath of nuclear spins (directly addressing the "central spin problem" -- a topic of hot theoretical interest). This work was also submitted to and was accepted at Physical Review Letters.

Again, as a result of Yan's data, our close collaboration with the Dortmund and Bochum University groups of Professor Manfred Bayer and Dirk Reuter continues. We have just published a joint theoretical/experimental paper on the use of these new experimental techniques as a high-resolution spectroscopic tool. Again, this paper was accepted at the prestigious journal Physical Review Letters (Zapasskii et al).

In November 2012 Yan finished construction of the new ultra-stable single-quantum dot microscope, which works very well. Yan has shown that we can measure the absorption from a single quantum dot, which is a remarkable achievement. She is currently measuring noise signals from this quantum dot – thereby achieving our goals. We are currently writing up these results for publication.

Impact on National Missions

This project will build Laboratory capabilities in the development of novel measurement methods that enable new scientific discovery at Los Alamos National Laboratory. It is based on recent technological advancements that enable the use of FPGAs and on the very large data storage and manipulation capabilities that have now become available. Our basic approach to noise spectroscopy goes well beyond the specific example of electron spin noise that will be investigated here and the advantages of noise spectroscopy as an experimental probe are very general. The project will advance new Laboratory capabilities that underpin a wide variety of Laboratory missions. Demonstration of single spin noise spectroscopy measurements will generate worldwide attention and will form a robust platform for nanoscale spintronics at LANL. The team will work with DOE program managers to develop a BES Materials Science funded program and to obtain DARPA funding for extending this work.

Publications

Li, Y., N. Sinitsyn, D. L. Smith, D. Reuter, A. D. Wieck, D. R. Yakovlev, M. Bayer, and S. A. Crooker. Intrinsic spin fluctuations reveal the dynamical response function of holes coupled to nuclear spin baths in (In,Ga)As quantum dots . 2012. Physical Review Letters. 108: 186603.

Sinitsyn, N. A., Y. Li, S. A. Crooker, A. Saxena, and D. L. Smith. Role of nuclear quadrupole coupling on decoherence and relaxation of central spins in quantum dots . 2012. Physical Review Letters. 109: 166605.

Zapasskii, V. S., A. Greilich, S. A. Crooker, Y. Li, G. G. Kozlov, D. R. Yakovlev, and M. Bayer. Optical spectroscopy of spin noise . 2013. Physical Review Letters. 110: 176601.

Zhang, S. X., S. A. Dayeh, Y. Li, S. A. Crooker, D. L. Smith, and S. T. Picraux. Electrical spin injection and detection in silicon nanowires through oxide tunnel barriers . 2013. Nano Letters. 13: 430.

Determining the Origin of the Highest Energy Cosmic Rays with TeV Gamma-ray Observations

Brenda L. Dingus
20110749PRD3

Abstract

Ultra-high energy cosmic rays are the most energetic particles known. The highest energy cosmic rays (CR) have energy greater than 1020 eV, the energy an average person expends throwing a baseball. Where do they come from? How do they get their energy? One idea is that they are accelerated in the flares of active galactic nuclei (AGN). To test the AGN flare idea, my research goal has been to measure and characterize AGN flares with TeV gamma rays – when CR are accelerated, very high energy gamma rays are also created. My instrument for this purpose is the High-Altitude Water-Cherenkov (HAWC) Gamma-ray Observatory. HAWC is a new ground-based, wide field-of-view instrument that operates in the 100 GeV to 100 TeV band. It is currently under construction in Mexico. It is an ideal instrument for measuring TeV transients from AGN.

My main objectives for this research project were to assist in the design and construction of the HAWC instrument and to develop the data analysis tools required to measure AGN transients. These objectives have been completed. During the construction and design of HAWC, I took a lead role in the mechanical design of the detector, the pre-installation testing of photo-sensors, analysis of muon events for calibration and verification, and the development of the software required to detect AGN transients. The HAWC instrument is scheduled to begin science operations by August 1, 2013. In the coming months we will collect data that will constrain the idea that flares from active galaxies accelerate the highest energy CR.

Background and Research Objectives

Cosmic rays (CR) are charged particles, mainly protons and atomic nuclei, that constantly bombard the earth from space. The highest energy CR have energy greater than 10^20 eV. The existence of these particles has been a mystery ever since they were first discovered several decades ago. In 2007, my colleagues and I showed that the arrival directions of the highest energy CR are correlated with the directions of nearby active galaxies [1, 2]. This suggests that active galaxies accelerated CR, but the body of evidence is far from conclusive. My research goal has been to observe active galaxies in high energy gamma rays for evidence of particle acceleration (gamma rays are created in the particle acceleration process). In particular, I have been interested in measuring the transient emission from active galaxies because there is theoretical guidance that the highest energy CR are accelerated in short lived flares (e.g., [3]). A thorough study of the transient emission of TeV gamma-rays from active galaxies will greatly increase our knowledge of the origin of the highest energy CR.

My tool for measuring transient phenomenon from AGN is the High-Altitude Water-Cherenkov (HAWC) Gamma ray Observatory. HAWC is a new ground-based instrument that observes about a third of the overhead sky with regardless of weather, Sun, or Moon. Its energy band is 100 GeV to 100 TeV. The instrument is comprised of an array of 300 water-Cherenkov detectors (WCDs). Each WCD consists of a 50,000 gallon steel water tank instrumented with four photomultiplier tubes (PMT). A recent picture of the HAWC observatory is shown in Figure 1. In Figure 2, we show pictures a WCD being constructed

LANL has taken a lead roll in designing and deploying the HAWC instrument. The HAWC fabrication project is funded by DOE, LDRD, NSF, and CONACyT (Mexico) moneys; however, these funds do not pay for the work of scientists on the fabrication. My main objectives for this research project were to provide additional inputs to the design and construction of the HAWC instrument that make possible observations of AGN transients, and to develop the data analysis tools required to measure them.

Scientific Approach and Accomplishments

Over the first year of this project, HAWC was mostly in the design phase and pre-deployment phase. During this time, I took on responsibilities in the areas of mechanical design and the pre-installation testing of the photo-multiplier tubes. Over the second year of this project, HAWC was mostly in the deployment phase. During this time, I have been involved in commissioning the part of the detector that is deployed (i.e., calibration and sanity checks) and developing data analysis methods. My accomplishments are described in the following subsections.

Pre-installation testing of PMTs

I have been in charge of all the pre-installation testing and characterization of the 1200 photo-multiplier tubes (PMT) for the HAWC detector. Nine hundred of the tubes are Hamamatsu R5912 (8") tubes and 300 are Hamamatsu R7081 (10") tubes. All the testing is performed at Los Alamos National Laboratory (LANL) by myself or by students under my direction. The raw data from the tests are reduced down to several parameters for each tube. These parameters include gain, relative quantum efficiency, dark rate, time response, after-pulse rate, pre-pulse rate and several other parameters particular to our data acquisition system design. I wrote a significant fraction of the software that reduces the raw test data into these parameters, and I designed how these parameters are organized and stored.

In Figure 3 we show the measured gain vs. the measured time-over-threshold (TOT) for single photo-electron events. TOT is the unit of amplitude that is used with the HAWC data acquisition system. This plot shows how a measurement of single PE events in TOT units can be used to determine the gain of a particular PMT.

I organized the PMTs into gain-matched batches and decided their order of deployment into the detector. Currently, 90% of the PMTs are tested and 60% of the PMTs are batched for deployment into the instrument. I authored an internal note describing the PMT testing [4].

Calibration and sanity checks

Because HAWC is deployed modularly, useful scientific data can be acquired before the full detector array is deployed. Indeed, at least 10% of the HAWC detector has been operating since September 2012.

It is important that the first data from the experiment is thoroughly checked and calibrated. For this purpose, I have developed a method of selecting muon events from the raw data. Muons are a part of the natural cosmic radiation, and they deposit a characteristic amount of energy into the HAWC WCD. Thus, muons are an excellent standard candle that can be used to test and calibrate the HAWC WCDs. I have developed an algorithm to use muon events for calibrating the instrument and verifying the detector simulation. This is a key step in the commissioning of the detector.

In Figure 4 we show the distribution of PMT signals in a single WCD after we select for times when the tank is hit by a vertical, centered (VC) muon. PMTs A & B have a similar signal distribution. PMT D has a different distribution which may indicate this tube has a higher quantum efficiency or in rotated in such a way that is has greater efficiency at collecting PEs for the geometry of a VC muon event.

Algorithm to search for transients

The analysis of data from the HAWC instrument is not trivial. Higher energy events have better angle and energy resolution and better background rejection. This has to be taken into account to get the most information from HAWC data. With this in mind, I developed a method to search for AGN transients using a binned log-likelihood method.

The method compares two hypotheses. The null hypothesis is that a particular AGN is in a quiet (normal) state. The alternative hypothesis is that the AGN is in a loud (active) state of a certain amplitude and duration. The data is binned in time and in a parameter that is a proxy for energy. The size of the time bin is ~10 minutes (e.g., HAWC will detect 1 photon with an energy greater than 2 TeV from the crab every 10 minutes – the method does not assume large-number statistics). The number of energy proxy bins is 14 (i.e., there are 14 different data streams).

If the alternative hypothesis fits the data significantly better, taking into account the additional two degrees of freedom, the AGN is judged to be in a loud state. The significance level can be set to any level.

This algorithm will be setup to run automatically for a predetermined set of AGN (i.e., a targeted search). If an AGN is determined to be in a loud state, HAWC personnel will be notified. A person will then judge whether to send out an alert to the broader astronomical community (e.g., for multi-wavelength observations). The alert will contain our estimated amplitude and current duration of the flare and a post-trial significance.

This works well with the complex data stream that comes from the HAWC instrument. In Figure 5, we show a simulated detection of a transient event. The event, though barely noticeable by eye, is judged by the algorithm to be a flare with high significance. The fitted loud state is quite similar to what was simulated.

Involvement with the Pierre Auger Collaboration
During this project, I have maintained my affiliation with the Pierre Auger Collaboration, which operates the world's largest aperture, ultra high energy cosmic ray observatory in Argentina. I have been an Auger collaborator since 2005. My science objectives for this project are not only part of the HAWC Collaboration's science objectives but they are also part of Auger's.

I am currently affiliated with the Auger group at the University of New Mexico. I attended meetings of the Auger groups in the United States in 2011 and 2012. I have been working with a student from Case Western on extending an idea about constraining the angular size of UHECR sources, which I published in 2011. I will be giving a review talk at the International Cosmic Ray Conference in July 2013 on UHECR in the Galaxy. Following this conference, I will be operating a shift at the Auger Observatory.

Impact on National Missions

This work is most closely tied to the High Energy Physics program of the DOE Office of Science. The HAWC observatory has been recognized by several National Academy studies as an important project and as making fundamental observations of the high energy Universe. More broadly, projects involving this sort of measurements at the extremes bring to the Laboratory talent and ideas that carry over to sensing missions for homeland security and nuclear non-proliferation.

Figure 1. The HAWC Site in May 2013. The instrument is ~30% deployed.

Figure 2. On the left, a custom jack-stand being installed by Patrick Younk. On the right, a work crew assembling the roof of the WCD structure.

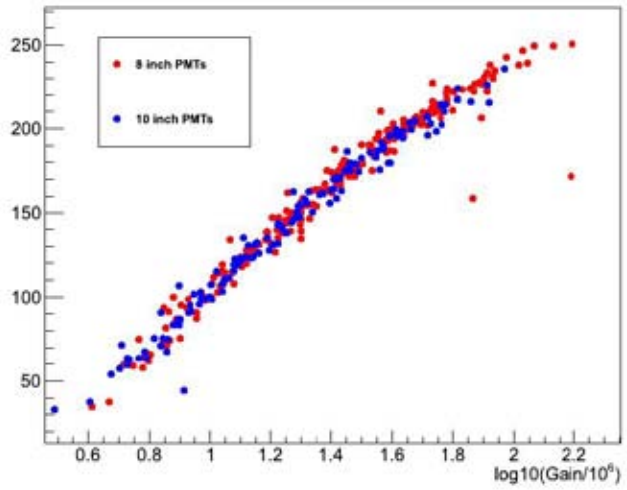

Figure 3. Time Over Threshold (ns) vs. Gain for HAWC PMTs.

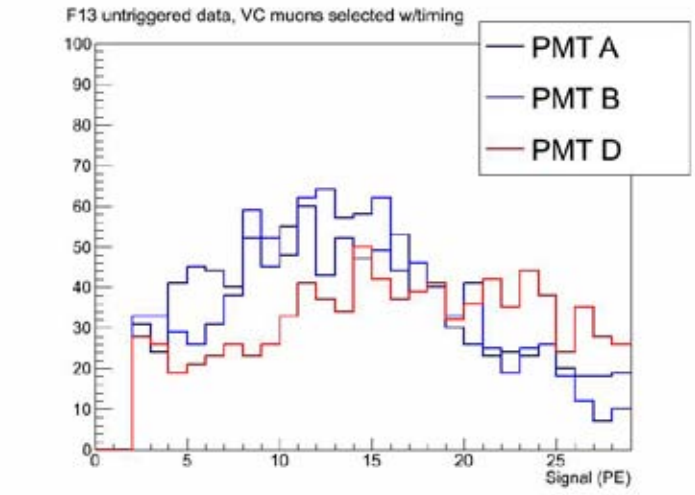

Figure 4. Signal distribution for PMTs in a single WCD for vertical, centered muon events.

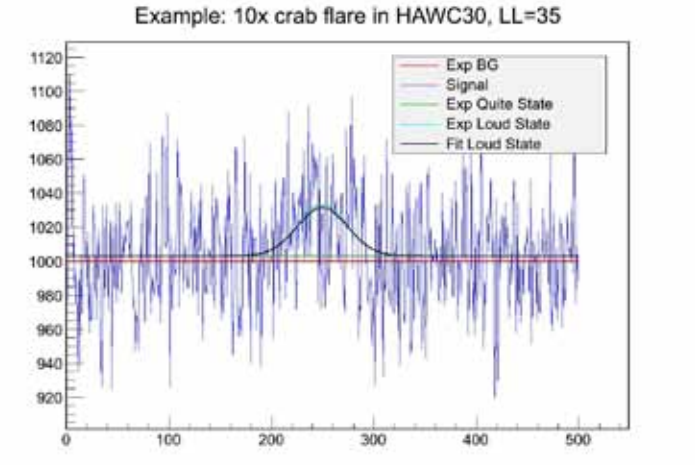

Figure 5. Detection of a simulated flare of the crab nebula. The unit of the x-axis is time / (30 minutes). The unit of the y-axis is number of particles.

References

1. Collaboration, P. Auger. Correlation of the Highest-Energy Cosmic Rays with Nearby Extragalactic Objects. 2007. Science. 318 (5852): 938.

2. Collaboration, P. Auger. Correlation of the highest-energy cosmic rays with the positions of nearby active galactic nuclei. 2008. Astroparticle Physics. 29 (3): 188.

3. Farrar, G. R., and A. Gruzinov. Giant AGN flares and cosmic ray bursts . 2009. Astrophysical Journal. 693: 329.

4. Karn, P., R. Lauer, and P. W. Younk. The pre-installation testing of the HAWC photomultiplier tubes. 2013. HAWC Internal Technical Note.

Publications

A method to constrain the characteristic angular size of the brightest cosmic-ray sources observed above 57 × 1018 eV. 2011. Astrophysics and Space Sciences Transactions. 7 (3): 403.

Abreu, P., M. Aglietta, E. J. Ahn, I. F. M. Albuquerque, D. Allard, et.al, Measurement of the Proton-Air Cross Section at root s=57 TeV with the Pierre Auger Observatory. 2012. PHYSICAL REVIEW LETTERS. 109 (6): -.

Abreu, P., M. Aglietta, E. J. Ahn, I. F. M. Albuquerque, D. Allard, et. al, Search for signatures of magnetically-induced alignment in the arrival directions measured by the Pierre Auger Observatory. 2012. ASTROPARTICLE PHYSICS. 35 (6): 354.

Abreu, P., M. Aglietta, E. J. Ahn, I. F. M. Albuquerque, D. Allard, et. al., The Lateral Trigger Probability function for the Ultra-High Energy Cosmic Ray Showers detected by the Pierre Auger Observatory (vol 35, pg 266, 2011). 2012. ASTROPARTICLE PHYSICS. 35 (10): 681.

Abreu, P., M. Aglietta, E. J. Ahn, I. F. M. Albuquerque, D. Allard, et.al, Search for first harmonic modulation in the right ascension distribution of cosmic rays detected at the Pierre Auger Observatory. 2011. ASTROPARTICLE PHYSICS. 34 (8): 627.

Abreu, P., M. Aglietta, M. Ahlers, E. J. Ahn, I. F. M. Albuquerque, D. Allard, et. al., A search for anisotropy in the arrival directions of ultra high energy cosmic rays recorded at the Pierre Auger Observatory. 2012. JOURNAL OF COSMOLOGY AND ASTROPARTICLE PHYSICS. (4): -.

Abreu, P., M. Aglietta, M. Ahlers, E. J. Ahn, I. F. M. Albuquerque, D. Allard, et.al., CONSTRAINTS ON THE ORIGIN OF COSMIC RAYS ABOVE 10(18) eV FROM LARGE-SCALE ANISOTROPY SEARCHES IN DATA OF THE PIERRE AUGER OBSERVATORY. 2013. ASTROPHYSICAL JOURNAL LETTERS. 762 (1): -.

Abreu, P., M. Aglietta, M. Ahlers, E. J. Ahn, I. F. M. Albuquerque, D. Allard, et., al, LARGE-SCALE DISTRIBUTION OF ARRIVAL DIRECTIONS OF COSMIC RAYS DETECTED ABOVE 10(18) eV AT THE PIERRE AUGER OBSERVATORY. 2012. ASTROPHYSICAL JOURNAL SUPPLEMENT SERIES. 203 (2): -.

Abreu, P., M. Aglietta, M. Ahlers, E. J. Ahn, I. F. M. Albuquerque, D. Allard, et. al., A SEARCH FOR POINT SOURCES OF EeV NEUTRONS. 2012. ASTROPHYSICAL JOURNAL. 760 (2): -.

Abreu, P., M. Aglietta, M. Ahlers, E. J. Ahn, I. F. M. Albuquerque, D. Allard, et. al., SEARCH FOR POINT-LIKE SOURCES OF ULTRA-HIGH ENERGY NEUTRINOS AT THE PIERRE AUGER OBSERVATORY AND IMPROVED LIMIT ON THE DIFFUSE FLUX OF TAU NEUTRINOS. 2012. ASTROPHYSICAL JOURNAL LETTERS. 755 (1): -.

Abreu, P., M. Aglietta, M. Ahlers, E. J. Ahn, I. F. M. Albuquerque, D. Allard, et. al., Ultrahigh Energy Neutrinos at the Pierre Auger Observatory. 2013. ADVANCES IN HIGH ENERGY PHYSICS. : -.

Abreu, P., M. Aglietta, M. Ahlers, E. J. Ahn, I. F. M. Albuquerque, I. Allekotte, et.al., Interpretation of the depths of maximum of extensive air showers measured by the Pierre Auger Observatory. 2013. JOURNAL OF COSMOLOGY AND ASTROPARTICLE PHYSICS. (2): -.

Settimo, M., P. Abreu, M. Aglietta, M. Ahlers, E. J. Ahn, I. F. M. Albuquerque, D. Allard, et. al., Measurement of the cosmic ray energy spectrum using hybrid events of the Pierre Auger Observatory. 2012. EUROPEAN PHYSICAL JOURNAL PLUS. 127 (8): -.

Younk, P., and M. Risse. Sensitivity of the correlation between the depth of shower maximum and the muon shower size to the cosmic ray composition. 2012. ASTROPARTICLE PHYSICS. 35 (12): 807.

Probing the Nucleon Structure via Spin Observables

Ivan M. Vitev
20110755PRD4

Abstract

Understanding the nucleon structure in terms of its basic building blocks (quarks and gluons) is of fundamental importance to science, and has entered a new era in recent years. Although there is great progress in the past few decades in understanding the longitudinal motion of quarks and gluons inside fast moving nucleons in high-energy collider experiments, their transverse motion is still largely unknown because these momentum components are small. In order to reliably extract this information and, thus, build a three dimensional image of the nucleon, we developed theoretical techniques and computational tools to describe the experimental data in both semi-inclusive deep inelastic lepton-proton scattering and proton-proton collision experiments in a unified framework. In particular, we derived the evolution equations for the relevant quark and gluon distributions inside the nucleon, which enable us to describe simultaneously the experimental data at different collision energies. We performed a first global fitting of available experimental data and successfully extracted the information on the quark and gluon's transverse motion. Results from our project were shown to be critical for the accurate modeling and reliable interpretation of the data from the current and future high energy nuclear experiments, in particular those at Jefferson Lab and Brookhaven National Laboratory. This research has helped position LANL as a major player in the theoretical effort to understand the quark and gluon transverse motion in nucleons, relevant to experiments at all collider facilities that push the limits of our understanding of the theory of strong interactions at very high energies.

Background and Research Objectives

The exploration of the internal structure of the nucleon in terms of quarks and gluons (partons), the degrees of freedom of Quantum Chromodynamics (QCD), has been and still is at the frontier of high-energy nuclear physics research. Concurrent advances in the experimental use of high energy scattering processes and theoretical breakthroughs in understanding "asymptotic freedom" and developing the perturbation theory of strong interactions have provided a way of mapping out the internal landscape of protons and neutrons. Specifically, perturbative QCD allows one to prove "factorization theorems" for high-energy processes, which state that the physics observables can be written as a convolution of short-distance partonic cross sections and long-distance parton distribution functions (PDFs) that encode the bound state properties, or structure, of colliding nucleons. Armed with these theorems, theorists are then able to extract the low-energy properties of the nucleon structure from the experimental data. In past decades, a one-dimensional picture of nucleons has emerged, in the sense that we "only" learned about the longitudinal motion of partons in fast moving protons and neutrons, as encoded in the so-called collinear PDFs. A boosted nucleon is Lorentz-contracted but its transverse size is still about 1 fm, which is large in comparison to the scale of the strong interactions. An important and yet unresolved question is what role the parton's transverse motion may play. To describe the quarks in the transverse plane in momentum space, one introduces the so-called Transverse Momentum Dependent PDFs (TMDs). TMDs provide new and much richer information on the nucleon structure: they allow for the first time to carry out 3D imaging of the nucleon. This novel concept will also help address the long-standing questions concerning the motion of quarks and gluons inside the nucleon. How do they move in the transverse plane? Do they orbit, and carry orbital angular momentum? Is there a quantum correlation between the motion of quarks, their spin and the spin of the nucleon?

Spin-dependent observables are the most sensitive probes of nucleon TMDs, as the spin can correlate with the transverse momentum of the partons. The main goal of our project is to develop a solid theoretical framework that will be used for reliable extraction of TMDs from experimental data in high-energy spin-dependent ex-

periments. To achieve this goal, we need both better first-principle understanding of TMDs and new simulation tools. We will first focus on the novel Sivers function, which has become the hottest topic in the field. It represents the distribution of unpolarized quarks in a transversely polarized nucleon through a correlation between the quark's transverse momentum and the nucleon polarization vector. A unique property of the Sivers function is that it is expected to be non-universal, while all the collinear PDFs are universal. The Sivers function changes sign when probed in semi-inclusive lepton-proton deep inelastic scattering (SIDIS) and in Drell-Yan (DY) production in proton-proton collisions. This dramatic prediction is deeply rooted in the fundamental properties of QCD and its experimental verification is among the highest DOE Nuclear Physics priorities. Some initial efforts to extract the Sivers functions from SIDIS have begun, though the method is very crude. We will improve the theoretical methods by resuming subsets of partonic scattering processes to all orders in perturbation theory. This, in turn, will allow for rigorous understanding of the Sivers effect. On the other hand, to link all the experimental TMD efforts together, one needs to derive the energy evolution of the relevant TMDs. Once both ingredients are developed, we will perform a global analysis of the experimental data currently available at Jefferson Lab, HERMES at DESY, COMPASS at CERN, and the Relativistic Heavy Ion Collider (RHIC) at BNL to reliably extract the Sivers function.

Scientific Approach and Accomplishments

In the past year we have achieved the major goals outlined in our proposal. Specifically, one most important ingredient in the unified theoretical formalism for analyzing the quarks and gluon TMDs has been developed. With this formalism in hand we performed for the first time the global fitting of the world data from the spin-dependent experiments and extracted successfully and consistently the quark and gluon transverse momentum distributions inside the nucleon. We focused mainly on the Sivers function and studied the associated quark and gluon dynamics and its implications for the fundamental spin theory.

We first derived the evolution equations for the quark and gluon distributions inside the nucleon. They are related to the first transverse-momentum moment of the Sivers function and, thus, describe the average transverse motion for quarks and gluons inside a transversely polarized nucleon. These evolution equations tell us how quark and gluon distributions change as a response to the momentum scale of the external experimental probe. They provide a way to link and describe all the experimental data with different collision energies in a unified and consistent manner. Our work was recently published in Physics Letters B [1].

To improve the current theoretical formalism and provide an analysis tool for the phenomenology, we further worked out the spin-dependent cross section in the SIDIS process too much higher precision (known as next-to-leading order). We verified the consistency of the theory to an even higher order in perturbation theory. By doing so, we provided for the first time the next-to-leading order spin-dependent quark and gluon cross sections at the short-distance. Coincidently, we derived the QCD evolution for their distribution. We found that our evolution equations agree with those derived from a different approach in our previously published paper [1]. Our new results appeared this year in Physical Review D [2]. It has already attracted attentions from a large experimental group, the COMPASS experiment at CERN. COMPASS plans to perform analysis of the data using our improved formalism in the future.

There are two different reactions, used world wide, to study the spin-dependent observables and thus to extract the parton transverse motion. The first one is the so-called semi-inclusive deep inelastic lepton-proton scattering, with experiments performed at Jefferson Lab and at CERN. The other one is the polarized proton-proton collisions, with experiments currently performed at RHIC at BNL. These two processes involve very different quark and gluon dynamics at the partonic level. At the same time, they are operated in very different collision energies and kinematic regime. Thus, it has been a great challenge, see Ref. [3], to describe both reactions within a unified theoretical framework. Recently, we carefully analyzed the relation between these two processes and were able to find a close connection between them. Combining this newly discovered relation with the evolution equations we derived, we are ready to analyze these world spin data within a unified theory. Such an analysis has just been finished and our paper [4] has been submitted to Physical Review Letters.

The community has recognized the importance of this work. As a result, Dr. Kang was recently invited to present a plenary talk at the upcoming fifth Workshop of the APS Topical Group on Hadronic Physics.

We were able to achieve a reasonable description for both lepton-proton and proton-proton collisions and validate our theoretical formalism, see Figures 1 and 2. To further test our approach and the theoretical formalism developed by us, we recently also proposed to make new measurements at RHIC. The new observable is related to prompt photon production. This proposal and prediction has now been published in Physics Letters B [5]. It has already been adopted as part of the suite of future spin measurements at RHIC. Figure 3 shows the projected experimental error bars compared to our theoretical predictions.

We have recently also studied the Sivers effect in the Drell-Yan process to test the non-universality (sign change) of the Sivers function. This result is now published in Physical Review D Ref. [6].

We made significant progress and laid the foundation for the future investigation of the internal partonic structure in fast moving nucleons in high-energy collisions. This LDRD project supported the publication of five peer-reviewed papers and one conference proceeding. We gave a total of eight invited presentations that include the results from this research. The current Director's Postdoctoral Fellow Dr. Zhongbo Kang was recently awarded the distinguished J. Robert Oppenheimer Fellowship.

Impact on National Missions

Spin physics is one of the cornerstones of the Nuclear Physics program in the DOE Office of Science portfolio. To understand transverse momentum distributions is one of the major goals in this field. Besides providing 3D-imaging information for the nucleon structure, TMDs are also deeply connected to the fundamental QCD properties - the color gauge invariance and the dynamics at very short distances. This research will allow scientists to accurately and reliably extract such information from the existing experimental facilities at Jefferson Lab, HERMES, COMPASS and RHIC, thus providing new insights into the nucleon structure and associated novel QCD dynamics. It also provides much-needed theoretical guidance for, and interpretation of, the experimental results from the flagship hadronic and nuclear physics program at LANL. In the future, the outcome of our theoretical work will help firm the scientific case for a future Electron Ion Collider, and, in particular, its spin program.

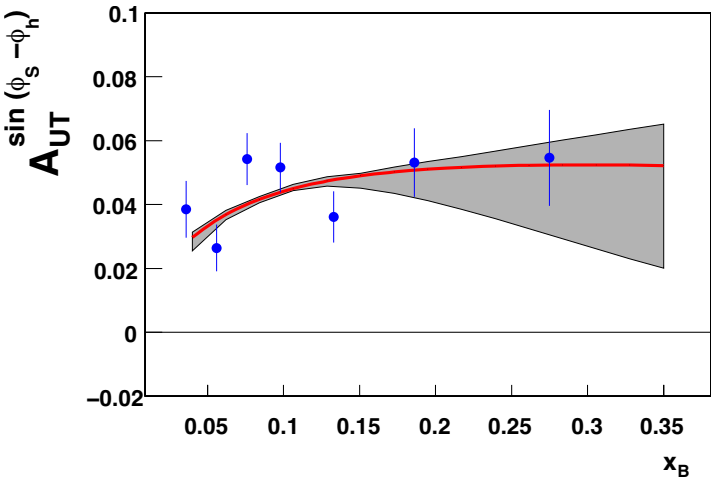

Figure 1. Description of SIDIS Sivers asymmetry from HERMES in Ref. [4].

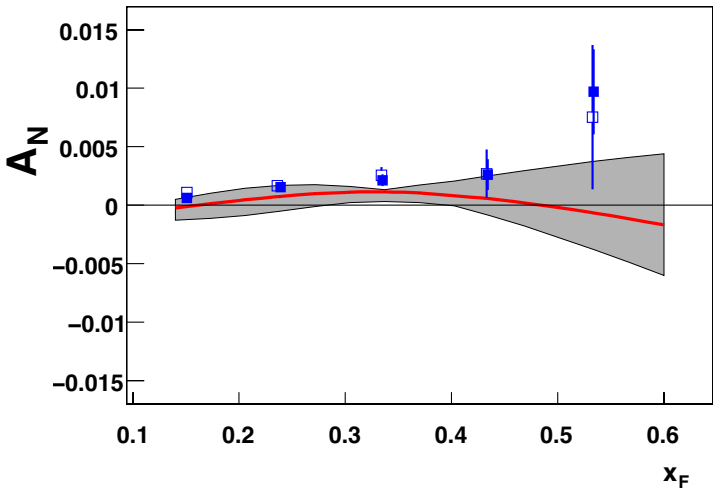

Figure 2. Description of single inclusive jet production in polarized proton-proton collisions in Ref. [4].

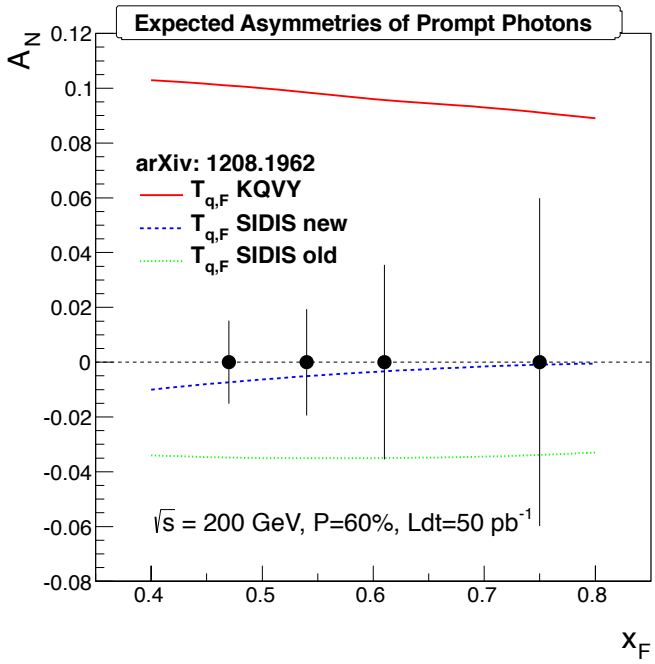

Figure 3. Experimental projection on prompt photon production compared with various theortical predictions in Ref. [5].

References

1. Kang, Z., and J. Qiu. QCD evolution of naive-time-reversal-odd parton distribution functions. 2012. PHYSICS LETTERS B. 713 (3): 273.

2. Kang, Z., I. Vitev, and H. Xing. Transverse momentum-weighted Sivers asymmetry in semi-inclusive deep inelastic scattering at next-to-leading order. 2013. PHYSICAL REVIEW D. 87 (3): 034024.

3. Kang, Z., J. Qiu, W. Vogelsang, and F. Yuan. An observation concerning the process dependence of the Sivers functions. 2011. PHYSICAL REVIEW D. 83: 094001.

4. Gamberg, L., Z. Kang, and A. Prokudin. Indication of the process-dependence of the Sivers effect. PHYSICAL REVIEW LETTERS.

5. Gamberg, L., and Z. Kang. Single transverse spin asymmetry of prompt photon production. 2012. PHYSICS LETTERS B. 718: 181.

6. Kang, Z., and B. Xiao. Sivers asymmetry of Drell-Yan production in small-x regime. 2013. PHYSICAL REVIEW D. 87: 034038.

Publications

Kang, Z. B., I. Vitev, and H. Xing. Transverse momentum-weighted Sivers asymmetry in semi-inclusive deep inelastic scattering at next-to-leading order. 2013. Physical Review D. 87 (3): 034024.

Kang, Z. B., L. Gamberg, and A. Prokudin. Indication on the process-dependence of the Sivers effect . Physical Review Letters.

Kang, Z. B., and B. W. Xiao. Sivers asymmetry of Drell-Yan production in the small-x regime. 2013. Physical Review D. 87 (3): 034038.

Kang, Z. B., and J. W. Qiu. QCD evolution of naive-time-reversal-odd parton distribution functions. 2012. Physical Letters B. 713 (3): 273.

Kang, Z. B., and J. W. Qiu. QCD evolution of naive-time-reversal-odd quark-gluon correlation functions . 2012. In QCD EVOLUTION WORKSHOP 2012. (Newport News, VA, USA, 14-17 May 2012). Vol. 20, p. 118. Singapore: International Journal of Modern Physics.

Kang, Z. B., and L. Gamberg. Single transverse spin asymmetry of prompt photon production. 2012. Physics Letters B. 718 (1): 181.

Data Mining for the M-sigma Relation

Aimee L. Hungerford
20110757PRD4

Abstract

The surprising discovery of a tight relationship between the mass of a supermassive black hole and the properties of its host galaxy's bulge has shaped the direction of extragalactic astronomy research over the past decade. To test the leading theory for the origin of this relation, the major merger of two galaxies, we turn to the Cosmic Assembly Near-Infrared Deep Extragalactic Legacy Survey (CANDELS). The data from this largest ever allocation of Hubble Space Telescope time has provided us with the first snapshot of the rest-frame optical properties of high-redshift AGN (active galactic nuclei) and their hosts. Our comparison of the host galaxy morphologies of X-ray and infrared-selected AGN in CANDELS indicates that mergers may indeed be responsible for driving the growth of AGN and their hosts, at least at high luminosities, high-redshifts, and/or large obscuration. A detailed photometric study of these objects, enabled by LANL's supercomputing resources, will continue to provide much needed information about these elusive sites of black hole growth, and will inform our understanding of the growth of structure in the Universe.

Background and Research Objectives

Supermassive black holes (SMBHs) are now known to reside at the center of nearly all-massive galaxies. When actively accreting as active galactic nuclei, or AGN, they can be observed across much of the Universe. However, despite their large masses, SMBHs exert little gravitational influence on their host galaxies. The observed tight correlation between the mass of SMBHs and the mass, luminosity, and stellar velocity dispersion of their host galaxy's bulges is therefore surprising.

This correlation, known as the M-sigma relation, points to a connection between the growth of galaxies and their central SMBHs that was put in place during the formation of the galaxy. Understanding how galaxies form provides a link between the initial density seeds from the big bang and the currently observed structures in the Universe today. As such, it is a necessary step in constraining cosmological models and our understanding of the origins of the Universe in which we live.

The primary goal of this research is to use the latest galaxy survey data from Hubble Space Telescope and the data intensive computing resources at LANL to test the origin of the M-sigma relation by constraining the morphological, AGN, and host galaxy properties of intrinsically dust-obscured active galactic nuclei. As discussed below, this study provides the best test to date on the origin of this important relation.

Scientific Approach and Accomplishments

Research Summary: The currently favored model for the M-sigma relation is one in which major galaxy mergers drive and then subsequently quench the formation of both SMBHs and their host galaxies. In this model, the merger of two gas-rich disk galaxies, each similar to our own Milky Way, drives gas and dust down into the central regions of the merging galaxy. This gas and dust fuels the formation of new stars and feeds the growing SMBH. When the accretion disk surrounding the SMBH becomes sufficiently luminous, radiation pressure halts the infall of additional material, shutting off further SMBH growth in a process referred to as 'feedback'. If this feedback is sufficiently strong, it removes the remaining dust and gas from the newly formed spheroidal galaxy or central bulge, preventing future star-formation and leaving the galaxy with a central SMBH and bulge/spheroid whose masses are now correlated.

To test this model, many studies have looked for evidence of major mergers among galaxies that host X-ray selected AGN. Nearly all of these studies have found that, contrary to expectations, X-ray selected AGN appear not to be triggered by major mergers, but by more benign processes incapable of driving global correlations between SMBH and galaxy mass.

X-ray-selected AGN samples benefit from the fact that AGN are the only luminous X-ray sources in the Universe. X-rays therefore allow astronomers to identify clean samples of AGN down to relatively low luminosities. X-ray selected AGN, however, are not the correct sample with which to test this major-merger scenario. The majority of AGN are intrinsically obscured by dust and gas that lies along our line of sight to the accretion disk, and if the quantity of gas between an AGN and us is sufficiently high, the AGN will be missed in the X-ray. The effects of obscuration are particularly important if we hope to catch AGN in the act of merging, as AGN in mergers are expected to be even more heavily obscured, and thus harder to detect, in the X-ray.

To overcome this limitation, I have developed a method of identifying AGN on the basis of their infrared emission (Donley et al. 2012). This color selection method, illustrated in Figure 1, has the advantage that it is able to identify both unobscured as well as heavily obscured AGN. Equally important, however, is the fact that this selection method is biased towards the most luminous AGN, which tend to lie at large redshifts. It is exactly this sample of AGN (high-luminosity, high-redshift, heavily obscured) for which the major merger scenario described above is thought to be most relevant. The infrared AGN I select using my new method are therefore the ideal sample with which to test the major-merger origin of the M-sigma relation.

To study the rest-frame optical/visible morphologies of AGN at high redshift, we require deep, high-resolution, near-infrared imaging data. (The near-infrared requirement comes from the fact that visible light from a distant galaxy is redshifted into the near infrared by the expansion of the Universe.) Prior to 2009, astronomers had no way of obtaining deep, high-resolution near-infrared imaging data. This changed with the successful installation of WFC3 on the latest (and last) Hubble Space Telescope servicing mission.

Following the servicing mission, Hubble placed a call for large, multi-cycle treasury observing proposals. One of the few successful programs, on which I am a Co-I, is CANDELS: the Cosmic Assembly Near-Infrared Deep Extragalactic Legacy Survey. With the largest ever allocation of Hubble Space Telescope time, we are obtaining deep, near-infrared imaging data across five extragalactic fields that also contain significant multi-wavelength coverage from both ground and space-based observatories. The CANDELS survey therefore provides us with the first deep rest-frame optical (observed near-infrared) images of the host galaxies of AGN at high-redshift.

To determine if major mergers are indeed the drivers of luminous AGN, I have been leading a study of the host galaxies of AGN in the CANDELS/ COSMOS field. (COSMOS is one of the five surveyed fields, and is also the field in which I defined my infrared AGN selection criteria.) The primary goal of this study is to determine if the morphologies of the host galaxies of infrared-selected AGN (high-luminosity, high-redshift, often heavily obscured AGN) are substantially different from those of X-ray selected AGN (lower-luminosity, lower-redshift, less heavily obscured AGN), as predicted.

To determine the morphologies of the AGN host galaxies, we turned to visual classification using a scheme developed by the CANDELS collaboration. This scheme allows us to determine both the morphological properties of the sample (e.g., disk, spheroid, irregular), as well as its interaction characteristics (e.g., merger, interaction, non- interacting companion, etc.). While astronomers have developed a number of quantitative parametric and non-parametric measures of morphology, all have shortcomings that impact their ability to identify merging galaxies, particularly at high-redshift. Visual classification, while somewhat subjective, overcomes these limitations. For an example, see Figure 2.

The preliminary results of my study (Donley et al. 2013, in prep.) suggest that the morphologies of infrared-selected AGN are indeed different from those of X-ray AGN in exactly the sense that we would expect if mergers only become important at the highest luminosities, redshifts, and/or obscurations (see Figure 3). Very few of the X-ray AGN has irregular or asymmetric hosts, and they are most likely to be undisturbed or undergoing interactions that have not (yet) led to large disturbances in the host galaxy. In contrast, infrared AGN tend to have irregular, asymmetric hosts, and are most likely to be either interacting or merging in a way that is disturbing the galaxy, or disturbed though not clearly interacting (a classification consistent with the late, more dynamically relaxed, phase of a major merger). Furthermore, the fraction of isolated disk galaxies, galaxies assumed not to have undergone a merger in the recent past, is significantly lower for the infrared selected AGN than the X-ray AGN, as expected.

This work is providing intriguing evidence that, contrary to the results from X-ray studies, mergers may indeed be responsible for driving the M-sigma relation. In order to fully understand this population of AGN, however, additional work must be done. In particular, because infrared AGN are often heavily obscured, they tend to be faint in the UV and optical. As such, the traditional method of obtaining accurate redshifts (e.g. distances) for these AGN via optical spectroscopy is often unsuccessful.

For the brightest sources, we can turn to near-infrared

spectroscopy, a relatively new capability in astronomy. While I have been working with collaborators to obtain deep, NIR spectra of the brightest infrared AGN, spectral-energy distribution fitting provides the only way to estimate the redshift for most sources. In this method, redshifted templates of well studied AGN and galaxies are compared to the observed photometry of the AGN to constrain the possible redshift of the source. Not surprisingly, this method depends on measuring accurate photometry in as many wavebands as possible.

To measure accurate crowded-field photometry in ground and space-based wavebands with greatly varying resolution, members of the CANDELS collaboration have developed a photometry package called TFIT. Motivated by LANL's supercomputing resources, I then wrote a pipeline that streamlines the image preparation and TFIT photometric steps. This pipeline, which has now been adopted by the CANDELS team, has greatly sped up the rate at which we compute multi-band photometry, and by running this pipeline on LANL's supercomputers, I have been able to process in a matter of days a number of large narrow-band datasets that our team would otherwise have lacked the manpower to analyze (see Figure 4 for an example). This additional data will help to optimize both photometric redshift and stellar mass estimates not only for the AGN, but also for all galaxies in CANDELS fields.

Additional Papers: In addition to the work in progress described above, I was a co-author on the following papers during my Director's Fellowship:

Mateos et al. 2012, "Using the Bright Ultrahard XMM-Newton survey to define an IR selection of luminous AGN based on WISE colours"

The infrared selection method I developed in Donley et al. (2012) identified infrared AGN on the basis of their Spitzer Space Telescope colors. The primary goal of the Mateos et al. paper was to develop a complimentary technique using the colors from the new infrared all-sky survey, WISE.

Perez-Gonzalez et al. 2013, "SHARDS: An Optical Spectrophotometric Survey of Distant Galaxies"

This paper presents an overview of the SHARDS survey, a narrow-band imaging survey in the GOODS-N field (one of the CANDELS fields) designed to provide detailed spectral energy distributions from which accurate photometric redshifts and stellar masses can be measured.

Talks:

During my tenure as Director's Fellow, I spoke at the CANDELS team meeting in Santa Cruz, CA, in September 2012, and also gave an invited talk at an invitation-only conference in Ringberg, Germany.

Community Service:

In June, 2012, I served on the Chandra X-ray Observatory Time Allocation Committee, and in August, 2012, I served on the NASA ADAP Proposal Review Committee. I also served as co-leader of the CANDELS junior scientist working group.

Impact on National Missions

The work presented here ties primarily to the Scientific Discovery and Innovation Mission, through the topics of Information Sciences and Cosmology. The analysis from this work relies on cross correlations with multi-wavelength datasets containing millions of sources. Using this science problem and datasets as a test bed for data mining algorithm research will directly benefit the growing interest in data-intensive computing by members of the Information Science communities.

In addition, this study provides a unique analysis of the observational survey data returned from NASA's CANDELS survey (the largest program ever undertaken by the Hubble Space Telescope).

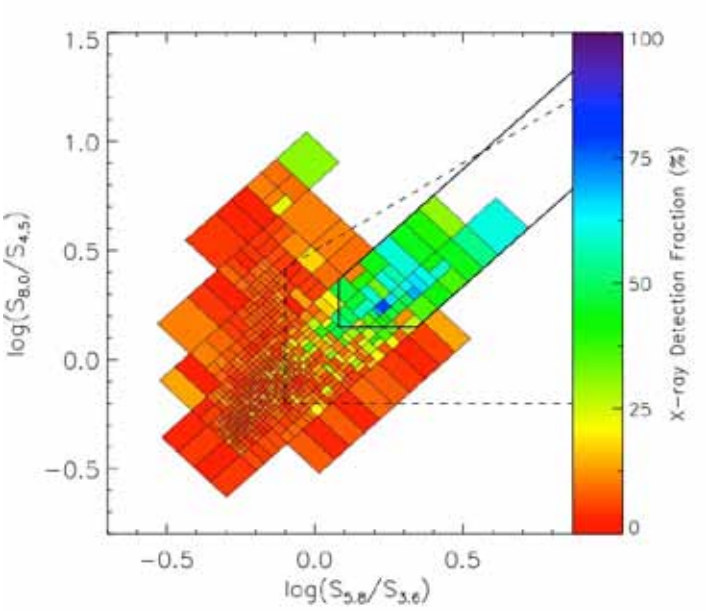

Figure 1. Infrared AGN selection region defined by Donley et al. (2012)

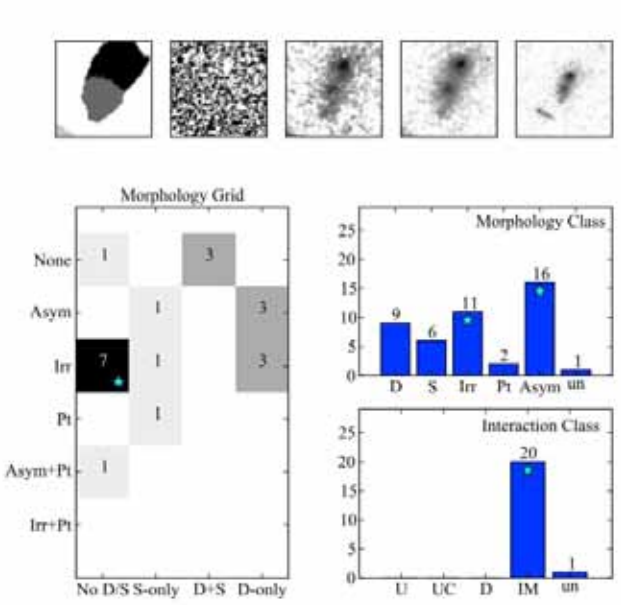

Figure 2. Example of the visual classification scheme for an infrared-selected AGN. The thumbnails show the segmentation map and the i-band, J-band, and H-band Hubble images. The grid shows the combinations of morphological parameters (asymmetric, irregular, point source, dis, spheroid) chosen by each of the 21 classifiers. Likewise, the histograms show the various morphology and interaction classes, with the consensus classes marked by cyan stars.

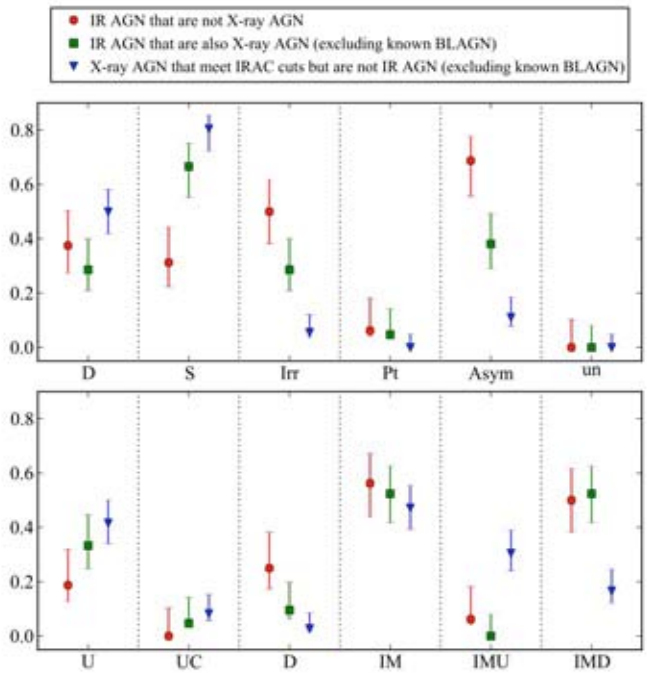

Figure 3. Preliminary comparison between the morphologies of X-ray and infrared-selected AGN. The histograms give the fraction of each sample that fall in various morphological classes (disk, spheroid, irregular, point source, asymmetric) and interaction classes (undisturbed, undisturbed with a companion, disturbed, interacting or merging with or without disturbance).

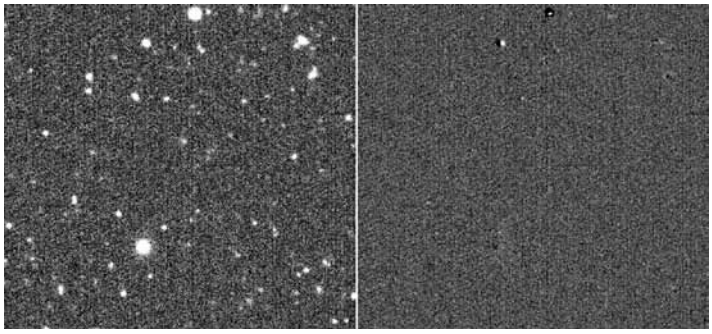

Figure 4. Output from the TFIT photometric pipeline run on the LANL supercomputers. The image on the left is the raw data, and the image on the right shows what remains once each source has been modeled and subtracted.

References

1. Perez-Gonzalez, P. G., A. Cava, G. Barro, V. Villar, N. Cardiel, I. Ferreras, J. M. Rodriguez-Espinosa, A. Alonso-Herrero, M. Balcells, J. Cenarro, J. Cepa, S. Charlot, A. Cimatti, C. J. Conselice, E. Daddi, J. Donley, D. Elbaz, N. Espino, J. Gallego, R. Gobat, O. Gonzalez-Martin, R. Guzman, A. Hernan-Caballero, C. Munoz-Tunon, A. Renzini, J. Rodriguez-Zaurin, L. Tresse, I. Trujillo, and J. Zamorano. SHARDS: An Optical Spectro-photometric Survey of Distant Galaxies. 2013. The Astrophysical Journal. 762: 46.

Publications

Caputi, K. I., J. S. Dunlop, R. J. McLure, J. -S. Huang, G. G. Fazio, M. L. Ashby, M. Castellano, A. Fontana, M. Cirasuolo, O. Almaini, E. F. Bell, M. Dickinson, J. L. Donley, S. M. Faber, H. C. Ferguson, M. Giavalisco, N. A. Grogin, D. D. Kocevski, A. M. Koekemoer, D. C. Koo, K. Lai, J. A. Newman, and R. S. Somerville. The Nature of Extremely red H - [4.5] > 4 galaxies revealed with SEDS and CANDELS. 2012. Astrophysical Journal, Letters. 750 (1): L20 (7 pp.).

Modeling X-ray Bursts

Christopher J. Fontes
20120733PRD1

Abstract

Zach Medin in XCP Division carried out this Director's Funded postdoctoral project. The goal of this work was to model radiation transport through the atmosphere of X-ray-bursting neutron stars (XRBs), using the LANL xRAGE and CASSIO codes. During the course of this work, Zach expanded the goals of the project by writing his own stand-alone radiation transfer code to investigate deficiencies in the LANL codes. This work put the LANL codes on a more sound theoretical footing, allowing him to proceed with simulating XRBs in ways that have not been previously considered. He also mentored a graduate student at Stony Brook University to help in the modeling of these XRBs. In the middle of his second year of working on this project, Zach was converted to a staff member in XCP Division.

Background and Research Objectives

The focus of this work was on modeling the transport of radiation through the atmospheres of X-ray-bursting neutron stars. Neutron stars provide some of the most extreme physical conditions in the universe, from the super-strong magnetic fields surrounding and threading these stars to the super-nuclear densities in their interiors. Many of these conditions can not be recreated in the laboratory, making neutron stars an important and unique probe of fundamental physics. X-ray telescopes such as Chandra and XMM-Newton have allowed astronomers to make detailed observations of the surface emission from a large number of neutron stars. One particularly interesting class of neutron stars is X-ray bursters. The hydrogen and helium accreted by an X-ray burster is periodically consumed in runaway thermonuclear reactions that cause the entire surface to glow brightly in X-rays for a few seconds. During these bursts, both the radius and the gravitational redshift of the neutron star can be measured. By probing neutron star radii, X-ray bursts are one of the strongest diagnostics of the nature of matter at extremely high densities. However, due to the strong surface gravities and high temperatures involved, the atmospheres where these X-ray bursts occur are far from ideal, making accurate determinations of the neutron star radius very difficult. Observations can potentially place extremely strong constraints on nuclear matter, once uncertainties in current atmosphere models have been reduced.

The main objective of this work is to model the atmospheres of X-ray bursters during the bursts. At the lab we have the tools to solve this problem while including a lot of important physics that has been ignored in previous calculations: the xRAGE radiation-hydrodynamics code in tandem with the LANL Opacity Library provides radiation transport schemes with accurate transport coefficients; the hydrodynamics module in xRAGE enables modeling of atmosphere expansion during bursts; the CASSIO code contains an iterative Monte Carlo algorithm for treatment of Compton scattering at a level beyond the diffusion approximation; and new non-thermodynamic-equilibrium techniques developed at the lab permit investigation of particle acceleration due to strong magnetic fields in the atmosphere. X-ray burster atmospheres are highly non-ideal and accurate models require tracking radiation transport across multiple frequency groups. Therefore, an additional goal was to add a new capability to the radiation module of xRAGE, the ability to use two-temperature opacities in the multigroup calculations.

Scientific Approach and Accomplishments

Zach spent the first year learning to use and apply the LANL xRAGE and CASSIO to this research topic. Initial comparisons for the case of elastic scattering produced significant differences with results in the literature by Madej et al [1], which motivated Zach to write his own, stand-alone radiative transfer code. While he was unable to obtain good agreement with the Madej results, he was able to use this code to identify and fix certain bugs in the LANL codes. In addition, he became involved in an external collaboration with the University of Chicago

to compare results obtained with their FLASH code and xRAGE. These comparisons further contributed to the identification of code errors as well as certain numerical limitations, resulting in improved methods in the xRAGE code. This work resulted in a paper that appeared in the Proceedings for NECDC 2012.

During the second year of this project, Zach implemented the more realistic approach of Compton scattering in his stand-alone code. He was able to obtain good agreement with the work of Suleimanov et al [2], using both his stand-alone code and CASSIO, suggesting that the earlier work of Madej may be inaccurate. In connection with this work, Zach became involved with an ongoing collaboration with the Department of Physics & Astronomy at Stony Brook University in New York. He mentored a graduate student, Marina Von Steinkirch, on the subject of applying his stand-alone code to a wide range of conditions relevant to X-ray bursters: 360 variations of composition, gravities and luminosities. Zach proceeded with the next goal of the project by attempting to model the XRBs with hydrodynamic effects included in xRAGE and CASSIO simulations. This approach did not produce significantly different results, so Zach proceeded to incorporate the next most likely piece of physics that is expected to produce a significant difference, general relativity, in his stand-alone code. During the implementation of this general relativistic effect, Zach was converted to a staff member in XCP around April 2013 and so was unable to complete this investigation, as well as to implement the two-temperature, multigroup opacity approach. He continues to work on this XRB project, as time permits, and intends to submit this work for publication when it has reached a suitable stage of completion.

While working on this LANL project, Zach was also a coauthor of a Physical Review E paper about phase transitions in multicomponent plasmas. This publication was a result of his previous affiliation as a postdoctoral fellow at McGill University.

Impact on National Missions

This project has resulted in the discovery of a number of deficiencies and subsequent improvements in the LANL xRAGE and CASSIO codes. These codes are used extensively throughout the lab to model a broad range of plasma conditions in support of high energy density programs.

References

1. Madej, J., P. C. Joss, and A. Rozanska. Model atmospheres and X-ray spectra of bursting neutron stars: Hydrogen-helium comptonized spectra. 2004. ASTROPHYSICAL JOURNAL. 602 (2): 904.
2. Suleimanov, V., J. Poutanen, and K. Werner. X-ray bursting neutron star atmosphere models using an exact relativistic kinetic equation for Compton scattering. 2012. ASTRONOMY & ASTROPHYSICS. 545: A120.

Publications

Hughto, J., C. J. Horowitz, A. S. Schneider, Z. Medin, A. Cumming, and D. K. Berry. Direct molecular dynamics simulation of liquid-solid phase equilibria for a three-component plasma. 2012. PHYSICAL REVIEW E. 86 (6): -.

Medin, Z., J. Wohlbier, C. Fryer, R. Rauenzahn, M. Fatenejad, D. Lamb, C. Graziani, and B. Fryxell. Collaborative comparison of high-energy-density physics codes. Presented at 2012 NUCLEAR EXPLOSIVES CODE DEVELOPMENT CONFERENCE. (LLNL, Livermore, CA, 22-26 Oct. 2012).

Experimental and Computational Studies of Engineered Nanoparticle Aggregation in Human Tissue Models

Charles Reichhardt
20120760PRD2

Abstract

This project focuses on computational modeling of non-equilibrium phenomena for particles undergoing aggregation. Particular emphasis is on particles undergoing aggregation for different types of dynamics as well as understanding the effects of a substrate or a combination of a substrate and bulk driving on aggregation. We find that a strong substrate can arrest aggregation; however, under an applied drive the system with a substrate can aggregate much faster than systems without a substrate. This opens a new route for controlling pattern formation in aggregating materials. Additionally, we show that aggregation can lead to enhanced diffusion or mobility in cases where there is an asymmetry in the substrate, which can be useful for particle separation.

Background and Research Objectives

In nature there are many examples of aggregation where individual particles can stick to one another or stick to some type of surface. The problem of aggregation is rather complicated since it is related both to spatial length scales as well as to time scales. In the simplest case of Brownian particles sticking to one another, a straightforward question is whether a single clump or multiple clumps will form as a function of time. In many mathematical limits this question can be addressed analytically, and it is known that under thermal fluctuations and for lower dimensions a single clump will form. In most real world situations there will be additional complications such as the presence of quenched disorder. The question is just how strong the quenched disorder has to be to arrest aggregations, and whether there are other regimes as well. In addition, there are situations in which the motion of the aggregating particles is not thermal but is driven by some type of correlated noise, such as turbulence, or by some type of external drive. In this case, the aggregation could be arrested or it could be possible to increase the aggregation rates. Our goal has been to understand aggregation under the effect of substrates and under different driving conditions.

Scientific Approach and Accomplishments

Our approach has been to use large scale simulations of different aspects of particles that exhibit aggregation. The first problem we address is that of particles with short range repulsion and longer range attraction. This interaction was modeled with two Bessel functions. Previous work showed that this model forms multiple clump and stripe phases; however, we demonstrated that these are not the true ground states, and that instead the system forms a single clump under long time thermal motion. The next question we addressed was to understand what happens to aggregation in the presence of quenched disorder. We model both random and periodic substrates and identify three regimes. (1) For weak substrates, the system completely phase separates. (2) For intermediate substrates, the substrate is effectively wetted by a portion of the particles while the remaining particles form a single clump. (3) For strong substrates, the substrate dominates the behavior and there is little or no aggregation. We next address the question of what happens under an applied drive. We found that even systems with strong substrates can exhibit dynamically induced aggregation when driven, and that the shape of the aggregation can be controlled and can take the form of stripe or labyrinth patterns. We also examined the effects of self-driven aggregating or flocking particles, and found that if the substrate is asymmetric, a novel ratchet effect occurs in which the aggregate exhibits a net dc motion even when there is no applied dc drive. We also show that the size of the particles in the aggregate can lead to motion in different directions, so that a new type of particle separation can be achieved.

Impact on National Missions

Toxicology. Certain nanoparticles can have very toxic effects; however, the toxicity can be altered if the particles aggregate, and in certain cases the aggregates are non-toxic even though their component particles are toxic. This suggested that controlled aggregation could be used to reduce the toxicity of many types of materials that are

byproducts of missions relevant to the Nation. Our results suggest that moving nanoparticles over a substrate with a strong applied drive can enhance the aggregation.

Particle separation. There are many examples of processes relevant to the mission where one would want to separate out different components of a mixture on the nanoscale. Our work suggests that the addition of actively aggregating particles can be used to create a ratchet effect in which aggregates of one size move in one direction while aggregates of another size move in the opposite direction, leading to enhanced sorting.

Aging processes in aggregation. Aggregation can be a long-time process and is relevant to the aging of materials that must sit for long periods of time. Aging is typically understood as a diffusive process; however, we have shown that in the presence of quenched disorder, aggregation can be suppressed, so that simple forecasts based on Brownian motion can fail. Additionally, if there is an external driving present, then the aggregation will be much faster than thermal diffusion, leading to a superdiffusive behavior.

Publications

Drocco, J. A., C. J. Reichhardt, and C. Reichhardt. Characterizing plastic depinning dynamics with the fluctuation theorem. 2011. European Physical Journal E. 34 (10): 117 (7 pp.).

Drocco, J., C. J. Reichhardt, and C. Reichhardt. Bidirectional sorting of flocking particles in the presence of asymmetric barriers. 2012. Physical Review E (Statistical, Nonlinear, and Soft Matter Physics). 85 (5): 056102 (6 pp.).

Drocco, J., C. Reichhardt, C. J. O. Reichhardt, and A. R. Bishop. Statics and dynamics of wetting-dewetting transitions for particles with attractive interactions on periodic substrates. 2012. Proceedings of SPIE. 8458: 84581J.

Drocco, J., L. M. Lopatina, C. Reichhardt, and C. J. O. Reichhardt. Dynamics of self-driven and flocking particles on periodic arrays. 2102. Proceedings of SPIE. 8458: 84581I.

Reichhardt, C. J. Olson, J. Drocco, T. Mai, M. B. Wan, and C. Reichhardt. Active matter on asymmetric substrates. 2011. In Optical Trapping and Optical Micromanipulation VIII ; 21-25 Aug. (2011 ; San Diego, CA, USA). Vol. 8097, p. 80970A (13 pp.).

Reichhardt, C., J. Drocco, C. J. O. Reichhardt, and A. R. Bishop. Statics and dynamics of vortex matter with competing repulsive and attractive interactions. 2013. Journal of Superconductivity and Novel Magnetism. 26: 2041.

Reichhardt, C., J. Drocco, C. J. Olson Reichhardt, and A. R. Bishop. The effect of pinning on vortex states with attractive and repulsive interactions. 2012. Physica C: Superconductivity and its Applications. 479: 15.

Quantum and Correlation Effects in High-energy Density Plasmas

Jerome O. Daligault
20120763PRD2

Abstract
The goal of the work was to achieve a theoretical understanding at the microscopic level of transport properties of dense plasmas in regimes where traditional theories break down, and to foster and validate models that can be used in the design codes. We review the main accomplishments of Dr Scott Baalrud obtained during his appointment as a Feynman postdoctoral fellow in T-5 between July 2012 and July 2013.

Background and Research Objectives
The attainment of inertial confinement fusion (ICF) for energy production relies on our understanding of microscopic transport properties in multi-component, high energy density plasmas (HEDP) over a wide range of physics regimes. These properties are still not fully understood because imploding plasmas can reach conditions in which quantum and many-body correlation effects influence Coulomb collisions between charged particles; regimes where traditional theories break down. In particular, the combined effects of quantum mechanics and statistics govern the behavior of conduction electrons, while at the same time the ions are in a moderately to strongly coupled, liquid-like state since their average interaction energy is of the order of or greater than their thermal energy. These effects contribute to the various transport mechanisms such as the thermal conductivity, energy relaxation rates, viscosity, and stopping power. A challenge in HEDP physics is to understand how the interplay of correlation and quantum effects gives rise to the physical properties of dense plasmas and to develop and validate practical models that can be used in the hydrodynamic design codes.

We propose to develop and validate with ab-initio molecular dynamics (MD) simulations a transport theory that accounts for quantum and correlation effects. The results will be applied to ICF by including the new transport model in a fluid code. The theoretical portion of the proposed research will be to extend an existing method to include quantum effects, and more general kinetic effects in the transport theory. We will then carry out a detailed comparison of the theory against classical and quantum molecular dynamics simulations. Finally, verified transport coefficients will be included in a hydrocode fluid code to investigate how quantum and correlation effects alter ICF implosion dynamics.

Scientific Approach and Accomplishments
We have performed a theoretical study of transport properties in plasmas that spans weak to strong coupling regimes. The results have been published in the Physical Review Letters (PRL 110, 235001 (2013)). Although collisional transport in weakly coupled plasmas has been understood for decades, it has proved to be a formidable challenge for theory to capture the strongly coupled regime where correlation effects become important. Some understanding of these regimes has been developed using particle simulations, such as molecular dynamics, but these are computationally expensive. Analytic theory is needed both to elucidate the physics underlying the transport properties, and to provide equations that can be practically implemented in fluid simulations.

We have developed an analytic transport theory that is physically motivated (explaining the physics underlying how correlations affect transport), versatile (it fits within the Chapman-Enskog transport model, which can be used to calculate virtually any transport property), computationally efficient to evaluate, and spans weak to strong correlation. The theory can be thought of as a generalization of conventional plasma theories to include correlation effects. The accuracy of the theory has been verified by comparison with ab-initio molecular dynamics simulations and recent experiments. These show that the theory is valid from the weakly coupled plasma limit, through the liquid-like regime, approaching the liquid-solid phase transition at very large coupling strength (around 100 for a one component plasma). This range of coupling strength covers most of the modern

experiments.

In addition to the PRL publication on our effective potential theory, we are preparing a longer manuscript that explains the theory in much greater detail and applies it to many more transport processes than were considered in the PRL. These include diffusion in Yukawa plasmas, temperature relaxation using semiclassical potentials and diffusion in ionic mixtures. We have been invited to submit this paper to Physics of Plasmas in November to document Dr. Baalrud's invited address at the 2013 APS Division of Plasma Physics meeting.

We are preparing a manuscript devoted to calculating the viscosity of one-component plasmas using molecular dynamics simulations and our effective potential theory. Viscosity is a particularly challenging transport coefficient to calculate, which provides a rigorous test of both the simulation technique and theory. Our contribution provides the most accurate simulation data to date, and our theory has elucidated how viscosity at strong coupling is a balance of kinetic and potential energy contributions. We emphasize that this balance was missed in the previous standard theory on this topic, which considered only the kinetic energy component.

We have begun collaboration with Dr. Charlie Starrett and Dr. Didier Saumon (XCP-5) to combine their average atom model for the pair distribution function in quantum plasmas, with our approach to calculate transport properties. Their results provide input to our model, and when combined, these provide an efficient way to predict ionic transport properties of warm dense matter. We plan to test this approach by making a comparison with quantum molecular dynamics simulations predictions of interspecies diffusion.

We have begun collaboration with Dr. Grisha Kagan, T-5, to understand ion species mix in ICF plasmas. Dr. Kagan has a theory for mix that takes transport coefficients as input. With our collaboration, he can extend his theory to strong coupling regimes relevant in ICF. We are working together to provide the necessary transport coefficients that he requires as input in his theory.

In addition to the transport theory discussed above, Dr. Baalrud published a paper on the incomplete plasma dispersion function and its uses for describing wave properties near plasma boundaries [S.D. Baalrud, Physics of Plasmas 20, 012118 (2013)]. This paper focuses on the basic mathematical properties of this interesting and useful function, but also applies it to describe ion acoustic and Langmuir wave properties near electrostatic potential barriers such as sheaths or double layers, which are common in plasmas.

Dr Baalrud also published a reply to comment paper [S.D. Baalrud and C.C. Hegna, Plasma Sources Science and Technology 21, 068002 (2012)], which was a response to a comment made by another researcher on an earlier paper of mine, which had criticized a yet earlier theory of his. The topic of this ongoing discussion is a kinetic theory for how fast ions leave a plasma (this is called the kinetic Bohm criterion). In this reply, we used experimental and numerical simulation data to defend our approach, which is based on a formalism that takes velocity moments of the kinetic equation.

Dr. Baalrud is preparing a manuscript on the collisionless kinetic theory of tearing instabilities, which is a continuation of work that began at U. New Hampshire (Scott's previous postdoc) in collaboration with A. Bhattacharjee and W. Daughton from LANL XCP-6. Scott has discussed this work in several meeting with Dr. Daughton over the past year. The theory is an extension of the previous standard to account for oblique modes that become stabilized by diamagnetic drifts. These are not considered in the standard theory. We have used our theory to explain this stabilization effect, which was observed in Daughton's previous large-scale PIC simulations of 3-D magnetic reconnection, but was not understood.

Impact on National Missions

The results of this research project provide a fundamental theoretical contribution to the burgeoning area of warm dense matter, with potentially significant impact on inertial confinement fusion (ICF) modeling. They will also have direct impact in a wide range of fields involving strongly coupled plasmas, including fast ignition physics, ultracold plasma physics, dusty plasma physics, and astrophysics (giant planets, white dwarfs and neutron star crusts).

Publications

Baalrud, S.. The incomplete plasma dispersion function: properties and application to waves in bounded plasmas. 2013. Physics of Plasmas. 20: 012118.

Baalrud, S., and C. Hegna. Reply to comment on `kinetic theory of the presheath and the Bohm criterion'. 2012. Plasma Sources Science and Technology. 21: 068002.

Baalrud, S., and J. Daligault. Effective Potential Theory for Transport Coefficients across Coupling Regimes. 2013. Physical Review Letters. 110: 235001.

Genetically Encoded Materials: Libraries of Stimuli-responsive Polymers

Jennifer Martinez
20120029DR

Introduction

Nature creates adaptable materials that respond dynamically to their environment, converting one type of signal into another. Likewise, man-made "smart polymers" can adapt, sense or react to their environment, converting one type of signal into another signal or functionality. These polymers impact diverse fields such as drug delivery, diagnostics, tissue engineering, and molecular electronics, and are only skimming the surface of their potential. In vivo polymers are engineered protein polymers with control over structure and function unparalleled by synthetic polymers. We can create large, diverse libraries of in vivo polymers that react biologically and/or optically, and rapidly identify functional materials using a genetic technique akin to evolution. Our libraries will be based on elastin- and silk- combined with functional units [diverse peptides (small proteins); light and electrically active polymers; and fluorescent metal-complexes]. Our goal is to develop a platform technology that allows us to select materials that are biologically, thermally, or optically responsive. Realization of this potential requires three significant breakthroughs: 1) creation of polymer libraries with incorporated functionalities; 2) development of methods for selecting stimuli-responsive polymers based on functions; and 3) understanding of functional polymers. These Materials are expected to impact diverse fields such as regenerative medicine (i.e. niches to grow cartilage or bone) and optical electronics and solar harvesting (i.e. stimuli responsive fluorescent or elastic charge-transfer materials).

Benefit to National Security Missions

We are creating the infrastructure to develop materials for regenerative medicine, biosensing, drug delivery, wound healing, and molecular electronics. Within the NIH we will be well positioned to respond to requests for proposals (i.e. http://grants.nih.gov/grants/guide/pa-files/PAR-10-141.html, which cites the need for complex scaffold materials to promote 3D tissue regeneration). In addition to the biomedical application domain, this month DOD (DTRA) listed active structural elastomers among its most highly sought enabling technologies. Further, DHS and DTRA has an active interest in wound healing, which requires biodegradable, cell recruiting, and biocompatible polymers, as we will produce in this project. On the molecular electronics frontier, the DOE sites the need for "soft materials with tailored bandgaps, optical cross-sections, (and) luminescence efficiencies," to meet a BES Grand Challenge, to "…design and perfect atom- and energy-efficient synthesis of revolutionary new forms of matter with tailored properties."

Progress

We seek to create optical and biologically reactive polymers for application in optoelectronics and regenerative medicine. Ultimately we aim to create polymer libraries in vivo and display them in a format that enables facile selection of bio- and photo-reactive polymers, out of a mixture of millions of different polymers. For ease in discussion our work is divided into biologically and optically active sections; however, we note that both sections of the project overlap experimentally (techniques, in vivo polymers, libraries and application of the polymers).

Biologically active polymers. We have shown that elastin-like polymers (ELP) can be easily displayed on bacterial phage (M13) and yeast. Diverse libraries of ELP with different lengths of peptides (~10^8 members) have been created and we find that the library diversity is maintained while displayed on phage and yeast. We have utilized these libraries to select polymers that bind specific integrins (proteins on the surface of cells) and for those that bind directly to progenitor stem cells. We are characterizing the polymers for biological activity (attachment, proliferation, migration, and differentiation). Further, we have made significant progress toward selections of polymers important for the initiation of cartilage development from stem cells, as well as those polymers that can bind growth factors.

Toward creating polymers that can be self-assembled over large length-scales, we have developed coiled-coil assemblies. Our first targets assemble into cubes and triangles. Similar coils have been combined with ELP to form assemblies called "HELP". These stimuli responsive polymers have temperature transitions and form hierarchical assemblies, as determined by microscopy.

Optically active polymers. Our goal is to expand the genetic code and enrich in vivo polymers with new functionalities from a suite of conjugated oligomers and a series of transition-metal complexes, to enrich polymers with tunable optical or electrochemical properties.

Toward that goal, DNA vectors have been created to allow the conjugation of optical moieties in defined location and number within individual ELP. We have also begun to utilize rolling circle amplification to create libraries of ELP and resilin that contain random placement and number of conjugation sites. Further, we have begun to develop an enzymatic method that will allow us to conjugate the optical moieties to libraries of ELP, while on phage and yeast, thus enabling our final goal of in vivo selection of optical properties.

A series of PPVO (p-phenylene vinylene oligomer) derivatives with functional groups of varying electronegativity, which impact the molecular electronic and optical properties of the PPVOs, have been synthesized. These suites of PPVO have broadly tunable and efficient UV absorption and photoluminescence spectra and have been incorporated and characterized in organic LED devices.

As proof of concept, we first conjugated the PPVO oligomers to a stimuli-responsive polymer (PNIPAM) with important industrial applications. This material exhibits thermoresponsive optical properties as the solution temperature exceeds the lower critical solution temperature (LCST) of the polymer. We have found that the polymer conjugate solution turns opaque and has a five-fold increase in fluorescence intensity as temperature exceeds the LCST. Such distinct increase in fluorescence intensity is likely due to the rigidchromism, that is, the change in optical properties due to confinement of the chromophores within a restricted polymer conformational state.

PPVO have now been conjugated to ELP and we are characterizing the temperature and stimuli-responsive properties of the monomeric polymer. Further, PPVO has been utilized as a cross-linking agent to incorporate the fluorescent oligomers into elastin hydrogels. These highly luminescent polymer gels have temperature dependent physical changes. We are currently investigating the temperature and pressure induced changes in optical properties.

We have designed and prepared three related classes of transition-metal (ruthenium) complexes with polypyridyl derivatives. In class I, the side-chain length of functional groups have been varied systematically. In class II, alterations in substituent groups were used to modulate the strong metal-to-ligand charge-transfer absorptions. We find that conjugates of the ruthenium polypyridyl complexes with ELP have temperature dependent optical properties. Above the LCST of elastin (~37oC) the complex exhibits 10-times higher fluorescence intensities, than the conjugate below the LCST. Our results suggest that the increased optical properties result from a more rigid environment of the ruthenium complex in the aggregated state of the polymer.

Future Work

Future goals/tasks for in vivo polymer libraries and selection methods:

- Select polymers adhesive to mammalian cells and/or extra cellular matrix milieu.
- Characterize the elastin transition to aggregation, as a function of salts, protein concentration, and temperature.
- Conjugate optically active materials to the in vivo polymers and study their assembly, stimuli response, and optical activity.
- Develop co-block libraries of: conjugation residues/elastin; silk/elastin; resilin/silk/collagen.
- Develop stimuli responsive selection techniques.
- Develop techniques to modify, with optical moieties, in vivo polymers specifically while displayed on the surface of phage and/or yeast.

Future goals/tasks for optically-reactive moieties:

- Vary the type and length of side chains with ending amine/carboxylic groups to afford a spectrum of reactivities.
- Characterize the assemblies and optical/electronic properties of modified elastins.
- Develop new conjugated oligomers.
- Conjugate conductive species to helical peptides and characterize the optical reactivity and assembly.

Future goals/tasks for modeling of polymer structure and designing polymer scaffolds:

- Develop LEGO-like building blocks exploiting regular local structural properties of protein units to create new polymers.

- Experimentally define the nature of elastin at the molecular and aggregate level.

Conclusion

We will create polymers that: change stem cells into bone cells; and emit light with environmental-dependent fluorescence (i.e. pH or heat triggered). Given that materials for cellular niches and optical electronics are large industries, and that our selection techniques are routine methodologies for many biotech companies, we anticipate that the technology developed from this DR will have broad utility and straightforward deployment to industry and government. Realization of this potential requires three significant breakthroughs: 1) creation of polymer libraries with incorporated functionalities; 2) development of methods for selecting stimuli-responsive polymers based on functions; and 3) understanding of functional polymers.

Publications

Ghosh, K., E. R. M. Balog, P. Sista, D. Kelly, J. S. Martinez, and R. C. Rocha. Morphological control of flower-shaped nanopatterns through stimuli responsive biopolymers. Biomaterials Science.

Jha, R. K., and C. E. M. Strauss. 3D structure analysis of PAKs: A clue to the rational design for affinity reagents and blockers. 2012. Cellular Logistics. 2: 69.

Park, Y. I., B. Zhang, S. Mallapragada, J. S. Martinez, Y. W. Park, and H. -L. Wang. Stimuli Responsive Poly-N-isopropylacrylamide- polyphenylene vinylene Oligomer Conjugate. 2013. Journal of Physical Chemistry C. 117: 7757.

Wang, H. -L., Y. I. Park, C. -Y. Kuo, S. Tretiak, J. S. Martinez, A. Zhugayevych, and O. Postupna. Tailored electronic structure and optical properties of conjugated systems through aggregates and dipole-dipole interactions. 2013. CAS Applied Materials and Interfaces. 5: 4685.

Using Microreactors for Efficient Plutonium Separations (U)

Stephen L. Yarbro
20130003DR

Introduction

Chemical separations, especially difficult separations depend on many factors. Fundamentally, reactions and rates are controlled by mass and heat transfer characteristics of the equipment. In equipment where the length scales are very large with respect to the boundary layers and therefore turbulent eddies are formed, mass and heat transfer are controlled by the contact area and 'mixing' energy per volume. In equipment such as microreactors, where the length scales are small with respect to the boundary layer and the flow is predominantly laminar, heat and mass transfer are controlled by different mechanisms. In this work, we propose to conduct studies with a difficult separation problem with importance to LANL missions and examine the fundamental roles of how heat and mass transfer effect the separation efficiency at these small scales.

Benefit to National Security Missions

The U.S. has an ongoing need for efficient actinide separation methods. Specifically, the will develop our ability to deploy advanced separation methods for weapons materials purification, advanced nuclear systems, nuclear forensics, and environmental management. It will also expand our capabilities in detection, measurement, and analysis of nuclear and radiological materials. In addition, it will provide an ability to conduct small-scale research and development with scarce and unique materials.

Progress

In FY 13, the project has made progress and completed the following activities scoped on the project plan:

Develop and model design concepts

- Completed workshop with LLNL on chemistry and engineering fundamentals
- Completed engineering design evaluation on bounding test cases
- Initiated continuum-based fluid dynamics calculations using COTS software
- Initiated Lattice-Boltzmann fluid dynamics calculations using LANL software
- Initiated examination of alternative design concepts including electrochemical

Fabricate/test integrated device

- Developed fabrication procedure for single channel device
- Initiated fluid flow testing to optimize fabrication method
- Characterized counter current and co current flow regimes

Characterize single stage system

- Completed tests on baseline extractant system
- Completed tests on equilibration times and extractant behavior
- Completed tests on alternative extractant system for comparison
- Measured mass transfer rates for baseline system
- Completed survey on ionic liquids for these systems

Design/test process diagnostics

- Initiated testing on microscope system to characterize interfaces
- Initiated testing on laser fluorescent system to characterize interface deformation
- Qualified analytical procedures for measuring concentrations

Other separations

- Completed engineering survey on three different candidate elements

Future Work

In FY14, the project will continue to further develop design concepts and verify them with multiscale modeling including continuum and Lattice-Boltzmann. Fabrication and testing of the equipment operating conditions will occur in parallel with refinement of the various chemical systems chosen for study. These devices will be tested with actual plutonium solutions and parameters developed for simple mixing, separation and reduction-oxidation methods. In addition, the project will continue testing design and development of on-line process diagnostics and testing of the radiolytic effects of radioactive materials on the chemical systems. This work will result in developing the design and initiating the fabrication of a more complex system based on the selected chemical system and scale-up of the preliminary contacting equipment.

The goals are the following:

- Develop and model countercurrent/crossflow contacting module
- Refine conditions for the selected extraction system
- Link simple contact systems to test cascades
- Design and initiate fabrication of intermediate system

Conclusion

The United States has an ongoing need for efficient actinide separation techniques. Our technical goal is to engineer a system based on a new understanding of the mass and heat transfer effects at small length and time scales to build a robust capability to carry out difficult separations. This will result in a processing capability that can meet new programmatic needs in a variety of national security, research, space and non-proliferation programs.

Battlefield MRI

Michelle A. Espy
20130121DR

Introduction

We propose to develop a portable "Battlefield" MRI (magnetic resonance imaging) machine based on SQUID (superconducting quantum interference device) sensor technology and ultra-low field MRI techniques developed at LANL. The device will provide a diagnostic quality image in a field deployable package, and use a novel "adaptive" open-coil shield to replace the tons of metal typically required in conventional MRI. The imager will employ very low magnetic fields, which can be completely turned off during transport or when not in use. Most importantly, because the device operates in a fundamentally different regime than a high field MRI machine, it will be able to perform unique imaging tasks that traditional MRI cannot, such as imaging in the emergency room or in the presence of metal. Battlefield MRI will bring the power of MRI to settings where it is presently not possible.

High field (HF) MRI, typically at high magnetic fields > 1.5 T, is the gold standard for diagnosis of mild to moderate brain injury. However, HF MRI is generally not used in emergency situations (emergency rooms or disaster relief), or the battlefield hospital because of the issues of cost and safety associated with high magnetic fields.

LANL is a world-leader in the technique of ultra-low field (ULF) MRI for imaging the human brain , ULF MRI operates at pulsed magnetic fields from 100 mT down to 10 microT. Because fields are very low, and can be completely removed, the system is safe to use in the presence of metal , without heating or movement; safe for surgical theaters or emergency situations where the presence of metal nearby or in the subject cannot be precluded.

Benefit to National Security Missions

This effort represents a critical and timely "next step" in LANL's development of a world-leading capability in ULFMRI and applications. Customers from DHS, DARPA, and ONR have explicitly issued calls grounded in this capability. This work will provide a rapid medical diagnostic tool for to serve these agencies e.g. disaster/terrorist event response, non-invasive screening. We anticipate a broad range of applications for NIH, e.g. ULFMRI combined with functional methods, fundamental understanding of brain, novel contrast at ULF for new diagnostics and basic biomedical research. We also anticipate significant potential for transition to industry partners. Outside of the battlefield application, the most compelling need for this technology is in developing countries. Sharing our prosperity in health care with the world is a national security interest as well as a humanitarian imperative. NIH may also have interest in MRI for more rural or underserved populations within the US. The technological advances of ULF MRI made here also serve other applications that would benefit from low-cost MRI or novel contrast instrumentation e.g. environmental monitoring (e.g. water or nutrient transport in trees); non-proliferation (non-invasive inspection of materials through pipes or in packaging). The unique contrast of ULF MRI has already served in materials studies including polymer science, and the detection of liquid explosives.

Progress

Sensor array development

We successfully implemented an existing 7-channel gradiometer system for the detector portion of the MRI system, and met the goal of demonstrating operation of the array outside the magnetically shielded room (MSR). Inside MSR, where characterization of the imaging system is presently being performed, the noise performance of the array is satisfactory at 1-3 fT/sqrt(Hz) depending on sensor position. The performance of this 7-channel array has also now been characterized in the presence of the MRI pulse sequence - and has demonstrated acquisition of 1-D images. The SQUIDs operate satisfactorily.

Pulse sequence development
Our goal for the previous year was to implement low-noise current delivery that would enable the use of projection imaging or "fast" imaging techniques so we could maximize available signal and minimize imaging time. A major accomplishment has been moving to entirely amplifier driven current sources without corrupting the low noise characteristics required of the imager. This has been successfully accomplished. All field generation is now in place, and low-noise operation has been verified. The practical ramifications are that we are now able to generate any field in any direction without the limitation of slow battery-driven supplies. We anticipate demonstration of pulse sequences that can capitalize on this success is on track for the end of FY2013.

Field Coils and Adaptive Shielding
All 10 field coils are designed, constructed, and being tested. We have also designed and implemented a simple set of compensation coils that are presently being characterized. We have also simulated and down-selected the control hardware for the adaptive shield. This control hardware has been procured and is at LANL now being characterized. The field-cancellation coils are under construction and we are on-schedule for benchmarking the field cancellation from DC to < 1 kHz in 2013. These steps are critical to achieving our milestone of a V1 system demonstration by the end of 2013.

Cryo-system development
We have made significant progress in characterizing the cooling needs, and simulating various cooling schemes. Refrigerator designs are presently being assessed for cost/benefit analysis, which will be completed in FY2013. We have also made some preliminary noise measurements of at least one cryo-cooling design to understand the implications for the SQUIDs.

Version 1 system
We have accomplished the goals for refurbishment and testing of the pre-polarization coil. We elected to pursue a liquid nitrogen design, and have determined that we can effectively insulate the coil such that it is suitable for imaging a human subject. Further, this coil can deliver ~ 300 mT in field - far surpassing our desired goal of 100 mT. Thus we have plenty of head-room in this design. We have a complete MRI set-up at this time, and are presently working on first imaging. This puts us on schedule for the V1 system milestone. 6) Low temperature Bp development: We have conducted extensive simulation of materials for the low-temperature Bp option. It appears that a true superconducting coil will produce too many issues with residual field and eddy currents. We have manufactured and tested a bench-marking coil based on high purity aluminum. This coil has been characterized via simulation and validating experimental tests have been performed. The coil appears to be at the edge of suitability for performance, largely based on our ability to construct a suitable cryostat. We are presently conducting a more extensive simulation and engineering design to determine if an additional test coil is warranted, or if we ought to pursue a less-costly (but more power intensive) chilled-water cooled version at this juncture.

The results of the first year's efforts have been included in a publication on the technique of ULF MRI (appeared in Journal of Magnetic Resonance), and have already helped in program development exercises with DARPA and NNSA.

Future Work

Sensor array development
We will upgrade the sensor system to include additional channels required for noise cancellation.

Pulse sequence development
We will demonstrate projection imaging and compressed sensing methods that will enable faster data acquisition than our previous linear approaches.

Field Coils and Adaptive Shielding
We will test and optimize the measurement and adaptive shielding coils constructed in Year 1 on the V1 system. Based on our results, we will iterate and upgrade the coil design.

Cryo-system development
We will develop the cooling system for the pre-polarization coil sub-system, and begin cryo-system fabrication as required.

Version 1 system
A milestone at the Year 1 to Year 2 transition is demonstration of an image from the V1 system.

Low temperature Bp development
In year two we will will down-select materials and develop (as required) a bench-scale coil for evaluation. A Milestone in Year 2 is a critical design review of the magnet design we plan to move forward with in the V2 (final) system.

V2 system
In the second year of the project we will begin design and fabrication of all upgraded magnetic field generation hardware.

Conclusion

The design goals for our proposed system are: 1) a diagnostic quality image as defined by image SNR > 20 and voxel size 2×2×4 mm3; 2) compact system footprint 2×2×2

m3 with open design; 3) infrequent cryogen replenishment, e.g. maintenance interval at >6 months; 4) 20 minute scan time; and 5) production cost of ~$ 500 k, 10X less than a HFMRI. Key innovations are the use of ultra-sensivite SQUID detection, pulsed-magnet technology, low-noise cryorefrigeration, and an adaptive noise cancellation approach. This approach will enable field-deployable MRI that is presently is not available.

Publications

Espy, M.. Applications of SQUID Detected MRI. Invited presentation at International Society for Magnetic Resonance in Medicine. (Salt Lake City, Utah, 4-7 April, 2013).

Espy, M.. Applications in ULF MRI. To appear in Ultra-Low Field NMR and MRI. By Kraus, R. H., M. Espy, P. Magnelind, and P. Volegov.

Espy, M.. Chapter 8 - Hardware Developments: Detection using Squids and Atomic Magnetometers . To appear in Mobile NMR and MRI. Edited by Johns, M..

A Time Reversal Non Contact Acoustical Source for NEWS (Nonlinear Elastic Wave Spectroscopy)

Pierre-Yves Le Bas
20120116ER

Introduction

The goal of this project is to develop a novel noncontact high amplitude acoustic source. The motivation for this is to be able to use Nonlinear Elastic Wave Spectroscopy (NEWS) techniques for non destructive testing. These techniques have been shown to be more sensitive to early damage than any other techniques; however they do require higher amplitude that can currently be generated by standard non contact transducers and bonding transducer is time consuming and can be prohibited on certain samples, thus reducing the field of application of those techniques.

Our objective is to use Time Reversal, a technique to focus wave energy, to develop a new non contact source that will be able to generate amplitude high enough to apply NEWS. In order to create a working device, we will (1) develop the electronics and algorithms to generate arbitrary waveforms with a minimal amount of calibration; (2) design the chaotic cavity to optimize the time reversal process while preserving a flat bandwidth through modeling and experimental validation; and (3) test the transducer on a variety of samples of different materials and shapes. At the end of this project, we expect to have a complete system comprised of hardware and software that, when supplied with an arbitrary waveform and a standoff distance, will generate the desired signal in the sample at amplitudes much higher than any non-contact transducer currently available. Success in development of the time reversal non-contact source will lead to broad application of NEWS. Of particular interest are applications to objects that cannot be touched or are too small to have transducers attached

Benefit to National Security Missions

A non-contact acoustical source has many applications. Within LANL, it will enhance the NDE capabilities of parts that cannot be touched, namely weapon components and actinides. There is also potential for external commercialization of the source; Polytec Inc. expressed interest in adding a mature non-contact acoustical source to their range of products.

Progress

In FY13, Marcel Remillieux has been hired as a post-doc for developing the modeling aspect of this project. This hire happened later than expected in the project as the first candidate rejected the offer from LANL. However, since Marcel's arrival, the modeling that was until now handled by Belgian collaborators has received the full time attention of Remillieux and thus a large degree of progress has been made. We now have a better understanding of the physical mechanisms involved in the operation of the device that will allow us to better exploit these mechanisms for a higher degree of focusing efficiency (e.g. efficient sound radiation from the device). The first numerical results are already giving indications on how to change the cavity shape to create a more efficient system.

Experiments for validating modeling results are underway. In-plane generation has been demonstrated, reinforcing the uniqueness of this non-contact source.

Experiments conducted this year have shown great improvements in the focal signal in terms of the focal quality and the ability to customize the focal signal

The software for driving all the elements of the system has been developed and should make the use of this emitter easy for any user even without the knowledge of how the source works.

Unfortunately, the critical patent application related to this project has been dropped by the USPTO due to a lack of response in time by our LANL tech transfer legal department. We are currently evaluating what solutions are remaining to protect IP, but options might be limited because of the following publications that were made after the patent application became publicly available.

Results have been shared with the scientific community in several meetings:

Invited presentation at the Acoustical Society meeting in Hong-Kong: "Toward a high power non-contact acoustic source using time reversal," Pierre-Yves Le Bas , TJ Ulrich , Brian Anderson , J. James Esplin, J. Acoust. Soc. Am. 131, 3461 (2012).

Invited presentation at the Acoustical Society meeting in Montreal: "Improving the focal quality of the time reversal acoustic noncontact source using a deconvolution operation," Brian E. Anderson , Timothy J. Ulrich , Pierre-Yves Le Bas, J. Acoust. Soc. Am. 133, 3497 (2013). International Congress on Ultrasonics in Singapore: "Simulations of a High Amplitude Air Coupled Source based on Time Reversal," Steven Delrue, Koen Van Den Abeele, Pierre-Yves Le Bas, TJ Ulrich and Brian Anderson, proceeding to be published.

International Congress on Nonlinear Elasticity in Materials, in Cefalu, Italy: "Improving time reversal focusing through deconvolution: 20 questions," T. J. Ulrich, Brian Anderson, Pierre-Yves Le Bas, Cedric Payan, Johannes Douma, and Roel Snieder, Proc. Meet. Acoust. 16, 045015 (2012).

Several papers have been published, are under review, or are in preparation:

"A high amplitude, time reversal acoustic non-contact excitation (trance)," Pierre-Yves Le Bas , T. J. Ulrich , Brian E. Anderson , J. James Esplin, J. Acoust. Soc. Am. 134, EL52-EL56 (2013). "Improving the focal quality of the time reversal acoustic noncontact source using a deconvolution operation," Brian E. Anderson, TJ Ulrich, and Pierre-Yves Le Bas, Proc. Meet. Acoust. 19, 065069 (2013). "Comparison and visualization of the focusing wave fields of various time reversal techniques in elastic media," Brian E. Anderson, TJ Ulrich, and Pierre-Yves Le Bas, J. Acoust. Soc. Am., under review."Optimization of time reversal focusing and source reconstruction through deconvolution," TJ Ulrich, Johannes Douma, Brian E. Anderson, and Roel Snieder, submitted to Wave Motion. "Numerical study and optimization of a non-contact acoustic source," Marcel C. Remillieux, Brian E. Anderson, Pierre-Yves Le Bas, and T. J. Ulrich, to be submitted to J. Acoust. Soc. Am.

This project has been featured in LANL 1663 and the Acoustical Society of America newsletter, Echoes.

Future Work

During FY14, the focus of this project will be on optimizing the shape of the prototype and active element positioning by using the results of numerical modeling to guide experimental redesign for improved results. Software and hardware allowing a larger number of channels to be used to create higher amplitudes will be finalized. Signal processing that improves the quality of the focal signal will be added to the software driving the system. A final prototype will be built and tested. If budget allows, a second prototype working at higher frequency will be tested (electronic equipment has been identified). The final prototype will be tested for non-destructive testing using nonlinear acoustic techniques. Tech transfer communications will continue regarding IP protection and the search for potential partner for further development and potential commercialization (Polytec, Inc. and Chevron have shown interest in such technology).

Collaborations with the Katholieke Universiteit Leuven Campus Kortrijk, Belgium (KULAK) and the Colorado School of Mines (CSM) will continue. Publications and presentations at international scientific meetings will continue.

Collaborators at KULAK are: Koen Van Den Abeele (Koen.VanDenAbeele@kuleuven-kortrijk.be) and Steven Delrue (Steven.Delrue@kuleuven-kortrijk.be).

Collaborators at CSM are Roel Snieder (rsnieder@mines.edu) and Johannes Douma (jdouma@mines.edu)

Conclusion

In this project, we will developed a noncontact acoustic source able to generate large amplitude waves. This will allow the use of nonlinear techniques for non destructive testing. These techniques are the most sensitive to early damage and thus their use could reduce early part replacement based on statistics and eliminate outliar for critical parts. The use of a contact source slow down and reduce the use of nonlinear techniques. This source has also the potential to generate in-plane motion which is critical to detect some defects normal to the surface. Currently, no commercial source can do this without contact.

Publications

Anderson, B. E., T. J. Ulrich, and P. -Y. Le Bas. Improving the focal quality of the time reversal acoustic noncontact source using a deconvolution operation . 2013. In International Conference on Acoustics. (Montreal, Canada, 2-7 June 2013). Vol. 19, POMA Edition, p. 030080. Montreal: Acoustical Society if America.

Anderson, B. E., T. J. Ulrich, and P. -Y. Le Bas. Comparison and visualization of the focusing wave fields of various time reversal techniques in elastic media. To appear in Journal of the Acoustical Society of America.

Bas, P. Y. Le, T. J. Ulrich, B. E. Anderson, and J. J. Esplin. Toward a high power non-contact acoustic source

using time reversal. 2012. In 163rd Meeting of the Acoustical Society of America. (Hong-Kong, Hong-Kong, 13-18 May, 2012). Vol. 131, p. 3461. N.A: Journal of the Acoustical Society of America.

Bas, P. Y. Le, T. J. Ulrich, B. E. Anderson, and J. J. Esplin. Toward a high power non-contact acoustic source using time reversal. 2012. Echoes, Newsletter of the Acoustical Society of America.

Bas, P. Y. Le, T. J. Ulrich, B. E. Anderson, and J. J. Esplin. A high amplitude, time reversal acoustic non-contact excitation (trance). 2013. JOURNAL OF THE ACOUSTICAL SOCIETY OF AMERICA. 134 (1): EL52.

Remillieux, M., B. E. Anderson, P. -Y. Le Bas, and T. J. Ulrich. Numerical study and optimization of a non-contact acoustic source. Jounrtal of the Acoustical Society of America.

Ulrich, T. J., B. E. Anderson, P. Y. Le Bas, C. Payan, J. Douma, and R. Snieder. Improving time reversal focusing through deconvolution: 20 questions. 2012. In International Conference on Nonlinear Elasticity in Material. (Cefalu, Italy, 1-8 July, 2012). Vol. 16, POMA Edition, p. 045015. Cefalu, Sicily, italy: Acoustical Society of America.

Ulrich, T. J., J. Douma, B. E. Anderson, and R. Snieder. Optimization of time reversal focusing and source reconstruction through deconvolution. Wave motion.

Measurement of Pressure and Temperature in Thermal Explosions

Markus P. Hehlen
20120247ER

Introduction

Pressure (P) and temperature (T) are the key quantities that enable a detailed understanding of the mechanisms of ignition, subsonic burning (deflagration), and the final transition to a violent response of plastic bonded explosives. Pressures of hundreds of MPa and temperatures >1000 oC develop during the final few microseconds of a thermal explosion. Conditions are even more violent in the supersonic regime of detonation. There are no commercially available P/T sensors which can be used under such extreme conditions. The goal of the proposed research is to design, construct, and test an active fiber-optic sensor that provides a dynamic optical measurement of both pressure and temperature within a thermal explosion. Our new sensor concept will offer high spatial and temporal resolution in a P/T regime that is not accessible by any existing sensor technology. We have already largely proven the feasibility of our concept. This work will therefore focus on delivering a well-engineered fiber-optic P/T sensor that can be calibrated, reproduced, and readily deployed into a variety of dynamic experiments. Predicting the "reaction violence" of high explosives has been the holy grail of many large programs for years as it is the foundation for understanding the performance and assessing the safety of these materials. Success of the proposed research will enable measurement of accurate P/T time-trajectories within a thermal explosion for the first time. This will allow calculation of the burn velocity, quantification of the complex interplay of chemical reactions, and prediction of the final transition to a subsonic or supersonic violent event. This insight is essential to a full understanding of the ultimate response of the metal case under both normal and accident scenarios.

Benefit to National Security Missions

An intrinsic dynamic P/T measurement within a thermal explosion is not currently possible, yet this data is critical to the understanding of explosives response at both a fundamental and an applied level. The proposed fiber-optic P/T sensor directly addresses this capability gap. If successful, we will establish a new diagnostic capability that will benefit LANL and the explosives community as a whole. It will enable new scientific discovery in the field of high explosives and provide previously unavailable data to many ongoing programs that address performance, safety, and accident scenarios of our nuclear weapons and conventional munitions stockpile. It will also advance our multidisciplinary capability in measurement science and diagnostics under extreme conditions and thereby directly benefit future LANL missions such as MaRIE.

Progress

Fiber-optic pressure sensor

We have successfully conducted an important first test of the fiber-optic pressure sensor for hydrostatic loads of up to 100,000 psi on a load frame. The system performed well, and the measured optical reflectivity of the multi-layer dielectric coating in the sensor tip decreased with increasing pressure, as expected. There was an excursion of the response at higher pressures which may be due to compliance in the pressure cell. This is currently being analyzed further to identify any changes that need to be implemented for the next load frame experiment. In parallel, we have created a first numerical model of the multi-layer dielectric coating that can predict the optical reflectivity of the coating as a function of probe wavelength, pressure, and temperature. First results from this model indicate that the coating layer thicknesses should be adjusted to minimize a temperature-induced response of the pressure sensor. The calculations are currently being refined, and we expect to place an order for a new batch of coated fibers later this FY that will undergo testing on the load frame setup.

Fiber-optic temperature sensor

The baseline architecture for the fiber-optic temperature sensor consists of a single-mode optical fiber that has a short (typically <100 um) section of erbium-doped fiber

spliced onto the end. Earlier this FY we have developed a gold/silica coating that was deposited over the end-face of the fiber in order to (1) block any external light (from the reacting explosive) from entering the fiber and (2) reflect the pump laser light and obtain a double-pass pumping of the short erbium-doped fiber section. We have conducted extensive characterization of this fiber-optic sensor and found that it shows useful temperature sensitivity in the 300-700 K range which is due to temperature-induced changes in the erbium luminescence spectrum. The erbium related response is expected to diminish above 700 K, and for those temperatures we intended to rely on thermal emission from the coating. Our experiments showed that the gold coating had excellent reflectivity. This meant conversely that it had very minimal thermal emission, which in fact was too low for use as a local temperature probe. Based on our success with a chromium fiber-cap for the pressure sensor, we have since developed a revised architecture that will use a small amount of europium-doped yttria phosphor at the fiber tip. This material is known to have a characteristic change in quantum efficiency over a wide range of (high) temperatures, allowing us to use the luminescence intensity relative to a room temperature standard as a thermometer. This architecture is currently being set up and first tests will be conducted later this FY.

The project was selected for a presentation at the 2012 LANL LDRD Day. Furthermore, the results from the pressure sensor development are being presented at the Conference on Lasers and Electro-Optics (CLEO) in San Jose in June 2013. Two publications are currently in development and will be submitted to peer-reviewed journals.

Future Work

Pressure sensor

The refined version of the pressure sensor will be fabricated, characterized using methods developed in FY12 (spectroscopy, load frame), and then tested in an DDT and/or cook-off explosives experiment. A second explosives test is planned to us the 6-channel system for the simultaneous measurement of several pressures at different locations in the confined experiment.

Temperature sensor

A refined version of the temperature sensor will be fabricated and tested in a high temperature furnace. A set of temperature sensors will be tested in an explosives cook-off experiment.

The results of these activities will be published in the peer-reviewed literature and, if possible, at a national conference (e.g. CLEO 2014).

Conclusion

Individual pressure (P) and temperature (T) sensors capable of calibrated measurement of 10–1000 MPa and 20–500 oC, respectively, with 1 µs response will be demonstrated. An integrated P/T sensor with these properties will be fielded in DDT and HEVR shots to demonstrate simultaneous calibrated P/T measurement with ~175 µm spatial resolution. We will publish our results in the peer-reviewed literature and present at conferences, including the International Detonation Symposium and SPIE.

Publications

Hehlen, M. P., B. W. Asay, G. R. Parker, L. B. Smilowitz, and B. F. Henson. Fiber-optic measurement of high temperatures with sub-millimeter spatial resolution. 2012. CLEO Technical Digest. : CM1F.6.

Hehlen, M. P., G. R. Parker, A. M. Novak, P. Rae, G. Rivera, D. W. Schmidt, K. C. Henderson, B. M. Patterson, and L. B. Smilowitz. Fiber-optic point measurement of high pressures in thermal explosions. 2013. In Conference on Lasers and Electo-Optics. (San Jose, 9-14 June 2013). , p. CTu2H.6. Washington, DC: Optical Society of America.

Hehlen, M. P., L. B. Smilowitz, G. R. Parker, A. M. Novak, M. D. Holmes, K. C. Henderson, G. Rivera, and D. W. Schmidt. Measuring Pressure and Temperature inside a Thermal Explosion. Invited presentation at LDRD Day 2013. (Pojoaque, NM, 23 October 2012).

High-Energy Segregated Fuel-oxidizer Solid Rocket Propulsion System

Bryce C. Tappan
20120285ER

Introduction

The aim of the proposed effort is to develop a segregated fuel-oxidizer propellant system that could be a major break-though in solid rocket propulsion in terms of safety and energy. The proposed system is a combination of novel materials that allow for a radically new engineering design. Because of the development of high-nitrogen/high hydrogen energetics at LANL that contain little or no oxygen, a segregated tandem system can be designed such that the energetic material will provide fuel from their decomposition that will be oxidized in a separate chamber by reaction with a solid oxidizer. Because the fuel and the oxidizer will remain separated until combustion of the fuel is initiated, and are both are relatively (or completely) insensitive to shock, the chance of accidental detonation or initiation of the rocket is dramatically reduced. These technologies that will allow for both a higher energy and much safer solid propellant propulsion system then is currently offered the state-of-the-art.

While solid propellant systems have proven reliable over the decades, they have long since reached their limit in terms of achievable safety and performance. However, the US DoD, NASA and commercial organizations continue to request increasingly higher-energy systems with an increased level of safety. These two characteristics, however, are almost always mutually exclusive, being that typically the higher energy systems almost always have the penalty of being higher hazard. Thus, in our current risk-adverse times, in order to have a system qualified as an "insensitive munition" by the DoD, a loss in performance is often accepted. Here we propose that a segregated fuel/oxidizer system can be designed such that it will provide an unprecedented level of safety and will thus allow for the utilization of higher energy components and will therefore be a much higher performing system than state-of-the-art solid propellants.

Benefit to National Security Missions

The applicability of this work to the US DoD, NASA and commercial organizations is due to the higher-energy systems with an increased level of safety. The DoD runs the Joint Insensitive Munitions Technology Program, with a specific topical area to fund 6.2-6.3 levels of development of insensitive propellants systems, which will be a perfect fit for transition of this work owing safety of this system.

NASA has various programs such as NextGen Concepts and Technology Development Project or Heavy Lift Propulsion Technology that could also benefit from the transitioning of research gains from this program.

Progress

A simplified model was developed to determine nozzle specifications and instantaneous pressure-time profiles for solid rocket experiments. This was then used to predict a series of nozzle diameters and pressure profiles for TAGzT burning under specific operating conditions and propellant geometry. As the nozzle size is decreased, the chamber pressure increases, thus decreasing burning time. Continued testing is ongoing to find the correct nozzle geometry to provide a neutral pressure-time profile using TAGzT end burner grains. One of the key observations of this project is that high-nitrogen/hydrogen fuels are subject to greater combustion instability than classic propellants, which often leads to over or under-pressurization in the chamber. This problem is being addressed by evaluation of new propellant formulations, a number of which have been evaluated and pressure vs burning rate graphs have been determined. To aid in the more rapid completion of this work, a new strand burner was built and provided by Penn State, which is now in place at LANL and is awaiting evaluation and approval by the LANL Pressure Safety Committee.

Additionally, the mechanism of this instability leading to failure is under investigation in collaboration with C-PCS using their fast x-ray imaging technique. For this an x-ray transparent motor has been designed and is currently being built. A series of opposed flow tests at atmospheric pressure to determine the burning rate of TAGzT as a function of oxygen flow rate have been performed. It was demonstrated that there is a critical amount of oxygen that is required to accelerate the burning rate until the heat transfer overwhelms the energy liberated by the combustion process. Finer resolution testing between 0 and 1 liter/minute oxygen flow will commence in the near future. As the delivery rate of the oxygen supplied to the surface is increase, the slope of the position time profile also increases; indicating the available oxygen to the surface increases the heat feedback to the surface. Under high pressures, this phenomenon may be less significant. In the next stage of this study a solid propellant opposed flow burner for elevated pressures has been designed and is currently beginning fabrication at Penn State. This will be used to examine gap distance and pressure effects on burning rate of the fuels and oxidizers, and will provide kinetic data of interactive reaction of the two materials. Interestingly, in the full motor testing of TAGzT formulations feeding product gases into AP pellets has shown that the rate of AP reaction is dependant mostly on the rate of the fuel products delivery to the oxidizer material, which was one of the main goals of this work, and will greatly simplify future utilization of this technology. The solid propellant opposed flow burner should be able to quantify this effect with various different fuels and oxidizers.

Efforts were also put into evaluation of the flame structure and temperature of the combustion of high-nitrogen fuel materials. The flame structure of a propellant is one of the important components for modeling input to predict the behavior of a rocket motor. This information is typically obtained simply from high-speed visual records of the combustion. With the combustion of high-nitrogen fuels, however, the flame structure is non-luminous, so a structure has never been observed. We, for the first time ever, observed the flame structure of the combustion of high-nitrogen materials using a Forward-Looking Infrared (FLIR) high-speed camera, while simultaneously obtaining temperature throughout the various flame zones. These data will be transferred to the modeling effort associated with this project. Work on this area is on-going this fiscal year, in which we are planning to obtain filters for the FLIR camera to provide real-time product determination for selected gases (such as carbon monoxide or carbon dioxide). This will allow the tracking of specific gases in the flame, and thus provide information on the rate of reaction of fuel products with the oxidizer in the product gases of the motor.

A scaled-up motor (2" ID) and thrust stand was produced and will begin this FY.

The initial patent for this technology was filed this year, and the Technology Transfer Division initiated interaction for possible industrial partnerships with ATK and Boeing.

Future Work

The goals and tasks for FY14 include continued characterization of new fuels with modified burning rates to build upon those produced in FY12-13, and most importantly to determine the reaction kinetics of oxidizer regression with fuel reaction products at high temperatures and pressures. This will be achieved using the duel fuel-oxidizer instrumented opposed flow reactor developed at Penn State in FY12-13. Results from these tests will allow for better modelling of motors due to a greater understanding of reaction rates at high temperatures and pressures. This task as well as small motor testing will allow for the milestone of thermoequilibrium maximization and a working counterflow model to be developed.

Work has begun in FY12 to measure thrust and chamber pressure in initial systems at small diameters. Goals for FY13 include perfecting these measurements and instrumentation, and scaling up to larger motor sizes, and the realization of one of the projects milestones of the development of a safe and reliable test bed for testing this system.

Data from thrust stands and chamber pressure measurements will allow for the down selection of fuel and oxidizer ingredients. Once this is achieved, explosives hazard analysis can be performed on ingredients of verify their safety properties, as one of the major overall goals of this project is to demonstrate the inherent safety of the concept. FY14 will include the bulk of these tests when final formulations have been down-selected such that the technology can be transitioned to industry more easily.

Conclusion

The US DoD, NASA and commercial organizations continue to strive for increasingly higher-energy propellant systems with an increased level of safety. These two characteristics, however, are almost always mutually exclusive. Higher energy systems almost always carry the penalty of being higher hazard. Here we propose designing a novel segregated fuel/oxidizer system that will provide an unprecedented level of safety, allowing previously inaccessible utilization of higher energy components, thereby exceed-

ing performance of state-of-the-art solid propellants.The expected result at the end of this project is to produce a breakthrough solid rocket motor design that is safer and higher performance than existing technology.

Publications

Regression rate of TAGzT with various oxidizers in a stagnation flow configuration. Journal of Propulsion and Power.

Observations of the kinetic isotope effect in the combustion of nanoaluminum and liquid water. Journal of the American Chemical Society .

Combustion performance of HTPB-based solid fuels containing TAGzT. Journal of Propulsion and Power.

High Performance Thin Film Super Capacitors

Aditya Mohite
20130527ER

Introduction

An electrochemical double layer capacitor (EDLC), also known as a supercapacitor, is an energy storage device that has energy densities typically 100-1000 times greater than conventional electrostatic capacitors. In contrast with traditional capacitors, electric double layer capacitors do not have a conventional dielectric material. Instead two high surface area electrodes (typically activated carbon) are separated by an electrolyte. Upon application of a voltage, an "electrical double layer" is formed at the electrode surfaces with atomic scale charge separation (on the order of a few nanometers) creating a very large charge storage capacity. Microscale supercapacitors provide an important complement to batteries in a variety of applications, including portable electronics. Although they can be manufactured using a number of printing and lithography techniques, continued improvements in cost, scalability and form factor are required to realize their full potential. A major bottleneck in their wide spread use is achieving high energy and power densities at a low cost. In this project, we directly confront these issues by developing a graphene oxide (GO) based thin film micro supercapacitor first demonstrated by a team member of this proposal (W. Gao) that uses an innovative and industrially scalable laser pattering approach. In our device, GO acts as solid-state electrolyte/separator that separates the laser exposed/electrically conducting reduced graphene oxide (RGO). As discussed below, such devices can (theoretically) outperform existing state-of-the-art thin film micro supercapacitors. In this proposal, we will 1) increase the energy density of the GO supercapacitor to a level comparable to Li-ion batteries, 2) increase the power density while maintaining fast charging/discharging rates and 3) improve the mechanical strength and flexibility of the thin film GO supercapacitor.

Benefit to National Security Missions

This proposed work addresses a critical energy related challenge, i.e., development of lost cost materials to store energy. As such, this work fits into the Materials Pillar as well as the EES grand challenge, while being focused on the engineering challenges needed to optimize the very impressive properties already demonstrated for patterned graphene oxide supercapacitors. Suc-cessful optimization of the thin film GO supercapacitors will be useful for a range of applications in industry (e.g., car starters), defense and intelligence agencies, which always needs low cost, light weight materials.

Progress

Our goals of this project were to a) increase the energy density by using a NIR laser and by reducing the dimensions to micron scale b) increase ionic conductivity by chemical modification of GO and c) develop supercapacitors on flexible substrates. Since the beginning of the project we have successfully accomplished the patterning of Go based supercapacitors with tens of microns of resolution. We find that the measured capacitance is an order of magnitude larger than the defined area. We have also shown that the ionic conductivity of GO increases by 4 times by ozonating its surface, which helps in proton conductivity. We have also developed hybrid GO based composites like GO paper and GO-PEO based to increase mechanical strength – mechanical testing of GO and RGO films and composites underway (Collaborator: Nate Mara, MPA-CINT).

In addition, we are working with the AET division (Engineering) on several applications using the thin film GO supercapacitors such as skin sensors to wings of aircrafts that will help us detect stresses on the aircraft by measuring the changes in the capacitance of the GO supercapacitor. We are also working to build an aerial mobile sensor node whose fuselage is built from capacitive GO paper. GO paper will serve the roll as structure and

energy storage. Some challenges during this project that we solved were making low resistance contacts to RGO electrodes for micron scale devices due to alignment

issues, lesser degree of reduction using femtosecond laser for patterning and the total output of number of devices using femtosecond laser patterning. These are solved and we are on track for achieving our goals for the project.

Future Work

- Demonstrate GO based supercapacitors with three different dimensions and how they could be applied for a variety of applications.
- Connect these supercapacitors in series and parallel to generate large amount of useful energy for portable electronics; This will be performed by using a shadow mask.
- Demonstrate higher energy density and ionic conductivity by functionalization of GO and explore better methods of exfoliation.
- Demonstrate the use of thin film supercapacitors as a capacitive skin sensor.

Conclusion

In this project, we will 1) increase the energy density of the GO supercapacitor to a level comparable to Li-ion batteries, 2) offer high power density while main-taining capacitance densities and 3) improve the mechanical strength and flexibility of the thin film GO supercapacitor.

This proposed work addresses a critical energy related challenge, i.e., development of lost cost materials to store energy. Successful optimization of the thin film GO supercapacitors will be useful for a range of applications in industry (e.g., car starters), defense and intelligence agencies, which always needs low cost, light weight materials.

Publications

Gao, W., C. Galande, A. Mathkar, T. Narayanan, A. Mohite, and P. Ajayan. Science and Engineering of Graphene Oxide. To appear in Particle and Particle Systems, Wiley.

Sharp, N., A. Kuntz, C. Brubaker , S. Amos, W. Gao, C. Farrar, A. Mohite, G. Gupta, and D. Mascarenas. Endowing Structures with a Nociceptive Sense Enabled by a Graphene-Oxide Sensing Skin. Presented at International Modal Analysis Conference. (Orlando, Feb3-6 2014).

Emittance-reduction System for Future Accelerator Solutions

Kip A. Bishofberger
20130688ER

Introduction

More than any other measure, the beam brightness has been the driving force for technological development in beam physics. Until recently, the beam's "emittances" (the rms area in phase space, comparable to temperature) were considered constants of linear motion, and nonlinear forces only increased them, thereby reducing the beam brightness.

However, within the past couple of years, a breakthrough has developed, largely originating with scientists at LANL. The term "eigen-emittances" refers to the emittances that a beam would possess if there were no additional correlations. The new discovery is that, by generating a beam with specific initial correlations, the eigen-emittances can be substantially reduced, and through beam optics that unravel the correlations, the final, observed emittances will take on these improved values.

The technology development capability supported by this proposal enhances our ability to design Engineered Systems. Additionally, compact, advanced accelerator technology supports a wide array of accelerator-based solutions to National Security missions. Two examples include Global Security, such as Warfigher Support (high-power FELs) and Countering Weapons of Mass Effect (active interrogation).

Benefit to National Security Missions

Los Alamos is an accelerator-centric National Laboratory. Major accelerator facilities at LANL include LANSCE and DARHT, and successful implementation of the proposed MaRIE signature science facility will require developing new accelerator capabilities.

Additionally, several emerging major Global Security work-for-other missions require state-of-the-art accelerator technology.

The work in this project directly supports future light sources (such as that proposed for the MaRIE XFEL) and future linear colliders, which are major DOE Office of Science projects. In turn, light sources support the Materials: Discovery Science to Strategic Applications grand challenge and linear colliders support the Beyond the Standard Model grand challenge.

More directly, the technology development capability supported by this project enhances our ability to design Engineered Systems, another grand challenge. Additionally, compact, advanced accelerator technology supports a wide array of accelerator-based solutions to National Security missions. Two examples include Global Security, such as Warfigher Support (high-power FELs) and Countering Weapons of Mass Effect (active interrogation).

Progress

This past year, we established several ideal candidate accelerators to demonstrate the emittance-reduction system. With widely ranging particle species, energies, parameter ranges, and availabilities, this optimization took several months of simulation work and comparisons. The simulation work defined important parameters of the individual system components, and generated more understading of the underlying physics and science behind this new emittance-reducing technique.

More specifically, it was discovered that beamlines of low energy are more constrained than higher energy. Passing the beam through a foil is not as fruitful for these low-energy beams as a canted-undulator technique. At higher energy, the simpler foil option is ideal for significant emittance reduction. However, another constraint is the beam-position stability; tests at on-site facilities have shown that significant position jitter prevents optimal emittance improvement. Adjusting the technique's parameters accomodates the high jitter, at somewhat reduced optimization.

Interested collaborators from several facilities, both onsite and outside Los Alamos, have expressed interest in our technical progress. Several presentations at international conferences have been generated. A significant amount of effort has been devoted to future publications.

Future Work

During the next year, this project intends to establish the ideal candidate accelerator to demonstrate the emittance-reduction system. With widely ranging particle species, energies, parameter ranges, and availabilities, this optimization will take several months of simulation work. The simulation work will also define the parameters of the individual system components. Simulation by itself is publishable work, and it is critical to the success of the project.

Simultaneously, construction of the various beamline elements will need to commence to be able to perform experiments and a full demonstration of the process. By the end of the year, the project will have developed an optimized emittance-reducing scheme which is scaleable to numerous types of accelerator and beamline applications.

Conclusion

This project intends to develop a new, revolutionary concept in accelerator physics. In particular, theory has shown that setting specific correlations within the particle distribution, and finally unraveling those correlations, the final transverse emittances will be superior to previous capabilities. This project intends to demonstrate and optimize this technique, in order to generate particle beams of exceptional brightness.

Updates to existing accelerator facilities (such as LANSCE and DARHT), future construction of the MaRIE signature-science facility, and Global Security missions all depend on the technology of this project.

Technology

Harnessing Nonlinearity for Transformative Metamaterial Technology

Houtong Chen
20110027DR

Abstract

New classes of nonlinear metamaterials are developed to combine the exquisite control of electromagnetic radiation offered by artificial metamaterials and various functionalities supported by nonlinear elements embedded in the metamaterial fabric. In particular, we developed two signature applications of nonlinear metamaterials, namely a compact source of millimeter electromagnetic waves and highly efficient nonlinear optical modulators. We developed modeling and simulation tools for nonlinear metamaterials based on circuit theory, modal expansions, and in-house numerical software. Furthermore, this project has had several other scientific spin-offs, including novel designs for metamaterial perfect absorbers, polarization control, anomalous reflection and refraction, and even nonlinear high-temperature superconducting metamaterials. The results of this project are of strategic importance to the laboratory and national mission since it allowed us to advance the science and technology of artificially engineered nonlinear metamaterials and devices for sensing and measurement for Global Security applications. We expect that this DR project will transition to external funding opportunities from the Mesoscale and Advanced Manufacturing National Initiatives, as well as puts us in an excellent position to respond to the upcoming DOE/BES calls for EFRCs.

Background and Research Objectives

During the past decade many unusual properties of metamaterials have been demonstrated for unique control of electromagnetic waves. However, the most severe issues that prevent metamaterials from transitioning to practical applications are the inherent high loss and strong dispersion. Overcoming metamaterial loss and dispersion requires gain, frequency mixing, or other requisite nonlinear functionalities, which are weak in many natural materials. In 1999, John Pendry pointed out that the resonant behavior in split-ring resonators (SRRs) could localize electromagnetic energy within the capacitive “gap”, which could be used to enhance nonlinear phenomena. Yet the whole concept was largely forsaken at the time, and many phenomenological questions dominated nonlinear metamaterials research. Prior to the start of this DR project, there were little validation and few or no useful devices. Nonlinear metamaterials research activity, particularly adding gain, was increasing, but demonstrations remained few or marginal.

The objective of this project is combining the exceptional wave control of metamaterials with the exclusive functions of nonlinearity to unleash metamaterial technology, through creating dramatically improved or completely new electromagnetic devices, suitable for all manner of sensing and measurement purposes. In order to accomplish this objective, this project requires a com¬p¬rehensive, multi-disciplinary, experi¬mental and theoretical effort. In experiments, we worked toward development of two signature applications, a compact powerful source of millimeter or sub-mm electromagnetic waves and a class of highly efficient nonlinear photonic devices. In theory, we developed new predictive models and design and simulation tools for creating and optimizing nonlinear metamaterials and their derived electromagnetic devices.

Scientific Approach and Accomplishments

Metamaterial-Based Electromagnetic Sources

Self-oscillations in gain loaded metamaterials: A challenge for metamaterials has been the introduction of gain in order to overcome the inherent losses. In the GHz or even into the THz spectrum, electronic elements, such as resonant tunneling diodes (RTDs) can provide direct amplification of the induced current within the metamaterial elements. The introduction of gain to a metamaterial array would facilitate self-oscillation if sufficient feedback is designed into the constituent elements, which would lead to a metamaterial-based emitter (metamitter). With the integration of RTDs with appropriately structured metamaterial elements, a THz

based metamitter could be achieved operating at room temperature with only an applied DC bias voltage as a power source.

The initial proof of concept metamitters was designed to operate at microwave frequencies. We used a double gap single ring (DGSR) structure as the metamaterial element, with one gap integrated with a gain device (tunneling diode), as shown in Fig. 1(a). When this metamitter element was biased at appropriate voltage, a sharp self-oscillation signal was observed at 2.4 GHz, much higher than (35 dB) the noise floor, shown in Fig. 1(b). It was shown that the direct transition to multiple-element metamitter designs for single frequency operation is challenging mainly due to the strong coupling among the elements as well as the attribution from the necessary electrical leads.

We then designed metamitter targeting a frequency range 90-110 GHz. A major portion of this effort was to design and fabricate high frequency gain device (resonant tunneling diode) and integrate them with metamaterials. The semiconducting RTD layers were grown by MBE technique. The challenge of this nonlinear metamaterial sample lies in the fabrication of the air-bridges, which were used to connect the metamaterial resonator and the resonant tunneling diode. Collaborated with Sandia National Laboratories, we were able to form bridges that withstood the fabrication process, however, the air-bridges revealed visible cracks, with the cause of cracks unknown at this point. This results in an open circuit that prevents the application of the required voltage bias to observe self-oscillation.

Frequency Mixing and Pulling: When an external RF field (2.39 GHz), slightly offset from the self-oscillation frequency (2.40 GHz), was applied to the nonlinear DGSR metamitter, frequency mixing was observed as the external field strength was increased. The gradual appearance of the mixing components was only present on the high frequency side of the resonance, as shown in Fig. 1(c). The fundamental self-oscillation frequency for the DGSR shifted toward the external source frequency shown in Fig. 1(d). Eventually, as the external field strength further increased, the discrete frequency components appeared to collapse into a broad continuum, which often indicates the transition to chaotic behavior. The apparent discrete behavior in Fig. 1(d) at higher external RF levels was an artifact of the data collection process and plotting. The actual mixing process demonstrated a continuous response with increasing external RF amplitude. Similar frequency mixing and pulling were observed when the external driving field (2.41 GHz) was slightly offset to be higher than the self oscillation, except that the mixing components were at the low frequency side. The frequency mixing phenomena was not evident when there was a large difference between the external field and the self-oscillation frequencies, indicating that the fundamental resonance of the DGSR played an important role in the coupling from free space into the metamaterial resonances.

Bi-Stablility: We designed and fabricated nonlinear metamaterials exhibiting bistable and hysteretic behavior using the 1) double gap double ring (DGDR) and 2) DGSR with parasitically coupled single gap single ring (SGSR), with the latter shown in the inset to Fig. 2(a). Numerical simulations of the both structures revealed a low frequency fundamental resonance near 1 GHz attributed to the larger SRR component, a resonance near 2 GHz attributed to the smaller SRR component, and a higher frequency broad dipole resonance at 3 GHz. These samples were tested and demonstrated two different operational regimes dependent upon the bias voltage, as shown in Fig. 2(b) for the DGDR structure. At a lower bias voltage (70 mV), it started self-oscillating, supporting simultaneously the fundamental (865 MHz), second harmonic, and third harmonic (mixing) modes. At a higher voltage bias (140 mV), the metamitter supports only the second harmonic signal only. Similarly, the DGSR+SGSR metamitter element displayed the same dual operational states depending on the bias voltage, as shown in Fig. 2(c). The device exhibited hysteretic behavior, shown in Fig. 2(d) for the second harmonic signal as a function of the bias voltage.

We further performed experiments to switch the metamitter states using external RF field. While appropriately biased (120 mV), the DGSR+SGSR metamitter supported self-oscillation at all the three frequencies. When an external field at the second harmonic frequency (1.632 GHz) was applied, we observed that the self-oscillation mode immediately switched to mimic the driving field and continued in the second harmonic field only mode even after the external field was turned off. Simulation results are shown in Fig. 2(e) and (f), demonstrating that the observed experimental behavior was correctly modeled, and this required both the geometric designed resonances and gain to support this nonlinear behavior.

Frequency Down-Conversion: When the DGSR+SGSR metamitter was biased with under a sub-threshold voltage, there was no observable signal. However, if we applied an external RF radiation at a frequency coincided with a supported resonance, we observed the other harmonic oscillations. This observation could have specific impact on implementing heterodyne detection through frequency down conversion. For example, when the external RF source is exciting the sub-threshold metamitter element at 2.4 GHz (the third harmonic), a very strong signal is generated at 0.8 GHz. This could become innovative and significant at THz frequencies, as commercial electronics have an

upper limit on frequency response into 100's of GHz. The down conversion of THz signal could be detected directly with available electronics. This single element could then be treated as a pixel, with an ordered array of pixels forming a focal plane array for THz radiation and is a promising technological advance that can compete with other more complicated and technically immature THz imaging schemes.

Theoretical Developments for Nonlinear Metamaterials
Equivalent Circuit Models for Stability and Harmonic Behavior: A simple circuit model shown in Fig. 3(a) was chosen for a split-ring resonator (SRR) integrated with a tunneling diode at the gap, which was motivated by our experimental configuration. The physical circuit element consists of a resonator in series with a tunnel diode. Such circuits can exhibit self-oscillations when biased in the negative resistance portion of the tunnel diode characteristics (Fig. 3(b)). We examined the dynamics of such a circuit at sufficiently low loss and for a DC bias in a certain range, which revealing unstable solution and exhibiting self-oscillation. A corresponding frequency domain picture shows a rich spectrum of harmonics is generated, as shown in Fig. 3(c) and (d), consistent with the experiments. In addition, we observed an amplitude dependence of the response such that sufficiently large drive amplitudes tend to lock the response to the drive frequency, suppressing significant harmonic generation, as shown in Fig. 3(e), also qualitatively confirmed in the experiments.

A model for bistable metamaterials was devised to explain the experimental observations of bistability and hysteresis. The model is based on the dynamics of a pair of coupled nonlinear oscillators, and the method of analysis is based on the multiple time scale averaging technique we developed in previous years of this program. This leads to an analytic criterion on the metamaterial parameters for the situation where bistability can occur. Results of this numerical approach are shown in Fig. 2(e) and (f) demonstrating both "ground" and "excited" states behavior in this gain loaded metamitter element.

Progress on PEEC Methods for Nonlinear Metamaterials: Work has progressed in understanding and implementing the Partial Element Equivalent Circuit (PEEC) method in our nonlinear metamaterial problems. This method is valuable in being able to correctly incorporate inter-element delays, which in turn allows us to extend our nonlinear time domain models to high frequencies. We have undertaken a study of the mechanisms affecting stability of the time domain solutions. For simple sytems, in our case a strip line, we have formulated a stability criterion in the Laplace domain which shows the absolute stability of a passive system, even with embedded inter-cell delays. Our intent is to extend this analysis to more complex systems, which should lead to a method for extracting spurious roots to produce stable time domain solutions. This work is currently in progress and has the potential of leading to new funding opportunities, as this is a relatively unexplored methodology.

Modal Approach to Metamaterials: We have applied rigorous eigenmode analysis to study the electromagnetic properties of linear and weakly nonlinear metamaterials. The general goal of this approach is to find eigenmodes and the corresponding eigenfrequencies of a metamaterial comprised of periodically patterned metallic structures fabricated on top of a planar homogeneous substrate. The nonlinear response can be totally described by the linear eigenmodes when weak nonlinearities are attributed to metamaterials. We have used this theory to interpret second-harmonic spectroscopy on metallic metamaterials. Our study indicates that metamaterial eigenmodes play a critical role in optimizing a nonlinear metamaterial response to the extent that a poorly optimized modal pattern overwhelms the widely recognized benefits of plasmonic resonant field enhancements.

Metamaterial Enhanced Electro-Optic Modulation
One of the components of our project is to demonstrate enhanced nonlinearity induced electro-optic (EO) effect. The EO effect is described as a change of the refractive index (birefringence) of a material in response to the applied DC or quasi-DC electric field, which alters the polarization state of the light that propagates through the medium. This behavior has been utilized to design and fabricate EO amplitude and intensity modulators. However, the EO effect is generally very small, and traditional EO modulation systems require a longer EO crystal and extremely high quasi-DC field to achieve detectable signals. Metamaterials open a new avenue to enhance the EO modulation, as predicted by Pendry that the field concentration in the critical regions of SRRs at resonance could dramatically improve the weak nonlinearity of natural materials, which could significantly reduce the magnitude of the applied electric field or reduce the length of the nonlinear medium to realize a measurable EO effect.

Metamaterial Electro-Optic Modulator on ZnTe: A series of numerical simulations were performed to obtain SRR designs that could be fabricated with resonance frequencies within the scope of our measurement capabilities. We have selected ZnTe <110> as the electro-optic crystal for our demonstration. The SRR samples were fabricated on ZnTe crystal (Fig. 4(a)), or a FR4 substrate where a piece of ZnTe crystal could be mounted to obtain EO modulation. The samples were characterized using an experimental setup where the laser pulses were synchronized with the

microwave signal and the relative phase was precisely controlled. The EO signal as measured was proportional to the applied quasi-DC electric field, which was dramatically enhanced at resonance. Our experimental results were shown in Fig. 4(b) and (c), in which we obtained the spatial distribution along the vertical and horizontal directions, as shown by the green lines in the insets. As predicted, the maximum was obtained at the center of the capacitive gap of the SRR where the microwave field was concentrated due to the resonance, about five times enhancement as compared to other regions. Fig. 4(c) also shows that the distribution of EO signals on the left and the right of the gap had the similar amplitudes but opposite signs, meaning the presence of opposing fields as expected.

Metamaterial Electro-Optic Modulator on GaAs: As a step towards even higher efficiency EO modulation, we chose GaAs as the nonlinear crystal with much smaller ohmic loss at RF frequencies as compared to ZnTe, and by improving the impedance matching using a scheme shown in Fig. 4(d). It turned out that loaded Q-factors varied from 40 to 90, roughly 10 times improvement as compared to the case of ZnTe. The EO effect mapping experiment with the metacell excited at resonant frequency confirmed the resonant electric field enhancement with the electric field maximum inside the SRR gap. As shown in Fig. 4(e), the EO signal at the SRR gap exhibited qualitatively an order magnitude enhancement compared to that on ZnTe. The experimental results support our theoretical prediction.

Other Accomplishments

Metamaterials for Antireflection, Perfect Absorption, Polarization Conversion, and Anomalous Reflection/Refraction: We developed an interference-based theory which is able to explain the near unity absorption and/or antireflection observed in experiments and numerical simulations. The metamaterial forms a Fabry-Pérot-like cavity that the incident light will be trapped inside, with great enhancement of field intensity and light-matter interaction time, and therefore has promising potential for nonlinear applications. On the other hand, we successfully employed this interference mechanism for the development of metamaterial linear polarization converters and the demonstration of generalized law of reflection/refraction. For example, we demonstrated ultrathin (Fig. 5(a)), broadband, and highly efficient metamaterial-based terahertz polarization converters that are capable of rotating a linear polarization state into its orthogonal one (Fig. 5(b) and (c)). On the basis of these results, we created metamaterial structures capable of realizing near-perfect anomalous refraction (Fig. 5(d) and (e)) using a super-unit-cell shown in Fig. 5(d). The result shown in Fig. 5(e) is equivalent to a flat thin film prism without the need of prism shape. Our work opens new opportunities for creating high-performance photonic devices and enables emergent metamaterial functionalities for applications in the technologically difficult terahertz-frequency regime, particularly for sensing applications.

Nonlinear High-Temperature Superconducting Metamaterials: While metals have been used for the conductive elements in the vast majority of metamaterial structures, the use of superconductors is of rapidly growing interest. In contrast to metals, the complex conductivity of superconductors intrinsically depends on the magnetic field, temperature, and applied optical fields. Active metamaterial structures can therefore be realized by directly controlling the conductivity of the superconducting elements without introducing additional elements. In addition, superconductors exhibit superior conductivity at low temperatures and the potential to integrate elements exhibiting quantum behaviour. We demonstrated a nonlinear terahertz response of split-ring resonator arrays made of high-temperature superconducting films. Intensity-dependent transmission measurements indicate that the resonance strength decreases dramatically (i.e. transient bleaching) and the resonance frequency shifts as the intensity is increased. Pump-probe measurements confirm this behaviour and reveal dynamics on the few-picosecond time scale.

Impact on National Missions

This project is of strategic importance to the laboratory and national mission since it is advancing the science and technology of artificially engineered nonlinear metamaterials and devices for sensing and measurement for Global Security applications. Whether it is imaging, chem/bio sensing, signature science or any other mission, electromagnetic devices are at the heart of information-gathering efforts. The electromagnetic technologies developed in this project are particularly relevant to mission areas, including threat reduction, treaty monitoring, intelligence gathering, nonproliferation, basic science, and others. All such missions will benefit from electromagnetic devices that offer smaller size/weight, greater efficiency, lower cost, higher sensitivity or dynamic range, etc. The nonlinear metamaterials and devices developed in this project offer these advantages. The initial thrust of the experimental work was toward a compact, room temperature array that would oscillate in the THz region of the spectrum. However, the uncovered potential to develop a heterodyne focal plane array for THz imaging would greatly enhance national security in both threat detection and chemical sensing. This would enable the use of commercial off-the-shelf GHz technologies to access THz detection. Likewise, bistable externally triggered GHz oscillator could act as low detectability RF tagging and identification system which could impact covert surveillance activities. Likewise, the EO

modulator can encode microwave frequency information on an optical beam providing the potential to have a compact free space microwave to optical repeater for secure line-of-sight communication systems.

As such, nonlinear metamaterials can support mobile, covert, or space-based platforms, where energy efficiency, size, and weight are critical challenges. Given the ubiquity of electromagnetic devices, these same benefits may apply almost universally to other missions. The understanding of nonlinear metamaterials developed in this project also supports basic sciences including emergent phenomena and materials science such as building deliberate material functionality, nano-to-bulk synthesis, and detector technologies.

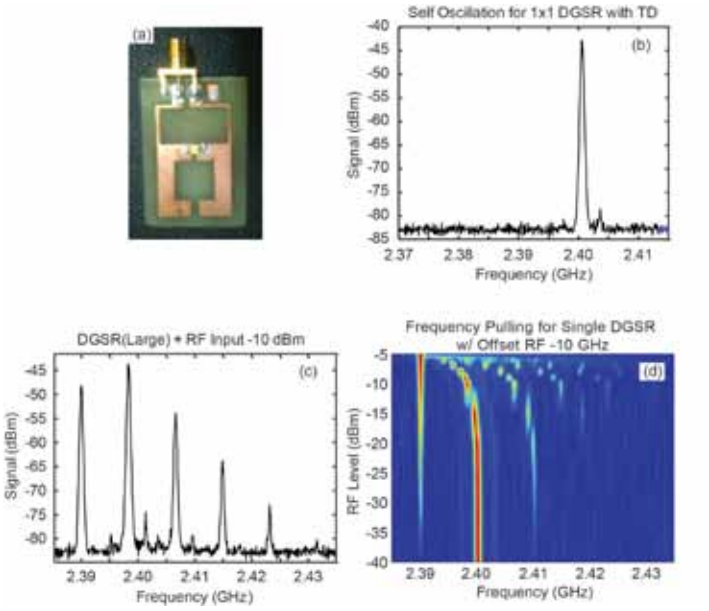

Figure 1. (a) DGSR metamitter element with tunnel diode and SMA connected to bias leads. (b) Measured self-oscillation signal at 2.4 GHz under 160 mV DC bias. (c) Oscillation spectrum with moderate external field at 2.39 GHz. (d) Oscillation spectra as a function of external RF power. The gradually increasing signal at 2.39 GHz was the external power source ramping up corresponding to the y-axis of the surface plot.

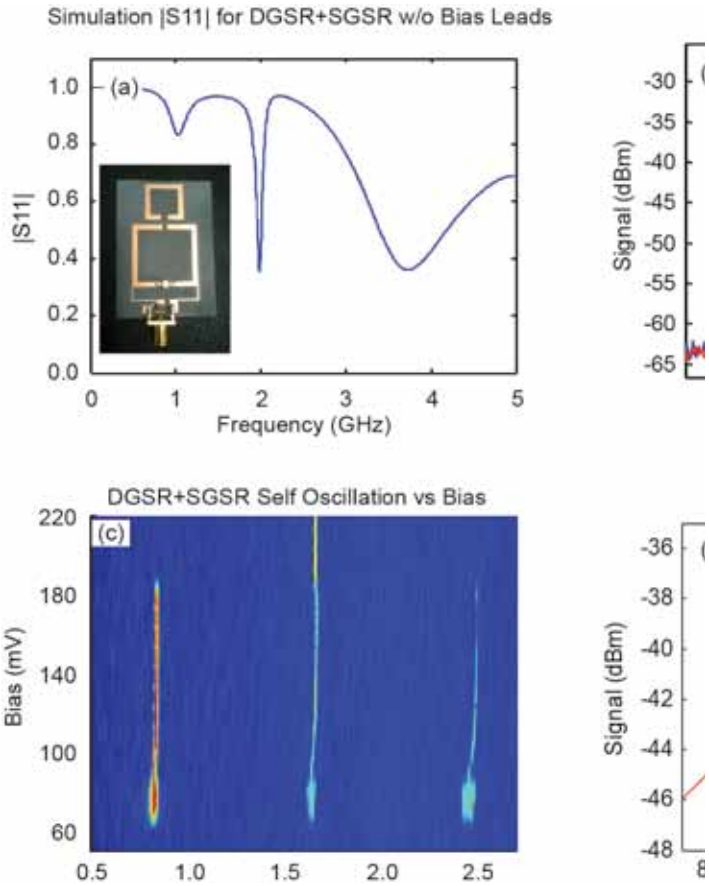

Figure 2. (a) DGSR plus parasitic single gap single ring (DGSR+SGSR) with simulated resonance. (b) Self oscillation spectra of the two dominant modes of the DGSR + SGSR metamitter, "ground state" and "excited state" at 70 and 140 mV respectively. (c) Surface plot of the self-oscillation spectra of the DGSR+SGSR as a function of bias. Note the transition between modes at 190 mV bias, from three harmonics to second harmonic only. (d) Hysteresis curves of the DGSR+SGSR for bias following peak second harmonic signal at 1.63 GHz. (e) Spectral response of numeric model after external stimulation at fundamental frequency with time domain response in inset. (f) Spectral response of model after external stimulation at second harmonic with the corresponding time domain response in inset.

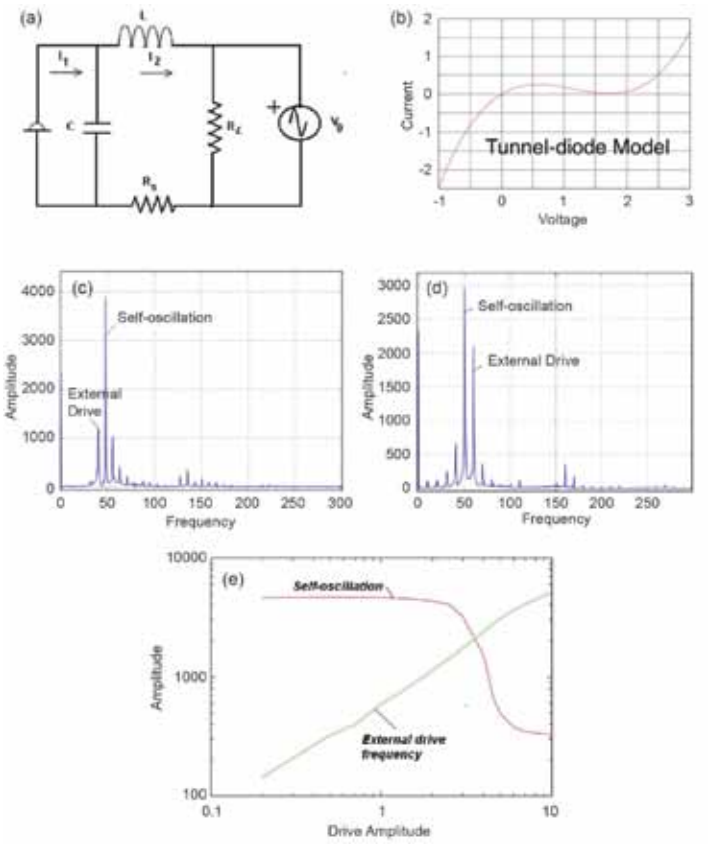

Figure 3. (a) Lumped element circuit model. An RLC circuit includes a series tunnel diode. An external source V0 is used to drive the system though coupling impedance Rs. (b) Modeled I-V curve for a tunnel diode. (c) Spectral response for excitation below the self-oscillation frequency. Upper sidebands appear, consistent with frequency sum rules. (d) Spectral response for excitation above the self-oscillation frequency. Lower sidebands are dominant. (e) Frequency locking as a function of drive amplitude.

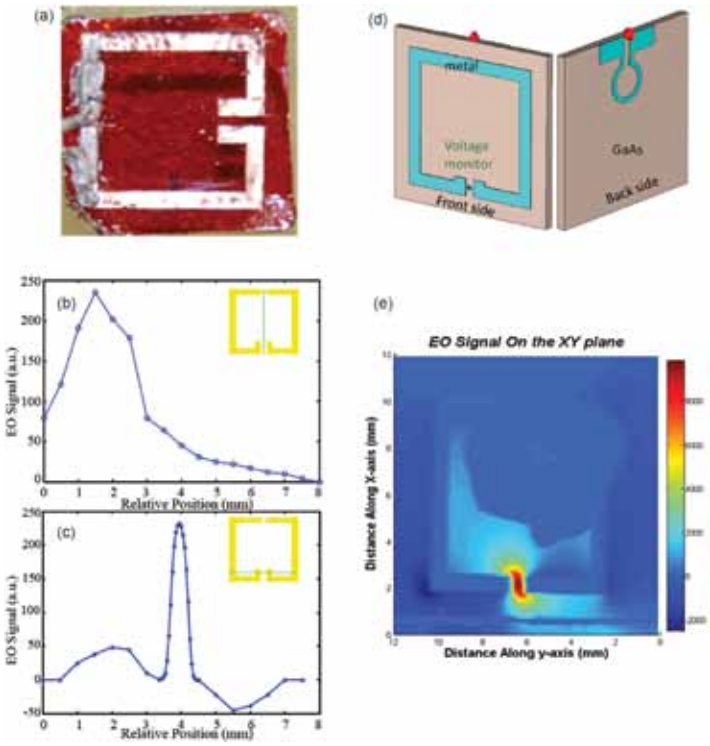

Figure 4. (a) Optical images of the sample fabricated on ZnTe substrate. Spatial distribution of EO signals (b) along the gap vertically shown by the green line from bottom to top and (c) along the horizontal line shown by green line from left to right. (d) Excitation scheme of SRR on GaAs nonlinear crystal using magnetic loop. (e) Measured EO signal of GaAs-based metamaterial EO modulator.

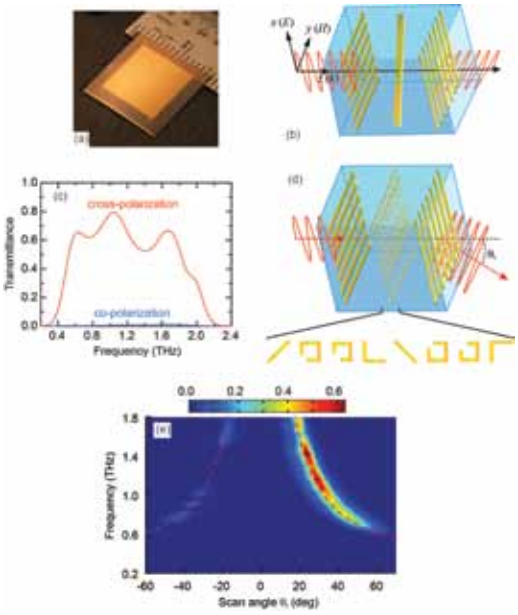

Figure 5. (a) Photograph of freestanding ultrathin (72 μm thick) metamaterial sample. (b) Schematic and (c) performance of transmission mode polarization converter. (d) Schematic of the anomalous refraction sample with super-unit-cell showing the shape of each resonator. (e) Transmission as a function of angle and frequency: each vertical stripe is a transmittance spectrum at a given angle.

Publications

Chen, H. T.. Interference theory of metamaterial perfect absorbers. 2012. Optics Express. 20 (7): 7165.

Chen, H. T., H. Yang, R. Singh, J. F. O'Hara, A. K. Azad, S. A. Trugman, Q. X. Jia, and A. J. Taylor. Tuning the resonance in high-temperature superconducting terahertz metamaterials. 2010. Physical Review Letters. 105 (24): 247402.

Chen, H. T., J. F. O'Hara, A. K. Azad, and A. J. Taylor. Manipulation of terahertz radiation using metamaterials. 2011. Laser & Photonics Reviews. 5 (4): 513.

Chowdhury, D. R., R. Singh, A. J. Taylor, H. T. Chen, and A. K. Azad. Ultrafast manipulation of near field coupling between bright and dark modes in terahertz metamaterial. 2013. APPLIED PHYSICS LETTERS. 102 (1): 011122.

Chowdhury, D. Roy, R. Singh, A. J. Taylor, H. T. Chen, W. Zhang, and A. K. Azad. Coupling schemes in terahertz planar metamaterials. 2012. International Journal of Optics. 2012: 148985.

Chowdhury, D. Roy, R. Singh, J. F. O'Hara, H. T. Chen, A. J. Taylor, and A. K. Azad. Dynamically reconfigurable terahertz metamaterial through photo-doped semiconductor. 2011. Applied Physics Letters. 99 (23): 231101.

Chowdhury, D. Roy, R. Singh, M. Reiten, H. T. Chen, A. J. Taylor, J. F. O'Hara, and A. K. Azad. A broadband planar terahertz metamaterial with nested structure. 2011. Optics Express. 19 (17): 15817.

Chowdhury, D. Roy, R. Singh, M. Reiten, J. Zhou, A. J. Taylor, and J. F. O'Hara. Tailored resonator coupling for modifying the terahertz metamaterial response. 2011. Optics Express. 19 (11): 10679.

Colestock, P. L., M. Reiten, and J. O'Hara. Modeling of nonlinear metamaterials. 2011. Proceedings of SPIE. 8093: 809327.

Colestock, P. L., M. T. Reiten, and J. F. O'Hara. Modeling of active and passive nonlinear metamaterials. 2012. Metamaterials. 6: 8.

Grady, N. K., B. G. Perkins Jr., H. Y. Hwang, N. C. Brandt, D. Torchinsky, R. Singh, L. Yan, D. Trugman, S. A. Trugman, Q. X. Jia, A. J. Taylor, K. A. Nelson, and H. T. Chen. Nonlinear high temperature superconducting terahertz metamaterials. To appear in New Journal of Physics.

Grady, N. K., J. E. Heyes, D. R. Chowdhury, Y. Zeng, M. T. Reiten, A. K. Azad, A. J. Taylor, D. A. R. Dalvit, and H. T. Chen. Terahertz Metamaterials for Linear Polarization Conversion and Anomalous Refraction. 2013. SCIENCE. 340 (6138): 1304.

Gu, J. Q., R. Singh, A. K. Azad, J. G. Han, A. J. Taylor, J. F. O'Hara, and W. L. Zhang. An active hybrid plasmonic metamaterial. 2012. OPTICAL MATERIALS EXPRESS. 2 (1): 31.

Gu, J., R. Singh, X. Liu, X. Zhang, Y. Ma, S. Zhang, S. A. Maier, Z. Tian, A. K. Azad, H. T. Chen, A. J. Taylor, J. Han, and W. Zhang. Active control of electromagnetically induced transparency analogue in terahertz metamaterials. 2012. Nature Communications. 3: 1151.

Huang, L., D. Roy Chowdhury, S. Ramani, M. T. Reiten, S. N. Luo, A. J. Taylor, and H. T. Chen. Experimental demonstration of terahertz metamaterial absorbers with a broad and flat high absorption band. 2012. Optics Letters. 37 (2): 154.

Huang, L., D. Roy Chowdhury, S. Ramani, M. T. Reiten, S. N. Luo, A. K. Azad, A. J. Taylor, and H. T. Chen. Impact of resonator geometry and its coupling with ground plane on ultrathin metamaterial perfect absorbers. 2012. Applied Physics Letters. 101 (10): 101102.

Huang, L., and H. T. Chen. A brief review on terahertz metamaterial perfect absorbers. 2013. International Journal of Terahertz Science and Technology. 6: 26.

Intravaia, F., P. S. Davids, R. S. Decca, V. A. Aksyuk, D. Lopez, and D. A. R. Dalvit. A quasi-analytical modal approach for computing Casimir interactions in periodic nanostructures. 2012. Physical Review A. 86: 042101.

O'Hara, J. F., M. T. Reiten, P. Colestock, L. Earley, and A. Taylor. Tunnel-diode loaded split-ring resonators as a foundation for nonlinear metamaterials. 2011. Proceedings of SPIE. 8093: 809304.

O'Hara, J. F., P. L. Colestock, and A. K. Azad. A partial-element analysis method for determining resonator coupling in terahertz metamaterials. 2013. International Journal of Terahertz Science and Technology. 6: 95.

Ramani, S., M. Reiten, P. Colestock, T. Taylor, A. Azad, and J. O'Hara. Electromagnetic response of finite terahertz metafilm arrays excited on total internal reflection boundaries. IEEE Trans. THz Sci. Technol..

Shchegolkov, D. Y., A. K. Azad, J. F. O'Hara, and E. I. Simakov. Perfect subwavelength fishnetlike metamaterial-based film terahertz absorbers. 2010. PHYSICAL REVIEW B. 82 (20): 205117.

Shchegolkov, D. Y., M. T. Reiten, J. F. O'Hara, and A. K. Azad. Direct observation of electro-optic modulation in a single split-ring resonator. 2013. Applied Physics Letters. 102 (9): 091109.

Shchegolkov, D. Y., N. A. Moody, E. I. Simakov, A. Azad, and J. F. O'Hara. Controlling terahertz waves with metamaterials and photonic bandgap structures. 2011. Proceeding of Wireless and Microwave Technology

Conference (WAMICON), 2011. : 5872861.

Singh, R., A. K. Azad, Q. X. Jia, A. J. Taylor, and H. T. Chen. Thermal tunability in terahertz metamaterials fabricated on strontium titanate single-crystal substrates. 2011. OPTICS LETTERS. 36 (7): 1230.

Singh, R., D. R. Chowdhury, J. Xiong, H. Yang, A. K. Azad, A. J. Taylor, Q. X. Jia, and H. T. Chen. Influence of film thickness in THz active metamaterial devices: A comparison between superconductor and metal split-ring resonators. 2013. APPLIED PHYSICS LETTERS. 103 (6): 061117.

Singh, R., J. Xiong, A. K. Azad, H. Yang, S. A. Trugman, Q. X. Jia, A. J. Taylor, and H. T. Chen. Optical tuning and ultrafast dynamics of high-temperature superconducting terahertz metamaterials. 2012. Nanophotonics. 1 (1): 117.

Zeng, Y., D. A. R. Dalvit, J. O'Hara, and S. A. Trugman. A modal analysis method to describe weak nonlinear effects in metamaterials. 2012. Physical Review B. 85: 125107.

Zeng, Y., H. T. Chen, and D. A. R. Dalvit. The role of magnetic dipole and non-zero-order Bragg waves in metamaterial perfect absorbers. 2013. Optics Express. 21: 3540.

Zhang, S., J. Zhou, Y. S. Park, J. Rho, R. Singh, S. Nam, A. K. Azad, H. T. Chen, X. Yin, A. J. Taylor, and X. Zhang. Photoinduced handedness switching in terahertz chiral metamolecules. 2012. Nature Communications. 3: Article No.: 942.

Zhou, J., D. Roy Chowdhury, R. Zhao, A. K. Azad, H. T. Chen, C. M. Soukoulis, A. J. Taylor, and J. F. O'Hara. Terahertz chiral metamaterials with giant and dynamically tunable optical activity. 2012. Physical Review B. 86 (3): 035448.

Exploiting Hamiltonian Properties of Beams to Revolutionize X-ray Free-electron Laser Architectures

Bruce E. Carlsten
20110067DR

Abstract

This project focused on developing the new underlying theory, analysis, and simulation tools that will be required for the next generation of hard X-ray sources, for both discovery science and for supporting the Laboratory's nuclear weapons program. These sources will be X-ray free-electron lasers (XFELs), and they will operate in regimes different from previous XFELs. In this project, we focused on the three most critical and difficult areas for these machines. Two of these areas are concerned with generating and maintaining the required electron beam brightness and the third is focused on decreasing the spectral bandwidth of the X-rays. As a result of this project, we are recognized as world leaders in the first two areas and highly regarded in the third. The capability developed through this project is essential to take free-electron lasers beyond their present-day limits. In rough numbers, through this project we have added a half dozen highly functional early and mid-career XFEL scientists to the Laboratory's overall XFEL capability.

Background and Research Objectives

Existing X-ray free-electron lasers (XFELs), most specifically the LCLS XFEL at the SLAC National Accelerator Laboratory (SNAL), operate in regimes that can tolerate lower quality electron beams than will be required for future XFELs, including the XFEL proposed for the Laboratory's future MaRIE facility. The LCLS produces the shortest wavelength (1.5 Å) coherent photons in the world today, with photon energy of about 8 keV. Future XFELs will be built to produce sub-angstrom photons (for example, the design point for the MaRIE XFEL is 0.3 Å, or 42-keV photons), and will require nearly an order of magnitude increases in the brightness of the electron beam that is used to generate these photons. In recognition that the foundational science and technology for this next step did not exist, the FY11 LDRD Directed Research Strategic Institutional Plan called out the priority: "Accelerator concepts, especially next-generation photon sources: emittance exchange, pre-bunching, seeding, and other FEL techniques to increase the number of photons and improve control over the temporal shape of the light pulse."

An XFEL is schematically shown in Figure 1. An electron bunch (typically 100 pC) is generated in an injector and accelerated to 10 to 20 GeV in a linear accelerator. The beam is compressed in one or more magnetic compressors to reach a peak current of a few kiloAmperes and then passed through an undulator where the X-rays are generated through the electron bunch's coherent synchrotron radiation. The transverse electron beam quality is defined through a metric called emittance, which corresponds to the rms area in each dimension's phase space (where the conjugate variable is angle with respect to be beam axis, or (x,dx/dz=x') for the horizontal dimension where the beam direction is z), with as low an emittance as possible desirable. The longitudinal electron beam quality is defined by the combination of peak current and energy spread within the bunch. To quantify the improvements needed, the transverse emittance of the electron beam driving the LCLS XFEL has a transverse emittance of 0.3 μm and energy spread of 0.1% whereas an electron beam that would drive a 42-keV XFEL would need to have an emittance no larger than 0.1 μm and energy spread no larger than 0.01%. Coherent synchrotron radiation (CSR) in the bunch compressors tend to be the limiting factor in achieving small emittances. (Unfortunately CSR is especially hard to model and existing numerical codes are missing important physics.) Additionally, an XFEL can self-oscillate, in a mechanism known as self-amplified spontaneous emission (SASE), or amplify a seed signal. SASE operation leads to a relatively broad X-ray spectrum (about 0.1%); our goal, a seeded XFEL, can run transform limited (with a relative spectrum as small as 0.001%).

The objectives of this LDRD DR project were to develop the underlying science and technology required to develop a new generation of ultra high-brightness electron

beams. The specific goals were to learn how to exchange phase-space area between the three dimensions (through a novel scheme known as eigen-emtittance partitioning) , develop a CSR modeling tool that leads to unprecedented accuracy, and understand the limitations of beam-based seeding (which is done by micro-bunching the electron beam before the undulator).

Scientific Approach and Accomplishments

In this section, we separately describe our progress and accomplishments in each of the three areas of study, in the order of eigen-emittances, CSR modeling, and seeding. Roughly a third of the DR's resources went to each of these areas, with a little more emphasis on eigen-emittances in FY11 and more in FY13.

Eigen-emittances: When generated, an electron beam tends to be equipartitioned in terms of how much phase space area each of its three dimensions (x, y, and z) occupy. However, the constraints on transverse phase space are more stringent than that on the longitudinal phase space. We realized that by tailoring the beam's eigen-emittances we could provide arbitrary control on the electron beam's partitioning of its emittances. The eigen-emittances are rms quantities, and are invariant under all linear symplectic transformations, which includes ensemble electron beam evolution in an accelerator (the limitation of this is discussed in the following paragraph). We can control the formation of the beam's eigen-emittances by controlling correlations between dimensions when the beam is generated (at the electron beam cathode). We can exchange these eigen-emittances among the three dimensions, and we recover them as the actual beam emittances when all correlations are removed with accelerator components. We derived a formalism to define eigen-emittances and to calculate them, and several schemes to implement this idea. We found novel combinations of correlations that would lead to two low eigen-emittances and one high, ideal for a very high-energy XFEL.

We determined that a two-stage approach is best, where first emittance is exchanged between the x and y dimensions and then separately exchanged between the x and z dimension. The initial x-y partitioning is straightforward – a scheme known as a "flat-beam transform", where there is nonzero axial magnetic field at the cathode causes an initial correlation through the electron's canonical angular momentum. This correlation can be removed after the beam has been focused with three "skew" quadrupole magnetics, where the quadrupoles are rotated 45o which leads to coupling between the horizontal and vertical dimensions. The second stage partitioning requires a non-symplectic interaction with the beam. The Lorentz force on electrons arises from a Hamiltonian. The resulting electrodynamic motion satisfies Liouville's theorem (hence there is conservation of the 6-dimensional phase space). In general, this motion leads to a nonlinear symplectic map. The linear part of the transformation (from the quadratic part of the Hamiltonian obtained by expanding the motion about a reference trajectory) satisfies the symplectic condition which conserves rms eigen-emittances. If the Hamiltonian is higher order in phase space variables, the rms eigen-emittances are no longer necessarily conserved. We show two possible second stage schemes in Figure 2, where the non-symplectic interaction is through beam energy attenuation in a transversely tapered wedge or through single-particle synchrotron radiation in an undulator that has a transverse field gradient. Using the undulator scheme, we have designed a practical two-stage emittance partitioning scheme that could be used on the LCLS accelerator and which would lead to a decrease in transverse emittance of factors of 2 to 3. (The resulting beam brightness would be the same for a conventional electron bunch with ten times less electrons in it.)

CSR Modeling: We developed a new first-principles, massively parallel CSR code, CSR3D, which solves the exact Lienard-Wiechert fields from a rotating bunch of particles at points of interest. We developed the CSR3D code as a tool of discovery to explore CSR physics and its potential impact on the design of future light sources. Using a real-world number of simulation particles (600 M to 6 B for 100-pC to 1-nC bunches) we have seen novel CSR phenomena for the first time ever, much of which is important to the design of future XFELs. The most important observation we made was to determine the limits of the common 1-dimensional CSR approximation. In Figure 3 we see the CSR fields of electron bunches that are formed as a tilted disk and a round ball with equal rms sizes, which are very nearly equal for this case. However, we verified where this 1-dimensional approximation starts to break down. We also uncovered a significant enhancement of the CSR field for micro-bunched beams (up to two orders of magnitude). This finding is especially relevant because CSR coupled with the beam's own longitudinal space charge force leads to the microbunching instability (MBI). MBI is the limiting factor for the LCLS XFEL performance and we have shown that all previous MBI calculations are flawed. Detailed analysis of the CSR fields have shown that reduced dimensional modeling (specifically keeping just two dimensions) can be accurate; surprisingly, the dimension that can be ignored is the one along the bend's radius. We calculated the CSR field's statistics, which can only be done while simulating the full number of electrons in a bunch. We found the noise in the CSR field grows as the beam energy squared while the correlation length of the noise scales inversely to

the third power of the beam energy. This leads to an unexpected energy diffusion due to CSR, where even mono-energetic particles rotating in a bend will begin to spread out in energy, in addition to the usual quantum-based energy diffusion of single particle synchrotron radiation.

From a beam dynamics point-of-view, we decomposed the CSR fields into radiation and velocity field components. This allowed us to do the first ever full calculation of the convective radiation term (coming from the derivative of the radial vector potential). This term is the dominant term for a particle's transverse equation of motion, and we were able to estimate the emittance growth from it, which is certainly important for emittances required for high energy XFELs. We developed a 1-dimensional integrated Green's function (IGF) model which captures the microbunching field enhancement and developed the groundwork required for a future 2-dimensional IGF numerical model.

Beam-based Seeding: XFEL seeding can be done either by pre-microbunching the electron beam before it enters the undulator or by manipulating the FEL interaction process (by filtering the X-rays are they are produced). We made contributions to both areas. Beam-based seeding would be done by modulating the electron beam 's energy via the inverse FEL interaction in a short undulator known as a "modulator". By passing this modulated beam through a dispersive section, current modulation can be produced. Because the shortest wavelength high power laser available for the modulation is about 200 nm, the modulation wavelength needs to be compressed. There are several schemes available for this, such as compressed harmonic generation (CHG), high gain harmonic generation (HGHG), and echo enhanced harmonic generation (EEHG). We developed a formalism to describe the beam's modulation, through the Fourier transform of the beam's physical coordinates. We used this formalism to determine the debunching of a micro-bunched beam due to the energy diffusion of quantum-based synchrotron radiation in magnetic elements, such as ones required for the schemes just described. We developed and evaluated novel schemes, such as a hybrid HGHG/EEHG configuration, shown in Figure 4. There are several factors that degrade the spectral bandwidth of the seeded light, in fact the first seeded extreme ultraviolet experiments did not show reduced bandwidth. Main among these factors is the shot noise on the electron beams itself and the spectral bandwidth of the seeding itself. We developed a new code that includes all these non-ideal effects for the evaluation of different approaches, specifically the bunching factor of the electron beam (where unity is a fully bunched beam) and the spectral bandwidth of the beam. The bunching factor and spectral width is shown for two EEHG cases in Figure 5.

Our seeding work let to a novel microbunching scheme, related to what is known as enhanced SASE, or eSASE. Originally, eSASE was developed to overcome having too large an emittance for ideal lasing: the electron beam is modulated and microbunched before it reaches the undulator and the resulting increase in peak current allows one to lase anyway. In our version, we are not trying to get around excessive emittance, rather microbunching the beam to ~ 100 spikes with say 3-kA of peak current instead of a single longer bunch of 3-kA suppresses deleterious effects from CSR and the undulator resistive wall wake. We studied the physics of this eSASE version, including developing a new model for the beam's own space-charge forces.

The work from this LDRD was recognized throughout the XFEL community. Our team has been recognized as the world's experts in eigen-emittances and CSR modeling. Our seeding work has also been highly regarded. We've published (or have in review) 10 refereed papers, had 8 invited talks, and 14 oral talks at conferences.

Impact on National Missions

This project has had a defining impact on the MaRIE XFEL project. It is not an understatement to say we could not have developed the conceptual MaRIE XFEL design without the foundational science and technology developed through this project. Nearly every aspect of the conceptual MaRIE XFEL design is based on ideas and concepts from this project (the notable exception is the MaRIE XFEL photoinjector which produced sufficiently low emittances that eigen-emittance schemes were not necessary). Through this project, we funded several postdocs who were subsequently converted to staff as well as developed XFEL capabilities with existing staff. The majority of the current MaRIE XFEL capability at the Laboratory has resulted from this project. Outside of the Laboratory, our work has begun to impact the design of high-brightness electron beam projects (most notably the ASTA project at FNAL) and other XFELs. It is likely that the SLAC version of the NGLS XFEL will benefit from our seeding studies.

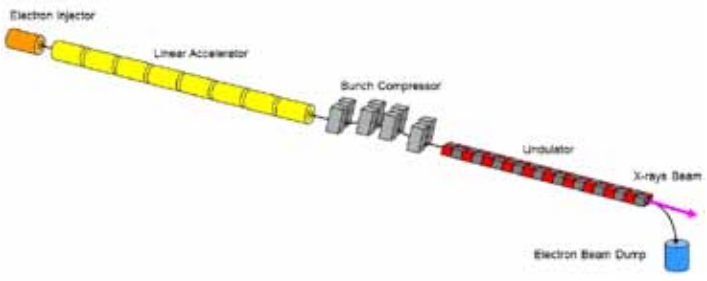

Figure 1. XFEL schematic

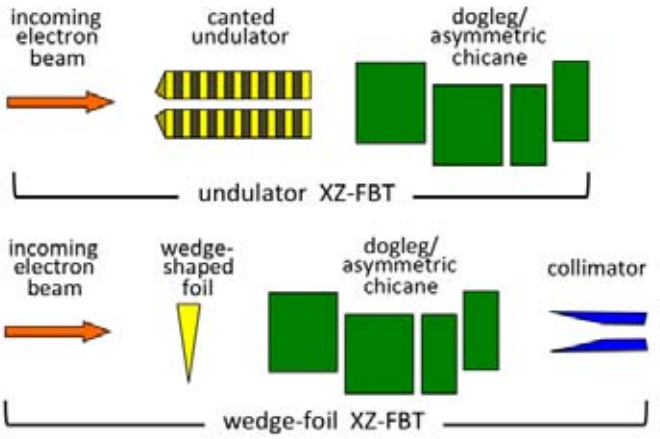

Figure 2. Schemes for non-symplectic emittance partitioning. Both cases use a dogleg or asymmetric chicane for removing an imposed correlation. Top: Electrons pass through a canted undulator, where the magnetic field is larger at one horizontal end of the beam than the other, and those electrons radiate more synchrotron radiation, causing a horizontal-energy correlation. Bottom: Electrons pass through a wedge-shaped foil; electrons lose more energy in the thick part than the thin part, causing a horizontal-energy correlation.

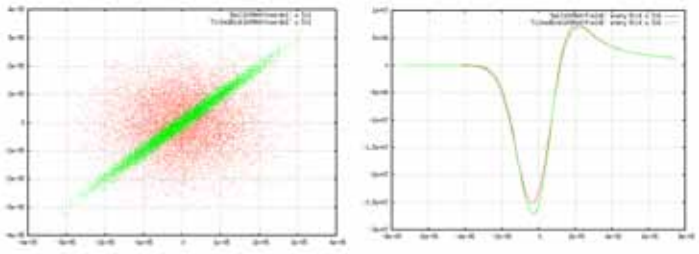

Figure 3. Left: Two beam distributions with the same rms sizes bending in the x-z plane; the red distribution has no correlations but the green distribution is highly correlated (it is a tilted disk in real space); the vertical axis is horizontal position and the horizontal axis is longitudinal position. Right: The longitudinal CSR field is plotted for both distributions along the "axis" of the beam (along the origin of the vertical coordinate); the vertical axis is the CSR field in V/m and the horizontal axis is longitudinal position.

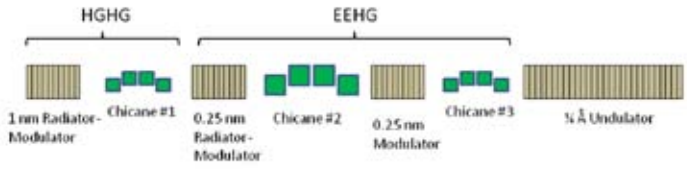

Figure 4. Novel HGHG/EEGH scheme requiring only one external laser (previous schemes required two external lasers).

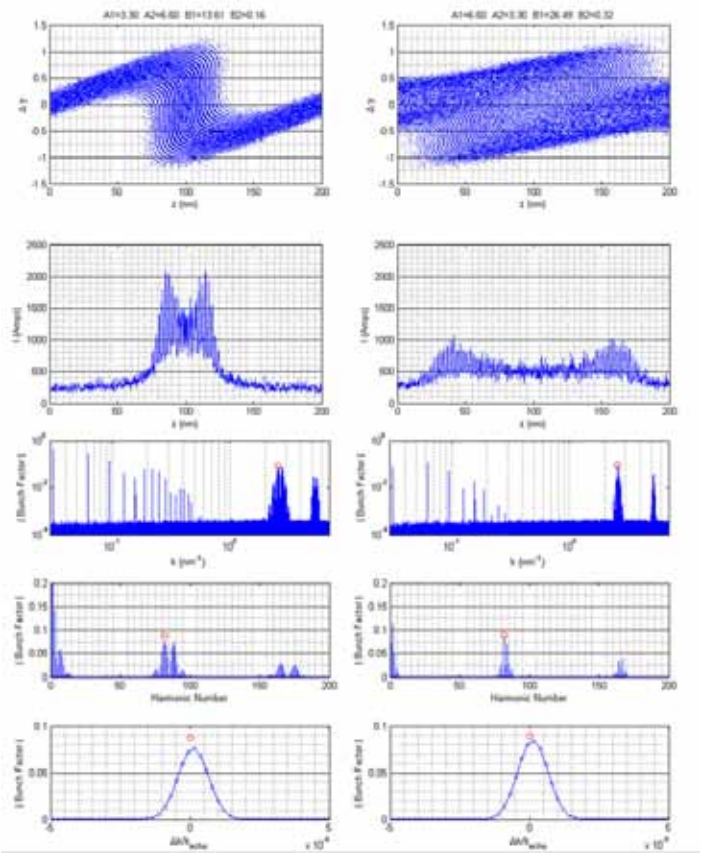

Figure 5. Plots comparing two EEHG schemes for the 82nd harmonic with our developed seeding analysis tool. The scheme on the left is the conventional EEHG configuration, with a stronger first compressor and weaker second compressor. The alternative scheme on the left has a stronger second compressor. The alternative scheme will be susceptible to more CSR effects, but has a more constant bunched current profile and thus will be less affected by slippage. Both have the same overall bunching factor and spectral bandwidth. Top row: Final longitudinal phase space. Second row: Current profiles. Third row: Resulting spectra (the red circle is the analytic computation of the echo amplitude). The effect of the noise floor is clear, but this signal is significantly above it. Fourth row: Spectra on a linear plot as a function of harmonic number. Bottom row: Zoom on the 82nd harmonic showing its spectral width.

Publications

Carlsten, B. E., K. A. Bishofberger, L. D. Duffy, C. E. Heath, Q. R. Marksteiner, D. C. Nguyen, R. D. Ryne, S. J. Russell, E. I. Simakov, and N. A. Yampolsky. New X-ray free-electron laser architecture for generating high fluxes of longitudinally coherent 50 keV photons. 2011. Journal of Modern Optics. 58 (16): 1374.

Carlsten, B. E., K. A. Bishofberger, L. D. Duffy, J. W. Lewellen, Q. R. Marksteiner, and N. A. Yampolsky. Using emittance partitioning instead of a laser heater to suppress the microbunch instability. To appear in Physical Review Special Topics - Accelerators and Beams.

Carlsten, B. E., K. A. Bishofberger, L. D. Duffy, S. J. Russell, R. D. Ryne, N. A. Yampolsky, and A. J. Dragt. Arbitrary emittance partitioning between any two dimensions for electron beams. 2011. Physical Review Special Topics - Accelerators and Beams. 14: 050706.

Carlsten, B. E., K. A. Bishofberger, S. J. Russell, and N. A. Yampolsky. Using an emittance exchanger as a bunch compressor. 2011. Physical Review Special Topics - Accelerators and Beams. 14: 084403.

Duffy, L. D., K. A. Bishofberger, B. E. Carlsten, A. Dragt, Q. R. Marksteiner, S. J. Russell, R. D. Ryne, and N. A. Yampolsky. Exploring minimal scenarios to produce transversely bright electron beams using the eigen-emittance concept. 2011. Nuclear Instruments and Methods in Physics Research A. 654: 52.

Mitchell, C. E., J. Qiang, and R. D. Ryne. A fast method for computing 1-D wakefields due to coherent synchrotron radiation. 2013. NUCLEAR INSTRUMENTS & METHODS IN PHYSICS RESEARCH SECTION A-ACCELERATORS SPECTROMETERS DETECTORS AND ASSOCIATED EQUIPMENT. 715: 119.

Prokop, C. R., P. Piot, B. E. Carlsten, and M. Church. Beam dynamics performances and applications of a low-energy electron-beam magnetic bunch compressor. 2013. NUCLEAR INSTRUMENTS & METHODS IN PHYSICS RESEARCH SECTION A-ACCELERATORS SPECTROMETERS DETECTORS AND ASSOCIATED EQUIPMENT. 719: 17.

Walstrom, P. L.. Dipole-magnet field models based on a conformal map. 2012. PHYSICAL REVIEW SPECIAL TOPICS-ACCELERATORS AND BEAMS. 15 (10): -.

Yampolsky, N. A.. Description of modulated beam dynamics. To appear in Physical Review Special Topics - Accelerators and Beams.

Yampolsky, N. A., and B. E. Carlsten. Bunching smearing due to ISR-induced energy spread. To appear in Physical Review Special Topics - Accelerators and Beams.

Development of an Interface-dislocation Dynamics Model to Incorporate the Physics of Interfaces in Predicting the Macroscopic Mechanical Properties of Nanoscale Composites

Jian Wang
20110573ECR

Abstract

Experimental measurements at LANL show that metallic nanolayered composites have over two orders of magnitude higher strength than bulk single crystal metals while still preserving high deformability. Atomistic modeling shows that interfaces are strong traps for single defects which provides insight on the fundamental mechanisms that impart unusually high strengths in nanocomposites. However, currently, there are no models available to predict macroscopic properties (such as strength, work hardening rate, ductility, etc) of nanocomposites; hence, there is a gap between experiments and atomistic models that probe the defect-interface interactions. We propose to develop the first of its kind interface-dislocation dynamics (Interface-DD) model that captures the dynamics of defect ensembles at interfaces at higher length scale. The development of this Interface-DD model will provide a way to tailor the macroscopic properties of nanolayered composites to make the strongest and most damage tolerant metals known to humankind, with strengths within a factor of two or more of the theoretical limit. Without such a predictive model to guide materials design, further developments in the properties of nanocomposites can only come from Edisonian approaches.

Background and Research Objectives

Nanocomposites developed at LANL have shown unprecedented levels of strengths, ductility and damage tolerance in extreme irradiation environments. For example, experimental measurements on 5nm Cu/5nm Nb multilayers show flow strengths approaching 2500 MPa, whereas the bulk, single-crystal metals have strengths < 50 MPa. These experiments, performed on bulk samples (sample sizes varying from tens of micrometers to several millimeters), measure macroscopic properties such as yield strength, work hardening rate and strain to failure (ductility). Atomistic modeling is able to elucidate the unit process of interaction of a single dislocation with a bi-metallic interfaces but cannot predict macr-oscopic properties measured experimentally. The continuum models of plasticity treat interfaces phenomenologically, i.e., as boundaries without any structural characteristics, and consequently, do not capture the defect physics at interfaces. Given the high area per unit volume of interfaces, the behavior of nanoscale materials is dominated by defect interactions at interfaces. This calls for a breakthrough in materials modeling to bridge the micron gap from atomistic to continuum. This EC project will pioneer a interface-Dislocation Dynamics model that links the atomistic-scale physics of dislocation-interface interactions with macroscopic (experimentally measured) mechanical properties, and will provide a path towards filling the gap in materials modeling between atomistic and micro/macro-scales. Since engineering design is based on macroscopic properties such as strength, ductility and toughness, but the defect-interface interactions govern the behavior of nanomaterials, our ability to predict and control the performance of bulk nanocomposites in engineering applications will depend on the ability to link interface physics with average behavior measured in bulk.

Recent workshop reports from DOE, Office of Science observe that current engineering materials fail at one-tenth or less of their intrinsic limits in unpredictable ways. To meet the demands of the future applications, material properties and performance need to be increased by over an order of magnitude that is not possible by incremental improvements in current structural materials. Nanocomposites developed at LANL have shown unprecedented levels of strengths, ductility and damage tolerance in extreme irradiation environments. Experimental and atomistic-scale studies show that the behavior of nanomaterials is dominated by defect interactions at interfaces. The current continuum models treat interfaces phenomenologically, and consequently, do not capture interface physics. DD models show promise for single crystal but cannot capture interface roles. This EC program pioneers the first Interface-DD model

(Figure 1) to incorporate the defect-interface interactions with macroscopic mechanical properties, and will fill the gap of materials modeling between atomic-scale model and macro-scale model. The developed model can be validated with existing experimental measurements, and in the future will be applied to predict and control mechanical behavior of nanomaterials in extreme conditions.

Scientific Approach and Accomplishments

We advance a concept of "interface strengthening" in designing ultra-high strength, damage-tolerant nanocomposites. Interfaces become crucial in determining the properties of nanoscale materials due to the change of deformation mechanisms from phase-dominated to interface-dominated as length-scale is reduced from micro- to nanoscales. To succeed in this effort, the key challenges are: Understanding the role of interface structures and properties during deformation and Developing a design principle for high strength composites through control of interfaces.

The breakthroughs achieved in this project will be realized through the development of an interface-DD model to link atomic-scale interface structures and properties with macroscopic material deformation. The development of interface-DD model mainly relies on the understanding of dislocation processes both in the bulk and at the interfaces. Here we summarize the key accomplishments corresponding to the tasks defined in this project. Correspondingly, we have published more than 20 journal papers, and one of them was awarded ScienceDirect Top 25 Hottest Articles in the field of Engineering.

Task 1: Develop reaction rules of defects interactions at interfaces using atomistic simulations.

These rules are necessary in developing interface-DD model, and were not systematically studied at interfaces yet. To do so, we first study the motion of dislocations (lattice and interfacial) at interfaces. Three motion mechanisms are glide, climb, and cross-slip.

We have developed a rule used in the DD-interface code by which we can deal with the weak interface shear accompanying with the slip transmission for a single dislocation across the interface.

Task 2: Develop interface structure description using topological model coupled with atomistic simulations. Interface roles that were not incorporated in current existing models are ascribed to the lack of interface model. The interface governs the motion, storage, reassembly (recovery and nucleation), and emission of dislocations. The interface structure includes the atomic arrangement and the basic geometric features (orientation relationship and interface plane).

We have been developing a geometrical classification scheme by which we can classify the interface into four types. Corresponding to each type of interface, we are analyzing the intrinsic defects, interface shear response, and the influence of interface structure on the interface-dislocation interactions.

Task 3: Develop Green function (GF) for forces calculation. The current DD models do not have stress calculation for defects in anisotropic, multiple interface nanocomposites. GF theory shows promise in solving stress/strain fields of a defect in anisotropic bi-materials that could be applied to a curved dislocation in multilayered composites.

We have been developing GF's solution for dislocations in anisotropic, multiple interface nanocomposites, and have applied the solution to calculate (1) Elastic fields of dislocation loops in three-dimensional anisotropic bimaterials and (2) predict the critical thickness of the shell in defect-free core-shell nanowires.

Task 4:Develop an interface-DD code through implementing reaction rules, interface models, and GF for force calculation into existing DD codes.

Currently, we are implementing the rule of slip transmission across a weak interface and twin boundaries. We have performed some simulations in understanding the plastic deformation in Cu-Nb metallic multilayers.

Impact on National Missions

This project addresses two themes of our Materials Grand Challenge: Defects & Interfaces and Extreme environments. This LDRD project will develop a new modeling tool that is of great significance to programmatic work at LANL, such as the materials science underlying stockpile stewardship and a number of DoD missions, as well as energy applications e.g. turbines. The capabilities to be developed are relevant to DOE/BES objectives also. Through this project, we will develop the first Interface-DD code that can be used in predicting mechanical response of nanocomposites with the interface physics. Moreover, we also provide insight in describing interface structures and properties and building the reaction rules of defect-interface interactions, which can be applied to other continuum scale models, as well as developing a Green function solution for dislocations in multi-phase composites.

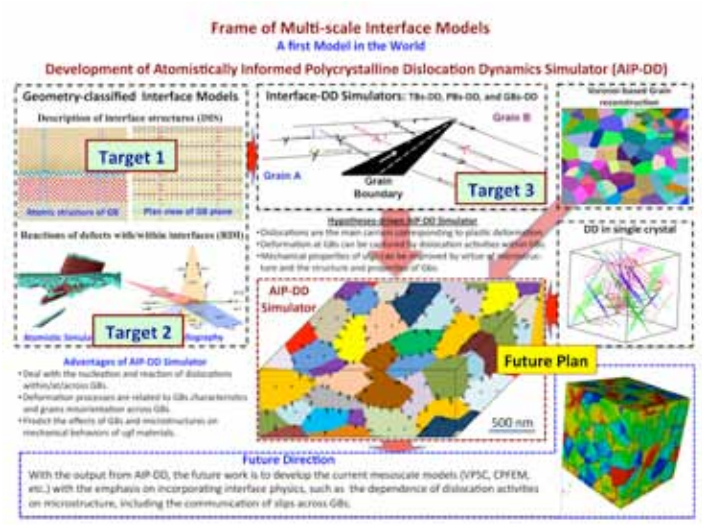

Figure 1. Frame of Multi-scale Interface Models, showing the current effort and the future plan.

Publications

Chu, H. J., E. Pan, J. Wang, and I. J. Beyerlein. Elastic Displacement and Stress Fields Induced by a Dislocation of Polygonal Shape in an Anisotropic Elastic Half-space. 2012. Journal of Applied Mechanics . 79 (2): 021011.

Chu, H. J., E. Pan, X. Han, J. Wang, and I. J. Beyerlein. Elastic fields for dislocation loops in three-dimensional anisotropic bimaterials. 2012. Journal of the Mechanics and Physics of Solids. 60 (3): 418.

Chu, H. J., E. Pan, X. Han, J. Wang, and I. J. Beyerlein. Elastic fields of dislocation loops in three-dimensional anisotropic bimaterials. 2012. JOURNAL OF THE MECHANICS AND PHYSICS OF SOLIDS. 60 (3): 418.

Chu, H. J., J. Wang, C. Z. Zhou, and I. J. Beyerlein. Self-energy of elliptical dislocation loops in anisotropic crystals and its application for defect-free core/shell nanowires. 2011. Acta Materialia . 59: 7114.

Chu, H. J., J. Wang, and I. J. Beyerlein. Anomalous reactions of a supersonic coplanar dislocation dipole: Bypass or twinning? . 2012. Scripta Materialia . 67 (1): 69.

Chu, H. J., J. Wang, and I. J. Beyerlein. Anomalous reactions of a supersonic coplanar dislocation dipole: Bypass or twinning?. 2012. Scripta Materialia. 67 (1): 69.

Chu, H., C. Zhou, J. Wang, and I. Beyerlein. Misfit Strain Relaxation Mechanisms in Core/Shell Nanowires. 2012. JOM. 64 (10): 1258.

Chu, H., J. Wang, I. Beyerlein, and C. Zhu. Self-energy of elliptical dislocation loops in anisotropic crystals and its application for defect-free core/shell nanowires. 2011. Acta Materialia . 59: 7114.

Kang, K., J. Wang, S. J. Zheng, and I. J. Beyerlein. Minimum energy structures of faceted, incoherent interfaces. 2012. Journal of Applied Physics. 112 (7): 073501 (10 pp.).

Kang, K., J. Wang, and I. J. Beyerlein. Atomic structure variations of mechanically stable fcc-bcc interfaces. 2012. Journal of Applied Physics. 111 (5): 053531 (10 pp.).

Li, N., J. Wang, A. Misra, X. Zhang, J. Y. Huang, and J. P. Hirth. Twinning dislocation multiplication at a coherent twin boundary. 2011. Acta Materialia. 59 (15): 5989.

Li, N., J. Wang, X. Zhang, and A. Misra. In-situ TEM Study of Dislocation-Twin Boundaries Interaction in Nanotwinned Cu Films. 2011. JOM. 63 (9): 62.

Li, N., N. A. Mara, J. Wang, P. Dickerson, J. Y. Huang, and A. Misra. Ex situ and in situ measurements of the shear strength of interfaces in metallic multilayers. 2012. Scripta Materialia. 67 (5): 479.

Wang, J.. A Multi-scale Perspective of Interfaces-dominated Mechanical Behavior. 2011. JOM. 63 (9): 57.

Wang, J., I. J. Beyerlein, A. Misra, S. M. Valone, and T. C. Germann. ATOMISTIC MODELING OF DISLOCATION-INTERFACE INTERACTIONS. 2011. In 3rd International Conference on Heterogeneous Material Mechanics (ICHMM 2011) ; 20110522 - 20110526 ; Shanghai Univ, Shanghai, PEOPLES R CHINA. , p. 39.

Wang, J., I. J. Beyerlein, N. Mara, A. Misra, and C. N. Tome. Deformation twinning mechanisms in FCC and HCP metals. 2011. In 3rd International Conference on Heterogeneous Materials Mechanics, ICHMM 2011 ; 20110522 - 20110526 ; Shanghai, China. , p. 88.

Wang, J., I. J. Beyerlein, and J. P. Hirth. Nucleation of elementary {-1 0 1 1} and {-1 0 1 3} twinning dislocations at a twin boundary in hexagonal close-packed crystals. 2012. Modelling and Simulation in Materials Science and Engineering . 20 (2): 024001.

Wang, J., K. Kang, R. F. Zhang, S. J. Zheng, I. J. Beyerlein, and N. A. Mara. Structure and Property of Interfaces in ARB Cu/Nb Laminated Composites. 2012. JOM. 64 (10): 1208.

Wang, J., K. Kang, R. F. Zhang, S. J. Zheng, I. J. Beyerlein, and N. A. Mara. Structure and property of interfaces in ARB Cu/Nb laminated composites. 2012. JOM. 64 (10): 1208.

Wang, J., R. G. Hoagland, X. Y. Liu, and A. Misra. The influence of interface shear strength on the glide dislocation- interface interactions. 2011. Acta Materialia. 59 (8): 3164.

Wang, J., and I. Beyerlein. Atomic Structures of Symmet-

ric Tilt Grain Boundaries in Hexagonal Close-Packed (hcp) Crystals. 2012. METALLURGICAL AND MATERIALS TRANSACTIONS A-PHYSICAL METALLURGY AND MATERIALS SCIENCE. 43A (10): 3556.

Wang, J., and I. Beyerlein. Atomic structures of [0110] symmetric tilt grain boundaries in Hexagonal Close-Packed (hcp) crystals. 2012. Metallurgical and Materials Transactions A: Physical Metallurgy and Materials Science. 43 (10): 3556.

Wang, J., and I. J. Beyerlein. Atomistic modeling of interactions of lattice dislocation with [0-110] symmetrical tilt grain boundaries in Mg. 2012. Metallurgical and Materials Transactions A. 43 (10): 3556.

Wang, J., and I. J. Beyerlein. Atomic structures of symmetric tilt grain boundaries in hexagonal close packed (hcp) crystals. 2012. Modelling and Simulation in Materials Science and Engineering. 20 (2): 024002.

Zhang, R. F., J. Wang, I. J. Beyerlein, A. Misra, and T. C. Germann. Atomic-scale study of nucleation of dislocations from fcc-bcc interfaces. 2012. ACTA MATERIALIA. 60 (6-7): 2855.

Zhang, R. F., J. Wang, I. J. Beyerlein, and T. C. Germann. Twinning in bcc metals under shock loading: a challenge to empirical potentials. 2011. PHILOSOPHICAL MAGAZINE LETTERS. 91 (12): 731.

Zhang, R. F., J. Wang, I. J. Beyerlein, and T. C. Germann. Dislocation nucleation mechanisms from fcc/bcc incoherent interfaces. 2011. SCRIPTA MATERIALIA. 65 (11): 1022.

Zhang, R. F., T. C. Germann, J. Wang, X. -Y. Liu, and I. J. Beyerlein. Role of interface structure on the plastic response of Cu/Nb nanolaminates under shock compression: Non-equilibrium molecular dynamics simulations. 2013. Scripta Materialia. 68 (2): 114.

Zhang, R. F., T. C. Germann, J. Wang, X. -Y. Liu, and I. J. Beyerlein. Role of interface structure on the plastic response of Cu/Nb nanolaminates under shock compression: Non-equilibrium molecular dynamics simulations. 2013. Scripta Materialia. 68 (2): 114.

Exploration of Megawatt Heat Pipe Reactor Concepts

Patrick R. Mcclure
20110141ER

Abstract

An important niche for nuclear energy is the need for power at remote locations removed from a reliable electrical grid. Nuclear energy has potential applications at strategic defense locations, theaters of battle, remote communities, and emergency locations. With proper safeguards, a 1 to 10-MWe (MegaWatt electric) mobile reactor system could provide robust, self-contained, and long-term power in any environment.

Heat pipe-cooled fast-spectrum nuclear reactors have been identified as a candidate for these applications. Heat pipe reactors, using alkali metal heat pipes, are perfectly suited for mobile applications because their nature is inherently simpler, smaller, and more reliable than "traditional" reactors.

The goal of this LDRD project was to develop a scalable conceptual design for a compact reactor and to identify scaling issues for compact heat pipe cooled reactors in general. Toward this goal two detailed concepts were developed, the first concept with more conventional materials and a power of about 2 MWe and a the second concept with less conventional materials and a power level of about 5 MWe. A series of more qualitative advanced designs were developed (with less detail) that show power levels can be pushed to approximately 30 MWe. Each of these designs had to overcome several limitations including:

- Limits on the number of heat pipes in a single block,
- Limits on heat-pipe performance,
- Limits on design imposed by the design-basis accident conditions,
- Limits on thermal and mechanical performance imposed by selected materials,
- Other limits imposed by material used to make the reactor core.

A vital part of overcoming these limits was research into double-ended heat pipes that can improve the heat pipe performance by a factor of at least 2 and possibly by a factor of 4. A series of experiments were performed to verify these limits.

Background and Research Objectives

A goal of the Army Nuclear power Program that ran from 1954 through 1977 was to provide power in remote (and even possibly hostile) locations. Settlements and installations at remote locations have historically relied on diesel power, which has significant logistic implications. Heat pipe reactors are perfectly suited for mobile applications because their nature is inherently simpler, smaller, and more reliable than "traditional" reactors that rely on pumped coolant through the core. Instead of the single point failure of a pumped loop, hundreds to thousands of heat pipes passively remove heat (including decay heat) from the core using simple and well-characterized physics. These reliability and safety advantages are especially important for remote sites. The robust, solid-state characteristics of the core are also advantageous for potentially damaging transport conditions or perhaps hostile operating environments.

The concepts of fast-spectrum reactors and heat-pipe-cooled reactors were pioneered at Los Alamos National Laboratory (LANL) during the 1950s and 1960s respectively. Heat-pipe-cooled reactor designs to date have had limited power output, reflecting the needs of their times. Now that compact reactors are under consideration for numerous remote applications, demand exists heat pipe cooled reactors at much higher power. This type of reactor is conceptually simple and potentially much more reliable than other reactor cooling technology. An example of a heat pipe reactor is presented in Figure 1.

The advantages of heat pipe reactors are many and include:

- Size (heat pipe reactors are small),
- Orientation (heat pipe reactors can be vertical or horizontal),
- Safety (heat removal by passive physics that avoid single point failures),
- Self-regulating (a feature of fast spectrum reactors),
- Solid state construction (a feature of heat pipe reactors),
- Surface area outside core (allows for a working fluid like air),
- Choice of working fluids (flexibility in construction), and
- High temperature output (a feature that allows for diverse application).

A heat pipe transfers heat between two bodies with little temperature change from hot to cold. This ability makes heat pipes an ideal means to extract thermal power from a nuclear reactor. To date, most proposed heat-pipe reactors were designed to far less than 1 MWe in power. This is, in some part, result of historical applications, where typical power needs were in the 10's to 100's of kilowatts electric range (early space power applications.) Today, many industrial and government applications require power levels that are much greater than 1 MWe. The design of heat-pipe reactors with powers much greater than 1 MWe was the focus of this LDRD project. Several issues must be overcome to scale heat-pipe reactors to this size. This paper presents the key issues that must be addressed and the necessary engineering advances to overcome these issues. Each of these designs had to overcome several limitations including:

- Limits on the number of heat pipes in a single block,
- Limits on heat-pipe performance,
- Limits on design imposed by the design-basis accident conditions,
- Limits on thermal and mechanical performance imposed by selected materials,
- Other limits imposed by material used to make core.
- To address the limits two approaches were used.
- A series of point design were done with LANL reactor design tools to evaluate the normal operating conditions and response to accident conditions;
- A set of experiments were performed to evaluate a new type of heat-pipe, the double ended heat pipe, to demonstrate its improved performance.

Scientific Approach

For the design portion of the project, LANL has a methodology that involves a preprocessor know as ALLGEN. ALLGEN has been developed so that it can be used for almost any reactor technology so it can perform rapid design or trade study calculations. The versatility is in part provided by MCNP6, the LANL Monte Carlo neutronics tool. Initially, calculations are performed to identify a design or designs that meet reactivity design requirements. Once a design is identified, a time-history nuclear analysis is performed. For these calculations, the MCNP core model and the MONTEBURNS depletion calculations are performed interactively. These calculations confirm the as-designed end-of-life reactivity margin calculated with ALLGEN. Next, simplified calculations are performed by the FRINK code, a system code that models heat transfer and coupled neutronics based on MCNP6 results. Two analyses are performed: one that assesses overall system performance, and one that calculates core response to bounding transient events. The transient analyses investigate how the system responds to accident conditions. The reactor thermal design analysis is the evaluated by a computer code called TMSS. The analysis performed uses as-calculated temperatures to determine thermal expansions, material properties, fuel performance, clad stress and stress limit, clad creep strain.

For the experimental portion of this project, a double-ended heat pipe was tested in two different apparatus, one in a vacuum quartz tube to test the operation of the heat pipe, and the other in a calorimeter to evaluate the operational limits of the heat pipe. Both apparatus' applied heat to the evaporator section of the pipe by radio frequency induction. High frequency power was generated to provide surface heating to simulate feasible applications. A water-cooled calorimeter was built to quantify the heat rejected from the heat pipe. The calorimeter fits over the condenser section and interfaces with the quartz over the evaporator section to create a closed system. The calorimeter is coupled to the heat pipe with a He-Ar mixture gas gap. By controlling gas composition and conductivity, the flow rate and difference in temperature between the water inlet and outlet are the properties that are measured to quantify the overall performance of the heat pipe.

Accomplishments

The limits to heat pipe reactor scaling were investigated using both the design approach described above and using the results of the experiments into double ended heat pipes.

The first design study examined two detailed design configurations. These two configurations involve using a

metal for the monolithic block with fuel in traditional pin configurations, where the cladding is the monolithic block wall. The goal behind these choices was a simple reactor configuration with known materials and a more advanced configuration with a less conventional fuel and materials. The two configurations were:

- Stainless steel with Uranium Oxide fuel pellets
- Molybdenum alloy (TZM) with Uranium Nitride fuel pellets

The second design study examined seventeen more design configurations in a qualitative study (less detailed than the previous study). These configurations involved the following changes:

- Replacing the metal monolithic block with graphite or silicon carbide using the block as fuel cladding;
- Replacing the metal monolithic block with graphite or silicon carbide using metal as fuel cladding;
- Replacing the metal monolithic block with a liquid metal pool of lead bismuth using metal fuel cladding;
- Dispersing the fuel in the monolithic block matrix, where the fuel was either Uranium Oxide or Uranium Nitride and the block material was stainless steel, molybdenum, or graphite.
- This then gave the following design configurations:
- Stainless steel with Uranium Nitride fuel pellets;
- Graphite with Uranium Oxide fuel pellets (clad and no clad);
- Silicon Carbide with Uranium Oxide fuel pellets (clad and no clad);
- LBE metal pool with steel clad at three thicknesses and Uranium Oxide pellets;
- Uranium Oxide fuel dispersed in stainless steel with either a small amount of gadolinium as a chemical stabilizer or no gadolinium;
- Uranium Oxide fuel dispersed in graphite with a small amount of gadolinium as a chemical stabilizer or no gadolinium;
- Uranium Oxide fuel dispersed in molybdenum with a small amount of gadolinium as a chemical stabilizer or no gadolinium;
- Uranium Nitride in dispersed in stainless steel;
- Uranium Nitride in dispersed in graphite;
- Uranium Nitride in dispersed in molybdenum.

The final design study utilized the results of the double-ended heat pipe experiments. The results of the experiments were incorporated into three advanced designs.

- Stainless steel with Uranium Oxide fuel pellets with double-ended heat pipes;
- Molybdenum alloy with Uranium Nitride fuel pellets with double-ended heat pipe;
- LBE metal pool with steel cladding, Uranium Oxide pellets and double-ended heat pipes.

Each of these designs had to overcome several limitations describe earlier. The impact of designs on limits is discussed below.

Limits on the number of heat pipes in a single block
A simple solution to this issue is to simply breaking the core into smaller segments. A heat-pipe reactor can be broken into segments that are mechanically and thermally isolated but are neutronically connected. An example of this configuration with eight segments is shown in Figure 2.

Limits on heat pipe performance
Heat pipes have a limit on the heat transfer rate per unit area on a per-heat-pipe basis. These limits are shown in Figure 3 included the following physical issues.

- The sonic limit is the power level where vapor approaches the sonic velocity at the evaporator exit.
- The capillary limit is the power level that produces mass flow rates sufficient for liquid and vapor pressure drops to exceed the maximum capillary head potential of the wick.
- The entrainment limit is the power level at which counter-flowing vapor sweeps liquid out of the wick, depriving the evaporator of returning liquid.
- The boiling limit is the power level at which incipient boiling of liquid occurs at the superheated wall.

The dual heat pipe configuration with uniform heating and cooling enhances capillary and viscous limits by up to a factor of four. The sonic and entrainment limits are enhanced by up to a factor of two. The dual configuration has no affect on boiling limit. Test results in both the quartz tube and the calorimeter apparatus have confirmed the functionality of the dual ended heat pipe configuration.

Limits on design imposed by accident conditions
A heat-pipe reactor must be designed to survive accident conditions and for a heat pipe reactor the accident of greatest concern is the failure of one or more heat pipes leading to cascade failure. Cascade failure is the loss of a

single or multiple heat pipes, causing the failure of surrounding heat pipes in a cascade. Cascade failure is mitigated by designing the reactor for the failure of one or more adjacent heat pipes for the limiting (highest power) fuel pin. An example of the analysis done for a heat pipe reactor is shown in Figure 4.

Limits on thermal and mechanical performance
For the design-basis case of two heat-pipe failures adjacent to a fuel pin, the solid-core block is designed to not exceed the ASME limits for thermal stress for the given material in the reactor core block. This was a limit imposed in the design studies.

Other material limits
The reactor working temperature helps determine the range of available materials. New materials are examined to see if new problems are introduced. For example, many materials have great properties but may not be compatible with oxygen or high-radiation environments. The new materials are also examined for an impact on neutron transport. Materials have to perform well over a range of conditions in order to be considered as a solution to scaling heat pipe reactors.

Summary of design studies
The results show that a heat pipe reactors can easily be scaled to the low (1 to 2) MWe range using well-characterized materials like Uranium Oxide fuel pellets and stainless steel. Advance concepts using Uranium Nitride fuel, molybdenum metal and double-ended heat pipes can push this limit to 15 MWe. This reactor concept is shown in Figure 5. Other advanced fuels and materials, plus changes to the reactor core have the potential to push this limit to 50 MWe. Past this point, it is postulated to be easier to build multiple reactors than to push the limits inherent in heat pipe reactor technology.

Impact on National Missions

The potential use of mega-watt size reactors for military purposes has been the focus of several recent studies. These studies have called for the Department of Defense to re-investigate the use of nuclear power for applications outside the continental U.S. In addition, a call for a new study to examine reactor technology with power levels below 10 MWe was added to the current Defense Authorization Act currently before Congress. Given the interest in reactors in this size range, LANL has further developed the base concept from this study into a complete conceptual reactor design.

The Uranium Dioxide fuel with a stainless steel monolithic block concept was further developed into a mobile reactor concept that utilized shipping cask technology developed for spent nuclear fuel as a permanent outer shell for the reactor concept. The concept uses existing on site power conversion technology to produce power (an open air Brayton turbine). The reactor is brought to the site and simply heats the air to the appropriate temperature before it enters the turbine. Only a heat pipe cooled reactor concept can use for open-air concept and not activate the air. On this concept the air does not pass through the reactor core but through heat exchangers on the condenser end of the heat pipes.

LANL will continue to pursue options for using the heat pipe cooled reactor technology for the U.S. government applications. Its benefits make it ideal for many applications in remote environments were mobile or transportable technology is needed.

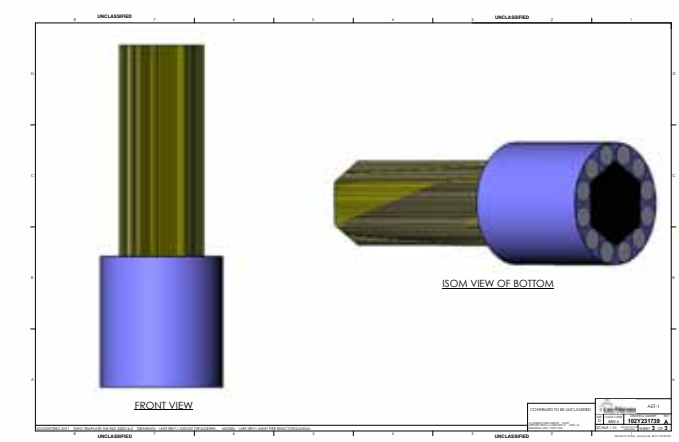

Figure 1. Heat Pipe Reactor Concept

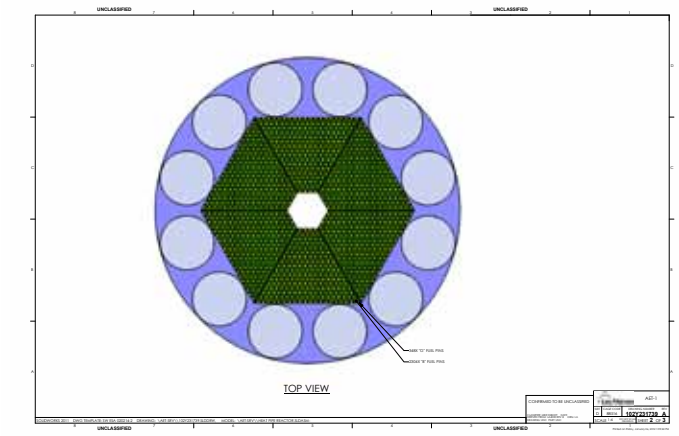

Figure 2. Core View Showing Eight Core Segments

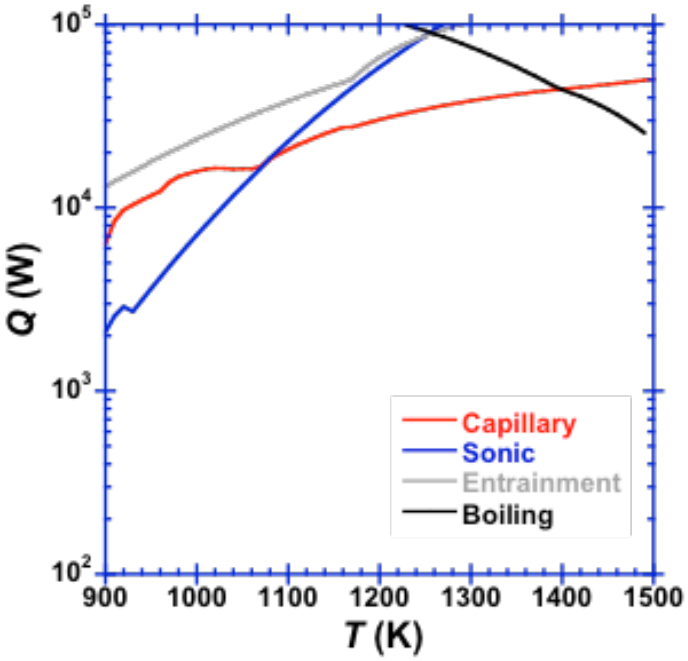

Figure 3. Heat Pipe Performance Limits

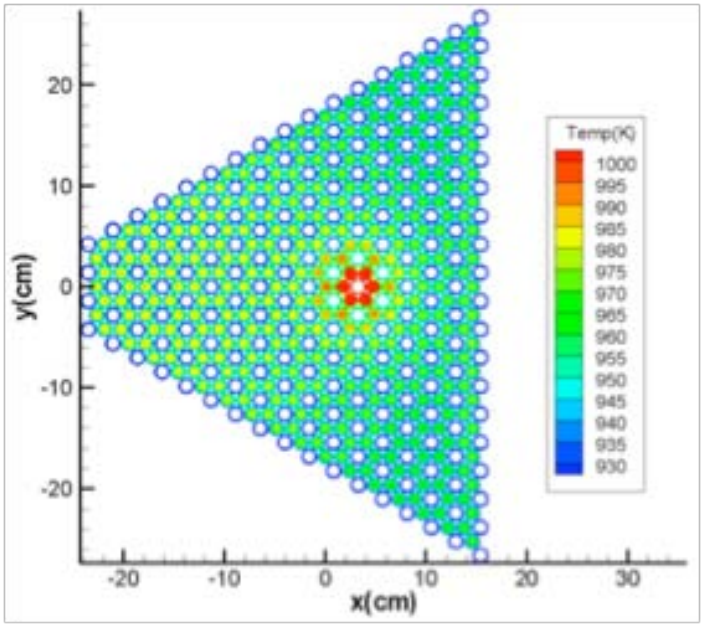

Figure 4. Temperature Response of Heat Pipe Reactor to Accident Conditions

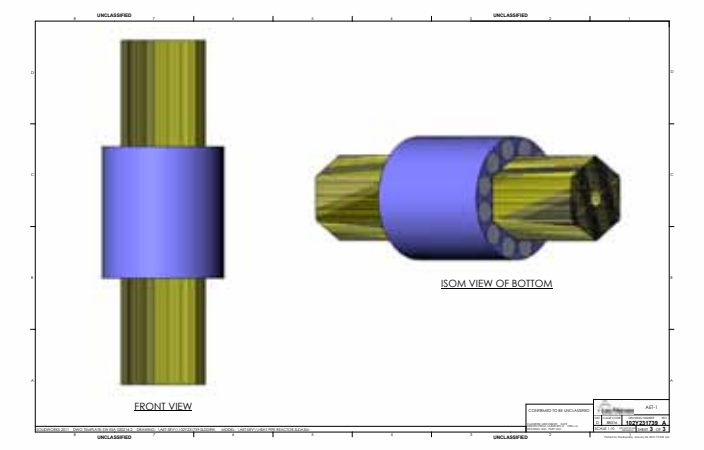

Figure 5. Double Ended Heat Pipe Reactor Concept

Publications

McClure, P. R., R. S. Reid, and D. D. Dixon. Advantages and applications of megawatt-sized heat-pipe reactors. 2012. In Proceedings of International Congress on Advances in National Power Plants 2012. (Chicago, 24-28 June 2012). , p. 101. Chicago: American Nuclear Society.

Poston, D. I., and R. Kapernick. Design and analysis of megawatt-class heat-pipe reactor concepts. 2012. In Proceedings of International Congress on Advances in National Power Plants, 2012. (Chicago, 24-28, June 2012). , p. 155. Chicago: American Nuclear Society.

Full-frame Programmable Spectral Imagers Based on Micro-mirror Arrays

Steven P. Love
20110267ER

Abstract

This project developed and demonstrated a powerful new class of programmable spectral imagers based on rapidly addressable spatial light modulators such as micro-mirror arrays. In these instruments, the micro-mirror array (MMA) and associated optics act as a rapidly reconfigurable many-band spectral filter wherein any combination of dozens or hundreds of spectral bands can be selected and used to form a chemical-specific image. In essence, the MMA performs hyperspectral image (HSI) processing directly in the optical hardware, rather than in post-processing. This technology represents a major advance over earlier MMA-based spectral imager concepts in the following crucial respect: Previous concepts suffered from a large variation of the selected wavelengths with image position, necessitating a time consuming spatial scan to acquire a two-dimensional image, and negating the speed advantages that are the major attraction of a programmable filter. Our new technology eliminates this problem through a revolutionary re-thinking of the optical system, so that MMA spectral processing can now be performed on an entire 2D image at once, allowing sophisticated background-suppressing matched filters to be implemented at real-time video rates. This new capability opens up applications ranging from rapid broad-area search for proliferation telltales (with the time required to scan and process data from a given area reduced 2-3 orders of magnitude over traditional hyperspectral imagers), remote imaging of natural gas leaks at production fields and pipelines, real-time medical imaging, spectral monitoring of rapid transients, spectrum-based tracking of vehicles, and (when coupled with the appropriate ultra-fast detector) ultra-fast spectral imaging on ns timescales.

Background and Research Objectives

Hyperspectral imaging (HSI), in which each pixel contains a high-resolution spectrum consisting of dozens to hundreds of contiguous spectral bands, has proven indispensible for remote detection and identification of gaseous and solid chemicals, in applications ranging from reconnaissance to medical imaging. But because they image only a single line of the spatial scene at a time and acquire the other spatial dimension by "push-broom scanning" that line across the scene, current HSI instruments are inherently slow, typically requiring several seconds to obtain a single spatial/spectral image cube. Monitoring phenomena on timescales faster than this has necessitated sacrificing either spectral specificity (e.g. reducing the spectral component to a simple band-pass filter in front of a fast camera), or sacrificing spatial information and simply aiming a spectrometer at a point (or, at most, a line). The aim of this project is to use programmable micro-mirror arrays (MMAs) to achieve an optimal compromise: collecting enough spectral information to reliably distinguish the target of interest from a spectrally cluttered background, while maintaining the speed and simplicity advantages of a simple filter. By performing all spectral manipulations instantaneously in the optics to produce already-processed imagery, this also drastically reduces data volume and processing time, two well-known logistical headaches that have long plagued conventional HSI.

The idea of an MMA-based programmable filter is not new, but prior to our work, essentially all such filters [1-10] were incapable of 2D imaging and worked as follows: Light from the scene is collimated and presented to a diffraction grating. Often, but not always, a slit restricts the field of view to a thin line. After the grating, light is focused to a spectrally dispersed image of the scene (cropped by the slit if one is included) at the MMA. The MMA acts as a multi-band spectral selector, with columns of micro-mirrors programmed to the "on" orientation to direct desired wavelengths toward the detector, while other columns are turned off to reject undesired wavelengths. The spectrally manipulated light is recombined by a second grating, and a non-dispersed, spectrally-filtered quasi-white-light image is focused onto the detector. The fundamental limitation, as seen in Figure

1(a), is that location within the scene is unavoidably intertwined with wavelength: different spatial locations have different angles of incidence onto the grating, and so light of a given wavelength does not arrive at a unique location on the MMA [1]. Therefore these instruments, like conventional hyperspectral imagers, can only image one line of the scene at a time, and require a push-broom scan to produce a 2D spatial image – a major limitation on data acquisition speed. The goal of this project is to overcome this limitation and produce MMA programmable filters capable of acquiring a full 2D image at once.

Scientific Approach and Accomplishments

The scheme outlined above, which is only a slight modification of a standard HSI setup, initially appeared to be the only conceivable choice, putting the goal of programmable spectral processing applied simultaneously to the entire 2D image out of reach. This project began with the realization that fundamentally different approaches do exist and are in fact workable. Our patent-pending new concept [11,12] begins by recognizing that, in order for the MMA to spectrally manipulate an entire 2D image at once, without any wavelength shifts with image position, it must be placed at a location where light of any given wavelength converges to a well-defined location that is unique for each wavelength, regardless of where in the 2D scene it originated. The original breakthrough concept was the realization that such a location can be produced if the grating is placed not at a non-imaging collimated-light location, but at an image plane in which light arrives at the same angle of incidence for all image points. With light striking the grating at the same angle of incidence for all image points, it follows that light of a given wavelength will emerge from the grating traveling in the same unique direction for all image points, and can therefore be focused to a well-defined spot on the spectral selector, where it can be turned on or off for the entire 2D image.

While simple in concept, the trick lies in actually producing that initial image plane having a spatially invariant angle of incidence. Our original concept involved using a microlens array near the image plane to redirect the light into the desired direction, but that strategy was found to be unworkable. A simpler strategy is simply to restrict the rays reaching the image plane to those traveling in the right direction, and reject the others. This strategy led to our first successful prototype, illustrated in Figure 1(b), and was the focus of the project's first year. Directional restriction was achieved using a capillary array, essentially a bundle of 100μm diameter hydrogen-blackened glass tubes, the whole bundle being approximately 2 cm in diameter and half an inch long. Instead of a micro-mirror array, the spectral selector in this first prototype was a liquid crystal device (LCD) spatial light modulator array between crossed polarizers. While not as good at rejecting unwanted wavelengths and limited in its wavelength range, the LCD had the advantage of being amenable to very simple optical setups. Images from a prototype designed to cover the entire visible spectrum are shown in Figure 2(a).

Several shortcomings of this early prototype immediately became apparent. First, the capillary array rejects off-axis rays in both the spectral and orthogonal dimensions, unnecessarily discarding a large fraction of the available light and making this a very low-throughput system. Secondly, because the hydrogen blackening process put strict limits on the length of the capillary tubes, disappointingly low spectral resolution was achieved (longer, thinner tubes more effectively restrict the light to just those rays traveling along the tube axis, and the resolution, in turn, depends on how precisely the light rays are aimed toward the diffraction grating). Abutting two or three identical capillary arrays end-to-end did improve the spectral resolution in the expected manner, but registration of the segments was extremely problematical.

A far better approach [12], and the next major breakthrough of the project, was developed in the second year. This improved approach grew out of the recognition that the required condition of constant angle of incidence at the grating imaging plane can be met using telecentric imaging optics to form the first image; in fact, the condition that chief rays (the center of the ray bundles) for every image point be parallel to each other is the definition of telecentricity. The simplest way to construct a telecentric imager is to place the initial aperture – the entrance pupil – one focal length in front of an ordinary lens. To achieve the angular restriction requirements – greatly restricted in the spectral dimension and essentially unrestricted (in order to admit as much light as possible) in the orthogonal dimension – the entrance pupil becomes a slit. This strategy has the advantages of having 1-2 orders of magnitude greater throughput than the capillary array approach, much higher spectral resolution, and can be realized using conventional optics. A simple system based on this principle is illustrated in Figure 1(c). A comparison of Figure 2(a) and 2(c) shows the much higher image quality and spectral resolution potential of the telecentric imaging strategy.

Although the first prototype used an LCD array as the spectral selector, micro-mirror arrays offer several significant advantages, and the aim of this work from the outset had been to produce MMA-based full-frame programmable spectral filters. These advantages include the following:

1. MMAs offer a much wider useful spectral range, extending from the ultraviolet into the mid-infrared,

whereas LCDs are limited to the visible and a small part of the near-infrared.

2. MMAs do not require polarizers, hence more light gets used (the LCD's initial polarizer immediately discards half the light).

3. MMAs offer a well-defined "off" state with essentially no light leakage, and high throughput in the "on" state, whereas considerable off-state rejection leakage occurs with LCD setups, depending on the quality of the polarizers and field of view.

Micro-mirror arrays, however, particularly the only readily available commercial array, the Texas Instruments DLP® (Digital Light Processor), present unique challenges of their own, in particular some rather problematic diffraction effects. The DLP® micro-mirror array used here consists of a 1024x768 array of 13.68µm-square micro-mirrors. Each micro-mirror can be set to tilt along its diagonal at either +12 or -12 degrees with respect to the device plane, the two orientations representing the "on" and "off" states in this application. Importantly (and inconveniently), the flat, plane-of-device orientation is not a settable position for the micro-mirrors. Given these properties, the DLP array is, in essence, a two-dimensional diffraction grating. As described in detail in [1] and [12], the angular directions of the various diffraction orders are determined solely by the spacing of the micro-mirror grid, just as the diffraction angles of a grating are determined by the groove spacing, while the 12-degree tilt of the micro-mirrors, in direct analogy with the blaze angle of a conventional diffraction grating, determines which of these diffraction orders will receive most of the light.

Left uncorrected, diffraction from the DLP micro-mirrors would have two major consequences for our programmable spectral imagers. First, the grating-like DLP diffraction would produce spectral dispersion in the final image, producing a rainbow-smeared version of the scene rather than a sharp white-light image. Secondly, the multiple diffraction orders of the DLP would produce multiple images, each with its own degree of spectral dispersion. At first, these problems appeared to rule out the use of DLP arrays in our full-frame programmable filter strategy, but a there is a solution: simply undo these diffraction effects using a second DLP [12].

This strategy is realized in our patent-pending DLP-based prototype [11-13], shown in Figure 3. As in Figure 1(c), a slit-shaped aperture one focal length in front of the first lens leads to a telecentric image on the grating. But in this case, the "slit" is actually a programmed pattern on the first of two DLP micro-mirror arrays. This first DLP introduces diffractive dispersion that eventually is reversed by the second DLP, which acts as the spectral selector. Not only is this design extremely compact, but it also enables rapid adjustment of spectral resolution and throughput simply by varying the slit pattern programmed onto the first DLP.

With this prototype we have been able to demonstrate all the key capabilities aimed for in this project: rapidly reprogrammable high resolution spectral imaging; background-suppressing matched-filter imaging; display of the final results as real-time video, already spectrally processed by the micro-mirror optics to highlight faint targets in a spectrally cluttered scene; and, when desired, full hyperspectral imaging using the Hadamard transform technique (which is a way of efficiently encoding spectral information, described in detail in [12,14]). An early demonstration of these capabilities is illustrated in Figure 4. Here our test scene consists of two light bulbs: an ordinary incandescent bulb, and a compact fluorescent lamp (CFL). While the incandescent bulb emits a continuous spectrum covering all visible wavelengths, the CFL emits only a few sharply defined discrete wavelengths dominated by the mercury vapor spectrum. In this demonstration we treat the CFL spectrum as the "target" and the incandescent as the "background." The spectral selection MMA is programmed to implement a background-suppressing matched filter [12,13] that emphasizes the target and suppresses the background, with an intricate selection of spectral bands and weights determined using a well-established mathematical framework [13]. The result is an image – displayed to the user as real-time video – in which the incandescent lamp is so effectively suppressed that it appears to be turned off (both lamps are actually on), and the faint reflection of the CFL (the target) is clearly visible on the incandescent bulb's surface. This is analogous to one of the major applications of this technology – detecting the faint spectral signatures of trace gases against much stronger background clutter – with the CFL reflection playing the role of the gas.

In the project's final year, we joined forces with another LDRD project, "Terrestrial Vegetation, CO2 Emissions, and Climate Dynamics" (20110014DR, Nathan McDowell, PI), and deployed our instrument at that project's vegetation survival/mortality (SUMO) test-bed to perform spectral imaging of trees subjected to varying degrees of drought- and heat-induced stress. Figure 5 shows example results from this first field deployment, in which the instrument implemented both programmed multi-band imaging and Hadamard full-hyperspectral imaging to explore the spectral signatures of these climate-stressed trees.

With its many successes, this work has already attracted

follow-on projects, most notably a CRADA with Chevron to adapt our technology to remote detection of natural gas leaks at production fields, "fracking" operations, and pipelines.

Impact on National Missions

This new technology, by offering a 2- to 3-order-of-magnitude speed improvement over standard hyperspectral instrumentation, directly addresses the long-standing need for a broad-area search capability for the DOE proliferation detection remote sensing mission, and it is already being considered for imaging of proliferation-related materials. The elimination of traditional HSI's slow scanning also enables a range of more general military and national security missions, such as tracking of vehicles and real-time imaging of chemical agent plumes. Coupling with LANL-developed high-speed imaging capabilities would add an as yet unexplored spectral dimension to these technologies. By working with industrial partners, like the follow-on project on natural gas leak detection, our advance is already showing significant potential impact on energy and environmental missions. New scientific applications seem likely as well, such as ultra-fast spectral imaging of shock waves and explosions, planetary missions, volcanic gas monitoring, and real-time medical imaging. The project successfully supported a postdoc, who is now on track to become a staff member supporting proliferation detection missions.

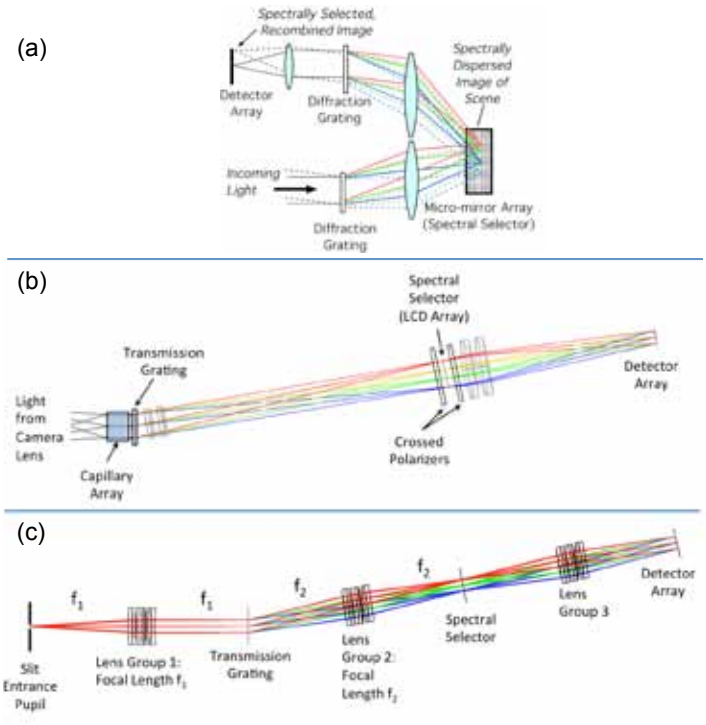

Figure 1. Full-frame programmable spectral filter principles of operation. (a) Basic scheme used by all previous micro-mirror array (MMA) programmable filters, which were incapable of full-frame imaging. Light impinging on the diffraction grating is collimated, and the MMA is placed at a spectrally-dispersed image plane. MMA-selected wavelengths are then recombined with a second grating and imaged onto the detector. Only a single line of the scene can be imaged at one time because the wavelength at a given position on the MMA varies with position in the scene, necessitating a push-broom scan to form a full two-dimensional image. The slitless design shown here, based on a non-full-frame prototype we produced in a 2009 project [1], performs the scan internally, by moving the spectral pattern across the MMA. (b) Realization of a full-frame programmable filter using a capillary array. Light is imaged onto the capillary array – basically a bundle of blackened tubes – which passes only those rays traveling down its axis and rejects all others, resulting in an image with spatially invariant angle of incidence at the diffraction grating. Because the light strikes the grating at the same angle for the entire image, each wavelength can be imaged to the same unique location at the spectral selector (an LCD array rather than an MMA in this example), regardless of where in the scene it originated. The selected wavelengths are then focused to a full 2D image at the detector. (c) Realization of a full-frame programmable filter realized using telecentric imaging onto the grating. A slit-shaped entrance aperture is placed one focal length in front of the first imaging lens, ensuring that the image at the grating is telecentric, i.e. that the chief ray from every image point strikes the grating at the same angle. As in (b), this produces a spectral plane where the MMA or LCD spectral selector can manipulate an entire 2D image at once. The slit entrance pupil restricts the light propagation direction only in the spectral dimension (the plane of the page in this picture). In the orthogonal dimension (out of the page) the tall slit allows a wide range of light propagation directions, without affecting the spectral resolution, thus greatly improving the throughput compared to the capillary array strategy.

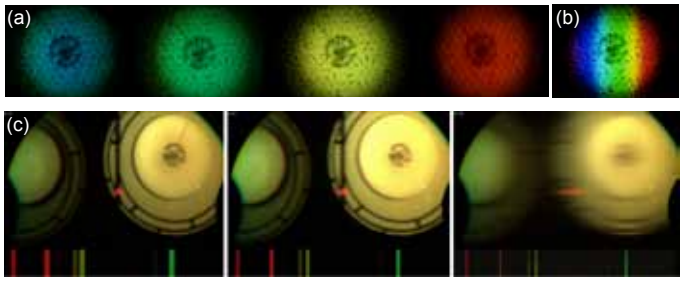

Figure 2. Sample images and spectral/spatial resolution trade results obtained from early prototype capillary-array and telecentric full-frame programmable filters. (a) Actual color images of a light bulb (note the "100 W" and manufacturer's label visible near the center of each image) obtained with a prototype capillary-array- and LCD-based full-frame programmable spectral filter similar to Fig. 1(b). In each image, the LCD array is programmed for a single moderate-width spectral band (~50 nm), corresponding to, from left to right, the visible colors blue, green, yellow, and red. The hexagonal structure of the capillary array can be seen superimposed on the images. The key aspect to note is that the color is the same throughout each image, indicating negligible wavelength shift with image position. (b) Conceptual depiction of how the image would look if it were obtained using

non-full-frame design as in Fig. 1(a), with a single narrow band programmed onto the selector; the passed wavelength varies with image position. (c) White-light images and spectra obtained with a telecentric full-frame spectral filter system similar to that shown in Fig. 1(c). Narrowing the slit entrance pupil to improve spectral resolution produces diffraction that degrades the spatial resolution; this is a fundamental performance trade of this system. These three images and spectra illustrate that trade. The scene in each image consists of two desk lamps (one partially obscured on the left) and a laser spot in the center. The laser spot, used as a spectral reference, consists of several co-aligned lasers of various wavelengths. Across the bottom of each frame is the spectrum of this laser reference, obtained by moving the detector array from the image plane to the spectral plane, illustrating the spectral resolution for the settings used to obtain the image. From left to right the spectral resolutions are 2.7 nm (150 spectral bands across the spectral range), 1.8 nm (225 bands), 0.4 nm (1000 bands). Only in the last case does diffraction significantly degrade the spatial image quality.

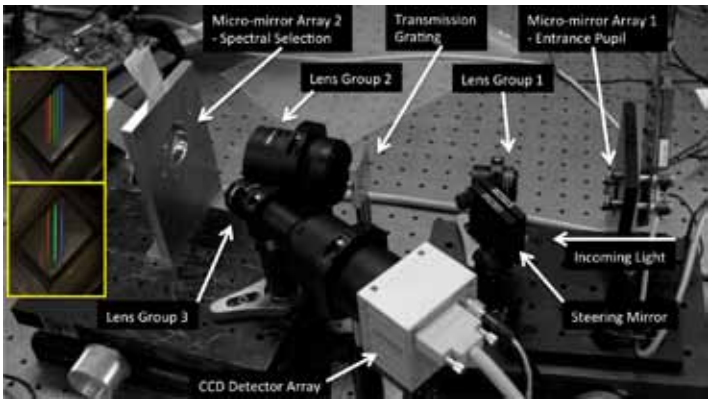

Figure 3. Photograph of a working prototype full-frame programmable spectral imager employing a Texas Instruments DLP® micro-mirror array as the spectral selector, with diffraction compensation by means of a second DLP. Incoming light strikes the compensating DLP first, introducing a "pre-compensating" diffractive dispersion. This first DLP, programmed to display a slit function, also serves as the entrance pupil for the telecentric imaging onto the grating. The spectral selection DLP reverses the effects of the pre-compensating DLP to produce a final non-dispersed image at the detector. Inset shows the spectral selection DLP array, programmed with two example spectral band selections, as viewed from the detector position. The optical design is described in detail in [12].

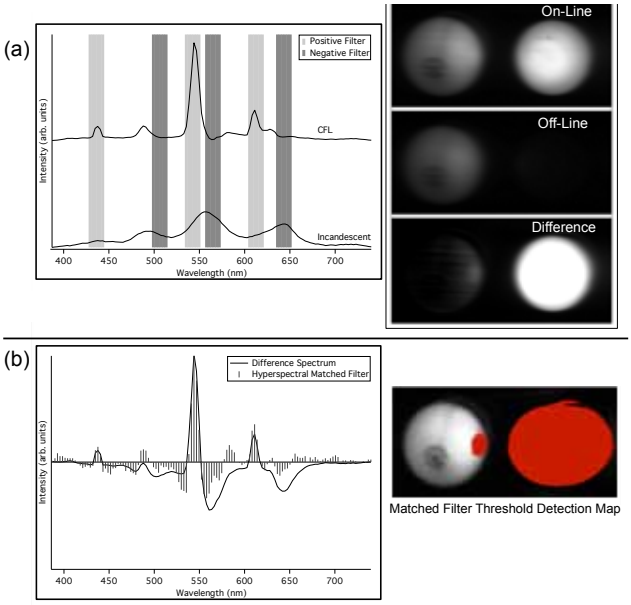

Figure 4. Examples of matched-filter imaging with background suppression using the full-frame programmable spectral imager prototype shown in Fig. 3. The scene for this example consists of two light bulbs: an incandescent bulb on the left and a compact fluorescent lamp (CFL) on the right. (a) A simple few-band matched filter. On the left side are 128-band spectra of the two bulbs, obtained with the prototype using the Hadamard transform technique [1,14]. The CFL spectrum consists of several sharp lines, whereas the incandescent bulb has a continuous spectrum. On the right, the top image results when the DLP micro-mirrors are programmed to pass three bands (light gray bars over the spectra on left) corresponding to CFL emission lines; the middle image is obtained with three different programmed bands (dark gray bars in the left figure), chosen to miss the CFL emission. The difference between these two images is shown at bottom. Note that, in the difference, the incandescent emission is so effectively suppressed that the only illumination visible is the reflection of the CFL. (b) A full 128-band matched filter, derived using rigorous hyperspectral image processing algorithms, as described in detail in [13]. Each spectral band is assigned a positive or negative weight, indicated by the histogram on the left, which is implemented on the DLP array using its duty-cycle-based grayscale capability, with negative values obtained by taking two frames and subtracting as in (a). The duty-cycle grayscale weighting works by flipping a micro-mirror "on" for only a fraction of the detector integration time, with the fraction determining that micro-mirror's apparent brightness. The resulting threshold detection map at right highlights in red all areas containing the CFL target spectrum, including a well-defined reflection on the incandescent bulb.

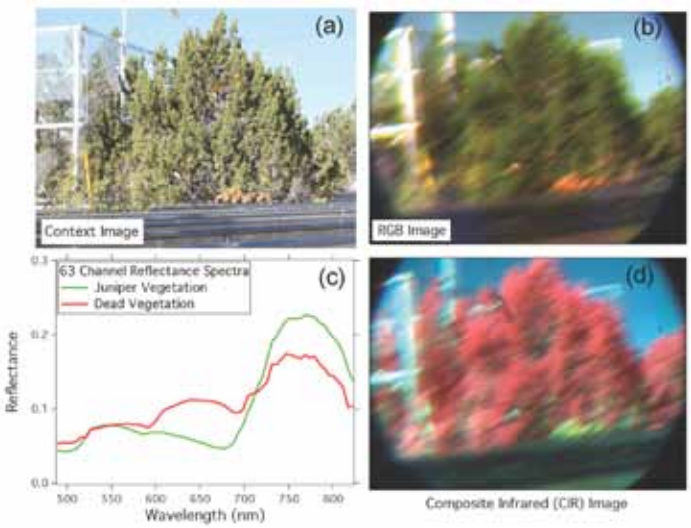

Figure 5. Results from the field deployment of the prototype full-frame programmable spectral imager at LANL's tree Survival/ Mortality (SUMO) test site. (a) Context image obtained with an ordinary digital camera. (b) Red-Green-Blue (RGB) color image obtained with the prototype by setting the programmable filter to pass three 30 nm wide bands centered 495, 560, and 640 nm. In both (a) and (b), note the orange/brown dead branch in the lower part of the image, just to the right of center. (c) Vegetation spectra obtained with the prototype operating in full hyperspectral mode. The healthy and dead vegetation spectra shown were extracted from selected pixels of a full hyperspectral data cube. Note the high near-infrared reflectivity of the healthy vegetation. (d) A false-color composite infrared (CIR) image obtained with the prototype by setting the programmable filter to pass three 30 nm wide bands centered 560, 640, and 760 nm. In the CIR image, healthy vegetation appears red and dead vegetation is highlighted as bright green. With the programmable spectral imager, any combination of spectral bands can be selected and displayed as real-time false-color video, offering the potential for rapid remote-sensing surveys of forest health specifically tailored for particular tree species, diseases, and levels of climate-induced stress.

References

1. Love, S. P.. Programmable matched filter and Hadamard transform hyperspectral imagers based on micro-mirror arrays. 2009. Proceedings of SPIE. 7210: 721007.

2. Wagner, E. P., B. W. Smith, S. Madden, J. D. Winefordner, and M. Mignardi. Construction and evaluation of a visible spectrometer using digital micromirror spatial light modulation. 1995. Applied Spectroscopy. 49 (11): 1715.

3. Kearney, K. J., M. Corio, and Z. Ninkov. Imaging spectroscopy with digital micromirrors. 2000. Proceedings of SPIE. 3965: 11.

4. Wehlburg, C. M., J. C. Wehlburg, S. M. Gentry, and J. Smith. Optimization and characterization of an imaging Hadamard spectrometer. 2001. Proceedings of SPIE. 4381: 506.

5. Wuttig, A., and R. Riesenberg. Sensitive Hadamard transform imaging spectrometer with a simple MEMS. 2003. Proceedings of SPIE. 4881: 167.

6. Hanf, M., A. Schaporin, R. Hahn, W. Dotzel, and T. Gessner. Novel Hadamard transform spectrometer realized using a dynamically driven micro-mirror array as light modulator. 2005. Proceedings of SPIE. 5717: 117.

7. Quyen, N. T., E. Da Silva, N. Q. Dao, and M. D. Joulan. New Raman spectrometer using a digital micromirror device and a photomultiplier detector for rapid on-line industrial analysis. 2008. Applied Spectroscopy. 62 (3): 273.

8. Goldstein, N., P. Vujkovic-Cvijin, M. Fox, B. Gregor, J. Lee, J. Cline, and S. Alder-Golden. DMD-based adaptive spectral imagers for hyperspectral imagery and direct detection of spectral signatures. 2009. Proceedings of SPIE. 7210: 721008.

9. Goldstein, N., M. Fox, S. Alder-Golden, and B. Gregor. Infrared adaptive spectral imagers for direct detection of spectral signatures and hyperspectral imagery. 2013. Proceedings of SPIE. 8618: 86180D.

10. Newman, J. D., B. V. Brower, P. P. K. Lee, A. D. Cropper, M. Gibney, and M. Pellechia. MEMS-based spectral-polarimetric imaging and target tracking architecture for airborne broad-area search. 2011. Proceedings of SPIE. 8053: 805302.

11. Love, S. P., and D. L. Graff. Full-frame programmable spectral imager. 2012. International Patent Application PCT/US2012/000417.

12. Love, S. P., and D. L. Graff. Full-frame programmable spectral filters based on micromirror arrays. 2013. Proceedings of SPIE. 8618: 86180C.

13. Graff, D. L., and S. P. Love. Real-time matched-filter imaging for chemical detection,using a DMD-based programmable filter. 2013. Proceedings of SPIE. 8618: 86180F.

14. Harwit, M., and N. J. A. Sloane. Hadamard Transform Optics. 1979.

Publications

Graff, D. L., and S. P. Love. Real-time matched-filter imaging for chemical detection,using a DMD-based programmable filter. Presented at SPIE Photonics West, Confer-

ence on Emerging Digital Micromirror Device Based Systems and Applications V. (San Francisco, 5-6 February, 2013).

Graff, D. L., and S. P. Love. Real-time matched-filter imaging for chemical detection,using a DMD-based programmable filter. 2013. Proceedings of SPIE. 8618: 86180F.

Graff, D. L., and S. P. Love. Real-time matched-filter imaging using a DMD-based programmable filter. To appear in Journal of Micro/Nanolithography, MEMS, and MOEMS.

Love, S. P.. Full-frame programmable spectral filters based on micro-mirror arrays. Presented at SPIE Photonics West, Conference on Emerging Digital Micromirror Device Based Systems and Applications V. (San Francisco, 5-6 February, 2013).

Love, S. P., T. C. Hale, and P. Chylek. Advanced Instrumentation for Hyperspectral Imaging. Invited presentation at LDRD Day 2011. (Santa Fe, NM, Sept. 13, 2011).

Love, S. P., and D. L. Graff. Full-frame programmable spectral filters based on micromirror arrays. 2013. Proceedings of SPIE. 8618: 86180C.

Love, S. P., and D. L. Graff. Full-frame 2D imaging programmable spectral filters based on micro-mirror arrays. To appear in Journal of Micro/Nanolithography, MEMS, and MOEMS.

Novel Broadband Tera Hertz Sources for Remote Sensing, Security and Spectroscopic Applications

John Singleton
20110320ER

Abstract

This project deals with the design, construction, testing and assessment of new antennas based on superluminal (faster than light) polarization currents. One is based on a magnetic field that rotates at frequencies between 1 and 4 GHz. Higher frequency emission from polarization currents in a surrounding dielectric is demonstrated, giving proof-of-principle of a new type of broadband THz source for spectroscopic, communications and security applications. Various dielectrics and metamaterials are screened to optimize higher frequency emission. A developing understanding of the computer modeling, control, and uses of superluminal polarization currents leads to antennas that could be optimized for communications applications, and a superluminal antenna is shown to give better performance than conventional technologies over distances of up to 76 km. A CRADA is established with industrial partners to develop the technology for commercial applications. Various models of astronomical objects employing superluminal polarization currents are explored.

Background and Research Objectives

Investigation of electromagnetic fields generated by charged particles moving superluminally (faster than light) started in the 1890s ([1-5] and references therein), but the publication of Special Relativity in 1905 discouraged further work; charged particles possess rest mass and cannot move superluminally. However, in the 1970s, Bolotovskii and Ginzburg pointed out that disturbances caused by the relative motion of differently charged particles –polarization currents – are not restricted to subluminal speeds. Polarization P (the dipole moment per unit volume) results from relative displacement of positive and negative charges (Figure 1(a,b)); a polarization current occurs when polarization moves or changes with time [1-5].

If a polarization current oscillates or accelerates, it emits radiation, just like a conventional electron current. However, in contrast to electrons, which are limited to speeds below c, the speed of light, polarization currents may travel arbitrarily fast, as the displacement of their constituent charged particles is minimal. While the radiation source travels faster than c, the individual massive particles' speeds remain subluminal [1-5].

In 2008, the PI and some members of the current research team, in collaboration with H. Ardavan of Cambridge and A. Ardavan of Oxford University undertook the project LDRD20080085DR: Construction and Use of Superluminal Emission Technology Demonstrators with Applications in Radar, Astrophysics, and Secure Communications. This project demonstrated the feasibility of superluminal polarization currents as antennas, designing, testing and proving the control electronics, antenna elements and electrical hardware necessary for the concept. It also produced a patent for a superluminal RADAR system that has garnered industry interest [6], and led to several awards, including Universe Today - Top 10 Story, Business Weekly - Who's Who in Technology, Federal Laboratory Consortium for Technology Transfer Notable Technology Development Award for Superluminal Radar System, and Los Alamos National Laboratory - Top 10 Science and Technology Development. Summaries of the papers produced in that project are given in [2-5] and references therein.

Though proof-of-principle had been demonstrated, the field of superluminal sources is still wide open, with many scientific and technological aspects to be explored. The current project therefore sought new ways to generate and manipulate superluminal polarization currents, and explored novel aspects of the emitted radiation, such as the production of much higher frequencies.

Figure 1 shows the principles of the superluminal antennas explored in this project (a third type, developed in Russia [1], requires a high-power laser). A dielectric (insulator) containing charged ions is depicted in Figure

1(a), whilst 1(b) shows the dielectric subject to a moving electric or magnetic field. Positive and negative ions are displaced in opposite directions, giving a region with net P. The movement of the polarized region gives rise to a polarization current. The principles of electrostatic superluminal antennas (ESAs) [2-5] are shown in Figure 1(c); blue shading represents a dielectric. Below is a metal ground plate, and above is a series of metal electrodes. If a voltage is applied between electrodes and the ground plane, a polarized region is created; turning electrodes off and on (Figure 1(d)) moves the polarized region. Creating a superluminal polarization current is thus just a matter of timing. An ESA in the form of an arc (Figure 1(f)) was built in this project in response to a growing understanding of the use and control of superluminal polarization currents, and as a validation of computer models.

However, a primary project aim was to create a superluminal polarization current using a rotating magnetic field. Figure 1(e) shows a rotating magnetic dipole; at sufficient distance from the rotation axis, the magnetic field lines are traveling faster than c. These superluminal field lines induce polarized currents in a dielectric that emit radiation [2-5]. Such emitters are known as magnetic superluminal antennas (MSAs). Our MSA employs orthogonal coils (Figure 1(g,h)); it is of interest because superluminal polarization currents in the dielectric can emit high frequency radiation, providing the basis for Terahertz (THz) sources. In tandem, experiments and computer models with ESAs led to discoveries useful in communication, radar and other applications that are the subject of two active patent applications and a further five planned patents.

Scientific Approach and Accomplishments

Initially, objections to superluminal antennas were raised by an examiner dealing with the Radar patent and by a potential sponsor. Therefore, experiments to demonstrate understanding and control of superluminal polarization currents were carried out. Selected data are in Figure 2.

Conventional Cerenkov radiation is known as the blue glow seen in storage ponds holding nuclear fuel rods; it is caused by radioactive particles traveling faster than the speed of light in water [1,4]. The discovery and explanation of the Cerenkov effect was rewarded with a Nobel Prize. By contrast, superluminal polarization currents should emit vacuum Cerenkov radiation, i.e., radiation due to disturbances traveling faster than the speed of light in a vacuum [1-5]. A linear ESA (Figure 2(a)) was used to demonstrate that this indeed occurs. Polarization currents were driven along the ESA at speeds from -4c to +4c. Figure 2(b) shows the power emitted versus ESA orientation. The peak emission position versus speed is in Figure 2(c); the faster the polarization current, the smaller should be the emission angle. The data match these expectations, and fit the theoretical angle-speed relationship for vacuum Cerenkov closely [1]. (Note that experiments involved two emission frequencies, 2.4 and 2.6 GHz). Figure 2(d) shows emitted power versus speed; again, agreement between theory [1] and experiment is good, showing unambiguously that superluminal polarization currents give the emission from the ESA, and their speed is controlled precisely.

Concern was expressed (by the LDRD Engineering panel) that a polarization current in alumina may not respond fast enough to generate THz. In response, currents traveling at up to 100c were demonstrated; e.g. Figure 2(e) shows received power (10.5 km away) versus angle for the ESA shown in Figure 1(f) run at speeds of 3c and 100c. There is little difference in power, showing that the polarization current “keeps up”; the emission process works at ultra-high speeds.

Applications of MSAs depend on the focusing properties of rotating superluminal sources. Once a source both exceeds the speed of the waves it emits and accelerates (via centripetal acceleration), unusual properties are expected; waves emitted over an extended period of the source’s time frame can arrive simultaneously at an observation point [2-7]. This is known as temporal focusing- focusing in the time domain [2-6]. One consequence is that some of the radiation from a rotating superluminal source will have a power that falls off as 1/distance, rather than as the 1/(distance)^2 dependence of conventional antennas [2-7]. Figure 2(f) shows power versus distance and pan angle for a rotating superluminal source with a speed of 3.3c, and Figure 2(g) shows the data from (f) processed to give the exponent n that describes how the power P falls off with distance d ($P \alpha d^n$); n is plotted versus pan angle. Notice that, as expected [2-7], at many angles, the power falls off more slowly than that from conventional antennas, though slight imperfections prevent the ideal n=-1 from being reached.

A primary objective was to design, model and fabricate a method for rotating a magnetic field at high speed (Figure 3(a)). This required a novel approach; two orthogonal coils driven by GHz alternating currents. Extensive electromagnetic modeling and engineering were necessary (Figure 1(h)) to achieve an optimized design that is compact and matched to 50 Ohm electronics. At GHz frequencies, the coil parameters (impedance and radiation resistance) are sensitive to the exact dimensions and geometry of the coils. The situation is complicated by the tendency for MSAs to behave resonantly, so that the time-averaged current is no longer uniform around the conductor, distorting the field. The pivotal breakthrough was a resistive load,

behind the coils, that suppresses the tendency to resonate, and yet allows maximum power to be coupled into the region where the field is produced. The completed coil system (Figure 3(b)) operates at 1-4 GHz, a first in electrical engineering; never before has such a rapidly rotating field been produced in such a large, open volume.

Following successful coil tests, various dielectric cylinders (Figures 3(a,b)) were used for higher frequency generation. Figure 3(c) gives typical data for two different materials; higher frequencies, not present in the electronic signals driving the coils, are emitted, showing up as second and third harmonics whose intensities depend on the dimensions and composition of the dielectric. This is proof-of-principle that the proposed THz source is feasible. The experiments also validate pulsar models based on superluminal currents [2-5].

To emphasize higher (THz) frequencies, the dielectric must be replaced with a metamaterial with an enhanced dielectric constant at a few tens of GHz. Various recipes of metamaterial were considered; multilayered arrays of copper structures (Figure 3(d)) were found to be the best. Unfortunately a mechanical failure of the coil system during extensive tests (June 2013) delayed experiments on the metamaterial; these are scheduled for late 2013.

Radiation from superluminal antennas cannot be calculated using conventional electromagnetic design packages, for reasons discussed in [2]. Consequently, another aim is to develop computational methods for simulating superluminal antennas; eventually, this will provide commercial design tools. Figure 4 shows the calculated (a) and measured (b) power versus distance and pan angle for the ESA shown in Figure 2(a); agreement between calculation and data is good. Computer simulations also designed future ESAs with tightly focused, steerable radiation pattern; e.g., Figure 4(c) shows a simulated power distribution from an array of five linear ESAs. The tightly-defined beam pattern is suitable for steered radar beams.

Progress was made on astronomical models based on superluminal polarization currents. Several papers have been presented at conferences of the American Astronomical Society; a Master's thesis [4] and a long paper on supernovae were completed [8]. Further papers are in preparation. Figure 4(d) depicts a simulation of the Crab Pulsar; the curve is theoretical, and points include recent data. The superluminal model requires only 3 adjustable parameters to fit the Crab spectrum over 18 orders of magnitude of frequency, an achievement beyond that of any rival model for pulsars.

Demonstrations helped to establish a CRADA with ComScope, a leading US telecommunications company. These included the first transmission of an audio signal using a superluminal antenna. As mentioned above, a remarkable prediction about superluminal antennas is that in certain directions, the emitted power should fall off as 1/d, rather than the 1/d^2 obeyed by conventional sources [2]. Experiments during the current project were able to demonstrate this effect over long distances for the first time. Figure 5(a) shows propagation tests of a circular ESA over distances 1.05, 10.5 and 76 km. As these prototype antennas produce wide beams, these tests involved comparisons with non-directional dipoles. Figure 5(b) shows the angle dependence of the power detected from the ESA using receivers at 1.05, 10.5 and 76 km relative to power received from the dipole. The advantage of the superluminal antenna- the transmitted power falls off more slowly with distance than that from the dipole - is clearly visible. Antennas with a wide angular spread suffer from losses due to destructive interference from ground reflections [7]. Nevertheless, comparisons of the superluminal antenna were made with commercial, directional dish antennas. Figure 5(c) shows power received from the superluminal antenna relative to that received from a dish with a tight beam not subject to destructive interference. The green curve connects observed data, the blue curve shows the expectations for conventional antennas, and the red curve the theoretical best performance of a superluminal antenna without ground reflections. In spite of ground reflections, the superluminal antenna still beats the dish. Collaborations with Professor Alicia Kim (LANL, Bath University) will apply the new field of antenna topology optimization to improve this performance towards the theoretical red curve.

A commercial quadrature amplitude modulation (QAM) signal [9] was transmitted using the ESA shown in Figure 1(f). Figure 5(d) shows a spectrum analyzer plot of the 64-QAM feed signal; Figure 5(e) depicts the transmitted signal. In the latter, the characteristic 8*8 points of the 64-QAM are smeared due to saturation of the vector modulators in the ESA, which, as part of a bench-top experiment, were not designed for the >10 dB excursions above mean signal level inherent in 64-QAM. Nevertheless, the demonstration shows that there is no potential problem in using superluminal antennas for telecommunications.

Four prototype passive feed networks were designed and built for economical ESAs (Figure 5(f)). Figure 5(g) shows a complete linear, 64 element, passive, ESA, intended for use in cellular telephone base stations. Successful tests of the passive feed networks open up the possibility of extreme power, pulsed, directed-energy superluminal antennas.

Many of the experimental results are currently tied up in

patents, both planned or in progress. Once these are resolved, internal reports on the technology will be modified for dissemination as publications in the scientific literature [9].

Impact on National Missions

One of LANL's aims is to "strengthen the core Laboratory capabilities in engineering to enable developing practical implementations of "discovery" successes". Superluminal emission is such a discovery, and by studying this approach to THz emission, directed energy and communications, this project applies basic science discovery to solve real-world problems. Broadband THz sources have a wide range of applications in remote sensing (e.g. detection of concealed controlled substances or explosives) and non-intrusive medical applications, whilst superluminal sources in general have potential applications in communications and homeland security; all are relevant to the core mission of LANL to be the leading laboratory for National Security Science. The project also develops and maintains expertise in metamaterials and simulation. Through a LANL Technology Transfer CRADA, technology is being licensed to US industries, spinning out applications from superluminal work; thus, any intellectual property will positively impact US job-creation. The project has increased collaboration between nanotechnology group MPA-CINT and LANL engineering groups, pointing toward new antenna technologies. It has strengthened connections between LANL and one of the world's leading experts in topology optimization (Professor Kim) that could lead to benefits in a variety of engineering fields. A Masters student employed in the project is now undertaking a PhD in Electrical Engineering on the topic and will bring expertise in unusual antenna design to LANL.

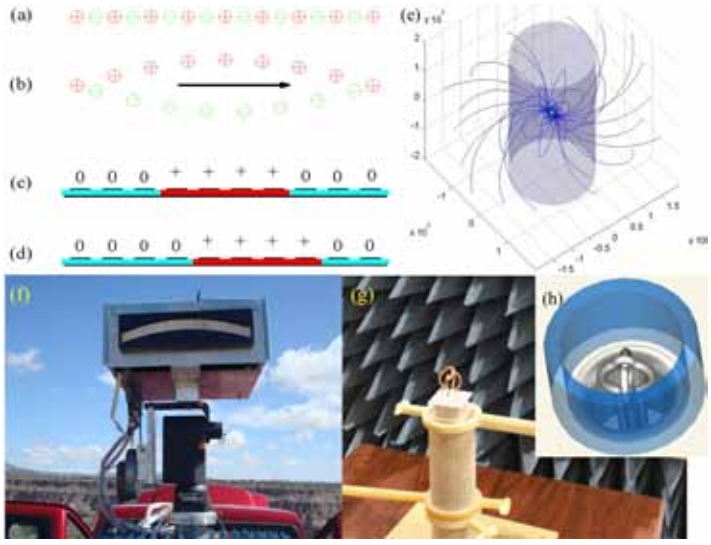

Figure 1. (a) Cartoon of dielectric solid containing positive (red) and negative (green) ions. (b) The same solid as in (a), but subject to a varying, vertical electric field that is strongest in the middle of the picture. Positive (red) ions have been displaced upwards and negative (green) ions have been displaced downwards, to form a region with net polarization, P. If the polarized region moves in the direction of the arrow, a polarization current flows. (c) Schematic of an electrostatic superluminal antenna. The blue region represents a dielectric solid such as alumina. The black line below is a metal ground plate, and the upper black lines represent metal electrodes. If a voltage is applied between some of the electrodes and the ground plane, a polarized region (red) is created in the dielectric. (d) Moving the polarization is accomplished by turning one electrode off and another on, so that the polarized region (red) shifts to the right; a polarization current has been formed. (e) Schematic of magnetic superluminal antenna. The blue curves are field lines of a magnetic dipole rotating in a horizontal plane. The gray cylinder represents the radius at which the field lines move fater than the speed of light. If a dielectric is placed around the dipole, the field lines will induce polarized regions similar to that shown in (b). (f) Electrostatic superluminal antenna with 32 electrodes built during the current project; the alumina dielectric (white region on the front of the antenna) is an arc of a circle of 1 m radius. In the photograph, the antenna is undergoing outdoor tests, beaming to a receiver 76 km away. (g) Orthogonal coils designed to produce a magnetic field rotating at frequencies between 1 and 4 GHz to energize a magnetic superluminal antenna. (h) Computer model of the coils in (g), used as a basis for finite-element simulations.

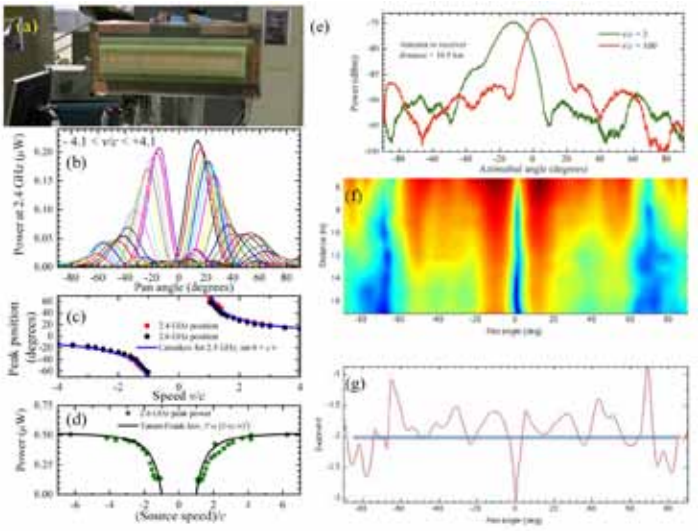

Figure 2. (a) Linear electrostatic superluminal antenna (the white dielectric visible on the front of the antenna is alumina) used to demonstrate the vacuum Cerenkov effect. (b) Power from the antenna in (a) versus emission angle. Each color represents the polarization current being driven at a different constant speed, ranging from -1.1 c (leftmost peak) to -4c (peak just below 0 degrees) and from +1.1c (rightmost peak) to +4c (peak just above 0 degrees). (c) Measured peak emission angle versus speed; points are data and the curve is the theoretical expectation for vacuum Cerenkov radiation. (d) Measured peak emission power versus speed; points are data and the curve is the theoretical (Tamm-Frank) expectation for vacuum Cerenkov radiation. (e) Received power versus angle for the superluminal antenna shown in Fig-

ure 1(f) run at speeds of 6c and 100c. There is little difference in peak power, showing that the emission process is effective even at very high speeds. (f) Received power (logarithmic color scale) versus distance and pan angle for a rotating superluminal source with a speed of 3.3c, measured in an anechoic range. (g) Data from (f) processed to give the exponent that describes how the power falls off with distance versus pan angle; the horizontal line (-2) is the expectation for a conventional antenna.

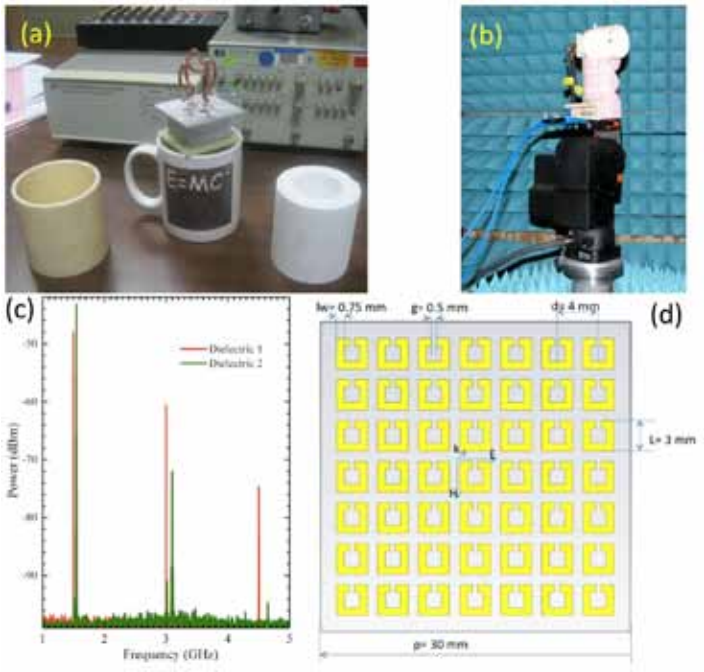

Figure 3. (a) The orthogonal coils used in the magnetic superluminal antenna inside a coffee cup for scale. On either side are examples of the different dielectric cylinders that are placed around the coils. The rotating field induces the polarization current in the dielectric, which subsequently emits radiation. (b) The coils inside a dielectric cylinder under test in an anechoic chamber; the antenna is mounted on a telescope mount that allows the antenna to be panned and tilted. (c) Experimental data showing harmonic generation from two different materials. So that the two data sets can be distinguished easily, the base (rotation) frequency used to excite dielectric 1 is 1.5 GHz and that for dielectric 2 two is 1.55 GHz. (d) Metamaterial (copper on insulator) designed to promote the emission of higher harmonics of the rotation frequency.

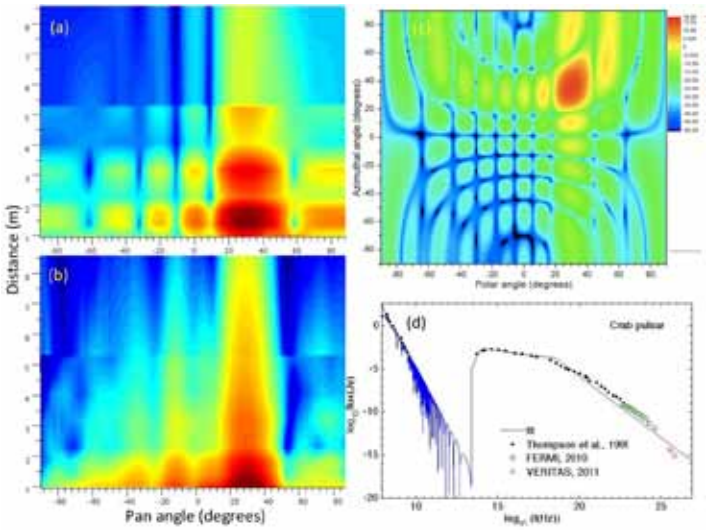

Figure 4. Calculated (a) and measured (b) power (logarithmic color scale) versus distance and pan angle for the superluminal antenna shown in Figure 2(a). The "moguls" seen in the power plot are less sharply defined in the experimental data because of small errors in the phase of the signals fed to the electrodes. (c) Simulation of the power (logarithmic color scale) versus pan and tilt angles from an array of five linear, superluminal antennas. The beam pattern is tightly defined, with side lobes >10 dB lower than the central maximum. (d) Simulation of the observed spectrum of the Crab Pulsar; the curve is theoretical, and points are experimental data. The superluminal model requires only 3 adjustable parameters to fit the spectrum over 18 orders of magnitude of frequency.

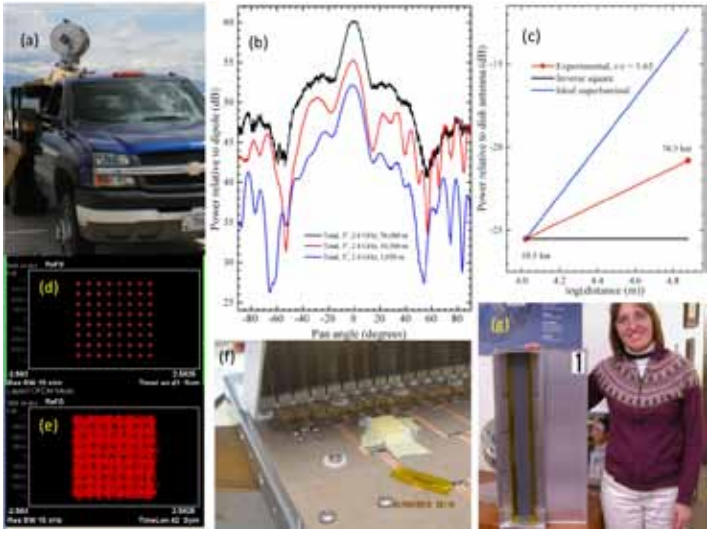

Figure 5. (a) Propagation tests of a circular superluminal antenna (mounted on the truck) over distances 1.05, 10.5 and 76 km. (b) Angle dependence of the power detected from the superluminal antenna using identical receivers at 1.05 (blue), 10.5 (red) and 76 km (black) relative to power from a conventional dipole antenna. The advantage of the superluminal antenna- transmitted power falls off more slowly with increasing distance than that from a conventional antenna - is clearly visible. (c) Power received from the superluminal antenna relative to that recieved from a highly

directional dish antenna versus log(distance). The red curve connects observed data, the black curve shows the expectations for a conventional antenna, and the blue curve the theoretical best performance of a superluminal antenna. (d) Spectrum analyzer plot of a 64-QAM signal fed to the superluminal antenna shown in Figure 1(f); (e) Corresponsing detected signal. The characteristic points of the 64-QAM are smeared due to saturation of the vector modulators in the superluminal antenna. (f) Prototype passive feed network for a superluminal antenna. (g) Complete linear, 64 element, passive, electrostatic, superluminal antenna, intended for use in cellular telephone base stations.

References

1. Bolotovskii, B. M., and A. V. Serov. Radiation of Superluminal Sources in Vacuum. 2006. Radiation Physics and Chemistry. 75: 813.

2. Ardavan, H., A. Ardavan, J. Singleton, J. Fasel, and A. Schmidt. Inadequacies in the Conventional Treatment of the Radiation Field of Moving Sources. 2009. Journal of Mathematical Physics. 50: 103510.

3. Schmidt, A., H. Ardavan, J. Fasel, J. Singleton, and A. Ardavan. Occurrence of Concurrent 'Orthogonal' Polarization Modes in the Lienard-Wiechert Field of a Rotating Superluminal Source. 2012. MPE Report. 291: 124.

4. Ardavan, H., A. Ardavan, J. Singleton, and M. Perez. Mechanism of Generation of the Emission Bands in the Dynamic Spectrum of the Crab Pulsar. 2008. Monthly Notices of the Royal Astronomical Society. 388: 873.

5. Schmidt, A.. Terrestrial and Extraterrestrial Radiation Sources that Move Faster than Light. 2012. MS Thesis in Applied Mathematics, UNM. : 1:123.

6. Singleton, J., H. Ardavan, and A. Ardavan. Apparatus and Method for Phase Fronts Based on Superluminal Polarization Currents. 2010. United States Patent Application US 20100039324A1.

7. Singleton, J., A. Schmidt, and J. Wigger. Test of the Linear Superluminal Antenna. 2012. Internal LANL Report.

8. Middleditch, J.. Pulsar-driven Jets in Supernovae, Gamma-Ray Bursts, and the Universe. 2012. Advances in Astronomy. 898907: 898907 1.

9. Singleton, J., A. Schmidt, J. Wigger, and S. Redman. Experimental and theoretical Studies of SL Antennas. Journal of Applied Physics .

Publications

Middleditch, J.. Pulsar-driven Jets in Supernovae, Gamma-Ray Bursts, and the Universe. 2012. Advances in Astronomy. 898907: 898907 1.

Schmidt, A. C., J. Middleditch, H. Ardavan, A. Ardavan, and J. Singleton. Statistical analysis of the pulsars in the Parkes multibeam survey reveals evidence for violation of the inverse-square law. 2012. In American Astronomical Society 219th Meeting. (Austin, Texas, 8-14 January 2012). Vol. 44, 2 Edition, p. 21706. Washington DC: Bulletin of the AAS.

Schmidt, A. C., J. Singleton, H. Ardavan, and J. Middleditch. Fitting of Fermi LAT observations of gamma-ray emitting pulsars to the frequency spectrum of a faster-than-light source. 2011. In American Astronomical Society 218th Meeting. (Boston Massachusetts, 22-26 May 2011). Vol. 43, 4 Edition, p. 32002. Washington DC: Bulletin of the AAS.

Schmidt, A. C., J. Singleton, J. Middleditch, H. Ardavan, and A. Ardavan. On the anatmoy of a point charge in superluminal rotation and its relevance to pulsar radiation. 2013. In 222nd American Astronomical Society Meeting . (Indianapolis, 2-6 June 2013). Vol. 45(4), p. 20909. Washington DC: Bulletin of the American Astronomical Society.

Singleton, J., A. C. Schmidt, J. Middleditch, S. Redman, J. Wigger, A. Ardavan, and H. Ardavan. Pulsars in the Laboratory: Practical superluminal emitters mimic their Galactic cousins. 2013. In 222nd American Astronomical Society Meeting . (Indianapolis, 2-6 June 2013). Vol. 45(4), p. 20908. Washington DC: Bulletin of the American Astronomical Society,.

Singleton, J., A. C. Schmidt-Zweifel, and J. Wigger. Tests of the linear superluminal antenna. 2012. Internal report created for prioritization of (i) invention disclosures, (ii) patent issues and (iii) future publications in the scientific literature.

Singleton, J., A. Schmidt, H. Ardavan, and A. Ardavan. Quantitative and qualitative models in support of the Supraluminal model of pulsar emission. 2012. In American Astronomical Society 219th Meeting . (Austin, Texas, 8-14 January 2012). Vol. 44, 2 Edition, p. 21702. Washington DC: Bulletin of the AAS.

Singleton, J., A. Schmidt, Z. Wang, Q. Marksteiner, H. Ardavan, and J. Middleditch. Comparisons between Ground-based, Artificial Pulsars and Data from the Parkes Multibeam Survey. 2011. In AAS 217th Meeting, Seattle, Washington. (Seattle, Jan. 2011). Vol. 43, p. 2. Washington: Bulletin of the American Astronomical Society.

Singleton, J., J. Middleditch, A. Schmidt, P. Sengupta, and H. Ardavan. Violation of the inverse-square law deduced from a Maximum-Likelihood Analysis of observational data on fluxes and distances of radio pulsars. 2011. In American Astronomical Society 218th Meeting. (Boston Massachusetts, 21-26 May 2012). Vol. 43, 4 Edition, p. 32001. Washington DC: Bulletin of the AAS.

Pyroelectric Heat Engines: Highly Efficient, Environmentally Friendly Cooling

Markus P. Hehlen
20110425ER

Abstract

The goal of this study was to demonstrate a new type of refrigerator that can be fabricated in thin film form. The device consists of a layer of electrocaloric material sandwiched between two thin-film heat switches. We succeeded in demonstrating this novel device architecture for the first time and determined that it has the potential to provide refrigeration with an efficiency comparable to or even exceeding that of vapor compression devices. They key enabling element of the refrigerator is a novel liquid-based heat switch that can change its thermal conductivity by at least a factor of 55 by electrically controlling the convection of the fluid. Our device could be a disruptive technology with the potential to increase the efficiency of cooling while lowering the cost and removing hazardous chemicals. Follow-on studies will be aimed at quantitatively optimizing the heat-switch performance and incorporating the latest class of ferroelectric polymers as high-performance electrocaloric materials.

Background and Research Objectives

Cooling and thermal management are important for commercial and residential air conditioning, high-performance computing, and satellite performance. In the U.S. more than 90% of cooling is provided by systems based on vapor compression. Much of the electrical power used for refrigeration is derived from fossil fuels, and the efficiency of cooling technologies has therefore a direct impact on air pollution and global warming. Air conditioning and refrigeration account for more than 20% of the Nation's electrical power consumption [1]. Furthermore, the global warming potential of refrigerants used in these devices, such as hydrochloroflurocarbons (HCFC) and hydrofluorocarbons (HFC), is typically more than 1000 times that of CO2. Optimizing this mature refrigeration technology is not sufficient to address the current needs of these important applications. The goal of this project was to demonstrate a novel thin-film electrocaloric (EC) refrigerator. Our device could be a disruptive technology with the potential to increase the efficiency of cooling while lowering the cost and removing hazardous chemicals.

Refrigerators based on traditional bulk EC materials have been considered for some time. An EC material can change its temperature (ΔT) upon changing the electric field (ΔE) applied across it. This way it can act as the heat reservoir in a heat pump. In 2009, Epstein et al proposed a novel EC refrigerator concept that consists of a thin-film EC material placed between two thin-film heat switches (see Figure 1) [2]. The heat switches serve to block or allow the flow of heat into or out of the device, and the EC material between the heat switches is the heat reservoir. To use an analogy, the device works much like a lock gate that allows ships (heat) to be raised against gravity (thermal gradient). The transport of a packet of heat from the cold to the hot reservoir is then accomplished by a sequence of four steps (see Figure 1). The process begins with both heat switches in their open (thermally insulating) position and the EC material in the low temperature state. First, the cold-side heat switch is closed to allow heat to flow from the cold side into the EC material. Second, the cold-side heat switch is opened, and the temperature of the EC layer is raised by applying an electric field. Third, the hot-side heat switch is closed to allow heat to be expelled to the hot side of the system. Finally, the hot-side heat switch is opened, and the temperature of the EC layer is again lowered by removing the electric field. The cycle can then begin again. For this single-stage device, the maximum temperature difference that can be sustained between the hot and cold side is less than the temperature change produced by the electrocaloric effect (ΔT). Larger overall temperature differences can be achieved by stacking multiple EC refrigerator stages in which the cold side of one stage corresponds to the hot stage of the preceding stage.

The efficiency of such an electrocaloric refrigerator is fundamentally limited by thermodynamics (Carnot effi-

ciency). Epstein et al have shown that the device efficiency is determined by the heat-switch performance, specifically by the ratio of the heat switch thermal conductivity in the closed and open states [2]. Figure 2 shows the expected device efficiency as a function of this thermal conductivity contrast, K. Heat switches with K>10 would make thin-film EC refrigerators competitive with thermoelectric devices. EC refrigerators having heat switches with K>100 could displace conventional vapor-compression coolers and find novel applications that are enabled by their compactness and efficiency.

The magnitude of the EC effect depends on temperature. It is typically largest just above the temperature at which the material transitions from a polarization-ordered (ferroelectric) to a polarization-disordered (paraelectric) state [3, 4]. In the past 5 years, advances in thin-film ferroelectric polymers (such as poly(vinylidene fluoride-trifluoroethylene) [P(VDF-TrFE)] copolymer) have shown that sizeable EC effects at practical electric fields can be achieved near room temperature [3, 5, 6]. Given the existence of suited EC materials and rapid progress in this field it was decided to focus the project on developing the liquid-based thin-film heat switches, which had not been demonstrated before. The research objectives of the project were (1) to design, fabricate, and characterize a thin-film heat switch, and (2) to demonstrate a thin-film EC refrigerator using the novel heat switches. We successfully completed both research objectives as outlined below.

Scientific Approach and Accomplishments

In some fluids, motion can be induced in the liquid by the application of an electric field. This phenomenon is referred to as electrohyrodynamic (EHD) flow, and it is the result of the electric field acting on charges that are present within the fluid. EHD flows have been known since the early 20th century [7] and have been used to achieve fluid pumping, fluid mixing, and enhancement of heat transfer on the macroscopic scale [8-10]. In this work, we use EHD flows on the microscopic scale to create a thin-film heat switch for the first time. Our approach was to create a thin fluid layer (500 µm scale) between two electrodes and to initiate transverse fluid vortices by applying an electric field. Such a structure can then be switched between a thermally “closed” state (electric field applied) in which the fluid moves and heat is transported efficiently by convection, and a thermally “open” state (electric field removed) in which the fluid is largely at rest, and heat is transported inefficiently by conduction. Our hypothesis was that this device architecture would allow for sufficiently large thermal conductivity contrasts, K, to enable an efficient EC refrigerator (see Figure 2).

Our initial studies in project year 1 were based on earlier reports that EHD fluid motion is the result of charge injection from electrodes at very high electric fields (>100,000,000 Volts per meter) [7, 11-15]. In this regime, the electrode acts as a corona source that directly injects electrons into the fluid. Such high fields can be created at sharp objects, and our initial samples therefore explored a variety of microscopic tip arrays fabricated by lithographic techniques. In the course of extensive material and device characterization we observed that fluid motion was already present at much lower electric fields than previously reported. We discovered that fluid motion could be induced from planar rather than sharp electrodes at electric fields as low as ~10,000 Volts per meter. This was an important discovery because (1) planar electrodes can be fabricated very inexpensively on a variety of rigid and flexible substrates, (2) the electric fields of this magnitude are easily realized by applying a just few hundred Volts across a 500 µm thick fluid layer, and (3) low-field EHD flows may cause substantially less fluid degradation than was previously reported in the high-field regime of corona injection. For these reasons we focused our work on understanding and optimizing these microscopic EHD flows at low electric fields.

Figure 3a shows a schematic of the thin-film heat switch architecture developed in this study. The liquid was confined to a typically 500 µm thick layer extending over a lateral active area of 10 mm × 10 mm. One side of the fluid film was in contact with a patterned electrode and the other was in contact with a planar electrode. Applying an electric field to the electrodes induced fluid flow primarily in the transverse direction and thus enabled efficient heat transport from the hot to the cold side by fluid convection. The heat transport coefficient was much smaller in the absence of an electric field when the fluid was at rest (no convection) and heat was primarily transported by conduction.

A variety of dielectric fluids and electrode geometries were tested for their thermal conductivity contrast performance in the device shown in Figure 3a. EHD flows were readily achieved in the hydrofluoroethers HFE-7100, HFE-7300, and HFE-7500 (3M Company) at low fields. This is particularly advantageous since these dielectric fluids are commercially available in large quantities and have been shown to possess a low global warming potential [16]. The low electric fields used here (<1 MV/m) were well below the dielectric strength of these fluids (~10 MV/m [17]) and well below typical thresholds for corona injection, promising excellent long-term fluid stability. By far the greatest heat-switch efficacy was observed for an asymmetric electrode (G1 and G2 different; Figure 3b). A typical measure-

ment of heat switch performance is shown in Figure 4a. A heater was used to establish a thermal gradient across the fluid layer. Upon activating the electric field and corresponding EHD flow in the fluid, the thermal gradient across the fluid layer was essentially eliminated, indicating efficient convective heat transport across the device. These experiments yielded a thermal conductivity contrast, K, of at least 55. This represented the first ever demonstration of heat switching in liquid-based thin films. The thermal conductivity contrast of K>55 is shown by the red region in Figure 2, indicating that the present heat switches should enable EC refrigerators with efficiencies that rival or exceed those of vapor compression devices. This result represents the first major accomplishment of this study.

In addition to the thermal studies described above, we also performed extensive studies of the electrical performance of the heat switches. Measurements of currents as a function of time and electric field strength allowed us to formulate a model of the underlying mechanism of EHD flow at these low electric fields. In this model, fluid molecules pick up an electron at the surface of the cathode, and the resulting negatively charged fluid molecules are then accelerated towards the anode thereby dragging the bulk fluid along and inducing bulk fluid motion. The charge is then transferred to the anode, closing the electric circuit, and the neutral fluid molecules flow back to the cathode. This model also explains the importance of an asymmetric electrode geometry, because the strip pattern allows for areas of fluid back flow and thus the formation of ordered transverse vortices in the liquid layer. The model was further substantiated by density functional theory (DFT) calculations of the HFE fluid molecules. These calculations showed that transfer of an electron from the cathode to a neutral fluid molecule to produce an anion is possible at low electric fields, while removal of an electron from a neutral fluid molecule to produce a cation is much less likely. The predicted corresponding current flow from the cathode to the anode was confirmed by the experiments. These experimental and computational studies allowed us to establish a first version of a quantitative model of the heat switch using the COMSOL Multi-Physics software package. Figure 4b shows a representative calculation of transverse fluid vortices that form upon applying an electric field across the fluid layer. The calculated fluid velocities of ~5 mm/s were in agreement with the time-resolved thermal measurements.

In a final step, the heat switches described above were used to construct an electrocaloric refrigerator. We did not attempt to fabricate multi-layer ferroelectric polymers but instead used readily-available commercial ceramic chip capacitors as an alternative EC material for these first studies. Mathur, Israel, and Kar-Narayan et al have shown that commercial multilayer capacitors based on piezoelectric BaTiO3 inadvertently exhibit magnetoelectric [18-20] and electrocaloric [21] effects. These capacitors consist of a multilayer electrode built up from alternating nickel-based electrode layers (typically 2.0 μm thick) and BaTiO3 dielectric layers (typically 6.5 μm thick). Commercially available capacitors with dimensions of 4.50 mm × 3.20 mm × 2.80 mm (“1812” package) were used in the present study. They can contain up to 200 dielectric layers and thus offer a sizeable amount of thin-film EC material in a small volume, resulting in an electric field-induced ΔT of ~0.5 K and a useful heat change. The prototype EC refrigerator was formed by constructing an array of 3 × 5 densely packed 100 μF ceramic chip capacitors (TDK Corporation, C4532Y5V1A107Z) arranged between two 500 μm thick copper plates. This structure was then sandwiched between two liquid-based heat switches, and the device was then processed through the cooling cycle (see Figure 1). Figure 5 shows the resulting temperature difference between the cold and hot side of the device as a function of time. A temperature drop of 0.1 K was observed upon activating the heat switches, demonstrating for the first time operation of the EC refrigerator. This temperature drop is small on an absolute scale but rather sizeable compared to the maximum ΔT of ~0.5 K that was theoretically possible with the EC layer built from the commercial capacitors. This result is the second major accomplishment.

Follow on studies will be aimed at using much higher performing ferroelectric polymers as electrocaloric materials as well as quantitatively optimizing the geometry of the heat switches using the developed COMSOL model. Based on the accomplishments of the present study we expect that it will be possible to construct an EC refrigerator capable of cooling by up to 20 K near room temperature with useful heat lift.

Impact on National Missions

Heat engines are important to numerous National Missions including energy security, global climate improvement, cooling of electronics, computers and machinery, and air-conditioning for residences, businesses and military personnel. Currently, most cooling devices largely rely on vapor-compression technology, which has not significantly changed in decades. Some small-scale cooling utilizes the less efficient, but more compact Peltier or thermoelectric technology. These two technologies are also the dominant players in the conversion of waste heat to electrical power. The electrocaloric heat engine approach that we are developing has the potential to be more efficient and less costly than either vapor compression or thermoelectric devices. Additionally, the thin-film format of these devices allows

low-cost manufacturing and engenders countless new applications that would be impossible with conventional devices. For example, one use for these our electrocaloric heat engines could be harvesting electrical power from low-grade waste heat (i.e. hot water) from power plants. While, conventional technologies cannot effectively work in this area, thin-film electrocaloric heat engine could fill this niche. We estimate that thin-film energy scavenging in U.S. power plants could produce 0.24 quads of electricity and reduce carbon emissions by 800 million tons annually.

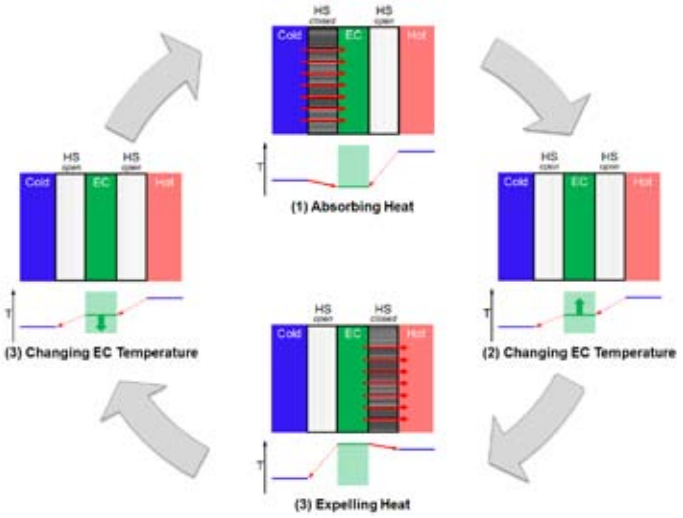

Figure 1. Conceptual operation of a single-stage cooler based on the electrocaloric (EC) effect. Each panel shows a heat pump, consisting of an electrocaloric layer (EC) sandwiched between two heat switches (HS), in contact with the cold side (left) and the hot side (right). The HS can be switched between an open (thermally isolating) or closed (thermally conducting) state. Heat is being transferred from the cold to the hot side by (1) the electrocaloric layer absorbing heat from the cold side, (2) increasing the EC temperature by application of an electric field, (3) expelling heat to the hot side, and (4) decreasing the EC temperature by removal of the electric field [2]. The lower half of each panel shows the temperature distribution across the device as well as the desired heat flows (solid arrows) and unwanted leakages (dashed arrows) (adapted from [2]).

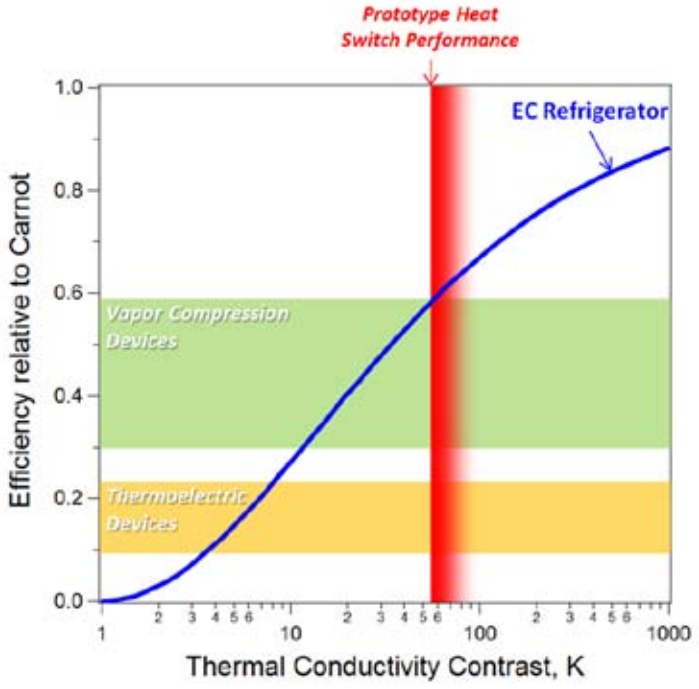

Figure 2. Theoretical efficiency of the electrocaloric (EC) refrigerator versus the thermal conductivity contrast of the heat switch in the closed and open state, K (blue curve). Ranges of efficiencies for thermoelectric (yellow) and vapor compression (green) refrigerators are shown for reference [2]. The prototype heat switches developed in this project achieved K>55 (as indicated by red range).

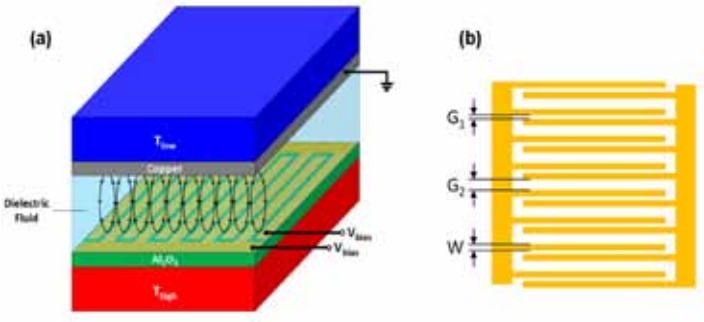

Figure 3. (a) Schematic illustration of the heat switch based on EHD flow in a thin layer of dielectric fluid. The fluid is contained between a gold-patterned Al2O3 electrode and a planar copper electrode. Each electrode is in thermal contact with its respective heat reservoir. Applying an electric field between the two electrodes induces transverse fluid flows (indicated by streamlines) that convectively transport heat from the hot side (Thigh) to the cold side (Tlow). The heat transport is reduced in the absence of the electric-field induced convection. (b) Layout of the interdigitated patterned electrode. The dimensions of the two gaps G1 and G2 and the trace width W are indicated.

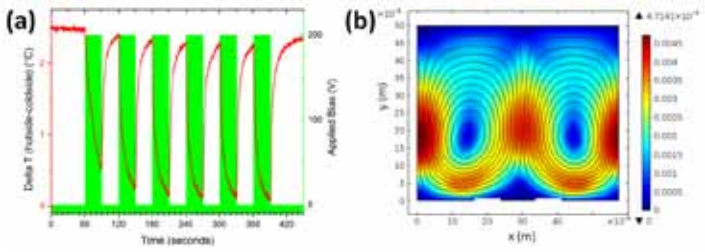

Figure 4. (a) Experimental demonstration of high-contrast thermal switching in a liquid-based heat switch. The red trace is the temperature difference between the hot and cold side of the thermal switch, and the green bars indicate when the electrical field (200 Volts across 500 um fluid layer) was switched on/off. (b) COMSOL model simulation of the fluid flow in the liquid-based heat switch. This is a cross-sectional view across the fluid layer, the colors indicate fluid velocity, and the black lines are the flow streamlines. The two electrodes at the bottom (shown as white rectangles) induce transversal vortices that enable efficient convective heat transport.

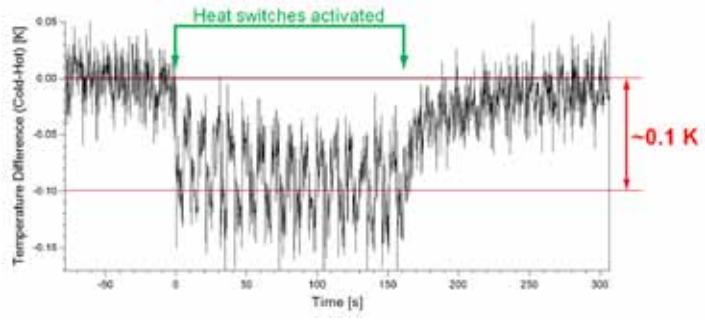

Figure 5. First demonstration of cooling in a thin-film electrocaloric refrigerator using liquid-based heat switches. This first prototype used multi-layer ceramic capacitors as electrocaloric material, offering a theoretical maximum temperature difference of ~0.5 K. The device was processed through the cooling cycle shown in Figure 1 at a rate of 0.1 Hz. The temperature drop of 0.1 K observed upon activating the heat switches indicates that heat was transported against the thermal gradient, successfully demonstrating our novel refrigerator concept.

References

1. Energy Information Administration / Annual Energy Outlook . 2008. Department of Energy.

2. Epstein, R. I., and K. J. Malloy. Electrocaloric devices based on thin-film heat switches. 2009. Journal of Applied Physics . 106: 064509.

3. Neese, B., B. Chu, S. G. Lu, Y. Wang, E. Furman, and Q. M. Zhang. Large electrocaloric effect in ferroelectric polymers near room temperature. 2008. Science. 321: 821.

4. Rose, M. C., and R. E. Cohen. Giant electrocaloric effect around Tc. 2012. Physical Review Letters. 109: 187604 .

5. Lu, S. G., and Q. Zhang. Electrocaloric materials for solid-state refrigeration. 2009. Advanced Materials. 21: 1983.

6. Liu, P. F., J. L. Wang, X. J. Meng, J. Yang, B. Dkhil, and J. H. Chu. Huge electrocaloric effect in Langmuir–Blodgett ferroelectric polymer thin films. 2010. New Journal of Physics. 12: 023035 .

7. Chattock, A. P., W. E. Walker, and E. H. Dixon. On the specific velocities of ions in the discharge from points. 1901. Philosophical Magazine. 1: 79.

8. Seyed-Yagoobi, J.. Electrohydrodynamic pumping of dielectric liquids. 2005. Journal of Electrostatics . 63: 861.

9. Grassi, W., D. Testi, D. Della Vista, and G. Torelli. Augmentation of heat transfer on the downward surface of a heated plate by ion injection. 2006. Annals of the New York Academy of Sciences. 1077: 602.

10. Grassi, W., and D. Testi. Electrohydrodynamic convective heat transfer in a square duct. 2009. Annals of the New York Academy of Sciences. 1161: 452.

11. Stuetzer, O. M.. Ion-drag pressure generation. 1959. Journal of Applied Physics. 30: 984.

12. Pickard, W. F.. Ion-drag pumping I – theory. 1963. Journal of Applied Physics. 34: 246.

13. Pickard, W. F.. Ion-drag pumping II – experiments. 1963. Journal of Applied Physics. 34: 251.

14. Krawinkel, G. H.. Zum Wirkungsgrad einer elektrostatischen Pumpe. 1968. Zeitschrift fur Angewandte Physik. 25: 302.

15. Sharbaugh, A. H., and G. W. Walker. The design and evaluation of an ion-drag dielectric pump to enhance cooling in a small oil-filled transformer. 1992. IEEE Transactions on Industrial Applications. 28: 310.

16. Owens, J. G.. Low GWP alternatives to HFCs and PFCs. 2000. 3M Specialty Materials, St. Paul, MN.

17. Novec(TM) Engineered Fluid HFE-7100 for Heat Transfer. 2013. 3M Specialty Materials.

18. Israel, C., N. D. Mathur, and J. F. Scott. A one-cent room-temperature magnetoelectric sensor. 2008. Nature Materials. 7: 93.

19. Israel, C., S. Kar-Narayan, and N. D. Mathur. Converse magnetoelectric coupling in multilayer capacitors.

2008. Applied Physics Letters. 93: 173501 .

20. Israel, C., V. M. Petrov, G. Srinivasan, and N. D. Mathur. Magnetically tuned mechanical resonances in magnetoelectric multilayer capacitors. 2009. Applied Physics Letters. 95: 072505 .

21. Kar-Narayan, S., and N. D. Mathur. Direct and indirect electrocaloric measurements using multilayer capacitors. 2010. Journal of Phyics D: Applied Physics. 43: 032002 .

Publications

Hehlen, M. P., A. H. Mueller, N. R. Weisse-Bernstein, and R. I. Epstein. Electrocaloric refrigerator using electrohydrodynamic flows in dielectric fluids . 2013. In Photonics West. (San Francisco, 4-7 Feb 2013). Vol. 8638, p. 86380D. Bellingham, WA: SPIE.

Spatial and Wavelength-diversity Lasercomm System

Anatoly V. Efimov
20120460ER

Abstract

Nearly all modern high-speed communication systems are optical due to the immense bandwidth allowed by the optical carrier frequencies. Optical data streams are typically transmitted through stationary preinstalled optical fibers. In contrast, wireless communication is more often facilitated by much lower-frequency radio waves, which are limited in bandwidth, heavily licensed and are susceptible to jamming and intercept. Optical frequencies can also be used for point-to-point wireless communication and a number of commercial lasercomm products exist. However, all existing systems suffer from signal degradation caused by atmospheric turbulence. In particular, the received signal shows strong fluctuations in amplitude, called scintillations, which increase with propagation distance. This issue restricts the typical range of commercial lasercomm systems to a couple of kilometers.

One solution to the turbulence problem on which most of the existing products are based is the use of multiple transmitters, which is called the spatial diversity approach. This technology was developed by AstroTerra and was sold to MRV for $100M in the early 2000s. The disadvantages of this approach include high cost, complexity and reliability issues.

We have developed and tested an alternative approach to mitigate atmospheric turbulence through the use of a single, spatially partially coherent beam (PCB) to transmit data. The use of PCBs for free-space optical communication was theoretically developed decades ago, but has not been demonstrated experimentally because there has been no practical way to generate proper PCBs, until now. We recently solved this problem and have demonstrated the PCB concept in a series of in-lab and open-air experiments. Using our PCB system we observed an up to an order of magnitude reduction in the scintillation index compared to a standard coherent beam, which translates into a factor of 10,000 reduction in the bit error rate for an actual lasercom system. Ranges of up to 6.5 kilometers were tested. Our solution allows for a much simpler implementation in hardware compared to the current multiple-transmitter systems, e.g. the optical head can be designed to be remotely fiber-coupled with no electronic components inside making the system immune to electromagnetic pulses and lightning damage.

Background and Research Objectives

Free-space communication at optical carrier frequencies (~100 THz) is a great alternative to RF communication in high-speed and secure links. Large application niches exist in both military and civil areas. US Navy and Air Force are looking for jamming-resistant communication modes and so far optics is the only alternative to RF. Remote access and rapid emergency response are examples of the civil markets for the lasercomm technology. A number of commercial companies currently supply lasercomm systems (e.g. LightPointe, fSona, SkyFiber and others). These systems, however, are limited to about 2 kilometer range at gigabit per second data rates. The limitation comes from the deleterious effect of atmosphere, which is always turbulent to a certain degree. Atmospheric turbulence results in strong signal fluctuations (scintillations), caused by beam fragmentation, wandering and self-interference on the detector. Error correction algorithms are capable to mitigate these scintillations only to a certain degree.

The turbulent eddies present in the atmosphere ever so slightly refract and bend portions of the laser beam. This refraction is the result of slight refractive index variations across the laser beam, which is a function of air temperature, pressure and water content. The spatial scale of atmospheric turbulence eddies comprise a wide spectrum (Kolmogorov spectrum) ranging from a few millimeters to meters. Small-scale eddies distort the phase front of the beam and lead to its break up and fragmentation; whereas large-scale eddies tend to refract the

laser beam as a whole, causing beam wandering.

The temporal scale of signal scintillations corresponds to the motion speed of the eddies, and is typically related to the wind across the beam (or the speed of the aircraft in the case when one lasercomm node is airborne). For the stationary system the characteristic time scale turns out to be a millisecond or slower. This observation precludes the use of direct averaging over signal fluctuations: it's just too slow.

A clever solution to signal scintillations mitigation was offered in [1] in which rudimentary spatial diversity was introduced. In this approach several mutually incoherent lasers are used to simultaneously transmit the same data stream in the direction of the receiver. The lateral spacing between the transmitters must be larger than the characteristic scale of the turbulence eddy and is typically a few inches in commercial systems. The premise here is that if one beam happens to result in a null on the detector, the others will likely result in a non-zero signal. Because the beams are mutually incoherent their overlapping will not result in destructive interference. Of course, the advantages of such spatial averaging diminish with increasing the propagation distance because closer to the receiver all the beams effectively propagate through the same turbulent eddies. The small company Astro-Terra that held the patent [1] was sold to MRV Communications for $100M in stock. With the technology developed by LANL we aim to achieve a similar feat simultaneously offering a simpler technology with a better performance.

The current approach to spatial diversity, as originally disclosed in the IDEA #11-51, is based on employing a spatio-temporal partially coherent beam (PCB) which does not require multiple independent lasers coupled to multiple apertures as in [1]. PCBs have been considered in theoretical literature more than 30 years ago as a way to reduce scintillations [2], however, no practical method for their generation was offered. For it to be useful in Gbps data rate lasercomm systems the PCB update rate must be at least an order of magnitude faster than the data rate. Currently described PCB generation methods (diffusers, spatial light modulators) are not capable of PCB rates of more than a few megahertz. In this project we designed and tested the first practical but simple PCB method capable to finally break the 2-km link range that was plaguing the industry up to now. To the best of our knowledge no similar work is being performed elsewhere.

Scientific Approach and Accomplishments

In the center of our PCB approach is a simple method to convert the spatially coherent light from a broadband optical source, such as a superluminescent laser diode (SLD) to a PCB using a suitable length of a multimode fiber (MMF) [3,4]. The multiple transverse modes excited in the MMF propagate at different speeds leading to an interference pattern at the output. Due to the short coherence time of the SLD this interference pattern is fluctuating on the time scale of the SLD coherence time, which is typically in the range of femtoseconds. In comparison, the duration of one data bit in a Gbps data stream is on the order of a 100 picoseconds. Therefore the detector will see and average many thousands of the interference patterns transmitted.

Only a few meters of MMF are required to scramble the modes well. The modal dispersion of the MMF will not be able to stretch the data pulse considerably. This is because efficient mode scrambling requires only a small phase difference to accumulate between the modes, while the modal dispersion needs intermodal time delays on the order of the data pulse duration to cause interpulse overlap.

This concept, in fact, was tested initially in our preliminary in-lab experiments, funded by the Office of Naval Research, using an artificial turbulence chamber built specifically for this purpose [5]. The results obtained during that phase of the experiment encouraged us to perform a series of open-air atmospheric experiments - the subject of this project.

A testbed consisting of mobile transmitter and receiver nodes was built, Figure 1. Both nodes were positioned on two-axis gimbal mounts to facilitate their alignment in the field. The transmitter featured five co-propagating lasers: three coherent units at 635, 980 and 1435nm and two PCB systems at 1550nm. The receiver was a single-element photodetector. Both units operated at about 10 centimeter beam aperture. In order to separate the signals from each individual lasers they were individually modulated at different frequencies and the specially written software on the receiving node performed real-time data acquisition and spectral decomposition at 2000 times per second. This approach allowed us to directly compare the performance of the five lasers, covering the turbulence frequencies of up to 1000 Hertz, which is more than enough bandwidth for stationary atmospheric experiments.

A series of open-atmosphere experiments was performed in October of 2012 in the mountains near Los Alamos, New Mexico, during various atmospheric conditions [6]. The measurement results for the scintillation index (SI) - normalized variation in received signal power - are summarized in Figure 2. The Figure shows the ratio of the SI obtained with a PCB to that obtained with a coherent beam as a function of the propagation range. The SI depends substantially on the transmitter and receiver apertures. The three theoretical lines (green, red, and

blue) correspond to the same receiver aperture radius of 5 centimeters and transmitter apertures of 8, 4, and 2 cm respectively. Each data point (circles) corresponds to an individual experiment and is computed from the SI data for the PCB at 1550nm and a coherent beam at 1435nm. In the experiments the transmitted aperture diameter was kept at 4 cm and we observe that the data points agree reasonably well with the red curve. Interestingly, the long-range data at 6.5 km shows better performance of the PCB than expected theoretically. This may be related to the limitations of the theory in this case, which is applicable to the low-turbulence regime. The data points represented by the crosses correspond to a separate set of experiments carried out with a smaller receiver aperture and supplement the main data in the Figure 2.

The main result of this work is that the performance advantage of our PCB approach is demonstrated clearly for the first time, suggesting that further advancements in free-space lasercomm technology are within reach. Open-air experiments at realistic gigabit per second data rates are required to finalize this stage of work and transition to a more advanced stage of technology readiness. At the same time, our experiments have proven that the wavelength diversity is not effective in mitigating the effects of the turbulence at the link ranges of up to 6.5 km.

Impact on National Missions

Atmospheric propagation and the goal of scintillation reduction is intimately related not only to optical communication, but also to such important areas as remote sensing, optical atmosphere monitoring and laser weapons. The effect of atmospheric turbulence is unavoidable in all these areas and our approach is now proven to be capable in mitigating the effects of turbulence. We developed a new capability previously unrealized at LANL allowing for a wider body of R&D to be performed. We applied due effort to extend and expand on the results obtained by contacting certain program managers, seek additional funding and press for IP protection with varying success.

Figure 1. Transmitter (top left and right) and receiver (bottom left) nodes near the completion of the development stage (left) and in the field (right).

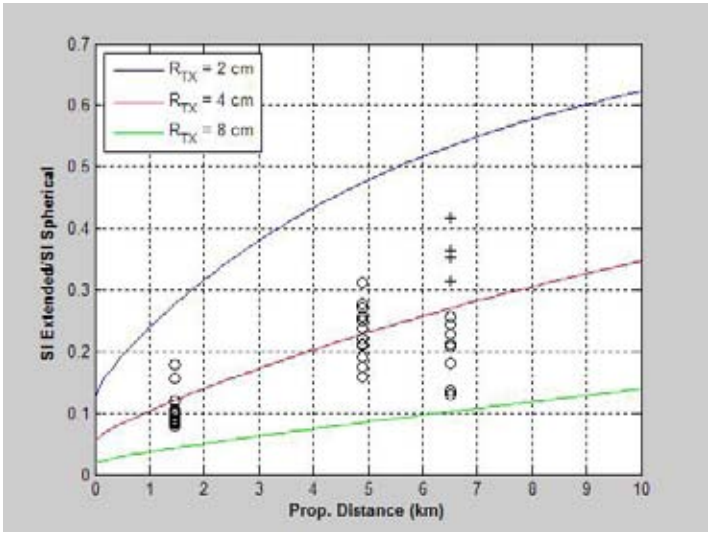

Figure 2. Scintillation index ratio of the PCB to the coherent beam of the same transmitter aperture diameter of 8cm as a function of the propagation distance. Solid lines - weak turbulence theory, circles - experimental data, crosses - experimental results for a reduced receiver aperture.

References

1. Korevaar, E.. Multiple transmitter laser link. 1998. US Patent 5,777,768 .

2. Leader, J. C.. Intensity fluctiations resulting from partially coherent lightpropagating through atmospheric turbulence. 1979. Journal of the Optical Society of America. 69: 73.

3. Efimov, A.. Lateral-sheering, delay-dithering Mach-Zehnder interferometer for spatial coherence measurement . To appear in Optics Letters.

4. Efimov, A.. Spatial coherence at the output of multimode optical fibers. Optics Express.

5. Efimov, A.. Scintillatioin of coherent and partially coherent beams in a laboratory turbulence. Optics Express.

6. Efimov, A., K. Velizhanin, and G. Gelikonov. Direct comparison of coherent and partially coherent beam propagation in an open atmosphere experiment. Optics Express.

Publications

Efimov, A.. Lateral-sheering, delay-dithering Mach-Zehnder interferometer for spatial coherence measurement. To appear in Optics Letters.

Efimov, A.. Spatial coherence at the output of multimode optical fibers. Optics Express.

Efimov, A.. Scintillatioin of coherent and partially coherent beams in a laboratory turbulence. Optics Express.

Efimov, A., K. Velizhanin, and G. Gelikonov. Direct comparison of coherent and partially coherent beam propagation in an open atmosphere experiment. Optics Express

Hyperspectral Intensity Correlation Interferometry

David C. Thompson
20120748ER

Abstract

Hyperspectral Intensity Correlation Interferometry (HICI) holds significant promise for overcoming low signal-to-noise ratio (SNR) that has hampered the practical application of standard Intensity Correlation Interferometry (ICI). Building on a previous LANL LDRD Science of Signatures (SoS) project that developed an HICI system concept, we have built an improved experimental arrangement that both has higher throughput for improved signal-to-noise ratio and much improved ease of alignment. It also features spectral and temporal fiducials and calibrations that are essential to performing the photon data correlations that are at the heart of the technique. A considerable quantity of data was taken prior to the end of the project, and most of the needed calibrations were performed. However the temporal fiducial signal was not strong enough to extract and therefore additional data collection with a stronger temporal fiducial will be needed before correlations can be performed and HICI demonstrated.

Background and Research Objectives

Interferometry has long been used to improve resolution beyond what is possible with conventional single-aperture imaging. However standard Amplitude Interferometry (AI) places high demands on the quality, stability and equality of length of the multiple optical paths used. Moreover it is significantly limited by atmospheric turbulence. Intensity Correlation Interferometry (ICI) has been an alternative technique since the 1950's, with many attractive features including much-reduced requirements on optics, only data rather than light being combined, and insensitivity to turbulence. But it has generally suffered from poor signal to noise ratio (SNR) performance in comparison to AI. Hyperspectral ICI (HICI) promises to overcome the SNR issue, increasing the SNR by dividing the light into many spectral channels, but it has never been experimentally demonstrated. The key to enabling this technique is the use of ps time resolution photon counting imagers developed at LANL. Experimental verification in this proposed work would make the technique practical for many imaging applications.

The task list for the project (as amended for the FY12 effort) was as follows:

Task 1: Theory, simulations and algorithms

Subtask 1a: Develop a model that simulates the system SNR for a variety of system configurations.

Subtask 1b: Write software for data acquisition and cross correlation.

Task 2: Laboratory system test with coherent and incoherent targets and two NCam detectors

Set up 2 NCam detectors with optics suitable for HICI; perform timing calibration and sensor time resolution characterization; perform a laboratory test of HICI using a small incoherently illuminated target.

An initial LDRD reserve effort in FY10 began this experimental verification, but the experimental apparatus was fairly elaborate and proved be somewhat difficult to align and to have some throughput limitations that would significantly reduce SNR. In FY11 we rearranged the experimental arrangement and successfully addressed these problems. Initial data was taken, and spectral and spatial calibration carried out, but difficulties were encountered in extracting the timing calibration signal from the data. Some of this analysis extended into FY12 with a small extension of funding.

We also made further progress with the numerical simulation, and it should be possible to compare future experimental data with this code, benchmarking the code with the experiment and providing a means to extrapolate performance for possible further experimental efforts.

Scientific Approach and Accomplishments

Figure 1 shows the basic concept of the experimental arrangement. Light from the target is collimated and analyzed by a pair of spectrometers with high-time-resolution photon-counting sensors (NCam's) at the focal planes. The two spectrometers sample different parts of the pupil plane and the data from the two sensors is correlated wavelength by wavelength. The variation in the correlation as a function of the relative position of the spectrometers in the pupil plane allows the geometry of the target to be determined.

To address the issues related to the HICI experimental optics, our first step was to eliminate the dual rectangular pinhole arrangement and replace it with two separate fiber coupled LED sources with the pair of fiber ends (200 μm diameter) closely-spaced (250 μm separation of centers). The LED's have a center wavelength of ~520nm and a FWHM of ~30nm. By using the fiber ends directly, we achieved a large improvement in the overall incoherent light source radiance, which is directly related to eventual HICI SNR. Also, by using two independent incoherent light sources, we more closely matched the usual conditions for HICI, with two completely independent light sources and with less reliance on arguments about independent speckle in multimode optical fibers. This change also required a small modification to the SNR simulation since the fiber ends are round and not rectangular.

Given the 15m collimator effective focal length (~1.5m OAP focal length combined with a 10X demagnification of the target) the speckle size in the pupil plane can be calculated at the 532 nm center wavelength. In Figure 2 we see that in the x direction the first zero is at 49 mm separation, while in y the separation of the two fiber ends gives an additional 18mm modulation period. The plotted functions do not include the smearing effects of the finite (36mm in x and 20mm in y) spectrometer entrance pupil, which must be convolved with the functions shown.

With respect to simplifying HICI optical alignment, we made changes to the opto-mechanical arrangement to improve stability and will develop improved optical alignment procedures to periodically test and realign the system. In particular we used the combination of a large off-axis parabola (60-inch focal length and 12 inch aperture) and a large reference flat (acquired from another program) that facilitated collimation of the source and boresighting of alignment lasers. We also redesigned the spectrometers, using an intermediate focal plane and a wide-field 10X microscope objective to reimage that plane to the sensor.

For alignment through the spectrometers we acquired a full format DSLR camera with video capability as a surrogate detector before adding NCams into the spectrometers. This facilitated alignment by not needing complete darkness, and also protected the much more valuable NCam sensors from possible exposure to excessive laser light.

The system includes spectral and temporal fiducials, and means for calibrating out any spatial nonuniformities using an etalon. A schematic of the experimental layout is shown in Figure 3.

The spectrometers can be moved so that their entrance pupils sample different parts of the overall pupil area in the collimated space formed by collimation of the target light by the off-axis parabola. Each spectrometer uses a high efficiency 1800 lines/mm Volume Phase Holographic Grating (VPHG) with center wavelength of 532 nm. The spectrometers have no slit - the target acts as the slit. The grating dispersion and the overall effective focal length of 7.5m result in an overall spectrometer band of approximately 1.3 nm or 1380 GHz across the 25mm diameter of the NCam sensor focal plane. For a spectral resolution of 11 GHz, this gives 120 effective spectral channels across each sensor. A cylindrical lens spreads the light vertically so that in the vertical direction the spectrometer entrance pupil is imaged onto the sensor. This allows higher pupil resolution in the vertical direction (where the fiber end separation gives higher spatial frequency structure).

The fiducial laser outputs are diverged to fill the aperture of the collimating mirror and match the geometry of the beam from the target. The temporal fiducial consists of a fiber laser system (Calmar Laser) generating a 50 kHz train of ~10ps pulses. The laser output was quite broad, much broader than the ~1.3nm band of the spectrometers.

The spectral fiducial consists of a Nanolase Q-switched microchip laser, which generates pulses of several ns width at a repetition rate of about 15 kHz. Figure 4 shows the extraction of this fiducial signal from the data.

In order to be able to correctly perform wavelength-by-wavelength correlation of the data, which is they key to the SNR enhancement expected for HICI, we must calibrate the spectral plate scale for both spectrometers and ensure that spatial distortions in the optical system and detector are properly accounted for. To accomplish this calibration, an etalon with 2 cm-1 (60 GHz) free spectral range and a measured finesse of 5.8 was placed in the optical path, in the collimated beam prior to the beamsplitter that sends light to the two spectrometers. This results in wavelength-dependent transmission of the light from the target and fringes in the two spectrometer image planes. Since the wavelengths of these fringes are in common, both spec-

tral calibration of the two sensors and cross calibration between them can be performed. In Figure 5, we see data from one of the sensors with the etalon in place.

Small-scale distortions in the optical system and sensors were corrected for by taking a number of images as the etalon was tilted to shift the fringe pattern. A total of 8 etalon tilts were used, spanning just over one fringe period. Figure 5 also shows the resulting measurement of distortion in the x (frequency) for one of the sensors. The corrections are small compared to the sensor resolution of ~80 µm, but not negligible. These measurements can then be used to correct photon positions to remove these effects and ensure that the frequency positions on the detectors correspond.

Following alignment of the system and prior to the end of the project, we collected a large initial dataset, with sufficient photon events so that correlations should be evident. However we were unable to extract the temporal fiducial from the data, despite trying a number of analysis techniques and therefore it is not possible to correlate the photon times to sufficient accuracy. It appears that the signal was not strong enough and more data collection will be required with an increase in the Calmar laser power.

Impact on National Missions

The Grand Challenge for Sensing and Measurement Science for Global Security explicitly calls out sensing and measurement science in support of national security in areas such as support for the warfighter, areas that HICI could significantly enhance. This work leverages previous LANL–developed technology and begins to develop a novel imaging capability with multiple applications in areas of growing national security interest and significant potential for the development of major programs. A successful demonstration of HICI would help to grow the remote sensing and single photon imaging portfolios at LANL.

For terrestrial imaging, success here would be an important first step towards single pupil HICI, with many potential applications for imaging through turbulence both in the laboratory and for long range tactical imaging. It is likely that we would then be looking for further funding to pursue an experimental demonstration of this application.

Other applications in the field of quantum imaging such as time coincidence (or shadow) imaging could benefit from a successful demonstration since coincidence imaging experiments have been limited to relatively slow frame rate time resolution or high speed single-element detectors. It has also been suggested that ICI techniques may be used for detection of exo-planets, by detecting small periodic variations in the relative position of a star relative to nearby stars in the sky. There are a number of other astronomical applications: since only the photon timing data is combined, extremely long baselines are possible – even between satellites; it may be possible to measure the size and oblateness of much smaller stars or to resolve spectroscopic binaries. Spectral information from HICI may also provide important information about limb darkening.

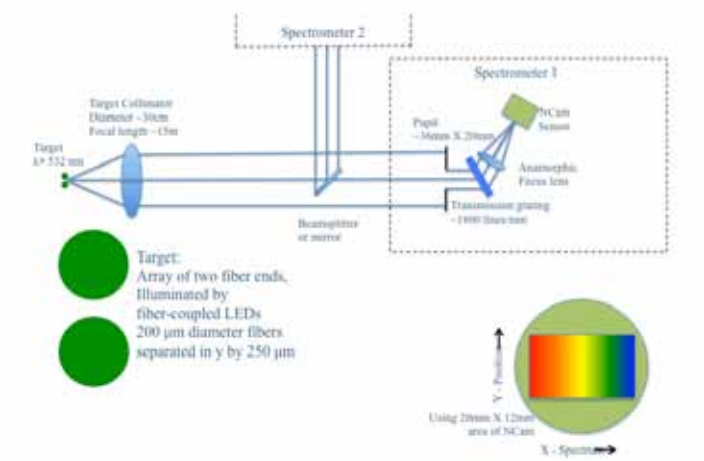

Figure 1. Conceptual arrangement of HICI experiment. A target (lower left) consists of a pair of LED-illuminated fiber ends. Light from the target is collimated and a pair of spectrometers sample light from different parts of the pupil area. The spectrometer's focusing optics is anamorphic so that the detector x coordinate corresponds to optical wavelength or frequency, and y corresponds to position in the spectrometers entrance pupil.

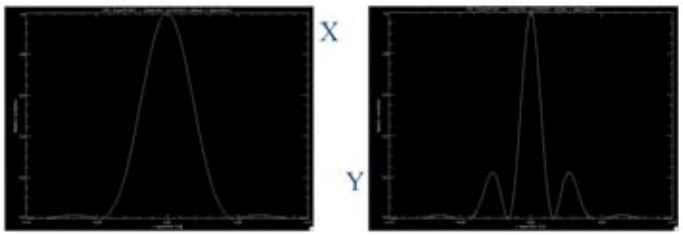

Figure 2. Theoretical correlation functions in x (left) and y (right).

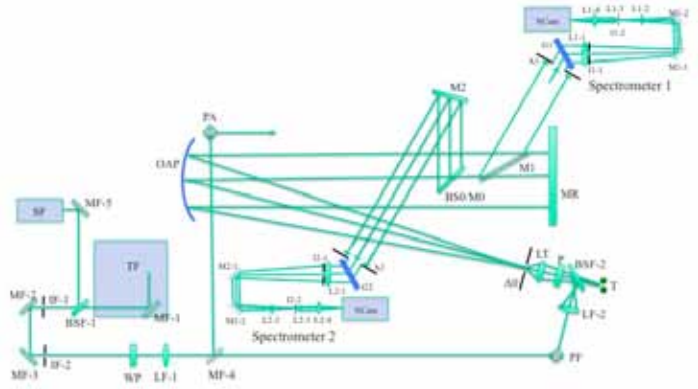

Figure 3. Schematic of the ICI experimental arrangement. Target T is imaged by a 10X microscope objective onto aperture A0 that marks the focus of off-axis parabolic mirror OAP. A polarizer P

selects a single polarization. Light from the target expands to fill OAP and is collimated by OAP. A large flat mirror MR can be used to check collimation and that the light is parallel to the OAP axis. Depending on the parts of the pupil to be sampled by the Spectrometers 1 and 2, either a beamsplitter BS0 or a mirror M0 directs light to Spectrometer 2, while mirror M1 directs light to Spectrometer 1. Each spectrometer has an entrance aperture A1/A2 that defines its 36mm wide by 20mm high entrance pupil; light is dispersed by a volume holographic grating G1/G2 and then focused by achromatic doublet lens L1-1/L2-1 to an intermediate focal plane defined by iris I1-2/I2-2. Mirrors M1-1/M2-1 and M1-2/M2-2 fold the spectrometer optical path and cylindrical lens L1-2/L2-2 images the spectrometer entrance pupil to the intermediate focal plane in the vertical direction only. Finally the intermediate focal plane is reimaged onto the sensor focal plane by a 10X microscope consisting of a wide-field objective L1-3/L2-3 and tube lens L1-4/L2-4. Laser fiducial beams from spectral fiducial SF and timing fiducial TF are combined with beamsplitter BSF-1 and co-aligned with mirrors MF-5, MF-2 and MF-3 and irises IF-1 and IF-2, and collimated with lens LF-1. A wave-plate WP aligns the polarizations of the two fiducials. The fiducial beam is brought to the target area using periscope PF, focused with microscope objective LF-2 and co-aligned with the light from the target with beamsplitter BSF-2. Mirror MF-4 can be inserted into the fiducial beam and periscope PA can direct the resulting alignment beam parallel to the axis of the OAP for alignment of the spectrometers.

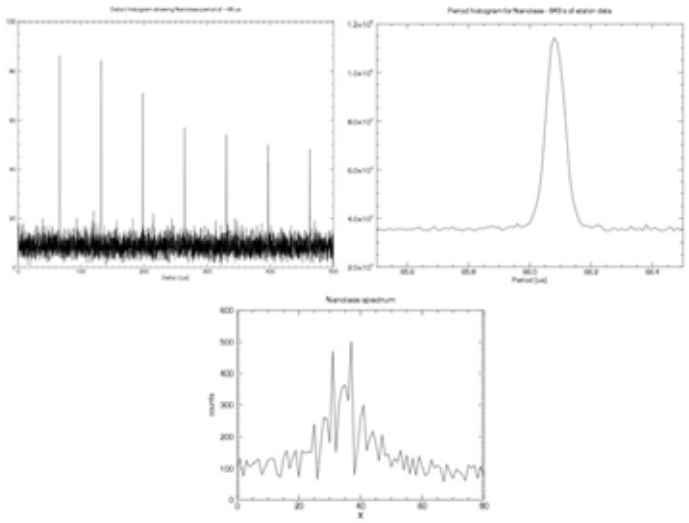

Figure 4. Data for the spectral fiducial laser extracted from the photon data. (Top left) periodogram showing the periodic laser pulses; (top right) histogram of laser period; and (bottom) spectrum of laser.

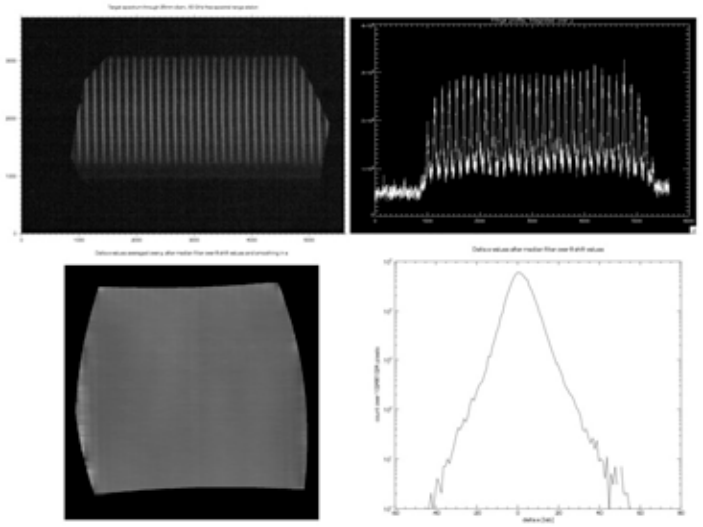

Figure 5. (Top left) image from one spectrometer with the calibration etalon in place; (Top right) an image cross section showing the horizontal profile of the fringe pattern; (Bottom left) plot of x corrections for one of the sensors; (Bottom right) histogram of x corrections. X units are NCam lsb's (least significant bits) where one lsb is about 2.1 µm.

Microfluidic Uranium Enrichment through Electrochemically Driven Solvent Extraction

Kirk R. Weisbrod
20130335ER

Abstract

Based upon examples provided in a 1968 Japanese patent, the potential for selective transport of uranium ions through ion exchange membranes is explored. The process may have applicability as an alternative method of uranium enrichment. After characterizing mass transfer in an electrodialysis stack, a feedstock containing a known ratio of uranyl sulfate to uranous sulfate was electrochemically prepared. Uranium transport rates were measured to determine membrane transference numbers and the relative ratio of valence transport rates. To date, the measurements indicate that the process would be impractical. Since the initial tests were performed at a higher acidity that those in the patent, it is recommended that the test be re-run at the acidity levels described in the patent.

Background and Research Objectives

Chemically based uranium enrichment processes were developed by the French and Japanese in the 1960's through 1980's. Multiple technical challenges limited the overall success and implementation of the technologies. Mass transfer represented one of the main limitations for both processes. A new opportunity is emerging for enrichment through use of enhanced mass transport in microfluidic systems.

The initial proposal defined the demonstration of uranium enrichment through use of multi-phase countercurrent extraction on the microfluidic scale. Further investigation indicated that this approach was too challenging for the resources of this ER project. An alternative chemical enrichment approach, which utilized many of the components suggested in the original proposal was found in the form of a 1968 Japanese patent [1]. High enrichment levels for a single stage electrodialysis (ED) cell were reported (seven times the expected level), but with limited detail. This discovery led to a re-directed effort to measure the transport rates more fully that reported in the patent.

Scientific Approach and Accomplishments

An electrodialysis stack was constructed to measure the relative transport rates of uranyl (UO2+2) and uranous (U+4) sulfate through ion exchange membranes. A stack, containing five independent flow loops was assembled, along with a flow loop that would fit in a chemical hood (Figure 1). The ED stack, model ED 64 0 04, was manufactured by PCCell, GmbH and purchased along with the original flow system from Electrosynthesis, Inc. The flow system was subsequently re-built to allow operation in a chemical hood. The uranium valences were determined by visual/ near IR spectrum analysis with a Cary 500 spectrometer.

Measurements consisted of the following:

- Characterize the mass transport within the ED cell to insure that transport rates through the ion exchange membranes was not limited by mass transfer.
- Configure the ED stack to convert uranyl sulfate to uranous sulfate. An equal molar mixture would subsequently be used in the uranium transport measurements.
- Measure the relative transport rate of uranyl sulfate to uranous sulfate through both the cation and anion exchange membranes. Also, determine the isotopics of the products.

Mass Transport Characterization

An ED stack consisting of two dilute chambers, two concentrate chambers and anode and cathode chambers was assembled. Mass tranfer limiting current was measured by the method developed by Cowan and Brown [2]. Mass transfer rates, measured in this study, are compared to values obtained by other investigators in Figure 2. While the flow channels contain a woven fabric mesh that separates the membranes, the mass transfer rate is compared to the correlation for an open channel. The correlation is given as follows:

Sh = 0.6 Sc1/3 NRe1/3

Where:

Sh = Sherwood number

Sc = Schmitt number

NRe = Reynolds number

Over the Reynolds number range of this study, the mass transfer rate follows the open channel correlation given by Isaacson and Sonin [5]. This agreement may be expected in a low Reynolds number regime. Heidekamp used the same model of ED module that we did but obtained significantly lower mass transfer rates. Our initial measurements showed a similar trend until we realized that the anode and cathode chambers must be operated at higher pressure than the dilute and concentrate chambers to insure that the membranes are in contact with the support mesh and bipassing is not occuring.

Reduction of uranyl sulfate to uranous sulfate

Uranyl sulfate trihydrate was purchased and part was converted to uranous sulfate. This approach not only produced the needed feedstock for the uranium transfer reactions, but also provided essentially pure uranyl and uranous sulfate for spectral analysis. The reduction reaction was accomplish in the ED cell with 0.1M H2SO4, and 0.25M uranyl sulfate solution as feed for the cathode chamber with 0.5M Na2SO4 circulated through the anode chamber. A PCCell anion exchange membrane (PC-SA) separated the two chambers. With a flow of 2 liters/min through both chambers at a current density of 1.5 A/cm2, the current efficiency began at 100% and dropped to 34% as the mass transfer limiting current fell. One liter of 0.25 M uranous sulfate in 0.1M H2SO4 was produced in a day.

Electro-migration of uranyl and uranous sulfate through ion exchange membranes

The ED stack was re-assembled to form five independent flow loops for measurement of uranium transport through both anion and cation exchange membranes (Figure 3). The feed solution was 0.1 M H2SO4 with 0.125 M of both uranyl and uranous sulfate. Concentrate solutions initially contained 0.1M H2SO4. Since the solution acid content is low, it was assumed that most of the uranium would be in the cationic form. The experiment was designed, however, to measure the transport of uranium anions as well. Isolation of the cation and anion concentrate compartments from the anode and cathode electrodes assured that the valence state of the transported ions would be maintained without further reaction.

Table 1 summarizes the results of the transport tests. The Neosepta CMX-S membrane is selective for monovalent ions. Transport rates were, however very similar to a CMX membrane. Fraction of the current attributed to ion transport through the membrane (tm) totalled less than 10%. It was hoped that passage of the other 90 percent of the current represented passage of hydronium ions (H3O+) from the feed to the cation concentrate so the acid content of the feed would be reduced with time. While there was a slight indication of this trend, the pH remained quite stable. Little improvement in the uranium transference number was seen with run time. When the composition of the cation concentration was compared to the feed, a 7:1 selectivity for UO2+2 over U+4 was observed. This value is reasonably promising, but the low transference number would make a multi-stage process impractical.

The cation exchange membrane was finally changed to a Nafion 117 membrane. The CMX series of membranes are probably composed of a sulfonic acid group attached to a styrene-divinyl benzene copolymer backbone. Nafion 117 is composed of perfluorinated sulfonic acid polymer. These membranes demonstrate higher uranium transference numbers but at lower selectivity.

The composition of the anion concentrate indicated that minimal uranium transport occurred during the tests. It is unclear whether the uranium was transported as an anion species or by diffusion through the membrane. Transport rates were about 1/10 as great the cation membrane rates.

The series of experiments were designed around an acid concentration of 0.1M instead of 0.025M as described in the Japanese patent. There are two reasons for this change. First, during the uranium reduction process, there was concern that concentration gradients would lead to precipitation of uranous sulfate in the flow channel or on the membrane. Second, if the pH drops near the cation exchange membrane, operation of the transport experiment is suseptable to uranous precipitation as well.

In retrospect, the low transport numbers for uranium indicates that a lower acid concentration should be used. It is our hope to re-run the experiment under patent conditions to obtain results that are more comparible. This change is now plasible since spectra are available for both the uranyl and uranous sulfates. The literature indicates that over the proposed acidity range, the spectra will not change significantly. It is hoped that these tests may be run in order to conclusely determine whether the Japanese patent has merrit.

Impact on National Missions

If the 1968 Japanese patent was proven accurate, chemical enrichment through electrodialysis could provide a practi-

cal method for enriching uranium. Advances in microfluidics, realized through improved woven mesh flow fields, would add to this advantage. This potential advance would allow a system that is generally seen as treating waste water to function as an isotopic enrichment system. Without exploring this potential advance, inspectors would not anticipate such an operation.

To date, the uranium transport rate and selectivity have been sufficiently low that the technology does not appear practical. Results from isotopic measurements are currently not available. It is recommended that the test be rerun at the acidity level described in the patent to determine whether an opportunity for further development is merited.

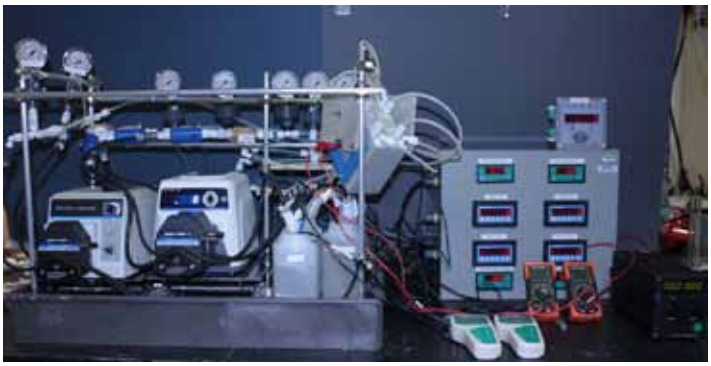

Figure 1. Electrodialysis system with left section in basin ready for hood installation

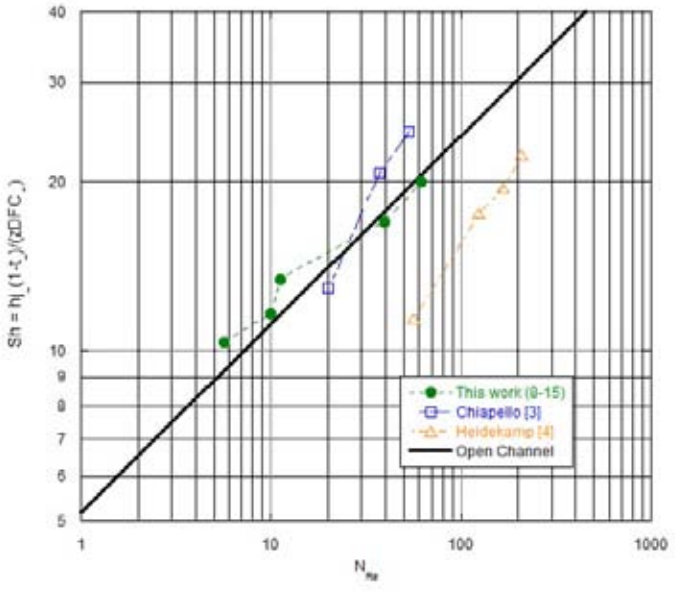

Figure 2. Comparison of measured mass transfer rates with literature values

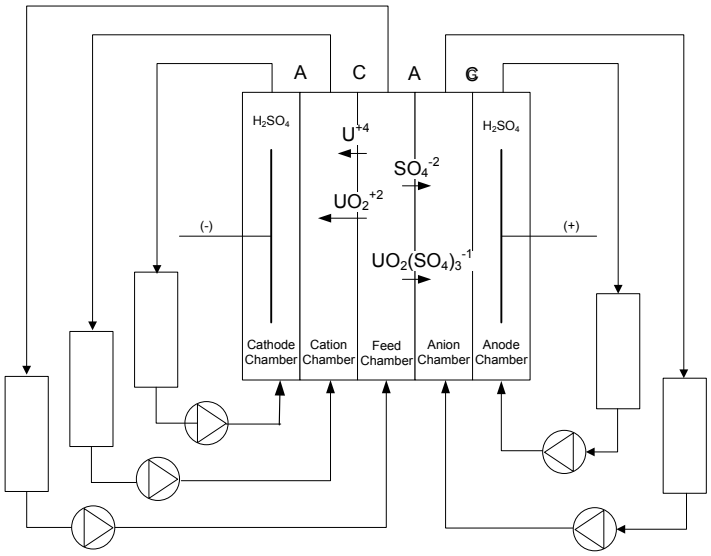

Figure 3. Flow diagram of the uranium transport experiment

Membrane	Anion or Cation Exch. Membrane	Stack Current (A)	Total A-min	$t_{m,U+6}$	$t_{m,U+4}$	$\frac{C_{concentrate}(U^{+6}/U^{+4})}{C_{feed}(U^{+6}/U^{+4})}$
CMX-S	C	1	111	0.022	0.062	6.5
CMX	C	1	317	0.025	0.065	7.1
Nafion 117	C	1.5 to 2	1046	0.073	0.061	1.3
Nafion 117	C	0.77	477	0.088	0.087	1.2
AMX	A	1 to 2	1141	0.0045	0.004	2.8

Figure 4. Summary of uranium transport across ion exchange membranes

References

1. Kakihana, H., and M. Seko. Method of Separating Isotopes. 1968. US Patent 3414500.

2. COWAN, D. A., and J. H. BROWN. EFFECT OF TURBULENCE ON LIMITING CURRENT IN ELECTRODIALYSIS CELLS. 1959. INDUSTRIAL AND ENGINEERING CHEMISTRY. 51 (12): 1445.

3. CHIAPELLO, J. M., and M. BERNARD. IMPROVED SPACER DESIGN AND COST REDUCTION IN AN ELECTRODIALYSIS SYSTEM. 1993. JOURNAL OF MEMBRANE SCIENCE. 80 (1-3): 251.

4. Heidekamp, M.. Mild desalination of cooling tower blowdown water with electrodialysis and membrane capacitive deionization: a comparative study. 2013. Master's Thesis, Delft University of Tech..

5. ISAACSON, M. S., and A. A. SONIN. SHERWOOD NUMBER AND FRICTION FACTOR CORRELATIONS FOR ELECTRODIALYSIS SYSTEMS, WITH APPLICATION TO PROCESS OPTIMIZATION. 1976. INDUSTRIAL & ENGINEERING CHEMISTRY PROCESS DESIGN AND DEVELOPMENT. 15 (2): 313.

Utilization of Conducting Polymers for Embedded Electrical Circuits (U)

Kevin M. Hubbard
20130554ER

Abstract

The goal of this project was to develop an electrically conducting, UV-curable, resin suitable for the preparation of electronic materials. Inherently conducting polymers (ICP) and carbon nanotubes (CNT) were used as conductive fillers, and several mixing methods were investigated. Electrical conductivity and resin viscosity were measured as a function of filler content. These quantities are strongly correlated – the development of percolating conducing pathways also inhibits motion of the resin polymer chains and increases viscosity. CNT were found to provide a lower percolation threshold than ICP fillers. However the ICP was found to provide higher composite conductivity. The combined use of ICP and CNT fillers improved conductivity further still, suggesting a synergistic effect between the materials. The measured conductivities of the test samples were found to be consistent with the best results published for similar composites, and adequate for a variety of applications.

Background and Research Objectives

Inherently conducting polymers (ICP) are well-established materials. Many are available commercially or have well-known synthesis routes. ICP derive their electrical conductivity from a structural backbone that consists of alternating single and double bonds ("conjugated bonds"). Carbon atoms have four outer shell electrons available for chemical bonding. In conjugated structures, however, each carbon atom forms only three directional covalent bonds (known as "sigma" bonds) with its nearest neighbors. The remaining outer shell electron forms what is known as a "pi" bond that is orthogonal to the three sigma bonds. These pi bonds overlap with each other and form a single set of delocalized electron orbitals along the polymer backbone. The resulting delocalized electrons provide the means for electrical conductivity, analogously to the "free" electron states in metals. Carbon nanotubes (CNT) are another example of a conjugated system. The carbon atoms in CNT are arranged in hexagons, with each atom forming three sigma bonds with its nearest neighbors. As with ICP, the remaining outer shell electrons form overlapping pi bonds leading to extended delocalized electronic states and high electrical conductivity.

Both ICP and CNT (and composites thereof) have been used successfully in the production of modern microelectronics. Although the conductivity of the best of these materials is two-three orders of magnitude lower than copper, published data show that functional circuitry can be prepared, an increasingly common example being organic LEDs.

These materials have also been extensively studied for the production of electrically conducting polymer composites. These composites consist of conductive fillers that are dispersed within an insulating polymer matrix. When the concentration of the filler exceeds a certain value (the percolation threshold) continuous conductive pathways are formed within the insulating matrix, leading to bulk conductivity. The percolation threshold can be rather low (3-10 wt.%) for ICP, and much lower still (0.1-1 wt.%) for high aspect ratio fillers such as CNT. The low filler concentration allows many of the bulk properties of the matrix material, such as mechanical strength, to be retained. Conducting resins are typically prepared by solution mixing, in which the filler is dispersed in a solution of the matrix material, followed by evaporation of the solvent. Polymers such as polymethylmethacrylate (PMMA) have been used for this process, but much of the published work focuses on epoxy or acrylic resins.

With respect to acrylics, there have been several published reports on the use of UV-curable materials. The purpose of this project was to develop an improved understanding of this technology, and the interrelated practical considerations that must be addressed to reduce it to reliable practice. These considerations are: 1) the filler concentrations must be sufficient to generate

adequate conductivity in the cured plastic; 2) the resin viscosity must be low enough to enable spin coating, screen printing, etc.; 3) the resin must be free of large aggregates that would potentially clog delivery lines or filters used for processing; 4) the modified resin must cure properly. The success of this effort will enable LANL to more effectively use this technology for a variety of applications.

Scientific Approach and Accomplishments

Resin - The UV-curable resin used as the matrix material was obtained commercially. The resin consists of a mixture of acrylic monomers and oligomers, as well as a photoinitiator that initiates curing upon exposure to UV-A radiation. It is transparent and colorless, enabling visual evaluation of the dispersion of the conductive filler.

Carbon Nanotubes - Multiwall carbon nanotubes (MWNT) of several types were evaluated as conductive fillers. The primary variable of interest was the nanotube length. It is generally reported that the use of longer CNT decreases the percolation threshold for electrical conductivity. However, longer CNT are more difficult to disperse, and hence more likely to form aggregates in suspension that could disrupt processing. The main focus was therefore on shorter CNT of 1-5 micron length, although longer (5-20 micron) CNT were included to determine if they provided a significant improvement in composite conductivity. Several methods were examined to determine the most effective means of dispersing the CNT in the liquid resin. The best results were obtained by simple direct (without added solvent) mixing on a magnetically-driven stir plate.

Conducting Polymers – Two ICP were evaluated as conductive fillers. The most effective was found to be poly-3,4-ethylenedioxythiophene (PEDOT). Two commercial variations of PEDOT were investigated. The first is designated Aedotron C3-NM, which is a dispersion of 200-600 nm diameter PEDOT particles in an organic solvent. The conducting PEDOT chains in this material are capped on either end with organic groups meant to aid dispersion in organic liquids. However these groups are insulating, and so the disadvantage of this filler is decreased resin conductivity. The second PEDOT compound is designated Orgacon Dry, and consists of freeze-dried pellets that can be re-dispersed into organic solvents by high speed mixing. The PEDOT in this formulation is uncapped and so the resin conductivity is significantly higher. However, it is more difficult to produce aggregate-free dispersions. The PEDOT dispersions in each case were mixed with the acrylic resin on a magnetic stir plate and the solvent was allowed to evaporate under ambient conditions. The use of elevated temperature or vacuum to aid evaporation was avoided, because it was found to cause degradation of the resin.

Electrical Conductivity - Film samples were prepared for electrical conductivity measurements by painting the mixed resin onto glass substrates, followed by curing with a UV-A flood lamp. Conductivity was measured as a function of filler content in order to determine the percolation threshold and maximum achievable conductivity. Typical results are shown in Figure 1. Among the CNT, the lowest percolation threshold and highest conductivity were obtained for the material designated SMW200 – most likely because of higher purity relative to the other CNT evaluated (>98% vs. >95%). Note also that CNT length, for the two otherwise identical materials, had little/no effect on performance. For PEDOT, the conductivity difference between the Orgacon and Aedotron samples is clear. Both have a higher percolation threshold than the CNT, but the Orgacon in particular is capable of producing composites with significantly higher conductivity. Note finally that blends of PEDOT/CNT were found to be highly conductive, suggesting a synergy between the two fillers. Most likely the PEDOT polymer chains in this case wrap around the CNT, lowering the contact resistance between tubes. The measured conductivities of the test samples were found to be consistent with the best results published for similar composites, and definitely adequate for a variety of applications.

Rheometry - It is known that the addition of filler to acrylic resins increases viscosity. As with conductivity, a percolation threshold exists as a function of filler concentration. At the threshold, the filler particles become close enough to interact with each other and impede the motion of the resin polymer chains, increasing viscosity. This is a practical concern, as the viscosity must be low enough to enable deposition by spin coating, screen printing, etc. Furthermore, if the polymer chains in the resin have insufficient mobility, the crosslinking reactions that occur during UV curing may be inhibited. A balance must therefore be achieved between the viscosity of the resin and the conductivity of the final composite. The viscosity of the filled resins was measured as a function of filler content. The correlation between viscosity and conductivity is evident from the data presented in Figure 2. The data for the three CNT types exhibit similar behavior, with viscosity increasing by 1500x even as the conductivity increases by only 250x. The data for Orgacon-PEDOT show considerably more scatter. The Orgacon pellets are highly hygroscopic. The observed scatter may be caused by variations in water content which would likely affect dispersion behavior, and hence both viscosity and conductivity. It is clear, however, that the viscosity increase for Orgacon is not quite as severe, perhaps because the PEDOT has a smaller geometric aspect ratio and is less prone to entanglement in suspension. From this perspective, Orgacon therefore appears to

be the preferred filler material for many applications.

Curing Evaluation - The curing behavior of the filled resin is another practical consideration. The addition of filler may inhibit curing in two ways. First, the viscosity data suggest that the presence of the filler may inhibit motion of the resin polymer chains to the extent that curing/crosslinking is inhibited in turn. A number of experiments were performed to evaluate this effect. Thin resin films were painted onto sapphire substrates that were then incrementally exposed to UV-A radiation from a spot curing system. Infrared absorption spectroscopy was used to directly monitor the progression of the curing reactions as a function of UV dose. Typical results are shown in Figure 3. Both fillers are found to slightly inhibit crosslinking in the initial 0.1-0.2 seconds of curing. However the effect becomes very small for longer exposures and is not expected to degrade processing.

The second concern for the curing of filled resins is unwanted absorption of the applied UV radiation by the filler particles. This was found to be a minor issue for CNT-based resins. Especially for higher loadings (and hence higher conductivity), films more than about 50 microns thick did not uniformly cure throughout their thickness. The deposition of thicker layers must therefore be performed incrementally. In contrast, PEDOT has very low absorption in the wavelength range of UV-A radiation. As a result, even 1 mm thick samples could be uniformly cured in a matter of seconds.

Dispersion and Aggregate Formation – Another practical consideration for material performance is the dispersion quality, specifically the presence or absence of aggregates that could clog transfer lines or in-line processing filters. This is a subtle issue that can be understood from the simple schematic illustration in Figure 4. At low filler concentration optimal filler dispersion does not produce conductivity, because few or no continuous conductive pathways are formed (left). A relatively high filler concentration is required in this case, which could lead to unacceptably high viscosity. Some degree of self-assembly (middle), without the formation of large aggregates (right), is therefore necessary in order to provide effective conducting pathways at low filler concentration. However, the resulting filamentary pathways have the potential to clog transfer lines and any in-line filters that may be present.

This is illustrated by experiments performed with two PEDOT-based resins, one based on Orgacon and the other on Aedotron. The top photos in Figure 5 show the relatively coarse filamentary nature of the more highly conductive Orgacon-filled resin, and a hand-painted film cured from this resin. As a result of the coarse structure, passage of the resin through an 18 micron in-line filter was found to almost completely strip away the conductive filler. In contrast, the Aedotron filler is specifically formulated for dispersion in organic liquids. The lower photos in Figure 5 illustrate the absence of the coarse filamentary structure in both resin and cured film, suggesting dispersion at something closer to a molecular level.

The interrelationship between conductivity/viscosity/dispersion is also evident from experiments on the use of viscosity modifiers. Several of these compounds were tested with both PEDOT and CNT fillers. The addition of modifiers did generally decrease resin viscosity significantly. However, this in turn appears to have aided dispersion of the filler, actually lowering conductivity. The net result is translating down the conductivity/viscosity correlation curve (Figure 2), so that no significant benefit is obtained relative to simply decreasing the filler concentration.

Discussion and Conclusions – Highly conductive UV-curable resins using both ICP and CNT as filler materials were successfully prepared. The composite conductivities were found to be consistent with the best literature data, and are adequate for many applications. There are several conflicting practical considerations involved with the use of these materials – conductivity, viscosity, curing behavior, and dispersion quality. Overall, the conducting polymer PEDOT appears to be the preferred filler material. It is capable of providing very high conductivity (Orgacon) or very fine dispersion (Aedotron) at reasonable viscosity. Additional optimization of Orgacon processing may be able to combine these traits, while maintaining acceptable viscosity. Finally, PEDOT has very low absorption in the UV-A region, enabling rapid curing of even very thick films.

Impact on National Missions

The development of organic electronics is a very fast growing field, with many potential applications of relevance to LANL missions. The specific use of composites is difficult – optimization of the several important resin properties is to some extent mutually exclusive. The work reported here has aided in understanding these complexities, and will help position LANL to better make use of this technology.

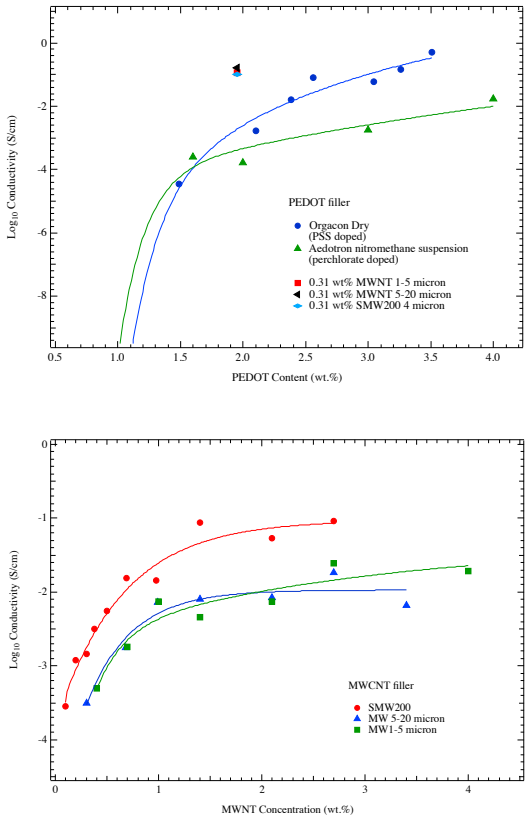

Figure 1. Electrical conductivity as a function of filler content for PEDOT (top) and CNT (bottom) filler materials.

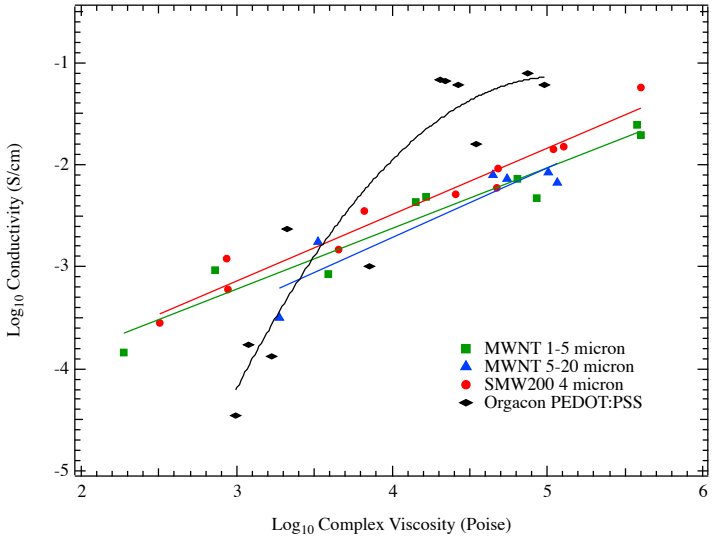

Figure 2. Log-log plot showing the correlation between resin viscosity and composite conductivity for PEDOT and CNT filler materials.

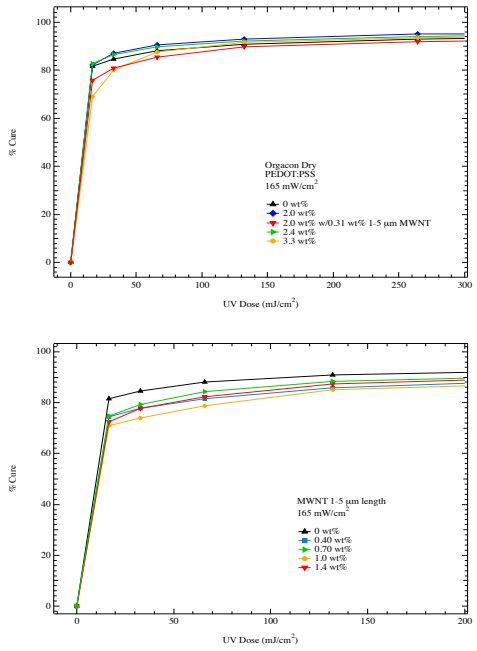

Figure 3. Curing progression as a function of UV exposure for PEDOT (top) and CNT (bottom) filler materials.

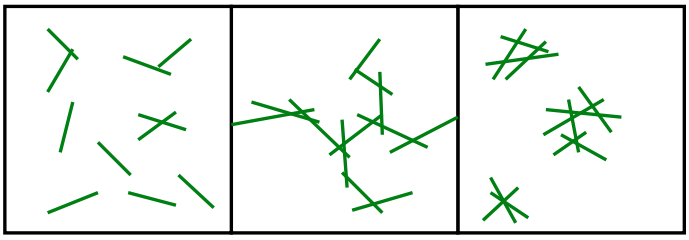

Figure 4. Schematic illustration of possible filler dispersion distributions.

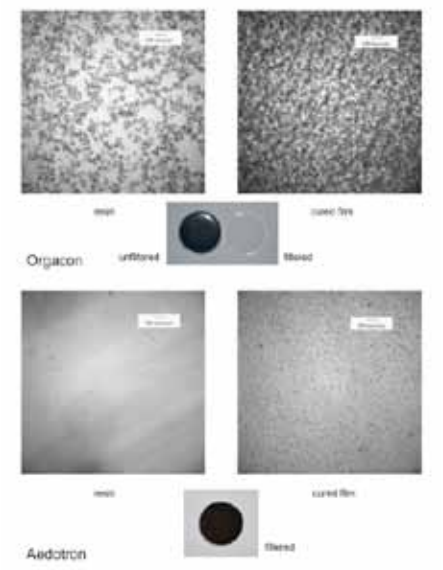

Figure 5. Photographs of PEDOT-loaded resins and cured films for Orgacon (top) and Aedotron (bottom) filler materials.

Toward Development of a Uniquely Specific and Sensitive Detection Technology

Antonietta M. Lillo
20130791ER

Abstract

The most specific and sensitive bio-detection assays currently available use ligand pairs binding to the molecule that one wishes to detect [1-3]. These assays are ideal for use in mission-relevant applications, including detection of bio-threat agents. Unfortunately obtaining ligand pairs is not trivial. Typically, bio-ligands are selected from display libraries and subsequently tested, by pair-wise screening, for their ability to simultaneously bind to orthogonal sites of the target molecule [4-6]. This stepwise approach: 1) is time consuming; 2) does not guarantee obtainment of affinity pairs; 3) is not suitable for small molecule detection. The long term goal of the work here described is to establish a method for simultaneous selection of ligand pairs that: 1) is time and cost effective; 2) is likely to afford ligand pairs with high specificity and affinity; 3) can be applied to target molecules of various size and complexity. Here we present proof-of-principle of the feasibility of direct ligand pairs selection and sorting, from libraries of yeast and phage-displayed antibody fragments (single-chain variable fragment, scFv). We show that: 1) scFv pairs, previously selected for binding to B. tuberculosis antigen 85 (Ag85) [4], work as phage and yeast-displayed ligands, in a flow cytometry-based sandwich assay; 2) preselected phage and yeast display libraries can be enriched for sequences that bind specifically to Ag85, by sorting phage-Ag85-yeast complexes. We also describe intrinsically fluorescent phage particles (fluorophage) that we have engineered as an unintentional side project. We demonstrate that this novel phage construct is suitable for high-throughput specificity screening of phage-displayed affinity ligands.

Background and Research Objectives

Phage and yeast display are well-established technologies that allow random ligands (peptides or antibodies) to be expressed on the surface of bacterial viruses (phage) or yeast, respectively [7-9]. In display libraries, each phage particle or yeast cell carries one ligand, together with the gene that encodes that ligand, thus enabling the selection and identification of antibodies or peptides that bind the target of interest. Phage display libraries include as many as 1012 unique ligands, with each phage particle expressing a variable number of copies of a single ligand. In contrast, yeast libraries tend to be smaller (typically 106 unique clones), while expressing roughly 30,000 copies of a single ligand per cell. The higher display level of yeast, together with their larger physical size, results in significant advantages, among which is the ability to use flow cytometry to provide immediate feedback on the progress of a selection.

One of the most efficient, recently described methods for selection of antibody pairs binding Ag85 [4] utilizes phage display libraries for the first few rounds of ligands selection and yeast display in later rounds of selection and for single ligands screening. In this method, as in many others used for selection of antibody pairs, binders are selected from libraries of potential ligands, with no consideration as to whether they bind to similar or different sites. These preselected affinity reagents are subsequently tested by pair-wise screening for their ability to simultaneously bind to orthogonal sites of the target molecule. Since the preselected reagents might be biased towards a specific region of the target molecule, there is no guarantee of finding affinity pairs. Current methods for selection of affinity pairs allow for screening of no more than 400 (20x20) potential interactions in no less than 1 week. Given that there may be thousands of different individual specific binders, an exhaustive survey takes months. Furthermore, small molecules often do not have distinct binding domains that can be recognized independently by different recognition ligands. Therefore, current “stepwise” approaches do not allow for selection of affinity pairs binding to small molecules.

In order to address these many issues, while providing LANL with a new capability, we have proposed a method that allows for direct selection of binding pairs, from large yeast and phage display libraries, as yeast-antigen-

phage complexes that can be sorted by flow cytometry (Figure 1). This approach offers an unsurpassed level of throughput (106 clones can be screened simultaneously), speed (2 weeks from naïve library to ligand pairs), and probability of finding high affinity and specificity pairs. Furthermore, the proposed "one-pot" selection method potentially allows for selection of affinity pairs binding to small molecules, since the second ligand would bind the complex "small molecule-first ligand" (which might be structurally different than the free small molecule and first ligand), eliminating the absolute need for two separate binding domains on the target molecule. This opens the door to specific detection of small molecules, like chemical warfare agents, which has not been possible utilizing currently available selection methods. The purpose of the work here described, was to gain proof-of-principle for this method. Toward this goal, we have proposed and achieved: 1) expression of already available antibody pairs binding Ag85 as phage and yeast-displayed proteins, 2) detection of yeast-antigen-phage complexes by flow cytometry; 3) mock selection of antibody pairs from libraries preselected for binding to Ag85; 4) deep sequencing of sorted yeast and phage libraries. We currently have sequences of a candidate pair that needs to be tested for specificity of binding. We originally intended to use previously engineered, intrinsically fluorescent phage particles (fluorophage-GFP2), which turned out to be too dim for selection and testing of the "phage-displayed-half" of the ligand pairs. Instead we used phage labeled with a set of primary and secondary antibodies bound to a fluorophore. In the meantime, we have engineered a more fluorescent fluorophage, which, while still unsuitable for the objective of this work, was demonstrated to be suitable for high-throughput specificity screening of phage-displayed affinity ligands.

Scientific Approach and Accomplishments

The proposed method for direct selection of binding pairs (Figure 1) comprises the following steps: 1) a large naïve phage display library (of antibodies and/or peptides, 1012 clones) is preselected for binding to a specific target; 2) the preselected library (106 clones) is sub-cloned for display on yeast and phage; 3) the yeast and phage sub-libraries are incubated with the target molecule; 4) unbound phage and target are washed away, while yeast-bound target molecule and phage are labeled; 5) doubly labeled complexes "yeast-target-phage" are detected and sorted by flow cytometry; 6) sorted yeast and phage are separated and amplified; 7) the sorting/amplification cycle (steps 3-6) is reiterated several times.

The first step toward demonstrating the feasibility of this method was to demonstrate the visibility of yeast-target-phage complexes. We displayed the best set of previously selected scFv pairs, binding to Ag85 [4], on yeast and phage. We incubated these constructs with biotinylated Ag85 (B-Ag85) and we analyzed the resulting mixture by flow cytometry. When two different versions of intrinsically fluorescent phage (fluorophage GFP2 and GFP11) were used, and B-Ag85 was labeled with streptavidin-Alexa632(APC), we saw APC-labeled yeast, but we failed to detect the doubly fluorescent complexes "yeast-Ag85-phage". However, when phage was labeled with a set of primary and phycoerytrin (PE)-labeled secondary antibody, we could see the doubly fluorescent complexes (Figure 2A). These complexes were demonstrated to derive mostly from specific interaction of the ligand pair with Ag85, as they were present at a much lower percentage when a naïve phage library, or yeast expressing polyclonal antiCBPT1 were used instead of phage or yeast-displayed anti Ag85 scFv respectively (Figure 2B and C). An even lower percentage of yeast-phage complexes were observed when Ag85 was omitted (Figure 2D). The visibility and the specificity of yeast-target-phage complexes were therefore proven.

Next, the feasibility of the selection method was tested by utilizing a phage display scFv sub-library derived from 3 rounds of selection for binding to Ag85 [4]. This sub-library was expressed on yeast and phage. The yeast sub-library was pre-incubated with B-Ag85, while the phage sub-library was pre-incubated with untreated yeast library (to subtract phage-scFv interacting with the yeast sub-library independently of Ag85). Bound yeast and pre-subtracted phage were mixed and analyzed by flow cytometry. Doubly labeled complexes were sorted, and the correspondent yeast and phage were amplified separately. Two rounds of selection were performed and complementarity-determining regions (CDR3) of the sorted scFv (on sorted phage and yeast) were deep-sequenced. The sub-libraries derived from the second sort were tested for the specificity of their interaction with Ag85 (Figure 3). These sub-libraries contained phage and yeast capable of forming doubly labeled complexes (blue dots in Figure 3 graphs), presumably derived from the simultaneous binding of yeast and phage to the target molecule. 47% of those complexes occurred only in mixtures of sorted libraries and Ag85, as demonstrated by a drop (from 9.1, in Figure 3A, to 5.2 in Figure 3B) in percentage of complexes formed when sorted libraries and Ag85 were used (Figure 3A) vs when a naïve phage library was used instead of sorted phage (Figure 3B). The average amount of total, a specific yeast-phage complexes (blue + turquoise dots) in the presence (Figure 3B and C) or absence of Ag85 (Figure 3D) was calculated to be 9.0±0.5% of total yeast, whereas the total amount of yeast-phage complexes in the presence of sorted yeast and phage and Ag85 (Figure 3A) was 16.9% of total yeast. This further

confirms that 47% of complexes yeast-Ag85-phage seen in Figure 3A derive from a specific interaction of sorted phage and yeast with Ag85. The deep sequencing results obtained for unsorted and sorted libraries showed that some complementarity-determining regions (CDR3, part of scFv) sequences were progressively being enriched during sorting, as demonstrated by the decrement of unique CDR3 sequences in each phage and yeast sort analyzed (Figure 4A). These results together with the QC of the second sort libraries, described above, support the feasibility of direct selection of antibody pairs specific to a target molecule of interest, using the proposed method.

Two highly represented CDR3s sequences (CDR3y, CAKDGDFWSGYYYWYFDLW and CDR3p, CARFIRGVNVDYW), found by deep sequencing, displayed an interesting trend. The representation (% of total sequences) of CDR3y dropped in the phage component of the first and second sort, but it increased in the yeast component of those same sorts; the opposite happened for CDR3p (figure 4B). This might mean that these 2 CDR3s belong to a set of antibody pairs binding Ag85, as phage (CDR3p) and yeast (CDR3y)-displayed molecules. Additional works is needed to confirm this theory.

As an unintentional side project, we have engineered a phage particle (fluorophage GFP11) displaying green fluorescent protein loop 11 [10 and 11] on the major coat protein 8 (p8). We show that this phage is produced in similar yields as the wild type (wt) phage, and it displays intense fluorescence, upon complementation with green fluorescent protein loops 1-10 (GFP1-10) (Figure 5A). We produced fluorophage GFP11 displaying anti-Ag85, and successfully tested this phage in a bead-based flow cytometry assay, for specificity of binding to Ag85 in a mixture containing negative control antigen UPS11 (Figure 5B). These results show that fluorophage GFP11 can be used for testing antibodies specificity, in high throughput.

The work here presented is the topic of two separate manuscripts ("Direct selection of antibody pairs from yeast and phage-display libraries" and "Fluorophage GFP11: a new tool for user-friendly immunoassays") currently in preparation that will be shortly submitted for publication in peer reviewed journals. Additionally we intend to initiate patenting of the antibody pairs selection method and fluorophage GFP11.

Impact on National Missions

This project supports the DOE mission in Biosurvelliance by enhancing our ability to specifically recognize molecules of interest, for application in chem/biothreat reduction and the biosciences missions of the DOE Office of Science. Additionally this work lays the foundation of a brand-new capability, "direct selection of ligand pairs for bio-recognition", of the laboratory. Further, we are working with program managers to attract external sponsors and to develop new proposals and funding opportunities.

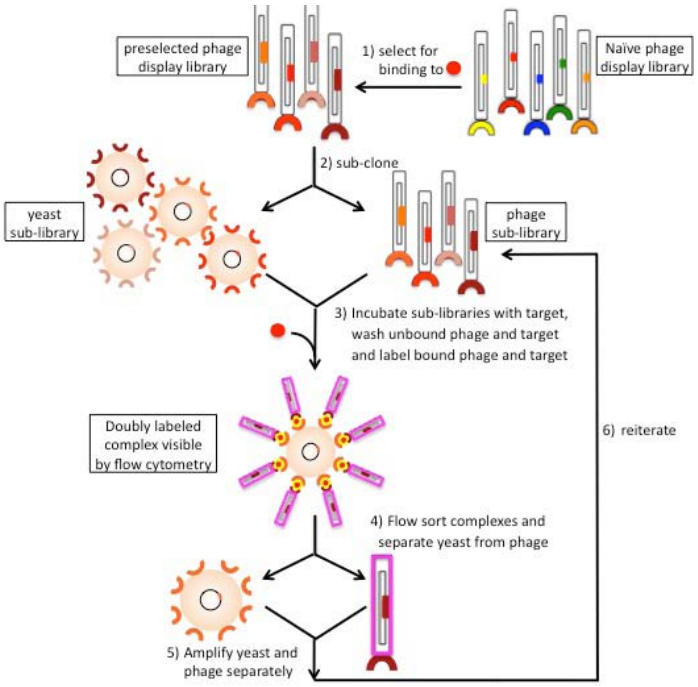

Figure 1. Strategy of ligand pairs selection. A naïve phage display library (of antibodies and/or peptides, 1012 clones) is preselected (1-2 rounds of selection) for binding to a specific target (step 1). The preselected library (106 clones) is sub-cloned for display on yeast and phage (step 2). Yeast and phage sub-libraries are incubated with the target molecule, free phage and target are washed, and bound phage and target are labeled (step 3). Doubly labeled complexes, derived from simultaneous binding of ligand pairs to the small molecule, are detected and sorted by flow cytometry and subsequently separated (step 4). Sorted yeast and phage are amplified separately (step 5). Steps 3 through 5 are reiterated several times (step 6).

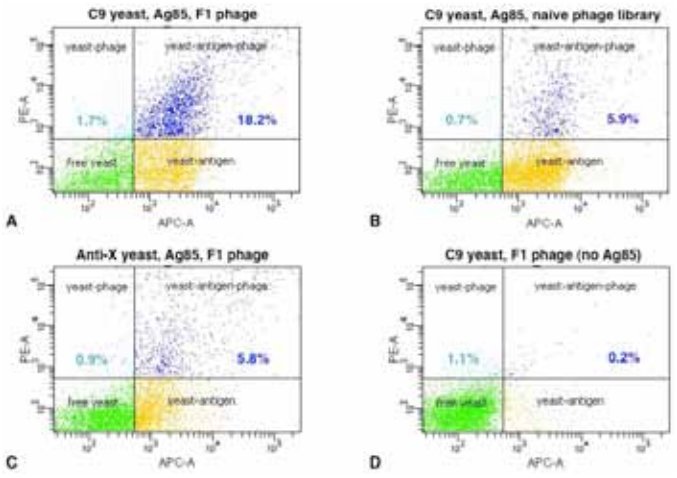

Figure 2. QC of yeast-antigen-phage binding flow assay. In the assays corresponding to graphs A, B and C, phage was incubated

with yeast that were pre-incubated with Ag85. Ag85 was labeled with Alexa632 (APC fluorescence, λex = 635 , λem = 660/20) and phage was labeled with phycoerythrin (PE fluorescence λex = 488, λem = 575/25). The green, yellow, blue and turquoise dots are yeast that are either unlabelled, Alexa632-labelled, Alexa632+phycoerythrin-labelled or phycoerythrin-labelled respectively. Therefore, the doubly labeled yeast (blue dots) derive from some sort of binding interaction between yeast, Ag85 and phage. These complexes are visible in all the experiments that include yeast, Ag85 and phage (graphs A, B and C). These complexes represent 18.2% of the total yeast population when C9 yeast Ag85 and F1 phage were used (A). This percentage drops to 5.9 and 5.8% when a naïve phage library (negative ctrl phage) and yeast expressing polyclonal anti-CBPT1 scFv (negative ctrl yeast), are used instead of F1 phage and C9 yeast respectively (graphs B and C). This indicates that 68% of complexes yeast-Ag85-phage seen in A derive from a specific interaction of scFv F1 and C9 with Ag85. Only 1.3% of total C9 yeast bind to F1 phage in the absence of Ag85 (graph D) indicating that aspecific yeast-phage interactions are minimal.

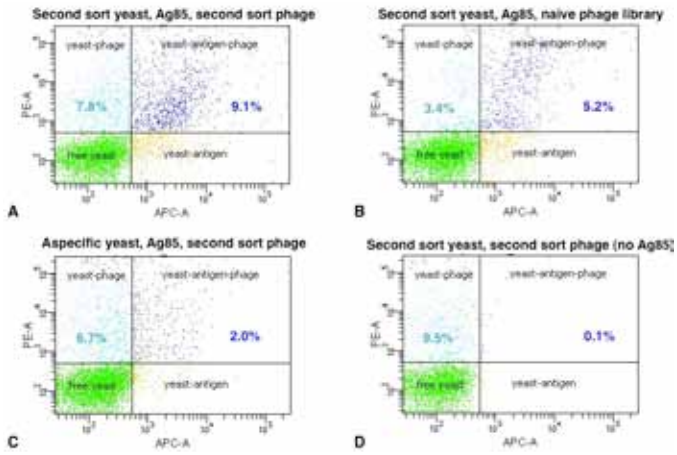

Figure 3. QC of second sort yeast and phage. Phage was incubated with yeast that were pre-incubated with Ag85. Ag85 was labeled with Alexa Fluor 632 (APC fluorescence, λex = 635 , λem = 660/20) and phage was labeled with phycoerythrin (PE fluorescence λex = 488 , λem = 575/25). The green, yellow, blue and turquoise dots indicate yeast that are either unlabelled, APC-labelled, APC+phycoerythrin-labeled or phycoerythrin -abeled respectively. Therefore, the doubly labeled yeast (blue dots) represent some sort complex "yeast-Ag85-phage". These complexes are visible in all the experiments that include yeast, Ag85 and phage (graphs A, B and C). They represent 9.1% of the total yeast population, when second sort yeast, Ag85 and second sort yeast are used (A). This percentage drops to 5.2% when a naïve phage library is used instead of second sort phage (B). This indicate that the interaction "second sort yeast-Ag85-second sort phage" is 43% specific. The amount of aspecific yeast-phage complexes (blue and turquoise dots) in the presence (B and C) or absence of Ag85 (D) was calculated to be 9.0±0.5% of total yeast, whereas the total amount of yeast-phage complexes in the presence of sorted yeast, sorted phage and Ag85 (A) is 16.9% of total yeast. This indicates that 47% of complexes yeast-Ag85-phage seen in A derive from a specific interaction of phage and yeast-displayed scFv with Ag85.

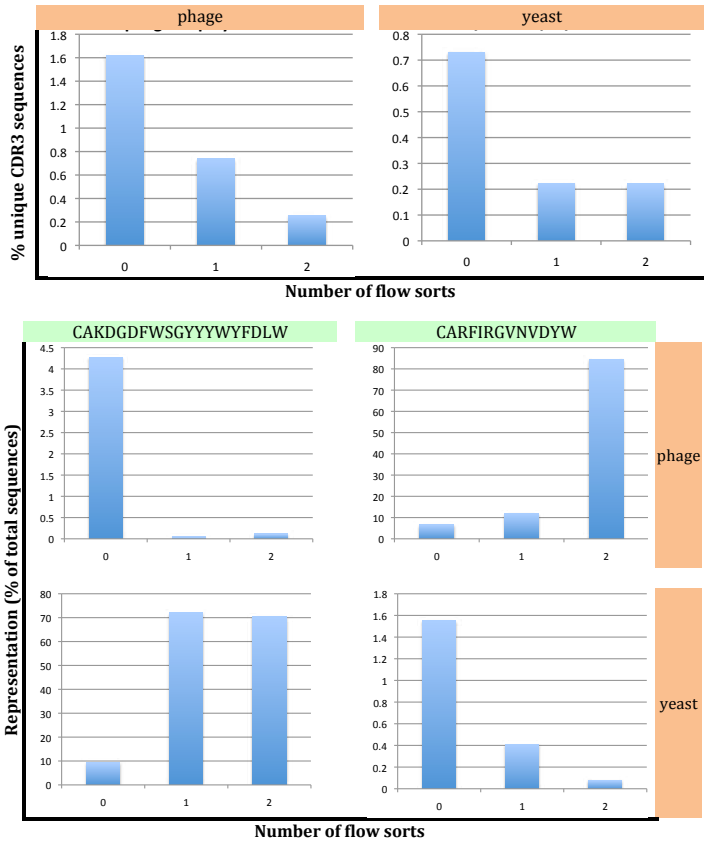

Figure 4. Deep sequencing results. A) Analysis of complementaritiy-determining regions (CDR3) sequences found in phage and yeast display libraries, before and after sorting. The decrement of unique sequences after the first and second flow sort in yeast and phage, indicates enrichment of some CDR3s. B) Fate of 2 CDR3s during sorting. CDR3y, CAKDGDFWSGYYYWYFDLW, is enriched 9-fold (from 9 to 80% of total sequences) after just one sort on yeast, whereas the same sequence is 36-fold less represented after just one sort on phage. CDR3p CARFIRGVNVDYW is enriched 13-fold (from 7 to 85% of total sequences) after two sorts on phage, whereas the same sequence is 19-fold less represented after two sorts on yeast. Since both CDR3 are the most enriched during the yeast-phage complex sorting (on yeast and phage respectively) it is possible that they are a ligand pair binding to Ag85.

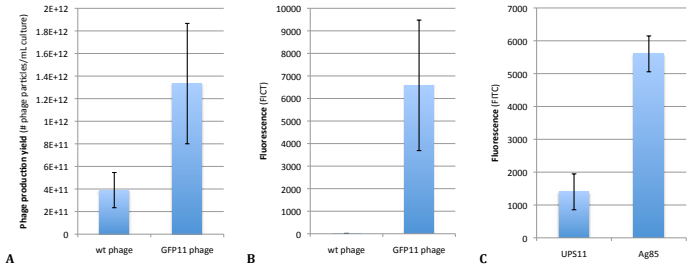

Figure 5. Fluorophage characterization. A) Phage production yield. The number for phage particles obtained per milliliter of culture was calculated by UV/Vis spectrometry using the following formula (Abs269-Abs320) x 6E+16/5300). Averages of 3 preps, with corresponding standard deviations are presented. B) Phage fluorescence. Average fluorescence (FITC, λEx 488 nm,

λEm 530 nm) and corresponding standard deviation of two equimolar solution of wild type (wt) phage and phage engineered to express GFP11 on major coat protein p8 (GFP11 phage), complemented with GFP1-10 is presented. C) Assessment of specificity of phage-displayed scFv interaction with antigen-coated luminex beads. Anti Ag85 scFv F1, was incubated with a duplex of luminex beads, coated with antigen UPS11 (negative control) or antigen 85 (Ag85). The duplex was analyzed by flow cytometry. The beads were separated based on their intrinsic fluorescence, and the phage-derived fluorescence (FITC, λEx 488 nm, λEm 530 nm), associated to each beads, was measured. Averages of two experiments with corresponding standard deviations are presented.

References

1. Mukundan, H., S. Kumar, D. N. Price, S. M. Ray, Y. J. Lee, S. Min, S. Eum, J. Kubicek-Sutherland, J. M. Resnick, W. K. Grace, A. S. Anderson, S. H. Hwang, S. N. Cho, L. E. Via, C. Barry, R. Sakamuri, and B. I. Swanson. Rapid detection of Mycobacterium tuberculosis biomarkers in a sandwich immunoassay format using a waveguide-based optical biosensor. 2012. TUBERCULOSIS. 92 (5): 407.

2. Hasan, S., J. Dong, Y. Hara, Y. Morizane, F. Shibasaki, and H. Ueda. Protein-based open sandwich immuno-PCR for sensitive detection of small biomarkers. 2013. Analytical Sciences. 29 (9): 871.

3. Lee, S., S. Kim, J. Malm, O. C. Jeong, H. Lijia, and T. Laurell. Improved porous silicon microarray based prostate specific antigen immunoassay by optimized surface density of the capture antibody. 2013. Analytica Chimica Acta. 796: 108.

4. Ferrara, F., L. A. Naranjo, S. Kumar, T. Gaiotto, H. Mukundan, B. Swanson, and A. R. M. Bradbury. Using Phage and Yeast Display to Select Hundreds of Monoclonal Antibodies: Application to Antigen 85, a Tuberculosis Biomarker. 2012. PLOS ONE. 7 (11): -.

5. Safsten, P.. Epitope mapping by surface plasmon resonance. . 2009. Methods in Molecular Biology. 524: 67.

6. Bembenek, M. E., A. Burkhardt, J. Y. Ma, Z. Li, H. K. Loke, D. Y. Wu, Q. Xu, O. Tayber, L. Y. Xie, P. Li, and L. Li. Determination of complementary antibody pairs using protein A capture with the AlphaScreen assay format. 2011. ANALYTICAL BIOCHEMISTRY. 408 (2): 321.

7. SCOTT, J. K., and G. P. SMITH. SEARCHING FOR PEPTIDE LIGANDS WITH AN EPITOPE LIBRARY. 1990. SCIENCE. 249 (4967): 386.

8. Bradbury, A. R. M., and J. D. Marks. Antibodies from phage antibody libraries. 2004. JOURNAL OF IMMUNOLOGICAL METHODS. 290 (1-2): 29.

9. Boder, E. T., and K. D. Wittrup. Yeast surface display for screening combinatorial polypeptide libraries. 1997. NATURE BIOTECHNOLOGY. 15 (6): 553.

10. Pedelacq, J. D., S. Cabantous, T. Tran, T. C. Terwilliger, and G. S. Waldo. Engineering and characterization of a superfolder green fluorescent protein. 2006. NATURE BIOTECHNOLOGY. 24 (1): 79.

11. Cabantous, S., T. C. Terwilliger, and G. S. Waldo. Protein tagging and detection with engineered self-assembling fragments of green fluorescent protein. 2005. NATURE BIOTECHNOLOGY. 23 (1): 102.

Neutron Sensor based on Integrated Scintillator and Photodiode

Kiril D. Ianakiev
20130795ER

Time Reversal Acoustic Communications for Rescue Operations

Brian E. Anderson
20130799ER

Abstract

The purpose of this project was to demonstrate the use of time reversal technologies as a means for communications in air and along solid structures. Applications of this work include communicating with hostages and survivors in rescue operations, communicating imaging and operational conditions in deep drilling operations, monitoring storage of spent nuclear fuel in storage casks without wires, or clandestine activities requiring signaling between specific points. This technology provides a solution in any application where wires and radio communications are not possible or not desired. It also may be configured to self calibrate on a regular basis to adjust for changing conditions. These communications allow two people to converse with one another in real time, converse in an inaudible frequency range or medium (i.e. using ultrasonic frequencies and/or sending vibrations through a structure), or send information for a system to interpret (even allowing remote control of a system using sound).

The time reversal process allows one to focus energy to a specific location in space and to send a clean transmission of a selected signal only to that location. In order for the time reversal process to work, a calibration signal must be obtained. This signal may be obtained experimentally using an impulsive sound, a known chirp signal, or other known signals. It may also be determined from a numerical model of a known environment in which the focusing is desired or from passive listening over time to ambient noise.

This research demonstrates two of the many potential applications: audio communications in a conference room and signal transmissions along a pipe encased in concrete. Our results will allow us to meet the global security mission needs for a range of government agencies within the U.S. Department of Defense and to provide U.S. industrial companies new technologies that help the U.S. develop its energy independence.

Background and Research Objectives

Time Reversal (TR), a fairly new technique providing spatially localized energy focusing[1-2], has been shown to provide secure and optimized underwater acoustic communication between two locations [3-5].

Vibrational communications in solid media, let alone using TR, have not been explored extensively in the literature aside from studies done on how certain animals communicate through the ground [6-7]. A recent study presented a very basic use of TR for seismic communications using a sledgehammer in a field demonstration with a communication rate of about 1 bit/s [8]. The purpose of the current research was to explore the use of TR for vibrational communication along a pipe at much higher bit rates with computer controlled sources, which could allow rescuers to audibly communicate with survivors of a building collapse about their location and health, communications of drilling operational conditions and imaging information, and allow for secure transmissions of information in situations where radio and wired communication is not desirable. Additionally this research set out to determine whether the ability to focus energy using TR along any of three Cartesian axes (developed by the authors for nondestructive evaluation purposes [9]) could provide an increase in the communication rate of at least 3 times, which has not been shown for any communication technologies to date, whether underwater or otherwise.

It was found that TR communications along a concrete-encased, steel pipe could be done at transmission rates of at least 20 kbit/s. Additionally it was found that transmission rates may in fact be tripled between a single source and a single receiver by focusing the energy in 3 different directions at the receiver location. These findings provide an excellent proof of concept that may lead towards further research and development funds for practical implementations.

In addition to vibrational communications, the authors also explored the use of TR for audible communications through the air. There have been a few studies that have explored the use of airborne TR communications in highly reverberant environments (i.e. racquet ball courts, parking garages) for Morse-code communications [10-11] and for imaging purposes [12-13], but these studies have not utilized typical room environments, nor have they focused on understanding real time speech communications. This research aims to determine whether TR may be used to communicate private, audible speech in a typical conference room environment, and to determine whether these communications may be realized with the sources and receiver placed outside the room.

It was found that private communications are possible in a typical conference room and that the communications can be made with the hardware outside of the room. Speech-like sounds could be heard at all locations in the room but observers of a live demonstration of the focusing could not understand the speech unless they were at the target location. It was also found that several types of signal processing methods could be used to further mask the intelligibility of the speech without destroying the ability to communicate to the desired focal location. A proof of concept of communicating to a target inside a room with the equipment outside the room was accomplished.

Scientific Approach and Accomplishments

For the vibrational communications, a buried pipe simulator was constructed using a 10 foot long steel pipe that was encased in a concrete trough (Figure 1). Ultrasonic signal transmissions and audio frequency transmissions were demonstrated under various conditions. These conditions included whether the pipe was buried in concrete or exposed to air and whether the pipe was filled with water or air. It was demonstrated that time reversal encoding greatly increases the signal transmission accuracy compared to broadcasting the signal without any encoding (the amount to which the accuracy improves depending on the complexity of the structure used), without affecting the transmission signal strength. The ultrasonic frequency communications provided cleaner signal transmissions than audible frequencies over the relatively short length of pipe tested due to the increased complexity of the ultrasonic wave propagation. Despite this fact, using a triaxial accelerometer for the audio signal transmissions, we demonstrated that one could send 3 independent signals between one source and one receiver when each of the accelerometer's vibration axes are employed (Figure 2). These independent signals allow 7 times higher transmission rates for communications (the factor of 7 is achieved if all combinations of x, y, and z are employed). It was found that the water filled pipe provided a signal transmission increase of up to 40 times and that the concrete casing reduced signal transmission only for the air filled pipe by a factor of up to 30 (the casing did not reduce the signal when the pipe was water filled).

In the case of the airborne communications, four loudspeakers, a microphone, and a laser vibrometer were setup in a conference room (Figure 3). To start with, successful private communications were demonstrated by placing the loudspeakers inside the room along with using a microphone for the calibration. A demonstration of simultaneously focusing two speech signals to two different locations was also done with audio frequencies (see the first video demo at Ref. [14]) and with ultrasonic frequencies (Figure 4). Further, we showed that a masking white noise could be added to the TR broadcast to mask the speech at most locations in the room but allow the target location to still understand the speech (see the second video demo at Ref. [14]). Private communications were also be made with the loudspeakers placed outside the room (along a wall with several windows) and by using a microphone for calibration (see the third video demo of focused pulses at Ref. [14], listen for the pronounced pop at the microphone location). Then communications were demonstrated using loudspeakers and a laser vibrometer in the same room (see the fourth video demo at Ref. [14]). In this case the laser was used to obtain the calibration signal to focus sound that one could hear at or near the location where the laser was shining. Finally, the loudspeakers and laser vibrometer were placed outside the room along a wall with many windows. Communication to a hostage from outside a room requires that the loudspeakers be outside the room and that a laser vibrometer be shined into the room on an object or wall near the hostage's head to obtain calibration signals from the loudspeakers to the object/wall used to focus speech to them. Either the laser would need to be shined through a window or be snaked into the room through a hole in the wall (using a fiber optic laser vibrometer for example). In this case, the sound from the specific loudspeakers used was not loud enough to transmit through the windows and vibrate a surface so that the laser could obtain a calibration signal. Higher amplitude loudspeakers perhaps with stronger directional characteristics and/or a more powerful laser vibrometer would likely allow this type of communication. However, the principle has been demonstrated, that a laser or a microphone may be used to obtain a calibration signal that may then be used for private audible communications. Additionally, one can envision using an infrared laser vibrometer to discretely obtain the calibration signals.

There is a lot of future work that should be done to ad-

vance these technologies to higher technology readiness levels and to determine under what conditions they may be applied. In the case of the airborne communications, various types of rooms with different acoustic conditions (i.e. different reverberation times) need to be studied in order to determine how many loudspeaker channels are necessary to ensure the privacy of the targeted communications. Additionally one could modify the design of the loudspeakers in order to provide extra scattering as is often done in nondestructive testing applications of time reversal [15]. Further research should look at additional means to obtain the required calibration signals, such as passive listening techniques which have been shown to provide the required signal. Because the goal of the audible communications is privacy at the target location, it is desirable to create a sound field that masks the communicated speech signals everywhere else in the room. For a given room and number of loudspeakers, this may be enhanced through various signal processing techniques. In the current project we showed preliminary results that suggest that additive white noise can help mask the speech everywhere but at the target location, however it is likely possible that an additive artificial reverberation may be used and/or other techniques may also prove promising such as wave decomposition methods [16]. Finally, there are several variants of the basic audible communications that should be studied, such as using headsets for ultrasonic communications with hardware to up shift and down shift to audible messages, and using time reversal focusing to sonically remotely control hardware or a device instead of using wireless technologies. In the case of vibrational communications, there is significant work that should be done to optimize the sources and receivers used for these communications, and the potential to obtain the calibration signal through passive listening as mentioned previously. Also there are other application areas for vibrational communications such as clandestine operations to listen to and locate sound sources of interest that may be underground for example. Thus while much of the future work is of an engineering nature for specific situations, there is a fair amount of fundamental science that needs to be explored.

Impact on National Missions

The Principle Investigator on this project, Brian Anderson, was hired at LANL 10 months ago in large part to develop his group's communication technology capabilities. This LDRD Reserve Funding provided the first opportunity to focus on this goal.

Secure acoustic communications are important to global security (GS) needs and we have been sought out for discussions with GS program managers Darryl Gardner, Kerry Habiger, Barry Charles, and Paula Knepper, as Dept. of Defense customers are looking for technologies to allow them to communicate with acoustic or vibration signals in situations where wires and radio communications are not feasible or not desired.

This work provides a significant research advance for energy resource extraction technologies. We have been developing joint intellectual property between LANL, Chevron, and JPL who have expressed interest in our vibrational communication capabilities. Our experiments on vibrational transmissions using time reversal have shown communication rates of at least 20 kbit/s and perhaps even 1 Mbit/s and may be able to operate during drilling operations. Additionally, this research provides a means to communicate monitoring information through sealed nuclear reactor vessels and storage casks for safe operations and reliable storage of spent fuel.

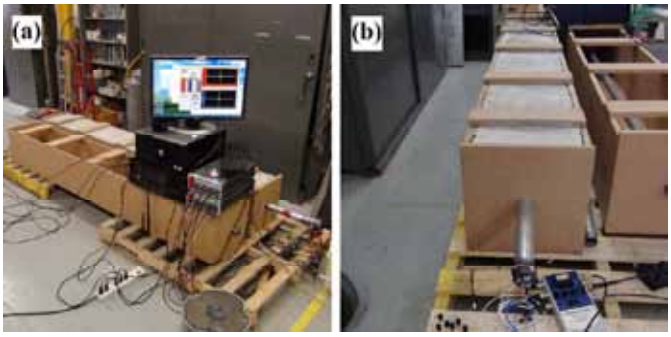

Figure 1. Photographs of the buried pipe setup used for demonstrations of vibrational communications. (a) Photo of the hardware and the pipe in the background. (b) Photo of the pipe with the concrete casing visible at the top of the wooden trough.

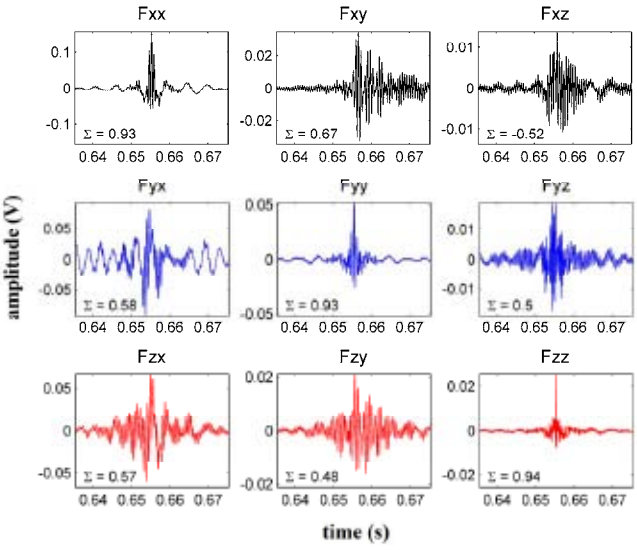

Figure 2. Plots of the amplitude versus time for three different types of focusing. Each row represents the results obtained for x focusing, y focusing, and z focusing. The focal signal, F, notation above each plot has two indices, the first representing the

calibration vibration direction, and the second representing the vibration in that direction obtained during each of the three types of foci. The focusing occurs more prominently in the direction in which the calibration signal is originally determined in. The Sigma values represent the temporal symmetry about the time of focus, which has been shown by the authors in previous work to indicate a time reversal focus.

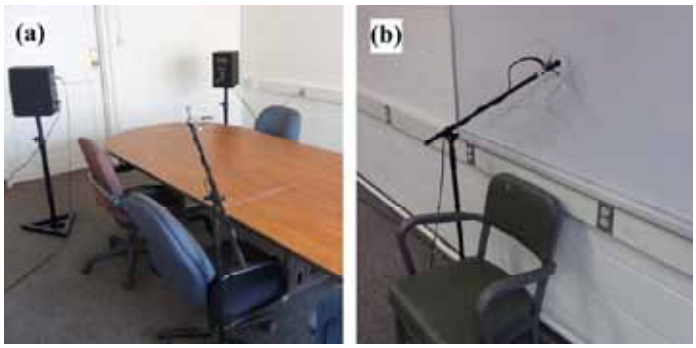

Figure 3. Photographs of the conference room setup used for demonstrations of audible private communications. (a) Photo of two of the loudspeakers used and the microphone placed at a seat location. (b) Photo of a small laser spot shining on a white board above a chair with an outline of a hostage drawn on the board (note that the microphone was placed at the same location in order to record what one would hear at that location.

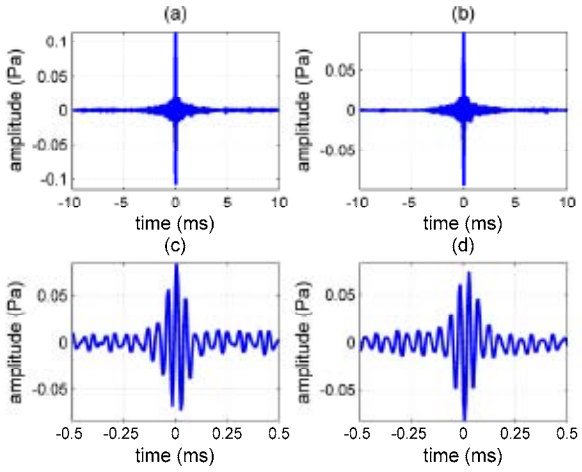

Figure 4. Plots of amplitude versus time representing time reversal focusing using ultrasonic frequency signals. (a) and (b) represent the focal signals obtained at two different locations using calibration signals specific to those locations when each focusing experiment is done independently. (c) and (d) represent a zoomed in look at the focal signals obtained at the two locations when the focusing is done simultaneously. These later results show that one can simultaneously send a positive phase focus to one location and a negative phase focus to a different location without these foci interfering with one another, demonstrating independent focusing to two locations.

References

1. Fink, M.. Time reversed acoustics. 1997. PHYSICS TODAY. 50 (3): 34.

2. Anderson, B. E., M. Griffa, C. Larmat, T. J. Ulrich, and P. A. Johnson. Time reversal. 2008. Acoustics Today. 4 (1): 5.

3. Parvulescu, A., and C. S. Clay. Reproducibility of signal transmission in the ocean. 1965. Radio and Electronic Engineer. 29: 223.

4. Song, A., and M. Badiey. Time reversal acoustic communication for multiband transmission. 2012. Journal of the Acoustical Society of America. 131 (4): EL283.

5. Song, H. C.. Time reversal communication in a time-varying sparse channel. 2011. Journal of the Acoustical Society of America. 130 (4): EL161.

6. O'Connell-Rodwell, C. E.. Keeping an 'ear' to the ground: Seismic communication in elephants. 2007. Physiology. 22 (4): 287.

7. Narins, P. M., E. R. Lewis, J. J. U. M. Jarvis, and J. O'Riain. The use of seismic signals by fossorial southern African mammals: A neuroethological gold mine. 1997. Brian Research Bulletin. 44 (5): 641.

8. Hanafy, S. M., and G. T. Schuster. Two applications of time reversal mirrors: Seismic radio and seismic radar. 2011. Journal of the Acoustical Society of America. 130 (4): 1985.

9. Ulrich, T. J., K. Van Den Abeele, P. Y. Le Bas, M. Griffa, B. E. Anderson, and R. A. Guyer. Three component time reversal: Focusing vector components using a scalar source. 2009. JOURNAL OF APPLIED PHYSICS. 106 (11): -.

10. Candy, J. V., A. W. Meyer, A. J. Poggio, and B. L. Guidry. Time-reversal processing for an acoustic communications experiment in a highly reverberant environment. 2004. Journal of the Acoustical Society of America. 115 (4): 1621.

11. Ribay, G., J. de Rosny, and M. Fink. Time reversal of noise sources in a reverberation room. 2005. Journal of the Acoustical Society of America. 117 (5): 2866.

12. Harker, B. M., and B. E. Anderson. Optimization of the array mirror for time reversal techniques used in a half-space environment. 2013. JOURNAL OF THE ACOUSTICAL SOCIETY OF AMERICA. 133 (5): EL351.

13. Mimani, A., C. J. Doolan, and P. R. Medwell. Multiple

line arrays for the characterization of aeroacoustic sources using a time-reversal method. 2013. Journal of the Acoustical Society of America. 134 (4): EL327.

14. Anderson, B. E.. Video demonstrations of time reversal acoustic communications in a conference room (LA-UR-13-27841). 2013. Los Alamos National Laboratory.

15. Damme, B. Van, K. Van den Abeele, Y. F. Li, and O. B. Matar. Time reversed acoustics techniques for elastic imaging in reverberant and nonreverberant media: An experimental study of the chaotic cavity transducer concept. 2011. JOURNAL OF APPLIED PHYSICS. 109 (10): -.

16. Blanc, C., M. C. Remillieux, J. M. Corcoran, and R. A. Burdisso. Generation of impulsive sound with speakers. 2012. NOISE CONTROL ENGINEERING JOURNAL. 60 (2): 148.

Remote Raman-LIBS Spectroscopy: Preliminary Tests for the Next Mars Rover

Samuel M. Clegg
20130801ER

Abstract

Raman and LIBS spectroscopy are highly synergistic analytical techniques that will be proposed for the next Mars rover mission. Raman is sensitive to the sample molecular structure while the elemental composition is determined by LIBS. The proposed work was designed to use a spare ChemCam flight laser, add a doubling crystal to convert the 1067 nm fundamental to 533.5 nm, and to collect remote Raman spectra with a LANL designed miniature transmission spectrometer. The samples were also probed with the ChemCam testbed with an identical ChemCam laser. These experiments demonstrate that the frequency doubled ChemCam flight laser and the transmission spectrometer could detect the Raman signatures from most geological samples at a 9 m standoff distance.

Background and Research Objectives

While independent Raman spectroscopy and LIBS experiments are routinely done in our laboratory, we have not done both types of experiments on the same geologic samples for dual verification. In fact, we are not aware of any study of this type reported in the literature. This proposed work was designed to demonstrate that a frequency doubled (533.5 nm) ChemCam laser could be used to produce remote Raman spectra as well as LIBS spectra.

Specifically, the work will start with the integration of a Raman-modified ChemCam spare laser from our collaborators at the Institut de Recherche en Astrophysique et Planétologie (IRAP, Toulouse, France) with the transmission spectrometer LANL designed and built for SAGE (proposed Venus lander that went through NASA Phase A development). The integrated hardware was used to probe eight geological samples. The results of this work will be submitted to Spectrochimica Acta B. These experiments are critical to successfully proposing a Raman-LIBS instrument for the next Mars rover mission due December 23, 2013.

Scientific Approach and Accomplishments

The first task was to test the IRAP Nd:KGW laser (1067 nm) and the doubling crystal (533.5 nm) to verify that one could use it for remote Raman spectroscopy and to synchronize the laser with the breadboard transmission spectrometer created for the NASA SAGE concept study. This integrated instrument was used to probe a series of geologic samples at a 9 m standoff distance. Since the transmission spectrometer is only capable of detecting Raman and LIBS emission over the 500 – 900 nm spectral window, the ChemCam test-bench was used to collect LIBS spectra (240 – 900 nm) on the same samples. Note that the ChemCam test bench uses the same model laser as the one used in the Raman experiments.

The IRAP Nd:KGW laser design is exceptionally well-qualified as a Raman laser for future RLS proposals to Mars and Venus. The laser produces 30 mJ/pulse at the 1067 nm fundamental frequency and is currently operating on Mars in ChemCam. A frequency doubled laser beam was generated with a KDP crystal properly oriented in front of the IRAP laser and produced 20 mJ/pulse, an outstanding 67% conversion efficiency. One critical requirement to doing Raman spectroscopy is to generate enough Raman scattering while preventing photochemical changes to the sample or LIBS. This 20 mJ/pulse is more than enough laser energy to generate Raman signals from most geologic samples and could be easily reduced when necessary.

Synchronizing the laser and the ICCD detector on the miniature transmission spectrometer took a little effort. Note that the Raman signal lifetime is as long as the pulse width of the laser, ~4.5 ns. The power supply that drives the laser diode pumps and the pockel cell contains a trigger monitor port. The diode pump trigger was used to externally trigger a DG535 Stanford Research Systems (SRS) Delay Generator. The SRS was used to separately trigger the intensifier with a 40 ns pulse width and the CCD detector. This ICCD uses a Sony

CCD that is readout noise limited. While the intensifier effectively transmitted a 40 ns window around the Raman signal, the CCD was held open for 10 seconds to record the Raman signal from 10 laser pulses. The resulting spectra were co-added by the software to record up to 500 laser shots.

The LIBS spectra were collected with the ChemCam testbed that uses the same model laser. The same samples were placed in a vacuum chamber and filled with 7 Torr CO2 to simulate the Martian surface pressure. Each sample was probed with 50 laser shots, which is the typical number of shots used to probe samples on Mars.

We selected a series of minerals that are important for future Mars and Venus mission proposals and include aragonite (CaCO3), barite (BaSO4), calcite (CaCO3), dolomite (CaMg(CO3)2), gypsum (CaSO4·2H2O), olivine ((Mg, Fe)2SiO4), quartz (SiO4), and talc (Mg3Si4O10(OH)2). The Raman and LIBS spectra for these 8 minerals are depicted in Figures 1a – h. The gypsum and talc samples produced significant fluorescence that made it difficult to detect the Raman emission but a better detector is expected resolve this problem. Olivine produces a very weak Raman signal and was not detected with the miniature ICCD.

Impact on National Missions

NASA has just released the call for proposals for the next Mars rover payload. This mission is a NASA HQ directed mission which is a national priority. This remote Raman – LIBS analytical approach could be a key instrument on the next mission and these experiments were are critical first step to selection.

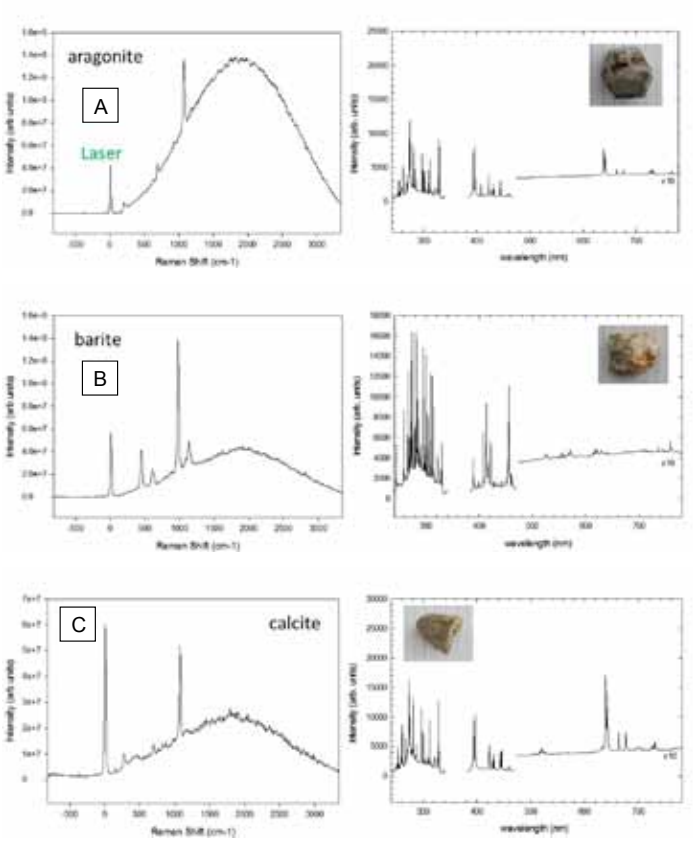

Figure 1. The Raman spectra (left) , LIBS spectra (right), and pictures of the rocks probed.

Optimization of Heterogeneous Sensing Systems for Risk-minimized Decision Making

Charles R. Farrar
20110575PRD1

Abstract

This research had two primary focus areas: 1) The development of a Bayesian experimental design framework for the optimal design of surveillance systems and 2) Designing optimal algorithms for non-destructive evaluation using measurement-rich, full-wavefield measurements. In both research thrusts, prototype algorithms and software packages were designed, written, and then demonstrated on a set of example test cases, including a loose-nuke surveillance optimization scenario and the detection of a composite delamination in a modern aerospace component. The success of this research supports a myriad of national missions, including nonproliferation, global security, and asset readiness.

Background and Research Objectives

Plug-and-play Surveillance System Optimization

Forward deployment of LANL sensing systems requires a design strategy. Consider surveillance networks: How many sensors? What kind? Where should they be placed? How should their data be processed? With an expanding canvas of national security challenges in the face of increasingly restrictive budgets, questions of how to optimize resource allocation become increasingly important. In other words, how can we do more with less?

We saw two major problems that need to be addressed in the area of sensor system design optimization. First, the standard approach to sensor optimization, which maximizes observability, does not consider the most important facets of the problem. It does not directly address the real goal of the system (e.g., no dirty bomb detonations and few, if any, unnecessary evacuations); it does not account for life-cycle costs (fabrication, deployment, and maintenance) of the sensor system itself; and it is unable to consider robustness to contingencies like sensor failure. Second, because the task of deriving the statistical expectations needed for optimization is often so labor intensive and the outcome is so narrowly applicable and sensitive to modeling assumptions, formal sensor system design optimization is regularly overlooked.

Our aim was to develop an application-independent process for rapidly generating risk-minimizing designs of distributed sensing systems using Bayesian analysis and sampling-adapted search strategies.

Full-Wavefield Data Processing for NDE

Our goal was to design and build a revolutionary laser-based non-destructive evaluation (NDE) hardware-software system for automated, rapid, remote imaging and assessment of structural properties and defects. The system excites and measure ultrasonic waves using scanning, non-destructive pulsed laser excitation and a laser-Doppler vibrometer (LDV). It generates quantitative images that provide estimates of structural features and defects using one-of-a-kind, LANL-derived signal and image processing technology. We envision an eventual system sufficiently compact, automated, and non-intrusive to enable previously-far-reaching technologies such as in-line inspection of conveyed parts, “smart hangars” for drive-in-drive-out full body inspection, fixed installation NDE-based monitoring of plant facility components, and mobile robotic platforms for on-demand inspection tasks.

Scanning laser Doppler vibrometer (LDV) technology enables the measurement of full-field time histories of propagating ultrasonic waves in a structure. Typically, damage detection approaches involving these systems rely on short, narrowband wave pulses for excitation. This is because the change in the pattern of a transient wave is readily apparent as the wave interacts with discontinuities (such as defects) in the structure. However, because these waves are transient and have so little energy, and because LDV systems typically have a high noise level, there are several limiting requirements for this inspection approach: 1) Many (often hundreds) of sequential measurements must be taken at each spatial sample point and averaged in order to achieve a satisfac-

tory measurement signal level. 2) A delay of as much as 40 ms must be allowed between measurements to allow the previously excited wave to "die out". 3) Surface preparations, short stand-off distances, and near-normal laser incidence are necessary to achieve sufficient laser backscatter.

Our goal was to develop a hardware-software system that makes use of steady-state excitation in place of transient wave excitation to rapidly image defects in plate-like structures. The use of steady-state waves provides three significant benefits: 1) Energy is effectively "pumped" into the structure, resulting in orders of magnitude higher displacement. 2) No delay is necessary between measurements. 3) Only a few cycles of the excited wave are sufficient to effectively capture the wave behavior at each scan point.

Scientific Approach and Accomplishments

Plug-and-play Surveillance System Optimization

The proposed approach to optimal design was based on minimizing the expected loss (i.e. maximizing expected benefit), in terms of money, safety, or security, that implementation of the sensing system will incur. The expected loss, or Bayes risk [1], of a design, D, can be thought of as the sum of the costs associate with taking some action A (e.g. to evacuate or not), for some event E (e.g. nuclear source is present or not),) weighted by the probability of taking action A for state E and the prior probability of E occurring to the begin with. Added to that is the lifecycle cost of the sensing system design. Note that the event E collectively represents the unobserved states of the monitored phenomenon and the sensing system itself (e.g. sensors 3 & 14 are offline).

Although action A is a deterministic function of the measurement data, as dictated by the decision strategy, the measurement data is a nondeterministic function of the event E. The optimal sensing system design minimizes the risk over the possible physical events (including possible sensor failure) and the possible actions that can be taken. The expected benefit of the system is the difference between the expected loss with no sensor system, and the expected loss with some design D. If the benefit is negative, then the design should not be implemented.

In practice, design optimization is often skipped because the apparent value doesn't justify the overhead associated with setting up and solving the optimization problem. Risk-based optimization seeks to address the apparent value, while the development of what we call "rapidly-deployable" optimization seeks to address the overhead. The difficulty lies in determining the probability of A given E and D which entails the often intractable task of propagating uncertainty through models of the phenomenon, the sensing system, the data acquisition and processing, and the decision strategy. Monte Carlo simulation is a minimum-human-effort solution to this problem, requiring only a forward model of the phenomenon, and sensing system, parameterized by the system design and uncertainties. The approach then builds performance estimates by drawing random samples of the uncertainties (such as a radiation source's location, or a sensor's status) and running them through the parameterized phenomenon and sensing simulations.

Monte Carlo simulations are computationally intensive while optimization search algorithms require a large number of performance evaluations. This typically makes them a poor pair. We addressed this using the following novel strategy: Generate and process samples for designs only to the point where the designs can be rejected as unviable (with reasonable confidence). While having precise performance estimates among the top designs is important [2], knowing the precise performance of a poor design is of little value in optimization. In applying this strategy to a genetic algorithm, for example, the population is only "subjected" to a small set of samples in each round. Those who performed the worst are eliminated, while those who survive to the next generation retain their previous samples. As such, poor members are eliminated with little wasted computation, while the performance estimates for surviving members become more precise as new samples are added each round. We demonstrated that these techniques dramatically reduce computation time.

Accomplishments

- Development of a Bayesian Experimental Design framework for general surveillance systems
- Development of a tool for extracting and visualizing live traffic flow over a computer network
- Design, software implementation, and testing of a novel hybrid Monte-Carlo-Genetic-Algorithm for optimal search
- Development of a prototype general software tool for quickly setting up and solving surveillance design problems (Figure 1)
- Demonstration of a solved urban loose-nuke optimal surveillance design problem (Figure 2)

Full-Wavefield Data Processing for NDE

Most previously proposed processing approaches are rendered ineffective when inducing steady-state responses as they rely on the transient interaction of the excited waves with structural defects [3]. The key then to using steady-state waves is the ability to extract time-invariant

properties of the wave that are indicative of damage. In particular, we developed an approach to estimate local wavenumber using these steady-state response measurements. Wavenumber, the inverse of wavelength, is the spatial analogy of frequency and is fixed for a given frequency, wave-mode, thickness, and set of material properties (in anisotropic plates, it's also a function of propagation direction). As such, changes in wavenumber can be a clear indicator of a damage, which often alters the material geometry or effective properties.

We achieved several technical breakthroughs for extracting and exploiting this previously untapped wave field information. Using equipment from LANL and borrowed from our university partners, we have demonstrated full wave measurement and processing using both transducers and Q-switched lasers as excitation sources. Among the inspected structures was a 40 cm composite panel with four stringers, a stiffening spar, and an invisible delamination, all on the far side of the featureless scanning area.

We have produced sets of 2D maps of local wavenumber estimates versus wave mode and frequency for several composite, metallic, flat, and substantially curved (pipe) structures[4,5]. For all specimens, including the composite, just one of the maps provided unprecedented NDE information for identifying all hidden components and defects, including some previously unknown composite features.

Accomplishments

1. Design, construction, and testing of a portable laser scanning NDE system
2. Record breaking inspection rate capability for ultrasonic NDE: five square meters per minute
3. Demonstration of effective imaging of hidden defects in metallic and composite structural components (Figure 3) and material distribution in UF6 containers
4. LANL-benefiting, ongoing collaboration with Chonbuk National University, Korea

Impact on National Missions

Plug-and-play Surveillance System Optimization

Our national security and scientific missions are dependent on increased sensing for future technical advancement. Applications include almost all sensing activities associated with Science of Signature including nonproliferation and global security, resilience of high-performance computing, global climate treaty verification, cyber security, space situational awareness. By providing a sensor system design methodology that is robust and optimized both to the cost of the sensor and to the value of the information, these myriad applications can be addressed in a principled manner.

Full-Wavefield Data Processing for NDE – Summary of Potential Applications

Energy Infrastructure: Improve the reliability and economic efficiency of nuclear, renewable, and other energy facilities through permanent monitoring and on-demand inspection. From 1970-2008, 3611 nuclear cooling pipe-line degradation incidents were logged to OPDE[6]. Of those, 2131 were found after leaking and 159 after structural failure. For wind turbines, blade damage is the most costly to repair and can cause serious secondary damage [7].

Nuclear Materials Accountability: Make rapid, automated measurements of the material levels and material properties of containment vessel contents in order to supplement existing radiation and weight measurement technologies for unattended verification of in-process nuclear materials, reducing the likelihood of spoofing.

Stockpile Stewardship: Rapid, less intrusive inspection of gas bottles and other weapons components for improved asset readiness.

Emergency Response: Rapidly assess components of nuclear facilities following natural or malicious events, which threaten structural integrity. Remotely analyze structural components of unfamiliar devices.

Maintenance of Lab Assets: New NDE technology would benefit all lab scientific assets that require NDE for safe, reliable use, including pressure & containment vessels, and pipelines.

DoD Support: Maintenance of military air, ground, and naval assets accounts for the majority of system lifecycle cost [8]. New lightweight composite materials confound the problem. This new technology could support "smart hanger" systems for rapid inspection.

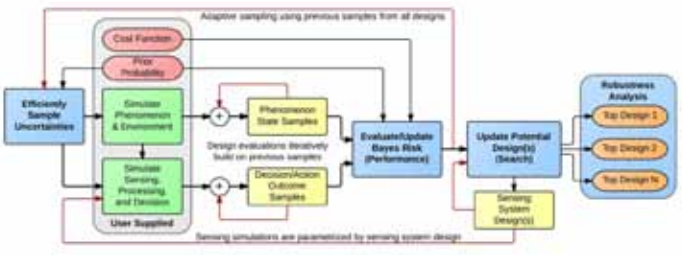

Figure 1. Flow diagram of the Bayesian optimal survielance system design framework and software.

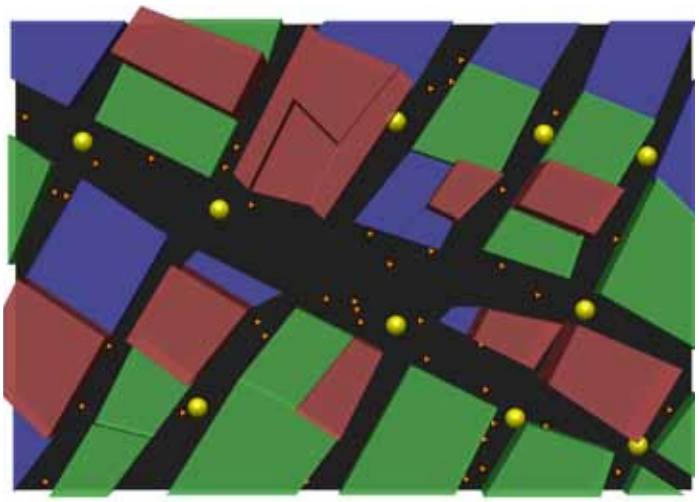

Figure 2. Optimal design result for placing radiation sensors in an urban enviroment for detecting a loose nuke.

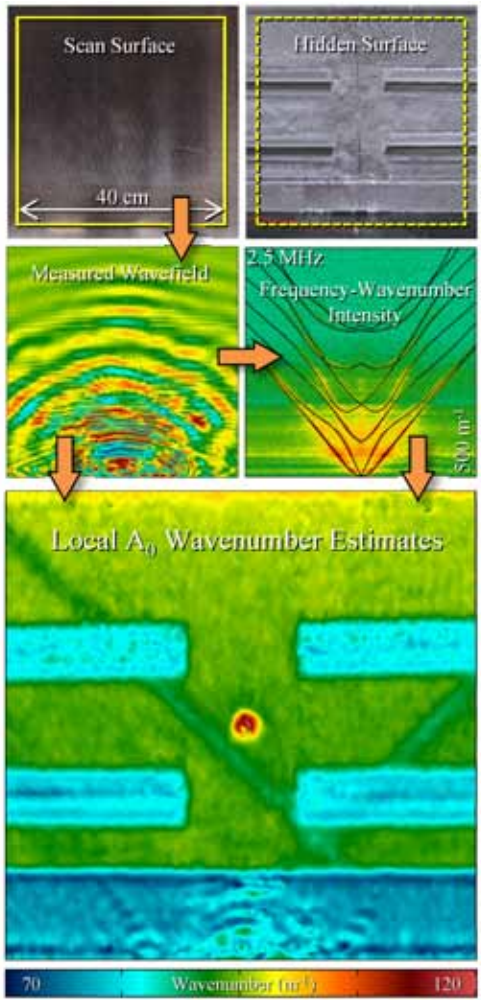

Figure 3. Wavenumber estimation procedure and results for imaging structural features and defects in a composite specimen using scanning laser technology

References

1. Flynn, E. B.. A Bayesian experimental design approach to structural health monitoring with application to ultrasonic guided waves. 2010. Doctoral Dissertation, Department of Structural Engineering, University of California - San Diego.

2. Arnold, D. V.. Noisy optimization with evolution strategies. 2002.

3. Lee, J. R., C. C. Ciang, C. Y. Park, and H. Jeong. Laser ultrasonic anomalous wave propagation imaging method with adjacent wave subtraction: Algorithm. 2012. Optical Laser Technology. 44: 1507–1515.

4. Flynn, E. B., J. R. Lee, and G. J. Jarmer. Frequency-wavenumber processing of laser-excited guided waves for imaging structural features and defects. 2012. In 6th International Workshop on Structural Health Monitoring. (Dresden, Germany, 3-6 July, 2012). , p. 788. Berlin: DGZFP.

5. Flynn, E. B., S. Y. Chong, G. J. Jarmer, and J. R. Lee. Imaging structures through local wavenumber estimation of guided waves. 2013. Internationa Journal of Nondestructive Testing and Evaluation. : 1.

6. OECD/NEA Pipe Failure Data Exchange (OPDE) Project. 2009. Nuclear Energy Agency: Committee on the Safety of Nuclear Installations. .

7. Ashwill, T. D.. Some recent trends & activities in turbines and blades . 2006. Sandia National Laboratory.

8. Boller, C.. Ways and options for aircraft structural health management. 2001. Smart Materials and Structures. : 432.

Publications

Dhital, D., J. R. Lee, C. Y. Park, and E. Flynn. Laser excitation and fully non-contact sensing ultrasonic propagation imaging system for damage evaluation. 2012. In Industrial and Commercial Applications of Smart Structures Technologies 2012 ; 20120312 - 20120313 ; San Diego, CA, United States. Vol. 8343, p. var.pagings.

Flynn, E. B., C. R. Farrar, S. Y. Chong, J. Lee, and G. Park. Structural imaging using laser-excited guided waves with advanced frequency-wavenumber processing. Presented at 2012 Annual Spring Conference of Korean Society for Nondestructive Testing. (Daegu, South Korea, 24-25 May 2012).

Flynn, E. B., E. F. Holby, and J. L. Disterhaupt. Taming the Grid: Dynamic Load Composition Quantification at the Distribution-Transformer Level . 2013. Los Alamos National Laboratory.

Flynn, E. B., G. J. Jarmer, S. Y. Chong, and J. R. Lee. Defect characterization using scanning-laser-generated guided

waves. 2012. In The First International Conference on Advances in Structural Health Management and Composite Structures. (Jeonju, South Korea, 29-31 Aug. 2012). , p. 57. Jeonju, South Korea: Chonbuk National University.

Flynn, E. B., G. J. Jarmer, S. Y. Chong, and J. R. Lee. Imaging and Characterizing Structural Defects through the Estimation of Local Dispersion Curves. Presented at 10th International Conference on Damage Assessment of Structures . (Dublin, 8-10 July 2013).

Flynn, E. B., J. Lee, G. J. Jarmer, and G. Park. Frequency-wavenumber processing of laser-excited guided waves for imaging structural features and defects . 2012. In The 6th European Workshop on Structural Health Monitoring. (Dresden, Germany, 3-6 Jul. 2012). Vol. I, p. 788. Berlin, Germany: DGZfP.

Flynn, E. B., S. Y. Chong, G. J. Jarmer, and J. R. Lee. Structural imaging through local wavenumber estimation of guided waves. 2013. NDT & E International. 59: 1.

Flynn, E. B., S. Y. Chong, G. J. Jarmer, and J. R. Lee. Full Field Measurement of High Order Ultrasonic Guided Wave Modes for Detecting and Visualizing Structure Defects. Presented at The 15th Asia Pacific Vibration Conference. (Jeju, 2-4 June 2013).

Flynn, E., M. Todd, S. Kessler, and C. Dunn. Identiying scatter targets in 2D space using in situ phased-arrays for guided wave structural health monitoring. 2011. In International Workshop on Structural Health Monitoring. (Palo Alto, CA , 13-15 Sept. 2011). , p. 200. Lancaster, PA: DEStech.

Haynes, C., M. D. Todd, E. B. Flynn, and A. Croxford. Statistically-based damage detection in geometrically-complex structures using ultrasonic interrogation. 2013. Structural Health Monitoring. 12 (2): 141.

Jarmer, G. J., E. B. Flynn, and M. D. Todd. Dispersion curve estimation via phased array beamforming methods. 2013. Journal of Intelligent Materials and Structures. : 1.

Jarmer, G. J., M. D. Todd, and E. B. Flynn. Phased Array Beamforming for the Detection of Damage in an Aluminum Plate. 2012. In The 1st International Conference on Advances in Structural Health Management and Composite Structures. (Jeonju, South Korea, 29-31 Aug. 2012). Vol. I, p. 56. Jeonju, South Korea: Chonbuk National University.

Mascarenas, D. [Los Alamos National Laboratory]., C. [Los Alamos National Laboratory]. Farrar, null. Chong, J. R. Lee, null. Park, and E. [Los Alamos National Laboratory]. Flynn. Application of Compressed Sensing to 2-D Ultrasonic Propagation Imaging System data. 2012. DOE/LANL.

Laboratory Directed Research & Development
Los Alamos National Laboratory
PO Box 1663, MS M708
Los Alamos, NM 87545
505-667-1235 (phone)